



**Aalborg University, Copenhagen, Denmark
4-5 October 2023**

43rd AIVC Conference

11th TightVent Conference

9th venticool Conference

**Ventilation, IEQ and health in sustainable
buildings**

PROCEEDINGS

Supporting Organizers:



Conference scope

As we spend most of our time in commercial and residential facilities, it is important for our society to look at how these spaces impact the environment and the people in them. This task is important for building and facility managers, maintenance managers, energy managers as well as expert and researcher concerned with adopting sustainable and healthy practices for an organization.

From indoor environmental quality point of view, sustainable buildings prioritize the quality of life and the wellbeing of the buildings' occupants and at the same time reduce negative environmental impacts. A building that, in its design, construction or operation, reduces negative impacts on our climate, also reduces their occupants' risk of related health problems and provides a more pleasant indoor environment, as well as increases occupants' satisfaction.

The conference organisers welcome contributions on the role of smart ventilation, building and ductwork airtightness and ventilative and resilient cooling on IEQ and health in sustainable buildings.

Since its 40th year of operation and annual Conference, the AIVC board has been offering authors the opportunity for a peer review of their paper. The procedure is twofold including 2 separate calls for abstracts & papers depending on whether the authors are interested in the peer review of their papers or not.

The papers which have been peer reviewed are indicated in the table of contents.

Editors

Peter Wouters (*INIVE*), Arnold Janssens (*INIVE/Ghent University*), Alireza Afshari (*Aalborg University*), Maria Kapsalaki (*INIVE*)

Scientific Committee

Australia

Riccardo Paolini

University of New South Wales

Mat Santamouris

University of New South Wales

Austria

Peter Holzer

Institute of Building Research & Innovation ZT-GmbH

Belgium

Hilde Breesch

KU Leuven

Samuel Caillou

Buildwise

Arnold Janssens

Ghent University

Jelle Laverge

Ghent University

Peter Wouters

INIVE

China

Zhengtao Ai

Hunan University

Guoqiang Zhang

Hunan University

Denmark

Alireza Afshari

Aalborg University

Bjarne Olesen

Technical University of Denmark

Carsten Rode

Technical University of Denmark

Pawel Wargocki

Technical University of Denmark

Per Heiselberg

Aalborg University

Henrik N. Knudsen

Aalborg University

France

Francis Allard

University of La Rochelle

François Durier

CETIAT

Gaëlle Guyot

ADEME

Valérie Leprince

Cerema

Laure Mouradian

CETIAT

Germany

Gunnar Grün

Fraunhofer-Institut für Bauphysik IBP

Hungary

Laszlo Fulop

University of Pecs

Zoltan Magyar

Budapest University of Technology and Economics

Ireland

Marie Coggins

NUI Galway

Hala Hassan

NUI Galway

Simon Jones

Air Quality Matters

James McGrath

Maynooth University

Italy

Lorenzo Pagliano

Politecnico di Milano

Japan

Yoshihiko Akamine

NILIM

Takao Sawachi

Building Research Institute

Hiroshi Yoshino

Tohoku University

Netherlands

Wouter Borsboom
Willem de Gids
Jaap Hogeling

TNO
ventGuide
REHVA

New Zealand

Manfred Plagmann

BRANZ

Norway

Kari Thunshelle
Guangyu Cao
Natasa Nord

SINTEF Byggforsk
NTNU
NTNU

Republic of Korea

Yun Gyu Lee

Korea Institute of Construction Technology

Spain

Pilar Linares Alemparte

The Eduardo Torroja institute for Construction Science-
CSIC

Sonia García Ortega

The Eduardo Torroja institute for Construction Science-
CSIC

Sweden

Jan-Olof Dalenbäck

Chalmers University of Technology

United Kingdom

Benjamin Jones
Maria Kolokotroni

University of Nottingham
Brunel University London

United States of America

Andrew Persily
Max Sherman
Ian Walker
Don Weekes

NIST
LBNL
LBNL
IEQ-GA

ISBN: 978-2-930471-65-5

EAN: 9782930471655

Conference Organizers

INIVE (International Network for Information on Ventilation and Energy performance)

[INIVE](#) (International Network for Information on Ventilation and Energy Performance) was created in 2001. The main reason for founding INIVE was to set up a worldwide acting network of excellence in knowledge gathering and dissemination. At present, INIVE has as member organisations [Buildwise](#), [CETIAT](#), [Ghent University](#), [Fraunhofer-IBP](#), [KU Leuven](#)).

INIVE has multiple aims, including the collection and efficient storage of relevant information, providing guidance and identifying major trends, developing intelligent systems to provide the world of construction with useful knowledge in the area of energy efficiency, indoor environment, ventilation and airtightness of buildings. Building energy- and environmental performance regulations are another major area of interest for the INIVE members, especially in relation to the implementation of the European Energy Performance of Buildings Directive. With respect to the dissemination of information, INIVE aims for the widest possible distribution of information.

INIVE is coordinating and/or facilitating various international projects, e.g. the Air Infiltration and Ventilation Centre – [AIVC](#), [Dynastee](#), the Indoor Environmental Quality – Global Alliance – [IEQ-GA](#), the [TightVent Europe platform](#), and the [venticool](#) platform. INIVE has also coordinated the ASIEPI project (01/10/2007 – 31/03/2010) dealing with the evaluation of the implementation and impact of the EU Energy Performance of Buildings Directive, the QUALICHECK project and platform aiming towards improved compliance and quality of the works for better performing buildings, the European portal on Energy Efficiency – [BUILD UP](#) and the EPBD feasibility study 19a



AIVC

The AIVC (www.aivc.org) activities are supported by the following countries: Australia, Belgium, China, Denmark, France, Ireland, Italy, Japan, Netherlands, New Zealand, Norway, Republic of Korea, Spain, Sweden, UK and USA.

Created in 1979, the Air Infiltration and Ventilation Centre (www.aivc.org) is one of the projects/annexes running under the International Energy Agency's Energy in Buildings and Communities Programme. With the support of 16 member countries as well as key experts and associations (IEQ-GA, REHVA, IBPSA, ISIAQ), the AIVC offers industry and research organisations technical support aimed at better understanding the ventilation challenges and optimising energy efficient ventilation

Since 1980, the annual AIVC conferences have been the meeting point for presenting and discussing major developments and results regarding infiltration and ventilation in buildings. AIVC combines forces with the TightVent Europe and venticool platforms aiming at facilitating exchanges and progress on airtightness and ventilative cooling issues, which are major topics of this conference.



TightVent Europe

The [TightVent Europe](#) 'Building and Ductwork Airtightness Platform' was launched in January 2011. TightVent Europe aims at facilitating exchanges and progress on building and ductwork airtightness issues, including the organization of conferences, workshops and webinars. It fosters experience sharing as well as knowledge production and dissemination on practical issues such as specifications, design, execution, control, etc., taking advantage of the lessons learnt from pioneering work while keeping in mind the need for adequate ventilation. In September 2012, the TightVent Airtightness Associations Committee (TAAC) was also launched with the primary goal of promoting reliable testing/inspection and reporting procedures. TAAC gathers both TightVent partners and TAAC members (experts or representatives of airtightness testers in their countries).

TightVent Europe has been initiated by INIVE (International Network for Information on Ventilation and Energy Performance) with at present the financial and/or technical support of the following partners: [Lindab](#), [MEZ-TECHNIK](#), [Retrotec](#), [Acin Instrumenten](#), [BlowerDoor GmbH](#), BCCA, [dooApp](#), [Soudal](#), [Eurima](#), [Gonal](#), [SIGA](#) and [BPIE](#).



venticool

[venticool](#) is the international ventilative cooling platform launched in October 2012 to accelerate the uptake of ventilative cooling by raising awareness, sharing experience and steering research and development efforts in the field of ventilative cooling. In 2020, venticool decided to broaden its scope towards resilient ventilative cooling.

The platform supports better guidance for the appropriate implementation of resilient ventilative cooling strategies as well as adequate credit for such strategies in building regulations.

The platform philosophy is to pull resources together and to avoid duplicating efforts to maximize the impact of existing and new initiatives. venticool joins forces with international projects (in particular [IEA EBC Annex 62](#) (ventilative cooling) and, more recently, [IEA EBC](#)

[annex 80](#) (Resilient cooling for buildings)) and organizations with significant experience and/or well identified in the field of ventilation and thermal comfort like [AIVC](#) and [REHVA](#).

venticool was initiated by INIVE (International Network for Information on Ventilation and Energy Performance) with the financial and/or technical support of the following partners: NAVENTA, [Velux](#), [Reynaers Aluminium](#), [WindowMaster](#), [Active House](#), [CIBSE nvg](#), [Eurowindoor](#) and [REHVA](#).



Aalborg University

Aalborg University, founded in 1974, is Denmark's fifth largest university with 20.200 students. A young and international university with campuses in Aalborg, Esbjerg and Copenhagen, offering 76 undergraduate and 112 postgraduate studies with a real-world approach and provide world-class research.

Is divided into four faculties a) Technical Faculty of IT and Design, b) Faculty of Engineering and Science, c) Faculty of Social Sciences and Humanities, d) Faculty of Medicine.

Additionally, has a cross-cutting unit, AAU Innovation, tasked with strengthening entrepreneurship and innovation, and promoting the university's knowledge cooperation with society.

In 2018 an analysis by the elite US University MIT placed the AAU engineering programmes as the best in Europe and fourth best in the world. Respectively, in the QS World University Rankings by Subject, it is ranked 58th for Electrical Engineering and 25th in Petroleum Engineering worldwide. Aalborg University is very focused on developing engineers with experience from working with real companies in their semester projects. Also, focus is put on working in a team environment that develops the interpersonal skills, as well as team-working skills.

Additionally, in 2019 the Times Higher Education World University Rankins placed AAU at number 207, while among younger universities (under 50 years) AAU is number 18 in the world.

Common to all three campuses is AAU's strong focus on problem-based learning as well as interdisciplinarity and research-based innovation. Through strong interplay between staff and students and intense collaboration with public and private sectors, offers degree programmes with a real-world approach and provide world-class research.



AALBORG UNIVERSITY

Supporting Organizers



Event sponsors

The conference organizers are grateful to the following companies for their support to this event

TightVent Partners



Venticool Partners



Other Sponsors



Table of Contents

Tomorrow's Ventilation Solutions for Future Hospital Demands <i>Trond Thorgeir Harsem</i>	20
Users and practices in heating and ventilating homes – why do they behave different than we think? <i>Kirsten Gram-Hanssen</i>	22
What we know about smart ventilation <i>Gaëlle Guyot</i>	24
Dallying with DALYs: Why acceptable IAQ should consider harm <i>Benjamin Jones</i>	28
Human exposure against airborne pathogens in an office environment <i>Risto Kosonen, Sami Lestinen, Simo Kilpeläinen</i>	29
Discussion on minimum ventilation rates for infection control <i>Yuguo Li, Wei Jia</i>	31
Mitigation of airborne transmission of respiratory viruses by ventilation – past, present and future <i>Arsen K. Melikov</i>	33
Point source ventilation effectiveness in infection risk-based post-COVID ventilation design <i>Jarek Kurnitski, Martin Kiil, Alo Mikola, Karl-Villem Võsa</i>	35
Airborne transmission of disease in stratified and non-stratified flow <i>Peter V. Nielsen, Chen Zhang, Li Liu</i>	45
Acoustic method for measurement of airtightness – field testing on three different existing office buildings in Germany <i>Björn Schiricke, Benedikt Kölsch</i>	53
Pulse tests in highly airtight Passivhaus standard buildings <i>Xiaofeng Zheng, Luke Smith, Christopher Wood</i>	63
Correlation analysis between ACH50 and Air permeability considering the floor area of a residential buildings <i>Su-Ji Choi, Jae-Hun Jo</i>	72
Airtightness predictive model from measured data of residential buildings in Spain <i>Irene Poza-Casado, Pilar Rodríguez-del-Tío, Miguel Fernández-Temprano, Miguel Ángel Padilla-Marcos, Alberto Meiss</i>	79

Bridging The Mechanical / Enclosure Gap	89
<i>David de Sola, Nathaniel Fanning</i>	
Windows and ceiling fan occupant behaviour model coupling methodology with building energy models, a tropical case study	103
<i>Maäréva Payet, Maxime Boulinguez, Mathieu David, Philippe Lauret, François Garde</i>	
An innovative approach to better understand hot discomfort, based on the measurement of global human responses, including physiological and sensory indicators - application to end users of mixed mode cooled buildings under tropical climate conditions	112
<i>Gwénaëlle Haese, Maxime Boulinguez, Pierre Bernaud, Anthony Couzinet</i>	
An IAQ and thermal comfort coach prototype to improve comfort and energy consumption thanks to adequate management of natural ventilation: development and first feedback results	122
<i>Arnaud Jay, Pierre Bernaud, Franck Alessi</i>	
Towards an alternative cooling: Optimisation of the successive use of the cooling systems from passive to active - Development of design and control strategies of the hybrid cooling	124
<i>Arnaud Jay, Aurélie Fouquier, Maxime Boulinguez, Gwénaëlle Haese, Simon Thebault, Virginie Chantepie, Jean Castaing Lasvignottes, Maäréva Payet, Simon Rouchier, Jean-Marie Caous, Pierre Constant-Beraud</i>	
Introduction to IEA EBC Annex 78	134
<i>Bjarne W. Olesen, Pawel Wargocki</i>	
Air cleaner as an alternative to increased ventilation rates in buildings: a simulation study for an office	136
<i>Alireza Afshari, Alessandro Maccarini, Göran Hultmark</i>	
Exploring the Energy-Saving Benefits of Gas-Phase Air Cleaning in Nordic Buildings	138
<i>Sasan Sadrizadeh</i>	
Gas phase air cleaning effects on ventilation energy use and indicators for energy performance	140
<i>Dragos-Ioan Bogatu, Ongun B. Kazanci, Bjarne W. Olesen</i>	
On the integration of envelope pressure inhomogeneity and autocorrelation in fan pressurization uncertainty analysis	148
<i>Martin Prignon</i>	
Statistical analysis of the correlations between buildings air permeability indicators	160
<i>Bassam Moujalled, Benedikt Kölsch, Adeline Mélois, Valérie Leprince</i>	
Proposal for new implementations in ISO 9972	163
<i>Benedikt Kölsch, Valérie Leprince, Adeline Mélois</i>	

Which design parameters impact the resilience to overheating in a typical apartment building?	173
<i>Abantika Sengupta, Jef Kerckaert, Marijke Steeman, Hilde Breesch</i>	
Renewable ventilative cooling? Insights from an Irish perspective	183
<i>Adam O' Donovan, Theofanis Psomas, Paul D. O' Sullivan</i>	
Urban context and climate change impact on the thermal performance and ventilation of residential buildings: a case-study in Athens	194
<i>Maria Kolokotroni, May Zune, Thet Paing Tun, Ilia Christantoni , Dimitra Tsakanika</i>	
Thermography-based assessment of mean radiant temperature and occupancy in healthcare facilities	204
<i>Paul Seiwert, Quan Jin, Kai Rewitz, Ulrike Rahe, Dirk Müller</i>	
Analyzing natural ventilation and cooling potential in a communal space building in Belgium under future climate conditions	214
<i>Shiva Khosravi, Joost Declercq, Delphine Ramon</i>	
A study of indoor environment and window use in French dwellings monitored during a summer with heatwaves	222
<i>Mathilde Hostein, Bassam Moujalled, Marjorie Musy, Mohamed El Mankibi</i>	
Importance of thermal stack effect in ventilative cooling concepts for residential buildings	232
<i>Diederik Verscheure, Koen Maertens, Axel Deturck</i>	
Performance 2 project - Winter IAQ campaigns in 13 dwellings equipped with Humidity-based DCV systems: analyses of the ventilation performance after 15 years of use	239
<i>Adeline Mélois, Ambre Marchand Moury, Marc Legree, Juan Rios, Jérémy Depoorter, Nicolas Dufour, Sylvain Rebières, Gaëlle Guyot</i>	
Checking and assuring real IAQ and energy performances through demand control and cloud connectivity	248
<i>Ivan Pollet, Kevin Verniers, Steven Delrue</i>	
Data driven models for fault detection - Combining thermal and indoor air quality grey box models	251
<i>Gabriel Rojas, Romed Jenewein, Klaus Prenninger, Johannes Schnitzer</i>	
Evaluation of supply temperature set-points and airflow imbalance using smart ventilation data	261
<i>Kevin Michael Smith*1, Jakub Kolarik</i>	
Technologies in balanced ventilation systems to maintain optimal performance in energy and comfort	263
<i>Bart Cremers</i>	
Building and ductwork airtightness in Norway: national trends and requirements	265
<i>Tormod Aurlien</i>	

Building and ductwork airtightness in the Netherlands: national trends and requirements	267
<i>Niek-Jan Bink, Rob Dam, Marcus Lightfoot</i>	
Building and ductwork airtightness in Spain: national trends and requirements	269
<i>Timo Hoek, Irene Poza-Casado, Sergio Melgosa</i>	
Building and ductwork airtightness in Latvia: national trends and requirements	271
<i>Andrejs Nitijevskis, Vladislavs Keviss, Nolwenn Hurel</i>	
Air tightness and its impact on energy consumption in multi-family residential buildings in Montenegro	273
<i>Esad Tombarević, Igor Vušanović, Miloš Krivokapić</i>	
Resilient Cooling Technology Profiles from the EBC Annex 80	282
<i>Peter Holzer</i>	
Resilient Cooling Guidelines from the EBC Annex 80	284
<i>Vincenzo Corrado, Theofanis Psomas, Philipp Stern</i>	
Health risks of residential indoor and outdoor exposure to fine particle-bound phthalates	286
<i>Jiayao Chen, Francesco Pilla</i>	
HEPA filters to improve vehicle cabin air quality – advantages and limitations	290
<i>Dixin Wei, Anders Löfvendahl</i>	
Experimental study of an innovative wet scrubber concept in regards to particle filtration and pressure loss	303
<i>Nhat Nguyen, Martin Kremer, Hendrik Fuhrmann, Philipp Ostmann, Dirk Müller</i>	
An evaluation of CO2 emission rates by Chilean school children	313
<i>Nicolás Carrasco, Constanza Molina, Benjamin Jones</i>	
The Effects of Bedroom Mechanical Ventilation on Health and Sleep Quality	320
<i>Jeong Won Kim, Sun Ho Kim, Yong Kyu Baik, Hyeun Jun Moon</i>	
Analysis of PM_{2.5} indoor-outdoor ratio in lobby floor according to configurations of entrance	328
<i>So-Yi Park, Jae-Hun Jo</i>	
Proposal of an effort-benefit diagram to compare unit and room air-change rates applied to a literature review	337
<i>Sven Auerswald, Andreas Wagner, Hans-Martin Henning</i>	
Experimental Investigation of Indoor Air Quality in an Open Office Environment	346
<i>Altug Alp Erdogan, Mustafa Zeki Yilmazoglu, Umit Gencturk</i>	

Hygienic Air Handling Unit Certification Program: the new necessity for a guaranteed indoor air quality	355
<i>Ali Nour Eddine, Sylvain Courtey</i>	
Car traffic or emissions from heating sources: What is responsible for IAQ?	373
<i>Katarzyna Ratajczak, Maciej Siedlecki</i>	
Monitoring VOCs' concentrations in a circular biobased residential building using low-cost sensors	383
<i>Yannick Thienpont, Seppe Verbiest, Douaa Al Assaad, Hilde Breesch</i>	
Smart & Predictive Air Quality Solution	392
<i>Paul Brassler, Florian Käding</i>	
Energy Implications of Increased Ventilation in Commercial Buildings to Mitigate Airborne Pathogen Transmission	399
<i>Sean M. O'Brien, David Artigas, Ece Alan</i>	
Reflections on alternative modelling approaches regarding occupants' window operation behaviour	408
<i>Christiane Berger, Ardeshir Mahdavi</i>	
Development of air supplied ceiling radiant air conditioning system using the Coanda effect	416
<i>Satoshi Noguchi, Yasuyuki Shiraishi, Daishi Inoue, Hiroaki Tanaka</i>	
Wind Tunnel Experiment of Wind-Induced Single-sided Ventilation under Generic Sheltered Urban Area	423
<i>Zitao Jiang, Tomohiro Kobayashi, Toshio Yamanaka, Noriaki Kobayashi, Narae Choi, Mats Sandberg, Kayuki Sano, Kota Toyosawa</i>	
A study on desiccant system regenerated by waste heat from home-use solid oxide fuel cell cogeneration system	433
<i>Keita Mizuno, Isamu Ohta</i>	
Method for Evaluating an Air-Conditioning System with Natural Ventilation by Coupled Analysis of a Building Energy Simulation Tool and Computational Fluid Dynamics	443
<i>Ryuichi Yasunaga, Yasuyuki Shiraishi</i>	
Performance comparison of different ventilation strategies in elderly care homes in Belgium	451
<i>Douaa Al Assaad, Quinten Carton, Abantika Sengupta, Hilde Breesch</i>	
Sea Water Air Conditioning (SWAC): A Resilient and Sustainable Cooling Solution for hot and humid climates - Energy Performance and Numerical Modeling	462
<i>Kanhan Sanjiv, Olivier Marc, Franck Lucas</i>	

The Effects of Lowering Temperature Setpoints on Perceived Thermal Comfort – An experimental study in office buildings	471
<i>Beatriz Coutinho</i>	
Long-term energy performance of dew-point indirect evaporative cooler under the climate change world scenario	478
<i>María Jesús Romero-Lara, Francisco Comino, Manuel Ruiz de Adana</i>	
On the assessment of the pressure coefficient on the mixed ventilation modeling	487
<i>Marcos Batistella Lopes, Gaëlle Guyot, Nathan Mendes</i>	
Construction of operational control rules for an earth-to-air heat exchanger through transfer reinforcement learning	497
<i>Yuki Adachi, Yasuyuki Shiraishi</i>	
Ventilation and Thermal Performance Examination of Slot Line Diffuser for Perimeter Usage by CFD Simulation	507
<i>Shaoyu Sheng, Toshio Yamanaka, Tomohiro Kobayashi</i>	
Quantifying the Potential Health Impacts of Unvented Combustion in Homes - A Meta-Analysis	517
<i>Jacob Bueno de Mesquita, Núria Casquero-Modrego, Iain Walker, Brennan Less, Brett Singer</i>	
How to create a performance-based regulation on ventilation – the French Experience	527
<i>Valérie Leprince, Baptiste Poirier, Gaëlle Guyot</i>	
Comparative Analysis Between Indoor Temperatures of Dwellings at Urban Scale During a Typical and Extreme Summers in a Temperate Climate	537
<i>Ainhoa Arriazu-Ramos, Germán Ramos Ruiz, Juan José Pons Izquierdo, Ana Sánchez-Ostiz Gutiérrez, Aurora Monge-Barrio</i>	
Decarbonization and IAQ in Spain: a roadmap	547
<i>Rafael Villar Burke, Marta Sorribes Gil, Daniel Jiménez González</i>	
Ventilation behaviour of occupants driven by outdoor temperature: 12 case studies	556
<i>Sonia García-Ortega, Pilar Linares-Alemparte</i>	
Indoor air quality in Austrian classrooms – Assessing different ventilation strategies with a citizen science approach	566
<i>Simon Beck, Gabriel Rojas, Elena Krois, Sebastian Goreth, Christian Hechenberger</i>	
Measurement of ventilation effectiveness and indoor air quality in toilets at mass gathering events	575
<i>Ben M. Roberts, Filipa Adzic, E. Abigail Hathway, Christopher Iddon, Benjamin Jones, Malcolm J. Cook, Liora Malki-Epshtein</i>	

Impact of the building airtightness and natural driving forces on the operation of an exhaust ventilation system in social housing in Chile	585
<i>Gilles Flamant, Waldo Bustamante, Arnold Janssens, Jelle Laverge</i>	
Metal Oxide Semiconductor sensors (MOS) for measuring Volatile Organic Compounds (VOC) - performance evaluation in residential settings	594
<i>Jakub Kolarik</i>	
Towards performance-based approaches for smart residential ventilation: a robust methodology for ranking the systems and decision-making	604
<i>Baptiste Poirier, Gaëlle Guyot, Monika Woloszyn</i>	
Update on Resilient cooling and indicators from the IEA EBC Annex 80	616
<i>Peter Holzer</i>	
Ventilative Cooling Design In Practice: Where next?	618
<i>Paul D. O'Sullivan, Adam O'Donovan, Maha Sohail</i>	
Life cycle assessment: A design element for ventilation system selection	621
<i>Jannick K. Roth</i>	
Lessons Learned from Irish Schools: Early-stage Insights on Overheating	625
<i>Adam O' Donovan, Elahe Tavakoli, Paul D. O'Sullivan</i>	
Resilient cooling in office buildings: case study in Belgium	628
<i>Joost Declercq, Shiva Khosravi, Abantika Sengupta, Hilde Breesch</i>	
Design procedures for ventilative cooling integrated in new standards	630
<i>Christoffer Plesner, Jannick K. Roth</i>	
Sensitivity Analysis of CO2 Concentrations as Ventilation Metrics	634
<i>Oluwatobi Oke, Andrew Persily</i>	
Evaluation of Uncertainties of Using CO2 for Studying Ventilation Performance and Indoor Airborne Contaminant Transmissions	643
<i>Liangzhu (Leon) Wang, Ibrahim Reda, Shujie Yan, Eslam Ali, Dahai Qi, Theodore Stathopoulos, Andreas Athienitis</i>	
Effects of ventilation on airborne transmission: particle measurements and performance evaluation	653
<i>Huijuan Chen, Caroline Markusson, Svein Ruud</i>	
Impact and benefits of the air cleaning measures implemented in two schools	655
<i>Liang Grace Zhou, Chang Shu, Justin Berquist, Janet Gaskin, Greg Nilsson</i>	
Critical reflections on indoor-environmental quality constructs	665
<i>Ardeshir Mahdavi, Christiane Berger</i>	
Ventilation and sleep quality	674
<i>Pawel Wargocki, Mizuho Akimoto, Xiajoun Fan, Shin-ichi Tanabe, Chandra Sekhar, Li Lan</i>	

Applicability and sensitivity of the TAIL rating scheme using data from the French national school survey	677
<i>Minh-Tien Tran, Wenjuan Wei, Claire Dassonville, Corinne Mandin, Mickael Derbez, Christophe Martinsons, Pascal Ducruet, Valérie Héquet, Pawel Wargocki</i>	
An investigation of MVHR system performance based on health and comfort criteria in bedrooms of low-carbon social housing in South-Wales, UK	686
<i>Faisal Farooq, Emmanouil Perisoglou, Miltiadis Ionas, Simon Lannon, Jo Patterson, Phil Jones</i>	
Impact of optimized residential ventilation with energy recovery on health and well-being	696
<i>Martin Kremer, Kai Rewitz, Dirk Müller</i>	
A detailed investigation of the impact of an innovative dynamic façade system on indoor environmental quality in offices	706
<i>Magdalena Hajdukiewicz, Marcel G.L.C. Loomans</i>	
A methodology for evaluating the ventilative cooling potential in early-stage building design	715
<i>Valentina Radice Fossati, Annamaria Belleri, Dick van Dijk</i>	
Ventilation reliability: A pilot study on window opening behaviour in a primary school	727
<i>Lara Tookey, Mikael Boulic, Barry McDonald, Wyatt Page, Pawel Wargocki, Hennie van Heerden</i>	
A survey of building design practitioner perceptions of ventilative cooling in their building design processes	743
<i>Maha Sohail, Adam O'Donovan, Christoffer Plesner, Paul D. O'Sullivan</i>	
Can naturally ventilated office buildings cope with dusty outdoor air?	753
<i>Evangelos Belias, Flourentzos Flourentzou, Dusan Licina</i>	
Distribution of Particulate Matter Concentration and Temperature Stratification Examined by Zonal Model and Experimental Measurements in Room with A Novel Portable Displacement Ventilation Cooling Unit	762
<i>Toshio Yamanaka, Choi Narae, Tomohiro Kobayashi, Aya Essa, Noriaki Kobayashi, Miharuru Komori, Nobuki Matsui, Tetsuya Okamoto, Takeshi Arakawa, Yuki Yamoto, Shougo Otaka</i>	
Thermal comfort and risk of draught with natural ventilation – assessment methods, experiences and solutions	772
<i>Jannick Roth, Per Heiselberg, Chen Zhang</i>	
Evaluation of sensor-based air cleaners to remove PM_{2.5} and TVOC from indoors with pollutant sources of smoking and burning candles	782
<i>Kathrine Andersen, Stig Koust, Freja Rasmussen, Li Rong</i>	

Developing methodology for testing of gas-phase air cleaners based on perceived air quality	792
<i>Kanta Amada, Lei Fang, Bjarne W. Olesen, Shin ichi Tanabe, Pawel Wargocki</i>	
Evaluating the impact of air cleaning on bioaerosols and other IAQ indicators in Belgian daycare facilities	795
<i>Sarah L. Paralovo, Klaas de Jonge, Arnold Janssens, Jelle Laverge, Reinoud Cartuyvels, Koen Van den Driessche, Borislav Lazarov, Maarten Spruyt, Marianne Stranger</i>	
Removal of Odorants in Nursing Homes Using Air Cleaners	805
<i>Stig Koust, Freja Rydahl Rasmussen, Morten Stoltenberg</i>	
What can CO₂ measurements tell us about ventilation and infection risk in classrooms?	815
<i>Carolanne V.M. Vouriot, Paul F. Linden</i>	
Indoor air modelling and infection risk assessment in a naturally ventilated patient room	818
<i>Natalia Lastovets, Mohamed Elsayed, Ville Silvonon, Anni Luoto, Piia Sormunen</i>	
Performance of Local Ventilation System Combined with Underfloor Air Distribution as Preventative Measures for Infectious Diseases in Consulting Room	828
<i>Jun Yoshihara, Toshio Yamanaka, Narae Choi, Tomohiro Kobayashi, Noriaki Kobayashi, Aoi Fujiwara</i>	
The numerical investigation of human micro-climate with different human simulators	838
<i>Haruna Yamasawa, Sung-Jun Yoo, Kazuki Kuga, Kazuhide Ito</i>	
Introduction to IEA EBC Annex 87	844
<i>Bjarne W. Olesen, Ongun B. Kazanci</i>	
Indoor environmental quality (IEQ) and energy performance evaluation of PECS	846
<i>Douaa Al Assaad, Marco Perino, Dragos-Ioan Bogatu, Bjarne W. Olesen</i>	
Physiological sensing for thermal comfort assessment	848
<i>Dragos-Ioan Bogatu, Jun Shinoda, José Joaquín Aguilera, Bjarne W. Olesen, Futa Watanabe, Yosuke Kaneko, Ongun B. Kazanci</i>	
ASHRAE 241-2023 Control of Infectious Aerosols	859
<i>Max Sherman, Benjamin Jones</i>	
Can the Wells-Riley model universally assess airborne pathogen infection risk?	861
<i>Benjamin Jones, Christopher Iddon, Max Sherman</i>	
Flow dynamic of human cough and measuring techniques: A review	870
<i>Chen Zhang, Peter V. Nielsen, Simon Madsen, Li Liu, Chunwen Xu, Zhengtao Ai</i>	

Evaluating the impact of air cleaning and ventilation of airborne pathogens and human bio-effluents at two primary schools in Belgium	880
<i>Klaas De Jonge, Marianne Stranger, Sarah L. Paralovo, Maarten Spruyt, Borislav Lazarov, Tom Geens, Reinoud Cartuyvels, Koen Van den Driessche, Jelle Laverge, Arnold Janssens</i>	
Review of international standards describing air cleaner test methods	889
<i>Hannelore Scheipers, Arnold Janssens, Jelle Laverge</i>	
Rethinking different ventilation strategies in a post-pandemic era: a CFD assessment	899
<i>Alicia Murga, Kazuhide Ito, Makoto Tsubokura</i>	
How the COVID Pandemic and the Energy Crisis Have Influenced Indoor Environmental Conditions in non-residential Buildings	907
<i>Aurora Monge-Bario, Ainhoa Arriazu-Ramos, María Fernández-Vigil, Ana Sánchez-Ostiz Gutiérrez</i>	
The impact of increased occupancy on particulate matter concentrations in mechanically-ventilated residential buildings in a subtropical climate	917
<i>German Hernandez, Rafael Borge, Dan Blanchon, Terri-Ann Berry</i>	
On-Site Capture Efficiency of Kitchen Range Hood Based on Particle Diameters and Exhaust Flow Rates	927
<i>Shinhye Lee, Seoungjun Park, Donghyun Rim, Donghwa Kang, Myoungsok Yeo</i>	
An investigation of cooking-related pollutants in the residential sector	937
<i>Daniela Mortari, Gaëlle Guyot, Nathan Mendes</i>	
Fine dust measurement in ducts of balanced ventilation systems	947
<i>Bart Cremers, Jan de Vries</i>	
The Impact of Deep Energy Renovations on Indoor Air Quality and Ventilation in Irish Dwellings	954
<i>Hala Hassan, Asit Kumar Mishra, Hilary Cowie, Emmanuel Bourdin, Brian McIntyre, Marie Coggins</i>	
Financial impact of leaky ductwork in buildings – a calculation tool to raise awareness	960
<i>Nolwenn Hurel, Valérie Leprince, Marcus Lightfoot</i>	
Decoding 30 Years of Insights: Conclusions from ISIAQ's Landmark Webinar Series on Indoor Air Quality and Climate	970
<i>Ying Xu</i>	
Calculation of the effect of ventilation measures in existing dwellings to reduce the carbon footprint	971
<i>Wim Kornaat, Wouter Borsboom, Ruud van der Linden</i>	

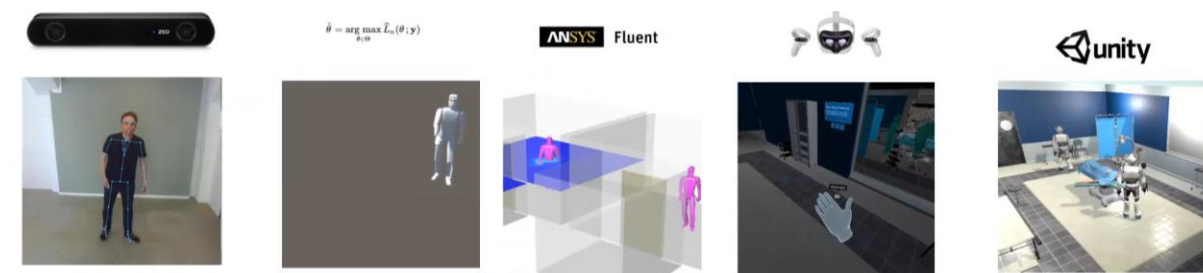
Tomorrow's Ventilation Solutions for Future Hospital Demands

Trond Thorgeir Harsem ^{1,2}

*1 Research and Development and Smart Technology, Norconsult AS, Sandvika, Norway -
2 School of Architecture and Built Environment, KTH Royal Institute of Technology, Stockholm, Sweden
t.thorgeir.harsem@norconsult.com*

SUMMARY

At hospitals and healthcare buildings, the ultimate objective is to save lives. According to the 2018 annual reports from the Norwegian Institute of Public Health, the incidence of postoperative wound infections (POSI) ranged from 1.6% to 13.4% depending on the surgical procedure. Surgical Site Infections (SSI) are severe complications in hospitals worldwide and Norway. SSI contributes to large societal costs through extended hospitalization, increased need for reoperation, and less participation in working life. The high occurrence of SSI increases the need for antibiotics, both preventive and treatment, increasing the risk of developing antibiotics resistance bacteria. Although it is well-known that most SSIs are caused by germs, the transport mechanism of such microorganisms is still a matter of debate. Recognizing the critical need for improved safety measures, Norconsult embarked on a groundbreaking project.

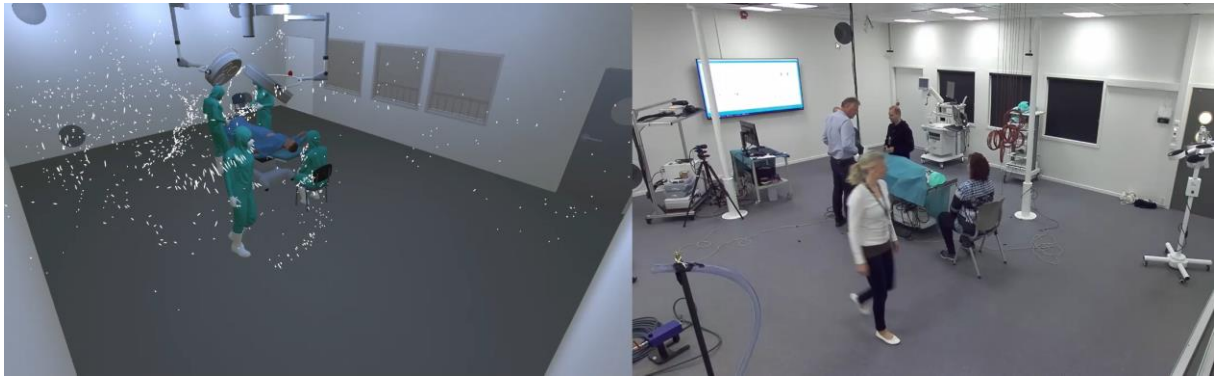


Norconsult's primary goal was to enhance the visualization and understanding of particle generation and ventilation flows within a 60m² operating room. To achieve this, they are developing an innovative Extended Reality (XR) solution. XR is a collective term for technologies that combine the real world with virtual elements. This cutting edge technology captures the dynamic interaction between healthcare personnel's movements and the virtual airflow and particle distribution in real time.

XR Technology can be used to visualize contaminants within an operating environment to increase staff awareness regarding their activity linked to air movement and airborne particle levels. The presented project has developed an XR tool to translate the numerical simulation results into an easy-to-understand 3D domain to increase the understanding of the interaction between the healthcare personnel and the operating room ventilation. Such dynamic behaviour is mapped using AI (Artificial Intelligence) powered stereo cameras and particle counters, which is then transferred to state-of-the-art Computation Fluid Dynamics (CFD) analysis. To further validate the results an ultra-clean operating room, 1:1 – 60 m², was build.

The operating laboratory is equipped with innovative particle reduction solution, that reduces the outside contaminants entering the operating room by more than 99%. Most importantly the operating room is equipped with possibilities to use different of ventilation solutions – Mixing Ventilation (MV) and a Laminar Air Flow ventilation (LAF) or a combination of this ventilation system.

Results from the solutions and measurements shows that in steady state measurements it is 50 times more particles in the wound with mixed ventilation than with laminar airflow ventilation. In the presentation more results will be shown for transient simulations and with operating persons moving around in the operating room.



Here medical staff and students can train to increase their knowledge and understanding about the airflow fields and airborne particles with the use of different ventilation system and their work practice on the level of contaminants within the operating room simulated in an interactive virtual environment.

KEYWORDS

SSI, AI, CFD, XR

ACKNOWLEDGEMENTS

The project is supported by the Research Council of Norway.

REFERENCES

Norconsult - <https://www.norconsult.com/>

Research Project POSIRed -

<https://prosjektbanken.forskningsradet.no/project/FORISS/317450?Kilde=FORISS&distribution=Ar&chart=bar&calcType=funding&Sprak=no&sortBy=date&sortOrder=desc&resultCount=30&offset=30>

Norconsult Health Buildings and Hospitals- <https://www.norconsult.com/services/building-and-property/health-buildings-and-hospitals/>

Users and practices in heating and ventilating homes – why do they behave different than we think?

Kirsten Gram-Hanssen

*BUILD, Aalborg University
AC Meyers Vænge 15
Copenhagen 2450 SV, Denmark*

SUMMARY

We need to improve the indoor air quality for the health of the building users, and we need to optimize and reduce energy consumption for heating, cooling, and ventilation for the sake of the global climate. In both cases the interplay between buildings, HVAC (heating, cooling, and ventilations) technologies and the users are central. Research show that technical optimization without considering the interaction and behaviour of the users may end in sub-optimal technical solutions, neither resulting in reduced energy consumption nor improved indoor air quality. This keynote will bring insight on how to understand users in the interaction between buildings and technologies, and it will provide a collection of research showing how users behaving different than what was expected, negatively impact the outcome related to either energy consumption or indoor air quality.

Understanding human behaviour has in some research traditions focused exclusively on the minds and attitudes of individuals. Research in relations between users, buildings, and technologies, however, shift this focus to understand how different types of technologies and buildings impact the practices of people in a more collective way where unconscious routines are in focus (Gram-Hanssen, 2014). A recent study comparing actual and calculated heating demand for residential buildings demonstrate how people in new efficient buildings in general over-consume whereas people in old inefficient home in general under-consume (Hansen & Gram-Hanssen, 2023). There is difference related to the socioeconomics of the residents, however, it is also clear how the buildings and technologies impact on the practices and comfort norms of the residents. This is also backed up in a large survey relating peoples heating and ventilation behaviour with their building type (Hansen et al., 2018).

From both policy and research, the optimization of indoor air quality and energy consumption is expected to be achieved by an increased use of smart technology assisting users in managing and controlling their indoor climate as well as their energy consumption. This keynote will bring insight from studies of how technology designers expect new smart technology to assist users in their everyday life (Aagaard, 2021) and compare this to the actual use by different types of residents (Larsen et al., 2023). Studies include gender difference in engagements with new technology (Strengers et al., 2022) as well as difference in competences, especially related to the age of resident (Larsen & Gram-Hanssen, 2020). Technological visions of managing indoor climate without the involvement of the resident is also compared to how occupants make workarounds to prevent technologies from working as intended if they do not understand or dislike their function.

Smart technology and digitalisation, including indoor air quality measurements, can also be used to give feedback to occupant, and be combined with incentives for residents to change their heating and ventilation behaviour. An experiment using this opportunity provide results on the possibilities and limitations of engaging residents (Gram-Hanssen et al., 2021). Economic incentives are often thought of as an efficient way to impact users' behaviour, however, research into studies of heating and ventilation behaviour show possible limitations and shortcomings. If people don't understand relations between their practices and the effect on energy consumption and indoor climate the incentives may not work as intended. Also, research into the consequences of the energy crisis with its rapidly increasing energy costs has showed how some resident may feel obliged to use unhealthy means of heating as well and reduce ventilation to save energy.

This keynote will conclude by relevant takeaways for technical research, design, and policy, when it comes to include user perspectives related to heating and ventilation.

KEYWORDS

User practices; smart home technology; residential heating; residential ventilation; human-building interaction

1 ACKNOWLEDGEMENTS

This presentation and the work behind are part of the project eCAPE, which is financed by the European Research Council (ERC) under the European Union's Horizon 2020 research and innovation program. eCAPE received an ERC Advanced Grant under the grant agreement number 786643.

2 REFERENCES

- Gram-Hanssen, K. (2014). New needs for better understanding of household's energy consumption – behaviour, lifestyle or practices? *Architectural Engineering & Design Management*, 10(1/2), 91–107. <https://doi.org/10.1080/17452007.2013.837251>
- Gram-Hanssen, K., Aagaard, L. K., Askholm, A. S. M., & Bonderup, S. (2021). Evaluering af projekt dynamisk varmeregnskab: Kvalitative interviews med beboere og driftspersonale. I *Evaluering af projekt dynamisk varmeregnskab* (Rapport Nr. 978-87-563-2015-3). Institut for Byggeri, By og Miljø (BUILD), Aalborg Universitet.
- Hansen, A. R., & Gram-Hanssen, K. (2023, juni 12). *Over- and underconsumption of residential heating: Analyzing occupant impacts on performance gaps between calculated and actual heating demand: NSB 2023: 13th Nordic Symposium on Building Physics*. NSB 2023: 13th Nordic Symposium on Building Physics - Aalborg University - CREATE, Aalborg, Denmark.
- Hansen, A. R., Gram-Hanssen, K., & Knudsen, H. N. (2018). How building design and technologies influence heat-related habits. *Building Research & Information*, 46(1), 83–98. <https://doi.org/10.1080/09613218.2017.1335477>
- Larsen, S. P. A. K., & Gram-Hanssen, K. (2020). When Space Heating Becomes Digitalized: Investigating Competencies for Controlling Smart Home Technology in the Energy-Efficient Home. *Sustainability*, 12(15), Article 15. <https://doi.org/10.3390/su12156031>
- Larsen, S. P. A. K., Gram-Hanssen, K., & Madsen, L. V. (2023). In Control or Being Controlled? Investigating the Control of Space Heating in Smart Homes. *Sustainability*, 15(12). <https://doi.org/10.3390/su15129489>
- Strengers, Y., Gram-hanssen, K., Dahlgren, K., & Aagaard, L. kryger. (2022). Energy, emerging technologies and gender in homes. *Buildings and Cities*, 3(1), 842–853. <https://doi.org/10.5334/bc.273>
- Aagaard, L. K. (2021). The meaning of convenience in smart home imaginaries: Tech industry insights. *Buildings and Cities*, 2(1), 568–582. <https://doi.org/10.5334/bc.93>

What we know about smart ventilation

Gaëlle Guyot^{1,2}

¹ Cerema,
BPE Research team,
46, rue St Théobald,
F-38080, L'Isle d'Abeau, France

² LOCIE
Univ. Savoie Mont Blanc
CNRS UMR5271,
F-73376, Chambéry, France

SUMMARY

The buildings 'sector is facing multiple challenges due to the need to generalize a sober approach and to reduce its energy consumption, its CO₂ emissions and its impact on climate change, to reduce its environmental impact and its carbon footprint, to reduce the burden of disease due to exposure to unhealthy indoor environments and to adapt and be resilient in the face of climate change and environmental changes such as the increase in pandemics, the urban heat island and outdoor pollution.

Ventilation in buildings is at the heart of all these challenges and is sometimes misunderstood, contrasting the need to reduce air flow to save energy with the need to increase air flow to provide healthy air for humans. We know that reality is never simple, as it is in this field. Building ventilation represents an incredible and underestimated factor in reconciling all these challenges, part of the solution. Firstly, because to achieve all these objectives, including IAQ, summer comfort and energy savings from heating and air conditioning, you really have to control the air flows in buildings. This means limiting unintentional infiltration due to air leaks and controlling voluntary air flows using ventilation system components. Secondly, through the concept of smart ventilation, which can be a solution for both new and existing buildings.

Indeed, providing a constant ventilation airflow rate throughout a building, whatever the boundary conditions (climate, outdoor pollution, seasons, ...), whatever the needs of the occupants, whatever the risks of damage to the buildings, seems totally unsuited to our challenging changing world and our need to adapt. Nevertheless, most buildings in developed countries are equipped with constant-airflow ventilation solutions, where ventilation exists.

Smart ventilation has been defined by the AIVC: “*Smart ventilation is a process to continually adjust the ventilation system in time, and optionally by location, to provide the desired IAQ benefits while minimizing energy consumption, utility bills and other non-IAQ costs (such as thermal discomfort or noise). (...)*”. Starting from this definition, demand-controlled ventilation (DCV) is considered as a specific subset of smart ventilation. This definition of smart ventilation includes a wide range of systems currently available in the literature and on the market depending on the type of sensing parameters (CO₂, humidity, occupancy, etc.), the type of sensing combinations, the type of installation (centralized/decentralized) and the types of control algorithms. A literature review on smart ventilation used in residential buildings, showed that with various smart ventilation systems based on CO₂-, humidity-, combined CO₂- and TVOC-, occupancy-, outdoor temperature-controlled ventilation, energy savings up to 60% could be obtained without compromising, and sometimes improving, IAQ (Guyot et al., 2018a).

While the terms “smart ventilation” were first used fairly recently by LBNL researchers (Walker et al., 2014; Less and Walker, 2016; Lubliner et al., 2016), and have been increasingly used since (Table 1), the concept of smart ventilation is older. Demand-controlled ventilation emerged after the oil crisis of the early 1980, with some research published at the time (Anon, 1983; Barthez and Soupault, 1984; Nicolas, 1985). More recently, a favourable context has been created to develop smart ventilation strategies, with DCV systems widely and easily available on the market in some countries, with more than 20-30 DCV systems approved and available in countries such as Belgium, France and the Netherlands (Guyot et al., 2018b).

The smart ventilation concept is also interesting because it demonstrates the **applicability of performance-based approaches** applied to ventilation. Even if the final report of the IEA EBC Annex 9 (1982-1986) already stated that in principle two approaches may be used to specify ventilation standards:

- i. The prescriptive approach, in which an outdoor air flow rate is stated.
- ii. The air quality approach, in which a limiting maximum pollutant concentration is defined and the building designer or user, is required to supply sufficient air to ensure that this is not exceeded.

To date, however, most national regulations and standards in this area still use the prescriptive approach.

In the field of smart ventilation, before being authorised or used in buildings, smart ventilation must undergo procedures/calculations in order to demonstrate that it is at least equivalent to traditional/reference ventilation, or

to demonstrated that the use of smart ventilation makes it possible to comply with IAQ requirements (Guyot et al., 2018b; Guyot, 2019; Guyot et al., 2019). To our knowledge, Spain is the only country in the world which generalized the performance-based approach for every type of ventilation in new residential buildings.

Smart ventilation is promising because such strategies can adjust the airflows in a changing world and changing outdoor conditions, like heat waves or outdoor pollution peaks. If balanced ventilation with heat recovery systems are often prioritized in strong winter climate conditions like in the European Scandinavian countries, smart ventilation could be very performing in several conditions (Laverge et al., 2013; Zukowska et al., 2020).

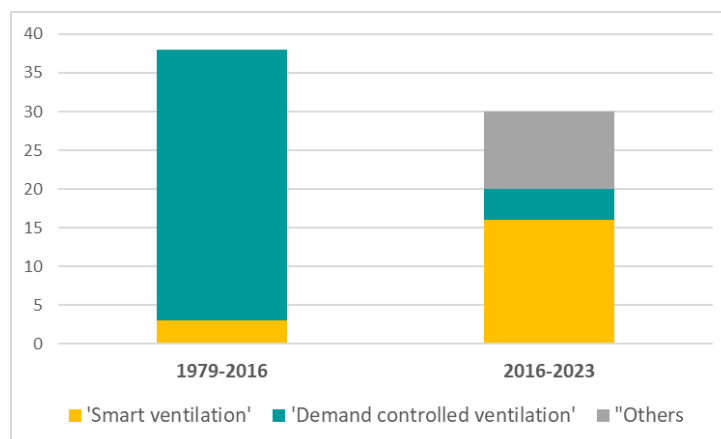
Several challenges can be addressed thanks to the use of smart ventilation: face to the lack of commissioning and the number of dysfunctions observed on ventilation systems, smart ventilation can offer online and continuing commissioning, and it can participate to the decrease of the carbon footprint of buildings. For all smart ventilation, robustness and resilience (to occupant, to life time, to other factors...) should also be taken into account. Indeed, durability of building performances is still a general crucial issue to be addressed. Nevertheless, with smart ventilation, we generally allow lower airflows at some times when needs are low (no occupancy, low emissions, etc...), but we have to secure even more than with other ventilation systems that expected ventilation airflows are still correctly provided, over the building life.

In the IEA-EBC Annex 86, and especially in the ST4-smart ventilation, we have been gathering and pushing and international effort about the promotion of smart ventilation strategies. ST4 includes a review work of existing knowledge about IAQ and energy performances of residential smart ventilation, their cost, and the choice of several smart ventilation strategies being highlighted as promising from the review analysis, and considered in the further work of the subtask as examples. This activity also includes a review of performance assessment methodologies, namely “performance-based” approaches used for smart ventilation, being used in the countries of the participants. At least, this activity is going to propose a performance-based rating approach for smart ventilation. The approach will be demonstrated by means of simulations, establishing a common exercise throughout the participating countries. We will propose quality managements schemes and inspection protocol for insuring the quality of implementation and address the issue of durability of smart ventilation systems and components. The keynote will give an overview of the recent knowledge on smart ventilation gathered through this Annex.

KEYWORDS

Ventilation, demand-controlled ventilation, performance, smart ventilation

Table 1. Number of studies dealing with smart ventilation



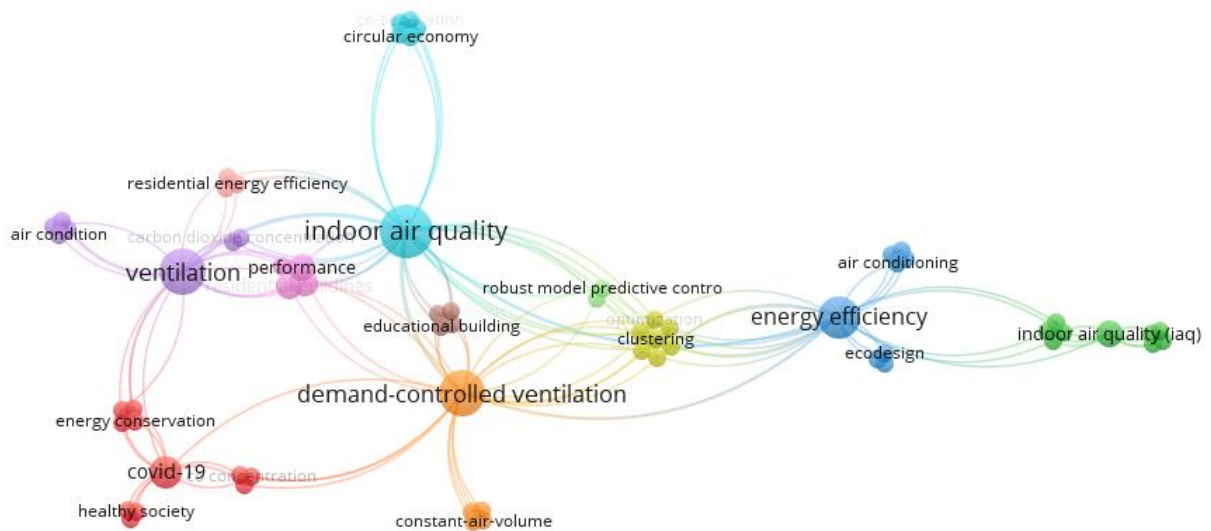


Figure 1: Keywords connection from the request “smart ventilation” and “demand-controlled ventilation” using Sciedirect database, February 2023. Source:VOS viewer

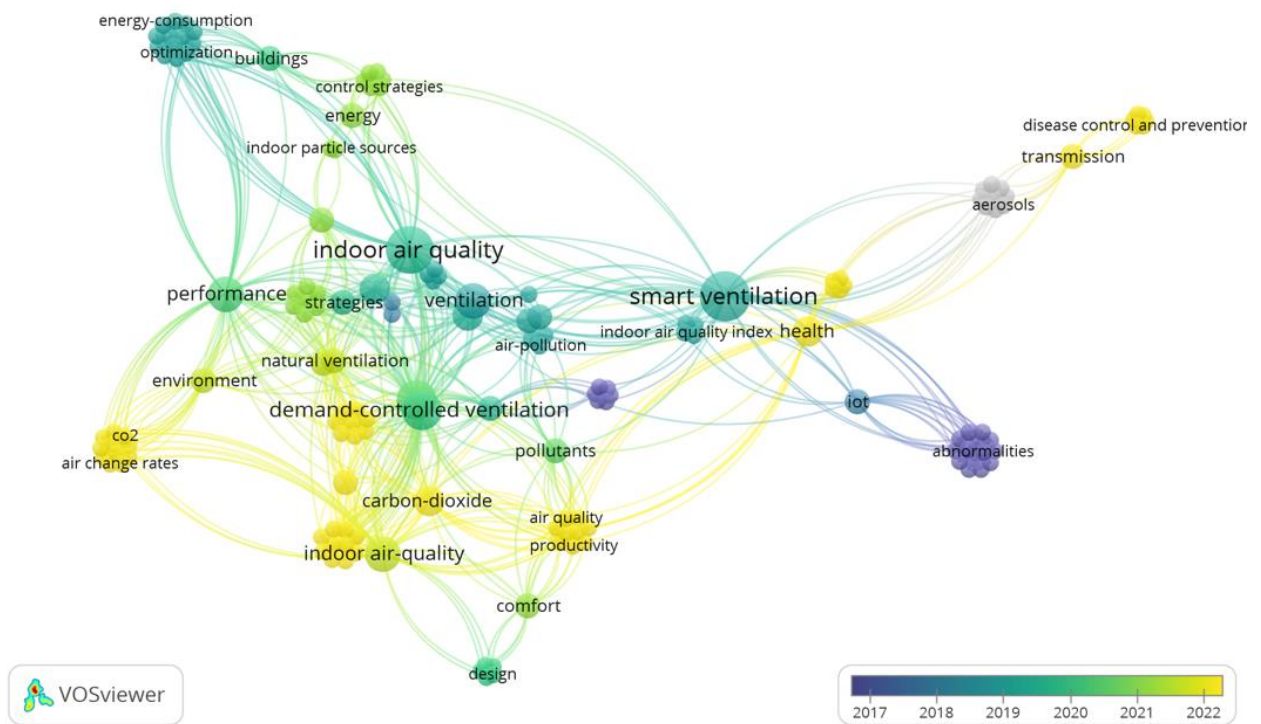


Figure 2: Keywords connection from the request “smart ventilation” using Sciedirect database, February 2023. Source:VOS viewer

ACKNOWLEDGEMENTS

I would like to thank Dr Daniela Mortari, from the PUCPR University, Brasil for our collaboration in University Savoie Mont Blanc on the topic of smart ventilation.
Thank you to all the colleagues from the IEA-EBC Annex 86 and particularly my co-leader of the ST4 smart ventilation Dr Jakub Kolarik.

REFERENCES

- Anon, 1983. Humidity-controlled ventilation. Un nouveau principe de ventilation mecanique - la ventilation hygromodulable. *Chaud Froid Plomb*. 37, p.107-109.
- Barthez, M., Soupault, O., 1984. Control of Ventilation Rate in Building Using H₂O or CO₂ Content, in: Ehringer, H., Zito, U. (Eds.), *Energy Saving in Buildings*. Springer Netherlands, pp. 490–494. https://doi.org/10.1007/978-94-009-6409-9_61
- Guyot, G., 2019. Introduction: Why performance-based assessment methods? Overview of the needs and the possibilities., in: *From Energy Crisis to Sustainable Indoor Climate 40 Years of AIVC*. Ghent, Belgium.
- Guyot, G., Sherman, M.H., Walker, I.S., 2018a. Smart ventilation energy and indoor air quality performance in residential buildings: A review. *Energy Build*. 165, 416–430. <https://doi.org/10.1016/j.enbuild.2017.12.051>
- Guyot, G., Walker, I., Sherman, M., Linares, P., Ortega, S.G., Caillou, S., 2019. VIP 39: A review of performance-based approaches to residential smart ventilation.
- Guyot, G., Walker, I.S., Sherman, M.H., 2018b. Performance based approaches in standards and regulations for smart ventilation in residential buildings: a summary review. *Int. J. Vent*. 0, 1–17. <https://doi.org/10.1080/14733315.2018.1435025>
- Laverge, J., Pattyn, X., Janssens, A., 2013. Performance assessment of residential mechanical exhaust ventilation systems dimensioned in accordance with Belgian, British, Dutch, French and ASHRAE standards. *Build. Environ*. 59, 177–186. <https://doi.org/10.1016/j.buildenv.2012.08.018>
- Less, B., Walker, I., 2016. Smart ventilation control of indoor humidity in high-performance homes in humid U.S. climates. Presented at the *Thermal Performance of the Exterior Envelopes of Whole Buildings*, pp. 272–280.
- Lubliner, Francisco, Martin, Walker, I., Less, B., Viera, Kuckle, Merrin, 2016. Practical Applications and Case Study of Temperature Smart Ventilation Controls, in: *Thermal Performance of the Exterior Envelopes of Buildings XIII*, ASHRAE/DOE/BTECC.
- Nicolas, C., 1985. Analysis of a humidity-controlled ventilation system. Evaluation des performances d'une ventilation hygromodulante., in: *Proceedings of the CLIMA 2000 World Congress on Heating, Ventilating and Air-Conditioning, Indoor Climate*. P O Fanger, Copenhagen, pp. p339-343.
- Walker, I., Sherman, M.H., Less, B., 2014. Houses are Dumb without Smart Ventilation. LBNL-6747E.
- Zukowska, D., Rojas, G., Burman, E., Guyot, G., Bocanegra-Yanez, M. del C., Laverge, J., Cao, G., Kolarik, J., 2020. Ventilation in low energy residences – a survey on code requirements, implementation barriers and operational challenges from seven European countries. *Int. J. Vent*. 1–20. <https://doi.org/10.1080/14733315.2020.1732056>

Dallying with DALYs: Why *acceptable* IAQ should consider harm

Benjamin Jones

*University of Nottingham
Department of Architecture and Built Environment
Nottingham, UK
benjamin.jones@nottingham.ac.uk*

SUMMARY

The ASHRAE Standard Project Committee on Ventilation and Acceptable Indoor Air Quality in Residential Buildings (62.2) has proposed an addendum to the standard that adds a harm-based Indoor Air Quality procedure as an alternative compliance method. The IAQ Procedure only considers 3 contaminants and only the sum of the harm from those three contaminants needs to be limited. This was determined by completing four stages of research.

The first stage considered the uncertainty in the concentrations of 45 airborne contaminants in dwellings was identified. Ethanol is the most common contaminant by mass (around 30%) and PM_{2.5} was the fourth most common (around 10%), but presence does not indicate harm.

Harm was evaluated using the disability adjusted life year (DALY) metric, a measure of time where a value of unity is one year of healthy life lost to some disease or injury. DALYs are calculated as the sum of years of life lost to premature mortality and morbidity in a population for some negative health effect. In the case of IAQ, the burden of disease is a measurement of the difference between the current health status of a population of building occupants and an ideal situation where they all live into old age, free of disease and disability.

The second stage of research required the development of a new metric, called a Harm Intensity, with units of DALYs per mean concentration per year. Its values were determined using epidemiological and/or toxicological models, depending on the availability of information.

The third stage combined the concentrations and harm intensities to identify the harm caused by each of the 45 contaminants in residential dwellings. PM_{2.5} (~66% of all harm), PM₁₀ (~13%), formaldehyde (~9%), and nitrogen dioxide (~8%), radon (~2%), and ozone (~1%) are the most harmful contaminants by around an order of magnitude. From these, ASHRAE 62.2 has chosen 3 contaminants of concern that account for ~83% of all harm: PM_{2.5}, formaldehyde, and nitrogen dioxide. The others were not included because they are principally outdoor contaminants or are otherwise not addressed by the existing ventilation rate procedure.

The fourth and final stage used the harm intensities to determine a relative weight of each contaminant that can be used to create a harm budget where the total harm caused by exposure to them is below an acceptable threshold. Reference concentrations for PM_{2.5}, formaldehyde, nitrogen dioxide are set at 8, 20, and 6 micrograms per cubic meter, respectively.

KEYWORDS

Disability Adjusted Life Years, health, IAQ, ventilation, harm intensity, ranking, health

Human exposure against airborne pathogens in an office environment

Risto Kosonen¹, Sami Lestinen¹ and Simo Kilpeläinen¹

¹Aalto University
Sähkömiehentie 4
FI-00076 AALTO
Espoo, Finland

SUMMARY

Airborne exposure has been highlighted during the COVID-19 pandemic as a probable infection route. This experimental study investigates different protection methods at an office workstation, where the concentration characteristics are studied under mixing ventilation conditions. The protection methods were the room air purifier, personal air purifier, face mask, and workstation partition panels. In experiments, the breathing machine, nebulizer, and syringe pump were used to generate an aerosol distribution of paraffin oil in the room. The breathing thermal manikin and the thermal dummy simulated the exposed and infected person, respectively. The concentration characteristics were measured from the manikin breathing zone. The temporal concentration characteristics were measured from zero concentration to steady-state conditions. The study provides insights into the effects of different protection methods for occupational health and safety decision-making for office indoor environments.

KEYWORDS

airborne transmission, air purifier, face mask, partition panel, protection method

1 METHODS

Test cases compare different protection methods at workstations (Figure 1). The measurement time was 1 hour and 40 minutes (6000 s) under the air change rate of 1.7 ACH. This included the concentration increase to a steady-state concentration during 3000-5000 seconds and the averaging of 1000 values with the sampling rate of 1 Hz in steady-state conditions.

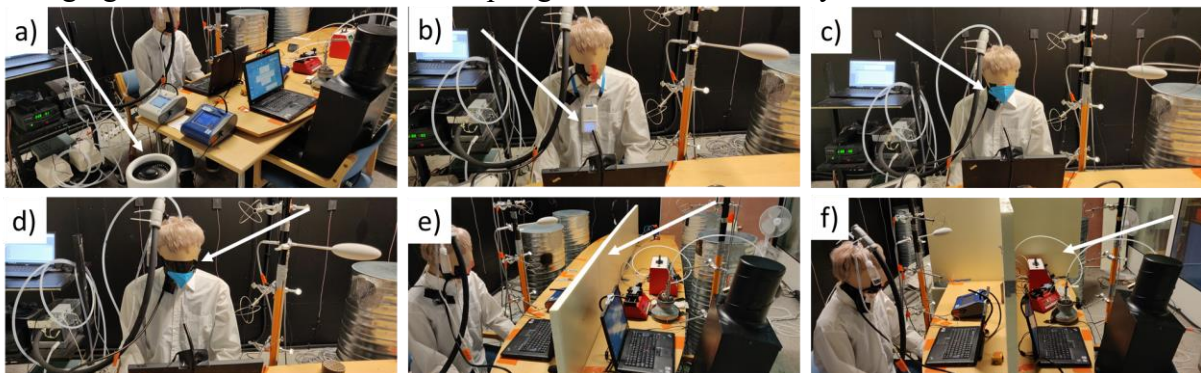


Figure 1: Protection methods: a) Room air purifier on the floor. b) Personal air purifier on the neck (20 cm below the mouth). c) FFP2-mask. d) FFP2-mask, sealed edges. e) Low partition panel on the table in the meeting setup (height 40 cm). f) High partition panels in front and side of workstation extending to the floor (height 80 cm).

The mixed ventilated mock-up room of the office and meeting spaces with internal dimensions of 5.5 m (L), 3.8 m (W) and 3.6 m (H) was used. The infected-to-exposed distance was 1.2 m. The infected person was created by using a respiratory exhalation simulator (CH Technologies Inc.) and a seated thermal dummy including light bulbs and a fan to equalize the heat inside. The seated breathing thermal manikin (P.T. Teknik Limited) was the exposed person.

2 RESULTS

The results at steady-state conditions are shown in Table 1. The concentration level increased to $166 \pm 11 \mu\text{g}/\text{m}^3$ (avg \pm sd) without any protection method whereas the room air purifier decreased the concentration to $84 \pm 7 \mu\text{g}/\text{m}^3$ and thus reducing the average level by 50%. The personal air purifier reduced the exposure concentration to the level of $137 \pm 9 \mu\text{g}/\text{m}^3$ which means about a 20% percent decrease in the average concentration. As a result, the experiments show evidence that the room air purifier can effectively reduce the exposure at the workstation if the purifier has been optimally designed. Another effective method was the FFP2-mask. The average concentration at the breathing zone falls to 65-103 $\mu\text{g}/\text{m}^3$ meaning from 40% to 60% (sealed) decrease in the concentration level.

Table 1: Averaged mass concentration (AVG) and standard deviation (SD) at the breathing zone of exposed manikin

Parameter	AVG ($\mu\text{g}/\text{m}^3$)	SD ($\mu\text{g}/\text{m}^3$)	reduction (%)
Without protection	166	11	reference
Room air purifier	84	7	-50
Personal air purifier	137	9	-18
FFP2-mask	103	38	-38
FFP2-mask, sealed	65	24	-61
Low screen:mid table meeting	153	12	-8
High screen:mid table meeting	168	11	0
High screen:table, mid+side office	165	11	-1
High screen:table+floor, mid+side office	154	10	-7

The results showed that the room air purifier and FFP2-mask could be a reasonable protection choice against the droplet nuclei aerosols. The room air purifier with HEPA filter effectively reduced the concentration. In this study, the circulating airflow rate was 2.5 times the ventilation airflow rate. The FFP2-mask reduced the exposure, but the user comfort can be poor if used the entire working day. In addition, sealing the face piece by proper fitting is important. The wearable personal air purifier had a relatively low effect on exposure and the location of the purifier seemed important because the clean air jet was narrow. However, it may be effective if the location can be adjusted with a holder, etc. The workstation partition panels had a negligible effect on the exposure. The partition panels may be better against coughing because those prevent droplets to reach other workstations.

3 ACKNOWLEDGEMENTS

The authors acknowledge the Finnish Work Environment Fund (Grant No. 210099), the Aalto University Campus & Real Estate (ACRE) and the city of Helsinki for the financial support of SUOJAILMA-project, and the Lifa Air Ltd for providing the protection solutions for the study.

Discussion on minimum ventilation rates for infection control

Yuguo Li and Wei Jia

*Department of Mechanical Engineering
The University of Hong Kong
Hong Kong, China
Email: liyg@hku.hk*

SUMMARY

There are several knowledge gaps that explains a lack of knowledge on minimum ventilation rates for intercepting airborne respiratory infection. One is a lack of unifying understanding of the roles of ventilation, filtration, settling, deactivation, and most importantly temporal and spatial variation. A recent finding on the equivalence of the occupied air volume per person and dilution and a generalized Wells-Riley equation are used to define a unified dilution air flow rate. The required threshold dilution air flow rate is not a function of the setting. I would suggest the use of the dilution air flow rate not the ventilation air flow rate for infection control.

KEYWORDS

Minimum ventilation, threshold ventilation, respiratory infection, SARS-CoV-2, risk assessment

1 A GENERALIZED WELLS-RILEY EQUATION

Consider a room with a volume V (m^3), N_σ susceptible individuals and N_I infectors. Each virus particle (virion) in the room might be inhaled by a susceptible individual and produce infection. Each point in the room is defined as $\mathbf{x}(x, y, z)$. Here we consider a setting where each susceptible individual ($i = 1, 2, \dots, N_\sigma$) has his/her position (\mathbf{x}_i) known. Individual i arrives in space at time $t_{1,i}$ and departs at time $t_{2,i}$, and $c_{Q,i}(\mathbf{x}_i, t)$ is the concentration of the infectious quantum at location \mathbf{x}_i and time t .

Following Jia et al (2022), the average infection risk of all individuals follows the generalized Wells-Riley equation.

$$\bar{p} = \frac{N_I}{N_\sigma} = \frac{1}{N_\sigma} \sum_{i=1}^{N_\sigma} \left(1 - e^{-\int_{t_{1,i}}^{t_{2,i}} q_{in,i}(t) c_{Q,i}(\mathbf{x}_i, t) dt} \right) \quad (1)$$

With one infector in a space, this equation may probably be converted somehow into the classical Wells-Riley equation at ideal uniform and steady-state setting.

$$\bar{p} = \frac{N_I}{N_\sigma} = 1 - e^{-Q \frac{q_{in} \Delta t}{q_d}} \quad (2)$$

It is noted that the effective dilution air flow rate for each susceptible individual depends on his/her trajectory in the space. In general, we may consider that the infectious quantum emission rate Q , the inhalation rate q_{in} , the effective dilution air flow rate q_d and exposure time Δt exhibit some probability distributions. Hence there is no single threshold dilution air flow rate.

2 FOCUSING ON VENTILATION ALONE IS NOT CORRECT

The vector for respiratory infection is respiratory particles (aerosols), which can be removed not only by ventilation air as for CO₂, but also by virus deactivation, particle settling, and filtration. The particle filtration can be counted for by using the clean-air flow rate (Shaughnessy and Sextro, 2006). The effect of crowding and non-uniform distribution of air also needs to be accounted for when the concentration $c_{Q,i}(\mathbf{x}_i, t)$ of the infectious quantum at location \mathbf{x}_i and time t is estimated from the mass conservation equation.

We first define a generalised *clean-air flow rate* per person q_c as the sum of the outdoor-air supply flow rate, q_v (ventilation), the equivalent clean-air flow rate due to virus deactivation, q_r , aerosol settling, q_s , and filtration, $\eta_f q_f$.

$$q_c = q_v + q_s + q_r + \eta_f q_f \quad (3)$$

We consider a typical setting with uniform concentration when infector and all susceptible individuals start to present at the same time in an indoor setting. In such situations, the concentration of the infectious quanta would build up from zero, and the individual infection risk can be written as.

$$p_i = \frac{N_t}{N_\sigma} = 1 - e^{-Q \frac{q_{in}}{q_c} \Delta t (1 - C_t)} \quad (4)$$

Where $C_t = \frac{1 - e^{-n\Delta t}}{n\Delta t}$, and the dilution air change rate $n = \frac{q_c}{V}$, and is the total *clean-air flow rate* of the room.

In non-uniform setting, we may use the zone air distribution effectiveness E_z in breathing zone (ASHRAE 62.1, 2019), $E_z = \frac{c_e}{\langle c_Q(x_i) \rangle} = \frac{Q}{\langle c_Q(x_i) \rangle q_c}$, where $\langle \cdot \rangle$ indicates the average concentration. c_e is the mean concentration of infectious quantum at exhaust.

The effective dilution air flow rate per person can thus be estimated as $q_d = \frac{E_z q_c}{1 - C_t}$.

3 ACKNOWLEDGEMENTS

The project was financially supported by RGC grants.

4 REFERENCES

- Shaughnessy, R.J. and Sextro, R.G. (2006). What is an effective portable air cleaning device? A review. *Journal of Occupational and Environmental Hygiene*, 3(4), 169-181.
- Jia, W., Cheng, P., Ma, L., Wang, S., Qian, H. and Li, Y. (2022). Individual heterogeneity and airborne infection: Effect of non-uniform air distribution. *Building and Environment*, 226, 109674.

Mitigation of airborne transmission of respiratory viruses by ventilation – past, present and future

Arsen K. Melikov

International Centre for Indoor Environment and Energy, Department of Environmental and Resource Engineering, Technical University of Denmark, Nils Koppels Alle Building 402, 2800 Kong. Lyngby, Denmark

SUMMARY

The importance of ventilation of spaces for occupants' health has been known for many years. Ancient Egyptians used natural ventilation to remove dust and thus to reduce respiratory diseases of stone carvers working indoors (Janssen 1999). In the past ventilation has been used to reduce airborne transmission of respiratory generated infectious agents in buildings. In the book "Natural and Artificial Methods of Ventilation" (Robert Byle & Son, London 1899), chapter X it is stated "The report on the influenza epidemic presented to Parliament by the Local Government Board indicates the extreme importance of proper ventilation – especially in schools – which is pronounced to be the only real safeguard against that disease." Several ventilation solutions in classroom and hospital patient rooms are suggested in the book with focus on the clean air distribution. Thus, already two centuries ago the importance of clean air distribution for fulfilling the main goal of ventilation, namely to provide occupants with clean air for breathing has been considered.

During the last two decades, the importance of ventilation for reduction of airborne transmission of SARS-CoV-1 and SARS-CoV-2 has been widely discussed in numerous research papers. Guidelines and standards on how to prevent the spread of respiratory generated infectious aerosols in spaces have been developed (REHVA COVID-19 Guidance 2021, ASHRAE Standard 241 2023). Unfortunately, the important role of air distribution, as recognised many years ago, has been ignored. Instead, either complete mixing of the supplied clean/disinfected ventilation air with the air in the entire occupied zone or the air in the "breathing zone" of the occupied space (ASHRAE Standard 241 recommends lateral flow velocity lower than 0.25 m/s in the breathing zone of the occupied space). However, in practice it is difficult to comply with these recommendations. The airflow distribution in occupied spaces, the transport and the exposure of occupants to infectious aerosols is result of complex interaction of ventilation flow, buoyancy flows (generated by occupants, warm/cold surfaces, etc.), occupants' activities and location, etc. In the literature related to ventilation for reduction of airborne transmission a minimum amount of clean/disinfected ventilation air (L/s person) supply is recommended (the validity of the recommended values can be discussed). However, the ventilation rate is important for energy performance assessment of ventilation system, but it is of secondary importance for the clean air distribution to the breathing zone of each room occupant. The word "ventilation" comes from the Latin word "ventus" meaning wind. Similar to the wind, room airflow is defined with the magnitude and the direction of the flow velocity. The supplied clean/disinfected ventilation air mixes with the infected room air reduces the concentration of infectious aerosols but it also spreads the infected exhaled air in the room. Therefore, increase of the ventilation rate as recommended in the standards may change the airflow direction and spread of infected air and this process will be difficult to control in practice. Increase of the supplied ventilation rate may generate high velocity causing draught for the occupants, will result in design of large air-handling units and duct systems in new buildings and rebuilding of existing HVAC systems which will be costly and not always possible. The increase of the ventilation rate will increase the energy consumption. Use of stand-alone room air cleaners is better option during pandemics.

The importance of air distribution for the exposure of room occupants to the infected air exhaled by one of the occupants is shown in Figure 1. The results reveal huge differences in the normalised concentration of infected air by the exposed occupants. This indicates large differences in the infection probability for the compared air distribution cases. The importance of air distribution for the reduction of airborne cross-infection is shown in Figure 2. Use of personalised ventilation dramatically reduces the reproductive number, i.e. the cross-infection.

The air distribution has huge potential for reduction of airborne infection. Yet, the main discussion at present is on how much should be the ventilation rate in order to reduce airborne cross-infection. As discussed above this approach will not provide beneficial results in practice. Successful reduction of airborne cross infection by ventilation requires different approach. Carefully designed advanced air distribution has to be applied selectively in practice depending on the ventilated space, occupants' activity and density, requirements for flexibility of space use. Ventilation solutions that make it possible to remove/disinfect the exhaled air at the location of the occupant before it is mixed with the room air has to be developed. Clean air delivery to the breathing zone without enhancing the spread of infected exhaled air to other occupants should be aimed. Personalised ventilation installed at workstations as well as personal wearable ventilation solutions performing independently of occupants' activities

has to be developed and used. This approach will bring shared values by reduction of both airborne cross infection, cost of ventilation systems, energy consumption, etc. Occupants should be trained to actively use the new solutions.

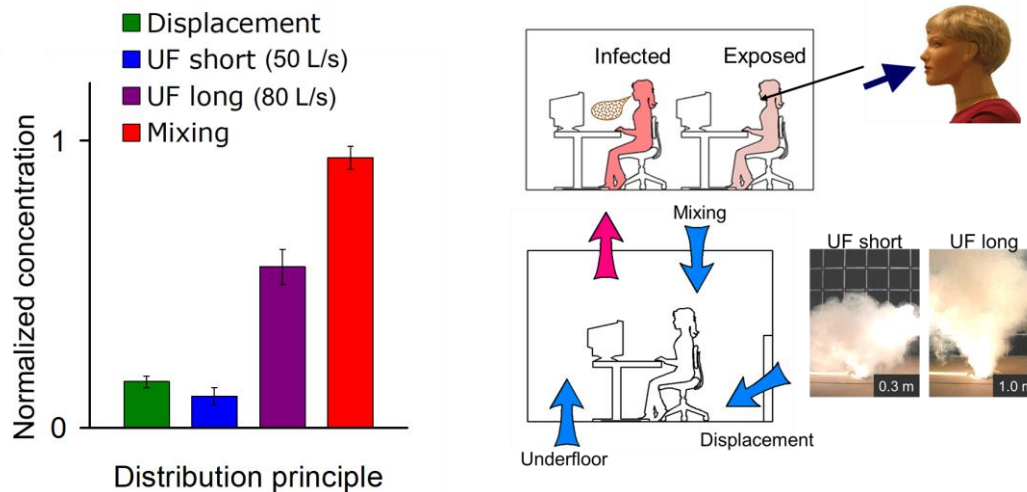


Figure 1: Experiments with full size breathing thermal manikin resembling two occupants in a room ventilated with different ventilation principles. Supply flow rate is 80 (50) L/s. Tracer gas concentration mixed with the air exhaled by the “infected occupant” is measured in the air inhaled by the exposed occupant. Normalised concentration is calculated as $(C_{in} - C_s)/(C_{ex} - C_s)$, where C_{in} , C_s , C_{ex} are respectively tracer gas concentration in the inhaled air, the supplied ventilation air and the exhaust room air. Details in (Cermak and Melikov 2006).

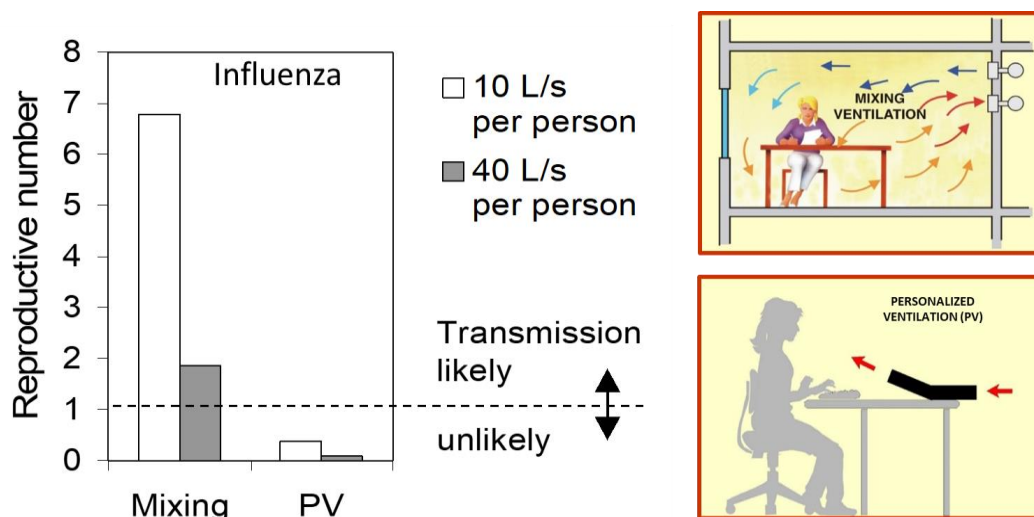


Figure 2: Comparison of the reproductive number defined as the number of secondary infections (influenza virus) that arise when a single infectious case is introduced into an office with 10 occupants where everyone is susceptible. The occupants spend 8 hours in the office ventilated by mixing ventilation or when each occupant has personalised ventilation. Comparison at 10 and 40 L/s person. Details in (Cermak and Melikov 2007).

KEYWORDS: Airborne transmission, air distribution, advanced ventilation

REFERENCES

- Janssen, J.E. (1999). The history of ventilation and temperature control - The first century of air conditioning. *Ashrae Journal*, 41 (10), 48-60.
- Natural and Artificial Methods of Ventilation. Robert Byle & Son, London 1899.
- REHVA COVID-19 guidance - How to operate HVAC and other building service systems to prevent the spread of the coronavirus (SARS-CoV-2) disease (COVID-19) in workplaces. REHVA 2021.
- ASHRAE Standard 241. Control of Infectious Aerosols. ASHRAE June 2023, p- 38.
- Cermak, R. and Melikov, A. (2006). Air quality and thermal comfort in an office with underfloor, mixing and displacement ventilation. *International Journal of Ventilation*, 5(3), 323-332.
- Cermak, R. and Melikov, A. (2007). Protection of occupants from exhaled infectious agents and floor material emissions in rooms with personalized and underfloor ventilation. *HVAC&R Research*, 13(1), 23-38.

Point source ventilation effectiveness in infection risk-based post-COVID ventilation design

Jarek Kurnitski^{*1,2}, Martin Kiil¹, Alo Mikola^{1,2}, and Karl-Villem Võsa¹

*1 Tallinn University of Technology
Ehitajate tee 5
19086 Tallinn, Estonia*

*2 Aalto University
Rakentajanaukio 4
02150 Espoo, Finland*

**Corresponding author: jarek.kurnitski@taltech.ee*

ABSTRACT

Measurement method for ventilation effectiveness, more specifically, for contaminant removal effectiveness with a point source corresponding to infector is analysed in this study with tracer gas measurements and infection risk calculations. Ventilation effectiveness is needed in infection risk-based ventilation design to take into account air distribution methods deviating from fully mixing. Tracer gas measurements were conducted with two source location in six non-residential spaces. Ventilation effectiveness calculated based on the infection risk probability assessment for every measurement point in the room was compared with calculation from the average concentration and calculation method proposed by REHVA accounting only 50% of measurement points with highest concentration. To conduct infection risk calculation, Wells-Riley model modification providing a relation between infection risk probability and ventilation rate at fully mixing was applied together with infection risk control concept based on the basic reproduction number $R_0 = 1$ during pre-symptomatic infectious period. By applying the required ventilation rate at fully mixing and individual probability of infection in each measurement point, ventilation effectiveness value corresponding to given event reproduction number was solved. With the method developed, the airflow rate at fully mixing and the airflow rate with actual air distribution, calculated with ventilation effectiveness, provide the same event reproduction number. Results show considerable differences compared to calculation based on average measured concentration, which overestimated the ventilation effectiveness and underestimated design ventilation rate. The method proposed by REHVA, taking into account only 50% of measurement points with highest concentration, revealed to be conservative in all studied cases, as ventilation effectiveness values ranged in between 0.34 – 1.29 compared to 0.62 – 1.44 solved from individual risk of all measurement points. Especially in the large open plan office, REHVA method considerably overestimated the design ventilation rate while in smaller spaces all three methods provided similar results. Results indicate that ventilation effectiveness determination from tracer gas measurements with a point source is not a trivial task. Calculation method developed, utilising individual probability of infection in each measurement point can be proposed to improve prediction accuracy.

KEYWORDS

Health-based ventilation, air distribution, tracer gas, contaminant removal effectiveness, air quality index.

1 INTRODUCTION

The impact of ventilation in reducing exposure to COVID-19 and other airborne respiratory infectious diseases has been widely discussed because SARS-CoV-2 and other respiratory pathogens have been shown to be effectively transmitted through the inhalation exposure route as concluded in the review by the Lancet COVID-19 Commission (2022). As a removal mechanism, outdoor air ventilation in buildings dilutes indoor-generated air pollutants (including bioaerosols) and reduces resulting exposures to occupants. Aerosol concentration reduction by general ventilation applies for the long-range transmission, while short-range transmission occurs via face-to-face interactions in proximity to an infected person that clearly dominates at distances < 1 m (Wagner et al. 2021). WHO (2021) has developed a

roadmap to improve and ensure good indoor ventilation in the context of COVID-19 that is divided into three settings – health care, non-residential and residential spaces. In this study we focus on ventilation design in non-residential buildings, where WHO recommends 10 L/s per person minimum ventilation rate with reference to EN 16798-1:2019. This value is recommended as the highest, Category I value defined in the existing standard. Beyond existing standards, an effective air change rate of 4-6 ACH has been proposed by Allen and Ibrahim (2021) to reduce long-range airborne transmission of SARS-CoV-2 by targeting this air change rate through any combination of outdoor air ventilation, recirculated air passing through effective filter, or passage of air through portable air cleaner. Their recommendation is based on exposure science and inhalation dose risk reduction but does not distinguish spaces with low and high occupant density and is intended for large group of indoor spaces such as classrooms, retail shops, and homes if guests are visiting.

For all these recommendations it is common that no calculation method is provided for infection risk control. While L/s per person ventilation values may work both for spaces with low and high occupant density, highly different viral loads of breathing, speaking and physical activities (Buonanno et al. 2020) must be considered in the ventilation design. First steps towards infection risk-based ventilation rate calculation were taken in (Kurnitski et al. 2021) introducing a ventilation rate equation derived from Wells-Riley model modification that allows to calculate the required ventilation at given infection risk probability for fully mixing air distribution in the steady state. This is further developed in (REHVA 2022) by extending the risk control concept from the event reproduction number to full pre-symptomatic period, and by introducing ventilation effectiveness concept to take into account air distribution solutions deviating from fully mixing.

In this study we focus on the application of ventilation effectiveness and its measurement procedure with a point source corresponding to infector. Infection risk-based ventilation design method proposed in (REHVA 2022) is applied for classrooms, offices, meeting rooms and gyms where tracer gas measurements were conducted to determine ventilation effectiveness. By conducting infection risk probability assessment for every measurement point in the room, the required ventilation rate at fully mixing is increased to the value satisfying the event reproduction number and allowing to determine corresponding ventilation effectiveness value. These values are compared with ones calculated by robust and simplified method proposed in (REHVA 2022). As a result, less conservative method is proposed for accurate ventilation effectiveness calculation from tracer gas measurement results.

2 METHODS

Wells-Riley model modification providing a relation between infection risk probability and ventilation rate is applied together with infection risk control concept based on the basic reproduction number $R_0 = 1$ during pre-symptomatic infectious period. With this concept, a room specific event reproduction number and ventilation rate can be calculated applying for fully mixing air distribution. This ventilation rate needs to be adjusted with ventilation effectiveness for an actual air distribution, which measurement and application is especially studied in this paper.

2.1 Infection risk assessment

For the infection risk assessment, Wells-Riley model modification providing an explicit equation for ventilation rate in the steady state at given infection risk probability and fully mixing air distribution (Kurnitski et al. 2021) was used:

$$Q = \frac{(1-\eta_i)IqQ_b(1-\eta_s)D}{\ln\left(\frac{1}{1-p}\right)} - (\lambda_{dep} + k + k_f + k_{UV})V \quad (1)$$

where

- Q outdoor air ventilation rate (m³/h)
- p probability of infection for a susceptible person (-)
- q quanta emission rate per infectious person (quanta/(h pers))
- Q_b volumetric breathing rate of an occupant (m³/h), see Table 1
- I number of infectious persons (-), default value $I = 1$
- η_s facial mask efficiency for a susceptible person (-)
- η_i facial mask efficiency for an infected person (-)
- D duration of the occupancy (h)
- λ_{dep} deposition onto surfaces (1/h)
- k virus decay (1/h)
- k_f filtration by a portable air cleaner (1/h)
- k_{UV} disinfection by upper room ultraviolet germicidal irradiation UVGI (1/h)
- V volume of the room (m³)

An acceptable individual probability p for a specific room can be calculated based on the event reproduction number R , defined as the number of new disease cases divided by the number of infectors $R = N_c/I$. Considering that the number of new cases $N_c = p N_s$ an acceptable individual probability for a specific room can be calculated as follows:

$$p = \frac{RI}{N_s} = \frac{RI}{(N-I)(1-f_v\eta_v)} \quad (2)$$

where

- R event reproduction number (-)
- N_s the number of susceptible persons in the room, $N_s = N - I$ if no vaccinated/immune persons
- f_v fraction of the local population who are vaccinated, $f_v = 0$ for no vaccination (-)
- η_v the efficacy of the vaccine against becoming infectious, $\eta_v = 1$ for ideal protection (-)

Acceptable R during one room-occupancy event can be based on the assumption that the likelihood of infecting others (i.e. the number of infections per unit time) is approximately constant over the infectious period. In such cases, an infectious person will not infect more than one person during the infectious period:

$$\frac{R}{R_0} \cong \frac{D}{D_{inf}} \implies R \leq \frac{D}{D_{inf}} \quad \text{when } R_0 \leq 1 \quad (3)$$

where:

- R event reproduction number, i.e. number of people who become infected per infectious occupant

- D room occupancy period, i.e. length of time when both infectious and susceptible persons are present in the room at the same time (h)
- D_{inf} the total interaction time when an infectious individual is in the vicinity of any susceptible persons during the whole pre-symptomatic infectious period (h)
- R_0 basic reproduction number that describes the spread of an epidemic in the population (-)

The pre-symptomatic infectious period ends typically at the onset of symptoms, when the infectious person self-isolates at home or is otherwise ‘removed’ from contact with susceptible individuals. This period may last some days, on average approximately 2 days for influenza and 2½ days for SARS-CoV-2.

It is possible to simplify Equation 1 by using the Taylor approximation of an exponential $e^n \cong 1 + n$ at low doses that allow for the rewriting of Wells-Riley equation $p = 1 - e^{-n}$ as follows:

$$n \cong \frac{1}{1-p} - 1 \quad (4)$$

where

n quanta inhaled by the occupant (quanta)

Taylor approximation provides reasonable accuracy at low p values, for instance, 2.4% at $p = 0.05$ and 4.7% at $p = 0.1$. By using another approximation $1/(1 - p) \cong 1 + p$ that applies if $|p| \ll 1$, Equation 1 can be rearranged as follows:

$$Q = \frac{(1-\eta_i)qQ_b(1-\eta_s)DN_s}{R} - (\lambda_{dep} + k + k_f + k_{UV})V \quad (5)$$

This equation enables us to calculate infection-risk-based ventilation rates in a simple fashion when substituting default values of quanta emission rate, breathing rate, and occupancy duration.

2.2 Ventilation effectiveness

Ventilation rate Q in Equation 5 applies at fully mixing air distribution. For an actual air distribution solution, deviating from fully mixing, the ventilation rate needs to be adjusted with ventilation effectiveness, known also as contaminant removal effectiveness (Mundt et al. 2004). Ventilation rate Q_s to be supplied by the ventilation system can be calculated as follows:

$$Q_s = \frac{Q}{\varepsilon_b} \quad (6)$$

where

Q target ventilation airflow rate for the breathing zone from equation 6 (L/s)

Q_s design ventilation airflow rate at actual air distribution solution (L/s)

ε_b point source ventilation effectiveness for the breathing zone (-)

To describe the situation with infector (=point source), a common ventilation effectiveness measurement with distributed tracer gas source describing contaminant emission from all occupants in the room, cannot be used. Thus, the point source with many possible locations in the room has to be used. It is proposed in (REHVA 2022) to calculate ventilation effectiveness as an average of two or more tracer gas measurements with different source locations. It is also proposed that concentrations of not all measurement points in the room, but only 50% of measurement points with the highest concentration are accounted for in measurement with each source location j :

$$\varepsilon_b^j = \frac{C_{je} - C_{j0}}{C_{jb} - C_{j0}} \quad (7)$$

$$\varepsilon_b = \frac{\sum_j \varepsilon_b^j}{m} \quad (8)$$

where

- ε_b^j point source ventilation effectiveness of measurement with source location j
- ε_b point source ventilation effectiveness for the breathing zone
- C_{je} measurement j concentration in the extract air duct
- C_{jb} measurement j concentration at the breathing level that is calculated as an average concentration of 50% of the measurement points having the highest concentrations
- C_{j0} concentration in the supply air
- m total number of measurements with different point source locations

In practice ε_b^j can be calculated from the values of the local air quality index:

$$\varepsilon_P = \frac{C_e - C_o}{C_P - C_o} \quad (9)$$

where

- ε_P local air quality index at the measurement point P
- C_P steady state concentration at the measurement point P

To account 50% of measurement points with the highest concentration means that ε_b^j is calculated from 50% of the points with lowest ε_P values as an average.

2.3 Calculating ventilation effectiveness from individual risk

ε_b^j calculation from 50% of measurement points is proposed by (REHVA 2022) to get a conservative value in the case of highly uneven concentration distributions. While infection risk can remarkably increase in locations with high concentration, the average concentration may underestimate it. In the following, we test how well this calculation rule holds by calculating individual infection risk in all measurement points and then summing these up to new disease cases, i.e. to event reproduction number. For the virus risk estimation at given room, the event reproduction number is solved from Equations 5 and 6:

$$R = \frac{(1-\eta_i)qQ_b(1-\eta_s)DN_s}{Q_s\varepsilon_b+(\lambda_{dep}+k+k_f+k_{UV})V} \quad (7)$$

Equation 7 is applied for every measurement point, which may represent one or more occupants, depending on the measurement grid:

$$R_i = \frac{(1-\eta_i)qQ_b(1-\eta_s)DN_{s,i}}{Q_s\varepsilon_{p,i}+(\lambda_{dep}+k+k_f+k_{UV})V} \quad (8)$$

where

- R_i reproduction number for susceptible persons at the measurement location (-)
- $\varepsilon_{p,i}$ is local air quality index at measurement point i (-)
- $N_{s,i}$ the number of susceptible persons represented by each measurement point i ,

The event reproduction number in the room is then calculated as a sum of all individual probabilities/reproduction numbers:

$$R = \sum_{i=1}^n R_i \quad (9)$$

In this calculation, ventilation rate Q_s needs to be solved for instance with goal seek to achieve given R value. To conduct the calculation, we use default values for virus, activity and occupancy parameters as proposed in (REHVA 2022):

- no facial cloth masks ($\eta_s = 0$, $\eta_i = 0$) and no vaccination ($f_v = 0$)
- surface deposition loss rate (Buonanno et al. 2020) $\lambda_{dep} = 0.24$ 1/h
- virus decay (Van Doremalen et al. 2020) $k = 0.63$ 1/h
- quanta emission rate time average values calculated based on median viral loads (Aganovic et al. 2023) of SARS-CoV-2, i.e. $q = 4$ quanta/(h pers) in classrooms, 6 quanta/(h pers) in offices and gyms, and 10 quanta/(h pers) in meeting rooms and restaurants
- number of infectious persons in the room $I = 1$ pers
- breathing rate time averaged values $Q_b = 0.60$ m³/h in offices, $Q_b = 0.57$ m³/h in classrooms, $Q_b = 0.65$ m³/h in meeting rooms and restaurants and $Q_b = 1.9$ m³/h in gyms
- occupancy duration $D = 2, 6,$ and 9 hours in meeting rooms, classrooms, and offices, respectively
- interaction time of an infectious individual is in the vicinity of susceptible persons, including traveling, lunches, and other out-of-home activities, $D_{inf} = 22.5$ h in offices and 16 h in schools over 2.5 days of the pre-symptomatic infectious period

3 RESULTS

Field measurements were conducted in 6 spaces to measure local air quality index with continuous dose method. In each space, two source locations were used. Measured air quality index and source locations are shown in Figure 1 for a large teaching space of 129.5 m². This

teaching space with room height of 2.9 m consisted of three classrooms with movable partitions. In the measurement it was one open space for 50 persons. There were 5 supply air ceiling diffusers and 3 extract air diffusers with total outdoor ventilation rate of 520 L/s. Tracer gas measurements were conducted with 3x9 measurement points equally distributed on 1.1 m height. Additionally, 3 extract air concentration measurements were conducted from which airflow weighted average extract air concentration was calculated. Outdoor air concentration was measured from supply air duct.

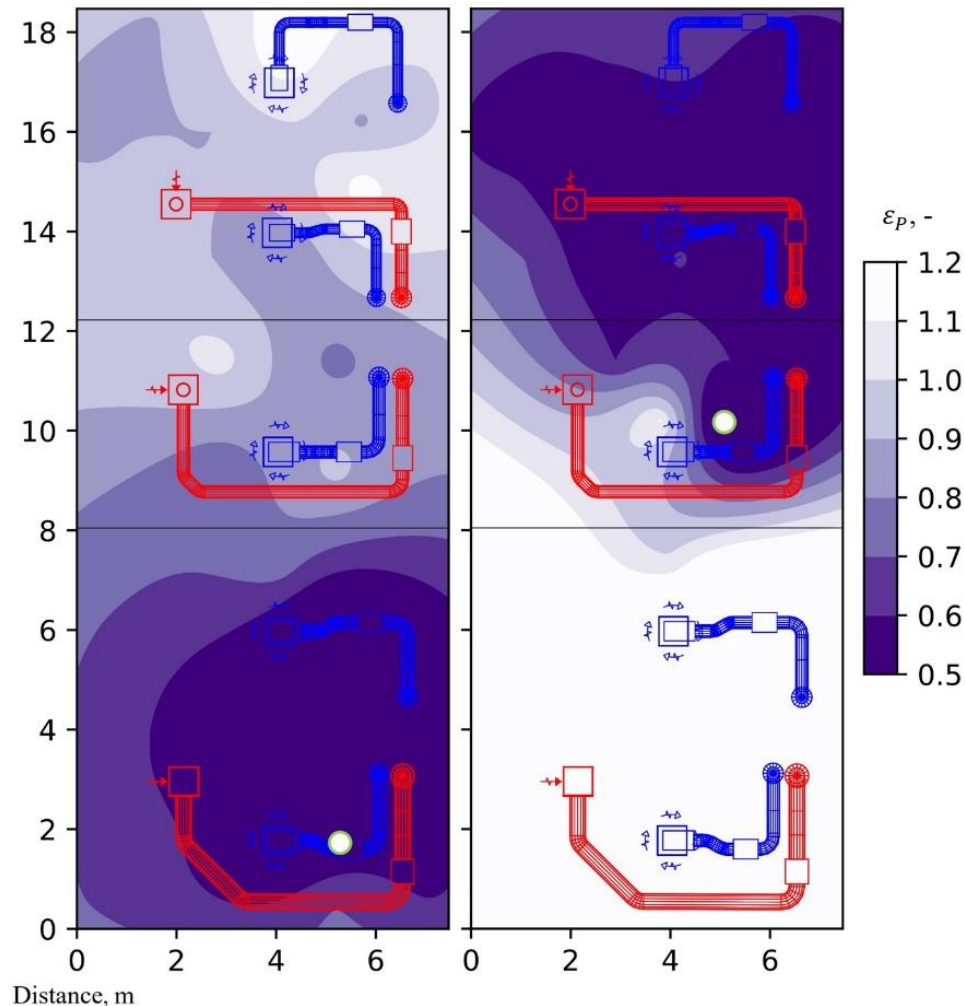


Figure 1: Local air quality index values with two locations of point source in the large teaching space of 129.5 m² with 4 L/(s m²) ventilation. Emission source is marked with green/white circle.

Another measurement example, showing the effect of extract air devices' location can be seen from 24-person meeting room in Figure 2. In this room with 52.5 m² floor area and 2.7 m height, 3x4 concentration measurement points were used from 1.1 m height and one measurement from extract air duct. Chilled beams with 3 L/(s m²) ventilation rate have resulted in reasonably well-mixed condition in the case of the left source location that is far from extract air devices. In this case, local air quality index values range 0.7–1.0 in most of the room area. In the case of the right source location close to extract air devices, the situation is completely different so that high concentration zone forms close to the source and in the white area in the figure, local air quality index values range 1.5–2.

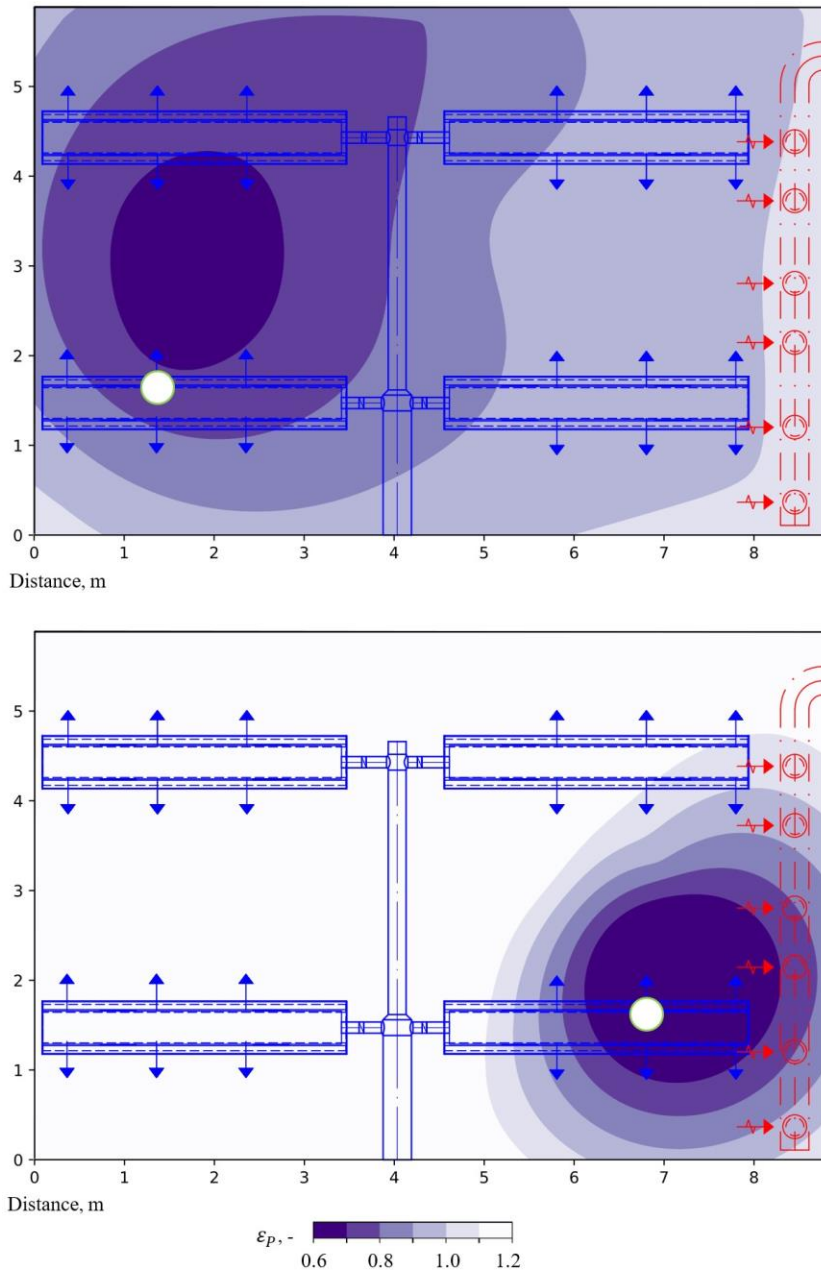


Figure 2: Local air quality index values with left and right locations of point source in the meeting room of 52.5 m² with 3.0 L/(s m²) ventilation. Emission source is marked with green/white circle.

Point source ventilation effectiveness values for all measurement cases are reported in Table 1. ϵ_b values were calculated with Equation 8 and 9, i.e., based on the individual probability of infection in each measurement point and resulting in design ventilation rate Q_s corresponding to specified event reproduction number ($R = 0.375, 0.0889$ and 0.4 in classrooms, meeting rooms and gyms, and offices respectively).

ϵ_b , 50% -rule represents the calculation from 50% of the lowest local air quality index values that revealed to be a conservative estimate in all cases. ϵ_b , avg, is calculated as an average from all local air quality index values. In this case, some high local values easily bias the result so that the ventilation effectiveness is considerably overestimated, leading to under sizing the ventilation rate. While in smaller rooms all three methods provide similar results, in the large open plan office, the differences are remarkable. 50% -rule strongly overestimates and average of all points strongly underestimates the required design ventilation rate.

Table 1: Point source ventilation effectiveness values and resulting design ventilation rates resulting from three calculation methods.

Room	Measurement	ε	ε , 50% -rule	ε , avg	Q_s , L/s	Q_s , 50% -rule, L/s	Q_s , avg, L/s
Classroom 30.5 m ² , 13 persons	Meas. No 1	0.99	0.92	1.00			
	Meas. No 2	1.89	1.67	1.93			
	Average	1.44	1.29	1.46	70	78	69
	%		-10.2%	1.6%		11.4%	-1.6%
Teaching space 129.5 m ² , 50 persons	Meas. No 1	0.77	0.66	0.82			
	Meas. No 2	0.81	0.53	1.19			
	Average	0.79	0.59	1.01	513	683	404
	%		-24.9%	27.0%		33.2%	-21.3%
Gym 173.5 m ² , 12 persons	Meas. No 1	0.56	0.46	0.66			
	Meas. No 2	1.80	1.35	2.53			
	Average	1.18	0.90	1.59	548	716	406
	%		-23.5%	35.0%		30.7%	-25.9%
Meeting room 29.2 m ² , 6 pers.	Meas. No 1	0.90	0.83	0.91			
	Meas. No 2	0.96	0.87	0.97			
	Average	0.93	0.85	0.94	199	217	196
	%		-8.2%	1.4%		9.0%	-1.4%
Meeting room 52.5 m ² , 12 persons	Meas. No 1	0.86	0.78	0.88			
	Meas. No 2	1.18	1.02	1.44			
	Average	1.02	0.90	1.16	404	459	356
	%		-12.0%	13.4%		13.6%	-11.8%
Open plan office 173 m ² , 17 pers.	Meas. No 1	0.50	0.24	2.25			
	Meas. No 2	0.74	0.45	1.19			
	Average	0.62	0.34	1.72	406	732	146
	%		-44.5%	177.2%		80.3%	-63.9%

4 CONCLUSIONS

In this study ventilation effectiveness was calculated based on the infection risk probability assessment in every measurement point in the room, that was compared with calculation from average concentration and calculation method proposed by REHVA accounting only 50% of measurement points with highest concentration. With the method developed, the airflow rate at fully mixing and the airflow rate with actual air distribution, calculated with ventilation effectiveness, provide the same event reproduction number. Results show considerable differences compared to calculation based on average measured concentration, which overestimated the ventilation effectiveness and underestimated design ventilation rate. The method proposed by REHVA, taking into account only 50% of measurement points with highest concentration, revealed to be conservative in all studied cases, as ventilation effectiveness values ranged in between 0.34 – 1.29 compared to 0.62 – 1.44 solved from individual risk of all measurement points. Especially in the large open plan office, REHVA method considerably overestimated the design ventilation rate while in smaller spaces all three methods provided similar results. Results indicate that ventilation effectiveness determination from tracer gas measurements with a point source is not a trivial task. Calculation method

developed, utilising individual probability of infection in each measurement point can be proposed to improve prediction accuracy.

5 ACKNOWLEDGEMENTS

EU Horizon 2020 SmartLivingEPC project and Finnish Government's analysis, assessment, and research project ILMIRA, have supported this research.

6 REFERENCES

- Aganovic, A, Cao, G, Kurnitski, J, and Wargocki, P, 'New dose-response model and SARS-CoV-2 quanta emission rates for calculating the long-range airborne infection risk', *Building and Environment* (2023), <https://doi.org/10.1016/j.buildenv.2022.109924>
- Allen, J.G.; Ibrahim, A.M. Indoor air changes and potential implications for SARS-CoV-2 transmission. *Jama* 2021, 325, 2112–2113.
- Buonanno, G.; Morawska, L.; Stabile, L. Quantitative assessment of the risk of airborne transmission of SARS-CoV-2 infection: prospective and retrospective applications. *Environ. Int.* 2020, 145, 106112.
- CEN EN Standard. 16798-1. Energy performance of buildings—Ventilation for buildings—Part 1: Indoor environmental input parameters for design and assessment of energy performance of buildings addressing indoor air quality. *Therm. Environ. Light. Acoust. M1-6.(16798-1)* 2019.
- Kurnitski, J, Kiil, M, Wargocki, P, Boerstra, A, Seppänen, O, Olesen, B, and Morawska, L. Respiratory infection risk-based ventilation design method. *Building and Environment*, 206, 2021 <https://doi.org/10.1016/j.buildenv.2021.108387>
- Mundt, M.; Mathisen, H.M.; Moser, M.; Nielsen, P. V Ventilation effectiveness: Rehva guidebooks. 2004.
- Nordic Ventilation Group; Rehva Technology and Research Committee COVID-19 Task Force Health-based target ventilation rates and design method for reducing exposure to airborne respiratory infectious diseases. REHVA proposal for post-COVID target ventilation rates. REHVA 2022.
- The Lancet COVID-19 Commission Proposed Non-infectious Air Delivery Rates (NADR) for Reducing Exposure to Airborne Respiratory Infectious Diseases. November 2022;
- Van Doremalen, N et al., 'Aerosol and surface stability of SARS-CoV-2 as compared with SARS-CoV-1', *N. Engl. J. Med.*, vol. 382, no. 16, pp. 1564–1567, 2020.
- Wagner, J.; Sparks, T.L.; Miller, S.; Chen, W.; Macher, J.M.; Waldman, J.M. Modeling the impacts of physical distancing and other exposure determinants on aerosol transmission. *J. Occup. Environ. Hyg.* 2021, 18, 495–509.
- World Health Organization Roadmap to improve and ensure good indoor ventilation in the context of COVID-19; World Health Organization: Geneva PP - Geneva, 2021; ISBN 9789240021280 (electronic version)

Airborne transmission of disease in stratified and non-stratified flow

Peter V. Nielsen^{*1}, Chen Zhang¹, Li Liu²

*1 Department of the Built Environment
Aalborg University
Denmark*

**Corresponding author: pvn@build.aau.dk*

*2 Department of Building Science
Tsinghua University
Beijing
China*

ABSTRACT

Airborne transmissions take place as a transport of virus or bacteria via the aerosol flow in rooms. The distribution of aerosols tends to be evenly distributed if the flow in the room is fully mixed. The aerosols distribution will be different if the room air is stratified. A vertical temperature distribution may create stratified layers with either lower or higher concentrations of exhalation from the infected person. The use of the stratification effect made it possible to create a reduced cross-infection risk for long range airborne transmission in some situations, but we need research in system layout to find solutions which will give a safe environment in all practical situations. A solution must be followed up with some necessary restrictions/information of use, if necessary. Another possibility is to use mixing ventilation and accept a higher flow rate of outdoor air.

KEYWORDS

Airborne transmission, infectious disease, stratified flow, displacement ventilation, mixing ventilation, human exhalation.

1 INTRODUCTION

Airborne transmissions take place as a transport of virus or bacteria via the aerosol flow in rooms. The transmission can be part of the exhalation flow from the source of infection, it can move in the thermal flow from a warm or a cold source, be transported in the ventilation flow or other air movement in the room, and it can be spread by the turbulent diffusion in the room. The distribution of aerosols tends to be evenly distributed if the flow in the room is fully mixed.

Things will be different if the room air is stratified. A vertical temperature distribution may create stratified layers with either lower or higher concentrations of exhalation from the infected person (source person). Consequently, it could be interesting to use this effect to create a system with a low cross-infection risk between people in the room, (Bjørn and Nielsen 2002)(Kosonen et al. 2017). This possibility will be discussed in the following. Another effect in a system with vertically upward increasing temperature is the prospect of obtaining a cooling effect in the room with low location of the supply opening and high location of the return opening. This is the basic principle in displacement ventilation. Stratified flow can also occur in other air distribution systems if they are highly loaded, as in rooms with a mixing ventilation system. In the following when we write “MV”, we assume a fully mixed air distribution and by “DV” we assume stratified air distribution.

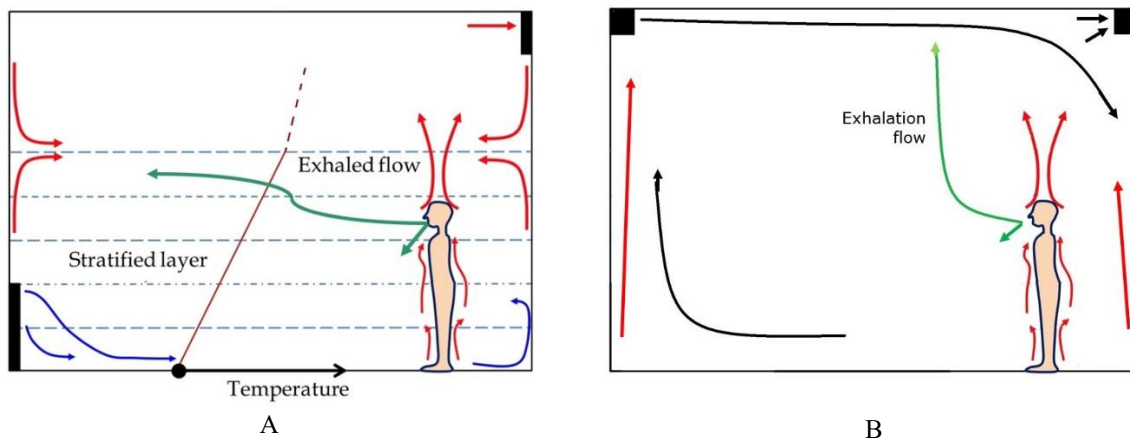


Figure 1. A) Air distribution in a room with displacement ventilation. The figure indicates the stratified flow (Zhou et al. 2017) and B) air distribution in a room with fully mixed flow. Both flows describe a cooling situation.

Figure 1 shows the principle of displacement ventilation. The air movements in the room consist of stratified horizontal flow and vertical movement from boundary layers and plumes. Heat loads, such as person and equipment, create a vertical upward movement; and vertical surfaces, such as windows and walls, create upward or downward movements depending on surface temperature, Figure 1. The flow in the stratified layer is locked into a horizontal temperature band. If we look at the flow from the diffuser, we will see that the height of the layer is rather constant through the whole room, and it is a function of the temperature difference between a reference room temperature and supply temperature (Nielsen 2000). There will only be an insignificant mixing in the horizontal layers because the turbulent mixing will be damped by the temperature gradient. The layer at the floor will have a velocity dependent on the diffuser, temperature difference and flow rate, and layers above may have an insignificant velocity level (Nielsen 2000)(Nielsen 1988). A passive release of tracer gas in any height, or a contaminant of equal density, will spread horizontally in the relevant temperature band in the room (lock-up height) (Bjørn and Nielsen 2002)(Zhou et al. 2017). The distribution of aerosols tends to be evenly distributed if the flow in the room is fully mixed, see Figure 1B. The exhalation will rise to the ceiling if the room temperature is below the exhalation temperature and the room air are entrained into the plume. Virus and bacteria will be fully mixed in the room air by turbulent diffusion. In principle many ventilation systems are based on mixing flow, but some room layouts may generate stratified flow in areas, and a high heat load can also generate stratified flow, as for example in case of direct solar radiation into a room.

2 EXHALATION AND INHALATION OF AEROSOLS

The airborne transmission of diseases in a stratified flow will occur via virus-laden aerosols (droplet nuclei) through human respiratory activities. Therefore, it is necessary to simulate the human exhalation and inhalation process in fine details. "Aerosol dynamic" measurements have hence been performed with breathing thermal manikins, which have the face geometry as described in Table 1, and Figure 2 (Bjørn and Nielsen 2002)(Nielsen et al. 2008)(Liu et al. 2017)(Nielsen and Xu 2022).

Table 1. Definition of nose and mouth.

<p>Nose: Two symmetrical jets. 30° between the jets Jets 60° inclined toward the chest 50 mm² each nostril opening (diameter 8 mm)</p> <p>Mouth: 100 mm² with semi-ellipsoidal shape Horizontal discharge of exhaled air</p>

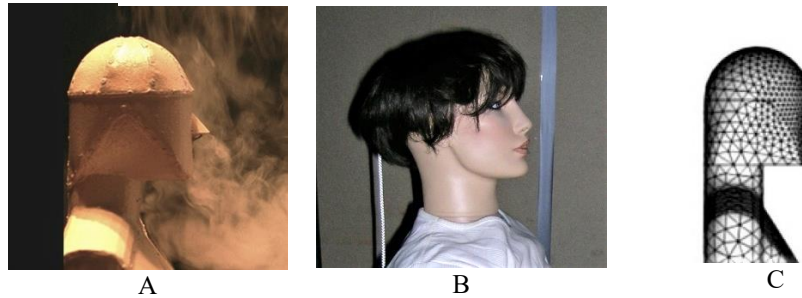


Figure 2. A) Thermal manikin with nose and mouth. B) Manikin with fine details. C) Detailed CFD Manikin.

The details of the face geometry are important as boundary conditions in experiments and in Computational Fluid Dynamics (CFD) predictions. Other important boundary conditions are the activity level of the person (heat release and thermal boundary layer), breathing frequency and volume flow rate. Movement of the face (direction of exhalation), height of person, movement of the person might also be important for a detailed description in an aerosol dynamic experiment. The airborne transmission of aerosols will increase when we investigate speaking, shouting, singing, and coughing. The parameters in Table 1 change. The mouth area and exhalation direction vary in speaking, singing, and coughing (Abkarian et al. 2020). The number of droplets and aerosols increase (Pan et al. 2022).

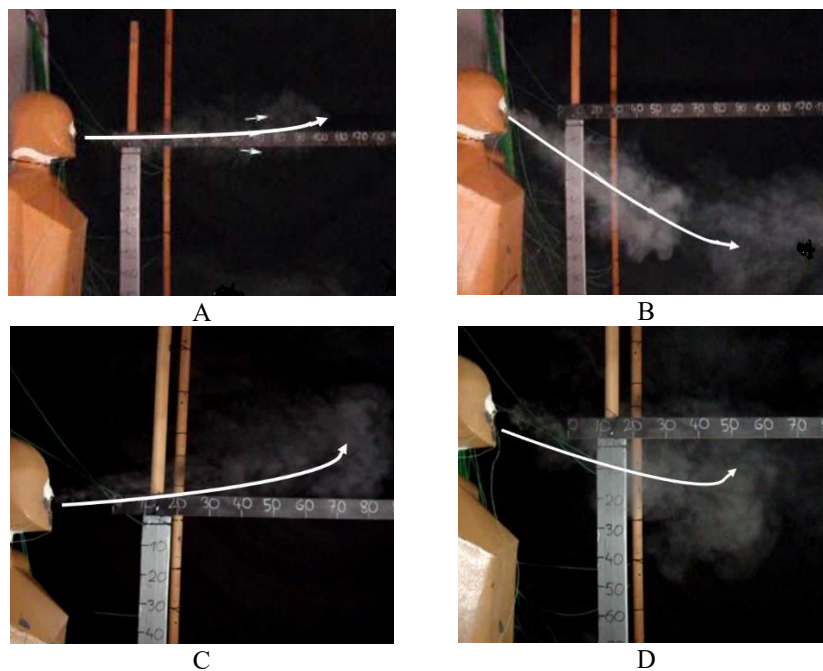


Figure 3. Exhalation 2.5 seconds after start of a sequence. A) DV and Exhalation through mouth. B) DV and Exhalation through nose. C) MV and exhalation through the mouth. D) MV and exhalation through the nose (Nielsen et al. 2009).

Several universities have agreed on both geometries described in Table 1 and Figure 2, and up until now, it is one of the most detailed mouth and face geometries used in experiments and CFD. They include an artificial lung creating the breathing function.

Figure 3A and B shows the flow in the microenvironment around a manikin in surroundings with a vertical temperature gradient of 2.0 K/m. Figure 3A for displacement flow shows that the exhalation from the mouth forms an initial horizontal jet, and the flow is locked up by the temperature gradient just above the mouth in this case. The exhalation through the nose is different from the mouth flow, cf. Figure 3B. It starts with a downward jet and turns into a horizontal flow at some distance because it is also ‘locking up’ in the vertical temperature gradient. The final flow has very different horizontal locations in the two cases. The initial exhalation temperature is 34° in both cases, but the exhalation jet mixes with the surrounding air and reduces the temperature to a local value in some distance.

Figure 3C shows the exhalation through the mouth in case of mixing flow. The exhalation turns upward due to an initial temperature of 34 °C and a surrounding temperature of 20.8 °C in this case. The upward velocity in the manikin’s thermal boundary layer is stronger in this MV case than in the DV case (Figure 3A), and this may explain the more upward directed exhalation. Figure 3D shows the exhalation through the nose. This flow is also influenced by a strong boundary layer around the manikin, and the flow will take an upward direction at some distance from the nose and, in principle, continue to the ceiling, as in Figure 3C.

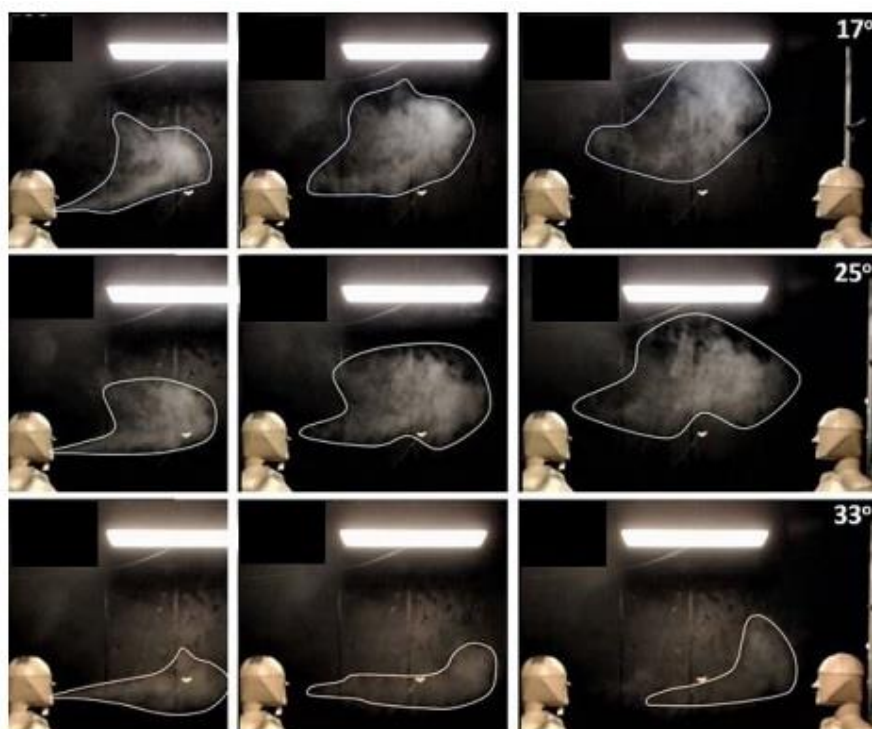


Figure 4 shows the movement of the pulsating exhalation flow based on the location of the tracer (smoke) at different time steps. Mixing ventilation. The smoke pattern is measured at three different room temperatures: 17 °C, 25 °C, and 33 °C (Nielsen et al. 2022).

The room temperature is an important parameter for the trajectory of the exhalation flow in a room with mixing ventilation as shown in Figure 4. The figure shows the pulsating exhalation as a time dependent flow. The position of exhaled tracer (smoke) is given at three different time steps, and the last time step is 1.66 sec of a total breathing cycle of 3.7 sec. It is clearly a more informative depiction of the instantaneous flow than the earlier Figure 3. It shows that the exhaled jet will have an upward movement in the beginning of an exhalation due to a combination of momentum and buoyancy. Later, when the velocity from the

exhalation is low, the exhaled volume of air will rise mainly due to buoyancy. The combined flow describes the true time dependent movement of the exhalation, and it expresses the flow as a combination of an instantaneous buoyant jet and a vortex flow (Nielsen et al. 2009). The middle row in figure 4 shows the exhalation flow in a room with a room temperature of 25 °C. This is close to the comfort temperature in a room, and it corresponds to most measurement in literature and to the situation in Figure 3. The upper row shows the situation in a cold room or outside. It is obvious that the horizontal distance in the exhalation is reduced in cold rooms or cold outdoor surroundings (Nielsen et al. 2022). The lower row shows the results for a room with a room temperature close to the exhalation temperature (34 °C) of a person. The exhalation moves horizontally through the room, but it do not reach the opposite manikin because this manikin's boundary layer and breathing are protecting the face regions. The inhalation of a person also dependent on several parameters. The air is inhaled from the thermal boundary layer around the body if the person does not move or turn around. Inhaling from the boundary layer means that a person will get his/her inhaled air from a lower level in the room than from the head height (Bjørn and Nielsen 2002)(Murakami 2004). This is a positive effect if there is a concentration gradient in the room since the concentration at the bottom of the occupied zone can be low in displacement ventilation. The effect of the body boundary layer will disappear when the person is moving forward with more than 0.2 m/s (Bjørn and Nielsen 2002).

3 MICROENVIRONMENT

The microenvironment around a person is the area where the air movement and the contaminant distribution processes are both influenced by the person and by the surrounding air conditioning system. The microenvironment can include two persons if they are standing in short distance $x < 1.5$ m.

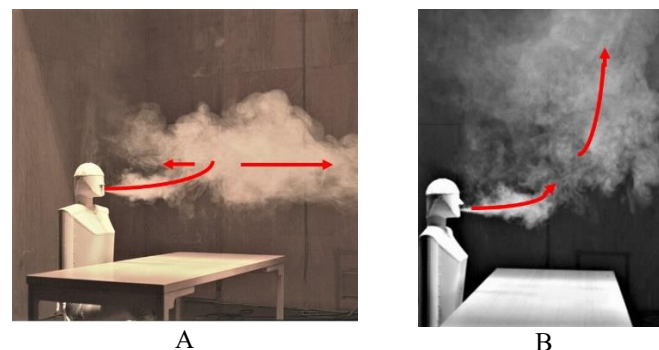


Figure 5. Exhalation flow from the mouth inside and outside the microenvironment. A) Surrounding stratified flow with a temperature gradient at head height of 0.5 K/m. B) Exhalation flow in a similar case with fully mixed surrounding flow without any temperature gradient, 0.0 K/m.

The vertical temperature distribution does influence the flow in the microenvironment. Figure 5A show the exhalation flow from the mouth in the case of DV with a gradient of 0.5 K/m. The flow is an instantaneous jet close to the mouth, and it moves upward, at some distance, and spreads horizontally at head height due to the lock-up effect in the case of Figure 5A. The situation is typical for DV, because a gradient of 0.5 to 1.0 K/m is within the comfortable conditions and a certain gradient is required to obtain an efficient energy solution. Figure 5B shows the situation in the case of fully mixed flow, MV, in the room. The exhalation from the mouth is first an instantaneous jet mixed with the surrounding air, but in principle it will move continuously up to the ceiling area as a plume due to the temperature difference. Although the exhalation flow will rise in both cases, it will be possible to stand closer to a person in the MV case without being influenced by the exhalation flow of the

opposite person. This effect is documented in many measurements of cross- infection risks between two persons at short distance inside the common microenvironment, (< 1.5 m) (Bjørn and Nielsen 2002)(Nielsen et al. 2008)(Liu et al. 2017)(Nielsen and Xu 2022).

Let us look at a situation where the cross-infection risk between two persons is expressed as the inhalation of tracer gas (aerosols) from one person to the other. Figure 6 shows the exposure of a target person expressed as normalized exposure $c_{exp}/c_R (= \epsilon)$, where c_{exp} is the exposure of inhaled tracer gas from an opposite source manikin and c_R is the concentration in return opening (fully mixed value). Although traces gas cannot be directly used as a measure for the health risk assessment, it can give an indication of this risk.

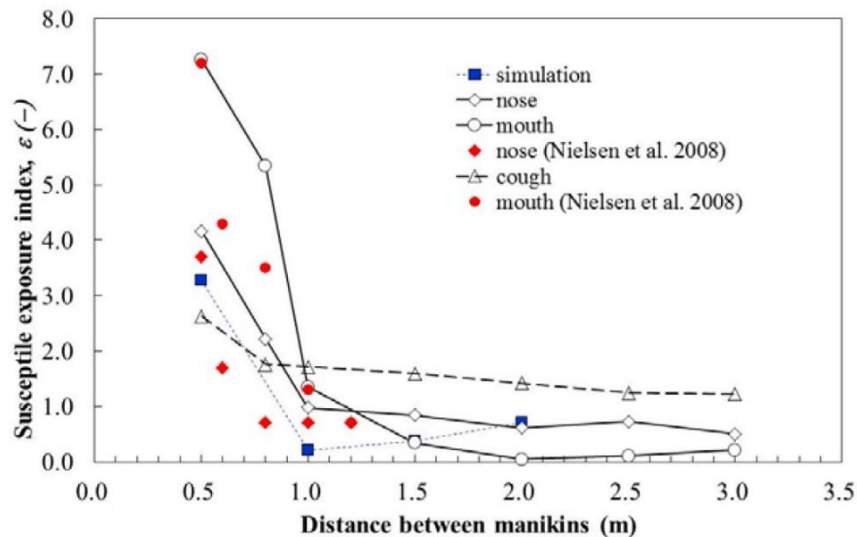


Figure 6. Exposure of target manikin versus distance between the two manikins of same height in a room with displacement ventilation. Results are shown for both breathing through the mouth, through the nose, for coughing and for CFD predictions (Liu et al. 2017).

It is obvious that there is a large increase in the cross-infection risk when the two persons are standing close to each other (in a common microenvironment, $x < 1.5$ m). This is both the case for breathing through the mouth and through the nose. It is also seen from (Nielsen et al. 2008) that the increase in this exposure is expected to be low in the case of MV, in agreement with the two situations shown in Figure 5. The effect is due to the influence of the temperature gradient on the exhalation flow, which is different for different ventilation systems. The normalized exposure, c_{exp}/c_R , at the distance 0.35 m for breathing through the mouth is, for example, around 7.0 for displacement ventilation, 4.3 for vertical ventilation, 1.8 for diffuse ceiling ventilation and only 1.5 for mixing ventilation (Nielsen and Xu 2022). Thermal stratification gives a high exposure in the microenvironment, and fully mixed (MV) conditions with a normalized exposure up to 1.5 (at 1.35 m) for breathing through the mouth are to be preferred. It should be noted that it can be difficult to obtain MV conditions at certain load conditions and at some certain geometries in the system.

4 MACRO-ENVIRONMENT

Figure 6 also shows the conditions in the macro-environment of a displacement ventilated room ($x > 1.5$ m). The normalized exposure is below the fully mixed value, and it is different for breathing through the nose (0.7) than for breathing through the mouth (0.2). The values are preferable values in a ventilated room, and they are achieved because people's inhalation is from the lower part of the room via the personal thermal boundary layer. The concentration of exhaled aerosols is often low in this lower part of a room with displacement ventilation. The results show that detailed boundary conditions for the breathing function of the source manikin must be very essential in the measurements and simulation of stratified flow.

What will challenge this overall low cross-infection risk between people in the room in case of DV? Let us look at the parameters discussed earlier. Results in Figure 6 are for people of same height and without moving. Walking and movement of persons could increase infection risk (Bjørn and Nielsen 2002). Blocking the target manikin's boundary layer by a table may increase infection risk. Breathing through the nose instead of the mouth could increase infection risk. The activity level of the person (heat release and thermal boundary layer), breathing frequency and volume flow rate will have an influence. Mouth area and exhalation direction vary in speaking, singing, and coughing (Abkarian et al. 2020) and could modify the lock-up height.

The position of the human exhalation layer depends on several variables as the size and location of the vertical temperature gradient in the room in addition this gradient is dependent on the heat load and temperature level in the room, on vertical and horizontal location of heat loads etc. Different situations obtained with a seated and a standing person (distance 4 m) in a room with different heat loads and flow rates, have normalized exposures from 0.6 to 1.75 (Bjørn and Nielsen 1997).

Fully mixed flow will be an alternative safe solution, but it requires a higher flow rate of outdoor air (Li, Nielsen, and Sandberg 2011). The system should be well-designed without creating any stratification at high heat load.

5 CONCLUSIONS

The use of the stratification effect made it possible to create a reduced cross-infection risk for long range airborne transmission in some situations, but we need research in system layout to find solutions which will give a safe environment in all practical situations. A solution must be followed up with some necessary restrictions/information of use, if necessary. Another possibility is to use mixing ventilation and accept a higher flow rate of outdoor air.

It is also a question whether or not it is acceptable to select a solution with the stratified flow, which shows high exposure at the close distance between people (< 1.5 m); if it can be solved with mixing ventilation where the cross-infection risk is lower at close distance, although a higher flow rate to the room is required to obtain an overall acceptable infection risk.

6 ACKNOWLEDGEMENTS

This research was supported by The Danish Agency for Higher Education and Science International Network Programme (Case no. 0192-00036B). It was co-supported by Martha og Paul Kerrn-Jespersens Fond (Exploring the potentials).

7 REFERENCES

- Abkarian, Manouk, Simon Mendez, Nan Xue, Fan Yang, and Howard A. Stone. 2020. "Speech Can Produce Jet-like Transport Relevant to Asymptomatic Spreading of Virus." *Proceedings of the National Academy of Sciences of the United States of America* 117(41):25237–45. doi: 10.1073/pnas.2012156117.
- Bjørn, E., and P. V. Nielsen. 2002. "Dispersal of Exhaled Air and Personal Exposure in Displacement Ventilated Rooms." *Indoor Air* 12(3):147–64. doi: 10.1034/j.1600-0668.2002.08126.x.
- Bjørn, Erik, and Peter V. Nielsen. 1997. *Passive Smoking in a Displacement Ventilated Room*. Dept. of Building Technology and Structural Engineering. Indoor Environmental Technology.
- Kosonen, Risto, Arsen Melikov, Elisabeth Mundt, Panu Mustakallio, and Peter V. Nielsen. 2017. *REHVA Guidebook No.23: Displacement Ventilation*. Federation of European

- Heating, Ventilation and Air Conditioning Associations.
- Li, Yuguo, Peter V. Nielsen, and Mats Sandberg. 2011. "Displacement Ventilation In Hospital Environments." *ASHRAE Journal* 53(6):86–88.
- Liu, L., Y. Li, P. V. Nielsen, J. Wei, and R. L. Jensen. 2017. "Short-Range Airborne Transmission of Expiratory Droplets between Two People." *Indoor Air* 27(2):452–62. doi: 10.1111/ina.12314.
- Murakami, S. 2004. "Analysis and Design of Micro-Climate around the Human Body with Respiration by CFD." *Indoor Air, Supplement* 14(SUPPL. 7):144–56. doi: 10.1111/j.1600-0668.2004.00283.x.
- Nielsen, Peter V., Rasmus L. Jensen, Michal Litewnicki, and Jan Zajas. 2009. "Experiments on the Microenvironment and Breathing of a Person in Isothermal and Stratified Surroundings." *9th International Conference and Exhibition - Healthy Buildings 2009, HB 2009*.
- Nielsen, Peter V., and Chunwen Xu. 2022. "Multiple Airflow Patterns in Human Microenvironment and the Influence on Short-Distance Airborne Cross-Infection – A Review." *Indoor and Built Environment* 31(5):1161–75. doi: 10.1177/1420326X211048539.
- Nielsen, Peter V. 2000. "Velocity Distribution in a Room Ventilated by Displacement Ventilation and Wall-Mounted Air Terminal Devices." *Energy and Buildings* 31(3):179–87. doi: [https://doi.org/10.1016/S0378-7788\(99\)00012-2](https://doi.org/10.1016/S0378-7788(99)00012-2).
- Nielsen, Peter V, F. V Winther, M. Buus, and M. Thilageswaran. 2008. "Contaminant Flow in the Microenvironment Between People Under Different Ventilation Conditions." *ASHRAE Transactions* (Part 2):632–40.
- Nielsen, Peter V, Chen Zhang, Kirstine M. Frandsen, Rasmus L. Jensen, Patrick Hundevad, Simon Madsen, Tonje Luckenwald, Najim Popalzai, Yuguo Li, Hua Qian, and Chunwen Xu. 2022. "Cross-Infection Risk between Two People in Different Temperature Surroundings Studied by Aerosol Dynamics." in *COBEE 2022*.
- Nielsen, Peter Vilhelm. 1988. *Displacement Ventilation in a Room with Low-Level Diffusers*. Vol. R8836. Aalborg.
- Pan, Shihai, Chunwen Xu, Chuck Wah Francis Yu, and Li Liu. 2022. "Characterization and Size Distribution of Initial Droplet Concentration Discharged from Human Breathing and Speaking." *Indoor and Built Environment* 0(66):1–14. doi: 10.1177/1420326X221110975.
- Zhou, Qi, Hua Qian, Haigang Ren, Yuguo Li, and Peter V. Nielsen. 2017. "The Lock-up Phenomenon of Exhaled Flow in a Stable Thermally-Stratified Indoor Environment." *Building and Environment* 116:246–56. doi: 10.1016/j.buildenv.2017.02.010.

Acoustic method for measurement of airtightness – field testing on three different existing office buildings in Germany

Björn Schiricke^{*1}, Benedikt Kölsch²

*1 German Aerospace Center (DLR),
Institute of Solar Research
Linder Höhe
51147 Cologne, Germany*

*2 German Aerospace Center (DLR),
Institute of Solar Research
Karl-Heinz-Beckurts-Str. 13,
52428 Jülich, Germany*

**Corresponding author: bjoern.schiricke@dlr.de*

ABSTRACT

Maintaining the airtightness of building envelopes is a key factor for the energy efficiency of buildings. A fast and reliable detection of leaks plays a decisive role, especially during building renovations. For this reason, work has been done in recent years to apply an acoustic beamforming method that enables the fast, simple, and large-area detection of leaks in building envelopes. This method is based on a microphone array technology and assumes that sound primarily follows the same paths as air through the building envelope. So far, these acoustic airtightness measurements have primarily been tested in the laboratory setting or on isolated facade parts with previously known leakages. Comprehensive field experience reports, particularly for use on a larger scale and on building envelopes with unknown leakages, have remained scarce.

This paper presents the results of large-scale testing and demonstration of acoustic air tightness measurements. Facades of 37 rooms of multi-storey buildings with unknown leakages were measured at three office buildings of different ages (built or renovated in 1990, 1995, and 2019) and heterogeneous building envelope structures. This represents, to the best of our knowledge, the most extensive field study to date for acoustic airtightness determination of building envelopes.

In the measurement campaign speakers emit white noise in the frequency range from 0.05 to 120 kHz from the inside with about 85 dB for a duration of four seconds. A microphone ring array with 48 microphones and a diameter of 0.75 m is located outside in a distance of up to 12 m from the observed facade. 57 measurements have been analysed and evaluated in a spectral range of 0.8 to 25 kHz.

As a result, hundreds of potential leaks were localized and visualized across a large area. Many of these were subsequently confirmed as plausible by visual inspection of the respective positions in the building envelope. Some were verified with a smoke stick test.

This paper introduces an Acoustic Assessment Score (ASS) for the evaluation of acoustic signals along with a colour code for their graphical representation. It enables a result representation that highlights the relevance of the signals concerning potential leakages. Furthermore, a Multi Frequency Assessment Score (MFAS) is defined, that allows a comparison of the acoustically determined airtightness of different rooms.

This field study has provided valuable experience into the practicality, speed, and interpretability of acoustic signals, along with the method's large-scale applicability and potential for further developments. The findings suggest, that a significant number of potential leakages can be detected, confirming the method's basic functionality for large buildings. Furthermore, a comparison of the distribution of the ASS and the MFAS within the different buildings suggests, that the applied acoustic method managed to discern the airtightness quality of the three buildings.

KEYWORDS

Airtightness, Beamforming, Leak detection, Building envelope, Field study

1 INTRODUCTION

The unintentional air exchange through a building envelope is estimated to account for 30 to 50 % of its heating and cooling energy. This unintentional airflow is a primary cause of heat loss in buildings, highlighting the need for effective airtightness measurements. Conventionally, the fan pressurization method (*ISO 9972:2015*, 2015) is used for this purpose. A fast and reliable detection of leaks plays a decisive role, especially in the renovation of buildings. However, identifying and quantifying leaks with standard methods in conjunction with a blower door test is challenging, time-consuming, and strongly depends on the experience of the respective energy consultant.

Recent advancements have seen the emergence of acoustic measurement methods, such as acoustic cameras, which hold the potential for identifying individual leaks in the building envelope. Unlike traditional methods, this non-destructive acoustic testing does not necessitate large volumes of air movement through the building envelope, allowing testing under naturally occurring unpressurized conditions. In contrast to the Blower-Door test, acoustic methods also do not rely on closed volume, enabling testing during the construction or renovation of a building.

In light of these advantages, there has been a focus on developing an acoustic beamforming method in recent years. Using an acoustic camera, this method enables the fast, simple, and large-area detection of potential leaks in building envelopes. This method is based on a microphone array technology, operating on the premise that sound primarily takes the same paths as air through the building envelope. In addition to other acoustic methods (Coltraco Ultrasonics, 2023), this presented method allows the detection of leaks on a large surface at once.

The aim of the acoustic measurements is to detect small openings in building enclosures and potential gas propagation pathways within buildings. A knowledge of leak location and estimates of leak sizes would enable a prioritized sealing of more substantial leaks (Walker & Wilson, 1998).

The objective of this work is to test and demonstrate the effectiveness of our acoustic air tightness measurement method on a larger scale. We applied this method to multi-storey buildings with unknown leakages and aimed to gain experience regarding the practicality, speed, and interpretability of the acoustic signals. Furthermore, we sought to assess the method's applicability method on a large scale, which has significant implications for its broader use.

2 TEST SITE AND MEASUREMENT CONFIGURATION

Within the framework of a project in which a heterogeneous building complex was also measured geometrically and thermally, the acoustic air tightness measurement was to be tested and demonstrated on a larger scale.

The test site selected for this study is a research institution consisting of five diverse buildings located in Villingen-Schwenningen, Germany. Figure 1 shows an aerial view and a 3D model of the investigated building complex. This measurement campaign focuses on office building parts A, D, and E, constructed or renovated approximately in 1990, 1995, and 2019. Building part B comprises clean rooms, and building part C houses a cogeneration unit. A total number of 57 acoustic measurements have been analysed, corresponding to 36 investigated rooms

(some of them had facades on different sides of the building so they required more than one measurement).

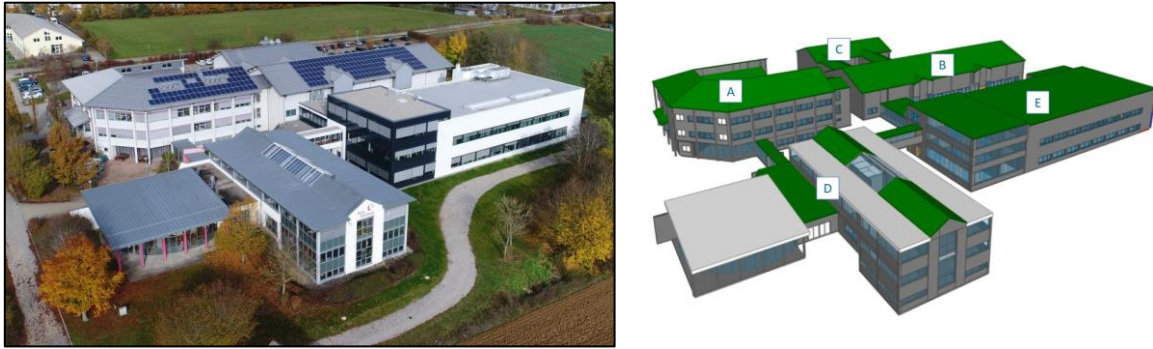


Figure 1: Aerial photo (left) and 3D-Model (right) of the investigated building complex, including labelling of the individual building parts

We used a microphone ring array with 48 uniformly spaced microphones with a diameter of 0.75 m for these measurements (see Figure 2, centre). This array functions optimally in a frequency range of 164 Hz to 20 kHz, although it can localize frequencies as high as 60 kHz. For this study, all signals were sampled at a frequency of 192 kHz and digitized with 32 bits. An optical camera positioned at the array's centre recorded a visual image of the measured scene, offering a resolution of 1920×1080 pixels.



Figure 2: Measurement setup: pair of loudspeakers inside (left), microphone array or acoustic camera outside (centre), visualization of the loudest noise sources on the facade (right).

In general, beamforming is a signal processing technique that enables the differentiation of sound sources from different directions using the microphone array. It operates by scanning a focus point \vec{x} on a pre-defined grid on the measured object. Equation 1 provides the time function $\hat{f}(\vec{x}, t)$ for this ring array for each focus point (Jaeckel, 2006):

$$\hat{f}(\vec{x}, t) = \frac{1}{M} \sum_{i=1}^M f_i(t - \Delta\tau_i) \quad (1)$$

During the evaluation, the individual microphones' time signals $f_i(t)$ are superimposed with a time delay $\Delta\tau_i$, corresponding to the time required for the sound wave to travel from the measured focus point on the building façade to the microphone. Subsequently, the time-corrected signals from all microphones are summed and divided by the total number of microphones M , yielding a time signal for each focus point. Equation 2 is then used to calculate the effective sound pressure $\hat{p}_{rms}(\vec{x})$ at the calculated focus point:

$$\hat{p}_{rms}(\vec{x}) \approx \hat{p}_{rms}(\vec{x}, n) = \sqrt{\frac{1}{n} \sum_{k=0}^{n-1} \hat{f}^2(\vec{x}, t_k)} \quad (2)$$

where n is the total number of corresponding discrete time samples, and t_k is the time value at the sample index k . The advantage for various applications using an acoustic camera is the visual result, typically overlaid with a visible image of the same scene. For more information about the operating principle of the acoustic camera, see Refs. (Kölsch, 2022; Kölsch et al., 2021; Teutsch, 2007).

A pair of speakers (see Figure 2, left) is situated on one side of the wall (inside), while the acoustic camera (see Figure 2, centre) is placed on the other (outside). The high-frequency speaker functions in an even frequency range of 15 to 120 kHz, while the low-frequency dodecahedron speaker operates from 0.05 to 16 kHz. The stationary setup of the acoustic camera and speakers allowed for consistent measurements, with the sound waves penetrating through the leaks in the wall, detectable as individual sound sources on the wall's other side by the acoustic camera. A computer-generated white noise signal was emitted inside at a sound pressure level of 85 dB for 4 seconds.

The data analysis is carried out with the software NoiseImage (GFaI, 2021), specifically the power beamforming option, which enhances image clarity and source representation sharpness. While this method disrupts the exact sound pressure levels, it does not critically impact this application.

While we were able to reduce the disturbing influence of external sound sources in the past by recording reference signals next to the speaker inside the building (Kölsch et al., 2021), we did not do so in this study for efficiency and time-saving reasons.

3 METHODOLOGY OF CATEGORISATION

3.1 Evaluation of acoustic measurements

This measurement campaign has shown that sound sources indicating potential leakages, with the given equipment, are typically found within the spectral range of 800 Hz to 25 kHz. Within this range, there are 16 third-octave frequency bands. In each of these bands, only the highest Δ dB of the recorded sound pressure levels (hereafter referred to as sound peaks) are shown superimposed on the visual image. The Δ is chosen individually to provide optimal visualization for each case.

Since sound peaks can occur at different locations across different frequency bands, thereby indicating potential leakages at different locations, it is rarely possible to display all leakages simultaneously. Most of the time, a series of images across different frequency bands is needed to illustrate the potential leakages in the building envelope. This is exemplified in Figure 3 using Room 106 (Building D, east façade), where only eight of the 16 examined frequency bands are shown. Here, the highest 1.7 dB ($\Delta = 1.7$) sound peaks are displayed for all third-octave frequency bands. To comprehend the need for illustrating the entire range of frequency bands, we consider the peak in the third window from the left. It is only visible at the frequency bands 2, 6.3, and 10 kHz. Conversely, the leakage at the lower window frame in the second window from the right, is only visible at 2.5, 3.2, 4, 5, and 6.3 kHz.

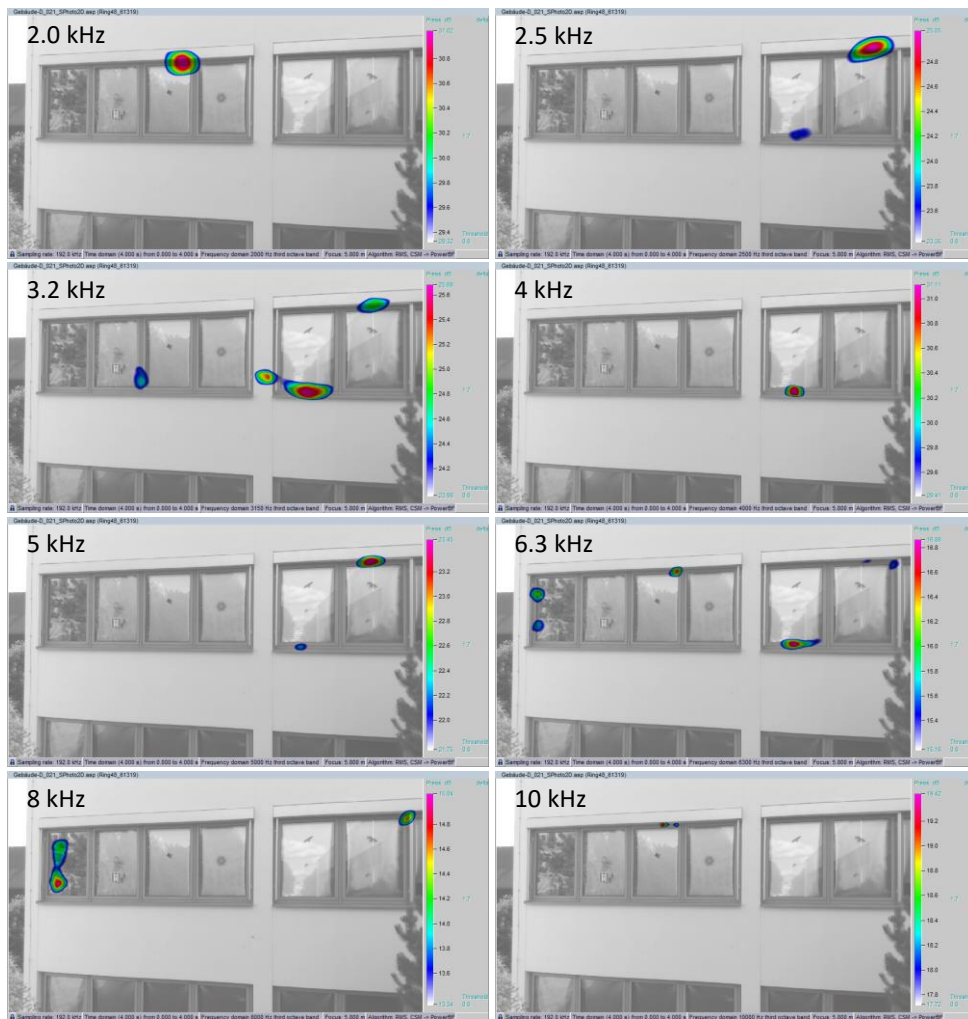


Figure 3: Representation of the results of the acoustic camera using the example of room 106 (building D, east facade). The highest 1.7 dB of the sound pressure level in each of the eight third-octave bands from 2 to 10 kHz are shown as coloured sound peaks. In the top left corner of each image, the average frequency of the third-octave band is noted.

Not every sound peak necessarily indicates a leakage; they can also result from sound reflections or structure-borne sound like vibrations, causing locally high sound levels. The sound peak on the pane of the left window in the 8 kHz example (Figure 3) is clearly located at an implausible place for leakage and is more likely caused by a vibration of the pane.

However, in many cases, a visual inspection at the locations of the sound peaks confirmed plausible causes for air leakage. An example is shown in Figure 4 (left), where a drilled hole from a previously installed window coincided with the position of the sound peak. In some rooms, a blower door and a smoke stick were employed, definitely confirming a leakage at the position of a sound peak (see Figure 4, right).

Often, however, the cause for a sound peak could not be clearly confirmed due to limited time resources. Therefore, these sound peaks required a subjective evaluation in terms of their plausibility for being leakage-related, which is further described in the following section.

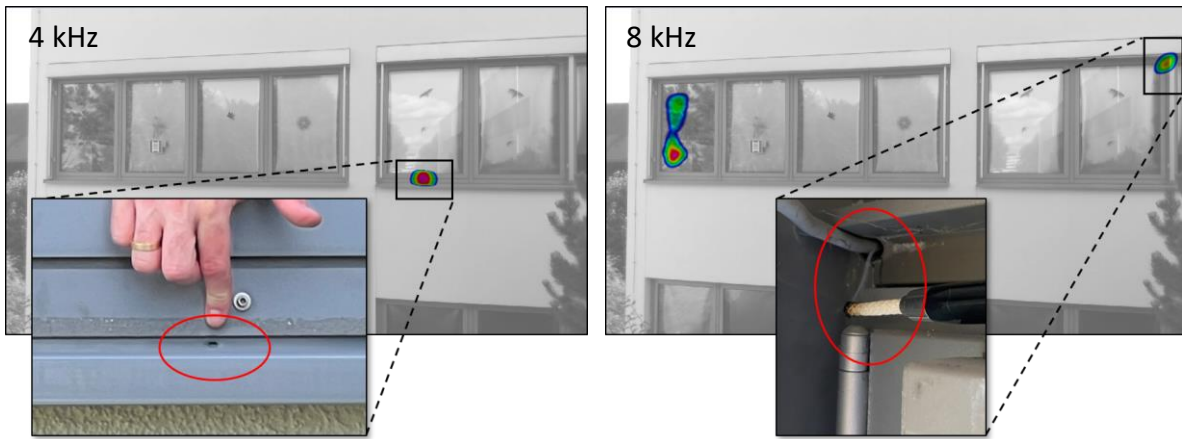


Figure 4: Examples of confirmed plausibility for air leakage as cause for sound peaks in room 106 (building D, east facade)

3.2 Categorization of the acoustic signals with regard to a possible leakage

The evaluation of individual peaks across all considered 16 third-octave frequency bands of all 57 measurements (in total 912 analysed frequency bands) required manual adjustment of the signal's peak Δ value in the software NoiseImage. This adjustment allowed the signal peak to be represented as the smallest possible area, thereby identifying the exact position of the source. The exact position of the peak is used to evaluate the plausibility of a leak being the cause of the sound source at that location. Table 1 describes the four evaluation categories with their colour code and scores.

Table 1: Description of the colour code for the evaluation of acoustic signals and their criteria

Colour Code	Acoustic Assessment Score	Evaluation of acoustic signals	Description of subjective criteria
○	0	very unlikely leakage	Peak of signal is at implausible location (e.g. on a window pane or facade panel, or outside the area under consideration)
●	1	unlikely leakage	Some indications that the signal is probably not caused by a leakage (e.g. wide spread shape of the sound source) or Peak of signal is at rather implausible location (e.g. close to a plausible location but just off the mark)
●	2	likely leakage	Peak of signal is at plausible location (e.g. joints between different materials or roof and wall), or even at particular plausible location, but with a much weaker signal.
●	3	very likely leakage	Peak of signal is at a particular plausible location (e.g. seals in door and window frames)

Identifying the exact location of the sound peak involves tedious manual work, and the assessment of the evaluation category is based on subjective criteria with fluid boundaries. Both tasks are time-consuming and susceptible to error, yet. Despite this, the method allows for documentation of the assessment in the facade representation using the corresponding colour code, as exemplified in Figure 5. Based on this representation, potential leakage locations on the facade can be identified for inspection and subsequent sealing if necessary. However, this process currently necessitates multiple images for the different third-octave frequency bands.

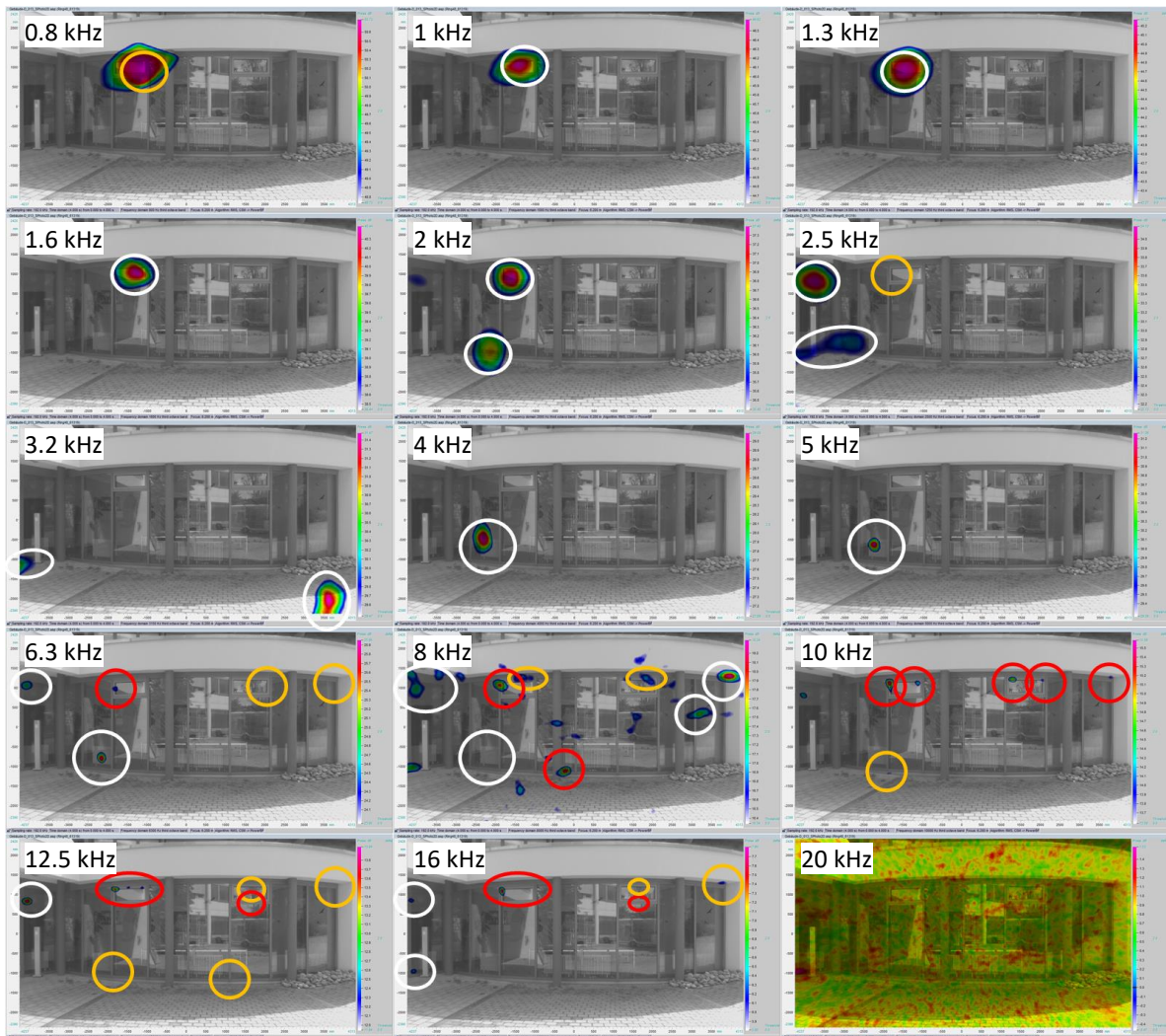


Figure 5: Representation of the evaluation of the sound peaks using the example of a corridor in building D with the colour codes of Table 1 for the third-octave bands from 0.8 to 20 kHz.

3.3 Evaluation of the airtightness of individual rooms on the facades

To summarise the evaluation of the airtightness of the individual rooms on the facades, the highest colour code assigned in the respective third-octave band is listed in a table (compare Table 2). This provides a visual summary indicating the frequency bands where signs of leakage were found.

As a quantitative metric for a certain room's airtightness, the so-called "multi frequency assessment score" is introduced. It is calculated as the sum of the "acoustic assessment scores" (see Table 1), corresponding to the highest colour codes assigned in each third-octave frequency band. This rules for calculation rule are admittedly arbitrary. We considered the possibility of weighting scores according to frequency range (e.g., giving less weight to lower frequency ranges), but we found no evidence to support this approach. Considering the number of sound peaks occurring for each third-octave band, instead of the score of the maximum occurring colour code, appeared to be less reproducible. Therefore, we opted for the simplest possible definition of the "multi frequency assessment score".

4 RESULTS AND DISCUSSION

Table 2 to Table 4 provide an overview of the evaluations for the building envelopes of the test site, representing all measured rooms/facades of buildings A, D, and E. The colour codes correspond to the “acoustic assessment score” (see Table 1), which are cumulatively represented in the “multi frequency assessment score”. In the second column, labelled “note”, we indicate the compass direction of the façade (if the room has more than one façade), or any special features of the measurement, such as detail shots or repetitions.

Table 2: Evaluation of acoustic signals for each measured room in Building D

Room		Third-octave frequency bands in kHz															Multi Frequency Assessment Score		
Name	note	0.8	1	1.3	1.6	2	2.5	3.2	4	5	6.3	8	10	12.5	16	20	25		
D-112	S	●	●	●	●	●	○	○	○	○	○	○	○	○	○	○	○	○	12
	S up	○	●	●	●	●	●	●	●	●	●	●	●	●	●	●	●	●	42
	SSW	●	○	○	○	○	○	○	○	○	○	○	○	○	○	○	○	○	15
	SW	○	○	○	○	○	○	○	○	○	○	○	○	○	○	○	○	○	36
	SW	○	○	○	○	○	○	○	○	○	○	○	○	○	○	○	○	○	39
	NW	●	●	●	●	●	●	●	●	●	●	●	●	●	○	○	○	○	28
D-112	NW	○	●	○	●	○	●	○	●	○	●	○	●	○	○	○	○	○	26
Corridor	N	●	○	○	○	○	○	○	○	○	○	○	○	○	○	○	○	○	19
	N detail	○	○	○	○	○	○	○	○	○	○	○	○	○	○	○	○	○	27
D-109		○	○	○	○	○	○	○	○	○	○	○	○	○	○	○	○	○	24
D-108	W	○	●	●	●	●	●	●	●	●	●	●	●	●	○	○	○	○	31
	S	○	○	○	○	○	○	○	○	○	○	○	○	○	○	○	○	○	35
D-107		○	○	○	○	○	○	○	○	○	○	○	○	○	○	○	○	○	36
D-106	S	○	○	○	○	○	○	○	○	○	○	○	○	○	○	○	○	○	36
	E	○	○	○	○	○	○	○	○	○	○	○	○	○	○	○	○	○	36
D-103		○	○	○	○	○	○	○	○	○	○	○	○	○	○	○	○	○	19
D-211		○	○	○	○	○	○	○	○	○	○	○	○	○	○	○	○	○	29
D-210		○	○	○	○	○	○	○	○	○	○	○	○	○	○	○	○	○	18
D-209		○	○	○	○	○	○	○	○	○	○	○	○	○	○	○	○	○	33
D-208	W	○	○	○	○	○	○	○	○	○	○	○	○	○	○	○	○	○	29
	S	○	○	○	○	○	○	○	○	○	○	○	○	○	○	○	○	○	37
D-207		○	○	○	○	○	○	○	○	○	○	○	○	○	○	○	○	○	33
D-206	S	○	○	○	○	○	○	○	○	○	○	○	○	○	○	○	○	○	33
	E	○	○	○	○	○	○	○	○	○	○	○	○	○	○	○	○	○	38
D-205		○	○	○	○	○	○	○	○	○	○	○	○	○	○	○	○	○	29
D-204		○	○	○	○	○	○	○	○	○	○	○	○	○	○	○	○	○	19
D-203		○	○	○	○	○	○	○	○	○	○	○	○	○	○	○	○	○	29
D-202		○	○	○	○	○	○	○	○	○	○	○	○	○	○	○	○	○	37
D-201		○	○	○	○	○	○	○	○	○	○	○	○	○	○	○	○	○	23
Bridge	S	○	○	○	○	○	○	○	○	○	○	○	○	○	○	○	○	○	19
	N	○	○	○	○	○	○	○	○	○	○	○	○	○	○	○	○	○	18
	N detail	○	○	○	○	○	○	○	○	○	○	○	○	○	○	○	○	○	21

Table 3: Evaluation of acoustic signals for each measured room in Building E

Room		Third-octave frequency bands in kHz															Multi Frequency Assessment Score		
Name	note	0.8	1	1.3	1.6	2	2.5	3.2	4	5	6.3	8	10	12.5	16	20	25		
E-Büro 2	2.floor (OG)	○	○	○	○	○	○	○	○	○	○	○	○	○	○	○	○	○	14
E-Büro 1	2.floor (OG)	○	○	○	○	○	○	○	○	○	○	○	○	○	○	○	○	○	20
E-Büro	2.floor (EG)	○	○	○	○	○	○	○	○	○	○	○	○	○	○	○	○	○	5
E-Büro		○	○	○	○	○	○	○	○	○	○	○	○	○	○	○	○	○	8
E-Bespr.		○	○	○	○	○	○	○	○	○	○	○	○	○	○	○	○	○	9
E-Bespr. 2	1.floor (UG)	○	○	○	○	○	○	○	○	○	○	○	○	○	○	○	○	○	21
E-Büro 1		○	○	○	○	○	○	○	○	○	○	○	○	○	○	○	○	○	15
E-Büro		○	○	○	○	○	○	○	○	○	○	○	○	○	○	○	○	○	24
E-Aufenth.	2.floor (EG)	○	○	○	○	○	○	○	○	○	○	○	○	○	○	○	○	○	10
E-Büro	1.floor (UG)	○	○	○	○	○	○	○	○	○	○	○	○	○	○	○	○	○	13

Table 4: Evaluation of acoustic signals for each measured room in Building A

Room		Third-octave frequency bands in kHz															Multi Frequency Assessment Score			
Name	note	0.8	1	1.3	1.6	2	2.5	3.2	4	5	6.3	8	10	12.5	16	20	25			
A-101	SW	●	●	●	○	○	○	○	○	○	○	○	○	○	○	○	○	12		12
	SW - detail	●	●	●	○	●	●	●	●	●	●	●	●	○	○	○	○	26		26
	NW	●	●	●	○	○	●	●	●	●	○	○	○	○	○	○	○	27		27
A-103	NW	○	○	○	○	○	○	○	○	○	○	○	○	○	○	○	○	9		9
		○	○	○	○	○	○	○	○	○	○	○	○	○	○	○	○	16		16
A-201/1		○	○	○	○	○	○	○	○	○	○	○	○	○	○	○	○	3		3
	detail	○	○	○	○	○	○	○	○	○	○	○	○	○	○	○	○	13		13
A-201/2		○	○	○	○	○	○	○	○	○	○	○	○	○	○	○	○	13		13
A-201/3		○	○	○	○	○	○	○	○	○	○	○	○	○	○	○	○	15		15
A-202	NW	○	○	○	○	○	○	○	○	○	○	○	○	○	○	○	○	16		16
	Diagrammbereich	○	○	○	○	○	○	○	○	○	○	○	○	○	○	○	○	16		16
	SW rep. 1	○	○	○	○	○	○	○	○	○	○	○	○	○	○	○	○	19		19
	SW rep. 2	○	○	○	○	○	○	○	○	○	○	○	○	○	○	○	○	12		12
	SW rep. 3	○	○	○	○	○	○	○	○	○	○	○	○	○	○	○	○	11		11
A-102		○	○	○	○	○	○	○	○	○	○	○	○	○	○	○	○	8		8

This overview can be used to assess if the applied acoustic method managed to discern any differences among the different buildings. This is reflected both visually in the distribution of the colour codes in Table 2 to Table 4 as well as in the frequency distribution shown in Table 5. As expected, Building D, which is the oldest building and was already identified as problematic by the building owner, exhibits the highest values in the "multi frequency assessment score". A high score indicates a strong acoustic evidence of leakage and, thus, a poor air tightness rating. Table 5 presents the frequency distribution of this numerical assessment of facades.

Table 5: Overall assessment of the acoustic leakage analyses for the three Buildings

Acoustic Multi Frequency Assessment Score	Number of measurements with that score per building		
	D (1990)	A (1995)	E (2019)
very low (0-9)	0	3	3
low (10-19)	8	10	4
mid (20-29)	10	2	3
high (30-39)	13	0	0
very high (40-48)	1	0	0
total number of meas.	32	15	10

5 CONCLUSIONS

This measurement campaign, to our knowledge, represents the most extensive field study conducted to date on the acoustic determination of airtightness of building envelopes. The method was successfully demonstrated on facades of multi-storey buildings of different ages and heterogeneous building envelope structures. Potential leaks were localized and visualized across large areas, with many of them confirmed as plausible by visual inspection. In selected rooms where smoke sticks were employed, some identified leakages were verified. In comparison to the well established infrared thermography method for visualizing leaks, this acoustic method does not rely on temperature or pressure differences across the building envelope.

This field study yields valuable insights regarding the practicability, speed, and interpretability of the acoustic signals and the broader applicability of the method. The findings suggest that a significant number of potential leakages can be detected, confirming the method's basic functionality for large buildings.

However, despite these advancements, further research is needed, particularly in interpreting the data. Possible developments include greater automation in the assessment of relevant leakage locations. This implies the need for systematic laboratory or field investigation with known leakages. Factors like wind influence or reflection of other outside sound sources on the shifting of acoustic peaks and the interpretation of results should also be accounted for.

Moving forward, we envision further detailed examinations at testing facilities and renovation sites. Enhancements to the measurement technology are also projected, such as combining infrared thermography with the existing acoustic camera setup to improve leak detection reliability. The development of a suitable ultrasonic transmitter is another area for exploration.

The potential of this methodology is significant. Noise reduction through reference signals (like done in (Kölsch et al., 2021)), the use of acoustic spectra to infer the type and size of leaks, and multi-perspective analysis to rule out reflections are promising future developments. Furthermore, visualizing leaks from various third-octave frequency bands in a single image could improve the leak-finding process.

6 ACKNOWLEDGEMENTS

This work is part of the research project “Pilotanwendung von Gebäudetomograph-Messmethoden an einem Institut der Innovationsallianz Baden-Württemberg (Gtom-innBW)” which was funded by the Ministry of Economic Affairs, Labour and Tourism Baden-Württemberg under the grant number: WM3-4332-157/64. The authors thank the “Hahn-Schickard-Gesellschaft für angewandte Forschung e.V.” in Villingen-Schwenningen for providing their office buildings as test cases. Additionally, the authors thank Dirk Döbler, Dr. Olaf Jaeckel and Dr. Fabian Knappe from “GFaI - Gesellschaft zur Förderung angewandter Informatik e.V.” for fruitful discussions regarding these measurement results.

7 REFERENCES

- Coltraco Ultrasonics. (2023). *Ultrasonic Airtightness, Leak Detection and Quantification System*. <https://coltraco.com/coltraco-products/portascanner-airtight/>
- GFaI. (2021). *Software: NoiseImage* (4.13.4.17964).
- ISO 9972:2015—*Thermal performance of buildings - Determination of air permeability of buildings - Fan pressurization method* (9972:2015). (2015).
- Jaeckel, O. (2006). Strengths and weaknesses of calculating beamforming in the time domain. *Proceedings of the 8th Berlin Beamforming Conference*.
- Kölsch, B. (2022). *Investigation of an improved acoustical method for determining airtightness of building envelopes* [Dissertation]. RWTH Aachen University.
- Kölsch, B., Schiricke, B., Lüpfert, E., & Hoffschmidt, B. (2021). Detection of air leakage in building envelopes using microphone arrays. *Proceedings of the 41st AIVC - ASHRAE IAQ Joint Conference*.
- Teutsch, H. (2007). *Modal array signal processing: Principles and applications of acoustic wavefield decomposition*. Springer.
- Walker, I. S., & Wilson, D. J. (1998). Field Validation of Algebraic Equations for Stack and Wind Driven Air Infiltration Calculations. *HVAV&R Research*, 1(2).

Pulse tests in highly airtight Passivhaus standard buildings

Xiaofeng Zheng^{*1}, Luke Smith², and Christopher Wood¹

1 Buildings Energy and Environment Research Group, Faculty of Engineering, University of Nottingham, University Park, Nottingham NG7 2RD, United Kingdom

2 Build Test Solutions Ltd., 16 St Johns Business Park, Lutterworth LE17 4HB, United Kingdom

**Corresponding author:*

xiaofeng.zheng@nottingham.ac.uk

ABSTRACT

Due to the minimal energy requirement, the Passivhaus standard has been widely recognised and adopted to deliver low carbon buildings. To achieve this standard, the thermal and physical properties of the building envelope have to meet a stringent criteria. It has set out the highest requirement for the building airtightness, which requires the envelope to achieve an air change rate less than 0.6 h⁻¹ when the building is subject to a pressure difference of 50 Pa. Building an envelope with such a high level of airtightness can be extremely challenging. However, with careful planning and conscientious implementation, the required airtightness can be achieved regardless of the construction method. Airtightness measurement plays an important role in the journey of delivering Passivhaus standard building as it allows the construction team to quality check its airtightness at the key construction stages and ensures its airtightness level meets the predefined target.

Current standard approach for measuring building airtightness is the conventional steady fan pressurisation method, which establishes a pressure difference across the envelop by drawing air out of or blowing air into the building and measures the corresponding air flow rate to establish the leakage-pressure correlation. Differing from this steady-state method by maintaining the building integrity and delivering a dynamic measurement, the novel Pulse technique releases compressed air from an air tank into the building over a short period of time and simultaneously measures the building and tank pressure responses to achieve the same purpose but at low pressures. Alongside the steady method, the Pulse technique has been used to measure the airtightness of 11 Passivhaus standard properties to understand its feasibility in measuring highly airtight buildings. The results show that measured airtightness ranged from 0.29 m³/h/m² @50Pa to 1.19m³/h/m² @50Pa. The average difference between the two methods at 4Pa is 0.0003 m³/h/m² @4Pa (11%) and 0.12 m³/h/m² @50Pa (18%) at 50Pa when using the Power Law as a means of extrapolation.

KEYWORDS

Passivhaus; Airtightness; Steady fan pressurisation; Low pressure Pulse technique

1 INTRODUCTION

The pulse technique measures the building airtightness at low pressures by releasing a known volume of air into the test building over 1.5 seconds from an air tank (Cooper et al, 2020). This in turn creates an instant pressure rise within the test building which is then followed by a steady pressure drop where the pressure variations in both the building and tank are monitored and used for establishing a correlation between leakage and pressure. The method used for the adjustment, which accounts for changes in background pressure, is achieved by deducting background pressure from the raw data.

A typical pulse test measurement is shown in Figure 1. The readings of building pressure consist of three key stages; background pressure before the pulse, pressure variation during a quasi-steady period (where the percentage of unsteady flow caused by flow inertia is negligible), followed by background pressures after the pulse. In a standard pulse setting, the solenoid valve opens after sampling the background room pressure for 2s, releasing compressed air from the air tank into the test building for 1.5 seconds, closing again at 3.5s. This Pulse setting allows a similar pulse shape to be obtained in most domestic buildings (typically with airtightness levels $>1.5 \text{ m}^3/\text{h}/\text{m}^2 @50\text{pa}$).

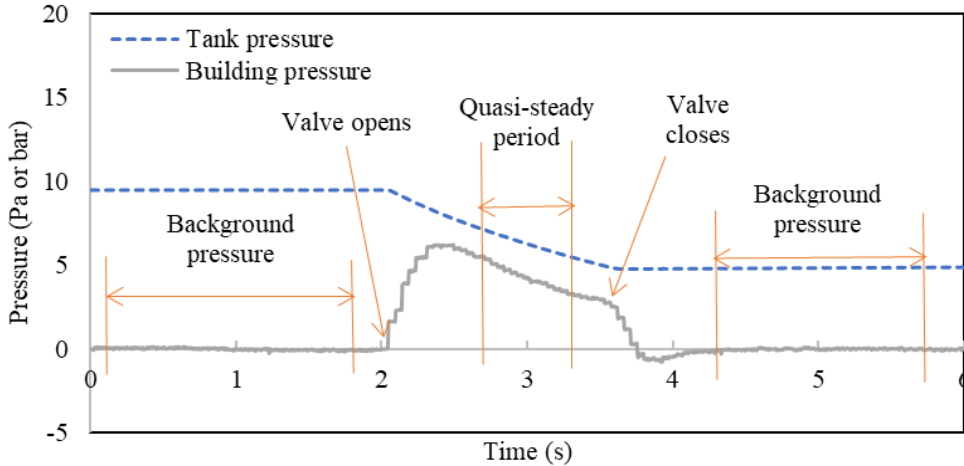


Figure 1: A typical pulse test by a pulse unit with 60 l tank (tank pressure measured in bar, building pressure in Pa) [Cooper et al, 2019]

When testing much more airtight dwellings, such as Passivhaus standard buildings, the pulse shape formed is different from that shown in Figure 1. It is seen that either the test property over-pressurises and saturates the room pressure sensor ($\pm 25\text{Pa}$ range) or there is a delay in the pulse peak leading to insufficient recording of the quasi-steady period in a standard pulse test setting. Figure 2 shows two typical examples of Pulse shapes experienced in highly airtight buildings.

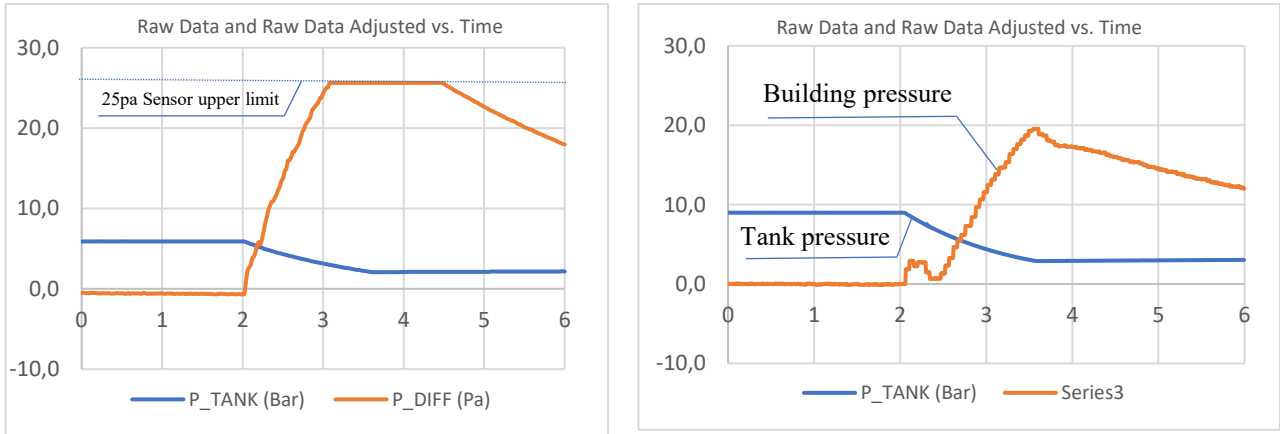


Figure 2: Example of unsuccessful pulse tests in highly airtight dwellings

The pulse shapes formed in each of the above tests are very different from that shown in Figure 1. In all such cases, we note it takes longer for the pressure pulse to reach the peak point with the rate of decay also becoming much more drawn out. This variation in shape is what has caused calculation failures for very airtight dwellings in early versions of the Pulse technology;

with timings becoming out of sync and the crucial ‘quasi-steady’ part of the measurement process not reliably captured. Acknowledging that this issue limits the operating range of the technology and would preclude the use of Pulse in Passivhaus buildings.

With a considerable body of data now at our disposal from our earlier field trials, an assessment of the impact of any proposed changes was able to be evaluated prior to undertaking any further field trial work. The two main changes made to the Pulse measurement device as a result of our investigations have been as follows:

- Air receiver volume and air outlet nozzle orifice
A major hardware change based on the field trial data has been to reduce the size of the air receiver and to constrain outlet flow by fitting it with a reduced sized outlet nozzle. This has the effect of creating a similar flow regime to the original 60 litre air receiver unit but simply reduces the overall capacity. This in turn makes the unit physically smaller and quicker to charge whilst also improving performance in the lower pressure range without considerably compromising the upper range. Conversely, where Pulse was found to be out of range in more leaky properties, two 60 litre tanks (120L) would often be excessive and thus two 40 litre tanks (80L) also provides a good balance at this upper end, with further air receivers able to be added as required with no upper limit.
- Valve opening time made adjustable
The second major change has been for the software to now enable a user adjustable valve opening duration. Much in the same way that a blower door fan operative may constrain flow by adding orifice plates to restrict the fan flow, a user of the Pulse system may now prolong the valve open period to ensure that a wider range of flowrate and Pulse shape is created. The logic here is that with the valve open for longer, the room pressure sampling duration is prolonged whilst the air flow rate of the Pulse itself also spans a wider range. Our revised user guidance is that standard Pulse valve open duration should be 1.5s for properties with a design airtightness of greater than $2 \text{ m}^3/\text{h}/\text{m}^2 @50\text{pa}$ and for a 4 second valve opening recommended when testing properties with a design air tightness of less than $2 \text{ m}^3/\text{h}/\text{m}^2 @50\text{pa}$.

With each of these changes assessed, next was to build an updated test unit and to evaluate the performance of the updated solutions across a range of airtight dwellings. For this exercise we specifically sought certified Passivhaus dwellings wherever possible.

2 METHODOLOGY

A total of 11 properties have been tested over the period October 2019 to January 2020 with a measured airtightness range of 0.48ACH @50Pa to 1.27ACH @50Pa (or 0.07ACH @4Pa to 0.38ACH @4Pa) and building volume ranging from 94m^3 to 637 m^3 . Here we specifically sought to measure as wide a range of property types as possible, ranging from new build certified Passivhaus properties through to Enerphit retrofits.



Figure 3: MVHR inlet and exhaust sealed both internally and externally

Each of the properties were prepared according to the building preparation method 2 in BS EN ISO 9972 (BS EN ISO 9972), i.e. all intentional openings were sealed, the doors and windows closed, traps filled. Mechanical ventilation with heat recovery unit is switched off and sealed with care, as shown in Figure 3.

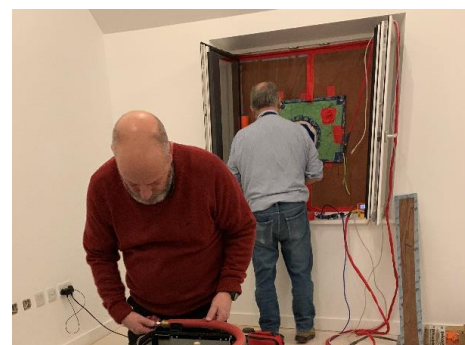
During the blower door testing, the junction where the blower door frame and door frame meet was also sealed up using airtight tapes to minimize any leakage around the blower door unit itself, as shown in Figure 4; a problem experienced in past lab-based testing of very airtight enclosures where agreement between the fan method and Pulse was being investigated (Zheng et al, 2022).



Figure 4: Blower door fan setup in a doorway and taped from inside



Complete 40L Pulse setup



Window mounted blower door

Figure 5: Blower door fan setup in window opening

Once set, a blower door fan test was first carried out by a qualified test engineer in both pressurisation and depressurisation mode. The door fan was then packed away and pulse tests using the latest hardware and software configuration were carried out immediately afterwards in each property under the same building preparation. However, some of the buildings were

tested using a window-mounted blower door unit by another onsite test engineer where the pulse test was performed with the blower door unit installed to minimise the envelope difference caused by the unit installation, as shown in Figure 5.

Table 1: Summary of tested dwellings

Property ID	Type	Envelope area (m ²)	Volume (m ³)	Setup Notes
001	Detached house	374	450	
002	Detached house	681	636.6	
003	Detached studio	138	94	
004	3-storey terraced house	344.4	360.6	Fan mounted in canvas in the doorway, frame taped
005	2-storey terraced house	244.4	186	
006	3-storey terraced house	344.4	322.5	
007	Flat	222.2	182.8	Carried out whilst door fan remained mounted in place of the window
008	Flat	213.4	125	Fan mounted in fixed panel within window opening and taped
009	Flat	123.2	138.3	
010	Flat	116.8	123.3	Carried out whilst door fan remained mounted in place of the window
011	0	344.2	322.5	Fan mounted in canvas in the doorway, frame taped

For the purposes of this report, all results are presented as volume of air leakage per hour per m² of floor area (m³/h/m²). This is in contrary to Passivhaus conventions where results are more commonly reported on the basis of volume of air leakage per hour per m³ of building volume (ACH). The differences between the test methods reported herein are however relative and apply regardless of the result being cited as Air Permeability (AP) or Air Change per Hour (ACH). The main findings from the testing may be summarised as follows:

Table 2: Pulse results at 4Pa compared to blower door fan results extrapolated down to 4Pa:

Property ID	N4 (BDT)	N4 (Pulse)	N4 Difference	N4 Percentage Difference
001	0.11	0.09	0.02	27%
002	0.14	0.13	0.01	3%
003	0.11	0.10	0.01	10%
004	0.13	0.20	-0.07	33%
005	0.05	0.06	0.01	7%
006	0.12	0.14	-0.01	10%
007	0.08	0.09	-0.01	9%
008	0.04	0.05	0.01	7%
009	0.11	0.11	0.00	2%
010	0.11	0.11	0.00	0%
011	0.36	0.31	0.05	17%

Here, the Pulse device results are presented based on an air leakage measurement directly at 4Pa with the Power Law used to extrapolate a 50Pa door fan result to estimate what its leakage measure would have been if run at the same 4Pa pressure difference. The average difference across the dataset between the blower door fan technique and Pulse is $-0.0003 \text{ m}^3/\text{h}/\text{m}^2 @4\text{Pa}$. In absolute percentage terms this equates to 11% which is broadly in line with expectation given the ISO 9972: 2015 declared measurement uncertainty of the fan method $\pm 10\%$, Pulse measurement uncertainty at $\pm 5\%$ and the further uncertainty associated with Power Law extrapolation.

Overall, the agreement between the two methods at low pressure is encouraging, especially given the challenge of sealing the fan method in an opening to a level comparable to that of the opening itself being closed (as it is for Pulse testing). This strong level of agreement is thought to be largely down to our specific attempts to take blower door fan leakage measurements across as wide a pressure range as possible to minimise extrapolation uncertainty. For instance, most of our fan results tested down to as low as 15-20pa, minimising the level of extrapolation required.

Of the notable outliers, property 004, goes to highlight that extrapolation isn't without its challenges. Here, the blower door fan pressurisation and depressurisation curves are on different paths, thus making the extrapolation down to 4Pa unreliable.

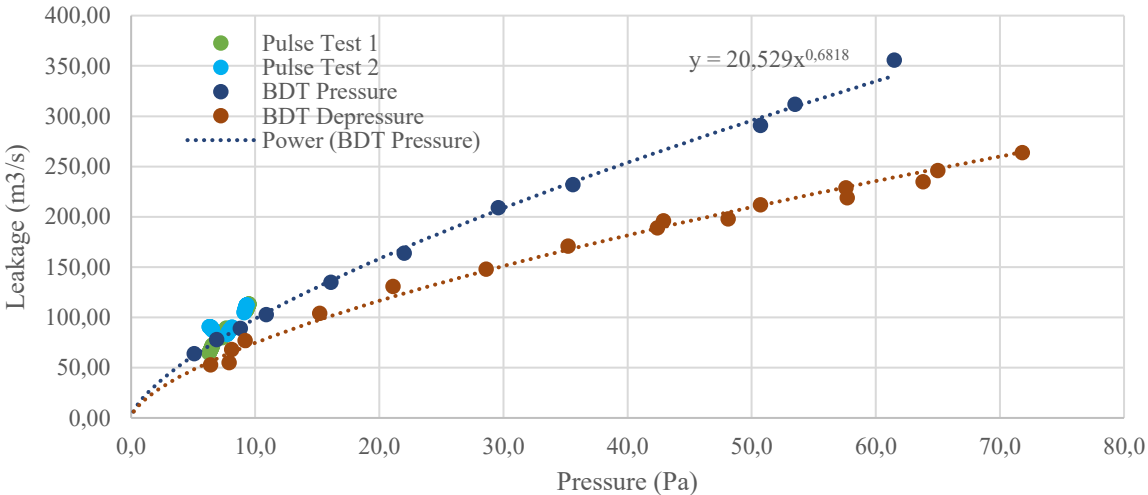


Figure 6: Property 004 blower door fan test power law extrapolation, with poor agreement between the pressurisation and depressurisation curves

Table 3: Blower door fan results at 50Pa compared with Pulse results extrapolated up to 50Pa

Property ID	N50 (BDT)	N50 (Pulse)	N50 Difference	N50 Percentage Difference
001	0.57	0.74	-0.17	22%
002	0.80	1.34	-0.55	41%
003	0.78	0.66	0.12	18%
004	0.73	0.82	-0.08	10%
005	0.45	0.50	-0.05	10%
006	0.78	0.74	0.04	6%
007	0.46	0.56	-0.10	17%
008	0.29	0.40	-0.11	28%
009	0.67	0.63	0.04	6%

010	0.65	0.80	-0.14	18%
011	1.19	1.53	-0.33	22%

In the above table, the blower door has been used to measure the air leakage directly at 50Pa and the Power Law has been used to extrapolate a 4Pa Pulse result to estimate what its leakage measure would have been if run at the same 50Pa pressure difference. The average difference across the dataset between the blower door fan technique and Pulse is $-0.12 \text{ m}^3/\text{h}/\text{m}^2 @50\text{Pa}$. In absolute percentage terms this equates to 18% which again is broadly in line with expectation given the measurement uncertainty of the fan method $\pm 10\%$, Pulse measurement uncertainty of $\pm 5\%$ and the uncertainty associated with Power Law extrapolation.

Note how the agreement between the two methods is notably worse when extrapolating in this upward direction. This is largely because there is absence of a known point at the high-pressure end for the leakage curve to follow while the origin provides a known point for the leakage-pressure curve to follow when extrapolation is done the other way around [Zheng et al, 2022]. There is also hydraulic dissimilarity between low pressure and high pressure, whereby it is widely recognised that n exponent values measured at low pressure and high pressure can be notably different, thus further compounding the uncertainties.

What is also particularly notable in the above table is the lack of a clear linear relationship between the results i.e. the fan method sometimes measuring the building to be more leaky, sometimes not. Factors beyond just extrapolation which can cause such uncertainty includes:

- Mounting of the blower door fan itself causing a door or window to potentially provide more or less leakage than the actual closed unit. In all of our test cases, the fan frame was actively sealed in place of a window or door opening in order to try to minimise this variation between its results and the Pulse test.
- Changes in weather conditions when conducting the comparative tests, particularly wind.
- Unreliable or inconsistent seating of window and door seals, especially in test scenarios where operatives were coming and going as part of the testing works. This was a particular issue with case P001 where all results are valid and repeatable but there is weak agreement between the two techniques.

Table 4: Blower door fan results at 50Pa:

Property ID	AP50 (BDT Pressurisation)	AP50 (BDT Depressurisation)	BDT Difference	BDT Percentage Difference
001	0.54	0.60	-0.06	11%
002	0.84	0.75	0.09	11%
003	0.75	0.81	-0.06	8%
004	0.86	0.61	0.24	28%
005	0.47	0.44	0.04	8%
006	0.83	0.73	0.10	12%
007	0.45	0.47	-0.02	5%
008	0.30	0.27	0.03	10%
009	0.66	0.68	-0.02	3%
010	0.67	0.64	0.04	5%
011	1.11	1.27	-0.16	14%

Although limited repeat-testing was conducted across the test properties due to time constraints, blower door fan testing was carried out in both pressurisation and depressurisation mode for all properties as required under standard Passivhaus conventions. Whilst neither the UK Building

Regulations nor the referenced approved procedure stipulate which mode is to be used for compliance reporting purposes, it is widely acknowledged that there can be variation between the two approaches for a wide range of reasons. Across these particular highly airtight 11 test cases, the average difference between the blower door fan pressurisation and depressurisation tests is $0.02 \text{ m}^3/\text{h}/\text{m}^2 @50\text{Pa}$. In absolute percentage terms this equates to 11% which is similar to the level of agreement seen between the two different test techniques and is again very close to expected levels of measurement uncertainty cited by the ISO 9972: 2015 standard. The closest match between both modes was 3% and biggest discrepancy was 28%. This isn't to discredit the fan method, rather to simply highlight that when working to measure such fine margins, even the established incumbent method has a level of associated uncertainty before further compounding with extrapolation.

3 CONCLUSIONS

Overall, the revised and updated Pulse unit has been tested across 11 very airtight dwellings, demonstrating an ability to reliably measure such properties just as effectively as the incumbent fan-based technique. There are however an inevitable number of challenges associated with working at this extreme end of the airtightness spectrum, especially when trying to compare methods whereby neither measure directly at the same pressure difference and where the fan technique must penetrate the envelope as part of the test procedure. Nevertheless, the average difference between the two methods at 4Pa is $0.0003 \text{ m}^3/\text{h}/\text{m}^2 @4\text{Pa}$ (11%) and $0.12 \text{ m}^3/\text{h}/\text{m}^2 @50\text{Pa}$ (18%) at 50Pa. Therefore, it seems reasonable to make the following conclusions:

- Pulse can measure very airtight dwellings just as reliably as the steady fan technique.
- Contrary to the previous BTS field trial-based recommendation of using a fixed conversion factor of 5.3 to convert a Pulse 4Pa result to a 50Pa air leakage value (Zheng and Cooper et al, 2019), this testing of very airtight dwellings illustrates how use of such a single number is not reliable across the full spectrum of buildings. The same applies to the divide-by-20 rule applied to all blower door fan results, as previously reported. Our recommendation having now conducted these additional tests is that the power law equation as detailed in the proposed updated TM23 document is used for all extrapolation purposes.
- Measurement of very airtight buildings is fraught with challenges, regardless of the measurement method being used. As ATTMA have already demonstrated with its TSL4 guidance document, expert preparation, specialist equipment and perfect conditions are all required in order to get a remotely reasonable assessment of air leakage from the technologies available on the market today. This, we believe, should be recognised by UK Government by continuing to support innovation in this field and by encouraging the development of further guidance and best practice.

4 ACKNOWLEDGEMENTS

The authors gratefully acknowledge funding received from: EPSRC ([EP/H023240/1](#)) Impact Acceleration Grant (United Kingdom).

5 REFERENCES

- Cooper E., Zheng X.F., Wood C.J. Numerical and experimental validations of the theoretical basis for a nozzle based pulse technique for determining building airtightness. *Build. Environ.* (2020), p. 107459
- Cooper E., Zheng X.F., Wood C.J., et al. Field trialling of a Pulse airtightness tester in a range of UK homes. *Int. J. Vent.*, 18 (1) (2019).

BS EN ISO 9972. Thermal performance of buildings-Determination of air permeability of buildings-Fan pressurisation method. BSI Standards Publication (2015)

Zheng X.F., Hsu Y.S., Pasos A.V., Smith L., Wood C.J. A progressive comparison of the novel pulse and conventional steady state methods of measuring the airtightness of buildings. *Energy and Buildings*, Vol. 261, 15 April 2022, 111983.

Zheng X.F., Cooper E., Zu Y.Q., Gillott M., Tetlow D., Riffat S., Wood C.J. Experimental Studies of a Pulse Pressurisation Technique for Measuring Building Airtightness. *Future Cities and Environment* (2019), 5(1): 10, 1–17.

Correlation analysis between ACH50 and Air permeability considering the floor area of a residential buildings

Su-Ji Choi¹, and Jae-Hun Jo^{*2}

*1 Inha University
Incheon
Republic of Korea*

*2 Inha University
Incheon
Republic of Korea
Corresponding author: jhjo@inha.ac.kr

ABSTRACT

Airtightness is presented through various expression according to the standards and measurement methods of each country. To compare the airtightness of buildings of different sizes, ACH50 and air permeability are mainly used to express the airtightness.

ACH50 and air permeability are airtightness expression methods calculated by dividing air flow into volume and surface area, respectively. As the size of a building increases, the airtightness value tends to decrease. However, the rate of change of ACH50 and air permeability according to the size of the building appears different, and it is necessary to compare the airtightness with an appropriate expression considering the characteristics of the building.

In this study, to analyze the correlation between ACH50 and air permeability according to the characteristics of the building, airtightness measurement data in multi-unit residential buildings were analyzed. The measurement target was a residential building built with the same construction method, and it was divided into three cases of small, medium, and large sizes, and 24 units were measured for each case.

As a result, the s/v ratio of the large floor area was 1, but the s/v ratio of the small floor area was 1.1. The S/V ratio tends to decrease as the floor area increases, and the area of the target building showed an s/v ratio close to 1, ranging from 1.02 to 1.11. This means that the larger the floor area, the smaller the effect of the airtightness expression. In the case of a small floor area, since the change in the value of ACH50 is relatively large, it is necessary to consider setting detailed standard for ACH50 according to the floor area. When the area is decreased to less than 100 m² or increased to more than 200 m², the change rate value is significantly different from 0.8 to 1.5, so it is necessary to evaluate the airtightness results considering the s/v ratio change rate by floor area.

KEYWORDS

ACH50, Air permeability, floor area, s/v ratio, Correlation

1 INTRODUCTION

Airtightness are presented through various expressions according to the standards and measurement methods of each country to compare the airtightness of buildings of different sizes.

Airtightness in a building is expressed as the air leakage rate for the area and volume of a building at a reference pressure difference, and is mainly expressed as ACH50, air permeability. ACH50 and air permeability are airtightness expressions calculated by dividing the air leakage rate by the volume and the envelope area, respectively. They are values calculated using dimensions such as airflow rate, volume, area, they can be converted to each other.

Due to the characteristics of the area and volume used in the two expressions, the rate of change of ACH50 and air permeability according to the size of the building appears different. In particular, the larger the size of the building, the larger the difference occurs. In small-sized buildings, ACH50 and air permeability are almost the same (AIRAH, 2017; Kyung-Hwan, J

et al., 2016), but in large-sized buildings, ACH50 expressed by volume is lower than air permeability, which seems to indicate tighter air tightness.

In this study, to analyze the correlation between ACH50 and air permeability, airtightness measurements were conducted on residential houses with the same construction technique in Korea, and correlations were derived by analyzing airtightness measurement data according to floor area.

2 AIRTIGHTNESS EXPRESSION

2.1 Airtightness expression according to the building geometry

Airtightness is expressed in various ways depending on the reference pressure difference and building geometry. To compare airtightness in buildings of different shapes and sizes, the airflow rate is divided into envelope area, volume, and floor area.

ACH50 and air permeability are commonly used airtightness expressions around the world. Air change rate (ACH50) is the air leakage rate (m^3/h) at 50Pa divided by the volume (m^3) of the building. Air permeability is the air leakage rate (m^3/h) at 50Pa divided by the envelope area (m^2) of the building. ACH50 indicates how many times the air in a room is leak out when a pressure of 50 Pa is applied to the building envelope, also expressed as n50. Air Permeability refers to the amount of leakage through the building envelope and is also represented by q_{50} (ISO9972, 2015).

2.2 Features of ACH50 and Air permeability

ACH50 and air permeability are expressed as volume and envelope area divided by the same airflow rate, respectively. Due to the characteristics of area increasing as a square and volume increasing as a cube, differences occur as the size of the building increases (Figure 1). Figure 2 shows the variation of the s/v ratio as dimension increases. For example, if the shape of a building is assumed to be a cube, a cube with a length of 1 has an s/v ratio of 6, which means that the area is much larger than the volume, but at a length of 6, the envelope area and the volume become equal, and exceeds 6, the s/v ratio becomes less than 1, which means that the volume appears larger. The envelope area and volume of a small building are approximately the same, so the s/v ratio for small building appears to be close to 1 (AIRAH, 2017; Kyung-Hwan, J et al., 2016). However, since the s/v ratio decreases as the size of the building increases, converting ACH50 and air permeability to the same ratio will cause a difference from the actual value, so it is necessary to evaluate the result by considering the correlation between the two expressions.

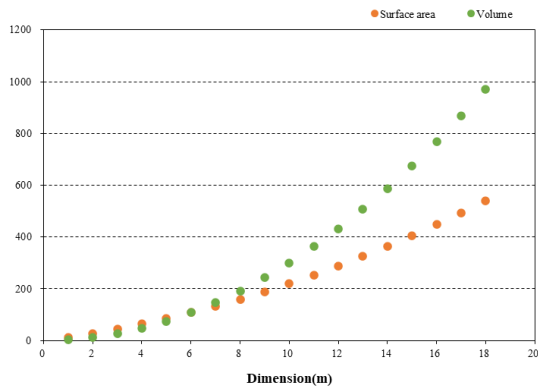


Figure 1: Area and volume change with dimensions

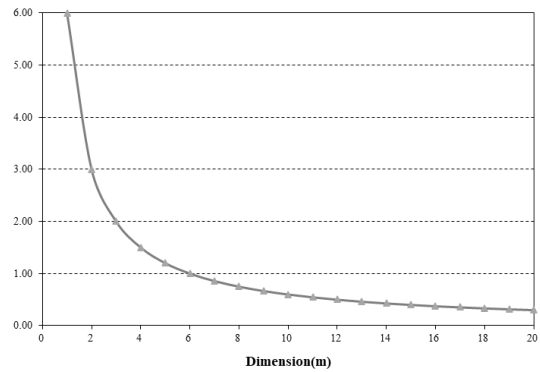


Figure 2: S/V ratio by dimension

3 FIELD MEASUREMENT OF AIRTIGHTNESS IN RESIDENTIAL BUILDINGS

3.1 Descriptions of residential buildings

The target building is a residential building in South Korea, constructed of reinforced concrete and completed in 2017. 274 units were measured and classified into small, medium, and large types according to floor area for analysis. To utilize the same number of data, we used 24 data points determined by random sampling. An overview of the target building is shown in Table 1.

Table 1: Descriptions of residential buildings

Classification	Small type	Medium type	Large type
Building site	Incheon, South Korea		
Construction	Reinforced concrete structure, Flat slab		
Building use	Multi-unit dwelling		
Number of stories	2 Basements, 42~44 stories		
Number of test unit	24	24	24
Floor area(m ²)	101.76 ~ 102.21	134.56 ~ 137.56	173.18

3.2 Airtightness results according to the floor area

Airtightness is measured according to ISO 9972, and ACH50 and air permeability are calculated from the airflow rate (Q) at 50Pa, the volume (V) of the unit, and the envelope area (S) of the unit. As shown in Figure 3, the ACH50(1/h) for the small type ranged from 1.49 to 3.32, with an average of 2.42. The ACH50 for the medium type ranged from 1.31 to 2.77, with an average of 1.79. The ACH50 of large type ranged from 0.87 to 2.37, with an average of 1.58. As shown in Figure 4, the air permeability(m³/h·m²) of the small type was measured between 1.32 and 3.07, with an average of 2.19. The air permeability of the medium type ranged from 1.24 to 2.63, with an average of 1.70. The air permeability of the large type ranged from 0.86 to 2.33, with an average of 1.56.

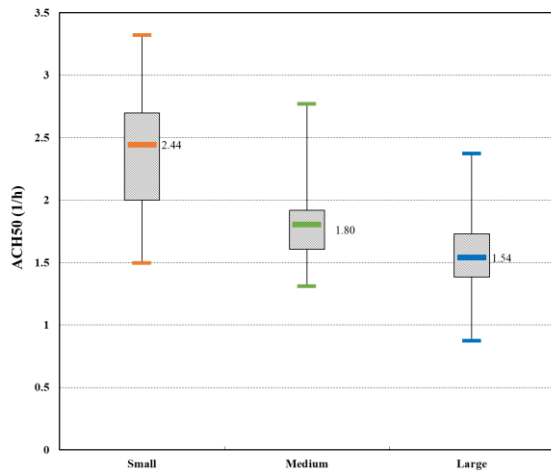


Figure 3: ACH50 by floor area

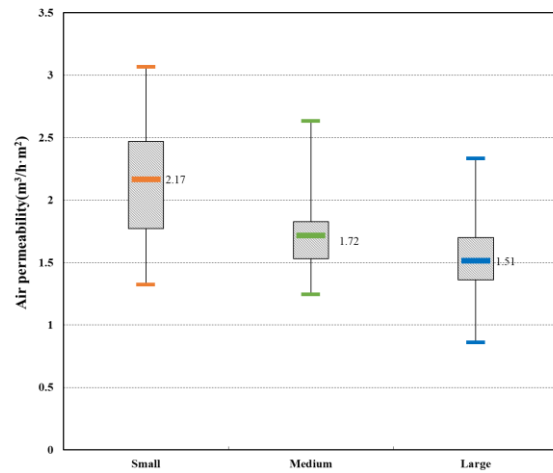


Figure 4: Air permeability by floor area

For both ACH50 and air permeability, the large type had the lowest values, with values decreasing as the floor area increased (Figure 5). When comparing the rate of change of ACH50 and air permeability according to floor area, the change of ACH50 is more rapid, and the difference is more noticeable for small. The difference between AHC50 and air permeability for each floor area was 11% for the small type, 5% for the medium type, and 2% for the large type. The small type has a higher airtightness value than the other two types, which is due to the relatively small volume and envelope area of the small type, although the Q of the small and medium types are similar.

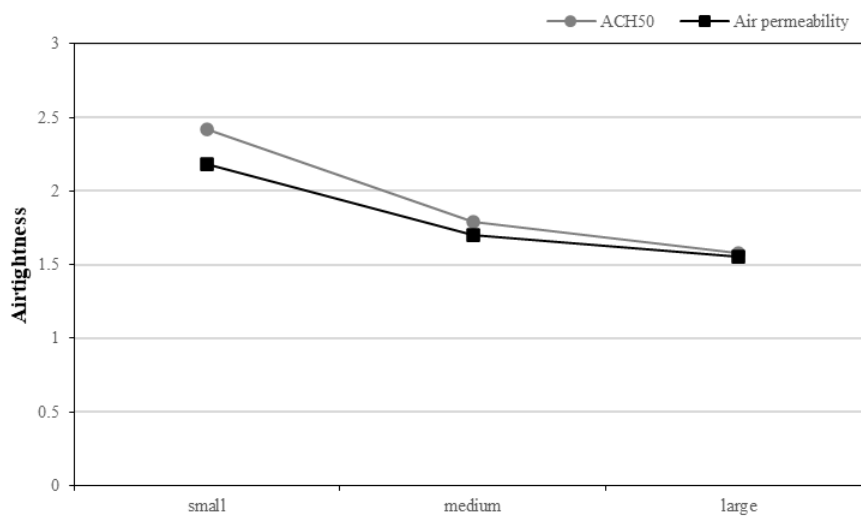


Figure 5: Change rate of ACH50 and air permeability by floor area

4 CORRELATION ANALYSIS BETWEEN ACH50 AND AIR PERMEABILITY

4.1 Correlation of ACH50 and Air permeability

To analyze the correlation between the two variables, ACH50 and air permeability, a scatter plot was used to analyze the correlation. ACH50 and air permeability are linearly related, with correlation coefficients of 0.99 for small type, 1.00 for medium type, and 1.00 for large type, indicating a strong positive correlation (Figure 6).

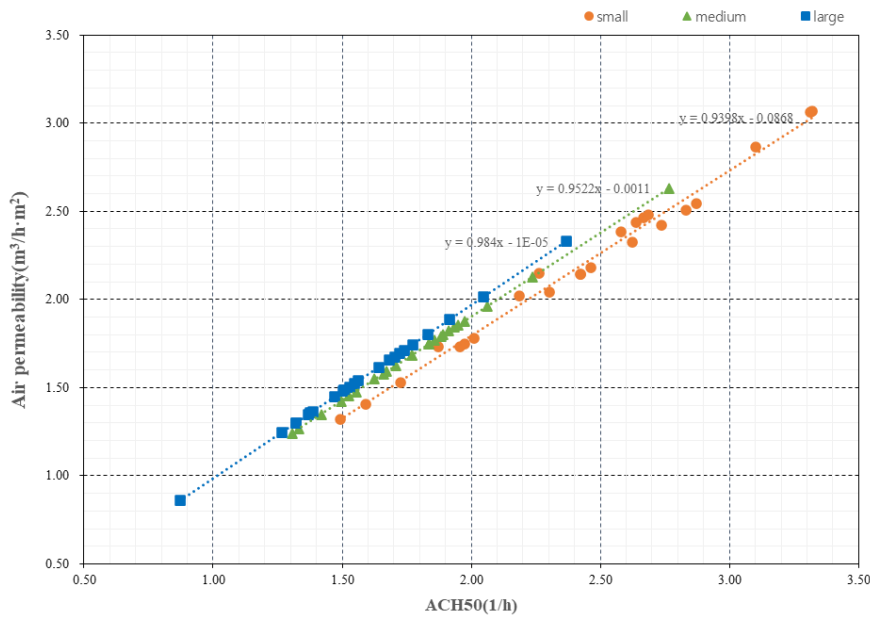


Figure 6: Correlation of ACH50 and air permeability

4.2 Analysis of ACH50 and Air permeability by floor area

ACH50 and air permeability are calculated as airflow rate divided by volume and envelope area, and the ratio of ACH50 to air permeability is equivalent to the s/v ratio, which is surface area divided by volume. As the floor area increases, the floor area ratio tends to decrease, which is shown in Figure 2 because the volume increases more rapidly than the area above a certain dimension. The average s/v ratio for small is 1.11, medium is 1.05, and large is 1.02, with ratios closer to 1 as the floor area increases (Figure 7).

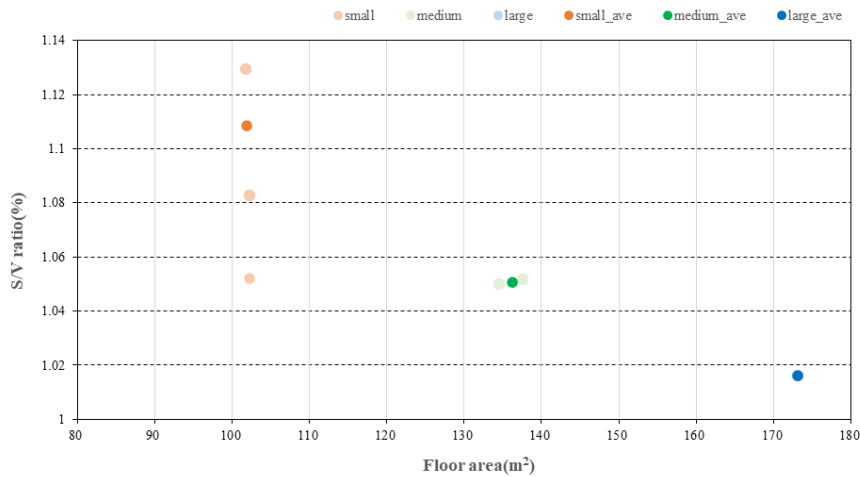


Figure 7: s/v ratio by floor area

To identify the changes in ACH50 and air permeability according to the floor area, we analyzed the s/v ratio according to the floor area (Figure 8). Assuming a hexahedron, the height was fixed at 3 meters for residential buildings, and the floor area ranged from 50m^2 to 1000m^2 . We considered three different floor types: 1:1, 1:2, and 1:5.

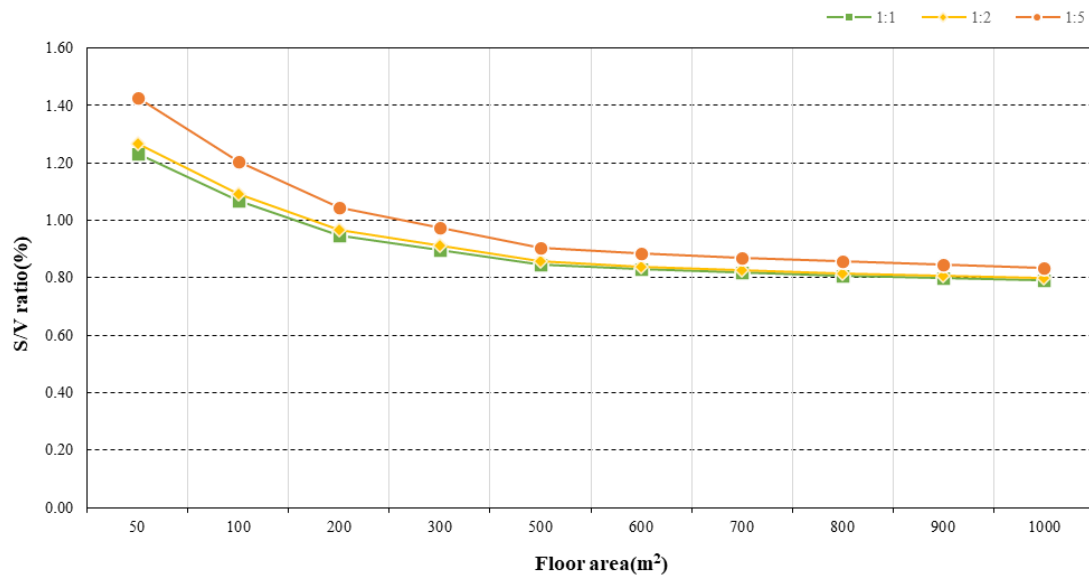


Figure 8: Change rate of s/v ratio by floor area

The s/v ratio tended to decrease as the floor area increased, with the closer to square the lower the ratio. The s/v ratio ranged from 1.23 to 1.43 for 50m² and 0.79 to 0.84 for 1000m², with a ratio of 1 between 100m² and 200m². The data applied to the residential building does not have a wide range of floor area, so the change of ACH50 and air permeability ratio, which have the same meaning as s/v ratio, shows a value like 1. When the area is decreased to less than 100 m² or increased to more than 200 m², the change rate value is significantly different from 0.8 to 1.5, so it is necessary to evaluate the airtightness results considering the s/v ratio change rate by floor area.

5 CONCLUSIONS

This study analyzed the correlation between ACH50 and air permeability, which is used to compare the airtightness of buildings of different sizes. ACH50 and air permeability were analyzed by classifying the measured data of residential buildings into small, medium, and large according to floor area. ACH50 and air permeability showed a strong positive correlation with the s/v ratio tending to decrease as the floor area increased, with the closer to the square shape showing a lower ratio.

The s/v ratio will have a value greater than 1 when the floor area is less than 100 m² and a value less than 1 when it is greater than 200 m². The area range in the target building is between 100m² and 200m², and the s/v ratio of the large type is closer to 1, but this is due to the small floor area of the target building, and it is necessary to consider the relationship between floor area and s/v ratio when converting the two expressions to evaluate the actual airtightness.

ACH50 is an expression of airtightness expressed by volume, and as the size of the building increases, it is more affected by volume, and the airtightness value changes more rapidly compared to air permeability and seems to have a better quality of airtightness. However, since airtightness is related to the flow of leakage rate through the envelope, the openings caused by each component present in the envelope must be considered. Therefore, it is more reasonable to evaluate the airtightness by air permeability, which has a smoother change in airtightness value and can consider the effect of leakage rate through the envelope. In this study, the correlation between envelope area and volume was considered to evaluate the airtightness according to the floor area, and further consideration of each component that affects the airflow rate required for airtightness evaluation is needed.

6 ACKNOWLEDGEMENTS

This work was supported by the National Research Foundation of Korea (NRF) grant funded by the Korea government (MSIT). (No. 2020R1A2C3013676)

7 REFERENCES

AIRAH. (2017). Air Tightness Metrics to Improve Australian Building Envelope Integrity.

Kyung-Hwan, J et al. (2016). Analysis of Airtightness Characteristics and Investigation of Leakage Point in High-rise Residential Buildings. *The Journal of KIAEBS* Vol. 10, No. 4, August 16, 308~313.

ISO 9972. (2015). Thermal performance of buildings - Determination of air permeability of buildings - Fan pressurization method. International Organization for Standardization.

Airtightness predictive model from measured data of residential buildings in Spain

Irene Poza-Casado^{*1}, Pilar Rodríguez-del-Tío², Miguel Fernández-Temprano², Miguel Ángel Padilla-Marcos¹, and Alberto Meiss¹

*1 GIR Arquitectura & Energía, Dpto. Construcciones Arquitectónicas, Ingeniería del Terreno y Mecánica de los Medios Continuos y Teoría de Estructuras, Universidad de Valladolid. E.T.S. de Arquitectura
Avenida Salamanca, 18
47014 Valladolid (Spain)*

*2 Dpto. Estadística e Investigación Operativa, E. de Ingenierías Industriales - Sede Doctor Mergelina
Paseo Prado de la Magdalena 3-5
47011 Valladolid (Spain)*

**Corresponding author: irene.poza@uva.es
Presenting author: Irene Poza-Casado*

ABSTRACT

The need for airtightness control is a reality given its impact on buildings' energy use and IAQ. For the past few years, this fact has resulted in energy performance regulations being established in many countries in Europe and North America. However, compliance proof is not always required, and on-site testing is often avoided. In this sense, predictive models have become useful in the decision-making process and to estimate input values in energy performance simulation tools. In Spain, maximum envelope permeability values were introduced recently, but pressurization tests rarely undergo. The most common approach to prove compliance is by means of reference values, which were proved to be inaccurate. This paper presents a predictive model for airtightness, which offers an alternative procedure for airtightness estimation. The model was developed from an airtightness database which included a representative sample of the residential building stock in Spain. A General Linear Model was considered to assess significant variables related to the climate zone, the age of the building, typology, building state, construction system, and dimensions. As a result, a predictive model that explains 42.9% of the variability of the response is presented, containing 12 main effects and 2 interactions. Overall, even if some limitations were identified, the relevance of the model proposed is warranted from the statistical point of view by the significance of the coefficients and the validity of its residual analysis.

KEYWORDS

predictive model; airtightness; blowerdoor; dwellings; database; statistical analysis

1 INTRODUCTION

The evaluation of airtightness is crucial for determining the energy performance of buildings and setting priorities for retrofitting strategies since airtightness is the main building characteristic that affects air infiltration (Dick 1950; Shaw 1907; Sherman and Chan 2004). This entails not only measuring airtightness but also detecting sources of leakage and the variables that affect overall performance.

When large datasets are available, statistical relationships among the variables can be determined and tools to analytically estimate the airtightness level from building characteristics can be developed. Predictive models are helpful to consider airtightness in energy performance (EP) simulation tools with the aim of controlling costs and time in the decision-making process before building construction or retrofitting actions.

The interest in approaches to analytically quantify airtightness has grown significantly (Bramiana, Entrop, and Halman 2016; Chan, Joh, and Sherman 2013; Khemet and Richman 2018, 2021; Krstić et al. 2014; McWilliams and Jung 2006; Pan 2010) despite the fact that airtightness estimation cannot substitute on-site testing (Relander, Holøs, and Thue 2012). The aforementioned models were created using built stocks with regionally distinct construction typologies, features, and configurations. This seems to be a shortcoming that prevents airtightness predictive models from being easily reproducible or exported to different contexts. This is also the scenario in Spain since previous predictive models (Fernández-Ag. era et al. 2016, 2019; Ibanez-Puy and Alonso 2019; Montoya et al. 2010) focused on specific regions and typologies.

1.1 Context in Spain

Spain and other Mediterranean countries with mild climates have only recently raised awareness for airtightness control. This can be explained given the traditional role of air infiltration as a source of air renewal in dwellings without controlled ventilation systems. However, the scenario has changed for the past few years, and the need for energy-efficient buildings led to mandatory controlled ventilation systems and airtightness control.

In 2019, regulations (CTE) introduced for the first time whole envelope airtightness limits depending on the volume-envelope area ratio of the dwelling (Ministerio de Fomento. Gobierno de España 2019). This requirement is only applicable for new and retrofitted dwellings for private use with a floor area greater than 120 m^2 . To prove compliance, pressurization tests can be performed, but reference values can also be used. The airtightness result obtained by either method is then introduced in the official EP calculation tool LIDER/CALENER (HULC) in order to verify the requirements established by regulations.

In reality, designers and practitioners typically prefer the analytical approach, and tests rarely undergo. Therefore, accurate estimation turns crucial. In this sense, a comparison of the results obtained from the analytical approach were compared to values obtained from pressurization tests performed in a representative sample of existing dwellings (382 observations). The model suitability was evaluated by means of a correlation analysis (Poza-Casado et al. 2022). A lack of linear association between the values of the CTE model and the test values was found concluding that the analytical approach is unsuitable to estimate the airtightness of existing dwellings.

Even though on-site testing is the only reliable method to determine airtightness, a precise estimate is key to address accurate energy performance calculation, as well as to set priorities and choose strategies for building design and renovation of existing buildings.

The authors developed a predictive model from representative experimental data to estimate the level of airtightness of the built stock in Spain (Poza-Casado et al. 2022). This approach is applicable at a national level and aims at understanding the factors that most impact airtightness in dwellings. This paper presents an adjusted model based on it, which introduces new significant variables and improves the variability of the response.

2 METHODS

2.1 Sample and airtightness testing

For the development of the model proposed, the INFILES national airtightness database (Feijó-Muñoz et al. 2019) was used. The database included existing dwellings, which were considered representative of the national residential built stock. Each case was tested and fully characterised including identification information, configuration, construction of the envelope, and building systems. The airtightness of the cases assessed was measured by

means of fan pressurisation tests, commonly known as blower-door tests, according to the International Standard ISO 9972 (ISO 2015).

2.2 Statistical model development

A General Linear Model (GLM) was considered as in Equation (1). In this way, categorical and quantitative variables with significant influence on the response variable were included. Both the main effects of the explanatory variables and first-order interactions among them were assessed.

$$Y = \beta_0 + \sum_{i=1}^p \beta_i X_i + \sum_{i < j} \tau_{ij} (X_i X_j) + \varepsilon \quad (1)$$

where: Y is the response variable to be predicted, X_i with $i=1, \dots, p$ are the explanatory variables, β_i are the main effects of the explanatory variables on the response, τ_{ij} are the first-order interactions among variables X_i and X_j , and ε are the random independent homoscedastic normal perturbations. For the qualitative explanatory variables, the usual decomposition in dummy indicator variables has been considered.

Outlier detection and elimination were performed and then a stepwise procedure was considered. This procedure starts with the model containing all variables and then an iterative procedure is performed ensuring that all variables in the final model are significant. Residual analyses were also performed at each step to check the GLM assumptions of linearity, homoscedasticity, independence and normality.

Due to the asymmetry exposed by n_{50} (Poza-Casado et al. 2022:7–8), we considered $\log(n_{50})$ as response variable Y in model (1). As for possible explanatory variables X_i to be included in the predictive model, variables related to location, age of the building, building typology, state, building systems, and dimensions were considered. First-order interactions among these variables were also considered. Table 1 contains a list of the variables initially considered, detailing which ones had a significant impact on the response variable. These significant variables are fully described below.

Table 1: Variables considered classified according to their type and their significance in the GLM model. Variables marked with * were introduced in the improved model.

Type of variable	Variables in the final model	Variables dismissed in the final model
Location	Climate zone (CTE)	City Winter severity climate Summer severity climate Simplified climate zone
Age of the building	Period of construction	Year of construction Decades of construction Applied regulations
Type of building	Typology Number of bathrooms*	Position within the building Height Number of floors Property developer Number of rooms Layout of the floorplan
Building state	Retrofitting state	Improvement of thermal bridges Identified cracks Closed balconies Integrated balconies Kitchen refurbishment Bathroom refurbishment Improvement of the envelope
Building system	False ceiling	Envelope layer composition

	Window permeability Window material Shutter position Heating system*	Outer cladding Insulation of the envelope Air chamber Windows opening system Double window Shutter type Partitioning system Cooling system Ventilation system Adventitious openings Ductwork Kitchen hood exhaust
Dimensions	Share of windows Share of opaque envelope	Floor area Volume Envelope area Compacity Ceiling height Share of wet rooms Windows joint length Window area Share of joint length

The relationship among variables and significance of the assessed variables on airtightness results were addressed through statistical analysis. The following variables were significant and, therefore, considered in the model proposed:

- Climate zone: climate was considered according to DB HE1 (Ministerio de Fomento. Gobierno de España 2019) regarding winter (zones A to E and α and summer severity (1-4). Climate severity combines degree-days and solar radiation in each location. From the international perspective, these zones would have the following equivalence in the Köppen-Geiger climate classification (Agencia Estatal de Meteorología (AEMET) 2011): A3 = Csa, B4 = BSk-Csa, C1 = Csb-Cfb, C2 = Csa, C3 = BSk, D2 = Csb, $\alpha 3$ = BSh.
- Period of construction: the age of the building is related to Energy Performance Regulations (EPR) over time. This fact was assessed by considering cases built before and after the first national regulations that established measures related to energy performance were implemented in 1980 (Ministerio de Obras Públicas y Urbanismo. Gobierno de España 1979).
- Typology: dwellings were classified as single-family or multi-family buildings given the impact that different construction systems and envelope features may entail. This variable is key in Spain, where multi-family housing prevails.
- Number of bathrooms: this variable considers the number of bathrooms of the dwelling, which are often associated with pipes and systems with an impact on the airtightness of wet rooms.
- Retrofitting estate: dwellings tested could be in their original state, or the envelope could have been retrofitted by their owners to a variable extent (windows replacement, external/internal insulation layer, etc.).
- False ceiling: the presence of this element can lead to the concealment of construction imperfections and, thus, leakages. A simplified characterisation was addressed considering dwellings with no false ceiling (FC0), dwellings with false ceiling only in corridor, kitchen and bathroom (FC1), and dwellings with false ceiling in all the rooms (FC2).
- Window permeability: the air permeability of windows was assessed according to UNE-EN 12207 (AENOR 2017) and classified as Class 0 (not tested windows), Class 1 (up to $50 \text{ m}^3/\text{h m}^2$), Class 2 (up to $27 \text{ m}^3/\text{h m}^2$), Class 3 (up to $9 \text{ m}^3/\text{h m}^2$), or Class 4 (up to $3 \text{ m}^3/\text{h m}^2$). It must be noted, though, that this information was not always available and could be just estimated from visual inspection.

- Window material: the impact of window frame material was considered (aluminium, PVC, wood, steel). The most representative material was considered when more than one type of window was found.
- Shutter position: shutters are widely used in Spain, and they have an important impact on the envelope airtightness since they constitute a discontinuity of the envelope. Rolling shutters were classified regarding their position: non-integrated shutters, external shutters, internal shutters, and no shutters, according to Figure 1. The most common solution is external shutters integrated into the inner layer of the envelope, whereas non-integrated shutters make reference to cases that originally had no shutter, and it is added constituting no additional leakages.

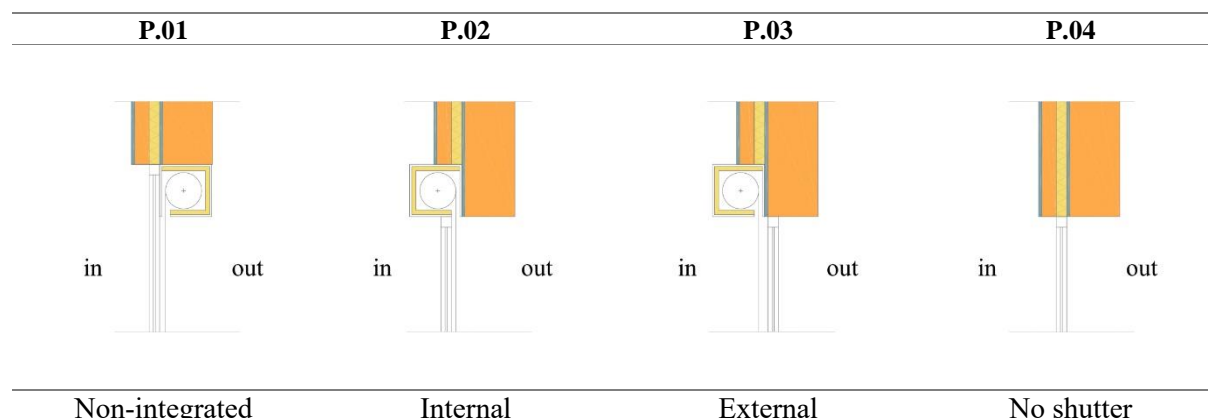


Figure 1: Shutter position classification.

- Heating system: this variable refers to the way in which the dwelling is heated, considering no heating system, heating units (e.g. radiators), underfloor heating, ducts, or other systems.
- Share of windows: it is the sum of the area of doors and windows related to the total envelope area. This parameter is closely related to A_h in the model proposed by Spanish regulations. This is a quantitative variable [m^2].
- Share of opaque envelope: it is the sum of areas of the opaque thermal building envelope with heat exchange with the outdoor air related to the total envelope area of the dwelling. This parameter is closely related to A_0 in the model proposed by Spanish regulations. This is a quantitative variable [m^2].

3 PREDICTIVE MODEL RESULTS

All analyses in this section: descriptive study, model estimation, variable selection and model validation, were performed with IBM SPSS software (IBM Corporation 2019).

3.1 Descriptive study

The outlier detection procedure mentioned in the previous section resulted in the elimination of 8 observations that had anomalous $\log(n_{50})$ values possibly due to measurement errors. Therefore, in the final model 392 observations are considered. Table 2 contains a descriptive study of the explanatory variables in the final model while

Table 3 gives a more detailed descriptive study of the initial response variable n_{50} and the final transformed response variable $\log(n_{50})$ and Figure 2 shows histograms of these two variables.

Table 2: Descriptive study for the explanatory variables in the final model. Variables marked with * were introduced in the improved model.

Variable	Value	N	%
Retrofitting state	Original	271	69.13%
	Retrofitted	121	30.87%
Climate zone	A3	33	8.42%

	B4	85	21.68%
	C1	47	11.99%
	C2	85	21.68%
	C3	112	28.57%
	D2	16	4.08%
	$\alpha 3$	14	3.57%
Period of construction	Before 1980	219	55.87%
	Since 1980	173	44.13%
Window permeability	Class 0 or 1	46	11.73%
	Class 2	196	50.00%
	Class 3	117	29.85%
	Class 4	33	8.42%
Window material	Steel	5	1.28%
	Aluminium	263	67.09%
	Wood	54	13.78%
	PVC	70	17.86%
Shutter position	P.01	19	4.85%
	P.02	290	73.98%
	P.03	21	5.36%
	P.04	62	15.82%
False ceiling	FC0	85	21.68%
	FC1	245	62.50%
	FC2	62	15.82%
Typology	Multifamily	317	80.87%
	Single-family	75	19.13%
Number of bathrooms*	0	3	0.76%
	1	159	40.56%
	2	166	42.35%
	3	43	10.97%
	4 or 5	21	5.36%
Heating system*	No heating	55	14.03%
	Underfloor heating	8	2.04%
	Ducts	36	9.18%
	Other systems	8	2.04%
	Heating units	285	72.70%
Share of windows	Mean	5.18	
	Std. Dev.	2.04	
Share of opaque envelope	Mean	25.07	
	Std. Dev.	17.52	

Table 3: Descriptive study for the variable n_{50} and the final transformed response variable $\log(n_{50})$.

	N	Minimum	Maximum	Mean	Standard deviation	Lower quartile	Median	Upper quartile
n_{50}	392	1.1930	39.4217	7.2238	4.2981	4.3371	6.2763	9.1672
$\log(n_{50})$	392	0.18	3.67	1.8291	0.5463	1.4672	1.8368	2.2156

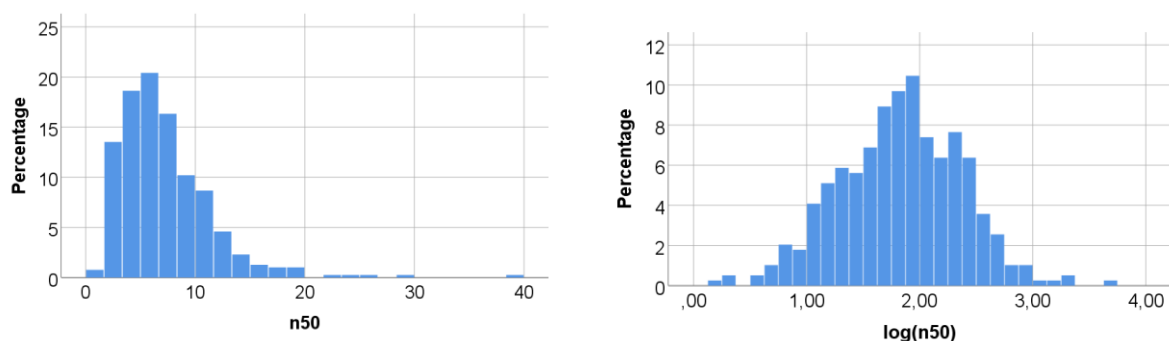


Figure 2: Histograms for the variable n_{50} and the final transformed response variable $\log(n_{50})$.

3.2 Predictive model

The improved predictive model contains 12 main effects and 2 interactions. The ANOVA table corresponding to this model is shown in Table 4. This table shows the variability of the response variable explained by each of the explanatory variables and interactions included in the model and whether this explained variability is statistically significant or not.

As a final caution, notice that we are not claiming that the variables that have been dropped in the selection procedure do not have any influence on airtightness. Their effect, as usual in multivariate statistical studies, may already be collected in the model by the variables that are already present in it.

Table 4: ANOVA table showing the variability of the response explained by each of the variables and interaction and its statistical significance. Variables marked with * were introduced in the improved model.

Source	Type III Sum of Squares	Degrees of freedom	Mean Square	F-value	p-value
Corrected model	49.997a	32	1.562	8.412	0.000
Intercept	18.359	1	18.359	98.845	0.000
Retrofitting state	1.120	1	1.120	6.030	0.015
Climate zone	9.226	6	1.538	8.279	0.000
Period of construction	2.612	1	2.612	14.063	0.000
Window permeability	4.688	3	1.563	8.412	0.000
Window material	1.985	3	0.662	3.563	0.014
Shutter position	1.841	3	0.614	3.304	0.020
False ceiling	3.172	2	1.586	8.540	0.000
Typology	1.227	1	1.227	6.606	0.011
Heating system*	1.832	4	0.458	2.465	0.045
Number of bathrooms*	2.844	4	0.711	3.828	0.005
Share of windows	2.904	1	2.904	15.634	0.000
Share of opaque envelope	0.553	1	0.553	2.976	0.085
Period of construction *	2.541	1	2.541	13.678	0.000
Share of opaque envelope					
Typology * Share of opaque envelope	1.112	1	1.112	5.985	0.015
Error	66.681	359	0.186		
Corrected Total	116.677	391			

a. $R^2 = .429$ (Adjusted $R^2 = .378$)

Table 5 contains the β_i and τ_{ij} coefficients of the equation of the final GLM model appearing in Equation (1) that can be used for predicting airtightness, together with the significance level of each coefficient. As usual in many studies, the convention used here is that p-values

between 0.10 and 0.05 showed weak significance, p-values between 0.05 and 0.01 showed strong significance, and p-values less than 0.01 show very strong evidence of significance.

Table 5: Equation of the final GLM predictive model for airtightness.

Parameter	Coefficient	Parameter	Coefficient
Intercept	0.273	Shutter position. P04	0a
Retrofitting state. Original	0.137**	False ceiling. FC0	-0.313***
Retrofitting state. Retrofitted	0a	False ceiling. FC1	-0.264***
Climate zone. A3	0.346**	False ceiling. FC2	0a
Climate zone. B4	0.545***	Typology. Multifamily	0.412**
Climate zone. C1	0.273	Typology. Single-family	0a
Climate zone. C2	0.630***	Heating system. No heating	0.074
Climate zone. C3	0.053	Heating system. Underfloor heating	-0.041
Climate zone. D2	0.575***	Heating system. Ducts	0.261***
Climate zone. $\alpha 3$	0a	Heating system. Other systems	0.173
Period of construction. Before 1980	-0.329***	Heating system. Heating units	0a
Period of construction. Since 1980	0a	Number of bathrooms. 0	0.610**
Window permeability. Class 0 or 1	0.596***	Number of bathrooms. 1	0.347***
Window permeability. Class 2	0.322***	Number of bathrooms. 2	0.183
Window permeability. Class 3	0.255***	Number of bathrooms. 3	0.090
Window permeability. Class 4	0a	Number of bathrooms. 4 or 5	0a
Window material. Steel	0.071	Share of windows	0.045***
Window material. Aluminium	0.074	Share of opaque envelope	0.003
Window material. Wood	0.298***	Period of construction. Before 1980 * Share of opaque envelope	0.010***
Window material. PVC	0a	Period of construction. After 1980 * Share of opaque envelope	0a
Shutter position. P01	0.195*	Typology. Multifamily * Share of opaque envelope	-0.009**
Shutter position. P02	0.144**	Typology. Single-family * Share of opaque envelope	0a
Shutter position. P03	-0.123		

a. This parameter is set to 0 as it corresponds to the reference class of the variable.

* stands for p-value ≤ 0.1 , ** for p-value ≤ 0.05 and *** for p-value ≤ 0.01

Figure 3 contains the residual analysis for this final GLM model. The graph shows that the main hypotheses of the model (linearity and homoscedasticity) can be assumed since no curvature or other shape is observed in the graph. Moreover, a single observation studentized residual appears outside the $[-3,3]$ interval, which is completely compatible with the absence of significant outliers in the model.

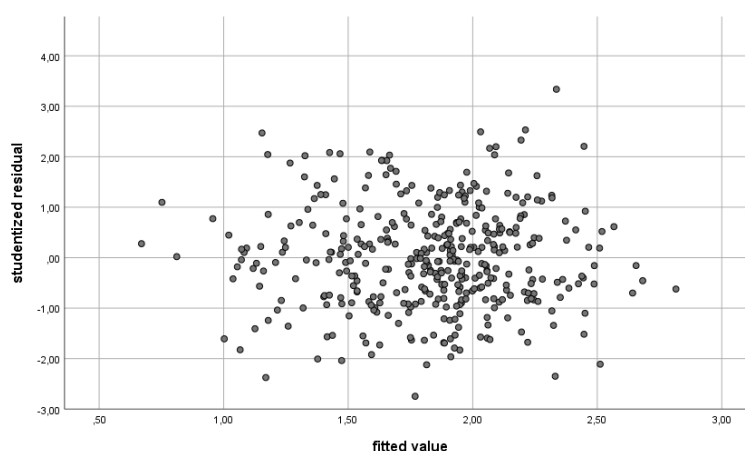


Figure 3: Residual analysis for the final GLM model proposed.

4 CONCLUSIONS

A GLM to predict the envelope airtightness was presented based on real test results obtained from a representative sample of existing dwellings in Spain. The methodology used to develop the model, although based on widespread strategies, offers added value regarding the origin of representative data, full characterization of the cases, standardised procedures, and the assessment of both quantitative and qualitative interactions.

The model allows the identification and analysis of factors with a significant impact on the level of airtightness. The variables that were found significant are in line with previously developed models: climate conditions, the age of the building, dimension-related characteristics, building systems, type of building, and conservation state. It considers, in addition, variables that refer to the singularities of the Spanish national built stock such as the effect of the position of rolling shutters, or the role of the share of the envelope to outdoors in the case of multi-family buildings. The improved model added the number of bathrooms and the heating system to obtain a better fit.

The R^2 value of this model is 0.429 so the model can explain 42.9% of the variability of the response, which slightly improves the R^2 value of the original model, which was 0.385. It should be noticed that, although this value may seem not too high, the relevance of the model is warranted by the significance of the coefficients and by the validity of its residual analysis.

In spite of identified limitations, the model is robust, and it provides valuable knowledge regarding the airtightness of dwellings and the factors that impact the most its performance. Therefore, it is intended as a useful tool although it cannot be seen in any way as a substitute of on-site testing.

5 ACKNOWLEDGEMENTS

The airtightness data assessed in this work was part of INFILES Project “Energy impact of the airtightness level in residential buildings in Spain: Analysis and characterization of the infiltrations” funded by the Economy and Competitiveness Ministry of the Spanish Government (reference BIA2015-64321-R). Attendance to the conference was possible thanks to the grant “Movilidad investigadores e investigadoras UVA-Banco Santander 2023”.

6 REFERENCES

- AENOR. 2017. “UNE-EN 12207:2017. Ventanas y Puertas. Permeabilidad Al Aire. Clasificación.”
- Agencia Estatal de Meteorología (AEMET). 2011. *Atlas Climático Ibérico (Iberian Climate Atlas)*. Ministerio de Medio Ambiente y Medio Rural y Marino de España.
- Bramiana, C. N., A. G. Entrop, and J. I. M. Halman. 2016. “Relationships between Building Characteristics and Airtightness of Dutch Dwellings.” *Energy Procedia* 96(October):580–91. doi: 10.1016/j.egypro.2016.09.103.
- Chan, Wanyu R., Jeffrey Joh, and M. H. Sherman. 2013. “Analysis of Air Leakage Measurements of US Houses.” *Energy and Buildings* 66:616–25. doi: 10.1016/j.enbuild.2013.07.047.
- Dick, J. B. 1950. “The Fundamentals of Natural Ventilation.” *J. Inst. Heat. Vent. Eng.* 18(179):123–24.
- Feijó-Muñoz, Jesús, Alberto Meiss, Irene Poza-Casado, Miguel Ángel Padilla-Marcos, Mario Rabanillo-Herrero, Andrés Royuela-del-Val, María Jesús Dios-Viéitez, Víctor Echarri-Iribarren, Cristina Pardal, Víctor José Del Campo-Díaz, Roberto Alonso González-Lezcano, Rafael Assiego de Larriva, Manuel Montesdeoca Calderín, and Jérica Fernández Agüera. 2019. *Permeabilidad Al Aire de Los Edificios Residenciales En España. Estudio y Caracterización de Sus Infiltraciones*. edited by A. Meiss and M. Á. Padilla-Marcos. Ediciones Asimétricas.

- Fernández-Agüera, J., Samuel Domínguez-Amarillo, Juan José Sendra, and Rafael Suarez. 2019. "Predictive Models for Airtightness in Social Housing in a Mediterranean Region." *Sustainable Cities and Society* 51:101695. doi: 10.1016/j.scs.2019.101695.
- Fernández-Agüera, J., Samuel Domínguez-Amarillo, Juan José Sendra, and Rafael Suárez. 2016. "An Approach to Modelling Envelope Airtightness in Multi-Family Social Housing in Mediterranean Europe Based on the Situation in Spain." *Energy and Buildings* 128:236–53. doi: 10.1016/j.enbuild.2016.06.074.
- Ibanez-Puy, Maria, and Jesus Alonso. 2019. "Airtightness in Spanish Residential Buildings. Case Study." Pp. 1–6 in *2019 IEEE International Conference on Engineering, Technology and Innovation (ICE/ITMC)*. Valbonne Sophia-Antipolis, France, France: IEEE.
- IBM Corporation. 2019. "IBM® SPSS® Statistics."
- ISO. 2015. "ISO 9972. Thermal Performance of Buildings. Determination of Air Permeability of Buildings. Fan Pressurization Method (ISO 9972:2015)."
- Khmet, Bomani, and Russell Richman. 2018. "A Univariate and Multiple Linear Regression Analysis on a National Fan (de)Pressurization Testing Database to Predict Airtightness in Houses." *Building and Environment* 146(September):88–97. doi: 10.1016/j.buildenv.2018.09.030.
- Khmet, Bomani, and Russell Richman. 2021. "An Empirical Approach to Improving Preconstruction Airtightness Estimates in Light Framed, Detached Homes in Canada." *Journal of Building Engineering* 33(June 2019):101433. doi: 10.1016/j.job.2020.101433.
- Krstić, Hrvoje, Željko Koški, Irena Ištoka Otković, and Martina Španić. 2014. "Application of Neural Networks in Predicting Airtightness of Residential Units." *Energy and Buildings* 84:160–68. doi: 10.1016/j.enbuild.2014.08.007.
- McWilliams, Jennifer, and Melanie Jung. 2006. *Development of a Mathematical Air-Leakage Model from Measured Data*.
- Ministerio de Fomento. Gobierno de España. 2019. *Código Técnico de La Edificación (CTE). Documento Básico HE 1: Limitación de La Demanda Energética*.
- Ministerio de Obras Públicas y Urbanismo. Gobierno de España. 1979. *Norma Básica de Edificación NBE-CT-79. Condiciones Térmicas En Los Edificios*. Spain.
- Montoya, María I., Elsa Pastor, François Rémi Carrié, Gaëlle Guyot, and Eulàlia Planas. 2010. "Air Leakage in Catalan Dwellings: Developing an Airtightness Model and Leakage Airflow Predictions." *Building and Environment* 45(6):1458–69. doi: 10.1016/j.buildenv.2009.12.009.
- Pan, Wei. 2010. "Relationships between Air-Tightness and Its Influencing Factors of Post-2006 New-Build Dwellings in the UK." *Building and Environment* 45(11):2387–99. doi: 10.1016/j.buildenv.2010.04.011.
- Poza-Casado, Irene, Pilar Rodríguez-del-Tío, Miguel Fernández-Temprano, Miguel-Ángel Padilla-Marcos, and Alberto Meiss. 2022. "An Envelope Airtightness Predictive Model for Residential Buildings in Spain." *Building and Environment* 223(July):109435. doi: 10.1016/j.buildenv.2022.109435.
- Relander, Thor-Oskar, Sverre B. Holøs, and Jan Vincent Thue. 2012. "Airtightness Estimation—A State of the Art Review and an En Route Upper Limit Evaluation Principle to Increase the Chances That Wood-Frame Houses with a Vapour- and Wind-Barrier Comply with the Airtightness Requirements." *Energy and Buildings* 54:444–52. doi: 10.1016/j.enbuild.2012.07.012.
- Shaw, W. N. 1907. *Air Currents and the Laws of Ventilation*. Cambridge University Press.
- Sherman, M. H., and Rengie Chan. 2004. *Building Airtightness: Research and Practice*. LBNL-53356.

Bridging The Mechanical / Enclosure Gap

David de Sola¹, Nathaniel Fanning²

*1 3iVE LLC
336 Windsor Street
Cambridge MA 02141 USA
Email: david.desola@3ive.com*

*2 Fitzmeyer & Tocci Associates, Inc.
300 Unicorn Park Drive, 5th Floor
Woburn, MA 01801 USA
Email: nfanning@f-t.com*

ABSTRACT

In the United States, the realm of building enclosure design and commissioning is separate and distinct from the realm of mechanical design and commissioning. This paper will illustrate how and why these disciplines have been historically separated and outline the consequences of this division and describe the opportunity that a closer relationship between the two represents in terms of costs and environmental impact.

Building Enclosure Commissioning (BECx) is a mature process designed to ensure a building's exterior and its environmental separating materials and assemblies meet an Owner's Project Requirements (OPR) in terms of durability and air tightness. The results of BECx efforts are both predictable and measurable. How can the BECx process better dovetail with the work of mechanical design and commissioning to inform mechanical design in terms of system type and size?

Today, mechanical systems continue to be designed and evaluated largely independent from a building's predicted or actual air leakage parameters. Given the significant carbon impact associated with the construction of new buildings, durability is a paramount value in the fight against climate change. Similarly, mechanical systems, in addition to providing the environmental conditions necessary for human comfort and health, also present an enormous energy draw and carbon contribution at the global level. While the importance of building air tightness and mechanical efficiency are symbiotically interlinked in terms of their function and importance, there is a fundamental practical and cultural divide in the practice of designing, constructing, and evaluating these systems. This divide represents a void of understanding as well as an enormous opportunity for cooperation among the design and commissioning professionals responsible for a building's enclosure and its mechanical systems.

State-of-the-art BECx processes include testing and metrics such as whole building air tightness protocols that reveal the actual air leakage of a constructed building. These tests can be conducted to include and exclude mechanical systems, thereby providing a wealth of information for the benefit of both designers and owners.

This paper first summarizes the existing BECx process by which building air tightness and durability can be predictably achieved and measured. It goes on to discuss ways the result of these efforts can be incorporated into mechanical design and commissioning efforts. Case studies from the authors' work together on a set of elementary schools in Massachusetts substantiate the assertion that a tight range of predicted results can be reliable in terms of design projections.

The paper will conclude with recommendations for a model with which the correlation of projected enclosure leakage rates can inform both the initial equipment as well projected energy cost of mechanical systems. When available and considered, this information can inform decision making models to dramatic effect: Because first and operational costs of mechanical equipment are variables that are dependent on equipment size, type, and efficiency, owner's equipped with accurate predicted mechanical performance are empowered to understand the impacts of their decisions in terms of payback duration, cash flow modelling, carbon impacts, and lifecycle costs.

KEYWORDS

Air Tightness, Enclosure Commissioning, Blower Door Testing, Infiltration Calculations, Equipment Sizing

1 INTRODUCTION

Understanding and addressing the mechanisms by which air is exchanged through a building enclosure is complex, challenging, and decidedly worthwhile effort (de Sola, Symonds 2019). Building Enclosure Commissioning (BECx) is a process designed to ensure a building's exterior enclosure and its environmental separating materials and assemblies meet an Owner's Project Requirements (OPR) in terms of durability and air tightness. The enclosure commissioning process relies upon a set of belt-and-suspenders tools and processes resulting in qualitative and quantitative assurances of a building's quality of construction in addition to its measured air tightness. In the US, for reasons we will touch upon in this paper, the relationship of the output measurements and feedback of the enclosure commissioning process have stood largely independent from the methods and analyses employed by mechanical engineers to specify and size the mechanical systems that will serve a given building and its users. In other words, there is a significant pool of reliable data readily available to impact mechanical design and the predicted function of mechanical equipment that is significantly underutilized.

A frequently cited statistic among building scientists asserts that the heating and cooling of buildings accounts for as much as 40 percent of the total energy consumed in the US. This is an enormous factor in terms of the total environmental impact of energy production as well as the cost of energy born by buildings. It stands to reason that even small improvements to such a major source of consumption can have a significant global impact. One of the places to look is in the category of air leakage and its direct impact on energy usage. How much energy is literally flying out our collective windows, doors, and holes in the wall? A salient statement on Oak Ridge Laboratory's Energy Savings and Moisture Transfer Calculator website (Oak Ridge, 2023) offers clear perspective: "In aggregate, infiltration accounted for greater energy losses than any other component of the building envelope, including fenestration and is responsible for over 4 % of all the energy used in the United States."

Our paper theorizes that incorporation of enclosure commissioning-based building performance data into mechanical design informs the selection and can result in reduced size of specified mechanical equipment. The resulting changes to smaller, more efficient equipment will, in turn, meaningfully reduce the global demand on energy and should therefore become a standard industry practice.

A problem arises with such a proposition: designing a system to measured values requires that measured values are available. Mechanical systems are specified in the design phase well in advance of a building's construction and completion where tools are available to measure it. Any proposed process would therefore necessarily rely upon predicted vs measured values. The question becomes, can the BECx process itself provide reasonable assurance to mechanical designers and building owners that high-performance values can safely be used for the purposes of selecting and sizing mechanical systems? For the effort to have meaning, the mechanical systems in question would need to become meaningfully smaller and more efficient. However,

smaller systems come with several corresponding risks: if the assumptions regarding a building's leakage and thermal resistance are not achieved in the field, undersized systems would:

- operate outside of efficient parameters
- operate at unsustainable internal loads and wear out quickly
- fail to reach design temperatures, resulting in occupant discomfort

In fact, several of these eventualities could become true over time. For high-performance predictions to be credible and reliable, a robust set of data would first need exist in the form of a statistically significant set of measured results from comparable projects in similar environments utilizing a BECx or similar protocol.

Additionally, to be considered sufficiently reliable for mechanical engineers to place stock in predicted high performance levels, there is another critical factor to consider: durability. It is one thing for a building to demonstrate a high level of performance near its date of completion; it is another thing all together that this performance will endure over time. Therefore, in addition to the introduction of commissioning data assessing performance to the realm of mechanical design, so must predictions of durability.

To address the attendant issues surrounding a need to improve the relationship between enclosure and mechanical systems, we will first look at the BECx process to unravel the focal points of the effort including air barriers and durability, and review the tool set used to achieve qualitative and quantitative assessments of building enclosures. We will then provide an overview of the current thinking used by mechanical designers and commissioning agents as it pertains to high performance buildings. Following this, we will describe three constructed projects featuring the BECx process and discuss their results to demonstrate how a growing body of similar results could be relied upon to inform mechanical design. Finally, we will broach the divide that separates enclosure design and commissioning from HVAC design and commissioning.

2 BECX: FOCUS AND PROCESS

2.1 An Overview of Air Barriers

Long and cold winters combined with severe building envelope failures stemming from early efforts to mitigate energy loss motivated Canada to invest in the research of building envelope assemblies as well as developing testing and verification processes to vet them. Canada's experiential and researched findings have flowed into the U.S. over the last three decades and now recognition of the importance of an air-tight exterior assembly for reducing a building's heating and cooling loads, as well as increasing indoor air quality, is becoming mainstream in the U.S.

Conceptually, an air barrier is like the placement of a balloon around all sides of a building, including the foundation; it is designed to fully encapsulate a building to eliminate the migration of air across its envelope. When functioning as designed this layer—often taking the form of a membrane only 20 - 60 mils thick—can affect dramatic reductions in the energy required for space heating and cooling. The function of an air barrier can be performed by numerous materials and assemblies including glass, metal, sealants, foams, as well as a variety of plastic and rubberized

sheets applied in sheets or by spray. Designing and specifying these materials and assemblies is only the beginning; numerous decisions and actions must be performed correctly in order for an air barrier system to function as intended:

- The air barrier materials—including its primers, sealants, and transition materials—must be compatible with those of its substrate, penetrating fasteners, and adjacent assemblies.
- When the air barrier is an applied sheet or membrane, it must be installed over clean and dry substrate under conforming weather conditions—usually dry conditions, not too hot, and not too cold.
- Air barriers must not be overexposed to dust, UV light, accidental mishandling, or field conditions that would otherwise degrade a full life expectancy.
- Air barriers must be correctly installed—not just over opaque wall conditions, but also where they connect to windows, skylights, storefronts, curtainwalls, louvers, vents, HVAC equipment, electrical and plumbing penetrations, the mechanical fasteners of the roof, brick ties, z-girt systems, and lintels, among other conditions.
- Air barriers must span and appropriately flex over movement joints between floors, differentially supported areas of the structure, and expansion joints, they must connect continually and without defect across major adjacent assemblies (e.g., roof-to-wall, wall-to-foundation, foundation-to-floor slab, etc.)

Studies have shown substantial energy savings resulting from tightening a building's exterior enclosure. Uncontrolled air flow into or out of a building can create performance problems including energy consumption, uncontrolled moisture concentration, and poor indoor air quality. Similarly, the addition of insulation in a balanced wall assembly can significantly increase occupant's thermal comfort as well as greatly reduce the costs associated with building heating and cooling expenses. Savings ranging from 20% to 40% are commonly associated with comparatively tight and well-insulated buildings against their leaky and uninsulated counterparts. With a high-performance exterior, HVAC units can be sized smaller as there is less risk of under sizing them. HVAC units are also capable of more precise control of the internal environment as there is less uncontrolled air flow in and out of the building. This, in turn, leads to higher rates of occupant comfort.

2.2 How Tight Is Tight Enough? The Development of Leakage Rate Standards

As we become increasingly aware of the need for functional air barriers in our buildings as well as the problems deficient installations may pose, efforts to codify and measure standards for air barrier systems have followed. Among the most influential voices to raise awareness of the value and establish standards for air tightness requirements is the U.S. Army Corps of Engineers (USACE). In May of 2012, in collaboration with the Air Barrier Association of America (ABAA), USACE issued a new Engineering and Construction Bulletin outlining requirements for building airtightness as well as building air leakage testing for both new and renovated building projects. The group also instituted a standard for air leakage for whole buildings: 0.25 cubic feet per minute (CFM) with a pressure differential of 75 pascal (1.57 PSF). (Zhivov, A., Bailey, et. al. 2012) The table below shows the minimum standards adopted by some of these.

Table 1: Standards and Requirements for Air Leakage

Standard	Requirement CFM@75 Pascal/ ft2
2009 IECC International Energy Conservation Code	.55
2012 IECC	.25
R-2000*	.13
LEED IV Multi-Family **	.09
Passivhaus	.05

*Standard for Energy Efficiency in New Construction developed by Natural Resources Canada

**50 Pascal, 2 Point Option, IECC Climate Zone 5-7

Table References: Genge, C. 2014; USGBC, 2018; USGBC LEED BD+C Homes Air Infiltration 2018

While the standards for permissible leakage vary widely, they are increasingly becoming more stringent. This is reflective of both the increasing understanding of the importance of airtightness as well as the growing body of evidence of test results demonstrating that extremely tight construction is both feasible and practical, even for large buildings.

2.3 Enclosure Durability

The required service life of a building is among the most important factors for an owner to address. An example of a framework is provided in Table 2.

Table 2: Durability Standards by Building Type

Classification	Service Life Requirement	Examples
Temporary	5 years	Annex Facility, Swing Space
Short	25 years	Big Box Stores, Strip Malls
Medium	50 Years	Airports, Hospitals, Data Centers
Long	75- 100 Years	Schools, College, Residence
Permanent	No End of Use Monument	Museums, Court Houses, Government University

Durability should be considered at micro-and macro-level assessment of the mechanisms of deterioration in the context of their placement is necessary. Detailed and specified materials and assemblies must be evaluated against environmental conditions; for example: heat, cold, moisture, UV exposure, storms, flooding, and salinity. Similarly, animals and insects can cause harm.

Easily accessible, low cost, and maintainable materials and assemblies may be appropriate for some low priority regions. Where difficult or impossible to access materials and assemblies are placed in a high priority region, the durability factor approaches the service life of the OPR. For example, mid-wall performance components, which are inaccessible without removal of the wall assembly, must have a durability greater than that of the OPR.

2.4 Overview of Building Enclosure Commissioning

In North America, a robust process designed to steward a building from inception through construction and occupancy is the Building Enclosure Commissioning (BECx) as outlined in ASTM E2813 – 12 Standard Practice For Building Enclosure Commissioning ASTM E2947 – 16 Standard Guide For Building Enclosure Commissioning and CSA Z320 :11 Building

Commissioning. The process features third party design review during the design process, includes submittal reviews, the development of mockup and building testing protocols, construction observation, and post-occupancy support. Buildings utilizing this process perform demonstrably better than those that don't.

A performance mockup that provides an opportunity to construct and test a given assembly in context can provide opportunities to improve both its design and execution. The mockup is tested for air, water, thermal, and structural performance. This can be performed in the laboratory or as a free-standing, fully enclosed mockup on the site.

Objectives of Building Envelope Commissioning are driven by building type, performance requirements, expected life cycle, geographic and climatic considerations, desired energy efficiency, and budgetary constraints, which all may vary considerably between projects. As there is much literature describing the tasks that comprise the BECx process, identifying these tasks is beyond the scope of this paper. However, to effectively compare BECx between typical and extreme climates, it is necessary to discuss the key action items common to most BECx programs. While the precise tasks and their frequency differ from project to project, basic practice generally follows a similar series of steps categorized into five phases: Pre-Design; Design; Pre-Construction; Construction, and; Operations and Maintenance (O&M).

A full-service Building Exterior Commissioning (BECx) process, as detailed in NIBS 3-2012 (NIBS 2012), has demonstrated the most impressive and reliable results. Evan Mills, PhD, a researcher at Lawrence Berkeley National Laboratory, called the BECx process “the single most cost-effective strategy for reducing energy, costs, and greenhouse gas emissions in buildings today.” (Sullivan, C. 2013)

2.5 Tools For Verifying Air Barrier Performance: Complexity and Challenges

In the U.S., projects have adopted a number of tools and techniques to decrease the probability of deficiencies in the performance plane. Of these, the process involves a qualified third party engaged at the beginning of the design process and serving through the construction process as an envelope auditor. The BECx process is intended to be comprehensive and typically includes the following key steps:

- Exterior envelope design reviews during the design and shop drawing documentation phases
- Development of BECx specifications
- A role in the contractor and subcontractor selection process
- Review of shop drawings
- Design and definition of the exterior functional performance testing protocol for mockups and field tests
- Contractor quality assurance and quality control auditing
- Site observation visits
- Deficiency logging
- Warranty and maintenance monitoring and audits

The BECx approach is sound and affordable relative to potential energy savings and reduced costs of repairs and maintenance; it is currently the best available option for owners to reduce the risks of a problematic exterior envelope. There remain numerous opportunities for problems to occur, however. For example, budgetary limitations limit the site visits made by the specialized consultants, engineers and/or architects, which decreases the possibility of identifying envelope issues as they occur and increases the potential for defects in the performance plane to be concealed behind permanent cladding systems; not every issue can reasonably be caught. The potential for issues to occur, even with consistent auditing, is a compelling reason to include a comprehensive mockup and field-testing protocol. A sensible deployment of recognized ASTM and AAMA protocols, for example: AAMA 501.1, AAMA 501.2, ASTM E1186, ASTM E783, and ASTM E1105, can identify hidden deficiencies during construction.

Whole Building Air Testing: Accumulating data from Whole Building testing are helping the industry to understand the types of envelope issues that persist, even under the highest quality standards. Kevin Knight and colleagues at the Building Envelope Technology Access Centre (BETAC) at Red River College in Manitoba, Canada, have advanced their airtightness testing program by means of laboratory testing as well as the study of previous whole building air testing. Their efforts have produced the following observations (Proskiw, G, Knight, et.al, 2016)

Leaks are common at:

- Exhaust and make-up air fans with one-way dampers
- Roof/wall intersections, especially on walls running perpendicular to roof deck flutes
- Unintentional bulkhead leakage into attic spaces
- Overhead doors, mainly at base and sides, not between sections
- CMU/floor slab intersections
- Curtain wall/floor slab intersections
- Unsealed walls above ceiling lines
- Ductwork and pipe penetrations
- Doors and windows (both broken and unbroken)
- Underground steam lines

Additionally, test results have prompted debate regarding the inclusion, exclusion, or partial inclusion of the mechanical system during the test, as has the idea of a pressure neutral result to simulate real world conditions. Knight and his colleagues have drawn a sensible conclusion to the question. The recommendation from the group is that two distinct sealing schedules be required for the mechanical system:

- Envelope Tests – Evaluate the integrity of the building envelope
 - Mechanical system is sealed
- Energy Tests – Evaluate the impact of air leakage on energy performance
 - Mechanical system is unsealed.

Whole building air testing, in the aggregate, can inform institutional Owners about the propensities of their buildings. The more data that is available, the more useful the tests become. While specific issues may be inaccessible, knowledge of their existence can prepare an Owner on what to watch as well as a sensible maintenance protocol. The data can establish institutional

benchmarks both helping measure new projects against previous standards as well helping inform design decisions—appropriate HVAC sizing being among the most recognized.

3 MECHANICAL DESIGN CONSIDERATIONS

3.1 Mechanical Design for New Construction

In the northeast of USA, general “rule of thumb” industry practices for the effect of building envelopes on mechanical equipment peak heating loads is shown in Table 3. As shown in this table, the results of improved building envelopes is staggering. Compared to older building envelope design practices, new high performance building envelope designs can support an approximately 400% smaller mechanical peak heating load.

Table 3: Building Envelope Design’s Effect on Heating Load Design “Rule of Thumb”

General Design Practices	Peak Heating Load (Btu/ft ² hr)	Peak Heating Load (W/m ²)
“Old” Designs	40	126
“New” Designs	20	63
High Performance	10	32
Passive House	<10	<32

These approximations should be viewed as general guidelines and not as a replacement for calculating peak heating loads. When performing these calculations, it is important to take into account the climate in which the building is being constructed, building envelop values, building air tightness, and anticipated internal heat loads which will be variable depending on the space type.

One of the largest changes to the design engineering industry, aside from building envelope improvements, is the topic of mechanical heating fuel switching, aka electrification. The rise of this topic coincides with growing social and environmental pressures to reduce the impact of climate change paired with industrial advancements such as heat pump technology. At first glance, designing a new construction building with a fully electrified mechanical heating system appears easy. Buildings can be designed with multiple configurations of infrastructure depending on building size, orientation, and usage. Electricity purchased for the building can be 100% renewable, and the “green” features can command premium rents from tenants. However, most electrical grid infrastructure was not designed or sized to support fully electrified buildings. As the demand for electricity increases, grid electrical infrastructure sizing will become more of an issue which could cause significant delays in the construction of new buildings if they are forced to wait until grid electrical infrastructure upgrades are completed.

The question then becomes, how can the anticipated total energy load of a building be reduced to mitigate or lessen the effect of these electrical grid issues? This is not a new question and most of the new construction industry already acknowledges the importance of building envelopes and their effects on the overall energy consumption of a building. This is evident in the emergence of “Passive House” and comparable design techniques. If the building envelope is designed and constructed to a low degree of heat loss tolerances, mechanical heating, cooling, and ventilation systems do not need to be as robust compared to standard design practices.

Herein lies the importance of mechanical commissioning and building envelope commissioning, as well as the marriage of HVAC and enclosure work. With significant emphasis on mechanical systems and envelopes performing to very high standards, efforts to ensure quality control are critical. Especially when it comes to building envelope as once the building is built, there will be very few options to correct mistakes without significant financial and schedule implications. Waiting to until a building is complete and performing a full building blower door test to see how a building performs without additional building commissioning efforts can be very risky. If tests come back with air leakage above acceptable levels, corrective actions for the building envelope may not be feasible and building mechanical systems may struggle to maintain heating loads. Similarly with mechanical systems, there will be high expectations of performance. With decreases sizing of mechanical equipment, the room for error in system performance is diminished.

3.2 Mechanical Design for Existing Buildings

“Around 80% of the buildings we have today will exist in 2050...” (Grainger, 2022). This is unmistakable throughout Europe and cities worldwide. That said, the buildings may exist, but building envelopes will inevitably degrade over time and mechanical equipment will need to be replaced. Due to the large capital expense required to repair building envelopes and replace mechanical infrastructure, considering sustainability is paramount. These sustainability considerations should include both energy efficiency and maintainability of systems.

When designing for replacement of mechanical systems, several questions must be considered.

- Why is the system being replaced?
 - Is it due to age, reliability, maintainability, operation, energy consumption, etc.?
 - Are there any changes to building codes, energy consumption limits, or Greenhouse Gas equivalent (GHGe) emission limits?
- Does the current system meet the building’s requirements?
 - Have there been changes to space use that would require more or less systems capacities?
 - Are there significant heating, cooling, ventilation complaints? If so, where?
- Does the building owner or tenant want to make changes to the building that would affect the current system’s effectiveness?
 - Is there a planned renovation that would change space usage? (e.g., office converted to labs)
- Do the existing generation, distribution, and/or terminal units need to be replaced?
 - Will new generation (e.g., water heater) equipment supply the correct temperature fluids to the terminal units?
 - Will the terminal units need to be replaced to receive lower temperature hot water?
- Will new system controls need to be added?
- Is the existing electrical infrastructure adequate to support a fuel switch (e.g., fossil fuel to electricity)?
- Will the electrical grid be able to serve an increased electrical load?
- How will the building envelope affect system performance?

Most of these questions can be answered by the design engineer and building owner with an acceptable level of certainty except for building envelope performance. Without performing existing building envelope commissioning and associated repairs, assumptions regarding building envelope performance will need to be made. These assumptions will normally be based on initial design criteria, tenant feedback, and visual observations. Due to these uncertainties and assumptions, many design engineers will just replace the system in-kind, but if fuel switching is also desired, replacement in-kind and considerations for downsizing of equipment may not be an option. This may lead the design engineer to oversize the replacement system to ensure that acceptable indoor conditions are met. In turn, this oversizing of equipment places additional stress on existing electrical infrastructure which may require costly electrical infrastructure upgrades.

A more thorough method of addressing uncertainty in building envelope performance is via the building envelope commissioning process. Through this process, critical information on building envelope performance is gathered and taken into consideration by engineering design professionals. Key testing components of this process are:

- Blower Door Testing ASTM E779 to identify total building air leakage.
- Fenestration Testing such as ASTM 783 to identify local air leakage. This can be combined with ASTM E1176 smoke detection to help source issues.
- Thermal Imaging Investigation ASTM C1153 to identify areas of concern for thermal bridging and heating/cooling energy loss. An additional benefit of this testing process is identifying areas of concern for water leakage into a building.

With this information, levels of certainty can be increased and the design engineer can make more accurate peak heating load calculations resulting with more appropriately sized mechanical infrastructure.

4 CASE PROJECTS AND VALUES

In the course of their collaboration over more than 10 years, the companies of this paper's authors have performed mechanical and enclosure commissioning on well over 20 institutional buildings together. As a result, a growing body of both qualitative and quantitative data to substantiate a basis of standards and predictability for our subject building types, specifically, K-12 academic buildings in Massachusetts, USA is available to us. Additionally, while our body of results for whole building air testing is still relatively small—the test is still gaining traction as a routine practice—the results have been both impressive and consistent. We now recognize that extremely tight high-performance academic buildings are not only possible but can be routinely achievable based upon the BECx process that we have consistently adopted for the vast majority of these projects. As a result, we have adopted an ambitious standard for air tightness, .1 CFM at 75 PA, that is specified as a performance requirements for all new academic projects supported by the state of Massachusetts. This rate represents just 25% of the allowable air leakage as dictated by the current building code for the state.

Table 4: Air Tightness Standards by Building Type

Case	Building Type	Measured Air Leakage Rate at 75 PA
1	Elementary School	.06
2	Library	.06
3	University Academic Building	.09
4	Elementary School	1.2*

*Project was constructed during the COVID pandemic; several of the BECx activities were not completed.

5 CONCLUSIONS

Building exterior enclosures are among the most critical, expensive, and energy consumptive of a building systems to construct. They represent an enormous carbon footprint, and they contribute mightily to overall energy usage. It is no trivial matter to make good decisions on this topic given both micro and macro considerations.

Governmental and other institutional / portfolio owners are challenged to evaluate the status of buildings with value-based and actionable terms. The escalating attention on energy efficiency, climate change, geo-political stability / national self-sufficiency, energy costs, and the increasingly competitive appeal of sustainable resources has placed additional focus and weight on high-efficiency and robust high-performance options for both enclosure and HVAC components.

Evaluating decisions for new and existing building stock in value-based terms requires data and the collaboration of multiple disciplines. Two of the most relevant of these to energy use are for enclosure and HVAC system design and evaluation.

We understand from the extensive studies performed on buildings over the years that among the pathways for energy loss, convective heat and cooling loss via air leakage is the most significant source of thermal transfer; buildings with the highest preponderance of leaky conditions are perform the worst in terms of thermal and energy efficiency.

The incorporation of measured air leakage and durability data into HVAC models can result in more efficient mechanical systems with low risk based upon the consistent results of the BECx processes outlined above.

We are optimistic that new means of calculating loads based on these inputs will become normalized over time as the data from tests such as Whole Building Air Testing becomes standardized and that increased reliance on such data will result in significant energy savings with benefits to both owners and the environment.

6 ACKNOWLEDGEMENTS

The Pioneering work by Kevin Knight of Retro-Specs LTD in the field of Building Science, Enclosure Commissioning, and Building Enclosure Testing has significantly influenced the content of this paper.

7 REFERENCES

de Sola, D, Symonds, T. (2019). *Benefits of Whole Building Air Leakage Testing For Higher Educational Institutional Buildings*. ASTM: STP161520180023 ISBN-EB: 978-0-8031-7676-8

Oak Ridge National Laboratory (2023). *Energy Savings and Moisture Transfer*. Oak Ridge National Laboratory Website

Zhivov, A., Bailey, D., and Herron, D. (2012) *U.S. Army Corps of Engineers Air Leakage Test Protocol for Building Envelopes Version 3.*. US Army Corps of Engineers Engineer Research and Development Center, Air Barrier Association of America.

Genge, C. (2014). *Air Leakage Testing of Commercial Buildings*. National Environmental Balancing Bureau (NEBB).

USGBC U.S. Green Building Council

USGBC. (2018). *LEED BD+C Homes Air Infiltration*. U.S. Green Building Council.

ASTM International, ASTM E2813 – 12 Standard Practice for Building Enclosure Commissioning

ASTM INTERNATIONAL, ASTM E2947 – 16 Standard Guide for Building Enclosure Commissioning

CSA Group (2011), CSA Standard Z320 :11 Building Commissioning

National Institute Of Building Sciences (2012). *NIBS Guideline 3-2012 Building Enclosure Commissioning Process BECx*. National Institute of Building Sciences.

Sullivan, C., (2013) *Calculating the ROI of Building Enclosure Commissioning*. Building Design + Construction.

Proskiw, G, Knight, K., Spewak,R., and Carson, C. (2016) *Commercial Building Airtightness Testing – Lessons Learned from the Red River College Airtightness Testing Program*. Thermal Performance of the Exterior Envelopes of Whole Buildings XIII International Conference 2016.

Grainger, G. (2022). *To create net-zero cities, we need to look hard at our older buildings*. World Economic Forum (weforum.org)

8 ADDITIONAL REFERENCES

ASTM E779-03 *Standard Test Method for Determining Air Leakage Rate by Fan Pressurization*. ASTM International.

ASTM E1827-11. (2017). *Standard Test Methods for Determining Airtightness of Buildings Using an Orifice Blower Door*. ASTM International.

National Building Code of Canada. (2003) Canadian Commission on Building and Fire Codes, National Research Council of Canada.

Air Tightness Testing and Measurement Assn. (ATTMA) Technical Specification 1 UK

CAN/CGSB-149.10 (2019) *Determination of the airtightness of building envelopes by the fan depressurization method*. Canadian General Standards Board.

CAN/CGSB-149.15 (1996), *Determination of the Overall Envelope Airtightness of Buildings by Fan Pressurization Method Using the Building's Air Handling Systems*. Canadian General Standards Board.

Lux, M.E., Brown, W.C., (1989). *Air Leakage Control In An Air Barrier for the Building Envelope*. Building Science Insight '86

Lstiburek, J. (2005). Understanding Air Barriers. *ASHRAE Journal*, Vol. 47, No. 7.

Di Lenardo, B., et. al. (1995). *Air Barrier Systems for Exterior Walls of Low-Rise Buildings*. CCMC Technical Guide Master Format 07195, Institute for Research in Construction, NRC Canada.

Ojanen, T., and Kumaran, K., (1996). Effect of Exfiltration on the Hygrothermal Behaviour of a Residential Wall Assembly. *Journal of Building Physics January, Vol. 19*. 215-227.

Emmerich, S. and Persily, A. (2011). *U.S. Commercial Building Airtightness Requirements and Measurements*. AIVC Conference 2011, Brussels. 134 – 137.

Brennan, T., Anis, W., Nelson, G. and Olson, C. (2013). *ASHRAE 1478: Measuring Airtightness of Mid- and High-Rise Non-Residential Buildings*. Proceedings of the Thermal Performance of the Exterior Envelopes of Whole Buildings XII International Conference 2013, Clearwater, FL. 1-6.

Emmerich, S., McDowell, T. and Anis, W. (2005). *Investigation of the Impact of Commercial Building Envelope Airtightness on HVAC Energy Use*. NIST Interagency/Internal Report (NISTIR), National Institute of Standards and Technology, Gaithersburg, MD

Straube, J. (2014). *BSD-040: Airtightness Testing in Large Buildings*. Building Science Digest 040.

Stanford University (2005). *Guidelines for Life Cycle Cost Analysis*. Stanford University Land and Buildings.

GreenSpec, (2018). *Airtightness and the 'Intelligent' membrane*. Greenspec.co

CSA Group (2019), CSA Standard S478:19 Durability in Buildings

Wiseman, A. (1997) *Durability Guidelines for Building Wall Envelopes, Public Works & Government Services, Canada Technology and Environmental Services, Ottawa, Canada.*

de Sola, D., Knight, K., Boyle, B. (2011) *Building Envelope Commissioning for Extreme Climates*, 9th Nordic Symposium on Building Physics Tampere, Finland.

E. Source Companies, LLC. (2003) *Managing Energy Costs in Colleges and Universities*. National Grid.

Conserval Engineering, Inc. (2018) *How the SolarWall® Technology Provides Fresh Air & Free Heat*. SolarWall®

Windows and ceiling fan occupant behaviour model coupling methodology with building energy models, a tropical case study

Maäréva Payet*^{1,2}, Maxime Boulinguez^{1,2}, Mathieu David², Philippe Lauret² and François Garde²

*1 LEU Réunion
139, rue François Isautier, 97410 Saint-Pierre
Ile de la Réunion, France*

**Corresponding author: mp@leureunion.fr*

*2 Laboratoire Physique et Ingénierie Mathématique
pour l'Énergie, l'environnement et le bâtiment
(PIMENT) University of Reunion Island, Sainte-
Clotilde 97715, La Réunion, France*

ABSTRACT

In this work, we propose a method to couple the behaviour models developed with Python in a previous paper with the dynamic thermal simulation software EnergyPlus, an advanced code used in research and design. The proposed coupling method is applied to the thermal model of an office building situated in the humid tropical climate of Reunion Island after calibrating and validating it with measured temperature and relative humidity data. Then, this resulting coupled model is compared with a typical design office energy model where behaviours are based on typical, deterministic scenarios. The comparison focuses on the power level of the ceiling fans employed, the level of opening use and the calculation time. The results obtained by coupling with the new behavioural models are better than in the conventional deterministic scenarios, providing a more faithful reproduction of user actions in the design phase.

KEYWORDS

Tropical climate, mixed-mode buildings, users behaviours modelling, operable windows, the power level of ceiling fans

1 INTRODUCTION

Buildings in humid tropical climates are witnessing a significant upsurge in their energy demands, primarily attributed to the use of cooling systems known for their substantial energy consumption. In low-energy buildings in such climates, occupants can employ both passive solutions, such as natural ventilation through windows, and low energy-consuming alternatives (in this study, we focus solely on using ceiling fans) to achieve thermal comfort, particularly during the hottest months. However, compared to other climatic zones, there needs to be more specific knowledge regarding occupant comfort and behaviour in this context. This leads to difficulties in the design phase for engineers who need to estimate the future operation of a building.

In a previous research paper (Payet, 2022), two deterministic methods based on machine learning supervised classification techniques (decision tree and random forest) and a probabilistic graphical model (bayesian network) were investigated to model occupant behaviour regarding windows and ceiling fans. In both cases, the random forest method obtained the highest performances. These techniques, explained in detail in (Payet, 2022), use historical measured data as explanatory variables for the variable to model (for example, in our

case, the power level of ceiling fans). The whole methodology elaborated is described in detail in this previous paper.

In this work, we present a novel approach to integrate the developed behaviour models with dynamic thermal simulation software, coupling Python and EnergyPlus, an advanced code used in research and design. The proposed coupling method is applied to the thermal model of a case study after calibrating and validating it with measured temperature and relative humidity data.

The first part of this paper provides an overview of existing methods for coupling behaviour models with dynamic thermal simulation software. Subsequently, the proposed coupling methodology is detailed, from the case study's presentation to the coupling method's integration, before discussing the results obtained in the last part.

2 STATE OF THE ART

Existing tools offer solutions of varying complexity to incorporate user behaviour into simulations (Sun, 2017; Darakdjian, 2017)

Direct modelling involves inputting user data into software modules but cannot create detailed occupancy profiles and conditioned behaviours.

Code customisation enables users to add personalised scripts to the source code, facilitating the incorporation of user behaviour into simulations (Sun, 2017). For EnergyPlus, the EnergyPlus Runtime Language of the Energy Management System is used (BigLadder, 2020). Another approach involves customising the core code of the software itself, offering significant flexibility but requiring proficiency in the underlying programming language.

Co-simulation offers a collaborative approach, combining the strengths of different simulation tools through information exchange at each time step. This method allows users to harness multiple tools' capabilities without extensive programming knowledge. Co-simulation can be achieved using functions like "External Interface" in EnergyPlus or by using communication intermediaries such as the Building Controls Virtual Test Bed (BCVTB) (Nihar, 2019; Kwak, 2016; Jia, 2020; Langevin, 2014)

A recent intermediary solution available since version 9.3 of EnergyPlus is the PythonPlugin interaction method. This new approach is positioned between code customisation and co-simulation. It allows engineers to write code within the EMS using Python, a widely used language known for its extensive functionalities and various libraries. This integration offers a significant advantage over the EnergyPlus Runtime Language, which has more limited capabilities.

To our knowledge, this last method chosen for this work has not yet been implemented in the existing literature to simulate occupant behaviour. Table 1 compares the different methods for integrating occupant behaviour into the dynamic thermal simulation.

Table 1: Comparison of existing user behaviour integration methods in dynamic thermal simulation

Method	Ease of implementation	Flexibility
Direct modelling	++++	+
Code customisation	++	++
Customisation of Core code	+	+++
Co-simulation	++	++++
Python plugin	+++	++++

3 METHODOLOGY

3.1 Case study and associated building model

The case study “Ilet du Centre” is a 310 m² design office, part of a residential building, exposed to the humid tropical climate of Reunion Island, a French island in the Indian Ocean. The office has two floors divided into several open-plan areas, with several offices organised side by side. There is a meeting room, a server room and two individual offices.

The 28 users can regulate temperature by generating crossed air flows, thanks to many manually adjustable and full-height louvre-type openings. They can also activate ceiling fans to reduce the temperature felt on the hottest days when air temperatures are high, and there is not enough natural airflow. There is no mechanical air conditioning system except for the server and meeting rooms.

Using specific power sub-meters, ceiling fans and electrical outlets were recorded between 2020 and 2022. In addition, air temperature and relative humidity, as well as the opening of windows using magnetic contacts, were monitored. The outdoor temperature, humidity, wind and solar radiation were recorded using a weather station.

From these actual measured data, we could calibrate a thermal model of the case study and then validate it to overcome modelling errors unrelated to occupant behaviour.



Figure 1: BEM model, view of the North façade (left) and South façade (right) displayed without shading

The calibration was performed manually using an iterative procedure in which various parameters are adjusted until the simulation results align with the measured data (Royapoor, 2015). Validation occurs when this iterative process is finished, and normalised metrics are used to determine the level of real-world representation achieved by the model.

Acceptable values for these metrics are provided by the American Society of Heating, Refrigerating, and Air-Conditioning Engineers Guideline 14 on Measurement and Energy

Demand (ASHRAE), the Federal Energy Management Program (Of Energy Efficiency & Renewables Energy), and the International Performance Measurement and Verification Protocol recommended in France by ADEME and the Ministry of Sustainable Development. Hourly and monthly thresholds must be verified.

However, these normalised threshold values were developed to validate building models based on measured energy data and do not enable objective comparisons when they relate to temperatures in °C or K. The existing literature offers limited guidance on validating building models using hourly temperature and humidity measurements (Baba, 2022), as in our case study, where indoor conditions were measured over a year using recording sensors.

To address this gap, we supplemented the existing normalised metrics, expressed as percentages, with the calculation of Mean Bias Error (MBE) and Mean Absolute Deviation (MAD), expressed in degrees Celsius (as described by Baba (2022)).

Following the method of O'Donovan et al. (O'Donovan, 2019) and to adjust the building parameters and avoid uncertainties related to user presence and their behaviours on controls, the model was calibrated during an unoccupied week (S1). Various adjustments on solar shading and thermal inertia were made during this week.

Internal load data (including the power demand of electrical outlets, ceiling fans, and window opening schedules) measured over 2020 were then integrated into the latest calibrated version. From this point, hourly validation metrics were then calculated based on indoor temperature and humidity data over different occupied weeks: a summer week (S2), a winter week (S3) and a mid-season week (S4). Metrics were also calculated for each month of the year 2020.

The hourly validation values obtained from indoor temperature data are:

- $0.05 \% \leq \text{NMBE}_h \leq 5.3 \%$
- $- 3.6\% \leq \text{CV(RMSE)}_h \leq 6.6$
- $- 1.8 \text{ }^\circ\text{C} \leq \text{MAD}_h \leq 2.8 \text{ }^\circ\text{C}$
- $- 0.01 \text{ }^\circ\text{C} \leq \text{MBE}_h \leq 1.2 \text{ }^\circ\text{C}$

As the values obtained were below the normalised thresholds, the model was considered validated based on indoor temperature data.

Once the building model was validated, the entries related to the use of ceiling fans and windows were modified in two ways: a case integrating the behaviour models developed using the PythonPlugin method and a case typically found in design office-type simulation (noted BE), where assumptions are made from expert knowledge.

3.2 Implementing random forest behavioural models in EnergyPlus with the Python Plugin method (case noted as “RF”)

This first case concerns the coupling of the Random Forest-based behavioural model with our BEM model.

The primary objective of the implemented method (noted as “RF” for Random Forest (Payet, 2022)) is to dynamically adjust the opening of windows and the use of ceiling fans in a thermal zone at each time step of an EnergyPlus simulation. This adjustment is based on data from the previous time step (T_n), ensuring the simulation accurately reflects real-time conditions. The process involves transmitting simulation outputs, such as indoor temperature and relative humidity, to the Python-coded behaviour models (one for windows and one for ceiling fans).

These models then estimate new control levels, subsequently updated in EnergyPlus to simulate the next time step (T_{n+1}).

For implementing the method on the EnergyPlus side, the Python module must be specified in the description file of the building model. On the Python side, a specific library allows us to create the link between the two software.

One notable advantage of this method is its user-friendly interface. Designers can seamlessly integrate the method into EnergyPlus, launching the simulation tool without additional technical complexities. This approach simplifies the workflow for designers, allowing them to incorporate occupant behaviour dynamics into their simulations effectively.

3.3 Comparison with a typical design office model (noted as “BE”)

The second case we conducted is based on a more conventional way of designer model behaviours in BEM models. This second case is a reference point to compare with the newly implemented method results of 3.2.

We conducted a simulation representing a typical design office scenario (noted as “BE”), where assumptions were formulated based on expert knowledge and no longer from the behavioural

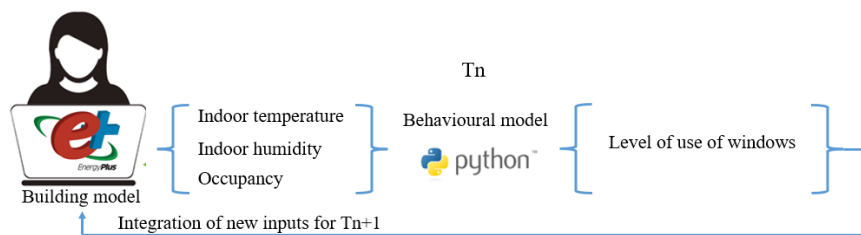


Figure 1: Simulation process with integration of the windows opening model

models developed in 3.2.

We have tried to make assumptions that reflect the standard practices employed by field professionals.

Concerning the ceiling fans, we assumed they were operated at full power during daytime hours in the summer period from January to the end of March, as well as during November and December. We estimated a reduced use of the ceiling fans during the transitional seasons (30% of use) and no use at all during the winter period from May to September. A power ratio of 5 W/m² was applied to calculate their impact.

Regarding the windows, we assumed the occupants would open them throughout the year during occupancy hours.

4 RESULTS AND DISCUSSION

The outputs of both the BE and RF simulations were analysed and compared with the actual data measured on “Ilet du Centre” in 2020.

In Figure 3, depicting the annual evolution of power demand for ceiling fans, it can be observed that the RF simulation more accurately replicates the triggering/extinction cycles of the ceiling fans compared to the BE simulation, which represents behaviours in the form of regular steps.

Nevertheless, discrepancies emerge as the simulated power levels during January and March are often below the maximum values observed in the measurements.

This can be attributed to the original nature of the behaviour models developed, which provide discrete classes rather than continuous values. To incorporate these models into the simulation, the results were transformed into single values by calculating the expected value using the median values of each class (as described in (Payet, 2022)). As a result, even if the highest class of ceiling fan use is estimated at a given time, the associated value will never reach the upper limit of that class.

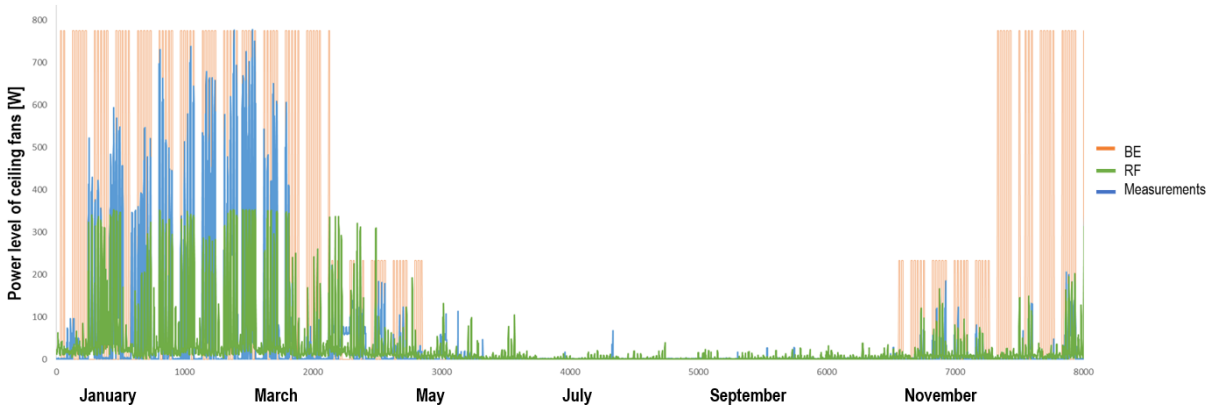


Figure 3: Comparison of the hourly average power level of the ceiling fans obtained by the BE method (in orange) and the coupling method (in green) with the actual measured data (in blue) for the year 2020

Various methods were tested to transform the original classes (such as calculating the expected value using the maximum and minimum values of the classes), but they yielded less accurate simulation results.

However, during the mid-season and summer periods in November and December, the simulated data from RF aligned much more closely with the measured data.

The use of the windows (Figure 4) simulated by RF follows the same trend as for the ceiling fans. It aligns more closely with the measured data compared to the results of the BE simulation.

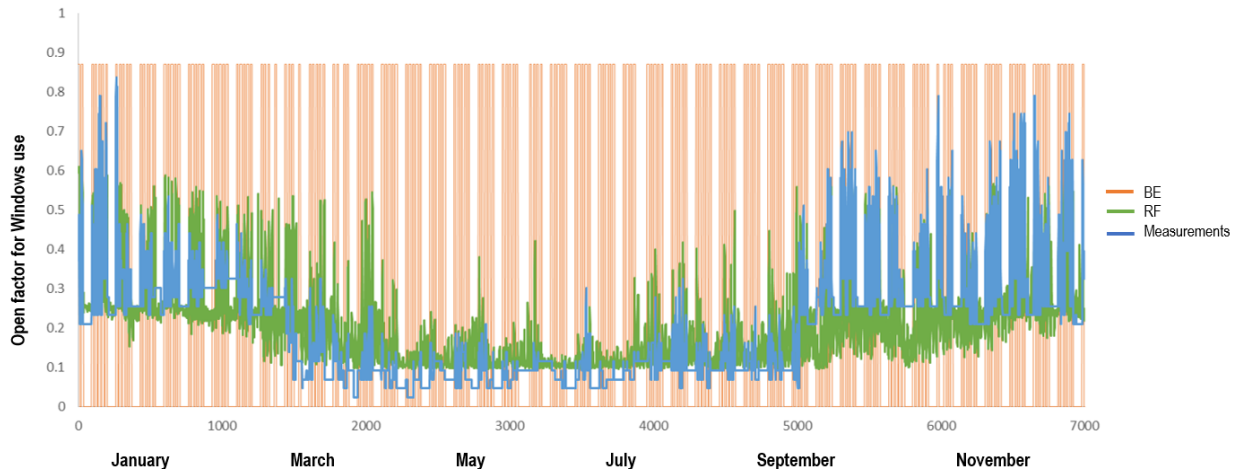


Figure 4: Comparison of the hourly open factor for the level of windows use obtained by the BE method (in orange) and the coupling method (in green) with the actual measured data (in blue) for the year 2020

The values of the various metrics calculated for each of the simulations are summarised in Table

Table 2: Comparison of the different simulations

		BE	RF
Calculation time		4 min 43s	2 h 21min
Indoor temperature	MBE (°C)	-0,59	0,19
	NMBE (%)	-2,4%	1,7%
	CV(RMSE) (%)	5,7%	5,2%
	MAD (°C)	4,89	4,53
	RMSE (°C)	1,43	0,80
Indoor humidity	MBE (%)	3,03	3,42
	NMBE (%)	5,5%	4,9%
	CV(RMSE) (%)	11,5%	8,6%
	MAD (%)	29,39	24,07
	RMSE(%)	7,95	5,95
Use of windows (opening factor)	MBE (%)	-0,12	-0,01
	NMBE (%)	-59,3%	-5,0%
	CV(RMSE) (%)	207,7%	45,8%
	MAD (%)	0,85	0,55
	RMSE(%)	0,43	0,10
Power level of ceiling fans	MBE (W)	-65,86	9,03
	NMBE (%)	-142,8%	19,6%
	CV(RMSE) (%)	480,2%	178,3%
	MAD (W)	774,80	661,54
	RMSE (W)	221,55	82,28

The obtained scores validate the observations made from the behaviour evolution curves, where the RF simulation outperforms the BE simulation. In the BE simulation, the average deviation (MBE) over the year is 66 W, while the RF simulation demonstrates a significantly lower deviation of only 9 W compared to the measured data.

5 CONCLUSION

We have introduced a novel approach to integrate user behaviour models into the EnergyPlus dynamic thermal simulation software using the recently developed PythonPlugin method. In this way, the use levels of louvres and ceiling fans are updated at each simulation time step of the simulation, based on data calculated at the previous time step in the BEM model.

To determine the performance of this method, we tested it on the Ilet du Centre building model, which had been calibrated and validated using temperature and humidity data for 2020. This step was necessary to eliminate modelling errors unrelated to user behaviour as far as possible. Once the building model was successfully validated, user behaviour was incorporated through two methods: a simulation based on assumptions derived from expert knowledge and a simulation incorporating random forest-based behavioural models.

A comparison between these two cases revealed that the method of coupling the building model with behavioural models allowed for more accurate replication of user actions compared to conventional practices employed by engineering and design firms.

Finally, it is worth noting that despite the evident advantages of the proposed coupling method during the design phase, it does result in relatively long simulation times (over 2 hours in our case study), which may pose challenges for some projects. To mitigate this issue, we replaced the random forest technique with decision trees in the developed behavioural models, achieving satisfactory simulation results while reducing computational time.

6 ACKNOWLEDGEMENTS

This work comes from a PhD thesis defended in 2022 in collaboration between LEU Réunion and the PIMENT laboratory of the University of Reunion Island.

This work will serve as input for the collaborative project CoolDown, funded by ANR under the number ANR-22-CE22-0014-06.

7 REFERENCES

Darakdjian, Q. (2017). *Prédiction des performances énergétiques des bâtiments avec prise en compte du comportement des usagers*, 249.

Payet, M., David, M., Lauret, P., Amayri, M., Ploix, S., & Garde, F. (2022). *Modelling of occupant behaviour in non-residential mixed-mode buildings: The distinctive features of tropical climates*. *Energy and Buildings*, 259, 111895.

Payet, M. (2022). *Simulation du comportement des usagers dans les bâtiments tertiaires à faible consommation énergétique, en zone tropicale*. Thèse de doctorat, Université de la Réunion.

- Sun, K., & Hong, T. (2017). *A framework for quantifying the impact of occupant behaviour on energy savings of energy conservation measures*. *Energy and Buildings*, 146, 383-396.
- Nihar, K., Bhatia, A., & Garg, V. (2019). *Optimal Control of Operable Windows for Mixed Mode Building Simulation in EnergyPlus*. *IOP Conference Series: Earth and Environmental Science*, 238, 012052.
- Kwak, Y., & Huh, J.-H. (2016). *Development of a method of real-time building energy simulation for efficient predictive control*. *Energy Conversion and Management*, 113, 220-229.
- Jia, M., & Srinivasan, R. (2020). *Building Performance Evaluation Using Coupled Simulation of EnergyPlus™ and an Occupant Behavior Model*. *Sustainability*, 12, 4086.
- Langevin, J., Wen, J., & Gurian, P. L. (2014). *Including occupants in building performance simulation: integration of an agent-based occupant behavior algorithm with EnergyPlus*. In *Proceedings of the ASHRAE/IBPSA-USA Building Simulation Conference* (pp. 10-12).
- Royapoor, M., & Roskilly, T. (2015). *Building model calibration using energy and environmental data*. *Energy and Buildings*, 94, 109-120.
- Ramos Ruiz, G., & Fernandez Bandera, C. (2017). *Validation of calibrated energy models: Common errors*. *Energies*, 10, 1587.
- ASHRAE. (n.d.). *Preview ASHRAE Standards and Guidelines*. Retrieved from <https://www.ashrae.org/technical-resources/standards-and-guidelines>.
- U.S. Department of Energy, Office of Energy Efficiency & Renewable Energy. (n.d.). *Federal Energy Management Program Publications*. Retrieved from <https://www.energy.gov/eere/femp/federal-energy-management-program-publications>.
- Baba, F. M., Ge, H., Zmeureanu, R., & Wang, L. L. (2022). *Calibration of building model based on indoor temperature for overheating assessment using genetic algorithm: Methodology, evaluation criteria, and case study*. *Building and Environment*, 207, 108518.
- Efficiency Valuation Organization. (n.d.). *International Performance Measurement and Verification Protocol (IPMVP)*. Retrieved from <https://evo-world.org/en/products-services-mainmenu-en/protocols/ipmvp>.
- O'Donovan, A., O'Sullivan, P. D. & Murphy, M. D. (2019). *Predicting air temperatures in a naturally ventilated nearly zero energy building : Calibration, validation, analysis and approaches*. *Applied Energy* **250**, 991-1010.

An innovative approach to better understand hot discomfort, based on the measurement of global human responses, including physiological and sensory indicators - application to end users of mixed mode cooled buildings under tropical climate conditions

Gwénaëlle Haese^{*1}, Maxime Boulinguez^{2,3}, Pierre Bernaud⁴, Anthony Couzinet¹

1 Technical and Scientific Centre for Building (CSTB), PULSE Laboratory,

11 rue Henri Picherit 44323 Nantes, France

**Corresponding author: gwenaelle.haese@cstb.fr*

2 Laboratoire Physique et Ingénierie Mathématique pour l'Énergie, l'environnement et le bâtiment

(PIMENT) University of la Réunion, Sainte-Clotilde 97715, La Réunion, France

3 Laboratoire d'Ecologie Urbaine Réunion 137 rue Isautier, 97410 Saint Pierre, La Réunion, France

4 Univ. Grenoble Alpes, CEA, Liten, INES 73375 Le Bourget du Lac France

ABSTRACT

Comfort modelling is a critical scientific barrier to reaching better thermal satisfaction in buildings. It allows designers to combine different cooling systems better to target comfortable low-energy buildings in hot and tropical climates. Increasing computer performance offers new perspectives to use more refined thermo-physiological models against traditional normative ones. Also, new types of coupled cooling alternatives arise and set a need for adequate comfort assessment models. The proposed article presents a methodology for better understanding human discomfort based on sensory response in hot conditions. It is an entry point to develop better and calibrate more generic bio-heat models for comfort prediction in the building industry. This study is part of a 48-month project called *CoolDown* funded by the French Nation Research Agency. It presents the first four months of field measurement. Preliminary results already give first insights into how relative humidity is predominant in hot climates when overreaching 68% and how temperature range is significant in occupant satisfaction when relative humidity is on the high side.

KEYWORDS

Thermal comfort, field survey, tropical climate, mixed-mode cooling, thermo-physiological models, bioheat model.

1 INTRODUCTION

In the current context of global warming, severe problems of overheating buildings in hot and humid climates arise. As a result, when natural ventilation (NV) is insufficient to target comfort, these hot periods lead to an overuse of air conditioning (AC), increasing energy consumption and electricity demand globally. However, alternative and original solutions exist to answer both comfort performance and energy savings in hot seasons. They are known as mixed-mode or hybrid cooling solutions and are aimed at drastically reducing AC energy use. They use ceiling fans coupled with either natural ventilation or air conditioning depending on the extremeness of climatic conditions. Nevertheless, although these mixed-mode solutions are gaining popularity nowadays, their use remains marginal in the Architecture Engineering and Construction (AEC) industry, especially in temperate and tropical climates. The lack of

quantitative and qualitative user experience feedback and knowledge of the actual comfort performance of combined active and passive systems partly explains this lack of interest by designers. Indeed, the normative approach to building comfort modelling, based on 20th-century research, highlights the dichotomy between analytical models (resulting from laboratory studies) and empirical models, such as the adaptive model (resulting from on-site surveys). This thus opposes air-conditioned buildings to naturally ventilated buildings. These two typologies are respectively governed by Fanger's PMV-PPD and the Adaptive Model, without foreseeing any real possibility of combining the two systems, or at least, without giving any clear prerogative as to the use of this, or that model in mixed-mode cooled buildings. (Yao et al., 2022). Both models have their field of application, advantages and disadvantages. On the one hand, the analytical model is based on all the environmental and individual variables without considering the notion of adaptability, thus, considering a passive user in the face of his comfort. On the other hand, the adaptive model hides them by focusing on the outside temperature alone. The case of mixed cooling then raises the question of combining the best of both worlds of air-conditioned and naturally ventilated buildings. The choice of the comfort model then becomes the priority question for understanding the transitions between the coupled cooling modes and the adaptability of the end user in such buildings. This study focuses on a more detailed approach accounting for a more dynamic way to assess thermal comfort based on physiological measurements on subjects working in a mixed-mode (MM) cooled building in la Réunion, an outermost French territory in a tropical climate. The cooling solutions consist of naturally ventilated and air-conditioned spaces, both coupled with high-performance ceiling fans. It aims at presenting the deployed methodology and preliminary results of a first summer campaign. This study is part of a French National Agency (ANR) funded *CoolDown* project focusing on mixed-mode cooling alternatives.

2 COMFORT MODELING IN BUILDINGS: TOWARD A PHYSIOLOGICAL APPROACH

The most commonly used thermal comfort models in the AEC industry are dedicated to uniform static environments. They are based on a right-here/right-now approach of body exchanges with its environment. They consider the human body to be a one-time physical body that does not react to varying environmental conditions and accounts neither for short/long term acclimatisation nor energy storage and dissipation mechanisms or adaptation of any kind. This dynamic should be considered in comfort modelling in NV and MM buildings as indoor ambient conditions is non-steady by nature. Furthermore, the human body does not detect the environmental condition directly. It is only made possible by thermoreceptors located in the outer skin layer. This skin layer is a strategic part of most common thermo-physiological models composed of two systems. They generally consist of a passive system representing all the human body's tissues and is the site of heat exchanges in the body and an active system which simulates physiological mechanisms such as shivering, cutaneous blood flow and sweating. Therefore, it becomes necessary to calculate the skin temperature to estimate the thermal sensation perceived by an individual in a given environment. This can be established through a thermoregulation model of the human body. Several complex thermoregulatory models exist to simulate the physiological responses of the human body and predict its skin and core temperatures (Fiala et al., 1999; Stolwijk, 1971; Tanabe et al., 2002; Salloum et al., 2007; Wissler, 2018). Some more simplified ones can also be found in the literature and are partially used in the AEC industry for specific applications (Urban comfort, Ashrae Elevated Air Speed Method) (Gagge, 1986; Walther, 2018; Walther, 2018; Ashrae Standard, 2020).

El Kadri (2020) developed a thermoregulation model based on neurophysiology, the NHTM (Neuro Human Thermal Model). Its passive system is based on Wissler's one developed for NASA (Wissler, 2018). The active system is based on signals from the skin and central thermoreceptors. Moreover, this model is individualisable; it can simulate several types of populations. The NHTM is coupled with Zhang's model (Zhang, 2003), which calculates sensation and thermal comfort in heterogeneous unsteady environments. In addition to calculating thermal comfort, the NHTM can estimate the health risks due to the exposure of individuals to thermal stress. This can be done by calculating core temperature and water loss through transpiration, sweating and evaporation.

Skin temperature plays an essential role in monitoring the thermoregulatory system of the human body. The skin is the physiological bridge between the human body and its environment. This sensory organ is therefore used as an indicator of thermal comfort.

Peripheral (skin) temperature was assessed as an index to estimate individual thermal sensation. The autonomic thermoregulation system uses peripheral blood vessels to maintain the temperature balance of the human body. In hot environments, cutaneous blood vessels dilate, allowing heat release. Thus, the skin temperature changes according to the blood flow. Field measurements must be carried out in labs or actual buildings to quantitatively estimate its influence on thermal sensation. Lan et al. (2014) reported thermal comfort levels during sleep for different air temperatures using mean skin temperature and responses to subjective thermal comfort questionnaires. Liu et al. (2013) studied the variations of mean skin temperature as a function of the skin surface in stable and unstable thermal environments.

A statistical analysis of the data collected according to different measurement methods, carried out by Yao et al. (2007), showed that the Burton model (3 points) obtains similar results for the average skin temperature compared to the other methods, for example, Colin/Houdas (10 points), Hardy/DuBois (12 points), Stolwijk/Hardy (10 unweighted points), and Mitchell/Wyndham (15 unweighted points). Due to its simplicity and convenience, Burton's model is quite suitable for in situ measurements for relatively long periods.

Burton minimises the number of sensors to three: on the heart chest side, the left forearm, and the right shin. He applies weighting coefficients to it to calculate the average skin temperature (T_{sk}), such as:

$$T_{sk} = 0.14 * T_{forearm} + 0.5 * T_{chest} + 0.36 * T_{shin} \quad (1)$$

Various technologies have recently been used to measure skin temperature, such as resistance thermometers, thermocouples applied to the skin's surface or infrared thermometers (Li et al., 2017). In the case of continuous measurements over a long period, the choice of thermocouples applied to the skin's surface is the least restrictive way to equip the participants.

3 MATERIALS AND METHODS

Three five days-long campaigns were organised during one working week from the 13th of February to the 31st of March 2023.

3.1 Buildings

Two buildings in Saint-Pierre in La Réunion, France, were selected to serve as demonstrators in this study. La Réunion is an outermost French territory in the Indian Ocean, governed by tropical climate conditions (Type Aw and As as from the Köppen Geiger classification). The average annual daytime temperatures [7 a.m. to 6 p.m.] do not drop below 23°C for Saint-Pierre. During the hot period, a daily temperature amplitude of 24 to 34 degrees Celsius with a relative humidity higher than 75% is expected. The design of buildings is thought to provide comfort,

avoiding space overheating. The first demonstrator “Ilet du Centre” building (IDC), is a large double floor open space office building built in 2008. As an experimental construction operation in a dense urban context, it was subject to a bioclimatic design primarily based on natural cross ventilation with louvres openings and double protection facades acting as fixed shadow devices. It is described by Payet et al. (2022). The second demonstrator, “CoArchitectes” (COA), is the first floor of an old basic concrete residential house on the city’s seaside. It has been recently renewed and extended as an office building. It does not benefit from natural cross ventilation in all spaces, and two third of the building has indeed single-sided openings. Those spaces are therefore equipped with AC units and ceiling fans for the hottest period of the year. May it be poorly insulated, solar impact on this building is limited by a second floor and very dense nearby vegetation.

3.2 Subjects

Twenty-one subjects (named SU_i with $i \in [1:21]$) (eleven females, ten males), aged from 25 to 52 (age mean: 35.2 ± 9.1), participated in the experiments. Their sensibility to cold and hot conditions was auto-evaluated by answering a questionnaire developed by CSTB; a sensitivity score was calculated to describe the panel. Based on the scores obtained from this group of participants, half can be considered “sensitive” to hot conditions, and the other half is “not very sensitive”. For the sensitivity to cold conditions, three categories can be defined: “not very sensitive” (2 participants), “moderately sensitive” (7 participants) and “very sensitive” (11 participants). These sensitivity levels can be used to analyse the results by sensitivity groups. The subjects are office workers. The studied population comprises architects, engineers and landscape designers working in their profession to reduce the impact of the AEC industry. By that means, they are sensitised to the AEC industry’s environmental impact and have a basic-to-good understanding of comfort components and their impact on energy use and carbon emission in buildings. SU_{1-8} were located in the IDC building, whereas SU_{9-21} was in the COA building.

3.3 Physiological measures

The physiological responses measured were skin temperatures and core temperature. Skin temperatures were measured by using stainless steel thermo buttons data logger 22L (ProgesPlus, France) at three localisations on the body (chest side of the heart, on the left forearm and on the right shin). Core temperature was measured using the same materials and placed under the armpit. The temperature acquisitions were made with a time step of 5 minutes. The average skin temperature (T_{sk}) was calculated according to Equation 1.

3.4 Comfort surveys

During the surveys, subjects were prompted to report their comfort status every 2 hours through a local executable written in French (Figure 1). The right side of the questionnaire concerns subject clothing and essential operable building elements such as sunshade deployment, doors and windows opening. Subjects could report any additional nuisance, such as noise, dust or glare and provide any comment in a free field. The left side of the questionnaire concerns comfort and air movement evaluation, such as thermal sensation (7-point scale), thermal comfort (6-point scale), satisfaction (4-point scale), acceptability (4-point scale), and preference (3-point scale). All results are gathered in tabulated format to speed up the data process and avoid transcription mistakes.

Comment vous sentez-vous maintenant, avez-vous ?

Très froid Froid Légèrement froid ni chaud ni froid Légèrement chaud Chaud Très chaud

Comment trouvez-vous l'environnement maintenant ?

0 - Très inconfortable 1 2 3 4 5 - Très confortable

Inacceptable Tout juste inacceptable Tout juste acceptable Acceptable

Etes-vous maintenant satisfait de cette ambiance thermique ?

Insatisfait Tout juste insatisfait Tout juste satisfait Satisfait

Souhaiteriez-vous avoir ?

Plus froid Pas de changement Plus chaud

Concernant les mouvements d'air, comment les jugez-vous ?

Inacceptable Tout juste inacceptable Tout juste acceptable Acceptable

Vous souhaiteriez en avoir ?

Moins Pas de changement Plus

Commentaires libres

vos vêtements

Haut : 1ère couche

sans manches manches courtes manches longues

Haut : 2ème couche

aucune manches longues pull

Bas (longueur)

court mi-long long

Bas (tissu)

tissu léger tissu épais

Pieds

pieds nus sandales nu pieds chaussures sans chaussettes chaussures avec chaussettes chaussures avec chaussettes épaisses

Y'a-t-il d'autres nuisances ?

sonore visuelle olfactive poussière

Ouvrants / Fenêtres

fermés ouverts

Portes

fermées ouvertes

Stores / Protections solaires

fermés ouverts

Merci de valider vos choix en cliquant sur le bouton ci-dessous :

Figure 1: Screenshot of the Cooldown project comfort application for comfort survey(in French)

3.5 Environmental measures

Indoor climatic conditions were recorded at two different levels, at the space level and the subject level.

The micro-climate around the participants was monitored using one hygro-button data logger for the air temperature (MC_T) and relative humidity (MC_RH). This sensor was pinned on the subject's top piece of the garment (at the chest level). These acquisitions were made with a time step of 5 minutes.

Air temperature and relative humidity were acquired with the PULSE box developed by CSTB every 10 minutes.

Environmental parameters for all spaces, such as dry bulb temperature, globe temperature, air velocity, and relative humidity, were recorded with various equipment, as in Table 1. All environmental parameters data are pre-processed to obtain a mean at 5 minutes time-step. For example, the environmental data from the PULSE box being acquired at a time step of 10 minutes, the value lying between two measured values corresponds to the average between these two values.

The meteorological data were extracted from the Mereen platform developed by CSTB, which combines solar radiation from satellite observations with classical weather station data, all at an hourly time step base. Results presented in this paper do not yet consider all granulometry of measurement at this early stage of the study.

Table 1: List of environmental parameters measure equipment

Supplier	Model	Probes	Measurements	Timestep
DeltaOhm	HD32.1 – Thermal Microclimate Data Logger	Combined temperature and relative humidity probe. Globe temperature probe Ø 150mm Omnidirectional hot wire probe (0°C...80°C)	Tdb, Tg, Va, RH	15 s
Testo	400	CO ₂ probe with Temperature and relative humidity sensors Globe temperature probe Ø 150mm TC type K Hotwire thermo-anemometer	Tdb, Tg, Va, RH	15 s
Kimo	VT 110 / VT 115	Hotwire thermo-anemometer	Va, Tdb	15 s
Campbell Scientific + Testo	CR1000	Combined temperature and relative humidity probe. Globe temperature probe Ø 152mm Thermal anemometer	Tdb, Tg, Va, RH	1 s

4 RESULTS & DISCUSSION

4.1 Quality of the data

The database was obtained by synchronising the data from the different sources of measurements. It contains 935 lines, corresponding to the 935 questionnaires obtained from the 20 participants over the three campaigns, and allowing the statistical analysis of the data to correlate all the environmental data, physiological and declarative data.

Due to the constraints of *in-situ* experimentation, some missing values exist in the database, depending on the sensors. The temperatures measured by the PULSE box showed a mean difference of 0.5°C with the temperature acquired with the comfort stations. The relative humidity recorded with the PULSE box showed a mean difference of 3.6% with the measures made with the comfort stations. These mean differences being sufficiently low compared to the uncertainty of the sensors, the missing values from the comfort stations were completed with the values of the PULSE boxes.

The number of missing values remaining after the database cleaning is 55 for the indoor temperature and indoor relative humidity measurements and 30 for the skin temperatures.

4.2 First results

The meteorological data indicate that the mean outside temperature during the three campaigns and the hours of response to the questionnaires was 28.5°C (min: 23°C, max: 31°C), and the mean relative humidity was 64.7% (min: 44.8%, max: 88.84%). Most of the time, the wind came from the southeast at a mean speed of 6.5 m/s (min: 0 m/s, max: 13.4 m/s).

The indoor temperatures in the IDC building were between 25.4°C and 29.4°C (mean: 28.3°C), and in the COA building, between 23.9°C and 31.3°C (mean 29.3°C) during the campaigns. The indoor relative humidity in the IDC building was between 51.5% and 81.8% (mean: 59.8%), and in the COA building, between 50% and 82.5% (mean of 67.1%). Windows were opened 85% of the time.

Regarding the responses to the questionnaire, 50% of the time, the subjects had a neutral thermal sensation, 30% slightly warm, 11% warm, and around 3% for the other choices. Only subjects in the COA building were declared “hot” when none of the subjects in the IDC building did.

The respondents declared they were satisfied 62% of the time, just satisfied 29%, just unsatisfied 7% and unsatisfied 2%. As for the thermal sensation, only occupants of the COA building chose the “unsatisfied” response. The same analysis can be made for comfort and acceptability. This result is consistent with the indoor conditions, which were hotter and more humid in the COA building than in the IDC one. The exact number of responses for each subject and each category of thermal sensation, comfort, acceptability and satisfaction is shown in Figure 2.

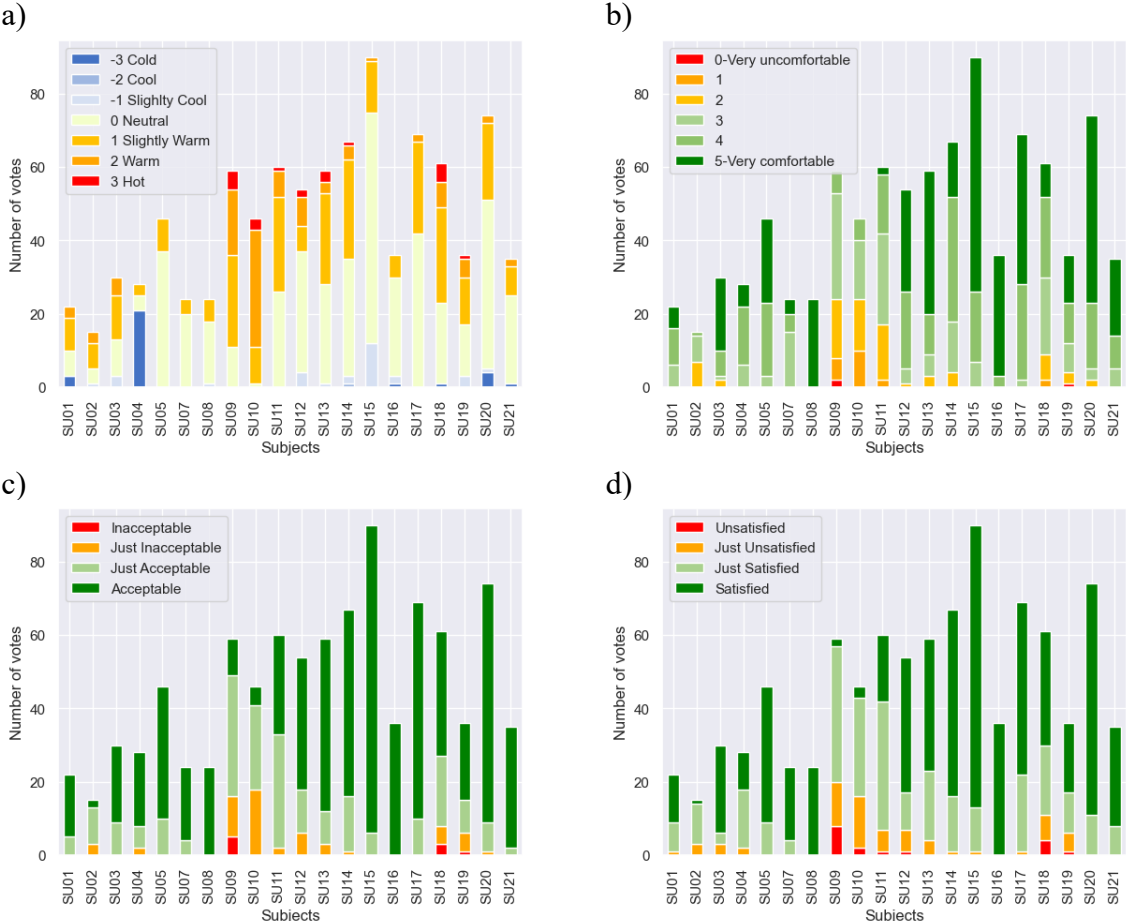


Figure 1: Number of votes for each subject and for each category of thermal sensation (a), comfort (b), acceptability (c) and satisfaction (d)

The four levels of satisfaction with the thermal environment are shown in Figure 3 as a function of the average values of air temperature and relative humidity. For each level, dissatisfaction increases with relative humidity. Confidence ellipses for the extreme satisfaction and dissatisfaction levels are constructed using the values of standard deviations of temperature and relative humidity. The correlation coefficient between temperature and relative humidity is used to calculate the angle of the confidence ellipse.

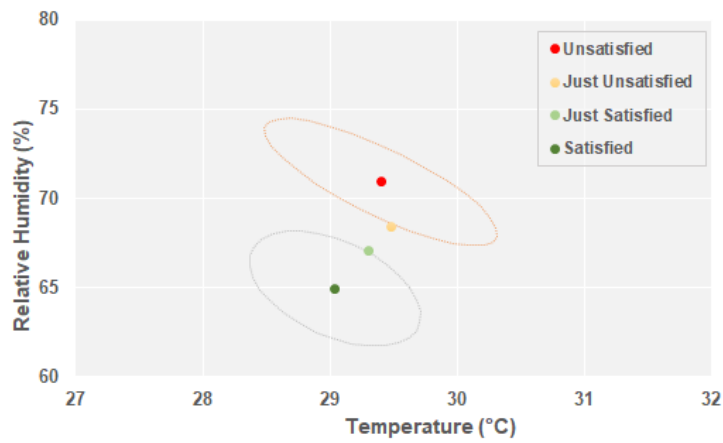


Figure 3: Evolution of the satisfaction level as a function of the temperature and relative humidity inside the buildings

Figure 3 shows that as dry as the air remains, the air temperature does not influence the level of satisfaction itself. On the contrary, a threshold value for relative humidity (68%) seems to condition the panel's dissatisfaction index.

Figure 4 shows the evolution of the skin temperature as a function of the microclimate temperatures and relative humidity. The results show that the main parameter influencing the skin temperature is the air temperature around the participants. The relative humidity is less linked to the skin temperature.

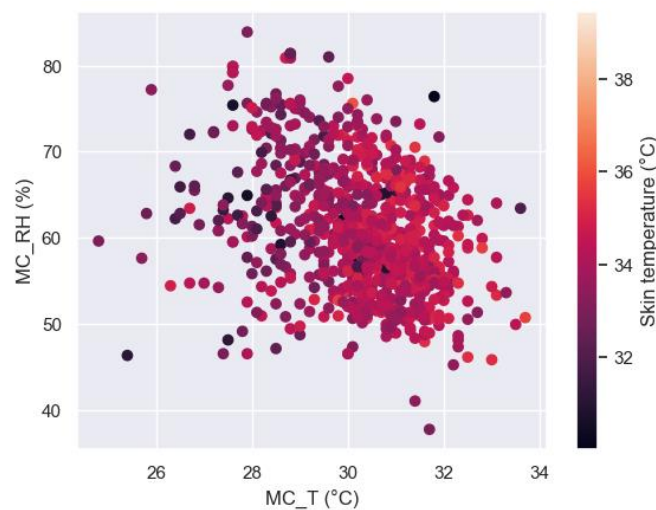


Figure 2: Evolution of the skin temperature as a function of the temperature and relative humidity given by the individual microclimate

5 CONCLUSIONS

This paper aims to present an overview of the methodology used in the ANR project CoolDown. Thus, the results presented in this paper are preliminary and do not show the whole set of data acquired.

These first results allow us to identify a trend regarding the strong influence of relative humidity on thermal satisfaction. A threshold value for relative humidity (68%) in this range of air temperatures seems to condition the panel's dissatisfaction index.

The skin temperature measurement is a good indicator of the ambient temperature around the subjects. This first set of declarative, physiological and environmental data constituted from the three campaigns will serve as entry data to build and optimise a thermal comfort prediction

model, which will be validated with the data from a second set of experimental campaigns while testing the optimised hybrid cooling solutions, identified during the CoolDown project.

6 ACKNOWLEDGEMENTS

The authors thank all the volunteers from Ilet du Centre and Coarchitectes who participated in the study for their interest and implication in the project. They also thank the members of their laboratory who helped in the preparation and deployment of the measures as well as their R&D Department for funding.

The project *CoolDown* is funded by ANR under the number ANR-22-CE22-0014-06

Maxime Boulinguez PHD Thesis is funded by LEU Réunion and French National Association for Research and Technology (ANRT) under the number 2020-1566

7 REFERENCES

El Kadri, M. (2020) *Thermo-neurophysiological Model of the Human Body for the Study of Thermal Comfort in Non-uniform Transient Climatic Conditions* (In French), PhD Dissertation, La Rochelle University, La Rochelle.

Fiala, D., Lomas, K. J., & Stohrer, M. (1999). *A computer model of human thermoregulation for a wide range of environmental conditions: the passive system*. *Journal of Applied Physiology*, 87(5), 1957. doi:10.1152/jappl.1999.87.5.1957.

Payet, M., David, M., Lauret, P., Amayri, M., Ploix, S., & Garde, F. (2022). *Modelling of occupant behaviour in non-residential mixed-mode buildings: The distinctive features of tropical climates*. *Energy and Buildings*, 259, 111895.

Li, Q., Zhang, L. N., Tao, X. M., & Ding, X. (2017). *Review of flexible temperature sensing networks for wearable physiological monitoring*. *Advanced healthcare materials*, 6(12), 1601371.

Stolwijk, J. A. J. (1971). *A mathematical model of physiological temperature regulation in man*. NASA, WASHINGTON, United States, Technical Report 19710023925.

Salloum, M., Ghaddar, N., & Ghali, K. (2007). *A new transient bioheat model of the human body and its integration to clothing models*. *International Journal of Thermal Sciences*, 46(4), 453-464. doi:10.1016/j.ijthermalsci.2006.06.017.

Tanabe, S., Kobayashi, K., Nakano, J., Ozeki, Y., & Konishi, M. (2002). *Evaluation of thermal comfort using combined multi-node thermoregulation (65MN) and radiation models and computational fluid dynamics (CFD)*. *Energy and Buildings*, 34(1), 69-76.

Walther, E. (2018). *Modélisation du confort dans les espaces ouverts et semi-ouverts*. Constr. Responsible.

Walther, E., & Goestchel, Q. (2018). *The PET comfort index: Questioning the model*. *Building and Environment*, 137, 1-10.

Wissler, E. H. (2018). *Human temperature control*. New York, NY: Springer Berlin Heidelberg.

Yao, R., Zhang, S., Du, C., Schweiker, M., Hodder, S., Olesen, B. W., ... & Li, B. (2022). *Evolution and performance analysis of adaptive thermal comfort models – a comprehensive literature review*. *Building and Environment*, 109020.

Zhang, H. (2003). *Human Thermal Sensation and Comfort in Transient and Non-Uniform Thermal Environments*. PhD dissertation, University of California, Berkeley.

An IAQ and thermal comfort coach prototype to improve comfort and energy consumption thanks to adequate management of natural ventilation: development and first feedback results

Arnaud Jay*¹, Pierre Bernaud¹ and Franck Alessi¹

*1 Univ. Grenoble Alpes, CEA, Liten, INES
73375 Le Bourget du Lac
France*

**Corresponding author: Arnaud.jay@cea.fr*

ABSTRACT

Over time with thermal and energy regulations, buildings are increasingly insulated and airtight to control better the heat exchanges between the indoor and outdoor environments. The primary function of the mechanical ventilation system is to ensure healthy air by diluting odours and humidity with fresh air. However, in many situations, windows opening can be much more effective in terms of thermal comfort, air quality, or release heat loads due to a higher air change rate than the mechanical ventilation system itself. On the contrary, opening the windows can be counterproductive and, in particular, leads to overconsumption of energy because it is not necessarily obvious whether it is appropriate to open or close a window. In addition, opening a window can improve air quality and generate additional energy consumption, leading to a complex decision process.

This presentation presents a coaching tool developed to help occupants to know whether it is a good option to open or close their windows. The objective of this coach is to consider the three components: thermal comfort, indoor air quality (IAQ) and energy consumption. The coaching tool is based on environmental data monitored thanks to 3 sensors in its first version: indoor and outdoor air temperature and indoor CO₂ concentration. The outside air temperature is first used to calculate the outdoor running temperature based on the last three days of measuring data. This running outdoor temperature is used to define the adaptive comfort temperature range. The indoor air temperature is then compared to both instantaneous outdoor air temperature and adaptive comfort temperature range to check if the thermal potential (heating or cooling) is in accordance with the thermal need of the indoor environment. In parallel, the IAQ is monitored thanks to the CO₂ concentration sensors and compared to different ranges to define whether opening the window might be necessary to bring cleaner air into the room. All these data are integrated into a rule-based algorithm to determine the coaching advice, which might take three states: Open, Close or Free. The last one means open or close will neither improve nor deteriorate the indoor environment quality (IEQ). One of the challenges of this tool is to be autonomous in energy for at least one season. Energy consumption of the tool, frequency of computation of the algorithm and advice displayed to the user are other bottlenecks developed in parallel with the algorithm's performance.

A testing campaign with five prototypes was run at the end of summer 2022 in an office building at Le Bourget-du-Lac (73) in France. Some first feedbacks are presented in Figure 1 within the upper graph, the measured data: indoor air temperature in orange, outdoor air temperature in green, the bandwidth of adaptive thermal comfort in red, and CO₂ concentration in blue. In the lower graph, the status of the windows is presented in yellow, and the advice from the coach is in blue. Unfortunately, in this first period, the outdoor conditions were inappropriate for testing the coach at full capacity.

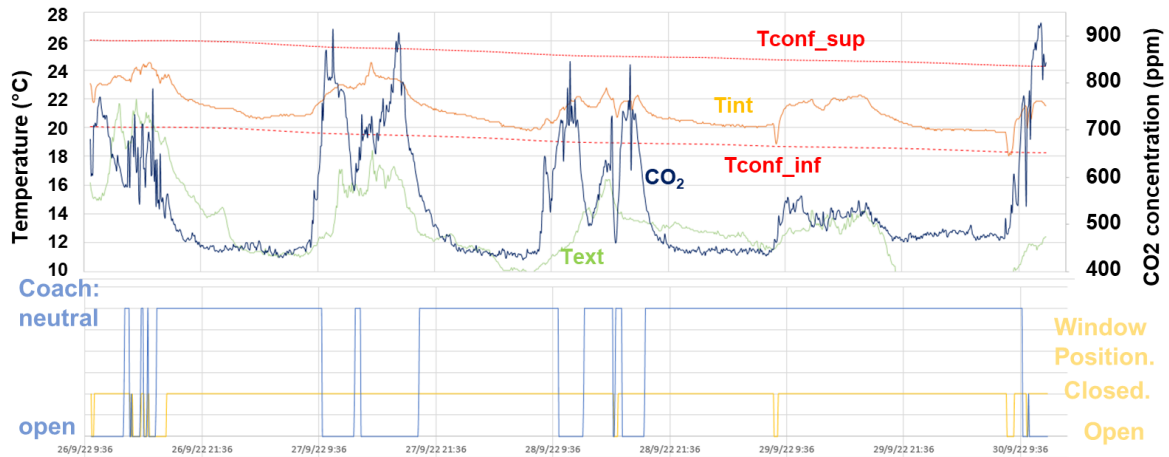


Figure 1 - 1st test of the coaching in a summer week

In parallel, a second version of the prototype has been developed and is shown in Figure 2. This second version will help in qualifying the algorithm during the summer of 2023.

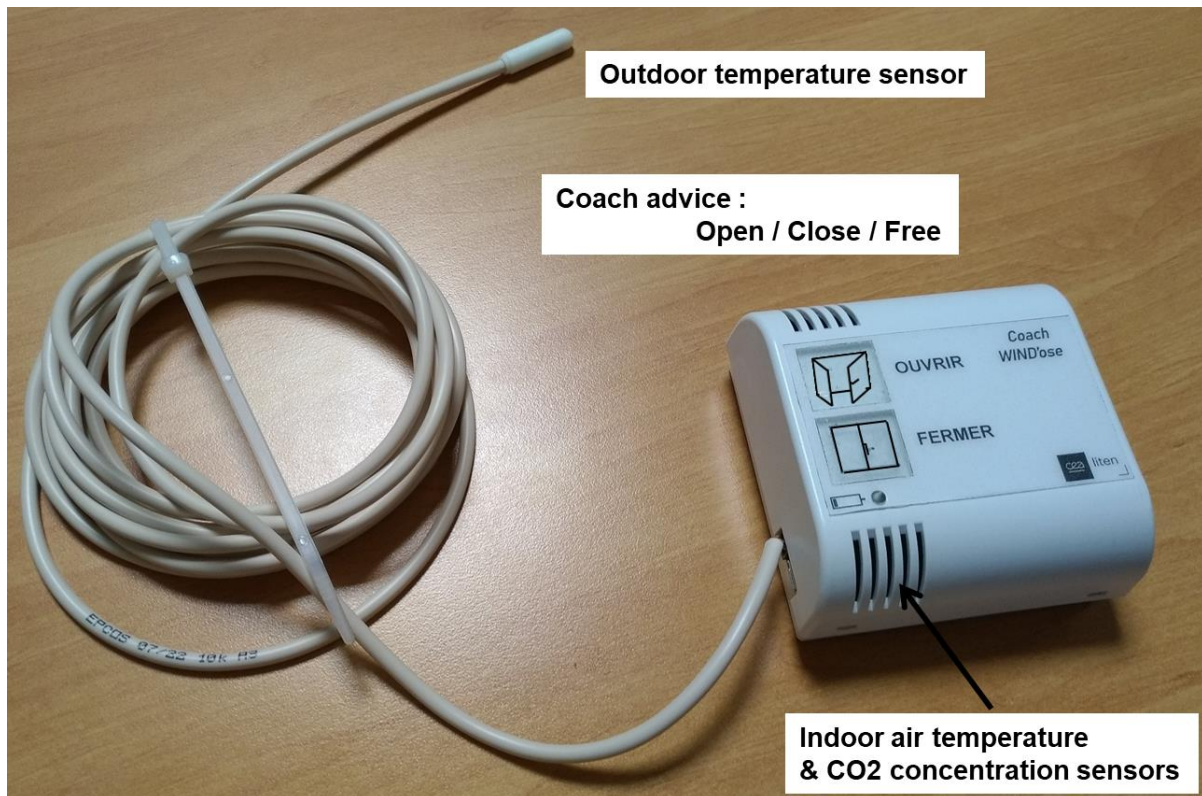


Figure 2: V2 of Wind'Ose prototype

More extended feedback on this coaching tool is necessary to quantify its impact on the three components: Thermal Comfort, IAQ and energy consumption.

1 ACKNOWLEDGEMENT

French Region Auvergne Rhone Alpes supported the project in the scope of the EasyPOC e-fair project.

Towards an alternative cooling: Optimisation of the successive use of the cooling systems from passive to active - Development of design and control strategies of the hybrid cooling

Arnaud Jay*¹, Aurélie Foucquier¹, Maxime Boulinguez^{2,3}, Gwénaëlle Haese⁴,
Simon Thebault⁴, Virginie Chantepie⁵, Jean Castaing Lasvignottes², Maäréva
Payet³, Simon Rouchier⁶, Jean-Marie Caous⁵, and Pierre Constant-Beraud⁵

*1 Univ. Grenoble Alpes, CEA, Liten, INES
73375 Le Bourget du Lac
France*

**Corresponding author: Arnaud.jay@cea.fr*

*2 Laboratoire Physique et Ingénierie Mathématique
pour l'Énergie, l'environnement et le bâtiment
(PIMENT) University of la Réunion, Sainte-Clotilde
97715, La Réunion, France*

*3 LEU Réunion
139, rue Francois Isautier, 97410 Saint-Pierre
Ile de la Réunion, France*

*4 Technical and Scientific Centre for Building,
PULSE Laboratory,
11 rue Henri Picherit 44323 Nantes, France
Corresponding author: gwenaelle.haese@cstb.fr

*5 Bluetek
ZI Nord Les Pins BP 13 - 37230 Luynes
France*

*5 Univ. Savoie-Mont-Blanc - Locie
Boulevard du Lac Léman, 73370 Le Bourget du Lac
France*

ABSTRACT

Due to global warming, severe problems of buildings overheating during summer in temperate and hot climates arise. Thus, there is an increasing use of air conditioning. However, alternative passive and soft cooling systems exist to address comfort and energy savings issues, such as natural ventilation or ceiling fans, that consume less energy. Although they are well-known today, their use remains under-enhanced. CoolDown project, funded by the French National Research Agency (ANR), aims to define the tools and methodology to optimise the successive use of passive, soft and active systems to maximise comfort for occupants while minimising energy consumption in summer, hot seasons or heat waves. The methodology of this project is hereafter presented to achieve two mainly two types of outputs: (1) the definition of metrics to quantify the building potential and performance from thermal comfort and energy perspectives, and (2) the development of tools and algorithms to optimise the coupling of building passive and active cooling systems, both in the design and operation phases.

KEYWORDS

Summer comfort, Mixed mode buildings, Hybrid Cooling Solution, IEQ, Multi-criteria optimised control strategies, Performance Guarantee

1 INTRODUCTION

In the current context of global warming, severe problems of buildings overheating during summer in temperate and hot climates arise. As a result, these hot periods lead to an increase in the use of air conditioning and, thus, to an increase in energy consumption and peak electricity demand at the global scale. However, alternative and original so-called combined passive and soft cooling solutions exist to address both comforts in hot climates and energy savings issues,

such as natural ventilation and ceiling fans that consume much less energy. Furthermore, the COVID-19 crisis highlights the importance of building ventilation with clean air in the foreground of natural ventilation. Some cooling solutions combining passive and low energy (soft) solutions with active, more energy-consuming systems can reduce energy consumption drastically. Nevertheless, although those mixed-mode solutions begin to be well-known today, their uses remain underwhelming in the building field, especially in temperate and tropical climates. To overcome this issue, 5 main scientific and technical barriers have been identified. The first Scientific and Technical Barrier (STB1) lies in a need for knowledge of the actual performance and the impact of the passive and soft cooling solutions and especially their combined uses with active systems (STB2). Moreover, in this notion of performance, both the energy and the comfort aspects are important issues. However, if the quantification of the energy consumed through an indicator is quite easy to reach, it is challenging to quantify and ensure thermal comfort in diverse hot climates considering a mixed-mode cooling solution combining passive, soft and active systems (STB3). Indeed, considerations of comfort are different in according to the cooling system and the occupant habits. It has been notably shown that the occupants' comfort expectancy is much higher when using Air Conditioning (AC) than for Naturally ventilated (NV) buildings. Mixed mode cooling solution being at the edge of those AC and NV ones, comfort should be quantified in accordance. Two other challenges appear then. First, if the energy performance guarantee is largely studied in the state of the art in heating conditions, energy performance guarantee in cooling conditions (STB4) remains less investigated, especially in the presence of natural ventilation and use of ceiling fans providing a consequent air velocity. Second, considering comfort in the verification protocols (STB5) is usually not considered in those works. Finally, the economic and environmental aspects also need to be considered to ensure the potential and consistency of optimised solutions.

The objective of this article is to present the methodology which will be developed during the *CoolDown* project. Its overarching objective is to define tools and methodology to optimise the successive and combined use of passive, soft and active solutions to maximize controlled comfort for occupants while minimising energy consumption in summer, hot seasons or heat waves to face the climate change impact in the Architecture and Engineering Industry (AEC) industry with a focus on existing office buildings.

2 STATE OF THE ART

As mentioned hereabove, the current context of global warming leads to a drastic increase in air-conditioning use and, consequently, energy consumption. Natural ventilation and ceiling fans showed their efficiency as alternative solutions, but their cooling potential tends to be reduced with higher outdoor air temperatures, especially during heat wave periods. Therefore, natural ventilation by itself, even coupled with ceiling fans, may not be sufficient to ensure the comfort of occupants throughout the year. In this context, there is an intermediate solution, defined as mixed cooling (MM: mixed mode cooling) according to the definition of (Brager, 2006). This solution, called *changeover*, is defined as cooling by air conditioning and natural ventilation operating in a differentiated manner on a seasonal or daily basis. In addition, the use of ceiling fans (0.5-2.0 m/s) makes it possible to lower the perceived temperature and consequently delay the turning of the air conditioners and raise the setpoint temperatures of the latter. It is then possible to have a cascade sequence of different solutions (Natural Ventilation, Natural Ventilation + Fan, Fan + Air Conditioning). Unlike naturally ventilated and air-conditioned buildings, the mixed-mode building does not have a dedicated comfort model. More generally, two families of comfort models are today represented in standards and literature. The first contains models based on steady-state heat balance equations, such as the one-node (Fanger, 1970) or the two-nodes (Gagge, 1986) thermal regulation models. They

make it possible to calculate the PMV (Predicted Mean Vote) or SET (Standard Effective Temperature) indices and give a prediction of the comfort felt by the user after a physiological reaction caused by thermal stress (Gao et al., 2015). To do this, they require a multitude of input parameters (radiant and air temperature, airspeed, relative humidity, clothing, metabolism, etc.). The second contains models from satisfaction surveys in a heterogeneous selection in terms of building and location. These are the models of comfort zones on the psychometric diagram, initiated by (Givoni, 1992) and the American (based on the RP-884) and European (based on the SCAT) adaptive models. They put in linear relation the indoor climatic conditions of comfort with outdoor running mean temperature. There are also regional variations in the Chinese (GB/T 2000), Dutch (ISSO74) and Indian (IMAC) standards. These adaptive models emerge from the observation that the thermal sensation votes from the PMV, initially validated in laboratory conditions, were different from the real votes in naturally ventilated buildings where the occupants benefit from a great opportunity for adaptation to restore their comfort. A dichotomy is thus established between comfort model type and building cooling modes in the standards governing comfort in the AEC industry. It should be noted that in the standards, as in the literature, the recommendations are in line with the use of Fanger's PMV-PPD (Predicted Mean Vote, Predicted Percentage Dissatisfied) model in air-conditioned buildings and the Adaptive Model (AM) in naturally ventilated buildings. However, the most common standards, ANSI/ASHRAE Standard 55 (USA), ISO 7730-2009 and EN 16798 (Europe, ex EN 15251) do not mention any real guide for the evaluation of comfort for this type of mixed-mode cooling (Kim et al., 2019; Carlucci et al., 2018). This is particularly true in hot and humid climates which lack research in the field as mentioned (Rodriguez and D'Alessandro, 2019). EN 16798 or IMAC (India) do offer an openness towards the use of the adaptive model for mixed-mode buildings but specifies that it is only valid if no air conditioning system is in operation, which rules out the simultaneous use of fans and air conditioners. Our project will then address this question of the suitable metrics for quantifying the comfort in the presence of a mixed-mode cooling strategy in a large diversity of climates.

At a different comfort complexity level, a new neurophysiological human thermal model based on thermoreceptor responses, the NHTM model, has been developed by (El Kadri et al., 2020) to predict regulatory responses and physiological variables in asymmetric transient environments. The passive system is based on Wissler's model (Wissler, 2018), which is more complex and refined, it simulates heat exchange within the body and between the body and the surroundings. The active system is composed of thermoregulatory mechanisms, i.e., skin blood flow, shivering thermogenesis, and sweating. The skin blood flow model and the shivering model are based on thermoreceptor responses. The sweating model is that of (Fiala et al., 1998) and is based on error signals. This latter has also been used to improve the Gagge model (Vellei et al., 2020). In this project, this model will be implemented, and the results will be compared to the other classic thermal comfort models previously mentioned.

Afterwards, those suitable comfort metrics would be used to feed the mixed-mode cooling control strategies. In the literature, some authors have already proposed intelligent solutions to control cooling systems by combining alternatively an active energy-consuming air-conditioning and a passive natural ventilation device (Emmerich et al., 2006), (Zhai et al., 2011), (Hu et al., 2014), (Chen, 2019). However, the aspect of occupant comfort and the simultaneous use of the different cooling systems should have been considered in those works. Our project is to go further by associating simultaneously the passive, soft and active cooling systems with a double objective of both energy and comfort. To reach the flexibility of the control algorithm, the chosen method will be fuzzy logic. One advantage of this technique resides in the fact that it allows modelling the user behaviour of a system instead of the system itself. Given that, it requires global concepts to describe approximate variables instead of precise numerical values. It provides then a large flexibility of the control algorithm. Some authors have already shown the efficiency of the fuzzy logic for ventilation control (Dounis et

al., 1996), (Eftekhari et al., 2003), (Homod et al., 2014). Our methodology will be built on those works.

Once the mixed-mode control strategies are defined, they will be tested, and the following required stage will consist in the ability to guarantee their performance according to energy and comfort issues. Guarantee the energy performance in buildings is a research topic more and more investigated in the recent years. As shown in the two successive IEA EBA Annex #58 dealing the intrinsic thermal performance of an envelope and #71 focusing on the performance in-use. To estimate the intrinsic performance which is a key point to ensure the quality of the on-site work compared to the design phase, methodologies (co-heating (Bauwens et al., 2014), ISABELE (Thebault et al., 2018), SEREINE, QUB (Ahmad et al., 2020)) are developed to quantify the heat loss of an envelope through conduction and the infiltration flowrate (Jay et al., 2020). This is particularly interesting to estimate the active systems' energy needs, whether hot or cold (Jay et al., 2021). All these methods focus on the energy use performance only. They do not consider the impact of comfort and quantify the relevance of natural ventilation or ceiling fans in the final energy consumption and their impact of the comfort.

3 METHODOLOGY

To define tools and methodology to optimize the combined use of passive, soft and active solutions, *CoolDown* workplan is articulated around 4 pillars (Figure 1). First one will focus on occupant acceptability and comfort followed by some occupant surveys. Second pillar will focus on active cooling systems with the development of a methodology to fine tune their sizing. Third pillar aims at optimizing the combined use of passive, soft and active cooling systems in term of sizing and control strategies. Fourth pillar targets to develop methodology for guaranteeing the actual performance of the hybrid cooling strategies considering occupants' acceptability and energy use. Last but not least, the work developed in this project will be supported by five (5) office buildings in real different climate areas (2 in Auvergne-Rhône-Alpes, 1 in Centre, 2 in La Réunion). These buildings will be used throughout the project, first as a use case for the technical *CoolDown* development and then for alternative solution implementation to get real feedback on their efficiency.

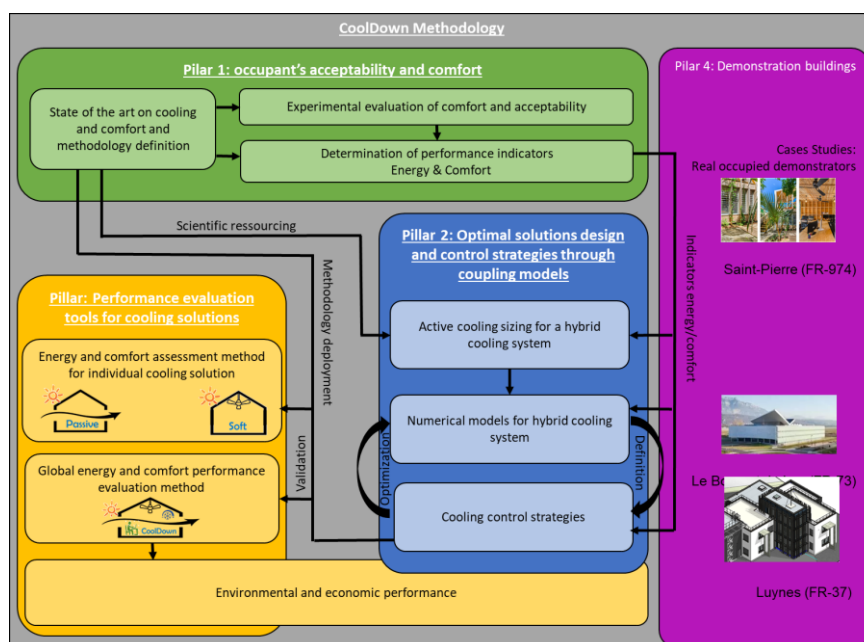


Figure 1: CoolDown methodology

3.1 Occupant acceptability and comfort

The acceptability of the occupants regarding the passive, soft and active cooling solutions is likely to be carried out by using a survey on a sample of a thousand people representative of the mainland and French outermost tropical population, by means of a telephone survey. This sampling will include a sample of occupants of non-equipped and equipped buildings. It will also integrate oversampling in regions experiencing recurrent episodes of high heat to anticipate future behavior induced by the effects of climate change.

Several experimental campaigns will be carried out in demonstrator buildings to obtain a first set of data corresponding to the initial state of the occupant's comfort. Twenty occupants' thermal comfort will be assessed using objective physiological measurements (skin temperature and heart rate) and declarative sensory questionnaires about their perceived thermal comfort. For each campaign, physiological and sensory responses will be recorded for one week for each participant, in a real occupied demonstrator in La Réunion. Their environment will also be monitored (temperature, humidity, radiation). This data set will contribute to building and optimising a thermal comfort prediction model, which will be validated with the data from a second set of experimental campaigns testing the optimized hybrid cooling solutions as described in *Figure 2*.

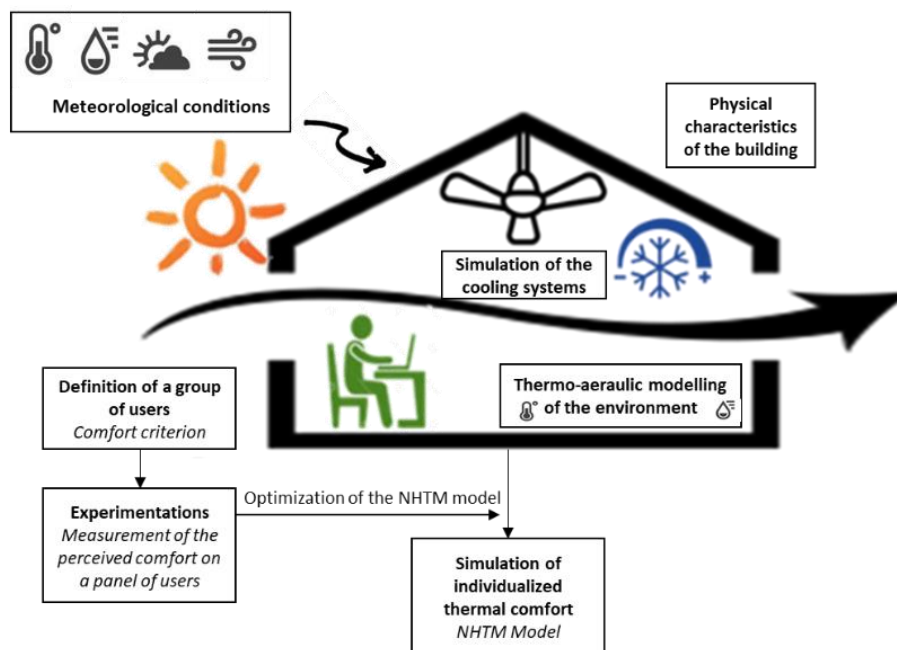


Figure 2: occupant acceptability surveys and model development process

3.2 Optimal solutions design and control strategies through coupling models

The project will target the optimization of the combined use of passive, soft and active cooling systems in term of sizing and control strategies. Better knowledge of active cooling system behaviour, flexibility, and complementarity regarding additional passive and soft modes are also studied. To do so, this task will combine numerical and laboratory experimentations with implementing and validating a hybrid cooling numerical model. To develop it as accurate as possible, numerical barriers appear through the choice and the coupling of the passive, soft and active cooling system sub-models. Furthermore, considering the metrics defined in the first axis, the mathematical optimization of the hybrid system sizing and control strategies will also be a major challenge.

STEP 1 : IMPLEMENTATION OF NUMERICAL MODELS FOR EACH COOLING MODE

Scientific challenges :

- In-situ less-informative measures
- Air velocity consideration without measure
- Transition from active cooling to fan or natural ventilation

Methods :

- Black box :
 - ❑ Linear or polynomial regression
 - ❑ SVR (support vector regression)
 - ❑ Neural networks
- Grey box : calibration
 - ❑ Meta-heuristic algorithms
 - ❑ Bayesian to deal with the uncertainties
 - ❑ Extended Kalman filter to deal with the non-linearities
- Mathematical identifiability :
 - ❑ Structural (Fischer matrix)
 - ❑ Practical through sensitivity analysis (Morris, RBD-FAST, SRC, Sobol)

looss and Lemaitre, 2014

STEP 2 : COOLING EFFICIENCY PREDICTION

Scientific challenges :

- Multi-criteria
- Generalisation of the indicators
- Comfort evaluation

Methods :

- State of the art on comfort models implemented in the first pillar of the COOL-DOWN project

Carlucci et al., 2018

- Comfort campaigns (ASHRAE June 2022, project demonstrators)

Outputs of the cooling models

Predictive models for indicators of characterisation and efficiency of the cooling

Resulting indicators

Predicted input data

- CO2 emitted by the electrical network
- Weather data
- Electrical network stress

STEP 3 : CONTROL

Scientific challenges :

- 5 modes
- 5 criteria
- Embedded control

Methods :

- Fuzzy logic algorithm for final command

Chevrie and Guely, 1998

Multi-objective and multi-mode embedded control

Objectives :

- Comfort,
- Energy,
- CO2,
- Electrical network stress
- Short circuit


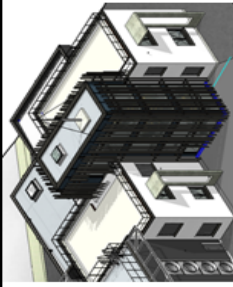
- Mathematical optimisation with meta-heuristic (PSO, NSGA, recuit simulé,...)

3.3 Performance evaluation tools for cooling solutions

Fourth pillar of *CoolDown* lies on performance assessment of the cooling solutions to ensure that the *CoolDown* solutions are efficient and to characterise their cooling potential and real performance. First, a work focuses on choosing and defining indicators to this end, then develops or adapting methodologies to measure and quantify these indicators. A two steps approach is foreseen. First indicators and methodologies are studied for standalone solutions including natural night ventilation, solar aperture, thermal inertia, and fans. Then, work is carried out on global methodologies and common indicators for the *CoolDown* solutions mixing different cooling modes. The target is to keep light monitoring strategies to replicate these methodologies at a large scale.

3.4 Case study to be used

Development and tests done in the other pillar of the project will be supported by four real occupied offices situated in different climate areas: Savoie (73), Indre et Loiret (37) and La Réunion (974). These buildings will first feed the other tasks as test cases thanks to the available monitored data and buildings characteristics to build on numerical models of these use cases. Following the results from Finally, each development will be implemented in at least one of the demonstrators to qualify its feasibility or quantify its impact.

	#1 La Reunion – Agence COArchitectes	#2 Mayotte Collège de Bouéni	#3 Hélios INES	#4 Bluetek
Picture				
Responsible partner // Crédit Photo	LEU Réunion//@Yannick Ah-Hot	LEU Réunion // LAB Réunion	CEA // CEA	Bluetek // Cub Architecture
Year built	Before 1980 – refurbishment 2017	2019	2014	2022
Position	Saint-Pierre 974	Bouéni, Grande Terre, Mayotte	Le Bourget du Lac (73)	Luynes (37)
Climate	Koppen Tropical dry savanna (As)	Koppen Tropical wet savanna (Aw)	Koppen (Cfb) RE2020: H1c	Koppen (Cfb) RE2020: H2b
Surface	150 m ²	5536 m ²	7000m ²	200m ²
Usage	Architecture offices	Middle school + Admin. Offices	Offices + Labs + Training rooms	Offices + conf. room + staircase
Cooling solutions	Openspace, Single Office, Meeting Room: AC + Fan + NV + double sided window doors openings Double Office : Fan + NV + Jalousies + louvers	We will only consider administration offices which is designed along a ventilation open atrium and benefits from AC and Ceiling fans. All opening are jalousie type.	In offices : Natural convection controlled manually with specific windows and jalousies in the offices Openings in the Atrium Automatic vertical shading	Natural ventilation manually activated but with notifications from a control system. Geothermal cooling. The building is designed from wind driven natural ventilation. The staircase is automated.
Monitoring	Temperature, Humidity, Energy Use, fan behaviour (from Mai 2022)	To be installed. Well known building as LEU Reunion is part of the design team	Part of the offices are monitored in term of temperature and occupants comfort thanks to a dedicated	Energy, temperature, Humidity, CO2, presence detector, Illuminance.

4 CONCLUSIONS

Centred on three different challenges of an innovative cooling solution among the comfort evaluation, the control and the performance guarantee, the *CoolDown* project will address efficiency and energy performance cooling strategies. Specifically, the objective of this project is to implement a cooling solution leading to energy savings by limiting the use of the air conditioning while providing optimal thermal comfort. To do so, three cooling modes will be employed with passive, soft and active systems. The passive mode will mainly be linked to natural ventilation through dedicated large openings. Concerning the soft solution, it will be reached by using fans (mainly ceiling fans in tropical climates). And finally, the active cooling will consist of an air conditioning system. Based on both comfort and energy considerations, a successive mode control strategy will be implemented to maximize the efficiency and performance of building cooling.

5 ACKNOWLEDGEMENTS

The project *CoolDown* is funded by ANR under the number ANR-22-CE22-0014-06

6 REFERENCES

- Ahmad, N., Ghiaus, C., & Thiery, T. (2020). *Influence of Initial and Boundary Conditions on the Accuracy of the QUB Method to Determine the Overall Heat Loss Coefficient of a Building*. *Energies*, 13(1), 284.
- Attia, S. (2015). *Impact of different thermal comfort models on zero energy residential buildings in a hot climate*. *Energy and Buildings*, 102, 1-5.
- Bauwens, G., & Roels, S. (2014). *Co-Heating Test: A State-of-the-Art*. *Energy and Buildings*, 82, 163-172.
- Bouchié, R., Alzetto, F., Brun, A., Boisson, P., & Thebault, S. (2014). *Short methodologies for in-situ assessment of the intrinsic thermal performance of the building envelope*. Sustainable Places, Nice.
- Brager, G. (2006). *Mixed-mode cooling*.
- Carlucci, S., Bai, L., de Dear, R., & Yang, L. (2018). *Review of Adaptive Thermal Comfort Models in Built Environmental Regulatory Documents*. *Building and Environment*, 137, 73-89.
- Chen, Y., & Z. T. (2019). *Achieving natural ventilation potential in practice: Control schemes and levels of automation*. *Applied Energy*, 235, 1141-1152.
- Chen, W., Zhang, H., Arens, E., Luo, M., Wang, Z., Jin, L., et al. (2020). *Ceiling-fan-integrated air conditioning: Airflow and temperature characteristics of a sidewall-supply jet interacting with a ceiling fan*. *Building and Environment*, 171, 1-10.
- Day, J. K., McIlvennie, C., Brackley, C., Tarantini, M., Piselli, C., Hahn, J., et al. (2020). *A review of select human-building interfaces and their relationship to human behavior, energy use and occupant comfort*. *Building and Environment*, 178, 1-14.

- Dounis, A. I., & Balaras, M. (1996). *Indoor Air-Quality Control by a Fuzzy-Reasoning Machine in Naturally Ventilated Buildings*. *Applied Energy*, 54, 11-28.
- Eftekhari, M. M., & Dascalaki, E. G. (2003). *Application of fuzzy control in naturally ventilated buildings for summer conditions*. *Energy and Buildings*, 35, 645-655.
- El Kadri, M., De Oliveira, F., Inard, C., et al. (2020). *New neurophysiological human thermal model based on thermoreceptor responses*. *International Journal of Biometeorology*, 64, 625-639.
- Emmerich, S. J. (2006). *Simulated performance of natural and hybrid ventilation systems in an office building*. *HVAC & R Research*, 12, 975-1004.
- Erba, S., Sangalli, A., & Pagliano, L. (2019). *Present and future potential of natural night ventilation in nZEBs*. *IOP Conference Series: Earth and Environmental Science*, 296, 1-6.
- Fiala, D. (1998). *Dynamic simulation of human heat transfer and thermal comfort (PhD dissertation)*. Institute of Energy and Sustainable Development, De Montfort University Leicester.
- Fanger, P. O. (1970). *Thermal comfort: Analysis and applications in environmental engineering*. New York: McGraw-Hill.
- Gagge, A. P., Fobelets, A. P., & Berglund, L. G. (1986). *A standard predictive index of human response to the thermal environment*. *ASHRAE Transactions*, 92(part 2B), 709-731.
- Gao, J., Wang, Y., & Wargocki, P. (2015). *Comparative Analysis of Modified PMV Models and SET Models to Predict Thermal Comfort*. *Building and Environment*, 92, 200-208.
- Givoni, B. (1992). *Comfort, climate analysis and building design guidelines*. *Energy and Buildings*, 18, 11-23. doi:10.1016/0378-7788(92)90047-K
- Homod, R. Z., & Shuayb, K. S. (2014). *Energy saving by integrated control of natural ventilation and HVAC systems using model guide for comparison*. *Renewable Energy*, 71, 639-650.
- Hu, J., & Kang, P. (2014). *Model predictive control strategies for building with mixed-mode cooling*. *Building and Environment*, 71, 233-244.
- Jay, A., Brun, A., Thebault, S., & Foucquier, A. (2020). *Dynamic infiltration airflow rate measurement thanks to tracer gas method: a case study at a dwelling scale*. In 15th ROOMVENT Conference, Torino.
- Jay, A., Fares, H., Rabouille, M., Oberle, P., Thebault, S., Challansonnex, A., & Anger, J. (2021). *Evaluation of the intrinsic thermal performance of an envelope in the summer period*. *Journal of Physics: Conference Series*, 2069(1), 012093.
- Johnston, D., Miles-Shenton, D., Farmer, D., & Wingfield, J. (2013). *Whole House Heat Loss Test Method (Coheating)*.

- Kim, J. T., Lim, J. H., Cho, S. H., & Yun, G. Y. (2015). *Development of the Adaptive PMV Model for Improving Prediction Performances*. *Energy and Buildings*, 98, 100-105.
- Marc, O., Anies, G., Lucas, F., & Castaing-Lasvignottes, J. (2012). *Assessing performance and controlling operating conditions of a solar driven absorption chiller using simplified numerical models*. *Solar Energy*, 86, 258-269.
- Payet, M., David, M., Lauret, P., Amayri, M., Ploix, S., & Garde, F. (2022). *Modelling of Occupant Behaviour in Non-Residential Mixed-Mode Buildings: The Distinctive Features of Tropical Climates*. *Energy and Buildings*, 259, 111895.
- Rodriguez, C. M., & D'Alessandro, M. (2019). *Indoor Thermal Comfort Review: The Tropics as the Next Frontier*. *Urban Climate*, 29, 100488.
- Thébault, S. (2017). *Contribution à l'évaluation in situ des performances d'isolation thermique de l'enveloppe des bâtiments (Doctoral dissertation)*. INSA de Lyon.
- Thébault, S., & Bouchié, R. (2018). *Refinement of the ISABELE method regarding uncertainty quantification and thermal dynamics modeling*. *Energy and Buildings*, 178, 182-205.
- Thébault, S., & Bouchié, R. (2015). *Estimating infiltration losses for in-situ measurements of the building envelope thermal performance*. *Energy Procedia*, 78, 1756-1761.
- Vellei, M., Herrera, M., Fosas, D., & Natarajan, S. (2017). *The Influence of Relative Humidity on Adaptive Thermal Comfort*. *Building and Environment*, 124, 171-185.
- Vellei, M., & Le Dréau, J. (2020). *On the Prediction of Dynamic Thermal Comfort under Uniform Environments*. *Conference WINDSOR*, 17, 1-6.
- Wissler, E. H. (2018). *Human temperature control: A quantitative approach (Doctoral dissertation)*. The University of Texas at Austin, Department of Chemical Engineering.
- Zhai, Z. J., & H. J. (2011). *Assessment of natural and hybrid ventilation models in whole-building energy simulations*. *Energy and Buildings*, 43, 2251-2261.

Introduction to IEA EBC Annex 78

Bjarne W. Olesen and Pawel Wargocki

*Intl. Centre for Indoor Environment and Energy
Technical University of Denmark
Nils Koppels Allé, Building 402
2800 Kgs. Lyngby, Denmark
Corresponding author: bwol@dtu.dk

SUMMARY

International Energy Agency (IEA) Annex 78 was launched in 2018. The title of the Annex is “Supplementing Ventilation with Gas-phase Air Cleaning, Implementation, and Energy Implications.” The objective of the Annex is to bring researchers and industry together to investigate the possible energy benefits of using gas-phase air cleaners (partial substitute for ventilation) and establish procedures for improving indoor air quality or reducing the prescribed ventilation rates by gas-phase air cleaning; a test method for air cleaners that considers perceived air quality ratings is also included in the activities with the potential of developing a new standard.

KEYWORDS

Air Cleaning; Gas-phase; Energy; Standard; Clean air delivery rate

1 INTRODUCTION

Ventilation accounts for approximately 20% of the global energy use for providing an acceptable indoor environment. The requirements for ventilation in most standards and guidelines assume acceptable quality of (clean) outdoor air. Worldwide, there is an increasing number of publications related to air cleaning and there is also an increasing sale of gas phase air cleaning products. This puts a demand for verifying the influence of using air cleaning on indoor air quality, comfort, well-being, and health. It is thus important to learn whether air cleaning can supplement ventilation with respect to improving air quality i.e., whether it can partly substitute the ventilation rates required by standards. Finally, the energy impact of using air cleaning as supplement of ventilation needs to be estimated. This topical session will provide an introduction to the objective/scope, activities, and intended outputs of the annex.

2 MAIN ACTIVITIES

The annex comprises five subtasks, and their activities are described in the following sections.

2.1 Subtask A: Energy benefits using gas phase air cleaning

The subtask aims at quantifying the energy performance of using air cleaning as part of the ventilation requirements. The baseline for calculating the energy benefits is the energy used to heat/cool the required ventilation air and the electrical energy to drive the fans. Possible energy reduction by decreasing the amount of outside air by use of air cleaning will be studied. The subtask will also establish a metric of assessing air cleaner efficiency in relation to energy: CADR/kWh where CADR is the clean air delivery rate

2.2 Subtask B: How to partly substitute ventilation by air cleaning.

This subtask will analyse how air cleaning can partly substitute for ventilation. Existing standards for IAQ-Ventilation and for testing air cleaners will be investigated. Measurement of perceived air quality and chemicals will be studied.

2.3 Subtask C: Selection and testing standards for air cleaners.

The main criteria for establishing required ventilation rates are based on perceived air quality. This subtask focuses on the need for standard testing procedures for air cleaners.

2.4 Subtask D: Performance modelling and long-term field validation of gas phase air cleaning technologies

The subtask will include activities like review of available models for predicting the performance of gas phase air cleaning technologies and perform long term field experiments to validate the selected gas phase air cleaning technologies.

2.5 Subtask E: Gas Phase Air cleaning Technologies

3 INTENDED OUTPUTS AND TARGET AUDIENCE

All subtasks will provide input to the final deliverables A-E

A: Energy benefits using gas phase air cleaning: A method for predicting the energy performance of gas phase air cleaning technologies and the possible reduction of energy use for ventilation. This will be of interest for consultants, manufacturers, government building codes in the goal to design and operate near zero energy buildings

B: How to partly substitute ventilation by air cleaning: A validated procedure for supplementing (partly substituting) required ventilation rates with gas phase air cleaning. This will be of interest for standards and guidelines setting requirements for indoor air quality and ventilation. This will also be of significant interest for manufacturers of air cleaning technologies

C: Selection and testing standards for air cleaners: A test method for air cleaning technologies that besides chemical measurements include perceived air quality as a measure of performance. This will be of interest for standard bodies writing test standards (ISO TC142/ CEN TC 195 and ISO TC 146) and related certification bodies. This will also be of significant interest for manufacturers of air cleaning technologies.

D: Performance modelling and long-term field validation of gas phase air cleaning technologies: A report on the long-term performance of air cleaning and model for the performance of gas phase air cleaning technologies. This will also be of significant interest for manufacturers, consultants, standard writing experts.

4 REFERENCES

- IEA EBC, Annex 78 - Supplementing Ventilation with Gas-phase Air Cleaning, Implementation and Energy Implications, Accessed 18-02-2020, <https://annex78.iea-ebc.org>.
- ISO 17772-1 2018 Part 1: Indoor Environmental Input Parameters for the Design and Assessment of Energy Performance in Buildings, ISO, Geneva, 2017.
- ISO 17772-2 2018: Part 2: Guideline for Using Indoor Environmental Input Parameters for the Design and Assessment of Energy Performance of Buildings., ISO, Geneva, 2018.
- Kolarik and Wargocki: Can a photocatalytic air purifier be used to improve the perceived air quality indoors? *Indoor Air* 2010;20, 255-262.
- Lei Fang, Pawel Wargocki, Adam Targowski, Toshio Tanaka, Kenkichi Kagawa, 2011, Performance of a Non-Thermal Plasma Air Purifier Examined with Sensory Assessments of Air Quality, 12th Int. Conf. on Indoor Air Quality and Climate.

Air Cleaner as an Alternative to Increased Ventilation Rates in Buildings: A Simulation Study for an Office

Alireza Afshari*¹, Alessandro Maccarini¹, Göran Hultmark¹

*1 Department of the Built Environment (BUILD)
Aalborg University
A. C. Meyers Vænge 15, 2450, Copenhagen Denmark*

SUMMARY

1 INTRODUCTION

Indoor air pollution is a significant concern due to its adverse effects on human health and productivity. With people spending most of their time indoors, exposure to indoor air contaminants can lead to various health issues, including respiratory problems, cardiovascular diseases, and even an increased risk of lung cancer and premature mortality. Additionally, poor indoor air quality can result in short-term symptoms like headaches, eye and throat irritation, fatigue, and asthma, impacting workplace productivity and absenteeism. To address these challenges, this study explores the potential of advanced air cleaner technology as an alternative to increased ventilation rates in buildings, focusing on an office environment.

2 BACKGROUND

The study begins by highlighting the sources of indoor air pollution, including outdoor pollutants from fossil fuel burning and waste incineration, as well as indoor sources such as cleaning products and biological activities. To enhance indoor air quality, traditional approaches involve using supply air filters in ventilation systems and reducing indoor pollutant sources while increasing outdoor air ventilation. However, this study investigates different air filtration methods, including central HVAC filters, room air cleaners, and combined active chilled beams with filters, to effectively remove both particulate and gaseous pollutants (Pope and Dockery, 2006), (Manisalidis et al., 2020).

3 DESIGN AND BUILDING MODEL

The research adopts a representative building model of a typical office room located on a middle floor of a high-rise building. The room has specific dimensions, and its surfaces are considered adiabatic, except for the south-oriented facade with a window. Shading devices are incorporated to block incoming solar radiation when it exceeds a certain threshold. The study includes hourly profiles for occupancy, appliances, and lighting to represent user behavior and internal heat gains. The building's heating and cooling system is designed to maintain a comfortable indoor air temperature within a specific range.

4 SYSTEM MODELS

Four different HVAC system configurations are implemented and evaluated in the study:

Reference case: A typical office ventilation system with a heat recovery unit, a heating coil, and supply and return fans. The system delivers outdoor air to the office room and maintains a specific air temperature.

4.1 System-based filter

A filter is integrated at the system level, allowing for lower outdoor air flow rates by filtering and recirculating return air from the room. This configuration reduces the need for larger ducts and offers potential energy savings. Room-based filter: A filter is placed at the room level, and air is filtered within the room using a small fan. Although this approach is less efficient in terms of fans, it offers localized air cleaning benefits.

Beam-based filter: A filter is incorporated into an active chilled beam unit, where room air is filtered by the device integrated into the beam. This system provides efficient recirculation of air through induction, resulting in energy savings.

5 RESULTS

The study presents the results of the four HVAC system configurations, focusing on their total primary energy use. Comparing the cases, the integration of a filter in the beam unit resulted in primary energy savings of approximately 26% compared to the reference case. The room-based and beam-based filter systems have similar energy demands for space heating, while the reference case requires slightly more energy due to the lack of air recirculation. For space cooling, the room-based and beam-based filter systems have higher energy demands, while the reference case has the lowest energy demand due to higher outdoor air supply. The system using filters has the lowest energy demand for the heating coil, while the reference case has the highest.

6 CONCLUSION

The study concludes that air cleaning technologies, such as portable air cleaners or combined chilled beams with air cleaners, can be effective solutions for mitigating indoor air pollution and improving air quality in specific rooms. However, it emphasizes the importance of considering energy performance when selecting air cleaners and ventilation systems for indoor environments. The appropriate choice of air cleaner and ventilation system can significantly impact energy efficiency and indoor air quality. The integration of filters in the HVAC system, particularly in active chilled beam units, demonstrates notable energy savings. Overall, the research provides valuable insights into optimizing indoor air quality while maintaining energy efficiency in office buildings. Please use the spell-check and grammar check before submitting your summary.

KEYWORDS

Air cleaning, Ventilation rate, Building, Simulation, Office

7 ACKNOWLEDGEMENTS

The project is financed by Aalborg University.

8 REFERENCES

Pope C. A. and Dockery, D. W. (2006) *Health effects of fine particulate air pollution: Lines that connect*, Journal of the Air and Waste Management Association, vol. 56, no. 6, pp. 709–742, 2006.

Manisalidis, E. Stavropoulou, A. Stavropoulos, and E. Bezirtzoglou, (2020) *Environmental and Health Impacts of Air Pollution: A Review*, Frontiers in Public Health, vol. 8, no. February, pp. 1–13, 2020.

Exploring the Energy-Saving Benefits of Gas-Phase Air Cleaning in Nordic Buildings

Sasan Sadrizadeh

KTH Royal Institute of Technology, Stockholm, Sweden

Mälardalen University, Västerås, Sweden

SUMMARY

This manuscript discusses the energy-saving benefits of gas-phase air cleaning in Nordic buildings. Ventilation systems are crucial in creating a healthy and comfortable indoor environment. These systems account for around 30% of building heat losses in cold climate regions. Indoor emissions from materials, occupants, and outdoor pollutants are key to ensuring acceptable indoor air quality levels. Therefore, this study focuses on using gas-phase air cleaning technologies in low-energy centralized air handling units. By simulating the heating performance of a typical residential and office building in central Sweden, we examine the impact of indoor air recirculation rates and air changes per hour on heating demand and indoor gaseous air pollution concentration. The results indicate that indoor air recirculation can reduce heating demand by approximately 10% for residential buildings and 20% for office buildings while maintaining acceptable indoor air quality.

KEYWORDS

Gas-phase air cleaning, Energy-saving benefits, Nordic buildings, Indoor air quality, Heating demand

1 INTRODUCTION

Meeting indoor air quality requirements and reducing indoor pollutants are crucial for ensuring a healthy and comfortable indoor climate for building occupants [1]. Heating, ventilation, and air-conditioning (HVAC) systems play a vital role in achieving these goals, but their configuration depends on factors such as building type, resident requirements, and climate conditions [2]. The transformation of the building sector towards zero-energy buildings that prioritize occupants' health, comfort, and productivity aligns with the United Nations' Sustainable Development Goals [3]. Ventilation accounts for approximately 9% of total primary energy use in some countries, with residential buildings in the U.S. consuming 30% of their energy for ventilation, heating, cooling, and domestic hot water needs [4]. However, increasing building airtightness has increased the significance of ventilation energy use, as well as the concern for carbon dioxide emissions [4, 5]. In order to reduce energy use to heat the ventilated air in cold climates, strategies such as improving building envelope airtightness, heat recovery, and preheating outdoor air have been implemented [6, 7]. However, these strategies can lead to increased concentrations of pollutants and the need for air-cleaning technologies. Integrating air cleaners into ventilation systems can improve indoor air quality and energy efficiency [8].

Nevertheless, optimization is required to balance parameters such as filtration pressure losses, fan power demand, and heating or cooling requirements [9]. The impact of ventilation rates, filter performance, and air exchange effectiveness on indoor air quality and energy usage in buildings has been studied [10].

This study aims to investigate the impact of recirculation rates on the energy usage of centralized air handling units (AHU) and buildings' heating demand in the central Swedish climate.

2 METHOD

To conduct our analysis, we used the TRNSYS software to perform annual transient simulations and assess variables. Additionally, a MATLAB code analyzed TVOC and CO₂ concentrations based on the building requirements modeled in TRNSYS. The study covered both residential and office buildings. Furthermore, we assessed the impact of implementing gas-phase air cleaners without a heat recovery system. More details can be found in an article by Nourozi et al. [11].

3 RESULTS AND DISCUSSIONS

Residential buildings with a heat recovery ventilation (HRV) system showed lower heating energy demand than those without. Recirculating indoor air had no significant effect on heating demand, with the energy requirement remaining unchanged. However, without heat recovery, the heating demand decreased by 3% increments for each 20% increase in the recirculation rate. In office buildings, the heating energy demand decreased with higher recirculation rates due to higher air change rates per hour (ACH). A 20% increase in the recirculation rate resulted in an approximately 8% reduction in energy demand. Gas-phase air cleaning and increased recirculation rate reduced heating demand for buildings without heat recovery. The effectiveness of heat recovery systems can vary

based on heat recovery efficiency and different building types. Real-time monitoring of air pollutants can optimize recirculation schedules.

Indoor CO₂ concentration was mainly influenced by outdoor concentration, with the occupancy rate having a minor effect. The recirculation rate had a negligible impact on indoor CO₂ concentration when outdoor concentration outweighed indoor sources.

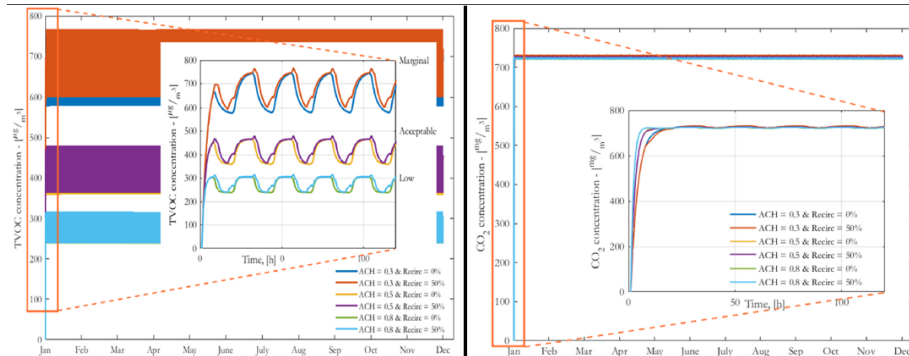


Figure 1: Impact of recirculation rate on TVOC and CO₂ concentration for different ACH values [11].

To conclude, using air cleaners as an extension to the building ventilation system can lead to energy savings and improved indoor air quality. Additionally, increasing the recirculation rate during rush hours in the mornings and evenings maintained CO₂ concentrations within acceptable ranges. In buildings without effective ventilation systems, gas-phase air cleaning and increased recirculation can be valuable strategies to optimize energy efficiency and indoor air quality.

4 ACKNOWLEDGEMENTS

This study contributes to the "IEA EBC Annex 78 - Supplementing Ventilation with Gas-phase Air Cleaning, Implementation, and Energy Implications" project. The financial support from the Swedish Energy Agency (Grant No. P50403-1) is greatly appreciated.

5 REFERENCES

[1] M. Liddament, A guide to energy efficient ventilation, *Phys. Rev. B* 51 (1996) 274.

[2] ASHRAE Environmental Health Position Document Committee, ASHRAE position document on infectious aerosols, *Ashrae* (2020) 1–24.

[3] A/RES/70/1 - Transforming Our World: the 2030 Agenda for Sustainable Development Goals (SDGs), 2021.

[4] F.M. Jesús, P.C. Irene, G.L.R. Alonso, et al., Methodology for the study of the envelope airtightness of residential buildings in Spain: a case study, *Energies* (2018) (2018) 704, 2018; 11:704.

[5] O.A. Seppänen, Association of ventilation rates and CO₂ concentrations with health and other responses in commercial and institutional buildings, *Indoor Air* (1999) (1999) 226–252.

[6] B. Nourozi, *Sustainable Building Ventilation Solutions with Heat Recovery from Waste Heat*, 2019.

[7] B. Nourozi, A. Ploskić, Y. Chen, et al., Heat transfer model for energy-active windows – an evaluation of efficient reuse of waste heat in buildings, *Renew. Energy* 162 (2020) 2318–2329.

[8] Y. Zhang, J. Mo, Y. Li, et al., Can commonly-used fan-driven air cleaning technologies improve indoor air quality? A literature review, *Atmos. Environ.* 45 (2011) 4329–4343.

[9] ANSI/ASHRAE Standard 52.2-2007, Method of Testing General Ventilation Air-Cleaning Devices for Removal Efficiency by Particle Size, 2007.

[10] H. Willem, E.L. Hult, T. Hotchi, et al., Ventilation Control of Volatile Organic Compounds in New U.S. Homes: Results of a Controlled Field Study in Nine Residential Units, 2013, pp. 1–64.

[11] B. Nourozi, et al. "Heating energy implications of utilizing gas-phase air cleaners in buildings' centralized air handling units." *Results in Engineering* 16 (2022): 100619.

Gas phase air cleaning effects on ventilation energy use and indicators for energy performance

Dragos-Ioan Bogatu^{*}, Ongun B. Kazanci, Bjarne W. Olesen

International Centre for Indoor Environment and Energy – ICIEE, Department of Environmental and Resource Engineering, Technical University of Denmark

*Nils Koppels Allé, Building 402
2800 Kgs. Lyngby, Denmark*

**Corresponding author: drabo@dtu.dk*

ABSTRACT

Gas-phase air cleaners can be used to either reduce occupant dissatisfaction for the same outdoor air flow rate or to reduce the outdoor air flow rate for the same resulting occupant satisfaction based on its clean air delivery rate (CADR). The latter lowers the required ventilation rate for the same indoor air quality and can thus lead to a reduction in energy use for preheating/cooling and from transporting the outside air. However, there is no current method or metric for determining the energy benefit of installing a portable air cleaner. This study aimed to establish a framework and metric for assessing air cleaner efficiency in relation to energy use. The investigated gas-phase air cleaner (GPAC) represented a stand-alone (portable) unit equipped with an active carbon filter. In order to evaluate the proposed metric human subject experiments were conducted to investigate the effect of a gas-phase air cleaner on perceived air quality. The purpose of the experiment was to determine the CADR as a function of the percentage of subjects dissatisfied. The experiments were complemented by building energy simulations which were used to estimate the annual energy use for heating, cooling, and transporting the outside air (fan energy). A CADR of approximately 50% (12 L/s) was identified when the pollution source was only represented by building emissions and a CADR of approximately 30% (9 L/s) was found when both bio-effluents and building emissions represented the pollution source. The proposed indicator, clean air efficiency (CAE), can be used to compare different solutions used for providing clean air into the space. Based on the results shown for an air handling unit (AHU) and a stand-alone GPAC for Copenhagen, Denmark - dominated by a high heating load - the GPAC was a viable solution, i.e. higher CAE, only if the AHU was not equipped with a heat exchanger. The GPAC was also more efficient if both bio-effluents and building emissions were present as pollution sources.

KEYWORDS

KPI, air cleaner, ventilation, energy use, CADR

1 INTRODUCTION

Gas-phase air cleaning can be used to improve the Indoor Air Quality (IAQ) by removing gaseous pollutants with negligible effect on indoor CO₂ concentration (Zhang et al. 2011). They can be characterized by their clean air delivery rate (CADR), a measure for clean air delivery efficiency (Afshari et al. 2021).

A gas-phase air cleaner (GPAC) can be used to either reduce occupant dissatisfaction for the same outdoor air flow rate or to reduce the outdoor air flow rate for the same resulting occupant satisfaction based on its CADR. The former would lead to an improved air quality in polluted buildings (Bogatu, Kazanci, and Olesen 2021). The latter lowers the required ventilation rate for the same IAQ and thus reduces the energy use for preheating/cooling and from transporting the outside air (Bogatu et al. 2021; IEA EBC 2019).

Although air cleaners can be compared as a function of their ability to delivery clean air, i.e. as a function of their CADR, there is no current method or metric for determining the reduction in

energy use obtained by installing a stand-alone air cleaner. This study aims to establish a framework and metric for assessing air cleaner efficiency in relation to energy use. The metric could potentially be used for comparing the effectiveness of an air cleaner relative to another method, e.g. all-air system, for transporting clean air into the space.

2 METHODS

In order to evaluate the proposed metric, human subject experiments were used to investigate the effect of a gas-phase air cleaner on the perceived air quality. The purpose of the experiment was to determine the CADR as a function of the percentage of subjects dissatisfied. The experiments were complemented by building energy simulations which were used to estimate the annual energy use for heating, cooling, and transporting the outside air (fan energy). The investigated GPAC represented a stand-alone (portable) unit equipped with an active carbon filter.

2.1 Clean air delivery rate

In the experiments, two scenarios were investigated, one where either both bio-effluents and building emissions or only building emissions were used as pollution sources (Hu 2023). Three human subjects were used as sources for bio-effluents and old linoleum as building emissions. The room temperature was 23 °C and the relative humidity (RH) was 50%. Experiments were made for outdoor air supply rates of 2.5, 4.0, 7.0, and 10.0 L/s per non-adapted person as recommended in EN 16798:1-2019 (CEN 2019). When human subjects were used as emissions sources and the air cleaner was employed, an outdoor air supply rate of 4 L/s per person was used while the number of stand-alone air cleaners was varied between one and three.

Two rounds of experiments were made, one with and one without the air cleaner. When in use, the air cleaner operated at the highest setting. During the experiments a panel of 37 subjects were asked to rate their acceptability through a whole-body exposure by entering the polluted rooms. Their characteristics and those of the subjects used for bio-effluent generation can be seen in Table 1. Their acceptability was rated using a continuous scale divided into two parts, from clearly not acceptable (-1) to just not acceptable (-0.01) and from just acceptable (0.01) to clearly acceptable (1).

Table 1. Human subject characteristics

Column Title	Sensory assessment panel	Subjects used for bio-effluent generation
Total	37	3
Gender*	23 males, 14 females	2 male and 1 female
Age (mean ± SD) [years]	25.3±3.3	25±3.3

*Sex considered binary, assigned at birth.

Prior to the experiment subjects were asked to get sufficient rest. They were not allowed to consume alcohol, garlic and spicy food in the evening, night before, or during the day of the experiment. Subjects were not allowed to consume caffeine within less than one hour prior to the experiment. Participants were asked to use odourless products during the course of the experiment and were asked to shower the prior evening. During the experiment, the three subjects used for generating bio-effluents entered the room one hour earlier before the panel assessed the indoor air quality.

For each air flow rate and round (with and without air cleaner), the percentage of subjects dissatisfied (PD), in %, was calculated as follows (Wargocki 2004):

$$PD = \frac{\exp(-0.18 - 5.28 \cdot \overline{ACC})}{1 + \exp(-0.18 - 5.28 \cdot \overline{ACC})} \cdot 100 \text{ [%]} \quad (1)$$

Where \overline{ACC} represents the mean acceptability rating made by the panel. The clean air delivery rate (CADR) was then determined as the percentage decrease in outdoor air flow rate for which the same PD was obtained with the air cleaner employed.

2.2 Energy use for heating, cooling, and ventilation

The annual energy use for heating, cooling, and transporting the outside air was estimated using a building energy model developed in IDA ICE (EQUA Simulation AB 2013) of an office space with an area of 19.8 m² and total volume of 53.46 m³ (Bogatu et al. 2021). The office space had the same area and volume as the room employed in the experiments and was conditioned by an air-handling unit (AHU) consisting of an air-to-air counterflow heat exchanger (HEX), pre-heating and cooling coils, and supply and return fans. Two sets of simulations were made, one with and one without the HEX. A HEX effectiveness of 85% was assumed when the HEX was operating. The simulations were made using the IWEC2 climate data for Copenhagen, Denmark (IWEC 2001).

Except for an external wall having a 5 m² window, the office was assumed to be part of a multi-storey office building and thus surrounded by identical spaces. An external blind shaded the upper part of the window when the incident solar radiation on the outside of the glazing exceeded 100 W/m². A high level of airtightness was assumed and thus infiltration was zero. The internal heat gains consisted of two occupants (1.1 met), appliances with a long-wave radiation fraction of 0.5, and lighting with a convective fraction of 0.5. The occupants, appliances, and lighting amounted to a total internal heat load of 35.7 W/m². All internal heat gains were active on weekdays from 9:00 to 12:00 and 13:00 to 16:00.

A constant air volume (CAV) ventilation was used for conditioning the space. The AHU supply air temperature setpoint was 16 °C. Outside occupancy the air flow rate was set to 0.15 L/(s·m²) while during work hours (9:00 to 16:00) the maximum air flow rate was 21 L/s or 28 L/s depending on the building type analysed, very low polluting (VLP) or low polluting (LP) (CEN 2019), respectively. An ideal heater and ideal cooler which operated only from 09:00 to 16:00 were installed in the office space to further condition the indoor thermal environment and maintain it between 20 °C and 26 °C.

In the simulations, the effect of a stand-alone air cleaner was analysed by reducing the maximum air flow rate proportional to the assumed clean air delivery rate (CADR). The annual energy use was determined for three CADRs (0%, 30%, and 50%) when the air cleaner was assumed to remove both bio-effluents and building emissions and one CADR of 50% when the air cleaner was assumed to remove only building emissions.

2.3 Air cleaner energy use

The annual air cleaner energy use was estimated from the power of the air cleaner and the total working hours. The total number of working hours during the simulation was 1560, assuming six work hours per day. At the setting used in the experiments for which the CADR was determined, the GPAC consumed 22 W. The same primary energy use factor of 1.9 was used for the electricity as in the simulation study (Bogatu et al. 2021).

2.4 Clean air efficiency

The clean air efficiency (CAE) is proposed as a key performance indicator (KPI) for comparing the efficiency of the AHU for heating, cooling, and transporting outdoor air and the efficiency

of the stand-alone air cleaner for recirculating and cleaning the same amount of air. The CAE in L/s per kWh was calculated as the ratio between the CADR [L/s] and the energy used for providing that amount of clean air [kWh]:

$$CAE = \frac{CADR}{Energy\ use} \quad [L/s\ per\ kWh] \quad (2)$$

3 RESULTS

3.1 Clean air delivery rate

Figure 1 shows the relationship between the PD and the outdoor air flow rate (q) for the two scenarios analysed in the human subject experiments. As observed, no matter the pollution source, the air cleaner reduced the dissatisfaction rate for the same outdoor air flow rate. Moreover, Figure 1b shows that the outdoor air flow rate can be reduced if the air cleaner is employed for the same resulting dissatisfaction rate. The figure also shows that increasing the number of GPAC units did not improve the perceived air quality.

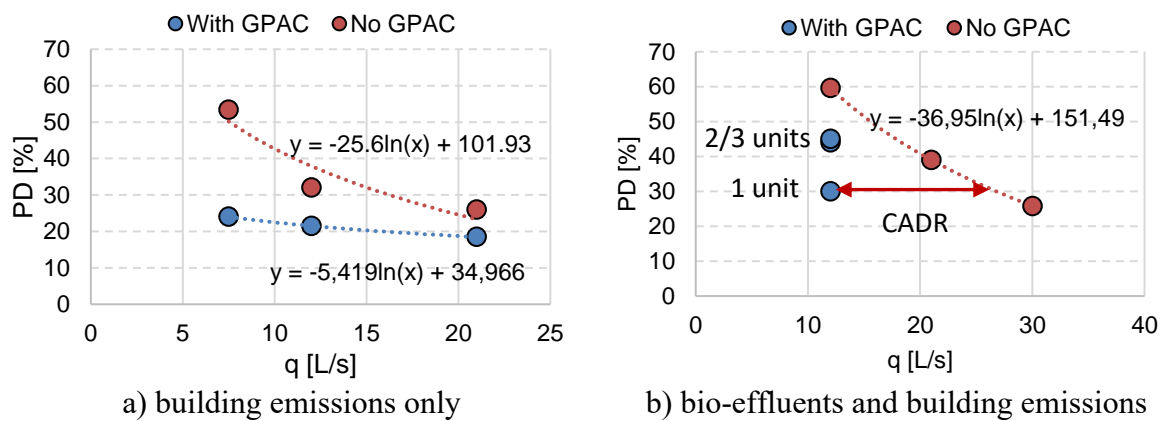


Figure 1. Relationship between PD and outdoor air flow rate for the two scenarios analysed where the pollution source consisted of both bio-effluents and building emissions or building emissions only (PD: percentage of subjects dissatisfied, q; outdoor air flow rate).

From Figure 1a, where only building emissions were used as pollution source, it can be seen that a CADR of 50% (12 L/s) was obtained for a PD of 20% (Category II) which is the target Category for office buildings (CEN 2019). However, when both bio-effluents and building emissions were present as sources (Figure 1b), a PD of 20% was not achieved and the CADR varied as the number of air cleaners was increased, with an average value of 30% (9 L/s).

3.2 Energy use of AHU and air cleaner

Figure 2 shows the primary energy use of the AHU as a function of the CADR for the scenarios where the air cleaner removed both bio-effluents and building emissions obtained by Bogatu et al. 2021. Heating energy and the energy use for transporting the outside air (AUX) decreased as the CADR increased, while the cooling energy increased. Nevertheless, a linear relationship was found between the heating, cooling, and AUX energy use and CADR.

The heating energy use decreased when the HEX was operating. The HEX did not influence the cooling energy use, although it led to an increase in the AUX energy as the pressure drop in the AHU increased. The cooling energy use was however lower for the LP building type since the maximum required air flow rate was higher. Although not shown in the figure, as the resulting air flow rate was slightly lower when the air cleaner removed only building emissions

for the same CADR (50%), the energy use for heating and transporting outdoor air decreased while cooling increased (Bogatu et al. 2021).

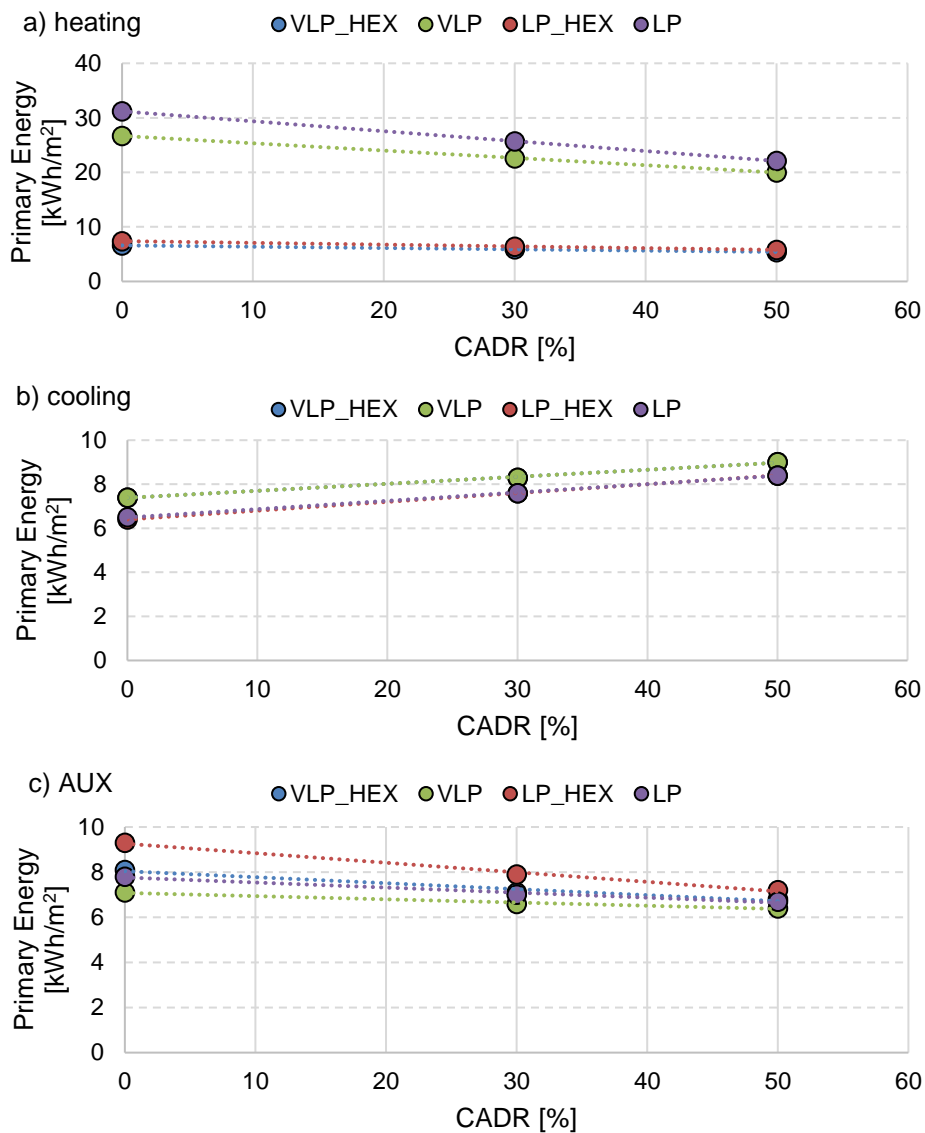


Figure 2. AHU primary energy use for heating, cooling, and transporting the outside air (AUX).

Assuming the GPAC ran at the highest setting for all working hours, its total energy use was estimated to be 3.3 kWh/m². This meant that the total energy use would increase by 3.3 kWh/m² in the scenarios where the GPAC was operating. However, at the medium setting (10.6 W) the total energy use would increase by only 1.6 kWh/m².

3.3 Clean air efficiency

The resulting CAE is shown in Figure 3 depending on the source of pollution. In the figure, the CAE of the AHU represented by bars is compared to the CAE of the GPAC represented by horizontal lines. The calculation was made for a CADR of 50% (12 L/s) when the air cleaner removed only building emissions and a CADR of 30% (9 L/s) when the air cleaner removed both building emissions and bio-effluents, as reported in section 3.1. The CAE values are given relative to the total annual AHU energy use (AHU), AHU fan energy use (AHU_{AUX}), i.e. AHU energy use without considering the energy use for heating and cooling the supplied air, energy used by the GPAC at high setting (GPAC_{HIGH}), energy use by GPAC at medium setting (GPAC_{MED}).

From the figure it can be seen that the CAE increases as less energy is used for supplying the respective clean air, 9 L/s in case of removal of both bio-effluents and building emissions and 12 L/s in case of removal of building emissions only. Thus, if the bar is higher than the horizontal line, the AHU should operate as less energy is used for heating, cooling, and transporting the outside air than for operating the GPAC.

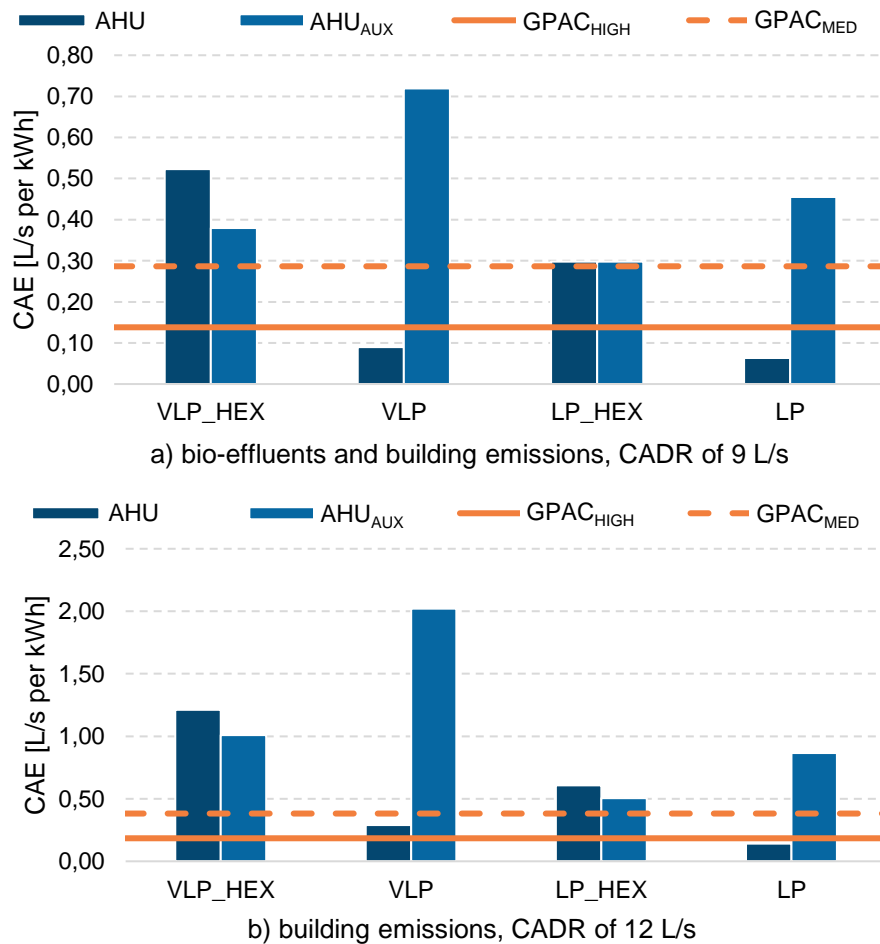


Figure 3. Clean air efficiency (CAE) relative to the total annual AHU energy use (AHU), AHU fan energy use (AHU_{AUX}), energy used by the GPAC at high setting (GPAC_{HIGH}), and energy use by GPAC at medium setting (GPAC_{MED}) by scenario.

For the investigated space and scenarios, the results show that the GPAC should be operated only when a HEX is not included in the AHU. When the GPAC removes only building emissions it may only lead to energy savings if the GPAC could be operated at a medium setting. The GPAC is never more efficient than simply supplying outdoor air if the energy use for heating and cooling the outdoor air is not taken into account as shown by the AHU_{AUX} bars.

4 DISCUSSION

The experiments showed that the CADR of the gas-phase air cleaner (GPAC) varied depending on the pollution source, namely both bio-effluents and building emissions or only building emissions. Moreover, increasing the number of GPACs for the same room volume did not improve the perceived air quality. This requires further consideration as the room size and number of people were not varied. Thus, for a higher building volume and occupancy where spatial distribution may also influence particle, odour, and volatile organic compound (VOC) distribution, multiple air cleaners may be required to achieve a uniform indoor air quality.

Moreover, the air cleaner was only tested at the maximum setting. Further investigation is required if the same perceived air quality may be obtained at a lower setting or if the fan speed is varied between settings instead of running continuously, i.e. an improved control.

From the comparison made for Copenhagen, Denmark between the stand-alone air cleaner and the AHU, it was found that the GPAC could only save energy if employed in buildings where the AHU is not equipped with a HEX according to the clean air efficiency (CAE). In the simulations a constant supply air temperature setpoint of 16 °C was used while the space was equipped with ideal heater and cooler to cover the remaining load. An optimal control of the supply air temperature and the source for the room-side conditioning systems may further influence the energy use and thus the CAE.

Higher energy savings would be achieved if the energy use of the air cleaner could be decreased for the same resulting perceived air quality. The energy use varies though as a function of climate while primary energy factors vary as a function of the grid energy mix. These factors would thus influence the CAE of both the AHU and the GPAC. A higher electricity primary energy factor would make the GPAC less efficient while the primary energy use of the AHU would be further influenced by the source for heating and cooling and their respective primary energy factors. A warmer climate would reduce the effectiveness of the HEX (Bogatu et al. 2021) and would thus make the GPAC a viable solution.

5 CONCLUSIONS

From the experiments a CADR of approximately 50% (12 L/s) was identified when the pollution source was only represented by building emissions and a CADR of approximately 30% (9 L/s) was found when both bio-effluents and building emissions represented the pollution source. The assessed indicator, clean air efficiency (CAE), can be used to compare different solutions used for providing clean air into the space. Based on the results shown for AHU and stand-alone GPAC for Copenhagen, Denmark - dominated by a high heating load - the GPAC was competitive only if the AHU was not equipped with a heat exchanger. The GPAC was also more efficient if both bio-effluents and building emissions were present as pollution sources.

ACKNOWLEDGEMENTS

This study is part of IEA-EBC Annex 78 supported by Danish government funding EUDP project No.: 64018-0599. The authors would like to recognize Kanta Amada, Zhengchai Hu, Pawel Wargocki, and Lei Fang for their efforts in planning and execution of the experiments and data processing of the experimental results.

REFERENCES

- Afshari, Alireza, Olli Seppänen, Bjarne W. Olesen, and Jinhan Mo. 2021. "Effect of Portable Gas-Phase Air Cleaner on Indoor Air Quality." *REHVA Journal* (2):28–35.
- Bogatu, Dragos-Ioan;, Ongun Berk; Kazanci, and Bjarne W; Olesen. 2021. "Gas-Phase Air Cleaning Effects on Ventilation Energy Use and the Implications of CO2 Concentration as an IAQ Indicator for Ventilation Control." Pp. 2919–26 in *Proceedings of Building Simulation 2021*.
- CEN. 2019. "EN 16798-1:2019 Energy Performance of Buildings – Ventilation for Buildings – Part 2: Interpretation of the Requirements in EN 16798-1 – Indoor Environmental Input Parameters for Design and Assessment of Energy Performance of Buildings Addressing Indoor A." *EN*.

- EQUA Simulation AB. 2013. "IDA-ICE Indoor Climate and Energy."
- Hu, Zhengchai; 2023. "Evaluation of Air Cleaning Technologies for Indoor Air Contaminants Control and Energy Performance." Technical University of Denmark.
- IEA EBC. 2019. "IEA EBC Annex 78 - Supplementing Ventilation with Gas-Phase Air Cleaning, Implementation and Energy Implications." Retrieved (<https://annex78.iea-ebc.org/>).
- IWEC. 2001. "Weather Data by Region | EnergyPlus." *EnergyPlus*. Retrieved April 21, 2018 (https://energyplus.net/weather-region/europe_wmo_region_6/GBR).
- Wargocki, Pawel; 2004. "Sensory Pollution Sources in Buildings." 14(Suppl 7):82–91. doi: <https://doi.org/10.1111/j.1600-0668.2004.00277.x>.
- Zhang, Yiping, Jinhan Mo, Yuguo Li, Jan Sundell, Pawel Wargocki, Jensen Zhang, John C. Little, Richard Corsi, Qihong Deng, Michael H. K. Leung, Lei Fang, Wenhao Chen, Jinguang Li, and Yuexia Sun. 2011. "Can Commonly-Used Fan-Driven Air Cleaning Technologies Improve Indoor Air Quality? A Literature Review." *Atmospheric Environment* 45(26):4329–43. doi: 10.1016/j.atmosenv.2011.05.041.

On the integration of envelope pressure inhomogeneity and autocorrelation in fan pressurization uncertainty analysis

Martin Prignon¹

¹*Buildwise*
Kleine Kloostersraat, 23
1932 Zaventem, Belgium

ABSTRACT

Improving the knowledge on uncertainty for fan pressurization measurement is of first importance. It allows to assess the reliability of the measurement, which is essential when comparing the results with benchmarks or standards, but it also gives a better understanding, and thus a chance of improving, the measurement procedure. In this context, recent studies on alternative regression techniques highlights the importance of identifying and quantifying the sources of uncertainty. This paper investigates the integration of two new aspects in the measurement procedure: an uncertainty source related to the inhomogeneity of pressure difference along building envelope, and the autocorrelation of successive pressure difference measurement due to wind fluctuations. Those are integrated in the framework of uncertainty calculation and are then applied to a series of 30 tests conducted in repeatability conditions in an apartment in Brussels. Results show the relatively low impact of those additions to the determination of building characteristics (n , C_{env} and q_{50}) and their large impact on both results variability and uncertainty assessment.

KEYWORDS

Fan pressurization test ; Uncertainty calculation ; Autocorrelation ; Measurement functions

1 INTRODUCTION

Fan pressurization test provides the user with a metric related to the capacity of a building to avoid undesired airflows between inside and outside. Furthermore, it is a good indicator of the care taken in the implementation and execution during construction. This test is of first importance, given the importance of air leakage on the energy consumption and occupant's comfort. An indication of the quality of the measurement should always be provided alongside with the test result, since, as expressed in the guide to the expression of uncertainty in measurement: "*without such an indication, measurement results cannot be compared, either among themselves or with reference values given in a specification or standard*" (JCGM, 2008).

Research on the quantification of fan pressurization uncertainties started in mid-90's with (Sherman and Palmiter, 1995). They already mentioned the inadequacy of an OLS (Ordinary Least Square) method to conduct the linear regression required in the post-processing of the data. Recently, (Delmotte, 2017) suggests using WLOC (Weighted Line of Organic Correlation) as an alternative to OLS. Since then, multiple studies (Kölsch and Walker, 2020; Prignon et al., 2020) showed that using WLOC results in a lower uncertainty of the obtained metric, and a better reliability of the calculated uncertainty.

In the WLOC method, each airflow and pressure difference measurements is weighted by its uncertainty. Consequently, while it is not relevant for the OLS method, the WLOC method requires to determine and estimate the different sources of uncertainty. This paper aims at integrating inhomogeneity and autocorrelation in the existing framework for uncertainty analysis. The impact of these new additions is then observed on a series of 30 tests realized in repeatability conditions presented in a previous study (Prignon et al., 2019). Although this paper brings the knowledge about uncertainty in fan pressurization test one step further, it does not pretend to draw up an exhaustive list of uncertainty sources.

The paper is presented as follows. The methodology section illustrates the framework for uncertainty analysis and describes different sources of uncertainty considered in this study, including two new integrated concepts. The methodology section although provides information about the dwelling used for the repeatability study, and the methodology for result analysis. The results of the repeatability study are presented and discussed in the result and discussion sections respectively. Lastly, the paper concludes with a summary of the findings, their limitations and the further work needed in this domain of research.

2 METHODOLOGY

When a measured quantity (y) is a function (f) of multiple input quantities (x_i), one can simply define the measurement function with (1):

$$y = f(x_1, x_2, \dots, x_n) + 0 \quad (1)$$

Compared to what is generally found in the field of airtightness measurement, this measurement function includes a “plus zero” term that does not alter the value of y . However, in the uncertainty calculation, this term accounts for the fact that the model approximates reality (Mittaz et al., 2019).

The uncertainty of the measured quantity, $u(y)$, is obtained from the measurement function using the propagation law (2):

$$u(y) = \sqrt{\sum_{i=1}^n c_i^2 u_c^2(x_i) + 2 \sum_{i=1}^{n-1} \sum_{j=i+1}^n c_i c_j u_c(x_i) u_c(x_j) r(x_i, x_j)} \quad (2)$$

In this equation, c_i and c_j are the sensitivity coefficients, $u(x_i)$ is the standard uncertainty related to the input quantity x_i and $r(x_i, x_j)$ is the correlation coefficient linking input quantities x_i and x_j .

2.1 Measurement functions for fan pressurization test

The fan pressurisation test aims to determine the building characteristics (n and C_L) based on multiple measurements of pressure difference – airflow couples (Δp ; q_{env}). This measurement is made of five different steps, and each of them lead to a different measurement function. In this section, uncertainty trees (figures 1 to 3) are used to illustrate the measurement functions and the sensitivity coefficients at each step.

First step is to determine the pressure difference induced by the fan on both sides of the building envelope. In practice, two pressure probes placed inside and outside the building measure a

pressure difference (Δp_m), which is the sum of the pressure difference induces by the fan (Δp_f) and by other effects (Δp_0) as such as wind pressure and stack effect. It is not possible to determine which part of the total pressure difference recorded is attributed to Δp_0 and Δp_f while the fan is working. Therefore, Δp_0 is measured before ($\Delta p_{0,1}$) and after ($\Delta p_{0,2}$) the test, and is assumed being constant during the test. Then, the pressure difference induced by the fan measured at the location of the pressure probes (Δp_f) is assumed equal to the pressure difference induced by the fan along the whole building envelope (Δp). Figure 1 illustrates this step with the uncertainty tree related to the pressure difference measurement.

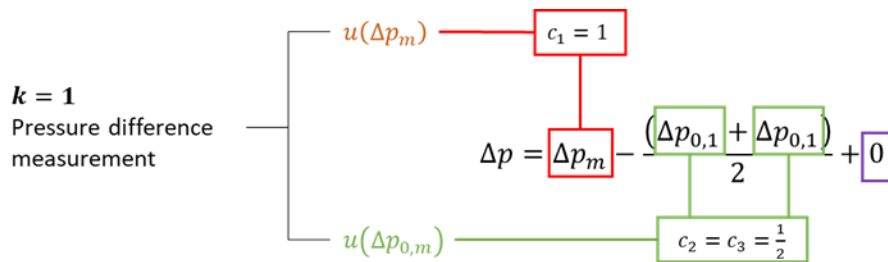


Figure 1: Uncertainty tree for the determination of pressure difference along building envelope.

Second step is the determination of airflow through building envelope openings. Since the mass of air inside the building is assumed constant in steady-state conditions and the pressure difference is considered small compared to atmospheric pressure, temperature ratio is used as a proportionality coefficient between airflow through the fan (q_m) and the building envelope (q_e). Note that, in this study, the uncertainty in temperature measurement is assumed equal for T_i and T_e . Figure 2 shows the uncertainty tree for the second step.

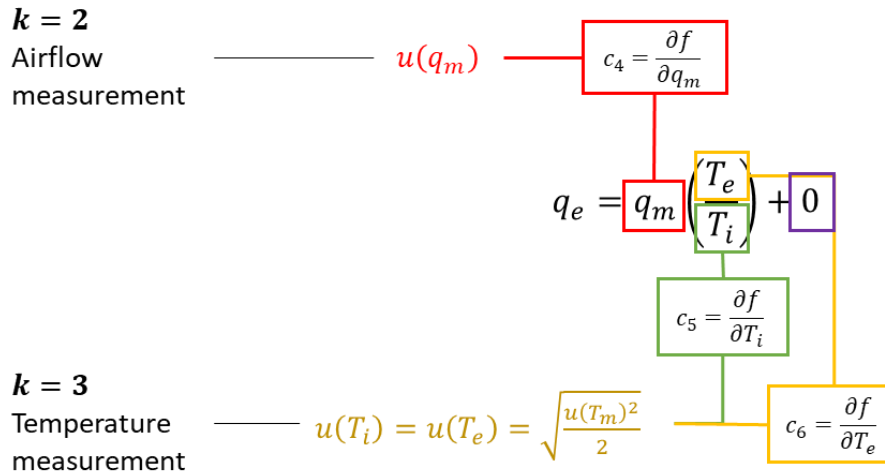


Figure 2: Uncertainty tree for the determination of airflow through building envelope.

Steps one and two provides q_e and Δp , and the combined uncertainty of each. Third step consists in average a series of single point measurements made at the same pressure difference, in order to reduce the uncertainty. Since each measurement is recorded with the same instrument and in a short period of time, those are expected to be correlated. This is particularly true for the pressure difference that is highly impacted by wind direction and speed. In the literature authors generally use a conservative but unrealistic assumption where the uncertainty of the average is equal to the uncertainty of a single measurement (Prignon et al., 2019). This study suggests an alternative between that conservative assumption and the unrealistic

hypothesis of uncorrelated measurements: taking into account that variables are autocorrelated. The uncertainty of the average of N fully uncorrelated measurements is given by the variance of the observations divided by N . In case of autocorrelated variable, an effective sample size N_{eff} depending on the level of autocorrelation is considered instead of N in the calculation. This takes into account the fact that a measurement made at time t depends on a series of measurements made before this one (depending on the level of autocorrelation). For a detailed calculation of N_{eff} , the reader should refer to (Warsza, 2013) or (Zhang, 2006).

The fourth step consists in fitting the series of couples $(\Delta p ; q_e)$ determined at multiple pressure difference with linear regression model. In this study, two different regression techniques are investigated: OLS (generally used) and WLOC (alternative suggested in previous studies). The reader should refer to previous works (Delmotte, 2017; Prignon et al., 2020) for an extended description of those methods and their mathematical expressions. Those regression techniques provide following values as a result: n , $\ln(C_{env})$, $u(n)$, $u(\ln(C_{env}))$ and $r(n, \ln(C_{env}))$.

Building regulations or specifications generally refer to quantities based on the airflow at 50 Pa (q_{50}), which is deduced in the fifth step. While n and $u(n)$ are directly extracted from the regression technique, the determination of the second building characteristics (C_L) referred to in the power law is more complicated. To avoid the complexity of dealing with n and C_L correlation, this study determines q_{50} directly based on n and $\ln(C_{env})$ and does not analyse the behaviour of C_L . Figure 3 shows the measurement function and the uncertainty tree for this last step.

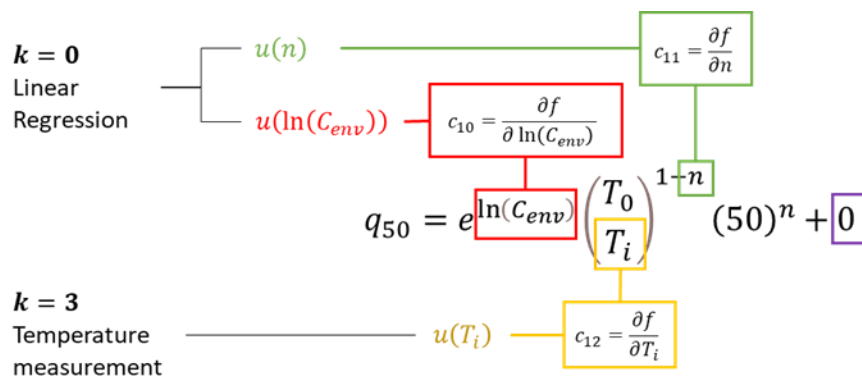


Figure 3: Uncertainty tree analysis for the determination of airflow at 50 Pa.

One may be interested in uncertainty in the combination of pressurization and depressurization, or in derived quantities rather than q_{50} . For both cases the methodology is similar to what was previously showed: define a measurement function that includes the new terms (e.g., building volume for n_{50}). This will also include a new source of uncertainty which must be propagated to the final value. Regarding its lack of interest in a methodological standpoint, those steps are not included in this study.

2.2 Sources of uncertainty

Based on previous section, 9 uncertainty terms divided in three types are included in the process of fan pressurisation measurements (Table 1).

Table 1: Uncertainty terms and type for fan pressurization measurement protocol.

Uncertainty term	Type of uncertainty
$u(T_m)$	Measurement uncertainty
$u(\Delta p_m), u(\Delta p_{0,m})$	Measurement uncertainty
$u(q_m)$	Measurement uncertainty
$u(0_{\Delta p})$	Assumption uncertainty (plus-zero term)
$u(0_{q_e})$	Assumption uncertainty (plus-zero term)
$u(0_{q_{50}})$	Assumption uncertainty (plus-zero term)
$u(n)$	Combined uncertainty from regression
$u(\ln(C_{env}))$	Combined uncertainty from regression

Values for the five terms coming from measurement uncertainty are provided in Table 2. Those are the uncertainty considered in this study, based on the experiment presented in (Prignon et al., 2019), and calculated based on data provided by the manufacturer.

Table 2: Measured quantity and measurement uncertainty for the three measured variables.

Measured quantity	Measurement uncertainty
Airflow rate – $u(q_m)$ [m ³ /h]	$\sqrt{\left(\frac{\max(0.04*q_m; 1.70)}{\sqrt{3}}\right)^2}$
Pressure difference – $u(\Delta p_m)$ and $u(\Delta p_{0,m})$ [Pa]	$\sqrt{\left(\frac{\max(0.01*\Delta p_m; 0.15)}{\sqrt{3}}\right)^2 + \left(\frac{0.1}{\sqrt{12}}\right)^2}$
Temperature – $u(T_m)$ [°C]	$\sqrt{\left(\frac{0.5}{\sqrt{3}}\right)^2 + \left(\frac{0.1}{\sqrt{12}}\right)^2} = 0.29$

The uncertainties due to assumptions are included in the uncertainty analysis through the “plus zero” terms in the measurement functions. This study considers two assumptions related to the determination of pressure differences, which should be included in the $u(0_{\Delta p})$ term. Although those hypotheses are often mentioned and discussed in the literature, to the authors’ knowledge only one of them was quantified (H1 hereunder). In this paper, in addition to the previously quantified, one additional hypotheses-related uncertainty component is investigated and quantified (H2).

H1: the zero-flow pressure during the test is defined as the arithmetic mean of the zero-flow pressure measurements conducted before and after the test. This hypothesis was extensively discussed in (Prignon et al., 2021, 2019). Those studies show that the uncertainty strongly depends on the standard deviation of the zero-flow pressure measurements ($\sigma_{\Delta p_0}$) and can be approached with (3):

$$u(\Delta p_{0,a}) = \frac{0.11 + 0.98 * \sigma_{\Delta p_0}}{1.35} \quad (3)$$

Although $\sigma(\Delta p_0)$ is easy to obtain during a fan pressurisation measurement, one could consider a conservative value of 1.5 Pa for $u(\Delta p_{0,a})$ in the absence of more information.

H2: the pressure difference between inside and outside the building is homogeneous along the building envelope. This hypothesis is a large approximation and is expected to lead to consequent uncertainties, especially at low pressure measurements. This study suggests a simplified way to quantify this uncertainty term, based on the methodology for uncertainty calculation in the context of climatic chambers. In that field of expertise, the uncertainty due to the inhomogeneity of temperature is defined as the maximum difference observed between two different locations in the chamber, divided by $\sqrt{3}$ (Nakahama, 2007).

To transpose this method for fan pressurization test requires first to determine the distribution of pressure differences along the façade. To that extent, let's consider a simple one-story building with a flat roof. Depending on the façade and the wind direction, the minimum and maximum pressure coefficient are $c_{p,max} = 0.5$ and $c_{p,min} = -0.9$ (ASHRAE, 2009). Those coefficients are then used to compute the minimum and maximum wind pressure, p_w , with (4):

$$p_w = \frac{c_p * v_w^2 * \rho}{2} \quad (4)$$

Where v_w is the wind speed [m/s] and ρ is the air density [kg/m³]. Assuming a constant air density of 1.244 kg/m³, the related uncertainty is deduced from the difference in pressure coefficients along the facade and the wind speed following (5):

$$u(\Delta p_{0,u}) = 0.36 * (c_{p,max} - c_{p,min}) * v_w^2 \quad (5)$$

In this study, the wind speed is known for each test, and $u(\Delta p_{0,u})$ can then be computed individually. Without those information, the user can use the Beaufort scale to define a wind speed based on observations, and compute $u(\Delta p_{0,u})$. H1 and H2 can be combined with (6):

$$u(0_{\Delta p}) = \sqrt{\left(u(\Delta p_{0,a})^2 + u(\Delta p_{0,u})^2 + 2 * r_{\Delta p_{0,a}; \Delta p_{0,u}} * u(\Delta p_{0,a}) * u(\Delta p_{0,u}) \right)} \quad (6)$$

In this study, the average of 30 repeated test (see section 2.3) showed an average value of $u(\Delta p_{0,u}) = 1.6$ Pa. Since $\Delta p_{0,a}$ and $\Delta p_{0,u}$ are computed for each test, it was possible to deduce $r_{\Delta p_{0,a}; \Delta p_{0,u}} = 0.48$. This value seems logical since both terms are largely impacted by wind speed.

Note that this work does not investigate the uncertainty related to the assumptions $u(0_{q_e})$ and $u(0_{q_{50}})$. The uncertainty terms $u(n)$ and $u(\ln(C_{env}))$ are directly deduced from the linear regression process, which is not described here.

2.3 Repeatability testing

To study the impact of those new variables in the fan pressurization measurement protocol, those modified protocols were applied on a series of 30 tests conducted in repeatability conditions. Those tests were performed on a newly constructed apartment within a period of 15 days in October 2017. The apartment was a masonry construction of 228 m³ located on the second floor of a 3-storey building in Brussels. Only two perimetral walls were exposed to the outside. During the tests, a weather station (Ahlborn FMD 760) placed on the roof above the apartment measured the outside air temperature, wind speed and wind direction every 10 s. The wind speed varied from 0.0 to 3.8 m/s during the tests (with an average of 1.3 and a standard deviation of 0.8). A thermometer (Testo 417) was used to measure the inside air temperature before each test. For more details about the tested dwelling, the reader could refer to a previous paper (Prignon et al., 2019).

For each test five different cases are investigated. First is obtained using OLS method, which is not impacted by the source of uncertainty considered in previous section. Other cases are

obtained applying WLOC method considering different sources of uncertainties as presented in Table 3.

Table 3: Five cases investigated and their integrated aspects in the uncertainty calculation

Integrated aspects	WLOC-1	WLOC-2	WLOC-3	WLOC-4
Measurement uncertainty	X	x	x	x
$u(\Delta p_{0,a})$		x	x	x
$u(\Delta p_{0,u})$			x	x
Autocorrelation				x

3 RESULTS

3.1 Uncertainty in the plus zero term

The two uncertainties related to specific assumptions described previously (H1 and H2) were computed individually for each test. Considering normally distributed data, Table 4 provides average and 95% confidence intervals for those two sources of uncertainty based on the 30 repeated tests.

Table 4: average and 95% confidence interval for $u(\Delta p_{0,a})$ and $u(\Delta p_{0,u})$ for the 30 tests conducted in repeatability conditions.

Uncertainty source	Average [Pa]	95% CI [Pa]
$u(\Delta p_{0,a})$	1.1	[0.0 ; 2.1]
$u(\Delta p_{0,u})$	1.6	[0.0 ; 4.2]

Based on those values, one can use (6) and previously mentioned information in order to deduce a value of 2.34 Pa for $u(0_{\Delta p})$.

3.2 Effective sample size due to autocorrelation

Autocorrelation is computed individually at each measurement. Figure 4 provides the 95% confidence interval of the effective sample size (N_{eff}) at each pressure difference step for pressurization (red) and depressurization (blue) based on the 30 repeated tests.

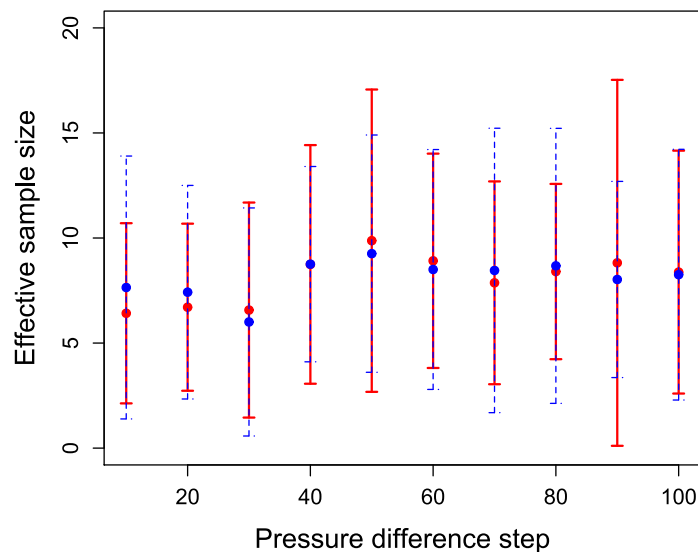


Figure 4: Mean and 95% CI for effective sample size in pressurization (red) and depressurization (blue).

3.3 Impact on building characteristics and uncertainty calculations

Following figures illustrate the values, the observed uncertainty (dash blue) and the calculated uncertainty (red full) of n , $\ln(C_{env})$ and q_{50} in pressurization and depressurization for each investigated case. Note that the exact values are given in tables in appendix.

For n and $\ln(C_{env})$, same observations are found and illustrated in Figure 5 and Figure 6 respectively. The observed uncertainty is lower for WLOC-2 and WLOC-3 than for other cases. WLOC-2 and WLOC-4 are the cases where the calculated uncertainty is the more reliable (i.e., smaller difference between observed and calculated uncertainty). Note that the uncertainty calculated with WLOC-3 largely overestimates the observed uncertainty. This was expected since two new terms increase the uncertainty, without considering the reduction due to the autocorrelation aspect.

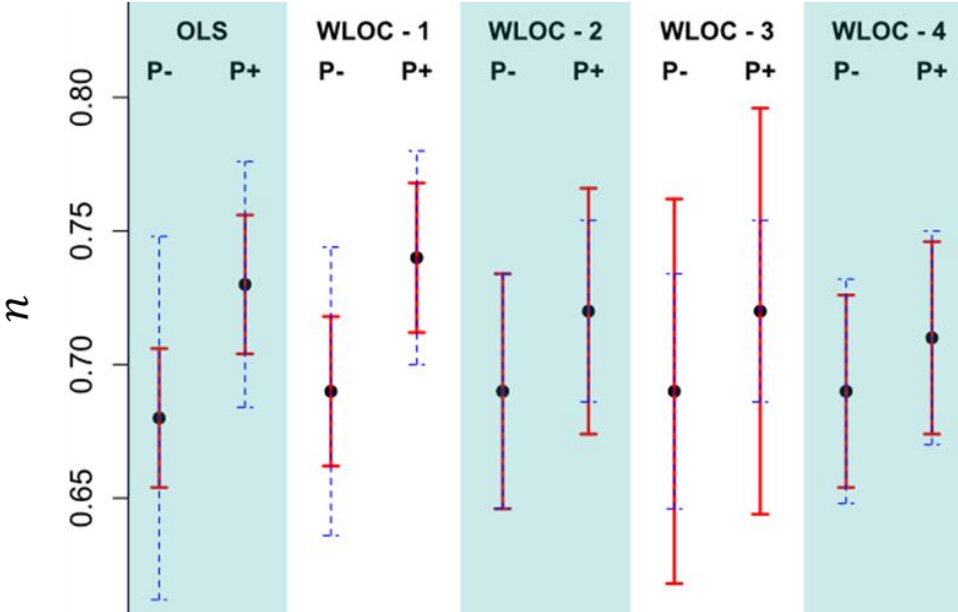


Figure 5: average (black dot), observed uncertainty (blue dashed line) and calculated uncertainty (red full line) for n for the 5 investigated cases based on 30 repeated fan pressurization tests.

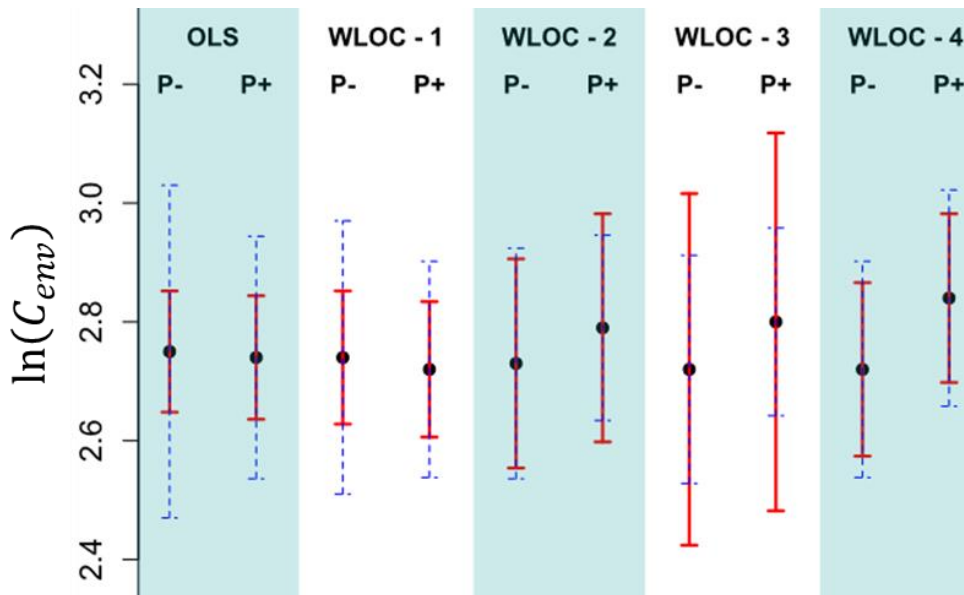


Figure 6: average (black dot), observed uncertainty (blue dashed line) and calculated uncertainty (red full line) for $\ln(C_{env})$ for the 5 investigated cases based on 30 repeated fan pressurization tests.

Figure 7 shows that the observations made for n and $\ln(C_{env})$ are not translated to q_{50} . In that case, the most reliable uncertainty calculation is for WLOC-3 while other are found performing equivalently.

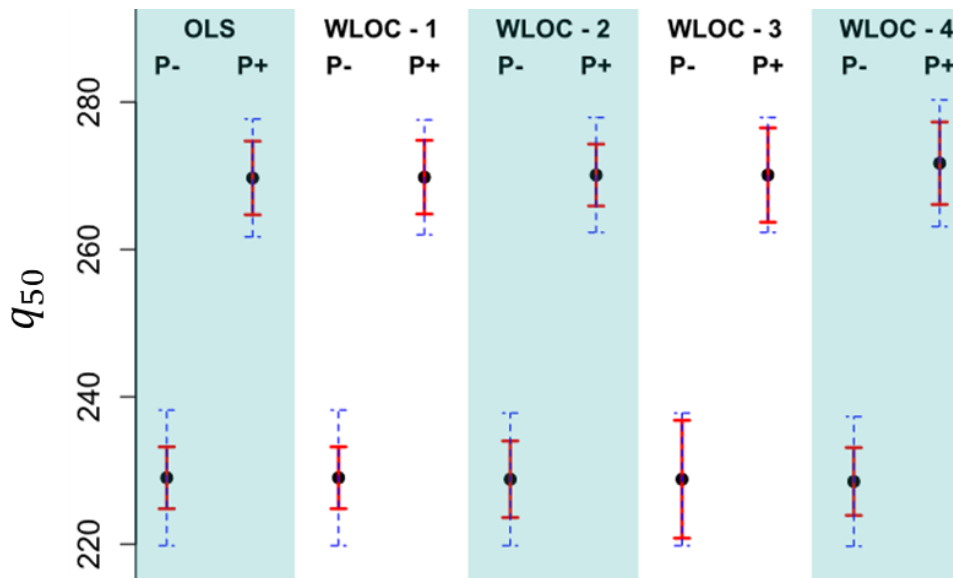


Figure 7: average (black dot), observed uncertainty (blue dashed line) and calculated uncertainty (red full line) for q_{50} for the 5 investigated cases based on 30 repeated fan pressurization tests.

4 DISCUSSION

The results presented in section 3.2 have three main outcomes. First, the uncertainty observed on n and $\ln(C_{env})$ are lower when using WLOC methods than when using OLS method. This is in line with existing literature and is confirmed in this study since it is found for all cases of WLOC, whatever the uncertainty sources considered (WLOC 1 to 4). Second, the fit between observed and calculated uncertainties for flow exponent and flow coefficient are found good for WLOC – 2 and WLOC – 4, and poor for WLOC – 3. Consequently, the inclusion of the

new suggested uncertainty term $u(\Delta p_{0,u})$ should always be considered when taking into account the autocorrelation of pressure difference measurement (WLOC – 4) since the conservative assumption $N_{eff} = 1$ used in previous studies induces an overestimation of the uncertainty. Third, the trends observed for n and $\ln(C_{env})$ hereabove are not transferable to airflow at 50 Pa. It was shown in previous research that the improvement using WLOC found for airflow exponent and air leakage coefficient is not seen at 50 Pa (Prignon et al., 2020), but is well found at higher and lower pressure differences. This can be explained either by a problem in the calculation of the correlation between n and $\ln(C_{env})$, or by the fact that this is not an exhaustive list of uncertainties. Other sources of uncertainty could be considered in the framework including, but not limited to, the location of the pressure probe, the impact of wind on airflow measurement and the deterioration of the equipment over time. The calculation for inhomogeneity of pressure difference along the envelope (section 2.2) could be adapted to consider the location of the pressure probe. However, this would require to study the pressure fields around the building.

Those observed trends are case specific. While the methodology – including the formulae – should be transferable to other cases, specific attention should be paid to using the suggested values of this paper when applying this to buildings of different shapes and sizes. This is especially true for buildings where the stack effect plays a large role in the Δp_0 measured.

5 CONCLUSION

This study investigates how the integration of two new aspects in the framework of uncertainty analysis impacts the fan pressurization test regarding the calculated and the observed uncertainties of n , $\ln(C_{env})$ and q_{50} . The study demonstrates that the use of WLOC should be preferred over OLS, but the choice of sources of uncertainty should be carefully conducted. It also provides methods to integrate the inhomogeneity of envelope pressure difference and the autocorrelation of pressure difference measurements in the uncertainty analysis. These results bring the scientific community one step further in the uncertainty analysis for fan pressurization measurements.

Although the study provides strong and useful results, two limitations inherent to the methodology should be mentioned. First, the conclusions are driven by a set of tests conducted on one specific building. Although those trends are expected to be found for other buildings, this generalization work is still to be done, especially when considering the values found in this study for $u(\Delta p_{0,u})$ and N_{eff} . Second, by definition the repeatability testing considers only precision errors since bias errors are expected to repeat from one test to another. Consequently, this study does not consider the bias errors that could be included in the fan pressurization test. In addition, the repeatability testing does not include the uncertainty related to a change in the operator since all tests are performed by the same person. This is expected to have a strong impact on the uncertainty of fan pressurization measurements as shown by (Delmotte and Laverge, 2011).

This work highlights the fact that uncertainties are still not well quantified for fan pressurization test. Further work should focus on having a better understanding of the sources of uncertainty through the generalization of the trends observed in this study, and on the study of a more comprehensive list of sources of uncertainty. This in order to improve the measurement method and to provide a reliable uncertainty value when conducting the experiment.

6 REFERENCES

- ASHRAE, 2009. Handbook of fundamentals (SI Edition). American Society of Heating, Refrigerating and Air-Conditioning Engineers, Inc.
- Delmotte, C., 2017. Airtightness of buildings-considerations regarding the zero-flow pressure and the weighted line of organic correlation. Presented at the 38th AIVC Conference.
- Delmotte, C., Laverge, J., 2011. Interlaboratory tests for the determination of repeatability and reproducibility of buildings airtightness measurements. Presented at the 32nd AIVC conference and 1st TightVent Conference.
- JCGM, 2008. Evaluation of measurement data - Guide to the Expression of Uncertainty in Measurement.
- Kölsch, B., Walker, I.S., 2020. Improving air leakage prediction of buildings using the fan pressurization method with the Weighted Line of Organic Correlation. Building and Environment 181, 107157.
- Mittaz, J., Merchant, C.J., Woolliams, E.R., 2019. Applying principles of metrology to historical Earth observations from satellites. Metrologia 56, 032002.
- Nakahama, H., 2007. Estimation method for temperature uncertainty of temperature chambers (JTM K 08) (No. 26), Espec Technology Report. Espec Test Center Corp.
- Prignon, M., Dawans, A., Altomonte, S., Van Moeseke, G., 2019. A method to quantify uncertainties in airtightness measurements: Zero-flow and envelope pressure. Energy and Buildings 188, 12–24.
- Prignon, M., Dawans, A., van Moeseke, G., 2021. Quantification of uncertainty in zero-flow pressure approximation. International Journal of Ventilation 20, 248–257.
- Prignon, M., Delmotte, C., Dawans, A., Altomonte, S., van Moeseke, G., 2020. On the impact of regression technique to airtightness measurements uncertainties. Energy and Buildings 215, 109919.
- Sherman, M., Palmiter, L., 1995. Uncertainties in fan pressurization measurements. Presented at the Airflow Performance Conference.
- Warsza, Z.L., 2013. Evaluation of the type A uncertainty in measurements with autocorrelated observations, in: Journal of Physics: Conference Series. IOP Publishing, p. 012035.
- Zhang, N.F., 2006. Calculation of the uncertainty of the mean of autocorrelated measurements. Metrologia 43, S276.

7 APPENDIX

Table 5: average, observed and calculated uncertainties for the flow exponent in pressurization.

Quantities	OLS	WLOC-1	WLOC-2	WLOC-3	WLOC-4
Average calculated value (n)	0.73	0.74	0.72	0.72	0.71
Standard deviation ($u_0(n)$)	3.2 %	2.8 %	2.4 %	2.4 %	2.9 %
Average calculated uncertainty ($u_c(n)$)	1.8 %	2.0 %	3.2 %	5.3 %	2.5 %

Table 6: average, observed and calculated uncertainties for the flow exponent in depressurization.

Quantities	OLS	WLOC-1	WLOC-2	WLOC-3	WLOC-4
Average calculated value (n)	0.68	0.69	0.69	0.69	0.69
Standard deviation ($u_0(n)$)	4.9 %	4.0 %	3.3 %	3.2 %	3.1 %
Average calculated uncertainty ($u_c(n)$)	1.9 %	2.1 %	3.1 %	5.2 %	2.6 %

Table 7: average, observed and calculated uncertainties for the flow exponent in pressurization.

Quantities	OLS	WLOC-1	WLOC-2	WLOC-3	WLOC-4
Average calculated value ($\ln(C_{env})$)	2.74	2.72	2.79	2.80	2.84
Standard deviation ($u_0(\ln(C_{env}))$)	3.7 %	3.3 %	2.8 %	2.8 %	3.2 %
Average calculated uncertainty ($u_c(\ln(C_{env}))$)	1.9 %	2.1 %	3.4 %	5.7 %	2.5 %

Table 8: average, observed and calculated uncertainties for the flow exponent in depressurization.

Quantities	OLS	WLOC-1	WLOC-2	WLOC-3	WLOC-4
Average calculated value ($\ln(C_{env})$)	2.75	2.74	2.73	2.72	2.72
Standard deviation ($u_0(\ln(C_{env}))$)	5.1 %	4.2 %	3.6 %	3.5 %	3.4 %
Average calculated uncertainty ($u_c(\ln(C_{env}))$)	1.9 %	2.0 %	3.2 %	5.5 %	2.7 %

Table 9: average, observed and calculated uncertainties for the flow exponent in pressurization.

Quantities	OLS	WLOC-1	WLOC-2	WLOC-3	WLOC-4
Average calculated value (q_{50})	270	270	270	270	272
Standard deviation ($u_0(q_{50})$)	2.0 %	2.0 %	2.0 %	2.0 %	1.9 %
Average calculated uncertainty ($u_c(q_{50})$)	0.9 %	0.9 %	1.1 %	1.8 %	1.0 %

Table 10: average, observed and calculated uncertainties for the flow exponent in depressurization.

Quantities	OLS	WLOC-1	WLOC-2	WLOC-3	WLOC-4
Average calculated value (q_{50})	229	229	229	229	229
Standard deviation ($u_0(q_{50})$)	1.5 %	1.5 %	1.4 %	1.4 %	1.5 %
Average calculated uncertainty ($u_c(q_{50})$)	0.7 %	0.7 %	0.9 %	1.3 %	0.7 %

Statistical analysis of the correlations between buildings air permeability indicators

Bassam Moujalled^{1,2*}, Benedikt Kölsch^{1,3}, Adeline Mélois^{1,2}, Valérie Leprince³

*1 Cerema
BPE Research Team, 46, Rue St Théobald, F-38080,
L'Isle d'Abeau, France*

**Corresponding author: bassam.moujalled@cerema.fr*

*2 Univ. Savoie Mont Blanc,
CNRS, LOCIE,
73000 Chambéry, France*

*3 Cerema
2 rue Antoine Charial
Lyon, France*

FOREWORD

The content presented comes from the paper under review “Quantitative correlation between buildings air permeability indicators: statistical analyses of about 500,000 measurements” (Moujalled, 2023a).

KEYWORDS

Building airtightness, measurements, database, field data, statistical analysis

1 COMPARISON OF AIR PERMEABILITY INDICATORS

Several building performance databases were created in recent years in many European countries thanks to the development of commissioning tests. This is particularly the case of building airtightness, where mandatory requirements with justification by measurement were introduced in France, UK, Belgium. This has led in these countries to the creation of national databases on building airtightness that includes more than 500,000 tests in France and the UK.

Comparing building performance across different countries can be challenging, as various indicators are used to measure the air permeability of buildings (table 1). These indicators depend on the specific application and the nation’s regulation. The most frequently used indicators, calculated from the airflow rate and the structure dimensions, are the specific air leakage rate per envelope area and the air change rate. While in the majority of countries, the reference pressure is 50 Pa, countries such as the Netherlands or France adopt 10 and 4 Pa as their respective reference points (de Hoon 2016) (Moujalled, 2023b). Calculating the specific air leakage rate requires knowledge of the building envelope area. According to ISO 9972, this area is calculated from internal dimensions, including floor areas and junctions of internal walls. However, in French and Belgium regulations, the calculation considers the thermal loss envelope area A_{TE} , which includes the areas of the building envelope directly in contact with the exterior environment, but also in contact with adjacent unheated spaces or the ground (Moujalled, 2023b)(Van Gelder, 2023). Further, the French regulation excludes the lower floor area in this calculation, and the Belgium regulation refers to the external envelope area. Furthermore, the building volume, as required for air change rate calculation, is defined in the ISO standard as the internal building volume without considering the volume of walls, floors, cavities or furniture. However, the internal volume calculation in some countries differs from this definition. In Germany, it is the net room volume as a product from the net room area and

the middle of the room height (GEG, 2020). These are all heated (or cooled) spaces. Besides, rooms that are only accessible from the outside can be excluded from the calculation if their air volume is less than 5% of the total volume. All these exceptions in national regulations make it even harder to compare the indicators.

Table 1. Comparison of air permeability indicators in five European countries

Country	Indicator	Definition	Calculation	Requirement
France	$Q_{4Pa-surf}$ [m ³ .h ⁻¹ .m ⁻²]	Specific air leakage rate at 4 Pa divided by heat loss area excluding the basement floor	$Q_{4Pa-surf} = q_4 / A_{TBAT}$ q ₄ : air leakage rate at 4 Pa [m ³ .h ⁻¹] A _{TBAT} : thermal envelope area excluding the basement floor [m ²]	Mandatory for new residential buildings
	n ₅₀ [h ⁻¹]	Air change rate at 50 Pa	$n_{50} = q_{50} / V$ q ₅₀ : air leakage rate at 50 Pa [m ³ .h ⁻¹] V: internal volume [m ³]	Optional, commonly used
Germany	n _{L50} [h ⁻¹]	Air change rate at 50 Pa	$n_{L50} = q_{50} / V_L$ q ₅₀ : air leakage rate at 50 Pa [m ³ .h ⁻¹] V _L : internal air volume [m ³]	Mandatory under certain conditions
	q _{E50} [m ³ .h ⁻¹ .m ⁻²]	Specific air leakage rate at 50 Pa divided by the internal envelope area	$q_{E50} = q_{50} / A_E$ q ₅₀ : air leakage rate at 50 Pa [m ³ .h ⁻¹] A _E : envelope area [m ²]	Additionally mandatory for buildings of an internal air volume > 1.500 m ³
Belgium	V ₅₀ [m ³ .h ⁻¹ .m ⁻²]	Specific air leakage rate at 50 Pa divided by heat loss area	$V_{50} = q_{50} / A_{test}$ q ₅₀ : air leakage rate at 50 Pa [m ³ .h ⁻¹] A _{test} : thermal envelope area [m ²]	Indicator of the regulation
	n ₅₀ [h ⁻¹]	Air change rate at 50 Pa	$n_{50} = q_{50} / V_{int}$ q ₅₀ : air leakage rate at 50 Pa [m ³ .h ⁻¹] V _{int} : internal volume [m ³]	Optional
UK	AP ₅₀ [m ³ .h ⁻¹ .m ⁻²]	Specific air leakage rate at 50 Pa divided by the internal envelope area	$AP_{50} = Q_{50} / A_E$ Q ₅₀ : air leakage rate at 50 Pa [m ³ .h ⁻¹] A _E : envelope area [m ²]	Required for new buildings > 500 m ² floor area
Netherlands	q _{v10} [m ³ .s ⁻¹]	Volumetric air flow at 10 Pa	q _{v10} : volumetric air flow at 10 Pa [m ³ .h ⁻¹]	Optional

2 CORRELATIONS BETWEEN BUILDINGS AIR PERMEABILITY INDICATORS

Statistical analysis was conducted on the French database with a total of 406,717 measurements. The analysis of the geometric data showed that the compactness factor is thus a good characterisation of the building geometry. It considers both the shape of the building and the contact with adjacent buildings or parts of buildings: around 0.8 for a typical single-family house and non-residential buildings, low values for multi-family apartments, especially for apartments on an intermediate level with one or two facades (0.2). However, this factor was calculated with the thermal envelope area as calculated in France without the lower floor area. If the entire thermal envelope area is used to calculate the compactness factor, this may introduce a bias that needs to be estimated.

Regarding the pressure exponent, the results are in close agreement with the literature, with a median and mean of around 0.66 and a standard deviation of around 0.06, whatever the type of building or its geometry. No parameter that could influence the pressure exponent has been identified, except for the presence of some specific leakages only for non-residential buildings. The correlations between the different indicators have been calculated according to the building type and compactness. Results show strong linear correlations between the different indicators with correlation coefficients between 0.80 and 0.99. The correlations between the specific air leakage rates $qE4$, $qE10$ and $qE50$ depends only on the pressure exponent. It does not vary with the buildings' geometry, same for the correlations between the air change rates $n10$ and $n50$. However, the correlations between the specific leakage rate and the air change rate are dependent on the geometry of the buildings. The more compact the building (i.e., the smaller the compactness factor), the greater the slope of the regression line. Using these tables, we can increase the reliability of the estimation of the indicators by knowing the right building type and geometry. A general correlation can be used with a higher estimation error if the geometry data is missing. The full results of the correlations according to the building type and the building compactness can be found in (Moujalled, 2023a).

As the thermal envelope area in the French database excludes the lower floor area, it would be interesting to perform analysis with other databases that include both the volume and the total envelope area to create a similar conversion equation for every existing indicator. In addition, cross analyses between databases are needed to compare the geometry parameters calculated according to different national regulations (i.e., internal and external volumes with and without walls). Finally, the correlations between airflow rates at 4, 10 and 50 Pa need to be compared to other data using directly measured airflow rates.

3 REFERENCES

- B. Moujalled, B. Kölsch, A. Mélois, V. Leprince, Quantitative correlation between buildings air permeability indicators: statistical analyses of about 500,000 measurements, under review. (2023).
- B. Moujalled, A. Mélois, VIP 45.6: Trends in building and ductwork airtightness in France, AIVC. (2023). <https://www.aivc.org/resource/vip-456-trends-building-and-ductwork-airtightness-france>.
- Gesetz zur Einsparung von Energie und zur Nutzung erneuerbarer Energien zur Wärme- und Kälteerzeugung in Gebäuden (Gebäudeenergiegesetz - GEG), 2020.
- German Institute for Standardization, DIN EN ISO 9972:2018-12. Thermal performance of buildings - Determination of air permeability of buildings - Fan pressurization method, (2018).
- HM Government, The Building Regulations 2010 - Approved Document L, Conservation of fuel and power, Volume 1: Dwellings, 2021 edition incorporating 2023 amendments, 2021. <https://www.gov.uk/government/publications/conservation-of-fuel-and-power-approved-document-l>.
- L. Van Gelder, M. De Strycker, C. Delmotte, A. Janssens, AIVC VIP 45.5: Trends in building and ductwork airtightness in Belgium, AIVC. (2023).
- M. de Hoon, Air Tightness - Predicting the performance of a building envelope, Delft University of Technology, Delft, 2016. <http://repository.tudelft.nl/>.

Proposal for new implementations in ISO 9972

Benedikt Kölsch*^{1,2}, Valérie Leprince¹, and Adeline Mélois^{2,3}

*1 Cerema,
Direction Territoire et Ville
2 rue Antoine Charial
69426 Lyon, France*

*2 Cerema,
BPE Research Team
46 rue Saint Théobald
38081 L'Isle d'Abeau, France*

**Corresponding author: benedikt.koelsch@cerema.fr*

*3 LOCIE
Université Savoie Mont Blanc
CNRS UMR 5271
73376 Le Bourget-du-Lac, France*

ABSTRACT

This article provides a summary of a comprehensive examination of the current ISO 9972 standard, focusing on the enhancements needed to improve its reliability and validity for airtightness tests in buildings. A working group composed of international experts has identified a list of issues warranting a potential revision of the standard. New recommendations are proposed based on research and consultation, including detailed considerations of previous guidelines and existing scientific literature. Key areas addressed include the definition and symbolism of terms, measurements of air temperature and wind speed, regression analysis, and airflow corrections. Significant alterations include a weighted line of organic correlation (WLOC) to improve the predictability of airflows. The article also sheds light on the significance of the zero-flow pressure difference and the requirements of measurement equipment.

These improvements aim to ensure that the ISO 9972 standard is adequately adapted to the evolving demands of building airtightness testing, in line with the increasing legal and financial implications of this field.

KEYWORDS

Building airtightness, ISO 9972, Fan pressurization method, Measurement uncertainty

1 INTRODUCTION

The global concern for the conservation of finite energy resources has significantly increased over the past few decades, and notably more so in recent months. Prominently, the building sector is tasked with confronting significant challenges, given that it accounts for a large fraction of the world's energy consumption and carbon dioxide emissions. Beyond thermal transmission, unintended airflows through the building envelope contribute to about 20 – 40% of a building's heating and cooling energy (Leprince et al., 2011), potentially increasing mold formation, decreasing thermal comfort due to drafts and cold surfaces, and possibly interfering with the operational efficiency of existing ventilation systems.

Consequently, the demand for airtightness tests has risen in various European countries, becoming an indispensable element of energy performance regulations, particularly in new buildings. This applies to several countries, including Denmark, France, Germany, Ireland, and the UK (Leprince et al., 2017; Poza-Casado et al., 2020). These tests serve critical purposes such as measuring air leakage in buildings to comply with energy performance regulations,

comparing the relative airtightness of various buildings, and quantifying the reduction in building air permeability following the execution of improvements.

The fan pressurization method, known as the Blower-Door test, is the most commonly employed technique for assessing the airtightness of buildings. The procedure for this measurement and the calculation methods for determining the air permeability of buildings using the fan pressurization method are defined in the ISO 9972 standard (*ISO 9972:2015*, 2015).

For outcomes to be comparable and trustworthy, the methods of measurement and calculation described in the standard must exhibit reliability, reproducibility, and consistency. The approach should ideally apply to all building types, and the results must retain their validity even under changing environmental conditions such as strong winds or solar radiation. In scenarios with unstable external conditions, a reliable estimate of the result's uncertainty becomes important. Recent developments and the growing number of tested buildings have underscored the need to improve the reliability of the method used for measuring a building's air leakage rate, as described in this standard (Hurel & Leprince, 2021).

This article aims to introduce a project and its methodology that intends to collect data and expertise from professionals in the field of airtightness to submit a proposed revision for ISO 9972 and proposals for potential new inclusions in the standard. It is important to clarify that the objective is not to officially revise the standard but to provide the best applicable knowledge for the official revision process in the ISO/TC 163/SC 1 technical committee (ISO committee for test and measurement methods). The project aims to propose a revised version of ISO 9972 while maintaining the existing process for testers. The ultimate goal of this project is to revise ISO 9972 so that it:

- allows the execution of the test under challenging conditions, including windy environments, extreme indoor-outdoor temperature differences, or high-rise buildings,
- enhances the reliability of the calculation process and provides a more accurate estimation of the uncertainty of measured and derived quantities,
- improves overall reliability and aligns more cohesively with other standards.

2 METHODOLOGY

The overall objective of this project is to offer a revised version of ISO 9972 to enhance the reliability of airtightness measurements in the building industry. To this end, Cerema has initiated and now leads a working group of about 30 international specialists from 13 countries, all experts in building airtightness testing. This diverse assembly of experts, with substantial research contributions and experience as testers, manufacturers, and distributors of measurement systems, is spread across the globe. Figure 1 visually represents the institutions and geographical locations associated with these working group members.

This project is structured into three principal stages:

1. Identification of the areas requiring revision in the current standard and formulation of research questions essential for addressing the existing problems.
2. Production of collaborative research with the working group members for issues to be clarified or added to the existing literature.
3. Integration of the research findings into the standard and proposition of a revised standard at the ISO level.

The initial stage of the project involved the construction of a comprehensive list of issues associated with the current version of ISO 9972, which:

- are inaccurate or irrelevant,
- induce challenges in the execution of the test,
- manifest inconsistencies with other standards,
- represent gaps in the standard (elements that need to be added for enhanced clarity or to encompass new aspects).

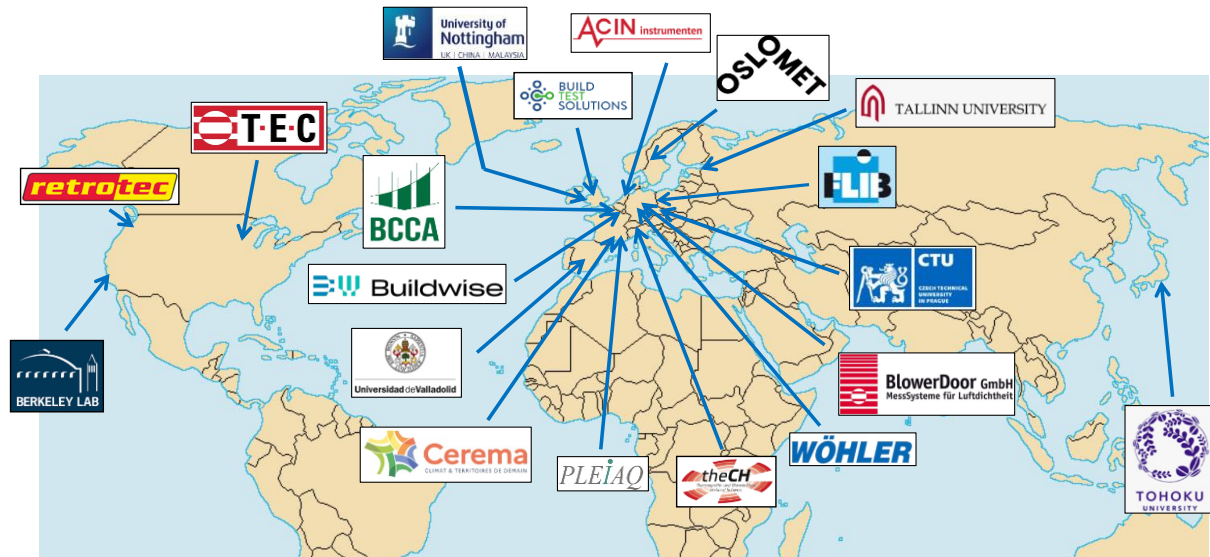


Figure 1: Affiliations of working group members, including universities, research institutions, and relevant companies

To create a comprehensive list of all relevant issues, an exhaustive survey was conducted among all working group members. Subsequently, the working group was divided into smaller sub-groups based on the members' areas of expertise and interests.

3 PROPOSED MODIFICATIONS TO ISO 9972

The working group has identified a comprehensive list of issues for a potential revision of the standard to enhance the method's reliability and validity. A more detailed description of these issues and the reasons behind a necessary revision is provided in Kölsch et al. (Kölsch et al., 2023). This section introduces the initial considerations for proposed modifications.

3.1 Terms, definitions, and symbols

The current version of ISO 9972's terms and definitions are globally considered unsatisfactory in their formulation. We have revised this section to ensure consistency and alignment with established definitions present in ISO 80000-1 (ISO 80000-1:2022, 2022) and ISO 704 (ISO 704:2009, 2009). Moreover, we have incorporated definitions for the following missing key terms: air leakage, flow rate, zero-flow pressure difference, and induced pressure difference. These revised definitions can be found in Appendix 7.1.

3.2 Apparatus – maximum permissible measurement error

Chapter 4 of ISO 9972 outlines the necessary measurement devices. However, these are frequently presented as definitions, which is not correct. Consequently, we have proposed more precise and improved formulations and have recommended a consistent maximum permissible measurement error (MPME) for each instrument. The MPME is defined as the maximum difference between the reading of an instrument and the quantity being measured (*ISO/IEC Guide 98-4:2012*, 2012). This MPME can serve as an input parameter in the uncertainty calculation. These MPMEs can be found in Appendix 7.2. Additionally, we have decided to delete the paragraph concerning the periodic calibration of the measurement system, because general requirements regarding equipment maintenance and calibration of the equipment are already specified in ISO/IEC 17025 (*ISO/IEC 17025:2017*, 2017). Hence, there is no necessity to reiterate this in ISO 9972. We are considering providing an informative annex about the verification of measurement systems.

3.3 Temperature and wind speed measurements

The current version of ISO 9972 lacks explicit guidance on the need and the appropriate locations for measuring ambient temperature and wind speed during the testing. We have incorporated recommendations based on the Czech national guideline (Novák, 2019).

Measurement of the air temperature, both internally and externally, and in the environment from which the air flows enter the air flow rate measuring system (if it differs from inside or outside air temperature), is critical for correcting the air flow measurements for air density. In chapter 5.3.2 of the standard, the existing language merely requires that the temperature inside and outside the building be recorded before, during, or after the test. We have added instructions in this section, specifying that thermometers should be preconditioned for a sufficient time in the environment where the temperature will be recorded. Additionally, it is important to conduct measurements at multiple locations within the building to ascertain an average temperature that represents the internal air temperature. An informative annex is also planned to provide further recommendations on considerations during the measurement process.

Currently, wind speed and direction measurements are not required as input in any calculations within the standard, serving only as supplementary information. Nonetheless, higher wind speeds may indicate discrepancies in the results of repeated tests of the same building. The existing standard allows for the estimation of wind speed and force through visual assessment of tree movement in terms of the Beaufort scale. We have extended this to include the option of recording wind speed with an anemometer at ground level and obtaining data from a nearby meteorological weather station.

3.4 Zero-flow pressure difference

The zero-flow pressure difference is the pressure difference between the interior and exterior of a building when it is not artificially pressurized. The measurement is taken at the start and end of each test and provides an estimation of the actual wind and stack effects present in the building.

ISO 9972 enforces a strict condition for a test to be valid, insisting that the absolute value of the zero-flow pressure difference must be lower than 5 Pa. This stringent constraint on the zero-flow pressure difference is intended to limit the test uncertainty due to wind speed and stack effect. To mitigate the influence of high-frequency wind gusts that may act on the external pressure sampling, we have extended the recording period from 30 seconds to 60 seconds, capturing 1 data point per second, ensuring that each point is the average of at least 10 measurements as recommended by Hurel et al. (Hurel & Leprince, 2021) and Prignon et al.

(Prignon et al., 2021). Furthermore, the restriction to be lower than 5 Pa excludes high-rise buildings from being tested according to ISO 9972 as there is a high likelihood that such buildings exhibit a zero-flow pressure difference exceeding 5 Pa. As such, we recommend specifying in the standard that the absolute value of zero-flow pressure difference should ideally be lower than 5 Pa and also propose including the zero-flow pressure difference (and potentially its variability) in the uncertainty calculation of the derived quantities. The method to include the impact of the zero-flow pressure in the uncertainty is currently under investigation.

3.5 Regression analysis

The ISO standard prescribes the use of a least squares technique to deduce the airflow coefficient (C) and pressure exponent (n) from the collected experimental data. In most cases, an ordinary least square method (OLS) is used to calculate these coefficients, accomplished by minimizing the sum of the squared differences between the measured values and the predicted values from the model only in the y-direction ($y_i = \ln(Q_i)$)).

However, Delmotte (Delmotte, 2013) observed that the application of OLS is only valid if all measured values in the y-direction are equally uncertain and the uncertainty in the x-direction ($x_i = \ln(\Delta P_i)$) is negligible, a condition rarely met during an actual measurement.

This limitation has been addressed by the German national annex DIN EN ISO 9972 (*DIN EN ISO 9972:2018-12*, 2018) and the Canadian standard CAN/CGSB-149.10-2019 (*CAN/CGSB-149.10-2019*, 2019), which introduce a weighted least squares (WLS) method. This WLS method acknowledges that measurements taken at low pressures have higher uncertainty and show a more significant influence on the regression, attributed to the nonlinearity of the pressure-flow relationship. Thus, the measured data are weighted using the square of the volume flow in the regression. Delmotte (Delmotte, 2013) advises using WLS only when uncertainty in the x-direction is insignificant. Despite this, Delmotte (Delmotte, 2017) asserts that this condition is rarely satisfied in practice, and introduces an alternative: the weighted line of organic correlation (WLOC). The WLOC uses the standard uncertainty at each pressure-flow data point as a weight and optimizes the distances in both x and y-directions. Studies (Delmotte, 2017; Kölsch & Walker, 2020; Prignon et al., 2019, 2018) have demonstrated that this method significantly enhances airflow predictability and reduces the variability of flow coefficient and pressure exponent. A comparison of the regression results of the OLS and WLOC methods is shown in Figure 2. It reveals that data points with greater measurement uncertainty have less impact on the regression. Consequently, we propose integrating the WLOC into the revised version of the standard. Integrating this method will also have an impact on the uncertainty calculation.

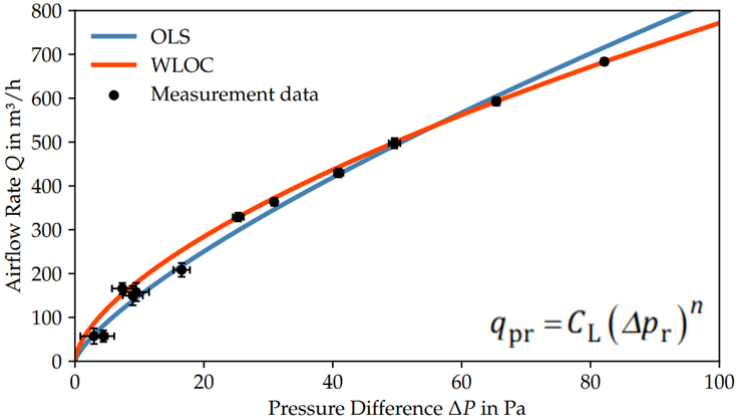


Figure 2: Comparison of OLS and WLOC - linear display (Kölsch & Walker, 2020)

3.6 Airflow corrections

For the resulting airflows to be both valid and comparable, it is important to correct them to standard temperatures and pressure conditions. This ensures the comparability of tests even when they are conducted under varying conditions. Unlike ASTM E772-19 (*ASTM E779-19*, 2019) and CAN/CGSB-149.10-2019, ISO 9972 currently requires only simplified corrections. These simplifications are suitable when the barometric pressure is negligible, the blower door calibration is near the reference conditions, and the pressure exponent is close to 0.5 (Walker et al., 1998). However, the airflow rates through system components and leaks are influenced by factors such as air viscosity, air density, and pressure exponent. Given modern computational equipment, the necessity and appropriateness of simplifying these corrections have been questioned (Carrié, 2014). Therefore, we propose the implementation of the following corrections for airflow and flow coefficient (here as an example for pressurization), as stipulated in the ASTM standard (with airflow rate q , airflow coefficient C , pressure exponent n , air density ρ , and dynamic viscosity of air μ):

$$q_{env} = q_m \left(\frac{\rho_e}{\rho_{int}} \right) \quad (1)$$

$$C_L = C_{env} \left(\frac{\mu_e}{\mu_0} \right)^{2n-1} \left(\frac{\rho_e}{\rho_0} \right)^{1-n} \quad (2)$$

4 CONCLUSION AND OUTLOOK

Due to rising awareness regarding building airtightness and an increasing number of performed airtightness tests, the experiences and knowledge regarding test reliability and validity are increasing. Because of related legal and financial issues, reliable and valid tests have become more critical. Therefore, Cerema started a project and set up a working group of international experts to improve and revise the ISO 9972 standard. This article presents a selection of the suggested improvements to the standard.

In addition to the aspects elaborated in this article, the project aims to address several other vital factors, including:

- Building preparation: It might be beneficial to describe the basic principles of building preparation in the current version of the standard more precisely and avoid ambiguities.
- Placement of external pressure taps: The location of the external pressure taps is important, as it serves as a reference for every pressure difference measurement, including zero-flow pressure measurements. It is crucial that ISO 9972 provides clear guidance on whether the pressure difference across the building envelope or the equilibrium internal pressure should be measured, as it directly impacts the location of external measurement probes.
- Comprehensive calculation of measurement uncertainty: The standard should offer a unified and comprehensive approach to calculating measurement uncertainty, considering all potential error sources. This includes instrumentation inaccuracies, environmental influences, and methodological factors.

5 ACKNOWLEDGMENTS

The authors thank the working group members for participating in this project and for their valuable contribution to this work.

6 REFERENCES

- ASTM E779-19—Standard Test Method for Determining Air Leakage Rate by Fan Pressurization. (2019).
- CAN/CGSB-149.10-2019—Determination of the airtightness of building envelopes by the fan depressurization method. (2019).
- Carrié, F. R. (2014). Temperature and pressure corrections for power-law coefficients of airflow through ventilation system components and leaks. Proceedings of the 35th AIVC Conference.
- Carrié, F. R., & Leprince, V. (2016). Uncertainties in building pressurisation tests due to steady wind. *Energy and Buildings*, 116, 656–665. <https://doi.org/10.1016/j.enbuild.2016.01.029>
- Carrié, F. R., Olson, C., & Nelson, G. (2021). Building airtightness measurement uncertainty due to steady stack effect. *Energy and Buildings*, 237, 110807. <https://doi.org/10.1016/j.enbuild.2021.110807>
- Delmotte, C. (2021). Airtightness of buildings – Assessment of leakage-infiltration ratio and systematic measurement error due to steady wind and stack effect. *Energy and Buildings*, 241, 110969. <https://doi.org/10.1016/j.enbuild.2021.110969>
- Delmotte, C. (2013). Airtightness of buildings—Calculation of combined standard uncertainty. Proceedings of the 34th AIVC Conference.
- Delmotte, C. (2017). Airtightness of Buildings – Considerations regarding the Zero-Flow Pressure and the Weighted Line of Organic Correlation. Proceedings of the 38th AIVC Conference.
- DIN EN ISO 9972:2018-12—Thermal performance of buildings - Determination of air permeability of buildings - Fan pressurization method (9972:2018-12). (2018). Beuth Verlag.
- Hurel, N., & Leprince, V. (2021). Impact of wind on the airtightness test results. AIVC Ventilation Information Paper No 41.
- ISO 704:2009—Terminology work - Principles and methods. (2009).
- ISO 9972:2015—Thermal performance of buildings - Determination of air permeability of buildings - Fan pressurization method. (2015).
- ISO 80000-1:2022—Quantities and units - Part 1: General. (2022).
- ISO/IEC 17025:2017—General requirements for the competence of testing and calibration laboratories. (2017).
- ISO/IEC Guide 98-4:2012—Uncertainty of measurement — Part 4: Role of measurement uncertainty in conformity assessment. (2012).
- Kölsch, B., Mélois, A., & Leprince, V. (2023). Improvement of the ISO 9972: Proposal for a more reliable standard to measure air leakage rate using the fan pressurisation method. Proceedings of the 13th International BuildAir-Symposium.
- Kölsch, B., & Walker, I. S. (2020). Improving air leakage prediction of buildings using the fan pressurization method with the Weighted Line of Organic Correlation. *Building and Environment*, 181, 107157. <https://doi.org/10.1016/j.buildenv.2020.107157>

- Leprince, V., Bailly, A., Carrié, F. R., & Olivier, M. (2011). State of the Art of Non-Residential Buildings Air-tightness and Impact on the Energy Consumption. Proceedings of the 32nd AIVC Conference.
- Leprince, V., Carrié, F. R., & Kapsalaki, M. (2017). Building and ductwork airtightness requirements in Europe – Comparison of 10 European countries. Proceedings of the 38th AIVC Conference.
- Novák, J. (2019). Implementation of the EN ISO 9972 standard into the Czech Republic. Proceedings of the 11th International BuildAir-Symposium.
- Poza-Casado, I., Cardoso, V. E. M., Almeida, R. M. S. F., Meiss, A., Ramos, N. M. M., & Padilla-Marcos, M. Á. (2020). Residential buildings airtightness frameworks: A review on the main databases and setups in Europe and North America. *Building and Environment*, 183, 107221. <https://doi.org/10.1016/j.buildenv.2020.107221>
- Prignon, M., Dawans, A., Altomonte, S., & Van Moeseke, G. (2019). A method to quantify uncertainties in airtightness measurements: Zero-flow and envelope pressure. *Energy and Buildings*, 188–189, 12–24. <https://doi.org/10.1016/j.enbuild.2019.02.006>
- Prignon, M., Dawans, A., & Van Moeseke, G. (2021). Quantification of uncertainty in zero-flow pressure approximation. *International Journal of Ventilation*, 20(3–4), 248–257. <https://doi.org/10.1080/14733315.2020.1777020>
- Prignon, M., Dawans, A., & Van Moeseke, G. (2018). Uncertainties in airtightness measurements: Regression methods and pressure sequences. Proceedings of the 39th AIVC Conference.
- Walker, I. S., Wilson, D. J., & Sherman, M. H. (1998). A comparison of the power law to quadratic formulations for air infiltration calculations. *Energy and Buildings*, 27(3), 293–299. [https://doi.org/10.1016/S0378-7788\(97\)00047-9](https://doi.org/10.1016/S0378-7788(97)00047-9)

7 APPENDIX

7.1 Revised terms and definitions

air leakage

passage of air through unintended path in the shell of an enclosure

Note 1 to entry: This passage includes flow through joints, cracks, and porous surfaces, or a combination thereof, induced by the fan used in the procedure described in this document (see Clause 4).

flow rate

quotient of the amount of fluid passing a given plane by the duration

air leakage rate

quotient of the amount of air leakage by the duration

building envelope

shell separating the inside from the outside environment or another building

volumic air leakage rate

deprecated term: air change rate

quotient of the air leakage rate by a reference volume

Note 1 to entry: In this document, the reference volume is the internal volume of the building.

areic air leakage rate

deprecated term 1: air permeability

deprecated term 2: specific air leakage rate

quotient of the air leakage rate by a reference area

Note 1 to entry: The reference area is commonly the area of the building envelope or the floor area of the building.

equivalent leak area

area of a single orifice which, for the same applied pressure difference, would pass the same air flow rate as the leaks of the building envelope under consideration

areic equivalent leak area

deprecated term: specific effective leakage area

quotient of the equivalent leak area by a reference area

Note 1 to entry: The reference area is commonly the area of the building envelope or the floor area of the building.

to close an opening

to make an opening hermetic by an appropriate means

Note 1 to entry: Examples of appropriate means are adhesives, inflatable balloons, or stoppers.

zero-flow pressure difference

admitted term: natural pressure difference

pressure difference prevailing between inside and outside a building when no air flow is generated by forces other than wind and stack effect

induced pressure difference

pressure difference generated between inside and outside a building by forces other than wind and stack effect

Note 1 to entry: In the present document, the other force is a fan (see clause 4.2.1).

7.2 Revised maximum permissible measurement errors (MPME)

Table 1: MPME of measurement instruments

Measurement instrument	MPME
Monometer	not larger than ± 1 Pa or 1 % of the reading, whichever is greater for the measurement interval that includes the measured quantity
Air flow rate measuring system	not larger than ± 5 m ³ /h or 7 % of the reading, whichever is greater
Thermometer	not larger than ± 1 °C in the range of -30 °C to 50 °C
Barometer	not larger than ± 300 Pa
Hygrometer	not larger than ± 5 % of relative humidity

Which design parameters impact the resilience to overheating in a typical apartment building?

Abantika Sengupta^{*1}, Jef Kerckaert¹, Marijke Steeman², and Hilde Breesch¹

Gebroeders de Smetstraat 1

9000, Gent, Belgium

**Corresponding author :*

abantika.sengupta@kuleuven.be

Presenting author: Abantika Sengupta

2 Ghent University

Campus Boekentoren - Plateau

Jozef Plateaustraat 22

9000 Gent, Belgium

ABSTRACT

Airtight, highly insulated, and passively cooled buildings in the EU are designed under typical outdoor and indoor thermal conditions. With increasing risk and uncertainty with regards to climate change and associated heatwaves (HW), the design thermal performance of these buildings is not guaranteed. It is crucial to focus on improving thermal resilience to overheating and futureproof these buildings. “Thermal resilience to overheating” is the characteristic that describes the extent to which buildings and their cooling strategies can maintain habitable conditions during or post shocks. Thus, a new design approach to improve the thermal resilience to overheating of existing and newly built buildings is a growing need in the building sector. Within the framework of IEA EBC Annex 80-Resilient Cooling of Buildings, the aim of this study is to determine the most influential building and system design parameters that impact the thermal resilience to overheating. To achieve this aim, building energy simulation (BES), is conducted on a reference typical apartment building in Belgium. A 2 bedroom apartment for 3 occupants is simulated in Open Studio and EnergyPlus during summer (April-September) of typical meteorological year (TMY). The apartment is evaluated with its default design (very heavy thermal mass, window to wall ratio (WWR) 10% and with no shading and no passive cooling strategy (in this case natural night ventilation -NNV). Apart from the default design, design parameters were altered such as thermal mass (very heavy-medium-light), WWR (10-30%), implementation of solar shading and NNV. The impact of the worst, improved and the optimized designs are also evaluated during a 6 day intense heatwave period. Overheating are most likely to occur in current buildings with higher WWR (>30%), no shading and with lighter thermal mass. WWR has highest impact on the thermal resilience followed by thermal mass. Apartment with very heavy thermal mass, WWR 10%, with NNV and solar shading shows the best result (80% reduction in the percentage of occupied hours above 25°C threshold). However, in buildings with higher WWR (>30%) and lighter thermal mass, thermal resilience can be improved with implementation of solar shading and passive cooling strategies such as NNV. Even during heatwave, an apartment without NNV has better (45%) thermal resilience to overheating than an apartment with NNV if the WWR is < 30%) and has a medium thermal mass rather than a light thermal mass.

KEYWORDS

Thermal Resilience, Overheating-risk, Apartments, Heatwaves, Design parameters

1 INTRODUCTION

A recent study in Europe, shows the cooling degree days (CDD) value was almost four times higher in 2022 than in 1979, indicating that the need for cooling (air conditioning) significantly increased over the last decades [1]. Additionally, Intergovernmental Panel on Climate Change (IPCC)s 2022 report warns about the severity of the climate change impacts (frequent and severe heatwaves) in future climate scenarios and also stresses on adaptation and mitigation plans[2]. Thus, overheating risk in buildings is expected to increase as global warming continues [3]. Apartment buildings accounts for a large share of building stocks and have implemented energy efficient technologies and practices (e.g., high-insulation, airtight envelopes, improved glazing). However, overheating has become a recurring problem in these buildings proving that “excessive striving for energy efficiency” could compromise a building’s

ability to maintain comfortable thermal conditions in future climate scenarios and during HWs[3][4]. Thus, to avoid any health risks such as sleep deprivation, heat stress and even mortality due to overheating in these buildings, the thermal resilience to overheating of apartments should be assessed and improved. A buildings' thermal resilience can be defined as "An ability of the building to withstand disruptions; and to maintain capacity to adapt, learn and transform" [5][6]. Thus, apart from energy performance, resilience is gaining importance to assess building performance [7] [8] and can be considered as a primary function of the building [9]. However, in order to improve the thermal resilience to overheating, the impact of different building and system parameters on the thermal resilience should be evaluated.

Building design parameters such as, building setting and micro-climate, building orientation and space zoning, window orientation and window to wall ratio (WWR), envelope properties (U-values, thermal mass, air-tightness), glazing properties, implementation of solar shading and passive cooling strategies impact the thermal resilience to overheating. Window orientation and WWR has significant impact on thermal resilience to overheating [10]. Norwegian residential building with WWRs greater than 50% experienced higher indoor temperatures and greater overheating risk during HWs compared to buildings with lower WWRs [11]. A study conducted to evaluate the most optimal WWR in different European climates concluded that although there is an optimal WWR in each climate and orientation, most of the ideal values can be found in a relatively narrow range ($0.30 < \text{WWR} < 0.45$). Apart from WWR, thermal mass of a building impacts the thermal resilience to overheating [12]. Incorporating materials with high thermal mass, such as concrete or brick, into the building envelope can help to absorb and store heat during the day, and release it at night when temperatures are lower. A recent study on an educational nZEB in Belgium showed that heavy thermal mass performs well in short-term shocks like short HWs when the building takes longer time to absorb the heat but once the heat enters the building, without proper ventilation, the heat is retained in the building for longer period and negatively impacts the buildings' thermal resilience to overheating C. A simulation study [13] evaluating the performance of solar shading in offices in several climates shows cooling energy use reductions by 5 to 77%. A study to evaluate the recovery aspect of thermal resilience of a residential building equipped with solar shading showed that when shading is active in a typical meteorological year (TMY) scenario, the temperature in the living room reaches below 25°C after peak within 9 hours. However, same building takes significantly higher recover time (takes 62 hours without the shading in a TMY period and 84 hours during HW period). Sengupta et al. [14] evaluated the thermal resilience of a Belgian dwelling during the HW of 2020 with and without natural night ventilation (NNV). The results showed that with implementation of NNV, the building recovers 90% faster from the HW and decreases maximum temperatures indoors by 4.3°C compared to the building without NNV.

The objective of this paper is to evaluate the impact of building design parameters and implementation of solar shading and passive cooling strategy (NNV) on the thermal resilience to overheating in a typical Belgian apartment. For this a base case scenario of the apartment (with default construction, no shading or no NNV) during TMY scenario is evaluated altering the design parameters. The worst, improved and optimized design cases are then assessed during a 6 day long HW.

2 CASE STUDY BUILDING

In order to perform parametric study, typical apartment building floor plans, while maintaining some degrees of freedom, has been developed by Renson [15] and KU Leuven. The floor plans are based on new buildings (2016-2020) data from Valaams Energie-en Klimaatagentschap (VEKA)[16] and are evaluated against EPBD guidelines [17]. The developed individual apartment floor plans have multiple bedrooms (ranging from 1 to 3). The surface of the living

room, kitchen, utility room and bathroom increase in function of the number of bedrooms. Multifamily dwellings (in Belgium) typically have an open plan kitchen and living area. Based on the VEKA [16] data (Figure 1), the most common type of apartment (2 bedroom apartment) has been selected for this study. The gross and net floor area of the apartment is 101.5 m² and 85.2 m² respectively with each floor height of 2.55 m. The apartment has a very heavy thermal mass according to the EN ISO 13790 [18] and n50 value of 1.89. The default apartment is north-south oriented and has been divided into 7 thermal zones (TZs) (see Figure 2 and Table 1). Table 2. shows building envelope properties. The apartment has double glazed windows (u-value: 1.00 W/m²K, g-value: 0.56) with window-to-wall ratio (WWR) of 18% on the South, 25% on East and 15% on west facade. The window-to-floor ratio is 14%. The windows on South and West are equipped with external solar shading ($g_{tot} = 0.04$), which activates when the radiation on the window is above 250 W/m². The apartment is designed for 3 occupants with internal gains (people and equipment) calculated according to EN 16798-1[19]. The building is equipped with balanced mechanical ventilation system with heat recovery, with a total supply airflow of 200 m³/h. The ventilation air flow rates are calculated according to the NBN D50-001[20] (see Table 1).

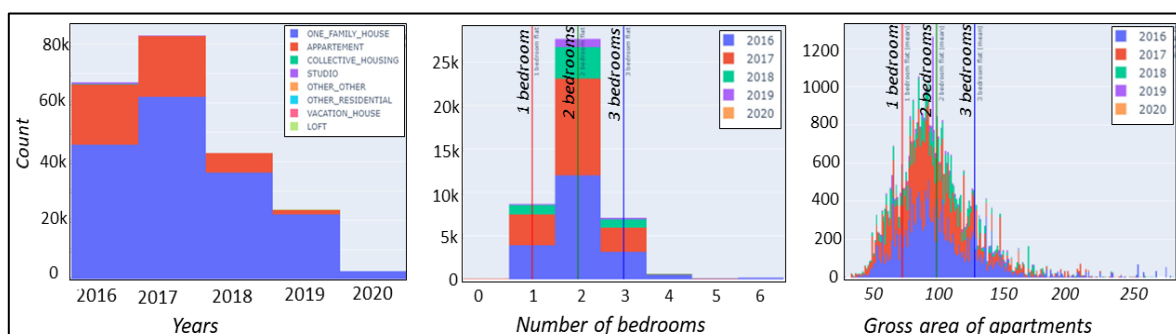


Figure 1. VEKA[16] data from 2016 to 2020 (new buildings) showing the typology of buildings, number of bedrooms and gross area of each apartment

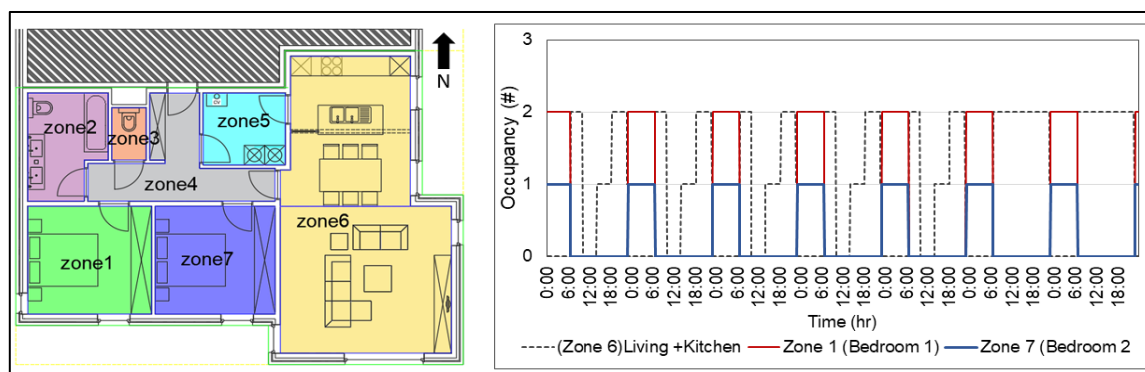


Figure 2. Floor plan with thermal zones (left) and occupancy pattern in different thermal zones (1 week)

Table 1. Thermal zones

Thermal zone	Area (m ²)	Ventilation flow rates (m ³ /h)
TZ 1 (Bedroom 1)	11.9	Supply =50, Extract =0
TZ 2 (Washroom)	2.5	Supply =0, Extract =50
TZ 3 (WC)	5.5	Supply =0, Extract =25
TZ 4 (Corridor)	9.0	Supply =0, Extract =0
TZ 5 (Utility room)	5.3	Supply =0, Extract =50
TZ 6 (Living+ kitchen)	38.9	Supply =100, Extract =75
TZ 7 (Bedroom 2)	11.6	Supply =50, Extract =0

Table 2. Construction packages and u-values

Construction package	Description	u-value (W/m ² K)
External Wall	Brick with air layer and 8 cm PUR	0.24
Common wall	Concrete reinforced with 3 cm rockwool	0.60
Internal wall	Gypsum board and brick	2.10
Separating floors	Concrete with screed and 6 cm rockwool	0.50

3 METHODOLOGY

To access the impact of design parameters on the thermal resilience to overheating in a typical Belgian apartment, different building parameters such as thermal mass, WWR implementation of solar shading and passive cooling strategy were altered.

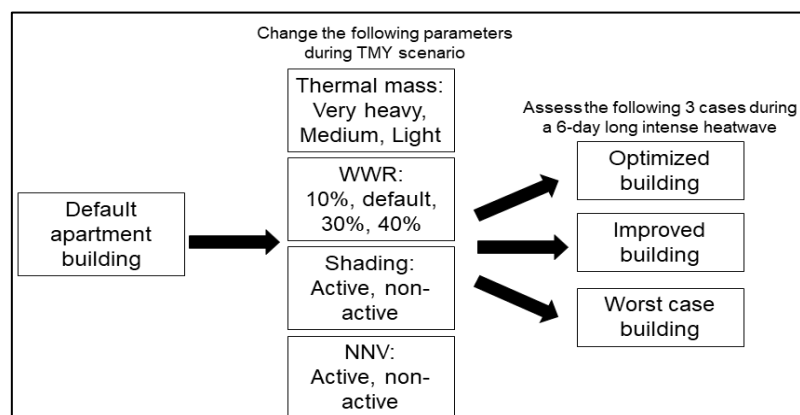


Figure 3. Altering the design parameters and testing the optimized, improved and worst-case scenario during the HW period

3.1 Design parameters

Thermal mass

Apart from the default (very-heavy) construction set, a medium and light thermal mass construction set was evaluated. For the default construction set (very heavy) to medium thermal mass, floor construction was altered and for light thermal mass, the external wall was altered. Table 3 gives an overview of the altered construction sets.

Table 3. Design alternatives for thermal mass

		Construction sets	d [m]	ρ [Kg/m ³]	C (J/KgK)	λ [W/(m.K)]	R [(m ² .K)/W]	U [W/(m ² .K)]
Default (very heavy)	Floor (i-e)	Tiles	0,03	1700	1000	1,10	0,03	
		Screed	0,06	2000	1000	0,40	0,15	
		Polyurethane (PUR)	0,06	30	1400	0,02	2,73	0,34
		Heavy reinforced concrete	0,14	2240	900	1,75	0,08	
	External wall (i-e)	Gypsum	0,01	1120	840	0,52	0,02	
		Light brick	0,14	850	880	0,80	0,18	
Polyurethane (PUR) Non ventilated air layer 25 =< d < 50		0,08	30	1400	0,02	3,64	0,24	
Medium thermal mass	Floor (i-e)	Wooden boarded floor	0,02	600	1880	0,15	0,13	
		Pressure-resistant wood fibre cement board	0,04	1000	1470	0,23	0,17	
		OSB 18 mm	0,02	600	1700	0,13	0,14	0,34
		Glass wool + wooden slats	0,15	139	1138	0,06	2,38	
		Promatect plate 2x	0,03	900	1000	0,18	0,14	
	External wall (i-e)	Light brick Non ventilated air layer 25 =< d < 50	0,14	880	850	0,80	0,18	
Light thermal mass	External wall (i-e)	Mineral wool (MW) - plates or blankets	0,04	10	1030	0,04	1,05	0,24
		Hempcrete	0,19	340	1700	0,07	2,76	
		Gypsum	0,01	1120	840	0,52	0,02	

Window to wall ratio (WWR)

A range of WWR between 10%-40% was tested. Table 4 gives an overview of the window areas varied to set WWR between 10%-40%.

Table 4. Design alteration to set WWR between 10%-40%

	Area (m ²) when WWR=10%	Area (m ²) when WWR=30%	Area (m ²) when WWR=40%
Zone 6 (Living+ Kitchen)	9,1	20,3	27,1
Zone 1 (Bedroom 1)	1,1	6,9	9,2
Zone 7 (Bedroom 2)	1,1	2,1	2,8

Shading

The building was assessed with and without solar shading to evaluate the impact of solar shading on the thermal resilience to overheating.

Natural Night ventilation

Natural night ventilation (NNV) is implemented as passive means to cool the building. TZ1, TZ 6 and TZ 7 are provided with operable windows which are automatically controlled. The effective area of these windows is calculated based on the method proposed in [21] taken into account the window area, height and opening angle. The total effective area of all windows is 2.7% of the gross floor area. Once open, the window will remain open for at least 15 min. The windows are open between 10 pm to 6 am from in summer period (April-September) if the following conditions are met:

- Room temperature exceeds both the heating set point (=22°C) and the external temperature +2°C
- External temperature is higher than 12°C
- Internal relative humidity is smaller than 70%
- There is no rainfall and the wind velocity on site is smaller than 10 m/s

3.2 Weather Data

Two types of weather data sets for Ghent, Belgium were used- (a) Typical meteorological year (TMY) 2010s to benchmark and (b) mid-term 2050s HW to assess the resilience of the building during shock. These weather data files were formulated adapting the method of Weather data task force of IEA Annex 80 and Ouzeau et al. [22]. The 6 day HW occurs between June 29th and July 4th with mean temperature of 28.6°C and peak outdoor temperature of 41.6°C[12].

3.3. Thermal resilience evaluation

To assess the impact of design parameters, the following indicators were used:

Adaptive thermal comfort

For buildings without cooling systems (default case): adaptive model with adaptive temperature limits (ATL), Category II is applied. The allowed indoor operative temperature is calculated as a function of the running mean outdoor temperature based on the ISO 17772-1 Annex H.2 [23].

Standard effective temperature

During the HWs, the occupants face health risks or even life-threatening consequences. Therefore, the threshold for the indoor environment should be selected by considering the impact on occupants' health. In this study, Standard effective temperature (SET) is adapted (ASHRAE 55-2017 [23] recommended to evaluate human response to heat stress). To calculate the SET, a clo of 0.5, airspeed of 0.1m/s and metabolic rate of 1 in bedrooms and 1.4 in living-dining-kitchen was assumed[24].

Unmet degree hours

Unmet degree. hours (K.h) was used as the resilience key performance indicator [25]. For this study, a fixed temperature limit (FTL) of 24°C for bedrooms and, 25°C, 26°C and 28°C for the living-dining-kitchen was chosen as the overheating threshold for European buildings (CIBSE TM52 standard [26]). The acceptable threshold according to the same standard is equal to 6 K.h./day. A SET threshold of 28 °C for the building under a HW was used calculate the unmet hours.

Percentage of occupied hours above threshold

To compare the impact of different design parameters, Method A as described in Annex F of the EN 16798 [27] was selected. Following this method, the percentage of occupied hours when the zone operative temperature is above FTL and ATL was evaluated. A percentage of occupied hours below 5% is considered as acceptable and below 3% is considered good.

3.4. Building Energy Simulations (BES) and scenarios

For the evaluation of impact of different design parameters, annual hourly BES were performed using Open Studio[28] and EnergyPlus [29]. In the BES model, the separating floors and common walls were assumed to be adiabatic. Results were evaluated for summer period (April-September).The simulation is started two weeks prior and was run for four weeks after the studied period. Table 5 shows the simulation scenarios during the TMY period. Furthermore, 3 cases –(a) worst, (b) improved and (c) optimized designs from both no cooling and cooling strategy implemented will be analysed during a 6 day HW period.

Table 5. Simulation scenarios during TMY period

Scenario No	Thermal mass	WWR	Shading	cooling strategy	Scenario No	Thermal mass	WWR	Shading	cooling strategy
A1	Heavy	10%	NO	None	A19	Heavy	10%	NO	NNV
A2	Medium	10%	NO		A20	Medium	10%	NO	
A3	Light	10%	NO		A21	Light	10%	NO	
A4	Heavy	30%	NO		A22	Heavy	30%	NO	
A5	Medium	30%	NO		A23	Medium	30%	NO	
A6	Light	30%	NO		A24	Light	30%	NO	
A7	Heavy	40%	NO		A25	Heavy	40%	NO	
A8	Medium	40%	NO		A26	Medium	40%	NO	
A9	Light	40%	NO		A27	Light	40%	NO	
A10	Heavy	10%	Yes		A28	Heavy	10%	Yes	
A11	Medium	10%	Yes		A29	Medium	10%	Yes	
A12	Light	10%	Yes		A30	Light	10%	Yes	
A13	Heavy	30%	Yes		A31	Heavy	30%	Yes	
A14	Medium	30%	Yes		A32	Medium	30%	Yes	
A15	Light	30%	Yes		A33	Light	30%	Yes	
A16	Heavy	40%	Yes		A34	Heavy	40%	Yes	
A17	Medium	40%	Yes		A35	Medium	40%	Yes	
A18	Light	40%	Yes		A36	Light	40%	Yes	

4 RESULTS AND DISCUSSION

4.1 Base case scenario (No solar shading, no cooling strategy)

In base case scenario (with default design), TZ6 is the most critical zone due to high solar and internal gains (occupancy and equipment). With fixed temperature limit (FTL) of 24°C and 25°C, unmet degree hours are above daily limit of 6 (K.h). With FTL of 26°C and 28 °C, unmet

degree hours in TZ 6 is within daily limit of 6 (K.h). In both the bedrooms (TZ 1 and TZ7), with FTL and ATL, daily unmet degree hours were below daily threshold.

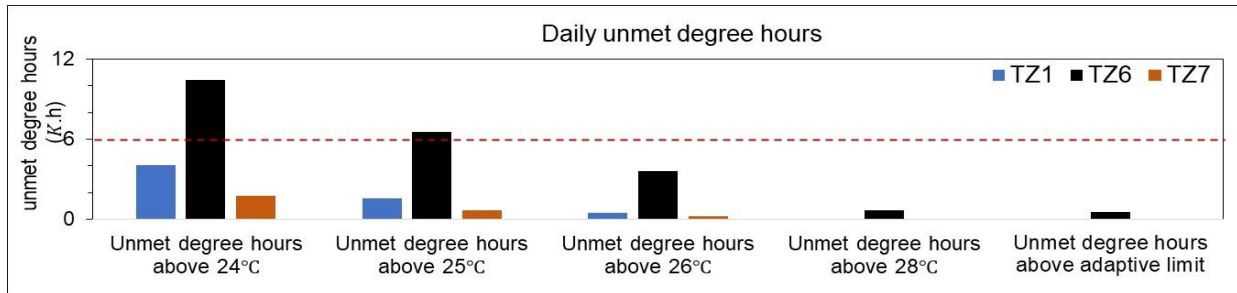


Figure 4. Unmet degree hours with fixed (24°C, 25 °C, 26°C and 28°C) and ATL in the base case model (default design)

Between June and August, more than 5% occupied hours were higher than FTL and ATL in TZ6. In TZ1 and TZ7, there were no occupied hours above FTL of 28°C and ATL during the entire summer period (April to September). With 26°C threshold, for TZ1, June and July was overheating period and for TZ7 only July was overheating period. Between June and August, more than 5% occupied hours were above FTL of 24°C and 25°C for TZ1 and TZ7. For further assessments, only the most critical zone (TZ 6) will be discussed.

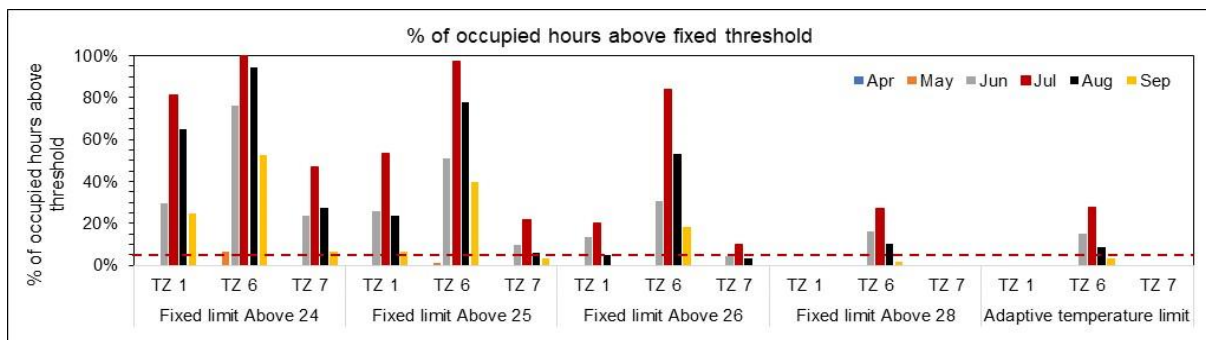


Figure 5. Percentage of occupied hours above fixed (24°C, 25 °C, 26°C and 28°C) and ATL in the base case model (default design)

4.2 Impact of design parameters and solar shading

Figure 6 shows the % of occupied hours above ATL for the whole summer period (April-September) for the altered design parameters (see Table 5).

Keeping 10% WWR, thermal mass is altered from very heavy to medium to light, (case 01-03). When thermal mass is altered from very heavy to medium, and from very heavy to light, there is a 3.1% and 8.2% increase in % of occupied hours above ATL. For all 3 thermal zones, % of occupied hours above adaptive threshold increases with increase in WWR. For TZ6 with default (very heavy) thermal mass, if WWR is increased from 10% to 30%, there is 66.5% increase in the % of occupied hours above ATL. Additional 10% increase i.e., 40% WWR, increases % of occupied hours above ATL by 83.1% compared to 10% WWR. However, it is interesting to notice that with 40% WWR, the % of occupied hours decreases as the thermal mass is altered from very heavy to medium (-0.8%) and further when thermal mass is light (-2.5%). The increased solar gains due to increase in WWR is flushed out faster by a lighter thermal mass compared to heavier thermal mass.

With implementation of solar shading, there is significant (9-70%) decrease in the percentage of occupied hours above ATL. With solar shading, in the default design case, % of occupied hours above ATL decreases from 9.2% to 0.07%, i.e., it is within 5% acceptable limit. The default apartment (no shading, 10% WWR, very heavy thermal mass) has 2.5% lower percentage of occupied hours above ATL than a building with solar shading with light thermal mass and 30% WWR. It can be concluded that to improve the thermal resilience to overheating,

along with implementing solar shading to reduce solar gains, it is crucial to find optimal balance between thermal mass and WWR of the building.

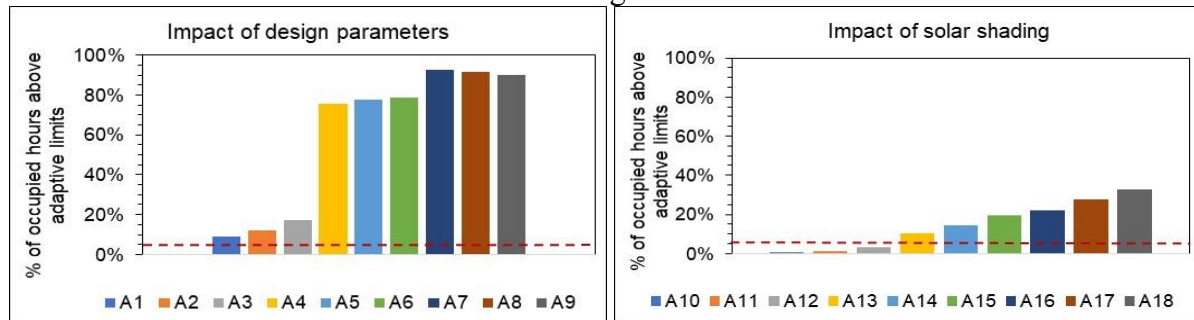


Figure 6. Impact of different design parameters and solar shading on the thermal resilience to overheating

4.3 Implementation of NNV and NNV+ solar shading

Even with NNV implemented, the % of occupied hours (with FTL 25°C and 26 °C) is above 5% accepted limit. With 28°C FTL, only with 10% WWR, the % of occupied hours above threshold is below 5% acceptable limit. With implementation of NNV, the % of occupied hours above FTL (25°C) decreased significantly (average 45%) except when WWR is increased to 30% and 40% without the solar shading (increased in occupied hours above threshold by 50% compared to base case). With solar shading, even if the WWR is increased to 30% and 40%, there is an average decrease of 35% in occupied hours above threshold limit. With NNV+ solar shading implemented, with 26°C FTL, the 5% limit is violated if WWR is above 30% and the thermal mass is medium. Thus, with increased 30% WWR, NNV with solar shading can reduce overheating risk. Case A28 (very heavy thermal mass + 10% WWR + NNV+ solar shading) shows the best result with 80% reduction in the percentage of occupied hours above FTL 25°C.

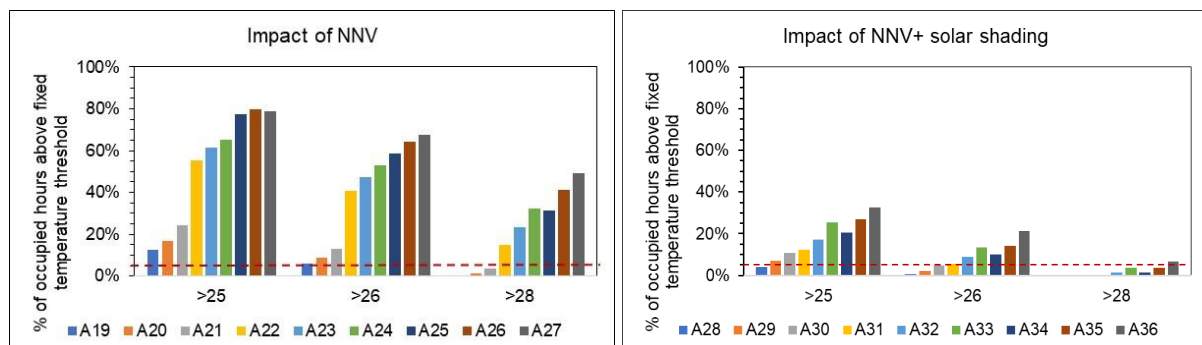


Figure 7. Impact of different NNV and NNV+ solar shading on the thermal resilience to overheating

4.4 Impact of heat wave

Table 6 shows the worst, improved and the optimized cases selected to evaluate the impact of HWs on the design parameters.

Table 6. Worst, improved and optimized design cases

	Scenario		Thermal Mass	WWR	Shading	Cooling
	No	Case				
Worst	E1	A9	Light	40	No	No cooling
Improved	E2	A14	Medium	30	Yes	
Optimized	E3	A10	Heavy	10	Yes	
Worst	E4	A27	Light	40	No	NNV
Improved	E5	A32	Medium	30	Yes	
Optimized	E6	A28	Heavy	10	Yes	

To evaluate the impact of design parameters during HWs, % of occupied hours above 28°C SET is assessed. With the worst design case (Light thermal mass+WWR40%+No shading+ No NNV), 97% of occupied hours are above 28°C SET limit. The thermal resilience of the building

is poor and the occupants are under heat stress. The optimized design case (Heavy thermal mass+WR10%+ solar shading+NNV), the % of occupied hours above 28°C SET is within 5% threshold even during HW. The result also demonstrates that implementing a passive cooling strategy such as NNV will not improve the thermal resilience unless it is coupled with the building design parameter. For example, case E3 has 45% less occupied hours without NNV than case E4 with NNV. This is due to higher solar gains (no shading and higher WWR) and also due to lighter thermal mass when absorbs the heat faster during a HW.

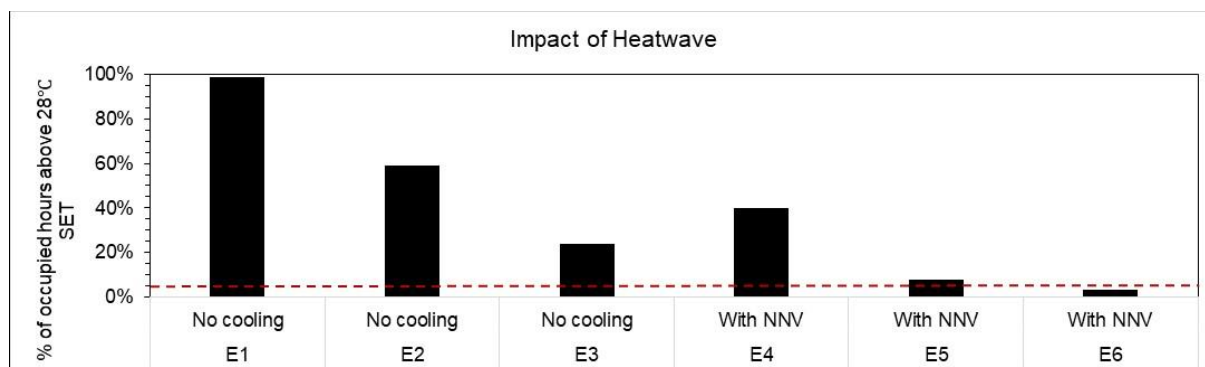


Figure 8. Impact of design parameters, solar shading and NNV on the thermal resilience to overheating during a 6 -day HW

5 CONCLUSIONS AND FUTURE OUTLOOK

The aim of this paper is to evaluate the impact of design parameters on the thermal resilience to overheating. The study demonstrates:

- a) Overheating is most likely to occur in current buildings with high WWR, no solar shading and with lighter thermal mass. WWR has highest impact on the thermal resilience followed by thermal mass. However, in buildings with higher WWR and lighter thermal mass, thermal resilience can be improved with implementation of solar shading and passive cooling strategies such as NNV.
- b) NNV and solar shading can improve the thermal resilience and heat stress during a short and intense HW. However, the thermal mass should be between medium and heavy and WWR should be between 10-30%. Buildings without NNV, but with heavy thermal mass and low WWR during HW performs better than buildings with light thermal mass and high WWR. NNV is not effective during a HW period as the diurnal variations of temperature are limited during HW period. To improve the buildings' thermal resilience to overheating, implementation of solar shading and WWR has the highest impact.
- c) Apart from the design parameters that were evaluated in this study, there is a need to evaluate other building design parameters such as orientation of the building, level of insulation, air-tightness, type of glazing, type of solar shading etc. There is also a need to evaluate other passive and active cooling strategies coupled with different building parameters. Future work will include a sensitivity analysis to evaluate the most influential building and system design parameters that impact the thermal resilience to overheating.

6 ACKNOWLEDGEMENT

This study is performed under the framework of International Energy Agency's Energy in Buildings and Communities (IEA EBC) Annex 80 - Resilient Cooling of Buildings. This work has been supported by FWO long stay grant (ID V427023N) and Flanders Innovation and Entrepreneurship in the Flux 50 Project 'ReCOVer++: Improving resilience of buildings to overheating.'

7 REFERENCES

- [1] Need to heat buildings down by a fifth since 1979 - Products Eurostat News - Eurostat, (n.d.). https://ec.europa.eu/eurostat/en/web/products-eurostat-news/w/ddn-20230227-2?pk_campaign=ENER Newsletter MARCH 2023 (accessed April 11, 2023).
- [2] Climate Change 2022: Impacts, Adaptation and Vulnerability | Climate Change 2022: Impacts, Adaptation and Vulnerability, (n.d.). <https://www.ipcc.ch/report/ar6/wg2/> (accessed March 25, 2022).
- [3] AECOM, Investigation into Overheating in Homes: Literature Review., 2012. https://www.gov.uk/government/uploads/system/uploads/attachment_data/file/7604/2185850.pdf.
- [4] Z. Ren, X. Wang, D. Chen, Heat stress within energy efficient dwellings in Australia, *Archit. Sci. Rev.* 57 (2014) 227–236. <https://doi.org/10.1080/00038628.2014.903568>.
- [5] M. Palme, A. Isalgué, H. Coch, Avoiding the Possible Impact of Climate Change on the Built Environment: The Importance of the Building's Energy Robustness, (2013) 191–204. <https://doi.org/10.3390/buildings3010191>.
- [6] A. Mavrogianni, J. Taylor, M. Davies, C. Thoua, J. Taylor, M. Davies, C. Thoua, J.K. Urban, A. Mavrogianni, J. Taylor, M. Davies, C. Thoua, Urban social housing resilience to excess summer heat Urban social housing resilience to excess summer heat, *Build. Res. Inf.* 00 (2015) 1–18. <https://doi.org/10.1080/09613218.2015.991515>.
- [7] J. Plumblee, L. Klotz, Marlo's windows: Why it is a mistake to ignore hazard resistance in LCA, *Int. J. Life Cycle Assess.* 19 (2014) 1173–1178. <https://doi.org/10.1007/s11367-014-0741-2>.
- [8] T. Kesik, L. O'Brien, A. Ozkan, A. Chong, Thermal Resilience Design Guide, (2019).
- [9] M. Pizzol, Life Cycle Assessment and the Resilience of Product Systems, *J. Ind. Ecol.* 19 (2015) 296–306. <https://doi.org/10.1111/jieec.12254>.
- [10] T. Psomas, P. Heiselberg, K. Duer, E. Bjørn, Overheating risk barriers to energy renovations of single family houses: Multicriteria analysis and assessment, *Energy Build.* 117 (2016) 138–148. <https://doi.org/10.1016/j.enbuild.2016.02.031>.
- [11] E.W. Conditions, Evaluation on Overheating Risk of a Typical, (2020).
- [12] A. Sengupta, D. Al Assaad, J.B. Bastero, M. Steeman, H. Breesch, Impact of heatwaves and system shocks on a nearly zero energy educational building: Is it resilient to overheating?, *Build. Environ.* 234 (2023). <https://doi.org/10.1016/j.buildenv.2023.110152>.
- [13] L.G. Valladares-Rendón, G. Schmid, S.L. Lo, Review on energy savings by solar control techniques and optimal building orientation for the strategic placement of façade shading systems, *Energy Build.* 140 (2017) 458–479. <https://doi.org/10.1016/j.enbuild.2016.12.073>.
- [14] A. Sengupta, M. Steeman, H. Breesch, Analysis of Resilience of Ventilative Cooling Technologies in a Case Study Building, *ICRBE Procedia.* (2020). <https://doi.org/10.32438/iCRBE.202041>.
- [15] Binnenklimaat verbeteren? Kies Renson: ruim 110 jaar ervaring | Renson, (n.d.). <https://renson.net/nl-be> (accessed April 11, 2023).
- [16] Over het Vlaams Energie- en Klimaatagentschap (VEKA) | Vlaanderen.be, (n.d.). <https://www.vlaanderen.be/veka/over-het-vlaams-energie-en-klimaatagentschap-veka> (accessed April 11, 2023).
- [17] EPBD – ERKENDE EPB-PRODUCTGEGEVENS, (n.d.). <https://epbd.be/nl/home/> (accessed April 11, 2023).
- [18] C. Sigauke, M.M. Nemukula, Modelling extreme peak electricity demand during a heatwave period: a case study, *Energy Syst.* 11 (2020) 139–161. <https://doi.org/10.1007/s12667-018-0311-y>.
- [19] Norm NBN EN 16798-1:2019 | NBN Shop, (n.d.). https://www.nbn.be/shop/nl/norm/nbn-en-16798-1-2019_8687/ (accessed November 29, 2022).
- [20] Ventilatievoorzieningen in residentiële gebouwen : NBN D50-001 en bijlage V : principes en eisen Conventies in de presentaties, (2005) 1–51.
- [21] 1998 van Paassen A H C, Liem S H, Groninger B P, Control of night cooling with natural ventilation. (Sensitivity analysis of control strategies and vent openings). | AIVC, (n.d.). <https://www.aivc.org/resource/control-night-cooling-natural-ventilation-sensitivity-analysis-control-strategies-and-vent> (accessed June 11, 2020).
- [22] G. Ouzeau, J.M. Soubeyroux, M. Schneider, R. Vautard, S. Planton, Heat waves analysis over France in present and future climate: Application of a new method on the EURO-CORDEX ensemble, *Clim. Serv.* 4 (2016) 1–12. <https://doi.org/10.1016/j.cliser.2016.09.002>.
- [23] ISO 17772-1:2017 - Energy performance of buildings — Indoor environmental quality — Part 1: Indoor environmental input parameters for the design and assessment of energy performance of buildings, (n.d.). <https://www.iso.org/standard/60498.html> (accessed April 12, 2023).
- [24] Z. Chen, O.B. Kazanci, S. Attia, R. Levinson, S.H. Lee, P. Holzer, R. Rahif, A. Salvati, M.; Machard, Anaïs; Pourabdollahtookaboni, A.; Gaur, B. Olesen, P. Heiselberg, IEA EBC Annex 80 - Dynamic simulation guideline for the performance testing of resilient cooling strategies - Version 2. DCE Technical Reports No. 306, (2023) 30.
- [25] K. Sun, W. Zhang, Z. Zeng, R. Levinson, M. Wei, T. Hong, Passive cooling designs to improve heat resilience of homes in underserved and vulnerable communities, *Energy Build.* 252 (2021) 111383. <https://doi.org/10.1016/J.ENBUILD.2021.111383>.
- [26] TM52: The Limits of Thermal Comfort: Avoiding Overheating in European Buildings | CIBSE, (n.d.). <https://www.cibse.org/knowledge-research/knowledge-portal/tm52-the-limits-of-thermal-comfort-avoiding-overheating-in-european-buildings> (accessed November 15, 2022).
- [27] EN 16798-1:2019 - Energy performance of buildings - Ventilation for buildings - Part 1: Indoor, (n.d.).
- [28] OpenStudio | OpenStudio, (n.d.). <https://www.openstudio.net/> (accessed August 27, 2020).
- [29] EnergyPlus, (n.d.). <https://energyplus.net/> (accessed December 9, 2021).

Renewable ventilative cooling? Insights from an Irish perspective

Adam O' Donovan^{1,2,*}, Theofanis Psomas³, Paul D. O' Sullivan^{1,2}

1 MeSSO Research, Munster Technological University, Rossa Avenue, Bishopstown, Cork Ireland

2 MaREI Centre for Energy, Climate, and Marine Ireland.

3 Department of Architecture and Civil Engineering, Chalmers University of Technology, Gothenburg, Sweden

*Corresponding author: adam.odonovan@mtu.ie

ABSTRACT

The future needs of indoor spaces in our buildings are likely to be cooling focused. With the widespread use of air-conditioning (AC) on the horizon there is now a need to ensure our systems perform as renewables (under the relevant definitions). A key part of tackling the uptake in energy intensive AC is likely to be the balancing of AC with renewable natural and mechanical ventilative cooling (VC). It is evident that a total reliance on AC could have significant ramifications for any building sector emissions targets but could also leave building occupants vulnerable to power outages from increased pressure on electricity grids. It is therefore critical that existing design practices encourage the use of passive systems, which take advantage of natural and renewable sources of energy be they as primary, supplementary, or secondary cooling systems or featured as part of a hybrid cooling system. To address this, the aim of this work was to determine the potential renewable energy contribution that natural ventilative cooling systems (NVCs) or mechanical ventilative cooling systems (MVCs) can have under favourable conditions in a temperate climate. Three different stages to this evaluation are presented: 1) a cooling demand using cooling degree hour (CDH) analysis in current and future conditions, 2) a simplified design stage evaluation of the potential of single-sided NVC and MVC, and 3) a calculation of the seasonal performance factor for NVC and MVC systems. In addition to this, the potential for NVC is discussed in relation to the existing building stock in Ireland. Initial results indicate that the NVC potential in supply terms is currently outstripping demand by greater than 3.5 times. Current calculations for NVC and MVC renewable status show a strong basis for their consideration in future, but more detail is required. The results also indicate that NVC and MVC systems are likely to be a renewable source that is currently not officially accounted for.

KEYWORDS

Renewable status, ventilative cooling, natural ventilation, mechanical ventilation

1 INTRODUCTION

The future needs of our buildings are going to be cooling focused. With the widespread use of air-conditioning (AC) on the horizon there is now a need to ensure our systems perform as renewables (under relevant definitions). A key part of tackling the uptake in energy intensive AC is likely to be the balancing of AC with renewable natural and mechanical ventilative cooling (VC). It is evident that a total reliance on AC could have significant ramifications for any building sector emissions targets but could also leave building occupants vulnerable to power outages (Attia et al. 2021). It is therefore critical that existing design practises encourage the use of passive systems, which take advantage of natural sources of energy be they as primary, supplementary, secondary cooling systems or featured as part of a combined cooling system. The use of natural or mechanical VC systems have been shown to be very effective at cooling buildings (O'Sullivan and O'Donovan 2018) and has been shown to have potentially very high co-efficients of performance (COP's) (Holzer and Stern 2019). Indeed, where systems like NV are used it is likely that COP's or seasonal performance factors (SPFs) could be particularly high if humans operate openings, even if actuation energy is considered it is

likely that SPFs for NV or MV systems will be well in excess of the SPFs required for heat pumps for them to be considered renewable (Nowak 2011; O’ Donovan and P. O’ Sullivan 2023).

Up until now the renewable status of VC has been presented very little, this is because previous iterations of renewable cooling calculations have excluded passive cooling systems based on building design (e.g. insulation, green roofs, building mass) or VC systems that supplied fresh air for air quality purposes (see sections 2.6.2.3 in (Kranzl et al. 2021)). However, it is now understood that “free cooling” which uses natural heat flow from hot to cold which is intentional and is supplied by pumps or fans (Kranzl et al. 2021) can be classified as a renewable for cooling purposes. To qualify as a renewable system for space cooling purposes a minimum SPF must be achieved, which is similar to definitions for heat pumps using for heating or cooling. In this paper, we present an example of renewable NVC and MVC and how this could be accounted for at design stage under the mild conditions of Ireland and consider an argument to consider NV to be a renewable when “intentional” through when it is actuated via a control system. This work is particularly relevant as currently Ireland is indicated as having no energy consumption requirement for cooling its residential building stock (SEAI 2022). This work will be presented in three stages: 1) a cooling demand assessment using cooling degree hour (CDH) analysis in current and future conditions, 2) a simplified design stage evaluation of the potential of single-sided NVC and MVC, and 3) a calculation of the seasonal performance factor for NVC and MVC systems.

2 MATERIALS AND METHODS

2.1 Case study building used

As part of this paper a case study building will be used in order to demonstrate the cooling demand and supply. The selected building presented in this paper was studied previously (O’Donovan, Psomas, and O’ Sullivan 2022) and is example of a deep energy retrofit. The building is a bungalow located in an inland location, this type of building has been seen as being vulnerable to overheating based on previous overheating assessments in Ireland (Washan 2019). Table 1 indicates the buildings thermo-physical characteristics which have been taken from its energy certificate file.

Table 1: Thermo-physical characteristics of case study building used to evaluate renewable NVC and MVC

Variable	Units	Value
Roof U-value	W/m ² K	0.13
Wall U-value	W/m ² K	0.2-0.23
Floor U-value	W/m ² K	0.12-0.13
Window U-value	W/m ² K	1.4
Effective air change rate	h ⁻¹	0.522
Floor area	m ²	182.09
Volume	m ³	491.64
Heat loss co-efficient	W/K	292

Previous work focused on this building (O’Donovan et al. 2022) highlighted that it was vulnerable to overheating in the living space if evaluated using Category I of EN16798-1 (CEN 2019) (i.e. considering vulnerable occupants), however, it should be noted that despite this overheating in the living space was limited to less than 1% of the occupied hours less than 28°C

(O'Donovan et al. 2022). Additionally, the empirically calculated overheating escalation factor for the same building indicated a degree of resistance to external conditions that was favourable.

2.2 Cooling demand and ventilative cooling supply

Cooling energy demand calculations

Cooling demand in buildings can be estimated by using a cooling degree hour (CDH) approach (De Rosa et al. 2015). In this example, we will use a base temperature that is more appropriate to low energy buildings (Rahif et al. 2021) (e.g. 14°C). However, this could be lower or higher depending on the building characteristics. Therefore, we present CDH's for different base temperatures initially before focusing on low energy buildings. The cooling demand for the case study building was calculated using Equation 1 below (which is similar to (De Rosa et al. 2015)):

$$CD_h = \sum_{h=1}^{h=8760} (T_e - T_b)^+ \quad (1)$$

Where, CD_h are the number of cooling degree hours (°Ch), T_e is the hourly external air temperature and T_b is the base temperature for cooling. The demand in energy terms (kWh) was calculated using Equation 2 (which is similar to (Rosa et al. 2014; De Rosa et al. 2015)), this was done assuming that the building had a 5% opening area to floor area ratio (or POF) (in line with national regulations (Dept of Housing 2019)).

$$E_{tot,c} = \frac{H \cdot CD_h}{1000} \quad (2)$$

Where, $E_{tot,c}$ is the energy demand for cooling (in kWh) for a specific building (which is similar to other relevant work in this area (Li, Allinson, and Lomas 2020), taken from Table 1 above).

Ventilative cooling potential (natural and mechanical supply)

To account for natural ventilative cooling potential or supply at the design stage, the approach of O'Donovan and O'Sullivan was adopted (O' Donovan and P. D. O' Sullivan 2023). In this approach, the work of Warren and Parkins (Warren and Parkins 1985) is used which evaluates airflow rates independently for two momentum sources: buoyancy and wind. The most widely used buoyancy driven airflow equation is shown in Equation 3 (taken from (Fan et al. 2021)) and, for wind driven airflow, indicated in Equation 4 (using reference wind speeds). There are many limitations in the use of the wind speed local at the opening, (also recommended by Warren and Parkins) not least that data on the local wind at the opening is seldom available to practitioners or may not be suitable for a given location. Therefore, the reference conditions were used to calculate NV airflow rates which would offer a maximum potential value for NVC. Equations 3 and 4 are presented below.

$$Q_b = \frac{1}{3} C_d A_{op} \sqrt{gH \frac{T_i - T_e}{T_i}} \quad (3)$$

$$Q_w = F_R A_{op} U_R \quad (4)$$

Where, Q_b is the volumetric airflow rate due to buoyancy (in m^3/s), C_d is the discharge coefficient (-), A_{op} is the effective opening area (in m^2), T_i is the internal temperature (in K), T_e is the external air temperature (in K), H is the opening height in metres, U_R is the reference wind velocity (in m/s). It was proposed by Warren and Parkins (Warren 1977) that for single-sided flow with one opening (typically abbreviated as SS1) that the maximum of either buoyancy or wind driven flows be taken, as is indicated in Equation 5.

$$Q_{nv} = \max(Q_b, Q_w) \quad (5)$$

To scale the wind velocities to the building height, Equation 6 (taken from CIBSE AM10 (CIBSE 2005)) was used:

$$U = U_{met} k z^a \quad (6)$$

Where, U is the wind speed (in m/s) at height z (in m) and k and a are coefficients determined by the terrain in which the building lies. For all VC supply estimates considered in this paper a value of $k = 0.35$ and $a = 0.25$ was used with a building height of 10m. This is closer to an urban environment than a rural one. As this is intended as a design stage NVC potential assessment, the internal air temperature (T_i , see Equation 3) is assumed depending on the outside conditions. The exponentially weighted external mean temperature was calculated using Equation 6 for the first day and using Equation 7 for every day after this according to TM52 (CIBSE 2013). For external mean temperatures of greater than or equal to 10°C the internal temperature was assumed to follow the neutral operative temperature (t_c) according to EN 16798-1 (CEN 2019) (see Equation 8) for external mean values less than 10°C a fixed internal condition of 22°C was adopted.

$$t_{rm} = (T_{od-1} + 0.8T_{od-2} + 0.6T_{od-3} + 0.5T_{od-4} + 0.4T_{od-5} + 0.3T_{od-6} + 0.2T_{od-7})/3.8 \quad (7)$$

$$t_{rm} = (1 - \alpha)T_{od-1} + \alpha t_{rm-1} \quad (8)$$

$$t_c = 0.33t_{rm} + 18.8 \quad (9)$$

Where, T_{od-1} is the daily average temperature from the day before today and so on, and α is a weighting factor which was assumed be 0.8. It should be noted that in order to calculate the cooling energy available by NVC all summations of energy were made with data greater than or equal to the base temperature. To calculate the energy supplied by NVC, Equation 10 was adopted.

$$E_{sup,nv} = \frac{Q_{nv} \cdot \rho_a \cdot C_{p,a} \cdot (T_i - T_e)}{1000} \quad (10)$$

Where, $E_{sup,nv}$ is the total available energy from natural ventilation (in kWh), ρ_a is the density of air (assumed to be $1.2 \text{ kg}/\text{m}^3$) and $C_{p,a}$ is the specific heat capacity of air (assumed to be $1000 \text{ J}/\text{kg K}$). To estimate a typical MV system an air change rate (ACR) was assumed to be delivered by fans only. Equation 11 indicates this relationship,

$$Q_{mv} = \frac{ACR_{MV} \cdot V}{3600} \quad (11)$$

Where, ACR_{MV} is a designed ACR (in h^{-1}) for a hypothetical MVC system being used in said dwelling and V is the dwelling volume (in m^3). Equation 12 indicates how the total energy available from MVC is calculated (which is similar to (Wouters et al. 1987)).

$$E_{sup,nv} = \frac{Q_{mv} \cdot \rho_a \cdot C_{p,a} \cdot (T_i - T_e)}{1000} \quad (12)$$

Where, Q_{mv} is mechanical ventilation rate (in m^3/s).

2.3 Seasonal performance factor calculation for NVC and MVC

To confirm and illustrate the renewable status of ventilative cooling, it was assumed that the natural and mechanical systems were actuated and that they were deliberately operated, based on a schedule. This aspect fulfils the intentionality requirement in the operation of the system which was a key aspect of the RED II definition in order to achieve renewable cooling status. The seasonal performance factor (SPF) for renewable cooling was calculated using Equation 13.

$$SPF_{vc} = \frac{Q_{supply}}{E_{INPUT}} \quad (13)$$

Where, Q_{supply} is calculated as the potential heat removed from a building using VC (in kWhs) for natural and/or mechanical systems and E_{INPUT} is the energy input for actuation of openings, energy use by fans, and energy use by control systems (see Table 2 for more information typical power consumption values for NVC and MVC systems from the literature). It should be noted that generally ventilation is considered passive cooling under current definitions (see section 2.6.2.3 (Kranzl et al. 2021)), however, where ventilation is intentional for cooling purposes, (which is ventilation supplied in excess of ventilation supplied for hygienic purposes) this can be considered as part of the renewable definition. To satisfy this renewable definition, heat loss for ventilation purposes should be excluded. To do this, all-annualised NVC or MVC energy supply values were calculated to exclude a value of $0.3l/s/m^2$ to comply with Irish regulations (Dept of Housing 2019) (this equates to $197m^3/h$ for the specific building studied in this paper). In this example, we present the SPF for a NVC system and a MVC system separately, however, a combined system could also be used. The potential SPF was calculated using design stage information, without the use of any dynamic simulation. This was done during the typical during the periods of time where demand was present (i.e. $>14^\circ C$ outside).

Table 2: Examples of typical energy consumed to operate MVC or NVC systems

Reference	System type	Units	Values reported
(Cho et al. 2021)	Hybrid systems	kWh/m ² /a	0.3 – 2.8
(Agency and Programme 2018)	NVC	kWh/m ² /a	~1.2
(Santos, Hopper, and Kolokotroni 2016)	NVC + phase change materials	kWh/m ² /a	~0.77
(Yan et al. 2022)	NVC	kWh/m ² /a	0.7-1.3
(Holzer and Stern 2019)	MVC	W/(m ³ /s)	<200
(Holzer and Psomas 2018)	MVC	W/(m ³ /h)	0.07 - 0.14

Additionally, the SPF for both daytime and night-time performance is taken into account (Day-time hours considered between 8am to 8pm). In this study, we assume that the NVC system will use about 2.4 kWh/m²/a (50W of continuous consumption) for the operation of controls and actuation of openings. For the MVC system we assume that the system will consume about 0.1W/(m³/h) for fans and controls. However, it is evident from the literature that NVC and MVC systems can consume less energy than this.

2.4 Weather data and boundary conditions

To calculate the cooling demand, supply as well as estimating the SPF for VC a series of local meteorological station data from Ireland's Met Éireann were downloaded from Met Éireann's historical weather databases (Met Éireann 2023). Table 3 indicates the locations considered and any substitutions that were made where data wasn't present. All future weather files were produced using Meteotest version 8.1.4 (Meteotest 2022).

Table 3: Weather data used for different aspects of the work presented

Location (Name, County)	Elevation (m)	Weather files considered for demand estimates	Weather files used for case study demonstration
Athenry, Galway	40		
Belmullet, Mayo	9		
Shannon Airport, Clare	15	2022,	
Cork Airport, Cork	155	2030 (RCP 2.6), 2030	
Phoenix Park*, Dublin	48	(RCP 4.5), 2030 (RCP	
Valentia, Kerry	24	8.5), 2040 (RCP 2.6),	2022,
Ballyhaise, Cavan	78	2040 (RCP 4.5), 2040	2050 (RCP 8.5)
Malin Head, Donegal	20	(RCP 8.5), 2050 (RCP	
Gurteen, Tipperary	75	2.6), 2050 (RCP 4.5),	
Johnstown Castle, Wexford	62	2050 (RCP 8.5)	
Finner, Donegal	33		

*Wind speed and wind direction for Dublin Airport used in the absence of available data

3 RESULTS AND DISCUSSION

3.1 Cooling demand in Ireland (Current and Future)

Despite recent research indicating that there is no cooling needs in Ireland (Agency and Programme 2018; SEAI 2022) or at least that NV systems are sufficient at present (O'Donovan, Murphy, and O'Sullivan 2021), it is evident that there will be a need for cooling in Ireland in the future and this is starting to manifest itself now, where existing software may be behind the trend of cooling need for Ireland in even the worst emissions scenarios.

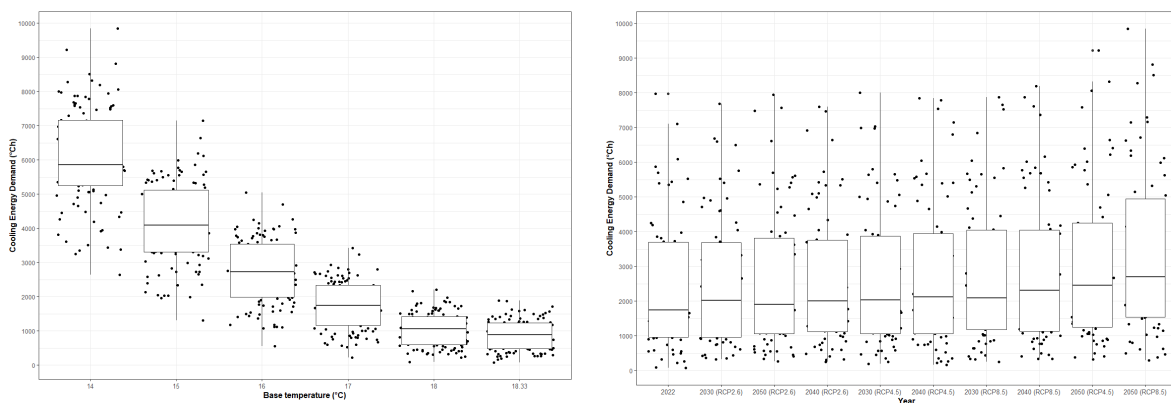


Figure 1: Relationship between cooling degree hours and base temperature and different climate scenarios

What is evident is that change in cooling demand because of the assumptions around base temperatures has a much greater effect in this case than that of existing projections for changes in the climate going forward (see Figure 1). The effect of different weather files in climate scenario has less of an overall effect on cooling demand. Overall, it is expected that demand (in CDH terms) for cooling in Ireland could increase by 591% on average by lowering the base temperature for cooling (through the retrofit of exiting building stocks or increasing fabric performance, from 18.33°C to 14°C), whereas the projected increase in external air conditions could lead to an increase of 41% on average in cooling demand between conditions in 2022 and 2050 in the projected worst case (2050 RCP8.5).

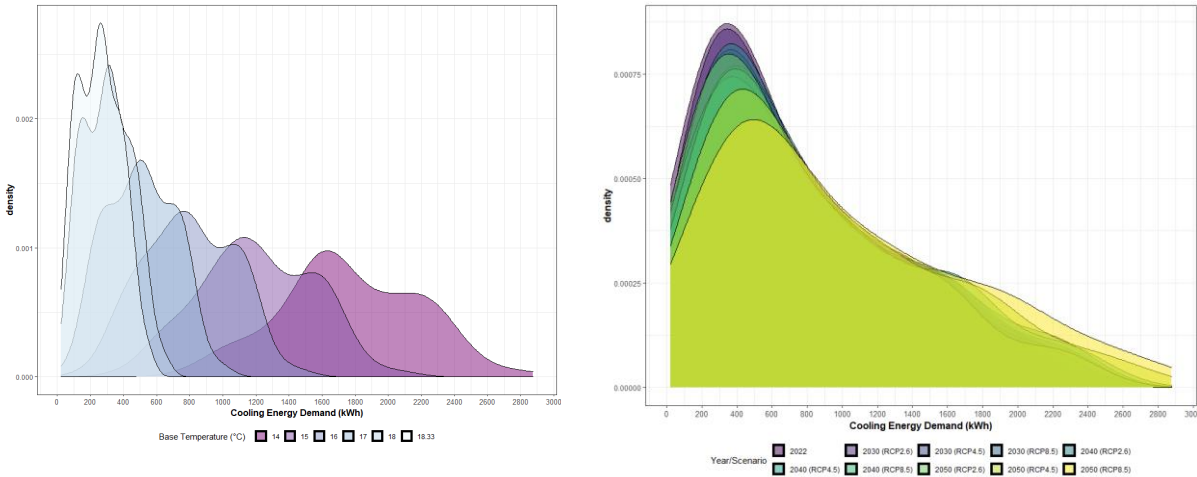


Figure 2: Density plots of estimated cooling energy demand (in kWh) for the case study building indicated in section 2.1. (Left: cooling demand different base temperatures, Right: cooling demand for different years and climate scenarios)

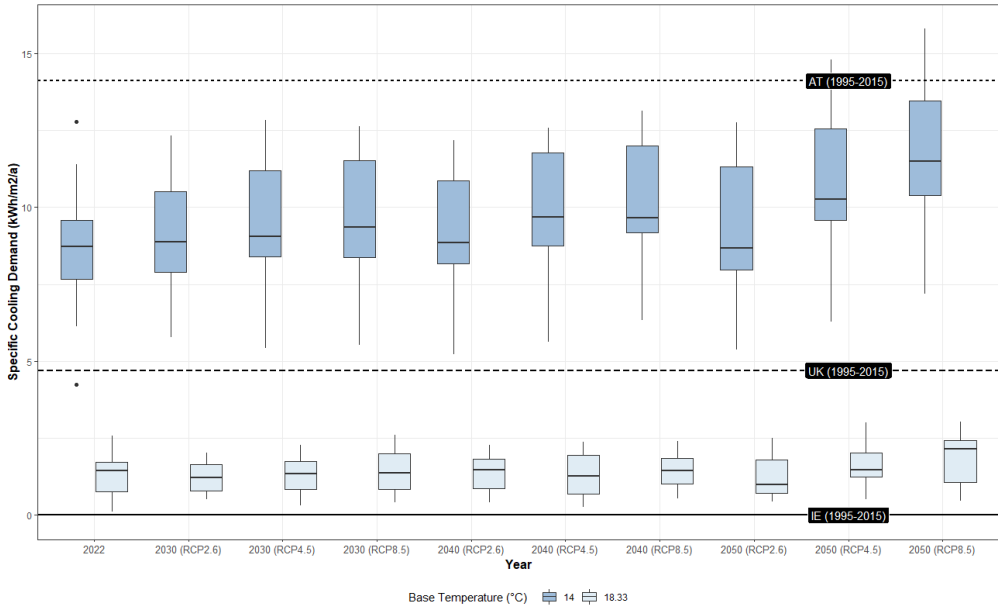


Figure 3: Boxplots of specific cooling demand with respect to climate scenario and different assumptions for base temperature. (Dashed lines indicate different specific cooling demands indicated in the work of (Jakubcionis and Carlsson 2018), for Ireland (IE), United Kingdom (UK), and Austria (AT)).

It should be noted that the use of a standardised base temperature for cooling (e.g. 18.33°C) can result in very different conclusions when compared to a base temperature that is more

appropriate for cooling demand in low energy buildings (e.g. 14°C). If we take a specific building as an example (see Figure 2), this can become more evident that the base temperature chosen leads to very different conclusions. It is therefore important that future research considers an effective calculation procedure for the determination of the base temperature for cooling in more detail, given its relative importance in the Irish context. Figure 3 indicates the specific cooling demand for the same building and indicates different reference levels of specific cooling demand from a cognate study in residential buildings in Europe (Jakubcionis and Carlsson 2018). This indicates that current demand levels in Ireland are above previous thresholds irrespective of assumptions on base temperatures. Additionally, current and future cooling demand levels in Ireland are likely to be above that of the UK in specific cooling demand terms (between the period 1995-2015).

3.2 Comparison of demand and supply of VC

Despite demand levels increasing in the coming years, currently it is estimated that MVC and NVC systems are capable of supplying enough cooling energy to offset the existing demands of low energy buildings. Figure 4 highlights the difference between current and future demand and supply levels depending on different VC systems (i.e. MVC or NVC). Based on the results presented in Figure 4, it can be observed that currently supply outstrips demand by between 4.0 to 5.8 times in 2022 and by between 3.5 and 4.9 in 2050 on average depending on the two proposed systems. The reduction in the ratio between supply and demand between now and 2050 would appear to be driven by increases in mean cooling demand levels between now and 2050.

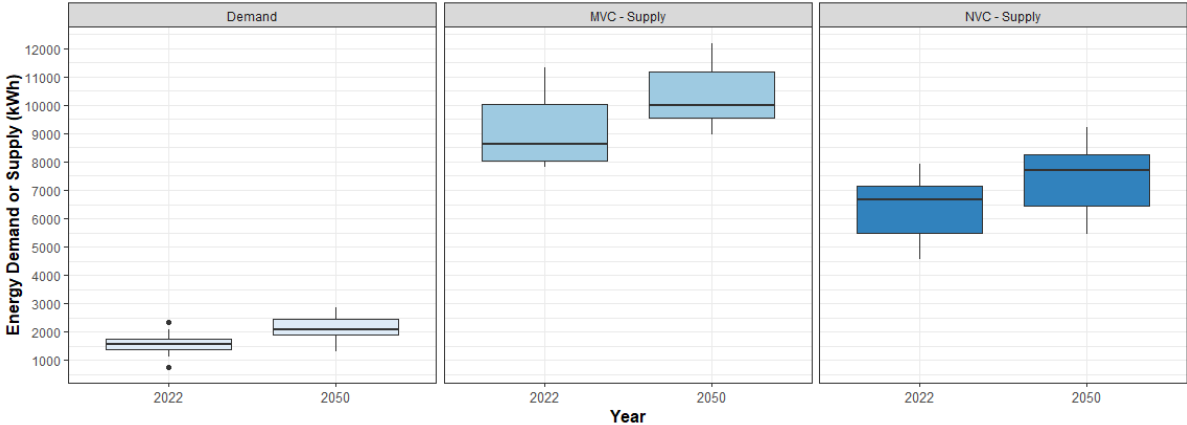


Figure 4: Boxplots of energy demand and supply for cooling with respect to year. (Facet grid represents demand, or supply type for MVC and NVC systems. Note: 2050 refers to RCP 8.5 scenario).

It should be noted that by in large these cumulative demand and supply values, highlight the total per annum performance, but this may not account for seasonal variance where overheating may be present despite cooling potential existing. This is because the cumulative value presented does not indicate hourly or sub-hourly periods where the supply of NVC or MVC is not sufficient. Additionally, because of the supply and demand being calculated based on external temperatures being greater than 14°C, and because this temperature will be below the neutral temperature, this leads to more supply accounted for in parts of the year where supply may not be typical. Resultantly, it is expected that 2% to 6% more hours of the year will have cooling needs in 2050 compared with 2022. This leads to increase in supply terms of between 4% and 39% for the NVC system studied and between 7% and 26% for the MVC system studied is observed between 2022 and 2050. This change is also highlighted by (Bravo Dias, Soares, and Carrilho da Graça 2020) where in their work it is expected that the potential for NV will

increase by 6 weeks in Northern Europe (between now (1971-2000) and the future (2070-2100)). It should also be noted that Bravo Diaz et al. highlighted that Dublin is likely to see no change in days that are too warm (TW), a decrease in days that are too cold (TC), less weeks where NV is possible, but an increase in the number of weeks where VC is applicable. Regarding the removal of energy for hygienic ventilation, it should be noted that the reduction of available supply for NVC and MVC was reduced by 10-15% to remove the ventilation need from each system for calculating SPF. This ventilation supply is likely to contribute to cooling supply in reality but has been excluded in this case.

3.3 SPF calculations

Considering the definition described in previous sections it is important to note that some countries set a minimum thresholds or ranges for renewable cooling these typically lie between 2.8 and 9.5 (Kranzl et al. 2021). Examples of MVC in the real world indicate that these systems can achieve COP values of up to 20 (Holzer and Stern 2019). With hybrid VC systems achieving COP's of 18.3 in reality (Yan et al. 2022). Figure 5 indicates the performance of NVC and MVC in both 2022 and in future conditions where demand is likely (>14°C outside). What is evident is that both MVC and NVC systems are likely to achieve very high SPFs in both 2022 and 2050 (RCP 8.5). On average NVC and MVC systems are likely achieve SPFs of 63 and 23 respectively (considering all years). Overall, the NVC system studied is likely to be providing between 25.1kWh/m²/a and 50.6 kWh/m²/a of specific cooling energy supply for the studied building, while, MVC systems are likely to be providing between 42.9 kWh/m²/a and 66.9kWh/m²/a in specific cooling energy supply for the same building type depending on the location and climatic year considered.

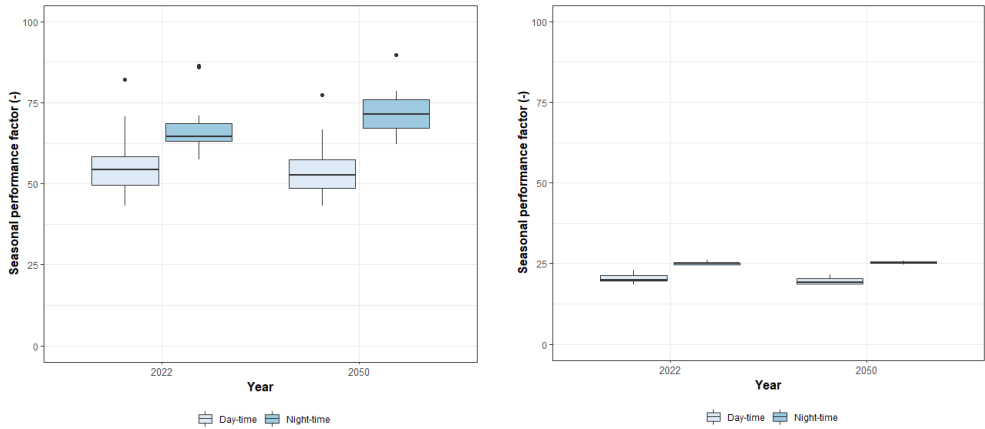


Figure 5: Boxplots of seasonal performance factor with respect to year (Left: SPF values for NVC, Right: SPF values for MVC, colour indicates SPF for day or night-time)

3.4 General discussion and future work in relation to Irish residential stock

The most recent report on the housing stock in Ireland indicated that there were 2,003,645 houses or apartments in Ireland in 2016 (CSO 2016), most of these homes use single-sided natural ventilation for cooling purposes, which are stipulated in current building regulations for purge ventilation purposes. A survey in 2019 by the CSO in Ireland indicated that the average floor area for dwellings in Ireland was 111m² (CSO 2019). Based on the combination of these two facts as well as the typical specific cooling energy supply values shown earlier it is estimated that between 5.6TWh/a and 11.3TWh/a is currently available from NVC in Ireland. Based on the ratio between demand and supply (shown earlier) it is likely that over one third of

this potential is being utilised by the housing stock on a per annum basis. This cooling energy is supplied as amongst the most energy efficient compared with even modern MVC systems as the energy usage for opening windows is likely to be manual in nature. As such, NVC is currently offsetting a significant amount of the existing cooling demand and currently this is not officially recognised as a renewable energy source. The work in this paper indicates that it is likely that if these systems are controlled or actuated that a significant amount of renewable cooling potential is available for the Irish housing stock and that the extent of this needs further examination. Future work should; 1) consider the effective determination of the cooling base temperatures for different building types, but particularly for low energy buildings as this value can have a significant effect on cooling demand calculations (see section 3.3), 2) consider simulating different archetypal buildings to interrogate the SPF values that can be achieved, 3) evaluate the SPF of real NVC and MVC systems in-use and 4) evaluate the current cooling energy supply in the building stock by using available energy rating databases for Ireland (as the estimates presented here are subject to variation).

4 CONCLUSIONS

In this paper, three stages were proposed to evaluate the status of renewable ventilative cooling in Ireland. Firstly, a cooling degree hour analysis was used to estimate the current demand levels for different base temperatures and weather data. Secondly, the potential for cooling energy supplied by a NVC and MVC system was estimated. Finally, the potential seasonal performance factor was calculated for an NVC and MVC system. The results presented have indicated that the current cooling energy supplied by VC appears to be outstripping estimated demand levels (on an annualised basis). The results also indicate that NVC and MVC systems are likely to be a renewable source that is currently not officially accounted for.

5 ACKNOWLEDGEMENTS

This research has been funded by the Sustainable Energy Authority of Ireland (SEAI) RD&D fund 2019, under grant number RDD/00496.

6 REFERENCES

- Agency, International Energy, and Communities Programme. 2018. *Ventilative Cooling Design Guide Energy in Buildings and Communities Programme*.
- Attia, Shady, Ronnen Levinson, Eileen Ndongo, Peter Holzer, Ongun Berk Kazanci, Shabnam Homaei, Chen Zhang, Bjarne W. Olesen, Dahai Qi, Mohamed Hamdy, and Per Heiselberg. 2021. "Resilient Cooling of Buildings to Protect against Heat Waves and Power Outages: Key Concepts and Definition." *Energy and Buildings* 239:110869. doi: 10.1016/j.enbuild.2021.110869.
- Bravo Dias, João, Pedro M. M. Soares, and Guilherme Carrilho da Graça. 2020. "The Shape of Days to Come: Effects of Climate Change on Low Energy Buildings." *Building and Environment* 181(April). doi: 10.1016/j.buildenv.2020.107125.
- CEN. 2019. "EN 16798-1 - Energy Performance of Buildings - Ventilation for Buildings - Part 1: Indoor Environmental Input Parameters for Design and Assessment of Energy Performance of Buildings Addressing Indoor Air Quality, Thermal Environment, Lighting and Acoustic."
- Cho, Haein, Daniel Cabrera, Sylvain Sardy, Romain Kilchherr, Selin Yilmaz, and Martin K. Patel. 2021. "Evaluation of Performance of Energy Efficient Hybrid Ventilation System and Analysis of Occupants' Behavior to Control Windows." *Building and Environment* 188(November 2020):107434. doi: 10.1016/j.buildenv.2020.107434.
- CIBSE. 2005. *AM10: Natural Ventilation in Non-Domestic Buildings Natural Ventilation in Non-Domestic Buildings*.
- CIBSE. 2013. *TM52 (2013): The Limits of Thermal Comfort: Avoiding Overheating in European Buildings*.
- CSO. 2016. "Census of Population 2016 - Profile 1 Housing in Ireland." Retrieved July 18, 2023 (<https://www.cso.ie/en/releasesandpublications/ep/p-cp1hii/cp1hii/hs/#:~:text=Ireland's housing stock in 2016,occupied by guests or visitors.>).

- CSO. 2019. "DOMESTIC BUILDING ENERGY RATINGS QUARTER 1 2019." Retrieved July 18, 2023 (<https://www.cso.ie/en/releasesandpublications/er/dber/domesticbuildingenergyratingsquarter12019/>).
- Dept of Housing, Planning &. Local Government. 2019. *Technical Guidance Document Part F*.
- Fan, S., M. S. Davies Wykes, W. E. Lin, R. L. Jones, A. G. Robins, and P. F. Linden. 2021. "A Full-Scale Field Study for Evaluation of Simple Analytical Models of Cross Ventilation and Single-Sided Ventilation." *Building and Environment* 187(July 2020):107386. doi: 10.1016/j.buildenv.2020.107386.
- Holzer, Peter, and Theofanis Psomas. 2018. *Ventilative Cooling Sourcebook Energy in Buildings and Communities Programme*.
- Holzer, Peter, and Philipp Stern. 2019. "Key Findings on Ventilative Cooling." *REHVA Journal* (September 2018):28–33.
- Jakubcionis, Mindaugas, and Johan Carlsson. 2018. "Estimation of European Union Service Sector Space Cooling Potential." *Energy Policy* 113(December 2016):223–31. doi: 10.1016/j.enpol.2017.11.012.
- Kranzl, Lukas, Philipp Mascherbauer, Mostafa Fallahnejad, and T. U. Wien. 2021. *Renewable Cooling Definition Options and Calculation Methodology*.
- Li, Matthew, David Allinson, and Kevin Lomas. 2020. "Estimation of Building Heat Transfer Coefficients from In-Use Data Impacts of Unmonitored Energy Flows." doi: 10.1108/IJBPA-02-2019-0022.
- Met Éireann. 2023. "Historical Data - Met Éireann." Retrieved July 1, 2023 (<https://www.met.ie/climate/available-data/historical-data>).
- Meteotest. 2022. "Meteonorm Version 8."
- Nowak, Thomas. 2011. "Heat Pumps – a Renewable Energy Technology?" *REHVA Journal* (August):10–12.
- O' Donovan, Adam, Michael D. Murphy, and Paul D. O'Sullivan. 2021. "Passive Control Strategies for Cooling a Non-Residential Nearly Zero Energy Office: Simulated Comfort Resilience Now and in the Future." *Energy and Buildings* 231:110607. doi: 10.1016/j.enbuild.2020.110607.
- O' Donovan, Adam, and Paul O' Sullivan. 2023. *DesignforIU : Comparison of Certified versus Operational Performance of Energy Efficient Technologies*.
- O' Donovan, Adam, and Paul D. O' Sullivan. 2023. "The Impact of Retrofitted Ventilation Approaches on Long-Range Airborne Infection Risk for Lecture Room Environments: Design Stage Methodology and Application." *Journal of Building Engineering* 106044. doi: 10.1016/j.job.2023.106044.
- O'Donovan, Adam, Theofanis Psomas, and Paul D. O' Sullivan. 2022. "Evaluating the Present Day Ambient Warming Resilience of Passively Cooled Dwellings in Ireland : A Data-Driven Approach." in *42nd AIVC-10th TightVent & 8th Venticool Conference, October 5-6, 2022, Hilton Hotel*. Rotterdam.
- O'Sullivan, Paul, and Adam O'Donovan. 2018. "Ventilative Cooling Case Studies Energy in Buildings and Communities Programme." (May):191. Retrieved January 31, 2021 (<http://venticool.eu/wp-content/uploads/2016/11/VC-Case-Studies-EBC-Annex-62-May-2018-Final.pdf>).
- Rahif, Ramin, Abdulrahman Fani, Piotr Kosinski, and Shady Attia. 2021. "Climate Change Sensitive Overheating Assessment in Dwellings : A Case Study in Belgium." in *Proceeding of the International Building Simulation Conference*.
- Rosa, Mattia De, Vincenzo Bianco, Federico Scarpa, and Luca A. Tagliafico. 2014. "Heating and Cooling Building Energy Demand Evaluation ; a Simplified Model and a Modified Degree Days Approach." *Applied Energy* 128:217–29. doi: 10.1016/j.apenergy.2014.04.067.
- De Rosa, Mattia, Vincenzo Bianco, Federico Scarpa, and Luca A. Tagliafico. 2015. "Historical Trends and Current State of Heating and Cooling Degree Days in Italy." *Energy Conversion and Management* 90:323–35. doi: 10.1016/j.enconman.2014.11.022.
- Santos, Thiago, Nick Hopper, and Maria Kolokotroni. 2016. "Performance in Practice of a Ventilation System with Thermal Storage in a Computer Seminar Room." *12th CLIMA REHVA World Congress* (May):11.
- SEAI, Sustainable Energy Authority of Ireland. 2022. *Heating and Cooling in Ireland Today (National Heat Study)*.
- Warren, P. R. 1977. "Ventilation Through Openings on One Wall Only." *International Conference on Heat and Mass Transfer in Buildings*. doi: 10.1017/CBO9781107415324.004.
- Warren, P. R., and L. M. Parkins. 1985. "SINGLE-SIDED VENTILATION THROUGH OPEN WINDOWS." in *Thermal Performance of the Exterior Envelopes of Buildings*. Florida.
- Washan, Pratima. 2019. *Research Report on Overheating Risk in Dwellings*.
- Wouters, P., W. F. De Gids, P. R. Warren, and P. J. Jacknan. 1987. "VENTILATION RATES AND ENERGY LOSSES DUE TO WINDOW OPENING BEHAVIOUR."
- Yan, Bin, Xu Han, Ali Malkawi, Tor Helge, Pete Howard, Jacob Knowles, Tine Hegli, and Kristian Edwards. 2022. "Energy & Buildings Comprehensive Assessment of Operational Performance of Coupled Natural Ventilation and Thermally Active Building System via an Extensive Sensor Network." *Energy & Buildings* 260:111921. doi: 10.1016/j.enbuild.2022.111921.

Urban context and climate change impact on the thermal performance and ventilation of residential buildings: a case-study in Athens

Maria Kolokotroni^{*1}, May Zune¹, Thet Paing Tun¹ Ilia Christantoni², and Dimitra Tsakanika²

*1 College of Engineering, Design and Physical Sciences,
Brunel University London, UK.
*Corresponding author:
Maria.Kolokotroni@brunel.ac.uk*

*2 DAEM SA,
City of Athens IT Company
144 Peiraios, 11854 Athens
Greece*

ABSTRACT

Urban settings and climate change both impact energy use, thermal comfort and ventilation of buildings. This is more noticeable in hot urban areas where the urban heat island effect is more pronounced; also, in densely built urban areas where thermal comfort in naturally ventilated buildings is affected by changes in natural ventilation rates because of surrounding obstructions. In some cases, overshadowing might alleviate the impact. This paper presents a study of changes in energy demand in residential buildings considering the overlapping effect of climate change and urban heat island intensity in Athens representing a hot European climate and a dense urban setting. The case study building is a real residential building in an urban canyon in central Athens with data obtained from the PRELUDE H2020 project. The impact of urban parameters on air temperature wind speed and solar overshadowing was considered. Urban air temperature was calculated by using the Urban Weather Generator which includes a number of indices such as site coverage, façade to site ratio and average building height; it also considers the building construction materials as well as anthropogenic heat emissions by the operation of the buildings. Urban wind speed was modified using the URBVENT urban canyon model for the computation of wind speed; this model was validated by its proposers in 2005 by measurements in Athens. Solar overshadowing was calculated for the case-study building considering the surrounding buildings. Current-urban and future-urban weather files were generated, and simulations were run considering energy demand and indoor thermal comfort. The thermal simulation results show that in the hot European climate of Athens with densely built urban areas and for a building within an urban canyon, current weather files which include overshadowing, urban heat island and canyon wind will increase the cooling demand by 24% in comparison to using a typical current weather file. However total energy demand (heating and cooling) increased only 3% for lower floors and 12% for higher floors due to the reduction of heating demand. Simulations using future weather files indicated a 66% increase of cooling demand in comparison to using a typical weather file. Future total energy demand increased by 32% for higher floors and 13% for lower floors. If the building is free floating an adaptive thermal comfort analysis indicated that only 25% of the summertime will be comfortable in comparison to the 50% prediction by the current typical weather file. Therefore, the use a suitable weather file to include urban external conditions in thermal simulations is essential for more accurate predictions of energy demand and internal avoidance of overheating in free-floating buildings.

KEYWORDS

Microclimate, climate change, urban heat island, ventilation, thermal comfort, energy use

1 INTRODUCTION

As reported by (Salvati and Kolokotroni, 2022) ‘in thermal simulations studies of buildings, ambient conditions are accounted for by using weather files of the building’s location, providing hourly values of typical ambient conditions: temperature, humidity, solar radiation and wind. Weather files are built using historical observational data usually over 30 years; they are based on measurements at meteorological stations usually at airports. Therefore, weather files do not account for characteristics of the urban environment which modify climatic conditions, especially those of air temperature and wind. In addition, buildings designed and built today, will last for many years. Therefore, future climate projections should be used to predict how our buildings will perform in 30 or 50 years. Using such climate projections can ensure that energy and comfort performance simulations can more realistically predict future performance.’

(Salvati and Kolokotroni, 2022) presented to the AIVC Conference in 2022, proposed a methodology based on the use of urban climate models (Urban Weather Generator -UWG) and detailed microclimate models (ENVImet) for urban microclimate simulation, in order to investigate the overlapping effects of climate change and urban effects on the future performance of urban buildings. This was applied to two case study buildings in London, UK and Cadiz, Spain.

The present paper is developed along the same methodology using the UWG (Bueno et al, 2013) to obtain modified urban temperatures, overshadowing calculations to consider restrictions in impending solar radiation by adjacent buildings and URBVENT (Ghiaus and Roulet, 2004) models to obtain modified wind speeds in an urban canyon. The case-study building is located in an urban canyon in Athens, Greece and its data were obtained from the PRELUDE H2020 (PRELUDE, 2023) project.

The paper presents the urban climate modifications – both for ambient temperature and urban canyon wind by generating site-specific urban weather files for the location of the case-study in Athens; section 2. The weather files are generated for both current and future urban weather scenarios and are used for EnergyPlus (DesignBuilder, 2023) energy and thermal simulations which include the effect of urban overshadowing; section 3. The results of simulations (energy and comfort) are presented in section 4.

2 CASE STUDY LOCATION AND BUILDING DESCRIPTION

2.1 Climate of case-study location

The Mediterranean climate of Athens (Köppen climate classification: Csa) represents a dominant alternation between prolonged hot and dry summers and mild, wet winters with moderate rainfall. July and August are the driest months for Athens with the highest outdoor dry bulb temperatures, and diurnal variations in outdoor temperatures are notable (Figure 1). The dominant southwest wind comes with higher wind speeds to Athens throughout the year (Figure 2). The heating degree days and cooling degree days for the current climate of Athens showed that the buildings in Athens need both heating and cooling for comfort (Figure 2).

The building in Athens is located in a very dense urban texture within a well-defined urban canyon street and in a climate region with high solar radiation and summer air temperatures, where the urban heat island (UHI) intensity has the highest negative impact.

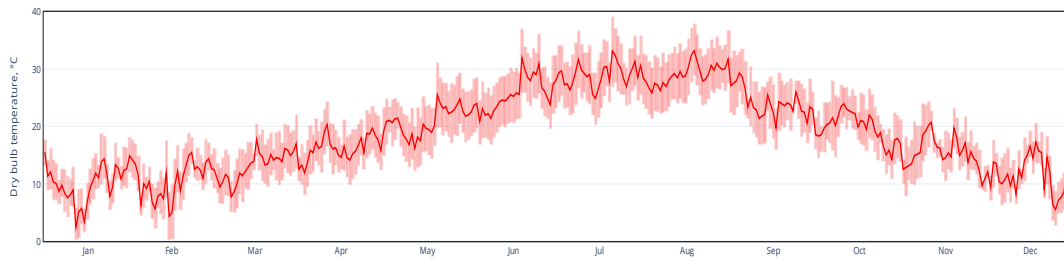


Figure 1: Daily outdoor dry bulb temperature profiles of Athens

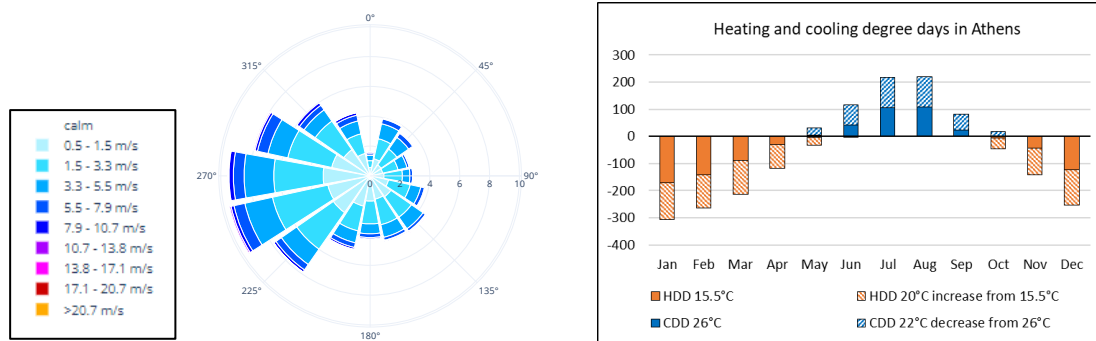


Figure 2: A wind rose, heating degree day and cooling degree day profiles of Athens

2.2 Case-study building description

The case-study building is a five-storey residential building in Athens. It is highly representative of low-rise multi-apartment buildings that were built during the 1930s. It was renovated in 2005 by adding rooftop insulation, installation of double aluminium windows to minimise thermal losses, replacement of outdated lighting with LED lamps etc. It is used as a hostel for the homeless and houses support staff with maximum capacity of 60 occupants. The total floor area is 1080 m² and it has a ground-floor, 5-storeys and a basement. It is located in Patission Street which is a long street surrounded by similar in-height buildings starting from the centre of Athens and extending to the north. The building is located about 3 km from the centre of Athens (Omonia Square). A typical floor plan and an external view of the building are presented in Figure 3. The heating and hot water system operates with natural gas, the lamps are LED and all windows are double-glazed aluminium. The apartments of the tenants are hotel-like rooms including a room and bathroom with TV and fan, heating & cooling thermostat. The thermal properties of the external envelope are presented in Table 1.

For this paper, two “intermediate levels” – level 2 (above the ground floor) and level 4 (below the top floor) were chosen. Each floor consists of 6 rooms – three single rooms (SR) and three twin rooms (TR). The single room (SR) is for one occupant and the twin room (TR) is for two occupants. Each room has one bath and there is a balcony with one window/door on either the east or west side. The communal areas, which include the kitchen, lift and stair core, are located in the middle of the building.

Table 1: Thermal properties of the building envelope

Building envelope	Thermal transmittance (W/m ² K)
External wall	1.739
Party wall	2.038
Ground floor	1.834
Internal floor	0.788
Roof	0.639
Internal door	2.672
Window	2.5 (light transmission 0.78)



Figure 3: External view and typical floor plan of the case-study building.

3 METHODOLOGY FOR GENERATING URBAN WEATHER FILES

The methodology for generating urban weather files to be used in thermal simulations is presented in Figure 4. Two rural weather files (current and future) from Meteonorm were used (Meteotest, 2020) as the starting point. The future weather was considered for the RCP8.5 scenario which is the worst-case, high-emissions scenario for the year 2050 caused by “business as usual” without efforts to cut greenhouse gas emissions (IPPC, 2014).

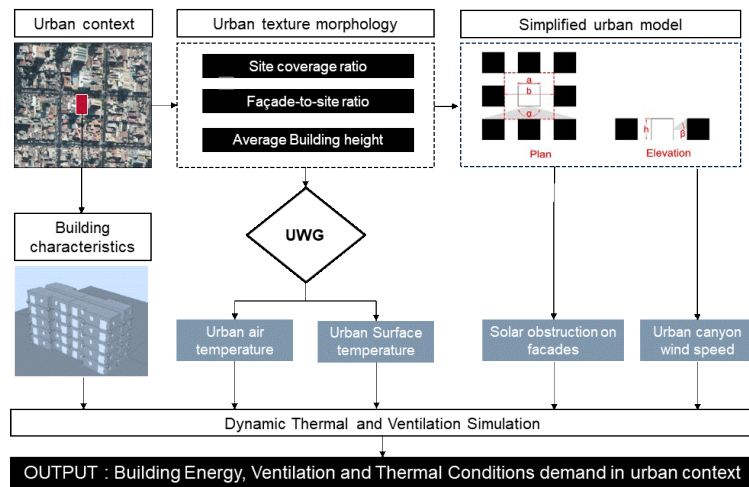


Figure 4: Urban considerations in building simulation (adapted from Salvati et al, 2020)

Autodesk *Revit* was used to generate the required building information for the UWG program. The 3D model was computed over an area of about 250m in length, as suggested for local urban climate studies (Salvati *et al.*, 2016) (Stewart and Oke, 2012). The case studied building is located on the road (yellow arrow shown in Figure 5) where the urban canyon wind was to be calculated. The topography of the site was modelled according to its location above sea level; the south is lower than the north. The buildings were represented in the Revit massing models that allow calculating the façade and floor areas of the site, and average building height for the UWG program. The building types were defined for each 3D model that allows calculating the energy consumption for residential, primary and secondary schools, retail shops, hotels, restaurants, supermarkets etc. The building density, urban buildings’ vertical-to-horizontal ratio

and green area coverage are then calculated through the Revit area scheme. Evergreen trees were considered for the vegetation growing seasons. The massing models of urban buildings for the selected site are shown in Figure 5. After the UWG's .xslm files and other source files are co-simulated using Matlab, two urban weather files for current and future scenarios were obtained. Table 2 presents the input values calculated.

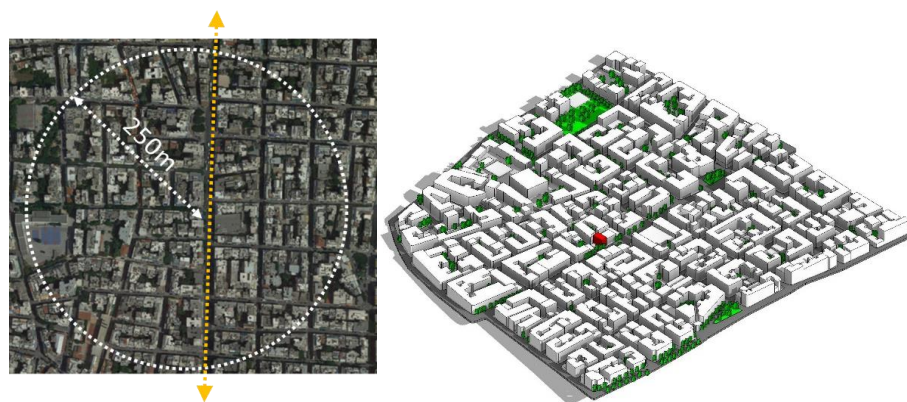


Figure 5: Site plan and 3D massing model of the case study location (Case study building is shown in red colour)

Table 2: Input data used in UWG's .xslm file

Urban Characteristics	Input data	Vegetation Parameters	Input data
Average Building Height	15.78	Urban Area Veg Coverage	0.0157
Fraction of waste heat into the canyon	1	Urban Area Tree Coverage	0.0245
Building Density	0.473	Veg Start Month	1
Vertical to Horizontal Ratio	1.078	Veg End Month	12
Urban Area Characteristic Length	250	Vegetation Albedo	0.25
Max Dx	62.5	Latent Fraction of Grass	0.5
Road Albedo	0.1	Latent Fraction of Tree	0.5
Pavement Thickness	0.5	Rural Road Vegetation Coverage	0.8
Sensible Anthropogenic Heat (Peak)	20		
Latent Anthropogenic Heat (Peak)	2		

The hourly wind speed was calculated using the algorithms of (Ghiaus et al 2005) as presented by (Salvati *et al.*, 2020). The terrain type with a roughness of 5.0 was assumed for the urban area. The average urban height, building density and vertical-to-horizontal building area ratio were considered referring to the data generated for the UWG program. The length-to-width ratio of the road is more than 20 hence, the canyon height-to-width ratio was checked, and it was identified that the case study building is exposed to the urban canyon wind. The case studied building has five stories; the urban canyon wind was therefore required to calculate from its relative building height above the ground level. It was considered 7m above street level for level 2 and 15m height for level 4 r. Hourly wind speed values of canyon wind were calculated for the undisturbed wind and wind direction values found in the rural weather files. The urban canyon wind speed values were then replaced with the urban weather files generated from the UWG program.

4 RESULTS AND DISCUSSION

EnergyPlus simulations were carried out using the generated weather files and overshadowing effect as presented in Figure 6. Data obtained from the building were used to define inputs such

as construction, schedules and internal heat gains, supplemented by values from (BS EN 16798-1, 2019) where data were not available.

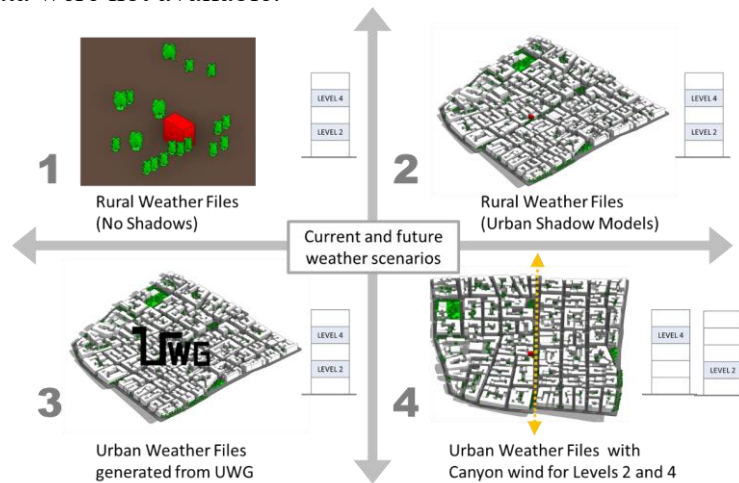


Figure 6: Tested cases for current and future weather scenarios

4.1 Comparison of weather files

The differences between different weather files are compared in Figure 7. As expected, higher temperature values were found in the urban weather files compared to the rural weather file. It can also be seen that the temperature values were increased in future weather conditions, but the annual mean temperatures were lower than 21°C in all scenarios. However, when the temperature values were assessed for the summer period only, a significant temperature increment could be observed in future weather conditions, reaching its summer average temperature above 31°C. On the other hand, significantly lower wind speed values were found in the urban weather file with the urban canyon wind modification. The average urban canyon wind speed, generated for level 4 rooms which are located at 15m height above the ground level, was as low as 1.5m/s and mostly still throughout the year. That implies decreasing natural ventilation efficacy in urban areas overshadowed.

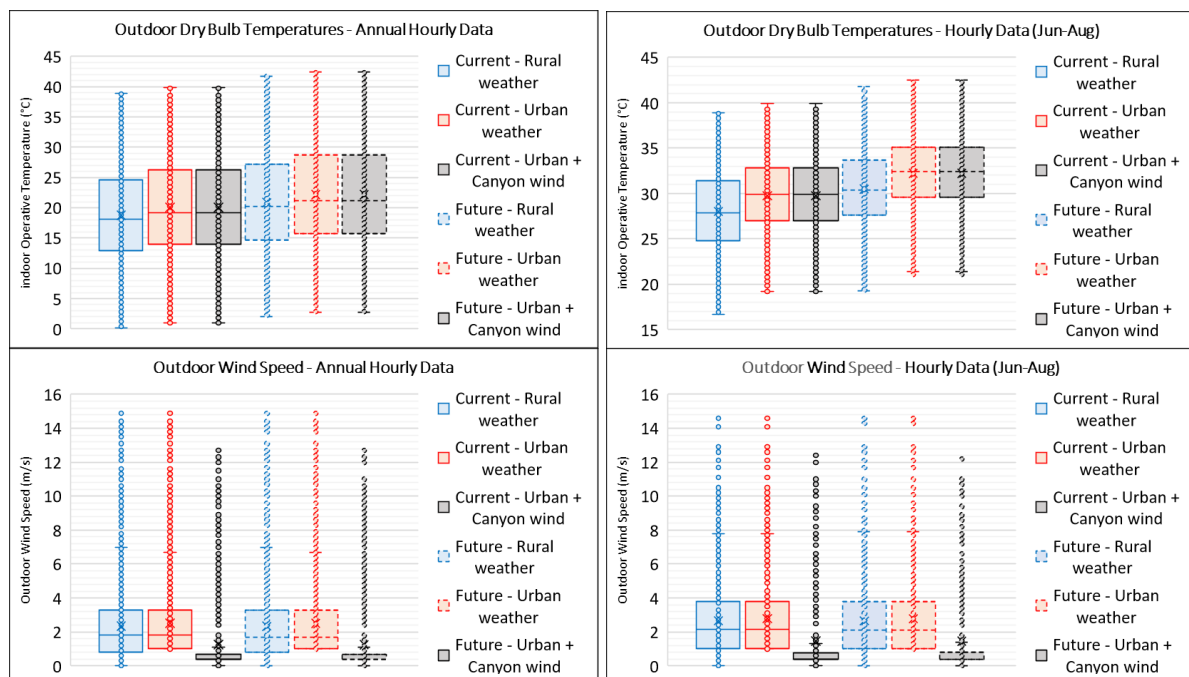


Figure 7: Comparison of outdoor dry bulb temperature and wind speed in different weather files

4.2 Energy use results

4.2.1 Annual energy demand

The annual heating and cooling demand for current and future weather conditions are presented in Figure 8 and

Table 3 for a lower floor (L2) and higher floor (L4) of the building; on all cases overshadowing has been considered. The impacts of building height and building density on energy demand were noted due to its exposure to the Urban Heat Island, overshadowing by surrounding buildings and lower urban canyon wind resulting to higher cooling demand and lower heating demand. A higher floor would demand more cooling and less heating compared to a lower floor due to lower wind speeds near the ground reducing infiltration and ventilation losses. As expected, future weather will demand higher cooling and lower heating because of an increase in external temperature. The highest total energy demand would be for higher floors in the future.

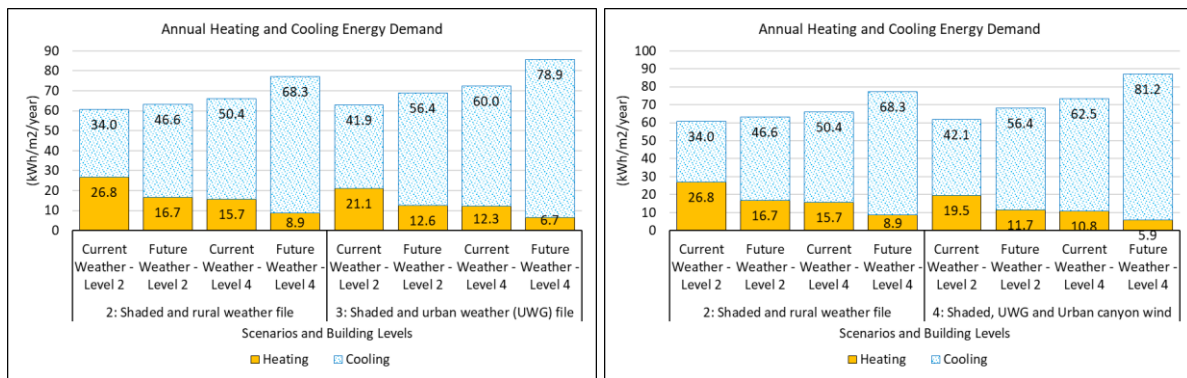


Figure 8. Annual heating and cooling demand of level 2 and level 4 rooms for scenarios 2 and 4.

Table 3: Heating, Cooling and Total energy demand for the various weather scenarios

Weather file	Heating	Change ratio	Cooling	Change ratio	Total	Change ratio
Current Weather	15.7		50.4		66.1	
Current Urban Weather (UWG)	12.3	0.78	60	1.19	73.1	1.11
Current UWG, Urban canyon Wind	10.8	0.69	62.5	1.24	74.0	1.12
Future Weather	8.9	0.57	68.3	1.36	77.8	1.18
Future Urban Weather (UWG)	6.7	0.43	78.9	1.57	86.0	1.30
Future UWG, Urban canyon Wind	5.9	0.38	81.2	1.61	87.5	1.32
Building Level 2						
Current Weather	26.8		34		60.8	
Current Urban Weather (UWG)	21.1	0.79	41.9	1.23	63.8	1.05
Current UWG, Urban canyon Wind	19.5	0.73	42.1	1.24	62.3	1.03
Future Weather	16.7	0.62	46.6	1.37	63.9	1.05
Future Urban Weather (UWG)	12.6	0.47	56.4	1.66	69.5	1.14
Future UWG, Urban canyon Wind	11.7	0.44	56.4	1.66	68.5	1.13

4.2.2 Monthly energy demand

The impacts of weather and microclimatic conditions on monthly heating and cooling demand are presented in Figure 9, considering the difference between rural and urban weather files, and the overshadowing and urban canyon wind effects on urban buildings; a higher floor (L4) is

presented as it was shown to perform worse than lower floors. The overshadowing impact is included in the results presented.

Figure 9 shows that heating demand is mainly from December to March due to the cold season in Athens. The heating demand of a single building exposed to the open terrain was less than the urban building as the urban building could be shaded by surrounding buildings limiting useful solar gains. Overshadowing considerations are important as would affect (increase) the heating demand significantly in all cases. As expected, using urban temperatures and future weather would reduce heating demand because of the increase in outdoor air temperatures. Because of the urban canyon wind, the heating demand could reduce.

Figure 9 also shows that cooling demand which is mainly during the summer months of June to September. As expected, the cooling demand of a single building exposed to the open terrain was higher than the urban building due to its exposure to solar radiation. Overshadowing considerations are important and would reduce the prediction of cooling demand. As expected, using urban temperatures and future weather would increase the cooling demand. Urban canyon wind, does not seem to impact monthly cooling demand significantly.

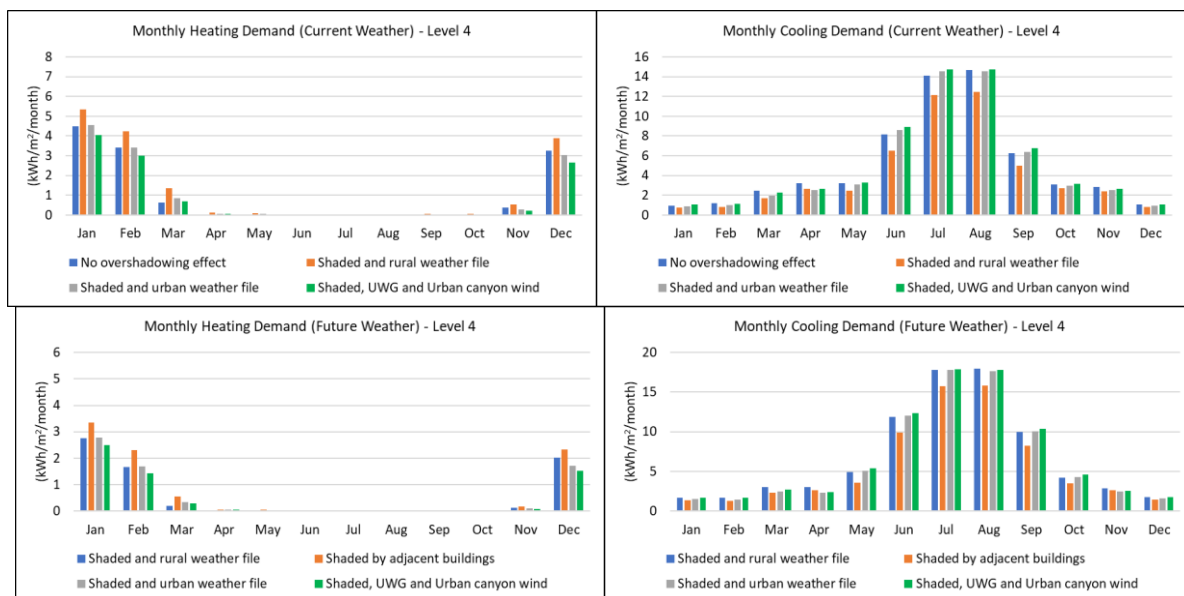


Figure 9: Monthly heating demand of level 4 rooms

4.3 Thermal comfort results

The impacts of weather and microclimatic condition on thermal comfort in the absence of air-conditioning are presented in Figure 10 as percentage of overheating hours during the summer (June to September). In calculating these, Category II (EN 16798-1-2019) limits were considered, hence, adaptive comfort temperature range can be expected by widening the upper limits to +3°C and lower limits to -4°C. Within these upper and lower limits of adaptive comfort, the temperature is assumed to be comfortable range, which is presented as yellow colour in Figure 10. If the indoor temperature is above the upper limits, it is the condition with overheating, which is presented as red colour for active cooling requirements. It can be seen that the overheating time was increased in the urban weather condition and future weather conditions. In the future weather condition with urban canyon wind, the SR2 room has less than 10% of summertime for adaptive comfort range, and more than 90% of summertime hours overheating.

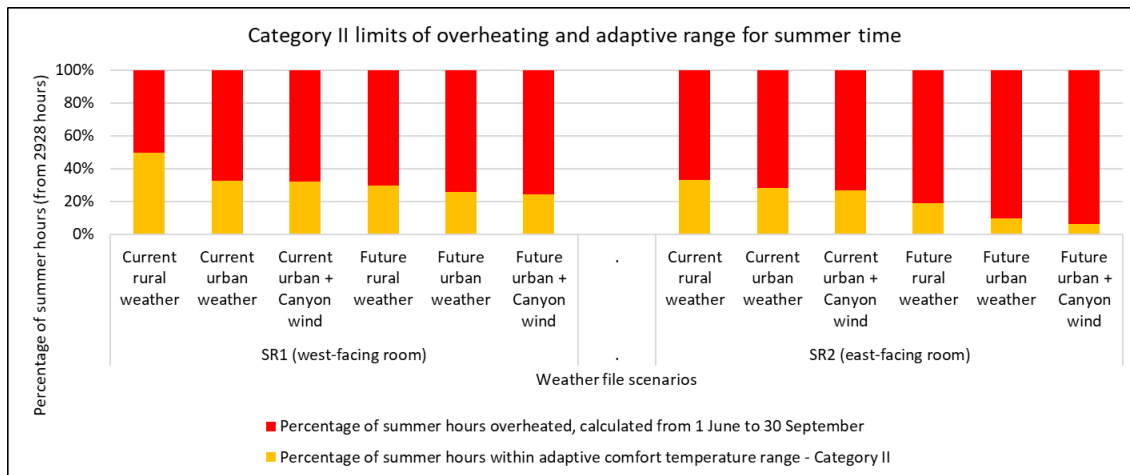


Figure 10. The percentage of summer hours for adaptive comfort and overheating time.

5 CONCLUSIONS

The confounding effects of urban density, urban textures and exposure to the wind, building design and human activities chemically and physically alter weather characteristics over and around urban areas. This paper aimed to identify the effects of changes in urban air temperatures and urban canyon wind on building energy performance and thermal comfort compared to rural conditions. Six weather files were generated from the UWG program and urban canyon wind calculation, and a total of eight weather files (two were the rural weather files generated from the Meteorom) were used to compare how different weather impacts building performance. The overshadowing effects from the surrounding buildings were considered as it is relevant to an urban setting. The case study building is located in Athens within an urban canyon with data obtained from the PRELUDE H2020 project.

The results of the simulation experiment showed that in hot European climate regions with densely built urban areas and for buildings within urban canyons, thermal simulation using current climate considering overshadowing, urban heat island and canyon wind will reduce the heating demand in future while the cooling demand could increase due to the increment in outdoor dry bulb temperature. The urban canyon wind caused lower wind speed which influences the efficacy of natural ventilation and energy consumption. The adaptive thermal comfort potential could reduce in the future while the overheating period could extend.

Specifically, for the case-study building in Athens the simulation results show an increase of the cooling demand by 24% in comparison to using a typical current weather file. However total energy demand (heating and cooling) increased only 3% for lower floors and 12% for higher floors due to the reduction of heating demand. Simulations using future weather files indicated a 66% increase in cooling demand in comparison to using a typical weather file. Future total energy demand increased by 32% for higher floors and 13% for lower floors. If the building is free floating an adaptive thermal comfort analysis indicated that only 25% of the summertime will be comfortable in comparison to 50% prediction by current typical weather.

Therefore, the use of a suitable weather file to include urban external conditions in thermal simulations is essential for more accurate predictions of energy demand and internal avoidance of overheating in free-floating buildings.

6 ACKNOWLEDGEMENTS

This study was funded by the European Union's Horizon 2020 research and innovation programme under Grant Agreement N° 958345 for the PRELUDE project (<https://prelude-project.eu>).

7 REFERENCES

- BS EN 16798-1 (2019) Energy performance of buildings. Ventilation for buildings. Indoor environmental input parameters for design and assessment of energy performance of buildings addressing indoor air quality, thermal environment, lighting and acoustics. Module M1-6. UK: BSI.
- Bueno, B., Norford, L., Hidalgo, J. and Pigeon, G. (2013) 'The urban weather generator', *Journal of Building Performance Simulation*, 6(4), pp. 269-281.
- Design Builder software <https://designbuilder.co.uk/> (assessed 23 June 2023)
- IPCC. 2014. Synthesis Report. Contribution of Working Groups I, II and III to the Fifth Assessment Report of the Intergovernmental Panel on Climate Change. edited by Core Writing Team, R. K. Pachauri, and L. A. Meyer. Geneva, Switzerland: IPCC.
- Georgakis, C. and Santamouris, M. (2008) 'On the estimation of wind speed in urban canyons for ventilation purposes — Part 1: Coupling between the undisturbed wind speed and the canyon wind', *Building and Environment*, 43(2008), pp. 1404–1410.
- Ghiaus, C., F. Allard, M. Santamouris, C. Georgakis, Ca Roulet, M. Germano, F. Tillenkamp, N. Heijmans, Jf Nicol, E. Maldonado, M. Almeida, G. Guarracino, and L. Roche. 2005. "Natural Ventilation of Urban Buildings - Summary of URBVENT Project." Pp. 29–33 in International Conference "Passive and Low Energy Cooling for the Built Environment." Santorini, Greece.
- Meteotest. (2020) Meteonorm Available at: <https://meteonorm.com/en/> (assessed 23 June 2023)
- PRELUDE project, Prescient building Operation utilizing Real Time data for Energy Dynamic Optimization (<https://prelude-project.eu>) (assessed 23 June 2023)
- Salvati A and Kolokotroni M (2022), Urban microclimate impact on ventilation and thermal performance of multi-family residential buildings: two case studies in different climates and urban settings, 42nd AIVC conference: Ventilation Challenges in a Changing World, 5-6 October 2022, Conference, Rotterdam, The Netherlands.
- Salvati A, Palme M, Chiesa G, and Kolokotroni M (2020). Built form, urban climate and building energy modelling: case-studies in Rome and Antofagasta. *Journal of Building Performance Simulation*. <https://www.tandfonline.com/doi/full/10.1080/19401493.2019.1707876>
- Salvati, A., Coch, H. and Cecere, C. (2016) 'Urban Heat Island Prediction in the Mediterranean Context: An Evaluation of the Urban Weather Generator Model', *ACE: Architecture, City and Environment, Arquitectura, Ciudad y Entorno*, 11(32), pp. 135–156. DOI: 10.5821/ace.11.32.4836.
- Santamouris, M., Georgakis, C. and Niachou, A. (2008) 'On the estimation of wind speed in urban canyons for ventilation purposes — Part 2: Using of data driven techniques to calculate the more probable wind speed in urban canyons for low ambient wind speeds', *Building and Environment*, 43(2008), pp. 1411–1418.
- Stewart, I.D. and Oke, T.R. (2012) 'Local Climate Zones for Urban Temperature Studies', *Bulletin of the American Meteorological Society*, 93(12), pp. 1879–1900. DOI: 10.1175/BAMS-D-11-00019.1.

Thermography-based assessment of mean radiant temperature and occupancy in healthcare facilities

Paul Seiwert¹, Quan Jin², Kai Rewitz¹, Ulrike Rahe³, Dirk Müller¹

*1 RWTH Aachen University
Mathieustraße 10
52066 Aachen, Germany*

**Corresponding author: pseiwert@eonerc.rwth-aachen.de*

*2 Chalmers University of Technology
Chalmersplatsen 4
412 96 Gothenburg, Sweden*

*3 Hochschule Wismar
Philipp-Müller-Straße 14
23966 Wismar; Germany*

ABSTRACT

Abstract. Due to its high demands regarding indoor environmental conditions, healthcare facilities are associated with high energy consumption. To move forward towards more demand driven and energy reduced conditioning, information on occupancy and temperature boundary conditions are crucial. Thermography-based systems enable data acquisition regarding both aspects in high local resolution. In this publication, we propose a thermography system that may be used for monitoring of rooms in healthcare facilities. It is set up using a 160 x 120 px thermography sensor and Raspberry Pi computer for data acquisition and processing. The sensors are mounted on walls to capture the inside of the room including patients, staff, and visitors. We evaluate the mean radiant temperature based on the individual inner surfaces of the room. The algorithm aggregates wall, floor and ceiling surface temperatures within the field of view of the sensor. For occupancy estimation inside the room, we apply a convolutional neural network (CNN). It is based on a pre-trained network and retrained using a partial dataset collected during the field study. To improve robustness of the algorithm several data pre-processing steps are conducted, that include image filters and redundancy testing. The system is evaluated based on data collected in a field study conducted inside MHH Hospital in Hannover, Germany. Several patients' rooms and a staff room are monitored over a period of 6 weeks, with the goal of evaluating indoor environmental data. The measurement period is inside the heating period in winter and different room layouts are considered. For reference, an indoor environmental quality measurement device is used to simultaneously measure air temperature, globe temperature and other IEQ parameters. Measured data of the reference system agree well with the thermography system. Deviations between both are less than 1 K in radiant temperature for most scenarios and measurement setups. Estimated occupancy is compared to a ground truth derived from manual processing of the captured thermography data. Finally, results of the field study are discussed together with the systems advantages and limitations with regard to privacy considerations.

KEYWORDS

Thermography, Occupancy detection, Mean radiant temperature, Computer Vision

1 INTRODUCTION

Continuous stress on the healthcare sector due to increasing life expectancy and threats from diseases has shifted public focus towards the conditions in healthcare facilities. Convalescence time and thus capacities in hospitals and other healthcare facilities are significantly influenced

by indoor environmental conditions (Shajahan et al., 2019). The high regulatory requirements for indoor conditions in these building types regarding ventilation rates and set temperatures, however, result in increased energy demand compared to other public buildings.

The methods and results presented within this publication are part of a pilot study to investigate measures for the improvement of well-being of patients and staff in hospitals as well as to convalescence and productivity. Furthermore, investigations into energy saving potentials are subject of the pilot study. It has been conducted between mid of November and mid of December 2020 in a ward of Medizinische Hochschule Hannover (MHH) and included both patients and staff's rooms.

Both the detection of occupancy and measurement of mean-radiant temperature (MRT) are crucial factors for efficient control of building energy systems. We propose a thermography-based system that enables the assessment of both aspects within one system.

1.1 Occupancy detection

During regular building operation indoor environmental conditions in healthcare facilities are typically not monitored under consideration of real-time occupancy. However, demand-controlled ventilation (DCV) enabled by occupancy detection can contribute to a significant decrease in heating, ventilation and air-conditioning (HVAC) related energy consumption in hospitals (Čongradac et al., 2014; Rätz et al., 2020).

For occupancy detection in indoor rooms several technologies have been proposed and investigated (Liu et al., 2019; Ahmad et al., 2021) In many applications, Pyroelectric Infrared Sensors (PIR) are used to detect presence of people, but they are not capable to retrieve information on the number of occupants. Derivation of occupancy from CO₂ measurements allows inexpensive and non-invasive detection, however with drawbacks in terms of accuracy, which can be improved with additional sensors in fusion with the CO₂ sensor (Dedesko et al., 2015; Rätz et al., 2022). Camera-based systems using machine learning algorithms are another option with high accuracy, but are sensitive with regards to the occupants' privacy.

Long-wave infrared (IR) sensors for occupancy detection are applied in different resolution and positions within indoor environments (Tyndall et al., 2016; Zhao et al., 2018). Analogous to camera-based systems, machine-learning algorithms are applied for classification based on the thermographic image. In most indoor conditions the high temperature difference between background and skin/clothing surface yields a good contrast for detection. The sensors can operate independent of illumination of the room and have become economically more viable. In terms of privacy, IR sensors are less critical as their lower resolution reveals less distinct features and less contrast than conventional cameras. Technical solutions for privacy implications have already been discussed (Pittaluga et al., 2016; Ahmad et al., 2021; Dubail et al., 2022).

1.2 Mean radiant temperature

According to ASHRAE standard 55 mean radiant temperature is – besides air temperature, air humidity and air speed – a required parameter to predict thermal comfort in thermal environments (ASHRAE, 2020). It is a key parameter for the quantification of radiative heat transfer between a person and its surrounding surfaces and is usually measured by means of a

globe temperature sensor, air temperature sensor and air velocity sensor. Further measurement methods include the two-sphere radiometer and the constant air temperature sensor (International Standardization Organization, 2002). As the radiative heat transfer is influenced by many factors including wavelength of radiation, view factors between objects and their surface temperature, its precise measurement is challenging, and it is associated with a high measurement uncertainty.

IR sensors allow continuous, non-intrusive measurement of surface temperatures. Using these measured surface temperatures and the view factors between the evaluation position and the surroundings, mean radiant temperature can be calculated analytically.

2 METHODS

2.1 Experimental setup and data acquisition

The experimental study is conducted as a field study within 5 different rooms of MHH: 4 patient rooms and 1 physicians' room. The rooms are equipped with mechanical ventilation systems and radiators for heating. Windows can be opened to allow for hybrid ventilation. In each of those rooms both IR sensor systems and an indoor environmental quality (IEQ) sensor system are installed.

Table 1: List of rooms with usage type and window orientation

Room	Type of room	Window Orientation	Number of beds
R1	Physicians room	North	-
R2	Patient room	North	2
R3	Patient room	South	2
R4	Patient room	South	3
R5	Patient room	South	2

The IR sensor system consists of a FLIR Lepton 3.5 160x120 px microbolometer sensor, the corresponding evaluation board for radiometric determination of object temperatures and a Raspberry Pi 3B+ microcomputer for data processing and transmission to storage. The sensor is specified with a typical accuracy of ± 5 K within regular operating conditions in buildings. In each room 2 of these sensors have been installed in opposing upper corners of the rooms, facing towards the occupied zone of the room, to cover as much wall, ceiling, and floor surface area as possible with the field of view (FOV) of the sensors. The low FOV angle of $57/71^\circ$ (horizontal/diagonal) compared to many other sensors limits the covered surface to mainly wall and floor sections.

The IEQ sensor system is used as a reference for the mean radiant temperature. The BAPPU-evo sensor device features among others air temperature (± 0.5 K), air humidity (± 4 % rH) and a globe temperature sensor (± 0.5 K). Due to restrictions regarding interference with care operations, the sensor system had to be placed on shelves slightly above the occupied zone at 2 m height.

In Figure 1 the positions of one of the IR sensor systems in a patient's room and one of the IEQ measurements systems are indicated.

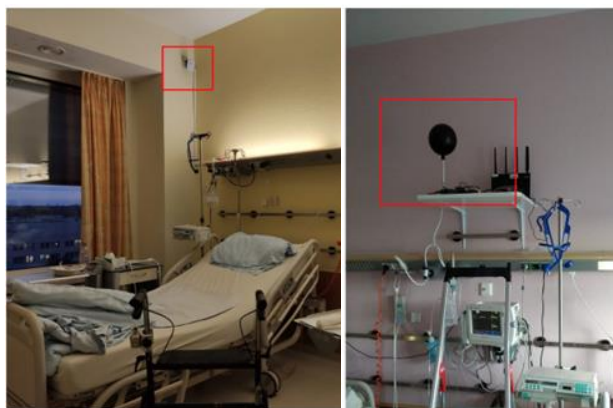


Figure 1: Positions of IR sensor system (left) and IEQ measurement system (right) inside a patient's room

2.2 Data pre-processing

The IR sensor system records frames with a frequency of 10 seconds. The frames are temporarily stored locally. In pre-processing the frame is analysed regarding its redundancy and validity. For redundancy testing the frame is compared to the previous frame based on the structural similarity index. In case the structural similarity is higher than 97% the frame is discarded. Occasionally, the sensor provides corrupted images which are detected based on a histogram comparison between frames. The frames are normalized and saved on a server in batches of 30 frames for further processing.

2.3 Occupancy

2.3.1 Data pipeline

The normalized frames are annotated manually by creation of labels for each occupant inside a room as shown in Figure 2. We have used one class of labels which includes occupants in different postures. These are standing, sitting, and lying. The images and annotations are saved and converted to the tfrecords format for further processing with machine learning platform TensorFlow (TensorFlow Developers, 2022).



Figure 2: Label annotations for occupants in patients' room

2.3.2 Network training

The TensorFlow platform provides pre-trained network architectures, which can be used for further individualized training of networks. The models suited for detection purposes are pre-

trained on the COCO 2017 dataset, which features images in the visual domain (Lin et al., 2014). We have selected the Faster R-CNN Inception ResNet V2 640x640 architecture (Szegedy et al., 2016). It is a very deep convolutional neural network with a good trade-off between accuracy and computational speed/ memory requirements. As the present frames are in the long-wave IR domain, the training process is cross-domain.

For transfer learning, we use a dataset of 800 frames, compiled randomly from 9 of the IR sensor systems. Data from one IR sensor system have been excluded due to faulty data. The network is trained in 100 000 steps with a batch size of 1. The development of the total loss metric for network training is shown in Figure 3. It includes classification loss, localization and objectness loss.

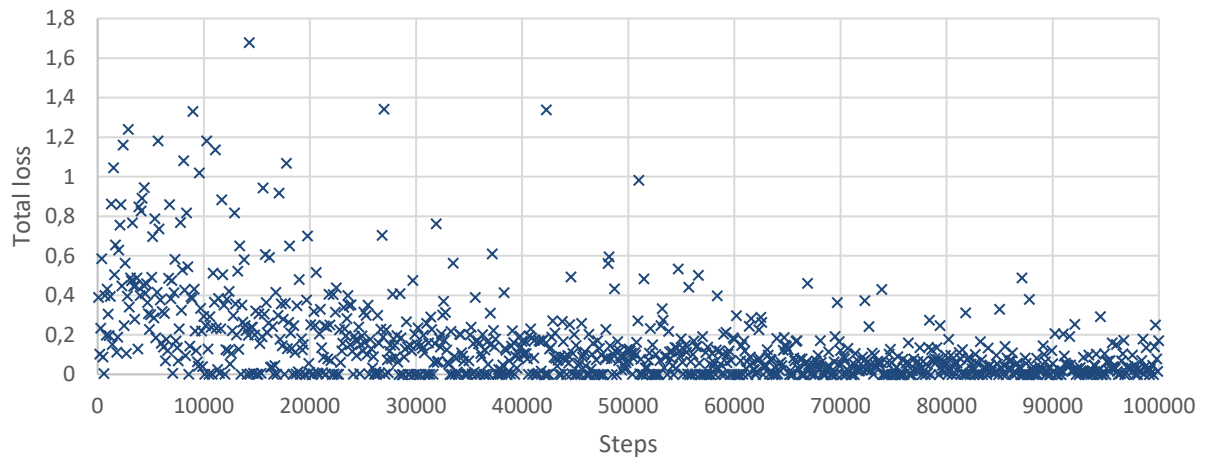


Figure 3: Total loss of network training process for each step

2.3.3 Training evaluation

For the evaluation of the networks training performance, COCO detection metrics are used. The confidence scores predicted by the classifier represent the probability that a bounding box contains a person. Precision indicates the reliability of the network's positive prediction, whereas recall describes the ability to determine the relevancy of predictions. The average precision is the average of precision values for all different levels of recall. The Intersection over Union (IoU) value represents the ratio of intersection area and union area of a predicted boundary box and a ground truth bounding box. The mean average precision (mAP) is calculated over different levels of IoU. The evaluation is based on an evaluation dataset of 200 frames from different sensor systems.

2.4 Mean radiant temperature

2.4.1 Algorithm for calculation

To determine MRT analytically both the surface temperatures t_i and view factors between the evaluation position and the surfaces F_{p-i} have to be known. According to ISO 7226 the following equation applies for the calculation of MRT indoor environments assuming high emissivity surfaces:

$$MRT^4 = \sum_{i=1}^N t_i^4 \cdot F_{p-i} \quad (1)$$

For small temperature differences, which are typical for surfaces in indoor environments it can be simplified to a linear equation:

$$MRT = \sum_{i=1}^N t_i \cdot F_{p-i} \quad (2)$$

The indoor surfaces temperature can be determined with the data captured by the IR sensor system. The surfaces are separated into segments based on their material properties, especially their emissivity. The assignment is done manually for the static position of the sensor after installation. For simplification of view factors, we substitute the view factors by arithmetic weighting according to the surface area A_i of each segment as shown in equation 3. This approach does not account for individual positions inside the room.

$$F_{p-i} = \frac{A_i}{\sum_{i=1}^N A_i} \quad (3)$$

Each surface is captured with one of the systems inside the rooms. The low angle of incidence between the sensor and ceiling results in a high share of reflected radiation. For this reason, the ceiling is not further considered for calculation. The expected error from this simplification is low for standing occupants, as projection factors according to ISO 7726 are small for ceiling and floor, compared to those for walls. However, for occupants in recumbent body position the expected error becomes more significant as the projection factor increases. An exemplary surface segmentation for a patient's room is shown in Figure 4.

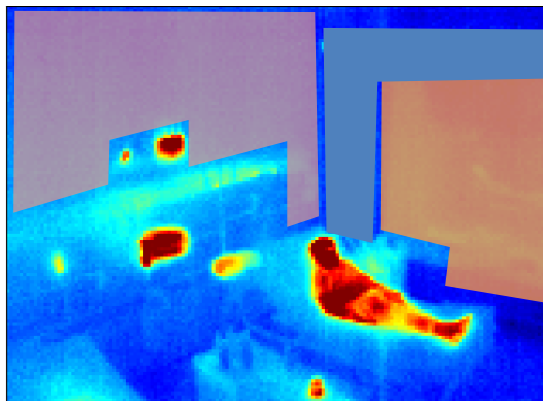


Figure 4: Exemplary selection of surfaces for MRT calculation for Room 4

After calculation of MRT, we filter not plausible outlier data by an Hampel-filter-function (based on a moving median) of MATLAB R2021a for a duration of five minutes. To reduce the noise of the sensor signals and to account for partial obstructions of surfaces by moving people, we finally calculated the moving mean value over five minutes for the data.

As a reference for the MRT, the globe temperature data from the IEQ measurement system are used. According to ISO 7226, MRT can be calculated from globe temperature t_g for forced convection based on equation 4, with air velocity v_a and air temperature t_a .

$$MRT = \left[(t_g + 273)^4 + 2.5 \cdot 10^8 \cdot v_a^{0.6} \times (t_g - t_a) \right]^{1/4} - 273 \quad (4)$$

The estimated deviation boundaries between globe temperature and calculated mean radiant temperature according to ISO 7226 are less than 0.8 K based on measured differences between air temperature and globe temperature of less than 2 K and air velocities of < 0.05 m/s.

3 RESULTS

3.1 Occupancy

In Figure 5 six exemplary frames from 4 different sensor systems with predicted boundary boxes are depicted. The green boundary boxes show the predicted position and area. The confidence scores at the top of the boundary boxes indicate the classifier confidence of the prediction being true.

In the top left frame both predictions are true positives. Also in the top right, bottom left and bottom center frame the predictions are correct. However, in the top right frame the IoU is lower than for the other predictions as only a part intersects with the ground truth (marked in red). In the top center frame the person lying in the bed is not detected (false negative) and in the bottom right frame a person is predicted, where nobody is present (false positive) indicating overfitting of the model.

The mean average precision (mAP) of the network for the evaluation data set is 0.4679 compared to the 0.377 of the pre-trained network on the COCO dataset. For an IoU of 0.5 the mAP significantly increases to 0.8028. For an IoU of 0.75 it is 0.4753. This means that the position of boundary boxes can be predicted well, but the intersection with annotated boundary box is not high for all cases as can be seen in the top right frame.

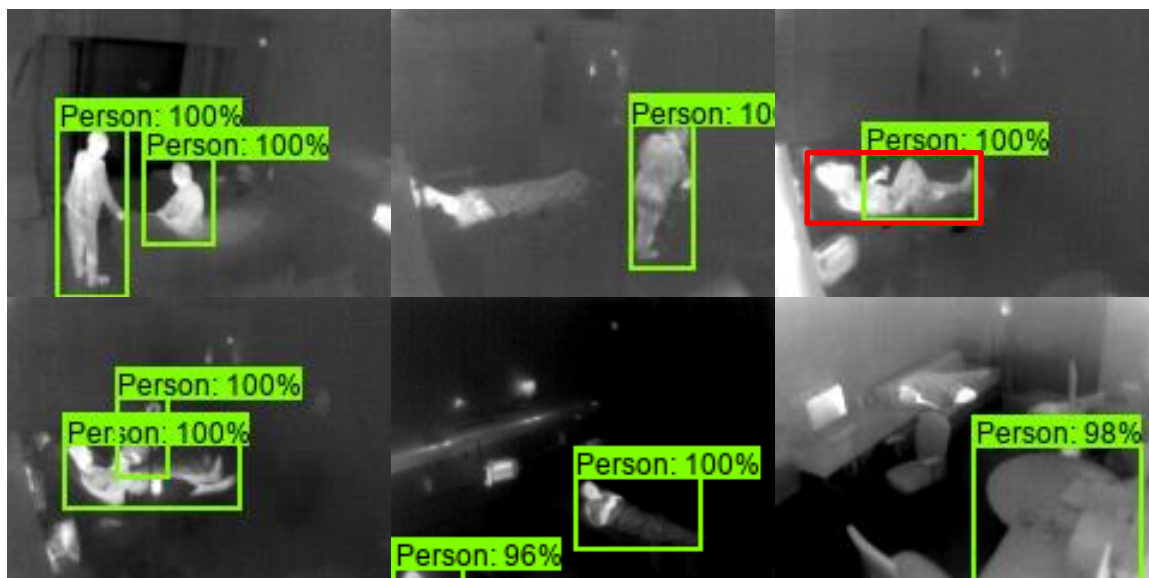


Figure 5: Selected frames of evaluation data set with predicted boundary boxes for persons marked in green

3.2 Mean radiant temperature

In Figure 6 the calculated MRT, air temperature and globe temperature as reference are depicted for Room 2 over the course of 18 days. Daily variations occur for the temperature profiles with

highest temperatures typically in the afternoon. A general trend with increasing temperatures from the beginning of the measurement period till the end can be observed.

Overall, the calculated MRT follows the globe temperature with little deviations. While in the beginning the difference between both values is continuously < 0.5 K, the difference increases after December 9th but stays within < 1 K. The RMSE between the MRT and the globe temperature for the whole measurement period in this room is 0.47 K.

Occasionally, short time temperature peaks occur for only one of the variables. For example, on December 5th the increase in globe temperature is significantly higher than for the MRT. A contrary effect can be observed on December 8th. Similar characteristics and effects can be observed for other rooms as well.

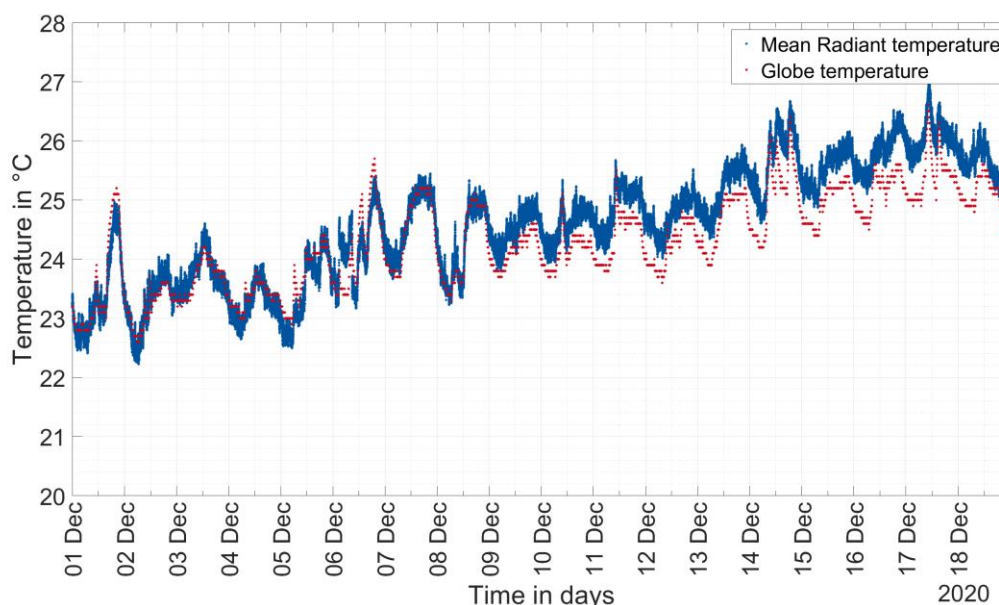


Figure 6: Calculated mean radiant temperature and measured globe temperature for Room 2

4 DISCUSSION

In terms of occupancy detection, the trained network yields good results for an estimation of occupancy in the rooms. In all different body postures, persons are detected by the network, although some predicted boundary boxes have a low IoU with the annotated boundary box. False negatives occur most frequently when the contrast between the person and the background is too low. High room temperatures lead to low differences between human skin or clothing temperature and the room temperature and thus lower contrasts, as we used normalized frames based on fixed temperature limits. Dynamic temperature limits may be a solution here, however implications for network training need to be considered as well.

As the pre-trained network was trained on visual domain images, features for classification are different in the frames used for further training and evaluation. Overfitting issues especially for specific sensor installation point may be caused by the low number of different installation points and fixed sitting and standing positions of patients and staff. Further classes (e.g. differentiation between postures) as well as more training data with different installation positions could reduce these issues.

Regarding privacy, the chosen installation position, sensor resolution and distance between sensor and person prevent direct identification of people as facial features are not recognisable. However, with further contextual information identification might be possible and technical

solutions must be implemented to reduce the associated concerns. Local data processing on the device and transfer of non-sensitive data to central building control systems can be part of the solution.

For the presented experimental setup, the applied calculation method for MRT shows only minor deviations compared to the reference globe temperature measurement and can therefore be considered valid. The homogenous boundary conditions comply with the assumptions made for the application of the method concerning view factors and temperature differences. As pointed out in the results section, some influencing and noise factors may have more significant impacts on the calculation methods which leads to limitations with regards to accuracy. These include ambient conditions such as air temperature and velocity but also body positions of occupants and distances between surfaces and evaluation positions. Further comfort relevant parameters such as radiation asymmetry and vertical temperature gradient may also be predicted based on the recorded data and could further enhance the capabilities of the system (Seiwert et al., 2018).

5 CONCLUSION

An IR sensor-based measurement system for occupancy detection and determination of mean radiant temperature has been presented in this work. The developed methodologies rely on image-based evaluation of data and comparison with measurements and manually annotated occupancy information.

For both aspects the results of the pilot study show promising results. The trained network can detect occupants inside the rooms with good precision and enables not only binary detection of occupancy but also a count of occupants. With further development and networks, which are exclusively trained on IR domain data, precision and recall may be further improved and model overfitting reduced. Privacy preserving algorithms can be implemented directly on the sensor system to reduce associated concerns.

With the calculation of mean radiant temperature, thermal boundary conditions inside rooms can be evaluated more accurately. The deviations measured in the observed rooms are within an acceptable range given the generally high uncertainty associated with its determination. Requirements regarding the boundary conditions have been fulfilled in this study, however they limit transferability to similar environments and require further validation.

6 ACKNOWLEDGEMENTS

We thank Tobias Schilling, Katharina Band and Iman El-Sayed from Medizinische Hochschule Hannover for their contribution in the preparation and conduction of the field study. Furthermore, we thank HeinzTrox Wissenschafts gGmbH and the Swedish Energy Agency for financial support of the study.

7 REFERENCES

- Ahmad, J., Larijani, H., Emmanuel, R., Mannion, M. and Javed, A. (2021). Occupancy detection in non-residential buildings – A survey and novel privacy preserved occupancy monitoring solution. *Applied Computing and Informatics*, 17(2), 279–295.
- ASHRAE (2020). Standard 55-2020: Thermal Environmental Conditions for Human Occupancy.
- Čongradac, V., Prebiračević, B. and Petrovački, N. (2014). Methods for assessing energy savings in hospitals using various control techniques. *Energy and Buildings*, 69, 85–92.

- Dedesko, S., Stephens, B., Gilbert, J.A. and Siegel, J.A. (2015). Methods to assess human occupancy and occupant activity in hospital patient rooms. *Building and Environment*, 90, 136–145.
- Dubail, T., Peña, F.A.G., Medeiros, H.R., Aminbeidokhti, M., Granger, E. and Pedersoli, M. (2022). Privacy-Preserving Person Detection Using Low-Resolution Infrared Cameras. <https://arxiv.org/pdf/2209.11335>.
- International Standardization Organization (2002). ISO 7726:2002: Ergonomics of the Thermal Environment - Instruments for Measuring Physical Quantities. Geneva.
- Lin, T.-Y., Maire, M., Belongie, S., Bourdev, L., Girshick, R., Hays, J., Perona, P., Ramanan, D., Zitnick, C.L. and Dollár, P. (2014). *Microsoft COCO: Common Objects in Context*.
- Liu, J., Luo, H. and Zhang, W. (2019). An Overview of Real-time Occupancy Information Acquisition Method for Demand-driven Building Energy Management. In: Hajdu, M. (ed.), *Proceedings of the Creative Construction Conference 2019: 29 June-2 July 2019, Budapest, Hungary*. Budapest: Budapest University of Technology and Economics; Diamond Congress Ltd, 625–634.
- Pittaluga, F., Zivkovic, A. and Koppal, S.J. (2016). Sensor-level privacy for thermal cameras, *2016 IEEE International Conference on Computational Photography (ICCP): Evanston, Illinois, 13-15 May 2016 : proceedings*. Piscataway, NJ: IEEE, 1–12.
- Rätz, M., Kalliomäki, P., Mathis, P., Koskela, H. and Müller, D. (2020). Analyzing the Energy-Saving Potential of Demand-Controlled Ventilation in Hospitals via Dynamic Building Simulations, 1026–1031.
- Rätz, M., Koskela, H., Kalliomäki, P., Müller, D. and Kremer, M.T. (2022). Real-Time Occupancy Detection in Hospital Patient Rooms Using Sensor Fusion, *Ventilation 2022: 13th International Industrial Ventilation Conference for Contaminant Control*.
- Seiwert, P., Schmitt, L., Wesseling, M.T. and Müller, D. (2018). Detection of Vertical Air Temperature Distribution by Long-Wave Infrared Thermography. In: Finnish Society of Indoor Air Quality and Climate (ed.), *Proceedings: Roomvent&Ventilation 2018: Excellent Indoor Climate and High Performing Ventilation*. Helsinki, Finland: SIY Indoor Air Information Oy.
- Shajahan, A., Culp, C.H. and Williamson, B. (2019). Effects of indoor environmental parameters related to building heating, ventilation, and air conditioning systems on patients' medical outcomes: A review of scientific research on hospital buildings. *Indoor Air*, 29(2), 161–176.
- Szegedy, C., Ioffe, S., Vanhoucke, V. and Alemi, A. (2016). Inception-v4, Inception-ResNet and the Impact of Residual Connections on Learning. arXiv. <https://arxiv.org/pdf/1602.07261>.
- TensorFlow Developers (2022). *TensorFlow*. Zenodo.
- Tyndall, A., Cardell-Oliver, R. and Keating, A. (2016). Occupancy Estimation Using a Low-Pixel Count Thermal Imager. *IEEE Sensors Journal*, 16(10), 3784–3791.
- Zhao, H., Hua, Q., Chen, H.-B., Ye, Y., Wang, H., Tan, S.X.-D. and Tlelo-Cuautle, E. (2018). Thermal-Sensor-Based Occupancy Detection for Smart Buildings Using Machine-Learning Methods. *ACM Transactions on Design Automation of Electronic Systems*, 23(4), 1–21.

Analyzing natural ventilation and cooling potential in a communal space building in Belgium under future climate conditions

Shiva Khosravi^{*1, 2}, Joost Declercq¹, Delphine Ramon²

*1 archipelago architects,
Remylaan 2b,3018,
Leuven, Belgium
* skhosravi@archipelago.be*

*2 Department of Architecture,
KU Leuven
Kasteelpark Arenberg 1
3001 Leuven, Belgium*

ABSTRACT

Due to climate change, Western Europe is experiencing a surge in cooling demand, leading to higher summer temperatures accompanied by longer and stronger heat waves, thereby intensifying the toll on our buildings. This signals the need for architects to design buildings that take advantage of passive techniques to provide thermal comfort. In recent years, natural ventilation has become a widely used method for reducing energy consumption and expenses. However, the utilization of natural ventilation can be restricted due to heatwaves and the impacts of climate change. To reduce the effects of these extreme conditions on the thermal comfort of the buildings, immediate guidance and decisions on architectural strategies are crucial. This study evaluated and compared the effectiveness of natural ventilation in current and future climate scenarios, particularly during extreme warm years.

The primary goal is to highlight the importance of increasing cross ventilation in order to reduce internal cooling loads during the summer months. The thermal performance of the building and the effect of natural ventilation was analyzed by the energy simulation tool 'IDA ICE'. As a case study, we considered a cultural building with communal spaces located in Belgium.

According to our observation, indoor thermal comfort can be improved by determining an optimum set of input parameters such as the temperature setpoint, the discharge coefficient of the night ventilation, and the window operation behavior (opening and closing schedule).

The results of this study indicate that natural ventilation can substantially reduce overheating risks and cooling demand during a typical year both in current and future climate scenarios. However, it is important to keep in mind that during heatwaves, natural ventilation becomes less efficient and cannot guarantee full thermal comfort to all occupants.

KEYWORDS

Thermal comfort, cooling demand, climate change, heatwave

1 INTRODUCTION

The vast majority of people spend most of their time indoors and rely on mechanical heating, ventilation, and air conditioning (HVAC) systems to keep the indoor environment comfortable. (Luo M, et al. 2021). The International Energy Agency (IEA) has released a report indicating that emissions from air conditioning are one of the primary factors contributing to global warming (Marschall, et al. 2020; IEA: 2018). Consequently, In future architectural design, it

will become increasingly important to reduce the use of mechanical cooling and air conditioning (Lomas, 2007; Chen, 2009).

In recent years, natural ventilation has become a widely used method for reducing energy consumption and reducing expenses. Natural ventilation systems have been estimated to save up to 60% of the energy required for ventilation and air conditioning in moderate climates (Elnagar et al. 2022).

While many studies have highlighted the benefits of natural ventilation, the actual application of natural ventilation can be affected by a variety of factors, making it challenging. A major challenge in integrating natural ventilation is that it creates uncertainty; as it relies on ever-changing weather conditions, the architectural layout of the building, as well as it entrusts the occupants with the task of regulating the indoor environment. However, the effectiveness of their behavior patterns cannot be guaranteed (Costanzo et al. 2019; Marschall et al. 2020). Moreover, the impact of the internal microclimate in complex spatial designs needs to be taken into account during the design phase. For example, many different spaces within a building can affect wind flow patterns, which may cause adverse consequences (Elnagar et al. 2022; Marschall et al. 2020). In general, sustainable design necessitates designers engaging with it at an early stage of the architectural design process and utilizing suitable metrics to simulate and visualize the performance of their proposals. However, even when buildings and their systems succeed in providing energy-efficient comfortable environments, they are often designed based on anticipated weather and operational conditions such as occupancy loads and solar heat gains, which may not always align with reality. Throughout the lifetime of buildings, they can be confronted with unexpected shocks and events, resulting in deviations from the originally intended comfort conditions and causing instances of over- or underheating.

Several studies indicate that the low-energy cooling strategies currently in use may become ineffective under long-term climate change, or in the event of an extreme event such as a heat wave or a power outage (Zhang et al. 2021). A report released by the Intergovernmental Panel on Climate Change (IPCC) in 2022 warns of the severity of climate change impacts and stresses the importance of adaptation and mitigation strategies (Sengupta et al. 2022).

With the continuation of global warming, building overheating is expected to increase. Summers that are warmer and more frequent heatwaves will lead to higher outdoor temperatures, which in turn will increase the risk of overheating inside buildings. There have been 18 warmest years in Europe over the last two decades, and extreme weather events are more frequent and intense than ever before (European Commission. 2018 ; Sengupta et al. 2023).

Despite the moderate climate in Belgium, buildings are subject to climate change and more frequent heatwaves, which increase overheating risk and cooling energy requirements (Jenkins et al. 2013; Sengupta et al. 2023). There are two essential aspects that must be considered in order to predict the building's thermal performance in the future: (1) an applicable energy simulation model that can accurately predict building performance and (2) high-quality future weather data (Ramon 2019).

Due to high occupant density, intermittent use, increased airtightness, and high glazing ratios, educational and cultural buildings, which represent a significant portion of the building stock, are responsible for high energy consumption. For this reason, in order to prevent any health risks associated with overheating in these types of buildings, it is important to evaluate and assess overheating separately from the buildings' energy efficiency. This paper aims to assess the thermal performance of a conference room with high occupant density, and presents preliminary findings regarding the influence of thermal mass and natural ventilation on the thermal comfort provided in a refurbished cultural building in Flanders (Belgium). To determine the effect of the aforementioned parameters on future energy performance, we analyzed the effects of current and future weather data for Typical Meteorological year (TMY) and Extreme Warm Year (EWY) in the building energy simulation.

Analyzing future climate change scenarios in simulations can be a useful approach to determining the optimal design of buildings based on their future thermal performance (Berger et al.2014; Andrić et al.2017). For this reason, the base case scenario was simulated with current weather data, and the results were compared to future weather files with no shock or power outage and EWY with heatwave scenarios.

2 METHODOLOGY

The thermal performance of the conference hall was assessed in this study using the IDA ICE v2.9.9 (EQUA) software (<https://www.equa.se/en/ida-ice>). As mentioned earlier, the case study building is a theoretical design of a conference hall in a cultural building located in Geel, Belgium (51°10'N 05°00'E). The floor area and the volume of the conference room are 320 m² and 5767.2 m³ respectively. The conference hall has external insulation with a concrete external wall and concrete slab floor. Table 1 summarizes the thermal property of the building material.

Table 1: thermal property of the building envelope

Construction Package	U-value (W/m ² K)
External wall	0.13
Roof	0.15
Floor	0.15

Figure 1 shows IDA ICE model of the cultural building and conference hall. To accelerate the simulation process, the other zones of the cultural building were treated as adiabatic.

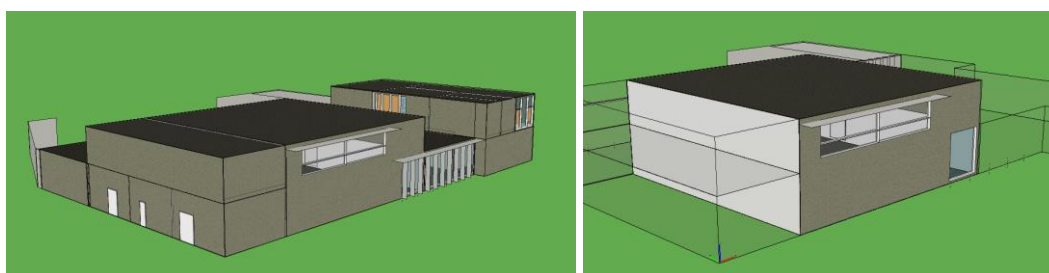


Figure 1: IDA ICE model (left : the cultural building, right: conference hall)

Windows are facing northeast and southwest and the area of each one is 24m². There are triple-glazed windows (U-value: 0.65 W/m²K, g-value: 0.52).

There are external shadings, which are controlled automatically (shading is ON when the radiation on the windows is above 250W/m²). In this study, the control strategy of natural ventilation is based on the indoor temperature, the temperature difference between indoor and outdoor temperatures, as well as the occupancy schedule for each scenario. Specifically, the natural ventilation system is activated from 7am to 6pm on working days when the indoor temperature is higher than 23 degrees Celsius and the outdoor temperature is higher than 14 degrees Celsius. During the night time, the ventilation system is activated if the interior temperature is higher than 21°C and the exterior temperature is lower than the interior and the exterior temperature is higher than 8°C.

The conference hall has a seating capacity of 170 individuals. It is utilized for three days each week, with a closure period from mid-July until the end of August. Figure 2 displays the occupancy schedule for one week.

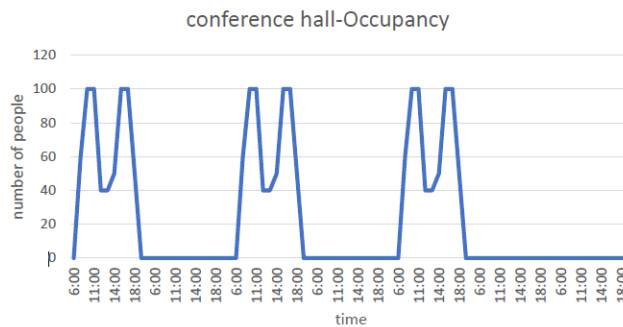


Figure 2: occupancy schedule

2.1 Weather data

Outdoor air quality is one of the most critical parameters in a natural ventilation strategy. It is necessary to conduct a qualitative assessment of the boundary conditions prior to proceeding with a quantitative approach. In this study, to determine whether the boundary conditions are suitable for natural ventilation, we conducted an analysis of the outdoor air quality and noise pollution (CIBSE, 2014). The Flanders Environment Agency (Vlaamse Milieu Maatschappij, VMM) monitors the outdoor air quality of Flanders and develops models to predict outdoor air quality. In general, air quality is improving. Except for Ozone, in almost all locations in Flanders, the European targets are met (VMM, 2018). Due to the property's location, near a forest and away from main traffic corridors, PM_{2,5}, PM₁₀, NO₂, and Black Carbon concentrations are below European standards. Noise levels are deemed acceptable due to the location of the building which is situated in the middle of a green area.

The weather files typically used in building performance simulation software represent the weather data recorded for specific months in a given year. In this study, all simulations were conducted using two types of weather data, namely “Typical Meteorological year (TMY)” (Thevenard & Brunger 2002) and “extreme warm year (EWY)” (Nik 2016) for current and future climate data (Regional Climate Models (RCMs)). The weather files are extracted for the recent past (1976-2004) and for an RCP 8.5 climate change scenario for the end of the 21st century (2070-2100). In Belgium, a climate model with a spatial resolution of 2,8 km is available through the CORDEX.BE project (Ramon 2021; Termonia P. et al. 2018). With a spatial resolution of 2,8 km, this model offers a better representation of extreme weather events and includes more local effects, such as urban heat islands, compared to RCMS with a spatial resolution of up to 10 km (Prein, A. F., et al. 2015), More information about the climate model can be found in Ramon et al. (2020)

3 RESULTS AND DISCUSSIONS

To evaluate the thermal performance of the conference hall, passive cooling strategies were applied, such as natural ventilation, shading, and thermal mass. Figure 3 presents the annual

indoor and outdoor temperature distribution, as well as, thermal comfort in the conference hall for the base case (scenario1). These outcomes are derived from dynamic simulation conducted for the base case, taking into account the current weather data. The results demonstrate that indoor temperatures are mainly affected by occupancy, as evidenced by a decrease in operational temperature from mid-July to the conclusion of August.

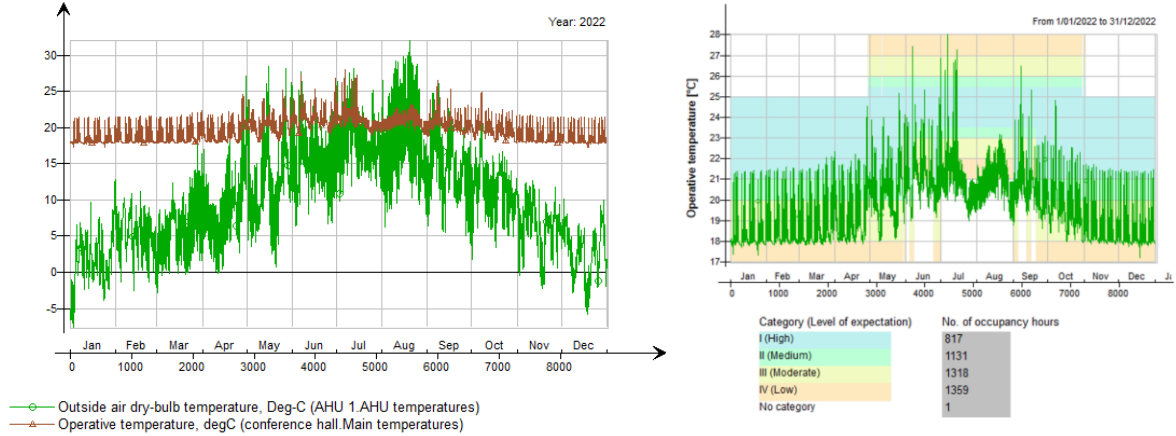


Figure 3: left: outside and operative temperature and right: thermal comfort

In order to demonstrate the impact of passive cooling strategies such as natural ventilation and thermal mass, a thermal dynamic simulation was conducted for 12 case studies. Each scenario is outlined and explained in Table 2.

Table 2: case study description

scenarios	Type of weather data	Passive cooling strategy	Thermal mass
Scenario 1	TMY current	Natural ventilation	high
Scenario 2	TMY current	Natural ventilation	low
Scenario 3	TMY current	No passive cooling	high
Scenario 4	TMY future	Natural ventilation	high
Scenario 5	TMY future	Natural ventilation	low
Scenario 6	TMY future	No passive cooling	high
Scenario 7	EWY Current	Natural ventilation	high
Scenario 8	EWY Current	Natural ventilation	low
Scenario 9	EWY Current	No passive cooling	high
Scenario 10	EWY future	Natural ventilation	high
Scenario 11	EWY future	Natural ventilation	low
Scenario 12	EWY future	No passive cooling	high

Figure 4 illustrates the annual occurrence of operative temperatures surpassing different thresholds (27°, 25°, and 30°) in the conference hall for the aforementioned scenarios. To highlight the impact of passive cooling figure 5 compares cooling demand for each case study. The frequency of annual operative temperature exceedances shows a significant contrast between scenarios without natural ventilation, whereas the variation is minimal when altering the thermal mass.

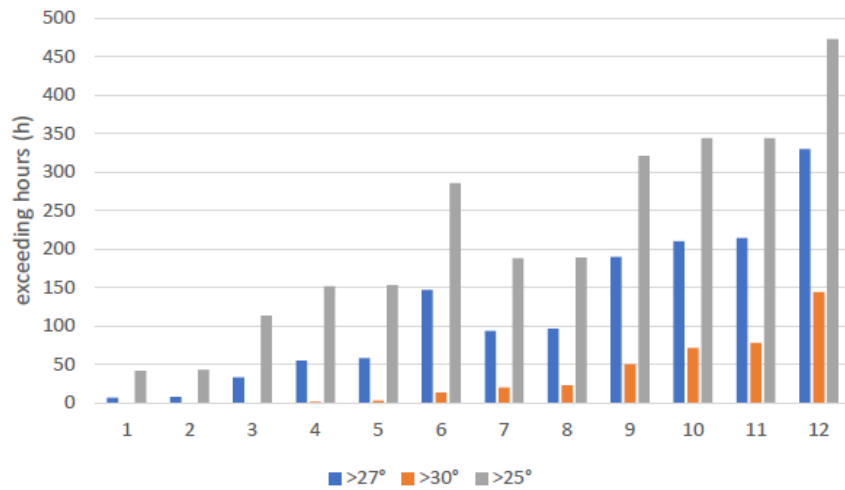


Figure 4: yearly exceedance of operative temperature

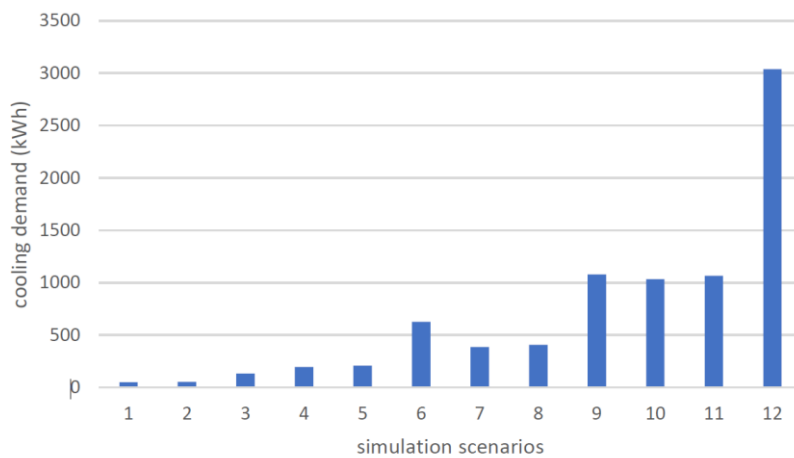


Figure 5: Annual cooling demand

This observation implies that, despite the challenges posed by rising temperatures due to global warming, natural ventilation remains a viable strategy for cooling indoor spaces. The graph depicted in Figure 4 emphasizes the reduction in indoor temperature resulting from the implementation of the natural ventilation strategy. However, future climate and heat waves will impose certain constraints on the utilization of night ventilation. Night ventilation effectively resets a building's thermal inertia by harnessing cooler outdoor air during nighttime hours to dissipate the heat accumulated within the building's walls throughout the day. However, the effects of global warming and extended duration of heatwaves are anticipated to diminish the potential of night ventilation, primarily due to the increasing temperatures during nighttime. As nights become warmer, the contrast between indoor and outdoor temperatures decreases, thereby reducing the effectiveness of night ventilation in dissipating heat. To address these challenges, alternative strategies and adaptations may be required. This could involve incorporating additional cooling methods, such as mechanical ventilation or air conditioning, to supplement natural ventilation during periods of reduced effectiveness. Additionally it is worth noting that a combination of natural ventilation and suitable thermal mass can result in an optimal indoor environment for thermal comfort.

4 CONCLUSION

This study examined the potential for passive cooling techniques, including natural ventilation and thermal mass, in a conference hall with a high occupancy rate located in Belgium. IDA ICE software was applied to analyze the thermal performance of the case studies. In this study, we assessed the impact of both natural ventilation and thermal mass on thermal comfort. Our findings clearly indicate that natural ventilation combined with thermal mass has a greater influence. According to the results of the study, Despite the difficulties presented by the increasing temperatures caused by global warming, natural ventilation continues to be a feasible approach for cooling indoor environments. In anticipated future climate scenarios, the inclusion of mechanical cooling becomes essential to achieve summer comfort under all circumstances. However, the potential energy savings achieved by combining mechanical cooling with natural ventilation are projected to be even greater compared to the present climate. This is due to the fact that the duration in which natural ventilation can effectively reduce the cooling load is expected to expand, thereby providing more opportunities for energy-efficient cooling.

5 REFERENCES

- Luo M, Hong Y and Pantelic J (2021). Determining Building Natural Ventilation Potential via IoT-Based Air Quality Sensors. *Front. Environ. Sci.* 9, 634570.
- Marschall, M., Burry, J., Tahmasebi, F. (2020). Simulating Natural Ventilation in Early Stage Design: Combining an Occupant Behavior Model with an Airflow Network Approach. In: Gengnagel, C., Baverel, O., Burry, J., Ramsgaard Thomsen, M., Weinzierl, S. (eds) *Impact: Design With All Senses*. DMSB 2019. *Springer, Cham*.
https://doi.org/10.1007/978-3-030-29829-6_10
- IEA (2018). *The Future of Cooling: Opportunities for energy-efficient air conditioning*, IEA, Paris.)
- Lomas K.J. (2007). Architectural design of an advanced naturally ventilated building form. *Energy and Buildings*, 39(2), 166-181
- Chen Q.(2009). Ventilation performance prediction for buildings: A method overview and recent applications. *Building and Environment*, 44(4), 848-858
- Elnagar E., Zeoli A., Lemort V.(2022), Performance Evaluation of Passive Cooling in a Multi-Zone Apartment Building Based on Natural Ventilation, *CIMA 2022 The 14th REHVA HVAC World Congress*, Rotterdam, Netherland
- Costanzo, V., Yao, R., Xu, T., Xiong, J., Zhang, Q., and Li, B. (2019). Natural Ventilation Potential for Residential Buildings in a Densely Built-Up and Highly Polluted Environment. A Case Study. *Renew. Energy*. 138, 340–353.
doi:10.1016/j.renene.2019.01.111
- Zhang C. , Berk Kazanci O., Levinson R. , Heiselberg P. , W. Olesen , Chiesa G., Sodagar B., Ai Z., . Selkowitz S., Zinzi M., Mahdavi A., Teufl H., Kolokotroni M., Salvati A., Bozonnet E., Chtioui F., Salagnac P., Rahif R., Attia S., Lemort V., Elnagar E., Breesch H., Sengupta A., Leon Wang L., Qi D., Stern P., Yoon N., Bogatu D., Forgiarini Rupp R., Arghand T., Javed S., Akander J., Hayati A., Cehlin M., Sayadi S., Forghani S., Zhang H., Arens E., Zhang G.(2021). Resilient cooling strategies – A critical review and qualitative assessment, *Energy and Buildings*, 251(15), 111312
- Sengupta A., Breesch H., Al Assaad D., Steeman M. (2023) Evaluation of thermal resilience to overheating for an educational building in future heatwave scenarios, *International Journal of Ventilation*

- Sengupta A., Al Assaad D., Borrajo Bastero J., Steeman M., Breesch H (2023), Impact of heatwaves and system shocks on a nearly zero energy educational building: Is it resilient to overheating? , *Building and Environment*, 234, 110152
- European Commission. (2018). *Going climate-neutral by 2050. Facilities*, 3–19. <https://doi.org/10.2834/508867>
- Ramon D. (2021) Towards Future-Proof Buildings In Belgium Climate And Life Cycle Modelling For Low-Impact Climate Robust Office Buildings, PhD thesis, Ku Leuven, Belgium
- Termonia, P., Van Schaeybroeck, B., Tabari, H., De Troch, R., Caluwaerts, S., Giot, O., Hamdi, R., Vannitsem, S., Duchêne, F., Willems, P., Gobin, A., Van Uytven, E., Hosseinzadehtalaei, P., Van Lipzig, N., Wouters, H., Vanden Broucke, S., Van Ypersele, J., Marbaix, P., Villanueva-Birriel, C. M, Vannitsem, S. (2018). The CORDEX.be initiative as a foundation for climate services in Belgium. *Climate Services*, 11, 49–61. <https://doi.org/10.1016/j.cliser.2018.05.001>
- Ramon D., Allacker K., P. M. Lipzig N., Troyer F., Wouters H. (2019), Future Weather Data for Dynamic Building Energy Simulations: Overview of Available Data and Presentation of Newly Derived Data for Belgium. *Energy Sustainability in Built and Urban Environments*
- Berger, T., Amann, C., Formayer, H., Korjenic, A., Pospischal, B., Neururer, C., Smutny, R. (2014), Impacts of climate change upon cooling and heating energy demand of office buildings in Vienna, Austria. *Energy Build.* 80, 517–530.
- Andrić, I., Pina, A., Ferrão, P., Fournier, J., Lacarrière, B., Le Corre, O.: The impact of climate change on building heat demand in different climate types. *Energy Build.* 149, (2017)
- Vlaamse Milieu Maatschappij (2018). Annual Air Report –Flanders (Belgium) – Emissions 2000-2016 and air quality in Flanders in 2017.
- Thevenard, D. J., & Brunger, A. P. (2002). The development of typical weather years for international locations: Part II, production. *ASHRAE Transactions*, 108.
- CIBSE (2014). Natural Ventilation in Non-Domestic buildings AM10. CIBSE Publications, London (UK).
- Declercq J., Ramon D., Deryn F., Allacker K. (2021), The feasibility of natural ventilative cooling in an office building in a Flemish urban context and the impact of climate change, BS2021 conference, Bruges, Belgium
- Prein, A. F., Langhans W., Fosser G., Ferrone .A, Ban N., Goergen N., Keller M., Tölle M., Gutjahr O., Feser F., Brisson F., Kollet S., Schmidli J., Lipzig N., and Leung R. (2015), A review on regional convection-permitting climate modeling: Demonstrations, prospects, and challenges, *Rev. Geophys.*, 53, 323–361
- Ramon, D., Allacker, K., De Troyer, F., Wouters, H., Van Lipzig, N. P. (2020). Future heating and cooling degree days for Belgium under a high-end climate change scenario. *Energy Buildings*
- Nik, V. M. (2016). Making energy simulation easier for future climate—Synthesizing typical and extreme weather data sets out of regional climate models (RCMs). *Appl Energy*, 177, 204-226.

A study of indoor environment and window use in French dwellings monitored during a summer with heatwaves

Mathilde Hostein*^{1,2}, Bassam Moujalled^{1,3}, Marjorie Musy^{1,3}, and Mohamed El Mankibi²

*1 Cerema, BPE Research Team
46 rue Saint Théobald
38081, L'Isle d'Abeau, France
*Corresponding author:
mathilde.hostein@cerema.fr*

*2 Univ. Lyon, ENTPE, Ecole Centrale de Lyon,
CNRS, LTDS, UMR 5513
3 Rue Maurice Audin
69518, Vaulx-en-Velin, France*

*3 Univ. Savoie Mont Blanc,
CNRS, LOCIE, UMR 5271
60 rue du lac Léman, Savoie Technolac
73376, Le Bourget-du-Lac, France*

ABSTRACT

Heatwaves are extreme events that will become more frequent and intense with climate change. Maintaining a comfortable and healthy indoor environment becomes crucial during these periods. The occupants are not just passive individuals who undergo the evolution of their environment. They can act to ensure their thermal comfort, in particular by opening or closing windows in summer.

This article thus aims to examine the thermal environment and indoor air quality during the summer period in French dwellings. Window use is studied in order to identify the physical and contextual factors influencing the occupants' behaviour thanks to a feature selection algorithm.

Four dwellings, three in a multi-family building and one in a single-family house, were monitored between June and September 2022. Three heatwaves occurred during this summer in the French region Auvergne-Rhône-Alpes. In addition to measurements of the indoor and outdoor environments, occupant actions on windows, fans and air conditioners were recorded. Three types of surveys were conducted with the occupants to understand their perceptions, experiences, and overall use of the dwellings.

The results show that the four households have different window use behaviours. Analysis of the data revealed that the variables influencing occupants' window behaviour are indoor and outdoor air temperatures, indoor CO₂ and light VOC concentrations, global horizontal irradiation and time of day.

KEYWORDS

Occupant Behaviour, Window use, Monitoring, Heatwave, Summer

1 INTRODUCTION

Windows are a link between the indoor and outdoor environment that occupants can control (Carlucci et al., 2020) to ensure their thermal comfort (Rijal et al., 2018) and indoor air quality (Marchand et al., 2018). However, noise or pollution can be disincentives to window opening (Rijal et al., 2018). Occupants have to make a compromise in their search for thermal, visual or acoustic comfort, or indoor air quality. It is therefore understandable that window use is influenced by **physical variables** of the indoor and outdoor environment.

However, although opening them could help to cool the room, closed windows can be observed at night during hot weather. Indeed, **context** matters. Occupants are not only looking for good indoor environmental quality, but also for their needs for security and privacy, as the dwelling is a shelter (Marchand et al., 2018). Moreover, each person acts differently. In addition to social

and cultural factors (Rijal et al., 2018), **individual** habits and preferences can be drivers to window openings or closings (Carlucci et al., 2020).

Many studies analyse window use based on field data. In 2012, Fabi et al. (Fabi et al., 2012) conducted a literature review about window opening behaviour. They divide factors influencing occupant behaviour into five categories: physiological, psychological, social, physical environmental and contextual. Since this review, several studies on the residential context have been published on this subject. Table 1 summarizes the results of these studies. It shows the physical and contextual variables influencing window openings and closings. Green ticks indicate a driver, and red crosses a non-driver. The presence of a tick and a cross means that the results are different for opening and closing, or between studies for the literature review.

Table 1. Variables influencing window openings and closings in residential buildings

Variables	(Fabi et al., 2012) Review	(Cali et al., 2016)	(Barthelmes et al., 2017)	(Jones et al., 2017)	(Yao & Zhao, 2017)	(Rijal et al., 2018)	(Shi et al., 2020)	(Cho et al., 2021)
T_{int}	✓		✓	✓	✓	✓		✓
T_{out}	✓	✓	✓	✓	✓	✓	✓	
RH_{int}		✓	✓	✓	✓			
RH_{out}			✗	✓ ✗	✓		✓	
$CO_{2, int}$ level	✓	✓	✓		✓			✓
$PM_{2.5, ext}$ level					✓		✓	
Solar radiation	✓ ✗		✓	✗				
Illuminance			✗ ✓					
Wind speed	✓ ✗		✗ ✓	✓	✓		✓	
Wind direction	✗				✓			
Rainfall	✗			✓				
Time of day	✓	✓	✓	✓	✓	✓		
Weekday	✗		✗		✓			
Season	✓			✓	✓	✓		
Others contextual drivers	✓ ✗	✓ ✗				✓	✓	

These studies aim to model window-related occupant behaviour. Logistic regression is used in five of these articles (Cali et al., 2016; Jones et al., 2017; Rijal et al., 2018; Shi et al., 2020; Yao & Zhao, 2017). Barthelmes et al. (Barthelmes et al., 2017) perform a variable selection with a Kolmogorov-Smirnov test, then model window use with Bayesian Network. Cho et al. (Cho et al., 2021) also conduct a feature selection before modelling, using a generalized additive model.

Feature selection methods can be used in data preparation for machine learning algorithms with predictive purposes (Brownlee, 2020). Speiser et al. (Speiser et al., 2019) compared 13 of these methods based on random forest thanks to 311 classification datasets from multiple scientific fields. To our knowledge, random forest variable selection has never been used for occupants' window-use behaviour.

This study aims to identify physical and contextual drivers influencing window opening and closing during summer in dwellings. A field measurement campaign was therefore conducted in four occupied French dwellings during summer 2022. A variable selection method based on random forests was used to analyse the measurement data.

2 METHODOLOGY

2.1 Data collection

A measurement campaign was conducted as part of the CREATIV project, which aims to analyse the relationship between **thermal comfort** and **indoor air quality** in dwellings during **heatwaves**. Therefore, four dwellings were monitored during summer 2022. Three of them are social housing of a multi-family building located in Lyon, and the fourth is a single-family

house in Clermont-Ferrand. Both buildings are located in the South-Est of France. We will refer to dwellings A, B, C and D in the following. Their characteristics are detailed in Table 2.

Table 2. Dwellings monitored in the CREATIV project during summer 2022

Identifier	Dwelling A	Dwelling B	Dwelling C	Dwelling D
Location city	Lyon	Lyon	Lyon	Clermont-Ferrand
Dwelling type	Multi-family housing	Multi-family housing	Multi-family housing	Single-family home
Number of rooms	3	3	4	5
Living-room orientation	East	East	Southeast	South
Number of occupants	1	2	1	2
Household equipment	1 fan purchased during the summer thus not monitored	2 fans and 1 AC	-	1 fan
Start of monitoring	07/07/2022	17/06/2022	16/06/2022	13/06/2022 and 14/06/2022
End of monitoring	15/09/2022	15/09/2022	15/09/2022	07/09/2022 and 27/09/2022
Holidays	-	08/07/2022 to 19/07/2022	10/08/2022 to 27/08/2022	08/08/2022 to 17/08/2022

For the indoor environment variables, several types of sensors were used (Figure 1):

- **NEMO XT** monitoring stations measured air temperature (T_{int}), relative humidity (RH_{int}), CO_{2int} , light VOC_{int} and fine particles (PM_{1int} , $PM_{2.5int}$ and PM_{10int}) levels in the living room and master bedroom of each dwelling at a time step of 10 minutes.
- **HOBO U12-011** dataloggers measured air temperature and relative humidity at a 10-minute time step. They were placed in most of the rooms in each dwelling. The temperature and humidity measurements were therefore duplicated in the living room and the master bedroom.
- **HOBO UX90** change of state recorders captured the opening and closing of windows, French windows and some interior doors. Some openings in dwelling D were equipped with **HOBO U9** which operate similarly.
- For dwellings with fans or mobile air conditioners, **VOLTCRAFT Energy Logger 4000** wattmeters were installed ahead of the appliances to record power consumption at a time step of 1 minute.



Figure 1. Pictures of the sensors used during the measurement campaign

Two types of outdoor sensors were used:

- On both sites, a **NEMO Outdoor** monitoring station was installed: on the balcony of a second-floor apartment in Lyon and on the terrace of the house in Clermont-Ferrand. They measured outdoor air temperature, relative humidity, light VOC_{out} and fine particles (PM_{1out} , $PM_{2.5out}$ and PM_{10out}) at a 10-minute time step.
- At the Lyon site, a **HOBO U23-002** datalogger was placed on the 6th floor. It measured outdoor air temperature (T_{out}) and relative humidity (RH_{out}) at a time step of 10 minutes.

As the pitched roofs were not accessible, it was not possible to install weather station. Wind and solar radiation data were collected from nearby stations. For the Lyon site, the **ENTPE**

station (ENTPE, s. d.), located at about 10 km aerial distance from the monitored building, was used. Wind speed and direction (WS/WD), as well as global and diffuse horizontal irradiation (I_{hg}/I_{hd}) were extracted at a time step of 1 minute over the whole monitoring period, i.e. from 16/06/2022 at 16:00 to 15/09/2022 at 14:30. No stations were found for the Clermont-Ferrand site with the relevant variables and at a rather low time step, so these variables are not used for dwelling D.

In order to complete the measured data, three types of surveys were filled in with the occupants in order to find out how they used the dwelling and how they felt about it:

- **Logbook** was filled in by the occupants independently during a one-week period of heatwave during the summer. Occupants were called at the beginning of the week. This document recorded cooking practices, household chores, solar protection use, bathroom use, door use and occupation. Only the occupants of dwelling D completed this document from Friday 15/07/2022 to Thursday 21/07/2022.
- **Thermal comfort surveys** were completed by the occupants independently throughout the summer. At any time during the campaign, an occupant could fill in a page specifying the date and time, the perceived thermal ambience and personal parameters useful in thermal comfort study.
- **General questionnaires** were filled in with the occupant when the sensors were removed or afterwards by telephone if the first option was impossible. It concerns the use of the dwelling and the equipment during the summer, the general comfort as well as the differences identified during a heatwave.

2.2 Data processing and analysis

After extracting the data measured by each sensor, a code written in R is used to group the data by dwelling and by room. To ensure a **single time step**, the environmental measurements are interpolated, the ENTPE data are averaged, and the window status (open/closed) is filled in between the state changes. The choice of a 5-minute time step corresponds to a compromise between the dynamics of the thermal and aerualic variables, and the windows openings. Openings of less than a minute are neglected because we noticed some openings of a few seconds which seem to be due to a sensor failure rather than a real opening/closing.

Cleaning steps are then performed manually, i.e. the consistency of the measured values is checked for each sensor. Some malfunctions were identified on some sensors used for the openings. They are due to the fall of one of the sensor parts. They were recovered separately and therefore recorded an open position since their fall. Data from these sensors is deleted from the end of the last closure, i.e. just before the opening due to the fall. Some sensors were dropped the day or the day after they were installed, and therefore no data is used for these sensors.

After processing the data, an **exploratory analysis** of the physical data is conducted. The indoor environments of the four dwellings are compared statistically. Occupant behaviour is then studied during the summer and heatwaves, through the measured data and surveys. A focus is made on dwelling B and D.

Finally, in order to identify the variables influencing the use of windows, a **feature selection** algorithm is applied for each room of each dwelling. We are interested here in the use of the windows (opening/closing) and not the state of the windows (open/closed). For this reason, at this stage, only the observations that correspond to a change of state are kept.

Libraries have been created in different programming languages to automate feature selection. In particular, the *VSURF* package on R, based on random forests, allows variables selection for interpretation or prediction purposes (Genuer et al., 2015). In the second case, the set of predictor variables will be smaller because the redundant variables among all those that influence the target variable are removed in order to maximise performance in terms of

prediction. There are other libraries on R for random forest variable selection, such as *Boruta* (Kursa & Rudnicki, 2010) or *varSelRF* (Diaz-Uriarte, 2007). However, both are well suited to databases with more than 50 features according to Speiser et al. (Speiser et al., 2019).

The **VSURF** library (Genuer et al., 2015) is therefore used. This method is chosen because it is implemented in R, it is one of the two best random forest variable selection methods of all those compared by Speiser et al. (Speiser et al., 2019), and it provides a distinction between interpretation and prediction purposes. This former functionality is used. The objective is indeed to find all the influential variables even if they may be redundant among themselves.

In addition to the measured environmental variables, we add several contextual explanatory variables: the heatwave (HW) warning, the day of week and the time of day.

- **HW alert** is a binary categorical variable which allows to identify if a HW has been declared by *Santé Publique France*¹ at the time of the action. Indeed, during HW periods, awareness messages are broadcast in France to prevent health risks related to HW. According to *Santé Publique France*, three periods of HW occurred during summer 2022 for both locations. They were under orange vigilance from 15 to 22 June. The second HW occurred from 12 to 26 July, during which Lyon was under orange vigilance and Clermont-Ferrand under yellow vigilance. Finally, both locations were under orange vigilance from 31/07/2022 to 05/08/2022, with a HW extended to 13 August under yellow vigilance for Lyon (*Santé Publique France*, s. d.).
- **Weekday** is a categorical variable with seven factors.
- **Time of day** is a numeric variable that corresponds to the number of minutes since the beginning of each day. It represents the occupants' habits.

3 RESULTS

3.1 Indoor environment

Figure 2 shows the boxplots of the indoor temperature (T_{int}) in the different rooms of the dwellings. In the three monitored dwellings of the multi-family building, T_{int} values are above 28°C at least 44% of the time in the living room, and this value reaches 63% in dwelling C. Temperatures are much lower in dwelling D, with average values below 25°C for all rooms.

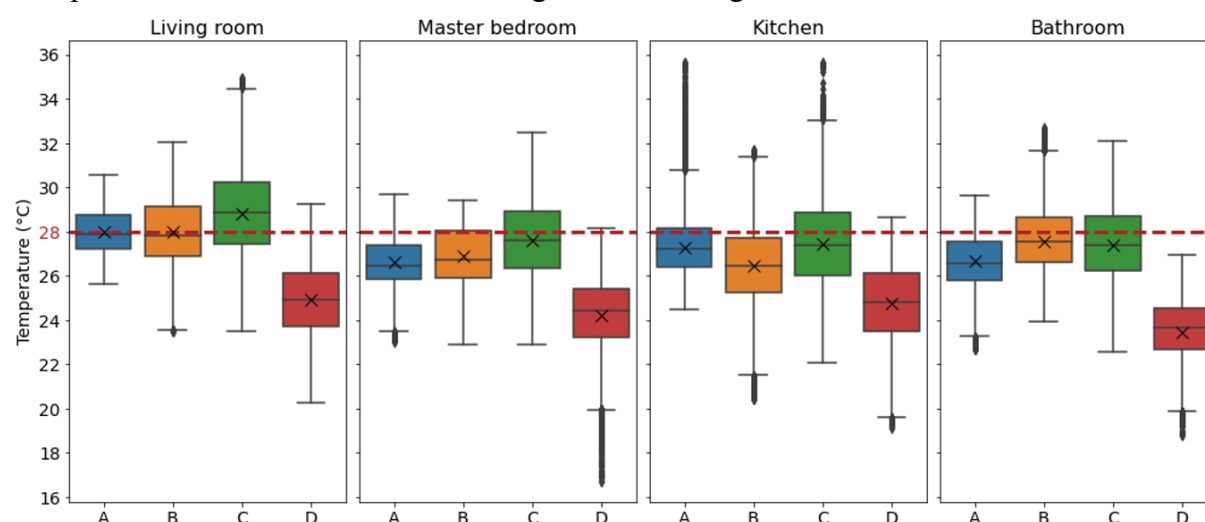


Figure 2. Comparison of T_{int} by room in the four dwellings using boxplot diagrams with means displayed

Dwelling D is a single-family house where the occupants are particularly active in keeping the temperature low, as we will see later. It is also the only dwelling where CO_2 level exceeds 1133 ppm half of the time at night in the main bedroom. Indeed, two occupants sleep in this room

¹ *Santé Publique France* is the national public health agency in France.

with the door and window closed, unlike the other dwellings where the master bedroom is occupied by one person. Figure 3 is a violin plot showing the distributions of CO₂ measurements with coloured density curves, and quartiles and medians as dotted lines.

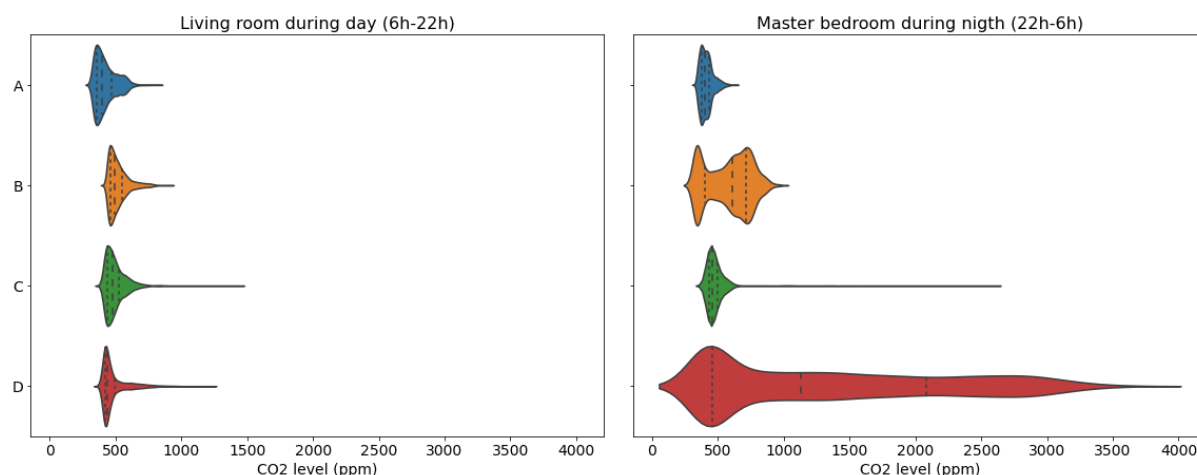


Figure 3. Distribution of CO₂ levels in the different dwellings using violin diagrams with quartiles displayed

In all monitored rooms of all dwellings, RH remains between 30 and 70% most of the time, and is outside this range less than 9% of the time. Dwelling C is the warmest and the most polluted, since it is the only one where the maximum daily average PM_{2.5} concentration exceeds the exposure limit set to 25 µg/m³ (Cony et al., 2017) in both monitored rooms. It is also the dwelling with the highest daily average concentration of light VOCs, up to 771 ppb in the living room and 308 ppb in the main bedroom.

3.2 Occupant behaviour

Household B is the only one with an air conditioner (AC). It also has two fans: one in the living room or bedroom 2 depending on the presence of the occupants, and one in the kitchen or master bedroom in the same way. Figure 4 shows the temporal evolution of the indoor air temperature and the CO₂ level in the living room during the third HW, highlighting the opening of the windows and the operation of AC and fan.

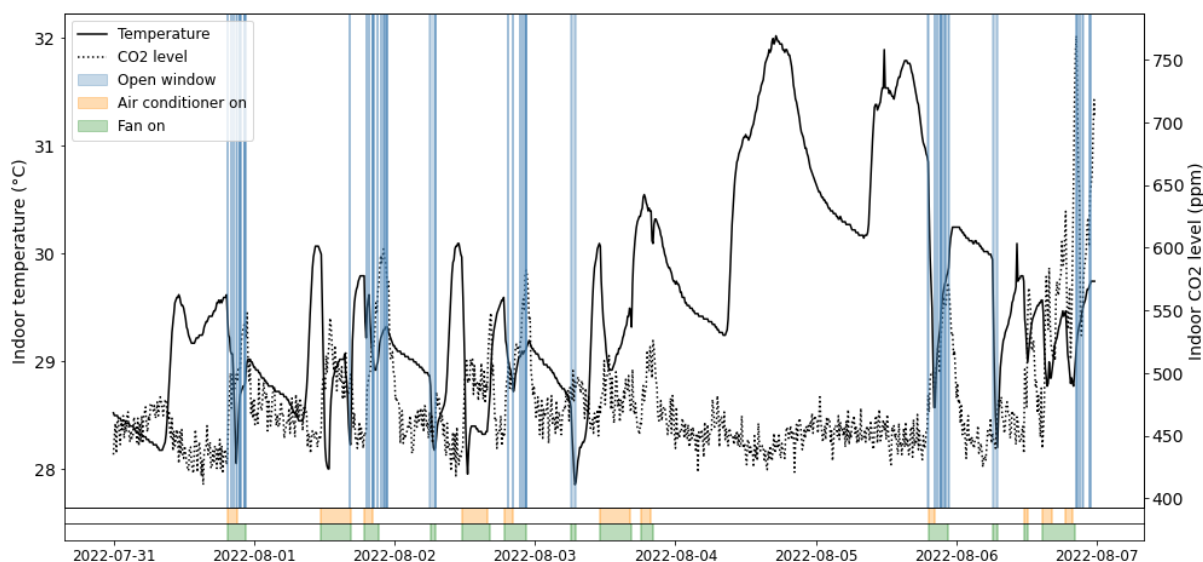


Figure 4. Evolution of the indoor environment with adaptation actions in the living room B during the 3rd HW

The window is opened mostly in the evening with some openings in the morning. The openings are short and frequent in the evening. This is a French window, so the openings can be a

response to heat, a habit or simply a means of accessing the balcony. From the evening of Wednesday 3 August, the occupants leave the house for two days, and T_{int} rises sharply.

During morning openings, fan is turned on but not AC. Fan and AC are turned on in the afternoon and evening when temperatures are hottest and occupants are present. During the night, AC is turned off and fan moved to the bedroom, to be turned on during sleep. When the fan is on, the window is closed 92.59% of the time in the living room. When AC is on, the living room window is closed 98.67% of the time.

According to the interview, the occupants of dwelling B open the windows for aeration and out of habit. They close the shutters against glare and heat. They feel restricted in their adaptive actions by external noise. The thermal environment is considered very hot and unacceptable in all main rooms in summer, with unbearable discomfort in the master bedroom during heatwaves. They sometimes leave the house for the day when the discomfort becomes unbearable. They feel powerless against the heat during heatwaves.

Occupants of dwelling D are the only one to have completed the logbook, which gives us detailed information on the use of solar protections. They also have a fan in the living room. Figure 5 plots the temporal evolution of the indoor temperature and the CO₂ rate in the living room during the second heatwave, by highlighting the opening of the windows and shutters, and the fan operation.

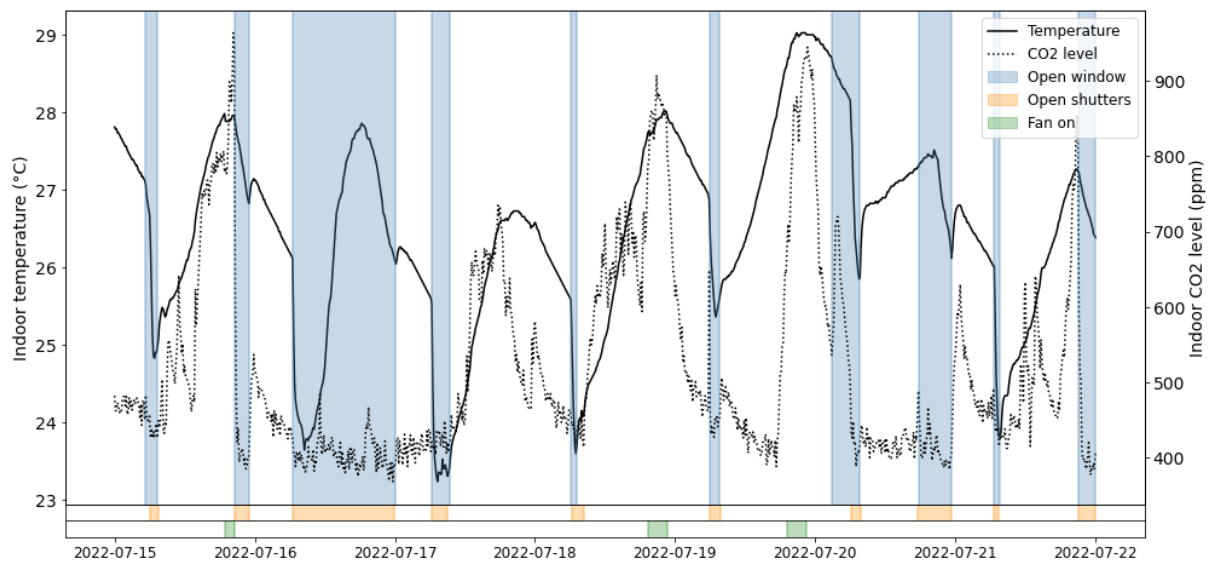


Figure 5. Evolution of the indoor environment with adaptation actions in the living room D during the 2nd HW

It can be observed that during this week, in all the rooms, the window is opened at the same time as the shutters. The window is always opened in the morning, which is the case during nearly the whole summer and for all the windows in the house. The opening durations are longer than in dwelling B. The fan is turned on in the evening. Compared to dwelling B, the occupants use the fan much less and it remains switched off 95.69% of the time. When the fan is on, the living room window is closed 64.58% of the time.

The interview revealed that the two occupants of dwelling D open the windows for aeration and close the shutters out of habit, for safety, and against glare and heat. The thermal environment is considered acceptable in all main rooms in summer, but unacceptable during heatwaves: very hot in the living room/kitchen and hot in the bedrooms and office. They mainly use windows and shutters to keep indoor temperatures low as shown in Figure 5. Fear of intrusion can limit their adaptive opportunities, because they live in a single-storey house. They feel that these adaptive actions are useful in summer, but that their effectiveness is limited during heatwaves, especially at night.

In order not to overload the article, we do not draw the same graphs for the other two dwellings but simply analyse the surveys. Dwelling A is a through apartment with two opposite orientations. It is located on the second floor. The occupant opens the windows for aeration and out of habit, and close the shutters against glare and heat. Her adaptive actions are restricted by the feeling of insecurity and the fear of intrusion. Thermal environment is perceived very hot throughout the summer in all the main rooms, hot during the night and extremely hot during the day during heatwave. Numerous adaptation actions are implemented: over-ventilation at night, solar protection lowered during the day, a fan in the living room, light clothing, cold drinks, a water spray and a shower in the evening.

Dwelling C is located on the sixth and top floor and has windows on three different orientations. The occupant opens the windows to ventilate, as a matter of habit, to get rid of odours and humidity, and against the heat. She cannot open them sometimes because of draughts, dust, and noise from outside. She closes the shutters against glare and heat, and opens them to access daylight and let in the sun's rays. When the heat becomes unacceptable, she can leave the dwelling for about a week. She does not have a fan or an air conditioner for economic reasons. During heatwaves, thermal environment is experienced in all the main rooms as slightly hot and acceptable during night, and extremely hot and unbearable during day. Indoor air quality is sometimes felt to be unacceptable during heatwaves.

3.3 Feature selection

For each room of each dwelling, Figure 6 shows the identified influencing variables with a green tick, according to *VSURF* library. On the right side of the figure, the percentage of rooms where the model finds these drivers is displayed. Some environmental variables are not measured in all rooms.

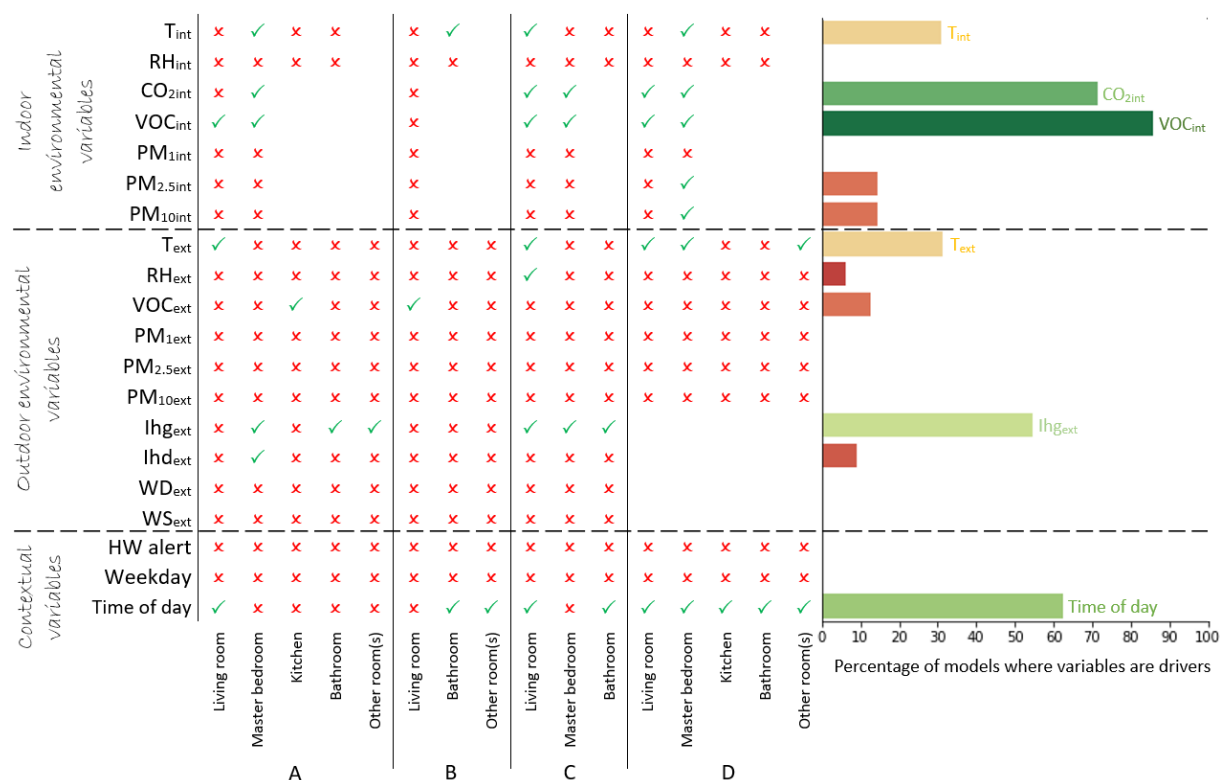


Figure 6. Variables influencing window use

Indoor and outdoor humidity, indoor and outdoor fine particle concentrations, outdoor VOC level, diffuse solar radiation, wind speed and direction, heatwave context and day of week have very little or no influence on window use. These variables are indeed identified as drivers for

maximum 1 room in all dwellings, except for the VOC_{out} which concerns 2 rooms out of all. We therefore find five variables that influence the opening of windows: VOC_{int} , $CO2_{int}$, Time of day, $I_{hg_{ext}}$, T_{int} and T_{ext} .

3.4 Discussions

In terms of environmental variables, our results show that indoor and outdoor temperatures, indoor CO_2 and light VOC concentrations, and global horizontal irradiation influence window use. These results are similar to the studies in Table 1. Solar radiation can be a driver or not depending on the article. However, we find that indoor and outdoor humidity, indoor and outdoor fine particle concentration, and wind speed and direction have no influence on window use. RH_{int} and $PM_{2.5, ext}$ were always found to be influential in Table 1 even though the second variable only concerns two studies. RH_{out} , WS and WD are controversial among the studies. It should be noted that in our case, WS and WD are not measured on site but at a nearby meteorological station. Draughts could have an impact.

To our knowledge, there are no residential studies that address the influence of indoor VOC concentration on window use. Fabi et al. (Fabi et al., 2014) address the issue for offices and find a small influence compared to other environmental factors. In our case, this factor is one of the most important, influencing window use in all living rooms and main bedrooms, the only rooms where it is measured, except in dwelling B. VOC_{int} may be one of the best indicators of perceived indoor air quality, as some of these pollutants have odours and may be associated with mucosal irritation (Fabi et al., 2014). However, the health impact depends very much on the VOC(s) considered, as this family includes many pollutants.

In terms of contextual variables, we only studied the HW alert, the day of week and the time of day. Only the last contextual variable is identified as a driver. These results are similar to those listed in Table 1 for time of day and day of week. Time of day variable represents the occupants' habits. We wanted to study the influence of HW on the use of windows, to see if the French government's message would have an impact. It does not seem to be important, and it is better to take into account directly the outside temperature.

4 CONCLUSIONS

Through a field measurement campaign in four French dwellings during the summer of 2022, this study seeks to identify the physical and contextual variables influencing window use, after looking at the indoor environment variations. Even if the indoor temperature distributions are different, surveys indicate that in all dwellings in Lyon, the thermal environment is perceived to be extremely hot during heatwave days. The house in Clermont-Ferrand is more thermally comfortable in the summer but the thermal environment is still considered unacceptable during heatwaves, especially at night.

Among the adaptive actions taken during heatwaves, all households reduce their calorific activities, open windows when the outside temperature drops and close solar protections during the hottest hours of the day. Some may also over-ventilate during night, use fans or air conditioners, leave or confine themselves to their homes, avoid some rooms, reduce their activity levels or adjust their clothing.

Using data analysis, we find that indoor and outdoor temperatures, indoor CO_2 and light VOC concentrations, global horizontal irradiation and time of day influence window use. Having identified the window use drivers using a feature selection method, we will be able to apply machine learning algorithms to model occupant behaviour. Future work will focus on assessing the indoor environment through indicators, and developing and evaluating behaviour models.

5 ACKNOWLEDGEMENTS

The authors would like to thank the Cerema colleagues who helped with the instrumentation. Data was collected as part of the CREATIV project funded by ADEME under agreement number 2062C0002. Data analysis was carried out as part of a PhD funded by the French Ministry of Ecological Transition.

6 REFERENCES

- Barthelmes, V. M., Heo, Y., Fabi, V., & Corgnati, S. P. (2017). Exploration of the Bayesian Network framework for modelling window control behaviour. *Building and Environment*, *126*, 318-330. <https://doi.org/10.1016/j.buildenv.2017.10.011>
- Brownlee, J. (2020). *Data Preparation for Machine Learning : Data Cleaning, Feature Selection, and Data Transforms in Python*. Machine Learning Mastery.
- Cali, D., Andersen, R. K., Müller, D., & Olesen, B. W. (2016). Analysis of occupants' behavior related to the use of windows in German households. *Building and Environment*, *103*, 54-69. <https://doi.org/10.1016/j.buildenv.2016.03.024>
- Carlucci, S., De Simone, M., Firth, S. K., Kjærgaard, M. B., Markovic, R., Rahaman, M. S., Annaqeeb, M. K., Biandrate, S., Das, A., Dziedzic, J. W., Fajilla, G., Favero, M., Ferrando, M., Hahn, J., Han, M., Peng, Y., Salim, F., Schlüter, A., & van Treeck, C. (2020). Modeling occupant behavior in buildings. *Building and Environment*, *174*, 106768. <https://doi.org/10.1016/j.buildenv.2020.106768>
- Cho, H., Cabrera, D., Sardy, S., Kilchherr, R., Yilmaz, S., & Patel, M. K. (2021). Evaluation of performance of energy efficient hybrid ventilation system and analysis of occupants' behavior to control windows. *Building and Environment*, *188*, 107434. <https://doi.org/10.1016/j.buildenv.2020.107434>
- Cony, L., Abadie, M., Wargocki, P., & Rode, C. (2017). Towards the definition of indicators for assessment of indoor air quality and energy performance in low-energy residential buildings. *Energy and Buildings*, *152*, 492-502. <https://doi.org/10.1016/j.enbuild.2017.07.054>
- Diaz-Uriarte, R. (2007). GeneSrf and varSelRF : A web-based tool and R package for gene selection and classification using random forest. *BMC Bioinformatics*, *8*(1), 328. <https://doi.org/10.1186/1471-2105-8-328>
- ENTPE. (s. d.). *Serveur de la station IDMP de l'ENTPE*. Accessed on 10 October 2022, at <http://idmp.entpe.fr/>
- Fabi, V., Andersen, R. V., Corgnati, S., & Olesen, B. W. (2012). Occupants' window opening behaviour : A literature review of factors influencing occupant behaviour and models. *Building and Environment*, *58*, 188-198. <https://doi.org/10.1016/j.buildenv.2012.07.009>
- Fabi, V., Maggiora, V., Corgnati, S., & Andersen, R. (2014, avril 10). Occupants' behaviour in office building : Stochastic models for window opening. *Counting the Cost of Comfort in a Changing World*. 8th Windsor Conference.
- Genuer, R., Poggi, J.-M., & Tuleau-Malot, C. (2015). VSURF : An R Package for Variable Selection Using Random Forests. *The R Journal*, *7*(2), 19.
- Jones, R. V., Fuentes, A., Gregori, E., & Giretti, A. (2017). Stochastic behavioural models of occupants' main bedroom window operation for UK residential buildings. *Building and Environment*, *118*, 144-158. <https://doi.org/10.1016/j.buildenv.2017.03.033>
- Kursa, M. B., & Rudnicki, W. R. (2010). Feature Selection with the Boruta Package. *Journal of Statistical Software*, *36*, 1-13. <https://doi.org/10.18637/jss.v036.i11>
- Marchand, D., Bonnefoy, B., Durand, F., Zhou, B., Heimer, A., & Robert, J. (2018). *Etude des représentations sociales de la qualité de l'air intérieur et évolution des comportements* (Projet NUDG' AIR, p. 62). ADEME.
- Rijal, H. B., Humphreys, M. A., & Nicol, J. F. (2018). Development of a window opening algorithm based on adaptive thermal comfort to predict occupant behavior in Japanese dwellings. *JAPAN ARCHITECTURAL REVIEW*, *1*(3), 310-321. <https://doi.org/10.1002/2475-8876.12043>
- Santé Publique France. (s. d.). *Fortes chaleurs, canicule*. Accessed on 21 October 2022, at <https://www.santepubliquefrance.fr/determinants-de-sante/climat/fortes-chaleurs-canicule>
- Shi, S., Li, H., Ding, X., & Gao, X. (2020). Effects of household features on residential window opening behaviors : A multilevel logistic regression study. *Building and Environment*, *170*, 106610. <https://doi.org/10.1016/j.buildenv.2019.106610>
- Speiser, J. L., Miller, M. E., Tooze, J., & Ip, E. (2019). A comparison of random forest variable selection methods for classification prediction modeling. *Expert Systems with Applications*, *134*, 93-101. <https://doi.org/10.1016/j.eswa.2019.05.028>
- Yao, M., & Zhao, B. (2017). Window opening behavior of occupants in residential buildings in Beijing. *Building and Environment*, *124*, 441-449. <https://doi.org/10.1016/j.buildenv.2017.08.035>

Importance of thermal stack effect in ventilative cooling concepts for residential buildings

Diederik Verscheure^{*1}, Koen Maertens¹, Axel Deturck¹

*1 Vero Duco NV
Handelsstraat 19
8630 Veurne, Belgium*

** Corresponding author: <firstname>.<lastname>@duco.eu*

ABSTRACT

This paper investigates the impact of ventilative cooling in residential buildings constructed from light-weight cross-laminated timber. Different temperature-controlled ventilative cooling concepts such as single sided ventilation, cross-ventilation and thermal stack based chimney ventilation concepts are simulated and compared in terms of impact on indoor temperature and robustness to external conditions such as the surroundings and the building orientation. Chimney ventilative cooling which makes use of the thermal stack effect has the largest impact on indoor temperature and is least affected by the external conditions.

KEYWORDS

Ventilative cooling, single-sided ventilation, cross-ventilation, chimney ventilation, thermal comfort, thermal stack, cross-laminated timber

1 INTRODUCTION

This paper investigates the impact of ventilative cooling in residential buildings constructed from light-weight cross-laminated timber and evaluates the robustness of different concepts with respect to environmental conditions such as the building orientation and the surrounding environment. Light-weight timber-based construction of residential buildings has received growing attention, and is increasingly implemented in order to realize serial prefabricated homes that can be installed on-site in a matter of days and to reduce the environmental footprint by use of sustainable materials. At the same time, these prefab construction styles also present new design challenges and questions on which heating, cooling and ventilation systems that should be used in order to realize low energy consumption and good thermal comfort, while also matching well with the serial production process. Ventilative cooling is an energy-efficient approach to cool buildings by utilizing natural airflow to regulate indoor temperatures. By harnessing cool outside air during favourable conditions, ventilative cooling reduces the need for active cooling, leading to cost savings and a smaller environmental footprint. Ventilative cooling solutions can be easily integrated in prefab walls and are considered an interesting concept for serial residential building production.

2 SIMULATION SETUP

2.1 Simulation environment

The simulations in this paper are carried out using Matlab/Simulink in a co-simulation setup where the building dynamics are modeled in the Modelica IDEAS library (Jorissen, et al., 2018) and the installation and control algorithms are implemented in Matlab/Simulink.

2.2 Inhabitant behaviour

Inhabitant profiles are generated using the StROBe model (Baetens & Saelens, Modelling uncertainty in district energy simulations by stochastic residential occupant behaviour, 2016;

Baetens, On externalities of heat pump-based low-energy dwellings at the low-voltage distribution grid, 2015; Baetens, StROBe, sd) which includes room occupancy, CO2, humidity and heat generation by occupants. Window opening behaviour is taken into account using an extension of this model (Verbruggen, Delghust, Laverge, & Janssens, 2021; Verbruggen, Window Use Habits as an Example of Habitual Occupant Behaviour in Residential Buildings, 2021; Verbruggen, EROB, sd). In this paper, only one inhabitant profile consisting of 2 full-time working adults with a school-going child is generated and used in the simulations.

2.3 Building geometry and properties

The building geometry considered is based on a terraced house used in the Dutch standards for ventilation calculations (VLA, TNO, Peutz BV, & Nieman Raadgevende Ingenieurs BV, 2018; ISSO 92, 2009). The 3 floors plan is shown in Figure 1 and the front and back view is shown in Figure 2. In this study, the building walls are modelled as layers of light-weight cross-laminated timber panels on the inside and outside with insulation material in between.

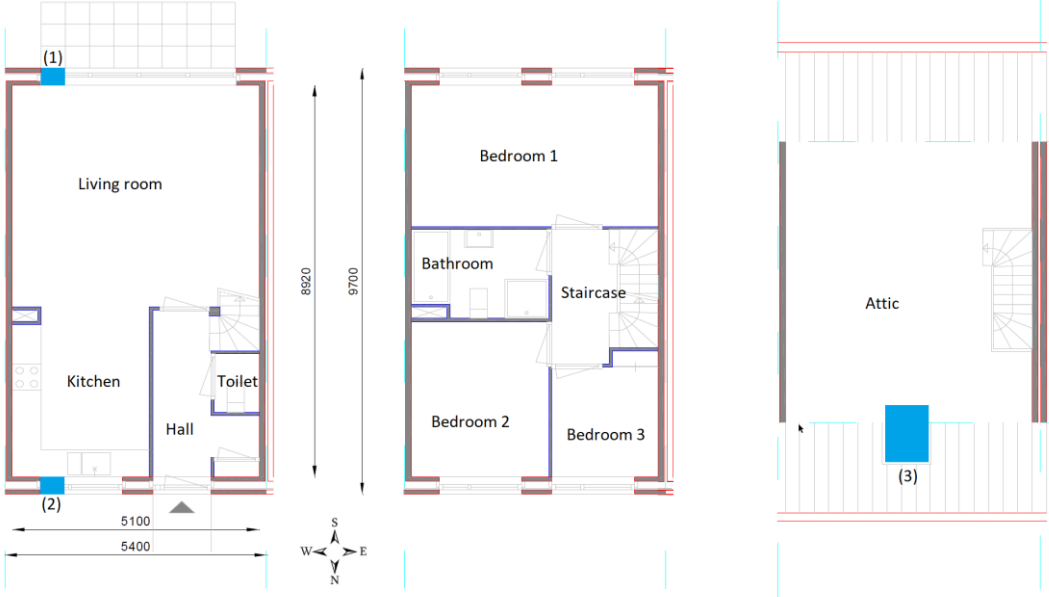


Figure 1: Terraced house floor plan

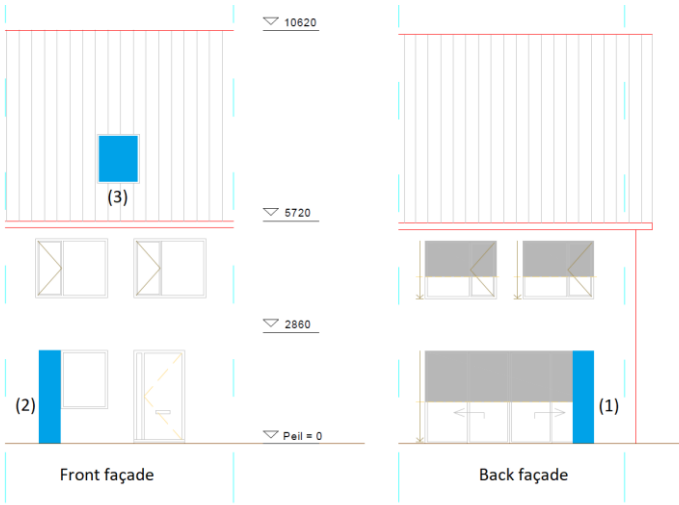


Figure 2: Terraced house front and back view

2.4 Environmental conditions

The climate data used in the simulations is based on data measured in Uccle, Belgium between 2000 and 2009, that is combined into a single climate file with some extremes including a hot summer to test the effect of challenging weather conditions. To evaluate the robustness of the ventilative cooling, the building is simulated in four different orientations and both in a suburban and urban environment. The effect of the surrounding environment on the wind speed is taken into account using a power-law correction (ASHRAE Handbook - Fundamentals, 1993). In the default orientation as shown in Figure 1, the front façade is facing north and the living room with the largest window is facing south.

2.5 Ventilative cooling concepts

The effect of three ventilative cooling automatic temperature-controlled concepts is investigated:

- Concept 1: Single-sided ventilation, where only one ventilative cooling component (1) of dimensions 2 m x 0.5 m with discharge coefficient of 0.2 in the living room is used (see (1) in Figure 1 and Figure 2). As this component is used on the ground floor, it is also burglary and insect-proof (Duco Louvres and grilles, sd).
- Concept 2: Cross-ventilation, where two ventilative cooling components (1) and (2) similar as above in the living room and kitchen are used (see (1)-(2) in Figure 1 and Figure 2).
- Concept 3: Chimney ventilation, where ventilative cooling component (1) similarly as above is located in the living room and a roof window (3) located in the attic (1.4 m x 1 m) are used and whereby an open staircase is assumed (see (1)-(3) in Figure 1 and Figure 2).

As a reference situation, manual ventilation by window opening of inhabitants is also simulated. It is important to remark that the results in this reference situation may depend heavily on the chosen inhabitant profile. This paper focusses mainly on the mutual comparison of the automatically controlled ventilative cooling, which is not directly affected by the absence or behaviour of inhabitants. In the simulations, it is assumed that the presence of the automatic ventilative cooling does not affect the window opening behavior of the inhabitants.

For the control of the ventilative cooling, a setpoint of 22 °C with a hysteresis of ± 2 °C is used and the ventilative cooling components are only opened when there is a cooling demand (above $22+2$ °C) and when there is cooling potential, namely when the outside temperature is lower than the inside temperature. Conversely, the ventilative cooling is closed when there is no more cooling demand (below $22-2$ °C) or when the outside temperature is higher than the inside temperature. Since the purpose of ventilative cooling is actually to reduce the temperature of the building mass and not just the air temperature, an estimate of the wall surface temperature of the building is used as the inside temperature.

3 SIMULATION RESULTS

In total 32 simulations are carried out ranging from May to September with four different building orientations, for a suburban and urban surrounding, and with manual window opening as the reference situation and as well as with the three temperature-controlled ventilative cooling concepts.

3.1 Impact of ventilative cooling on indoor temperatures

Figure 3 shows the influence of the ventilative cooling during a hot July week for a suburban environment with outside temperatures reaching 36 °C. With only window ventilation by inhabitants, the operative temperature in the living room is reaching 33 °C during the hottest day. With temperature-controlled ventilative cooling, the operative temperature is considerably

reduced to 30.4 °C with single-sided ventilation, 29.3 °C with cross-ventilation and 28.5 °C with chimney-ventilation. With cross-ventilation and chimney ventilation, temperatures at night go down with the outside temperature and the heat built up during the hottest day on July 20 is also evacuated more quickly during the following days. In bedroom 1, the operative temperatures with window ventilation, single-sided and cross-ventilation are quite similar, whereas only chimney ventilation is able to remove heat from the bedroom. However, even with chimney ventilation, the temperature in bedroom 1 is quite high and going up to 32.4 °C on the hottest day. An explanation for this is that the window opening in the inhabitant profile from the StROBe/EROB models is not dependent on the climate data and the temperatures in the building. In reality, inhabitants will also open their windows during hot summer nights which will enhance the ventilative cooling considerably.

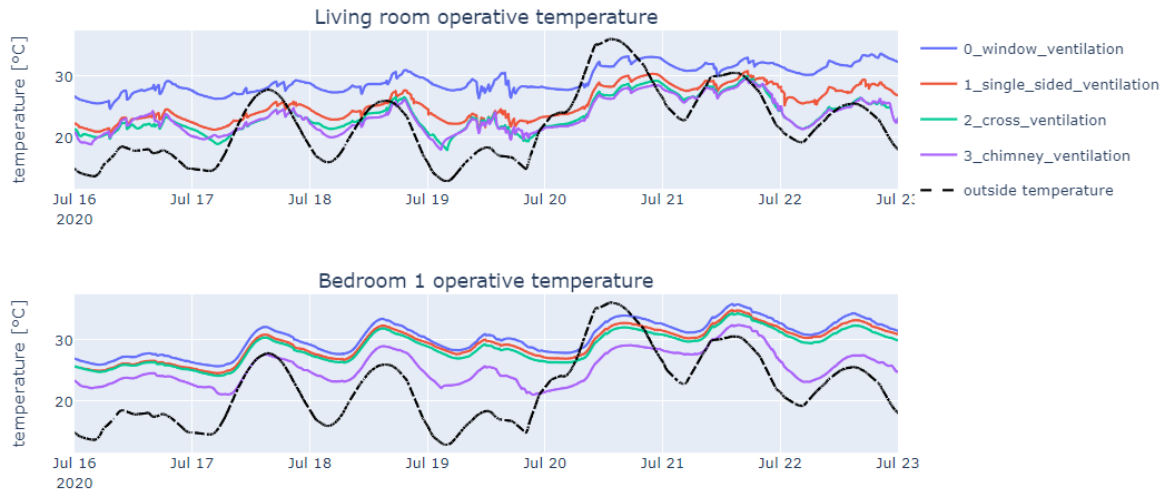


Figure 3: Living room and bedroom 1 operative temperature during a hot summer week

In Figure 4, the position of the ventilative cooling components during the hot July week is shown. Firstly, it can be seen that the ventilative cooling systems are open when the outside temperature is lower than the inside temperature and when the inside temperature is higher than 22 ± 2 °C. Secondly, the chimney ventilation is closing quicker than the other concepts when the outside temperature is rising above the inside temperature, because it is slightly better in evacuating the heat during the hot summer days.

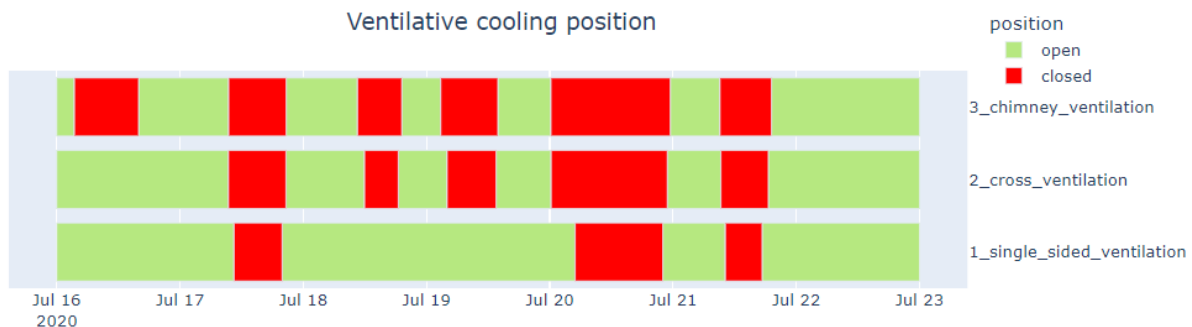


Figure 4: Ventilative cooling position for the different concepts during a hot summer week

3.2 Robustness of the ventilative cooling to external conditions

Figure 5 shows box plots of the daily average operating temperature in the living room for the different ventilative cooling concepts, aggregated from May until September over the different orientations with suburban surroundings on the left and urban surroundings on the right. Compared to manual window opening, which depends on the presence and behaviour of inhabitants, the temperature-controlled ventilative cooling concepts allow to keep the temperature in the living room under control most of the times. Single-sided ventilative cooling

performs worse than the other two concepts, whereas chimney ventilation performs best and is able to keep the temperature well around the setpoint of 22 ± 2 °C. In an urban environment, where wind speeds are reduced compared to unshielded or suburban surroundings, the cross-ventilation concept performs slightly worse than the thermal stack driven chimney ventilation.

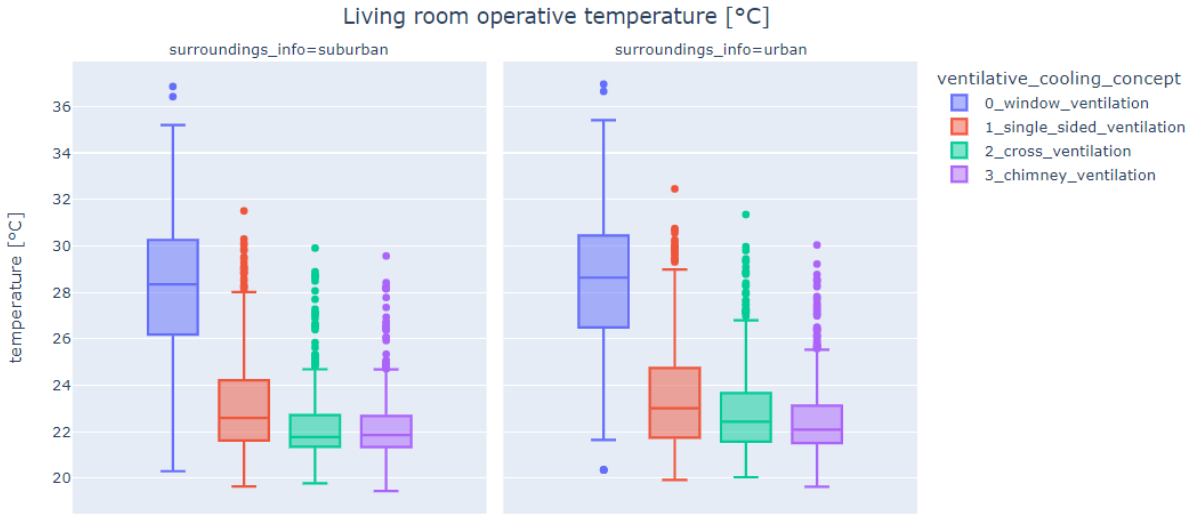


Figure 5: Box plots of the daily average living room operating temperature for suburban and urban surroundings

Figure 6 shows box plots of the daily average operating temperature in the living room for the different ventilative cooling concepts in urban surroundings, aggregated from May until September for the different building orientations from left to right. The orientation refers to the direction of the front façade, whereby 0° means that the front façade is facing north (as in Figure 1), 90° facing east, 180° facing south and 270° facing west. The single-sided and cross-ventilation concepts result in operative temperatures that depend on the orientation, with 270° being the worst case, whereas the chimney ventilation concept exhibits more constant temperatures, because the thermal stack effect is acting more consistently and independent of the orientation and the surroundings.

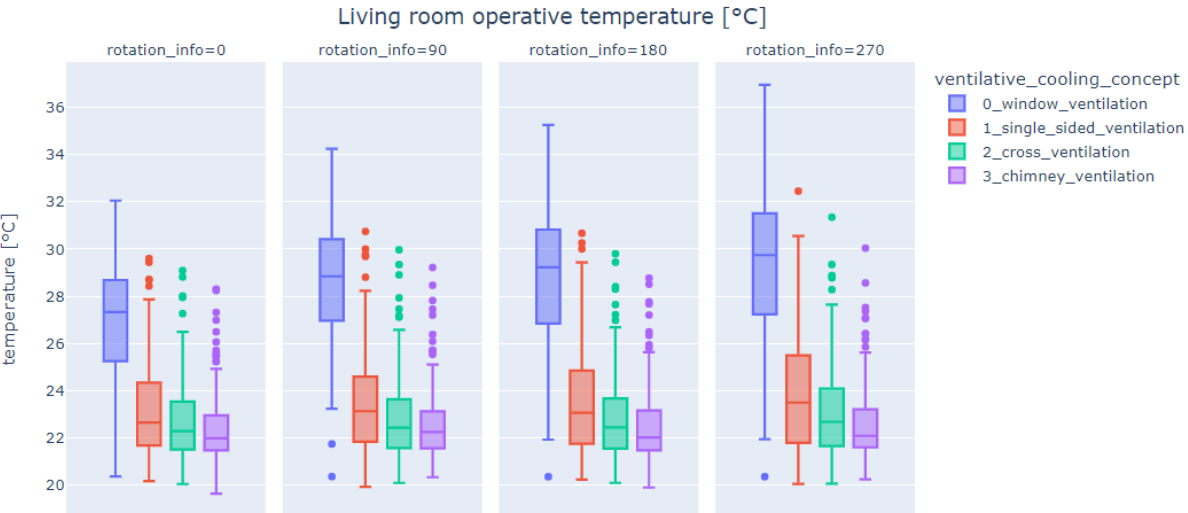


Figure 6: Box plots of the daily average living room operating temperature for urban surroundings and four different orientations

Figure 7 summarize the influence of the ventilative cooling concept, the environment and the orientation on the daily average operative temperature in the living room and bedroom 1. For

clarity we focus here on the mutual differences between the three ventilative cooling concepts and therefore the manual window ventilation is omitted from the comparison.

From Figure 7 it is clear that the single-sided ventilation concept with an orientation of 270° in an urban environment has the highest average temperature of around 23.9 °C (top) and the chimney ventilation concept with an orientation of 0° in a suburban environment has the lowest average temperature around 22.2 °C (bottom). It can also be seen that for the cross-ventilation concept in urban surroundings, the 270° orientation (bottom left) results in the highest temperature of the 4 orientations.

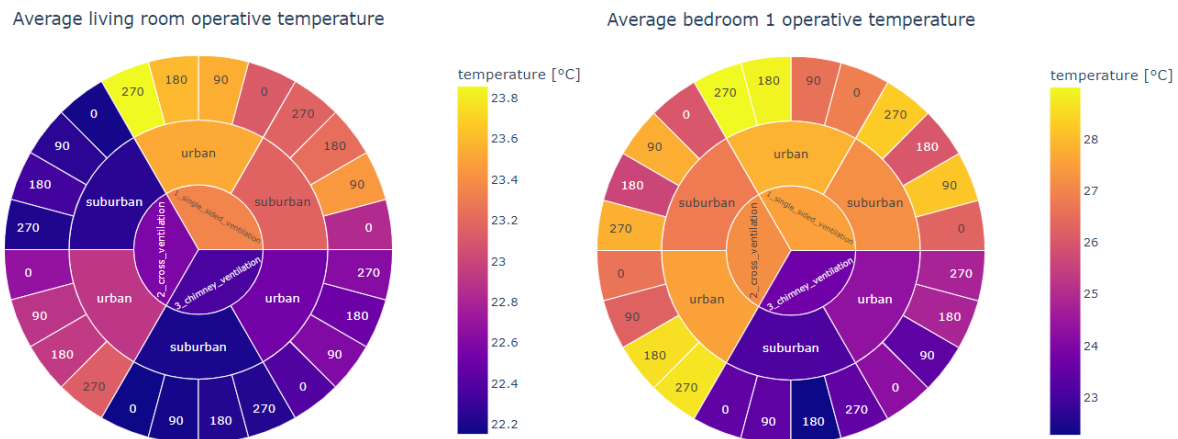


Figure 7: Sunburst plot of the influence of the ventilative cooling concept, the surroundings the orientation on the daily average temperature in the living room and bedroom 1

There are in fact two reasons that explain these results. Firstly, with the orientation of 270°, the living room with the largest window is oriented eastwards and is heating up by high solar gains from the morning until noon. This built-up heat can only be removed when the outside temperature starts to decrease towards the evening. Secondly, in the climate data, the wind is coming predominantly from the south, such that the cross-ventilation and single-sided ventilation concepts can benefit less from wind-driven ventilation when the wind is perpendicular to the ventilative cooling components. The chimney ventilation on the other hand is less impacted by the higher solar gains in the 270° orientation, as the driving thermal stack effect becomes also stronger when the temperature difference between inside and outside increases.

For bedroom 1, the highest average temperature of 28.9 °C also occurs for the single-sided ventilation with a 270° orientation in an urban environment, whereas the lowest temperature of 22.3 °C occurs for the chimney ventilation concept with a 180° orientation in suburban surroundings. The chimney ventilation is the only concept here that contributes significantly to reduction in bedroom temperatures.

4 DISCUSSION AND CONCLUSIONS

This paper investigates the impact of three ventilative cooling concepts in residential building constructed from light-weight cross-laminated timber on indoor temperatures and evaluates the robustness to external conditions such as the surroundings and the orientation of the building. The ventilative cooling concepts consist of temperature-controlled single-sided, cross-ventilation and thermal stack based chimney ventilation. Compared to manual window opening, automatically controlled ventilative cooling concepts do not require inhabitants to be present and allow to significantly reduce living room temperatures throughout the months of May to September thus avoiding the need for active cooling. The thermal stack based chimney ventilation concept is the only concept that also reduces bedroom temperatures significantly

and appears most robust to the external conditions such as the surroundings and the building orientation. From a cost and installation perspective, the chimney concept is also an interesting option, as it requires only one ventilative cooling component to be used in the living room in combination with a roof window that is often already present, but only needs to be automated. Further work will investigate the effect of thermal stack based chimney ventilation in pilot residential buildings.

5 ACKNOWLEDGEMENTS

The work in this paper was carried out as part of R&D project HBC.2019.2399 that was generously funded by VLAIO (Vlaams Agentschap Innoveren & Ondernemen).

6 REFERENCES

- (1993). *ASHRAE Handbook - Fundamentals*. American Society of Heating Refrigerating and Air-Conditioning Engineers.
- Baetens, R. (2015). *On externalities of heat pump-based low-energy dwellings at the low-voltage distribution grid*. KULeuven, Faculty of Engineering Science,, Leuven.
- Baetens, R. (sd). *StROBe*. Opgehaald van <https://github.com/open-ideas/StROBe>
- Baetens, R., & Saelens, D. (2016). Modelling uncertainty in district energy simulations by stochastic residential occupant behaviour. *Journal of Building Performance Simulation*, 9(4), pp. 431-447.
- Duco Louvres and grilles*. (sd). Opgehaald van <https://www.duco.eu/uk/products/intensive-ventilation/wall-and-window-louvres>
- Fanger, O. (1970). Thermal Comfort.
- ISSO 92. (2009). *Ventilatiesystemen met decentrale toevoer en centrale afvoer in woningen en woongebouwen*.
- Jorissen, F., Reynders, G., Baetens, R., Picard, D., Saelens, D., & Helsens, L. (2018). Implementation and Verification of the IDEAS Building Energy Simulation Library. *Journal of Building Performance Simulation*, 11(6), pp. 669-688.
- Verbruggen, S. (2021). *Window Use Habits as an Example of Habitual Occupant Behaviour in Residential Buildings*. Universiteit Gent, Departement Architectuurontwerp en bouwtechniek.
- Verbruggen, S. (sd). *EROB*. Opgehaald van <https://github.com/siverbru/EROB>
- Verbruggen, S., Delghust, M., Laverge, J., & Janssens, A. (2021). Evaluation of the relationship between window use and physical environmental variables:. *Journal of Building Performance Simulation*, 366-382.
- VLA, TNO, Peutz BV, & Nieman Raadgevende Ingenieurs BV. (2018). *VLA methodiek gelijkwaardigheid voor energiebesparende ventilatieoplossingen in woningen*.

Performance 2 project - Winter IAQ campaigns in 13 dwellings equipped with Humidity-based DCV systems: analysis of the ventilation performance after 15 years of use

Adeline Mélois^{1,2*}, Ambre Marchand Moury³, Marc Legree⁴, Juan Rios⁴, Jérémy Depoorter⁵, Nicolas Dufour⁵, Sylvain Rebières³, Gaëlle Guyot^{1,2}

¹ Cerema BPE research team, 46 rue St Théobald, F-38080, L'Isle d'Abeau, France

² Univ. Grenoble-Alpes, Univ. Savoie Mont Blanc, CNRS, LOCIE, 73 000 Chambéry, France

*Corresponding author: adeline.melois@cerema.fr

³ Cerema Centre Est – Agence d'Autun – Groupe Bâtiments, Boulevard Bernard Giberstein, 71400 Autun, France

⁴ AERECO SA, Z.I de Lamirault, 62 Rue de Lamirault, 77090 Collégien, France

⁵ ANJOS VENTILATION, Lot. Roche Blanche, 01230 Torcieu, France

SUMMARY

The Performance 2 project (2020-2024) is a French national research project that aims to evaluate the durability of Humidity-based Demand Controlled Ventilation (DCV) systems installed in two multi-family social housing buildings (Paris and Villeurbanne) over than 10 years ago. This evaluation includes the analysis of continuous measurements performed on the ventilation system (sensors located close to the air terminal devices) and two additional Indoor Air Quality (IAQ) campaigns including two other monitors placed in the “dry” rooms conducted in 13 dwellings. IAQ parameters such as CO₂, Relative Humidity (RH), Particulate Matters (PM), and Volatile Organic Compounds (VOC), as well as energy losses and consumption, are being analysed and compared to tenant usages to assess the performance of the ventilation systems. Finally, the results of the on-site campaigns will focus on three main factors:

- the performance of the ventilation systems by comparing, for different regulatory indicators regarding RH and CO₂, the values obtained 15 years ago during on-site campaigns (at commissioning), the values from the Performance 2 project (15 years later), and the results of a numerical approach based on nodal simulations;
- the IAQ, particularly with respect to PM and VOC, assessment based on the values obtained in the dwellings, considering the occupants' behaviour and the location of the sensors (15 years later);
- the energy consumption attributed to ventilation, by comparing the losses due to air renewal calculated 15 years ago and calculated in Performance 2 project.

KEYWORDS

Smart ventilation, residential ventilation, IAQ, energy efficiency, durability, humidity

1 INTRODUCTION AND OBJECTIVES

Relative humidity-controlled mechanical extract ventilation (RH-MEV) systems have been widely used in France for 40 years (Mélois et al., 2023). Most of the new residential buildings

complying with RT 2012 and now RE 2020 energy performance regulations, are equipped with such systems (Mélois et al., 2019) and currently they are considered as a reference system. In 2019, the “Performance 2” project was launched in three phases to (1) conduct a full winter analysis of the system after 13 years of in-situ operation using the installed sensors (non-recalibrated) and without major intervention, (2) collect the air terminal devices (inlet and exhaust units) and sensors for laboratory testing before and after cleaning and maintenance and finally, (3) reinstall the cleaned and maintained ventilation units (where the hygroscopic component remains intact) with new calibrated sensors. The phase (1) has been described in (Guyot et al., 2022) and phase (2) in (Mélois et al., 2023). This paper presents the methodology and the first results of the data analysis of the measurements collected over 2 years after these phases. The objectives of this study are as follows:

- To evaluate the durability of the RH-MEV systems in two buildings after 15 years, by comparing the current of the energy performance and IAQ (RH and CO₂ only) with the results obtained at the commissioning, as well as the theoretical performances evaluated 15 years ago;
- To assess the performance of the RH-MEV systems regarding other pollutants, including VOC, Formaldehyde, and PM, and regarding CO₂ and RH, using new analyses;
- To investigate the factors influencing “good” or “bad” performances through analyses of the evolution of ventilation systems conditions, changes in ventilation requirements (occupancy, pollutant emissions), and the impact of the occupants’ behaviour (components sealing, use of manual control, cleaning, ...).

2 METHODS

2.1 Case studies, on-site campaigns and previous diagnosis

The two social housing buildings studied are as follows:

- a building of Paris Habitat where 19 dwellings were instrumented by Aereco in 2007 (from the 4th to the 8th floor),
- a building of Lyon Métropole Habitat where 12 dwellings were instrumented by Anjos in 2007.

The Performance 2 campaigns include the following:

- continuous measurements close to the ventilation terminals, which already had CO₂, Temperature and RH sensors in place since the Performance 1 project 15 years ago. VOC and PM were added for Performance 2 for the building in Paris. Additionally, two outdoor weather stations have been installed on the Paris building;
- Two winter campaigns (one in winter 2021-2022 and another in winter 2022-2023) during which two NEMOs IAQ monitors were installed in each voluntary dwelling (one in the living room and one in the parental bedroom). These monitors measured CO₂, Temperature, RH, light VOCs, Formaldehyde and PM. Additionally, an outdoor NEMO was installed during each winter campaign.

An inventory of the ventilation installations was carried out, partly applying the French Promevent protocol (Bailly Mélois and Mouradian, 2018). A laboratory study of the terminals and sensors was conducted to characterize the state of the terminals, assess the current hygro-regulated performance of the ventilation terminals, and verify the operation and reliability of the on-board sensors (Mélois et al., 2023).

2.2 Evaluation of the durability of the RH-MEV systems performances

During Performance 1 project (2007-2009), 19 dwellings in Paris and 12 dwellings in Villeurbanne were monitored during the first months after commissioning. Several analyses

were conducted from these data and where possible, the same analyses will be performed from Performance 2 project to enable result comparison. The main analyses focused on energy performance, the fan consumptions and airflow rates (Figure 1). These measurements were compared to theoretical values obtained using French software SIREN, considering the number of rooms in the dwellings.

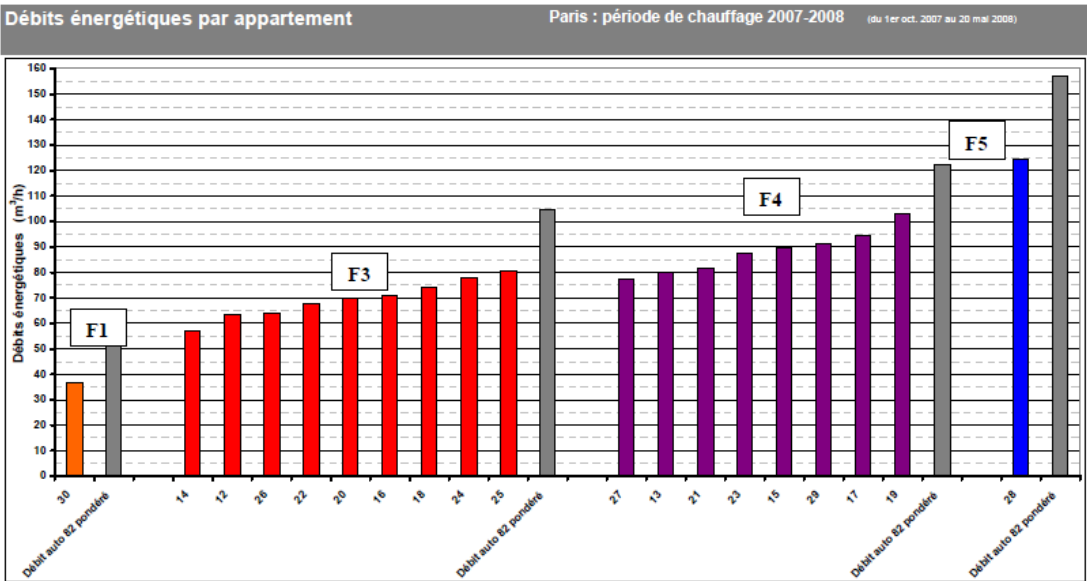


Figure 1: Average airflow rates (2007-2008 season) per apartment compared with weighted flow rates for March 1982 (SIREN evaluation) at the Paris site – Performance 1 project final report

For the CO₂ concentrations, the dynamic of the CO₂ were analysed during the year. The cumulative hours above 1000 ppm during heating season in bedrooms were calculated, and the correlation between CO₂ concentrations and intake airflows was analyzed (Figure 2).

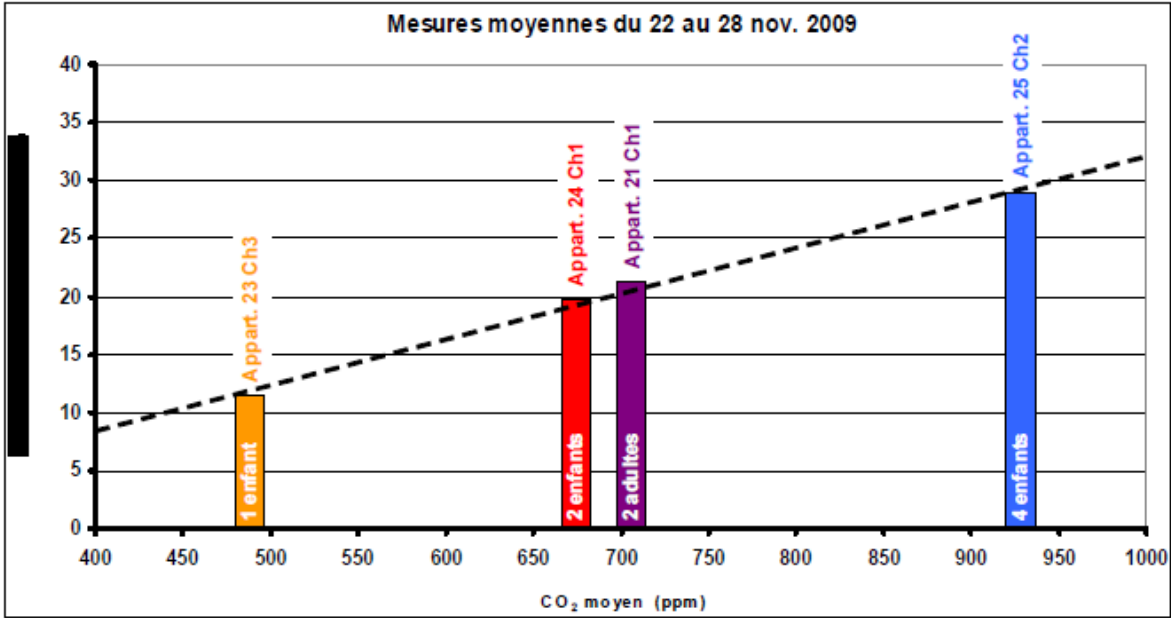


Figure 2: Evolution of the average air inlet flow rate at 10 Pa as a function of the average CO₂ level in a room for several dwellings – Performance 1 project final report

Regarding the relative humidity, calculations were performed to evaluate the risk of condensation on windows (Figure 3), as well as the number of hours with a RH above 75% has been evaluated for each room.

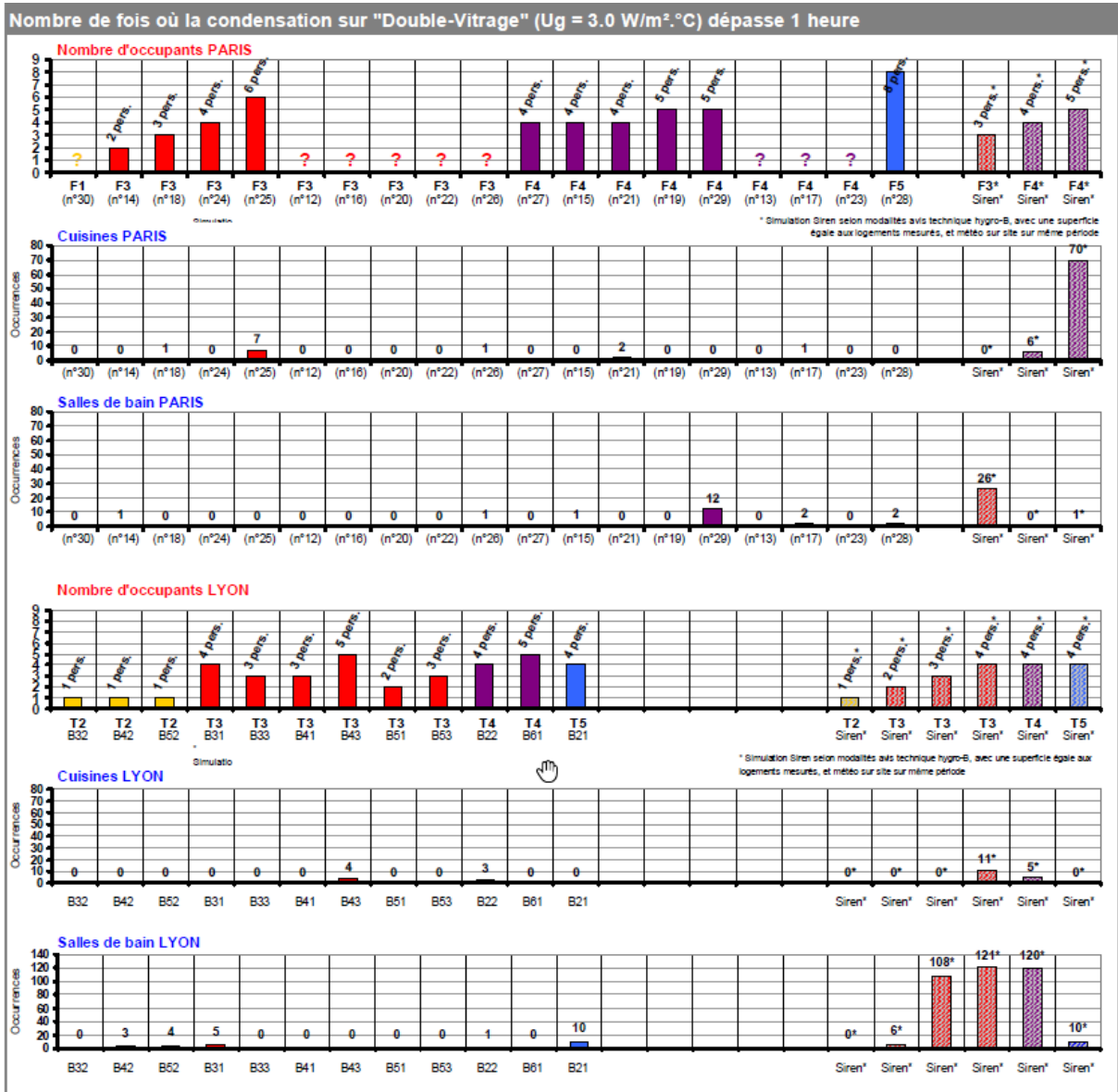


Figure 3: Comparison of condensation risks (occurrences) evaluated from on-site measurement and calculated by SIREN – Performance 1 project final report

2.3 Evaluation the performance of the RH-MEV systems regarding others pollutants

During Performance 1 project, no pollutant was measured. Therefore, the durability of the performance regarding the IAQ cannot be evaluated. However, the current performances can be assessed to determine when the system is adequate or not for providing good IAQ in the dwellings. In Paris, in order to have a representative measurement of the pollution in the room, the VOC and PM sensors were installed near the exhaust units and near the air inlets but out of their flow. Data was collected in 15 dwellings over 2 year period. Furthermore, data from the winter campaigns (two weeks at the end of 2021 for seven dwellings and two weeks at the end of 2022 for four dwellings) collected using the NEMOs monitors will be analysed. In Villeurbanne, since no additional sensors were installed, only the measurements taken with the NEMOs during the winter campaigns have been evaluated (two weeks at the beginning of 2021 for six dwellings and two weeks beginning of 2023 for five dwellings).

To characterize the IAQ, it is necessary to determine indicators and establish “good/bad” scales. These indicators are being defined according to:

- State of the art regarding health recommendations and thresholds;
- Previous large scale IAQ campaigns in dwellings on-site;
- Accuracy of the performed measurement.

2.4 Evaluation of the evolution of the ventilation systems conditions

A diagnostic was conducted for each dwelling at the beginning of the project to evaluate the condition of the terminal devices and the internally mounted air transfer devices. In certain dwellings, additional pressure difference measurements were conducted at the Air Terminal Devices (ATDs). Then, during the laboratory phase each collected ATD was classified depending on its condition (Mélois et al., 2023).

2.5 Evaluation of the evolution of the ventilation needs

In the past 15 years, the occupancy and the use of the dwellings have evolved. An interview was conducted in each voluntary dwellings during the winter campaigns to collect data regarding the number of occupants, their presence schedule, their bathrooms habits, and the potential sources of indoor pollution (household products, cosmetics, cooking habits, ...). Additionally, the occupants were asked to fill in a weekly log during the campaigns period (Mélois et al., 2022). The data collected from these documents will be compared to the data collected during Performance 1 project.

3 FIRST RESULTS

3.1 Data completeness

In order to be able to show statistical results that are representative of reality over a predefined period of time, a preliminary study of the data needed to be done. Figure 4 is an example of the percentage of the CO₂ data that has been collected over the year 2022, for each dwelling in Paris. In most cases, more than 98% of the period has been monitored. There were only three cases (rooms) where the collection partially failed (P10, bathroom, P11 in the kitchen, and P15, also in the kitchen). In the future analysis these specific cases will be considered.

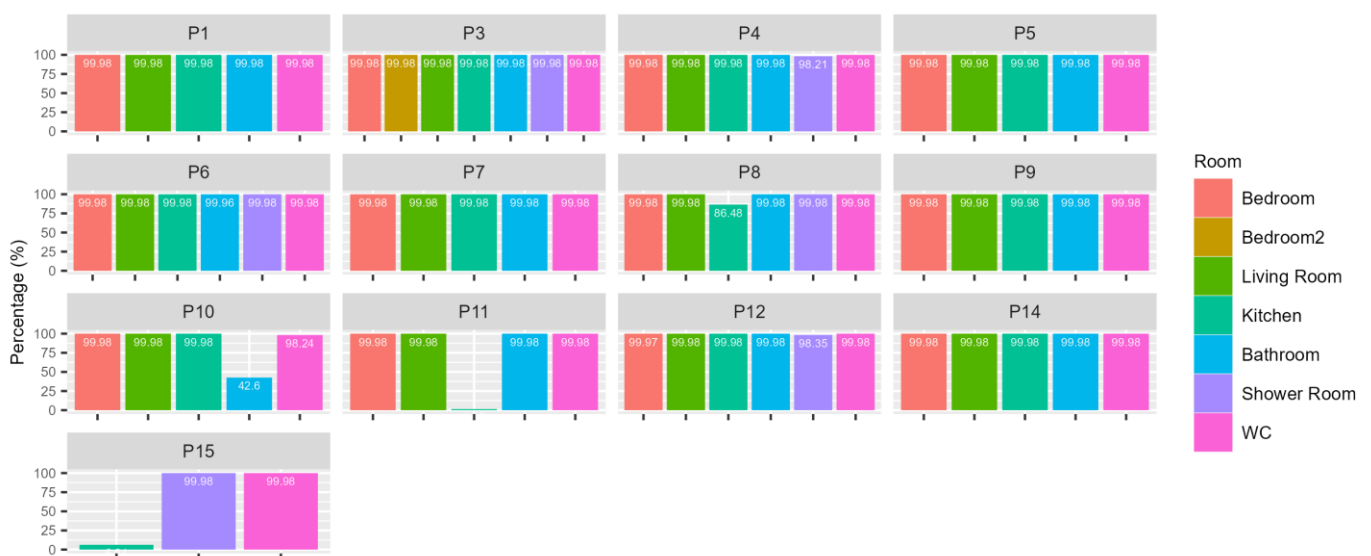


Figure 4: Percentage of CO₂ data collected in Paris over 2020

3.2 Comparison data during winter campaigns

Some parameters are measured by different sensors: continuous measurements from the sensors installed next to the ventilation ATDs and punctual IAQ campaigns from the NEMOs. To identify potential accuracy issues, additionally to the inter-comparisons carried out during the laboratory phase of the project, both acquisitions were compared (Figure 5).

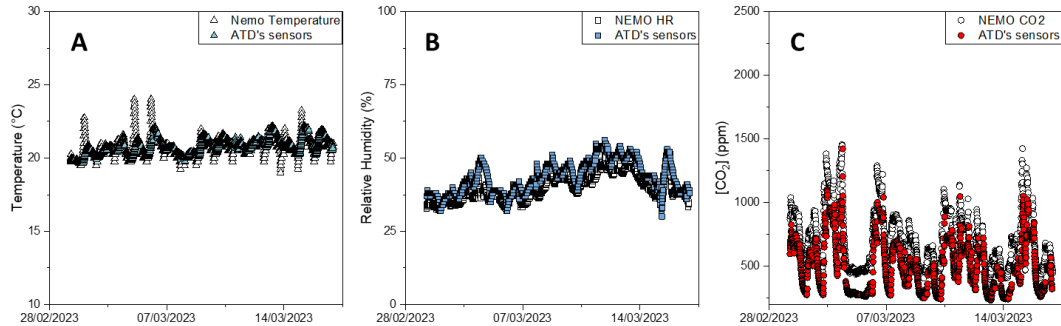


Figure 5: Comparison of data collected by two different sensors in one bedroom (Villeurbanne) for Temperature sensors (A), Relative humidity sensors (B) and CO₂ sensors (C).

3.3 CO₂ concentration depending on the type of room

With a RH-MEV system, the airflow is mechanically extracted from the kitchen, bathroom, and toilets, and enters naturally by the living room and the bedrooms due to the depressurization created by the extraction system. Figure 6 represents the CO₂ concentration for each apartment and room. It can be observed that for most of the dwellings, the CO₂ concentration is higher in the bedrooms (in red) compared to the other rooms.

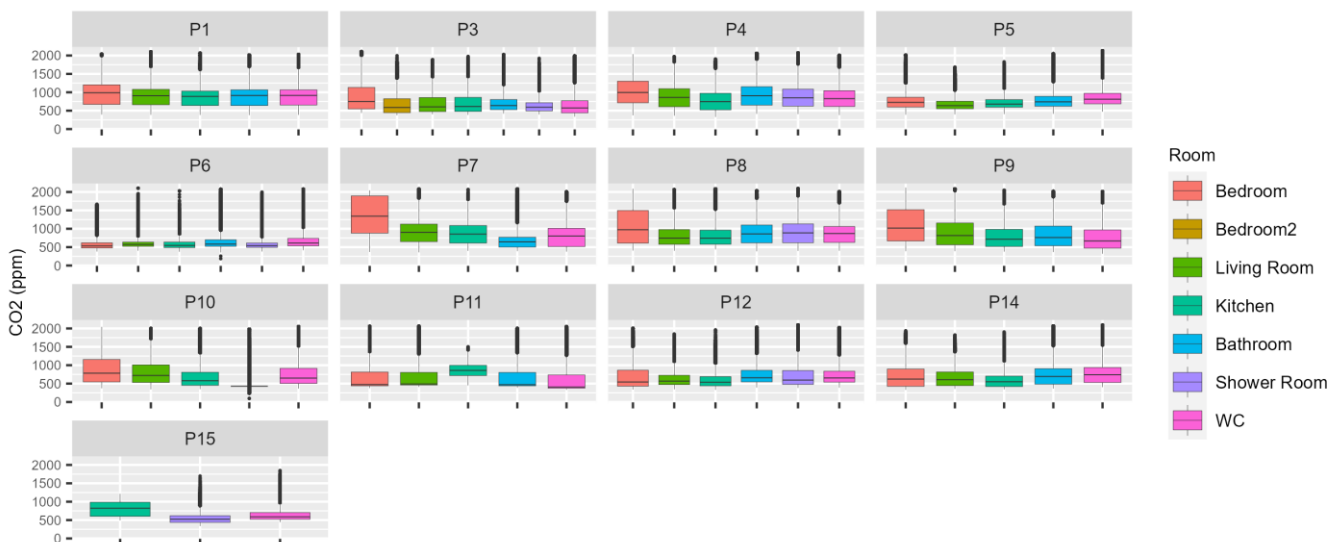


Figure 6: CO₂ concentrations measurements with continuous monitoring in Paris for each dwelling depending of the type of room

Additionally, regarding to the number of hours past above 2000 ppm for each room (described in Figure 7), it is observed that the ventilation is sometimes not enough to evacuate the CO₂ in the bedrooms (in red).

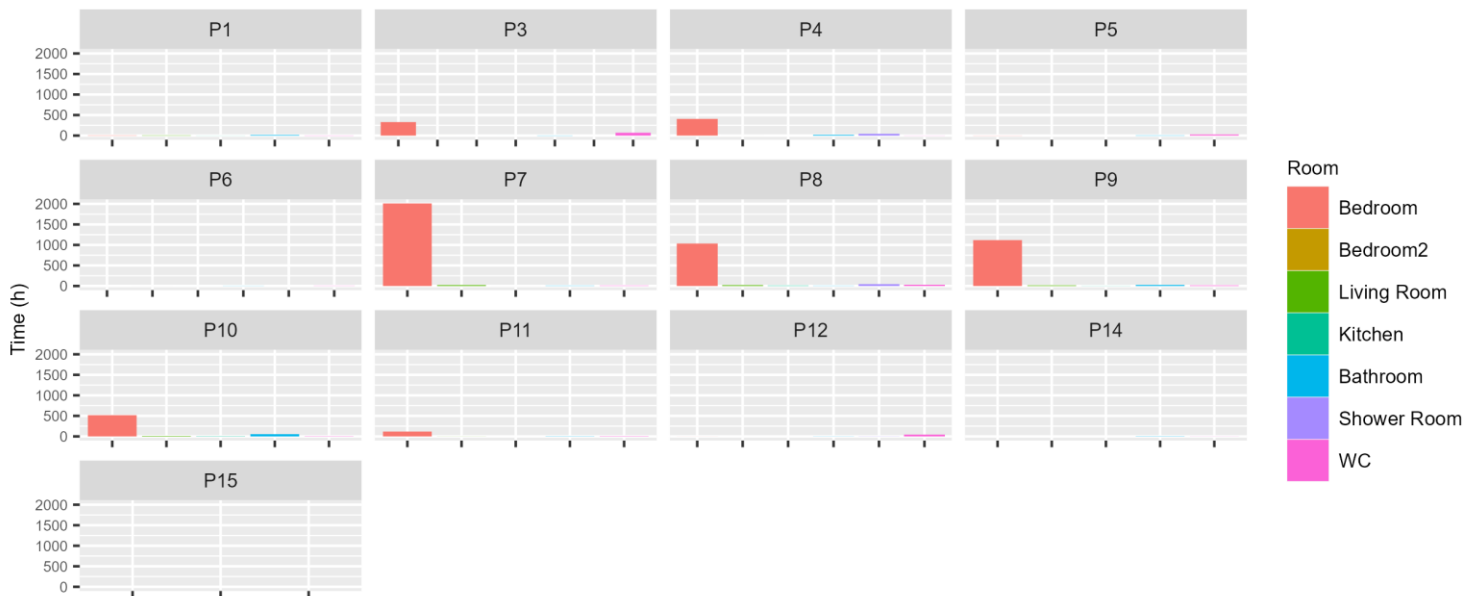


Figure 7: CO₂ concentrations - number of hours past above 2000 ppm for each room in each dwellings in Paris

3.4 Correlation between airflow at terminal devices and IAQ (CO₂ and RH)

The airflow at ATDs must depend on the RH. The good system operation was assessed in laboratory conditions (Mélois et al., 2023). A similar analysis is carried but in real conditions by verifying that the measured airflow rates correspond adequately to the measured RH (Figure 8).

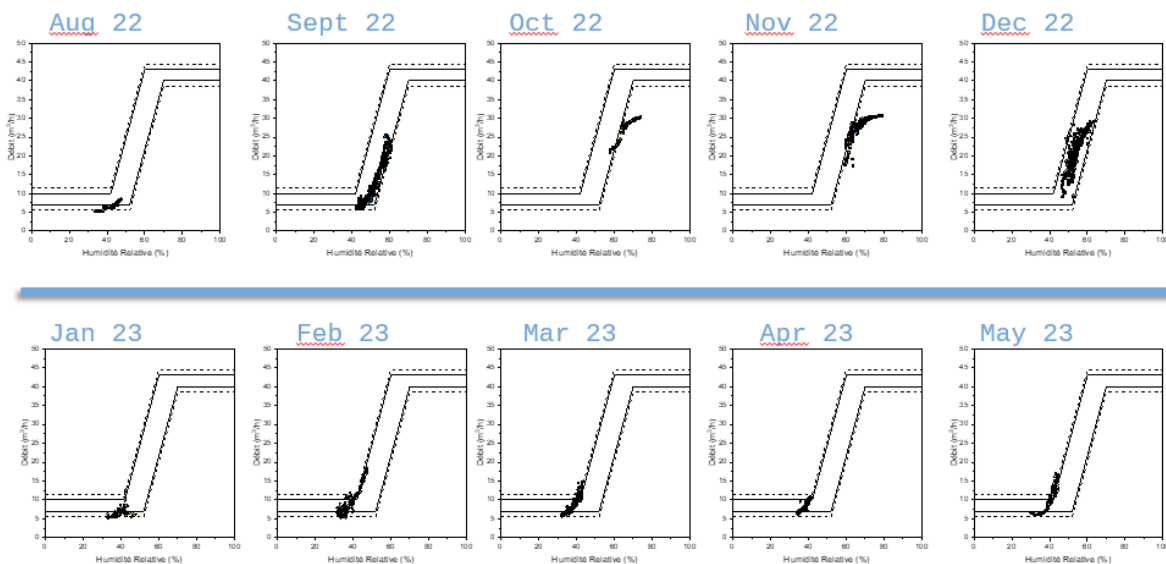


Figure 8: One year airflow rates measured at ATD depending on the measured RH in one bedroom (Villeurbanne)

The RH-MEV systems adapt the airflow only based on the RH. Therefore, the correlation between the measured airflow and the measured concentration of different pollutants was studied to evaluate the good regulation and then ensure a good IAQ in “normal conditions”. Figure 9 presents the correlation between CO₂ concentration and measured airflows at ATD in

a living room in Villeurbanne. As a result, it is shown that for high values of CO₂ the airflow is not maximal. A deep analysis is necessary to understand these specific cases.

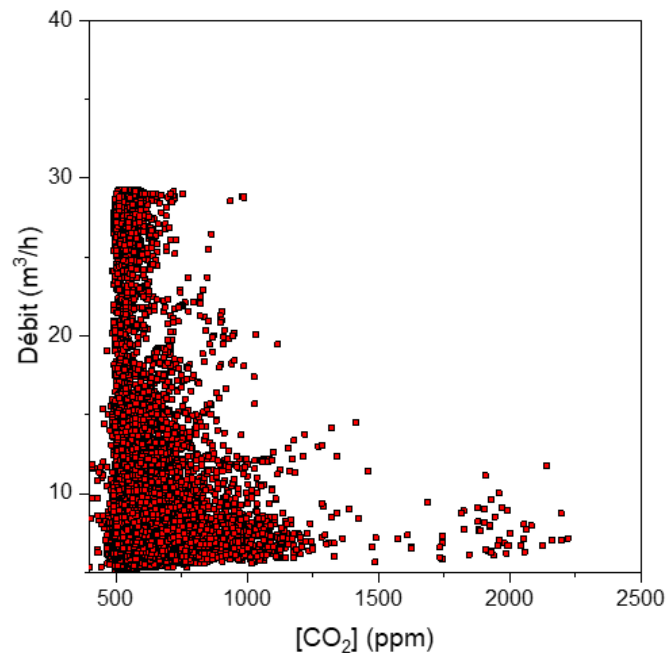


Figure 9: CO₂ concentration and airflow at ATD (with $\Delta P = 20$ Pa) in a living room (Villeurbanne)

4 CONCLUSIONS AND PERSPECTIVES

During Performance 2 project, data have been collected thanks to continuous monitoring, winter measurement campaigns and occupants interviews. The challenge now is to organize the analysis in order, first, to meet the initial objectives of the project: to evaluate the durability of the RH-MEV systems, and to identify their performances regarding energy consumptions and IAQ depending on the occupants 'use. First analyses of this data are being performed to compare the current performances to initial and theoretical performances. Deep analyses will be performed depending on these first results in order to identify the reasons behind the results. Data may be use for other purpose, for example to validate new model developed for the new regulation and to explore the feasibility of continuous evaluation of ventilation through cheap but reliable monitoring.

5 ACKNOWLEDGEMENTS

The authors acknowledge the support of ADEME under the contract number 2004C0014.

The laboratory campaigns have been carried out by AERECO, ANJOS and LOCIE.

The on-site campaigns have been prepared and conducted by different teams of the Cerema: Cerema Hauts-de-France (BED and ABV), Cerema Centre Est (Groupe Bâtiments Autun and Groupe Bâtiments D2T), Cerema Ile-de-France (Bâtiment) and Cerema Ouest (PsyCap).

6 REFERENCES

Bailly Melois, A., Mouradian, L., 2018. Applications of the Promevent protocol for ventilation systems inspection in French regulation and certification programs, in: Proceedings of the 39th AIVC Conference "Smart Ventilation for Buildings." Presented at the 39th AIVC conference "Smart ventilation for buildings," Antibes Juan-Les-Pins, France.

- Guyot, G., Jardinier, E., Parsy, F., Berthin, S., roux, E., Charrier, S., 2022. Smart Ventilation Performance Durability Assessment: Preliminary Results from a Long-Term Residential Monitoring of Humidity-Based Demand-Controlled Ventilation, in: IAQ 2020: Indoor Environmental Quality Performance Approaches Transitioning from IAQ to IEQ. AIVC-ASHRAE, Athens, Greece.
- Mélois, A., Legree, M., Sebastian Rios Mora, J., Depoorter, J., Jardinier, E., Berthin, S., Parsy, F., Guyot, G., 2023. Durability of humidity-based ventilation components after 13 years of operation in French residential buildings – Assessment of components performance in laboratory. *Energy Build.* 292, 113154. <https://doi.org/10.1016/j.enbuild.2023.113154>
- Mélois, A., Vala, N., MArchand-Moury, A., Nauleau, C., Jobert, R., 2022. How to collect reliable information regarding occupants' behavior during IAQ campaigns? Performance 2 project first feedbacks. Presented at the 42nd AIVC-10th TightVent & 8th Venticool Conference, Rotterdam, The Netherlands.
- Mélois, A.B., Moujalled, B., Guyot, G., Leprince, V., 2019. Improving building envelope knowledge from analysis of 219,000 certified on-site air leakage measurements in France. *Build. Environ.* <https://doi.org/10.1016/j.buildenv.2019.05.023>

Checking and assuring real IAQ and energy performances through demand control and cloud connectivity

Ivan Pollet^{*1}, Kevin Verniers¹ and Steven Delrue^{1,2}

*1 Renson Ventilation
Maalbeekstraat 10
Waregem, Belgium*

**Corresponding author: ivan.pollet@renson.be*

*2 KU Leuven
Faculty of Science, Kulak Kortrijk Campus
Etienne Sabbelaan 53
Kortrijk, Belgium*

KEYWORDS

Cloud-connected ventilation, demand control, big data, indoor air quality, energy consumption

EXTENDED ABSTRACT

Since 2018, Renson has introduced a range of cloud-connected residential ventilation systems, including central and decentral mechanical extract ventilation (MEV), as well as fully mechanical systems with heat recovery (MVHR) (see Fig. 1). These systems incorporate smart control mechanisms that utilize different IAQ sensors (CO₂, VOC, RH), to adjust the airflow rate(s) locally or centrally to the detected needs. The IAQ sensors are located at the control valves or at the central unit, but not within the rooms. In that way, the full control system is integrated within the ventilation unit itself. The central MEV system also allows to extract air directly from the bedrooms, in addition to the wet rooms, to improve the sleeping environment.



Figure 1: Central MEV system (left), central MVHR system (middle), decentral MEV (right)

Cloud connectivity of smart devices offers a dual aspect. It presents several challenges that need to be addressed, including:

- Adoption of big data technology in construction industry is slow and difficult
- Accessing relevant insights from massive amounts of data is difficult
- Exploiting data requires significant investments to be made
- Security and privacy rights need to be maintained.

Despite these challenges, wired/wireless IoT devices offer valuable opportunities by creating added value for the different stakeholders, including manufacturers, installers, service companies, building owners, and end users. This is achieved by monitoring big data, which serves two key purposes:

- Providing services through interaction with the person of interest
- Gathering insights into real-time operation to optimize/improve system performances.

The range of services facilitated through digital interactions is numerous and includes the following:

- Digital communication:
 - Communication with residents/installers: Via resident/set-up app & web portals
 - Project preparation & planning: The set-up app supports the installer throughout the installation process by retrieving project parameters prepared in web portal, assisting in system calibration, displaying the installation parameters, and inserting measurement results for the automatic preparation and creation of the measurement ventilation report in the web portal.
 - Push notifications on smartphone for filter warnings and error detection: These notifications serve as alerts for potential faults, such as defective valves or fans, or to the installation of a wrong valve type for a given room. For instance, a bathroom valve can be switched with the one for a bedroom and vice versa.
 - Visual representation of real time/historic air quality and ventilation levels: The user app provides a visual display of air quality and ventilation levels in the home, down to room level. Colors indicate the air quality per home/room.
 - Service management and follow-up: remote inspection of correct functioning and maintenance of the devices to save time and money.
 - Communication with smart home/home automation: via API and/or via switching module
- Sending automatic software updates

To obtain valuable insights into real-time performance of connected systems, especially the central MEV system data was anonymously analyzed in recent years on several characteristics: energy consumption, IAQ, maximum ventilation rate, pressure losses, user interaction with the system, etc.

De Mare *et al.* (2019) presented a large-scale analysis of the performance of the smart MEV system based on field data. Half of the units were installed as a smartzone system which involved additional mechanical extraction from habitable rooms like bedrooms. Indoor climate and IAQ were analysed with respect to design criteria set out in standards as well as fan characteristics and energy consumptions. The finding revealed that, on average, the CO₂ level in bedrooms were below 950 ppm for at least 90% of the nighttime. For the MEV system with smartzone, the ctrl-factor of 0.26 was substantially lower than the default values (0.43-0.50) currently used in regulations. Additionally, the auxiliary energy consumption of the MEV with smartzone was found to be less than 50% of the literature values reported on similar systems. The average total yearly energy cost related to the operation of the ventilation system (heating and auxiliary energy) was found to be limited to €100 (in 2023 half that high due to price increases), and at least comparable to the operating cost of a MVHR system. Since rooms are often unoccupied or occupied at a low level, advanced demand control technology proves to have a high potential to limit total energy consumption, while assuring a good IAQ.

Another performance study was carried out by Pollet *et al.* (2022) to analyse the maximal used extract ventilation capacity of dwellings equipped with local air flow control during the heating season. The study examined how ventilation control options can have an impact on the maximal simultaneous ventilation losses. The central MEV system was again investigated with respect to the maximal occurring total extract rate during the heating period, based on big field and simulated data of the smart connected ventilation system. A maximal used fraction of the nominal installed ventilation capacity down to 50% was found, impacting in that way the required heat generation power (kW).

A third study was performed by Verniers *et al.* (2022), in which the significant impact of critical versus non-critical path control on the mean operating pressure and auxiliary fan consumption for residential DC-MEV systems was examined by means of multizone simulations during the

heating season. Due to critical path control relative to non-critical path control, reductions of the fan power consumption in the range of 33 to 44% were obtained.

In today's context, residents have increasing expectations for simple and user-friendly solutions that minimize the need for complex manual adjustments. Besides, the ability to quickly react and adapt to indoor and outdoor changes (weather, occupancy, usage) is often expected. As a result, alongside smart ventilation systems, the integration of solar shading and ventilative cooling products as IoT devices into home automation has become common. These integrated systems work in harmony to enhance overall comfort and efficiency.

Furthermore, the use of model predictive control (MPC) is gaining recognition as a promising approach to improve occupant thermal comfort while reducing energy consumption. Instead of relying solely on rule-based control strategies, MPC leverages building design information, historical sensor data (e.g. indoor temperature), and weather forecasts to optimize building control. By considering predictive modelling, MPC allows for more proactive and efficient management of indoor conditions, resulting in enhanced occupant comfort and reduced energy usage.

The integration of smart ventilation systems, solar shading, ventilative cooling products, and the adoption of model predictive control represents a forward-thinking approach to building automation. These technologies work together to create responsive, comfortable, and energy-efficient living environments that align with residents' expectations for simplicity and adaptability.

REFERENCES

- De Maré, B., Germonpré, S., Laverge, J., Losfeld, F., Pollet, I. & Vandekerckhove, S. (2019). Large-scale performance analysis of a smart residential MEV system based on cloud data. *40th AIVC Conference*, Ghent (Belgium), 15-16 October 2019, 751-765.
- Pollet, I., De Maré, B., Losfeld, F., Delrue, S., Vandekerckhove, S. & Laverge, J. (2022). Performance analysis of the maximal used extract ventilation capacity of dwellings during the heating season. *41th AIVC – ASHRAE – IAQ2020 Conference*, Athens (Greece), 4-6 May 2022, C1253.
- Verniers, K., Losfeld, F. & Pollet, I. (2022). Critical versus non-critical path control in Residential DC-MEV. *Rehva Journal*, 59(3), 24-28.

Data driven models for fault detection - Combining thermal and indoor air quality grey box models

Gabriel Rojas^{*1}, Romed Jenewein¹, Klaus Prenninger², and Johannes Schnitzer³

*1 Unit for Energy Efficient Building & Digital
Science Center, University of Innsbruck
Technikerstrasse 13
Innsbruck, Austria*

*2 Smart Building Department
Salzburg University of Applied Sciences
Am Markt 156
Kuchl, Austria*

**Corresponding author: gabriel.rojas@uibk.ac.at*

*3 Forschung Burgenland
Steinamangerstraße 21
Pinkafeld, Austria*

ABSTRACT

The progressive digitalization is providing more and more measurement data from building operation, in particular from heating, cooling and ventilation (HVAC) systems. This work investigates the potential use of data-driven models to simulate indoor environmental conditions, i.e. temperature and CO₂ concentration, for fault detection applications. Herein, a grey-box model, depicting the thermal behaviour of building zones, is coupled with model representing the indoor air quality/ventilation condition in the respective zone allowing the combined use of measurement data from building operation. The models are applied to an office room of a case study building and the model parameters are identified with measurement data for a four-weeks long training period. The identified models are used to predict the timely evolution during a three-day long prediction period. By comparing residual metrics between training phase and prediction phase the model's capabilities to detect simple exemplary faults are evaluated. Herein, preliminary results with rather simple fault cases, like temperature or CO₂ sensor faults or (unintentionally) left-open windows are investigated. Results indicate that indoor temperature anomalies are detected well and that anomalies in CO₂-concentration are also detectable with this modelling approach but depend on the available occupancy estimation (or measurement). Further investigations are underway to test possible adaptations to the presented approach to allow for better occupancy estimation and/or account variable ventilation rates.

KEYWORDS

Fault detection, grey-box models, ventilation model, thermal model, CO₂ model, parameter identification

1 INTRODUCTION

The progressive digitalization is providing more and more measurement data from building operation, in particular from heating, cooling and ventilation (HVAC) systems (Kim and Katipamula 2018). The data is most often used for control and/or monitoring on component level. However, the combined use of measurement data from HVAC components, weather station and building volume (e.g. zone temperature, CO₂ concentration) opens new possibilities. This work investigates the potential use of data-driven models to simulate indoor environmental conditions, i.e. temperature and CO₂ concentration, for fault detection applications. Herein, grey-box (RC network) models, depicting the thermal behavior of building zones, are coupled with simplified models representing indoor air quality condition in the respective zone allowing the combined use of measurement data from building operation. The aim is to use such models to detect anomalous conditions stemming from faulty or misadjusted HVAC components or (unintentional) misused of building, e.g. window left open, misadjusted air inlet valve, etc., by comparing model predictions with current

measurement values. This paper presents first results from training such a combined model for a real case study office room and comparing predictions for periods with artificial or real faults.

2 MODEL DESCRIPTION

So-called grey box models were used for depicting the dynamic behaviour of the building (or the room in this case) (Bacher and Madsen 2011; Bauwens, Ritosa, and Roels 2021; Reynders, Erfani, and Saelens 2021). The thermal behaviour of buildings can be described by a series of first-order differential equations. These can be represented as simple resistance-capacity networks. The level of detail of the model can be determined by the number of dependent parameters. In the course of the case study, different models were applied. Simpler models have the advantage of having fewer model parameters which can be identified more reliably. However, oversimplified models might not be able to reproduce the dynamic behaviour sufficiently well. Starting from a simple RC model with only one capacity (1C), the complexity of the thermal model is increased by introducing a second capacity representing the thermal capacity of the external walls (2C). In a third step the 2C thermal model is coupled with a model representing the mass balance equation for CO₂ in the room, i.e. a ventilation model (2C+V). The mass balance model and the thermal model are coupled via the air exchange rate. In the following, these three models and their respective differential equations are documented in more detail.

2.1 1C Thermal model

This model is one of the simplest modelling variants. In this case, only the thermal behavior of the building is considered. The building envelope is represented by one resistance to the outside and has only one capacity to account for thermal mass, see Figure 1. It therefore has two free parameters (resistance R_{ie} and capacity C_i).

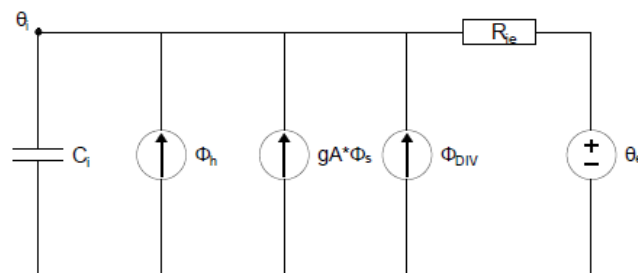


Figure 1: Resistance-Capacity network representing the 1C thermal model.

The model shown in Figure 1 can also be written as a differential equation as follows.

$$\frac{d\theta_i}{dt} = \frac{\theta_e - \theta_i}{C_i * R_{ie}} + \frac{1}{C_i} * \Phi_h + \frac{gA}{C_i} * \Phi_s + \frac{1}{C_i} * \Phi_{DIV} \quad (1)$$

It describes the energy balance of the internal room temperature node θ_i . The other variables are described in section 2.3. This modelling variant has proven to be robust in determining a good initialization value for the parameters.

2.2 2C Thermal model

To increase the level of detail of the model, another differential equation can be added. In this model, as shown in Figure 2, the external resistance is divided. Thus, the thermal capacity of the building can be considered better. As a result, this model has two more free parameters that need to be identified using measurement data.

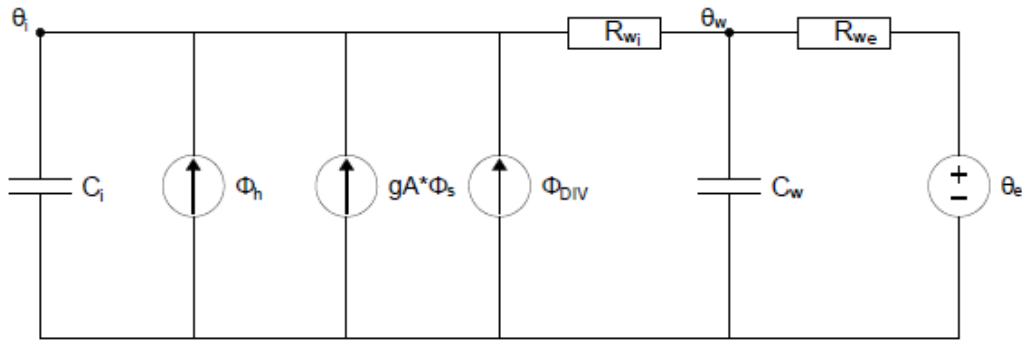


Figure 2: Resistance-Capacity network representing the 2C thermal model.

This model can be described by an additional differential equation representing the energy balance of the external wall node θ_w .

$$\frac{d\theta_i}{dt} = \frac{\theta_w - \theta_i}{C_i * R_{wi}} + \frac{1}{C_i} * \Phi_h + \frac{gA}{C_i} * \Phi_s + \frac{1}{C_i} * \Phi_{DIV} \quad (2)$$

$$\frac{d\theta_w}{dt} = \frac{\theta_i - \theta_w}{C_w * R_{wi}} + \frac{\theta_e - \theta_w}{C_w * R_{we}} \quad (3)$$

See the following section for a variable description.

2.3 2C+V Thermal and ventilation model

The two models above can describe the thermal behaviour of a building or a room. However, the heat flow through massive walls is, compared to heat flow through e.g. ventilation, considerably slower. To be able better reproduce dynamic events, like the influence of a controlled or uncontrolled air exchange with the ambient, the thermal model from section 2.2 can be supplemented with a ventilation model. This model describes the mass balance of CO₂ in the room and is shown Figure 3.

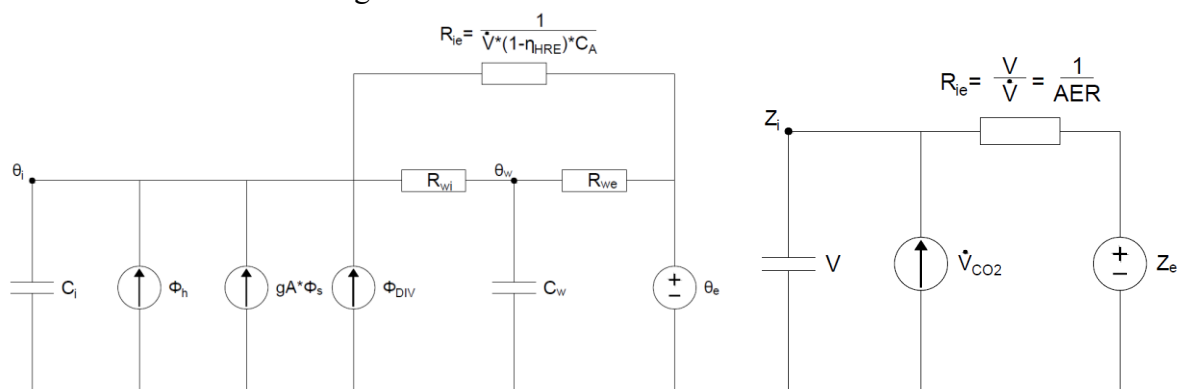


Figure 3: Resistance-Capacity network representing the 2C+V model. Left: Representation of thermal behaviour, i.e. heat flow through building/room envelope. Right: Representation of CO₂ concentration in the building/room.

The models in Figure 3 are coupled via the volume flow. In the thermal model, the volume flow is considered as part of an additional resistance. The idea behind this resistor is to consider the heat flows of the opaque envelope and the ventilation separately. Infiltration losses are estimated (stationary) and included in the effective heat recovery efficiency of the ventilation. The n_{50} -value of the room is estimated (1 h^{-1}) based on the building n_{50} -value.

$$\frac{d\theta_i}{dt} = \frac{\theta_w - \theta_i}{C_i * R_{wi}} + \frac{\theta_e - \theta_i}{C_i} * (1 - \eta_{HRE}) * \dot{V}_{AL} + \frac{1}{C_i} * \Phi_h + \frac{gA}{C_i} * \Phi_s + \frac{1}{C_i} * \Phi_{DIV} \quad (4)$$

$$\frac{d\theta_w}{dt} = \frac{\theta_i - \theta_w}{C_w * R_{wi}} + \frac{\theta_e - \theta_w}{C_w * R_{we}} \quad (5)$$

$$\frac{dz_i}{dt} = \frac{\dot{V}_{CO2}}{V} + (z_e * z_i) * \frac{\dot{V}_{AL}}{V} \quad (6)$$

The differential equations are composed of known input data, unknown parameters, and state variables. The variables for equations 1 through 6, are described here.

State variables:

- θ_i ... interior temperature [°C]
- θ_w ... wall temperature [°C]
- z_i ... CO₂ concentration in the interior [ppm]

Known input data:

- θ_e ... external temperature [°C]
- z_e ... external CO₂ concentration [ppm]
- η_{HRE} ... effective heat recovery efficiency [-]
- Φ_h ... heat load [kW]
- Φ_s ... solar radiation [kW]
- Φ_{DIV} ... combination of diverse heat flow's (internal gains from people; internal gains from electrical devices; the heat flow between the neighbour rooms) [kW]
- \dot{V}_{CO2} ... CO₂ volume flow caused by people present [m³/h]
- V ... room volume [m³]

Unknown(free) parameters:

- C_i ... interior capacity [kWh/K]
- C_w ... wall capacity [kWh/K]
- R_{wi} ... external wall resistance on inner side [K/kW]
- R_{we} ... external wall resistance on exterior side [K/kW]
- gA ... solar aperture [m²]
- \dot{V}_{AL} ... volume flow between the inside and the outside [m³/h]

Furthermore, for the training of the model and thus the determination of the unknown parameters, measurement equations are needed. For the 2C+V model the two trivial equations, where the observed state variables are set equal to the measured data are needed as documented in formula (7) and (8).

$$\theta_i = \theta_{i,measured} \quad (7)$$

$$z_i = z_{i,measured} \quad (8)$$

3 METHODS - MODEL TRAINING

3.1 Case study description

The described models were trained using measurement data from an office building in eastern Austria. The building belongs to the research institute Forschung Burgenland and is equipped with a great number of sensors, including room sensors for temperature, relative humidity, CO₂-concentration, supply and extract air flows, supply air temperature as well as an outdoor weather station. The office room number "02" was used for the following analysis. It is usually occupied by one person (occasionally by two) on three to five working days per

week. The nominal ventilation rate in this room is 55 m³/h. Room “02” is located in the upper floor and its glass façade faces south-south-east, see Figure 4. The relevant parameters are summarized in

Table 1.



Figure 4: Left: Picture of the south-south-east façade of the case study building “Energetikum”. Right: Upstairs floorplan with investigated room “02”. Source: Forschung Burgenland.

Table 1: Building and room parameters and assumptions

Parameters & assumptions	Value	Unit
Area external wall: Room “02”	18.8	[m ²]
U-value external wall: Room “02”	1.10	[W/(m ² K)]
Floor area: Room “02”	26.04	[m ²]
Height: Room “02”	3.17	[m]
Average U-value: Entire building	0.39	[W/(m ² K)]
Avg. thermal cap. estimate: Entire building	204	[Wh/(m ² K)]
Occupancy assumption (7:00-16:00)	5	[d/week]
Occupant sensible heat rate	76	[W]
Occupant CO ₂ emission	18	[L/h]

Table 2: Initial values and limiting bounds for free model parameters

Parameter		Source for initial value	Initial-value	Units	MIN	MAX
R	Resistance	Energy Performance Cert.	48.4	[K/kW]	1	500
$C_i(+C_w)$	Capacity	Estimate [PHPP]	5.3	[kWh/K]	0.01	500
L	Position of the wall-capacity	Estimate	0.50	[-]	0.1	0.9
gA	solar aperture	Estimate	5.00	[m ²]	0.1	50
\dot{V}_{AL}	airflow	Measurement data	mean	[m ³ /h]	50	300
HLC	Heat-Loss-Coefficient	=1/(R)	20.7	[W/K]		

3.2 Parameter identification

In order to obtain a suitable model that can be used for simulation, the unknown/free parameters described in section 2 had to be identified. For this purpose, the System Identification Toolbox from the software MATLAB was used. Therein the grey-box estimation algorithm was used to identify the free parameters that minimise the cost function,

i.e. the sum of squares of the difference between simulated and measured values from the training period. Initial values and limiting bounds were defined for the unknown parameters according to Results from the model parameter estimation are documented in Table 3. These should lie within a physically reasonable range. For the 2C models the resistance R is split using the factor L , representing the position of the effective wall capacity C_w . Results from the model parameter estimation are documented in Table 3.

Table 3: Estimated model parameters for 1C, 2C and 2C+V model. Initial value and design value (if known) are also listed for comparison.

Parameter		Initial-value	1C estimation	2C estimation	2C+V estimation	Design value	Units
HLC	Heat-Loss-Coefficient	20.7	14.5	16.6	9.6	20.7	[W/K]
$C_i(+C_w)$	Capacity	5.3	4.8	8.7	19.2	n.a.	[kWh/K]
L	Position of the wall-capacity	0.50	n.a.	0.67	0.39	n.a.	[-]
gA	solar aperture	5.00	1.45	1.9	2.6	unknown	[m ²]
\dot{V}_{AL}	airflow	4	n.a.	n.a.	134	55	[m ³ /h]

3.3 Exemplary tests for fault detection (FD)

In order to test the usability of the proposed combined model (2C+V) for FD the trained models were used to predict the temperature and CO₂ concentration for a three-day long period immediately after a four-weeks long training period. Note that the presented prediction is a simulation for the entire three-day prediction period and not a 1-step ahead prediction as often used in this context. As concluded in previous studies, evaluating the multi-step prediction (in this case even for three days), might provide a better model assessment (Reynders et al. 2021). The simulation was initialized with measured data at the beginning of the prediction period.

This paper presents the first results for testing with rather “simple” fault cases, see Table 4. They were produced artificially, by altering the measurement data, simulating e.g. a faulty sensor, or, they occurred in reality, as for the open window “fault”. Note that these simple faults may also be detected with simpler FD-schemes, e.g. rule-based FD techniques. However, the proposed method with physically based grey-box models has the potential to provide further capabilities like fault diagnosis, e.g. by continuously retraining the models and interpreting the identified parameters. Further, more complex and more realistic faults will be tested in this ongoing work.

Table 4: Preliminary fault detection test cases

Fault		Training start	Prediction start	Fault duration
Temperature sensor faulty	Sensor outputs +2 K (artificial)	2022-11-03 11:15	2022-12-01 11:15	60 hrs
CO ₂ sensor faulty	Sensor outputs +200 ppm (artificial)	2022-01-27 11:15	2022-02-24 11:15	60 hrs
Window left open	Window was left open unintentionally (real occurrence)	2022-09-01 7:40	2022-09-29 7:40	8 hrs
			2022-09-30 7:40	6 hrs

4 RESULTS

Using the thermal models one can detect only anomalies that alter the thermal behaviour, i.e. the temperature sensor fault and the open window in herein presented cases. Looking at evolution of the measured and simulated temperature during the training month one can see that the simple model with one thermal capacity (1C) follows the general trend fairly well, but

cannot follow the daily temperature variation fully, see Figure 5 (left). The 2C model is able to reduce the root-mean-square of the error/residuals (RMSE) by reproducing the daily variations slightly better, see Figure 5 (right). The temperature simulation of the 2C+V model is very similar to the 2C model, see Figure 6 (left). In all three cases the temperature sensor offset of +2 K can easily be identified by comparing the RMSE between prediction and training period. The RMSE increases by around 200%, i.e. triples, with all three models, see Table 5.

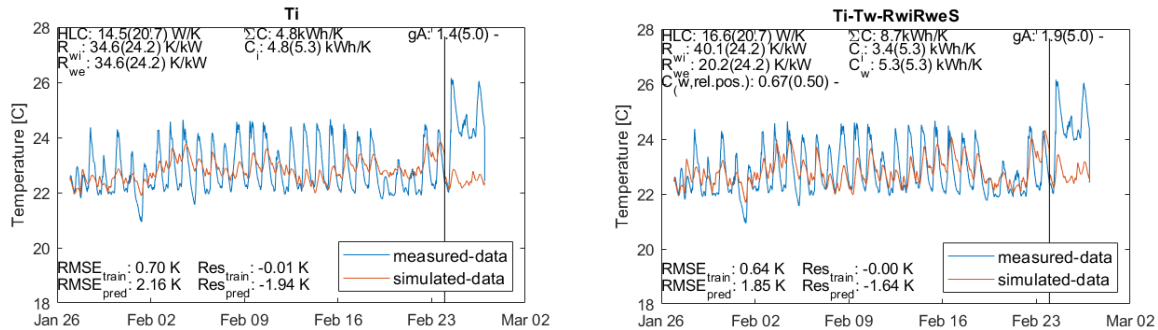


Figure 5: Result for 1C model (left) and 2C model (right) for temperature sensor fault case: Measured and simulated indoor temperature evolution during training (4 weeks) and prediction (3 days) phase. The end of training phase is marked with a vertical line.

As seen in Figure 6 (right) the simulated CO₂-concentration can reproduce the measured CO₂-concentration roughly, but the parameter identification algorithm seems to overestimate the ventilation rate (134 m³/h). Therefore, the simulated daily peaks fall short compared to the measured ones. Nevertheless, the CO₂-concentration is reproduced in a decent manner, considering that the occupancy (and the corresponding emission rate) is just based on the naïve assumption using a fix working schedule (Mo-Fr, 7:00-16:00) for the presented results. One of the difficulties in this case is, that the ventilation rate is controlled via schedule and CO₂ concentration and is therefore not a fix value. However, a varying ventilation rate cannot be depicted in this model variant. This issue was addressed in a model extension, see below. With that, a ventilation rate of around 90-100 m³/h was estimated during regular working hours. Note that the measurements provided by the building control sensors provided unrealistic values of around 10-15 m³/h.

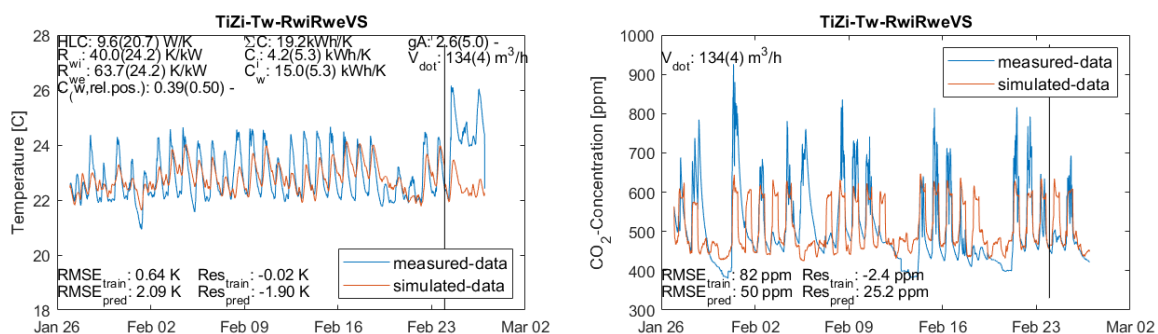


Figure 6: Result for 2C+V model for temperature sensor fault case: measured and simulated indoor temperature (left) and CO₂ concentration (right) evolution during training (4 weeks) and prediction (3 days) phase. The end of training phase is marked with a vertical line.

Figure 7 shows the prediction results for the case where a faulty CO₂ sensor is simulated. While the RMSE of the prediction period shows no increase, the RMSE of the predicted CO₂ concentration increases by almost 300%, allowing a fault detection if an occupancy estimate (or measurement) is available, see Table 5. When only rough occupancy estimates are available, then a prolonged prediction period would be advisable to average out the rough estimate. See “open window” test case, where inaccurate occupancy estimate hinders the fault

detection. Note that this model can be altered to allow for a prediction of CO₂ emission rate instead of indoor concentration, see below.

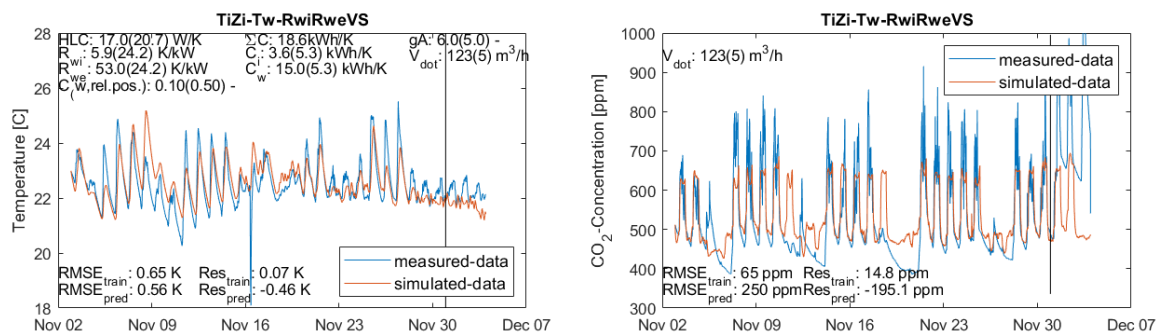


Figure 7: Result for 2C+V model for CO₂ sensor fault case: measured and simulated indoor temperature (left) and CO₂ concentration (right) evolution during training (1 month) and prediction (3 days) phase. The end of training phase is marked with a vertical line.

The results for the “open window fault case” is shown in Figure 8. As can be seen, the temperature drop due to the open window is clearly visible and increases the residuals (RMSE) between simulation and measurement substantially, see also Table 5. Looking at Figure 8 (right) one can also see that the difference between simulated and measured CO₂-concentration is rather large. However, due to the fact that the occupancy estimate is rough and due to the fact that the volume flow control is not depicted in this model, the RMSE is also rather high for the training period. Therefore, the RMSE increase of the CO₂-simulation cannot be used to detect the open window state for this particular case. Possibilities to increase CO₂ prediction accuracy by allowing better occupancy estimates are currently investigated further.

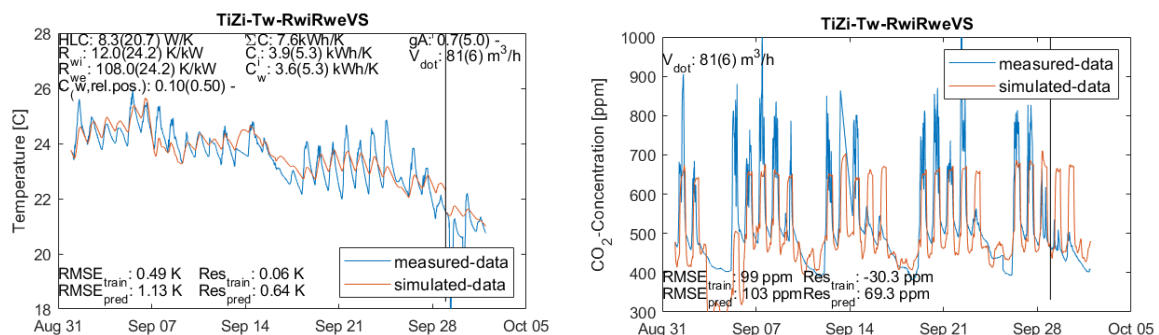


Figure 8: Result for 2C+V model for “open window fault” case: measured and simulated indoor temperature (left) and CO₂ concentration (right) evolution during training (1 month) and prediction (3 days) phase. The end of training phase is marked with a vertical line.

Table 5: Summary table of prediction results. The fields were coloured as follows. Green: fault present and RMS increase >100%; yellow: fault present and RMS increase >33%; red: fault present and RMS increase <33%.

		Failure type					
		T sensor offset (February)		CO ₂ sensor offset (November)		Window left open (September)	
		T [K]	CO ₂ [ppm]	T [K]	CO ₂ [ppm]	T [K]	CO ₂ [ppm]
1C	RMS train.	0.70	n.a.	0.74	n.a.	0.51	n.a.
	RMS pred. w/o fault	0.65	n.a.	0.37	n.a.	n.a.	n.a.
	RMS pred. with fault	2.16	n.a.	0.37	n.a.	1.10	n.a.
	RMS increase	209%	n.a.	-50%	n.a.	116%	n.a.
2C	RMS train.	0.64	n.a.	0.70	n.a.	0.77	n.a.

	RMS pred. w/o fault	0.52	n.a.	0.42	n.a.	n.a.	n.a.
	RMS pred. with fault	1.85	n.a.	0.42	n.a.	1.10	n.a.
	RMS increase	189%	n.a.	-40%	n.a.	43%	n.a.
2C-V	RMS train.	0.64	82	0.65	65	0.49	99
	RMS pred. w/o fault	0.58	50	0.56	137	n.a.	n.a.
	RMS pred. with fault	2.09	50	0.56	250	1.13	103
	RMS increase	227%	-39%	-14%	285%	131%	4%

5 OUTLOOK

5.1 Stepwise parameter identification

Previous work has shown that physical parameter identification can be challenging (Rojas et al. 2023). The tighter that certain free parameters, e.g. building thermal mass, can be bounded, the easier it is for the algorithm to find physical sensible values, in particular for more complex models with higher number of free parameters. In an ongoing work, the following stepwise identification procedures are being compared:

- IC1 (as used in for the results presented in section 4): The starting values of the parameters are defined via the energy performance certificate of the case study whenever possible and the bounding limits are left fairly loose.
- IC2: The parameters are first identified as in method IC1, but with training data in the winter period. The value of these parameters then serves as the starting value for the actual parameter identification. The lower and upper limit are defined +/-95% from this determined value in the winter period.
- IC3: With this method, the parameters are first determined with the simple model from section 2.1 (1C). The identified values are used as initial values and for defining boundaries (+/- 95%). Then the same procedure as within method IC2 is followed.

5.2 Emission rate prediction

The 2C+V model can be adapted to output CO₂-emission rate instead of the CO₂-room concentration. This could be used to extract room occupancy for improving FD prediction models or other application such as model predictive control. Figure 9 shows preliminary results with such an adapted model for the “open window test case”.

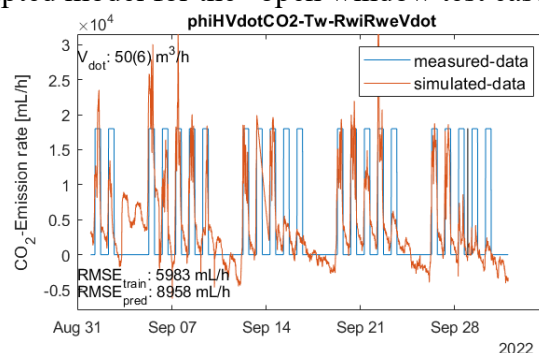


Figure 9: Result for adapted 2C+V model outputting CO₂ emission rate for “open window fault” case. “Measured value” refers to the naïve occupancy assumption. A validation with an actual measured occupancy profile has not been performed yet.

5.3 Accounting variable ventilation rates

As noted above, the 2C+V model has the limitation, that only a fix/static ventilation rate can be modelled and identified. Introducing model states with a modified external temperature

and modified external CO₂ concentration which use the ventilation flow control signal to alter the measured values accordingly, are being tested to account variable ventilation rates.

6 CONCLUSIONS

This paper documents work-in-progress for combining a thermal grey-box model with a simple ventilation mass balance model, i.e. a model that reproduces the CO₂ concentration in a room. Both models are coupled via the ventilation rate. The models are applied to an office room of a case study building. The model parameters are identified with measurement data for a four-weeks long training period. Their values compare well with design values from the energy certificate. The identified models are used to predict the timely evolution during a three-day long prediction period. By comparing residuals (measurement minus simulation) between training phase and prediction phase, this work investigates the model's capabilities to detect simple exemplary faults, like temperature or CO₂ sensor faults or (unintentionally) left-open windows. The preliminary results show that larger indoor temperature anomalies can be detected well with this approach. Anomalies in CO₂-concentration are also detectable but depend on the available occupancy estimation (or measurement). It should be noted that the herein investigated faults are simplified and additional testing is needed. Further investigations are underway to test possible adaptations to the presented approach to allow for better occupancy estimation and/or account variable ventilation rates.

7 ACKNOWLEDGEMENTS

This work was financed through the Austrian Research Promotion Agency (FFG) in the framework of the funding program "Stadt der Zukunft" by the Austrian Federal Ministry for Climate Action, Environment, Energy, Mobility, Innovation and Technology (BMK) (Grant Number 879437).

8 REFERENCES

- Bacher, Peder, and Henrik Madsen. 2011. "Identifying Suitable Models for the Heat Dynamics of Buildings." *Energy and Buildings* 43(7):1511–22. doi: 10.1016/j.enbuild.2011.02.005.
- Bauwens, Geert, Katia Ritosa, and Staf Roels. 2021. *IEA EBC Annex 71: Building Energy Performance Assessment Based on in-Situ Measurements - Physical Parameter Identification*.
- Kim, Woohyun, and Srinivas Katipamula. 2018. "A Review of Fault Detection and Diagnostics Methods for Building Systems." *Science and Technology for the Built Environment* 24(1):3–21. doi: 10.1080/23744731.2017.1318008.
- Reynders, Glenn, Arash Erfani, and Dirk Saelens. 2021. *IEA EBC Annex 71: Building Energy Performance Assessment Based on In-Situ Measurements - Building Behaviour Identification*. KU Leuven.
- Rojas, G., S. Metzger, M. Blöchle, M. Šipetić, R. Jenewein, and S. Öttl. 2023. *IEA Energie in Gebäuden Und Kommunen (EBC) Annex 71 : Bewertung Der Gebäudeenergie- Effizienz Mit Hilfe Optimierter in Situ Messverfahren*.

Evaluation of supply temperature set-points and airflow imbalance using smart ventilation data

Kevin Michael Smith*¹, Jakub Kolarik¹

*¹ Technical University of Denmark,
Department of Civil and Mechanical Engineering
Brovej, Building 118
Kongens Lyngby 2200, Denmark*

KEYWORDS

Smart ventilation, Continuous commissioning, Digitalisation, Heat recovery, Automatic balancing

1 BACKGROUND

The installation of central mechanical ventilation with heat recovery (MVHR) in renovated apartment buildings presents considerable challenges, primarily due to insufficient space for ductwork. Consequently, many renovation projects are installing decentralised MVHR units, catering to individual apartments. Many of these devices offer the option of communicating with their controllers via Modbus, BACnet, KNX, or internet APIs, provided the necessary resources are available for the connection. Unlike central MVHR units, which offer the opportunity for centralised commissioning and maintenance, these decentralised units are frequently located in suspended ceilings or cabinets in refurbished apartments. This placement makes them challenging to access without a coordinated effort. Therefore, monitoring these decentralised MVHR units via available communication links – a concept commonly referred to as 'smart ventilation' - proves to be more convenient and less labour-intensive. Most MVHR units come with standard data sets, which typically include supply and exhaust fan signals and temperature sensors located before and after the heat exchanger for both the supply and exhaust airflows. The controller uses these temperature measurements, as depicted in Figure 1, to adjust the bypass damper's opening position, thereby modulating heat recovery. This adjustment aims not only to achieve the specified supply temperature set-point but also to prevent frost accumulation by raising the exhaust temperature when necessary. During the commissioning phase, the installer seeks to balance the supply and exhaust airflows to maximise heat recovery and minimise infiltration or exfiltration. However, reaching the specified airflows for each zone proves difficult. Even when achieved, this balance could degrade over time due to dust accumulation on components or occupants' interference with the valves. 'Smart ventilation' data can be used to optimise heat recovery by ensuring balanced supply and exhaust airflows. By performing an energy balance, 'virtual sensors' can be created to indicate the airflow balance. In this study, we utilized 'smart ventilation' data from 100 apartments in Frederikshavn, Denmark, to assess the supply temperature set-points and airflow balance.

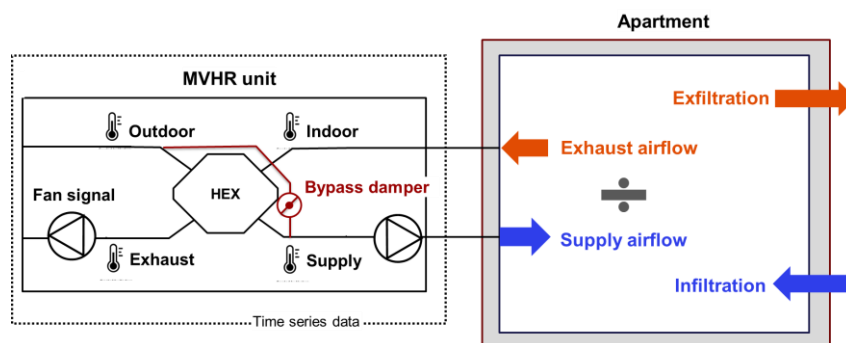


Figure 1. Common data from a residential AHU with a plate heat exchanger.

2 METHODS

We aimed to create a simple indicator assessing heat recovery. We started with the energy balance for heat transfer in the exchanger, where $Q_{supply} = \dot{m}_{supply} c_p (T_{supply} - T_{outdoor})$ was set equal to $Q_{exhaust} = \dot{m}_{exhaust} c_p (T_{indoor} - T_{exhaust})$. The validity of this equivalence depends on four key assumptions: (1) All mechanically driven supply and exhaust airflow pass through the heat exchanger. (2) The temperature changes are large enough to offset measurement errors. (3) The ratio of volume flows remains constant. (4) There is no condensation inside the heat exchanger. As such, we only consider data satisfying the corresponding conditions: (1) The bypass damper is fully closed. (2) The outdoor temperature is less than 10°C. (3) The exhaust fan signal remains un-boosted. (4) The exhaust temperature is above the dewpoint temperature of the indoor air. Ventilation heat exchangers have high nominal efficiencies, so the temperature difference between airflows is small longitudinally. Therefore, we assume the supply and exhaust airflows have roughly similar specific heat capacities (c_p) and air densities (ρ). This led to Equation 1 – the flow ratio (Fr) of supply and exhaust airflows.

$$Flow\ ratio, Fr = \frac{\dot{m}_{supply}}{\dot{m}_{exhaust}} = \frac{\rho_{supply}}{\rho_{exhaust}} \cdot \frac{\dot{V}_{supply}}{\dot{V}_{exhaust}} = \frac{(T_{supply} - T_{outdoor})}{(T_{indoor} - T_{exhaust})} \quad (1)$$

In the Danish temperate climate, the outdoor temperatures rarely rise above freezing, suggesting that the bypass damper should remain closed for nearly the entire heating season. If the bypass damper is open excessively, it could indicate that the supply temperature setpoint is too low, triggering unnecessary bypass of heat recovery (or an undetected sensor fault). We aimed to create a bar plot wherein the magnitude of each bar shows the balance of airflows while each bar's colour indicates whether the applied filters removed most (red) or very little (green) of the data. A red bar indicates an excessive opening of the bypass damper, potentially due to low supply temperature set-points or other errors. It also suggests a high degree of uncertainty, arising from the invalidity of the previously stated assumptions.

3 MAIN RESULTS AND CONCLUSIONS

Figure 1 shows the constructed indicators for all 100 ‘smart ventilation’ units in an apartment building. It indicates that the ventilation is poorly balanced in most units. Several apartments had most of their data filtered out (red), possibly due to low supply temperature setpoints or other faults. The next step involves manually investigating these problematic apartments.

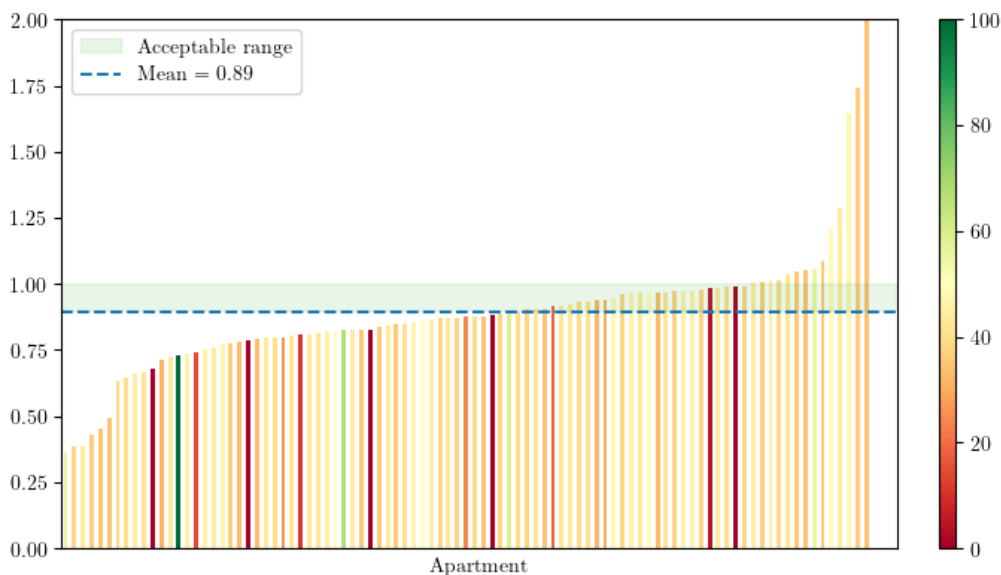


Figure 1. Flow ratios for 100 ‘smart ventilation’ units.

Technologies in balanced ventilation systems to maintain optimal performance in energy and comfort

Bart Cremers

*Zehnder Group
Lingenstraat 2
8028 PM Zwolle, The Netherlands
bart.cremers@zehndergroup.com*

SUMMARY

Measurements of the installed base of balanced ventilation systems in houses often show that optimal performance is not achieved. The installed base however, is a mix of various generations of units that have been developed over the years, starting in 1980. As a result, energy benefit and perceived comfort for residents is underestimated. Since 2015, improved knowledge has led to new technologies that have been implemented in the newest generation balanced ventilation units. In the following paragraphs, seven technologies are described that guarantee the fresh air flow as well as the balance between the supply and return air stream. This ensures a constant refreshment, an optimal energy benefit of recovery and resultingly a better comfort of the supplied fresh air flow for occupants.

KEYWORDS

Balanced ventilation, optimal heat recovery, adaptive comfort, modulating bypass, season detection

1.1 Automated fan speed adjustment during commissioning

For older units, produced before 2015, the factory-default fan speeds of supply and return fans should be adjusted to the resistances in the supply and return ducts during commissioning. This ensures the flow rates match the desired values. Adjusting the fan speeds is often omitted, forgotten, or done incorrectly by installers. In the contrary, newer units have an automated calibration cycle that 'senses' the resistances. Fan speeds are then automatically adjusted so that both airflows have the desired flow rate, and are balanced. This technology prevents incorrect settings, and therefore unnecessary noise, as well as unbalance and cold supply temperatures in winter.

1.2 Balance in mass flow rate rather than volume flow rate

In older units, airflow balance depends on the installer's measurements and fan speed settings. When temperature differences occurred between supply airflow and return airflow, the installer's measurement was not precise enough to balance the mass flow. Newer units continuously adjust mass airflow rates. This takes into account temperature differences. As a result, the mass flow is always balanced and there is optimal energy exchange between the airflows. This prevents varying recovery efficiency with varying temperature differences.

1.3 Automated fan speed correction (Flow Control)

In older units, the fan speed does not change over time. New units have a control for constant mass flow rate with changing system resistances. The resistance may change with condensation in the exchanger (medium-term) and with filter degradation (long-term). To avoid unwanted noise changes, short-term resistance changes due to for example wind pressure are not

corrected. This automatic speed control maintains optimal recovery efficiency (and thus prevents draughts) even if outdoor temperatures get colder and/or filters get dirty.

1.4 Comfort levels instead of values

Older units have a "comfort temperature" setting. This setting makes sure passive cooling by activation of a bypass comes into effect when the return temperature rises above the comfort temperature. The value of this comfort temperature can be adjusted by a resident, but is often misunderstood, leading to excessively low or high values. Newer units use a temperature profile (COOL, NORMAL or WARM). In COOL, the bypass is activated more often for passive cooling. With WARM, on the other hand, the bypass is activated less. This prevents incorrect settings by residents and is consistent with a resident's psychological well-being.

1.5 Adaptive comfort technology

Older units have a "comfort temperature" setting that does not change over time unless manually adjusted by the resident. Throughout the year, therefore, the comfort temperature is always the same. Newer appliances use three temperature profiles (COOL, NORMAL and WARM), within which the "comfort temperature" adapts to prevailing outdoor temperatures. This makes use of adaptive comfort, where people accept a slightly higher indoor temperature when outdoor temperatures are high. This prevents incorrect adjustment of the comfort temperature and therefore incorrect deployment of the bypass. In short, automatically more comfort for the resident.

1.6 Modulating bypass technology

Older units had a bypass that alternated between fully closed (maximum recovery) or fully open (maximum passive cooling). At outdoor temperatures below 13°C, the bypass could not open because condensation could occur directly on the outside of the supply ducts. Newer units have a bypass that can be continuously controlled from maximum recovery to full passive cooling. This controls the supply temperature between the outdoor and indoor temperatures. This allows passive cooling to be applied in well-insulated houses, even at outdoor temperatures lower than about 13°C, without condensation forming on the outside of the supply ducts. This prevents unnecessary and unwanted heat recovery in well-insulated houses in the mid-season and summer seasons.

1.7 Season detection

Older units assumed a fixed limit for the start of the heating season, regardless of the location of the house, its orientation to the sun, the degree of insulation and the resident's wishes. Newer units have settings for heating and cooling season limits. The default value for these limits can be adjusted according to the specific conditions of the home and the resident's wishes. In better-insulated houses, this prevents the bypass from being unused for a long time because the unit thinks that heating is still going on in the house.

Building and ductwork airtightness in Norway: national trends and requirements

Tormod Aurlien*¹

*1 Norwegian University of Life Sciences
Elizabeth Stephansens v. 15,
1430 Ås, Norway*

**Corresponding author: tormod.aurlien@nmbu.no*

FOREWORD

The AIVC is preparing a series of VIP on national regulations and trends in airtightness for various countries (numbered VIP 45.XX), detailing for both building and ductwork airtightness:

- the national requirements and drivers (regulations, incentives, justifications and sanctions)
- whether it is taken into account in the energy performance calculations and how;
- the test protocol (testers qualifications, national guidelines, requirements on measuring devices);
- the tests already performed and whether there is a results database;
- key documents.

This presentation focuses on the airtightness trends in Norway.

KEYWORDS

Building airtightness, ductwork airtightness, regulation, trends, Norway

1 BUILDING AIRTIGHTNESS

Building airtightness has been important for centuries in Norway, being a cold and windy nation. Quantifying airtightness of building came to our country around 1980, inspired from Sweden. The oil crisis in 1973 played an important role and European energy directives have played a central role, even though Norway only link to EU through the EUS-treatment.

For detached houses, requirements have changed gradually in steps from $n_{50} \leq 4$ /h to the ambitious level of $n_{50} \leq 0.6$ /h about 10 years back in time. Dwellings in general may still be documented according to a simplified «measures method», where $n_{50} \leq 0.6$ /h is the target value, but a maximum value of $n_{50} \leq 1.5$ /h is still allowed, if there is documentation of other extra energy means compensating for this. In general, all buildings must have airtightness $n_{50} \leq 1.5$ /h. For “other buildings” than dwellings this is unchanged since 1980; which is not very ambitious.

The official view in Norway is that all new buildings shall be tested, but in practice the percentage of new buildings being tested is probably much less than 100%. Ambitious n_{50} values are easy to achieve for large buildings, but very tricky for small apartments. A consequence is that contractors avoid measuring single flats in a block, and instead measure the whole building, with all doors to the stairway open.

2 DUCTWORK AIRTIGHTNESS

The energy legislation in Norway requires that balanced mechanical ventilation with heat recovery has to be used for all new buildings.

Airtightness of ventilation ducts is probably not an important topic in Norway, the way we build: We use spiro ducts with gaskets and the duct system is usually within the heat-insulated building construction. Small leakages may more be a topic related to internal vent adjustment and to a very small degree influencing energy or air quality.

Building and ductwork airtightness in the Netherlands: national trends and requirements

Niek-Jan Bink*¹, Rob Dam², and Marcus Lightfoot³

*1 ACIN instrumenten
Handelskade 76
2288 BG Rijswijk, The Netherlands
Corresponding author: NJ.Bink@acin.nl

*2 Retrotec Europe
Hardermaat 12
7244 PZ Barchem, The Netherlands*

*3 Ubbink Centrotherm group
Verhuellweg 9
6984 AA Doesburg, the Netherlands*

FOREWORD

The AIVC is preparing a series of VIP on national regulations and trends in airtightness for various countries (numbered VIP 45.XX), detailing for both building and ductwork airtightness:

- the national requirements and drivers (regulations, incentives, justifications and sanctions)
- whether it is taken into account in the energy performance calculations and how;
- the test protocol (testers qualifications, national guidelines, requirements on measuring devices);
- the tests already performed and whether there is a results database;
- key documents.

This presentation focuses on the airtightness trends in the Netherlands.

KEYWORDS

Building airtightness, ductwork airtightness, regulation, trends, Netherlands

1 BUILDING AIRTIGHTNESS

In the last few years there has been an increased level of awareness on the topic of climate change, and the required energy transition in the Netherlands. Laws and regulations such as the quality law (wet kwaliteitsborging) have been delayed but are slowly being implemented.

The Dutch Construction Law (Bouwbesluit 2012 article 5.4) provides an overall maximum air permeability of 0.2 m³/s (200 l/s for a maximum of 500m³ of building volume, after which the rate pro rata considered for larger volumes). This value should be measured as per the NEN 2686 standard. This leakage rate is not considered stringent, but is considered as a minimum baseline.

Generally speaking, contractors are more aware of the requirements of airtightness, but a knowledge gap still exists for some. Certain contractors are very active in improving their quality, others act as if they have never even heard of airtightness.

2 DUCTWORK AIRTIGHTNESS

In the Netherlands, there is currently no legal requirement to test the airtightness of ventilation systems. For residential building testing is close to zero. The testing of non-residential

construction is fully controlled by LuKa, the Dutch association of air duct manufacturers. They are actively involved in promoting the quality and performance of air duct systems in the Netherlands.

LUKA has developed its own quality assurance program, which includes testing and certification of air duct systems. This program aims to ensure that the manufactured air ducts meet the required standards and specifications, including aspects related to airtightness. While LUKA's certification is not a legal requirement, it is widely recognized in the industry and can provide assurance of the quality and performance of air duct systems. Builders and contractors often prefer to use LUKA-certified air ducts to ensure compliance with industry standards and best practices. Therefore, although not legally mandated, the involvement of LUKA and their certification program can play a significant role in promoting and ensuring the airtightness and quality of ventilation systems in the Netherlands. LUKA closely cooperates with the independent institute TÜV Rheinland Nederland B.V.. The quality officers of TÜV Rheinland Nederland B.V do regular checks on compliance with the standards.

Airtightness testing is now part of the overall energy performance calculation of a building according to the NTA 8800:2022. This NTA is aimed at improving the energy efficiency of buildings and reducing energy consumption.

Building and ductwork airtightness in Spain: national trends and requirements

Timo Hoek¹, Irene Poza-Casado^{*2}, and Sergio Melgosa³

*1 Carrer del Pintor Sisquella, 14,
08870 Sitges, Barcelona, Spain*

*2 University of Valladolid
Plaza de Santa Cruz, 8,
47002 Valladolid, Spain*

**Corresponding author: irene.poza@uva.es*

*3 eBuilding
Letonia 5, P4 5ªA
28760, Tres cantos, Spain*

FOREWORD

The AIVC is preparing a series of VIP on national regulations and trends in airtightness for various countries (numbered VIP 45.XX), detailing for both building and ductwork airtightness:

- the national requirements and drivers (regulations, incentives, justifications and sanctions)
- whether it is taken into account in the energy performance calculations and how;
- the test protocol (testers qualifications, national guidelines, requirements on measuring devices);
- the tests already performed and whether there is a results database;
- key documents.

This presentation focuses on the airtightness trends in Spain.

KEYWORDS

Building airtightness, ductwork airtightness, regulation, trends, Spain

1 BUILDING AIRTIGHTNESS

Building airtightness has not traditionally been a major priority in the Spanish construction industry. Because most dwellings did not have any controlled ventilation systems, air infiltration has been a supplemental source of air renewal together with window airing, that contributed to indoor space air renewal. However, current mandatory controlled ventilation strategies have changed the scenario.

The past few years have been key regarding building airtightness in Spain. For the first time, the recent incorporation of whole minimum building airtightness requirements on the last update of Basic Document for the Energy Saving in Buildings (DB HE1), although not too stringent, can be seen as a way to raise awareness on this parameter and familiarize with the existing tools and techniques to handle it, which encourages positive progress towards energy-efficient buildings.

It is important to note that airtightness testing is not mandatory to prove compliance and usually reference values are used in the energy performance calculation. So far, the main drivers for building airtight and testing have been certifications like Passivhaus, BREEAM or LEED. These certifications have given way to a broader knowledge on the airtightness tests.

2 DUCTWORK AIRTIGHTNESS

Ductwork airtightness is still an issue that does not entail much concern in the construction sector.

Currently, ductwork airtightness is required by “Reglamento de instalaciones térmicas de los edificios” (RITE). Section IT 1.2.4.2.3 provides airtightness requirements, which specifies that the ductwork must comply at least with Class B values. This is in force since 2007 and the requirement makes reference to new buildings and retrofitted ones.

On Section 2.2.5. of (RITE), airtightness tests are required while the system is still accessible for its testing according to UNE-EN 12599:01. However, this requirement is somehow recent and still there is not much concern among construction agents. Therefore, in practice, ductwork is still not always tested. There are no sanctions if a ductwork does not comply with the requirement.

Building and ductwork airtightness in Latvia: national trends and requirements

Andrejs Nitijevskis¹, Vladislavs Keviss¹, and Nolwenn Hurel*²

*1 IRBEST Ltd
Kurzemes prospekts 84 - 133
Riga, Latvia*

*2 PLEIAQ
2 Avenue de Mérande
73000 Chambéry, France*

**Corresponding author: nolwenn.hurel@pleiaq.net*

FOREWORD

The AIVC is preparing a series of VIP on national regulations and trends in airtightness for various countries (numbered VIP 45.XX), detailing for both building and ductwork airtightness:

- the national requirements and drivers (regulations, incentives, justifications and sanctions)
- whether it is taken into account in the energy performance calculations and how;
- the test protocol (testers qualifications, national guidelines, requirements on measuring devices);
- the tests already performed and whether there is a results database;
- key documents.

This presentation focuses on the airtightness trends in Latvia.

KEYWORDS

Building airtightness, ductwork airtightness, regulation, trends, Latvia

1 BUILDING AIRTIGHTNESS

The attention to building airtightness in Latvia started in 2010 when the European Union (EU) started to require blower door tests for buildings renovated with EU funds.

In 2015, Latvian Construction Standard (LBN 002-01) on thermal insulation and airtightness became stricter, with the following requirements in force for residential houses, homes for the elderly, hospitals, kindergartens, and public buildings:

- $q_{50} \leq 3,0 \text{ m}^3/(\text{h}\cdot\text{m}^2)$ for buildings with natural ventilation (airing);
- $q_{50} \leq 2,0 \text{ m}^3/(\text{h}\cdot\text{m}^2)$ for buildings with mechanical ventilation;
- $q_{50} \leq 1,5 \text{ m}^3/(\text{h}\cdot\text{m}^2)$ for buildings with mechanical ventilation equipped with a heat recovery system;
- $q_{50} \leq 4,0 \text{ m}^3/(\text{h}\cdot\text{m}^2)$ for industrial buildings.

There is however no mandatory justification that these requirements are achieved. And these required airtightness values are used as defaults values in the energy calculation, still without required justification, which is not a good incentive for airtightness tests.

In 2021 the government recommended to provide air tightness tests for the commissioning of all public buildings larger than 5000 m^3 , so about 70-80% of public buildings are tested, but probably only 5-10% of industrial buildings and 5-15% of dwellings.

2 DUCTWORK AIRTIGHTNESS

If awareness on building airtightness is emerging in Latvia, the ductwork airtightness is not really taken into account so far. There are no national regulations or guidelines on this subject, so there are no requirements on the airtightness level of ductworks.

There are only rare cases in which customers initiate a ductwork airtightness test. There are no data collected on these tests to quantify them and follow their evolution with time.

Air tightness and its impact on energy consumption in multi-family residential buildings in Montenegro

Esad Tombarević^{*1}, Igor Vušanović¹ and Miloš Krivokapić¹

*1 University of Montenegro, Faculty of Mechanical Engineering
Džordža Vašingtona bb
81000 Podgorica, Montenegro*

**Corresponding author: esad.tombarevic@ucg.ac.me*

Presenting author: Esad Tombarević

ABSTRACT

Airtightness is of key importance, both for indoor thermal comfort and for energy efficiency of buildings. Although formally regulated by the rulebook on minimum energy efficiency requirements for buildings, airtightness is not properly addressed in practice in Montenegro. Airtightness measurements are not mandatory, so there is no data in this regard for the building stock so far.

The paper presents the results of blower door measurements on a limited sample of apartments in multi-family residential buildings. Measurements were carried out in accordance with the ISO 9972:2015 standard. The aim of the measurements is to have an idea of the state of the buildings in Montenegro in terms of air permeability of their envelope, to determine which elements of the envelope contribute the most to infiltration and what is the potential of window replacement as an air tightening measure. The results of the measurements unequivocally showed that air tightness depends mostly on the type, quality of installation and maintenance of the windows. In one of the apartments, blower door measurements with wooden windows before and PVC windows after renovation showed that window replacement is an effective measure of increasing air tightness, which brought the number of air changes per hour at the reference pressure difference within the limits required by the rulebook.

In order to assess the energy impact of air tightness, energy consumption calculations were carried out for one of the apartments in accordance with the DIN 18599 standard, varying the climatic conditions, the U-value of the thermal envelope and the level of air tightness. The results of the calculations showed that the increase in air tightness is an effective energy efficiency measure, which achieves significant savings in energy consumption for heating, while savings for cooling are negligible. Furthermore, it is concluded that relative savings are significantly higher in buildings with an improved thermal envelope, located in a colder climate zone.

KEYWORDS

Air tightness, blower door, energy consumption, residential buildings, windows replacement

1 INTRODUCTION

At the local, regional and global level, various measures are being implemented to combat climate change. The European Union is leading the way in this, showing a strong determination to reduce greenhouse gas emissions. The well-known 2020 climate and energy package set by EU leaders in 2007 had three key targets: reducing GHG emissions by 20% compared to the 1990 level, increasing the share of energy from renewable sources to 20% and reducing energy consumption by 20% by applying energy efficiency measures. The European Green Deal, approved in 2020 is even more ambitious, setting an overarching aim

of making the European Union climate neutral by 2050. It is clear that the building sector is crucial for reaching the mentioned energy and environmental goals, as it is responsible for 40% of EU energy consumption and 36% of energy-related GHG emissions.

Increasing attention is now being paid to the air-tightness of the building envelope, given that strict requirements for energy efficiency cannot be achieved just by increasing the thickness of the insulation and installing more efficient heating systems.

Much more attention is paid to air tightness in countries in colder regions. In the USA, for example, air tightness of buildings has been developed as an area of research for decades and there are databases with the results of thousands of fan pressurization tests (Sherman & Dickerhoff, 1998). Air tightness is also extensively regulated and researched in countries of Northern and Central Europe. Examples include studies conducted in Finland (Jokisalo, Kurnitski, Korpi, Kalamees, & Vinha, 2009), Ireland (Sinnot & Dyer, 2012) and the UK (Pan, 2010).

In countries with milder climate such as Montenegro, heat losses due to infiltration are relatively smaller, so the problem of air tightness is given significantly less attention. However, recently the results of several studies in the countries of Mediterranean Europe were published: Greece (Sfakianaki, et al., 2008), Italy (D'Ambrosio Alfano, Dell'Isola, Ficco, & Tassini, 2012), Spain (Feijó-Muñoz, et al., 2018) and Portugal (Pinto, Viegas, & de Freitas, 2011). Studies on the assessment of the impact of air tightness on energy consumption in countries with milder climate are even scarcer. One Spanish study (Poza-Casado, Meiss, Padilla-Marcos, & Feijó-Muñoz, 2021) report that in the Mediterranean provinces the energy impact of infiltration is in the range 8.61–16.44 kWh/m²year for heating and significantly lower for cooling.

Although air-tightness in Montenegro is formally regulated by the rulebook on minimum energy efficiency requirements for buildings, measurements are not carried out and it is not known what the actual condition of building envelopes, whether old or new, is in this regard. The aims of the study, the results of which are presented in this paper, are: to get an idea of the state of the envelope of residential buildings in Montenegro in terms of air tightness, to determine which element of the envelope contributes the most to infiltration, to determine how much air tightness can be improved by replacing windows and finally, how different levels of air tightness affect energy consumption for heating and cooling.

2 BACKGROUND

Air tightness as the main envelope property impacting infiltration is usually defined as the flow of air that infiltrates the building at certain pressure difference, usually 50 Pa. The standard procedure for determining the airtightness of building envelope is the fan pressurization method. The procedure commonly known as the blower door test is explained in detail in the standard ISO 9972:2015 (International Organization for Standardization, 2015). It consists in placing a fan on the door which generates pressure difference across the envelope. The more leaky the building envelope, the more flow will be required to achieve the given pressure difference. The speed of the fan is varied so that pressure differences in the range of 10 to 75 Pa are generated, and the relationship between pressure difference Δp and air flowrate \dot{V} can be represented by a power law as:

$$\dot{V} = c_L \Delta p^n, \quad (1)$$

where c_L is the air leakage coefficient and n is the air flow exponent.

The generally adopted reference pressure difference is 50 Pa, since it is large enough so that the measurement is not affected by the weather conditions and small enough to be achieved in most buildings using blower door fan. In order to be able to compare buildings with each

other, metrics are defined that normalize air leakage at the reference pressure difference with something that scales with the size of the building. An overview of the metrics with their definitions is given in Table 1.

Table 1: Summary of air leakage metrics

Metric and definition	Equation	Unit
Air leakage rate at the reference pressure difference of 50 Pa, \dot{V}_{50}	$\dot{V}_{50} = C_L(50 \text{ Pa})^n$	m^3/h
Air change rate at the reference pressure difference of 50 Pa, n_{50} The air change rate at the reference pressure difference of 50 Pa, n_{50} , is calculated by dividing the air leakage rate at the reference pressure difference of 50 Pa, \dot{V}_{50} , by the internal volume, V .	$n_{50} = \frac{\dot{V}_{50}}{V}$	h^{-1}
Air permeability at the reference pressure difference, q_{50} The air permeability at the reference pressure difference of 50 Pa is calculated by dividing the air leakage rate at 50 Pa, \dot{V}_{50} , by the envelope area A_E .	$q_{50} = \frac{\dot{V}_{50}}{A_E}$	$\text{h}^{-1}\text{m}^{-2}$
Specific leakage rate at the reference pressure difference, w_{50} The specific leakage rate at the reference pressure difference of 50 Pa is calculated by dividing the air leakage rate at 50 Pa by the net floor area A_F .	$w_{50} = \frac{\dot{V}_{50}}{A_F}$	$\text{h}^{-1}\text{m}^{-2}$
Effective leakage area, ELA Effective leakage area is the area of a fictitious orifice that allows the same air flow as the building envelope at the pressure difference of 4 Pa.	$ELA = c_L 4^{n-0.5} \sqrt{\frac{\rho}{2}}$	m^2

3 MEASUREMENT OF AIRTIGHTNES ON A LIMITED SAMPLE OF APARTMENT BUILDINGS IN MONTENEGRO

The blower door tests were performed using Minneapolis Blower Door Model 4.1, product of BlowerDoor GmbH which has a flow range from 25 to 7800 m^3/h at 50 Pa. The fan was mounted on the front door. The calibrated fan was connected to the speed controller which is connected to the digital pressure gauge DG700 and a computer. The test was fully automated by the accompanying TECTITE Express software installed on the computer. The software processed the data, fit the regression curve through a set of points $(\Delta p, \dot{V})$, plotted the charts and calculated the airtightness metrics. Blower door fan mounted on the front door of one of the tested apartments is shown in Figure 1.



Figure 1: Blower door fan mounted on the front door of the apartment

In all tested cases, the apartments were kept depressurized for a certain period of time, during which the envelope was inspected to determine the most contributing leakage points. During all measurements, the requirements of the ISO 9972:2015 standard were met: the wind speed was less than 6 m/s and the product of the building's height and the indoor outdoor temperature difference was less than 250 mK.

The results of all blower door tests with calculated airtightness metrics are given in Table 2, while air leakage curves are shown in Figure 2.

Table 2: Results of the blower door tests

No.	Floor area A (m ²)	Volume V (m ³)	Year of construction	Air leakage rate V_{50} (m ³ /h)	Air change rate n_{50} (h ⁻¹)	Specific leakage rate w_{50} (m ³ /h/m ²)	Effective leakage area ELA (cm ²)	Building leakage curve		Windows type
								Air leakage coefficient c_L (m ³ /h/Pa ⁿ)	Air flow exponent n	
1	53	127	2006	1001	7.87	18.89	228.8	90.6	0.614	Wood
2	43	114	2011	679	5.95	15.78	148.5	57.4	0.631	Aluminium
3	58	162	2012	711	4.38	12.26	150.1	56.9	0.646	PVC
4	68	190	1963	1831	9.63	26.92	453.3	187.6	0.582	Wood
5	68	190	1963	1225	6.45	18.02	280.2	111.0	0.614	Wood/PVC
6	68	190	1963	305	1.60	4.48	63.1	23.6	0.654	PVC
7	85	227	1986	1418	6.25	16.69	334.5	134.8	0.602	Wood
8	85	227	1986	174	0.77	2.05	37.5	14.4	0.637	PVC

In all cases, most of the leaks were detected around the windows. The main air pathways were the gaps due to weak abutment of the sash on the frame, as well as between the frame and carcass opening. In addition, significant leakages were recorded around the wooden shutter boxes of the windows that had them. The current Montenegrin rulebook on minimum energy efficiency requirements stipulates that n_{50} must not exceed 3.0 h⁻¹ for buildings without mechanical ventilation and 1.5 h⁻¹ for buildings with mechanical ventilation. The results in Table 1 show that this condition is met in only 2 out of 8 cases, and in both cases, these are apartments where PVC windows were subsequently installed (blower door tests 6 and 8). In general, all apartments with wooden windows (blower door tests 1, 4 and 7) turned out to be poorly sealed. The reasons are the poor quality of the old wooden windows themselves, as well as their installation, the fact that they do not have rubber seals, age and lack of proper maintenance. The only analysed building with aluminium windows also performed poorly in terms of air tightness. The reason was the sliding balcony doors where brush seals cannot sufficiently prevent air leakage.

The potential of window replacement as a measure to increase air tightness can best be seen by comparing the blower door tests 4, 5 and 6, as well as the blower door tests 7 and 8.

4, 5 and 6 are three completely identical two-bedroom apartments in the same building. In apartment 4, all windows are original, wooden. In apartment 5, windows on the east side are still wooden, while those on the west side have been replaced with PVC windows. In apartment 6, all wooden windows were replaced with PVC windows. By partially replacing wooden windows with PVC ones, the air change rate decreases from 9.63 h⁻¹ to 6.45 h⁻¹, or by about 33%. By completely replacing the windows, the air change rate is reduced to 1.6 h⁻¹, that is, by 83%. In addition to the value of the number of air change rate, the replacement of the windows is reflected in the value of the air flow exponent, which indicates the size and shape of the dominant leaks. The value of the air flow exponent is 0.582 for wooden windows, 0.614 in the case when wooden windows are partially replaced with PVC ones and 0.654 in the case of PVC windows. Those values clearly indicate that by replacing the

windows there is a transition from leakage through short and relatively large openings to leakage through long and relatively narrow ones.

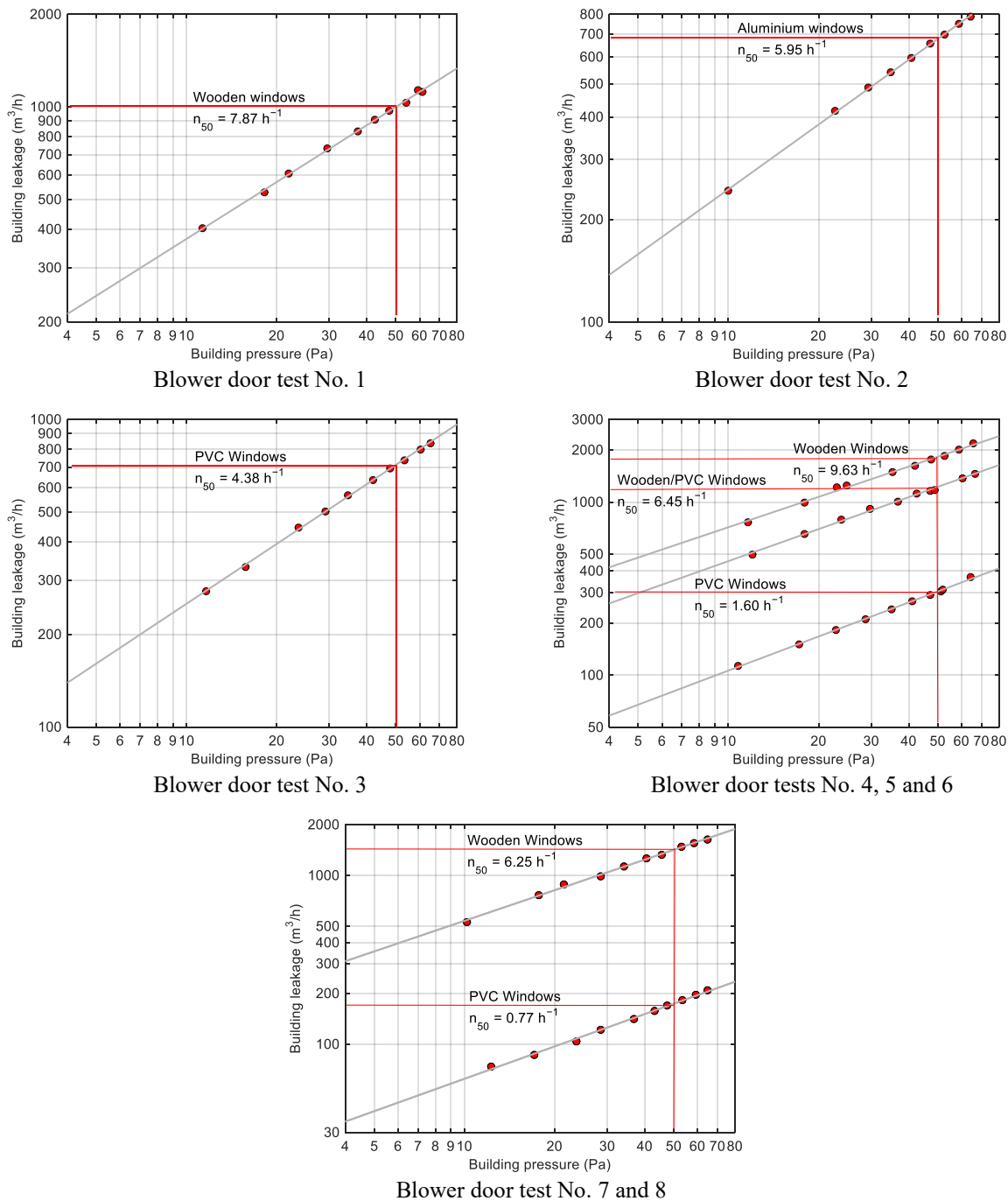


Figure 2: Air leakage curves (numbered in accordance with Table 2: Results of the blower door tests Table 2)

The most interesting blower door tests are those numbered 7 and 8. These are blower door tests conducted on the same three-bedroom apartment, before and after replacement of wooden windows with PVC windows. This apartment was convenient because the authors had the freedom to influence and interrupt the order and dynamics of the renovation works, to choose the windows to be installed and to supervise the quality of their installation. The building was materialized in the manner that was common for the last quarter of the 20th century. The external walls are uninsulated, mostly made of cast-in-place reinforced concrete. The former windows were wooden, casement type, double-glazed, where each pane was in its

own sash mounted on its own hinges and operated independently. Half of the windows and doors had roller shutters housed in wooden boxes. The windows did not have rubber seals. They were fully functional, although they lacked adequate maintenance. The new windows are made of Softline AD profile, a product of VEKA AG, Germany. These are five-chamber profiles, with a standard installation depth of 70 mm and with two seals. After the replacement, all windows were equipped with matching roller shutters of the same manufacturer. From the common diagram showing the leakage curves for blower door tests No. 7 and 8, it is clear that the air tightness was drastically improved by replacing the windows. The number of air changes at the reference pressure difference was reduced from 6.25 h^{-1} to 0.77 h^{-1} , i.e. by almost 90%, and now it not only meets the minimum requirement from the national regulation (3.0 h^{-1}), but also significantly approached the requirement for passive houses (0.6 h^{-1} in most countries).

Here, it is important to highlight that the objective was not to assess the complete building's airtightness or draw conclusions solely based on measuring the airtightness of a single apartment. When examining the airtightness of the entire building, several practical limitations arise. Often, the building's size makes it challenging to depressurize using a small blower door fan. Additionally, there may be numerous leaks in corridors, stairwells (such as elevator shafts, fire escape doors, basement, etc.) that are difficult to identify and control. Furthermore, accessing each individual apartment may be impractical if the building is already occupied. On the other hand, based on the measurement of airtightness of a single apartment, a general valid conclusion cannot be made about the airtightness of the entire building, because possible leaks that are not through the outer envelope but from the adjacent apartment or staircase would be taken into account even multiple times.

4 THE EFFECT OF AIR TIGHTNESS ON ENERGY CONSUMPTION

Energy use for heating and cooling was calculated using the national MEEC software for calculating the energy performance of buildings, developed by the Fraunhofer Institute for Building Physics. Software is based on German methodology for calculation of the net, final and primary energy demand for heating, cooling, ventilation, domestic hot water and lighting (German Institute for Standardization, 2018). The aim of energy calculations is to assess the effect of infiltration on energy consumption for heating and cooling, as well as the influence of the climate zone and the condition of the thermal envelope on the reduction of energy consumption due to the increase in air tightness. For this analysis, the usual systems used in Montenegro were adopted: biomass central heating system and multi-split cooling system.

The energy analysis was done for a three-room apartment (blower door test results 7 and 8 from Table 2). Calculations were made for both air tightness values. In order to analyse the influence of climatic conditions, calculations were made for all three climatic zones in Montenegro. Also, the calculations were made for the case when the building envelope is as it currently is and for the case when it is thermally improved so that it just meets the minimum requirements from the national regulation. The results of the calculations of delivered energy for heating and cooling before and after applications of measures to improve the thermal envelope and airtightness are given for all three climate zones in Table 3 and Figure 3.

For climate zone I (where the building is actually located), improving the air tightness by replacing the windows (reducing n_{50} from 6.25 h^{-1} to 0.77 h^{-1}) reduces the delivered energy for heating (including auxiliary energy) and cooling from $155.44 \text{ kWh/m}^2\text{year}$ to $142.63 \text{ kWh/m}^2\text{year}$, or by about 8.2%. Interestingly, almost all of the reduction in energy consumption is due to a reduction for heating, while the reduction for cooling is almost negligible. Relative contribution of the increase in air tightness to the reduction of energy consumption is even greater in the case when the building envelope is thermally insulated, and in that case it amounts to about 15.6%.

Increasing air tightness as a measure of energy efficiency has an even greater effect in regions with a colder climate. If the same building were to be located in the north of Montenegro (climate zone III), the delivered energy for heating and cooling is reduced by replacing the windows from 258 kWh/m²/year to 233.26 kWh/m²/year or by about 9.6%. In the case when the building is thermally insulated, increasing the air tightness results in a reduction in the delivered energy of as much as 20.9%.

The effect of different degrees of air tightness on the delivered energy for heating and cooling was also investigated by varying the number of air changes at the reference pressure difference of 50 Pa in the range from $n_{50}=1 \text{ h}^{-1}$ to $n_{50}=15 \text{ h}^{-1}$. It can be seen that with increasing air tightness, energy consumption for heating and cooling decreases linearly. By increasing n_{50} by a unit value, savings from 2.3 kWh/m²/year in climate zone I to 4.6 kWh/m²/year in climate zone III are achieved.

Table 3: Delivered energy for heating and cooling before and after the application of measures to improve the thermal envelope and air tightness

Climate zone	Building envelope	$n_{50} \text{ (h}^{-1}\text{)}$	Delivered energy (kWh/m ² /year)			
			Heating	Cooling	Auxiliary	Total
I	Existing	6.25	129.84	21.78	3.82	155.44
	thermal envelope	0.77	117.32	21.73	3.58	142.63
	Improved	6.25	63.60	12.67	2.68	78.95
	thermal envelope	0.77	51.57	12.67	2.37	66.61
II	Existing	6.25	196.01	8.84	4.85	209.70
	thermal envelope	0.77	176.70	9.06	4.61	190.37
	Improved	6.25	98.02	4.85	3.43	106.30
	thermal envelope	0.77	79.28	5.13	3.11	87.52
III	Existing	6.25	248.67	3.50	6.04	258.21
	thermal envelope	0.77	223.85	3.68	5.73	233.26
	Improved	6.25	112.25	1.49	3.92	117.66
	thermal envelope	0.77	87.95	1.75	3.41	93.11

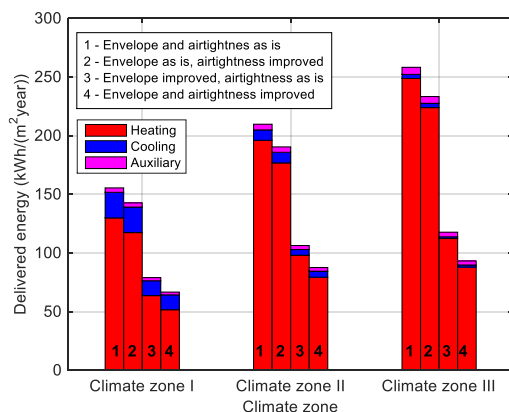


Figure 3: Delivered energy for heating and cooling

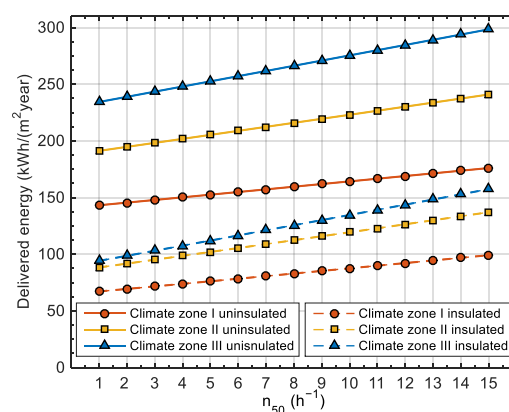


Figure 4: Delivered energy for heating and cooling as a function of n_{50}

It is important to acknowledge that when measuring the leakage of a single apartment's envelope using a blower door fan, the recorded results includes potential leaks that originate not only through the outer envelope, but also from the neighbouring apartments that are thermally conditioned. Consequently, there is a possibility that infiltration and the associated energy consumption might be slightly overestimated. However, the authors are convinced that these contributions are negligible considering the construction method and the fact that hand and smoke pen inspection during the depressurization did not indicate internal leakages.

Improving airtightness while neglecting adequate air exchange can result in poor indoor air quality. Among other things, there may be increased relative humidity; potentially leading to the formation of condensation and mould on interior walls if their temperatures fall below the dew point (the problem is more prominent when the envelope is not thermally insulated). In old buildings such as the one considered, there is often no ventilation system, except possibly extraction ventilation in kitchens and toilets, which is ineffective when, due to good airtightness, there is no possibility of sufficient air suction through the envelope. To mitigate these issues, regular window airing of the apartment becomes essential. However, experience from renovating existing buildings has shown that occupants often fail to modify their habits after airtightness improvements. It is worth emphasizing that when calculating energy consumption, the software adjusts the air change rate due to window airing as a function of infiltration and does not allow the total air change rate (infiltration plus window airing) to go below the value of 0.5 h^{-1} , which is widely accepted as a threshold value below which the perception of poor indoor air quality can occur.

The idea for future research is the use of whole-building energy simulation software such as EnergyPlus, which would enable the analysis of the impact of air tightness on infiltration and indoor air quality, above all on relative humidity.

5 CONCLUSIONS

The results of blower door tests on a limited sample of multi-family residential buildings in Montenegro indicate the poor performance of building envelopes in terms of airtightness and that this problem should be addressed in a way that it deserves. Examining the building envelope during the fan depressurization determined that windows are by far the most contributing cause of air leakage. In this respect, old wooden windows without rubber seals performed the worst. The replacement of windows proved to be an effective measure for increasing air tightness, which improves n_{50} almost to the standard applicable to passive houses.

The analysis of energy consumption at different levels of air tightness showed that with a decrease in air changes rate, energy consumption for heating is significantly reduced, while the reduction in energy consumption for cooling is practically negligible. Furthermore, in relative terms, the reduction of energy consumption due to the increase in air tightness is more pronounced in colder climate zone and when the thermal envelope of the building is improved by reducing its U-value. For the observed case study, with a reduction of n_{50} by a unit value, energy savings of $2.3 \text{ kWh/m}^2\text{year}$ are achieved when the apartment is located in climate zone I to $4.6 \text{ kWh/m}^2\text{year}$ when it is located in climate zone III.

The generality of the conclusions of this study is limited due to the fact that a relatively small sample of buildings was analysed. The idea for future research in this area is to consider a larger sample in order to obtain statistically credible results.

6 REFERENCES

- D'Ambrosio Alfano, F., Dell'Isola, M., Ficco, G., & Tassini, F. (2012). Experimental analysis of air tightness in Mediterranean buildings using the fan pressurization method. *Building and Environment*, 53, 16-25.
- Feijó-Muñoz, J., Poza-Casado, I., González-Lezcano, R., Pardal, C., Echarri, V., Assiego De Larriva, R., . . . Meiss, A. (2018). Methodology for the Study of the Envelope Airtightness of Residential Buildings in Spain: A Case Study. *Energies*, 11(4), 704.
- German Institute for Standardization. (2018). Energy Efficiency of Buildings—Calculation of the Net, Final and Primary Energy Demand for Heating, Cooling, Ventilation,

- Domestic hot Water and Lighting (DIN Standard V 18599). Retrieved from <https://www.beuth.de/de/vornorm/din-v-18599-1/293515783>
- International Organization for Standardization. (2015). Thermal Performance of Buildings—Determination of Air Permeability of Buildings—Fan Pressurization Method (ISO Standard 9972:2015). Retrieved from <https://www.iso.org/standard/55718.html>
- Jokisalo, J., Kurnitski, J., Korpi, M., Kalamees, T., & Vinha, J. (2009). Building leakage, infiltration, and energy performance analyses for Finnish detached houses. *Building and Environment, 44*, 377-387.
- Pan, W. (2010). Relationship between airtightness and its influencing factors of post-2006 new-build dwellings in the UK. *Building and Environment, 45*, 2387-2399.
- Pinto, M., Viegas, J., & de Freitas, V. (2011). Air permeability measurements of dwellings and building components in Portugal. *Building and Environment, 46*, 2480-2489.
- Poza-Casado, I., Meiss, A., Padilla-Marcos, M., & Feijó-Muñoz, J. (2021). Airtightness and energy impact of air infiltration in residential buildings in Spain. *International Journal of Ventilation, 20*, 258-264.
- Sfakianaki, A., Pavlou, K., Santamouris, M., Livada, I., Assimakopoulos, M., Mantas, P., & Christakopoulos, A. (2008). Air tightness measurements of residential houses in Athens, Greece. *Building and Environment, 43*, 398-405.
- Sherman, M., & Dickerhoff, D. (1998). Airtightness of U.S. dwellings. *ASHRAE Transactions, 104*, 1359-1367.
- Sinnot, D., & Dyer, M. (2012). Air-tightness field data for dwellings in Ireland. *Building and Environment, 51*, 269-275.

Resilient Cooling Technology Profiles from the EBC Annex 80

Peter Holzer¹

*1 Institute of Building Research & Innovation
Wipplingerstraße 23/3
1010 Vienna, Austria
peter.holzer@building-research.at*

SUMMARY

The world is facing a rapid increase of air conditioning of buildings. This is driven by multiple factors, such as urbanisation and densification, climate change and elevated comfort expectations together with economic growth in hot and densely populated climate regions of the world. The trend towards cooling seems inexorable therefore it is mandatory to guide this development towards sustainable solutions.

Against this background, it is the motivation of Annex 80 to develop, assess and communicate solutions of resilient cooling and overheating protection. Resilient Cooling is used to denote low energy and low carbon cooling solutions that strengthen the ability of individuals and our community as a whole to withstand, and also prevent, thermal and other impacts of changes in global and local climates. It encompasses the assessment and Research & Development of both active and passive cooling technologies.

A wide range of cooling technologies and solutions is already available. Nevertheless, significant joint efforts are still needed to really guide the mainstream development of cooling into the direction of sustainability and resilience. The Resilient Cooling Technology Profiles systematically assess existing cooling technologies, their potentials, limitations, qualities of resilience and identify barriers as well as conducive conditions to implementation. The aim is to provide well-structured collection of technology descriptions. The Technology Profiles shall support decision makers within the process of urban planning, building investment and building design with well-structured information to draw their attention towards resilient cooling options.

The list of technologies assessed is based on the list of technologies that have already been subject of the EBC Annex 80 State of the Art Report. A total of 16 Technology Profiles have been developed, each one having a maximum of 2500 characters and/or 5 pages, excluding images and tables. The following table presents a summary of the technologies covered.

Table 1: List of Resilient Cooling Technology Profiles

1.	Reducing Heat Loads to People and Indoor Environments
1.1.	Solar Shading Technologies
1.2.	Cool Envelope Materials
1.3.	Glazing Technologies
1.4.	Ventilated Façades
1.5.	Green Roofs and Green Façades
2.	Removing Heat from Indoor Environments (Production, Emission and Combined)
2.1.	Ventilative Cooling
2.2.	Thermal Mass Utilization
2.3.	Evaporative Cooling
2.4.	Sky Radiative Cooling
2.5.	Compression Refrigeration
2.6.	Adsorption Chillers
2.7.	Natural Heat Sinks
2.8.	Radiant Cooling

3.	Increasing Personal Comfort Apart from Space Cooling
3.1.	Comfort Ventilation and Elevated Air Movement
3.2.	Micro-cooling and Personal Comfort Control
4.	Removing Latent Heat from Indoor Environments
4.1.	Dehumidification

For every Technology Profile an author or team of authors within the Annex 80 group was assigned corresponding on the field of expertise.

Each Technology Profile is composed of 4 chapters. The description gives information about the physical principles, the function, and the characteristic applications of the specific Resilient Cooling Technology. Further, relevant subtypes are also listed. In the next chapter, called Key Technical Properties, information about relevant technical qualities and indicators of the specific Resilient Cooling Technology are given. Also, properties of the technology which are relevant when designing and/or purchasing the system are characterized. The third chapter, Performance and Application, gives information on the possible effect of the specific technology on the whole building performance, also describing synergies with others technologies. Special information is given, in which way the specific technology contributes to qualities of resilience in the meaning of the Annex 80's definition of resilience of a building against heat waves with or without power outage and against long-term climate change. Exemplary quantitative outputs from the simulation studies, for indicative building types in indicative climate zones in the midterm future is provided in most Technology Profiles. Information about the range of possible applications as well as about limitations of the specific technology is given, including aspects of climate dependency, building type, physical influences, such as internal gains, solar gains, ventilation, information about compatibility and incompatibility with other technologies and information about recent level of availability and about expected developments ahead. The final chapter, Further Reading, is offering links to further information to the reader if desired.

The outcome of the collaboration are 16 created Technology Profile Sheets giving recommendations for good implementation, commissioning and operation, barriers to application and opportunities. These shall support the Annex 80 mission of a rapid transition to an environment where resilient low energy and low carbon cooling systems are the mainstream and preferred solutions for cooling and overheating issues in buildings.

KEYWORDS

Cooling Technologies, Resilient Cooling, Resilience, Technology Profiles, Technology Descriptions

1 ACKNOWLEDGEMENTS

Authors

Bernhard Kling, University of Natural Resources and Life Sciences, Austria
 Constanze Rzhacek, University of Natural Resources and Life Sciences, Austria
 Dahai Qi, Université de Sherbrooke, Canada
 Dragos Bogatu, DTU, Denmark
 Emmanuel Bozonnet, La Rochelle Université, France
 Gamze Gediz Ilis, Gebze Technical University, Turkey
 Hilde Breesch, KU Leuven, Belgium
 Magdalena Wolf, University of Natural Resources and Life Sciences, Austria
 Mamak Pourabdollahtookaboni, Politecnico di Torino, Italy
 Michele Zinzi, ENEA, Italy
 Ongun Berk Kazanci, DTU, Denmark
 Peter Holzer, Institute of Building Research & Innovation, Austria
 Pierre Jaboyedoff, Effin'Art, Switzerland
 Ronnen Levinson, Lawrence Berkeley National Laboratory, USA
 Theofanis Psomas, Chalmers University of Technology, Sweden
 Thomas Keller, University of Natural Resources and Life Sciences, Austria
 Vincenzo Corrado, Politecnico di Torino, Italy

Resilient Cooling Guidelines from the IEA EBC Annex 80

Vincenzo Corrado¹, Theofanis Psomas², Philipp Stern³

*1 Politecnico di Torino
Corso Duca degli Abruzzi, 24
10129 Torino, Italy
vincenzo.corrado@polito.it*

*2 Chalmers University of Technology,
Chalmersplatsen 4
412 96 Gothenburg, Sweden
th.psomas@gmail.com*

*3 Institute of Building Research & Innovation
Wipplingerstraße 23/3
1010 Vienna, Austria
philipp.stern@building-research.at*

SUMMARY

The world is seeing a rapid increase of cooling of buildings¹. This is driven by multiple factors, such as urbanization and densification, climate change and elevated comfort expectations together with economic growth in hot and densely populated regions of the world. Additionally, disruptive events, such as extreme heat and heat waves are occurring more often and are expected to become a common phenomenon by mid-century. The trend towards cooling seems inexorable. It is therefore mandatory to steer this development towards sustainable solutions.

Against this background, it is the motivation of this guidebook to support practitioners to implement highly efficient, low-carbon, resilient cooling solutions, technologies, and strategies and contributing to a sustainable built environment. Resilient cooling aims to avoid heat stress to people and to maintain safe and operable conditions in buildings in the event of externally induced disruptions. It therefore goes beyond the upkeep of thermal comfort. This guidebook focuses on the design of resilient cooling against such disruptions.

The Resilient Cooling Guideline is based on findings of the international research project of the Energy in Buildings and Communities (EBC) programme Annex 80 Resilient Cooling of Buildings provided by a group of scientists from numerous institutions in various fields such as architecture, engineering, building science and building physics.

The Resilient Cooling Guideline addresses both free-running and mechanically cooled buildings and aims to answer the following question: How can I/we design a “resilient cooling” building?

For such, it is important to understand the underlying concepts of resilience regarding buildings, the available technological solutions, and the methods and tools used to evaluate options. Several chapters are sequenced to assist practitioners in these areas, as shown in Table 1.2. Two chapters provide practical examples of application of the guidelines for case-study buildings.

KEYWORDS

resilient cooling, guideline, framework, implementation

Table 1: Chapter overview

Chapter	Overview	Topics addressed
2	Provides a definition of disruptions and resilient cooling and explanations of the disruptive events identified in the context of resilient cooling design	✓ How can resilience be conceptualized? ✓ What is the definition of resilient cooling?
3	Provides concise information of resilient cooling solutions	✓ Which resilient cooling solutions exist to improve the building resilience (technology specific KPIs)? ✓ Which strategies and technologies to implement in building design process to be prepared for future disruptions? ✓ How to size these strategies considering future climate uncertainties? ✓ How to assess the performance of resilient cooling strategies prospectively?

¹ Birol, D. F. (2018). The Future of Cooling. 92.

4	Provides a selection of key performance indicators (KPI) that can be used for the evaluation of resilient cooling in buildings	✓ How can the resilience of a building/cooling system be quantified in the case of power outages and/or heat wave events?
5	Gives an overview of performance assessment methods and tools for the evaluation of operational and energy efficiency of buildings to identify potential improvements	✓ How to select input and output parameters for simulation and technology assessment? ✓ How to evaluate the resilience of a building against different disruptions? ✓ How to model specific resilient cooling technologies? ✓ How to calibrate a building simulation model?
6	Introduces climate data necessary for resilient cooling design	✓ How to account for future or extreme events? ✓ How to select future or extreme weather data sets for building simulation? ✓ How should future weather files be prepared for building simulations?
7	Discusses parameters related to people and their use of spaces, and incorporation of these issues in building performance simulation and analysis	✓ How do occupancy patterns impact building performance assessment? ✓ How does metabolic rate impact building performance assessment? ✓ What about internal gains?
8	Addresses performance influencing factors such as the setting of a building and its form, envelope characteristics or orientation.	✓ How does microclimate, location, landscape, and orientation affect building performance? ✓ What influence do fenestration design, shading systems and opaque envelope characteristics have on resilient cooling?

ACKNOWLEDGEMENTS

Editors

Vincenzo Corrado Politecnico di Torino, Italy
 Theofanis Psomas Chalmers University of Technology, Sweden
 Philipp Stern Institute of Building Research & Innovation, Austria

Authors

Abantika Sengupta, KU Leuven, Belgium
 Abhishek Gaur, Concordia University, Canada
 Amanda Krelling, Federal University of Santa Catarina, Brazil
 Anais Machard, CSTB, France
 Dahai Qi, Université de Sherbrooke, Canada
 Essam Elnagar, University of Liège, Belgium
 Fuad Baba, Université de Sherbrooke, Canada
 Gerhard Hofer e7, Austria
 Hilde Breesch, KU Leuven, Belgium
 Hua Ge, Concordia University, Canada
 Leticia Gabriela Eli, Federal University of Santa Catarina, Brazil
 Liangzhu (Leon) Wang, Concordia University, Canada
 Mamak Pourabdollahtookaboni, Politecnico di Torino, Italy
 Marcelo Salles Olinger, Federal University of Santa Catarina, Brazil
 Ongun Berk Kazanci, DTU, Denmark
 Peter Holzer, Institute of Building Research & Innovation, Austria
 Philipp Stern, Institute of Building Research & Innovation, Austria
 Radu Zmeureanu, Concordia University, Canada
 Rajat Gupta, Oxford Brookes University, UK
 Ramin Rahif, University of Liège, Belgium
 Shady Attia, University of Liège, Belgium
 Vincent Lemort, University of Liège, Belgium
 Vincenzo Corrado, Politecnico di Torino, Italy

Health risks of residential indoor and outdoor exposure to fine particle-bound phthalates

Jiayao Chen^{*1}, Francesco Pilla¹

1 School of Architecture, Planning and Environmental Policy, University College Dublin, Dublin, Ireland

**Corresponding author: jiayao.chen@ucd.ie*

ABSTRACT

We performed residential indoor fine particle (PM_{2.5}) measurement from 26 homes and three outdoor monitoring locations. Six PM_{2.5}-bound phthalate esters (PAEs) — including dimethyl phthalate (DMP), diethyl phthalate (DEP), di-n-butyl phthalate (DnBP), butyl benzyl phthalate (BBP), di(2-ethylhexyl) phthalate (DEHP), and di-n-octyl phthalate (DnOP) — were measured using a thermal desorption-gas chromatography/mass spectrometer method. Average concentrations of summation of six PAEs (Σ 6PAEs) in residential indoors (646.9 ng/m³) were slightly lower than the outdoor levels. DEHP was the most abundant PAE congener (80.3%) and was found at the highest levels, followed by BBP, DnBP, and DnOP. Strong correlations were observed between indoor DEHP with DnBP (rs: 0.88; $p < 0.01$), BBP (rs: 0.83; $p < 0.01$), and DnOP (rs: 0.87; $p < 0.01$). However, no apparent inter-correlations were shown for PAE congeners. Principal component analysis affirmed heterogeneous distribution and notable variations in PAE sources between residential indoor and ambient exposure. The results provide critical information for mitigation strategies, suggesting that PAEs from indoor and outdoor sources should be considered when exploring the inhalation risks of PAEs exposure.

KEYWORDS

Indoor air quality, particle-bound phthalates, DEHP

1 INTRODUCTION

Phthalate esters (PAEs) are a group of synthetic chemicals widely used in polyvinyl chloride (PVC) products and consumer products (such as commodities, medical products, cosmetics, and personal care products) and in households (building materials, furnishing, household goods) (Eichler, Cohen Hubal, & Little, 2019; Meeker, Sathyanarayana, & Swan, 2009). The negative impacts of PAEs on human health have raised global concerns due to their widespread use (IARC Working group, 2000; Katsikantami et al., 2016).

The International Agency for Research on Cancer and the United States Environmental Protection Agency (U.S. EPA) have classified DEHP and BBP as possible human carcinogens (Group B2 and Group C) (Caldwell, 2012; U.S. EPA, 1987). Given that a large proportion (> 85%) of daily time is spent indoors for the general population, research efforts have been made to address PAEs in different indoor microenvironments, including schools, offices, and residential homes (Otake, Yoshinaga, & Yanagisawa, 2004) and from indoor dust (Kang, Man, Cheung, & Wong, 2012). Buildings offer partial protection against ambient origin particulate pollutants, but indoor sources of PAEs enhance the potential for overall exposures. PAEs are physically bound to the plastic polymer and can be easily released into the ambient atmosphere and adhere to indoor particles and settled house dust (Clausen, Liu, Kofoed-Sorensen, Little, & Wolkoff, 2012; Zhang et al., 2021).

The research aims are to (1) examine the occurrence and variations of PM_{2.5}-bound PAE congeners (i.e., DMP, DEP, DnBP, BBP, DEHP, and DOP) in residential indoors; (2) characterize the within- and between- home variability of PAE congeners in residential indoor; (3) investigate the potential sources of PAEs in outdoor and residential indoors.

2 METHODOLOGY

PAE congener concentrations are reported in ng/m³. The Shapiro–Wilk test is used to check the normality of data. Seasonal variations of targeted PAEs were analysed using the Mann–Whitney U test. Differences in PAEs between ambient and residential indoor were calculated using *t* test. The mixed-effects model was used to calculate the within-home variance (σ^2_w) and between-home variance (σ^2_b) in residential indoors [37]. Statistical analyses were performed in R 3.5.1. A *p*-value < 0.05 was considered statistically significant.

Average indoor-to-outdoor (I/O) ratios for PAEs were calculated. We used Spearman's correlation coefficients (*r_s*) to characterize the associations of PAE congeners in and between exposure categories. In addition, we applied principal component analysis (PCA) to identify the potential sources of PAEs in ambient and residential indoor. PCA was performed by using IBM SPSS Statistics (Version 26.0, Armonk, NY, USA: IBM Corp).

3 RESULTS

3.1 Characteristics of PAEs in residential indoor

The reported Σ 6PAEs accounted for an average of $1.8 \pm 3.7\%$ indoor PM_{2.5} level (35.1 ± 19.0 $\mu\text{g}/\text{m}^3$). Daily residential indoor Σ 6PAEs concentrations varied from 0.8 to 3245.4 ng/m³ with an average of 646.9 ng/m³. Average DEHP (582.2 ng/m³) was presented at the highest level in residential indoor PM_{2.5}, followed by BBP (65.5 ng/m³), DnBP (27.1 ng/m³), and DnOP (20.5 ng/m³), accounting for 80.3%, 5.8%, 11.6%, and 1.6% of Σ 6PAEs concentrations, respectively. DMP and DEP concentrations were one to two orders of magnitude lower than other PAE congeners because these low-molecular-weight (LMW) PAEs tended to be present in the gas phase.

3.2 Ambient and residential indoor relationships

Comparing the average concentrations of PAEs indoors and outdoors, the average I/O ratios of PAE congeners and Σ 6PAEs ranged from 1.8 to 4.8 (Table 1). For paired data, indoor Σ 6PAEs exceeded the corresponding outdoor levels in 33.3%–50.0% of households. The median I/O ratios for PAE congeners < 1. As for individual PAE congeners, the highest average I/O ratio was shown for DnBP (4.8), and there were significant differences for outdoor with indoor DnBP exposure (*p* = 0.02), suggesting that DnBP sources are primary in some residential indoors. Further, DMP and DEP concentrations in different exposure categories demonstrated no significant differences but higher average and median I/O ratios compared with other PAE congeners.

3.3 Source identification

Significant correlations were shown between DMP and DEP (*r_s* = 0.72, *p* < 0.01) in residential indoor (Table 2). In addition, strong correlations for DEHP with DnBP (*r_s* = 0.88; *p* < 0.01), BBP (*r_s* = 0.83; *p* < 0.01), and DnOP (*r_s* = 0.87; *p* < 0.01) were shown in residential indoor. Similarly, strong correlations were demonstrated outdoors. There are moderate correlations between DnBP with DMP and DEP in residential indoor, suggesting that there might be common sources for these compounds. No such associations were found outdoors. Outdoor monitoring at fixed sites could not capture indoor origin pollutants.

We applied PCA to explore the sources of particle-bound PAEs in PM_{2.5} (Table 3). For residential indoor PAEs, three principal components accounted for 88.3% of the total variance. Component 1 explained 33.5% of the total variance and comprised BBP (0.90), DnOP (0.93), and a lesser extent of DEHP (0.58), indicating the influence of widely used plasticizers in PVC and other polymer products. Component 2 in residential indoors was loaded with DnBP (0.96)

and DEHP (0.76), which explained 28.0% of the total variance. Component 3 accounted for 26.8% of the data variance and had high loading of DMP and DEP, indicating the household's non-plastic sources (cosmetics, perfumes, and personal care products). The indoor sources of PAEs are more diverse and complicated compared to outdoor sources. It is difficult to disentangle these sources because of a lack of specific observations concerning factors influencing indoor PAE exposure (e.g., plastic products, wall coverings, furniture, and building characteristics).

Table 1. Summary statistics of PAE congeners and Σ_6 PAEs in residential indoor PM2.5

	Indoor (ng/m ³)							I/O ratio (no unit)			
	Mean \pm SD	Median	95th	Min – Max	N	σ_b^2 (%)	σ_w^2 (%)	Mean \pm SD	Median	Q1 – Q3 ^e	N ^d
DMP	0.17 \pm 0.17	0.12	0.43	0.01 – 1.08	61	30.3	69.7	1.9 \pm 4.3	0.81	0.52 – 1.46	57
DEP	3.22 \pm 3.07	2.21	9.25	0.05 – 16.11	62	23.7	76.3	2.3 \pm 5.8	0.84	0.36 – 1.75	60
DnBP	27.1 \pm 24.9	21.2	71.10	0.1 – 129.0	63	0	100	4.8 \pm 15.2	0.69	0.34 – 1.93	57
BBP	65.5 \pm 122.5	12.9	315.6	0.2 – 654.4	53	0	100	1.9 \pm 3.5	0.27	0.03 – 1.71	41
DEHP	582.2 \pm 604.8	409.5	2007.4	0.4 – 2330.6	59	3.7	96.3	1.8 \pm 3.3	0.46	0.16 – 1.75	50
DnOP	20.5 \pm 50.1	6.4	98.9	0.1 – 243.0	50	1.6	98.4	2.8 \pm 7.5	0.45	0.06 – 3.04	40
Σ_6 PAEs	646.9 \pm 734.1	471.8	2495.5	0.8 – 3245.4	63	7.2	92.8	3.2 \pm 11.6	0.46	0.16 – 1.76	55

Table 2. Spearman's correlation matrix for PAEs.

Residential indoor (I)	DMP	DEP	DnBP	BBP	DEHP	DnOP
DMP	1	0.72**	0.30*	-0.003	0.30*	0.05
DEP		1	0.07	-0.16	0.03	-0.04
DnBP			1	0.73**	0.88**	0.76**
BBP				1	0.83**	0.80**
DEHP					1	0.87**
DnOP						1
Outdoor (O)						
DMP	1	0.68**	0.09	0.11	0.11	0.07
DEP		1	-0.0005	-0.16	-0.11	-0.21
DnBP			1	0.77**	0.90**	0.81**
BBP				1	0.90**	0.93**
DEHP					1	0.93**
DnOP						1
I-O	0.14	0.02	0.03	-0.15	-0.13	-0.16
P-I	0.23	0.17	-0.18	0.07	-0.03	-0.02

Table 3. Factor loading of principal component analysis (PCA) on PAEs

Species	Residential indoor			Outdoor	
	PC1	PC2	PC3	PC1	PC2
DMP	*	*	0.86	*	0.87
DEP	*	*	0.91	*	0.87
DnBP	*	0.96	*	0.74	*
BBP	0.90	*	*	0.90	*
DEHP	0.58	0.76	*	0.93	*
DnOP	0.93	*	*	0.87	*
Eigenvalue	2.67	1.61	1.00	3.00	1.54
% of variance	33.5	28.0	26.8	50.0	25.7

4 CONCLUSIONS

This investigation revealed a comprehensive picture of the abundance and composition of PAE congeners in outdoor and residential indoors. The within-home variances dominated the total variability of indoor PAE congeners. DEHP was the dominant PAE congener, contributing to 80.3% of Σ_6 PAEs, followed by BBP, DnBP, and DnOP. The results showed strong

heterogeneity for PAE congeners, and no apparent intercorrelations were observed between outdoor and residential indoors. We further explored the emission sources of exposure to PAEs.

5 ACKNOWLEDGEMENTS

Jiayao Chen acknowledge the TwinAIR project.

6 REFERENCES

- Caldwell, J. C. (2012). DEHP: genotoxicity and potential carcinogenic mechanisms-a review. *Mutat Res*, 751(2), 82-157. doi:10.1016/j.mrrev.2012.03.001
- Clausen, P. A., Liu, Z., Kofoed-Sorensen, V., Little, J., & Wolkoff, P. (2012). Influence of temperature on the emission of di-(2-ethylhexyl)phthalate (DEHP) from PVC flooring in the emission cell FLEC. *Environ Sci Technol*, 46(2), 909-915. doi:10.1021/es2035625
- Eichler, C. M. A., Cohen Hubal, E. A., & Little, J. C. (2019). Assessing Human Exposure to Chemicals in Materials, Products and Articles: The International Risk Management Landscape for Phthalates. *Environ Sci Technol*, 53(23), 13583-13597. doi:10.1021/acs.est.9b03794
- IARC Working group. (2000). *Some Industrial Chemicals*. Lyon, France: IARC: World Health Organization International Agency for Research on Cancer.
- Kang, Y., Man, Y. B., Cheung, K. C., & Wong, M. H. (2012). Risk assessment of human exposure to bioaccessible phthalate esters via indoor dust around the Pearl River Delta. *Environ Sci Technol*, 46(15), 8422-8430. doi:10.1021/es300379v
- Katsikantami, I., Sifakis, S., Tzatzarakis, M. N., Vakonaki, E., Kalantzi, O. I., Tsatsakis, A. M., & Rizos, A. K. (2016). A global assessment of phthalates burden and related links to health effects. *Environ Int*, 97, 212-236. doi:10.1016/j.envint.2016.09.013
- Meeker, J. D., Sathyanarayana, S., & Swan, S. H. (2009). Phthalates and other additives in plastics: human exposure and associated health outcomes. *Philos Trans R Soc Lond B Biol Sci*, 364(1526), 2097-2113. doi:10.1098/rstb.2008.0268
- Otake, T., Yoshinaga, J., & Yanagisawa, Y. (2004). Exposure to phthalate esters from indoor environment. *J Expo Anal Environ Epidemiol*, 14(7), 524-528. doi:10.1038/sj.jea.7500352
- U.S. EPA. (1987). Butyl benzyl phthalate (BBP) (CASRN 85-68-7). In. U.S. Environmental Protection Agency, Washington, DC: Environmental Protection Agency Washington, DC.
- Zhang, J., Sun, C., Lu, R., Zou, Z., Liu, W., & Huang, C. (2021). Associations between phthalic acid esters in household dust and childhood asthma in Shanghai, China. *Environmental research*, 200, 111760.

HEPA filters to improve vehicle cabin air quality – advantages and limitations

Dixin Wei*^{1,2}, Anders Löfvendahl²

*1 Chalmers University of Technology
Division of Building Services Engineering
Gothenburg, Sweden*

*2 Volvo Car Corporation
Climate Department
Gothenburg, Sweden*

**Corresponding author: dixin.wei@volvocars.com;*

ABSTRACT

Maintaining a good indoor air quality level has received growing attention in the past years. Especially the smaller particles like PM_{2.5} (particles of aerodynamic diameter less than 2.5 µm) and UFP (ultrafine particles, aerodynamic diameter less than 100 nm) might lead to higher health risks. Vehicle cabin is one challenging environment due to the elevated particle concentrations from the surroundings.

The main protection against outdoor pollutants is from the filter in the vehicle HVAC (Heating, ventilation, and air conditioning) unit. During the past decade, the state-of-the-art solution has been synthetic filters with integrated activated carbons to also cope with gaseous pollutants. These conventional filters, however, are limited by factors including space, reduced efficiency whilst dust-loading, and relatively low efficiencies around the particle size of 100-300 nm. Widely varying efficiency values (20%-90%) have been reported from different vehicles.

There is now an interest to introduce filters with higher efficiencies, for example HEPA (High-Efficiency Particulate Air) filters in vehicles. Besides improved efficiencies, another advantage is that the efficiency does not decrease much whilst dust loading. The disadvantages are increased pressure-drop and space requirements, which make them harder to implement in the compact vehicle environment.

One potential improvement in the short run is to use a HEPA-filter placed in the engine bay as a pre-filter, to protect and potentially extend lifetime of the HVAC filter. The combined particle filtration efficiency is improved, and the increased pressure-drop can be acceptable when the HEPA-filter has relatively large dimension.

In this study two filter prototypes (EPA and HEPA level) were manufactured to investigate applications of pre-filter in a production vehicle. Vehicle test with generated particles (NaCl and Di-Ethyl-Hexyl-Sebacat) and road particles were performed. The inside and outside particle concentrations were measured simultaneously under different fan speeds and combinations of prototypes. One prototype was aged and tested in the vehicle as well.

The tested system showed considerably improved air quality, also with an aged filter. With pre-filters applied, the in-cabin UFP and PM_{2.5} removal could achieve 99%, much higher than the original filter alone (76% and 87% respectively). More importantly in the particle size range below 100 nm, higher than 97% removal was achieved for all sizes. The limitation of such system is mainly the added pressure-drop and space in the vehicle, which demands a balance with the improved filter efficiency.

KEYWORDS

Pre-filtration; HEPA; vehicle cabin; particulate matter

1 INTRODUCTION

Maintaining a good indoor air quality level has received growing attention in the past years. One important focus is the airborne particulate matter, especially small particles like PM_{2.5} (particles of aerodynamic diameter less than 2.5 µm) and UFP (ultrafine particles, aerodynamic diameter less than 100 nm). Epidemiology studies have stated their correlations with higher risks of respiratory and cardiovascular diseases (Mitsakou et al. 2007; Gan et al. 2011; Shiraiwa et al. 2017).

Vehicle cabin is one challenging indoor environment due to elevated particle concentrations from surrounding traffic (Ramos et al. 2016). The main protection against outdoor particles is achieved by the vehicle heating, ventilation, and air-conditioning (HVAC) system through filtration, combined with improved airtightness and air recirculation. The efficiency of common vehicle HVAC filters have a wide distribution between reported values of 20% to 90% (Xu et al. 2011). Electrostatically charged multi-layer filters containing active carbon exist in premium car models. However these filters are mainly limited by loss of efficiency as electrical charges deteriorate, together with increased pressure-drop (dP) due to dust loading. Besides, these filters normally provide lower removal (down to 20%) at the most penetrating particle size (MPPS) around 100-300 nm (Xu et al. 2011).

A comprehensive study on the state-of-the-art performance, including field measurements in cars (Wei et al. 2020), development of a model to simulate the air quality (Wei et al. 2022) and the energy use under different air recirculation (Wei et al. 2023) have been carried out.

There is now interest to introduce filters with higher efficiencies, such as HEPA (High-Efficiency Particulate Air) filters which have been used in appliances like air cleaners, clean rooms, nuclear industrial applications etc. (Xu et al. 2016). HEPA filters, according EN1822 (CEN: European Committee for Standardization, 2019), have efficiencies equal to or above 99.95% at the MPPS. EPA (Efficient Particulate Air) filters have efficiency equal to or above 85% at MPPS. The dust loading, unlike traditional cabin filters, normally elevates the filtration efficiency due to the domination of mechanical filtration. While the obvious limitation is the high pressure-drop from the dense material design. Accordingly, there is increased demand of space to limit the pressure-drop, which is more complex to meet in the vehicle context in comparison to more common building applications. Elevated pressure-drop in the vehicle climate system means higher energy consumption to deliver the same airflow, and higher risks of noise, vibration, and harshness (NVH) problems.

Xu et al. (2013) performed measurements on HEPA filters applied in airlines. Filter usage between 2000-8000 hours contributed to around 10% of efficiency increase, however 800% of pressure-drop increase. Lee and Zhu (2014) studied applying improved filters in vehicles, which showed up to 93% removal of UFP, yet lead to 7% to 22% decrease of the airflow rate. There have also been investigations of building an auxiliary HEPA filtration box inside a modified van to filter the in-cabin air, which showed that more than 97% of UFP was removed (Zhu et al. 2008). The application however requires large modification, e.g., the entire first row of seats was removed.

This study investigates one potential improvement, an EPA/HEPA-filter placed in the engine bay as a pre-filter for the original HVAC-filter. Both lab and road measurements were performed in a slightly modified vehicle, under common climate settings. Reduction of PM_{2.5} and UFP were compared under different filtration scenarios: original HVAC filter, two-step

filtration; and with different particle types: road, DEHS (Di-Ethyl-Hexyl-Sebacat) and NaCl. Other factors including pressure-drop, and practical installation limitations in the vehicles are investigated.

2 METHODS

2.1 Filter Prototypes

All the studied filters are listed in **Table 1**. Two pre-filter prototypes were manufactured in collaboration with an industry partner. The filter dimensions are designed according to available space in an existing production vehicle's thermal bay. The two prototypes (P1, P2) have similar design, pleated particle filter (no activated carbon) made of multi-layer synthetic fiber. P2 (HEPA level) has slightly higher efficiency than P1 (EPA level). The tested vehicle has an original HVAC filter, which is an electrostatically charged multi-layer synthetic filter with activated carbon. The main difference of pre-filters is the media design (e.g., material, diameter), which allow them to achieve much higher efficiencies than conventional HVAC filter. Both prototypes could be stacked with a coarse protection filter of the same dimension, for the purpose of extending the lifetime. P2 was also loaded with ISO 12103-1 A2 Fine Dust (International Organization for Standardization, 2016) and environmental cycle until pressure-drop increased by 50 Pa (80 L/s) compared to new status, to represent an aged filter status. Pictures of filters are shown in

Figure 1. The prototypes are also tested at certified filter test agency for pressure-drop, efficiency values following the standard for vehicle compartment filters DIN 71460-1 (German Institute for Standardization, 2006).

Table 1: Prototype dimensions and status

Filter	Type	size	status
P1	EPA synthetic filter	400*314* 30 mm	new
P2	HEPA synthetic filter	400*314* 30 mm	new
P2	HEPA synthetic filter	400*314* 30 mm	aged
P1 + protection filter (Two pieces stacked)	EPA synthetic filter + protection particle filter	400*314* 30 mm * 2 pcs	new
P2 + protection filter (Two pieces stacked)	HEPA synthetic filter + protection particle filter	400*314* 30 mm * 2 pcs	new
Original HVAC filter	Synthetic filter with activated carbon	247*289*40 mm	new

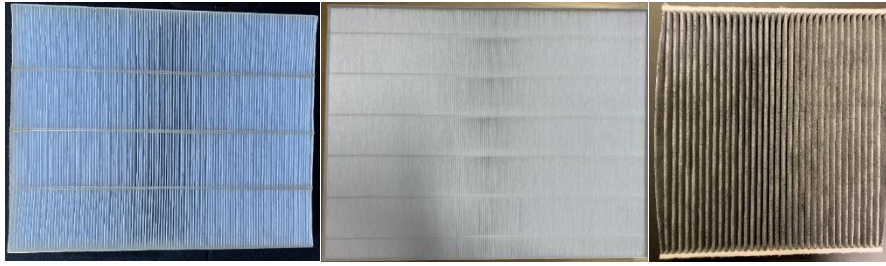


Figure 1 Filter prototypes. Left: P1, Middle: P2, Right: original HVAC filter

2.2 Instrumentation

Two inter-calibrated GRIMM MiniWRAS (Mini Wide Range Aerosol Spectrometer) model 1.371 were used in the rig and vehicle measurements. The instrument measures particles of aerodynamic diameter from 10 nm to 35 μm , distributed into 41 channels with log interval of one minute. The measurable mass concentration range is 0.1 $\mu\text{g}/\text{m}^3$ to 100 mg/m^3 (GRIMM, 2023). The mass and number concentration of all size channels are acquired, including $\text{PM}_{2.5}$, UFP counts from 10 nm to 100 nm. Annual calibration was performed by supplier and automatic self-test done by instrument at each start-up.

Two TSI Portable Test Aerosol Generators (Model 3073) were deployed to generate test dust of NaCl and DEHS. These atomizer-type devices generate particle concentrations from 85 $/\text{cm}^3$ to $>10^7 /\text{cm}^3$ and has an output flow rate adjustable from 0.3 to 4.5 L/min. According to specification the generated DEHS aerosol distribution has mode diameter between 0.15 to 0.3 μm , and for NaCl 0.05-0.2 μm (TSI, 2023).

2.3 Vehicle measurement

The prototypes (P1, P2) were installed in a production vehicle's thermal bay as pre-filters (VOLVO XC40 BEV model-year 2021) as shown in **Figure 2**. Part of the original storage accessory was removed and replaced with a 3D-printed filter holder, which was connected to the original HVAC system air inlet. The air intake to the pre-filter is from the front grille. The holder is designed so that the hood could be closed as normal. The vehicle measurements were performed both inside an indoor vehicle test room with generated particles, and in a road tunnel in Gothenburg, Sweden (at emergency parking). On both occasions the vehicle was standing-still with climate system operating.



Figure 2 Pre-filter prototype installation in an existing production vehicle's thermal compartment

Vehicle measurements were performed between February and June 2022. The measurement method is the same as described in the Methods section of a previous paper (Wei et al. 2020). Here a brief description is given.

The climate settings were AC off and desired temperature of 22 °C, as well as a constant ratio of airflow at panel and floor vents, no air recirculation. The varied climate parameters are mainly the airflow rates (extra low (Xlow), low, medium, high), which were controlled by a software connected to the vehicle climate control unit (Estimated airflow rates at these 4 levels are around 20, 40, 60, 85 L/s respectively). Different scenarios were tested: original HVAC filter alone, and pre-filter (P1 or P2) + original HVAC filter.

The in-cabin and outside particle concentrations were measured simultaneously. An outside sampling tube was placed in front of the pre-filter. The inside sampling tube was placed above the middle armrest between the front seats. A data collection interval of around 5-10 minutes is logged when the in-cabin concentration is relatively stable. At least 3 repetitions were logged for each combination of parameters, leading to in total 164 valid datasets collected.

3 RESULTS

3.1 Removal of UFP and PM_{2.5} from generated particles

The average in-cabin removal percentage of PM_{2.5} and UFP with generated particles are presented in **Table 2**. Different filter combinations are compared. The removal percentage is calculated from the simultaneously measured inside to outside (I/O) concentration ratio, i.e., Removal percentage = 1 – I/O ratio. The mass concentration of PM_{2.5} (µg/m³) and count concentration of UFP (N/cm³) are used in calculation. All the data points are the means of repetitions under the same test conditions.

Table 2 Comparison of in-cabin removal percentage of UFP and PM_{2.5} with different filter combinations and dust type (DEHS and NaCl). Original: the original HVAC filter alone. Airflow Low level (around 40 L/s), no recirculation. Standard deviations are not presented due to smaller than 3% units in all cases. Each arithmetic mean is based on around 20 repetition samples.

	PM _{2.5} removal percentage		UFP removal percentage	
	Arithmetic Mean		Arithmetic Mean	
	NaCl	DEHS	NaCl	DEHS
<i>Original</i>	94.6%	98.2%	94.5%	78.2%
<i>P2 + Original</i>	99.8%	99.9%	99.9%	99.1%
<i>P2 aged + Original</i>	99.9%	99.9%	99.9%	98.2%

Table 2 shows that application of P2 as pre-filter achieved removal percentage higher than 99% in all conditions for both PM_{2.5} and UFP. Even after P2 is loaded with dust to represent aged status, 98% removal was maintained. In comparison, when only the vehicle's original HVAC filter is installed, average removal of DEHS UFP is 78%, which is lower than NaCl UFP removal of 94%. The atomized aerosols in this study are not neutralized. According to investigation from Shi et al. (2013), DEHS is practically without electrical charges. This could result in the original HVAC filter has lower efficiency of removing the DEHS UFP.

Furthermore, independent sample t-tests were performed on results in **Table 2** and p-values are summarized in **Table 3**. All comparisons showed statistically significant difference, except that P2 aged+Original is able to maintain the same level of UFP NaCl removal as P2 + Original.

Table 3 P values of independent sample t-tests between three filter combinations, categorized by particle type and particle size.

	PM _{2.5}		UFP	
	NaCl	DEHS	NaCl	DEHS
Original & P2+Original	4.15E-11	3.62E-10	4.50E-09	2.44E-11
Original & P2 aged +Original	2.55E-11	5.73E-10	4.52E-09	2.38E-11
P2 + Original & P2 aged +Original	1.81E-03	1.48E-03	4.44E-01	1.32E-02

3.2 Removal of UFP and PM_{2.5} from road particles

Table 4 Comparison of in-cabin removal percentage of UFP and PM_{2.5} with different filter combinations. Measurements performed with road particles in Lundby tunnel, Gothenburg, Sweden. Original: the original HVAC filter alone. Airflow Low level (around 40 L/s), no recirculation.

	Removal percentage of road particles			
	PM _{2.5}		UFP	
	Arithmetic Mean	Standard Deviation	Arithmetic Mean	Standard Deviation
<i>Original</i>	86.8%	3.9%	75.7%	5.9%
<i>P1</i>	97.6%	0	93.1%	0
<i>P2</i>	98.3%	0.5%	98.7%	0.5%
<i>P1 + Original</i>	99.7%	0	96.0%	0
<i>P2 + Original</i>	99.1%	0.7%	99.3%	0.6%

In **Table 4** the similar comparison of particle removal percentage is presented for measurements performed on the road. Clearly the application of pre-filter, either P1 or P2 enhances the removal of particles. Especially with P2 as pre-filter, the removal of UFP and PM_{2.5} is 99%. The original filter removes only 76%-87% of particles. Applying P1 as pre-filter improves the UFP removal up to 96% and PM_{2.5} to 99%.

3.3 Size-resolved removal percentage of particles

Generated particles and road particles have different size distributions, and the removal percentages vary with size. **Figure 3** presents the comparison of size-resolved removal percentage of all particles. When only the HVAC filter is installed, the removal at MPPS is 69% for road particles, 70% for DEHS and 87% for NaCl. The combination of original HVAC filter with P2, either new or aged, lead to an enhancement. In all sizes, higher than 97%, up to 99% removal of particles are achieved. This enhancement is very important since UFP has more potential of entering human body, thus lead to cardiovascular problems.

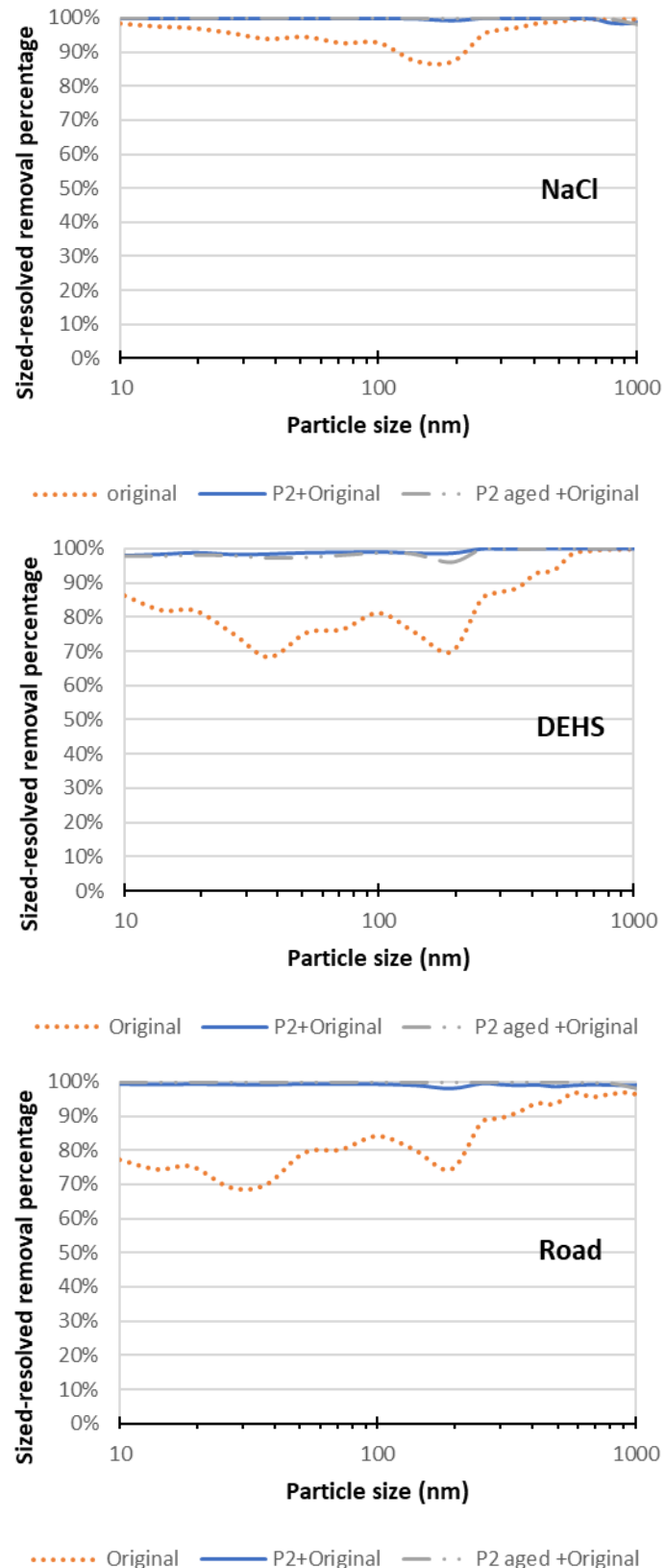


Figure 3 Size-resolved in-cabin removal percentage of particles in the vehicle measurements. NaCl, DEHS and road particles are compared. Plotted data are the average of all repetitions. Original: the original HVAC filter alone. Airflow Low level (around 40 L/s), no recirculation. The *P2 aged+original* line almost overlap with *P2+Original* line in all graphs.

3.4 Pressure-drop

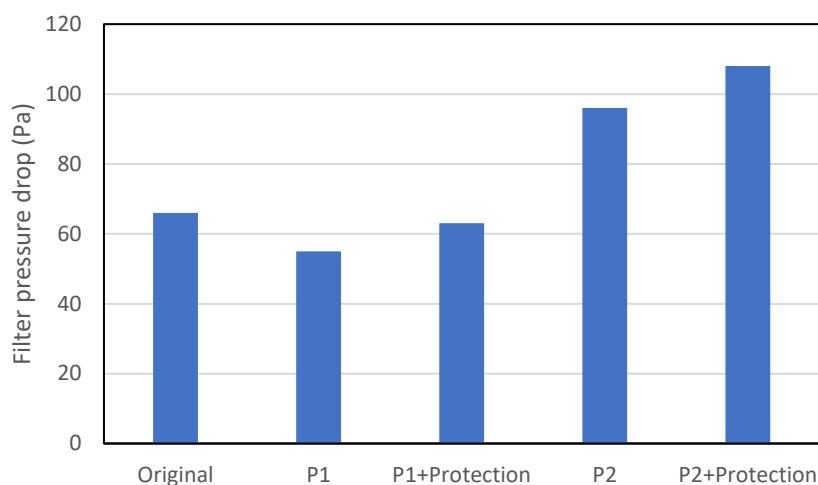


Figure 4 Pressure-drop of filter prototypes measured following standard DIN 71460-1. Test airflow 80L/s

Figure 4 presents the pressure-drop of filter prototypes under airflow 80 L/s measured in certified agency, following the standard DIN 71460-1, Air filters for passenger compartments. The pressure-drop of P2 is higher than P1 due to the filter media and layer design. When a protection filter is applied before, 8 Pa and 12 Pa are added on P1 and P2 respectively.

It should be noted that the dimension of original filter is smaller than the pre-filter (see **Table 1**). P1 has similar level of pressure-drop as the original HVAC filter, which means the application of pre-filter almost doubles the total pressure-drop from filters. The influence on the climate system operation, specifically the fan power depends on the fan control strategy.

4 DISCUSSION

The same filters showed somewhat different removal percentages when tested with different aerosols. This could be related to the particle characteristics such as size distribution, which influences the filtration performance, and also particle loss in the ducting etc. These factors are now discussed.

Figure 5 presents four examples of different particle size distributions, for NaCl, DEHS, road air in this study, and a previous road air measurement in China (Wei et al. 2020) respectively. All examples have outside $PM_{2.5}$ concentration around $100 \mu\text{g}/\text{m}^3$. While from the figure it's observed that the particle distributions are quite different.

The road measurement in this study has a large mass portion around 100 nm and 3 μm . The previous China measurement however has more mass in the nano-meter range, with two peaks around 100 nm and 3 μm . The NaCl and DEHS are more focused in only one peak, around 100 nm and 2 μm respectively. When the count distribution is compared, a different trend is that all the examples only have one mode around 70-100 nm. And DEHS has 5-15 times lower count concentration in the mode size than others.

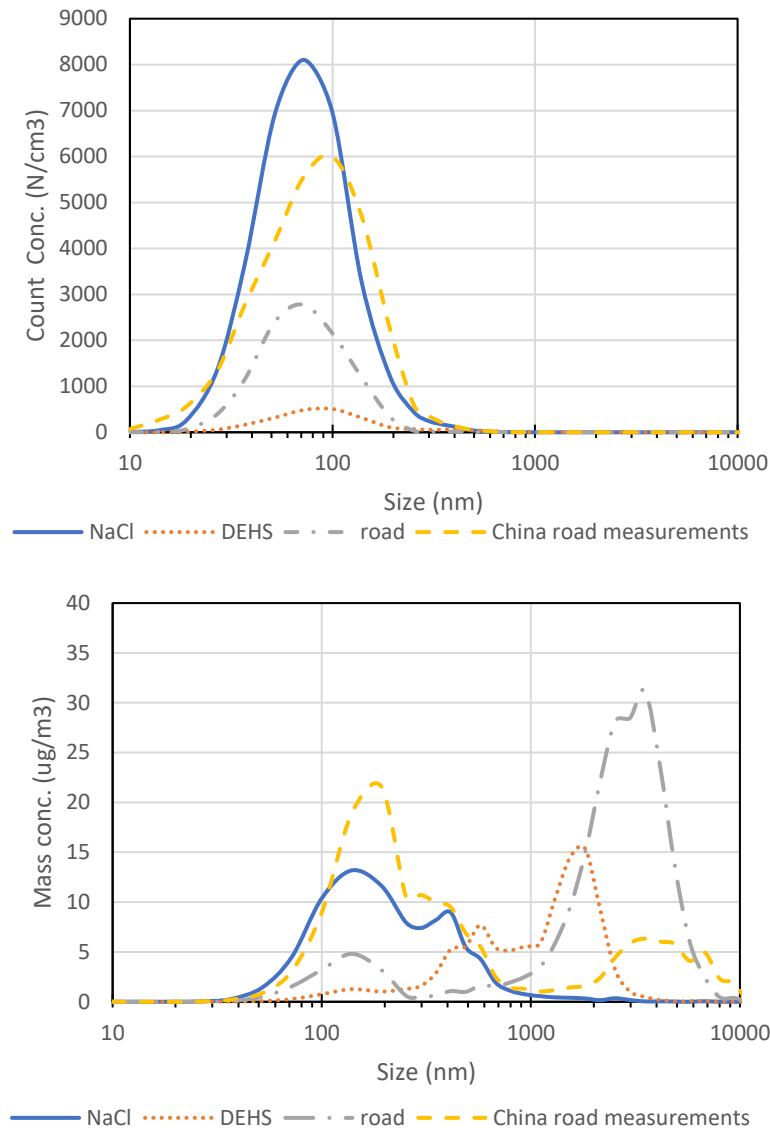


Figure 5 Outside air particle size distribution comparison of both count concentration (N/cm^3) and mass concentration ($\mu g/m^3$). Examples of the generated dust of DEHS, NaCl, road air in this study and a previous measurement in China 2019 (Wei et al. 2020) are compared. Four examples all have $PM_{2.5}$ concentration around $100 \mu g/m^3$

This comparison point out that, different aerosol types would mean different challenges for the filters, and thus different removal of $PM_{2.5}$ or UFP. For example, the NaCl mass size distribution is close to the MPSS which may lead to a low $PM_{2.5}$ removal as opposed to the case with DEHS in Table 2

Table 2 Comparison of in-cabin removal percentage of UFP and $PM_{2.5}$ with different filter combinations and dust type (DEHS and NaCl). Original: the original HVAC filter alone. Airflow Low level (around 40 L/s), no recirculation. Standard deviations are not presented due to smaller than 3% units in all cases. Each arithmetic mean is based on around 20 repetition samples.

	PM _{2.5} removal percentage		UFP removal percentage	
	Arithmetic Mean		Arithmetic Mean	
	NaCl	DEHS	NaCl	DEHS
<i>Original</i>	94.6%	98.2%	94.5%	78.2%
<i>P2 + Original</i>	99.8%	99.9%	99.9%	99.1%

<i>P2 aged + Original</i>	99.9%	99.9%	99.9%	98.2%
---------------------------	-------	-------	-------	-------

, which has a peak mass concentration at far larger particles where the filter efficiency is high.

On the other hand, when the MPPS efficiency is compared in **Figure 3**, DEHS and road particles show similar values around 70%, yet NaCl with substantially higher 84%. One possible reason could be that the NaCl aerosol can be expected to have more electrostatic charges.

It should also be noted that the removal percentages are reflecting the particles lost in the filter and other surface in the HVAC system. Qi et al. (2008) have reported 8% in non-winter condition and 39% in winter of particle removal when no filter is installed in the vehicle. This value would be influenced by the particle type. Moreover, the modification of ducting in this study added more surface and duct bends, where particle losses are more likely to happen compared with straight ducts (Jeong et al. 2009).

In general, vehicle tests with real particles from roadways may differ from the vehicle test and laboratory test with standardized particles (Lee and Zhu 2014). Road measurements are closer to the real application scenarios, while standardized test rigs provide stable and more repeatable conditions. A combination of extensive test methods would be beneficial. To correlate the results, for example the NaCl possibly need to be neutralized according to Shi et al., (2013). Another useful measure is to compare the MPPS efficiency in addition to the total removal of PM_{2.5} or UFP, where the comparison is more straightforward in a narrow size range.

5 CONCLUSION

This study investigates the application of a pre-filter in an existing vehicle with small modifications, which improves the overall particle removal, and thus the cabin air quality.

Two prototypes were tested feasible with regards to achieving better cabin air quality. The vehicle removal of PM_{2.5} was improved from 87% to 99% with both prototypes. The removal of UFP was improved from 76% to above 96% with prototype 1 and 99% with prototype 2. This performance was also maintained with an aged prototype 2. It means that the service interval is possibly mainly dependent on the pressure-drop increase and other aspects like gas absorption, microbial growth etc., not the particle efficiency.

On the other hand, the choice of filter quality in real vehicles would be a complex balance between filtration efficiency, dimension, cost, climate comfort and pressure-drop to reduce the fan power, i.e. the energy consumption and to reduce NVH problems. For example, the application of P1 would give considerable improvement on filtration as well as adding lower pressure-drop. The cost per filter unit is also normally lower for P1 than P2.

Furthermore, the pre-filters with a protection filter had similar performance and slight increase of the pressure-drop; around 10 Pa. It could possibly extend the pre-filter lifetime if space is adequate. The studied pre-filters could also be applied alone to filter particles effectively, which however demands proper design to required gas absorption.

This study also aimed at contributing to the development of vehicle particle filtration test methods, especially by comparing on road tests and lab tests with generated particles. Different

characteristics and behaviours of particles are observed. The same vehicle test setup of original HVAC filter removes 76% of road UFP, while corresponding values for DEHS and NaCl are 78% and 94%. This points out the need of further correlating standardized tests with real road conditions, where the latter is the user scenario.

The findings provide inputs to the design of vehicle climate system with good air quality and pressure-drop balance. Relationships among efficiencies, pressure-drop and filter age could be further studied to facilitate the decision on proper filter service interval.

ACKNOWLEDGEMENTS

This project is funded by the Swedish Energy Agency (Energimyndigheten).

REFERENCES

- CEN: European Committee for Standardization. (2019, April). EN1822-1 High efficiency air filters (EPA, HEPA and ULPA) - Part 1: Classification, performance testing, marking.
- Gan WQ, Koehoorn M, Davies HW, et al (2011) Long-term exposure to traffic-related air pollution and the risk of coronary heart disease hospitalization and mortality. *Environ Health Perspect* 119:501–507. <https://doi.org/10.1289/ehp.1002511>
- German Institute for Standardization. (2006). DIN 71460-1 Road vehicles - Air filters for motor passenger compartments - Part 1: Test for particulate filtration.
- GRIMM. (2023, Feb). MINI WIDE RANGE AEROSOL SPECTROMETER. Retrieved from <https://www.grimm-aerosol.com/products-en/indoor-air-quality/the-wide-range-hybrid/1371/>
- International Organization for Standardization. (2016). ISO 12103-1:2016 Road vehicles — Test contaminants for filter evaluation — Part 1: Arizona test dust.
- Jeong JW, Bem J, Bahnfleth WP, et al (2009) Critical review of aerosol particle transport models for building HVAC ducts. *J. Archit. Eng.* 15:74–83
- Lee ES, Zhu Y (2014) Application of a high-efficiency cabin air filter for simultaneous mitigation of ultrafine particle and carbon dioxide exposures inside passenger vehicles. *Environ Sci Technol* 48:2328–2335. <https://doi.org/10.1021/es404952q>
- Mitsakou C, Housiadas C, Eleftheriadis K, et al (2007) Lung deposition of fine and ultrafine particles outdoors and indoors during a cooking event and a no activity period. *Indoor Air* 17:143–152. <https://doi.org/10.1111/j.1600-0668.2006.00464.x>
- Qi C, Stanley N, Pui DYH, Kuehn TH (2008) Laboratory and On-Road Evaluations of Cabin Air Filters Using Number and Surface Area Concentration Monitors. *Environ Sci Technol* 42:4128–4132
- Ramos CA, Wolterbeek HT, Almeida SM (2016) Air pollutant exposure and inhaled dose during urban commuting: a comparison between cycling and motorized modes. *Air Qual Atmos Heal* 9:867–879. <https://doi.org/10.1007/s11869-015-0389-5>
- Shi B, Ekberg LE, Langer S, et al (2013) Intermediate Air Filters for General Ventilation Applications : An Experimental Evaluation of Various Filtration Efficiency Expressions Intermediate Air Filters for General Ventilation Applications : An Experimental Evaluation of Various Filtration Effici. 6826:.. <https://doi.org/10.1080/02786826.2013.766667>
- Shiraiwa M, Ueda K, Pozzer A, et al (2017) Aerosol Health Effects from Molecular to Global Scales. *Environ Sci Technol* 51:13545–13567. <https://doi.org/10.1021/acs.est.7b04417>
- CEN: European Committee for Standardization. (2019, April). EN1822-1 High efficiency air filters (EPA, HEPA and ULPA) - Part 1: Classification, performance testing, marking.
- German Institute for Standardization. (2006). DIN 71460-1 Road vehicles - Air filters for motor passenger compartments - Part 1: Test for particulate filtration.
- GRIMM. (2023, Feb). MINI WIDE RANGE AEROSOL SPECTROMETER. Retrieved from <https://www.grimm-aerosol.com/products-en/indoor-air-quality/the-wide-range-hybrid/1371/>
- International Organization for Standardization. (2016). ISO 12103-1:2016 Road vehicles — Test

contaminants for filter evaluation — Part 1: Arizona test dust.

- TSI. (2023, Feb). Portable Test Aerosol Generator 3073. Retrieved from https://tsi.com/getmedia/e5d8a77a-7533-4631-a85a-470f11828a1c/5002118_US_3073_Portable%20Test%20Aerosol%20Generator_Web?ext=.pdf
- Wei D, Nielsen F, Ekberg L, et al (2020) PM2.5 and ultrafine particles in passenger car cabins in Sweden and northern China—the influence of filter age and pre-ionization. *Environ Sci Pollut Res* 27:30815–30830. <https://doi.org/10.1007/s11356-020-09214-0>
- Wei D, Nielsen F, Ekberg L, Dalenbäck JO (2022) Size-resolved simulation of particulate matters and CO2 concentration in passenger vehicle cabins. *Environ Sci Pollut Res*. <https://doi.org/10.1007/s11356-022-19078-1>
- Wei D, Nielsen F, Karlsson H, et al (2023) Vehicle cabin air quality: influence of air recirculation on energy use, particles, and CO2. *Environ Sci Pollut Res*. <https://doi.org/10.1007/s11356-023-25219-x>
- Xu B, Chen X, Xiong J (2016) Air quality inside motor vehicles' cabins: A review. *Indoor Built Environ* 0:1–14. <https://doi.org/10.1177/1420326X16679217>
- Xu B, Liu J, Ren S, et al (2013) Investigation of the performance of airliner cabin air filters throughout lifetime usage. *Aerosol Air Qual Res* 13:1544–1551. <https://doi.org/10.4209/aaqr.2012.11.0330>
- Xu B, Liu S, Liu J, Zhu Y (2011) Effects of vehicle cabin filter efficiency on ultrafine particle concentration ratios measured in-cabin and on-roadway. *Aerosol Sci Technol* 45:215–224. <https://doi.org/10.1080/02786826.2010.531792>
- Zhu Y, Fung DC, Kennedy N, et al (2008) Measurements of ultrafine particles and other vehicular pollutants inside a mobile exposure system on Los Angeles freeways. *J Air Waste Manag Assoc* 58:424–434. <https://doi.org/10.3155/1047-3289.58.3.424>

Experimental study of an innovative wet scrubber concept in regards to particle filtration and pressure loss

Nhat Nguyen¹, Martin Kremer¹, Hendrik Fuhrmann¹, Philipp Ostmann¹ and Dirk Müller¹

¹ RWTH Aachen University, E.ON Energy Research Center, Institute for Energy Efficient Buildings and Indoor Climate, Mathieustraße 10, Aachen, Germany

ABSTRACT

The risen awareness of improved indoor air quality has resulted in an increased energy demand for HVAC systems due to higher air exchange rates and the additional operation of air purifiers. Therefore, the need for energy-efficient methods to improve indoor air quality has grown. In this experimental study, we develop an innovative wet scrubber concept to remove solid particles from the airflow. In contrast to conventional wet scrubbers, this concept uses a perforated plate and the hydrostatic pressure to feed water droplets into the air stream. The absence of injectors reduces the energy demand compared to common wet scrubbers, as the required pressure to generate the water droplets is significantly lower. In addition, the larger droplet sizes enable the usage of a matching droplet separator with negligible pressure drop. Within the scope of this work, we investigate the particle removal efficiency and the pressure drop for a range of ambient conditions, which represent the different seasons: summer, winter and transition period. Furthermore, we analyze three different volume flow rates of water to cover a broad spectrum of droplet formation regimes. In the scenarios investigated, we measure a pressure drop of 4 – 7 Pa and a particle removal efficiency of up to 38 %. The results show that the ambient conditions have little influence on the particle removal efficiency. However, the presented wet scrubber concept displays the same behavior as common wet scrubbers, where the particle removal is less efficient for smaller particles. The investigated wet scrubber concept demonstrates a significant decrease in particle removal efficiency for droplets with a diameter below 4 μm . Higher water flow rates improve the particle removal efficiency but also increase the pressure drop across the wet scrubber.

KEYWORDS

wet scrubber, removal efficiency, energy efficient, particle, pressure drop

1 INTRODUCTION

Air pollution is one of the greatest environmental risks to human health. Ambient air consists of many harmful substances, which originate from numerous natural and anthropogenic sources. Among the various pollutants, fine and coarse particulate matter is one major contributor. They can penetrate deeply into the respiratory tract and increase mortality and morbidity even at low concentrations (World Health Organization, 2016). Many studies have shown that particulate matter is positively associated with an increased risk for cardiovascular diseases and respiratory diseases that, as a result, lead to increased hospital admissions (Adar et al., 2014; Beelen et al., 2014; Lu et al., 2015; Hystad et al., 2020; Yee et al., 2021).

Therefore, the removal of fine and coarse particulate matter from the supply air of buildings is necessary to improve indoor air quality and reduce the risk to human health. Fabric filters and wet scrubbers are common and efficient technologies in practical applications. Fabric filters are easy to install and can filter up to 99.99 % of the particles contained in the air stream. However, they are only useable in dry conditions due to fouling and need to be replaced periodically due to clogging caused by particulate build-up over time. In comparison, wet scrubbers are less efficient at removing particulate matter, especially at small particle sizes. However, they have the advantage of filtering both solid and gaseous pollutants and can be used in high humidity conditions (Cheremisinoff, 2002).

There are different wet scrubber concepts, which differ in particle removal efficiency and pressure drop in the airflow. The simplest wet scrubbers are spray towers or spray columns.

They achieve particle removal efficiencies of 90 % or higher for particles that are larger than 5 μm . However, the efficiency drops to 50 % or less for particles that are smaller than 3 μm . Cyclonic wet scrubbers and venturi scrubbers achieve higher efficiencies due to higher relative velocities and higher turbulence at the expense of higher pressure drops. Venturi scrubbers can achieve up to 99 % particle removal efficiency for particles larger than 1 μm . For submicron particles, the efficiency drops to 50 %. The pressure drop across a venturi scrubber can vary between 2400 Pa and 37 000 Pa. Higher velocities in a venturi scrubber will result in higher efficiencies but also to increased pressure drops (Schiffner and Hesketh, 2017).

Table 1 shows the particle removal efficiencies, the pressure drops and the particle sizes investigated in previous particle removal studies of wet scrubbers. (Biswas et al., 2008) investigated the influence of various parameters on the hydrodynamics of a counter-flow spray column. They found that the pressure drop increases with rising gas flow rates, liquid flow rates and solid loading conditions in the inlet. The droplets were in the range of 80 – 200 μm . (Raj Mohan and Meikap, 2009) investigated a two-stage “spray-cum-bubble” column scrubber to remove particulate matter in the range of 1 – 200 μm . This concept consists of a bubble column mounted above a spray column with a twin fluid air-assist atomizer. They studied the particle removal efficiency for varying water heights, gas flow rates and spray liquid flow rates. The droplets were in the range of 80 – 200 μm . They found that the contribution of the spray section of the combined wet scrubber is prominent. However, the bubble section can remove very fine particles that escaped the spray section. (Zhao and Zheng, 2008) performed a numerical flow simulation analysis of a gravitational wet scrubber with electrostatically charged particles and droplets. They found that the electrostatic enhancement increases the removal efficiency. (Lee et al., 2013) developed a turbulent wet scrubber by using high-velocity supply gas to displace water in a water reservoir, which creates droplets and turbulence. They found that the particle removal efficiency and the pressure drop increased with increasing water levels and gas flow rates. (Hu et al., 2021) conducted an experimental study on the particle removal efficiency of a wet scrubber with a radial mixing impeller. The mixing impeller generates a fine mist with the supplied water and separates the water-dust mixture through centrifugal force. They varied the number of blades and the water intake. The mixing impeller with 16 blades and medium water intake achieved the highest particle removal efficiency. The pressure drop increased with increased water intake. However, the particle removal efficiency did not correlate linearly with the number of blades. (Qian et al., 2022) proposed a numerical model to consider particle aggregation and particulate removal with a cyclonic wet scrubber with swirling flow. The gas flow rate, spray flow rate and particle concentration were varied to investigate the particle removal efficiency. High turbulent kinetic energy facilitated the high particle removal efficiency because turbulence supports particle aggregation. Furthermore, a big contact area between droplets and particles due to higher water flow rates was also positively associated with particle removal efficiency.

Table 1: Literature overview of particle removal efficiency, pressure drop and particle sizes

Author	Particle removal efficiency / %	Pressure drop / Pa	Particle sizes / μm	Wet scrubber
Biswas		100 – 327	2 – 200	Counter-flow spray Columns
Raj Mohan	57.5 – 99.3		2 – 200	Spray & bubble column scrubber
Zhao	5		< 1	Gravitational wet scrubber, no charge
	99		< 1	Gravitational wet scrubber, charged
Lee	87 – 99	1176 – 2157	> 0.95	Turbulent wet scrubber
	43 – 79	1176 – 2157	< 0.95	Turbulent wet scrubber
Hu	96	170	0.8 – 75	Radial mixing impeller, 16 blades
	86	264	0.8 – 75	Radial mixing impeller, 20 blades
Qian	99.7		1 – 12.1	Cyclone water spray, swirling gas flow

Previous studies on wet scrubbers regarding particle removal mainly focus on different approaches to improve the removal efficiency of particulate matter, especially fine particles. These modified wet scrubber concepts can remove even fine particles very well. However, the studies do not consider the energy demand required to remove the particulate matter. With increasing particle removal efficiencies, the need for energy efficient methods has grown. Wet scrubbers are rarely used in residential buildings. They are mostly part of industrial applications with high particle loads in the exhaust air, such as coal combustion (Qian et al., 2022).

In this study, we investigate a wet scrubber concept, which aims at reducing the operational energy demand by reducing the pressure drop across the wet scrubber and by modifying the droplet generation method. We replace the spray injection of water droplets that wet scrubbers commonly use with a perforated plate and the droplets are fed into the airstream by dripping through the perforated plate. This reduces the required power to feed water into the wet scrubber because spray injections usually require a substantial pump head. Furthermore, the generated droplets in this wet scrubber feature a bigger diameter than droplets generated by spray injection. Hence, a droplet separator for bigger droplets with less pressure drop can be used to remove excess water droplets from the supply air vent (Bürkholz and Muschelknautz, 1972).

2 EXPERIMENTAL SETUP

2.1 Ventilation test bench

In order to analyze the removal efficiency and pressure drop of this wet scrubber concept we develop a test bench. Figure 1 shows the developed wet scrubber test bench and the positions of the utilized sensors. The air duct features a 300 mm x 300 mm cross-section, which tapers into a 130 mm diameter pipe at the end. The first HEPA filter at the beginning of the air duct removes ambient particulate matter in the supply air. An aerosol generator feeds the particles into the airflow downstream of the first HEPA filter. The particle feed's nozzle is positioned in the center of six horizontal cylinders that are staggered vertically. Each cylinder has a diameter of 35 mm. This cylinder arrangement introduces additional turbulence and facilitates a homogenous distribution of the particles within the air duct. A calming section of 1000 mm between wet scrubber section and cylinders enables particle mixing into the airflow and a homogenous flow structure. At the end of the wet scrubber section, a honeycomb structure with a depth of 80 mm and at an angle of 13° to the vent acts as a droplet separator. Another honeycomb structure with a depth of 40 mm directly downstream of the first one acts as a flow straightener. The honeycomb structures in this study have a diameter of 9 mm. The second HEPA filter downstream of the wet scrubber section protects the fan at the end of the pipe from the remaining particulate matter in the airflow.

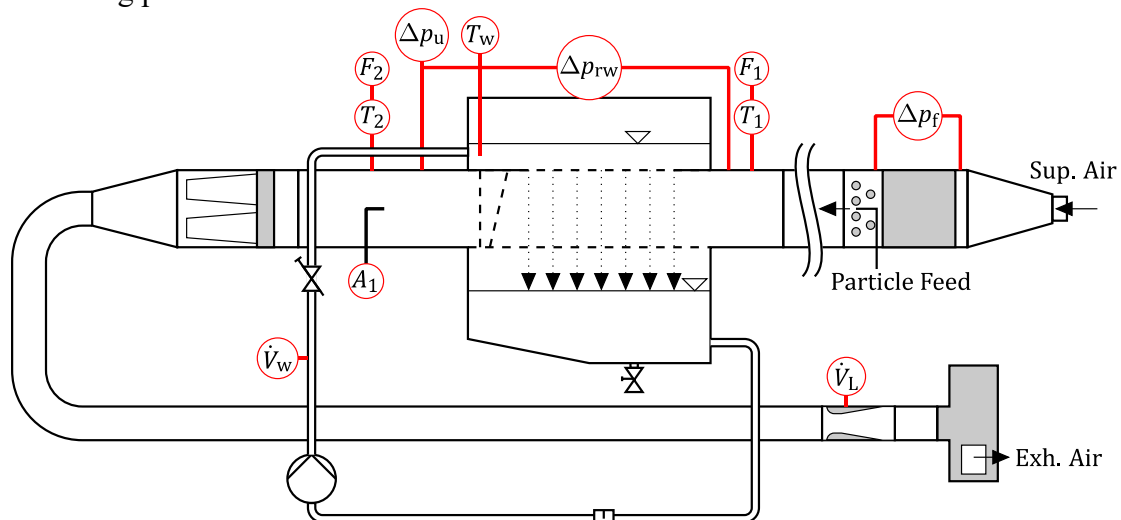


Figure 1: Schematic diagram of test bench

2.2 Wet scrubber section

The wet scrubber section consists of a water basin on top of the air duct, a perforated plate, a collection tank below the air duct, honeycomb structures, a pipe system and a pump. Figure 2 shows the perforated plate that separates the water basin from the air duct. The plate has a thickness of 1 mm.

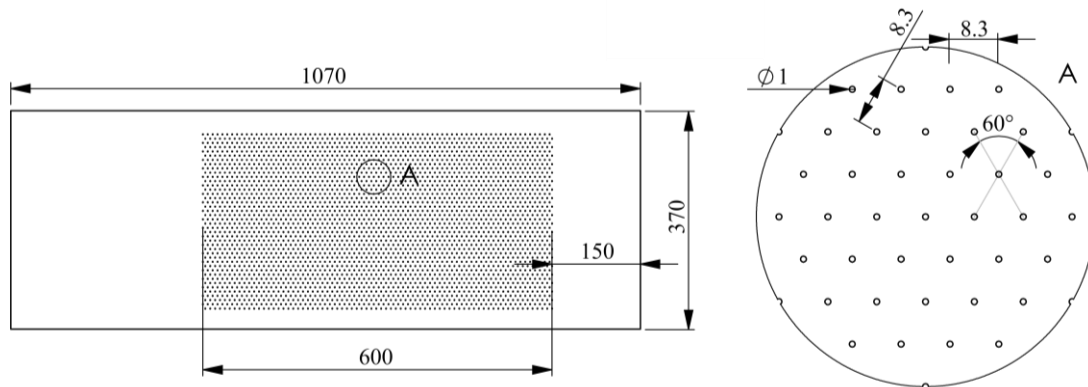


Figure 2: Perforated plate, dimensions in mm

Another horizontal honeycomb between the air duct and the collection tank prevents falling drops from bouncing back into the air duct after impinging on the water surface. A pipe system connects the water basin and the collection tank. It contains a pump, a line regulating valve and a filter. The pump circulates the water within the pipe system and controls the water mass flow. The line regulating valve supports pump control at low water flow rates by increasing the pressure drop and shifting the system's characteristic curve into the operating range of the pump. The filter has a 0.6 mm mesh and protects the pump from coarse particulate matter.

2.3 Sensors

A differential pressure sensor measures the pressure drop Δp_{rw} across the wet scrubber section. Another differential pressure sensor measures the pressure difference relative to the ambient air Δp_u . This measurement allows the pressure in the duct to be monitored and adjusted in the case of overpressure. The pressure within the duct has a significant effect on the droplet shape due to the low pressures used to generate the droplets in this wet scrubber concept. A third differential pressure sensor measures the pressure drop Δp_f across the first HEPA filter to monitor the clogging of the filter. We use combination sensors to measure the temperature and the relative humidity before (F_1, T_1) and after (F_2, T_2) the wet scrubber section. A temperature sensor measures the water temperature T_w within the water basin. The water temperature is not controlled in this study. An optical particle sizer (OPS) measures the particle sizes and particle size distribution. The measurable particle sizes range from 0.3 – 10 μm . A 9 mm probe in the center of the air duct is installed 470 mm downstream of the wet scrubber area (A_1). It is oriented parallel to the flow direction and guides the collected particles through a 90° elbow tube into the OPS. An external vacuum pump is connected to the probe to ensure isokinetic sampling. A venturi throttle in accordance to DIN 51678-1 measures the airflow rate \dot{V}_L . The fan of the test bench uses this measurement to adjust its fan speed according to the external air supply settings. An electromagnetic flowmeter measures the water volume rate \dot{V}_W in the pipe system. The programmable logic controller monitors the sensor values and adjusts the water and airflow rates. It measures the sensor data every 10 ms and averages the values.

An external air supply system provides the test bench with conditioned air via a tube. Figure 3 shows the setup of this external system. The air supply system consists of a sorption dryer, a fan, a cooler, a heater, a steam humidifier and various valves. The air supply system sucks in ambient air and conditions it according to the set boundary conditions. The different valves

regulate the airflow within the system and into the test bench. The supply system controls temperature and humidity using the sensor values of the wet scrubber test bench.

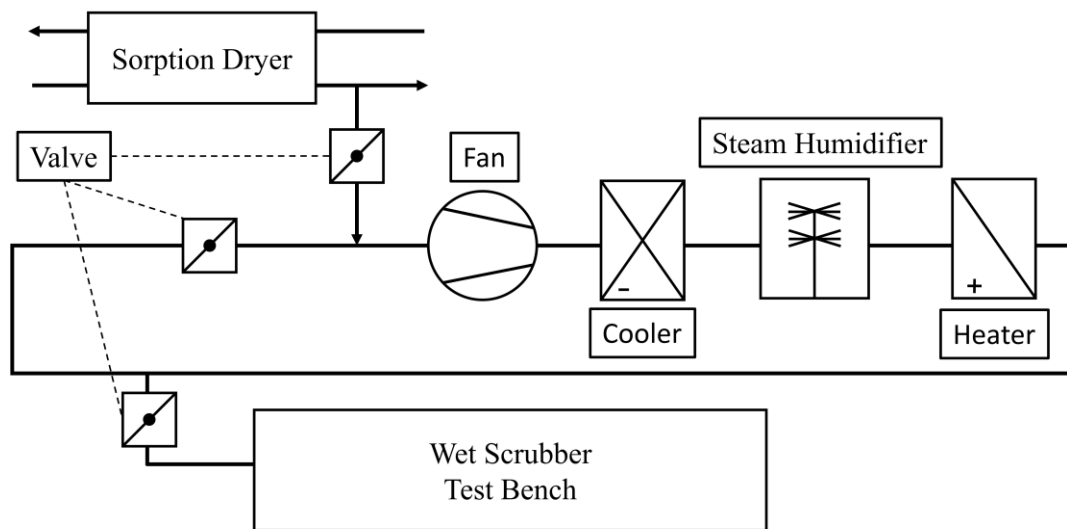


Figure 3: Schematic diagram of air supply system (Kremer and Mathis, 2020)

3 EXPERIMENTAL METHODS

During this study's experiments, the airflow rate is kept constant at 560 m³/h. The aerosol mass flow rate is also kept constant throughout all experiments at 1.11 g/h. To evaluate the performance of the wet scrubber we define the particle removal efficiency η as:

$$\eta = 1 - \frac{K_{wet}}{K_{dry}} \quad (1)$$

where K_{wet} and K_{dry} are the particle numbers per cubic meter with and without the wet scrubber running, respectively. The particle removal efficiency and the pressure drop are investigated for three different scenarios, which differ in temperature and humidity. Table 2 sums up the boundary conditions for each scenario.

Table 2: Boundary conditions of investigated scenarios

Scenario	Temperature [°C]	Rel. Humidity [%]
Summer	32	30
Transition	13	55
Winter	3	72

An experiment to determine the particle removal efficiency consists of two phases. In the first phase, the particle concentration is measured without the wet scrubber running. In the second phase, the measurement is performed under the same boundary conditions with an active wet scrubber. In each phase, the particle concentrations are measured for five minutes. These concentrations are used to calculate the particle removal efficiency. After each phase, a five-minute break is included to prepare for the next phase. The break after phase one ensures that there is sufficient time for the water in the water basin to reach a stationary level. The pause after phase two allows sufficient time for the water basin and the duct walls to dry.

The water flow rate is used to determine the critical Weber number. The critical Weber number defines the transition from dripping to jetting. (Clanet and Lascheras, 1999) experimentally determined the critical Weber number for the transition from dripping to jetting for needles. Although the present study does not investigate needle dripping, the findings from Clanet will be used to approximate the transition boundaries for our perforated plate. The critical Weber number for the transition from periodic dripping to chaotic dripping and from chaotic dripping

to jetting are approximately 1.07 and 3.16, respectively. Table 3 summarizes the regimes and the Weber number for the investigated water flow rates. The investigated water flow rates (2 m³/h, 4 m³/h and 6 m³/h) cover three different regimes.

Table 3: Droplet Regime

Water flow rate	Weber Number	Regime
2 m ³ /h	0.74	Periodic dripping
4 m ³ /h	2.96	Chaotic dripping
6 m ³ /h	6.65	Jetting

The OPS uses scattered light to determine the optical diameters of the particles. It divides the particle into 17 bins. From now on, unless otherwise noted, the diameter will always refer to the optical diameter. Table 4 shows the particle size ranges each bin covers. The OPS cannot size particles with a diameter greater than 10 µm and assigns them to bin 17.

Table 4: OPS bin particle size range

Bin	1	2	3	4	5
Range [µm]	0.3 - 0.374	0.374 - 0.465	0.465 - 0.579	0.579 - 0.721	0.721 - 0.801
Bin	6	7	8	9	10
Range [µm]	0.801 - 1.001	1.001 - 1.391	1.391 - 1.732	1.732 - 2.156	2.156 - 2.501
Bin	11	12	13	14	15
Range [µm]	2.501 - 3	3 - 4.162	4.162 - 5.182	5.182 - 6.451	6.451 - 8.031
Bin	16	17			
Range [µm]	8.031 - 10	> 10			

For each of the investigated cases ten experiments are performed. The measurements are averaged in each case and the uncertainty of the measurement is determined according to (JCGM, 2008).

4 RESULTS

Figure 4 illustrates the particle count for each bin on a logarithmic y-scale for a case without active wet scrubber. The bin with the smallest particles (0.3 – 0.374 µm) has the highest number of particles with a count of approximately two million particles. The particle count decreases with larger particle sizes. Bin 6 and bin 9 show a slight deviation from the overall trend as their particle count is higher than both their neighboring bins. The bin with the largest particle sizes (> 10 µm) consists of approximately 370 particles.

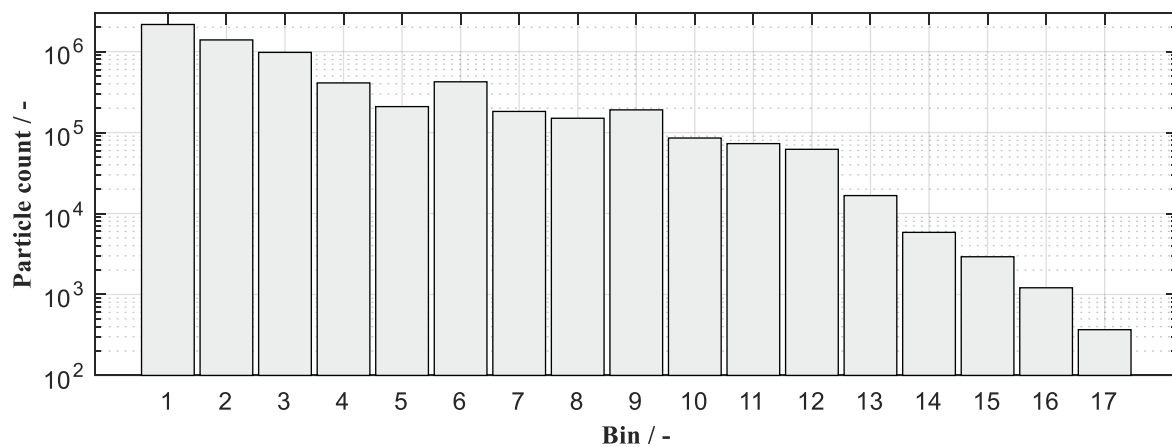


Figure 4: Particle count for one experiment without wet scrubber running

Figure 5 shows the pressure drop of the investigated wet scrubber over the water flow rate for all cases. The pressure drop increases with higher water flow rate. Depending on the water flow

rate, the pressure drop ranges from 3.6 Pa to 6.9 Pa. The difference in pressure drop among the first three settings is 1 Pa on average. There is, however, a slight jump of approximately 2 Pa in the pressure drop at the highest water flow rate investigated.

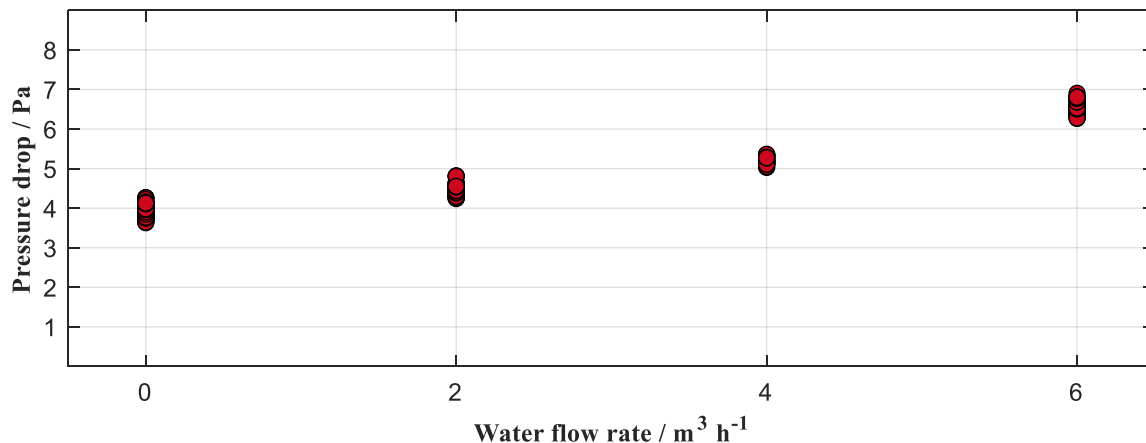


Figure 5: Pressure drop over water flow rate of all cases

Figure 6 displays the particle removal efficiency over the particle bins for the transition scenario at the three investigated water flow rates. The particle removal efficiency for bin 12 (3 – 4.162 μm) and lower bins is negative. This indicates that the particle count in the measurements with an active wet scrubber is higher than in the measurements with an inactive wet scrubber. In bin 13, the particle removal efficiency is positive for the highest water flow rate of 6 m³/h only. Starting from bin 14, the particle removal efficiencies are positive. In these bins, the particle removal efficiency increases with rising water flow rate and larger particle sizes. The efficiency rises up to 29 % for the largest particle sizes at the highest water flow rate. The uncertainty bars indicate a very good repeatability of the measurements at low bin numbers. The uncertainty increases with higher bin numbers to ± 3 percentage points (pp). The negative particle removal efficiencies range from -1.2 % to -3 % with an uncertainty of approximately ± 0.23 to ± 0.36 pp. The most negative particle removal efficiency occurs in bin 6 for a water flow rate of 4 m³/h. The described behavior can also be observed in the other scenarios.

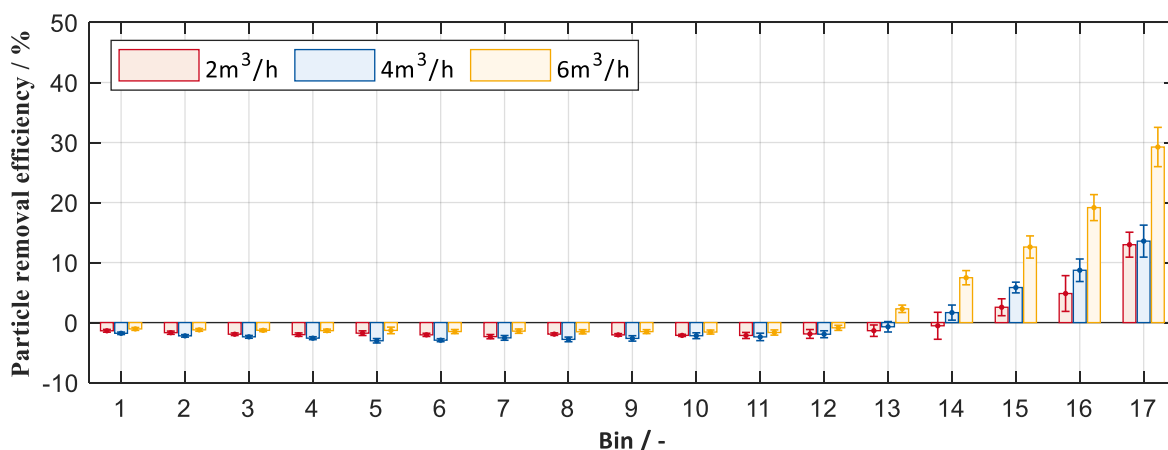


Figure 6: Particle removal efficiency for different water flow rates over the particle bins in the transition scenario

Figure 7 shows the particle removal efficiency for the various scenarios at a water flow rate of 2 m³/h (top), 4 m³/h (center) and 6 m³/h (bottom). At a water flow rate of 2 m³/h, negative particle removal efficiencies occur in bins 14 and lower. The transition scenario shows the highest particle removal efficiency at approximately 14 % for particle sizes larger than 10 μm . Overall, all scenarios achieve similar efficiencies in all bins except in bin 17, where the

transition scenario has an approximately 6 pp higher efficiency than the other scenarios. At a water flow rate of 4 m³/h, the efficiencies behave similarly to the cases with a water flow rate of 2 m³/h. However, in the higher bins, the positive particle removal efficiencies of the different scenarios are in the same range. At a water flow rate of 6 m³/h, the particle removal efficiency in the summer scenario is about 8 – 10 pp higher than in other two scenarios, which show similar efficiencies. Across all water flow rates similar negative particle removal efficiencies are detected in the lower particle bins. In analogy to Figure 6 the particle removal efficiency increases for higher water flow rates in all scenarios.

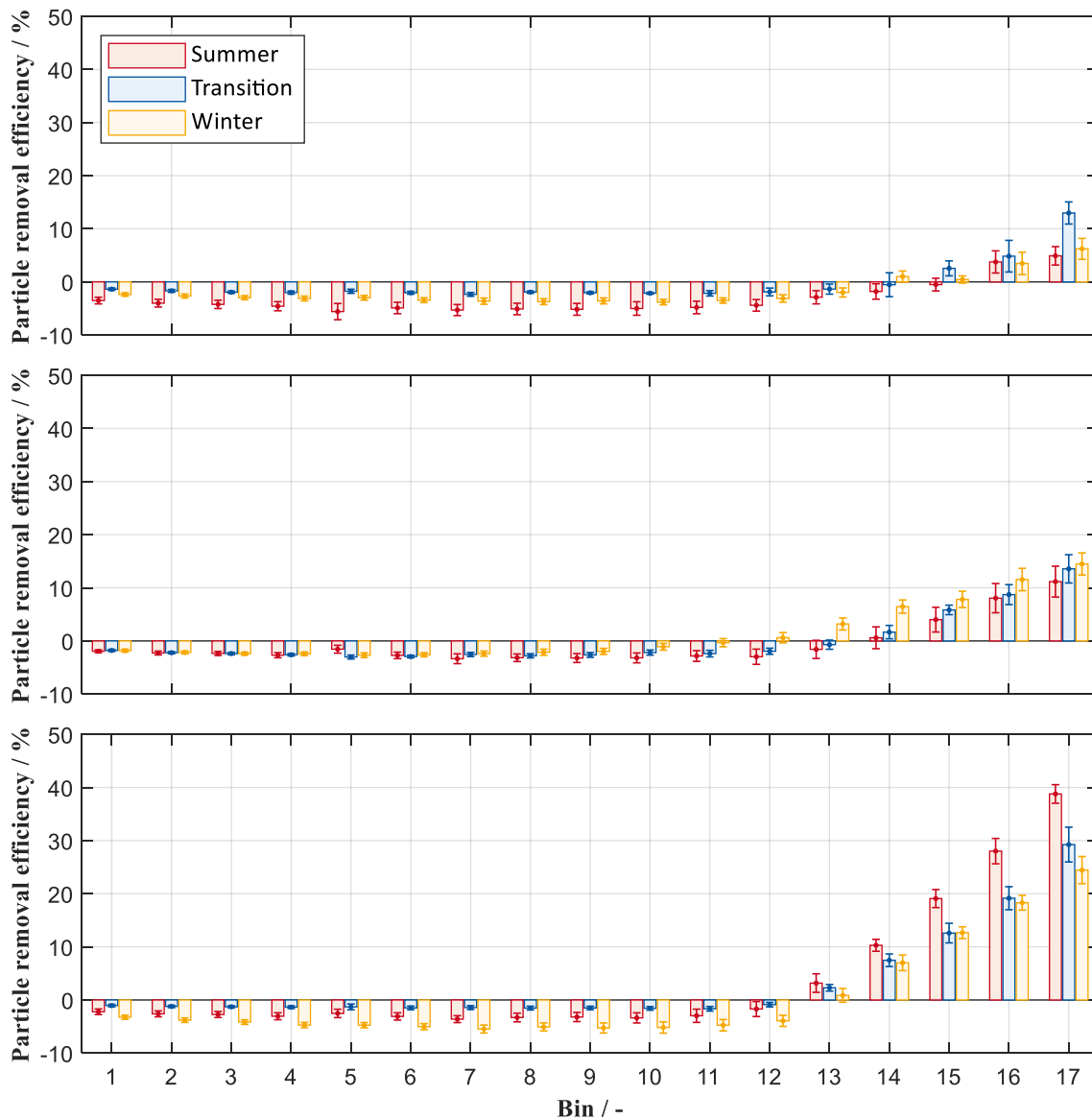


Figure 7: Particle removal efficiency for all scenarios at 2 m³/h (top), 4 m³/h (center) and 6 m³/h (bottom) for all particle bins

5 DISCUSSION

The high particle count in the lower bins allows for a better repeatability among the measurements because stochastic deviations are less significant compared to the total count. The pressure drop across the investigated wet scrubber is 1 – 2 orders of magnitudes less than in already existing wet scrubbers. This wet scrubber concept achieves a particle removal efficiency of up to 38 % depending on water flow rate and particle size. However, the particle

removal efficiency of the investigated wet scrubber is significantly lower than for existing wet scrubbers due to the relatively low number of droplets in this concept. The water is not atomized due to the low pressures applied. Therefore, the droplet sizes for the investigated concept are larger than those for existing wet scrubber concepts. The investigated wet scrubber concept has a smaller water surface area as it produces less droplets and droplets with larger diameters. This results in a lower particle removal efficiency because particle removal via interception is less likely with less contact area between the water and the particles. The generated droplets are also significantly larger than the hole diameter of the perforated plate because the water wets the plate surface and coalesces into larger droplets before falling. At a water flow rate of $6 \text{ m}^3/\text{h}$, the water forms ligaments through the plate holes without wetting the plate surface. These ligaments break into small droplets due to the relative velocity between the airflow and the water. The increase in particle removal efficiency at higher water flow rates is a result of the increased water surface area due to an increase in the number of droplets. The negative particle removal efficiencies may indicate an agglomeration of particles outside of the measureable range. However, the current OPS does not allow further investigation of particles smaller than $0.3 \mu\text{m}$ in diameter. Furthermore, the OPS detected an insignificant amount of particles in experiments with an active wet scrubber and an inactive particle feed. Hence, small water droplets that passed the droplet separator are not the cause of the significant increase in measured particles in the active wet scrubber measurements. Overall, the particle removal efficiency of each bin is approximately the same for the different scenarios. Therefore, temperature and humidity appear to have little influence on the particle removal efficiency. On the other hand, the particle removal efficiency increases with higher water flow rates.

6 CONCLUSION

We have developed a test bench to investigate our new wet scrubber concept. This wet scrubber concept reduces the energy demand by not using sprays to generate droplets and by having low pressure drops across the wet scrubber. The experimental results show, that the particle removal efficiency for coarse particles increases with higher water flow rates. A plate with a shorter perforated section may result in better droplet generation because the hydrostatic pressure is higher for the same water flow rate. Hence, the length of the perforated section shall be investigated in future studies. There is no particle removal detected for fine particles. However, if particle agglomeration occurs and increases particle sizes to larger diameters, this wet scrubber concept can be used as a pre-filter to another method that removes fine particles. Further investigations could also address the adhesion of water to the plate surface. The adjustment of the adhesion between plate surface and droplet can result in better dripping behavior and smaller droplets, which increase the water surface area. An increased water surface area facilitates the particle removal efficiency for fine and coarse particles. The adhesion can be influenced by altering the roughness of the plate surface or by applying a waterproof coating to the plate surface. Wet scrubbers can remove particulate and gaseous pollutant. Therefore, the removal of gaseous pollutant needs to be investigated in future studies to facilitate a holistic evaluation of this wet scrubber concept.

7 ACKNOWLEDGEMENTS

We gratefully acknowledge the financial support by the Federal Ministry for Economic Affairs and Climate Action (BMWK), promotional reference 03ET1606B.

8 REFERENCES

- Adar, S.D., Filigrana, P.A., Clements, N. and Peel, J.L. (2014). Ambient Coarse Particulate Matter and Human Health: A Systematic Review and Meta-Analysis. *Current Environmental Health Reports*, 1(3), 258–274.
- Beelen, R., Raaschou-Nielsen, O., Stafoggia, M. and others (2014). Effects of long-term exposure to air pollution on natural-cause mortality: an analysis of 22 European cohorts within the multicentre ESCAPE project. *Lancet (London, England)*, 383(9919), 785–795.
- Biswas, S., Rajmohan, B. and Meikap, B.C. (2008). Hydrodynamics characterization of a counter-current spray column for particulate scrubbing from flue gases. *Asia-Pacific Journal of Chemical Engineering*, 3(5), 544–549.
- Bürkholz, A. and Muschelknautz, E. (1972). Tropfenabscheider. Übersicht zum Stande des Wissens. *Chemie Ingenieur Technik - CIT*, 44(8), 503–509.
- Cheremisinoff, N.P. (2002). *Handbook of air pollution prevention and control*. Amsterdam: Butterworth-Heinemann.
- Clanet, C. and Lascheras, J.C. (1999). Transition from dripping to jetting. *Journal of Fluid Mechanics*, 383, 307–326.
- Hu, S., Gao, Y., Feng, G., Hu, F., Liu, C. and Li, J. (2021). Experimental study of the dust-removal performance of a wet scrubber. *International Journal of Coal Science & Technology*, 8(2), 228–239.
- Hystad, P., Larkin, A., Rangarajan, S. and others (2020). Associations of outdoor fine particulate air pollution and cardiovascular disease in 157 436 individuals from 21 high-income, middle-income, and low-income countries (PURE): a prospective cohort study. *The Lancet. Planetary health*, 4(6), e235-e245.
- JCGM (2008). Evaluation of measurement data - Guide to the expression of uncertainty in measurement.
- Kremer, M. and Mathis, P. (2020). *Feuchterückgewinnung für energieeffiziente RLT-Anlagen*, 112pp.
- Lee, B.-K., Mohan, B.R., Byeon, S.-H., Lim, K.-S. and Hong, E.-P. (2013). Evaluating the performance of a turbulent wet scrubber for scrubbing particulate matter. *Journal of the Air & Waste Management Association (1995)*, 63(5), 499–506.
- Lu, F., Xu, D., Cheng, Y., Dong, S., Guo, C., Jiang, X. and Zheng, X. (2015). Systematic review and meta-analysis of the adverse health effects of ambient PM_{2.5} and PM₁₀ pollution in the Chinese population. *Environmental research*, 136, 196–204.
- Qian, J., Wang, J., Liu, H. and Xu, H. (2022). Numerical Investigation of Fine Particulate Matter Aggregation and Removal by Water Spray Using Swirling Gas Flow. *International journal of environmental research and public health*, 19(23).
- Raj Mohan, B. and Meikap, B.C. (2009). Performance characteristics of the particulate removal in a novel spray-cum-bubble column scrubber. *Chemical Engineering Research and Design*, 87(1), 109–118.
- Schiffner, K.C. and Hesketh, H.E. (2017). *Wet scrubbers*. Routledge.
- World Health Organization (2016). *Ambient air pollution: a global assessment of exposure and burden of disease*. World Health Organization.
- Yee, J., Cho, Y.A., Yoo, H.J., Yun, H. and Gwak, H.S. (2021). Short-term exposure to air pollution and hospital admission for pneumonia: a systematic review and meta-analysis. *Environmental health : a global access science source*, 20(1), 6.
- Zhao, H. and Zheng, C.G. (2008). Modeling of Gravitational Wet Scrubbers with Electrostatic Enhancement. *Chemical Engineering & Technology*, 31(12), 1824–1837.

An evaluation of CO₂ emission rates by Chilean school children

Nicolás Carrasco¹, Constanza Molina^{*1}, and Benjamin Jones²

*1 Pontificia Universidad Católica de Chile
Vicuña Mackenna 4860, Macul, Santiago
Chile*

*2 Department of Architecture and Built Environment,
University of Nottingham
Nottingham, NG7 2UH, UK.*

**Corresponding author: cdmolina@uc.cl*

ABSTRACT

The predicted and measured carbon dioxide (CO₂) emitted by human respiration into an occupied space has been used as an indicator for controlling buildings' ventilation rates. However, this application assumes a constant emission rate for the entire population. Conversely, new knowledge has shown that this variable depends on the number of people in the room and their sex, diet, height, and above all, body mass and metabolic rate. This paper applies the latter model and a previously used sampling approach to identify the variability of CO₂ emission rates and excess CO₂ concentrations in school classrooms in Chile, and compares them with those in the USA. This time, we collected data from local sources and public databases to model an evidence-based average classroom of 29 students –15 men and 14 women– following the Chilean regulations and the ASHRAE 62.1 and SHRAE 241 standards for ventilation. Then, using Python and a Monte Carlo sampling approach, we calculated the emission rates for the local population in the classrooms of children between 5 and 18 years old. Results show that the mean body weights of the USA and Chilean child populations are statistically different, but the excess CO₂ concentrations can vary by only 4% between demographics. The difference in excess CO₂ concentrations between countries reflects their differences in occupancy densities. Finally, there is a significant difference in excess CO₂ concentrations for the two standards but little difference between countries for the same standard.

KEYWORDS

CO₂ concentrations; ventilation; indoor air quality; proxy indicator

1 INTRODUCTION

Carbon dioxide (CO₂) is a product of respiration and so is emitted in any spaces where people are present. Indoor CO₂ concentrations have long been used as a proxy indicator of the *per capita* ventilation rates, and a model of CO₂ generation rates has been developed that is based on principles of human metabolism and exercise physiology. It explicitly accounts for age, sex, and body mass (Persily & de Jong 2017). CO₂ has, however, been used without an adequate understanding or explanation of the limitations of doing so, and so ASHRAE (Laue, J., 2018) recently outlined key limitations. It states that when using CO₂ as an indicator of the outdoor air, ventilation rate, space type, occupant density, and occupant characteristics must be considered as factors into any analysis. Occupant characteristics include age, body mass (which is a function of sex), and activity levels. A recent investigation of uncertainty in the relationship between indoor steady-state CO₂ concentrations and ventilation rates in US school classrooms looked at the variation in emission rate of US children aged between 4 to 19 years (Molina et al. 2021). It showed that the rate of change and uncertainty in body mass is most significant in children between the ages of 4 and 14 years old. Furthermore, a global sensitivity analysis determined that the most important input into the emission rate model of Persily & de Jong is body mass. This means that standards and guidelines should use existing body mass data used by health services to determine appropriate values of mean emission rate to represent a local population. Molina *et al.* determined CO₂ emission rates for US children using government-published weight-for-age percentiles and sex ratios, and representative values of child metabolic rates in schools. The emission rates varied between 3.1 and 5.1 cm³ per person (or ppm m³ s⁻¹ per person).

As the body mass of US school children may not be comparable to those in other countries, the emission rates derived for them may not apply in other countries. Therefore, this study aims to determine if physiological data for another country may produce different emission rates, using Chilean school-age children as an example.

2 METHOD

A steady state indoor CO₂ concentration, $C_{i,ss}$, can be used to evaluate a *per capita* ventilation rate.

$$Q_o = \dot{V}_{CO_2} (C_{i,ss} - C_o)^{-1} = \dot{V}_{CO_2} C_{e,ss}^{-1} \quad (1)$$

Here, Q_o is the outdoor air ventilation rate per capita ($m^3 s^{-1}$ per person), \dot{V}_{CO_2} is the generation rate of CO₂ *per capita* ($cm^3 s^{-1}$ per person), $C_{i,ss}$ is the steady-state indoor CO₂ concentration (ppm), and C_o is the outdoor CO₂ concentration (ppm). The difference between $C_{i,ss}$ and C_o is known as the *excess CO₂* steady-state concentration $C_{e,ss}$ (ppm), which is typically a more useful metric because C_o varies by location and diurnally, and is steadily increasing over time. Here we note that ppm, which is equivalent to one μL of CO₂ per L of air, is used herein for CO₂ concentrations.

2.1 Model of CO₂ emission rates

A full description of Persily and de Jong's CO₂ emission rate model is given elsewhere (Persily & de Jong, 2017) and so only a summary is given here. The generation rate of CO₂ per capita ($cm^3 s^{-1}$ per person) is given by

$$\dot{V}_{CO_2} = BMR M RQ \dot{V}_{O_2} T P^{-1} \quad (2)$$

Here, BMR is the essential energy a person requires to sustain life, known as the *basal metabolic rate* ($J s^{-1}$ per person). We assumed it is a linear function of body mass requiring sex and age dependent gradients and intercepts, which are given in Table 1 of Persily & de Jong (2017). M is a dimensionless metabolic rate that describes the ratio of a person's energy demand required to complete a specific physical activity relative to their BMR. RQ is the ratio of the volumetric rate at which CO₂ is produced to the rate at which oxygen is consumed, known as the *respiratory quotient*. For well-nourished people in a normal weight range, its primary determinant is diet. Fractions of dietary carbohydrates, fats, proteins, and alcohol by sex are derived from the US National Health and Nutrition Examination Surveys (Wright & Wang, 2010). They are assumed to be constant because uncertainties in these values are not given, and we also assume that children do not consume alcohol. \dot{V}_{O_2} is a person's rate of oxygen consumption ($cm^3 J^{-1}$) and implicitly assumes that 1 kcal (4.2 J) of energy use requires 206 cm^3 of oxygen consumption. Finally, T is the ratio of the air temperature to 273.15 K, and P is the ratio of the air pressure to 101.325 kPa. We assume indoor temperatures and pressures are 293.15 K and 101.325 Pa, respectively, so T and P are 1.07 and 1.00, respectively, throughout.

2.2 Sources of information and assumptions

Child body mass and BMI values are sampled by age, and extracted from the standardized growth patterns for the child and adolescent population issued by the Chilean Ministry of Health (MINSAL, 2018). The corresponding age was allocated for each school grade following the grades given by the Ministry of Education of Chile. Each grade is mixed-sex and each class has 29 students, comprising 15 males and 14 females, reflecting the Chilean population sex ratios between 1950 and 2020.

The metabolic rate, M , is determined as a function of age, and three activities of different physical intensities are considered to occur in a classroom: *playing on the computer*, *watching*

TV, and *household chores*, with a time-weighted ratio of 0.75:0.15:0.1, respectively, to give a weighted M . This weighted factor accounts for high-intensity activities that do not usually occur for prolonged periods. Therefore, its values are higher than those used by Molina et al. (2020), and Equation (2) shows that this should increase the value of \dot{V}_{CO_2} . M is then calculated by age band following Pfeiffer (2017). Pfeiffer's analysis is for the US child population, so we compared the two population samples using the T -test.

An appropriate value of RQ for well-nourished children is around 0.85, following Wright et al. (2010). However, only around 37% of children in Chile can be considered *well nourished* (Lira, M., 2022), and so we assume it is normally distributed with a mean of 0.82 and a standard deviation of 0.07.

2.3 Sampling method

The sampling method uses a Monte Carlo (MC) approach written in Python code to interrogate the probability space. The model requires input variates that are specified deterministically or are described by continuous probability distributions. They are applied to the \dot{V}_{CO_2} model and,

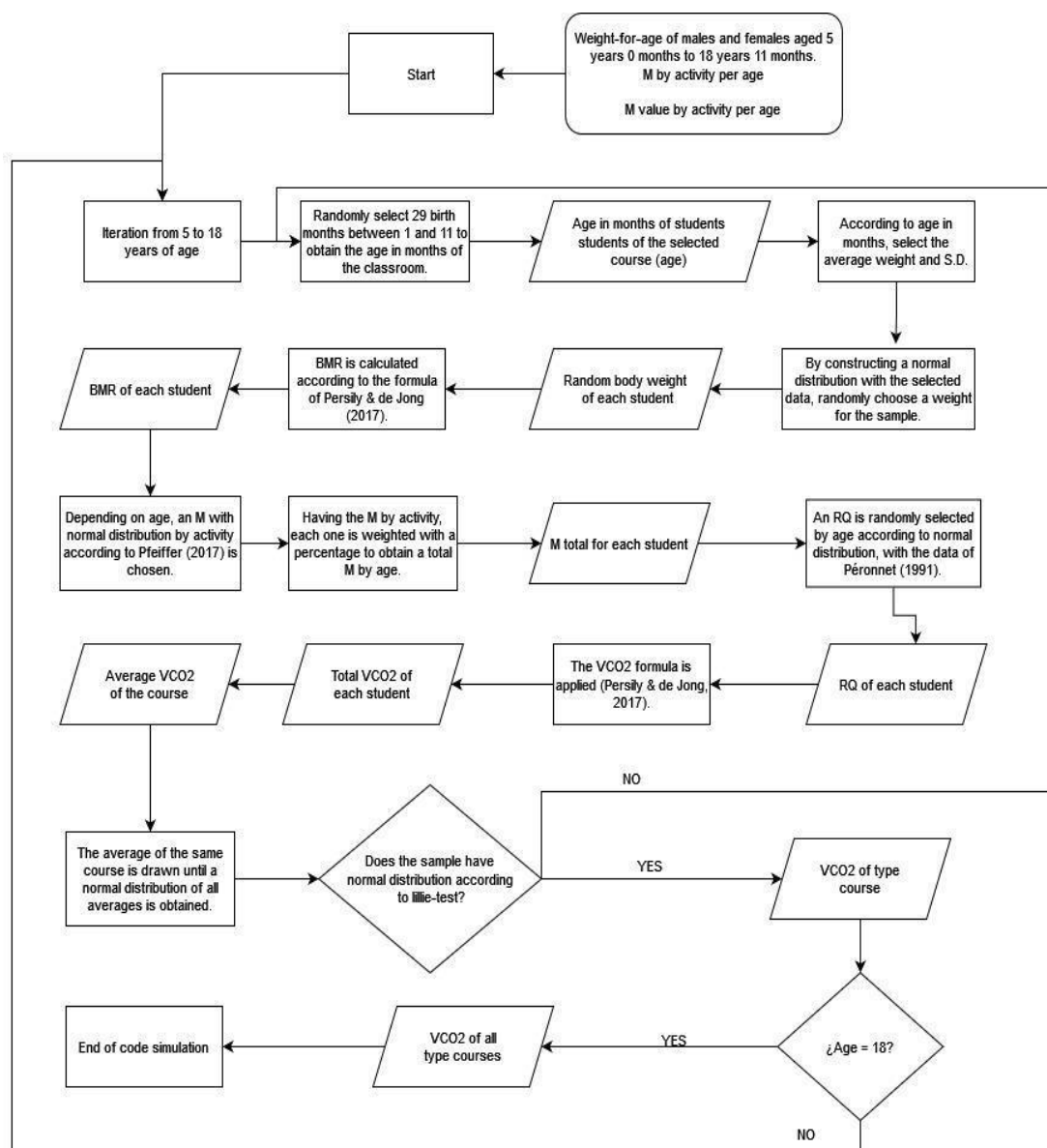


Figure 1: Model system diagram

by systematically varying the variates and running multiple simulations, distributions of \dot{V}_{CO_2} are generated that quantify the uncertainty in \dot{V}_{CO_2} . The modeling approach is shown in Figure 1.

Inputs were sampled to form a class of children for each age group. The Python code was run until a normal distribution of the means of each age class was obtained. A Lillie test is used to confirm the normality of the sampling distribution of means.

2.4. Comparison to standards

Classrooms in the US use ASHRAE standards 62.1. to determine outdoor air delivery rates, which comprise the sum of a *per capita* air flow rate and a flow rate of 0.6L/s per unit floor area. The *per capita* air flow rate and classroom occupancy density are different for children aged 5 to 8 years and those aged 9 or more years old. ASHRAE Standard 241 gives airflow rates designed to control of infectious aerosols, requiring 20L/s per person. Equation 1 is used to determine the excess concentration $C_{e,ss}$ and are compared for each age group and each standard (using default occupancy densities for 62.1).

3 RESULTS AND DISCUSSION

Figure 1 shows the distributions of \dot{V}_{CO_2} by age group. The change is non-linear, plateauing as the children reach around 14 years of age. It also shows a clear difference between 5 and 18-year-old children. This is reflected by the relationship between \dot{V}_{CO_2} and body mass, shown in Figure 3. The body weights of the USA and Chilean child populations are found to be different at a statistically significant level by using the T-test.

Figure 2 shows that the distributions of \dot{V}_{CO_2} are not normal, which agrees with the findings of Molina *et al.* Therefore, an appropriate representative statistic is the median, and so these are given in Table 1 for each age band.

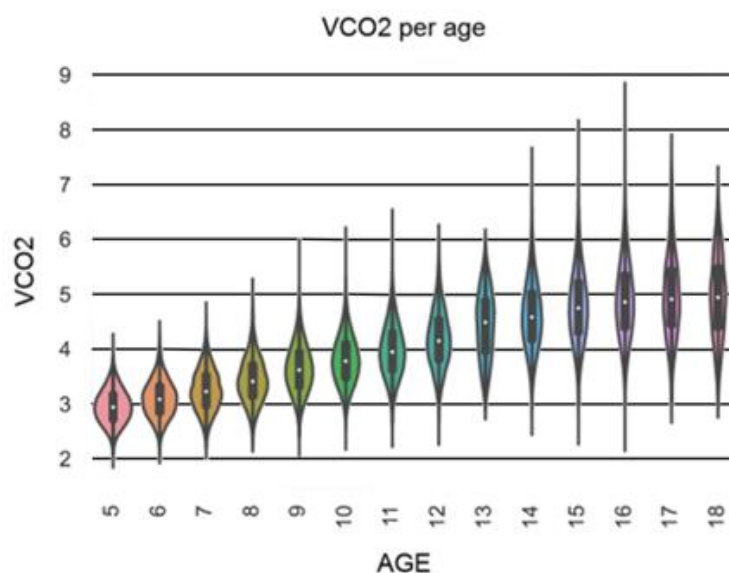


Figure 2: Distribution of \dot{V}_{CO_2} emission by age group

Table 1 also gives the excess concentrations $C_{e,ss}$ for each age group and for each standard (using default occupancy densities for 62.1) applying Equation 1. This shows that there is a significant difference in $C_{e,ss}$ for the two standards (T-test, $p \ll .01$; Cohen's d , *strong* effect for both countries), but there is very little difference between countries for the same standard (Cohen's d ; *above the minimum* for the ASHRAE 62.1, and *no effect* for the ASHRAE 241).

Table 1: \dot{V}_{CO_2} and $C_{e,ss}$ for ASHRAE standards governing classrooms.
All values given to 2 significant figures.

Age	Median \dot{V}_{CO_2}		Excess concentration, $C_{e,ss}$			
			ASHRAE 62.1		ASHRAE 241	
	USA	Chile	USA	Chile	USA	Chile
5	3.1	3.0	420	490	160	150
6	3.3	3.1	440	510	160	160
7	3.4	3.2	460	540	170	160
8	3.6	3.4	490	570	180	170
9	3.9	3.6	580	600	200	180
10	3.9	3.8	580	630	200	190
11	4.1	4.0	610	660	210	200
12	4.3	4.2	640	700	220	210
13	4.5	4.4	670	740	230	220
14	4.8	4.6	720	760	240	230
15	5.0	4.8	750	790	250	240
16	4.9	4.9	730	810	250	240
17	5.0	5.0	750	830	250	250
18	5.1	5.0	760	830	260	250

The reason for the higher excess concentrations in Chilean classrooms, despite their lower emission rates, is because occupancy densities are different, at around 60 people per 100m² as opposed to the 25 and 35 people per 100m² in the US for 5-8 year olds and over 9 year olds, respectively. This shows that standardized values of $C_{e,ss}$ need to be country specific if the occupancy densities differ.

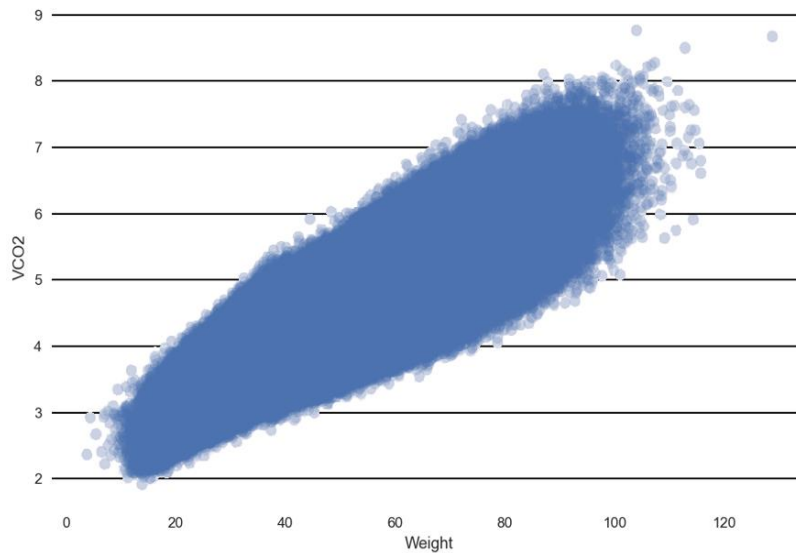


Figure 3: The relationship between \dot{V}_{CO_2} and body weight for both sexes combined.

The differences in $C_{e,ss}$ and \dot{V}_{CO_2} for the age bands of each country are small. The magnitude of \dot{V}_{CO_2} is heavily dependent on the body mass of the children. The difference between the distributions of body mass for each age band for each country is tested using a T-test to show that there is not enough evidence to conclude that their means are different ($p > .05$). When

considering emission rates for other countries, if the body mass of the new population is like those used for existing calculations of \dot{V}_{CO_2} , there is no need to revise them.

Finally, when a building is run in infection risk mitigation mode when ASHRAE Standard 241 applies, then an excess concentration of 150 ppm ensures the children of all age groups meet its requirements.

3.1 Limitations

When this same model was used by Molina et al. (2021) for the calculation of the US population, extensive databases were found with information on inputs, such as body mass, height, and BMI. For Chile, however, information on the nutritional status of the child and the adolescent population is scarce and unavailable to the general public. The Ministry of Health of Chile has some limited public reports, but they do not cover all age groups. It does project the body mass, height, and BMI of the child and adolescent population to compare them against the same projections made by the World Health Organisation.

4 CONCLUSIONS

Metabolic CO₂ emission rates for US and Chilean children for the same activities in school classrooms are broadly similar, and they follow the same age-related trends. This is because differences in the body mass of both populations of children are statistically insignificant. The existing uncertainties in estimating a per capita ventilation rate from a steady state carbon dioxide concentration mean that it is possible for other countries whose distributions of child body mass broadly agree with those in the US to use the emission rates derived for the US.

There are differences between the CO₂ emission rates of 5- and 18-year-old students, which range between 3 and 5 cm³ s⁻¹ per person. If the age of students is unknown, or if they may vary over some period, the smaller value should be used to determine an excess steady-state concentration threshold.

Finally, excess steady-state concentration thresholds should be determined locally if the standardized airflow rates are a function of the classroom floor area. This is because occupancy densities are inconsistent.

6. References

- Molina, C., Jones, P. B., & Persily, E. A. (2021) Investigating Uncertainty in the Relationship between Indoor Steady-State CO₂ Concentrations and Ventilation Rates.
- MINSAL.(2018). Patrones de crecimiento para la evaluación nutricional de niños, niñas y adolescentes desde el nacimiento hasta los 19 años de edad
- Laue, J. (2018). ASHRAE 62.1: using the ventilation rate procedure. *Consult. Spec. Eng*, 55, 14-17.
- Wright, J. D., & Wang, C. Y. (2014). Trends in intake of energy and macronutrients in adults from 1999-2000 through 2007-2008. NCHS data brief. 2010 (49): 1–8.
- Pfeiffer, K. A., Watson, K. B., McMurray, R. G., Bassett, D. R., Butte, N. F., Crouter, S. E., ... & Berrigan, D. (2018). Energy cost expression for a youth compendium of physical activities: Rationale for using age groups. *Pediatric exercise science*, 30(1), 142-149.

- Persily, A., & de Jonge, L. (2017). Carbon dioxide generation rates for building occupants. *Indoor air*, 27(5), 868-879.
- Lira, M. (2022). Informe Mapa Nutricional 2021. *JUNAEB: Santiago, Chile*.

The Effects of Bedroom Mechanical Ventilation on Health and Sleep Quality

Jeong Won Kim¹, Sun Ho Kim¹, Yong Kyu Baik², and Hyeun Jun Moon^{*1}

*1 Dankook University
152, Jukjeon-ro*

*Suji-gu, Yongin-si, Gyeonggi-do
Presenting author: underline First & Last name
Corresponding author: hmoon@dankook.ac.kr

*2 Seoil University
28, Yongmasan-ro 90-gil
Jungnang-gu, Seoul*

ABSTRACT

Sleep is essential for overall health and well-being. The quality and efficiency of sleep are strongly influenced by the sleep environment, including indoor air quality. This study investigates the influence of mechanical ventilation on bedroom air quality during sleep and its impact on sleep efficiency and quality. Objective and subjective measurements were conducted to assess the effects of operating a mechanical ventilation system. The results showed that both objective and subjective evaluations of sleep quality demonstrated the improvement of sleep quality when the ventilation system was in operation. Conversely, when the ventilation system was not used, the objective indicator of sleep efficiency was lower, indicating an increase in sleep disturbances. These findings suggested that maintaining low CO₂ concentrations could enhance the sleep efficiency and quality. These findings provide foundational insights for further studies on appropriate sleep environment.

KEYWORDS

Sleep efficiency, Sleep quality, Mechanical ventilation, Bedroom environment, CO₂ concentrations

1 INTRODUCTION

1.1 Background

Sleep is essential for energy restoration, physical and mental recovery, and maintaining bodily functions, accounting for approximately one-third of the total time (M.R. Opp, 2009). The quality of sleep is influenced by various internal factors, such as indoor environmental conditions, individuals' health status, and emotional state. Good sleep is generally crucial for human health and well-being, and many factors of indoor environmental quality (IEQ) affect the quality of sleep including air temperature and relative humidity, air velocity, concentration of particle matter, lighting levels, noise levels, and ventilation rates. While most people may not consciously perceive environmental changes during sleep, research findings are suggesting that indoor environmental factors such as indoor air quality, temperature, and relative humidity (RH) have a significant impact on sleep quality (Lan et al, 2017, He et al, 2019). Indoor air quality and thermal environment significantly contribute to the recovery of psychological and physical fatigue accumulated during sleep (Lan et al., 2014; Wang et al., 2015). To ensure sleep quality, it is important to have an appropriate thermal environment, lighting, noise control, and healthy indoor air quality. Zhang et al. (2021) suggest that the sleep environment, in contrast to factors like psychological state and physical conditions, can be easily modified and controlled. Therefore, conducting additional research is deemed valuable to gather conclusive evidence on the significant impact of indoor environmental factors, such as air quality, temperature, and

relative humidity, on sleep quality. Healthy indoor air refers to air that contains sufficient oxygen, has lower carbon dioxide levels, and contains normal air ions. Additionally, there is an increasing interest in creating healthier and safer indoor spaces due to the recent COVID-19 pandemic. Bedrooms in residential spaces often have smaller volumes compared to living rooms and are more likely to lack ventilation systems. As occupants may not consciously implement planned ventilation in the bedroom, adequate ventilation is crucial for maintaining good indoor air quality. There is limited research focusing on the impact of bedroom air quality and ventilation on sleep quality (Xiong et al., 2020; Storm-Tejsen, 2016). Therefore, this study aims to analyse the difference in sleep efficiency based on the operation of bedroom ventilation systems.

1.2 Scope of the study

In this study, we analyzed the difference in sleep efficiency depending on the operation of the ventilation system in an experimental testbed with two bedrooms, which was designed to replicate a real residential environment. A total of four university students participated in the experiment. Participants slept in separate bedrooms within the environmental chamber. The ventilation system was controlled while the participants were sleeping, and changes in carbon dioxide concentrations were monitored. Objective sleep efficiency was measured using Actigraph during sleep, and participants' subjective evaluation of sleep quality was conducted after the experiment to assess the appropriateness related to ventilation during sleep from a comfort perspective.

2 METHOD

2.1 Experimental facility and subjects

This study aimed to analyse the difference in sleep efficiency of occupants based on the operation of the ventilation system during sleep in a typical residential space. The study included a total of four healthy young adults, two males and two females in their 20s. The experiments were conducted in the Smart Living Testbed, a chamber designed to simulate a residential unit (dimensions: length (L) 8m x width (W) 5m x height (H) 2.7m) (Figure 1). The experimental testbed, as shown in Figure 1, was located inside a bigger indoor space with climate control systems. There are two bedrooms in the testbed, and participants of the same gender entered their rooms to sleep respectively. Participants were instructed to exclude factors that could affect the experiment, such as excessive physical exertion, alcohol consumption, smoking, and should try to maintain their normal lifestyle. Additionally, to eliminate factors that could affect the experiment, participants were provided with sleepwear and bedding, and were encouraged to sleep from 12 AM to 8 AM.



Figure 1: Images of the Smart Living Testbed for sleep experiments

2.2 Experimental design

To investigate the impact of indoor air quality on sleep, sleep experiments were conducted with a mechanical ventilation system. The experimental conditions were set to be identical except for the use of the ventilation systems. The ventilation system was operated within a range (150m³/h) that had been determined through pre-experiments to ensure it did not disturb the participants' sleep. The qualitative evaluation of sleep was conducted using a sleep questionnaire, and the quantitative evaluation was performed using Actigraph (Table 1). Actigraph is a research-oriented device based on technology that measures sleep and wakefulness activity, allowing for accurate investigation of sleep patterns in healthy adults or patients (Figure 2). Although Actigraph cannot classify sleep stages, it provides data on total sleep time, sleep onset latency, sleep efficiency, and the number of awakenings during sleep. The questionnaire used in this study evaluated subjective sleep quality based on the criteria proposed by Zilli et al., including 6 items such as calmness of sleep, ease of falling asleep, ease of awakening, freshness after awakening, satisfaction about sleep, and sufficient sleep (Zilli et al, 2009). Each item included five levels (Fully, Fairly, Moderately, Not much, and Not at all), with higher level indicating higher sleep quality. The question regarding sufficient sleep is scored on a 1-point scale, with "Yes" or "No" options. The total score for the 6 items is 26 points. Previous research has shown that the results of this questionnaire align with EEG measurements (Lan et al., 2014).



Figure 2: Sleep efficiency measurement bands (Actigraph)

Table 1: Sleep assessment methodology

Criteria	Variables	Unit/Range	Interpretation	Interval
Sleep quality (Zilli et al, 2009)	Survey	0-26	0 = bad, 26 = good (Sleep Quality)	Daily
Actigraph	Length of sleep	minutes	-	1 min
	No. of awakenings		-	1 min
	Sleep efficiency	0%-100%	-	Daily

Each experimental session was conducted from 22:00 (10:00 PM) to 8:30 the following day, as shown in Figure 3. The participants attended the orientation of the experiment and changed cloth into the provided sleepwear. They were provided with an 8oz standard bedding. On the day of each experiment, participants arrived at the experiment site 2 hours before the start of the experiment and wore the equipment, and acclimatized to the experimental environment. Sleep was initiated at 24:00 (12:00 AM) after lights were turned off, and the evaluation of the previous night's sleep was conducted upon waking up.

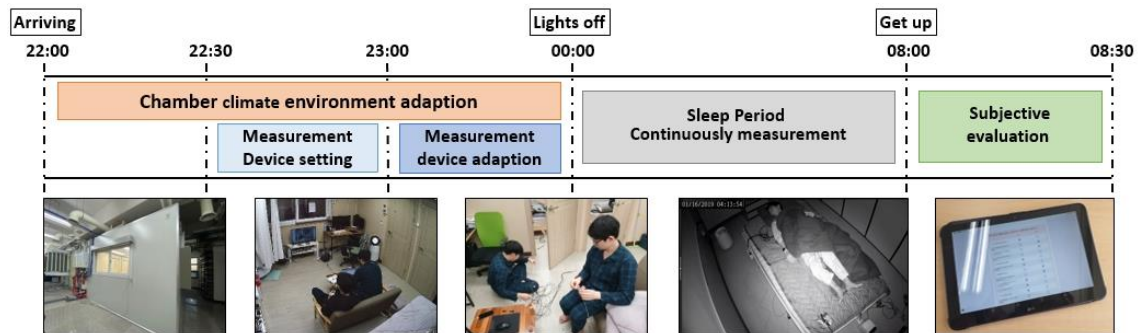


Figure 3: Experimental procedure

3 RESULT

The carbon dioxide (CO₂) levels according to the operation of the ventilation system are presented in Figure 4. In Case A, the ventilation system was operated, while in Case B, the ventilation system was not operated. In Case A, where the ventilation system was operating, the CO₂ concentrations ranged from a minimum of 394 to a maximum of 573 ppm. In contrast, in Case B, where the ventilation system was not operating, the CO₂ concentrations ranged from a minimum of 449 to a maximum of 1,321 ppm. Before the experiment, with no occupants in the bedroom, the initial CO₂ concentrations were measured between 394 and 575 ppm. Subsequently, in Case A (ventilation on) the CO₂ concentrations remained at similar levels to the initial measurements, whereas in Case B, the CO₂ concentrations gradually increased. The average CO₂ concentration in Case A was 492 to 537 ppm, while in Case B, it ranged from 1,019 to 1,152 ppm. In Case B, the CO₂ concentration increased from an initial average of 495 ppm to a maximum of 1,321 ppm. It can be concluded that without the operation of the ventilation system, the CO₂ concentration increased due to the occupants' respiration. Therefore, when the ventilation system was not in operation in this testbed, it was not able to meet the requirements for indoor CO₂ concentration levels specified in international ventilation standards such as ASHRAE and CEN.

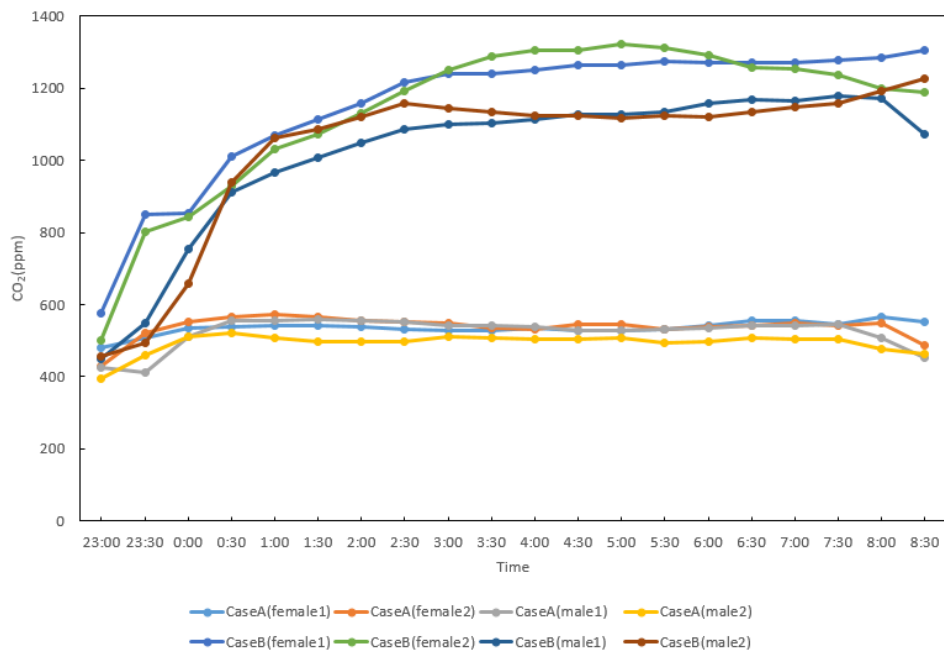
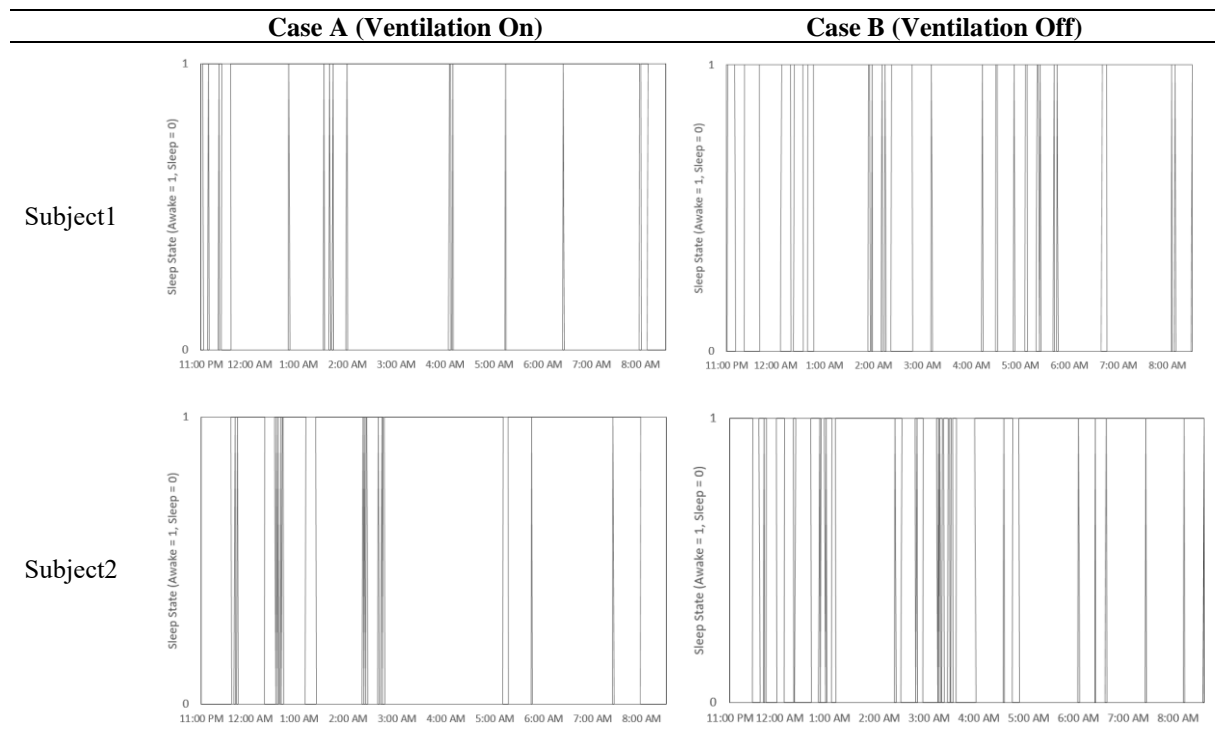
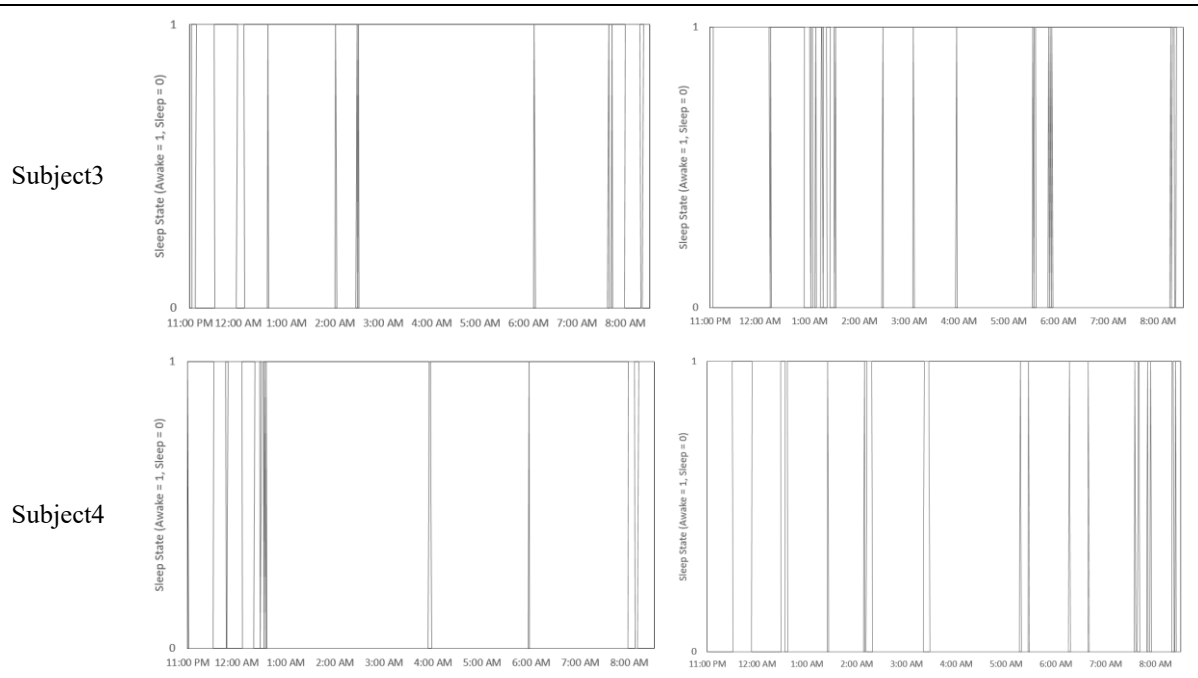


Figure 4: CO₂ Concentration

The quantitative evaluation of participants' sleep was measured using Actigraph. Table 2 presents the participants' sleep movements for each case. The more movements during sleep, the lower the sleep efficiency. In Case A, the average number of sleep movements ranged from 7 to 35, with a mean of 17.5. In Case B, the average number of sleep movements ranged from 29 to 94, with a mean of 52.3. Sleep movements decreased by approximately 66% when the ventilation system was operated during sleep.

Table 2: Subject's Sleep State





Investigating the individual evaluations of participants' sleep, in terms of quantitative evaluation results, the sleep quality of Subject 2 showed the most significant improvement, while Subject 3 showed the lowest improvement. The sleep efficiency of Subject 2 was the lowest in Case B, at 79%, and increased by 17.5% to 95.7% in Case A. The sleep efficiency of Subject 3 was the highest in Case B, at 92.8%, and increased by 3.7% to 96.4% in Case A. In subjective evaluation results, represented by the sleep questionnaire, Subject 2 also showed the most significant improvement, while Subject 3 reported similar sleep quality regardless of ventilation operation. The sleep quality of Subject 2 was the lowest in Case B, at 6 points, and improved by 57% to 14 points in Case A.

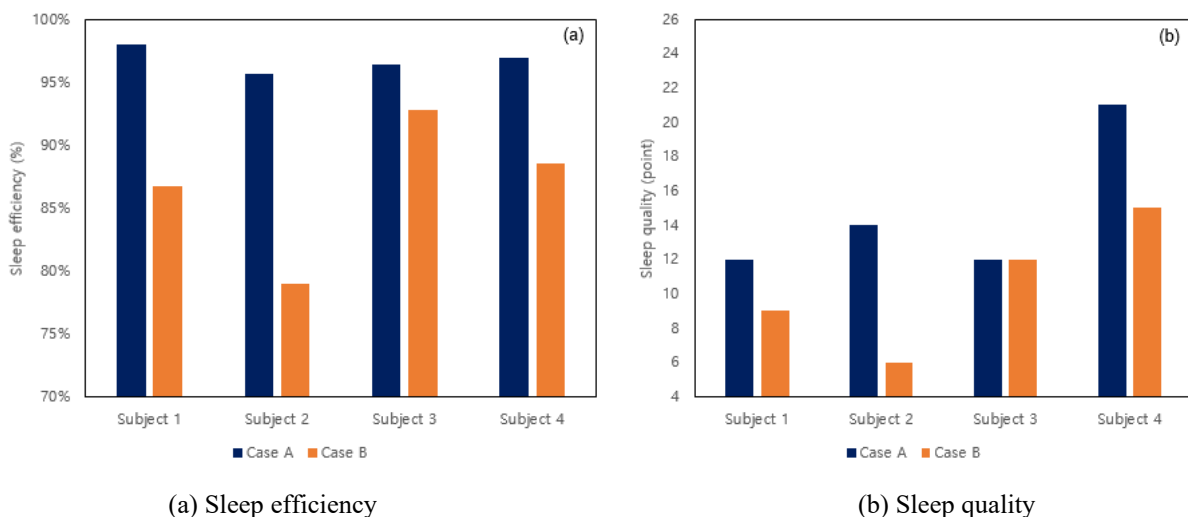


Figure 5: Sleep efficiency and quality depending on the operation of the ventilation system

The comprehensive analysis of the participants' sleep results revealed that in Case A, where the ventilation system was operational, the sleep efficiency ranged from 95.7% to 98%, with an average sleep efficiency of 97%. On the other hand, in Case B, where the ventilation system was not operational, the sleep efficiency ranged from 79% to 92.8%, with an average sleep

efficiency of 86% (Table 3). This indicates that the operation of a mechanical ventilation system can lead to a maximum improvement of 17.5% in sleep efficiency.

Furthermore, the qualitative assessment using a sleep questionnaire, with a total score of 26 points, showed that in Case A, the sleep quality ranged from 12 to 21 points, with an average sleep quality of 15 points. In Case B, the sleep quality ranged from 6 to 15 points, with an average sleep quality of 10 points (Table 3). This indicates that the operation of a mechanical ventilation system resulted in a maximum improvement of 57% in sleep quality.

Table 3: Sleep assessment scores using Actigraph and questionnaires

	Case A (Ventilation On)			Case B (Ventilation Off)		
	Avg	Min	Max	Avg	Min	Max
Sleep efficiency (%)	97.0	95.7	98.0	868.8	79.0	92.8
Awakenings (No.)	17.5	7.0	35.0	52.3	29.0	94.0
Sleep quality (points)	14.8	12.0	21.0	10.5	6.0	15.0

These results indicate that the operation of the ventilation system has a positive impact on sleep efficiency and sleep quality. By maintaining appropriate CO₂ levels in a bedroom, the sleep environment could be improved, leading to a positive influence on the participants' sleep.

4 CONCLUSIONS

In this study, we investigated the impact of mechanical ventilation in bedroom on sleep quality. Objective and subjective measurements of sleep efficiency were conducted according to the operation of the ventilation system. The results showed that both objective and subjective evaluations of sleep quality were improved in the case where the ventilation system was operated. In the case where the ventilation system was not operated, the objective indicator of sleep efficiency was lower, indicating an increase in the number of awakenings during sleep. Although these research findings may not be statistically significant, the overall results suggest that improving sleep quality and efficiency can be achieved by introducing outdoor air through a mechanical ventilation system. Future research should consider increasing the number of participants for further analysis and conducting experiments with various combinations of sleep parameters. These research findings could serve as foundational data for studies on appropriate sleep environment.

5 ACKNOWLEDGEMENTS

This research was supported by the National Research Foundation of Korea (NRF) grant funded by the Korea government (MSIT) (No. 2021R1A2B5B02002699). This work was supported by the Korea Institute of Energy Technology Evaluation and Planning (KETEP) and the Ministry of Trade, Industry & Energy (MOTIE) of the Republic of Korea (No. 20212020800120).

6 REFERENCES

Opp, M.R. (2009) Sleeping to fuel the immune system: mammalian sleep and resistanceto parasites. *BMC Evol Biol* 9:8-10

- Lan L, Tsuzuki K, Liu YF, Lian ZW. (2017). Thermal environment and sleep quality: a review. *Energy Build.* 149: 101- 113.
- He M, Lian Z, Chen P. (2019). Evaluation on the performance of quilts based on young people's sleep quality and thermal comfort in winter. *Energy Build.* 183: 174- 183.
- Lan, L., Pan, L., Lian, Z.W., Huang, H., Lin, Y.B. (2014). Experimental study on thermal comfort of sleeping people at different air temperatures. *Building and Environment* 73:24–31
- Wang, Y., Liu, Y., Song, C., Liu, J. (2015). Appropriate indoor operative temperature and bedding micro climate temperature that satisfies the requirements of sleep thermal comfort. *Building and Environment* 92:20–29
- Zhang, X., Luo, G., Xie, J., & Liu, J. (2021). Associations of bedroom air temperature and CO2 concentration with subjective perceptions and sleep quality during transition seasons. *Indoor air*, 31(4), 1004-1017.
- Xiong, J., Lan, L., Lian, Z. (2020). Associations of bedroom temperature and ventilation with sleep quality. *Science and Technology for the Built Environment* 26(9) 1274-1284
- Storm-Tejsen, P., Zukowska, D., Wargocki, P., Wyon, D.P., (2016). The effects of bedroom air quality on sleep and next-day performance. *Indoor air* 26(5): 679-686
- Zilli I, Ficca G, Salzarulo P. (2009) Factors involved in sleep satisfaction in the elderly. *Sleep Med.* 10(2): 233- 239.

Analysis of PM_{2.5} indoor-outdoor ratio in lobby floor according to configurations of entrance

So-Yi Park¹, Jae-Hun Jo^{*2}

1 Department of Architectural Engineering, Inha University, Incheon, Korea

2 Division of Architecture, Inha University, Incheon, Korea

**Corresponding author: jhjo@inha.ac.kr*

ABSTRACT

Outdoor PM_{2.5} has a continuous and significant effect on the indoor environment, and lobby floors, in particular, can be exposed to high concentrations due to entrance doors and greater airflow rates than other floors. In this study, the PM_{2.5} indoor-to-outdoor (I/O) ratio for lobby floors was evaluated according to the operation type and configuration of entrance doors. Airflow analysis was conducted for an office building with multi-zone network simulation, and the I/O ratio was evaluated for different entrance strategies according to the occupant traffic schedule. This study analyzed door configurations with and without vestibules using swinging doors and revolving doors. As airflow analysis results, the neutral pressure level is located at 40% of the total height of the building. The pressure difference across the envelope of the lobby floor was less than the top floor, whereas the airflow was the greatest within the building. As contaminant analysis results, PM_{2.5} I/O ratios reaching a steady state for the single-type (S-S, S-R) was higher than the box and combo-type (B-S, B-R, C-S, C-R) due to vestibule. Entrances consisting of a single door with no vestibule are directly connected to the outdoor environment and can be exposed to PM_{2.5} concentrations equal to or higher than outdoor levels. However, the boxed doorway with a vestibule was exposed to concentrations closer to the outdoors, with a maximum I/O ratio of 1.024 when there was no difference in operating time between the two doors. This indicates that the vestibule strategy is meaningless in a scenario where both doors open and close simultaneously. Therefore, architectural methods to design door configurations and additional measures to control door operations are needed to ensure and manage indoor air quality in lobbies.

KEYWORDS

Entrance Door, PM_{2.5}, Multi-zone Network Simulation, Indoor Air Quality

1 INTRODUCTION

In Korea, the number of days exceeding the World Health Organization's daily average criteria of 25 µg/m³ is greater than 50% in a year (Lee, 2014). The concentration of indoor PM_{2.5}, in the absence of an indoor source, is increased by penetration from the outdoor environment and 30%–75% of indoor PM_{2.5}, originating from the outdoor environment (Dockery et al., 1981, Xiong et al., 2004). Outdoor PM_{2.5} has a continuous and significant effect on the indoor environment.

Outdoor PM_{2.5} can be transported indoors by relying on airflow. In high-rise buildings, during winter, indoor-outdoor temperature difference causes to be drawn from the bottom of the building and rise along vertical paths (such as elevator shafts and stairwells) to carry PM_{2.5}. Many studies have confirmed the significant impact of PM_{2.5} on indoor environments on the lower floors of a multistory building (Lee et al., 2017, Fu et al., 2022, Park et al., 2022). Lobby floors, in particular, can be exposed to high concentrations due to entrance doors and greater airflow rates than other floors. Therefore, it is necessary to evaluate the impact of entrance doors on indoor PM_{2.5} to implement appropriate particle control measures.

The PM_{2.5} penetration between two zones through doors or cracks has been studied, providing insight into the transport of pollutants (Thatcher et al., 1995, Lv et al., 2018). The investigations

have suggested that architectural characteristics, such as airtightness level, affect the indoor particle concentration (Stephens et al., 2012). However, only a few studies have been conducted in high-rise buildings and multi-zones (Lee et al., 2017). In addition, there is a lack of research focusing on entrance doors as a main pathway for outdoor PM_{2.5}.

In this study, the PM_{2.5} I/O ratio for lobby floors was evaluated according to the operation type and configuration of entrance doors. Airflow analysis was conducted for an office building with multi-zone network simulation, and the I/O ratio was evaluated for different entrance strategies according to the occupant traffic schedule. The purpose of this is to provide a basis for designing entrance doors for lobby floors, which are the main penetration pathways for PM_{2.5} in high-rise buildings.

2 APPROACH

2.1 Penetration of PM_{2.5} through entrance doors

The mechanism of indoor PM_{2.5} concentration consists of indoor-outdoor exchange, exchange between indoor spaces, deposition on indoor surfaces, suspension, and generation (Raunemaa et al., 1989, Kulmala et al., 1999). In this study, it was assumed that no resuspension and generation occurred to focus on the penetration process of outdoor PM_{2.5}. Therefore, the indoor PM_{2.5} concentrations can be expressed as follows:

$$V \left(\frac{dC_i}{dt} \right) = Q_{io}PC_o - Q_{ij}C_i - KVC_i \quad (1)$$

Where,

V , volume of the room, m³

C_i, C_o , indoor and outdoor particle concentration, #/m³

Q_{io}, Q_{ij} , indoor-outdoor and zone i-j exchange rate, m³/s

P , penetration coefficient

K , particle deposition rate

The three terms on the left-hand side of equation (1) represent indoor-outdoor exchange, exchange between indoor zones, and deposition. The deposition process is affected by the gravity of the particle mass. The indoor concentration is determined by the air exchange rate (Q_{io}, Q_{ii}). Airflow in a building is defined by the following power law:

$$Q = C(\Delta P)^n \quad (2)$$

Where the pressure difference (ΔP) is determined by the geometry of the building and weather conditions, and C and n represent the characteristics of the opening through which the air passes. The airflow through an entrance door depends on its type of operation and configuration. In office buildings, swing, revolving, and sliding doors are typically used, along with vestibules if necessary. For effective lobby floor planning, the variation in the PM_{2.5} I/O ratio with door configuration was analyzed in a simulation case study.

2.2 Simulation conditions

CONTAM, a multizone network simulation software, was used to evaluate indoor PM_{2.5} concentrations under different door conditions. The model building is a 15-story educational facility located in South Korea. Table 1 summarized the building. The building has two main entrances on the first floor, a podium on floors 1st-4th, and a tower on floors 5th-15th. The

offices and classrooms are located in the tower section. Assuming an office building with constant occupancy traffic, we derived the expected occupancy load and traffic rate based on the floor area, as shown in Figure 1. The traffic rate can be divided into ranges I and II. Both ranges have the same number of occupants; however, the difference is that range I has a normal distribution over a five-hour range, whereas range II has a normal distribution over a seven-hour range.

Table 1 Summary of model building

Parameter	Content
Location	Incheon, Korea
Floor	15 F
Gross floor area	25,813 m ²
Office floor area	10,534 m ²
Occupant density (IBC, 2012)	9.3 m ² /people

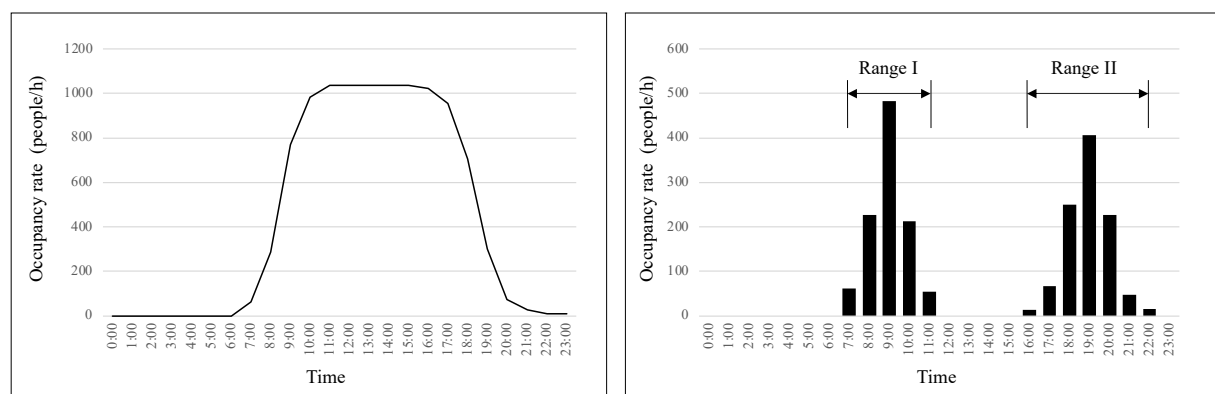


Figure 1 Occupancy schedule (right) and occupancy traffic rates (left) of model building

The input data for the airflow and contaminant analysis of the model building are listed in Table 2. The airflow analysis was performed for the entire building, while the contaminant analysis was focused on the lobby floor. The indoor and outdoor air temperatures and outdoor PM_{2.5} concentrations were kept constant to evaluate the PM_{2.5} I/O ratio for the entrance door conditions. Swing doors and revolving doors were used in this study, whereas sliding doors, which are mostly automatic, were excluded because they require analyzing the opening time. Swing doors and revolving doors, which are the focus of this study, differ in the rate of airflow when the door is operating, i.e., when it is open. Swing doors have an opening size of the door leaf, whereas revolving doors have minimal airflow due to the rotation of the door leaf (Lee et al. 2017). Therefore, while both doors had the same air leakage rate in the closed state, the data when the doors were open were different.



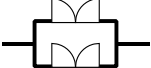
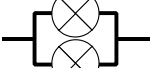
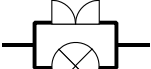
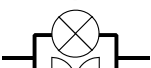
Table 2 Input parameters of model building

Parameter	Data	Unit	Reference	
Temperature	Indoor	20	°C	ASHRAE, 2017
	Outdoor	-10.2	°C	ASHRAE, 2017
Air leakage	Envelope	1500	cm ³ /s.m ² @75Pa	ASHRAE, 2017
	Elevator door	325	cm ² /item@10Pa	Jo et al., 2005
	Entrance door	Stop (close, stationary)	150	cfm@50Pa
Operating (revolving)		600	cfm@50Pa	Schutrum et al., 1961

		Operating (swing door open)	1.8 m ² /door	Opening area
Contaminants	Particle density		1.27 g/cm ²	Kim et al., 2018
	Particle diameter		0.001- 2.5 μm	-
	Outdoor concentration		31.2 μg/m ³	Lee, 2014

Case I consisted of a single type without a vestibule and a box/combo type with a vestibule. The PM_{2.5} I/O ratio was evaluated for the door operation type and entrance configuration. Case II evaluated the changes in the I/O ratios according to the difference in operation time between the two doors in the box type. The case consisted of a box-type entrance with two swing doors. The main variable in Case II was the time difference between the doors, which can be adjusted using the space between the doors of the vestibule entrance in an actual building. B-0 means that the doors operate simultaneously, B-5 means that the first door operates, and the other door operates 5 s later.

Table 3 Cases for contaminant analysis

Case I	Vestibule type	Operation type	Diagram
S-S	Single	Swing	
S-R	Single	Revolving	
B-S	Box	Swing+ swing	
B-R	Box	Revolving+revolving	
C-S	Box (Combo)	Swing(outside)+revolving(inside)	
C-R	Box (Combo)	Revolving(outside)+swing(inside)	
Case II	Vestibule type	Operation type	Time difference of door operation
B-0	Box	Swing+swing	0 s
B-1	Box	Swing+swing	1 s
B-2	Box	Swing+swing	2 s
B-3	Box	Swing+swing	3 s
B-4	Box	Swing+swing	4 s
B-5	Box	Swing+swing	5 s

3 IMPACT OF ENTRANCE DOOR ON PM_{2.5} I/O RATIO

3.1 Airflow analysis for model building

The airflow analysis was performed using CONTAM, a multi-zone network simulation, to determine the pressure difference and airflow rate in the lobby floor. The model building includes the entrance of B-S with a vestibule on swing doors, with the doors closed and in steady state. Figure 2 shows the pressure profile of the building and the airflow rate in the envelope.

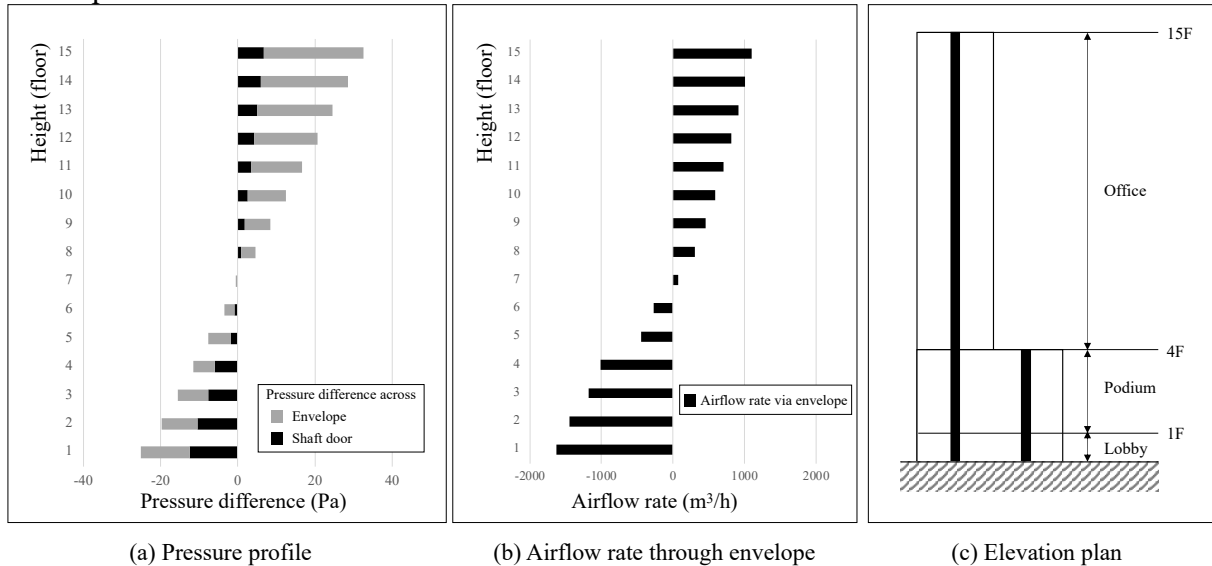


Figure 2 Results for airflow analysis of the model building

The neutral pressure level is located at the 7th floor, 40% of the total height of the building. It is located below the center of the building due to the large envelope area of the lower floors (1-4F) and the entrance doors. The envelope pressure difference on the first floor was 12 Pa, which was lower than the top floor (25 Pa). However, the lobby level, the first floor, had a higher airflow rate of 1,634 m³/h than the top floor (1,102 m³/h) due to the entrance door and large envelope area. Based on this airflow analysis, the air movement path of the lobby floor for the contaminant analysis was derived.

3.2 PM_{2.5} I/O ratio based on operation type

The simulation was conducted from 12:00 on January 1 to 12:00 on January 3, with 48 h intervals of 1 s. The target period was from January 2 at 0:00 to January 2 at 24:00, with 12 h of indoor concentration stabilization before and after the target period. In all cases, the initial indoor concentration was set to the outdoor concentration, resulting in an initial I/O ratio of 1. The pressure difference between the outside and lobby spaces was set to 12 Pa, which was derived from the airflow analysis. Figure 4 shows the concentration stabilization areas for Case I. The I/O ratio of concentrations reaching a steady state for the single type (S-S, S-R) was 0.518, which was higher than 0.491 for the box and combo types (B-S, B-R, C-S, C-R). This was caused by the decrease in airflow due to the use of the vestibule.

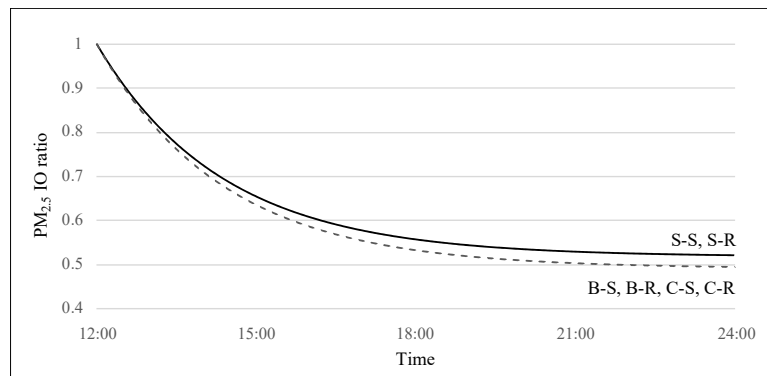


Figure 3 Stabilization of indoor $PM_{2.5}$ concentrations before the target period

Table 4 and Figure 4 show the I/O rate results for the 24 hours. The minimum value of each case is the steady state value, and the results were divided into single-type and box/combo-type. In the box/combo-type, the cases with at least one revolving door, B-R, C-S, and C-R tended to have similar behavior in the entire range.

Table 4 $PM_{2.5}$ I/O ratio of Case I during the target period

Case		S-S	S-R	B-S	B-R	C-S	C-R
$PM_{2.5}$ I/O ratio	Min.	0.518	0.518	0.491	0.491	0.491	0.491
	Avr.	0.768	0.522	0.504	0.492	0.492	0.492
	Max. (Range I)	1.293	0.531	0.551	0.494	0.495	0.495
	Max. (Range II)	1.21	0.53	0.521	0.493	0.494	0.494
Increase rate (%)	Range I	149.6	2.5	12.2	0.6	0.8	0.8
	Range II	106.5	2.1	5.5	0.4	0.6	0.6

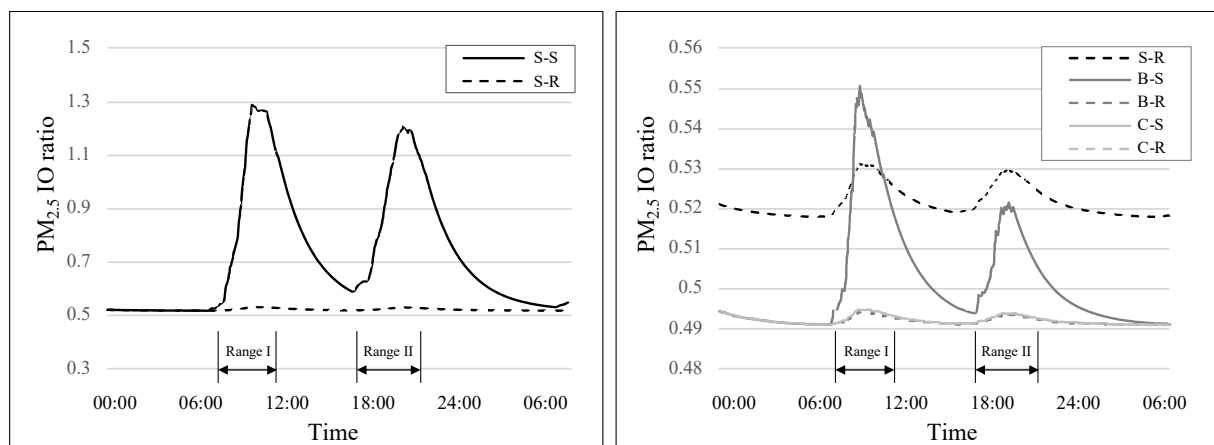


Figure 4 $PM_{2.5}$ I/O ratio of Case I during the target period (Single-type cases (left) and cases without P-S (right))

Figure 5 shows the I/O ratio for the results of single-type cases (S-S, S-R) and cases without P-S. In all cases, the I/O ratio increased more rapidly in range I, where the occupant traffic rate was higher. The I/O ratio for S-S was higher than the other cases and increased to 1.29 at the peak of occupant traffic, indicating that the lobby floor can be exposed to higher indoor $PM_{2.5}$ concentrations than outdoor concentrations. Due to the vestibule, the minimum value of S-R is higher compared to the box and combo cases (B-S, B-R, C-S, S-R), which can lead to higher background concentration. Cases except B-S included a revolving door, which had the smallest change in the ratio (within 1%). S-R had a relatively large range of 2.5% because it

included a revolving door but was a single type. B-S had the highest percentage increase from normal to peak concentration (12%). Depending on the door operation schedule, there were periods when the I/O rate in B-S was higher than in S-R. The I/O rates of the B-R, C-S, and C-R groups were not significantly different, suggesting that installing at least one revolving door at the entrance door can effectively block $PM_{2.5}$ inflow when occupants enter and exit.

3.3 $PM_{2.5}$ I/O ratio according to operation time difference

The lobby-to-outside I/O ratio was investigated for differences in door operation time. The case study was conducted at a box-type entrance consisting of two swing doors, while the door operation time in an actual building may vary depending on the space between the two doors. Table 5 and Figure 6 present the results of the I/O ratios during the target period.

Table 5 $PM_{2.5}$ I/O ratio of Case II during the target period

Case		B-0	B-1	B-2	B-3	B-4	B-5
$PM_{2.5}$ I/O ratio	Min.	0.491	0.491	0.491	0.491	0.491	0.491
	Avr.	0.663	0.504	0.504	0.505	0.504	0.503
	Max.	1.024	0.551	0.549	0.548	0.545	0.543
Increase rate (%)		108.5	12.2	11.8	11.6	11.0	10.6

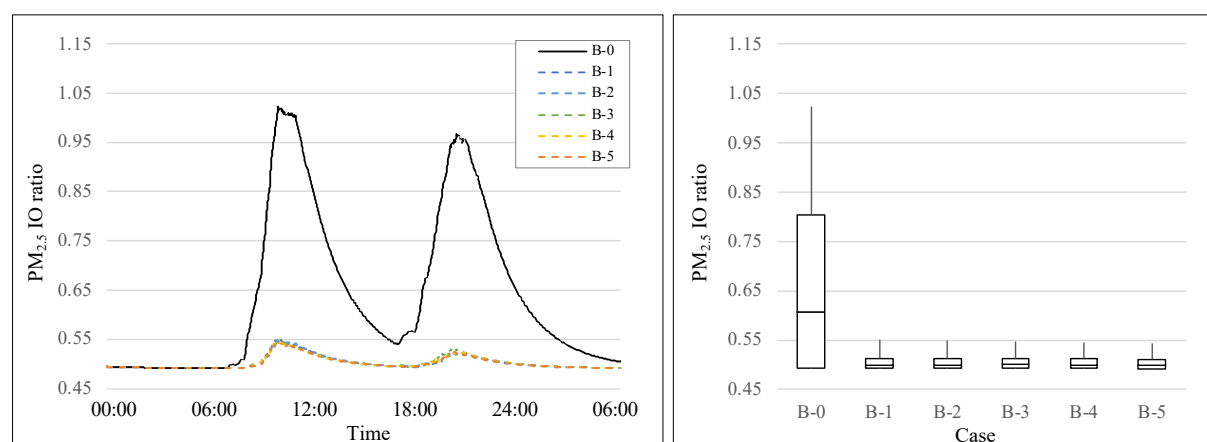


Figure 5 $PM_{2.5}$ I/O ratio of Case II during the target period (Time series data (left) and boxplot (right))

The I/O ratio of B-0 was higher than those of the other cases. The maximum ratio for this case in the high traffic range I was 1.024, showing that it can be exposed to $PM_{2.5}$ concentrations close to the outdoor concentration. B-0 is a scenario in which both doors open and close simultaneously, which is the same as the single-type operation. As the time difference increased from B-1 to B-5, the maximum ratio decreased; however, the difference was insignificant from 10.6% to 12.2%, which can be considered the same level. This means that even if an entrance with a vestibule strategy is applied, it is possible to achieve the same level of results as single-type depending on how the door is operated and controlled.

4 CONCLUSION

In this study, the I/O ratio of the lobby floor to the outdoor $PM_{2.5}$ concentrations according to the operation type and configuration of the entrance was evaluated with a case study. The outdoor $PM_{2.5}$ intake at the lobby space varied owing to different airflow rates, depending on the door operation. This was depicted in this study using swing and revolving doors and

analyzed based on the door configuration, with and without a vestibule. An entrance consisting of a single door without a vestibule is directly connected to the outdoor ambient. It can be exposed to PM_{2.5}, which is equal to or higher than the outdoor concentration level, depending on the occupancy schedule. Additionally, an entrance with a vestibule can be exposed to high concentrations when no difference exists in the operating times of the two doors. Therefore, in order to ensure and manage indoor air quality at the lobby, architectural methods to design the configuration of the doors and additional measures to control the operation of the doors are required.

5 ACKNOWLEDGEMENTS

This work was supported by the National Research Foundation of Korea(NRF) grant funded by the Korea government(MSIT). (No. 2020R1A2C3013676)

6 REFERENCES

- Lee, M. (2014). An Analysis on the Concentration Characteristics of PM_{2.5} in Seoul, Korea from 2005 to 2012. *Asia-Pacific Journal of Atmospheric Sciences*, 50 (Suppl 1), 585–594.
- Dockery, D.W. & Spengler, J.D. (1981). Indoor-outdoor relationships of respirable sulfates and particles, *Atmospheric Environment*, 15(3) 335-343.
- Xiong, Z. M., Zhang, G. Q., Peng, J. G. & Zhou, J. L. (2004). Research status of indoor inhalable particulate pollution. *HVAC*, 34(4), 32-36.
- Lee, B. H., Yee, S. W., Kang, D. H., Yeo, M. S., & Kim, K. W. (2017). Multi-zone simulation of outdoor particle penetration and transport in a multi-story building. *Building Simulation*, 10, 525-534.
- Fu, N., Kim, M. K., Chen, B., & Sharples, S. (2022). Investigation of outdoor air pollutant, PM_{2.5} affecting the indoor air quality in a high-rise building. *Indoor and Built Environment*, 31(4), 895-912.
- Park, S., Cai, Y., Lim, H., & Song, D. (2022). Analysis of vertical movement of particulate matter due to the stack effect in high-rise buildings. *Atmospheric Environment*, 279, 119-113.
- Thatcher, T. L., & Layton, D. W. (1995). Deposition, resuspension, and penetration of particles within a residence. *Atmospheric environment*, 29(13), 1487-1497.
- Lv, Y., Wang, H., Wei, S., Wu, T., Liu, T., & Chen, B. (2018). The experimental study on indoor and outdoor penetration coefficient of atmospheric fine particles. *Building and Environment*, 132, 70-82.
- Stephens, B., & Siegel, J. A. (2012). Penetration of ambient submicron particles into single-family residences and associations with building characteristics. *Indoor air*, 22(6), 501-513.
- Schutrum L.F., Ozisik N., Baker J.T., & Humphreys C.M. (1961). Air infiltration through revolving doors. *ASHRAE Journal*, 3(11), 43-50.
- Jo, J. H., Lim, J. H., Song, S. Y., Yeo, M. S., & Kim, K. W. (2007). Characteristics of pressure distribution and solution to the problems caused by stack effect in high-rise residential buildings. *Building and Environment*, 42(1), 263-277.
- Raunemaa, T., Kulmala, M., Saari, H., Olin, M., & Kulmala, M. H. (1989). Indoor air aerosol model: transport indoors and deposition of fine and coarse particles. *Aerosol Science and Technology*, 11(1), 11-25.
- Kulmala, M., Asmi, A., & Pirjola, L. (1999). Indoor air aerosol model: the effect of outdoor air, filtration and ventilation on indoor concentrations. *Atmospheric Environment*, 33(14), 2133-2144.

- IBC 2021. (2012). *2012 International Building Code*. International Code Council, Inc. Section 1004, 239-242.
- Lee, J., Go, B., & Hwang, T. (2017). Characteristics of revolving door use as a countermeasure to the stack effect in buildings. *Journal of Asian Architecture and Building Engineering*, 16(2), 417-424.
- American Society of Heating Refrigerating and Air-Conditioning Engineers. (2017). *2017 Ashrae handbook. fundamentals*. ASHRAE 2017.
- Jo, J. H., Yeo, M., & Kim, K. (2005). Simulation of pressure distribution and solving the pressure differentials problem in high-rise residential buildings. *Journal of the Architectural Institute of Korea: Planning & Design*, 21(11), 269-276.
- Kim, E., Seo, S., Kim, S., Jung, S., Lee, Y., Oh, S. H., ... & Bae, M. S. (2018). Determination of Hourly Density Using Real Time PM_{2.5} Mass and Volume Concentrations at the Road Side-OPS Correction Based on Optical Absorption of eBC. *Journal of Korean Society for Atmospheric Environment*, 34(6), 865-875.
- van Schijndel, H., Zmeureanu, R., & Stathopoulos, T. (2003, August). Simulation of air infiltration through revolving doors. *In Eighth International IBPSA Conference*, Eindhoven, Netherlands.

Proposal of an effort-benefit diagram to compare unit and room air-change rates applied to a literature review

Sven Auerswald^{*1}, Andreas Wagner², and Hans-Martin Henning^{1,3}

1 Fraunhofer Institute for Solar Energy Systems ISE
Heidenhofstraße. 2
79110 Freiburg, Germany
sven.auerswald@ise.fraunhofer.de*

*2 Building Science Group
Institute for Building Design and Technology at
Karlsruhe Institute of Technology (KIT)
Englerstr. 7,
76131 Karlsruhe, Germany*

*3 INATECH
Albert-Ludwigs-Universität Freiburg
Emmy-Noether-Straße 2
79110 Freiburg, Germany*

ABSTRACT

The main task of every ventilation system is to dilute and extract pollutants from indoor air, most importantly in occupied space. This is usually achieved by exchanging polluted indoor air with less polluted outdoor air. In the case of a mechanical ventilation system, this process requires a fan power to be provided which is approximately proportional to the power of three to the resulting airflow. Because of this, reducing the necessary airflow to be provided by the ventilation unit e.g., by 10% would lead to a reduced power supply of about 27%. Vice versa, a necessary increase of 10% of the airflow provided by the unit, would result in an increased power supply of about 33%. To determine whether a reduced unit airflow is feasible or an increase in unit airflow is required, it is important to evaluate the ventilation efficiency for the occupied zone and any other zone with certain air change rate requirements. Unfortunately, this evaluation process is time-consuming as well as labour-intensive and can't be done for every indoor zone separately yet. However, for those situations where it has been performed, a common procedure for comparing them in a comprehensible graphical way would be helpful. This paper proposes a diagram to visualize how efficiently certain ventilation systems provide their unit air change rate as a room air change rate. As characteristic physical limits and isolines the values for ideal mixed ventilation and plug flow are included as well. Furthermore, the diagram has been applied to visualize air change rates from a literature review. The overview indicates, other than often assumed, real buildings do not necessarily reach ideally mixed ventilation. Pointing out that, it must be admitted as well, that currently the available data for such a comparison is often not based on a uniform measurement and evaluation procedure. Nevertheless, the proposed diagram can be a useful tool to communicate the air exchange performance of ventilation systems.

KEYWORDS

air change rate, air change efficiency, literature review

1 INTRODUCTION

Due to the challenges we all face because of climate change, the building sector needs to contribute to energy savings by more airtight building envelopes combined with controlled ventilation systems. To keep the required power consumption of these systems as low as possible, it is essential to strive for a high ventilation or air change efficiency. However, this requires awareness in the design-phase of building of the fact that it is not sufficient to only move air, but also assure "fresh" or better younger air is provided where it is actually needed. Vice versa, a ventilation system has to efficiently extract polluted, or older air from the sources of these pollutants. Unfortunately, in practice, it is often assumed unit air change rates according to Equation (1) are equal to the air change rate present in any point within a ventilated space. This assumption is, for example, implicitly made in the German standard DIN 1946-6, which

means every ventilation system reaches by default the air change efficiency of ideal mixed ventilation or $\varepsilon_j^a = 50\%$. This is problematic because with such an assumption, there is no motivation to further improve the most relevant characteristic of a ventilation system.

$$n_j = \frac{\dot{V}_j}{V_j} = \frac{1}{\tau_j} \quad (1)$$

n_j	Nominal air change rate of a system j	$[\text{h}^{-1}]$
\dot{V}_j	Effective volume flow for a ventilated system j to exchange the air	$[\text{m}^3 \text{h}^{-1}]$
V_j	Entire volume of the system j to be ventilated	$[\text{m}^3]$
τ_j	Nominal time constant of the system j as a characteristic statistical measure for the time air spends at least within that system	$[\text{h}]$

2 THEORY

To better understand the theoretical background of air change efficiency, it helps to imagine a simplified real room like in Figure 1. Most importantly, a real indoor space cannot be ideally mixed, rather it can be viewed as a more or less coarse or fine discretized mesh of zones filled with air of different ages which interact with each other.

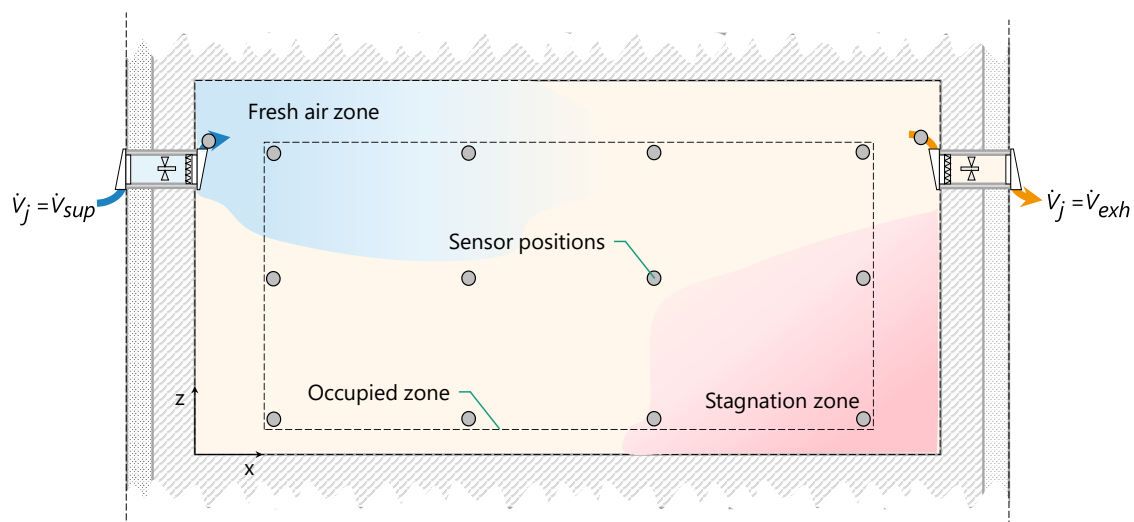


Figure 1: Simplified sketch of a ventilated room with various air ages, where the exhaust catches air of some room average air age. A fraction of older air is stagnating in few regions of the indoor space (Auerswald 2023).

The assumption of mixed ventilation means that the average air age $\langle \bar{\alpha} \rangle_j$ of all locations over the whole space equals the nominal time constant τ_j of that space. The condition of ideal mixed ventilation is a theoretical reference condition, where every location or zone \mathbf{x}_i has that average air age ($\bar{\alpha}(\mathbf{x}_i) = \langle \bar{\alpha} \rangle_j = \tau_j$, $\varepsilon_j^a = 50\%$). The other two theoretical reference conditions are complete short-cut ($\varepsilon_j^a = 0\%$), where the air age in every indoor location is infinity ($\bar{\alpha}(\mathbf{x}_i) = \infty$). And plug-flow ($\varepsilon_j^a = 100\%$), where the air crosses the indoor space on the most direct path from supply to exhaust without leaving a single location unventilated. The air age $\bar{\alpha}(\mathbf{x}_i)$ under plug flow conditions increases linearly from 0 at the supply to τ_j at the exhaust, which means the average air age is $\langle \bar{\alpha} \rangle_j = 0,5 \cdot \tau_j$. With this said, the definition of the absolute air change efficiency ε_j^a follows than Equation (2) (Skåret 1986; Mundt and Mathisen 2004; Sandberg and Sjöberg 1983; Sandberg 1981).

$$\varepsilon_j^a = \frac{\tau_j}{\langle \bar{t}_j \rangle} = \frac{1}{2} \frac{\tau_j}{\langle \bar{\alpha}_j \rangle} = \frac{1}{1 + \mu_2^*(\tau_j)} = \frac{1}{2} \frac{\langle \bar{n}_j \rangle}{n_j} = \frac{\langle \bar{n}_{e,j} \rangle}{n_j} \quad (2)$$

ε_j^a	Absolute air change efficiency of a system j	[-]
τ_j	Nominal time constant of the system j as a characteristic statistical measure for the time air spends at least within that system	[h]
$\langle \bar{t}_j \rangle$	Average residence time of air within the system j or air age in the exhaust plane of that system	[h]
$\langle \bar{\alpha}_j \rangle$	Average air age within the system j	[h]
$\mu_2^*(\tau_j)$	Dimensionless second order central moment or dimensionless variance of the statistical distribution of residence times outside the system	[-]
$\langle \bar{n}_j \rangle$	Average room air change rate	[h ⁻¹]
n_j	Nominal air change rate of a system j	[h ⁻¹]
$\langle \bar{n}_{e,j} \rangle$	Average room air change rate in the exhaust plane of the system j	[h ⁻¹]

However, often it is neither relevant nor practically feasible to measure or otherwise evaluate the absolute air change efficiency. One example is here air volumes, which are enclosed by furniture. Relevant for the air exchange is mostly the zone occupied by persons. In order to reduce the complex reality and to consider the relevance of various zone for the use cases of the indoor space, it is helpful to set up a model which discretizes an indoor space into subsystems. With this in mind, it is logical to define a relative air change efficiency $\langle \varepsilon_j^a \rangle_i$ for a subsystem i inside the system j , according to Equation (3).

$$\langle \varepsilon_j^a \rangle_i = \frac{\tau_j}{\langle \bar{t}_j \rangle_i} = \frac{1}{2} \frac{\tau_j}{\langle \bar{\alpha}_j \rangle_i} = \frac{1}{2} \frac{\langle \bar{n}_j \rangle_i}{n_j} = \frac{\langle \bar{n}_{e,j} \rangle_i}{n_j} \quad (3)$$

$\langle \varepsilon_j^a \rangle_i$	Relative air change efficiency of a subsystem i in j	[-]
$\langle \bar{t}_j \rangle_i$	Average residence time of air within the subsystem i or air age in the exhaust plane of that subsystem	[h]
$\langle \bar{\alpha}_j \rangle_i$	Average air age within the subsystem i in j	[h]
$\langle \bar{n}_j \rangle_i$	Average room air change rate in the subsystem i	[h ⁻¹]
$\langle \bar{n}_{e,j} \rangle_i$	Average room air change rate in the exhaust plane of the subsystem i	[h ⁻¹]

Since air change efficiencies are a ratio of the achieved room air change rate to the nominal air change rate provided by the ventilation unit, it can be seen as a ratio of the benefit in relation to the necessary effort.

3 EFFORT-BENEFIT DIAGRAM FOR THE AIR CHANGE EFFICIENCY

Even though the evaluation of the air change efficiencies provides a method to quantify the performance of a ventilation system's capability to exchange indoor air, it is rarely used. The reason for this is the effort it takes to measure or simulate it. Also, because of the wide range of individual definitions for $\langle \varepsilon_j^a \rangle_i$ and even sometimes an unclear differentiation from the absolute air change efficiency, ε_j^a makes it difficult to further optimize existing ventilation system configurations. However, for those cases where the air change efficiency has been, and more importantly, will be evaluated, the effort-benefit-diagram for ventilation systems in Figure 2 can be a graphical method to reduce the burden of comparing different ventilation systems.

Furthermore, the diagram can be used to better communicate expectations from standards and regulations for ventilation systems.

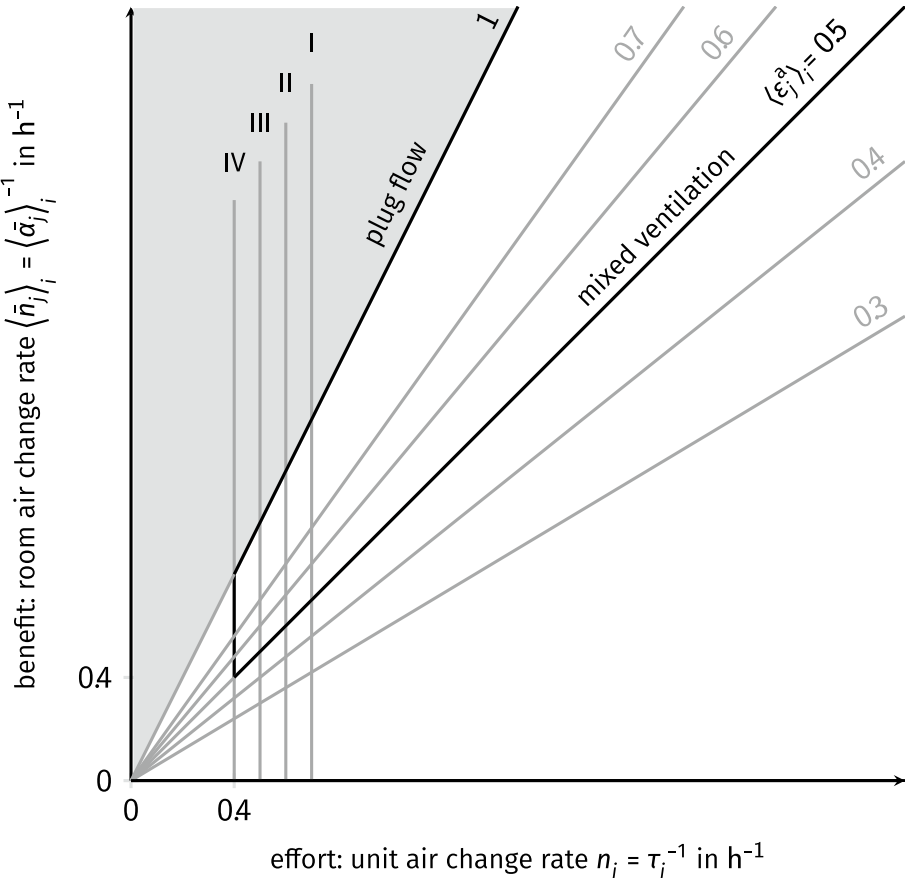


Figure 2: Effort-benefit-diagram to visualize how efficiently a ventilation system provides a certain unit air change rate to the indoor space (Auerswald 2023).

The proposed diagram shows the ratio between the provided nominal or unit air change rate n_j in relation to the achieved room air change rate $\langle \bar{n}_j \rangle_i$. As a result, the diagonal isolines correspond to the relative air change efficiency $\langle \epsilon_j^a \rangle_i$. If $\langle \bar{n}_j \rangle_i$ covers the entire indoor space where n_j has been provided to, these lines become the isolines for ϵ_j^a . The two bold diagonal lines mark the values for the two reference cases, mixed ventilation and plug flow. The grey area is physically not possible to reach. If $\langle \bar{n}_j \rangle_i$ considers the requirement zone like the breathing level and Skåret's (1986) rules are considered, then efficient ventilation systems shall be designed for a relative air change efficiency $\langle \epsilon_j^a \rangle_i$ above the 50%-level. Additionally, the four vertical lines mark, as an example, the reference air change rates for the four indoor air quality expectation categories (IEQ) for a residential indoor space according to DIN EN 16798-1 (p. 56, table B.11). Since the standard suggest assuring an IEQ well above IV and to design for II, the area framed in bold lines in the diagram represents the target range for ventilation systems.

4 REVIEW OF RESULTS FOR THE RELATIVE AIR CHANGE EFFICIENCY

The following section provides an overview of measured and simulated air change efficiencies based on a literature review of scientific publications. Besides Google-Scholar the [AIVC Airbase](#) has been used to search for publications regarding ventilation efficiency, air change efficiency and air age evaluations. From the publications found the review considers only the reported points of interest inside the evaluated space. In the case of centralized ventilation systems with a continuous unidirectional flow, this data is sometimes provided additionally to

the easier accessible data in the exhaust ductwork, which leads to an absolute air change efficiency ε_j^a . Especially for decentralized systems with alternating flow, the accessibility between ε_j^a and $\langle \varepsilon_j^a \rangle_i$ is precisely the opposite, since there is no such location which continuously represents the exhaust duct only measurement data for the indoor space can be measured directly. For all presented data, it must be considered that there is no common practice how to exactly install the trace gas measurement equipment and how detailed the uncertainties of these evaluations shall be determined. Even though it shall be mentioned that there are the standards DIN EN ISO 12569 (2018) and DIN ISO 16000-8 (2008) which describe the tracer gas technique and how to calculate $\langle \bar{n}_j \rangle_i$ or $\langle \bar{a}_j \rangle_i$ respectively based on the measurement data. Of these two standards the second is more detailed. Based on the procedure in DIN ISO 16000-8 (2008) Auerswald (2023) presents an improved evaluation method for the measurement data and their uncertainties.

The first results on air change efficiency were published by Lidwell (1960), Sandberg (1981), and Skåret and Mathisen (1982). They transferred the tracer measurement technique to ventilation systems and tested it in the laboratory using nominal air change rates higher than those used in common practice for most buildings nowadays. Further investigations in a laboratory environment were carried out by Tomasi et al. (2013). A comprehensive summary of field measurement results in non-residential buildings (NRB) can be found in Fisk and Faulkner (1992). Data on the air change efficiency of residential ventilation systems are published by Merzkirch (2015), Mikola et al. (2017) and FGK e. V. (ed.) (2019). The classification of the studies considered by building and system type is listed in Table 1. Figure 3 visualizes the results of these studies by the introduced effort-benefit diagram.

Table 1: References for evaluations of the nominal and room air change rate, as well the resulting relative air change efficiencies. TS = test facility or simulation, NRB = non-residential building, H = including a heat source

Reference	Building type			System type	
	TS	NRB	flat	centralized	decentralized
				continuous	alternating
Sandberg (1981)	•			•	
Sandberg and Sjöberg (1983)	•			•	
Sandberg (1984)	•	•		•	
Fisk et al. (1985)		•		•	
Offermann and Int-Hout (1987)		•		•	
Fisk et al. (1988)		•		•	
Persily and Dols (1991)		•		•	
Fisk et al. (1991)	•			•	
Bauman et al. (1992)	•			•	
Persily et al. (1994)		•		•	•
Manz et al. (2000)	•, H				•
Olesen et al. (2011)	•, H			•	•
Tomasi et al. (2013)	•			•	•
Merzkirch (2015)			•	•	•
Mikola et al. (2017)			•		•, H
FGK e. V. (ed.) (2019)	•			•	•
Auerswald (2023)			•		•

5 CONCLUSIONS

From this small overview it can be concluded, that ventilation systems installed in buildings tend to not achieve at least mixed ventilation and thus do not satisfy Skåret's (1986) rules. Especially for those systems in residential buildings in Germany, it seems they tend to be under-

dimensioned. From references found and considered here, most of the systems which satisfied the requirement $\langle \varepsilon_j^a \rangle_i \geq 0.5$ are test facilities. This indicates that there may be a transfer gap from accepted scientific knowledge for the indoor air exchange to real-world buildings.

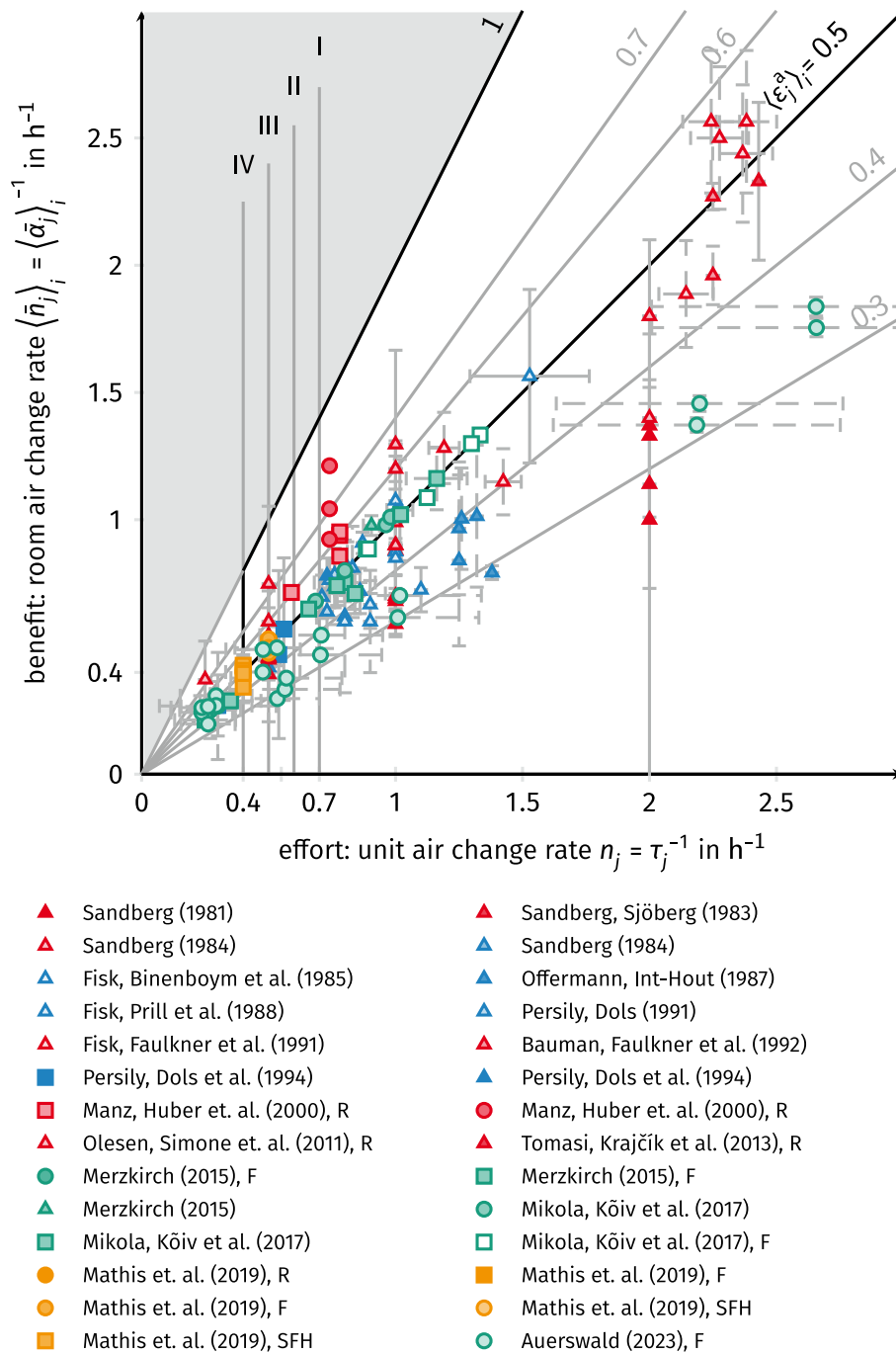


Figure 3: Effort-benefit-diagram applied to the comparison of data from a literature review about nominal air change rates to room air change rate, as well as the resulting air change efficiencies. Red = test facility, blue = non-residential building, green = residential building, orange = simulation (residential), triangle = centralized continuous system, rectangle = decentralized continuous system, circle = decentralized alternating system

6 ACKNOWLEDGEMENTS

This work was funded by the European Union’s research and innovation programme ‘[Horizon 2020](#)’ under Grant Agreement no. [101079961](#). The project „DigitAI and physical incrEMental

renovation packaGes/systems enhancing environmental and energetic behaviour and use of Resources“ ([AEGIR](#)) runs from 01.10.2022 to 30.09.2026.

7 REFERENCES

- Auerswald, Sven (2023): Dezentrale Fassaden-Integrierte Wohnungslüftungsgeräte. Kombinierte Bewertung des erzielten Luftaustausches und der Energieeffizienz. Dissertation. Albert-Ludwigs-Universität Freiburg, Freiburg im Breisgau. Fraunhofer ISE.
- Bauman, F. S.; Faulkner, D.; Arens, E. A. (1992): Air Movement, Comfort and Ventilation in Workstations. In *ASHRAE Transactions* (98). Available online at <https://escholarship.org/content/qt65s9f50g/qt65s9f50g.pdf>, checked on 1/13/2022.
- DIN EN 16798-1, 03.2022: Energetische Bewertung von Gebäuden – Lüftung von Gebäuden –. Available online at <https://www.beuth.de/de/norm/din-en-16798-1/349622591>, checked on 6/8/2022.
- Fachverband Gebäude-Klima e. V. (Ed.) (2019): EwWalt – Energetische Bewertung der dezentralen kontrollierten Wohnraumlüftung in alternierender Betriebsweise. Abschlussbericht. Aktenzeichen SWD-10.08.18.7-16.32. With assistance of Paul Mathis, Bernd Dipl.-Ing Klein, Thomas Prof. Dr.-Ing Hartmann, Christine Dipl.-Ing Knaus. Rheinisch-Westfälischen Technischen Hochschule Aachen (RWTH); Forschungsgesellschaft HLK Stuttgart mbH (HLK Stuttgart); Institute for Energy Efficient Buildings and Indoor Climate - E.ON Energy Research Center (EBC - E.ON ERC); Institut für Technische Gebäudeausrüstung Dresden - Forschung und Anwendung GmbH (ITG Dresden). Aachen (TGA Report). Available online at https://downloads.fgk.de/335_TGA-Report_06_EwWalt.pdf, checked on 7/8/2019.
- Fisk, William J.; Binenboym, J.; Kaboli, H.; Grimsrud, D. T.; Robb, A. W.; Weber, B. J. (1985): Multi-Tracer System For Measuring Ventilation Rates and Ventilation Efficiencies in Large Mechanically-Ventilated Buildings. In : AIC Conference. AIC Conference. Het Meerdal, NL, checked on 1/13/2022.
- Fisk, William J.; Faulkner, D. (1992): Air Exchange Effectiveness in Office Buildings: Measurement Techniques and Results. In. International Symposium on Room Air Convection and Ventilation Effectiveness. Tokyo, 1992-07-22/1992-07-24,. Available online at <https://escholarship.org/uc/item/29d9w25z>, checked on 10/13/2021.
- Fisk, William J.; Faulkner, D.; Prill, R. J. (1991): Air Exchange Effectiveness of Conventional and Task Ventilation for Offices. In : Healthy Buildings. IAQ'91 Conference. Washington, DC, USA, 04.09.1991/08.09.1991. Available online at <https://escholarship.org/uc/item/4799p1s0>, checked on 1/13/2022.
- Fisk, William J.; Prill, R. J.; Seppänen, Olli (1988): Commercial Building Ventilation Measurements Using Multiple Tracer Gases. In : Effective Ventilation. 9th AIVC. Ghent, Belgium, 12.09.1988/15.09.1988, checked on 1/14/2022.
- DIN ISO 16000-8, 12.2008: Innenraumluftverunreinigungen – Teil 8: Bestimmung des lokalen Alters der Luft in Gebäuden zur Charakterisierung der Lüftungsbedingungen (ISO 16000-8:2007). Available online at <https://www.beuth.de/de/norm/din-iso-16000-8/102342071>, checked on 5/18/2018.
- Lidwell, O. M. (1960): The Evaluation of Ventilation. In *The Journal of Hygiene* 58 (3), pp. 297–305. Available online at <http://www.jstor.org/stable/3861194>, checked on 9/17/2016.

- Manz, Heinrich; Huber, Heinrich Prof.; Schälin, A.; Weber, A.; Ferrazzini, M.; Studer, M. (2000): Performance of single room ventilation units with recuperative or regenerative heat recovery. In *Energy and Buildings* 31 (1), pp. 37–47. DOI: 10.1016/S0378-7788(98)00077-2.
- Merzkirch, Alexander (2015): Energieeffizienz, Nutzerkomfort und Kostenanalyse von Lüftungsanlagen in Wohngebäuden. Dissertation. University of Luxembourg (uni.lu), Luxembourg. RUES - Research Unit in Engineering Sciences. Available online at <https://www.shaker.de/de/content/catalogue/index.asp?lang=de&ID=8&ISBN=978-3-8440-3675-6&search=yes>, checked on 7/6/2021.
- Mikola, Alo; Kalamees, Targo; Kõiv, Teet-Andrus (2017): Performance of ventilation in Estonian apartment buildings. In *Energy Procedia* 132, pp. 963–968. DOI: 10.1016/j.egypro.2017.09.681.
- Mundt, Elisabeth; Mathisen, Hans Martin (2004): Ventilation effectiveness. With assistance of Peter Vilhelm Nielsen, Alfred Moser, Mats Prof. Ph.D (Eng) Sandberg, Dirk Prof. Dr.-Ing. Müller, Klaus Fitzner, Olli Seppänen, Derrick Braham. Bruselas: Rehva (Guidebook, 2). Available online at <https://www.rehva.eu/eshop/course-detail/no02-ventilation-effectiveness>, checked on 4/23/2023.
- Offermann, Francis J.; Int-Hout, Dan (1987): Ventilation Effectiveness and ADPI measurements of three supply/retrun air configurations. In : Indoor Air'87. 4th International Conference on Indoor Air Quality and Climate. Berlin, 1987-08-17/1987-08-21. Institute for Water, Soil and Air Hygiene. Available online at https://www.aivc.org/sites/default/files/airbase_2814.pdf, checked on 1/16/2022.
- Olesen, Bjarne Wilkens; Simone, Angela; Krajčák, Michal; Causone, Francesco; Carli, Michele de (2011): Experimental Study of Air Distribution and Ventilation Effectiveness in a Room with a Combination of Different Mechanical Ventilation and Heating/Cooling Systems. In *International Journal of Ventilation* 9 (9 // 4), pp. 371–383. DOI: 10.1080/14733315.2011.11683895.
- Persily, Andrew K.; Dols, W. Stuart (1991): Field Measurements of Ventilation and Ventilation Effectiveness in an Office/Library Building. In *Indoor Air* 1 (3), pp. 229–245. DOI: 10.1111/j.1600-0668.1991.03-13.x.
- Persily, Andrew K.; Dols, W. Stuart; Nabinger, Steven J. (1994): Air Change Effectiveness Measurements in Two Modern Office Buildings. In *Indoor Air* 4 (1), pp. 40–55. DOI: 10.1111/j.1600-0668.1994.t01-3-00006.x.
- DIN 1946-6, 12.2019: Raumluftechnik – Teil 6: Lüftung von Wohnungen – Allgemeine Anforderungen, Anforderungen an die Auslegung, Ausführung, Inbetriebnahme und Übergabe sowie Instandhaltung, checked on 1/15/2020.
- Sandberg, Mats (1981): What is ventilation efficiency? In *Building and Environment* 16 (2), pp. 123–135. DOI: 10.1016/0360-1323(81)90028-7.
- Sandberg, Mats; Sjöberg, Mats (1983): The use of moments for assessing air quality in ventilated rooms. In *Building and Environment* 18 (4), pp. 181–197. DOI: 10.1016/0360-1323(83)90026-4.
- Sandberg, Mats Prof. Ph.D (Eng) (1984): The multi-chamber theory reconsidered from the viewpoint of air quality studies. In *Building and Environment* 19 (4), pp. 221–233. DOI: 10.1016/0360-1323(84)90003-9.

- Skåret, Eimund (1986): Contaminant removal performance in terms of ventilation effectiveness. In *Environment International* 12 (1-4), pp. 419–427. DOI: 10.1016/0160-4120(86)90057-7.
- Skåret, Eimund; Mathisen, Hans Martin (1982): Ventilation efficiency. In *Environment International* 8 (1-6), pp. 473–481. DOI: 10.1016/0160-4120(82)90065-4.
- Tomasi, Roberta; Krajčák, M.; Simone, A.; Olesen, Bjarne Wilkens (2013): Experimental evaluation of air distribution in mechanically ventilated residential rooms: Thermal comfort and ventilation effectiveness. In *Energy and Buildings* 60, pp. 28–37. DOI: 10.1016/j.enbuild.2013.01.003.
- DIN EN ISO 12569, 04.2018: Wärmetechnisches Verhalten von Gebäuden und Werkstoffen - Bestimmung des spezifischen Luftvolumenstroms in Gebäuden - Indikatorgasverfahren (ISO 12569:2017); Deutsche Fassung EN ISO 12569:2017. Available online at <https://www.beuth.de/de/norm/din-en-iso-12569/272434270>.

Experimental Investigation of Indoor Air Quality in an Open Office Environment

Altug Alp Erdogan¹, Mustafa Zeki Yilmazoglu^{*2}, Umit Gencturk¹

*1 ÜNTES Heating Air Conditioning Company
Fatih Sultan Mehmet Blv., No:348
Kahramankazan, 06980
Ankara, Türkiye*

*2 Gazi University, Faculty of Engineering,
Department of Mechanical Engineering,
Ankara, Türkiye*

**Corresponding author: zekiyilmazoglu@gazi.edu.tr*

ABSTRACT

Open offices, where more than one person works, have been used frequently in recent years. However, there are many studies on the efficiency of the indoor air quality of the employees in these offices. It has also been shown that the risk of cross-contamination is higher in such offices during the COVID period, but this risk can be reduced by increasing the amount of fresh air. For both efficiency and a healthy working environment, an experimental investigation of indoor air quality (IAQ) according to scenarios was carried out experimentally with the living laboratory created in the R&D center. Working together with 8 engineers in the open office environment investigation was measured with an indoor air quality measuring device at different points throughout the day. With these measurements, both the comfort of the employees was compared and the possible improvements to be made in the devices in order to increase the indoor air quality were examined. According to the results obtained, it was found that suitable conditions in terms of thermal comfort are provided during working hours and the CO₂ level is generally kept below 1000 ppm.

KEYWORDS

HVAC, Indoor air quality (IAQ), Thermal comfort, Sustainability, Energy efficiency

1 INTRODUCTION

Rapid urbanization, ongoing climate changes, and previous epidemic periods such as COVID-19 have highlighted the importance of ensuring suitable indoor air quality (IAQ) in office areas. With employees typically spending more than 80% of their time indoors, IAQ becomes a critical factor in their overall well-being (Marc et al., 2018). The progression of climate change is expected to worsen outdoor air quality due to increasing CO₂ and temperature levels, leading to extreme conditions such as higher indoor temperatures, infiltration of outdoor airborne allergens, and humidity fluctuations (EPA, 2022). Poor IAQ can result in various health issues, including cross-infection, sick-building syndrome (SBS), eye irritation, respiratory illnesses, and allergies (Wojciech et al., 2007; Wyon and Wargocki, 2013), while prolonged exposure can cause up to a 15% decline in office employees' performance (Wargocki and Wyon, 2017). Thus, it is crucial to maintain acceptable IAQ in office environments. To achieve acceptable IAQ in office areas, reducing CO₂ levels through proper ventilation and meeting minimum thermal comfort requirements are essential. Thermal comfort depends on seven factors consisting of air temperature, humidity, radiant temperature, air velocity, metabolic heat rate, clothing, and possible occupant adaptations (Borowski et al., 2022). Recommended measures to provide thermal comfort in office environments include maintaining a temperature range of 20-24°C, a relative humidity range of 30-60% (Sakhare and Ralegaonkar, 2014), and a mean radiant temperature (MRT) range of 18-27°C (Choudhury et al., 2011), along with adequate ventilation. However, ensuring appropriate ventilation is a complex procedure that requires

detailed considerations. ANSI/ASHRAE Standard 62.1-2019 recommends a minimum outdoor air rate of 2.5 L/s per occupant at the breathing zone for acceptable IAQ in office spaces (ASHRAE, 2019). Controlling airflow patterns has also been emphasized in a position document (Stewart et al., 2020). In contrast, REHVA published a guideline for post-COVID target ventilation rates, emphasizing the adjustment of outdoor air supply based on indoor CO₂ levels. For health-based ventilation, maintaining a CO₂ setpoint of 550 ppm is recommended, while a setpoint of 650 ppm is suggested for comfort ventilation, resulting in a ventilation rate of 15-25 L/s.person during normal periods (REHVA, 2022). Given the energy consumption of HVAC equipment and the importance of meeting thermal comfort requirements, the potential impacts of these variations in outdoor air rates would obviously be crucial for design considerations. To enhance the precision of design-specific strategies, further studies are required that investigate the indoor air quality (IAQ) of various office environments and ventilation layouts experimentally.

Various experimental studies investigated several optimization strategies of IAQ, thermal comfort and energy for various HVAC applications. Table 1 shows a summary of several related studies. As can be seen, there are various strategies to improve IAQ and thermal comfort rather than directly increasing airflow rates inside the space. Up to 35% energy savings could be achieved by occupancy-based control (OBC) strategy with an acceptable air quality and thermal comfort (Kong et al., 2022). Studies also showed that energy consumption can be reduced by up to 55.8% via demand-controlled ventilation (DCV) strategies without reducing the IAQ (Sun et al., 2011).

Table 1: Several studies from the literature that investigate several strategies to improve IAQ in different indoor environments.

No	Reference	Space Type	Mechanical Applications	Control Strategies	Variable Parameters	Examined Parameters
1	Ming et al. (2023)	Office Meeting Room	4-Way Active Chilled Beam Ventilation	-	- Heat Gains - Terminal Layouts	- Operation Ranges - Contamination Removal Efficiency - Heat Removal Efficiency
2	Wang et al. (2023)	Lecture Room	Radiators & Natural Ventilation	- Occupant-Based Heating and Natural Ventilation Control	- Heat Losses - CO ₂ Concentrations	- Thermal Comfort - Energy Consumption
3	Yang et al. (2023)	Office	Personal Heating Devices	-	- Indoor and Ambient Temperatures - Indoor Temperatures	- Thermal Comfort Votes - Thermal Sensation Votes - Energy Consumption
4	Tsay et al. (2023)	Office	Fresh Air Heat Recovery Unit (HRU) & Air Conditioner	- Thermal Comfort Control - Energy Savings Control - Productivity Control	- Air Velocities - Predicted Mean Vote (PMV) - Predicted Percent Dissatisfaction (PPD)	- Thermal Sensation - Thermal Comfort - Air Quality - Energy Savings
5	Kong et al. (2022)	Office	Air Treatment Modules (ATMs) & Dedicated Outdoor Air Handler (DOA)	- Thermal Comfort Control - Energy Savings Control - Productivity Control	- Supply/Return Air Temperatures - Outdoor Air Temperature - Occupancy Rate	- Thermal Sensation - Thermal Comfort - Air Quality - Energy Savings
6	Sun et al. (2011)	Multi-Zone Office Building	Central Air Handling Unit (AHU) With Cooling Coils & Variable Air Volume (VAV)	- CO ₂ -Based Adaptive Demand Controlled Ventilation	- CO ₂ Concentrations	- Energy Consumption

Since the ventilation layout and airflow patterns inside office environments are as much important as the amount of minimum outdoor air supplied, further case-specific studies are required to improve IAQ in a sustainable and economical way. Also, ventilation layouts should be reoriented in a way to provide reduction in the cross-infection risks in office environments without increasing energy demands. In this study, the effects of a different ventilation strategy on IAQ of an open office environment are investigated experimentally. The results obtained from the measurements are evaluated in order to provide some alternatives for the improvement of IAQ inside the office. Also, design considerations for the HVAC&R system design were presented in detail.

2 METHODOLOGY

2.1 Layout of the Selected Office

The selected space is an R&D office, which is located in Ankara, Türkiye and has an open office layout as described in Figure 1. Except for the adjacent spaces shown in Figure 1, all envelopes of the office are open to outdoor environment. The R&D office is planned to be served by a dedicated HVAC&R system, which is separated from the system of adjacent conditioned areas. The office space is located on the attic floor and the structure of the roof did not allow a homogeneous ceiling height. Therefore, suspended ceiling through the long perimeters of the space, which covers the dotted areas presented in Fig. 1, has a clean ceiling height of 2.25 m, and the clean height at the middle area is 2.6 m. U-values of exterior walls, roof and windows were calculated to be 0.23 W/m²K, 0.67 W/m²K, and 2.45 W/m²K, respectively. Although the office was designed for 13 office employees, the office was occupied by 8 people during the measurements, while each occupant was using a laptop along with a monitor. Also, there are 8 LED lights placed to the ceiling, which have 20x20 cm² footprint area. The total cooling load caused by the equipment including laptops, monitors and the printer is calculated as 500 W, and the cooling load due to the lighting is assumed to be 10 W/m².

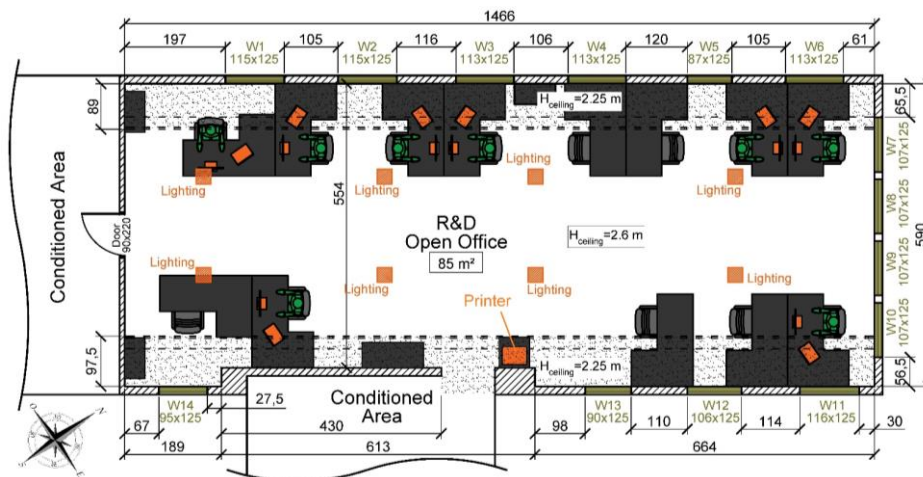


Figure 1: 2D layout of the considered R&D open office.

2.2 Design Calculations and Resulting HVAC&R System

Resulting design data for the considered R&D office were presented in Table 1. For the design of outdoor air and heating-cooling systems, minimum outdoor air rates were determined according to ANSI/ASHRAE 62.1 Standard (ASHRAE, 2019), whereas heating-cooling loads were calculated via Carrier HAP v4.90 software, which utilizes the methodology explained in S. Zaphar (2018). Annual design conditions for the outdoor air were retrieved from ASHRAE

Climatic Design Conditions, which were obtained from Ankara Murted Station as being the closest station to the R&D office. Since return air grills were planned to be located below 2.8 m and the occupancy in that space corresponds to 50% of the total of the ventilation zone, air distribution effectiveness (E_z) and system ventilation efficiency (E_v) were considered to be 0.8 and 0.66, respectively. As a result, required outdoor air rate with 30% safety factor (q_{safe}) was calculated to be 514 m³/h, whereas design outdoor air rate (q_{design}) was determined to be 600 m³/h.

Table 2: Design calculations for the HVAC&R system.

Design Conditions		Outdoor Air Rate		Cooling-Heating Load Calculations				
Parameter	Value	Parameter	Value	Load Source	Load Details	Cooling		Heating
						Sensible	Latent	Sensible
^a Latitude	40.079 N	^b q_{occ}	2.5 L/s.person	$Q_{windows}$	18 m ²	2733 W	-	1497 W
^a Longitude	32.566 E	N_{occ}	13 person	Q_{walls}	48 m ²	80 W	-	369 W
^a Elevation	843 m	^b q_{area}	0.3 L/s.m ²	Q_{roof}	84 m ²	1485 W	-	1910 W
<u>Design Heating</u>		Area	85 m ²	$Q_{lighting}$	8 lights	422 W	-	-
^a DB	-12°C	q_{req}	58 L/s (208.8 m ³ /h)	$Q_{equipment}$	8 laptops	500 W	-	-
Setpoint	22°C	^b E_z	0.8		1 printer			
<u>Design Cooling</u>		^b E_v	0.66	Q_{occ}	13 people	975 W	780 W	-
^a DB	31.9°C	^b q_{calc}	396 m ³ /h	Safety	10%	620 W	78 W	378 W
^a WB	16.8°C			$(Q_{tot})_{space}$	-	6815 W	858 W	4154 W
Setpoint	24°C	q_{safe}	514 m ³ /h	$(Q_{tot})_{vent}$	600 m ³ /h	976 W		6058 W
		q_{design}	600 m ³ /h	Q_{tot}		8649 W		10212 W

^a The data were retrieved from ASHRAE Climatic Design Conditions website (ASHRAE, 2021).

^b Values were retrieved from ANSI/ASHRAE Standard 62.1 "Ventilation for Acceptable Indoor Air Quality" (ANSI/ASHRAE, 2019). Minimum air requirements per each occupant (q_{occ}) and per unit area (q_{area}) were obtained by considering the space as an office, whereas the air distribution effectiveness (E_z) and system ventilation efficiency (E_v) were defined by evaluating the ventilation layout described in Figure 1 and Figure 2. The total amount of required outdoor air rate (q_{calc}) was calculated in accordance with the methodology presented in the standard.

The resulting 2D layout of HVAC&R systems and the airflow rates obtained from field measurements are presented in Fig. 2. Accordingly, the outdoor air is provided by UTFP-100 model heat recovery unit (HRU) operating with 100% fresh air. The outdoor air is supplied from 4 swirl diffusers and the air is then exhausted to the HRU from 4 return grills. Each utilized FCU has a heating capacity of 2.2 kW with the usage of 30% ethylene glycol, and there are 4 FCUs placed on the middle region of the suspended ceiling. All FCUs are served by a dedicated heat pump system having a maximum heating capacity of 16 kW. Aside from the literature, outdoor air supply diffusers were located at the middle region, and the return air grills were placed at the lower suspended ceiling. Thermal comfort measurements were carried out at M1, M2 and M3 points shown in Figure 2.

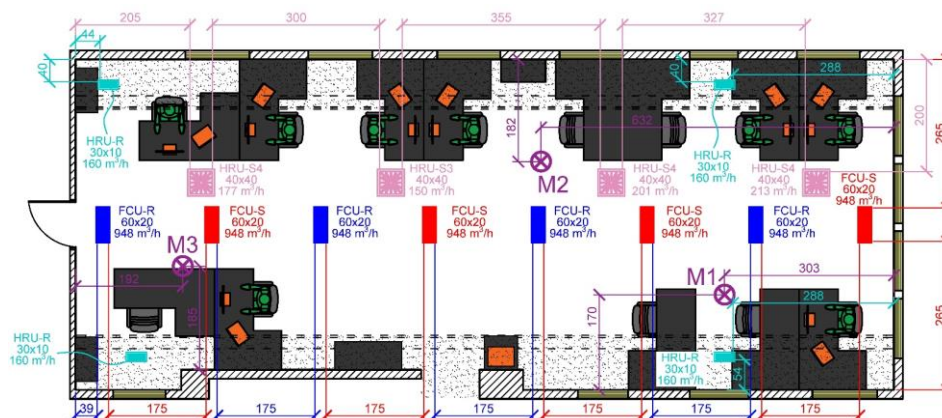


Figure 2: 2D layout of the considered R&D open office.

2.3 Experimental Procedure

IAQ measurements were carried out with Testo[®] 440 air velocity and IAQ measurement device, which has a turbulence probe ($0 - 5 \pm 0.03$ m/s), CO₂ probe ($0 - 10000 \pm 50$ ppm), humidity-temperature probe ($-20...+70 \pm 0.5^\circ\text{C}$, $0-100 \pm 2\%$ RH) and a globe thermometer ($0-120^\circ\text{C}$). Measurements were performed for the heights of 1.1 m (represents the breathing zone for sitting and working position) and 1.7 m (represents the breathing zone for standing position) at each location presented in Fig. 2.

3 RESULTS AND DISCUSSION

Measurement data for the location M1 were presented in Fig. 3. The dry bulb temperature increased at 1.7 m from noon. It remained approximately constant at 1.1 m. Although the CO₂ level showed an swinging during office usage hours at 1.7 m, it remained around 600 ppm on average at 1.1 m. PMV and PPD indices were found to be in the range where the space can be considered comfortable. The results of the second and third measurement points showed similar results in terms of thermal comfort. Detailed analysis results are given below.

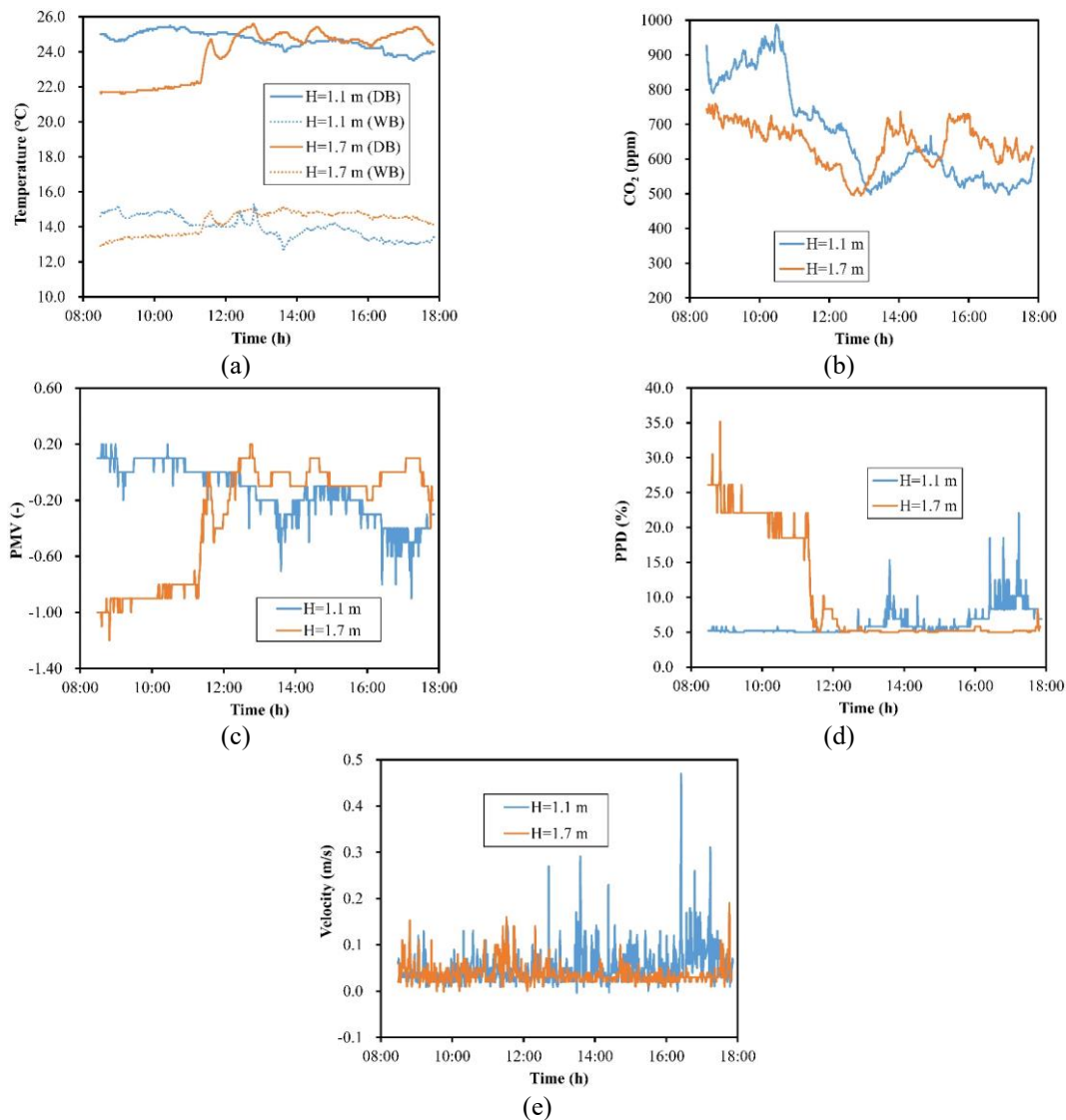


Figure 3. Measurement data from the location M1 against the time period. (a) DB and WB temperatures, (b) CO₂ concentrations, (c) Calculated PMV, (d) Calculated PPD, (e) Air velocity.

Measurement data for the location M2 were presented in Figure 4.

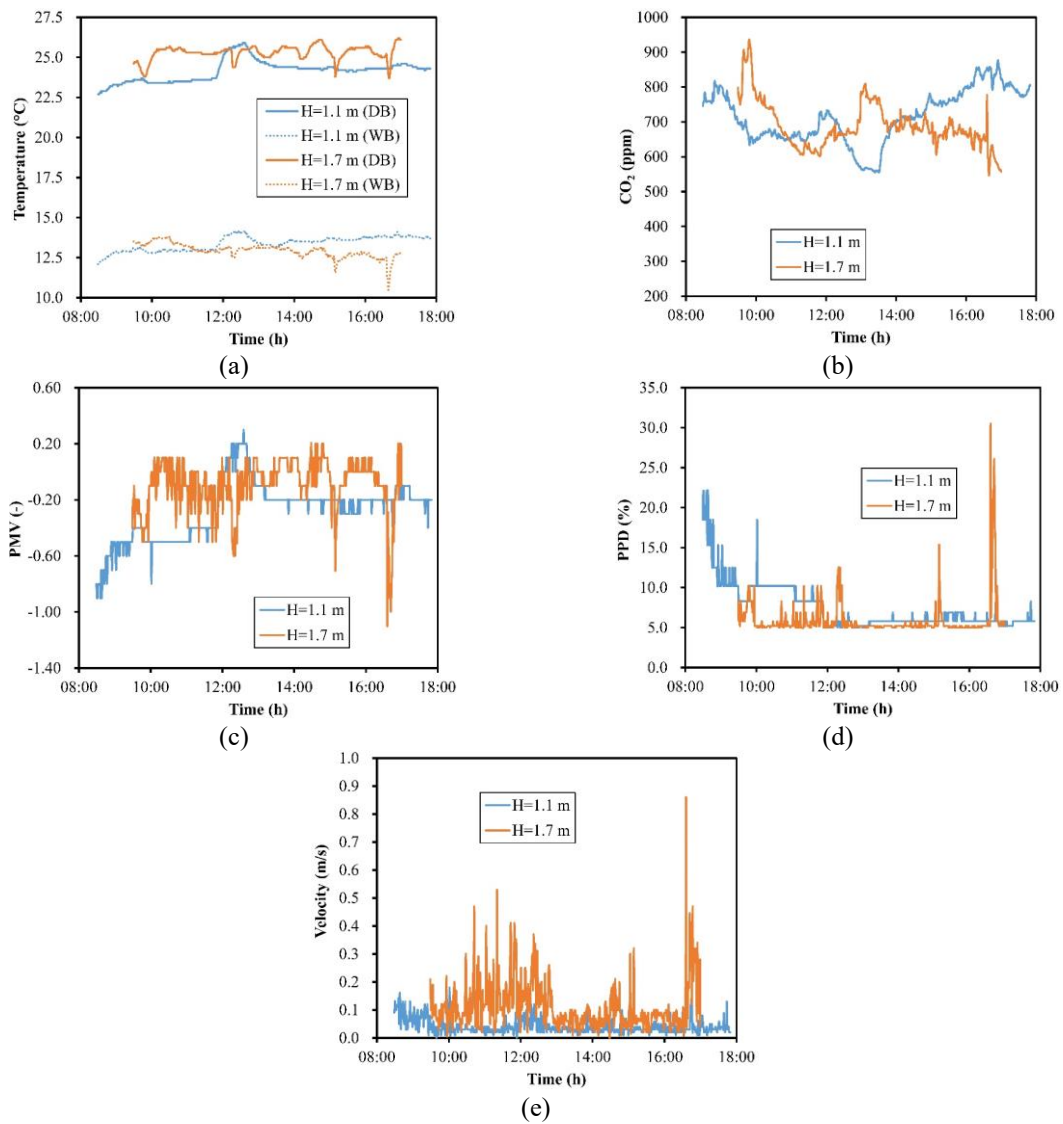
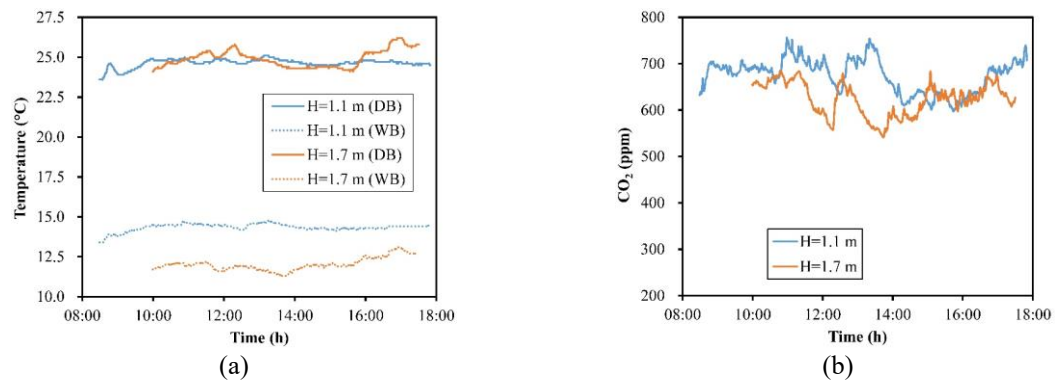


Figure 4. Measurement data from the location M2 against the time period. (a) DB and WB temperatures, (b) CO₂ concentrations, (c) Calculated PMV, (d) Calculated PPD, (e) Air velocity.

Measurement data for the location M3 were presented in Figure 5.



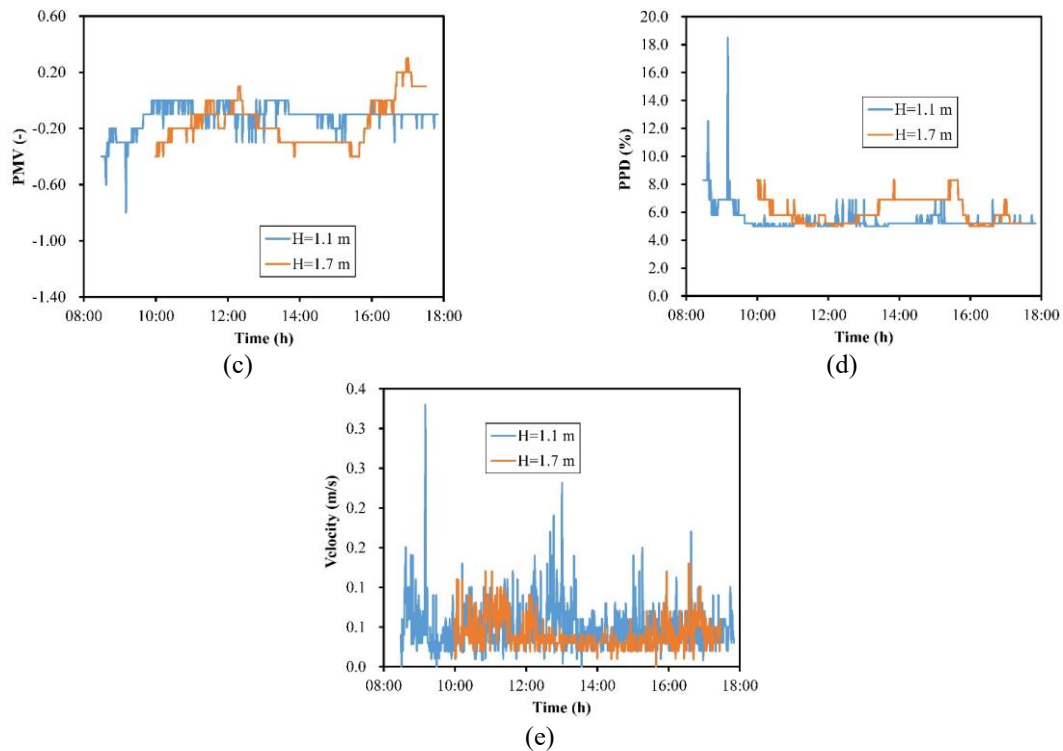


Figure 5. Measurement data from the location M3 against the time period. (a) DB and WB temperatures, (b) CO₂ concentrations, (c) Calculated PMV, (d) Calculated PPD, (e) Air velocity.

4 CONCLUSIONS

The importance of providing thermal comfort in open-plan offices, but choosing options that use energy efficiently and minimize the risk of contamination has come to the fore in the epidemic we live in. CO₂-based ventilation systems and their operating parameters are important in terms of marketing for device manufacturers. In addition, ensuring energy efficiency and determining the options to be offered in the devices should be evaluated within this scope. Ventilative cooling offers an important option in terms of energy efficiency. In the previous study (Birturk and Yilmazoglu, 2022), an annual utilization potential of 59% was determined in Ankara climate conditions. This percentage was found to be 67% for Istanbul and 73% for İzmir. Therefore, from the perspective of the device manufacturer, ventilative cooling should be considered as an important efficiency option for the Turkish HVAC market. For this purpose, studies are continuing to test this option on the date of uploading this text to the submission system (July 2023). Other alternatives to be considered are the humidifier option and improved CO₂-based ventilation.

5 ACKNOWLEDGEMENTS

Authors would like to thank ÜNTES Heating Air Conditioning Corp. for their support and allowance for our project.

6 REFERENCES

Stewart, E. J., Schoen, L. J., Mead, K., Olmsted, R. N., Sekhar, C., Vernon, W., ... & Conlan, W. (2020). ASHRAE position document on infectious aerosols. *ASHRAE: Atlanta, GA, USA*.

- U.S. Environmental Protection Agency (2022, December 5). *Indoor Air Quality and Climate Change*. Environmental Protection Agency (EPA). Retrieved June 4, 2023, from <https://www.epa.gov/indoor-air-quality-iaq/indoor-air-quality-and-climate-change#research>
- Choudhury, A. R., Majumdar, P. K., & Datta, C. (2011). Factors affecting comfort: human physiology and the role of clothing. In *Improving Comfort In Clothing* (pp. 3-60). Woodhead Publishing.
- ASHRAE. (2021). *Climatic Design Conditions 2009/2013/2017/2021*. <http://ashrae-meteo.info/v2.0/>. Accessed 5th July 2023.
- ANSI/ASHRAE. (2019). *Ventilation for Acceptable Indoor Air Quality* (ASHRAE Standard 62.1-2019). Atlanta, GA.
- Marć, M., Śmiełowska, M., Namieśnik, J., & Zabiegała, B. (2018). Indoor air quality of everyday use spaces dedicated to specific purposes—A review. *Environmental Science and Pollution Research*, 25, 2065-2082.
- Wojciech, H., Jansson, B., Komulainen, H., Ladefoged, O., Mangelsdorf, I., Steenhout, A., ... & Viluksela, M. (2007). Scientific Committee on Health and Environmental Risks opinion on: Risk assessment on indoor air quality. *Scientific Committee on Health and Environmental Risks*.
- Wyon, D. P., & Wargoeki, P. (2013). How indoor environment affects performance. *ASHRAE Journal*, 3(5), 6.
- Borowski, M., Zwolińska, K., & Czerwiński, M. (2022). An experimental study of thermal comfort and indoor air quality—a case study of a hotel building. *Energies*, 15(6), 2026.
- Sakhare, V. V., & Ralegaonkar, R. V. (2014). Indoor environmental quality: Review of parameters and assessment models. *Architectural Science Review*, 57(2), 147-154.
- Stewart, E. J., Schoen, L. J., Mead, K., Olmsted, R. N., Sekhar, C., Vernon, W., ... & Conlan, W. (2020). ASHRAE position document on infectious aerosols. *ASHRAE: Atlanta, GA, USA*.
- REHVA. Health-based target ventilation rates and design method for reducing exposure to airborne respiratory infectious diseases. In *REHVA Proposal for Post COVID Target Ventilation Rates*; REHVA: Brussels, Belgium, 2022.
- Ming, R., Mustakallio, P., Kosonen, R., Kaukola, T., Kilpeläinen, S., Li, B., ... & Yao, R. (2023). Effect of active chilled beam layouts on ventilation performance and thermal comfort under variable heat gain conditions. *Building and Environment*, 228, 109872.
- Wang, Z., Calautit, J., Tien, P. W., Wei, S., Zhang, W., Wu, Y., & Xia, L. (2023). An occupant-centric control strategy for indoor thermal comfort, air quality and energy management. *Energy and Buildings*, 285, 112899.

- Yang, B., Wu, M., Li, Z., Yao, H., & Wang, F. (2022). Thermal comfort and energy savings of personal comfort systems in low temperature office: A field study. *Energy and Buildings*, 270, 112276.
- Tsay, Y. S., Chen, R., & Fan, C. C. (2022). Study on thermal comfort and energy conservation potential of office buildings in subtropical Taiwan. *Building and Environment*, 208, 108625.
- Kong, M., Dong, B., Zhang, R., & O'Neill, Z. (2022). HVAC energy savings, thermal comfort and air quality for occupant-centric control through a side-by-side experimental study. *Applied Energy*, 306, 117987.
- Sun, Z., Wang, S., & Ma, Z. (2011). In-situ implementation and validation of a CO₂-based adaptive demand-controlled ventilation strategy in a multi-zone office building. *Building and Environment*, 46(1), 124-133.
- American Society of Heating, Refrigerating and Air-Conditioning Engineers (ASHRAE). (2021). *2021 ASHRAE Handbook Fundamentals*. Atlanta, GA.
- Birturk, A., Yilmazoglu, M.Z. (2022). Analysis of the application of ventilative cooling in different regions of Turkey, REHVA 14th HVAC World Congress, CLIMA 2022, Rotterdam, The Netherlands.

Hygienic Air Handling Unit Certification Program: the new necessity for a guaranteed indoor air quality

Ali Nour Eddine^{*1}, Sylvain Courtey²

*1 Eurovent Certita Certification
Rue Laffitte
Paris, France*

*2 Eurovent Certita Certification
Rue Laffitte
Paris, France*

**aa.nour-edine@eurovent-certification.com*

ABSTRACT

Nowadays, people spend most of their time indoors. Homes, offices, leisure and workplaces must meet people's needs and provide safe, healthy and productive environments. The supply of fresh air plays an important role in achieving these goals. Not only by providing the right temperature and humidity but even more with the purity of the air inside the rooms. A recent study of the World Health Organization showed a significant correlation between yesterday's particulate matters concentration in outdoor air and today's death rate counting 7 million deaths in 2022 caused by air pollution. In recent years, the Ecodesing regulation of the European Union has helped to solve the dilemma between reducing energy consumption and creating a healthy indoor environment by adding highly efficient energy recovery components. However, the variation between the real and the declared performances of air handling units shows a substantial difference between what is expected and the real quality of the air in the market. Eurovent Certita Certification is a third-party certification company that do market surveillance for HVAC products for more than 20 years now. A new Hygienic Air Handling Unit program has been created. This program has 59 additional verification criteria to those of the original AHU program and categorize the unit by number of stars depending on the application. This program provides the insurance that the unit provide the pure air ventilation when most needed.

KEYWORDS

Indoor Air Quality, Air Handling Unit

1 INTRODUCTION

11 March 2020, the date when the World Health Organization (WHO) director announced the beginning of the Covid-19 pandemic (World Health Organization, 2020) is the date that changed the world perception of the importance of the indoor air quality (IAQ) and ventilation inside buildings. Several studies followed later to find the mathematical relation between the outdoor air pollution, the IAQ and the global mortality rates. Vohra et al. (Karn Vohra et al., 2021) showed that the fossil fuel air pollution is responsible for 1 in 5 deaths worldwide. The results of Shetty et al. (Shetty et al., 2021) have concluded that long term exposure to indoor pollution had a significant effect on COPD deaths as well as its symptoms. The study of Ali et al. showed that the high level of indoor air pollution is leading to 3.55 million deaths annually among women and children. While the residential households usually use naturel ventilation or VMC, the air handling unit (AHU) remain the mostly used ventilation system in commercial buildings and hence the efficiency of these systems will have direct effect on the global mortality rates in the upcoming years(Ali et al., 2021).

The AHU was firstly introduced into buildings to provide clean dust free air the building occupants and it was mainly composed of fan and filters. The global need for air-conditioned air leaded the development of these units to be also responsible of heating and cooling, humidifying and dehumidifying and providing more specific filtration such as for hospitals

and white rooms. While including more complex components of these units and so the energy consumption, most of the previous studies focused on increasing the efficiency and reducing the consumption even if this meant sometimes to reduce the filtration capacity. Stephens et al. (Stephens et al., 2010) studied the impact of high efficiency filters on the energy consumption and showed that this theory should not be valid in residential HVAC systems. Moreover, some studies explored the economic model if the employee's productivity when exposed to more filtered air justify the additional on the building energy cost (Bekö et al., 2008). One common conclusion is that improving the air filtration result in an increase in the electrical consumption of the unit due to the increase in the pressure drop of the filter. This dilemma of the trade off between the efficiency of the unit and the IAQ was the main subject of the previous research era, where the balanced scaled more to reduce the building energy in the absence of any existing regulation for the AHU's in the market.

The AHU is a main player in the IAQ and though the health of the global population. However, regulating and controlling these units in the market present a great challenge for governments worldwide. In difference of the common residential HVAC units where the units are massively manufactured and easier to control, the AHU's are mostly customised units strictly dependent of each building's filtration needs and space limitations. A European association that unit the large players of the HVAC ecosystem provided a part of the solution by providing a detailed guideline (Abreu et al., 2021) of the recommended performances and required filtration for AHU's depending on the application. The other more complicated part of the solution was provided by third party certification that guaranteed the market surveillance of the AHU performances through a well elaborated fishnet that will be explained in this study. Even further in its hygienic AHU option, Eurovent Certita Certification (AHU / Eurovent Certita Certification, n.d.) provided the suitable solution to the historical trade-off between the energy consumption and filtration quality by categorising the AHU's depending on the application and though to use the right filter for the right application.

The market status of the AHU's, the certification fishnet and the Hygienic options in addition to the results of 2021 control campaign will be presented in this study.

2 MARKET STATUS OF AHU

To better understand the impact of the performance of the AHU on global health, one should understand the size of this market. The global air handling units market was valued at 11.6 billion USD in 2021 and is projected to reach 15.9 billion USD from 2021 to 2026 (Market and Markets, 2021). The rising usage of air handling units across various application sectors such as commercial buildings, hospitals, industries, universities, data centers and server rooms is expected to fuel the growth of the market.

According to Eurovent Market intelligence report 2021 (Eurovent Market Intelligence, 2022) 283604 were sold in Europe in 2021. Offices, health and educations represent 70% of our daily time and 40% of the AHU market share (Figure 2) and while the main sale channel of the AHU is through installers it is crucial to guarantee that the unit have the right performance and it is the best adapted to the application.

One more impact of the COVID 19 pandemic could be seen in Figure 1 where the importance of IAQ and Energy consumption in AHU is considered by the manufacturers as almost equal in 2022 with a small prevalence of Energy consumption. In 2025 slight increase in the importance of IAQ is expected, however, not very significant (+3%) to stimulate an active redesign of the product.

Figure 2: AHU main applications and sales channel in EU 2021

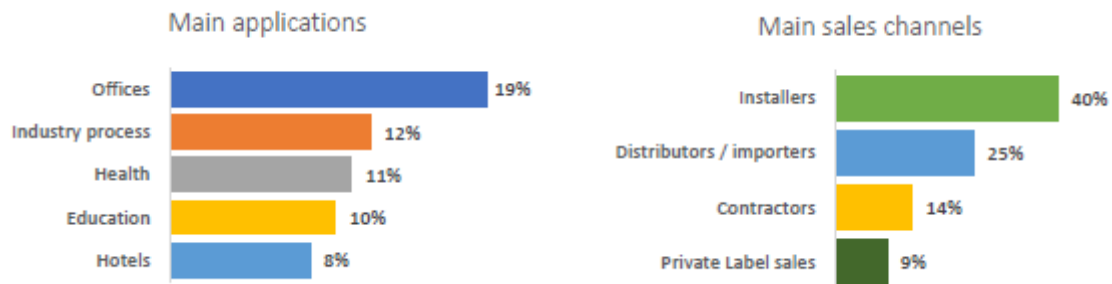
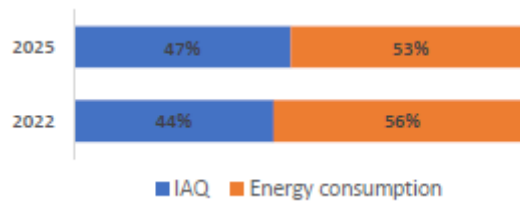


Figure 1: Trade-off between IAQ and Energy consumption



3 CERTIFICATION ROLE

The market surveillance is a key element in the HVAC eco system. For most of the HVAC systems it is the guarantee:

- for the designers that the specifications of the unit provided by the suppliers are compliant with the data sheet
- For the building owner that the declared energy consumption corresponds to the real consumption of the building

For the AHU it is more critical as it also have a great impact on the health of the occupants and the global mortality rates.

In this section the market surveillance process should be explained and the 2021 campaign results should be presented.

3.1 Air Handling Unit Certification Programme

The Ecodesign regulation and the ErP (Energy related Products) directive upcoming policy is to set a new energy efficiency criterion and control the quality of the units allowed to be released in the EU market. Ensuring the market surveillance and controlling the unit in the market is one of the main objectives of the certification fishnet.

3.1.1 Certification process

The program includes more than 10000 certified units. The units' performances and characteristics are verified through the manufacturer documentation and catalogues and audited in the selection software.

After the documentation study, a sampling of units is chosen for testing in independent accredited laboratory under the testing requirements:

- Mechanical characteristics: **EN1886**: Ventilation for buildings - Air Handling Units Mechanical performance
- Rating performances: **EN13053**: Ventilation for buildings - Air Handling Units - Ratings and performance for units, components and sections

The testing procedure for the mechanical characteristics includes:

- Casing strength
- Casing air leakage
- Filter bypass leakage
- Thermal transmittance of the casing
- Thermal bridging factor
- Acoustical insulation of casing

And for performances testing:

- Air flow rate - static pressure - power input (5 points)
- Octave band in-duct sound power level (at the inlet and outlet, with only supply air running)
- Airborne sound power level (only with supply air running)
- Heating capacity (2 conditions) if standard feature of the product range
- Cooling capacity (2 conditions)
- Heat recovery (1 condition)
- Heat recovery pressure drop (on both air sides)
- Pressure drop on water side* (2 conditions)
- Eurovent AHU Energy Efficiency Class

In addition to the product verification and testing, the factory is audited, and the manufacturing process is verified.

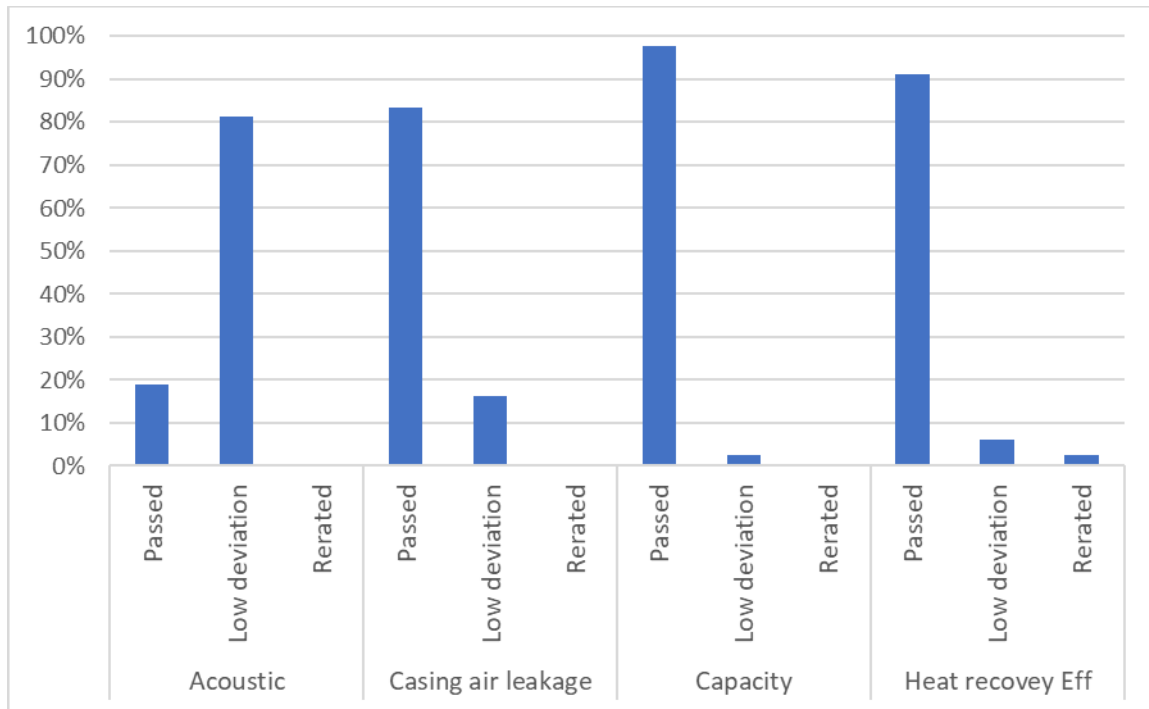
3.1.2 Results of the 2021 campaign

174 units has been tested for the 2021 certification campaign. And 186 factories have been audited.

Figure 3 show an extraction of the failed performances for the Acoustic, the Casing air leakage, the capacity (heating and cooling) and the heat recovery efficiency of the tested air handling units.

Each of the tested performance have a specific acceptance criterion for the deviation and the rerate, such as 3 dbA for acoustic, same class for the casing air leakage, and 3% for heat recovery efficiency. When the performance deviation is above these limits, the performance should be rerated. For the performances presented in Figure 3 3% of the declared heat recovery efficiencies has been rerated to the real tested value while all the tested capacities, casing air leakage and Acoustic performances are within the acceptable deviations limits.

Figure 3: example result of performances for 2021 campaign.



3.2 Hygienic Air Handling Unit programme

To answer to the trade off between the energy consumption and the IAQ, the hygienic option has been added to the AHU certification programme. The main objective of this programme is to categorise the AHU into three categories from the least hygienic with one star, to the best hygienic with three stars. In fact, the need for better filtration depends on the application. In an operation room in the hospital the need filtration is far greater than that in an ordinary office, and though choosing the unit performance depending on its application is the perfect solution for the historical trade off.

3.2.1 Levelling requirements:

The hygienic option of the AHU programme proposes 3 levels of certification defined as Level 1 to Level 3. The higher the rating, the more hygienic the AHU unit.

As a reference only:

- Level 1 would be appropriate for schools, offices and hotels
- Level 2 for hospital (except rooms with high hygienic requirements)
- Level 3 for food processes, pharmaceutical, white rooms, operating theatres and equivalent

The study to determine the star level of the unit includes 59 requirements which includes the whole process of the manufacturing of the unit starting from the planning and up to delivery:

3.2.1.1 Planning

R1. Coating, paints and sealing materials releasing harmful substances or odors are not allowed. Likewise, insulating materials, porous linings, or seals used within the airflow are prohibited.

Level 1, 2 & 3: Requirement applied

R2. Cleaning methodology, general arrangement and dimension of the AHU including location of doors and/or hatches shall be including in the IOM (Installation, Operation and Maintenance Manual) of the product.

Level 1, 2 & 3: Requirement must be included in the IOM of the product.

3.2.1.2 Manufacture

R3. All surfaces which are in contact with air stream shall be cleaned and particles removed after manufacture (e.g. with electrical broom, steam or mop)

Level 1: Procedure shall be included in the quality system of the manufacturer.

Level 2 & 3: Level 1 and Final disinfection requirement after mounting the modules of unit (before installing the filters) on site must be included in the IOM.

3.2.1.3 Shipment

R4. Flat packing delivery of units is not allowed.

In order to comply with restricted buildings accesses or transportation limits, units might be delivered in sections, blocks or sub-assemblies to be assembled together on site. In that case, the assembly method shall be explained in the IOM or the site assembly to be performed by personal trained by the manufacturers.

Level 1, 2 & 3: Procedure shall be included in the quality system of the manufacturer.

In case of blocks or sub-assemblies' delivery, requirements must be included in the IOM of the manufacturer or evidence showing that a qualified person is in charge of the assembly shall be provided.

R5. After manufacture, the AHU shall be fully dry, clean and properly packed with weather protection in order to protect the unit during shipment. The same rule applies for the components.

Level 1, 2 & 3: Procedure shall be included in the quality system of the manufacturer.

R6. Every component of the ventilation system shall be protected from potential damage and contamination after manufacture and this until the installation on site of the unit.

Level 1, 2 & 3: Procedure shall be included in the quality system of the manufacturer.

R7. Every component shall be covered before shipment to avoid any dust infiltration. Manufacturer shall ensure that the components are in clean and dry conditions.

Level 1, 2 & 3: Procedure shall be included in the quality system of the manufacturer.

R8. During the on-site storage every door, hatch and other type of openings (if applicable) shall be sealed.

Level 1, 2 & 3: Requirement must be included in the IOM of the product.

R9. Manufacturer shall ensure that no residue remains within the air flow after manufacture.

Level 1, 2 & 3: Procedure shall be included in the quality system of the manufacturer.

3.2.1.4 Unit Housing

3.2.1.4.1 Metallic Materials

R10. Metallic material shall be corrosion resistant, minimum requirements for internal surfaces are described under each "Level".

Internal surfaces include the following:

- a) Inside panels / door metallic surface
- b) Metallic parts which hold components (rails, holding constructions, etc.). Housings of the components (filter frame, coil frame, heat exchanger frame, fan frame)
- c) Ventilation component itself (coil fins, heat exchanger fins, fan's impeller)
- d) Motors

Fixing elements should correspond regarding corrosion resistance to the surfaces as indicated above.

If coating or painting is used, refer to coating section (R1)

Level 1 & 2: Minimum materials resistance according to corrosivity class C3 in accordance with EN ISO 12944-2:1998 or aluminum

AND Drain pans shall be in stainless steel with at least 18% Cr and 8% Ni (for instance EN steel 1.4301 - AISI 304; minimum corrosion resistance class CRC: II (2) according EN 1993-1-4:1995 EUROCODE 1-4) or aluminum (at least AlMg; in accordance with DIN 1946/4-6.5.1:2018)

Level 3: Minimum materials resistance according to corrosivity class C4 in accordance with EN ISO 12944-1:2017 or aluminum

AND Floor and drain pans shall be in stainless steel with at least 18% Cr and 10% Ni (for instance EN steel 1.4401 - AISI 316; minimum corrosion resistance class CRC: II (2) according EN 1993-1-4:1995 EUROCODE 1-4) or aluminum (at least AlMg; in accordance with DIN 1946/4-6.5.1:2018)

3.2.1.4.2 Non-Metallic Materials

R11. For all non-metallic parts excluding paints, cables and control equipment but including sealants, gaskets, filters, etc. (non exhaustive list) with surface in contact with the air > 5 cm² (summed up surface per each part type). Proof by test reports from hygiene institute as per EN ISO 846:2019 shall be presented. The maximum allowed growth rate for microorganisms according to Table 4 and 5 of ISO 846:2019 is 1 (0, 1a, 1b or 1c are accepted) and C (no growth or slight growth).

Level 1 & 2: Requirement applied

Level 3: Requirement applied and the cabling to electrical components shall not cross another section (or component space) than the space dedicated to this specific component.

R12. Porous or open cell materials as linings, insulating materials (except acoustic baffles) sealants and rubbers in contact with the airflow are not permitted.

Level 1, 2 & 3: Requirement applied

3.2.1.5 General AHU Arrangement

R13. The H-AHU certification is related to AHU within the scope of the Technical Certification Rules ECP 05, but with the following exclusions:

- a) For the H-AHU certification are considered only floor mounted AHU with horizontal air flows (no vertical units).
- b) For the maintenance are considered only AHU with lateral inspection doors / hatches.

Level 1, 2 & 3: Requirement applied

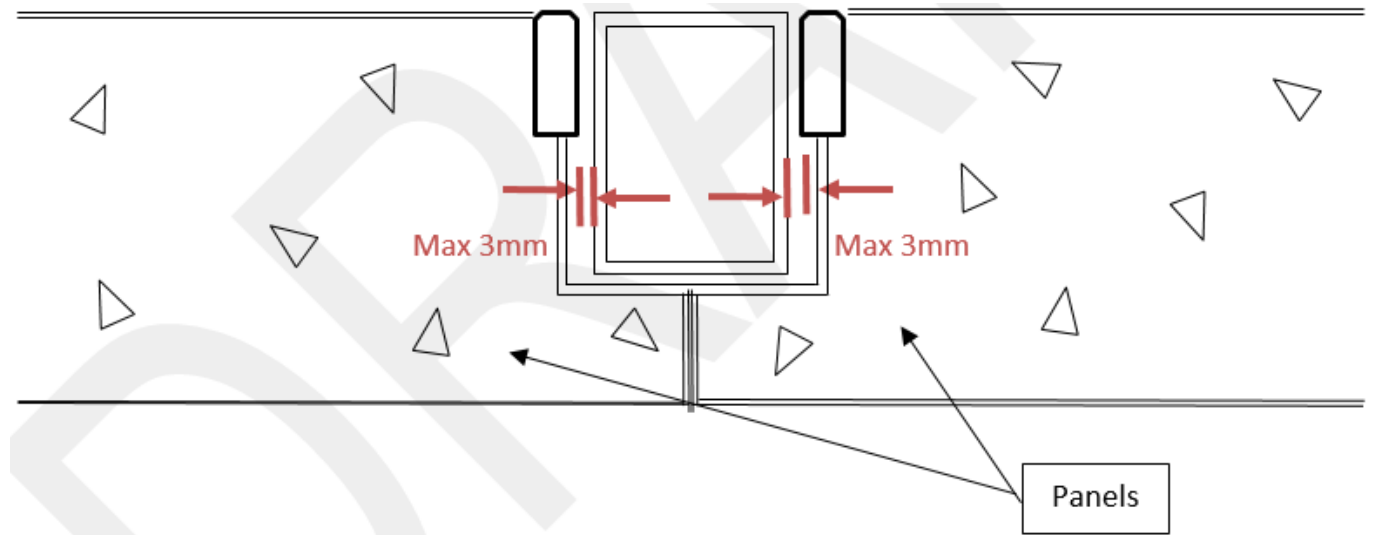
R14. Every component selected in the software (air filters, heat exchangers (energy recovery systems and coils, droplet separators, fans, humidifiers, dehumidifiers, silencers, dampers) shall be installed within/inside the AHU.

Level 1, 2 & 3: Requirement applied

3.2.1.6 Inner Casing Surface

R15. Except for doors and hatches grooves, joints and gaps between panels and gaps between panels and frame profiles shall have maximum width of 3mm (Figure 4).

Figure 4: Gaps between panels and frame profiles schematic



Level 1, 2 & 3: Requirement applied

R16. Except for doors and hatches grooves, joints and gaps between panels and also gaps between panels and frame profiles at the floor shall be sealed to create a smooth and closed surface

Level 1: No Requirements

Level 2 & 3: Requirement applied

R17. Except for doors and hatches grooves, joints and gaps between panels and also gaps between panels and frame profiles at the complete inner casing surface shall be sealed to create a smooth and closed surface

Level 1 & 2: No requirements

Level 3: Requirements applied

R18. Sealants for lids, hatches and doors for IMC shall be located directly at the inside casing surface to avoid any gap or groove.

Sealants for lids, hatches and doors shall be easily replaceable or otherwise installed in a mechanically protected position.

Sealants fixed by direct chemical bonding (FIPFG: Formed in Place Foam Gaskets) are considered as not replaceable. For proper mechanical protection these sealants shall be applied on the lid, hatch or door leaf (but not on the door frame).

Mechanically fixed sealants (inserted in or clamped on a profile) are considered as replaceable, thus they can be located on the lid, hatch or door leaf as well as on the frame.

For the sealants of lids, hatches and doors the requirements of *R11 and R12* shall be fulfilled independently from the surface of the sealant in the airstream.

For the fixation of sealants for lids, hatches and doors:

Level 1 & 2: Mechanical fixing (inserted in or clamped on a profile) or direct chemical bonding (FIPFG: Formed in Place Foam Gaskets) or fixation by a bi-adhesive film or a glue are allowed.

Level 3: Mechanical fixing (inserted in or clamped on a profile) or direct chemical bonding (FIPFG: Formed in Place Foam Gaskets) are allowed. Sealants fixed with a bi adhesive (film or a glue) are not allowed.

R19. To reduce the risk of injuries for the maintenance staff and to ensure safe and proper cleaning at the inside of the AHU, fasteners (e.g. self-tapping screws ...) shall not point inside the unit, sharp edges and open rivets are not allowed inside the housing.

Level 1, 2 & 3: Requirement applied

3.2.1.7 General Requirements to the Casing for Inspection, Maintenance and Cleaning (IMC)

R20. The design shall be such that a maintenance person can reach manually at any inner casing surface for:

- a) Cleaning with a sponge, a mop or similar. No residue shall remain after cleaning.
- b) Access to all components and relating fixing elements.

For the necessary IMC works, any component (air filters, heat exchangers (energy recovery systems and coils, droplet separators, fans, humidifiers, dehumidifiers, *dampers*, silencers, water trays of humidifiers and condense trays of cooling sections or energy recovery systems) in the air stream shall be easily accessible (*R22 & 0*) (installed in the AHU) **OR** alternatively quickly removable (*R21*).

In any case, sufficient space (*R23*) shall be available in the AHU allowing proper IMC. The underlined notions are specified in the following requirements (*R21, R22, 0* and *R23*).

Level 1, 2 & 3: Requirement applied

R21. Any component as defined under *R20* shall be quickly removable.

A component designed for the purpose of IMC as "quickly removable" shall have a weight of maximum 25 kg.

Quickly removable means that after opening the access door or hatch, the component is directly removable within a short time.

Note: For that reason, a water or a refrigerant coil cannot be claimed as "quickly removable". It is not allowed, that other installations (cables, instruments...) hinder the quick removal of the component.

Level 1, 2 & 3: Requirement applied

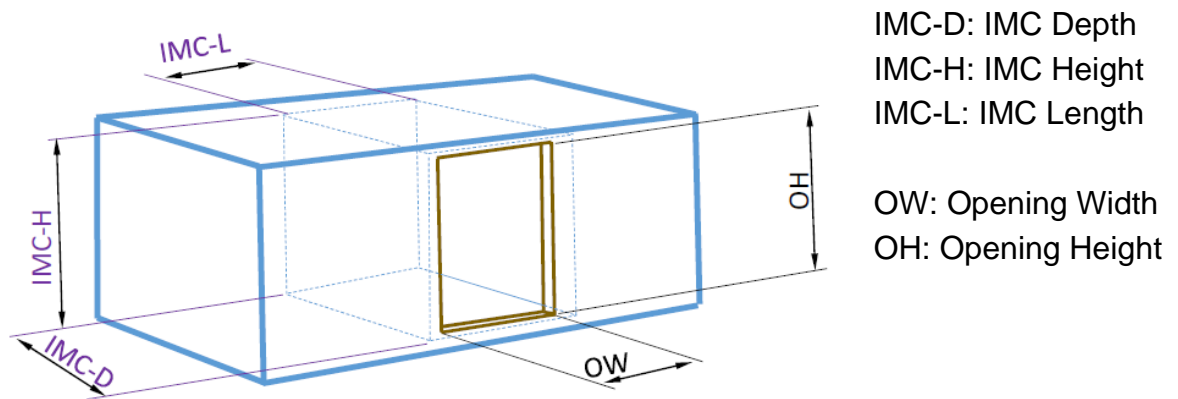
R22. Any component as defined under *R20* shall be easily accessible:

AHU components require a quick and easy access to the unit inside through access openings. As access opening for IMC is accepted only a (quickly removable) hatch or a hinged door, according to the following definition:

- c) The opening of any access opening with hinge (door or hatch) shall be possible within 20 seconds.

- d) For hatches (not hinged access doors) the maximum allowed weight is 25 kg and the maximum allowed width of the hatch is 600 mm (except for silencers). The hatches shall be equipped with handles for proper handling.
- e) For minimum free opening width [OW as per Figure 5] and minimum free opening height [OH according Figure 5] of the access opening, please refer to "j g certification manual.

Figure 5: Opening dimensions – IMC dimensions



Note: Panels which shall be unscrewed for the access are not accepted. At access openings, no installations shall be fixed (cables, instruments...) which hinder the quick opening.

Level 1, 2 & 3: Requirements applied

For any component defined under *R20*, an easy access shall be ensured **from both sides** (upstream and downstream):

For components, which are quickly removable according to *R21*, the component itself is deemed to be accessible from both sides. Nevertheless, the relating guides or frames, the casing ranges directly upstream and downstream of the component and any instruments installed inside the chamber of the relating component shall also be accessible for these quickly removable components.

For any component considered as quickly removable according to [R21](#) the empty space of the component itself can be utilized as part of the inspection section of the non-removable components located next to a quickly removable component.

Level 1: No requirements

Level 2 & 3: Requirement applied

R23. *Sufficient space:* To allow the necessary IMC work, sufficient space shall be available.

Level 1, 2 & 3

R24. Droplet separators downstream cooling coils shall be easily accessible and quickly removable or alternatively have an access door and plenum between cooling coils and droplet separator. In case that there is no compliant space between cooling coil and droplet separator and the droplet separator itself is easily removable, the length (in air direction) of the removed droplet separator can be used as available length for IMC of the cooling coil.

Level 1, 2 & 3: Requirement applied

R25. For easy removal of droplet separators, these shall be side removable in parts with maximum weight of 25 kg and maximum width of 1000 mm.

Level 1, 2 & 3: Requirement applied

3.2.1.8 Requirement regarding filter maintenance

R26. Filter change shall be possible from the dirty air side or by side removal. The installed filter frame shall correspond to the filter class installed and the manufacturer shall be certified minimum for the installed filter bypass leakage. In any case the requirements for sufficient space and easy access for IMC shall be maintained.

Level 1: Requirement applied

Level 2 & 3: Requirement applied and the complete filter(s) frame shall be sealed to the casing frame.

R27. Filter chambers shall be accessible for the IMC works. For unit with internal heights > 1600 mm; the access from both sides (upstream and downstream the filter) shall be possible. For that reason an access door on clean air side is mandatory. This requirement is achieved by default for side removable filter.

Level 1, 2 & 3: Requirement applied

R28. During filter maintenance gasket shall be checked and changed if necessary.

Level 1, 2 & 3: Requirement to be included in the IOM.

3.2.1.9 Other requirements related to casing

R29. To avoid condensation, the certified model box shall have a minimum thermal bridging class of **X**.

Level 1&2: X = TB3

Level 3: X = TB2

R30. The certified model box shall have at least a tightness class of **X** and the Real Unit shall have at least a tightness class of **Y**.

Level 1 & 2: X = L2 (M) & Y = L2 (R)

Level 3: X = L1 (M) & Y = L1 (R)

R31. All drain pans, condense trays and water tanks shall have a sufficient slope from any point of the bottom to the drain tube. The requirement is deemed to be fulfilled, if after filling them with 5 l/m² water, minimum the percentage **X** has been drained off over a period of 10 minutes.

Level 1, 2 & 3: X = 95% (25 cl/m² of remaining water)

Note: The manufacturer shall provide the appropriate material to test this requirement during the audit

R32. Drain pipes of unit shall have a diameter of at least 40 mm and sufficient slope and run via a siphon with free discharge into the sewer system. A backflow protection is mandatory for negative pressures. In case it is not provided by the manufacturer, it shall be stated in the IOM.

Level 1, 2 & 3: Requirement applied

R33. Drains with positive and negative pressure levels shall be constructed separately with each having an individual siphon.

Level 1, 2 & 3: Requirement applied

R34. All connecting pipes passing through the casing where there is a risk of condensation shall be insulated.

Level 1, 2 & 3: Requirement applied.

3.2.1.10 Air Treatment

3.2.1.10.1 Filter

R35. A minimum ePM10 50% filtration stage shall be installed before the first component of any air stream (except dampers or filter pre-heater)

Level 1, 2 & 3: Requirement applied

R36. Air filters shall be selected and arranged in order to ensure a good incoming air quality (as a minimum). The filter efficiency according to EN 16890:2016 of the filters shall be certified by a certification body accredited ISO 17065:2012.

Level 1 & 2: The filtration efficiency at 0.4 µm of all filters installed shall be equivalent to an ePM10 50% filter on the exhaust side and to an ePM1 50% filter on the supply side.

Level 3: The filtration efficiency at 0.4 µm of all filters installed shall be equivalent to an ePM10 50% filter on the exhaust side and to an ePM1 85% filter on the supply side.

R37. Manufacturer shall ensure that closed cell gasket is used and that the seal is properly fastened. The section related to non-metallic materials (test reports from hygiene institute according EN ISO 846:2019) shall be applied.

Manufacturer shall ensure that closed cell gasket is used and that the seal is properly fastened.

Level 1 & 2: Requirement applied

Level 3: Level 1 & 2 requirements **and** the gasket shall be either fixed on the filter frame and changeable or on the filter cell.

R38. Bag filter must be in vertical position (this requirement does not apply to rigid filters). It shall be clearly indicated in the IOM that the filter shall always be in a vertical position, it is also recommended to put a label on the unit.

Level 1, 2 & 3: Requirement applied

R39. To facilitate the maintenance of the air filter the following information shall be permanently indicated on the air-filter chamber:

- Dimensions
- Filter class:
 - For medium and fine filters, it shall be according to EN 16890:2016.
 - For high efficiency filters it shall be according to EN 1822:2019.
- Number of air filters
- Actual air volume of the installed system
- Final pressure drop based on the fan's characteristics.

Level 1, 2 & 3: Requirement applied

R40. Each filter stage shall be equipped with a differential-pressure gauge. The measuring display device shall be easily accessible and easily readable by future users.

Level 1 & 2: For each filter a visual signaling or an alarm in the control system is mandatory. For units to be installed outdoor liquid manometer is not allowed.

Level 3: For each filter an alarm in the control system is mandatory. For units to be installed outdoor liquid manometer is not allowed.

Note: Should the control system be delivered by the manufacturer, the requirements apply. Should they not, the requirement shall be written in the IOM.

R41. The supply side shall be filtered by two filter stages.

Level 1: No requirements

Level 2 & 3: Requirement applied **and** the first stage of filter class shall be at least **M5**.

Note: if a third stage filter is required, it can be present within the unit or outside the unit. Therefore, this is not in the scope of this programme.

R42. Recirculated air shall be filtered with the same requirement as defined under R35 for supply air filter.

Level 1 & 2: Requirement applied

Level 3: No recirculated air shall be allowed.

3.2.1.10.2 Cooling and Heating Coil

R43. For energy and hygiene reasons the distance between the fins of the coolers that can dehumidify shall be at a minimum **Y** mm, otherwise, the distance between fins shall be at a minimum **X** mm.

Note: This applies also to cooling coil within run around coil

Level 1 & 2: $X_{\min} = 2.0$ mm and $Y_{\min} = 2.5$ mm

Level 3: $X_{\min} = 2.5$ m and $Y_{\min} = 3.0$ mm

R44. Air heaters, which are used for drying before the first filter stage, shall guarantee a minimum distance between the fins of at least 4 mm.

Level 1, 2 & 3: Requirement applied

R45. The fins shall have a thickness of **X**.

Level 1, 2 & 3: $X_{\min} = 0.10$ mm

R46. For hygiene reasons, coolers with dehumidification shall not be arranged immediately before air filters or silencers. Fans, heaters *or droplet separators* shall be installed in between to limit the relative humidity.

Selection software to alert the user that cooler with dehumidification shall not be arranged immediately before air filters or silencers.

Level 1, 2 & 3: Requirement applied

3.2.1.10.3 Humidifier

R47. For clean application humidifier shall be installed with at least an element (Coil, fan, heat exchanger, droplet separator) between humidifier and final filter or silencers.

A maximum of 90% RH is allowed before each filter section or silencer.

Level 1, 2 & 3: Requirement must be included in the IOM of the product.

3.2.1.10.4 Dehumidifier

R48. Any solid or liquid absorbent shall be harmless, a test report showing the compliance of the product used shall be provided.

Filtration downstream the desiccant unit shall be minimum **X**.

Level 1 & 2: Requirement applied and X = ePM1 50%

Level 3: Requirement applied and X = ePM1 85%

R49. No moisture can carry over to the components or sections downstream of the coil.

Selection software to alert the user that cooler with dehumidification shall not be arranged immediately before air filters or silencers.

Level 1, 2 & 3: Requirement applied

3.2.1.10.5 Heat Recovery System (HRS)

R50. The coils in the run around coils shall comply with the requirements of coils.

Level 1, 2 & 3: Refer to 3.2.1.10.2.

R51. Heat exchangers shall be easy to clean and to disinfect in order to avoid any kind of contamination.

Level 1, 2 & 3: Requirement applied

R52. Cross contamination

Level 1: For rotary heat exchanger, cross contamination between extract air and supply air at design condition shall be limited to $EATR \leq 5\%$. To assess EATR, both the leakage across the heat recovery device and, if applicable, the leakage across partition walls between supply part and extract part shall be considered.

Evaluation of the leakage: Leakage shall be based on the calculated operating pressure in the unit sections at design pressure drop for components and design external pressure. External pressure in the calculation is set at 50 Pa at the non-building side (if ducted) and the remainder at the building side (EN 13053:2019 §5.2.3.1.1.1)

OR The final supply air shall be filtered as the supply air defined under IV.3a

OR The return air shall be filtered as the supply air defined under IV.3a.

OR No requirement if the air handling unit is equipped with a recirculation damper.

Level 2: For rotary heat exchanger, cross contamination between extract air and supply air at operational condition shall be limited to $EATR \leq 5\%$. To assess EATR, both the leakage across the heat recovery device and, if applicable, the leakage across partition walls between supply part and extract part shall be considered.

Evaluation of the leakage: Leakage shall be based on the calculated operating pressure for worst possible operational conditions. Worst possible operational conditions exist when pressure differential between supply part and extract part are the lowest:

- For the supply part the highest pressure drop of components upstream the fan and lowest pressure drop for components downstream the fan shall be considered for components with variable pressure drop (filters, dry/wet heat exchangers).
- For the extract part the lowest pressure drop of components upstream the fan and highest pressure drop for components downstream the fan shall be taken for components with variable pressure drop.

System failure do not have to be considered. External pressure in the calculation is set at 50 Pa at the non-building side (if ducted) and the remainder at the building side (EN 13053:2019 §5.2.3.1.1.1)

OR The final supply air shall be filtered as the supply air defined under IV.3a

OR The return air shall be filtered as the supply air defined under IV.3a.

OR No requirement if the air handling unit is equipped with a recirculation damper.

Level 3: For rotary heat exchanger, cross contamination between extract air and supply air at operational condition shall be precluded (EATR = 0%).

A positive pressure between supply side and extract side shall be ensured for the heat recovery section and, if applicable, partition walls between the two air streams.

Rotary heat exchangers shall be equipped with a purging sector with sufficient purge angle adapted to the nominal rotor speed.

A pressure control system with differential pressure sensor across the sections with the lowest possible pressure difference shall safeguard this requirement.

If a lower value is measured than the minimum permissible value set at 50 Pa, the control system will proportionally (further) close an extract air inlet damper and/or generate an alarm.

The system shall be evaluated as described under level 2.

OR No requirements if the two airstreams are fully separated by individual casings and split heat recovery.

3.2.1.10.6 Fans

R53. Fans and fan drives shall be used rather than belt drive fans.

If a belt drive fans or fans with housing are used refer to [3.2.1.7](#) for cleaning and maintenance.

In case of use of a V-belt driven fan (exception: flat-belt drives), an additional filtration stage shall be installed immediately downstream of the fan (before any other component). The filtration efficiency of this filtration stage shall be at least equal to the highest filtration efficiency installed upstream of the fan (with a minimum of ePM10 50%).

An inspection window plus inspection light for checking the visual aspect of the belt shall be installed (for any type of belt).

Level 1: Requirement applied

Level 2 & 3: Requirement applied and the inspection window and inspection light is mandatory for any type of fans for units with an internal height above 1.3 m.

R54. Fans shall be easily accessible for maintenance as described under [3.2.1.7](#).

Definition of removable fan:

- All screws or similar fixings visible when opening door or hatch.
- Enough space for screws or fixing to be loosen and replaced with a simple tool (spanner, screwdriver, etc. or no tool at all) unless a special tool is provided by Manufacturer.
- Withdrawal of the fan can be performed by maintenance personal only, without the help of an electrician (No need to undo electrical connection, only mechanical disassembly and only opening of electrical socket is allowed).

If fans can be removable no additional requirements, otherwise following requirements applied:

Level 1: Fan shall be accessible from one side according for 'Access and Space'.

Level 2&3: In case of plug fan only:

- On supply side: fan shall be accessible from both sides with at least half of the IMC-L downstream after the motor for 'Access and Space' upstream the fan.
- On extract side: fan shall be accessible from both sides, at least half of the IMC-L downstream after the motor for 'Access and Space' upstream the fan. If the fan is the last component before the damper, an access shall be ensuring for 'Access and Space' only upstream the fan.

For any other type of fans, fans shall be accessible from both sides for 'Access and Space'.

If no electrical connection is delivered with the fan and the variable speed drive (VSD), then the requirement shall be included in the IOM.

R55. If the water drain of a fan with housing is sealed it shall be easily accessible for cleaning and maintenance purposes. If not, the fan shall be removable.

- Plug is visible when opening the door or hatch.
- Enough space for plug to be open and removed with a simple tool (spanner, screwdriver, etc. or no tool at all), unless a special tool is provided by Manufacturer.
- Possibility to mop and wipe water below the fan (Min space about 3 cm below fan).

Level 1, 2 & 3: Requirement applied

R56. Fans with housing shall have an easily removable inspection lid (applicable for nominal impeller diameters greater than 400mm):

- Lid and all its fixings visible when opening the door or Hatch (Units with air flow height below 1,6 meter) **OR**
- When entering the unit (Units with air flow height larger or equal to 1.6 meter) enough space to open and close latch with a simple tool (spanner, screwdriver, etc. or no tool at all) unless a special tool is provided by Manufacturer.

Level 1, 2 & 3: Requirement applied

3.2.1.10.7 Silencer

R57. Supply air shall be filtered upstream the silencer with minimum ePM10 50% filter.

Level 1: No requirements

Level 2 & 3: Requirement applied

R58. Material lined with sound-absorbent components shall be abrasion resistant, harmless and shall resist to cleaning (e.g. fiber glass).

Proof by test reports from hygiene institute as per EN ISO 846:2019 shall be presented.

Certificate or technical report from supplier to be provided for fiber-glass compliance.

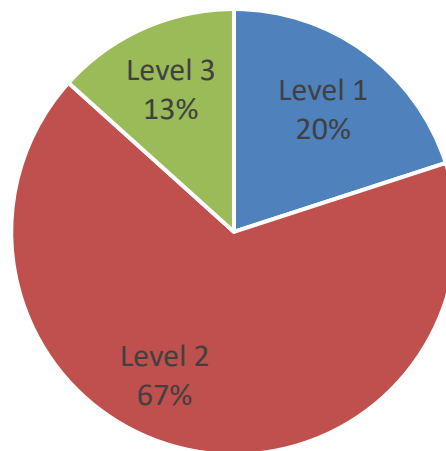
Level 1, 2 & 3: Requirement applied

3.2.2 2021 Campaign results

In 2021, 30 AHU units has been submitted for the Hygienic qualification. As Figure 6 shows, 20% of the units have the level 1, 67% have the level 2 and 13% have the level 3. This allows

any end user to filter the search of the unit depending on the required level of hygiene for a specific application, in addition it provide all the 59 requirement information.

Figure 6: 2021 campaign test results



4 CONCLUSIONS

Defining the rules and regulations for performances and efficiencies of any HVAC system including the air handling units is the responsibility of governments through internal or European regulations. However, ensuring the market surveillance of this type of units specially with a market with more than 11 billion USD size and growing requires third party entities experienced in the sector. In addition, the increasing interest of reducing the energy consumption of air handling unit for several reasons (net zero building objectives, the energy crises, energy cost), the COVID 19 pandemic increased the interest on the effect of IAQ on the human health. Eurovent Certita Certification in its certification programmes provided the both solutions to guarantee the performance of the unit and the hygienic level.

5 REFERENCES

- Abreu, C., Berg, G., Bijmans, A., Consalvo, P., & Courtney, S. (2021, October). *Air handling units eurovent guidebook everytHing you need to know about the heart of a ventilation system*. <https://Eurovent.Eu/Sites/Default/Files/2021%20-%20Eurovent%20AHU%20Guidebook%20-%20Second%20Edition%20-%20EN%20-%20Web.Pdf>. www.eurovent.eu
- AHU | Eurovent Certita Certification. (n.d.). Retrieved June 30, 2023, from <https://www.eurovent-certification.com/en/third-party-certification/certification-programmes/ahu>
- Ali, M. U., Yu, Y., Yousaf, B., Munir, M. A. M., Ullah, S., Zheng, C., Kuang, X., & Wong, M. H. (2021). Health impacts of indoor air pollution from household solid fuel on children and women. *Journal of Hazardous Materials*, 416, 126127. <https://doi.org/10.1016/J.JHAZMAT.2021.126127>
- Bekö, G., Clausen, G., & Weschler, C. J. (2008). Is the use of particle air filtration justified? Costs and benefits of filtration with regard to health effects, building cleaning and

- occupant productivity. *Building and Environment*, 43(10), 1647–1657.
<https://doi.org/10.1016/J.BUILDENV.2007.10.006>
- Eurovent Market Intelligence. (2022). *Air Handling Units Market report*.
<https://www.eurovent-marketintelligence.eu/reports/>.
- Karn Vohra, Alina Vodonos, & Joel Schwartz. (2021). *Fossil fuel air pollution responsible for 1 in 5 deaths worldwide – C-CHANGE / Harvard T.H. Chan School of Public Health*.
<https://www.hsph.harvard.edu/c-change/news/fossil-fuel-air-pollution-responsible-for-1-in-5-deaths-worldwide/>. <https://www.hsph.harvard.edu/c-change/news/fossil-fuel-air-pollution-responsible-for-1-in-5-deaths-worldwide/>
- Market and Markets. (2021, November). *Air Handling Units Market by application, type, capacity and region - global forecast to 2026*.
<https://www.marketsandmarkets.com/Market-Reports/Air-Handling-Units-Market-84723052.html#:~:Text=Air%20Handling%20Units%20Market%20Analysis,6.5%25%20from%202021%20to%202026>.
- Shetty, B. S. P., D'souza, G., & Anand, M. P. (2021). Effect of indoor air pollution on chronic obstructive pulmonary disease (COPD) deaths in southern Asia—a systematic review and meta-analysis. *Toxics*, 9(4), 85. <https://doi.org/10.3390/toxics9040085/S1>
- Stephens, B., Novoselac, A., & Siegel, J. A. (2010). The effects of filtration on pressure drop and energy consumption in residential HVAC systems (rp-1299). *HVAC and R Research*, 16(3), 273–294. <https://doi.org/10.1080/10789669.2010.10390905>
- World Health Organization. (2020, March 11). *WHO Director-General's opening remarks at the media briefing on COVID-19 - 11 March 2020*. <https://www.who.int/director-general/speeches/detail/who-director-general-s-opening-remarks-at-the-media-briefing-on-covid-19---11-march-2020>.

Car traffic or emissions from heating sources: What is responsible for IAQ?

Katarzyna Ratajczak*¹, Maciej Siedlecki

*1 Poznan University of Technology
Faculty of Environmental Engineering and Energy
M.Sklodowskiej-Curie 5
Poznan, Poland*

*2 Poznan University of Technology
Faculty of Civil and Transport Technology
M.Sklodowskiej-Curie 5
Poznan, Poland*

**Corresponding author:*

katarzyna.m.ratajczak@put.poznan.pl

ABSTRACT

The quality of indoor air in buildings depends on many factors. Some of these factors have internal sources, and some have external sources. The internal loads of the room include those generated by people: CO₂ and moisture emissions from breathing, heat emissions from room equipment: volatile organic compounds VOC. External sources are, for example, particulate matter present in the air, which is the result of emissions from cars and the burning of fossil fuels. The scientific literature states that car traffic can contribute a large share. However, it seems that this is largely dependent on the location of the building, including in a particular country.

An evaluation of the impact of car traffic on indoor and outdoor air quality was performed in different buildings located in the same district of a large city. Temperature, relative humidity, CO₂ concentration and PM_{2.5} and PM₁₀ concentrations were analyzed. The indoor air quality recorder was located in the room facing the busiest street. The way the room was used was unchanged. The external air quality recorder was located directly in front of the building. In addition to outdoor air, the number and type of vehicles that pass near the building were also recorded. Using the values of specific emissions of pollutants from vehicles of a given type, the number of pollutants emitted was determined in the vicinity of the building.

The analysis of the results addressed mainly the comparison of the concentration of particulate matter in the outside room with the value measured outside and the imposition of the number of cars and the determined emissions. The measurements were carried out over a period of month to eliminate differences in the emission of pollutants from heating sources, which was related to the temperature of the outdoor air.

The results showed that road transport does not have a significant effect on the concentration of pollutants in buildings. A discussion of the results was also held on a review of international studies. It turned out that of Poland a large share in outdoor air pollution has emissions from heat sources, which are caused by the use of nonrenewable fuels to heat houses and apartments. In Poland, there are more than half of the 50 most polluted cities in Europe. This results in increased exposure of people to the negative health effects associated with inhaling air contaminated with particulate matter.

The introduced EU regulations, including EPDB corrections and forcing thermomodernization to reduce heat demand, may result in limiting the use of fossil fuels, which will result in an improvement in the situation. The next step should be to look at the situation with regard to traffic pollution.

Research concerns Poland, where the use of low-efficiency heat sources that burn fossil fuels is a huge problem. The authors are aware that different socioeconomic conditions may occur in different countries.

KEYWORDS

Car traffic, Indoor air quality, Outdoor air quality, Poland

1 INTRODUCTION

Indoor activities and building equipment can be a burden on indoor air. In residential or public buildings, the main activities that affect indoor air are related to people staying indoors (Li et al. 2022; Sakamoto et al. 2022; Yan et al. 2023). Being indoors is associated with the emission of moisture and carbon dioxide from breathing (McMurray and Ahlborn 1982), as well as VOC (Wang et al. 2022) emissions. Moisture emission is also associated with showering and cooking (Liu et al., 2023). Furthermore, heat gains are emitted in rooms where people are present, which affect the temperature of the indoor air (Dharmasastha et al. 2023). To maintain comfortable parameters for people, installations are used to regulate air temperature - heating and air conditioning installations, while ventilation should be used to ensure proper concentration of carbon dioxide (Chai and Fan 2022; Khare et al. 2023; Ratajczak 2022; Sinacka and Mróz 2023; Sinacka and Szczechowiak 2021; Zender-wiercz et al. 2022). Air exchange in the room can take place through the use of mechanical ventilation with heat recovery or through natural ventilation, mainly through airing.

The efficiency of mechanical ventilation systems is high and allows for the maintenance of proper air parameters, including the possibility of its purification. However, the effectiveness of natural ventilation is not high and depends on many external factors. Most residential buildings in Poland do not have mechanical ventilation (Grygierek and Ferdyn-Grygierek 2022) and the type and configuration of ventilation affects energy usage and comfort (Amanowicz, Ratajczak, and Dudkiewicz 2023). The main burdens for outdoor air quality are two factors: transport and pollution emitted from the burning of fossil fuels to heat buildings. The pollutants emitted from car traffic are related to the type of the tested vehicle, the year of its production (meeting the emission standard) and the efficiency of the engine and non-engine exhaust gas treatment systems, as previously discussed. The amount of pollutant emissions is also related to the intensity of vehicle traffic, the speed of movement, and whether the passage of cars is smooth or whether there are numerous changes in speed, including stopping due to traffic congestion. The combustion of petroleum fuels is associated with the imperfection of this process because of the short time and insufficient mixing of fuel with air. This involves the creation of solid particles. The quantitative and qualitative structure of toxic compounds in exhaust gases depends on many factors, including the operating conditions of the unit, the way it is operated, and the type of fuel and engine used. This is especially important in cities with heavy traffic, where people can be directly exposed to the components emitted by motor vehicles. (Rymaniak et al. 2023; Siedlecki et al. 2019, 2021; Ziółkowski et al. 2022)

Outdoor air pollution related to fuel combustion for heating buildings is mainly particulate matter (PM), sulfur dioxide (SO₂), nitrogen oxides (NO_x), and various heavy metals related to the local combustion of mainly solid fuels. All of these compounds can have detrimental effects on healthy people (Munawer 2018). This takes place in many locations, even in large cities in Poland, although the burning of poor-quality fuels and garbage in small towns is a bigger problem. According to Forbes Reports, Poland has 29 out of 100 cities with the worst air quality in the world. This is related to the burning of fossil fuels, especially in the south of the country. The quality of outdoor air is linked to the quality of indoor air (Leung 2015), especially considering that the exchange of indoor air by introducing outdoor air is mainly through ventilation, which has been the subject of previous research (Basińska et al. 2021). In this case, air with a concentration of pollutants present in the outdoor air is introduced into the buildings. For countries with high outdoor air pollution, there is a high risk that indoor air will also be polluted. For these situations, solutions that will allow one to clean the air introduced into the room, e.g. through air purifiers or the installation of forced ventilation equipped with air filters (Rawat and Kumar 2023). However, it would be better to think about the reason for poor outdoor air quality and look for solutions on a larger scale than your own home.

The research was carried out in one district of a city in Poland, where four measurement points were located. A map with the location of the measurement points is shown in Fig. 1. Several aspects of indoor and outdoor air quality were recorded, and the number of cars passing near the analyzed building was recorded as well. Furthermore, the quality of the outdoor air in the district was recorded in the period before and after the experiment, to provide a general background for the quality of the outdoor air in this district.

2 METHODS

2.1 Experiment Locations and Background

The research was carried out in Poznan, Poland. It is a city with a population of 500,000. According to data from the Inrix report, which aims to verify traffic volume in cities, Poznan is ranked 44th globally, 120th among European cities, and 2nd compared to other cities in Poland. According to statistics, drivers in Poznan spend an average of 74 hours a year in traffic jams. In 2020, 527.5 thousand registered in Pozna. motor vehicles, including 415,000 passenger cars, which translates into 756 passenger cars per 1,000 inhabitants in Poznan.

The city has a heating network powered by a combined heat and power plant that generates heat in cogeneration, with a non-renewable primary energy input factor of 0.9. About 60% of city dwellers (40% of addresses) are supplied with heat from this source. Thanks to this solution, the emission of pollutants related to the preparation of heat for residents is small and does not significantly affect the quality of the outdoor air in the city (Xi et al. 2019).

About 40% of residents declare that they heat their buildings by burning solid fuels, the same percentage uses gas, and about 12% use electricity (mainly through heat pumps). Most multifamily buildings are connected to district heating, whereas single-family buildings use all four types of heat sources. However, the city has poor air quality during the winter, as previously described (Basińska et al. 2021).

The research was planned and conducted in a district of single-family homes. The choice of buildings was related to their location on streets with different intensities of traffic. The location of buildings, car traffic, and outdoor air quality measurement points is shown in Fig. 1a. The measurement point where the outdoor air parameters were continuously measured from April to June was also marked as a district baseline.

The indoor air recorders were placed in a room facing the street where the outdoor air parameters were measured. All rooms had no mechanical ventilation and air exchange was carried out by infiltration or opening a window. The occupants of the premises were to follow their normal mode of use of the premises. The map of the location of the measuring equipment is shown in Fig. 1b.

2.2 Location and dates of measurements

The measurements were carried out over a period of one month. A period of the year was selected in which the heat sources operate only for the preparation of domestic hot water. The study period was selected when the average outside air temperature was higher than 12 °C, at the time when the heating season ended in the city. The average outdoor air temperature measured at the district baseline point (Fig.1) for the first week of measurements was 13.5°C and the concentration of particulate matter was 15.7 µg/m³, while on the second week of measurements it was 20.7°C and 14.6 µg/m³, respectively.

In each location (A-D), measurements were carried out for one day from 8:00 am to 4:00 pm. Measurement dates: location A – April 26; location B – April 27; location C – May 20, location D – May 21.

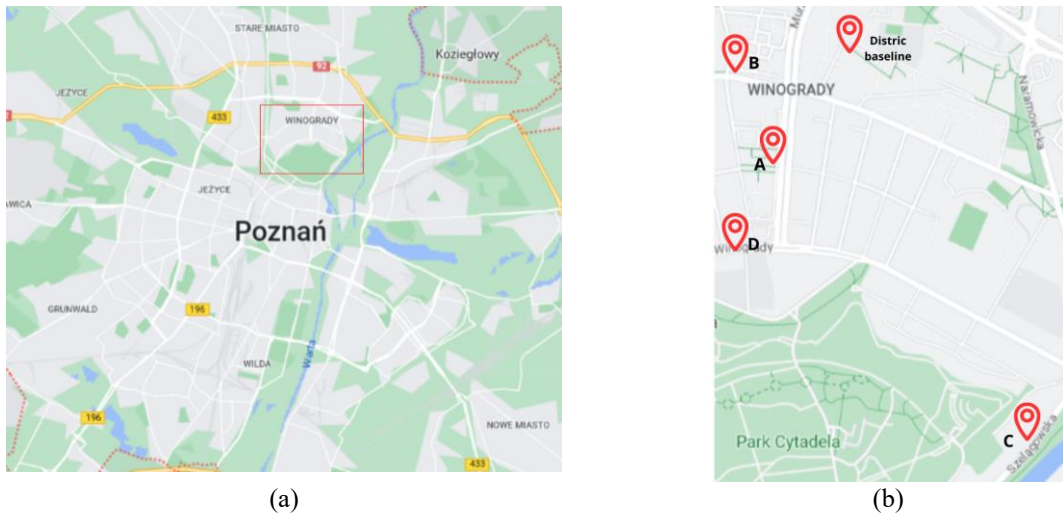


Figure 1: Analysed district of Poznań City (a) and localisation of measurement points (b) [Source: Google Maps]

2.3 Method of evaluating car traffic and pollutant emissions from car traffic

A device for measuring traffic intensity, i.e. Topo Vitronic, was used for the research. It is a compact device that contains properly configured measuring instruments (Fig. 2). This device uses high-frequency waves, which, after reflection, allow evaluating passing vehicles in several respects.



Figure 2: Device for traffic measurements - Topo Vitronic

The Topo Vitronic device, due to the fact that it uses technology that changes the frequency of waves, allows one to obtain measurements also in tunnels, roadwork zones, or curves. The basic data of the device are presented in Table 1.

Table 1: Description of the Topo Vitronic device

Size	Temperature range	Working time	Communication	Data transfer
42x35x18 cm	-30 to +50 °C	7 days	Bluetooth, GPRS	GSM, GPS

Six vehicle classes were analyzed: Class 1 - PC vehicle, Class 2 - motorcycle or very small vehicle, Class 3 - van and truck, Class 4 - vehicle with trailer, Class 5 - bus or vehicle combination, Class 6 - unclassified vehicle (bicycle, tram).

To evaluate the emission from car traffic previously obtained, unit emission of particulate matter was taken: 7 12 mg PM/km per each car.

2.4 Method for assessing air parameters

Outdoor air quality measurements were made using the NEMo Outdoor recorder (Ethera, France) to measure outdoor air parameters and NEMo Mini XT recorder (Ethera, France) for measuring indoor air parameters. The recorders measured and recorded the air quality parameters at 10-minute intervals. The parameters measured and measurement method are summarized in Table 2. A room with windows facing the street was selected for the location of the indoor unit. The external device with a shield was located directly next to the vehicle traffic measurement apparatus, in the immediate vicinity of the building where the indoor air parameters were measured.

Table 2: Measurements of outdoor air parameters

Parameter	Carbon dioxide	Temperature	Relative humidity	PM2.5, PM10
Detection method	Non-dispersive infrared spectrometry	Complementary Metal-Oxide-Semiconductor	Capacitive	Laser-based light scattering
Measuring range	0–5000 ppm	(–55)–(+120) °C	0–95%	0–1000 µg/m ³
Resolution	1 ppm	0.08 °C	0.08 %	1 µg/m ³
Accuracy	±50 ppm	±0.5 °C	±3 %	±5 %
Used in device	Mini XT	Mini XT; Outdoor	Mini XT; Outdoor	Mini XT; Outdoor

2.5 Assessment criteria

The choice of measurement date was assessed by evaluating the temperature of the outside air and the concentration of PM2.5 and PM10 at the measurement point for the district.

Because the high concentration of particulate matter in the heating season does not determine what is the reason for poor indoor air quality car traffic or combustion from heating source, the criterion for answering the question: Car traffic or emissions from heating sources: What is responsible for IAQ? will be assessing whether the concentration of particulate matter is low or high compared to the WHO standards. The criterion is the following:

- low concentration of particulate matter in the off-heating season period with high traffic intensity - car traffic does not generate high pollution,
- high concentration of particulate matter in the off-heating season period - car traffic generates a lot of pollution

For each measurement point, the following was assessed:

- a number of vehicles passing the building and PM2.5 concentration in the outdoor air,
- range of PM2.5 and PM10 concentrations in indoor and outdoor air,
- range of indoor CO₂ concentration values as the indicator of ventilation.

Historical data described in the publication (Basińska et al. 2021) where similar measurements were carried out, but in the colder period of the year, were also assessed.

The criterion to assess whether car traffic or heating sources have an impact on indoor air quality. The PM2.5 and PM10 concentration in locations with various vehicle traffic (based on the number of vehicles counted during the measurement period) will be evaluated.

3 RESULTS

3.1. Number of vehicles near the building

Using Topo Vitronic measuring equipment, the number of cars passing in 4 locations from 7:00 to 15:00 was calculated. The results for each location are presented in Fig. 3 and in Fig. 4 the total sum of vehicles is presented.

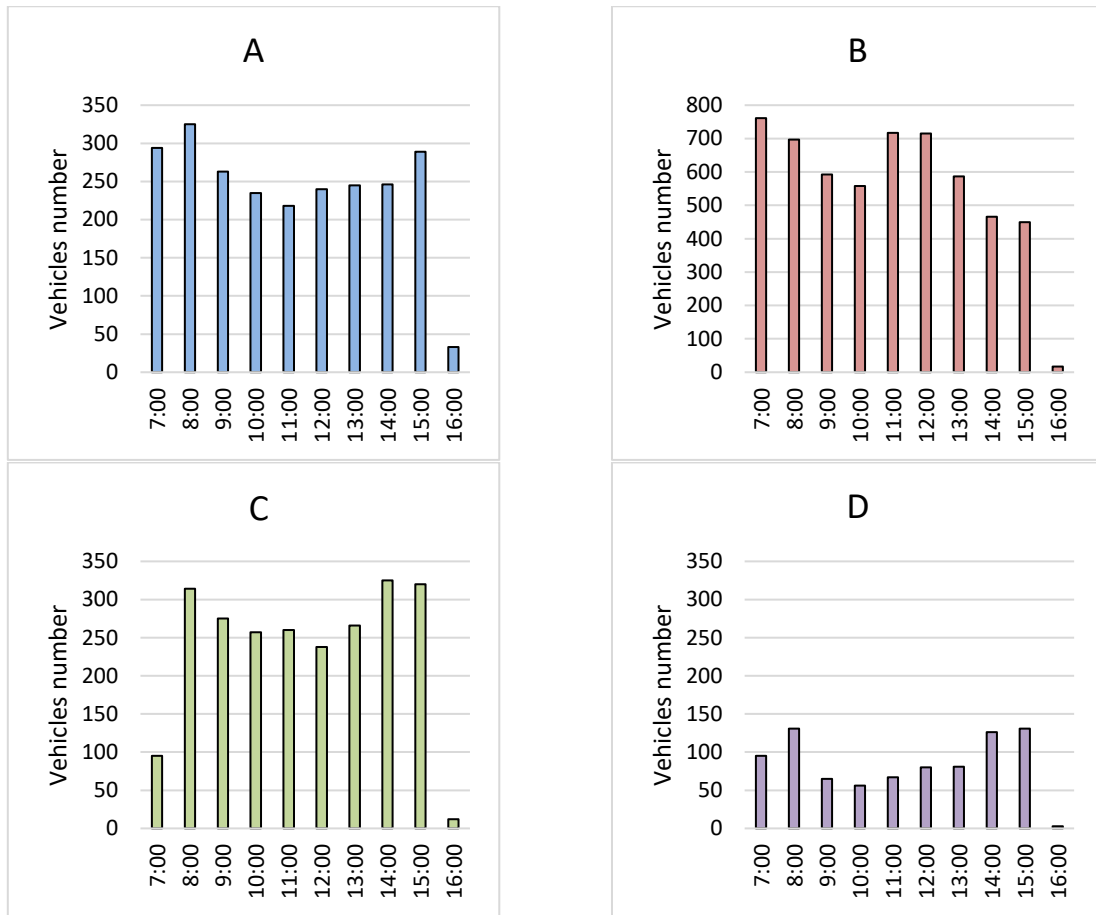


Figure 3: Number of vehicles at each location A, B, C, D during measurement day

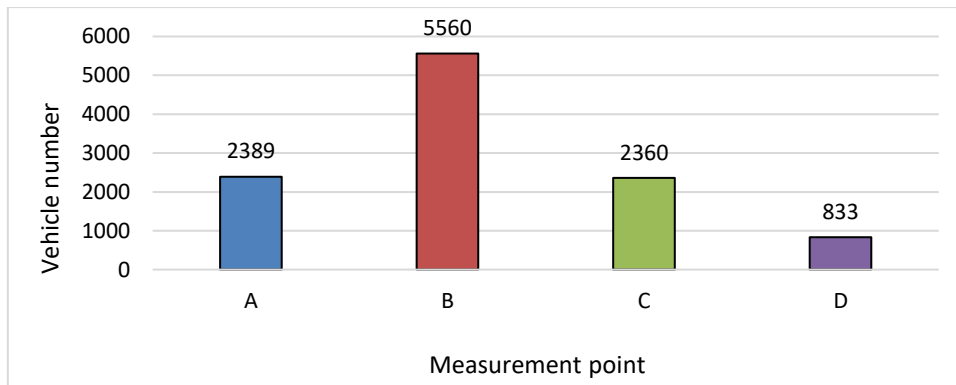


Figure 4: Total number of vehicles at each location A, B, C, D during measurement day

Measurement point B is located on a very busy street. The number of vehicles that passed the measurement point was almost as high as the total number of vehicles observed at the other three locations. Locations A and C are located on broad streets with moderate car traffic, while location D is not a main street. Car traffic in four chosen locations differs, so it should be seen in the results of air parameter measurements.

3.2. PM_{2.5} and PM₁₀ in indoor and outdoor air

Indoor and outdoor concentrations of PM_{2.5} and PM₁₀ were measured and the ranges of these parameters in each location are presented in Figure 5.

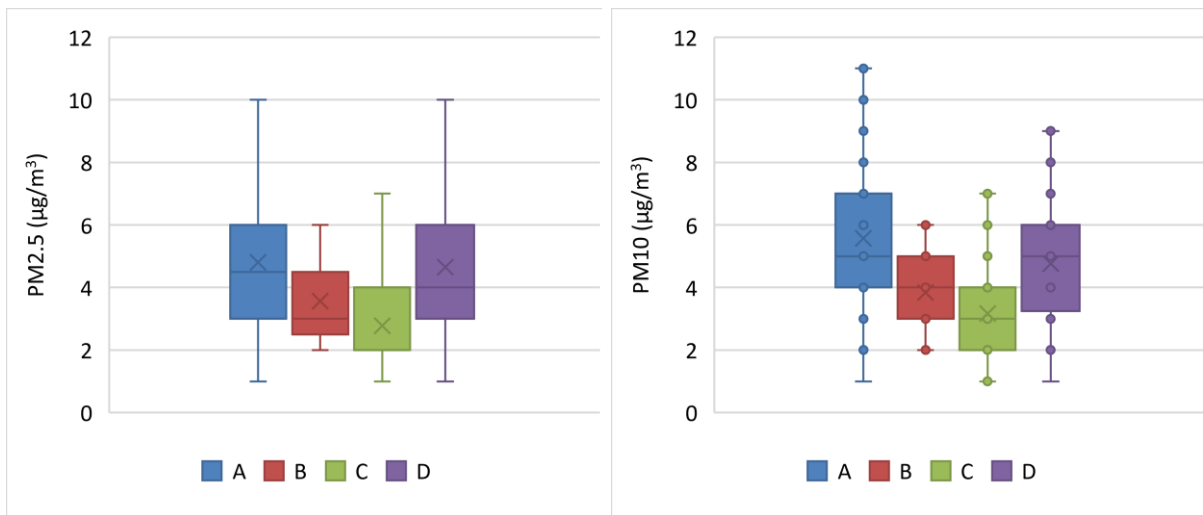


Figure 5: PM2.5 and PM10 in indoor air in locations A, B, C, D

As suspected, the concentration of particulate matter PM2.5 is lower than the concentration of PM10. Because the recommended values for PM2.5 are lower than for PM10, the results for PM2.5 will be discussed. The PM2.5 concentration was low in each location, with the average value ranging from 2.7 to 4.7 $\mu\text{g}/\text{m}^3$. It is below the value recommended by the World Health Organization - 15 $\mu\text{g}/\text{m}^3$. The maximum value was 10 $\mu\text{g}/\text{m}^3$. This suggests good air quality. The average carbon dioxide concentration during measurement day was for locations A, B, C and D 1102 ppm, 777 ppm, 806 ppm and 550 ppm, respectively. The difference in units results from the way the rooms are used and the number of people present in the room. This indicates that the air quality is not bad. But CO₂ concentration is not the topic of this study.

3.3. Concentration of PM2.5 outdoor air

To assess whether car traffic is responsible for air pollution in selected district of large city, the evaluation of concentration of PM2.5 in outdoor air is illustrated in Fig. 6.

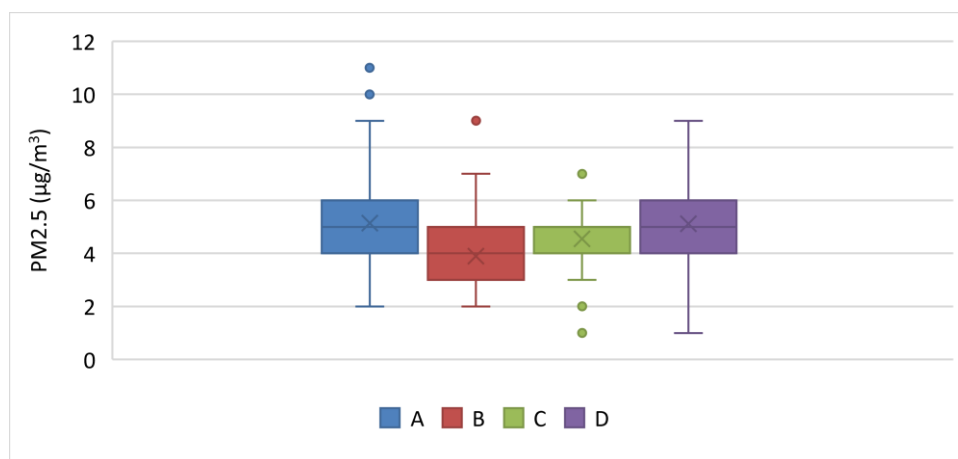


Figure 6: PM2.5 concentration in outdoor air in locations A, B, C, and D

The concentration of PM2.5 in the outdoor air is slightly higher than the concentration of this compound in the indoor air, with the average value for locations A, B, C and D 5.2 $\mu\text{g}/\text{m}^3$, 3.9 $\mu\text{g}/\text{m}^3$, 4.6 $\mu\text{g}/\text{m}^3$ and 5.1 $\mu\text{g}/\text{m}^3$. The highest concentration occurred at location D, while the lowest was at location B. PM2.5 did not correspond to the number of vehicles passing near the air parameter recorder. However, the concentration of PM2.5 corresponds well to the concentration in indoor air.

4 EVALUATION OF THE RESULTS

Previously described research on indoor and outdoor air quality in the same district, in the location located about 500 m from location A showed that there is a relationship between the PM2.5 concentration and the season, or more precisely, between the period of the heating season and the lack of the heating season. The results showing the relation between outdoor air temperature and PM2.5 concentration are presented in Fig. 7.

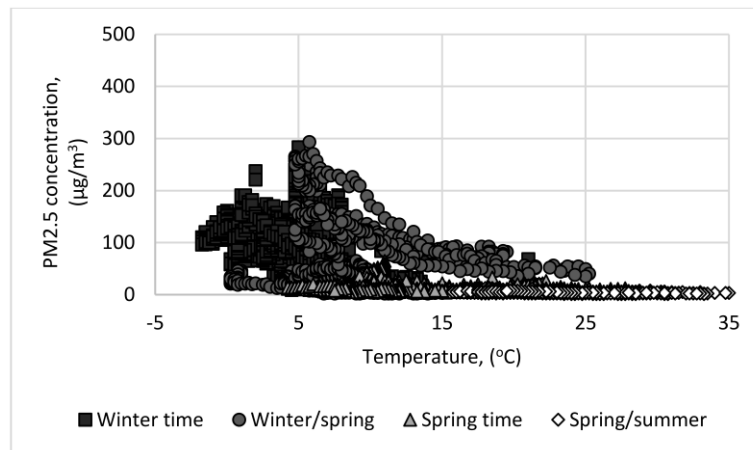


Figure 7: Concentration of PM2.5 in outdoor air in previously published research, based on (Basińska et al. 2021)

The research carried out, described in this article, was aimed at checking whether car traffic near the building affects the parameters of external and indoor air. A short experiment conducted showed that car traffic does not have an effect. Taking into account previous studies in which the seasonality of PM2.5 concentration in outdoor air occurs, it can be concluded that in the analysed location, the responsibility for air quality lies in the combustion of fuels for heating purposes. However, the results are not consistent with other studies conducted in Poland (Zender-Świercz and Polański 2022), but, the city where the other studies were conducted were in a more polluted part of Poland. This indicates the need for further research towards this objective.

The authors realize that the conducted experiment was short and included a small number of air parameters. But with their research, they wanted to draw attention to the fact that a significant problem related to air quality is the burning of fuels to heat buildings.

In this light, the provisions of the European Union related to the need to introduce more ecological ways of supplying buildings with heat seem necessary. By reducing the use of fossil fuels and replacing them with renewable fuels, while taking care to modernize buildings by reducing heat losses, it may be possible to achieve a state in which the quality of outdoor air will improve.

Research and analysis, however, require continuance.

5 CONCLUSIONS

In the studies described, it was important to assess air quality outside the heating season. The difference in the measured concentration of particulate matter in locations with fewer and more car traffic. Using the apparatus for measuring the number of passing vehicles and recorders of air parameters the quality of indoor and outdoor air was assessed in four locations located in one district of the big city.

The concentration of PM_{2.5} inside buildings indicates good indoor air quality. The maximum concentration of PM_{2.5} was 10 µg/m³, and the average was approximately 4 µg/m³. In location B, where the greatest traffic of vehicles occurred, the sum of vehicles that passed the measurement point at this point was 5,560 and was almost as high as the total number of vehicles in the other three locations. It was a point with the largest car traffic. At the same time, in this location, the measured concentration of PM_{2.5} in the outdoor air was the lowest and amounted to 3.9 µg/m³. Whereas at location D, where the vehicle traffic was the PM_{2.5} lowest (833 vehicles), the concentration was 5.1 µg/m³. In the experiment carried out, it was assessed that traffic in the examined district does not affect the quality of indoor air in rooms located on the side of the busiest street. But by analyzing historical data, it can be concluded that poor air quality in winter is caused by the fuels used to heat buildings.

6 REFERENCES

- Amanowicz, Łukasz, Katarzyna Ratajczak, and Edyta Dudkiewicz. 2023. "Recent Advancements in Ventilation Systems Used to Decrease Energy Consumption in Buildings—Literature Review." *Energies* 16(4): 1853.
- Basińska, Małgorzata et al. 2021. "The Way of Usage and Location in a Big City Agglomeration as Impact Factors of the Nurseries Indoor Air Quality." *Energies* 14(22): 7534.
- Chai, Jiale, and Jintu Fan. 2022. "Advanced Thermal Regulating Materials and Systems for Energy Saving and Thermal Comfort in Buildings." *Materials Today Energy* 24: 100925.
- Dharmasastha, K, D.G. Leo Samuel, S.M. Shiva Nagendra, and M.P. Maiya. 2023. "Impact of Indoor Heat Load and Natural Ventilation on Thermal Comfort of Radiant Cooling System: An Experimental Study." *Energy and Built Environment* 4(5): 543–56.
- Grygierek, Krzysztof, and Joanna Ferdyn-Grygierek. 2022. "Design of Ventilation Systems in a Single-Family House in Terms of Heating Demand and Indoor Environment Quality." *Energies* 15(22): 8456.
- Khare, Vaibhav Rai, Ravi Garg, Jyotirmay Mathur, and Vishal Garg. 2023. "Thermal Comfort Analysis of Personalized Conditioning System and Performance Assessment with Different Radiant Cooling Systems." *Energy and Built Environment* 4(1): 111–21.
- Leung, Dennis Y. C. 2015. "Outdoor-Indoor Air Pollution in Urban Environment: Challenges and Opportunity." *Frontiers in Environmental Science* 2. <http://journal.frontiersin.org/article/10.3389/fenvs.2014.00069/abstract> (June 28, 2023).
- Li, Mengze et al. 2022. "Human Metabolic Emissions of Carbon Dioxide and Methane and Their Implications for Carbon Emissions." *Science of The Total Environment* 833: 155241.
- Liu, Peng et al. 2023. "Understanding the Role of Moisture Recovery in Indoor Humidity: An Analytical Study for a Norwegian Single-Family House during Heating Season." *Building and Environment* 229: 109940.
- McMurray, Robert G., and Seth W. Ahlborn. 1982. "Respiratory Responses to Running and Walking at the Same Metabolic Rate." *Respiration Physiology* 47(2): 257–65.
- Munawer, Muhammad Ehsan. 2018. "Human Health and Environmental Impacts of Coal Combustion and Post-Combustion Wastes." *Journal of Sustainable Mining* 17(2): 87–96.
- Ratajczak, Katarzyna. 2022. "Ventilation Strategy for Proper IAQ in Existing Nurseries Buildings - Lesson Learned from the Research during COVID-19 Pandemic." *Aerosol and Air Quality Research* 22(3): 210337.

- Rawat, Nidhi, and Prashant Kumar. 2023. "Interventions for Improving Indoor and Outdoor Air Quality in and around Schools." *Science of The Total Environment* 858: 159813.
- Rymaniak, Łukasz, Bartosz Ziętara, Natalia Szymlet, and Daniel Kołodziejek. 2023. "Use of Toxicity Indexes in Reference to Carbon Dioxide for a Vehicle Equipped with a Two-Stroke Engine Without an Exhaust Aftertreatment System." *Journal of Ecological Engineering* 24(4): 228–36.
- Sakamoto, Mitsuharu et al. 2022. "CO₂ Emission Rates from Sedentary Subjects under Controlled Laboratory Conditions." *Building and Environment* 211: 108735.
- Siedlecki, Maciej et al. 2019. "Impact of the Use of Comfort Devices on the Exhaust Emission from a Hybrid Vehicle." *Combustion Engines* 179(4): 250–85.
- Siedlecki, Maciej, Jerzy Merkisz, Michał Dobrzyński, and Kamil Kubiak. 2021. "Impact of the Use of Comfort Devices on the Exhaust Toxic Compounds from a Modern PC Car with Spark Ignition Engine." *Combustion Engines*. <http://www.combustion-engines.eu/Impact-of-the-use-of-comfort-devices-on-the-exhaust-toxic-compounds-from-a-modern,142280,0,2.html> (June 28, 2023).
- Sinacka, Joanna, and Tomasz Mróz. 2023. "Novel Radiant Heating and Cooling Panel with a Monolithic Aluminium Structure and U-Groove Surface – Experimental Investigation and Numerical Model." *Applied Thermal Engineering* 229: 120611.
- Sinacka, Joanna, and Edward Szczechowiak. 2021. "An Experimental Study of a Thermally Activated Ceiling Containing Phase Change Material for Different Cooling Load Profiles." *Energies* 14(21): 7363.
- Wang, Nijing et al. 2022. "Emission Rates of Volatile Organic Compounds from Humans." *Environmental Science & Technology* 56(8): 4838–48.
- Xi, Xiaoqian et al. 2019. "Air Pollution Related Externality of District Heating – a Case Study of Changping, Beijing." *Energy Procedia* 158: 4323–30.
- Yan, Yan et al. 2023. "Emission Rate of Carbon Dioxide by Older Adults While Sleeping." *Building and Environment* 236: 110299.
- Zender-Świercz, Ewa, and Michał Polański. 2022. "Influence of Road Traffic on Indoor Air Quality." *Structure and Environment* 14(4): 142–52.
- Zender-Świercz, Ewa, Marek Telejko, Beata Galiszewska, and Mariola Starzomska. 2022. "Assessment of Thermal Comfort in Rooms Equipped with a Decentralised Façade Ventilation Unit." *Energies* 15(19): 7032.
- Ziółkowski, Andrzej, Paweł Fuć, Aleks Jagielski, and Maciej Bednarek. 2022. "Analysis of Emissions and Fuel Consumption in Freight Transport." *Energies* 15(13): 4706.

Monitoring VOCs' concentrations in a circular biobased residential building using low-cost sensors.

Yannick Thienpont^{*1}, Seppe Verbiest¹, Douaa Al Assaad¹, Hilde Breesch¹,
Alexis Versele¹

¹*KU Leuven, Department of Civil Engineering, Building Physics and Sustainable Design, Ghent Campus, Gebroeders De Smetstraat 1, 9000, Gent, Belgium*

ABSTRACT

Most current building materials are industrially processed, resulting in increased carbon emissions. Global annual carbon emissions due to construction materials reached its peak in 2013, 9.5 gigatons of CO₂ were produced. Upcoming circular economies can have a positive impact on the environment since reusing materials can lower carbon emissions. This economy encourages the use of more innovative materials (e.g., textile insulation, cellulose insulation, hemp, and cork) and recycling old materials. However, there is a lack of knowledge in the literature on the effect these innovative and recyclable materials have on the indoor air quality (IAQ) and human health. Most studies have been conducted in a lab environment and there is a need to monitor IAQ in a real test case study under dynamic indoor and outdoor climatic conditions. The aim of this work was to establish a monitoring campaign of volatile organic compounds (VOCs) in a circular biobased residential building in Belgium using new emerging low-cost VOCs sensors. Given their economic benefits, more sensors can be used covering a wider monitoring area compared to high-end sensors. Measurements were conducted for a trial of two weeks for a case of no ventilation and natural ventilation. Opening of the windows resulted in a large reduction in VOC concentrations, with several sensors measuring values underneath the most stringent threshold value of 300 µg/m³.

KEYWORDS

Indoor air quality, Biobased building materials, Volatile organic compounds, Residential building, Low-cost sensors

1 INTRODUCTION

In Belgium, the concentration of certain indoor pollutants can be higher indoors than outdoors, especially with increasing regulations on envelope air tightness (Hoge Gezondheidsraad, 2017). The modern European citizen spends about 90% of their time indoors, therefore exposure to environmental pollution mainly depends on the indoor air quality (IAQ) (Instituto de engenharia mecanica, 2008; Hoge Gezondheidsraad, 2017; de Kort, 2022). Moreover, nowadays, hybrid working has become more relevant in a lot of companies, so people are more than ever working from home (Van Tran et al., 2020). For this reason, the indoor air of dwellings is a key factor in determining the wellbeing of residents (Hoge Gezondheidsraad, 2017).

Existing pollutants indoors include volatile organic compounds (VOC), and particulate matter (PM) (Van Tran et al., 2020). VOCs are one the main pollutants of building materials, since they are easily vaporized entering the surrounding air (NHBC Foundation, 2009). Common residential building materials, such as wood parquet, gypsum board, PVC coverings, paint etc. are known to shed toxic compounds, such as toluene and formaldehyde (Van Tran et al., 2020). At high concentrations, toluene could cause liver, kidney, and brain damage in case of repeated exposure (New Jersey Departement of Health, 2016) and formaldehyde can cause skin burns and eye damage (National Library of Medicine, 2023). Therefore, materials used for composing the building envelope of new (or renovated) dwellings, should be carefully chosen (Ferreira Pinto Da Silva, 2017).

High performance biobased construction materials, which are produced sustainably and/or using waste products, offer an approach which is environmentally friendly (Keena et al., 2022). However, their effect on the IAQ in actual dwellings are not known. De Kort (2022), conducted laboratory tests on VOC emissions from expanded cork. These experiments showed that after 28 days no exceeded TVOC values were found with the tested expanded cork and the material meets the Belgian level of $1000 \mu\text{g}/\text{m}^3$. However, it should not be concluded that this will universally account for other present and future biobased envelope materials. Moreover, the research conducted thus far has been limited to a small selection of biobased materials under laboratory environments (de Kort, 2022; Maskell et al., 2015; Ferreira Pinto Da Silva, 2017). These studies are conducted under controlled conditions of temperature, solar radiation, RH, etc. while in real life this is not the case. They analyse each material separately and not as a whole working environment, which means that they are not capable to determine the influence of human exposure to indoor VOC concentrations. Therefore, these lab environments are non-representative scenarios. There is a need to monitor VOC emissions of biobased building materials on a real test case residential building with multiple biobased materials present at the same time, influenced by the surrounding environment (temperature, relative humidity (RH), air velocity, etc.).

This paper presents the results of a short-term monitoring campaign, to measure VOC concentrations, in a real circular and biobased residential building using low-cost sensors (LCSs). The emergence of LCSs can help to set up these monitoring campaigns that now rely on very expensive sensors. Due to their low cost, more sensors can be used with the same budget, covering a wider monitoring area. In that way it is also possible to measure differences and compare VOC concentrations between each sensor, in that way spatial trends can be identified. They also have the potential to become effective tools for introducing and engaging students in air quality matters. However, typically LCSs are less accurate and suffer from cross sensitivities with other pollutants. Nonetheless, they are still able to provide adequate reliability. Therefore, using low-cost sensing technology for monitoring IAQ must be encouraged. The number of studies with LCSs needs to increase, using them in bigger numbers and over a more extended measurement period. This study provides an overview of the quantitative capabilities of LCSs, using multiple LCSs in a broader environment. It will be one of many studies in which the use of LCSs will become increasingly reliable (Polidori et al., 2017; Alonso et al., 2022).

2 METHODOLOGY

2.1 Case study building: CBCI living lab.



Figure 1: CBCI Living Lab

The CBCI Living Lab project of Interreg was selected for this study. This building is a circular biobased residence which is located at the Technology campus Gent of KU Leuven (Faculteit

Industriële Ingenieurswetenschappen KU Leuven, 2021). The building consists of three floors: a ground floor with toilet, first floor with kitchen and second floor with technical installations. All rooms have a floor area of 20,73 m² and a space volume of 54,88 m³, except the third floor which has a smaller space volume due to the sloping roof. The Living Lab is equipped with a mechanical extract ventilation, denoted as system C in Belgium, which has a standard ventilation rate of 243 m³/h. The air is being extracted on the ground and first floor. During the monitoring campaign, the ventilation system was OFF due to malfunction. **Table 1** shows the materials exposed to the indoor environment.

Table 1: Inner envelope materials and furniture

Source	Material
Ceiling	Gypsum board + biobased paint
Wall	Gypsum board + biobased paint
Floor	Pine wood parquet
Furniture	MDF (Medium-density Fibreboard)
Staircase	CLT

2.2 Sensors

2.2.1 Benchmarking test

The low-cost sensors used were the SGP30 sensors of Sensirion (Sensirion, n.d.). To gain insight about the reliability of the LCS, reliability tests were performed in an empty experimental chamber. During this reliability test the LCS measurements were compared to the measurements of a more expensive indoor air sensor (Ethera Nemo). The Ethera Nemo sensor measures linear VOCs, this means less than 4 carbon atoms. The SGP30 sensor measures TVOCs, this is why no similar values were expected, only similar trends. The experimental setup was created to simulate a ventilated room. On one side of the cardboard box a ventilator was placed to have an inlet of air. On the other side of the box another hole was opened, to have an outlet for the inside air.

In **Figure 2** it was clear to see that both sensors followed similar trend. There was a big increase in values measured followed by a gradual reduction visible on both sensors. The SGP30 and the Ethera Nemo both reached their maximum values being 60 000 ppb and 47 000 ppb. The general conclusion of this measurement is that the SGP30 can be used for the intended purpose.

Table 2: Specifications sensors

Sensor	Price	Environmental parameters	Range (resolution)
SGP30 (RS Components Benelux, n.d.)	€ 21,19 (incl. BTW)	TVOC CO ₂ eq	0 – 60 000 ppb (6 ppb) 400 – 60 000 ppb (3ppm)
Ethera Nemo (Ethera, 2020)	€ 4 565 (excl. BTW)	Formaldehyde CO ₂ LVOC PID Temp RH Pressure	0 – 2 800 ppb (1 ppb) 0 – 5 000 ppm (1 ppm) 30 ppb – 5 ppm (1 ppb) 1 ppb – 50 ppm (1ppb) -55 - +125 °C (0,08 °C) 0 – 95 % (0,08 %) 260 – 1 260 hPa (0,02 hPa)

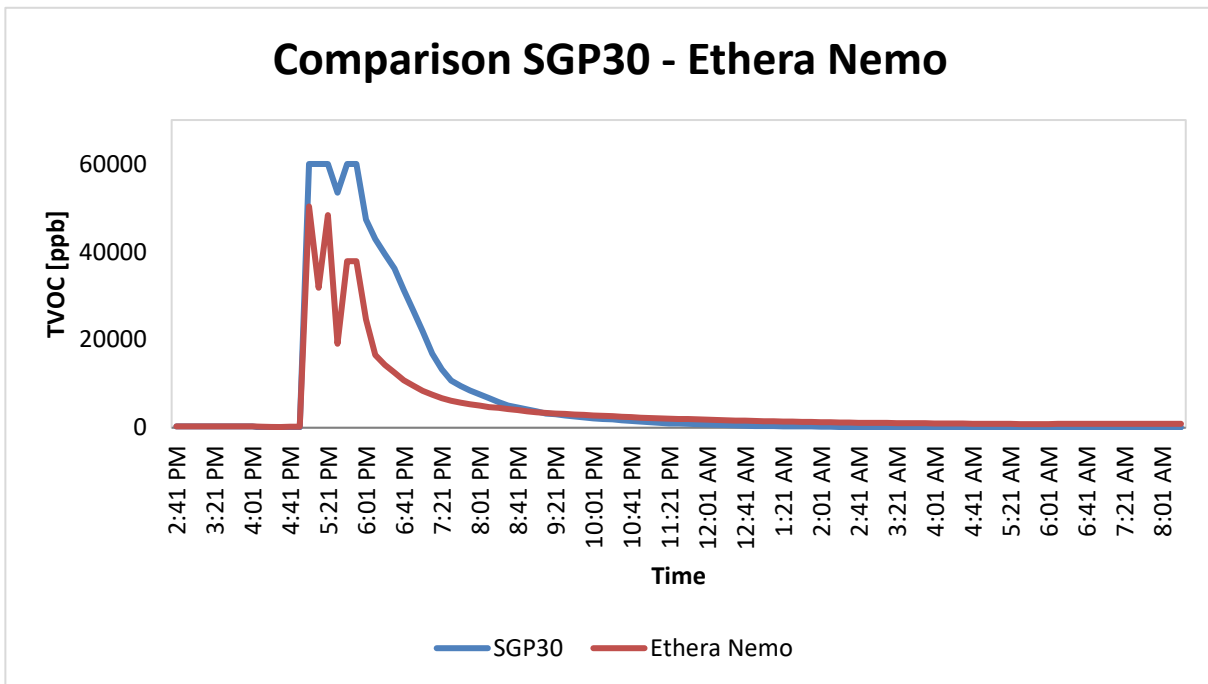


Figure 2: Comparison of SGP30 – Ethern Nemo sensors

2.2.2 Monitoring campaign

During the monitoring campaign, additional to TVOC measurements, temperature and RH were monitored using a HOBO U12 data logger (Onset Computer Corporation, 2008). This is a two-channel logger, which can provide reliable and accurate data since it has an accuracy of +/- 0,35 °C for the temperature and +/-2,5% for RH (Onset Computer Corporation, 2008). This sensor was placed in the centre of the first floor on the kitchen counter.

Multiple SGP30 sensors were placed at 15 cm from the envelope surfaces (floor, wall, and ceiling), see **Figure 3** and **Table 3**. To measure TVOC concentrations of the outdoor air, an additional sensor was placed outside of the CBCI Living Lab.

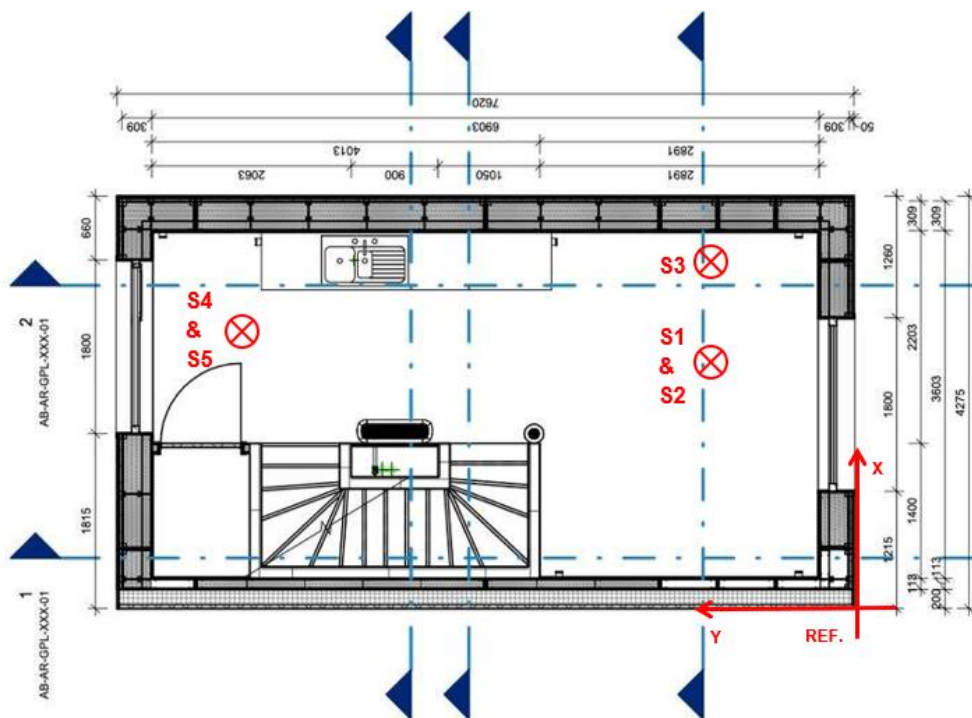


Figure 3: Sensor placement on first floor

Table 3: Sensor placement

Sensor ID	Position relative to reference	Purpose
S1	X: 3m Y: 1m Z: 0,15m ^a	Measuring VOC-concentrations close to floor
S2	X: 3 m Y: 1 m Z: 2,45 m ^a	Measuring VOC-concentrations close to ceiling
S3	X: 3,8 m Y: 1 m Z: 1,3 m ^a	Measuring VOC-concentrations close to wall
S4	X: 3 m Y: 4,3 m Z: 0,15 m ^a	Measuring VOC-concentrations close to floor
S5	X: 3 m Y: 4,3 m Z: 2,45 m ^a	Measuring VOC-concentrations close to ceiling
S6	At bicycle storage 20 m from CBCI	Measuring VOC-concentrations in outside air

^a: Heights were calculated to be 15 cm from surface. This 15 cm is determined based on two studies. The first one is the study of Huang and Haghghat (2002) where they presented VOC emission with a boundary layer. The intention was to install the sensors outside the boundary layer. The second one is a work of Du et al. (2015), they positioned their sensors 10 cm from the surface. During this monitoring campaign, an extra 5 cm margin was added resulting in the above heights. Ceiling: free height – 15 cm, floor: 15 cm from surface, wall: width – 15 cm and at breathing height.

To find the influence of ventilation, different measuring scenarios were devised, see **Table 4**. To be able to only measure the influence of the building envelope, the building had no occupancy during the measurements. In scenario 2, two windows were opened, one on the first floor and two on the second floor, creating an airflow through the building. The two windows on the second floor were Velux inclined roof windows located on each side. The window on the first floor was a tilt window (**Figure 3**).

Table 4: Scenarios for measurements

Scenario	Details	Duration of scenario
1	Reference case no ventilation	21/03/2023 15:30 – 23/03/2023 8:30
2	Reference case with configuration of open windows	24/03/2023 14:30 – 27/03/2023 7:40

3 RESULTS & DISCUSSION

3.1 Indoor air quality in the CBCI home

The results of the monitoring campaign were analysed based on ppb.hour values. This parameter was used to get an idea to what extent the VOC concentrations of each scenario exceeded the threshold value. According to the Flemish Indoor Air Decree these threshold values amount to a 66.7 ppb target value and 222.2 ppb intervention value (De Brouwere et al., 2022).

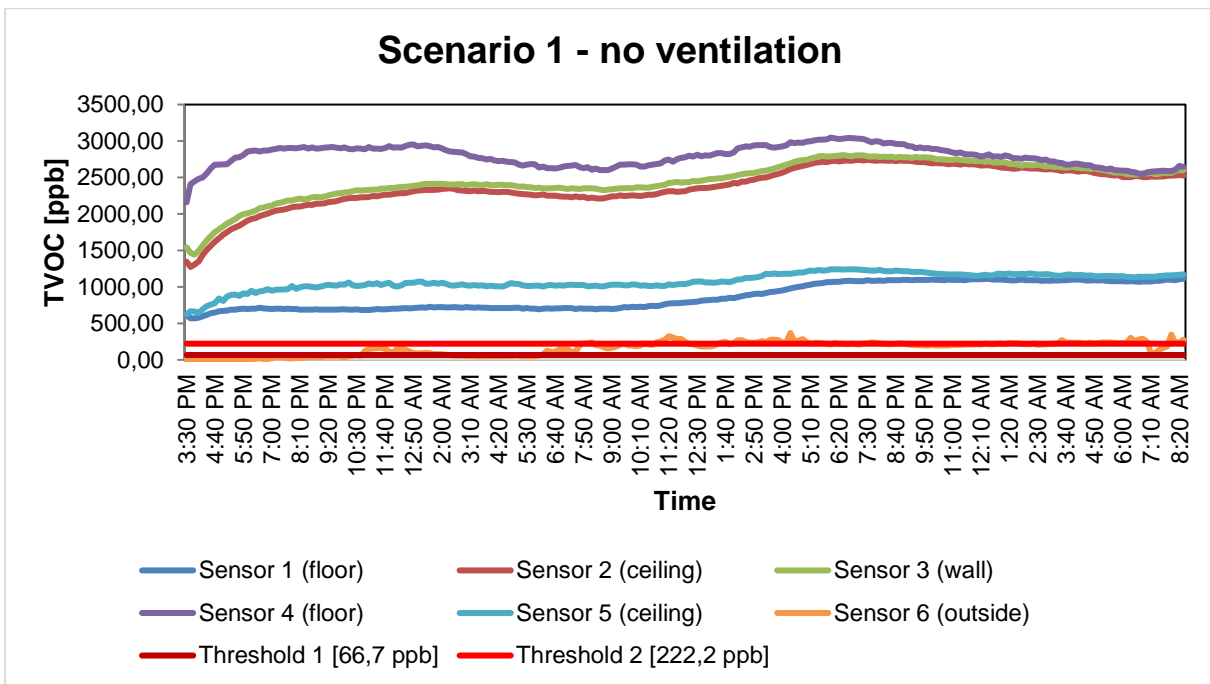


Figure 4: TVOC-measurements during Scenario 1

From **Figure 4**, it can be concluded that each of the five sensors exceeded both threshold values throughout the scenario due to the lack of ventilation and the build-up of VOCs over time. Sensor 4 measuring near the floor had the highest concentrations at an average of 2750 ppb, followed by sensors 2 & 3 (ceiling, wall respectively) at an average of 2250 ppb and finally sensors 1 & 5 (floor, ceiling) at an average of 1000 ppb and 750 ppb respectively. The difference between sensors measuring near the same source can be due to the device-to-device variety, (Sensirion, n.d.). Another reason may be the movement of the air in the room. Du et al. (2015) also showed the difference in air flow rate for different positionings of sensors. The third option is the possibility of a difference of environmental parameters at the different positions of the sensors. As only one sensor was used for temperature and RH during our monitoring campaign, no evidence of this can be provided.

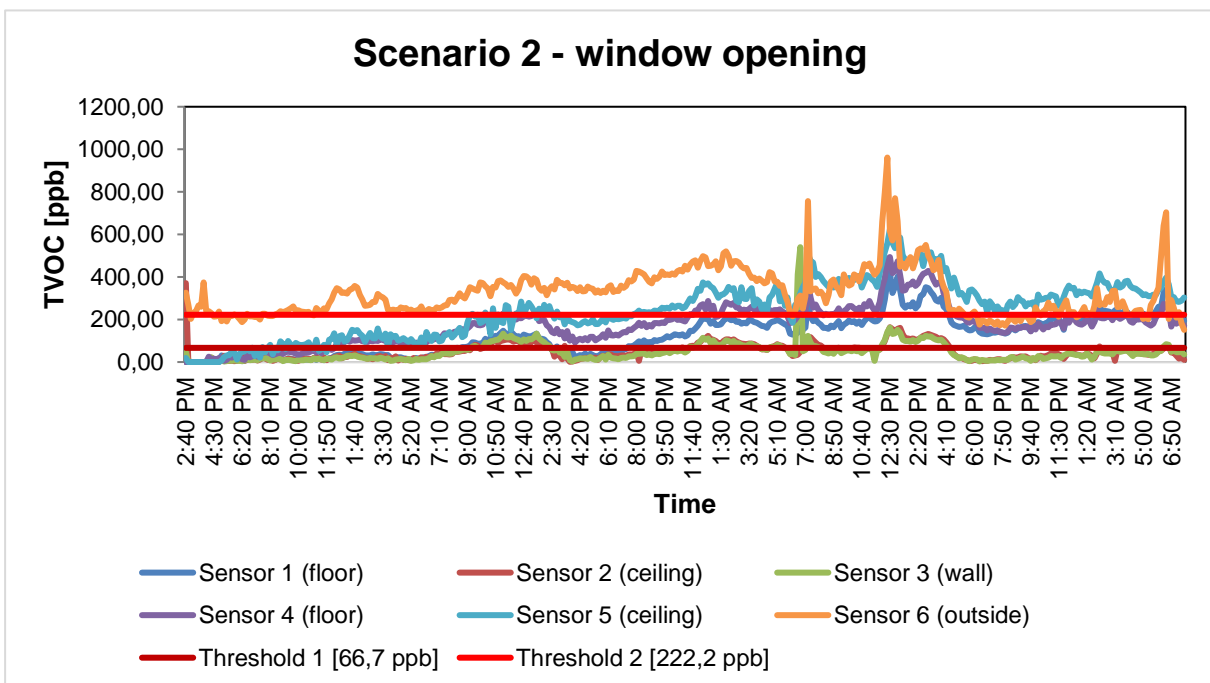


Figure 5: TVOC-measurements during Scenario 2

Opening of windows resulted in reduction of concentrations by 97 % compared to scenario 2a due to favourable wind directions. The lowest threshold limit was not violated for sensor 2 (ceiling) and sensor 3 (wall) throughout most of the scenario. The average values of these sensors were lower than the threshold limit of 66,7 ppb with 48 ppb for sensor 2 and 47 ppb for sensor 3. Sensor 1 (floor), sensor 4 (floor) and sensor 5 (ceiling) were measuring values around the highest threshold limit of 222,2 ppb. With average measurements of respectively 127 ppb, 174 ppb and 246 ppb. Indoor measurements followed the same trend as outdoor concentrations.

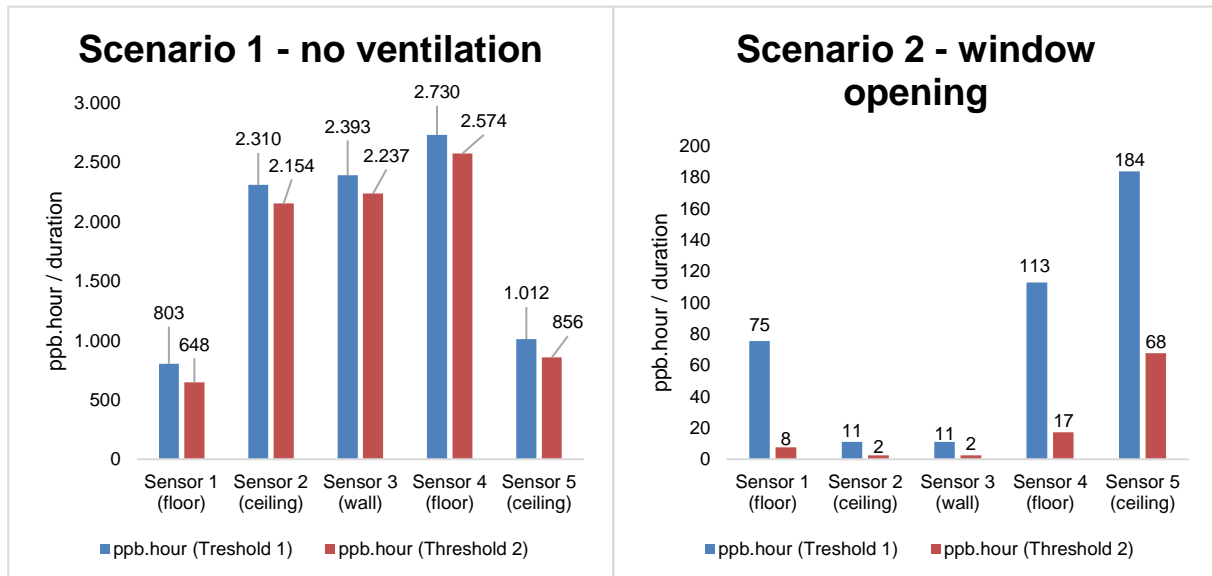


Figure 6: ppb.hour / duration values of Scenario 1 (a) and Scenario 2 (b)

4 CONCLUSIONS

In this study, a short monitoring campaign of VOC concentrations was set-up in a bio-based residential building in Belgium using low-cost sensors (LCS):

The key takeaways can be summarized below:

- In the case of no ventilation TVOC concentrations consistently exceeded both the intervention and target value due to excessive build-up over time.
- Opening of windows reduced the TVOC concentrations considerably. VOC concentrations for sensor 2 (ceiling) and sensor 3 (wall), dropped below the threshold values while it was slightly exceeded for sensor 1 (floor), sensor 4 (floor) and sensor 5 (ceiling).
- Differences in TVOC concentrations can be noticed between the sensors. This is probably due to the device-to-device variety of 25% (Sensirion, n.d.). A difference in air flow rate at each position of the sensor could also be an explanation. There could also be a difference of temperature and RH at each position of the sensors.
- The general conclusion of the reliability measurement is that the SGP30 is usable for the intended purpose. It can be used for a quantification of VOC emission in a case study where biobased materials were used. The trend of the measured values was comparable between the two sensors. This experiment proved that LCS can provide an indication of VOC emission and environmental parameters with a smaller budget. This provides many more opportunities for future work and IAQ monitoring.
- Future work includes benchmarking the obtained values of VOC concentrations in the bio-based home in a regular dwelling with commercial construction materials.

5 REFERENCES

- Alonso, M., Madsen, H., Liu, P., Bramming Jørgensen, R., Berg Jørgensen, T., Christiansen, E., Myrvan, O., Bastien, D., Mathisen, H. (2022). Evaluation of low-cost formaldehyde sensors calibration. *Building and Environment*, 222, 109380. <https://doi.org/10.1016/j.buildenv.2022.109380>
- De Brouwere, K., Bautmans, B., Benoy, S., Geerts, L., Stranger, M., & Van Holderbeke, M. (2022). “Establishing target and intervention guidance values for indoor air in dwellings and publicly accessible buildings: The Flemish approach”. *International Journal of Hygiene and Environmental Health*, 230, 113579. <https://doi.org/10.1016/j.ijheh.2020.113579>
- de Kort, J. (2022). Qualification and quantification of VOC emissions from (biobased) building materials. [Master thesis, Eindhoven University of Technology]. Retrieved January 23, 2023, from <https://research.tue.nl/en/studentTheses/qualification-and-quantification-of-voc-emissions-from-biobased-b>
- Du, Z., Xu, P., Jin, X., & Liu, Q. (2015). Temperature sensor placement optimization for VAV control using CFD–BES co-simulation strategy. *Building and Environment*, 85, 104- 113. <https://doi.org/10.1016/j.buildenv.2014.11.033>
- Ethera. (2020, January). Ethera Catalogue. Ethera. Retrieved April 15, 2023, from http://www.etheralabs.com/wp-content/uploads/2020/01/Catalogue_ethera_en_ld.pdf
- Faculteit Industriële Ingenieurswetenschappen KU Leuven. (2021, September 02). CBCI Living Lab KU Leuven. KU Leuven Building Physics and Sustainable Design. Retrieved April 02, 2023, from <https://iiv.kuleuven.be/onderzoek/building-physics-and-sustainable-design/cbci-living-lab-ku-leuven>
- Ferreira Pinto Da Silva, C.F. (2017). Interactions between volatile organic compounds and natural building materials. [PhD Thesis, University of Bath]. University of Bath. Retrieved March 11, 2023, from <https://researchportal.bath.ac.uk/en/studentTheses/interactions-between-volatile-organic-compounds-and-natural-build>
- Hoge Gezondheidsraad. (2017). Indoor air quality in Belgium. Federal Public Service Health, Food Chain Safety and Environment. Retrieved January 5, 2023, from https://www.health.belgium.be/sites/default/files/uploads/fields/fpshealth_theme_file/hgr_8794_advies_iaq.pdf
- Huang, H., & Haghghat, F. (2002). Modelling of volatile organic compounds emission from dry building materials. *Building and environment*, 37(11), 1127-1138. [https://doi.org/10.1016/S0360-1323\(01\)00089-0](https://doi.org/10.1016/S0360-1323(01)00089-0)
- Instituto de engenharia mecanica. (2008, October 31). Co-ordination action on Indoor Air Quality and Health Effects. Cordis EU research results. Retrieved February 21, 2023 from <https://cordis.europa.eu/project/id/502671>
- Keena, N., Raugei, M., Lokko, M., Etman, M., Achnani, V., Reck, B., & Dyson, A. (2022). A Life-Cycle Approach to Investigate the Potential of Novel Biobased Construction Materials toward a Circular Built Environment. *Energies*, 19(15), 7239. <https://doi.org/10.3390/en15197239>
- Maskell, D., da Silva, C., Mower, K., Rana, C., Dengel, A., Ball, R., Ansell, M., Walker, A., Shea, A. (2015). Properties of bio-based insulation materials and their potential impact on indoor air quality. *Academic Journal of Civil Engineering*, 33(2), 156-163. <https://doi.org/10.26168/icbbm2015.24>
- National Library of Medicine. (2023, April 08). Formaldehyde. National Library of Medicine. National Center for Biotechnology Information. Retrieved April 09, 2023, from <https://pubchem.ncbi.nlm.nih.gov/compound/712>

- New Jersey Department of Health. (2016, April). Hazardous substance fact sheet Toluene. NJ Health. Retrieved March 30, 2023, from <https://www.nj.gov/health/eoh/rtkweb/documents/fs/1866.pdf>
- NHBC Foundation. (2009, July). Indoor air quality in highly energy efficient homes – a review. NHBC Foundation. Retrieved March 15, 2023, from <https://www.nhbcfoundation.org/wp-content/uploads/2016/05/NF18-Indoor-air-quality-in-highly-energy-efficient-homes.pdf>
- Onset Computer Corporation. (2008). HOB0® U12 Temp/RH. HOB0. Retrieved April 28, 2023, from <https://www.onsetcomp.com/sites/default/files/resources-documents/7660-C%20MAN-U12-011.pdf>
- Polidori, A., Papapostolou, V., Feenstra, B., & Zhang, H. (2017). Field Evaluation of Low-Cost Air Quality Sensor. Air Quality Sensor Performance Evaluation Center. Retrieved April 28, 2023, from <https://www.aqmd.gov/docs/default-source/aq-spec/protocols/sensorsfield-testing-protocol.pdf>
- Sensirion. (n.d.). SGP30. Sensirion. Retrieved April 20, 2023, from <https://sensirion.com/products/catalog/SGP30/>
- Van Tran, V., Park, D., & Lee, Y.-C. (2020). Indoor Air Pollution, Related Human Diseases, and Recent Trends in the Control and Improvement of Indoor Air Quality. *International Journal of Environmental Research and Public Health*, 17(8), 2927. <https://doi.org/10.3390/ijerph17082927>
- RS Components Benelux. (n.d.). Seed Studio Grove-VOC and eCO2 Gas Sensor (SGP30) Gas Sensor for SGP30 Indoor Air Quality Application. RS. Retrieved April 28, 2023, from [https://benl.rs-online.com/web/p/sensor-developmenttools/1845085?cm_mmc=BE-PLA-DS3A-_-google-_-PLA_BE_NL_Raspberry_Pi_%26_Arduino_%26_ROCK_%26_Development_Tools_Whoop-_\(BE:Whoop!\)+Sensor+Development+Tools-_-1845085&matchtype=&pla338196066953&gclid=Cj0K](https://benl.rs-online.com/web/p/sensor-developmenttools/1845085?cm_mmc=BE-PLA-DS3A-_-google-_-PLA_BE_NL_Raspberry_Pi_%26_Arduino_%26_ROCK_%26_Development_Tools_Whoop-_(BE:Whoop!)+Sensor+Development+Tools-_-1845085&matchtype=&pla338196066953&gclid=Cj0K)

Smart & Predictive Air Quality Solution

Paul Brassler, Florian Käding

Prometech B.V.

Churchillaan 11 (Unit 17.07)

3527 GV Utrecht, The Netherlands

ABSTRACT

Monitoring and regulating the air quality inside critical infrastructure is essential for protecting occupants from external and internal airborne threats, such as pollutants, toxic chemicals, and pathogens. The outdoor air can be contaminated with agents such as diesel and car exhaust or with more toxic agents like Toxic Industrial Chemicals (TICs). In case of a pandemic, there is a threat of viruses and bacteria which can spread in the building. These airborne agents can penetrate and disperse inside the building via windows and doors or via the ventilation system. This gives insights into the transportation of these agents through the building. A smart software suite was built (HAVAC) for calculating the air flow through the building, combined with agent mass balances per room. Furthermore, once combined with a range of sensor systems, the tool can use the output of these systems to fine-tune the prediction on the way the agent will disperse into the building. Future predictions of concentrations per room can be generated. In case of a calamity or incident, this system can indicate which areas in the building are or will be “hot zones” in terms of agent concentration. Furthermore, a companioning expert system (MORTAL AI) can use these future prediction calculations to determine expected toxicological effects on occupants and provide decision support on possible further actions, such as evacuation of people or the decontamination of specific rooms. When designing a building, it can also - based on a large number of iterations - help design evacuation routes based on a range of different scenarios and provide recommendations on the best locations in the building to deploy IAQ (Indoor Air Quality) sensors and air purification filters.

KEYWORDS

Airflow modelling, agent dispersion prediction, air quality, decision support

1 INTRODUCTION

Monitoring and regulating the air quality in indoor areas such as large (cruise) ships and critical infrastructure is important¹. After an incident at – for instance – a nearby chemical plant, vapour or aerosol can escape into the surrounding area. The outdoor air can be contaminated with agents such as diesel and car exhaust or Toxic Industrial Chemicals (TICs). This pollution can have environmental effects and may have an effect on the health of persons in the polluted area. In case of a pandemic, there is a threat of viruses and bacteria which can spread in the building. These airborne agents can penetrate and disperse inside the building via windows and doors or via the ventilation system. To provide insight into these matters, there is a need for a holistic and comprehensive modelling and AI suite that takes into account indoor & outdoor air flow, agent dispersion, building information and human toxicology.

¹ See the EU Horizon ISOLA project for an example use-case (<https://isola-project.eu/>)

2 INDOOR AIR QUALITY & TOXICOLOGY MODELLING

For this reason, a software suite (HAVAC) was developed. It contains the necessary tools to safeguard occupants of critical infrastructure, by providing insight into current and future air quality issues and their potential impact on occupants of large structures. It includes an AI suite that specialises in a specific set of tasks related to the assessment and prediction of air quality and human comfortability / safety. It operates under a pre-defined range of contexts and is very good at handling these specific tasks. This approach is also known as Artificial Specialized Intelligence and can be integrated as a “smart” layer into new or existing air quality systems.

2.1 Air Quality

To model the indoor dispersion, a floor plan of a building is analysed in terms of rooms, windows, doors and the existence of a possible HVAC system. This 3 dimensional floor plan is used to calculate the airflow through the building, based on external factors, such as the outdoor wind velocity and temperature and also on the refresh rates of rooms, created by the HVAC system. If the exact structure of the HVAC is not known, the software tool is able to construct a virtual HVAC system for the building, depending on the required air refresh rate per room. This calculated air flow is used to predict the dispersion of possible contaminants through the building, which can originate from outdoors or from a source in the building.

In the HAVAC modelling suite a multi zonal approach is used, where every room in a building as well as every duct in the HVAC system is defined as a zone (Stuart Dols (2015), Feustel Helmut (2005), Brassler (2017a)). The outdoor environment is also defined as a zone. A zone can exchange air with a neighbouring zone via flow paths, which represent doors, windows and other leakages. The air flow through these flow paths can be present due to natural causes, such as outdoor wind pressure or as a result of ventilators, which are located in these flow paths (for instance in the HVAC system). The airflow through the entire building is then calculated by solving a set of equations, each describing the air mass balance per room (Brassler (2017b)). Outdoor wind pressures onto the building influence this air flow. Furthermore, an existing HVAC system also can supply fresh air into the building and suck away used air by incorporating an HVAC entrance and exhaust per room. In Figure 1, an example air flow and dispersion calculation for a single scenario is shown.

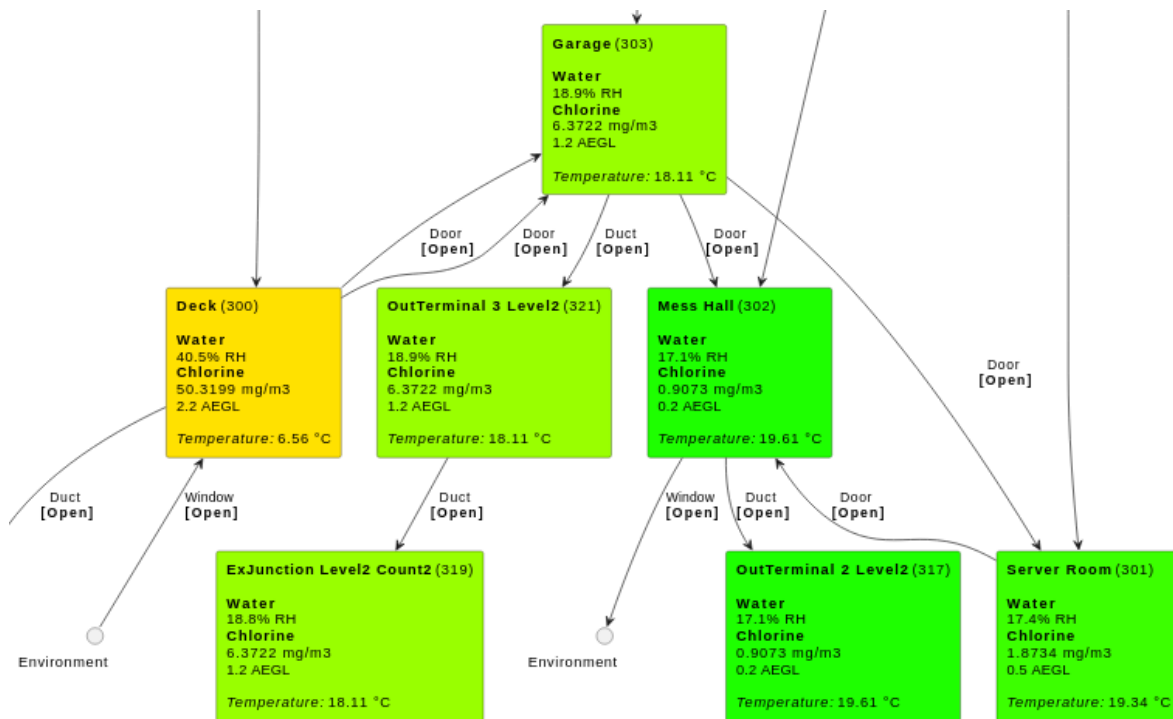


Figure 1: Example air flow and dispersion calculation for a single scenario

Temperature effects of airflow are also taken into account. For instance hot air will rise, resulting in a vertical air flow. Once this air flow through the building is known, it is also possible to calculate agent transport through the building. If an agent source is suspected or known (indoor or outdoor), this can be added into the software as well, resulting in the calculation of a dispersion of the agent through the building over time.

On top of that, the software tool is also able to incorporate sensory data of agent concentrations to fine tune the predicted agent dispersion through the building.

2.2 Toxicology

Chemical agents can have a toxic effect on humans. Obviously the amount (the concentration or the dose) of the agent plays a huge role in this toxicity. To keep track of the effects people encounter when present in the infrastructure, the software tool stores all challenge concentrations a person (or an entity, for that matter) encounters every timestep, while present in the building. Based on these values, the toxicological effects of these agents onto these persons are calculated.

Several different models are present in literature to predict the toxic effect, based on certain agent parameters and the agent dose. Based on the amount of known toxicity data present of the agent, one of these models will be chosen for the toxicity calculations. All models make a distinction between the severity of the effect onto the human. Three levels of severity are defined:

- Mild effects: Myosis, small blisters etc.
- Severe effects: Problems with breathing, larger blisters etc.
- Lethal effect: Complete cessation of bodily functions

To calculate the severity of the effect, toxicological data is required for each severity level. Obtaining the required data often is the crucial part in the toxicological calculations. Results (effects) of toxicity tests on animals (and sometimes on humans) with the specific agent are required for toxicological calculations. In literature several different standards are present. For instance:

- AEGL: Acute Exposure Guideline Levels, see NRC (2001)
- ERPG: Emergency Response Planning Guidelines, see AIHA (2023)
- TEEL: Temporary Emergency Exposure Limits, see DOE (2008)
- NATO Publishes standards by NATO, see NATO (2003)
- PAC: Protective Action Criteria, see OEE HSS (2016)

Output from the air flow and agent dispersion modelling is used as input to this model current and future predicted toxicological effects on occupants of critical infrastructure.

3 APPLICATIONS

In critical infrastructure planning and operation, predictive air quality monitoring and smart air purification systems play a vital role in ensuring a healthy, safe, and efficient environment. Combining scenario-driven design in the planning phase of critical infrastructure design with real-time monitoring and response during its operational phase can significantly improve infrastructure resilience and sustainability.

During the scenario-driven design phase, predictive air quality modelling is used to simulate various scenarios which the infrastructure might encounter throughout its life (see Figure 2). This includes considering the dispersion of pollutants, variations in air pressure, temperature, and humidity (see Brassler (2017c), Brassler (2017d)). These simulations are essential for optimising the layout, materials, and systems of the infrastructure to various air quality scenarios. Smart air quality reporting tools, which incorporate AI-powered analytics, play a pivotal role here by providing detailed calculations, analyses, and targeted recommendations for various threat scenarios. For example, these tools can guide the optimal placement of indoor air quality sensors and filters, ensuring maximum detection coverage and filtration efficiency. Furthermore, they advise on the appropriate efficiency needed for air filters and provide insights into HVAC system design, to ensure harmony with the air purification strategy.

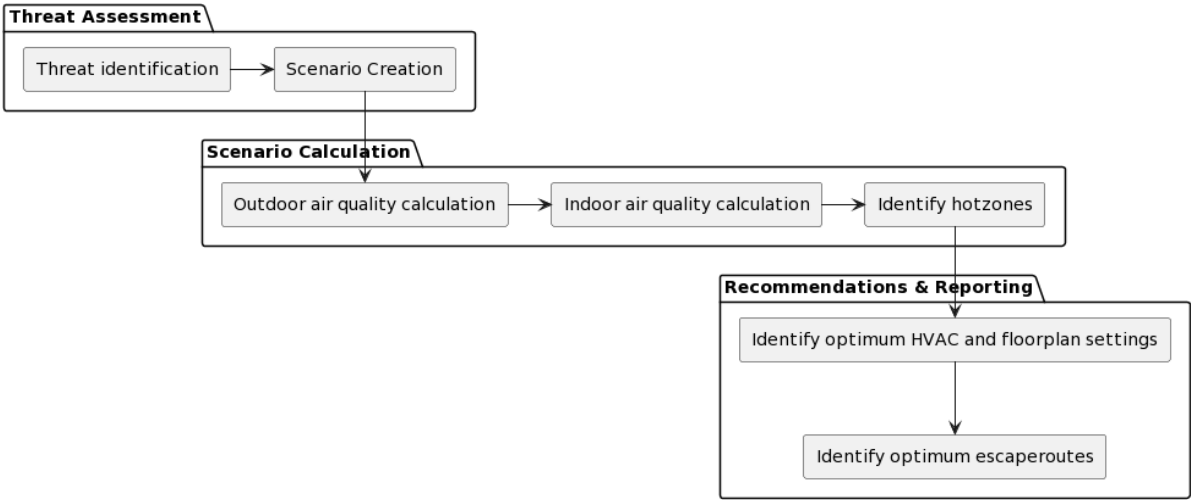


Figure 2: Flow of a scenario-driven design process

Similarly, during the operational phase, real-time air quality monitoring becomes crucial (see Figure 3). Here, smart air quality systems equipped with sensors continuously track air quality parameters, such as particulate matter, volatile organic compounds, and other pollutants. The HVAC tool analyses the data and predicts trends in air quality, enabling operators to receive alerts when air quality levels cross predefined thresholds. It can also identify potential contaminated areas or hot zones and localise potential sources of contamination (see Brassler (2017e)). It, too, relies on AI-powered analytics, which leverage data from various internal and external sources to provide actionable insights.

In both phases, the challenges often arise from poor ventilation leading to an accumulation of indoor pollutants, the lack of data-driven support for the placement of sensors, and the absence of standard operating procedures for emergency response. Additionally, ensuring compliance with air quality regulations and standards is a concern common to both phases. In the scenario-driven design phase, adherence to regulations is achieved by incorporating predictions into the design process. In contrast, in the operational phase, compliance is ensured by real-time monitoring and dynamic adjustments to ventilation and filtration systems based on the data received.

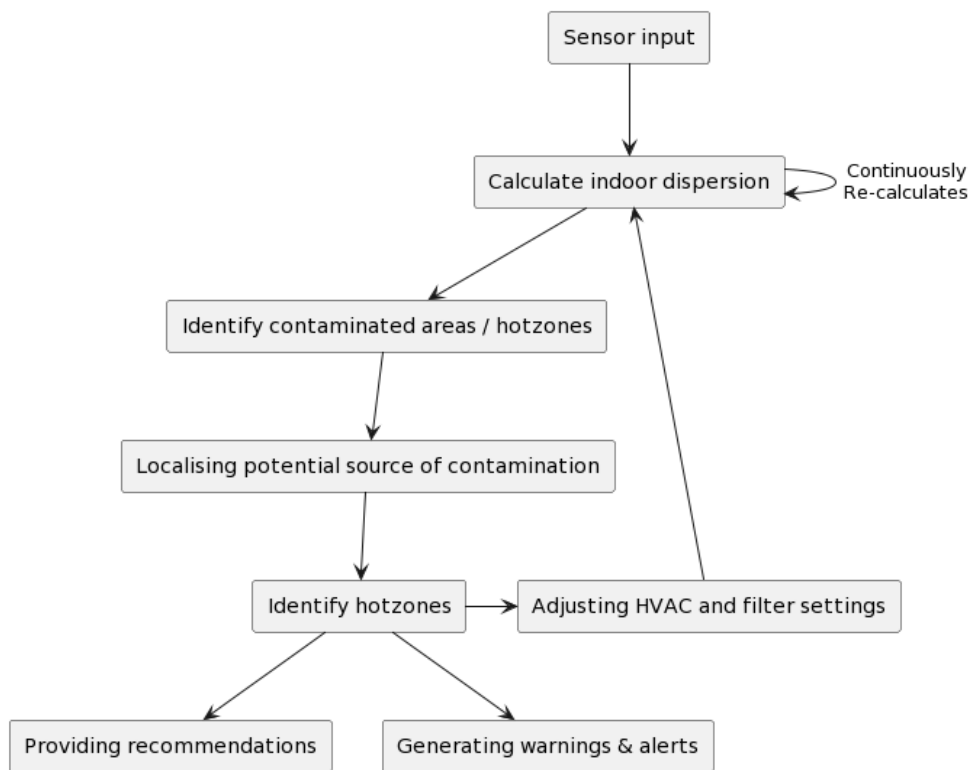


Figure 3: Real-time monitoring flow

A comprehensive solution to address these challenges in both phases involves integrating real-time air quality monitoring with data-driven insights, predictive modelling, and automation. This integrated approach offers facility managers an all-encompassing air quality management solution, empowering them to make rapid and informed adjustments in response to incidents or changes in air quality.

Additionally, situational awareness is critical in both phases. During the design phase, knowing potential threats and how they can impact the infrastructure is necessary for building

a resilient system. In the operational phase, continuous awareness of the indoor air quality conditions is vital for timely interventions (see Figure 4). In both cases, the integration of advanced technologies, including AI and analytics with air quality systems, is key to providing a robust and efficient air quality management solution.

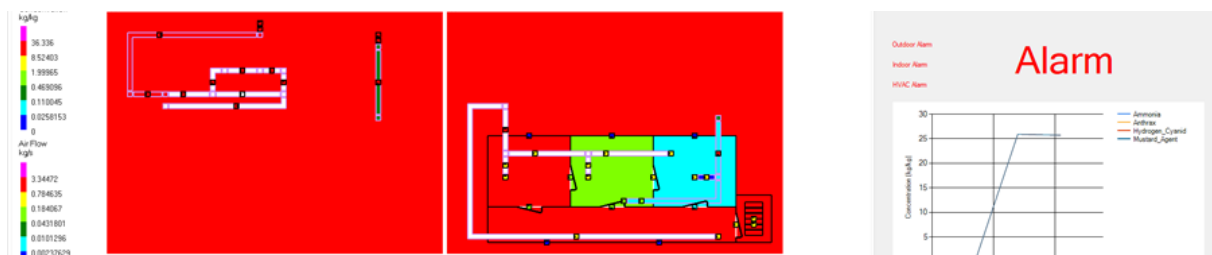


Figure 4: Example of agent concentrations in several rooms and floor levels in the floor plan of a building

In summary, by aligning the scenario-driven design process with real-time monitoring and response systems, critical infrastructure can be designed and operated with optimal efficiency and resilience to air quality challenges. This involves utilising predictive modelling in the design phase to anticipate and plan for various air quality scenarios, and implementing intelligent air quality monitoring systems during operation to ensure timely responses to changing conditions. Both phases necessitate the use of AI-powered analytics and integration with building management systems for a holistic and effective approach to air quality management.

4 CONCLUSION

A software suite was developed, which can be used to calculate the indoor airflow, dispersion of agents and toxicological effects. The tool predicts airflow by considering elements such as windows, doors, and the HVAC system. The tool quantifies the concentration of agents in each room over time and facilitates seamless incorporation of building structures, including rooms, corridors, and openings across various floor levels, effectively creating a digital twin for airflow analysis. Toxicological effects of existing contaminants are predicted.

Furthermore, escape routes can be generated in case of an incident, taking into account which rooms are least contaminated. It contains a decision support tool which is designed to provide a multifaceted simulation and analysis of air dynamics within buildings.

There are two major applications of the software suite: in the design phase of a building and during the operational phase of critical infrastructure. In the design phase of a building the smart air quality reporting tool generates detailed analyses and a plethora of recommendations, and serves as an invaluable resource for stakeholders in the design of critical infrastructure. During the operational phase of critical infrastructure, the primary value of the tool is to protect the health and well-being of occupants of the critical infrastructure, as autonomous response can save time (and therefore lives) in case of an emergency and help contain the possible threat.

All in all, this suite provides the necessary tools to safeguard the air quality within critical infrastructure, and therefore the health of its occupants.

5 REFERENCES

- Stuart Dols (2015), W. Stuart Dols and Brian J. Polidoro , *CONTAM User Guide and Program Documentation Version 3.2*, NIST Technical Note 1887 , National Institute of Standards and Technology, USA.
- Feustel Helmut (2005), E. Feustel and Brian V. Smith (Editors), (2005) *COMIS 3.2 - User Guide*, EMPA
- Brasser (2017a), Paul Brasser, Responsive Indoor Air Quality (RIAQ), *User Guide*, Deliverable 24 ,A-1152-RT-GP – JIP CBRN Call 2
- Brasser (2017b), Paul Brasser, Responsive Indoor Air Quality (RIAQ), *Scientific manual of the RIAQ software program*, Deliverable 25 , A-1152-RT-GP – JIP CBRN Call 2
- NRC (2001) National Research Council (US) Subcommittee on Acute Exposure Guideline Levels. *Standing Operating Procedures for Developing Acute Exposure Guideline Levels for Hazardous Chemicals*. Washington (DC): National Academies Press (US); 2001. <https://www.ncbi.nlm.nih.gov/books/NBK223427/> .
- AIHA (2023), *ERPGs Emergency Response Planning Guidelines* <https://www.aiha.org/get-involved/aiha-guideline-foundation/erpgs>.
- DOE (2008) Department of energy (US), *Temporary emergency exposure limits for chemicals: methods and practice*, doe-hdbk-1046-2008 , <https://www.standards.doe.gov/standards-documents/1000/1046-Bhdbk-2016/@/@images/file>.
- NATO (2003), *Assessment of effect levels of classical chemical warfare agents applied to the skin to be used in the design of protective equipment*, AEP-52, NATO.
- OEE HSS (2016), Office of Environment, Health, Safety & Security, *Protective Action Criteria (PAC) with AEGLs, ERPGs, & TEELs, PAC Database*, <https://pacteels.pnnl.gov/#/definitions>, <https://pacteels.pnnl.gov/#/>.
- Brasser (2017c), Paul Brasser, Responsive Indoor Air Quality (RIAQ), *Case description including Virtual Building* , Deliverable 16, A-1152-RT-GP – JIP CBRN Call 2
- Brasser (2017d), Paul Brasser, Responsive Indoor Air Quality (RIAQ), *Final report describing scenarios and effect of RIAQ system*, Deliverable 31, A-1152-RT-GP – JIP CBRN Call 2
- Brasser (2017e), Paul Brasser, Responsive Indoor Air Quality (RIAQ), *Hotspot Locations*, Deliverable 26, A-1152-RT-GP – JIP CBRN Call 2

Energy Implications of Increased Ventilation in Commercial Buildings to Mitigate Airborne Pathogen Transmission

Sean M. O'Brien^{*1}, David Artigas¹, Ece Alan¹

*1 Simpson Gumpertz & Heger Inc.
525 Seventh Avenue, 22nd Floor
New York, NY, USA*

**Corresponding author: smobrien@sgh.com*

ABSTRACT

One proposed mitigation to reduce transmission of the SARS-CoV-2 virus and other airborne pathogens is to increase ventilation in buildings. This measure can be difficult to implement in existing buildings and has the potential environmental costs of increased energy consumption to condition the additional airflow, as well as other potential costs such as the disposal of existing serviceable mechanical equipment and the manufacture and delivery of new equipment. This paper focuses on the increased energy consumption caused by increased ventilation rates in commercial buildings to mitigate airborne pathogen transmission. We used energy modelling software to compare energy use in different typical commercial buildings in different climates at current standard ventilation rates to the energy use in the same buildings with increased ventilation rates and filtration. Our analysis shows that increased filtration has little effect on energy used for air conditioning, but that increased ventilation has a significant effect.

KEYWORDS

Ventilation, airborne pathogens, SARS-CoV-2, COVID, energy

1 INTRODUCTION

During the recent SAR-CoV-2 (COVID) pandemic, public health officials and government agencies advocated, and in some cases distributed funds, for increased mechanical ventilation and air filtration rates as a preventive measure to mitigate the spread of the virus in interior spaces. Some have gone farther, recommending that increased ventilation rates be implemented at all times to promote general health, not just as a temporary pandemic mitigation measure. Although well-intentioned and seemingly pragmatic, the assumed benefits of increased ventilation and filtration must be verified and weighed against the potential increased energy consumption and resultant carbon emissions to move, condition, and filter the air.

1.1 Literature Review

The United States Centers for Disease Control and Prevention (CDC) provides the following recommendations for ventilation to mitigate airborne pathogen spread:¹

- Five air changes per hour (ACH) in occupied spaces (lower ACH could be used in large spaces with few occupants).
- Minimum Efficiency Reporting Value (MERV) 13 air filtration or greater.

- In non-residential settings *without* a known infectious source, operate the mechanical system at maximum outside airflow for 2 hours, or until the building has achieved at least 3 air changes, after the building no longer is occupied (i.e., “flushing” the building’s air).
- The CDC provides calculations that can be followed for the required ventilation to flush a building after a known infectious source was present.

The American Society of Heating, Refrigerating and Air-Conditioning Engineers (ASHRAE) states that policy makers should consider two states of building operation: a normal state (generally how buildings operated pre-pandemic), and an epidemic state during which higher levels of risk exist. Unlike many public health advocates, ASHRAE states that normal building operations result in low level of risk of airborne pathogen transmission due to public health measures implemented over time into Building Code and industry standard requirements. ASHRAE goes further, stating that operating in a pandemic state at all times will waste resources and that policy members should use caution when enacting policies that could force building managers to implement mechanical interventions for airborne pathogen transmission when less costly measures may be available. ASHRAE acknowledges a lack of empirical studies to establish the necessary ventilation rates to mitigate airborne pathogen spread, but still strongly recommends that increased ventilation be implemented as a pandemic mitigation measure when that risk is present.²

ASHRAE’s Epidemic Task Force Building Readiness Guide provides several recommendations for modifications to existing mechanical systems to reduce the potential for airborne pathogen transmission, which includes increased ventilation. However, ASHRAE also notes that doing so may make it difficult to maintain indoor setpoints in some climates and that it will increase the required chilled water (for cooling) and the pressure drop across the cooling coil, and that the demand on the cooling plant and could affect building or space pressurization. ASHRAE also notes that particles (including airborne viruses) do not behave as gases and should not be assumed to be evenly distributed in a space. ASHRAE recommends that airborne pathogen mitigation measures for building mechanical systems be limited to the pandemic period.³

Allen and Ibrahim cite observational studies that show lower ventilation rates correlate to increased viral transmission for several viruses and recommend minimum 4 to 6 ACH in most indoor applications with MERV 13 or greater filtration, but to increase the ACH in denser occupancy applications. These authors state that increased ACH would be of more benefit to reduce airborne viral transmission over greater distances than close contact. They also recommend making these modifications to mechanical system operation permanent to improve health overall.⁴ Chen et al cite research by others stating that aerosols remain suspended in air ten times longer in poorly ventilated spaces and recommend increasing ventilation and filtration to mitigate airborne viral transmission.⁵

Rothamer et al used a combination of mathematical models and a mock-up of a classroom setting using mannequins with “breathing” apparatuses for one hour with different rates of aerosol concentration and ventilation to estimate airborne pathogen spread. They found that increasing ventilation has diminishing returns: increasing ACH from 1.38 to 5.05 only reduced the potential for infection spread by a factor of 2, and further increasing the ACH to 10 further reduced the potential for infection spread only by a factor of 1.71 (i.e., diminishing returns).⁶

Pantelic and Tham used mathematical models to calculate the efficacy of ventilation to mitigate airborne pathogen spread. They found that for pathogens with lower infectiousness increased ventilation made little difference (due to the lower probability of infection spread), but that increasing ventilation did reduce, but not eliminate, the potential for infection spread for pathogens of higher infectiousness. However, they also found that the effect of increased ventilation decreased over time, such that within a few weeks increased ventilation had little effect on infection spread. This study shows that increased ventilation as a means to limit viral transmission mainly works for short-term exposure over shorter overall time periods.⁷

Citing research by others, Burkett notes that calculations of the time required to flush a building or space often assume perfect mixing of the air and that they underestimate the actual time required to flush a building or space. He also notes that the location of the exhaust vents relative to the infection source plays a significant role in the ability of ventilation to mitigate airborne pathogen spread, and that if the exhaust vent is not directly over the infection source increasing ventilation can have little effect (again, citing research by others). Burkett cites other research showing that increasing ventilation has little effect on the decay time for airborne pathogens when the mechanical system includes filtration of MERV 13 or better.⁸

2 EVALUATION OF ENERGY IMPLICATIONS OF INCREASED FILTRATION AND VENTILATION

We performed a series of energy models using the eQuest version 3.65 software developed by the United States Department of Energy (DOE) to evaluate the building-wide energy impact of both increased filtration and increased ventilation. We analysed a theoretical 2-story office building (2,320 m²) and a 22-story (25,520 m²) office building in both New York, NY and Miami, FL – predominantly heating and cooling climates, respectively. We based the building enclosure and mechanical system performance on the prescriptive requirements of the 2021 International Energy Conservation Code (IECC) for each climate zones, including requirements for minimum mechanical equipment efficiency and energy recovery systems for ventilation.⁹ We based internal loads and occupancy data on guidance from the 2021 ASHRAE *Handbook of Fundamentals*.¹⁰ For the New York building, we assumed gas-fired hot water coils for heating and direct expansion cooling. For Miami, we assumed direct expansion systems for both heating and cooling. In both cases, based on the parameters of the buildings we modelled, the energy code does not require the inclusion of energy recovery on the ventilation/exhaust systems, although we did model an air-side economizer in all cases. The intent of these models was not to predict actual energy use for a specific building, but rather to establish a reasonable baseline of performance that could be used for evaluating relative changes between the various models.

The first evaluation that we performed was of the impact of increased filtration for various ventilation rates on energy use. This was a relatively high-level assessment due to the lack of detailed data on the relationship between fan power and filtration quality (other than the two being directly proportional). We used data from the United States Leadership in Energy and Environmental Design (LEED) 4.1 Minimum Energy Performance Calculator on the impact of filtration on fan power for MERV 9-12 and MERV 13-15. This analysis is limited, but conveniently in the same ranges as typical buildings and those which utilize CDC recommendations for filtration to limit pathogen spread. For reference, MERV ratings describe the effectiveness of a filter at removing particulates in a certain size range. At the low end of the range we evaluated, a MERV 9 filter is >35% effective at filtering particles in the 1.0-3.0 µm range and >75% for 3.0-10.0 µm particles. A MERV 15 filter is >90% for the 1.0-3.0 µm range, >95% for 3.0-10.0 µm, and adds a level of >85% for 0.3-1.0 µm. Although

beyond the scope of this paper, it is interesting to note (and presents opportunities for further research) that the typical COVID virus particles are approximately 0.07-0.09 μm in size – smaller than any of the listed sizes in MERV filters and even smaller than most high efficiency particulate air (HEPA) filters are rated for (0.3 μm range).¹¹ While viral particles suspended in respiratory droplets are typically large enough to be caught by a moderately high-MERV filter, those droplets are also more likely to end up deposited on surfaces within the occupied space than to reach the filter via the return airstream. This demonstrates that there are many other factors beyond filtration that impact distribution of viruses or other contaminants.

Table 1 shows the impact only of adding filtration to the air distribution system of a building. The base case (no filter), while not practical, is presented to demonstrate the added fan power needed to push air through a filter within the system. We compare both system fan power (kW) and overall building source energy use intensity (EUI; kWh/m²yr). We performed this analysis only for the New York building case as fan power is relatively independent of heating type and climate.

Table 1: Filtration Impact on Fan Power and Building EUI

Filtration Level	System Fan Power (kW)	Increase over Baseline	Building Source EUI	Increase over Baseline
None	3.1	-	174	-
MERV 9-12	5.3	71.0%	180	4.0%
MERV 13-15	5.8	87.1%	182	4.7%

Since the primary goal of our analysis was to determine the impact of increased ventilation and filtration on overall building energy use, based on this initial study (which shows a negligible difference in source EUI for the two levels studied) we evaluated the remaining cases assuming MERV 13-15 (based on CDC guidelines) rather than modelling dozens of additional combinations of ventilation and filtration type. Table 2 shows the impact of increasing ventilation by various amounts over the typical code-minimum value (from the 2021 IECC).⁹ Since ventilation is typically a major contributor to building energy, we only analysed cases up to double the code-minimum value (4.72 L/s/person vs. 2.38 L/s/person).

Table 2: Increased Ventilation Impact on Building EUI (MERV 13-15 only)

	Low Rise - New York	Source EUI	Increase over Baseline
Fresh Air - L/s/person	2.38 (Baseline-IECC)	181.7	-
	2.83 (20% increase)	183.3	0.87%
	3.54 (50% increase)	185.5	2.08%
	4.72 (100% increase)	190.2	4.69%
High Rise - New York			
Fresh Air - L/s/person	2.38 (Baseline-IECC)	178.2	-
	2.83 (20% increase)	179.8	0.88%
	3.54 (50% increase)	182.7	2.48%
	4.72 (100% increase)	186.8	4.78%
Low Rise - Miami			
Fresh Air - L/s/person	2.38 (Baseline-IECC)	235.7	-
	2.83 (20% increase)	239.1	1.47%
	3.54 (50% increase)	243.9	3.48%
	4.72 (100% increase)	251.7	6.83%
High Rise - Miami			
Fresh Air - L/s/person	2.38 (Baseline-IECC)	225.9	-
	2.83 (20% increase)	229.0	1.40%
	3.54 (50% increase)	233.8	3.49%
	4.72 (100% increase)	241.0	6.70%

In addition to overall building energy use we also looked at the impact of increased ventilation on annual heating and cooling energy (kWh). It is worth noting that the zero heating energy in the Miami likely is not realistic, and more likely is due to our using an idealized model for these comparisons. However, as noted above the idealized model is useful for calculating differences between cases as opposed to absolute values which fits well with the intent of our study.

Table 3: Increased Ventilation Impact on Annual Heating and Cooling Energy

	Low Rise - New York	Heating Energy	Increase	Cooling Energy	Increase over Baseline
Fresh Air - L/s/person	2.38 (Baseline-IECC)	48.5	-	32.2	-
	2.83 (20% increase)	50.0	3.14%	32.8	1.82%
	3.54 (50% increase)	52.8	8.76%	33.7	4.64%
	4.72 (100% increase)	58.4	20.36%	35.3	9.64%
High Rise - New York					
Fresh Air - L/s/person	2.38 (Baseline-IECC)	305.7	-	379.5	-
	2.83 (20% increase)	327.9	7.29%	385.7	1.62%
	3.54 (50% increase)	362.8	18.70%	395.9	4.32%
	4.72 (100% increase)	426.7	39.60%	411.8	8.49%
Low Rise - Miami					
Fresh Air - L/s/person	2.38 (Baseline-IECC)	0	-	84.1	-
	2.83 (20% increase)	0	-	86.6	3.03%
	3.54 (50% increase)	0	-	90.4	7.49%
	4.72 (100% increase)	0	-	96.3	14.53%
High Rise - Miami					
Fresh Air - L/s/person	2.38 (Baseline-IECC)	0	-	853.4	-
	2.83 (20% increase)	0	-	880.4	3.16%
	3.54 (50% increase)	0	-	919.7	7.76%
	4.72 (100% increase)	0	-	982.1	15.08%

The data above represented cases of high-percentage but low-magnitude increases in ventilation rate on a L/s/person basis. To evaluate how these adjustments compare to more recent guidance regarding ventilation as a way to mitigate viral transmission, we ran an additional set of energy models using the CDC-recommended ventilation rate of 5 ACH for the New York low-rise building example (note that the IECC minimum of 2.38 L/s/person results in only 0.3 ACH for this case). For this building, 5 ACH results in a ventilation rate of 39.3 L/s/person – over 15 times higher than the IECC minimum requirement. Although the IECC requires energy recovery for this magnitude of ventilation, we did not include that feature in the models since our goal was to evaluate changes in existing buildings to accommodate higher ventilation rates (i.e., those buildings would not have been designed with energy recovery ventilation and are unlikely to add those systems to compensate for a temporary increase in ventilation rate). We summarize these results in Table 4.

Table 4: EUI and Space Conditioning Loads for 5 ACH vs. IECC Minimum Ventilation

New York Low Rise	Source EUI	Heating Energy	Cooling Energy (kWh)
Baseline IECC Ventilation	181.7	48.5	32.2
CDC Recommended 5 ACH	634.4	507.6	146.9
% Increase	249%	947%	356%

These increased in both source EUI and heating/cooling energy are commensurate with the 15x increase in ventilation, and as we will discuss below, make such an increase financially unfeasible at least and fully impossible at most.

3 DISCUSSION

3.1 General

One point that must be considered in evaluating increased ventilation as a way to reduce airborne pathogen spread is that most of the data supporting increased ventilation as reducing airborne pathogen spread is from observational studies, which can have confounding variables that the studies do not address but can affect the studies' results significantly. Also, people do not behave as mannequins with breathing apparatuses (stationary with a constant breathing rate), and it is likely that the infectious load varies with each breath, rather than a constant rate of "viral shedding" with each breath. People also do not behave uniformly nor predictably, as most mathematical models of airborne pathogen spread assume to simplify the calculations. Some studies (though limited) have shown that the positive effect of increased ventilation is short-lived with highly infectious pathogens, so it is possible that increased ventilation merely delays infection, rather than prevent it. That said, when in an emergency/pandemic state with little reliable data on a new pathogen, increasing ventilation to slow the spread of infection does make intuitive sense and likely is of some short-term benefit.

Both system heating and cooling capacity must be considered when adding ventilation. Although older buildings may have more "excess capacity" that can be utilized for ventilation, buildings designed more recently to stricter energy codes and using more accurate heating/cooling load calculations are less able to accommodate added service loads. While energy use is a major concern, occupant comfort cannot be discounted when increasing ventilation. There is a practical limit to how much ventilation can be added before the HVAC systems become ineffective at controlling interior conditions. Adding too much ventilation will reduce the ability of the system to control interior temperature and relative humidity (RH). While temporary discomfort for occupants may be an acceptable trade-off to reduced viral transmission risk, high interior RH (especially in more humid climates) can lead to "less acceptable" problems such as condensation, interior finish damage, and microbial growth on susceptible surfaces.

An additional aspect of ventilation that unfortunately often is ignored when adjusting ventilation rates is the importance of balance in the system. Forcing too much outside air into a zone without balancing it with exhaust or return air can create significant pressure imbalances between spaces within a building. Take the example of a school building with multiple occupied classrooms. The intent of increased ventilation in the classrooms is to dilute contaminants within the occupied spaces. However, over-ventilating individual classrooms without providing sufficient return/exhaust air will create positive pressure in those spaces, forcing excess (and potentially contaminated) air into adjacent spaces, corridors, etc., and defeating the purpose of adding ventilation in the first place – to reduce viral transmission. Similarly, arbitrarily adding more stringent filters to HVAC units without evaluating if the systems are designed to handle them can result in reduced airflow and increased load on fans. Mismatching filters and equipment can thus result in decreased ventilation and equipment life. Lastly, before making any adjustments to ventilation or airflow in a system, it is critical to evaluate the design and layout of those systems. For example, most large commercial airliners will have multiple independent ventilation zones with separate supply and return systems. This is in recognition of the risk of disease transmission in spaces with very high occupant densities. Thus, the risk of a first-class passenger infecting someone in the rear of the aircraft is very low. Buildings, conversely, often have highly centralized systems for air (including ventilation air) distribution. Moving more air through those systems may have little positive benefit, and may in fact simply allow

for greater air exchange (and viral transmission) between building areas. These examples highlight the danger of implementing changes to building systems which can, despite their apparent simplicity, result in a variety of unforeseen and potentially negative consequences.

3.2 Model Results

Our initial review of the energy model results showed that there is a significant difference in fan power requirements for the filtered vs. unfiltered (which is not realistic, but modelled for comparison) systems, a 71% increase in fan power and 4% increase in EUI. However, the increase to MERV 13-15 from MERV 9-12 only results in an additional 0.7% on EUI. At these levels, the added energy use is easily justified if there is demonstrable reduction in virus transmission but is also high enough so that some owners, whether for the sake of reduced utility bills or simple conservation of energy, will more carefully evaluate the potential benefits before implementing changes.

Our models show that moderately increasing ventilation has a modest impact on the energy used to operate the mechanical system in cold and hot climates, with the biggest increases for heating energy in the New York case. For the low-rise case, doubling the amount of ventilation relative to IECC minimums results in an approximately 20% increase in annual heating energy and a still-significant 10% increase in annual cooling energy. Looking at the Miami cases, heating energy is a non-issue but cooling energy increases by 15% when doubling ventilation rates. While these percentages are relatively high, a more useful metric is the building Energy Use Intensity – a measure of total energy consumed by the building normalized to building area. We use source EUI for this comparison, which includes the energy impacts of harvesting and generation/transmission. For the New York cases both building types see a 5% increase in source EUI, with a 7% increase for the Miami cases. Some of that added 2% is likely due to the energy type used, since the total energy used in Miami is all-electric, which is typically has a higher site-to-source conversion. These values demonstrate the potentially high operating cost increase associated with added ventilation, as well as the importance of carefully evaluating the benefits of this strategy for a specific building before implementing it.

Lastly, our evaluation of the CDC-recommended ventilation rate of 5 ACH for the New York City, low-rise building case shows that this approach is completely unfeasible from an energy use standpoint, with a 249% increase in source EUI. In addition, the resulting increases in heating and cooling energy (947% and 356%, respectively) mean that, barring a substantial upgrade to mechanical system capacity, the existing building systems would not be able to handle the added loads. This is in contrast to the more moderate increase in ventilation, where the 10-20% increase in heating and cooling energy likely could be accommodated by the existing systems due to excess capacity or operate at modified interior set points on a temporary basis, likely an acceptable compromise if the resulting increased ventilation has some short-term benefit to reducing viral transmission. Even if these systems were operated with the addition of energy recovery, at 5 ACH the magnitude of ventilation air required would still result in order-of-magnitude increases in both EUI and heating/cooling loads (regardless of building type or climate).

4 CONCLUSIONS

Our review of available literature indicates that there is some potential short-term benefit to viral transmission (i.e., reduced infection rates) associated with increased ventilation. The benefit may be more pronounced for highly infectious diseases such as COVID. The energy

analyses we performed show that there are relatively substantial increases in annual energy use and heating/cooling energy associated with increases in ventilation that are likely within the airflow and heating/cooling capacity of existing building equipment (up to double the IECC-minimum rates). For a 6-month to 1-year adjustment this energy use is likely feasible, but for longer-term implementation there will be significant increases in operating costs at a likely diminishing return on reduced viral transmission (not to mention the associated carbon emissions). In the case of the CDC-recommended ventilation rate, it would be completely impractical (if not impossible) to modify existing building systems to accommodate such a massive increase in ventilation rate. Without any long-term studies of effectiveness, there is no justification for this level of modification.

When adjusting ventilation rates, it is important to look not only at increased energy use but also internal airflow paths and balance between interior spaces. For example, if the full 5 ACH ventilation rate were possible with existing equipment, that level of airflow without sufficient exhaust would create significant interior building pressures and likely imbalanced between interior spaces. Building dynamics are relatively complex and making changes to one system can have far-reaching consequences in other. In addition, what works well in one building could be ineffective or even detrimental in another depending on the layout of the space and the zoning of the mechanical systems. While well-intentioned, much of the current guidance on increasing ventilation in buildings focuses solely on effectiveness in reducing viral transmission (often in the short-term) and assumes perfect mixing of air and pathogens, and focuses less on the practical implications and limitations of making those changes. Both must be considered, especially when evaluating these changes over the long-term.

5 REFERENCES

1. Centers for Disease Control and Prevention (2023). Ventilation in Buildings, updated May 12, 2023. <http://www.cdc.gov/coronavirus/2019-ncov/community/ventilation.html> (accessed on 21 June 2023).
2. American Society of Heating, Refrigerating and Air-Conditioning Engineers (ASHRAE, 2022). ASHRAE Positions on Infectious Aerosols, 13 October 2023. [http://www.ashrae.org/file library/about/position documents/pd_-infectious-aerosols-2022.pdf](http://www.ashrae.org/file%20library/about/position%20documents/pd_-_infectious-aerosols-2022.pdf) (accessed on 21 June 2023).
3. ASHRAE (2022). ASHRAE Epidemic Task Force Building Readiness Guide, updated 5-17-22. [http://www.ashrae.org/file library/technical resources/covid-19/ashrae-building-readiness.pdf](http://www.ashrae.org/file%20library/technical%20resources/covid-19/ashrae-building-readiness.pdf) (accessed 13 June 2023).
4. Allen, J. G. and A. M. Ibrahim (2021). Indoor Air Changes and Potential Implications for SARS-CoV-2 Transmission, *Journal of the American Medical Association*, 325(20), 2112-2113.
5. Chen, C., P. Chen, J. Chen, & T. Su (2021). Recommendations for ventilation of indoor spaces to reduce COVID-19 transmission,” *Journal of the Formosan Medical Association* 120, 2055-2060.
6. Rothamer, D., S. Sanders, D. Reindl, and T. Bertram (2021). Minimizing COVID-19 Transmission in High Occupant Density Settings, Part 2, *ASHRAE Journal*, 63(6), 12-20.
7. Pantelic, J. & K. W. Tham (2012). Assessment of the Mixing Air Delivery System Ability to Protect Occupants from the Airborne Infectious Disease Transmission Using Wells–Riley Approach, *HVAC&R Research*, 18(4), 562-574.
8. Burkett, J. (2021). Virus Transmission Modes and Mitigation Strategies, Part 3: Ventilation, Filtration, and UVGI, *ASHRAE Journal*, 63(8), 18-25.
9. International Code Council (2021). *International Energy Conservation Code, USA*: International Code Council.

10. ASHRAE (2021). *Handbook of Fundamentals*, Peachtree Corners: ASHRAE.
11. Lee, B. L. (2020). Minimum Sizes of Respiratory Particles Carrying SARS-CoV-2 and the Possibility of Aerosol Generation, *International Journal of Environmental Research and Public Health*, 17(19), 2-8.

Reflections on alternative modelling approaches regarding occupants' window operation behaviour

Christiane Berger^{*1} and Ardeshir Mahdavi²

*1 Department of Architecture, Design and Media
Technology, Aalborg University, Aalborg, Denmark
chbe@create.aau.dk

*2 Institute of Building Physics, Services, and
Construction, Faculty of Civil Engineering Sciences
Graz University of Technology, Graz, Austria.*

ABSTRACT

Computational predictions of buildings' indoor-environmental conditions and energy performance would presumably benefit from the inclusion of models that could reliably capture occupants' window operation behaviour. Frequently, models derived from empirical data have a black-box character. However, the utility of window operation models could be conceivably improved, if the model derivation process is preceded by specific hypotheses regarding the variables that are assumed to influence the frequency and timing of window operation actions. In the present contribution, we discuss the process of exploring explicit hypotheses regarding factors that could influence occupants' operation of windows prior to the model derivation step. To illustrate the potential of this approach, we utilize a specific window operation data set from an open plan office. This data set was used to test three distinct hypotheses regarding the factors that influence occupants' window operation actions upon arrival. The results suggest that the most plausible conjecture from the intuitive point of view is not supported by the data set. This observation encourages more in-depth reflections on the motivational background of occupants' behaviour. Purely data-driven black-box models arguably do not provide a similarly strong impetus toward an explicit understanding of occupants' behaviour patterns in buildings.

KEYWORDS

Natural ventilation, window operation, occupant behaviour, computational models

1 INTRODUCTION

Natural ventilation in general and manual operation of windows in particular represent the oldest and most primary means of modulating the rate of air change in buildings and hence influencing both indoor air quality and thermal conditions (Etheridge 2011). Besides indoor-environmental conditions, operation of windows can also influence buildings' energy use. Hence, computational predictions of buildings' indoor-environmental conditions and energy performance would presumably benefit from the inclusion of models that would capture occupants' window operation behaviour. These models may range from simple schedules to sophisticated probabilistic routines (Mahdavi et al. 2016, Tahmasebi and Mahdavi 2019, 2016). Either way, development and validation of window operation models must be ultimately based on observational data.

Frequently, models derived from empirical data are of a black-box type: Observed behaviour is statistically correlated with values of variables pertaining to, for instance, thermal conditions inside and outside buildings (D'Oca and Hong 2014). It is not suggested here that black-box models would be either deficient or ineffective. Depending on the application scenario, such models may be very useful. However, the utility and scalability of window operation models could be arguably improved if, at the outset of the model derivation process, specific hypotheses are stated regarding the variables that are assumed to influence the frequency and timing of

window operation actions, particularly when such hypotheses include transparent formulation of the reasoning (and respective narratives) regarding the mapping from independent to dependent variables. Instead of recurrent tweaking of coefficients of black-box models to fit ever new sets of data coming from different buildings, explicit hypotheses and their testing could help to: *i*) identify those independent variables that are more likely to constrain occupant behaviour, *ii*) shed light on the potential causal mechanisms involved, and *iii*) augment the scalability of local window operation models toward more generally applicable computational routines.

In the present contribution, we reflect on the process of formulating and testing explicit hypotheses regarding factors that could influence occupants' operation of windows. To illustrate the potential of this approach, we utilize a specific window operation data set from an open plan office (in a university building in Vienna, Austria). This year-long data set includes time series information on indoor and outdoor temperatures, occupants' presence, and their window operation actions (for the present study we focused on the warmer months of the year, i.e., from May to September). At the outset, examples of general hypotheses are formulated. These are basically conjectures about what factors (i.e., independent variables or predictors pertaining to indoor and outdoor conditions) could influence the dependent variables (i.e., the probability of window opening actions upon occupants' arrival in the office) and what reasoning or narrative is behind these conjectures. This approach is suggested to support the derivation of transparent and scalable window operation models that can be integrated in computational tools for the prediction of buildings' energy and indoor-environmental performance.

2 METHODOLOGY

As outlined in the introduction, the purpose of the present paper is to explore the process of testing explicitly formulated hypotheses regarding predictors of occupants' window operation against collected data. It is of course possible to confront an observational data set with a set of variables to see if patterns of influence on specific behavioural manifestations (window opening actions in the present case) can be extracted. However, in the absence of explanatory (e.g., causal) stories behind the pattern, the applicability of such a model to other settings (and respective data sets) remains questionable. It thus seems useful if the model development process would start with transparent hypotheses as to what influence mechanisms are postulated and why. To illustrate this possibility, we consider here, as a case in point, the occupant-driven window operation in an office building. Note that the purpose here is not to document a comprehensive instance of a related model development exercise. The illustrative case study involves neither a comprehensive and representative repository of monitored data, nor shall we conduct a detailed statistical analysis to develop or validate a full-fledged window operation model. Rather, the idea is to use a limited data set and simple descriptive statistics to conceptually illustrate the advantages of the proposed approach.

Predicting the timing and frequency of occupants' operation of windows is by all accounts a challenging endeavour, given the extensive set of circumstances that may trigger window operation actions. This set includes, amongst other factors, thermal, air quality, and acoustic conditions inside and outside buildings as well as factors related to individual occupants (activity, clothing, age, sex, health, preferences, habits, cognitive load). Moreover, occupants' position (for instance, in office buildings, the distance of the occupants' workstations from the window units), the quality of window opening interface (ease of opening, potential interference with shading operation, etc.) as well as social settings (e.g., hierarchical relationships amongst occupants in an open plan office) may play a role.

Given the illustrative nature of the present treatment, we focus here on a few factors only, consider a limited data set, and perform a rather simple descriptive statistical analysis. As dependent variable, we focus on the probability of window operation actions upon occupants'

arrival in the office. Hence, intermediate window operations are not considered. As to potential influencing factors, we consider only indoor temperature, outdoor temperature, and the so-called comfort temperature (i.e., the ambient air temperature assumed to be preferred by the occupants). Hence, individual occupants' characteristics are not taken into account, nor are workstation configurations and social settings.

Given these choices, we proceed to formulate a number of general (rather qualitative) hypothesis regarding the candidate independent variables and how they influence the dependent variable (window opening probability upon arrival in the office). Note that these hypotheses are in part contradictory, as at this stage (prior to being examined against observation), they entail only conjecture-type narratives as follows:

- H_i* The probability of opening a window upon arrival in the office is higher, if the temperature in the office deviates from the comfort temperature. In other words, the larger the perceived discrepancy between the comfort temperature and indoor temperature upon arrival, the higher the probability that occupants would open the windows to change indoor thermal patterns.
- H_{ii}* The probability of window opening upon arrival can be influenced by the thermally relevant cooling potential of the outdoor air. In other words, insufficient indoor-outdoor air temperature differences can reduce the thermal (cooling) potential of window opening and thus reduce the respective probability.
- H_{iii}* The probability of window opening upon arrival can be influenced by the pre-arrival thermal perception of the outdoor air temperature. In other words, larger deviation of outdoor temperature from occupants' comfort temperature can increase the tendency to open windows upon arrival.

To operationalize the hypothesis *H_i* above, we designate $\Delta\theta_{ic}$, that is the difference between indoor temperature (θ_i) and comfort temperature (θ_c), as the independent variable ($\Delta\theta_{ic} = \theta_i - \theta_c$). The dependent variable (window opening probability P_w) is operationalized in terms of the number of window opening actions n_{op} within a certain time interval divided by the number of first arrivals in the office n_{ar} within the same time interval ($P_w = n_{op} \cdot n_{ar}^{-1}$).

To operationalize the hypothesis *H_{ii}* above, we designate, aside from $\Delta\theta_{ic}$ (see *H_i* description above), the difference between indoor temperature (θ_i) and outdoor temperature (θ_e) as an independent variable ($\Delta\theta_{ie} = \theta_i - \theta_e$). The dependent variable is, as in case of *H_i*, the window opening probability P_w .

To operationalize the hypothesis *H_{iii}* above, we designate, aside from $\Delta\theta_{ic}$ (see *H_i* description above), the difference between comfort temperature (θ_c) and outdoor temperature (θ_e) as an independent variable ($\Delta\theta_{ce} = \theta_c - \theta_e$). The dependent variable is, as in case of *H_i*, the window opening probability P_w .

To test the above hypotheses empirically, monitored data from an open plan office area with eight workstations in a university building (in Vienna, Austria) was used (Mahdavi et al. 2019). Figure 1 shows the floor plan of the office area as well as the default position of the eight workstations. This office area was equipped with a comprehensive monitoring infrastructure. Collected data included occupants' presence, state of windows, and a number of indoor environment variables (including air temperature, humidity, and CO₂ concentration). Outdoor parameters (including air temperature, solar radiation, wind velocity, and precipitation) were also monitored using the building's roof-top weather station. For the purpose of the present exercise, 15-minute interval data over the course of five months (May to September) in a calendar year was drawn on. The data set comprised occupants' arrival time, window operation events, as well as indoor and outdoor temperatures. A window opening action is assumed to have occurred upon the occupant's arrival in the office if it is registered either at the same interval in which the arrival is observed or in the immediate next interval. Later actions are considered as intermediate actions and not included in the analysis. As the building is not

conditioned (neither heated nor cooled) in the selected time period, the adaptive comfort theory (and a respective comfort temperature equation) was deployed to derive the comfort temperature based on the mean monthly outdoor temperature (Nicol et al. 2012). Table 1 provides detailed information about the sensor types used to monitor indoor temperature and occupancy. Information regarding other indoor and outdoor sensors can be found in Mahdavi et al. (2019). Table 2 and Figure 2 provide an overview of monthly mean temperature for 2013 in Vienna. Note that, given the illustrative nature of the present treatment, potential confounding effects of other variables (e.g., humidity and wind speed) were not taken into consideration.

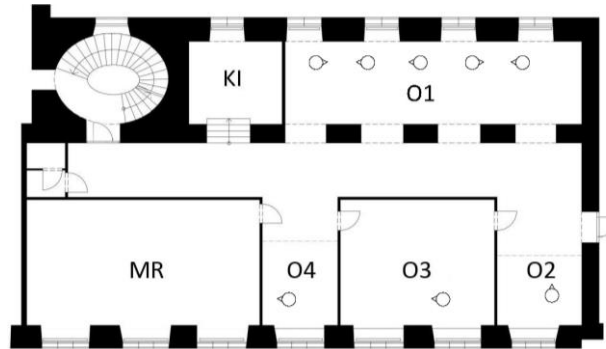


Figure 1: Floor plan of open plan office area (Mahdavi et al. 2019)

Table 1: Description of sensor types for indoor temperature and occupancy (Mahdavi et al. 2019)

Sensor type	Measured variable	Range	Accuracy
Thermokon-SR04 CO2 rH	Indoor air temperature	0 – 51 °C	± 1% of measuring range (typ. at 21°C)
Thermokon – SR -MDS Solar	Motion/ occupancy	0/1	-

Table 2: Monthly mean air temperature in Vienna in °C (GeoSphere Austria 2023)

Month	May	June	July	August	September
T_m	15.0	18.7	22.9	21.3	15.2

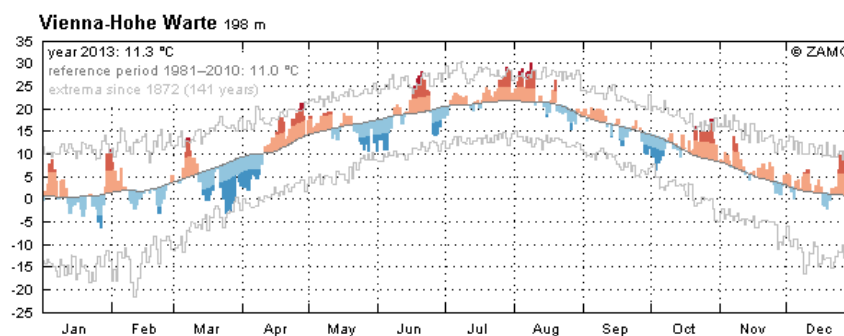


Figure 2: Monthly mean temperature, 2013, Vienna (GeoSphere Austria 2023)

3 RESULTS AND DISCUSSION

As alluded to before, the purpose of the present study is not to either develop or validate a window operation model. Limited monitored data from a single open-plan office and the small number of occupants are certainly insufficient for such a purpose. Rather, the intention is to illustrate the basic features of a process that, given sufficient data and advanced analysis, could lead to more informative and scalable models of occupants' interactions with buildings' control devices and systems. Accordingly, the emphasis is on the prior formulation of relevant hypotheses regarding the background and circumstances that allow for the estimation of the patterns and frequency of occupants' control actions. Accordingly, the observational data is not subjected to a detailed mathematical analysis for explicit model development purposes but applied toward a simple descriptive statistical inquiry. As such, the main findings can be summarized in terms of the information provided in Figure 3. In this Figure, the left-side y-axis marks the window opening probability (P_w) and the x-axis marks the value ranges (bins) of the term $\Delta\theta_{ic}$ (i.e., the difference between indoor temperature θ_i and comfort temperature θ_c). Also shown are the tendencies of $\Delta\theta_{ce}$ (dashed line) and $\Delta\theta_{ie}$ (continuous line) corresponding to the $\Delta\theta_{ic}$ bins of the x-axis. The respective values of these two variables can be obtained from the right-side y-axis.

Consideration of the aforementioned hypotheses H_i to H_{iii} in the light of the data depicted in Figure 3 warrants certain inferences. First, H_i is obviously not supported by observations. Indeed, a trend can be observed, but it is contrary to the one postulated by H_i : It seems the window opening probability is lower for larger deviations of occupants' comfort temperature from indoor temperature arrival times in the office. However, hypotheses H_{ii} and H_{iii} appear to be supported by the observations. The decreasing tendency in window opening probability seems to be consistent with both the outdoor air's diminishing thermal cooling potential as implied by lower $\Delta\theta_{ie}$ values (continuous line in Figure 3) and the lower level of thermal discomfort prior to entering the office space as implied by lower $\Delta\theta_{ce}$ values (dashed line in Figure 3).

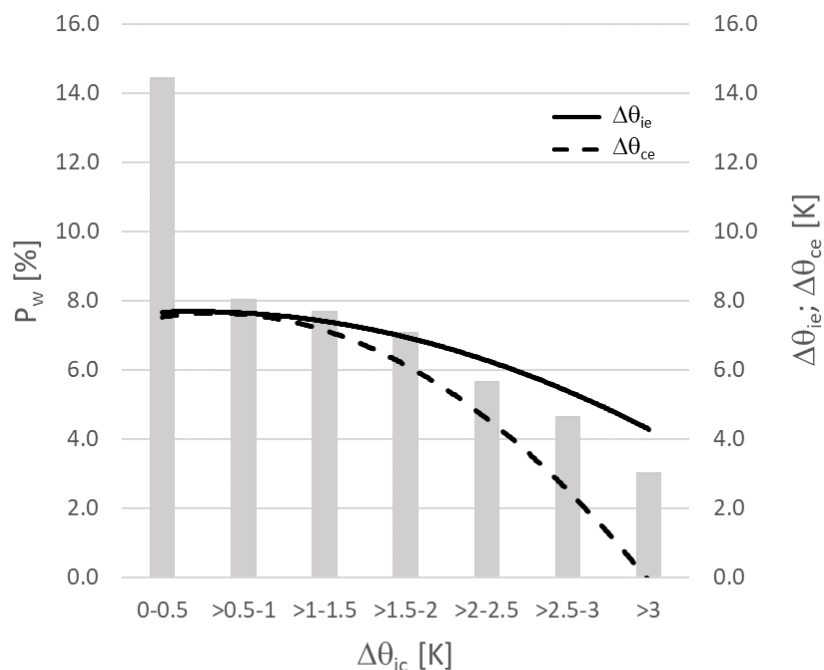


Figure 3: Probability of window opening actions (P_w) as a function of $\Delta\theta_{ic}$. Also shown are the tendencies of $\Delta\theta_{ce}$ and $\Delta\theta_{ie}$ corresponding to the $\Delta\theta_{ic}$ value ranges

These observations underline the initial argument regarding contrasting methodological approaches toward development of behavioural modes. Frequently, such models are based on extraction of patterns from locally and typologically limited data sets. They may be expressed in terms of various types of equations, which map various independent variables onto dependent variables that are meant to capture occupant actions. However, one typically ends up with black-box models, when the model derivation process is not preceded by hypothesised mechanisms mediating between independent and dependent variables. Black-box models can be of course useful in specific scenarios. For instance, a locally calibrated black-box model customised for use in an existing building, with well-documented system details and occupancy patterns, can effectively support building control operations. However, black-box models may be less effective in at least three regards. First, on their own, black-box models do not necessarily shed light on the motivational background and logic of occupants' control-oriented actions. Hence, their role in promoting transparent and knowledge-based design and operation strategies remains limited. Second, they may be less effective as generally deployable prediction models to be integrated, for instance, in building performance simulation applications: Their predictive performance can radically decline without recurrent recalibration to local data. Third, the efforts to further develop and enhance existing black-box models can be hampered by their lack of explicit insights into the intervening mechanisms between independent and dependent variables.

Let us further explain this point. The data underlying Figure 3 could be also analysed in a "theory-free" manner to arrive at a function for the computation of P_w . Equation 1 below provides an illustrative instance of such a function emerging from this data. Using this function, the window opening probability (P_w) can be estimated based on indoor air temperature at arrival time (θ_i) and the preceding mean long-term outdoor temperature ($\theta_{e,l}$), whereby a , b , c , d , and e represent coefficients with values that are adjusted to the data set:

$$P_w = a.\theta_i^2 + b.\theta_i + c.\theta_{e,l}^2 + d.\theta_{e,l} + e.\theta_i.\theta_{e,l} + f \quad (1)$$

Using such a function, one can perhaps obtain reasonably good predictions of the window operation frequency for our case study building and for the same set of occupants. It is also conceivable that others could use this general formalism and adapt the coefficients to match monitoring data from their own buildings. Yet it is not clear to which extent such a formalism could provide any essential insights regarding the logic of occupant behaviour, nor is it clear how the approach can be helpful in cases where local observational data is not available, which de facto includes the bulk of building design scenarios.

To put things in perspective, in our illustrative case study, scanning the data through the filter of the hypotheses does not confirm the conjecture (H_i): The magnitude of perceived thermal discomfort upon arrival cannot, on its own, explain the observed window operation tendency. As to the other conjectures, they are not rejected by the analysis: Both higher cooling potential of the outdoor air (H_{ii}) and the pre-arrival experience of thermal discomfort (H_{iii}) could have encouraged window opening behaviour immediately after entering the office space. However, given the simplistic nature of the analysis, it is important to emphasize that these two conjectures cannot be suggested to have been proven. But the study does suggest that they are worthy of further pursuit based on a richer set of data and more robust statistical methods of analysis.

4 CONCLUSIONS

Occupants' operation of windows can influence indoor-environmental conditions (temperature, humidity, and air quality) and hence occupants' comfort. It can also influence buildings' energy performance. Understanding and predicting window operation behaviour and the availability of related prediction models can thus inform the design and operation of high-performance buildings. In the present study, we contrasted two general approaches to developing such models. Put simply, one approach starts by formulation of prior explicit conjectures and examines those on the basis of available observational data, whereas the other approach starts by a theory-free pattern search in available observational data. We suggested that the former approach has certain advantages in that it can *i*) provide insights into the underlying logic of behavioural patterns, *ii*) support the development of more generally applicable models, *iii*) facilitate the successive improvement of existing models.

Even though the study was of illustrative character and was not meant to rigorously prove anything, it would be prudent to mention various simplifications and limitations it involved. As already mentioned, the observational data, collected over a period of six months, was limited to one space and a small number of occupants. Only thermal factors were considered. Even though both CO₂ concentration and indoor humidity were monitored, they were not used for hypothesis formulation and testing. It is worth mentioning though, that CO₂ concentration, even if it would be considered as a proper proxy of air quality, would have not yielded a proper predictor variable in this study, as its concentration was generally below 600 ppm. Likewise, given the location of the selected office space, which faced a rather quiet internal courtyard, outdoor noise did not represent a potentially relevant influencing parameter. More importantly, the window opening probabilities were aggregated over multiple occupants, thus disregarding inter-individual differences regarding age, gender, health, personal preferences, and habits.

Depending on the relevant application scenarios, the predictive models of occupant behaviour can be of course developed at various level of resolution and detail, that is from simple rule-based formulations to complex stochastic algorithms (Mahdavi and Tahmasebi 2016). Nonetheless, the main contention of the present contribution arguably applies irrespective of the selected level of resolution: More insights can be gained, and more scalable models can be developed, if researchers approach observational data with prior explicit hypotheses, use the verdict emerging out of data analysis to confirm or falsify those, and thus advance the state of their knowledge in this critical domain of inquiry.

5 ACKNOWLEDGEMENTS

In developing the ideas underlying the present paper, the authors benefited from discussions in the framework of IEA EBC Annex 79 – Occupant-Centric Building Design and Operation.

Ardeshir Mahdavi is supported by the FWF (Austrian Science Fund: "Der Wissenschaftsfonds") Project MuDoCo (Project I 5993).

6 REFERENCES

D'Oca, S., & Hong, T. (2014). A data-mining approach to discover patterns of window opening and closing behavior in offices. *Building and Environment*, 82, 726–739. <https://doi.org/10.1016/j.buildenv.2014.10.021>

Etheridge, D. (2011). *Natural Ventilation of Buildings: Theory, Measurement and Design*. Wiley.

GeoSphere Austria (2023). *Monthly Climate Report*. https://www.zamg.ac.at/cms/en/climate/climate-overview/current_climate/monthly_climate/klimawerte?monat=09&jahr=2013. Accessed 20.06.2023

Mahdavi, A., Berger, C., Tahmasebi, F., & Schuss, M. (2019). Monitored data on occupants' presence and actions in an office building. *Scientific Data*, 6(1), 290. <https://doi.org/10.1038/s41597-019-0271-7>

Mahdavi, A., Del Bolgia, M., Tahmasebi, F., & Schuss, M. (2016). Prediction of user-driven window operation in buildings. *Indoor Air 2016 - The 14TH International Conference of Indoor Air Quality and Climate*, Paper-Nr. 750.

Mahdavi, A., & Tahmasebi, F. (2016). The deployment-dependence of occupancy-related models in building performance simulation. *Energy and Buildings*, 117, 313–320. <https://doi.org/10.1016/j.enbuild.2015.09.065>

Nicol, F., Humphreys, M., & Roaf, S. (2012). *Adaptive Thermal Comfort: Principles and Practice*. Routledge.

Tahmasebi, F., & Mahdavi, A. (2016). An inquiry into the reliability of window operation models in building performance simulation. *Building and Environment*, 105, 343–357. <https://doi.org/10.1016/j.buildenv.2016.06.013>

Tahmasebi, F., & Mahdavi, A. (2019). Revisiting the benefits of diversity representation in window operation models for building performance simulation. *Bauphysik*, 41, 30–37. <https://doi.org/10.1002/bapi.201800022>

Development of air supplied ceiling radiant air conditioning system using the Coanda effect

Satoshi Noguchi¹, Yasuyuki Shiraishi¹, Daishi Inoue², and Hiroaki Tanaka²

*1 The University of Kitakyushu
1-1 Hibikino, Wakamatu, Kitakyushu, Fukuoka
Japan 808-0135*

*2 Nikken Sekkei Ltd.
4-15-32, sakae, nakaku, nagoya, Aichi
Japan 460-0008*

ABSTRACT

Air-supplied ceiling radiant air conditioning is expected to become more popular in Japan in the future because there is no leakage from pipes and no condensation on the surfaces of radiant panels. Coanda air conditioning, a type of air-supplied ceiling radiant air conditioning, uses the Coanda effect, which is the tendency a fluid passing near a wall to maintain contact with it. As used commonly, Coanda air conditioning cools the ceiling surface by blowing airflow horizontally along it from the top of the wall surface and cooling by radiation¹). In contrast, the line-type Coanda air-conditioning system proposed in this study (Figure 1) blows airflow to the ceiling in both directions from the air outlet, thereby enabling uniform cooling of the ceiling surface at low air volumes. As an initial study, this paper presents a case study involving the use of computational fluid dynamics to optimise the outlet shapes. The effectiveness of the proposed method is verified by using air diffusion performance index/predicted mean vote environmental assessment for a typical office space, and it is confirmed that the proposed method provides a comfortable thermal environment by radiant heat transfer mainly on the ceiling surface around the air outlet.

KEYWORDS

Coanda effect, CFD analysis, air supplied systems, ADPI

1 INTRODUCTION

Recently, ceiling radiant air conditioning systems have attracted attention owing to their high levels of comfort and energy-saving, and such systems are increasingly being adopted in office buildings. In particular, air-supplied ceiling radiant air conditioning systems are expected to become more widespread in Japan in the future since there is no leakage from pipes and no condensation on the surfaces of radiant panels. However, although general air-supplied systems are easier to install compared with water systems, the initial costs are higher than for general air-conditioning systems. In addition, there is much need for a simpler system that can be installed in existing buildings without complications such as the need to re-cover ceiling surfaces. Coanda air conditioning, a type of air-supplied ceiling radiant air conditioning, uses the Coanda effect, which is the tendency a fluid passing near a wall to maintain contact with it. As used commonly, Coanda air conditioning cools the ceiling surface by blowing airflow horizontally along it from the top of the wall surface and cooling by radiation¹). However, if the airflow is blown from the wall to the ceiling rapidly for a long time, a draft may occur where the blown airflow detaches from the ceiling. Therefore, this research aims to further improve the comfort of and ease of installing and retrofitting air-supplied radiant air-conditioning systems by developing a line-type Coanda air-conditioning system for installation in office spaces. The line-type Coanda air-conditioning system proposed in this study (Figure 1) blows airflow to the ceiling in both directions from the air outlet, thereby enabling uniform cooling of the ceiling surface at low air volumes. Also, air-supplied ceiling radiant air conditioning can be realised simply by installing a dedicated

protrusion at the outlet of the line-type air conditioning commonly used in offices, which is expected to reduce costs and lead to considerably improved workability.

In this paper, as an initial study of the proposed system, the projection shape is optimised in a computational fluid dynamics (CFD) case study, and the optimised projection shape in a general office space is subjected to CFD analysis to verify the effectiveness of the proposed system.

2 OUTLINE OF LINE-TYPE COANDA AIR CONDITIONING SYSTEM

Figure 1 shows an overview of a line-type Coanda air-conditioning system. A typical air-conditioning system in an office space tends to cause discomfort due to drafts. Therefore, in this system, the airflow direction is changed by installing protrusions and plates at the air outlets and cooling the ceiling surface by the Coanda effect. The coldness creates a radiative air-conditioning area near the air outlet and a convection one away from it, the aim being to improve the comfort of the entire space.

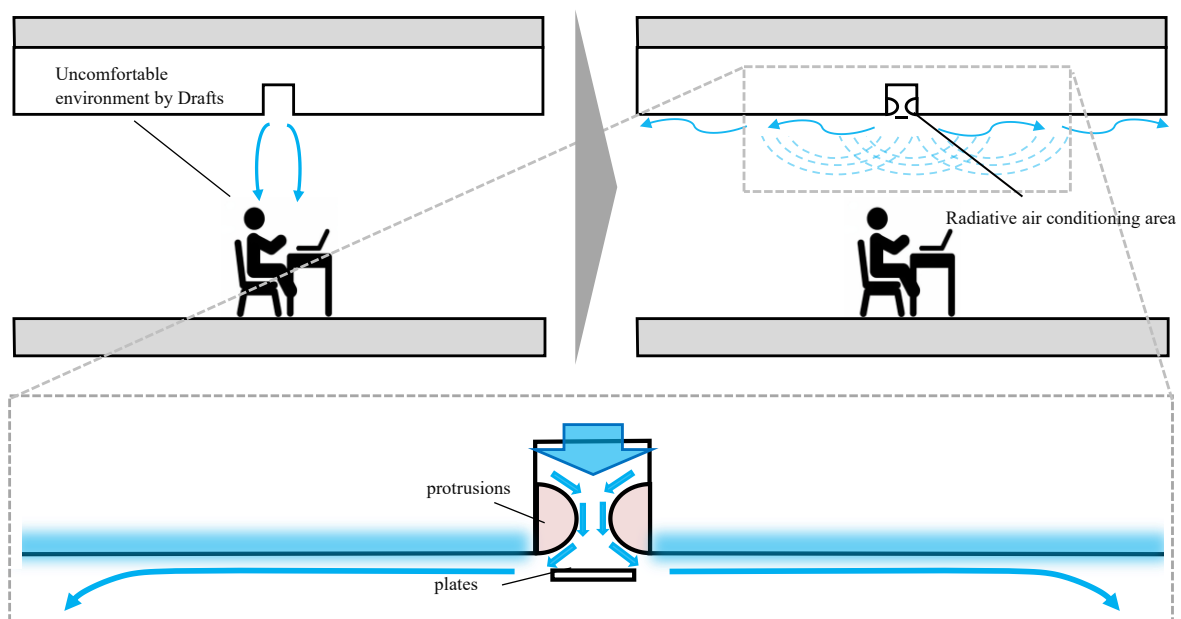
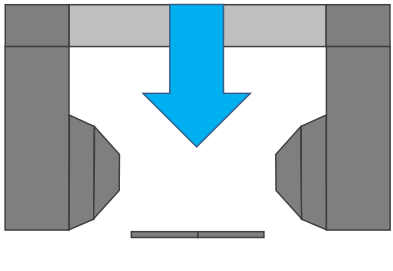
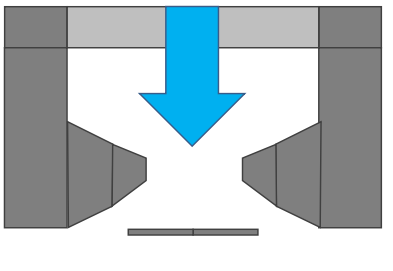
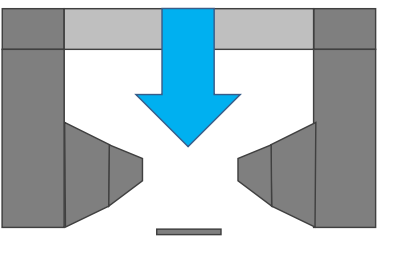


Figure1: Outline of line-type Coanda air-conditioning system

3 OPTIMIZATION OF OUTLET SHAPE (2D ANALYSIS)

The studied outlet shapes are described in Table 1, and to determine the case that gives the largest separation distance, the temperature, flow field, and radiation field are analysed here by means of steady-state CFD. In addition to determining the separation from the calculated streamlines, the distance until the blown airflow separates from the ceiling (hereafter the separation distance x_{max}) is calculated from how the distribution of wind velocity vectors varies along the z axis, and the shape that gives the largest separation distance is considered the optimal shape.

Table 1: Case table of outlet shape

Case1	Case2	Case3
		
Basic Case	A model with extended central projection	A model with half the plate width of Case 2

3.1 Analysis Model

Table 2 and Figure 2 show respectively the analytical conditions and model for optimising the outlet shape. The analysis is performed on a two-dimensional model for improved calculation accuracy and reduced calculation load. Although this system has a two-directional blowout, the centre of the outlet is the symmetry boundary and only one side is analysed. In addition, a heat load of 15.7 W/m^2 is given to the floor surface, and the exhaust is sufficiently far from the air outlet so that the airflow at the exhaust port affects neither the separation distance nor the entire wall surface. Since this analysis was performed at the design stage, comparison with experimental results to verify the validity of the analysis has not yet been performed. However, we have verified that the analytical model has sufficient grid resolution to analyze the flow and temperature fields.

Table 2: Analysis conditions for CFD analysis (2D Analysis)

Domain	10.00m(X)×3.35m(Z)	
Mesh	360(X)×199(Z)=71,640	
Outlet boundary conditions	Temperature: 18°C , Speed of moving fluid: 0.42m/s $k_{in}=(U_{in}/10)^2$, $\varepsilon_{in}=C_{\mu}^{3/4} \cdot k_{in}^{3/2}/l_{in}$	
Inlet boundary conditions	Speed of moving fluid: 0.42m/s	
Turbulence model	Linear Low Reynolds turbulence model	
Advection scheme	QUICK	
Wall boundary conditions	Velocity	Analytical wall function, Cutcell
	Temperature	above the ceiling: (28°C)External temperature, ($9.0 \text{ W/m}^2\text{K}$) overall heat transfer coefficient Ceiling interior side: Logarithmic law
Heat generation	Floor heating: 15.7 W/m^2	

U_{in} : Outlet air wind speed [m/s], k_{in} : Outlet air turbulence energy [m^2/s^2], ε_{in} : Dissipation rate of k_{in} [m^2/s^3], C_{μ} : Model constant (=0.09) [-], l_{in} : Length scale [m]

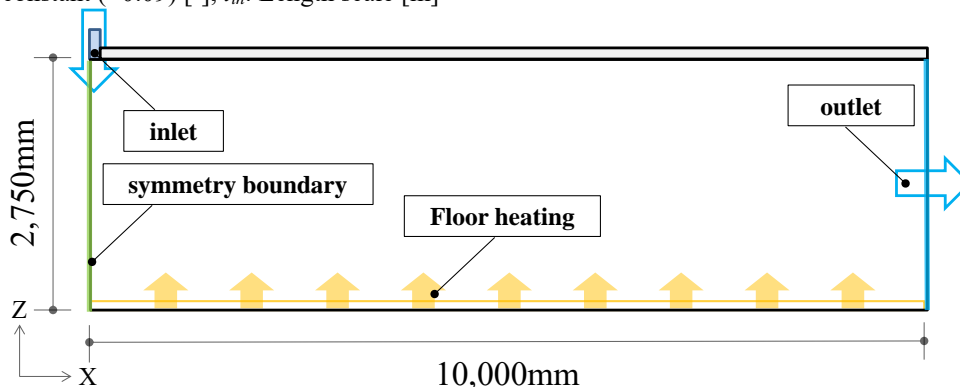


Figure 2: Analysis model (2D analysis)

3.2 Analysis case

The protrusion models are shown in Table 1. As the initial proposal, the cylindrical protrusion is Case 1. In Case 2, the protrusion is extended to the centre to increase the distance that the airflow travels along the surface of the protrusion just before it blows out into the occupied area. Finally, Case 3 has half the plate width of that in Case 2.

3.3 Analysis Results

Figure 3 shows the results of the streamline analysis for the three cases. As can be seen, Case 2 gives the longest separation distance, presumably because the separation distance is affected by the magnitude of the wind velocity vectors along the x axis between the protrusion and the plate. In the subsequent sections, the analysis is performed using Case 2 as the optimal shape.

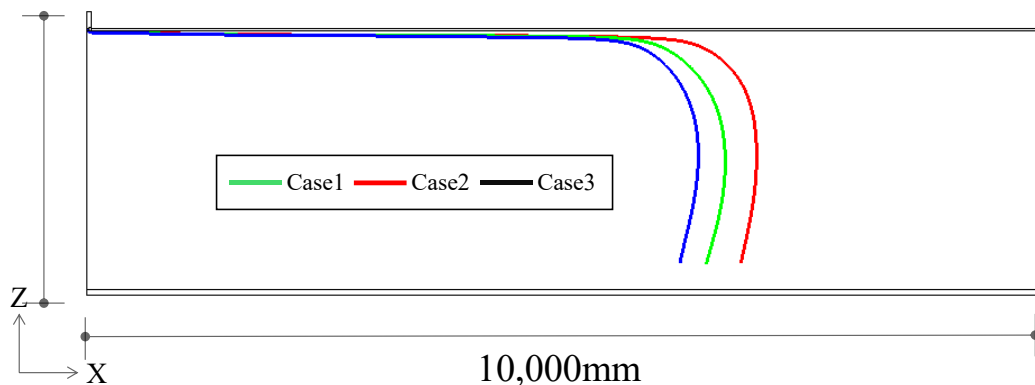


Figure 3: Streamlines analysis results

4 Validation using model office (3D analysis)

In this analysis, the temperature, airflow, and radiation fields are analysed by means of steady-state CFD to assess whether the proposed system forms a comfortable thermal environment.

4.1 Analysis model

Figure 4 and Table 3 show the three-dimensional analytical model and analytical conditions, respectively. A typical office span is assumed, and Case 2, which was the optimal shape from Section 3, is used for the outlet shape.

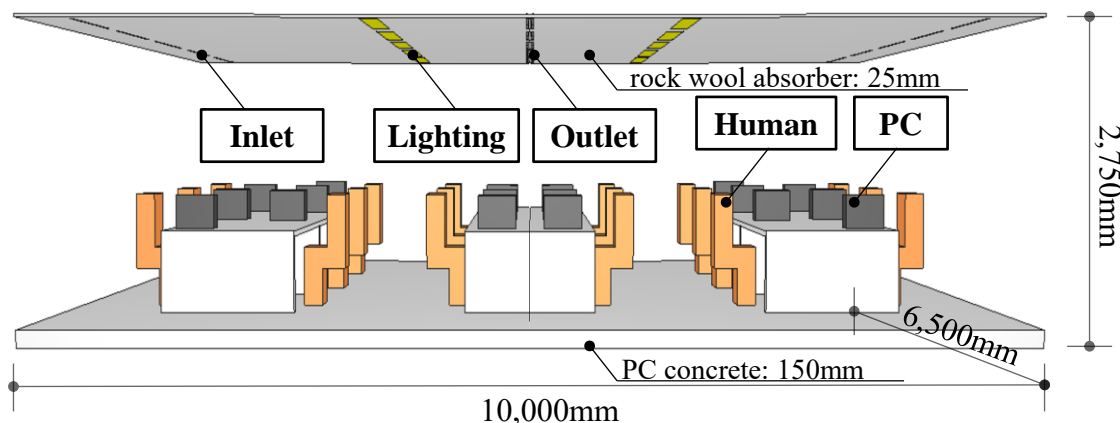


Figure 4: Analysis model (3D analysis)

Table 3: Analysis conditions for CFD analysis (3D Analysis)

Domain	10.00m(X)×6.5m(Y)×2.75m(Z)	
Mesh	127(X)×76(Y)×103(Z)=994,156	
Outlet boundary conditions	Temperature: 17.11 °C, Velocity: 190m ³ /h $k_{in}=(U_{in}/10)^2$, $\varepsilon_{in}=C_{\mu}^{3/4} \cdot k_{in}^{3/2}/l_{in}$	
Inlet boundary conditions	Velocity (5units): 190m ³ /h/unit	
Turbulence model	Linear Low Reynolds turbulence model	
Advection scheme	QUICK	
Wall boundary conditions	Velocity	Analytical wall function, cutcell
	Temperature	above the ceiling: (28°C)External temperature, (9.0 W/m ² K) overall heat transfer coefficient Ceiling interior side: Logarithmic law
Heat generation	Human (18 person): 69W/person, Lighting (10 lights): 40W/unit, PC (18 units): 32W/unit	

U_{in} : Outlet air wind speed [m/s], k_{in} : Outlet air turbulence energy [m²/s²], ε_{in} : Dissipation rate of k_{in} [m²/s³],
 C_{μ} : Model constant (=0.09) [-], l_{in} : Length scale [m]

4.2 Analysis case

Table 4 shows the analysis cases. To derive the optimal operating conditions for the proposed system, the cases were set up with a fixed air flow rate and different air temperatures at each outlet.

Table 4: Operating Conditions Case Table (Model Office Verification)

	flow rate [m ³ /h]	blowoff temperatures [°C]
Case2-1	190	19.11
Case2-2		18.11
Case2-3		17.11
Case2-4		16.11

4.3 EDT and ADPI

The effective draft temperature (EDT) is the temperature at which the human body is comfortable when exposed to a draft. If this temperature is between -1.7 and +1.1 and the air velocity does not exceed 0.35 m/s, then the majority of people in the room are considered to be comfortable. The EDT is calculated as given in (1).

$$\text{EDT} = (t_x - t_c) - 7.66(V_x - 0.15) \quad (1)$$

t_x : Room local temperature [°C]
 t_c : Average temperature of the living area [°C]
 V_x : local wind speed [m/s]

The air diffusion performance index (ADPI) is an index for draftiness indoors and is calculated as given in (2).

$$\text{ADPI} = \eta / \eta' \times 100\% \quad (2)$$

η : Area where EDT values meet the comfort range (-1.7 ≤ EDT ≤ 1.1) [m²]
 η' : Indoor floor area [m²]

4.4 Analysis Results

Figure 5 shows the ceiling surface temperature distribution, the predicted mean vote (PMV) distribution at 1.2 m from the floor, the horizontal surface EDT distribution, and the ADPI. The ceiling surface temperature distribution shows that the average ceiling surface

temperature also decreases as the air temperature at the outlet decreases, and it is confirmed that the cooling range of the ceiling surface is generally constant. It seems that because the cooling is blocked by the lighting between the air outlet and the inlet, the cooling range is limited to the space between the air outlet and the lighting. The PMV distribution is within ± 0.5 after Case 2-3, confirming the formation of a good indoor thermal environment. The horizontal EDT distribution and ADPI in Case 2-3 are confirmed to be more than 80% of ADPI, indicating a comfortable thermal environment with little draft and temperature irregularity. The above results confirm that a comfortable and good thermal environment forms at the present outlet air temperature of 17.11°C .

Figure 6 shows the temperature and mean radiant temperature (MRT) distributions of the line-type Coanda air-conditioning system under the air conditions of Case 2-3, that is, the optimal operating conditions. In the line-type Coanda air-conditioning system, the air temperatures at both ends of the room and the MRT at the centre of the room are low, seemingly because of the formation of convection and radiation air-conditioning zones as intended in the design.

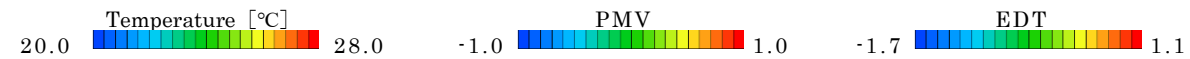
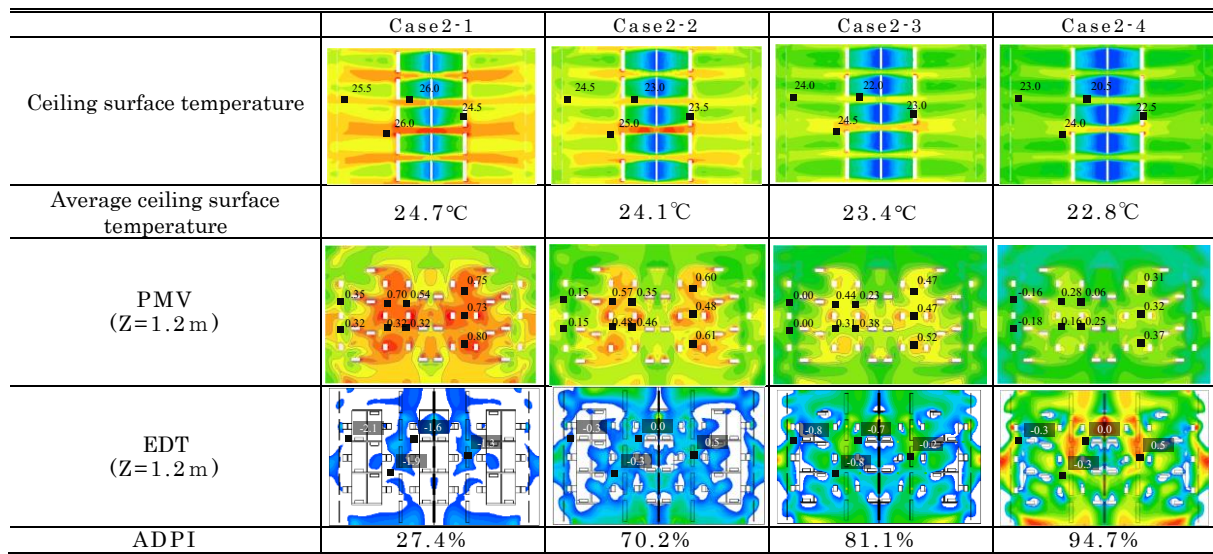


Figure 5: Ceiling surface temperature, MRT, PMV vertical distribution and 1.2m horizontal EDT distribution for each case

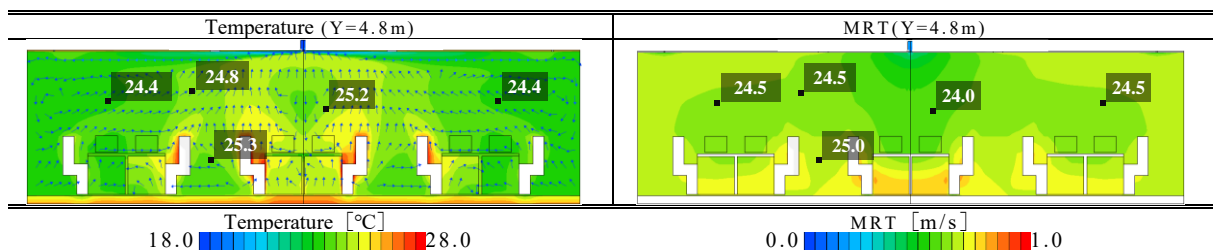


Figure 6: Case2-3 Temperature and MRT distributions of line type Coanda air conditioning and convection type air conditioning (Anemo type) under blowout conditions

5 CONCLUSION

In this study, as an initial investigation of a line-type Coanda air-conditioning system, the shape of the air outlet was optimized through a CFD analysis case study. Furthermore, CFD analysis was conducted for a typical three-dimensional office space to clarify the characteristics of a line-type Coanda air-conditioning system.

The followings are the findings of this study.

- 1) We proposed an outlet shape that efficiently cools the ceiling surface. Case 2, which has the shortest distance between the projection and the plate, was confirmed to have the longest separation distance. This is presumably because the separation distance is affected by the magnitude of the wind velocity vectors along the x axis between the protrusion and the plate.
- 2) It was confirmed that installing a line-type Coanda air-conditioning system in the model office formed a radiative and a convection air-conditioning area and a comfortable thermal environment with little draft and uneven temperature.
- 3) Comparison with general air-conditioning systems, the proposal of design conditions using Archimedes number, and confirmation of ventilation performance using Age of air and other indices are future issues to be considered.

6 REFERENCES

- 1) Igarashi H et al. (2022). Study of Coanda air-conditioning system compatible with variable air volume- Thermal comfort evaluation by full-scale experiments-, Architectural Institute of Japan (in Japanese)

ACKNOWLEDGMENT

This work was supported by JSPSKAKENHI Grant Number 22H01653.

Wind Tunnel Experiment of Wind-Induced Single-sided Ventilation under Generic Sheltered Urban Area

Zitao Jiang^{*1}, Tomohiro Kobayashi¹, Toshio Yamanaka¹, Noriaki Kobayashi¹,
Narae Choi³, Mats Sandberg², Kayuki Sano¹, and Kota Toyosawa¹

1 Osaka University

2-1 Yamadaoka

Suita City, Japan

**Corresponding author:*

jiang_zitao@arch.eng.osaka-u.ac.jp

2 University of Gävle

SE-801 7

Gävle, Sweden

3 Toyo University

5 Chome-28-20 Hakusan

Tokyo, Japan

ABSTRACT

The utilization of natural ventilation helps to reduce building energy consumption and improve indoor air quality. In the urban area, the performance of the natural ventilation is very sensitive to surrounding building density. However, the influence of surrounding buildings on ventilation rate was not well investigated in previous research. This paper presents a wind tunnel experiment to assess the influence of urban density on the wind-induced ventilation rate of single-sided ventilation. Spacing density, wind direction, and the number of openings were primary factors that were investigated in this experiment. The ventilation rate is evaluated by a continuous dose method of the tracer gas technique. The wind pressure coefficient at openings of the sealed model without openings was measured by pressure transducers. The streamwise velocity at the street canyon was measured by a split-film probe with a constant temperature anemometer unit. The ventilation rate, wind pressure coefficient fluctuations, and surrounding velocity of an isolated building are compared to that of a building with two layers of surrounding buildings with a spacing of 0.5 H (building height), 1 H, and 1.5 H. The relationship between the wind pressure coefficient of the sealed model and the ventilation rate was also discussed.

KEYWORDS

Natural ventilation, Wind pressure coefficients; Wind tunnel experiment, Urban canopy flow

1 INTRODUCTION

Accurately predicting natural ventilation rates and understanding its performance in different environmental conditions is crucial for optimizing building ventilation design. However, predicting natural ventilation rates can be challenging due to the complex interactions between wind flow, building geometry, and other factors. Moreover, the effectiveness of natural ventilation systems can be significantly affected by external factors such as wind direction and building orientation (Y. Jiang & Chen, 2002), especially in sheltered conditions (Ghiaus et al., 2006) where airflow is limited. The sheltering effect on cross ventilation was extensively investigated by wind tunnel experiments or numerical analysis (Tominaga & Blocken, 2015; Ikegaya et al., 2019; Shirzadi et al., 2019; Adachi et al., 2020; Golubić et al., 2020; Mohammad et al., 2021). In the urban context, compared to cross ventilation, single-sided ventilation is a more common ventilation feature because of the limitation of large indoor spaces. Focusing on single-sided ventilation in isolated and sheltered buildings, this research has two-fold purposes. The first objective is to investigate the sheltering effect of single-sided ventilation. The second aim of the present work is to look into the wind pressure fluctuation that is dominating wind-

induced ventilation and discuss the ventilation rate prediction methods of single-sided ventilation.

2 EXPERIMENT METHODS

2.1 Case and wind tunnel descriptions

The target building model is a cube with the dimension of 100 mm (Length) x 100 mm (Width) x 100 mm (Height). Two types of building models were used: one is the sealed model without openings, which was used to measure the wind pressure coefficient, and the other is the building model with openings, which was used to evaluate the ventilation performance. For the building model with openings, as shown in Fig.1(a), it is assumed the target building model has 1/2/3 square-shaped openings (15mm x 15mm) located on the same external wall, which are abbreviated as SS1, SS2 and SS3.

Both isolated and sheltering conditions were tested in the experiment. The surrounding buildings have the same dimension as the target cubical building but without openings, and two layers of surroundings were arranged in a regular array with equal spacing of d , which is $d=0.5H$, $d=1H$ and $d=1.5H$ respectively. The planar area ratio (λ_p) is defined as:

$$\lambda_p = \frac{LW}{(L+d)(W+d)} \quad (1.)$$

where L and W are the length and width of the target building, and d is the distance between adjacent buildings. λ_p is $\lambda_p=0.44$, $\lambda_p=0.25$ and $\lambda_p=0.16$ in three sheltering cases respectively.

The approaching wind direction is set to 0° (opening at windward side), 30° , 45° , 60° , 90° (opening at lateral side), 120° , 135° , 150° and 180° (opening at leeward side). The turntable was rotated to accommodate the different approaching wind directions. The combination of opening configuration, sheltering condition and approaching wind angle resulted in a total of 108 cases in this experiment.

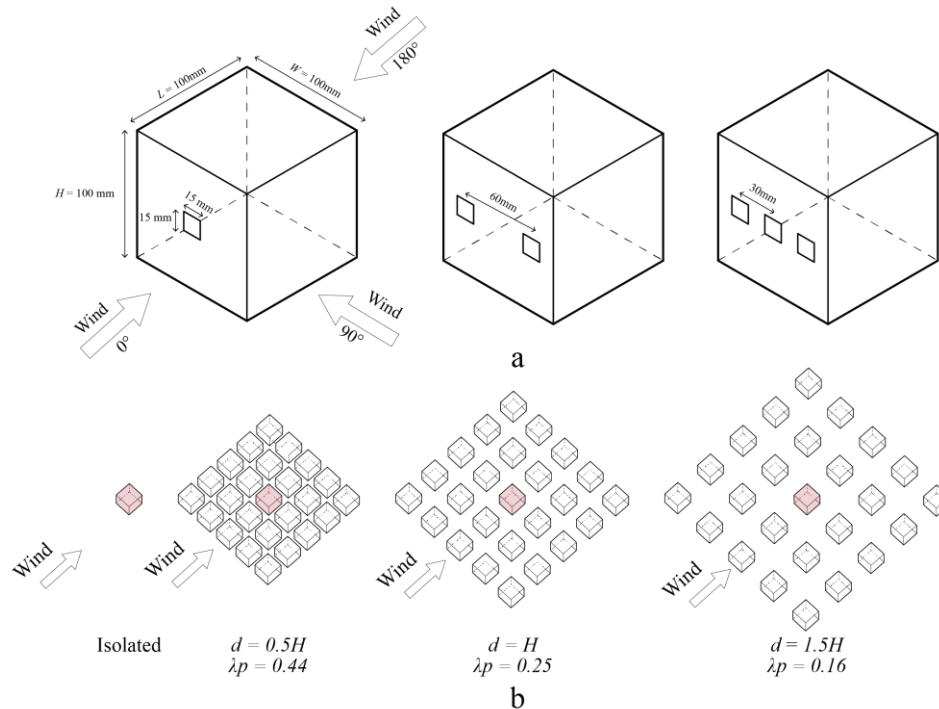


Fig. 1. (a) Schematic view of the studied cubic building model; (b) Surrounding building configurations.

The wind tunnel experiment was carried out in the atmospheric boundary layer wind tunnel at Osaka University. A combination of turbulence grid and roughness blocks were used to

create a neutral atmospheric boundary layer as shown in Fig.2(a). Fig.2(b) shows the experimental setup for the ventilation performance measurement. The vertical mean streamwise velocity profiles and turbulent intensity measured at the centre of the turntable without the physical models are shown in Fig.2(c) and Fig.2(d). The reference velocity at building height (U_H) was measured to be 6.44 m/s.

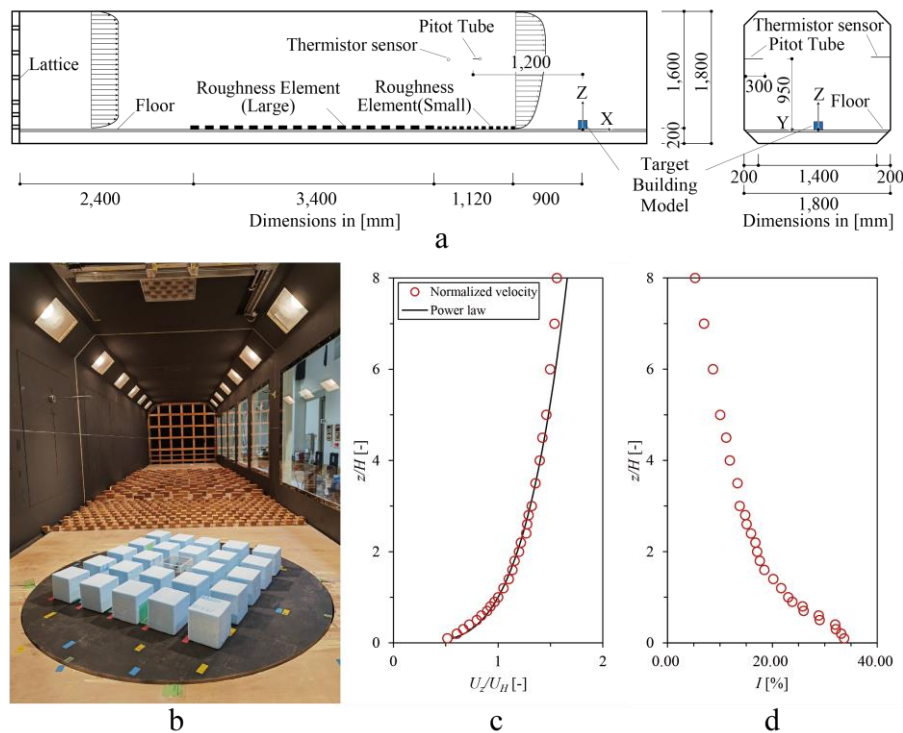


Fig. 2. (a) Wind tunnel schematic diagram; (b) Inside view of the wind tunnel; (c) Mean streamwise velocity of the boundary layer; (d) Turbulence intensity of the boundary layer.

2.2 Velocity measurement

The streamwise velocity component of flow (U_x) in the street canyon were measured by the straight split-fibre film probe (55R55, Dantec) in the wind tunnel experiment. The probe was operated using a constant-temperature anemometer and linearizer modules (Kanomax). Sampling was conducted at a rate of 1,000 Hz for a period of 60 s for the velocity measurements to obtain statistically stationary values.

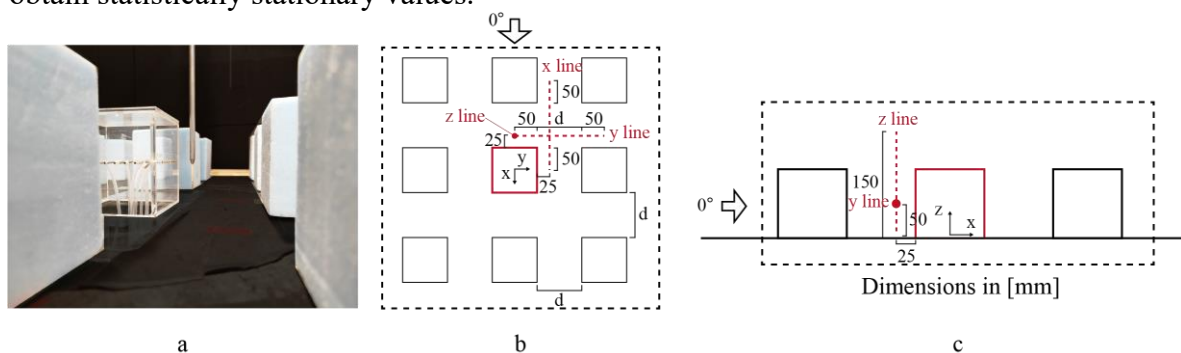


Fig. 3. (a) Photo of velocity measurement by split-fibre film probe; (b) Plan view of measurement lines; (c) Section view of measurement lines.

Fig.3(a) shows the velocity measurement set-up in the wind tunnel. The nearby velocity around the sealed model with 0° wind direction under different planar density cases was measured. Fig.3(b) and Fig.3(c) show three velocity measurement lines around the building. In

each condition, wind speeds are measured at a 25 mm distance from the building wall in three lines in the X-, Y- and Z-directions at 10 mm intervals. Measurement lines X and Y are 50 mm above the wind tunnel ground.

2.3 Pressure coefficient measurement

The mean and fluctuating pressure at the three opening positions at the sealed building model were measured as shown in Fig.4(a) and Fig.4(b). Wind pressure is commonly expressed by wind pressure coefficient (C_p), which is defined as the ratio of wind pressure at the point of the sealed body and the reference dynamic pressure in free-stream flow.

$$C_p = \frac{p - p_{ref}}{p_d} \quad (2.)$$

where p is the static pressure at the wall of the sealed model, p_{ref} is the reference static pressure in approaching flow and p_d is the dynamic pressure at building height (100 mm). Both mean and RMS of C_p are measured by connecting surface pressure taps and a pressure transducer (Validyne DP45). The pressure was measured at a frequency of 1000 Hz for 60 s in the experiment to obtain high-frequency data.

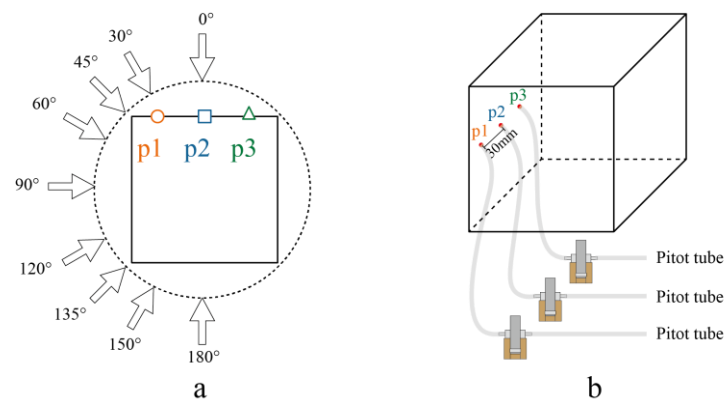


Fig. 4. (a) Wind pressure measurement points; (b) Pressure measurement system.

2.4 Ventilation rate measurement

In this study, the ventilation rate was evaluated by the continuous dose method of the tracer gas technique. CO_2 was used as the tracer gas in the experiment. Fig.5 shows the diagram of the ventilation rate measurement system. The tracer gas was evenly injected from 4 evenly distributed dosing pipes, the emission rate was controlled by a mass flow controller (Fujikin, FCS-T1005F). The tracer gas concentration at the centre of the physical building model was sampled by a sampling pipe, and concentration was measured by a gas analyser (LumaSence Technologies, Innova 1312).

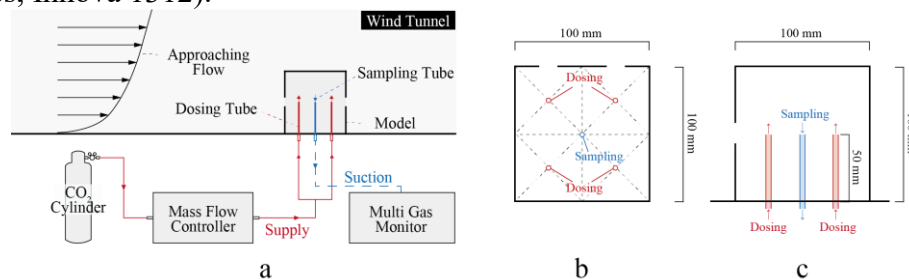


Fig. 5. (a) Schematic of the tracer gas measurement; (b) Plan view of tracer gas injection and sampling rods; (c) Section view of tracer gas injection and sampling rods

The wind tunnel was switched to open-circuit to prevent the influence of returning tracer gas from upstream. The measurement procedure involved first recording the indoor concentration without CO_2 emission for 5 minutes, during which the average value was taken as the mean outdoor concentration. Subsequently, measurements were carried out every 1 minute for 10 minutes after the indoor concentration reached a steady state.

$$Q = \frac{m}{C_r - C_o} \quad (3.)$$

where m is the constant volumetric emission rate of tracer gas [m^3/s], C_r and C_o are time-averaged steady-state indoor and outdoor concentrations respectively. In this study, the dimensionless ventilation rate Q' is defined ($Q' = Q / AU_H$) as the measured ventilation rate (Q , m^3/s) divided by the product of a single opening area ($A=2.25 \times 10^{-4} m^2$) and building height ($U_H = 6.44 m/s$).

3 RESULTS

3.1 Velocity results

Fig.6 shows the velocity measurement results, the positive velocity is the streamwise direction and the negative velocity is the reverse flow. Fig.6(a) shows the mean streamwise velocity along the X-direction measurement line. For isolated building, the obstruction of the windward wall makes the flow velocity experiences a gradual increase when approaching the building, and the velocity reaches the peak value ($U_x/U_H=0.94$) at a short distance downstream of the corner ($x/H=-0.4$). Fig.6(b) shows the mean streamwise velocity along the Y-direction measurement line. In all conditions, the velocity increases from the centre of the windward side ($y/H=0$) to the street ventilation corridor, and it reaches the peak at the centre of the ventilation corridor. It can be observed that the velocity in sheltering cases is negative outside of the ventilation corridor, which is caused by the recirculating flow in the wake region of the upwind building. Fig.6(c) shows the mean streamwise velocity along the Z-direction measurement line. For isolated buildings, the reverse flow only occurs at the lowest part of the measurement line. In sheltering cases, the reverse flows are observed from the ground up to the height of the building ($z/H=0.9$). Similar to velocity results along the Y measurement line, it is thought to be due to the effect of the circulation flow caused by the building on the windward side. Moreover, the higher position of reverse flow also indicates the centre of the eddy vortex in the street canyon moves higher.

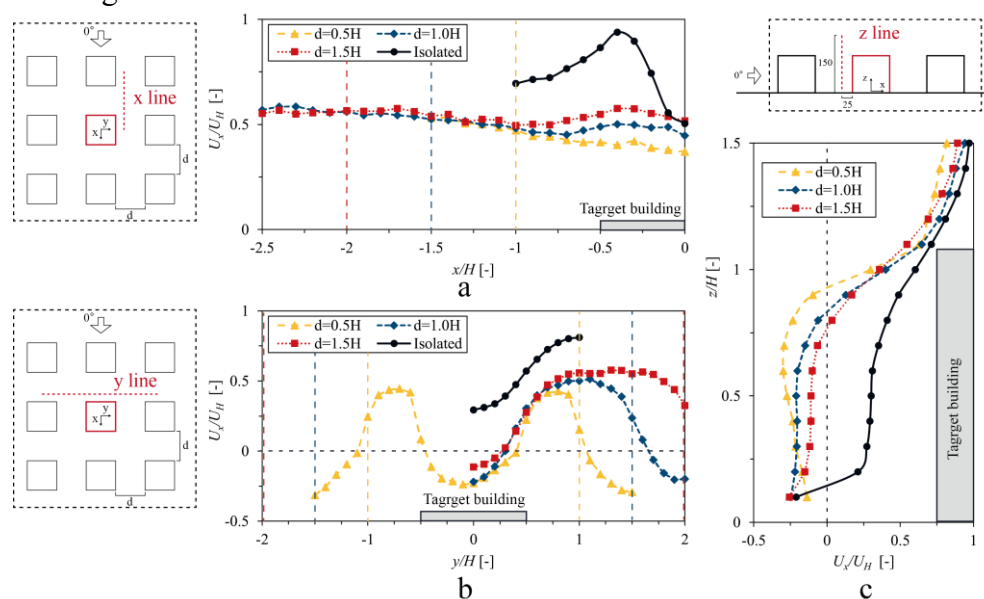


Fig. 6. (a) Mean streamwise velocity at X direction measurement line; (b) Mean streamwise velocity at Y direction measurement line; (c) Mean streamwise velocity at Z direction measurement line.

3.2 Wind pressure coefficient results

Fig.7 plots the time-averaged C_p ($\overline{C_p}$) and RMS of C_p (σ_{C_p}) at three measurement points against different wind directions under different conditions. The results show that for isolated cases, the value of $\overline{C_p}$ changes significantly as the wind direction changes. $\overline{C_p}$ decreases when the wind direction increases between 0° and 90° , and $\overline{C_p}$ increases between the wind direction of 120° and 180° . In the condition where there are surrounding buildings, the change becomes smaller as the building spacing becomes narrower and the $\overline{C_p}$ value also becomes smaller.

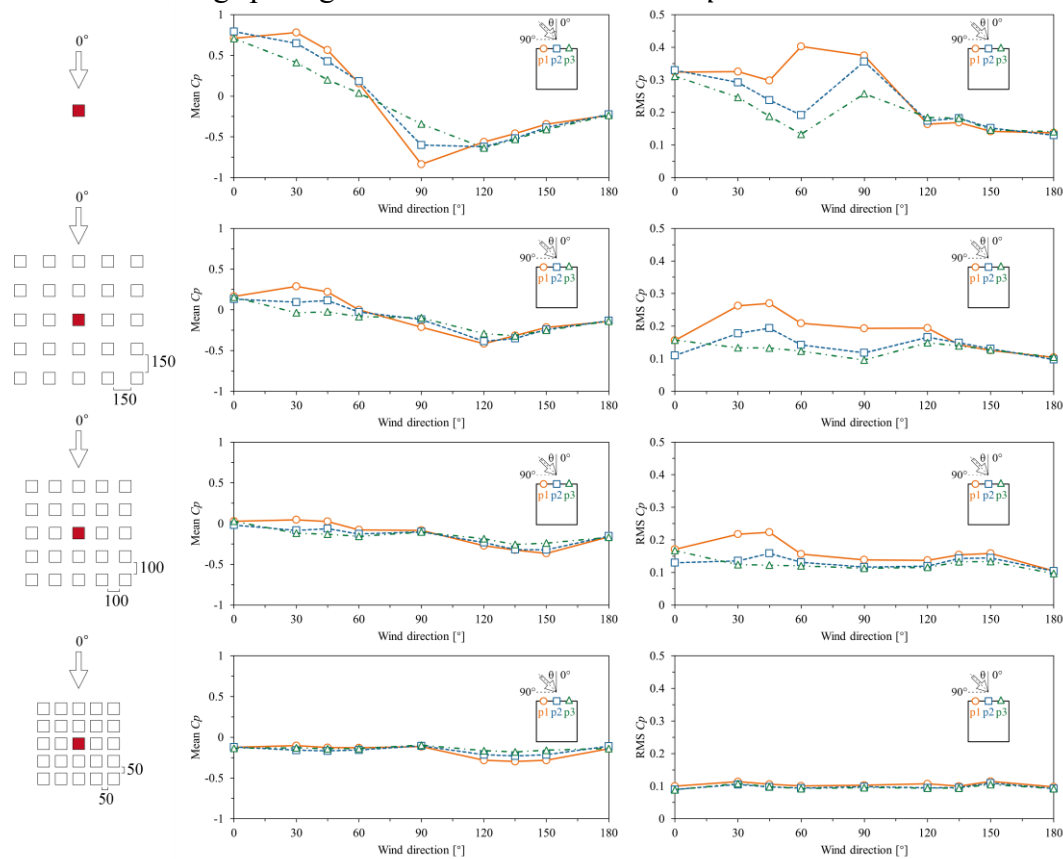


Fig. 7. Mean C_p of three measurement points against different wind angles under different sheltering conditions.

Considering the SS2 case, ventilation is predominantly determined by the pressure difference between point 1 and point 3. The mean wind pressure difference ($\overline{\Delta C_p}$) and RMS of the wind pressure difference between point 1 and point 3 is shown in Fig.8. Generally, compared to isolated cases, $\overline{\Delta C_p}$ becomes smaller when there are surrounding buildings.

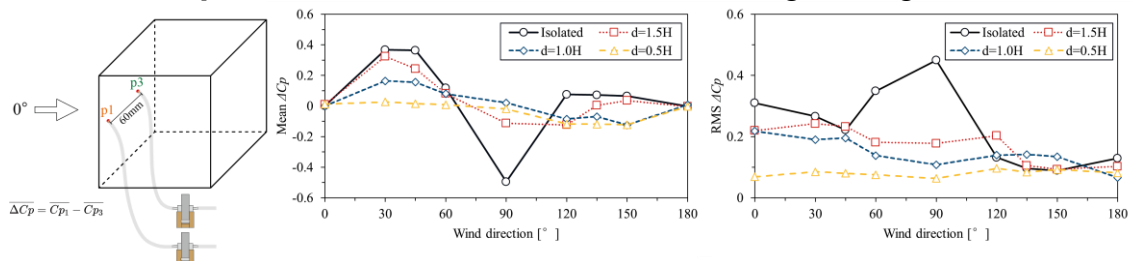


Fig. 8. Mean ΔC_p against different wind angles under different sheltering conditions.

3.3 Ventilation rate results

Fig.9 (a) shows the Q' against different wind directions classified by the number of openings. In SS1 case, Q' tends to be slightly higher when the opening faces upwind. In a higher density case (Case 0.5H), since the airflow in the street canyon and wind pressure fluctuations are more invariant to wind directions, the Q' are nearly unchanged wherever the approaching wind comes. The trend of Q' in SS2 cases and SS3 cases are rather similar, Q' is very sensitive to both sheltering conditions and wind directions. When the wind direction is between 0° and 60° , or at around 90° , Q' is relatively higher than others in wind directions. Fig.9(b) shows the Q' against different wind directions classified by the spacing between buildings. Q' of SS2 and SS3 cases are much higher than that of SS1 cases. The difference in Q' between SS2 and SS3 cases is insignificant.

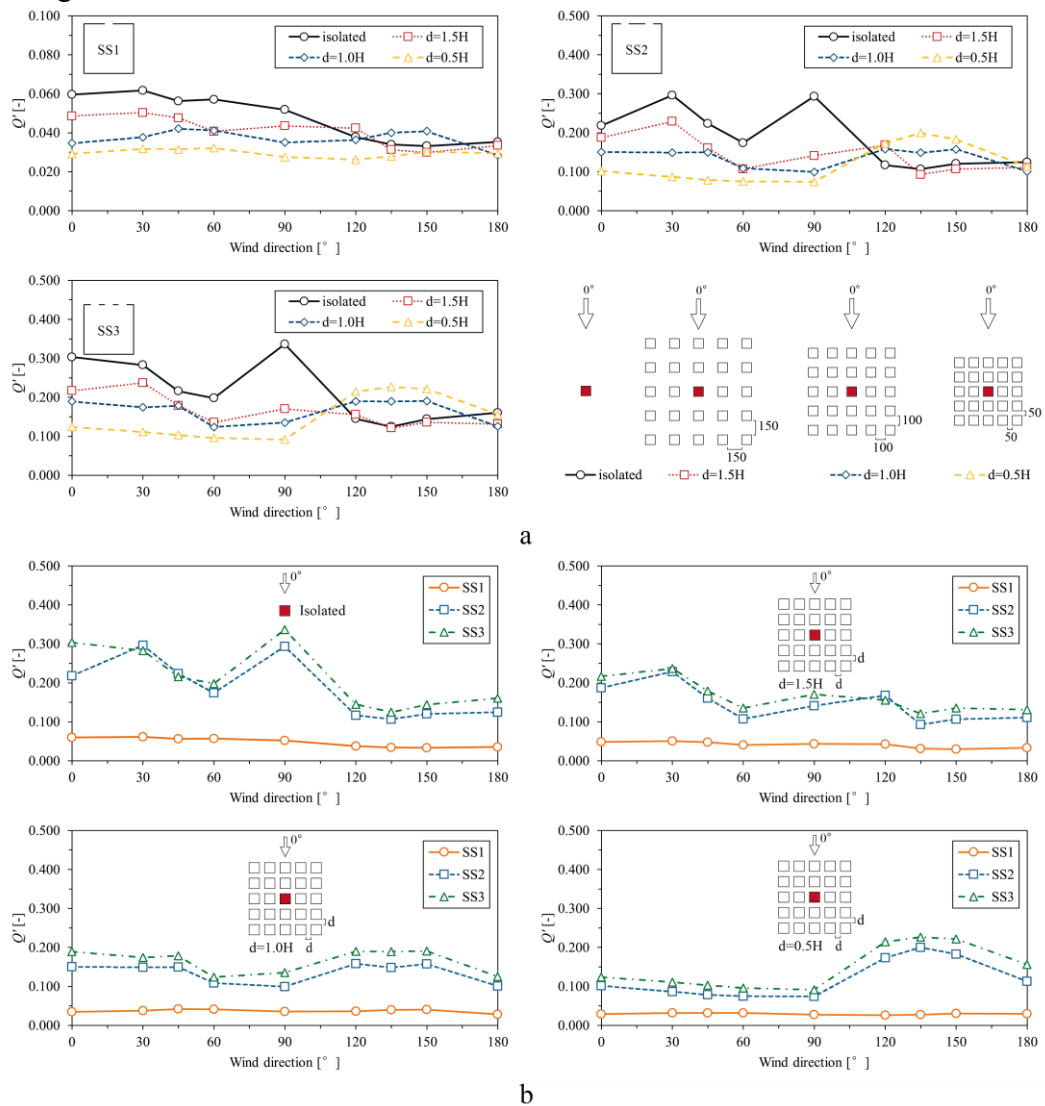


Fig. 9. (a) Dimensionless ventilation rate (Q') against different wind directions for SS1/SS2/SS3 cases; (b) Dimensionless ventilation rate (Q') against different wind directions for isolated/d=1.5H/d=1.0H/d=0.5H cases

3.4 Relation between SS1 ventilation rate and pressure

In SS1, it is assumed that time-averaged pressure between indoor and outdoor is almost the same, therefore, the pressure fluctuations at the openings mainly contribute to air exchange between indoor and outdoor air. Fig.10(a) shows the relations between $\sqrt{\sigma_{Cp}}$ and dimensionless measured ventilation rate Q' for SS1 cases. The Pearson correlation between $\sqrt{\sigma_{Cp}}$ and Q' was found to be 0.80, which indicates there is a relatively positive linear correlation between the

pressure fluctuations and the ventilation rate. The constant C was determined by the least square method, resulting in a value of 0.1022. Using σ_{Cp} , the ventilation rate can be simply estimated by Eq.(4).

$$Q = CAU_{ref}\sqrt{\sigma_{Cp}} \quad (4.)$$

Fig.10(b) plots the measured ventilation rate and predicted ventilation rate from Eq.(4). The absolute error in the prediction is defined as:

$$\frac{1}{n} \sum_{i=1}^n \left| \frac{Q'_{pre} - Q'}{Q'} \cdot 100\% \right| \quad (5.)$$

The dotted line in Fig.10(b) represents the 30% deviation from the $y=x$ line. Analysis of the data reveals that the majority of predicted ventilation rates exhibit an absolute error of less than 30%. Furthermore, the proposed prediction equation has an absolute error of 11% when applied to all measured values, indicating good accuracy.

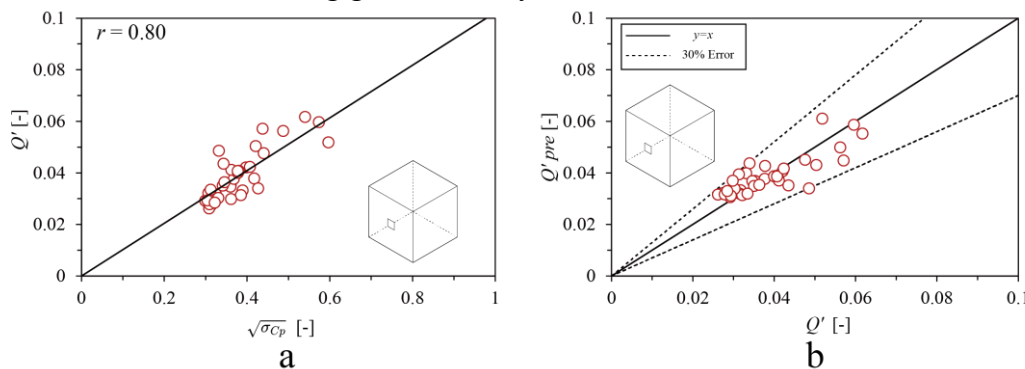


Fig. 10. SS1 ventilation prediction methods (a) Relations between $\sqrt{\sigma_p}$ and dimensionless ventilation rate Q' ; (b) Comparison between measured ventilation rate Q' and predicted ventilation rate Q'_{pre}

3.5 Relation between SS2 ventilation rate and pressure

As pointed out by much previous research, not only mean pressure difference but also pressure difference pressure contributes to part of the ventilation rate (Chu et al., 2015; Daish et al., 2016; Z. Jiang et al., 2022). Fig.11(a) shows the relations between $\sqrt{\sigma_{\Delta Cp}}$ and dimensionless measured ventilation rate Q' for SS2 cases. The Pearson correlation between $\sqrt{\sigma_{\Delta Cp}}$ and Q' was found to be 0.76, which indicates there is a relatively positive linear correlation between the pressure difference fluctuations and the ventilation rate.

In previous research, it was widely accepted that the Orifice equation fails to well predict the wind-induced ventilation rate when the $\overline{\Delta Cp}$ is small. It is the consequence of bi-directional airflow that makes the inlet and outlet alternatively change between two openings and the predicted ventilation rate based on $\overline{\Delta Cp}$ will underestimate the ventilation performance. In this study, instead of using the absolute value of the mean wind pressure coefficient ($|\overline{\Delta Cp}|$), the time average of the absolute wind pressure coefficient ($\overline{|\Delta Cp|}$) was used to predict the ventilation rate.

$$Q = (C_d A)_{eff} U_{ref} \sqrt{\overline{|\Delta Cp|}} \quad (6.)$$

Fig.11(b) plots the measured ventilation rate Q' and predicted values based on $|\overline{\Delta Cp}|$ and $\overline{|\Delta Cp|}$. It can be seen that predicted ventilation rate based on $\overline{|\Delta Cp|}$ generally agrees well with the measured values. The absolute error of the two methods is 104% and 17% respectively.

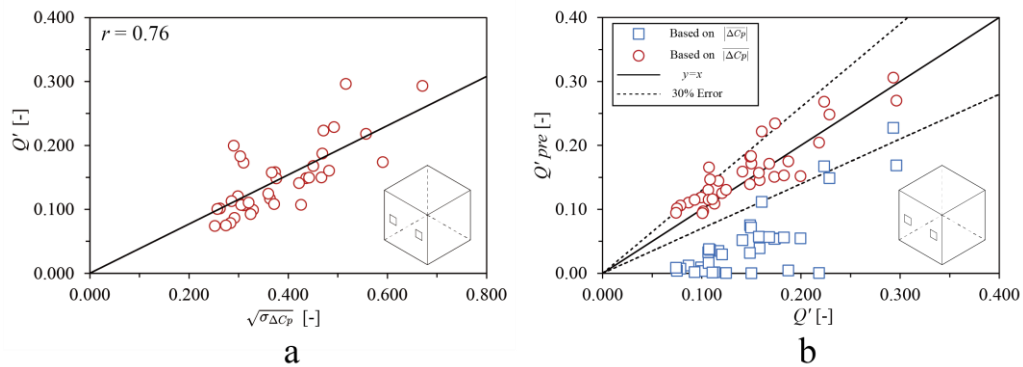


Fig. 11. SS2 ventilation prediction methods (a) Relations between $\sqrt{\sigma_{\Delta C_p}}$ and dimensionless ventilation rate Q' ; (b) Comparison between measured Q' and predicted ventilation rate Q'_{pre}

3.6 Relation between SS3 ventilation rate and pressure

To determine the flow rate at each opening for SS3, an initial guess is given to indoor pressure, and the flow rate through 3 openings can be solved independently assuming the flow is purely driven by the difference between indoor pressure and each wind pressure coefficient at the sealed model. The indoor pressure is iterated till the total inflow and outflow rate is conserved. The instantaneous flow rate is half of the total flow rate through 3 openings. Consequently, the ventilation rate of SS3 can be obtained by taking the time average of the instantaneous flow rate. Fig.12(a) shows the flow chart of prediction methods for the ventilation of SS3. This method can also be applied to SS3 or SSn. Fig.12(b) illustrates the predicted and measured ventilation rate. The absolute error of the proposed method is about 17%.

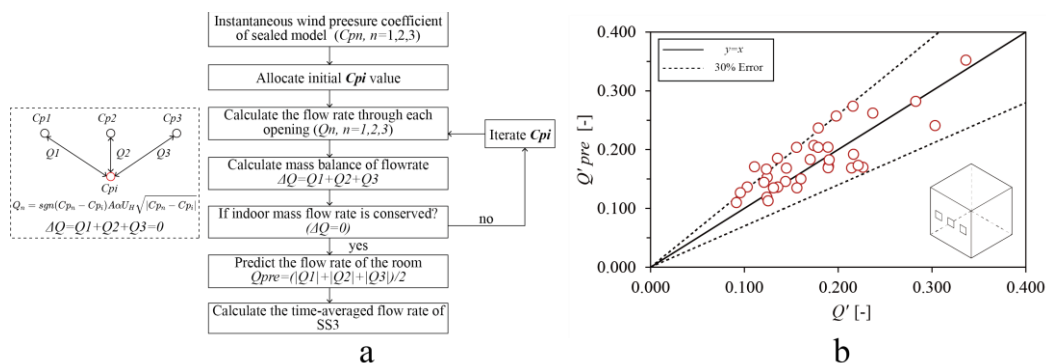


Fig. 12. SS3 ventilation prediction methods (a) The flow chart of prediction methods for ventilation rate of SS3 or SSn; (b) Comparison between measured Q' and predicted ventilation rate Q'_{pre}

4 CONCLUSIONS

The present work reported the wind tunnel experiment to investigate the influence of sheltering buildings as well as discuss simplified ventilation rate prediction methods for wind-induced single-sided ventilation. The following conclusions are summarized as the main understandings of this study:

- In both isolated or sheltered conditions, SS2 has a much higher ventilation rate than SS1, while the ventilation rate of SS3 is only slightly higher than SS2.
- The sheltering does not always reduce ventilation performance of single-sided ventilation. When the wind direction is 120° - 180° , higher building density enhances the ventilation performance.

- The ventilation rate of SS1 can be estimated by the wind pressure coefficient, which yields an absolute error of 11% in this study.
- The ventilation rate of SS2 can be predicted using the absolute value of the mean wind pressure coefficient ($|\overline{\Delta Cp}|$), which includes the influence of both steady pressure difference and unsteady pressure fluctuations. The predicted equation only caused a 17% absolute error.
- The ventilation rate of SS3 can be calculated by using the instantaneous wind pressure coefficient from the sealed model and iterating indoor pressure till the inflow and outflow flow rate is conserved, the time-averaged predicted flow rate produced an absolute error of 17%. However, the findings of this work are limited to a reduced-scale model. The similarity of velocity distribution and ventilation rate should be confirmed in the future study, which determines whether the conclusions from this study can be applied to a full-scale scenario.

5 ACKNOWLEDGEMENTS

We would like to thank the AIVC 2023 Reviewers for taking the time and effort necessary to review the manuscript. We sincerely appreciate all valuable comments and suggestions, which helped us to improve the quality of the manuscript.

Part of this work was supported by a JSPS Grant-in-Aid for Scientific Research in Japan (Grant-in-Aid for Scientific Research(B), Grant Number: JP20H02311, Principal Investigator: Tomohiro Kobayashi) and JST SPRING, Grant Number JPMJSP2138.

6 REFERENCES

- Adachi, Y., Ikegaya, N., Satonaka, H., & Hagishima, A. (2020). Numerical simulation for cross-ventilation flow of generic block sheltered by urban-like block array. *Building and Environment*, *185*, 107174. <https://doi.org/10.1016/j.buildenv.2020.107174>
- Chu, C.-R., Chiu, Y.-H., Tsai, Y.-T., & Wu, S.-L. (2015). Wind-driven natural ventilation for buildings with two openings on the same external wall. *Energy and Buildings*, *108*, 365–372. <https://doi.org/10.1016/j.enbuild.2015.09.041>
- Daish, N. C., Carrilho da Graça, G., Linden, P. F., & Banks, D. (2016). Impact of aperture separation on wind-driven single-sided natural ventilation. *Building and Environment*, *108*, 122–134. <https://doi.org/10.1016/j.buildenv.2016.08.015>
- Ghiaus, C., Allard, F., Santamouris, M., Georgakis, C., & Nicol, F. (2006). Urban environment influence on natural ventilation potential. *Building and Environment*, *41*(4), 395–406. <https://doi.org/10.1016/j.buildenv.2005.02.003>
- Golubić, D., Meile, W., Brenn, G., & Kozmar, H. (2020). Wind-tunnel analysis of natural ventilation in a generic building in sheltered and unsheltered conditions: Impact of Reynolds number and wind direction. *Journal of Wind Engineering and Industrial Aerodynamics*, *207*, 104388. <https://doi.org/10.1016/j.jweia.2020.104388>
- Ikegaya, N., Hasegawa, S., & Hagishima, A. (2019). Time-resolved particle image velocimetry for cross-ventilation flow of generic block sheltered by urban-like block arrays. *Building and Environment*, *147*, 132–145. <https://doi.org/10.1016/j.buildenv.2018.10.015>
- Jiang, Y., & Chen, Q. (2002). Effect of fluctuating wind direction on cross natural ventilation in buildings from large eddy simulation. *Building and Environment*, *37*(4), 379–386. [https://doi.org/10.1016/S0360-1323\(01\)00036-1](https://doi.org/10.1016/S0360-1323(01)00036-1)
- Jiang, Z., Kobayashi, T., Yamanaka, T., Sandberg, M., Kobayashi, N., Choi, N., & Sano, K. (2022). Validity of Orifice equation and impact of building parameters on wind-induced natural ventilation rates with minute mean wind pressure difference. *Building and Environment*, *219*, 109248. <https://doi.org/10.1016/j.buildenv.2022.109248>
- Mohammad, A. F., Ikegaya, N., Hikizu, R., & Zaki, S. A. (2021). Turbulence Effect of Urban-Canopy Flow on Indoor Velocity Fields under Sheltered and Cross-Ventilation Conditions. *Sustainability*, *13*(2), Article 2. <https://doi.org/10.3390/su13020586>
- Shirzadi, M., Tominaga, Y., & Mirzaei, P. A. (2019). Wind tunnel experiments on cross-ventilation flow of a generic sheltered building in urban areas. *Building and Environment*, *158*, 60–72. <https://doi.org/10.1016/j.buildenv.2019.04.057>
- Tominaga, Y., & Blocken, B. (2015). Wind tunnel experiments on cross-ventilation flow of a generic building with contaminant dispersion in unsheltered and sheltered conditions. *Building and Environment*, *92*, 452–461. <https://doi.org/10.1016/j.buildenv.2015.05.026>

A study on desiccant system regenerated by waste heat from home-use solid oxide fuel cell cogeneration system

Keita Mizuno¹, Isamu Ohta²

*1 Misawa Homes Institute of Research and Development Co., Ltd.
1-1-19, Takaidonishi
Suginami-ku, Tokyo, 168-0071, Japan
mizuno.k52@home.misawa.co.jp*

*2 Misawa Homes Institute of Research and Development Co., Ltd.
1-1-19, Takaidonishi
Suginami-ku, Tokyo, 168-0071, Japan
Isamu_Ohta@home.misawa.co.jp*

ABSTRACT

Since the spread of covid-19 in 2019, it is necessary to realize an indoor environment that takes measures against viral infections such as covid-19 and influenza virus. One method for realizing such an indoor environment is to control indoor humidity. In a high-humidity environment, mold grows, indoor air quality deteriorates, and physical fatigue increases. On the other hand, in a low-humidity environment, viruses easily suspend and the immune system gets weaker. Therefore, controlling indoor humidity is necessary for human health.

Furthermore, in order to achieve carbon neutrality by 2050, there is a need for significant energy savings in facilities. As energy-saving facilities, cogeneration systems such as those utilizing fuel cells are one of the effective methods. Exhaust heat from fuel cells is commonly used to supply hot water, but a lot of waste heat goes unused in summer and warm regions, because the demand for hot water supply is low. Therefore, by utilizing this unused waste heat to control indoor humidity, it is possible to save energy and improve the total energy efficiency of the fuel cells.

In this way, by researching a desiccant system that utilizes waste heat from home-use solid oxide fuel cell cogeneration system (hereafter Ene-Farm or EF), we aim to contribute to energy conservation and to realize an indoor environment that has a good influence on human health. The results were as follows:

- 1) Waste heat from the EF (about 450W) is transferred to desiccant system by water, and the amount of available waste heat at this system changes with the water flow rate. As a result of experiment how to maximize the amount of waste heat utilization, we were able to transfer 380W of heat, which is approximately 80% of the waste heat from the EF, to the desiccant system by setting the flow rate to 0.2L/min.
- 2) In order to maximize the dehumidification amount of the desiccant unit under the condition of 1), an experiment was conducted using the return air volume (RA) and outdoor air volume (OA) as parameters. A maximum dehumidification rate of 350g/h under summer conditions (outdoor:30°C75%, indoor:27°C50%) was obtained when RA was 160m³/h and OA was 160m³/h.
- 3) As a result of simulating the room size that can be controlled to an appropriate relative humidity environment (40% to 60%) with a dehumidification amount 350g/h, it is possible to control the room size of about 30 m² in Tokyo and about 20m² in Okinawa (the highest humidity environment in Japan).
- 4) As a result of a demonstration experiment in Okinawa, the indoor absolute humidity environment was 10g/kg' lower than the outdoor absolute humidity environment. Furthermore, we clarified the relationship between outdoor absolute humidity and indoor absolute humidity when this system was introduced.

KEYWORDS

desiccant, humidity control, fuel cell, waste heat utilization, cogeneration system

1 INTRODUCTION

Since the spread of covid-19 in 2019, it is necessary to realize an indoor environment that takes measures against viral infections such as covid-19 and influenza virus. One method for realizing such an indoor environment is to control indoor humidity. High humidity environments during summer promote mold growth, which can worsen air quality and have adverse effects on building materials and human health¹⁾. In addition, the high-humidity environment affects sweating and amplifies the feeling of physical fatigue²⁾. On the other hand,

in a low-humidity environment such as winter, viruses easily suspend and the immune system gets weaker³⁾⁴⁾⁵⁾. Therefore, it is necessary to control indoor humidity appropriately throughout the year in order to realize an indoor environment that takes human health into consideration.

Furthermore, COP21 held in Paris in 2015 proposed the goal of becoming carbon neutral by 2050, and COP27 held in 2022 reaffirmed the importance of achieving the 1.5°C target. Under such circumstances, building facilities are required to achieve significant energy savings to become carbon neutral, and waste heat recovery systems such as fuel cell systems (hereafter ENE-FARM or EF) are considered to be effective⁶⁾. However, EF usually use waste heat for hot water supply, but in summer and in hot and humid regions, the demand for hot water supply is low and unused waste heat is generated⁷⁾. The unused waste heat could be used for dehumidification in the summer and humidification in the winter. In addition to improving overall efficiency, the use of unused waste heat would also increase the operating hours and high-load operation of EF.

In this way, by researching a system that dehumidifies indoor air using the waste heat from the EF, the goal is to achieve an indoor environment that contributes to energy conservation while also being considerate of human health.

2 DESICCANT SYSTEM UTILIZING ENE-FARM WASTE HEAT

2.1 System Overview

Figure 1 shows the configuration of desiccant system utilizing the EF waste heat. The waste heat from the EF is recovered by the exhaust heat recovery heat exchanger and stored in the hot water storage tank. The hot water stored in the hot water storage tank is pumped from the top of the tank to the desiccant unit and used as pre-heat hot water for regeneration. After the water is used, it is returned to the lower part of the hot water storage tank and again pumped to the waste heat recovery heat exchanger. On the other hand, the desiccant unit is a rectangular rotor honeycomb element with a dehumidification/regeneration area ratio of 1:1, and uses a polymer sorbent that can be regenerated at low temperatures as the moisture absorbing material. On the dehumidification side, indoor air (RA) with high relative humidity, pre-cooled by medium-temperature cold water (20°C) generated by a chiller, is passed through the rotor to sorb moisture, and then the air, whose temperature rises due to sorption heat, is after-cooled to room temperature before being supplied (SA). On the regeneration side, outdoor air (OA) with low relative humidity due to waste heat from the EF is passed through the rotor to desorb moisture, and the rotor is regenerated, and the air containing moisture is exhausted to the outdoors (EA).

Table 1: EF and Desiccant unit specifications

EF specifications		Desiccant unit specifications	
Power generation capacity[W]	700	Desiccant	Polymeric sorbent
Waste heat utilization capacity [W]	430	Air volume of RA[m ³ /h] (Upper: Dehumidification experiment Lower: Humidification experiment)	120,140,160,180,200
Waste heat recovery temperature [°C]	65	Air volume of OA[m ³ /h] (Upper: Dehumidification experiment Lower: Humidification experiment)	80,120,160
Water flow rate from SOFC [L/min]	0.2,0.3		140,160,200
			200

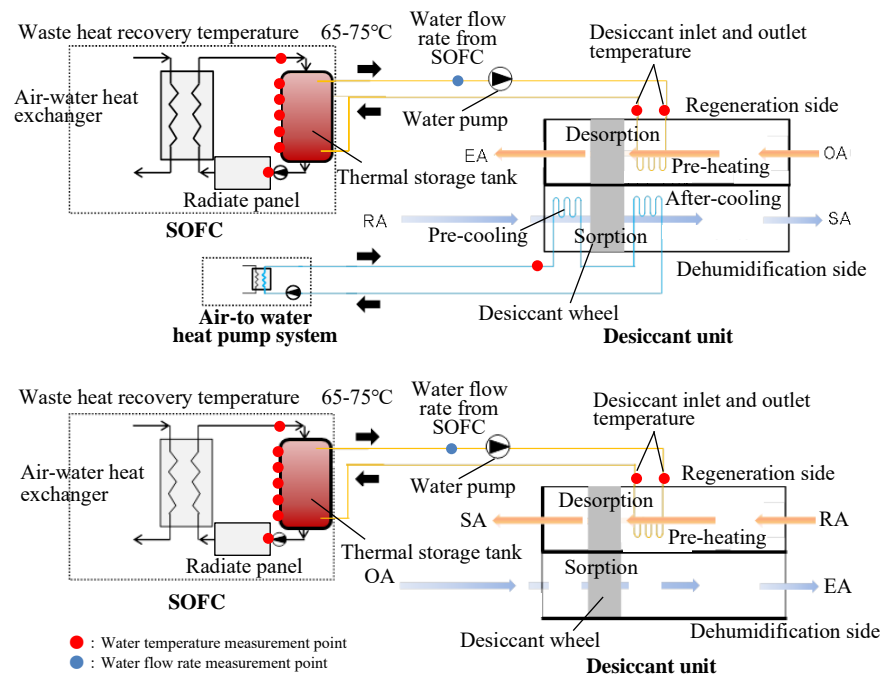


Figure 1: Diagram of desiccant system utilizing ENE-FARM waste heat
(Upper: Dehumidification, Lower: Humidification)

2.2 Optimization of waste heat utilization condition

2.2.1 Experiment Overview

Figure 2 and Table 2 show the 1st floor plan and measurement summary of the demonstration house. The EF has a 28L hot water storage tank and provides approximately 430W of waste heat at a rated power generation of 700W. The conditions for the use of EF waste heat were organized in a two-story wooden experimental housing in Aichi, Japan. The target rooms for measurement were the 1st floor LDK + Japanese-style room space, and the target rooms floor area and rooms volume were 44.5 m² and 110.4 m³, respectively. The measurement period was 6/4/2019-9/23/2019. The parameters of the demonstration are the flow rate of water supplied to the desiccant unit (0.2,0.3L/min).

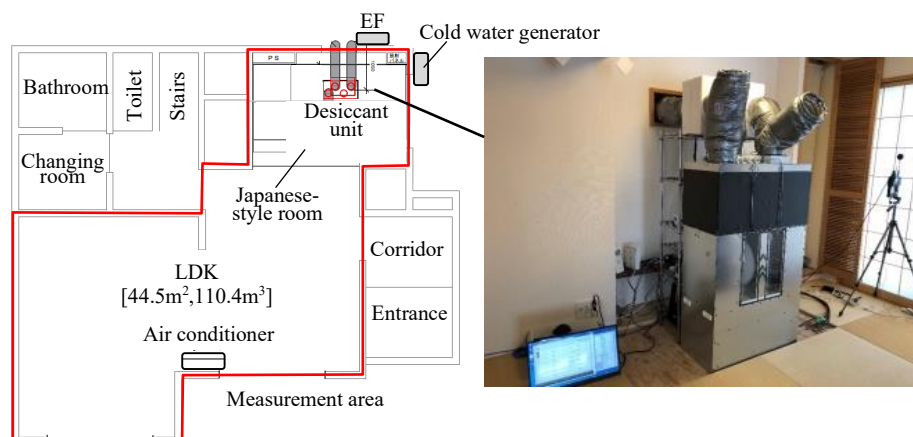


Figure 2: Experimental housing in Aichi, Japan

Table 2: Overview of experimental housing

Experimental housing	
Site	Aichi, Japan
Construction	Wooden framework method
Floor area[m ²]	67.8
Measurement area[m ²]	44.5
Measurement Volume[m ³]	110.4
Q (Heat loss coefficient) [W/(m ² · K)]	1.8
C (Equivalent leakage area) [cm ² /m ²]	2.5
Measurement period	6/4/2019-9/23/2019 (Excluding self-maintenance periods)

2.2.2 Results of experiments

The left panel of Figure 3 shows the outlet temperature of air-water heat exchanger for and the hot water temperature supplied to the desiccant at the flow rates of 0.2 L/min and 0.3 L/min. The outlet temperature of air-water heat exchanger was stable at about 65°C at both flow rates. However, the hot water temperature supplied to the desiccant was stable at 62–63°C, approximately 10°C higher when the flow rate was 0.2 L/min. This is because the 0.2L/min flow rate was generally consistent with the waste heat recovery flow rate, and the high-temperature water that remained at the top of the hot water storage tank could be used in a stable manner. The low flow rate and low return temperature to the hot water storage unit also reduced the amount of heat dissipated from the radiator.

The Right panel in figure 3 shows the amount of waste heat used in the desiccant unit during the mid-season and summer when the water flow rate is 0.2 L/min, which allows stable hot water to be obtained. Of the approximately 430 W of waste heat generated by the EF, approximately 355 W was used by the desiccant unit. This means that about 80% of the heat emitted from the EF was utilized in the desiccant unit in both the mid-season and summer seasons.

From the above, this condition is considered to be the condition that can maximize the use of the waste heat from EF. Therefore, using these conditions, the dehumidification capacity conditions of the desiccant unit were examined in the next chapter.

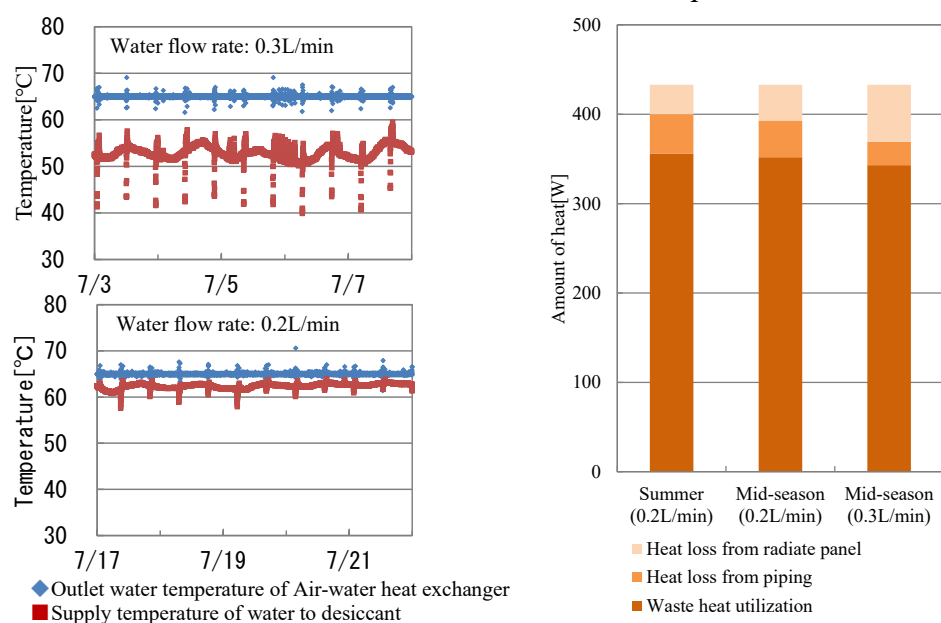


Figure 3: Experimental results graph

(Left panel: Relationship between outlet water temperature of air-water heat exchange and supply temperature of water to desiccant, Right panel: Breakdown of waste heat)

2.3 Experiments to maximize dehumidification and humidification capacity

2.3.1 Experiment Overview

Figure 4 and Table 3 show a plan of the environmental test chamber and an overview of the experiment. This experiment was conducted from 3/9-3/19/2020 in a 2-room environmental laboratory in Ibaraki, Japan. The area and volume of the warm room (WR) and cool room (CR) were 16.2 m² and 64.8 m³ and 24.3 m² and 97.2 m³, respectively. The temperature and humidity setting conditions for each room were 30°C and 75% (outdoor conditions) for WR and 27°C and 50% (indoor conditions) for CR. A desiccant unit was placed on the CR side, and OA and EA ducts were installed on the WR side using sleeves installed in the insulated partition wall. Parameters were determined based on prior numerical analysis and preliminary experiments; RA airflow rates of 120, 140, 160, 180, and 200 m³/h and OA airflow rates of 140, 160, and 200 m³/h were used as parameters. The optimum air volume that would result in the maximum dehumidification of this system under the above conditions was studied.

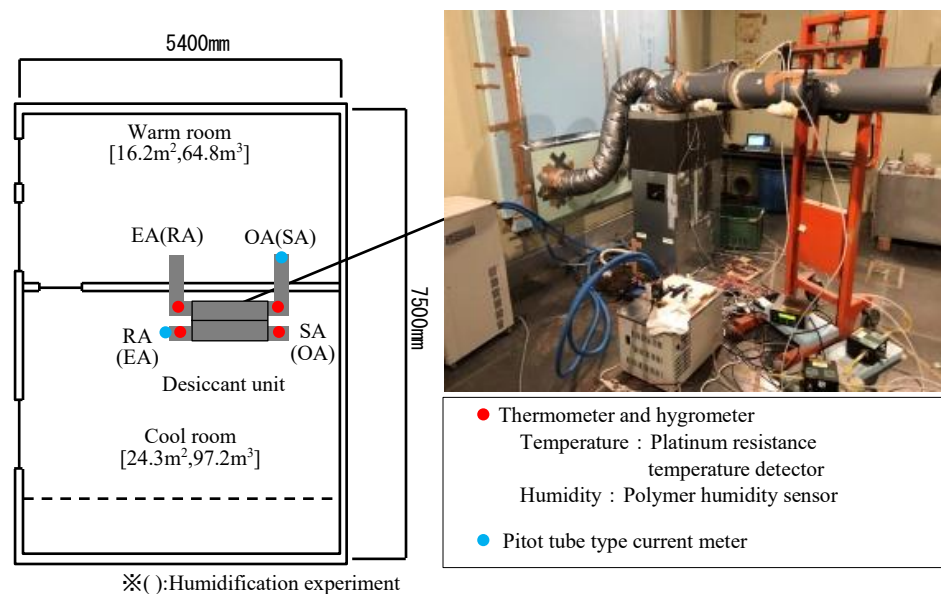


Figure 4: Environment test room

Table 3: Overview of environment test room

Environment test room	
Site	Ibaraki, Japan
Floor area[m ²]	Warm room:16.2 Cool room:24.3
Room capacity[m ³]	Warm room:64.8 Cool room:97.2
Setting temperature[°C] and humidity[%] (Upper: Dehumidification experiment Lower: Humidification experiment)	Warm room:30[°C],75[%],Cool room:27[°C],50[%] Warm room:22[°C],40[%],Cool room:5 [°C],50[%]
Measurement period	3/9/2020-3/19/2020

2.3.2 Results of experiments

The left panel of Figure 5 shows the amount of dehumidification for each RA and OA airflow rate. The peak dehumidification amount was at 160 m³/h for both air volumes, with a maximum dehumidification rate of 352 g/h. These conditions are the conditions under which the effects of pre-cooling and pre-heating can be greatly obtained. As for the effect of pre-

cooling, the air in front of the dehumidifying side wheel could be made low temperature and high humidity. As an effect of preheating, the air in front of the wheel on the regeneration side was made high temperature and low humidity. As a result, the relative humidity difference between the air in front of the wheel on the dehumidification side and the regeneration side became larger, which is thought to have increased the amount of dehumidification.

The Right panel of Figure 5 shows the dehumidification process at maximum dehumidification: RA at 27.5°C, 56.8%, 13.1 g/kg' became high relative humidity to 22.2°C, 76.1% by pre-cooling using cold water (20°C, 2L/min), and after passing through the wheel and after-cooling it became 25.2°C, 55.6%, 11.2 g/kg' and about 1.9 g/kg' of SA was dehumidified. The transition of SA from after pre-cooling is almost on the enthalpy on the air diagram. Furthermore, since it is close to the dehumidification limit, it can be assumed that the sorption and desorption process of the wheel is generally optimized.

On the other hand, the humidification rate tended to increase as the RA air volume decreased, reaching a maximum of 310 g/h at RA air volume of 80 m³/h and OA air volume of 200 m³/h. It is assumed that the low RA air volume and slow air velocity in the desiccant unit were the reasons for the large effect of preheating. As a result, the air before sorption could be made less humid and the humidification amount could be increased. In addition, looking at the humidification process, there is a possibility that further increase in humidification can be expected since the transition is not on the enthalpy.

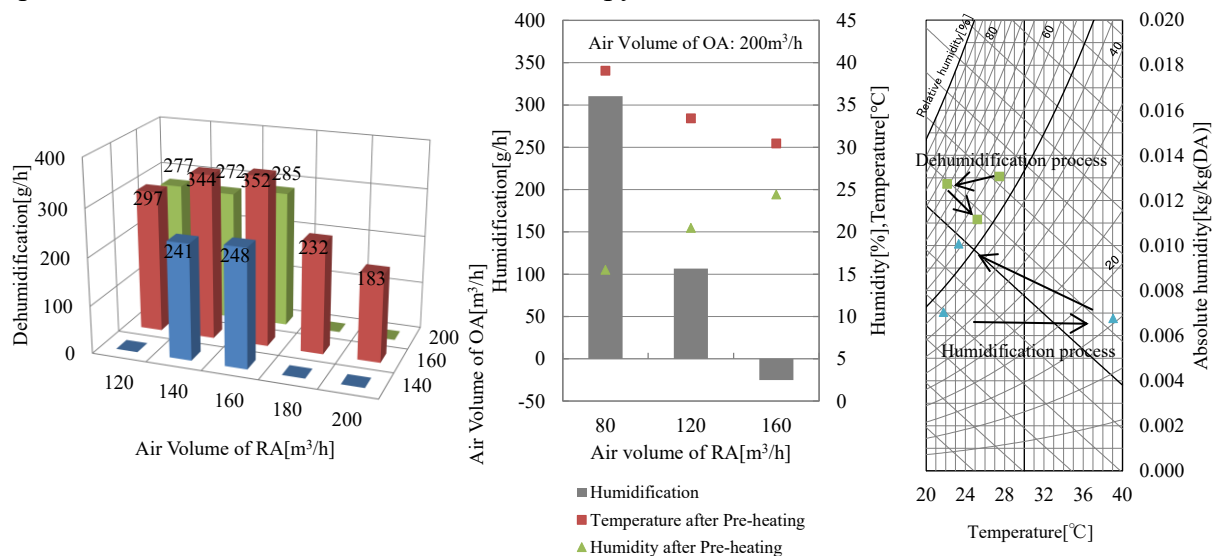


Figure 5: Diagram of the results of the experiment (Left panel: Dehumidification by air volume, Central panel: Relationship between humidification and humidity, Right panel: Dehumidification and humidification process)

2.4 Study of the effect of improving indoor humidity environment

2.4.1 Simulation Overview

The effect of this system on improving the indoor humidity environment was investigated. Figure 6, Table 4 shows a simulation outline. The system operating conditions were dehumidification operation (dehumidification volume 350 g/h) from the first day the outdoor air temperature exceeded 25°C since June, and humidification operation (humidification volume 300 g/h) from the first day the outdoor air temperature fell below 15°C since November. During the rest of the year, ventilation, air exchange rate, was set at 0.5 times/h. AE-CAD/SimHeat⁽⁸⁾⁽⁹⁾ was used as the simulation software, and standard year EA meteorological data 2000 (Tokyo) was used as the meteorological data. The housing model was designed with

a total floor area of 124.0 m², a room volume of 444.6 m³, a U_A value of 0.40 W/(m²K), and a latent heat capacity of 41.9 kJ/(m³(g/kg'))¹⁰, with the LDK (31.3 m², 88.9 m³) as the target living room. The heating/cooling schedule, human body humidification, and equipment humidification schedule were based on energy conservation standards of Japan. However, in order to evaluate the effect of the desiccant system's dehumidification and humidification capabilities, only sensible heat treatment was considered in the air conditioners, not latent heat treatment.

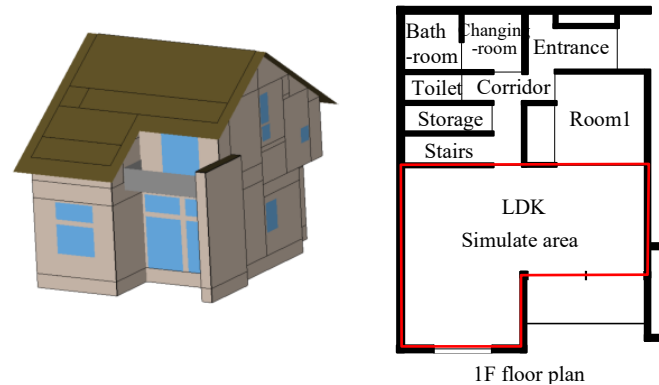


Figure 6: Simulation model

Table 4: Simulation outline

Simulation outline	
Simulation software	AE-CAD/SimHeat
Weather data	Standard EA weather data (Tokyo)
Number of people	4
Simulation room area and volume	LDK(1F):31.3[m ²],88.9[m ³]
U _A value	0.4[W/(m ² · K)]
Room latent heat capacity	41.9[kJ/(m ³ (g/kg'))]
Ventilation appliance	0.5[Times/hour] Temperature exchange efficiency: 70[%] Humidity exchange efficiency: 40[%]
Desiccant system	6/15-9/30: Dehumidity (350[g/h]) 11/1-4/15: Humidity (300[g/h]) Other than the above : Ventilation (air exchange rate:0.5[Times/h])

2.4.2 Results of simulation

The left panel of Figure 7 shows the absolute humidity transition with and without this system. During the dehumidification period, the indoor humidity could be dehumidified to less than 12 g/kg' while the outdoor humidity was more than 15 g/kg'. During the humidification period, the indoor was able to be humidified to about 7 g/kg' while the outdoor was dry at about 4 g/kg'. Generally, an indoor relative humidity of 40-60% is recommended. It can be determined that a comfortable indoor humidity environment can be achieved by increasing the time within this range. Therefore, The Right panel of Figure 7 shows the percentage of annual indoor relative humidity occurrence. Without the system, about 30% of the year's relative humidity fell within the 40-60% range, but with the system, about 67% of the year's relative humidity fell within the recommended range. There were time periods during the dehumidification period when the relative humidity fell below 40% and time periods during the humidification period when the relative humidity exceeded 60%. However, this could be resolved by controlling the start-up and shutdown of the system, and considering the control of the system, approximately 88% of the time periods were within the recommended range of 40-60% relative humidity.

From the above, it was found that this system, which performs dehumidification using about 355 W of waste heat of EF, can improve the indoor humidity environment in a living room of about 30 m².

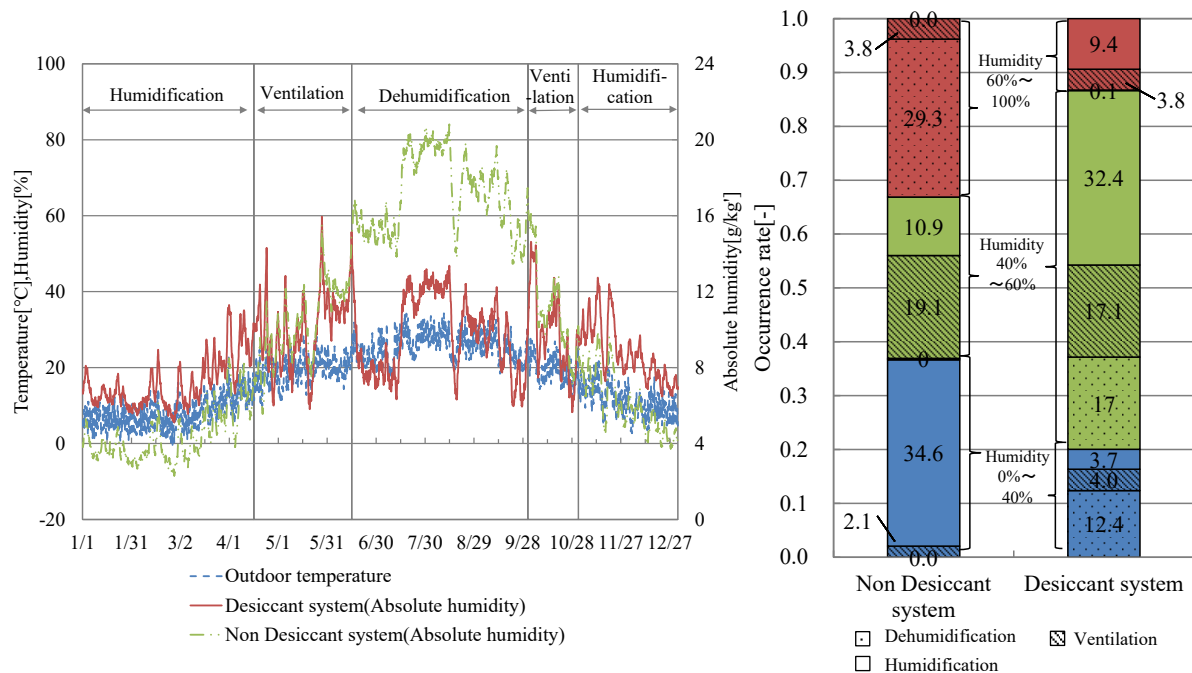


Figure 7: Diagram of the results of the simulation
(Left: Transition of outdoor temperature and indoor absolute humidity, Right: Occurrence rate of humidity)

2.5 Indoor environment measurement in actual environmental conditions

2.5.1 Demonstration Overview

Figure 8 shows an overview of the demonstration. In order to understand the effect of this system on the indoor humidity environment, a demonstration test was conducted in Okinawa, which has the harshest humidity environment in Japan and high demand for dehumidification. This demonstration was conducted in a room of a two-story RC building with an area of 16.5 m², assuming the LDK of a typical house. The measurement period was from 6/1/2021 to 8/31/2022, excluding the winter period. In addition, EF is operated as rated continuous operation, and the waste heat utilization conditions and the operating conditions of the desiccant unit are conducted under the conditions described in the previous chapter.



Experimental housing	
Site	Okinawa, Japan
Construction	Reinforced concrete (RC)
Floor area[m ²]	16.5
Volume[m ³]	39.6
C Value[cm ² /m ²]	1.8
Measurement period	6/1/2021-8/31/2022

Figure 8: Overview of the demonstration site

2.5.2 Demonstration Results

Figure 9 shows the indoor temperature, relative humidity, and absolute humidity for one day during the rainy season. By installing this system, the indoor relative humidity can be dehumidified to less than 60% even on days when the outdoor relative humidity exceeds 80%. The indoor absolute humidity was about 10 g/kg', which is about 5 g/kg' lower than the outdoor.

The left figure in Figure 10 shows dehumidification by indoor environment. No significant changes in dehumidification were observed under the summer environment, indicating that this system was able to demonstrate stable dehumidification capacity. Although the amount of dehumidification decreased in low-temperature environments such as the rainy season compared to the summer season, this was not considered a problem because the indoor environment was at the appropriate humidity level.

The right figure in Figure 10 shows the relationship between outdoor and indoor absolute humidity. Under the high humidity environment exceeding 20 g/kg', the indoor environment was able to achieve 5 to 10 g/kg' lower than the outdoor air. It can be said that this system has realized a humidity environment favourable to the building and human body throughout the year.

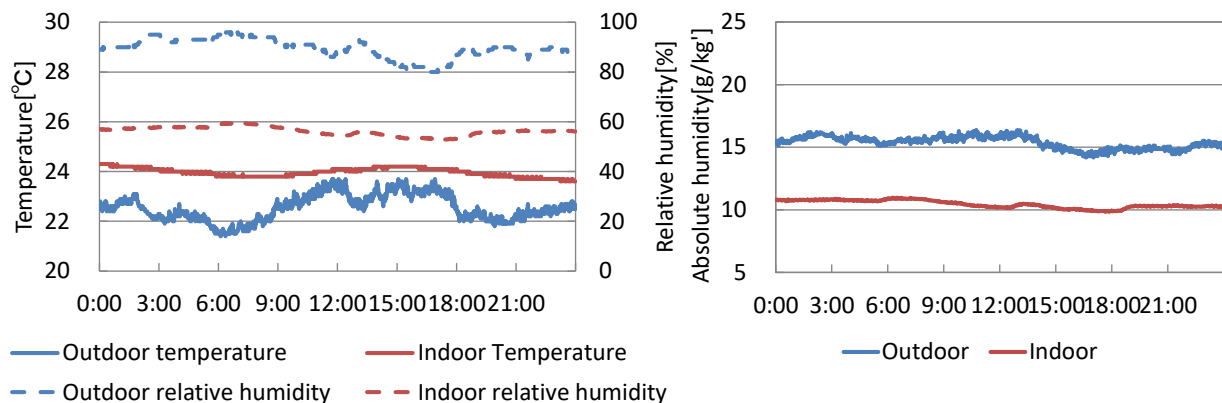


Figure 9: Indoor environmental transition during rainy season

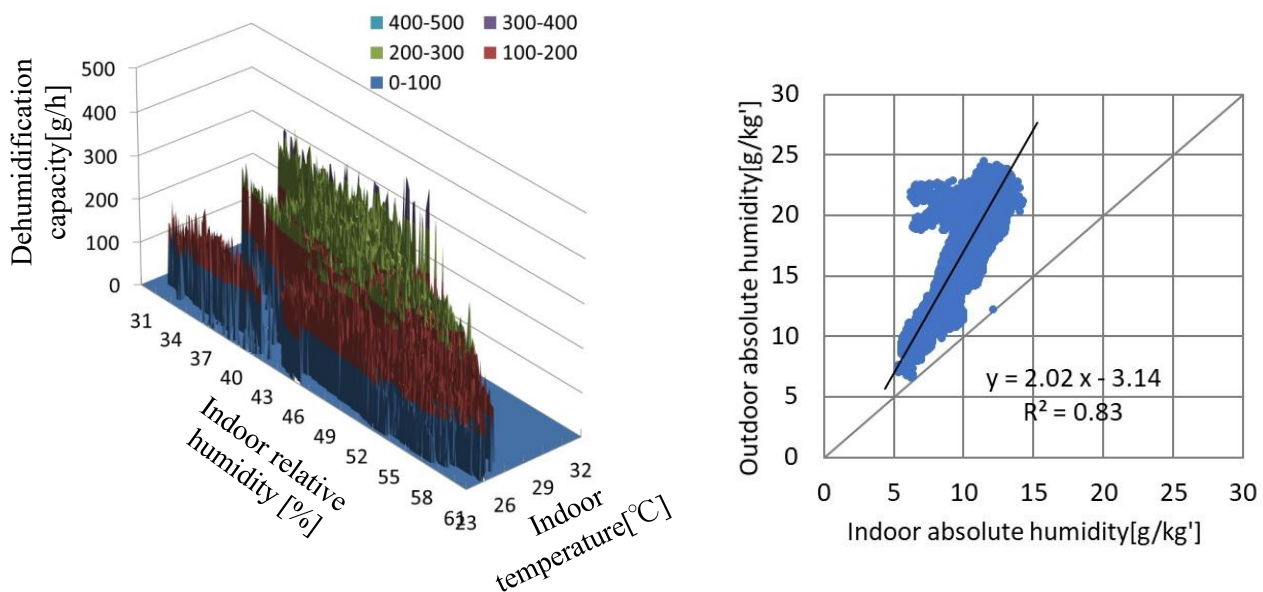


Figure 10: Left figure: Amount of dehumidification for each indoor environment, Right figure: Relationship between indoor and outdoor absolute humidity

3 CONCLUSIONS

A dehumidification system was proposed as a method of utilizing the exhaust heat from the EF, and the performance of the system was evaluated and the indoor environment was assessed through actual measurements. The following are the findings obtained.

- 1) Waste heat from the EF (about 450W) is transferred to desiccant system by water, and the amount of available waste heat at this system changes with the water flow rate. As a result of experiment how to maximize the amount of waste heat utilization, we were able to transfer 380W of heat, which is approximately 80% of the waste heat from the EF, to the desiccant system by setting the flow rate to 0.2L/min.
- 2) In order to maximize the dehumidification amount of the desiccant unit under the condition of 1), an experiment was conducted using the return air volume (RA) and outdoor air volume (OA) as parameters. A maximum dehumidification rate of 350g/h under summer conditions (outdoor:30°C 75%, indoor:27°C 50%) was obtained when RA was 160m³/h and OA was 160m³/h.
- 3) As a result of simulating the room size that can be controlled to an appropriate relative humidity environment (40% to 60%) with a dehumidification amount 350g/h, it is possible to control the room size of about 30m² in Tokyo.
- 4) As a result of a demonstration experiment in Okinawa, the indoor absolute humidity environment was 10g/kg' lower than the outdoor absolute humidity environment. Furthermore, we clarified the relationship between outdoor absolute humidity and indoor absolute humidity when this system was introduced.

4 REFERENCES

- 1)Pradeep Kumar (2021) *Biological contaminants in the indoor air environment and their impacts on human health, Air Quality, Atmosphere & Health 14, 1723-1736*
- 2)Jing Feng Zhang (2014).*A basic study on the effects of ambient air temperature and humidity on the heat stress of human body. Journal of the Japan research association for textile end-uses, Vol.55, pp.756-765.*
- 3)Jeffrey Shaman (2009). *Absolute humidity modulates influenza survival, transmission, and seasonality, Proc Natl Acad Sci USA., 106(9), 3243-3248*
- 4)Lisa M. Casanova (2010) *Effects of air temperature and relative humidity on coronavirus survival on surfaces, Applied and environmental microbiology, Vol.76, No.9, 2712-2717*
- 5)Seizaburo Harata (2004) *Relationship between absolute humidity and influenza prevalence in odate and akita cities, akita prefecture, in 2001 and 2002 (in Japanese), The Japanese Association for Infectious Diseases, Vol.78, 411-419*
- 6)Takahiro Yamamoto (2020). *Study of energy saving effect and catch up to electric demand of fuel cell for residence with detailed measurement survey in an actual house. (in Japanese) J. Environ. Eng., AIJ, Vol.85 No.767, 45-54*
- 7)Koki Yaku (2014). *Study on Performance Evaluation of Residential SOFC Cogeneration System. (in Japanese) The society of heating, air-conditioning sanitary engineers of Japan, No.203. 25-33*
- 8)Kenichi Miyajima (2005). *Development of CAD system for various environment simulation programs and combined simulation program of heat and ventilation. Part1 outline of CAD system and simulation program. (in Japanese), Proceedings of Academic Conference., AIJ, Environmental Engineering II, pp119-120*
- 9)AE-CAD/SimHeat, AE solutions inc. [online]http://ae-sol.co.jp/?page_id=66
- 10)Council for Coordination among Organizations involved in Home Performance Assessment (in Japanese) (2004). *Guidelines for Testing Based on Benchmark Test Results for Annual Heating and Cooling Load Calculation Methods for Thermal Environment*

Method for Evaluating an Air-Conditioning System with Natural Ventilation by Coupled Analysis of a Building Energy Simulation Tool and Computational Fluid Dynamics

Ryuichi Yasunaga¹, Yasuyuki Shiraishi¹

*1 The University of Kitakyushu
1-1 Hibikino, Wakamatsu Kitakyushu, Fukuoka, Japan*

ABSTRACT

In office buildings, an air-conditioning system with natural ventilation can reduce cooling loads and create a comfortable indoor environment. However, it is difficult to predict the performance of such systems and there is concern that the natural ventilation will create an uneven indoor thermal environment. In this paper, we propose a method for evaluating the performance of a natural-ventilation air-conditioning system by coupling a building energy simulation tool and computational fluid dynamics. In addition, we analysed the office building in which the system was installed and verified the prediction accuracy of the proposed method by comparing the simulation results with actual measurements. It was confirmed that the proposed method has sufficient accuracy.

KEYWORDS

Natural ventilation, Office building, Building energy simulation tool, CFD, Coupled analysis

1 INTRODUCTION

In recent years, air-conditioning (A/C) systems that incorporate natural ventilation to reduce cooling loads and achieve a comfortable indoor environment have attracted increasing attention. However, because the amount of natural ventilation is greatly affected by weather conditions, it is difficult to predict quantitatively, and there is concern that the natural ventilation will create an uneven indoor thermal environment. In addition, no uniform performance evaluation method for such systems has been established. Building energy simulation (BES) tools have attracted attention as a comprehensive analysis tool for evaluating the performance of buildings. However, such tools represent the physical quantity of the room as a single node and cannot consider the non-uniformity of the room environment.

Therefore, in this paper, we propose a method for evaluating the performance of an A/C system that considers the heterogeneity of the indoor environment by coupling the BES tool and computational fluid dynamics (CFD). In addition, we analysed a real office building in which the system was installed and verified the prediction accuracy of the proposed method by comparing the simulation results with actual measurements.

2 BUILDING CASE STUDY

In the office building targeted in this study (Fig. 1), outdoor air is introduced through inlets capable of supplying a constant airflow. These inlets are situated at the northern and southern ends of the workspace. The air travels through a shaft in the centre of the workspace and exits through the northern and southern outlets in the upper part of the shaft (Fig. 2). A building

energy management system (BEMS) is installed in the building, through which automatic control of the indoor environment, equipment, and facilities is carried out based on sensor information collected both inside and outside the building. The determination of whether natural ventilation is effective or not is made based on the conditions shown in Table 1, and if all conditions are met, the mechanism for natural ventilation will be activated.



Figure 1: Building exterior

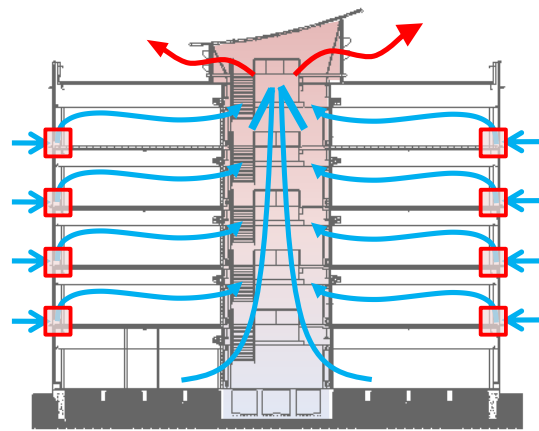


Figure 2: North-south vertical cross section

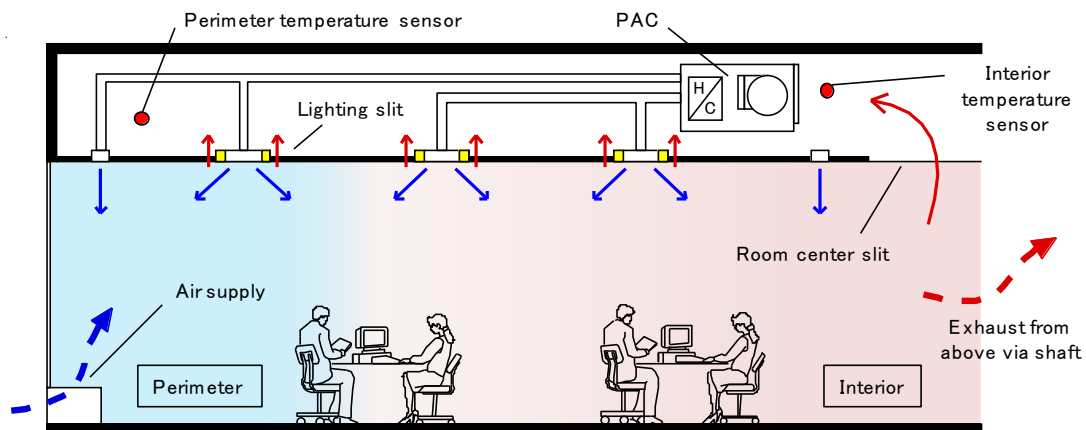


Figure 3: A/C system using natural ventilation

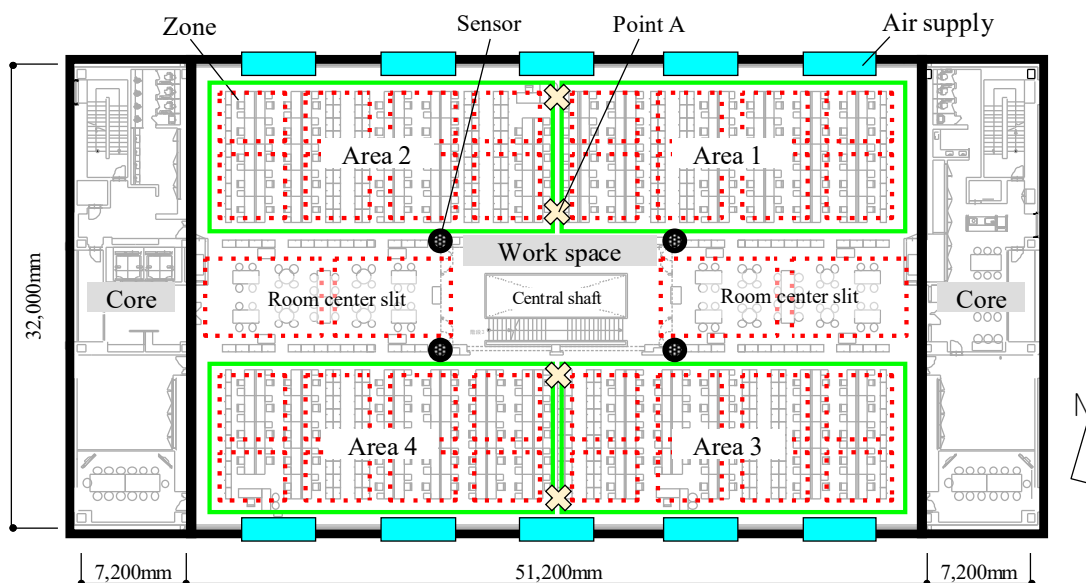


Figure 4: Floor plan

Table 1: Conditions for natural ventilation effectiveness

1. Enthalpy	Outdoor enthalpy < Indoor enthalpy
2. Outside temperature	16 °C < Outdoor temperature < 26 °C
3. Humidity	5 °C DP < Dew point (DP) < 16 °C DP
4. Indoor temp	Indoor temperature setting – 4 °C < Indoor temperature

3 MEASUREMENT

3.1 Overview of measurements

Measurements were performed for one month, from May 1 to 31, and the items for which data were collected are shown in Table 2. The estimated ventilation rate was calculated by multiplying the area of each air supply outlet by the wind speed value at the centre point of each air supply outlet. The accuracy of the estimation method was verified and correction methods were determined in advance based on preliminary measurements¹⁾. The heat generated by the equipment and lighting was estimated from the power consumption data of the BEMS. The solar load was measured by monitoring the amount of solar radiation on the north–south vertical surfaces on the third floor. In addition, the CO₂ concentration was used to estimate the human heat load. The vertical temperature distribution on the third floor was measured at 0.1, 0.6, 1.1, 1.6, 2.2, and 2.8 m above the floor at each point A (Fig.4).

Table 2: Measured parameters

Natural ventilation	Wind direction/speed
	Outdoor temperature
	Outdoor dew point temperature
	Outdoor/Indoor enthalpy
	Indoor temperature
	Status of supply air vents (open/close)
	Supply air velocity
Heat load	Solar radiation
	Electricity consumption of outlets
	A/C power consumption
Others	Vertical temperature distribution
	CO ₂ concentration

3.2 Measurement results

May 10 was selected as the representative day because it had the most suitable weather conditions for natural ventilation during the measurement period. Figure 5 shows the time series variations of outdoor air temperature, outdoor dew point temperature, and heat load due to solar radiation on the third floor for the day. It was confirmed that May 10 was a clear day with an outdoor temperature between 15°C and 20°C, which is suitable for natural ventilation. Figures 6 and 7 respectively show the time series variation of the ventilation rate and internal load on the third floor on the representative day. The heat processed by the A/C system and natural ventilation will be discussed later in conjunction with the analysis results.

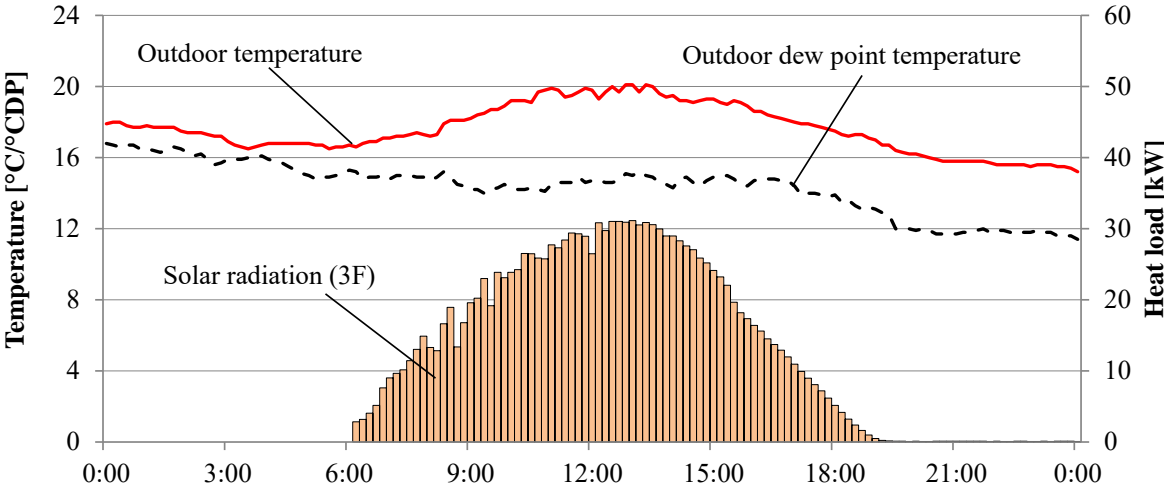


Figure 5: Outdoor temperature/dew point temperature and solar radiation

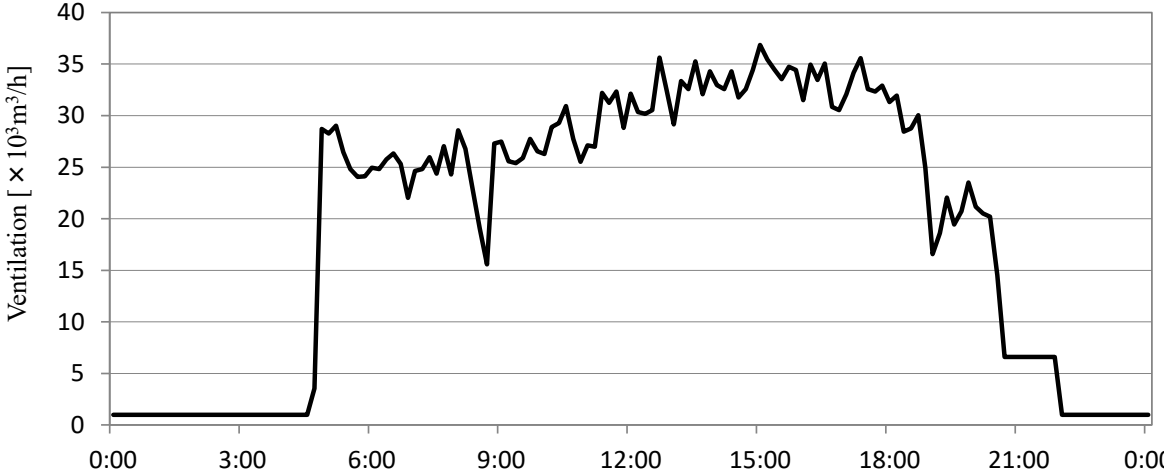


Figure 6: Ventilation volume on the 3rd floor

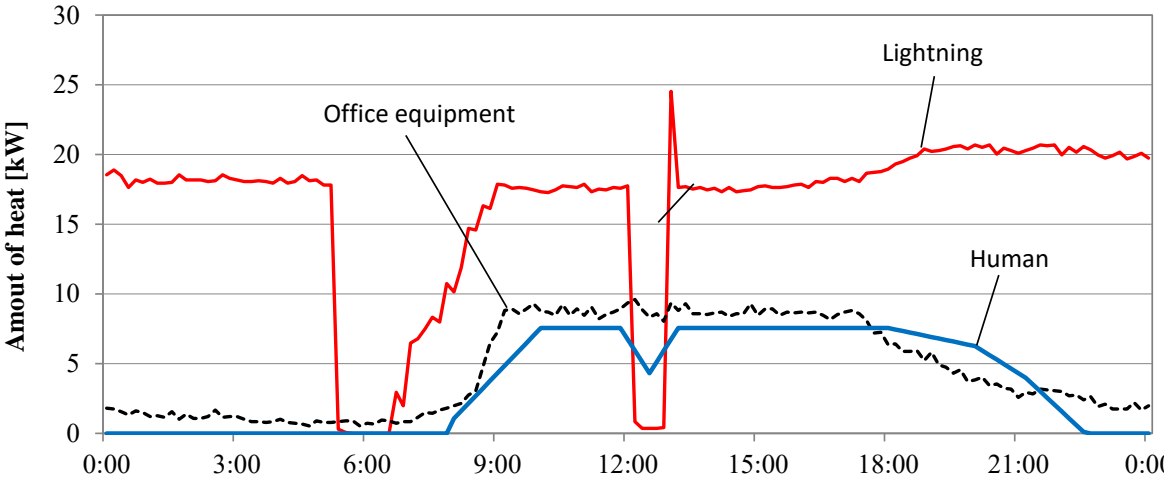


Figure 7: Internal heat load on the 3rd floor

4 ANALYSIS

4.1 Coupling analysis method for the BES tool and CFD

A CFD analysis was performed using the A/C module of BEST²⁾, a comprehensive BES tool (Figure 8). BEST creates a model of the A/C system by connecting various modules for the heating source, fans, and other components. We used a newly developed module for connecting CFD that was specifically designed for coupled analysis. In the steady-state analysis, we performed repeated non-steady coupled analyses between BEST and CFD and terminated the calculation when their fluctuations became sufficiently small.

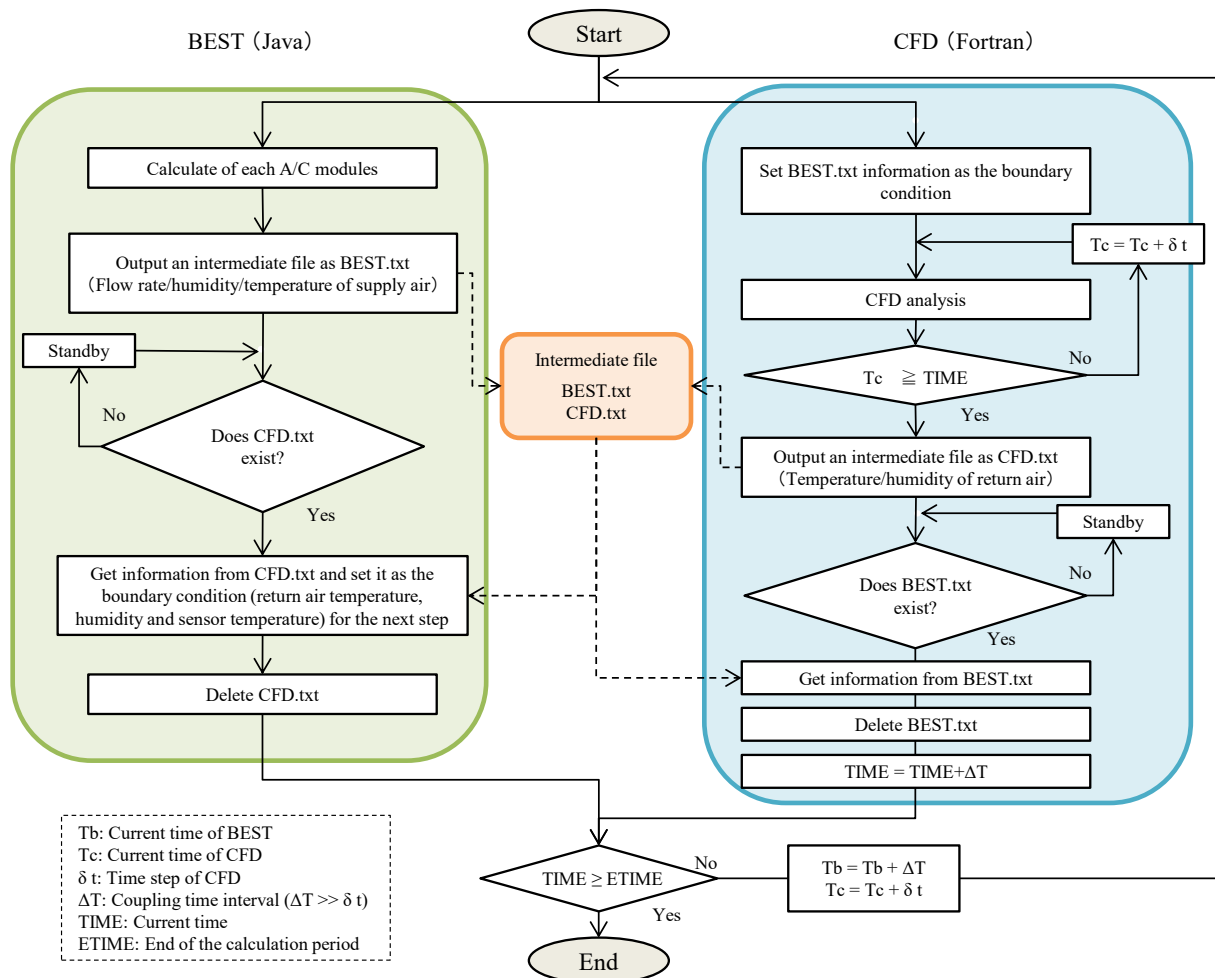


Figure 8: Analysis workflow

4.2 Analysis conditions

The analysis target was the office space on the third floor of the building. Table 3 shows the analysis conditions. Steady-state analyses were performed at five times (9:00, 11:00, 13:00, 15:00, 17:00) each day, and the accuracy of the analysis model was verified by comparing it with the measured values of the indoor A/C heat load and temperature distributions.

Table 3: Analysis conditions

Domain	32.0m(x)×51.2m(y)×4.45m(z)	
Mesh	452(x)×283(y)×39(z) = 4,988,724	
Mesh for radiation	7,291	
Turbulence model	Standard k-ε model	
Inflow conditions	A/C	Temperature: Proportional control Flow rate: 17.5 m ³ /min per unit $k_{in}=(U_{in}/10)^2$, $\epsilon_{in}=C_{\mu}^{3/4}k_{in}^{3/2}/\ell_{in}$
	Natural ventilation	Temperature: Outdoor temperature of the BEMS data Flow rate: BEMS data $k_{in}=3/2(U_{in}\times 0.05)^2$, $\epsilon_{in}=C_{\mu}^{3/4}k_{in}^{3/2}/\ell_{in}$
Outflow conditions	A/C	Fixed flow
	Natural ventilation	Fixed static pressure
Wall boundary conditions	Temperature: Fixed convection heat transfer coefficient 4.5 W/m ² K Speed: Generalized logarithmic law	
Outside boundary conditions	South/North: Sol-air temperature, Fixed heat transfer coefficient 23W/m ² K East/West: insulation	
Heating conditions	Lighting/Office equipment/Human/Solar radiation: Measured value	

U_{in} : supply wind speed [m/s]; k_{in} : turbulence energy [m²/s²]; ϵ_{in} : dissipation rate of k_{in} [m²/s³]; C_{μ} : model constant (= 0.09); ℓ_{in} : inlet length

5 RESULT

Table 4 shows the root mean square error (RMSE) value of the vertical temperature distribution for each time and Figure 9 also shows vertical temperature distributions at 9:00 and 15:00. The RMSE value was generally a low value of 1.0°C or less at all time points. Figures 10 and 11 show the measured and analytical values of the A/C heat load and the amount of heat removed by natural ventilation. The maximum error in the amount of heat was also a low value of about 10% at maximum.

The above results indicate that this analysis model has sufficient predictive accuracy, although actual phenomena such as airflow turbulence and unsteadiness due to fluctuations in natural ventilation cannot be reproduced in detail in this analysis.

Table 4: RMSE of vertical temperature distribution

Time	9:00	11:00	13:00	15:00	17:00
RMSE [°C]	0.45	0.66	0.98	0.75	0.97

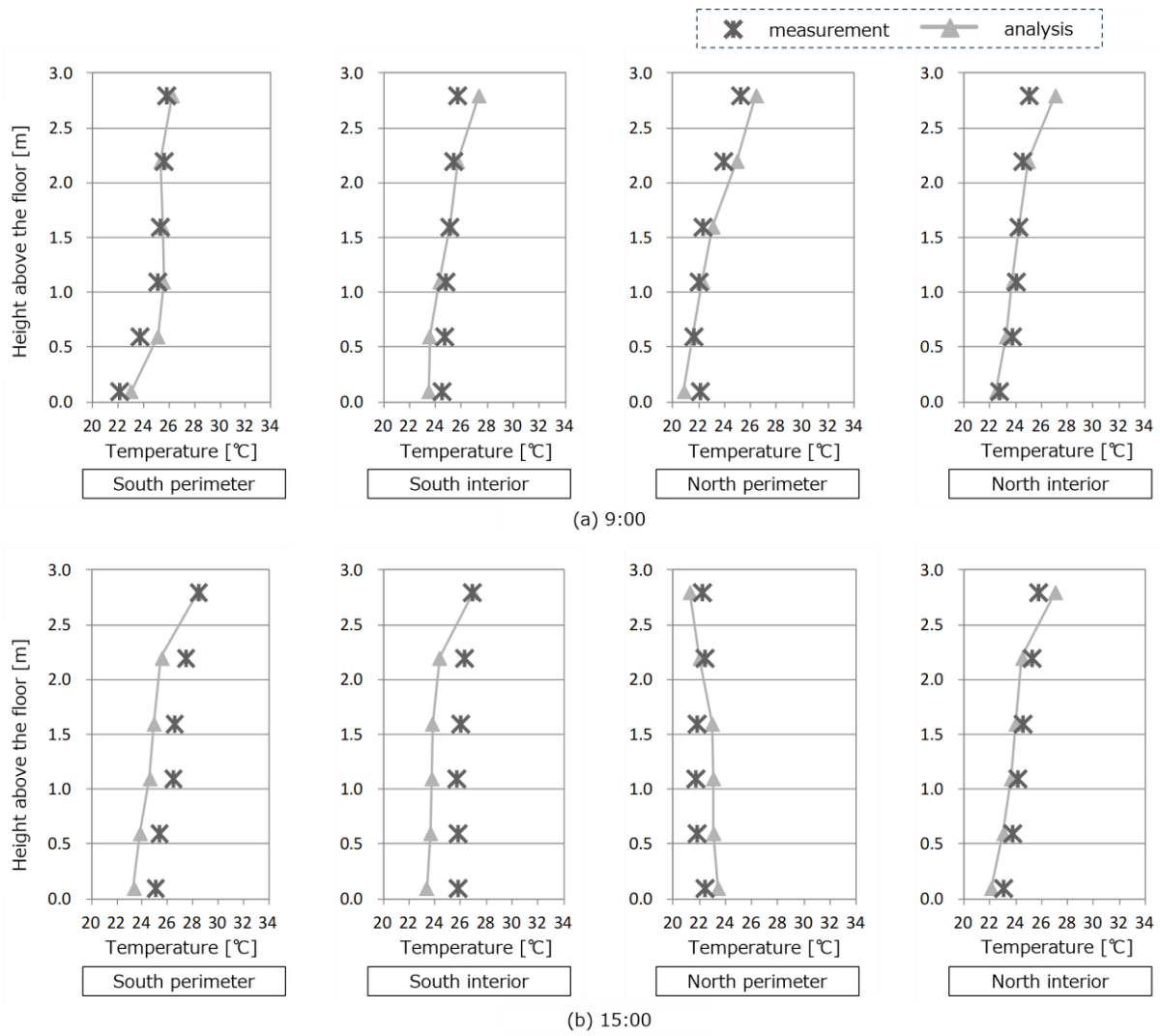


Figure 9: Vertical temperature distribution

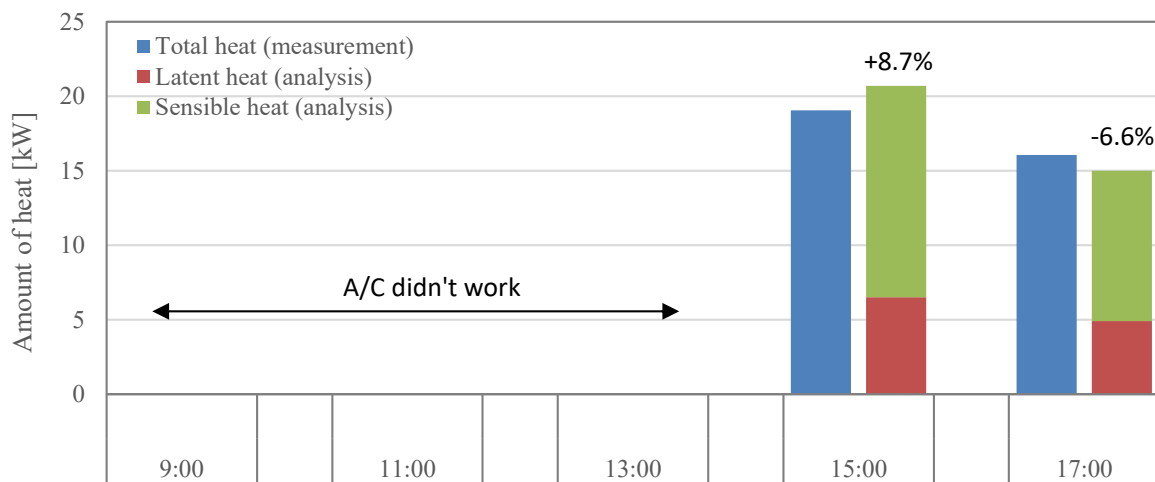


Figure 10: A/C heat load

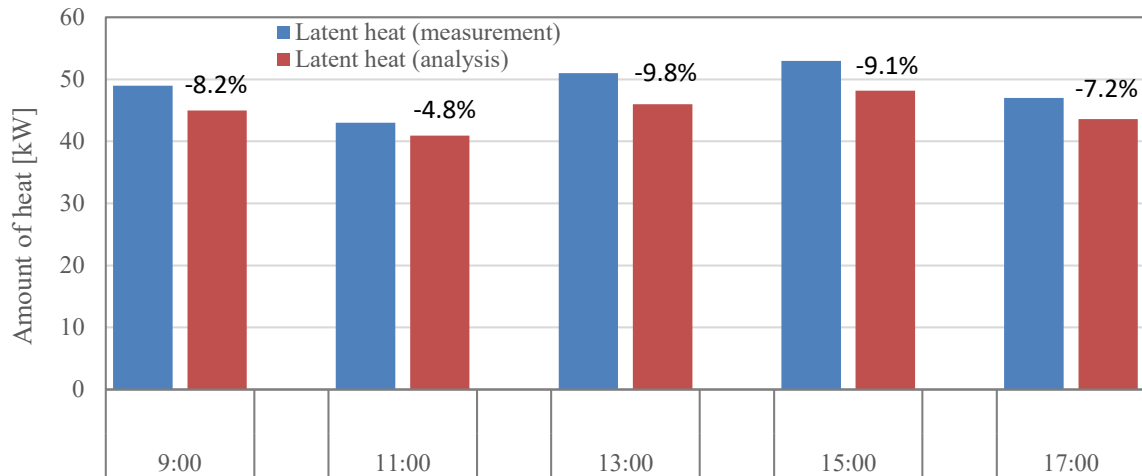


Figure 11: Amount of heat removed by natural ventilation

6 CONCLUSIONS

A method for evaluating the performance of A/C systems involving natural ventilation that combines a BES tool and CFD was proposed. A steady-state analysis was performed based on the proposed method for one floor of an existing office building, and the prediction accuracy of the proposed method was verified by comparing it with the measured values. The results confirmed that the proposed method has sufficient predictive accuracy. In the future, we plan to perform further verification of this analysis model under unsteady conditions and to verify the performance of this building's A/C system as a case study of the method.

7 REFERENCES

- 1) Yasunaga R., et al. (2012). Hybrid air-conditioning system using natural ventilation in an office building with flow control inlets and outlets (Part1), The Architectural Institute of Japan's Journal of Environmental Engineering, AIJ, Vol. 678, pp.681-688
- 2) Murakami S., et al. (2007-2014). Development of an Integrated Energy Simulation Tool for Buildings and MEP Systems, the BEST(Part 1-152), Technical Papers of Annual Meeting the Society of Heating, Air-conditioning and Sanitary Engineers of Japan, SHASE

ACKNOWLEDGMENT

This work was supported by JSPSKAKENHI Grant Number 20KK0102.

Performance comparison of different ventilation strategies in elderly care homes in Belgium

Douaa Al Assaad*¹, Quinten Carton¹, Abantika Sengupta¹, and Hilde Breesch¹

¹*KU Leuven, Department of Civil Engineering, Building Physics and Sustainable Design, Ghent Campus, Gebroeders De Smetstraat 1, 9000, Gent, Belgium*

ABSTRACT

Elderly people residing in nursing homes spend a vast majority of their times indoors and often in common recreation areas, to allow for socialization and interaction. Elderly people are a vulnerable age group. Hence, it is essential to provide them with good breathable air quality during these common activities and reduce cross contamination through ventilation. Prolonged exposures of elderly to contaminants may adversely affect their health, quality of life and increase medical expenditures due to frequent hospitalizations. In Belgian elderly care homes, 3 typical ventilation strategies are commonly found (natural ventilation, extract and balanced mechanical ventilation). The aim of this work is to determine the windows opening strategies and duration for the ventilation strategies to deliver good indoor air quality. The impact of window opening on thermal comfort and energy use during heating and cooling season will be assessed. To conduct this work, models of the common room and equipped systems were developed in Modelica. The performance was assessed using two indicators: ppm.hours (for CO₂), degree.hours, and days where RH(%) went outside the acceptable [30-70]% range.

KEYWORDS

Ventilation, elderly care homes, indoor air quality, energy use, occupant behaviour

1 INTRODUCTION

Indoor air pollution is a pressing public health issues given the fact that building policies are dictating airtight envelopes which gives rise to build-up of indoor contaminants. Thus, indoor concentrations of several contaminants can be significantly higher than those outdoors (Bruce et al., 2000). In modern day society, people spend 80-90% of their day in indoor environments. Notably, retired elderly people belonging to the vulnerable populations, residing in elderly care homes are likely to spend even more time indoors (Almeida-Silva et al., 2014). Thus, indoor air quality (IAQ) is of special concern in these types of spaces.

Many field studies in elderly care homes conducted in the EU have already shown poor IAQ and prolonged exposure to high levels of indoor pollution due to inadequate ventilation and its correlation to decreased health of elderly residents (Almeida-Silva et al., 2014; Annesi-Maesano et al., 2013). Exposure to indoor pollution is likely to become acute in the face of disruptive events or shocks such as pandemics. The COVID-19 pandemic has proven to be detrimental for elderly people's livelihoods. For vulnerable populations, acute exposure to high levels of contaminants or exposure to contagious pollutants can threaten their wellbeing and should be prevented with adequate ventilation.

During the pandemic, facility managers and health care workers operating the elderly care homes and taking care of the residents were advised to maximize window opening to dilute the concentration of contaminants, especially in common room areas. However, this can risk in increasing energy use and compromising thermal comfort without bringing much added benefits to IAQ.

The aim of this work is to determine the windows opening strategies and duration for the ventilation strategies to deliver good indoor air quality throughout the year. The impact of window opening on thermal comfort and energy use during heating and cooling season will be

assessed. Different building orientation were also considered. To conduct this work, models of the common room and equipped systems were developed in Modelica. The performance was assessed using two indicators: ppm.hours (for CO₂), degree.hours, and days where RH(%) went outside the acceptable [30-70]% range.

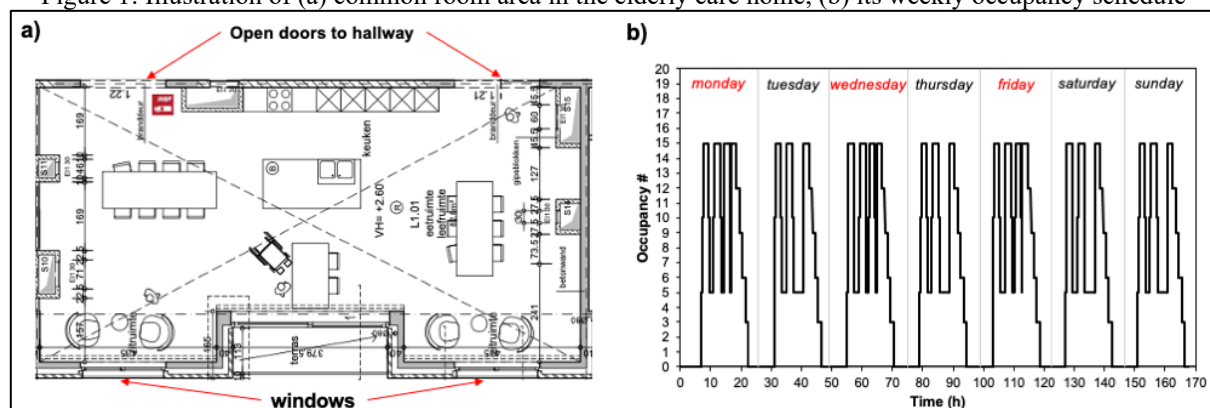
2 METHODOLOGY

2.1 Space and systems' description

Elderly care homes in Belgium are often multi-floor mid-sized buildings consisting of residential rooms, common rooms, utility rooms and offices for staff. Common rooms – of particular interest in this study, are recreational areas, where elderly residents take their meals (breakfast, lunch, and dinner), socialize, and/or conduct recreational activities (e.g., watching television). A typical common room (13.3 m × 6.8 m × 2.7 m) located in an elderly care home in the city of Gent, Belgium was considered in this work (**Figure 1a**). Based on the information provided by the Agency of care and health in Belgium (Home | Zorg En Gezondheid, n.d.), this room was occupied by a maximum of 15 people daily, corresponding to a maximum occupant density of 0.17 persons/m². The group of 15 residents of the elderly care home frequented the common room at least three times a day for meals. On average, there was always 5 people occupying the room. Three days of the week (Monday, Wednesday and Friday), group activities were conducted in the afternoon. The weekly occupancy schedule can be seen in **Figure 1b**.

The envelope of the common room consists of an external wall located on the southwest (SW) façade in the direction of prevailing winds (U-value = 0.21 W/m².K). The external wall had two double-glazed windows with a window to wall ratio of 0.48 and a U-value of 1.1 W/m².K. The opposite internal wall connected to the corridor and the rest of the internal walls connected to utility and laundry rooms. The rest of the boundaries (internal walls, floor, ceiling) were considered as 'adiabatic' to represent a zone within a larger floor plan with other floors above and below. The envelope was air-tight with a rate of 0.3 h⁻¹ (n-value).

Figure 1: Illustration of (a) common room area in the elderly care home, (b) its weekly occupancy schedule



In elderly care homes in Belgium, common rooms are usually ventilated by three types of ventilation systems depending on the type of construction:

1. **Natural ventilation** (found in old constructions): The windows served as inlet and a sanitary block located on the ceiling level in the hallway acting as a natural exhaust. Motorized windows opened automatically during occupied hours starting at 6:30 a.m. until 10:30 p.m. 4 different

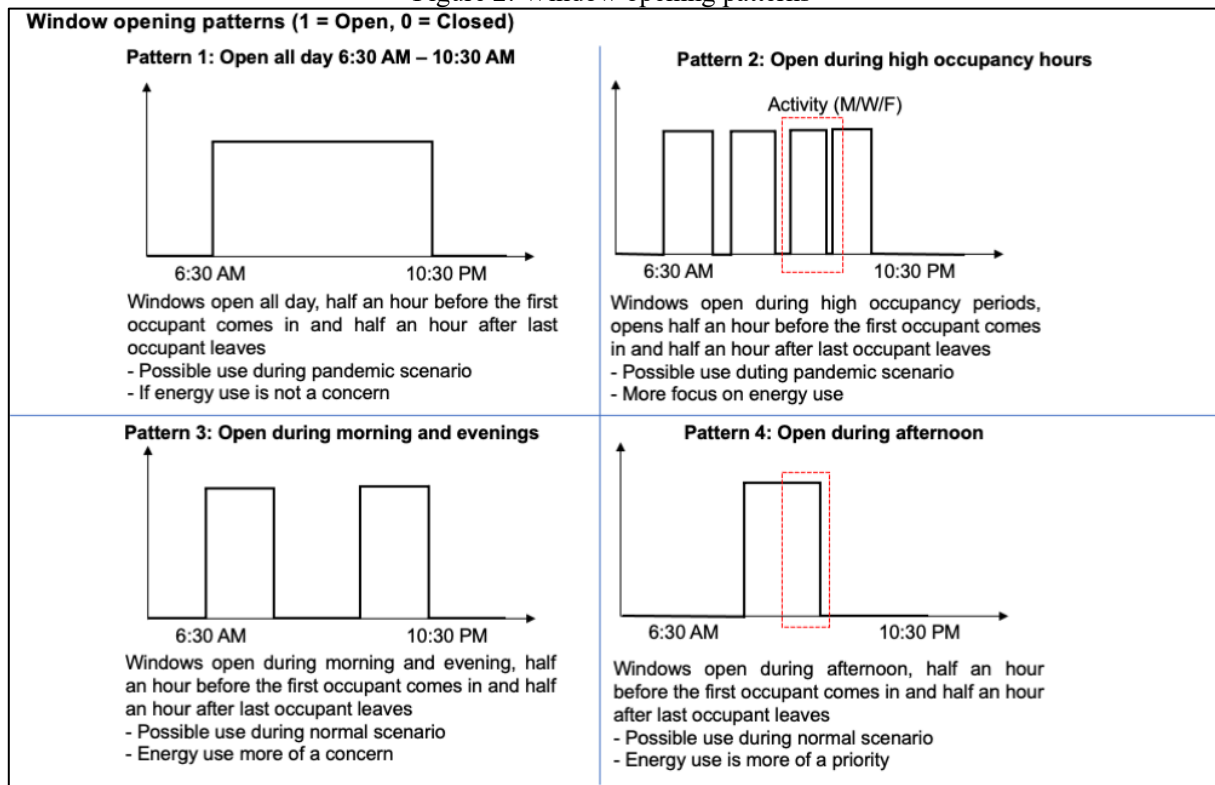
opening strategies will be tested and are illustrated in **Figure 2**. This system will be denoted as **System A** for the remainder of this work.

2. **System C** (found in more recent constructions): The polluted room air was exhausted from the room to the outdoors from a mechanical extract (local ceiling fan). For system C, the ceiling fan operated from 6:30 a.m. – 10:30 p.m. at a flow rate of 24 m³/h per person (IDA class 3) (Standard EN 13779), which is what is currently applied in elderly care homes in Belgium. The operation time of the fan was 16 hours. This might result in an insufficient ventilation capacity in current constructions which is why assistive window opening according to the strategies of **Figure 2** were applied. The effect of the different window opening strategies on energy costs will be reported and compared to an increase in mechanical ventilation capacity.

3. **System D** (found in more recent constructions): The polluted room air was exhausted from the room to the outdoors from a ceiling fan and replaced by outdoor clean air supplied from the ceiling level as well. For system D, the ceiling fan operated from 6:30 a.m. – 10:30 p.m. at a flow rate of 24 m³/h per person (IDA class 3) (Standard EN 13779), which is what is currently applied in elderly care homes in Belgium. The operation time of the fans was 16 hours. This might result in an insufficient ventilation capacity in current constructions which is why assistive window opening according to the strategies of **Figure 2** were applied. The effect of window opening on energy costs will be reported and compared to an increase in mechanical ventilation capacity.

The common room was equipped with radiators used to maintain the room temperature in the winter at an average of 22°C during occupied hours. During the cooling season, an active cooler was available and operated only if temperatures in the room exceed 26°C.

Figure 2: Window opening patterns



2.2 Pollution sources, IAQ and thermal comfort assessment

The pollution sources considered here were first CO₂ from outdoors and indoor generation due to occupancy respiration. The outdoor concentration was considered equal to 400 ppm and the occupant generation rate equal to 0.0037 l/s per person (Persily & de Jonge, 2017). For CO₂, the threshold in elderly care homes in Belgium was to be maintained at 1200 ppm, but that value was lowered to 900 ppm during the COVID-19 pandemic. In this work, an average threshold of 1000 ppm was assumed. Water vapor was also considered and was generated by occupancy (latent heat generation, 45 W under sedentary activities) and infiltrated from outdoors.

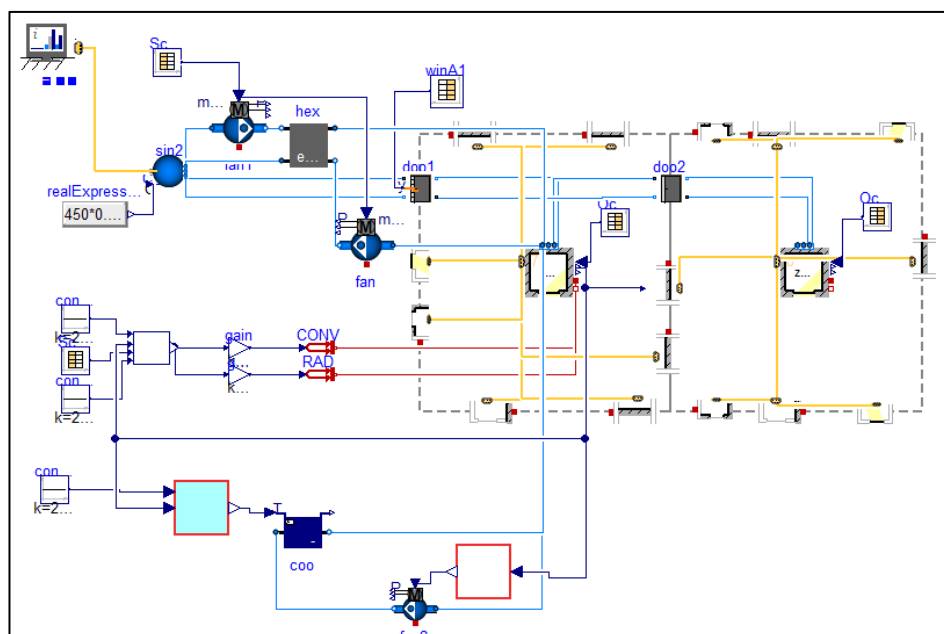
To compare the ventilation systems and the effect of the occupants' window opening patterns, the *ppm.hours* exceeding 1000 ppm were calculated for CO₂ during the occupied periods only. Thermal comfort was also assessed through the degree.hours of exceedance. The temperature threshold during the heating season (October through April) was equal to 22°C and 26°C during the cooling season (May through September). The amount of time that the RH(%) was spend outside the [30-70]% was also assessed as well as the cooling and heating energy usage.

2.3 Modelica models

To accurately compute the temporal variation of CO₂ concentrations in the common rooms, an appropriate model was needed. A simulation tool that can model the building dynamics, HVAC systems, their control, and varying events with different time scales, was needed. Hence, the Modelica language in the Dymola environment was selected (Dymola - Dassault Systèmes®) as it is an open-source, equation-based modeling language with an object-oriented structure. Modelica gives access to specific libraries that contain validated sub-models of the building envelope, systems, and their control. The “*Integrated District Energy Assessment by Simulation*” (*IDEAS*) library will be used in this work (Jorissen et al., 2018). Despite the use of validated sub-components, the full model still needs to be validated against measurement data. **Figure 3** shows the Modelica model of the common room as seen in Dymola for ventilation system D.

The model takes as input the TMY weather files and outdoor pollutants' concentrations using the simulation info manager as seen in **Figure 3**. The weather data collected from a weather station in Gent for the year 2022 was used (al Assaad Douaa et al., 2022). In the zone model, the envelope characteristics, occupancy schedule, sensible and latent heat generations from occupants (75 W and 45 W respectively during sedentary activities) were defined as well as the pollutants' generation rates. Sensible heat generation due to lights was defined in Modelica through the lux value (500 lux) in the zone model. The lights were LED that turned on during occupancy hours. Simulations were conducted for 1 day of the week (Monday) for no shock or base case scenario and shock scenarios.

Figure 3: Modelica model of the considered space with its heating, cooling, and ventilation system (illustrated is system D)



3 RESULTS AND DISCUSSION

The results section will first present an analysis of the indoor environmental quality in the elderly care home common room (IAQ, thermal comfort) and energy use while comparing the different systems during heating and cooling seasons. The results section will then conclude on the optimal window opening strategies for the different systems.

3.1 IAQ in the common room area

Figure 4 illustrates the ppm.hours of CO₂ exceeding the 1000 ppm threshold during heating and cooling seasons for systems A (natural ventilation), system C (mechanical extract, ACH = 1.5) and system D (balanced mechanical ventilation, ACH = 1.5), for 4 window opening patterns and for 4 different building orientations (window side facing either South, North, West and East).

According to **Figure 4**, the IAQ violations for all systems, for all building orientations and all window opening patterns were higher during the cooling season rather than the heating season due to unfavorable wind directions and speeds during the latter.

During the heating season, system D had the lowest IAQ violations followed by system A and finally system C. This applied to all four building orientations and for all the window opening patterns. System D had the best performance given the fact that it additionally supplies clean outdoor air unlike system C which only extracts contaminated air and relies on fresh air infiltration from the building envelope and trickle vents. Note that the infiltration was not that efficient given the airtightness of the building envelope. System A outperformed System C. This can be due to large pressure gradients created by opening of windows and the sanitary block in the hallway driving in considerable amount of fresh air to ventilate the room unlike system C, that relies on a mechanical extract.

During the cooling season, system D remained the highest performing for all building orientations and all window opening patterns. System C only outperformed system A for south oriented windows while system A outperformed system C. For all the different systems, when the duration of the window opening decreased, going from Pattern 1 to Pattern 4, the IAQ violations increased due to lower air change rates from natural ventilation. This was more pronounced in the heating season rather than the cooling season during which the wind directions and speeds were less favorable.

Figure 4: CO₂ ppm.hours for systems A, C and D for different window opening patterns during the heating and cooling seasons.

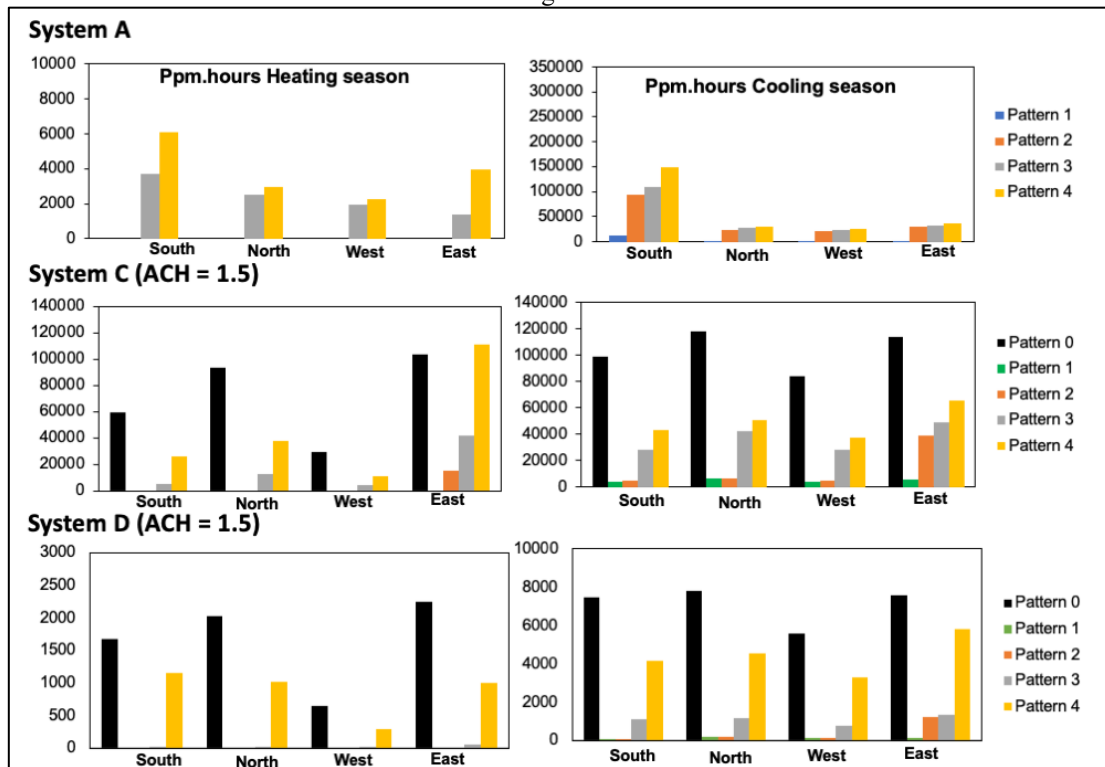
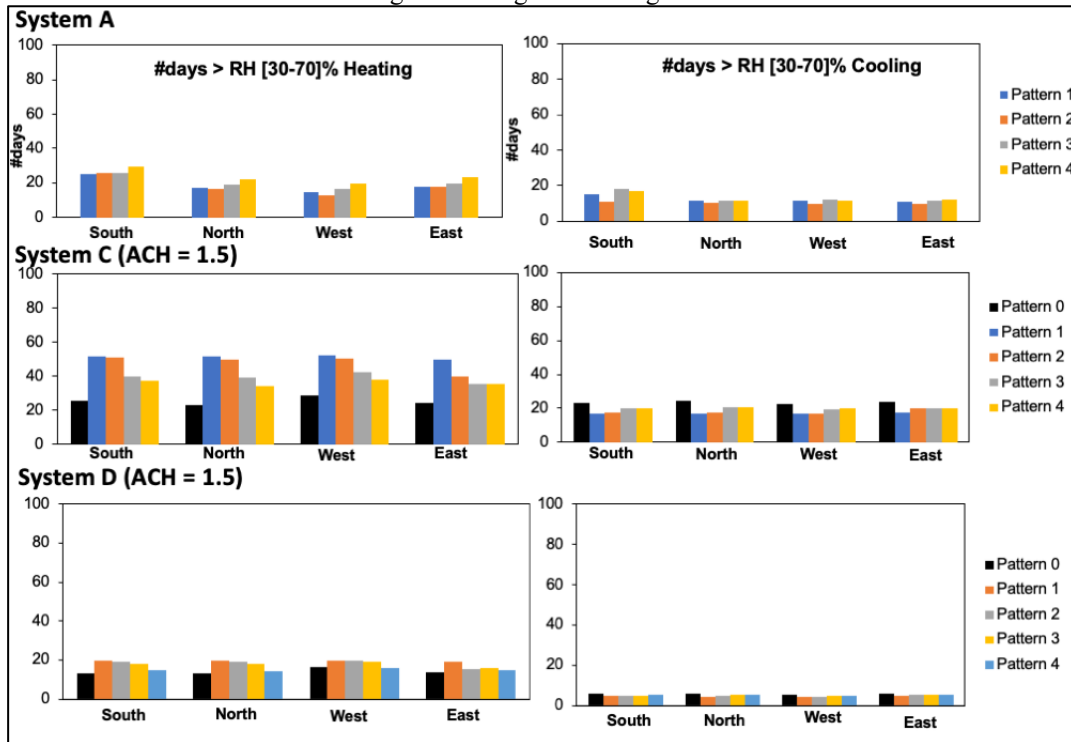


Figure 5 illustrates the number of days where RH(%) exceed the [30-70]% range during the heating and cooling seasons for systems A (natural ventilation), system C (mechanical extract, ACH = 1.5) and system D (balanced mechanical ventilation, ACH = 1.5), for 4 window opening patterns and for 4 different building orientations (window side facing either South, North, West and East). According to **Figure 5**, the number of days violating the RH(%) acceptable range were higher during the winter seasons than during the summer season. This was due to drier indoor conditions in winter due to heating and the longer duration of the heating season as compared to the cooling season. Additionally, with decreasing duration of window opening, the violations decreased during winter, however the effect was not that pronounced. It was even less pronounced during the cooling season. During the heating season and cooling seasons, similarly system D had the lowest violations followed by system A and closely by system C.

Figure 5: #days RH(%) exceeded [30-70]% range for systems A, C and D for different window opening patterns during the heating and cooling seasons.



3.2 Thermal comfort and energy use

Figure 6 illustrates the degree.hours exceeding the 22°C threshold during heating season and 26°C threshold during the cooling season for systems A (natural ventilation), system C (mechanical extract, ACH = 1.5) and system D (balanced mechanical ventilation, ACH = 1.5), for 4 window opening patterns and for 4 different building orientations (window side facing either South, North, West and East). **Figure 7** illustrates the corresponding heating and cooling power consumptions.

According to **Figure 6**, the violations during the heating season were much larger than those during the cooling season where the violations were rather negligible. In fact, during the cooling season, due to the moderate climate, the outdoor temperatures were not that high. Thus, no overheating occurred and the 26°C threshold was not violated. It follows that the power consumption during the cooling season was lower than during the heating season (**Figure 7**). Note that during the cooling season, the power consumption was comparable between the different systems. During the heating season, violations decreased with decreasing duration of window opening patterns given the lower amount of infiltrating outdoor air that needs to be heated. The same was observed during the cooling season but at lower rates.

Comparing the different systems, system C had the lowest violations due the low amount of infiltration as previously stated, followed by system D and finally A. It follows that the highest power consumption was for system A, followed by system D and closely by system C. Finally, between the building orientation, the south oriented windows had the lower power consumption demand given the high solar radiation on the south facades and thus a reduced amount of heating needed.

Figure 6: Degree.hours for systems A, C and D for different window opening patterns during the heating and cooling seasons.

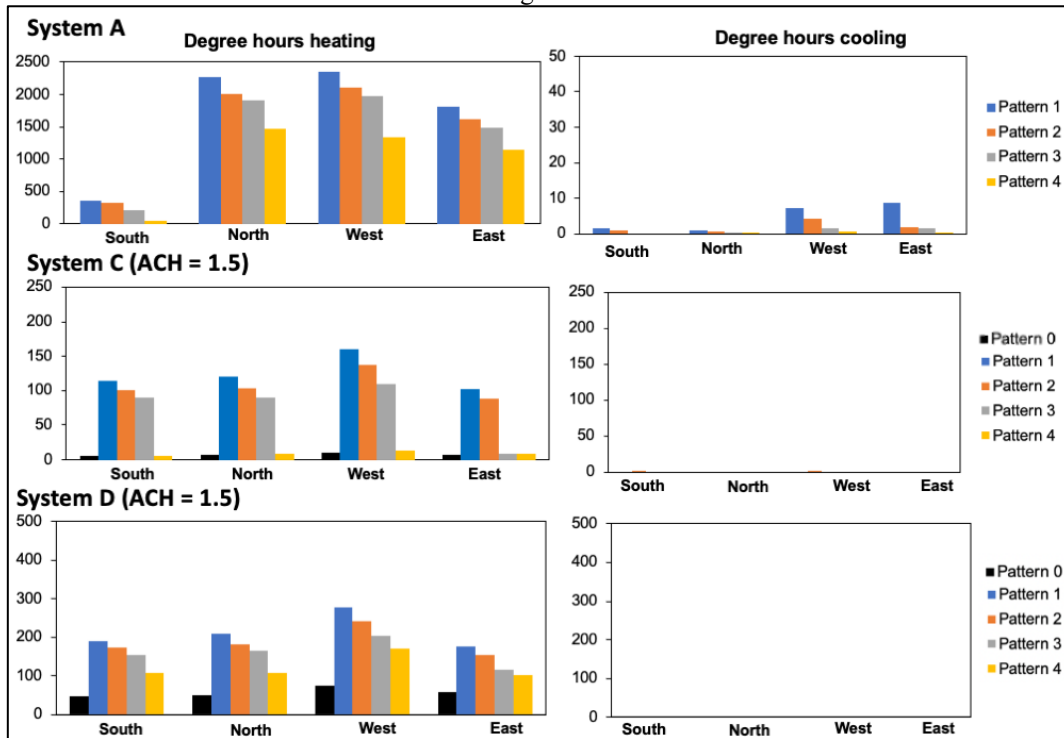
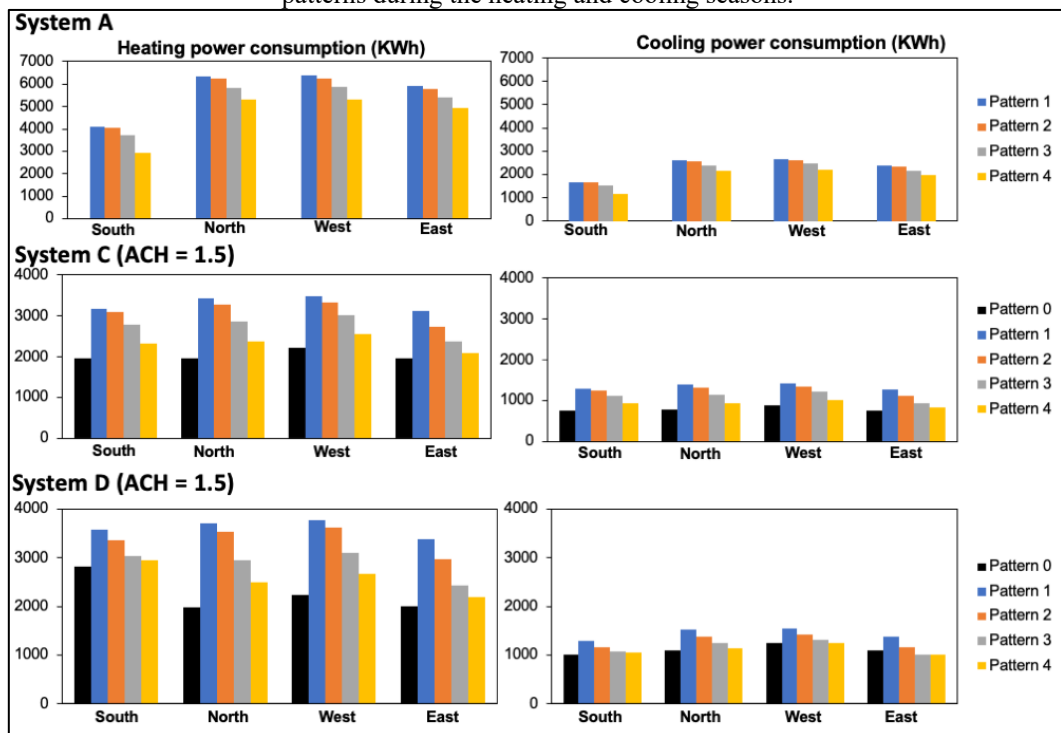


Figure 7: Heating and cooling power consumptions (KWh) for systems A, C and D for different window opening patterns during the heating and cooling seasons.



3.3 Window opening patterns

To determine the window opening patterns for each system, the analysis will rely on the ppm.hours and energy use. This is since the violations of degree.hours were not as high as the ppm.hours. Moreover, the discrepancy between the degree.hours of the different scenarios (systems, window patterns) were not as pronounced as the ppm.hours (**Figure 4-7**). In Belgium, there is no threshold values of acceptable yearly *ppm.hours*. A value of 30,000 ppm.hours was adopted in the Netherlands and was considered in this work. This was divided proportionally between the heating and cooling seasons (20,000 and 10,000 respectively).

For system A, during the heating season, windows can be kept open under Pattern 4 for IAQ benefits given the lower power consumption. During the cooling season, this can be Pattern 1 despite the higher power consumption due to the the significant IAQ violations of Patterns 2 to 4. This applies for all orientations.

For system C, during the heating season, for south oriented windows, an optimal case would be to replace the current fans with a fan that can supply an ACH of 2. For this scenario, the windows can be closed during the operation without having any IAQ violations and with the benefit of lower power consumption compared to an ACH of 1.5. However, if this is not possible, an ACH of 1.5 with a window opening Pattern 3 would be the better option as a compromise between IAQ and energy. The same applies for north and west orientations. However, for the East orientation, due to the significantly higher ppm.hours, it would be better to open the windows at Pattern 2 for slightly higher IAQ benefits. During the cooling season, for all orientations, it is better to resize the fan at ACH of 2 while closing windows as well. However, if this is not possible, an ACH of 1.5 with a window opening Pattern 1 would be the better option since energy use during the cooling season was not that high. Thus, it is better to take advantage of the IAQ benefits.

For system D, during the heating season, the windows can be opened even less (system D has higher IAQ performance). For all window orientations, an ACH of 1.5 with Pattern 0 can be suitable. During the cooling season, and for all window orientations, an ACH of 1.5 with Pattern 0 was also acceptable.

4 CONCLUSION

In this work, the possible window opening strategies in an elderly care home were studied for different existing pre-sized mechanical ventilation systems and natural ventilation strategies. The choice of window opening patterns were selected based on a compromise between IAQ and energy use between heating and cooling seasons since thermal comfort violations were not

as significant. Different building orientations were also considered. The obtained results are summarized in the table below:

Table 1. Window opening strategies

System type	Window opening strategy
Natural ventilation	Heating season: Pattern 4 (Open during afternoon): all orientations Cooling season: Pattern 1 (Open all day during occupied periods): all orientations
Mechanical extract (ACH = 1.5)	Heating season: Pattern 3 (open during morning and evening): south, west, north Pattern 2 (Open during high occupancy periods): east Cooling season: Pattern 1, all orientations
Balanced mechanical ventilation (ACH = 1.5)	Heating season: Windows can be kept closed (all orientations) Cooling season: Windows can be kept closed (all orientations)

5 ACKNOWLEDGEMENTS

The authors would like to thank the Flemish Fund for personal matters (VIPA) and the Agency of care & health for their support in this work.

6 REFERENCES

- [1] N. Bruce, ... R.P.-P.-B. of the W., undefined 2000, Indoor air pollution in developing countries: a major environmental and public health challenge, SciELO Public Health. (n.d.). <https://www.scielosp.org/pdf/bwho/v78n9/v78n9a04.pdf> (accessed January 13, 2023).
- [2] M. Almeida-Silva, H.T. Wolterbeek, S.M. Almeida, Elderly exposure to indoor air pollutants, *Atmos Environ.* 85 (2014) 54–63. <https://doi.org/10.1016/J.ATMOENV.2013.11.061>.
- [3] I. Annesi-Maesano, D. Norback, J. Zielinski, A. Bernard, C. Gratiou, T. Sigsgaard, P. Sestini, G. Viegi, Geriatric study in Europe on health effects of air quality in nursing homes (GERIE study) profile: objectives, study protocol and descriptive data, *Multidiscip Respir Med.* 8 (2013). <https://doi.org/10.1186/2049-6958-8-71>.
- [4] Home | Zorg en Gezondheid, (n.d.). <https://www.zorg-en-gezondheid.be/> (accessed January 11, 2023).
- [5] Standard EN 13779 | NBN Shop, (n.d.). https://www.nbn.be/shop/en/standard/nbn-en-16798-1-2019_8687/ (accessed January 11, 2023).
- [6] A. Persily, L. de Jonge, Carbon dioxide generation rates for building occupants, *Indoor Air.* 27 (2017) 868–879. <https://doi.org/10.1111/INA.12383>.
- [7] Dymola - Dassault Systèmes®, (n.d.). <https://www.3ds.com/products-services/catia/products/dymola/> (accessed February 11, 2022).
- [8] F. Jorissen, G. Reynders, R. Baetens, D. Picard, D. Saelens, L. Helsen, Implementation and verification of the IDEAS building energy simulation library, *J Build Perform Simul.* 11 (2018) 669–688. <https://doi.org/10.1080/19401493.2018.1428361>.

- [9] al Assaad Douaa, Sengupta Abantika, Breesch Hilde, Demand controlled ventilation in educational buildings: Energy efficient but is it Resilient?, *Building and Environment* . 226 (2022).

Sea Water Air Conditioning (SWAC): A Resilient and Sustainable Cooling Solution for hot and humid climates - Energy Performance and Numerical Modeling

Kanhan Sanjivy^{*1,2}, Olivier Marc³, and Franck Lucas¹

*1 GEPASUD, University of French Polynesia,
Faa'a, French Polynesia
*Corresponding author:
kanhan.sanjivy@doctorant.upf.pf*

*2 French Environment and Energy Management
Agency (ADEME)
20, avenue du Grésillé-
BP 90406 49004 Angers Cedex 01 France*

*3 PIMENT, University of Reunion Island,
Saint-Pierre, La Réunion, France*

ABSTRACT

Sea Water Air Conditioning (SWAC) is a highly efficient alternative to conventional air conditioning that uses deep seawater as a cooling source (Free Cooling). There are three SWAC installations in the world dedicated to cooling production in real-operating conditions, all located in French Polynesia due to its suitable bathymetry for SWAC installations and the high cooling needs of tropical climate. These installations provide cooling for two hotel complexes and a hospital center respectively in Bora Bora, Tetiaroa, and Tahiti.

The efficiency of SWAC has been demonstrated through the experimental assessment of the Tetiaroa installation, which showed that its Coefficient of Performance (COP) can range from 20 to 150, depending on the length of the distribution loop. These experimental results can also allow an accurate validation of a numerical model designed to study various operating scenarios to optimize performance, reduce costs, and expand the technology to areas with less favorable bathymetry than French Polynesia.

The development of such a design tool model is a necessary step for improving future installations and providing an accurate estimation of the capital costs (CAPEX) and operating costs (OPEX), which would greatly accelerate the development of SWAC technology and its visibility worldwide. This article presents a comprehensive examination of the SWAC technology as a resilient cooling solution for tropical climate. It includes a numerical model created using EnergyPlus and Python plugins, along with its experimental validation using Tetiaroa measurements for an operating period of one month.

KEYWORDS

Sea Water Air Conditioning (SWAC); Numerical Model; Experimental Validation; District Cooling (DC)

1 INTRODUCTION

The Intergovernmental Panel on Climate Change (IPCC) has identified an increase in cooling needs as one of the unavoidable consequences of global warming. This tendency is even more significant in tropical territories, where rising temperatures and changing weather patterns are already having a noticeable impact. The International Energy Agency (IEA) report titled “The Future of Cooling” also emphasizes the growing demand for cooling. The report states a need for space cooling expected to triple by 2050 because of combination of factors such as population growth, urbanization, and rising incomes. Such a surge will have a huge impact on energy consumption and greenhouse gas emissions as conventional air conditioning systems are energy-intensive and rely on refrigerants which are potent greenhouse gas (International Energy Agency (IEA) 2018). This article presents SWAC technology as a resilient cooling solution for tropical climates based on over two years of data from Tetiaroa installation. It includes a numerical model created using EnergyPlus and Python plugins, along with its experimental validation using an operating period of one month.

2 EXPERIMENTAL ANALYSIS

2.1 SWAC technology

Sea Water Air Conditioning (SWAC) is a type of free cooling system that uses Deep Ocean Water (DOW) as a cold source to cool buildings thanks to District Cooling (DC). SWAC technology has several advantages:

- Its efficiency is not limited by Carnot efficiency like mechanical refrigeration systems.
- Seawater temperatures remain relatively constant throughout the year.
- SWAC doesn't use any refrigerants like some other Air Conditioning (AC) system.

However, its deployment requires two main conditions, high cooling needs close to the sea and great depths near the coast.

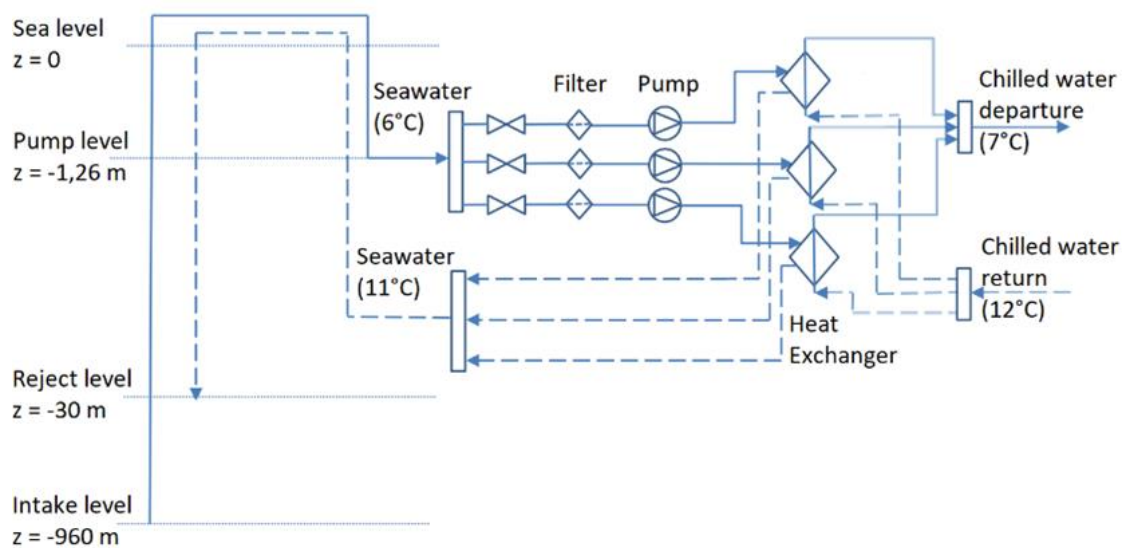


Figure 1: Operating process diagram of SWAC system

The SWAC system is represented above (Figure 1), it includes a drawing and a rejection pipeline. The drawing point is around 960 m depth, and the reject level is at 30 m depth with a technical area located 1.26 m deep in the ground. The technical area contains three pumps and three heat exchangers, combined with a district cooling system with the typical temperature regime 7/12°C. The seawater inlet temperature is about 6°C and 11°C for the return. The environmental impact of a deep seawater discharge was studied for an OTEC installation in Martinique and found that it had a minimal effect on the environment (Giraud, s. d.).

Table 1: Characteristics of SWAC installations in French Polynesia

Location	Year	Drawing pipeline length	Drawing pipeline diameter	Cooling power	Investment cost
Bora Bora	2006	2300 m	400 mm	1.6 MWf	5.5 M€
Tetiaroa	2011	2618 m	368/383 mm	2.4 MWf	10 M€
Tahiti	2022	3800 m	710 mm	6 MWf	30 M€

The SWAC alternative is a relevant solution for insular regions with a high energy cost, especially those having a suitable bathymetry with huge depths close to the shore like French Polynesia. There are three installations providing cooling for two hotel complexes and a hospital center respectively in Bora Bora, Tetiaroa, and Tahiti. Their characteristics are summarized in Table 1 (Sanjivy et al. 2023).

2.2 Experimental data

Experimental data of Tetiaroa SWAC system, including loop temperatures, heat flows, electric pump consumption and Coefficients of Performance (COP) will be presented over a two-year period. Data were averaged on a weekly basis after being processed using the Interquartile Range (IQR) method to remove outliers.

$$IQR = Q_3 - Q_1 \quad (1)$$

$$Q_1 - 1.5 * IQR < \mu < Q_3 + 1.5 * IQR \quad (2)$$

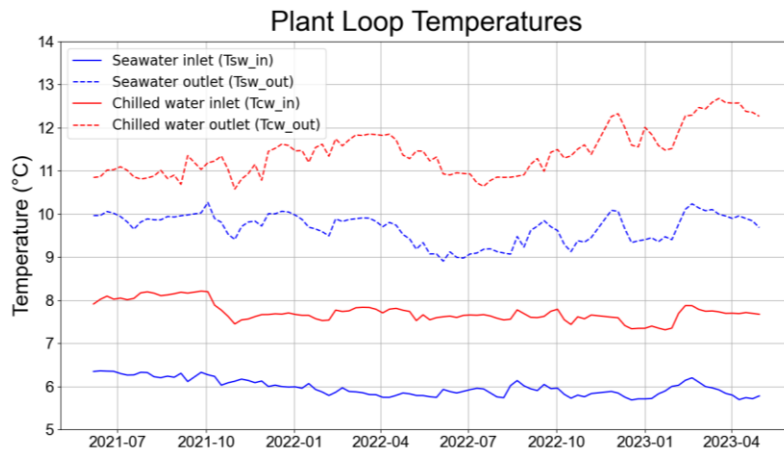


Figure 2: Seawater and chilled water temperatures

Temperatures at the heat exchangers inlet (T_{sw_in} ; T_{cw_in}) and outlet (T_{sw_out} ; T_{cw_out}) of each loop are depicted above. The seawater inlet temperature remains between 5.5 and 6.5°C throughout the year, depending on the primary flow rate. The greater the flow rate, the lower the thermal losses along the drawing pipeline. The chilled water inlet temperature is a constant temperature setpoint which controls the primary flow rate, it is generally fixed between 7.5 and 8°C. Both outlet temperatures vary depending on the building's cooling demand, around 9 and 10°C for the primary loop and 11 and 13°C for the secondary loop.

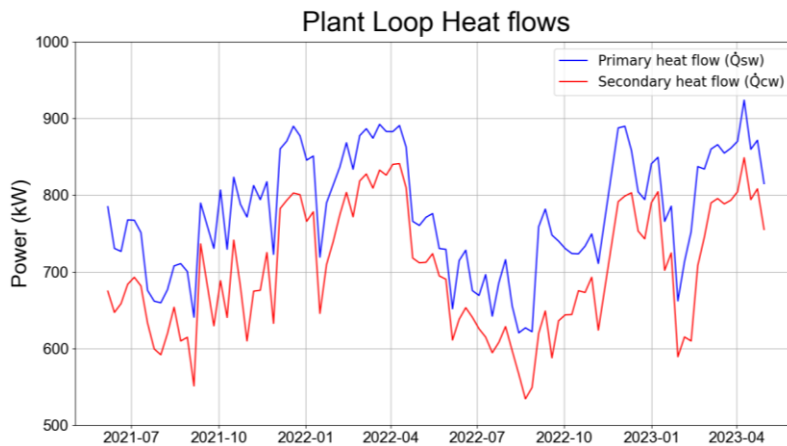


Figure 3: Seawater and chilled water heat flows

The heat flows on each side of the heat exchangers are plotted in Figure 3 and are calculated using (3) and (4).

$$\dot{Q}_{sw} = \rho_{sw} \cdot \dot{V}_{sw} \cdot c_{p_{sw}} \cdot (T_{sw_out} - T_{sw_in}) \quad (3)$$

$$\dot{Q}_{cw} = \rho_{cw} \cdot \dot{V}_{cw} \cdot c_{p_{cw}} \cdot (T_{cw_out} - T_{cw_in}) \quad (4)$$

The cooling demand of the District Cooling (DC) varies between 550 and 850 kW during the year, which is low compared to the nominal installation operation of 2.4 MWf.

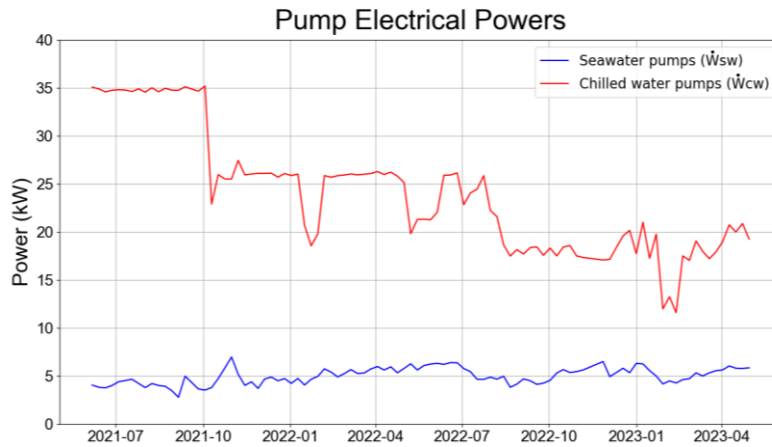


Figure 4: Seawater and chilled water pump electrical powers

The primary pumps consume about 5 kW (Figure 4), the secondary pumps are controlled either by a constant pressure setpoint or manually by the operator.

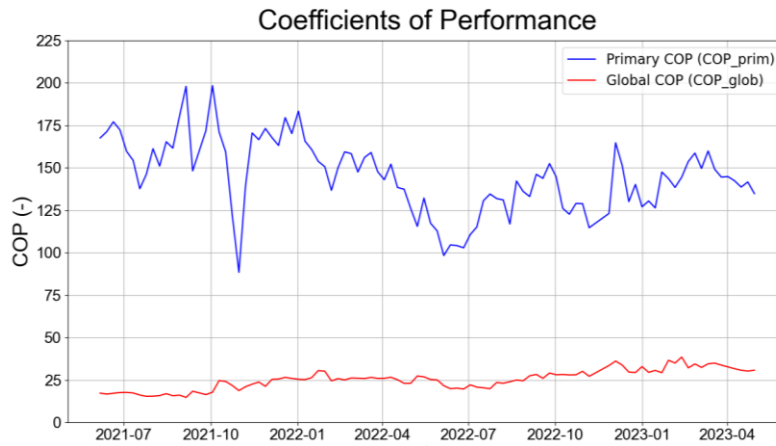


Figure 5: Primary and global COP

Using (5) and (6), two performance indicators have been estimated in Figure 5. The primary COP is excluding the distribution loop in order to compare SWAC performance to centralized AC and is the theoretical maximum of the global COP of its installation. The global COP includes both loop and represents the whole system's performance, it tends to be higher with increased cooling demand.

$$\text{COP}_{\text{prim}} = \frac{Q_{\text{cw}}}{W_{\text{sw}}} \quad (5)$$

$$\text{COP}_{\text{glob}} = \frac{Q_{\text{cw}}}{W_{\text{sw}} + W_{\text{cw}}} \quad (6)$$

Regarding the measurement period, we can consider seasonal variations of the system's performance by calculating the Seasonal COP (SCOP) with (7).

$$\text{SCOP} = \frac{1}{T} \int_0^T \text{COP}_{\text{glob}} \quad (7)$$

The Tetiaroa SWAC installation SCOP is 25.44 for the studied period.

3 NUMERICAL MODEL

3.1 EnergyPlus/Python co-simulation

EnergyPlus is a building energy simulation software used to model energy consumption for Heating Venting and Air-Conditioning (HVAC) and water use in buildings. It will allow us to create a coupled model of the SWAC system and the building in order to include mutual influence between both. EnergyPlus now provides a Python API which enables the integration of user-defined scripts. These scripts called plugins can be triggered at various simulation points, these points are the same as those defined for the EMS (Energy Management System) feature.

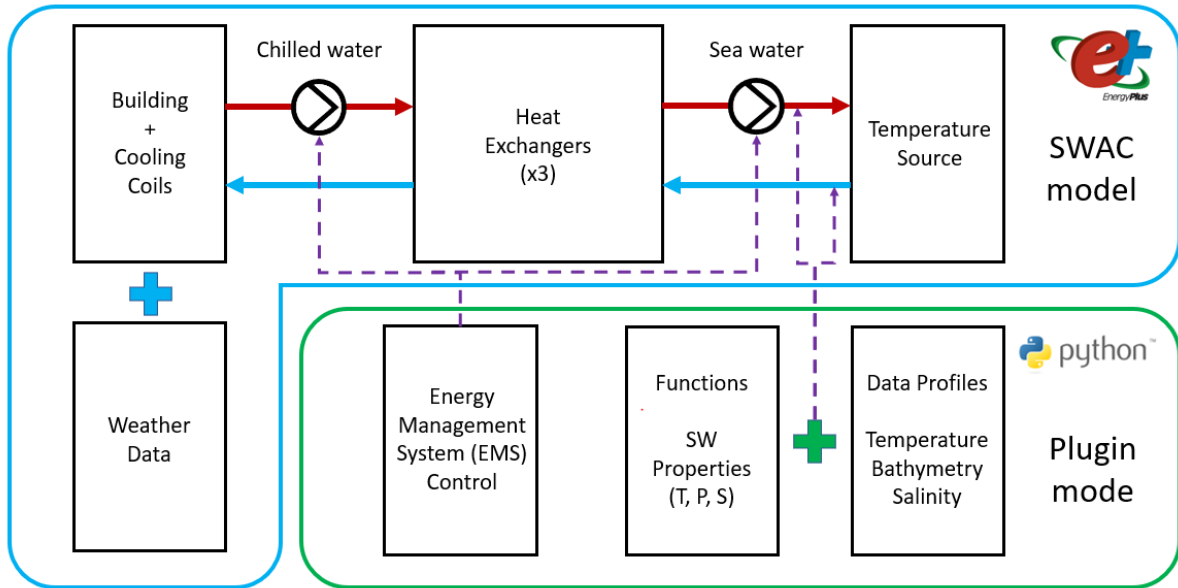


Figure 6: Block diagram of SWAC numerical model

The block diagram of the SWAC numerical model is represented in Figure 6. The blue block depicts the EnergyPlus built-in models used, and the green block represents the additional features from the plugins and their impact on the running simulation with violet arrows.

Python plugins are first used to accurately estimate the pump head of each loop depending on their respective flowrates (8) using the equivalent hydraulic resistance calculation in (9) and (10).

$$\Delta P = \rho g R \dot{V}^2 \quad (8)$$

$$R = \sum_{i=1}^n \left(\frac{\Delta H}{\dot{V}^2} \right)_n \quad (9)$$

$$\Delta H = \frac{\lambda L}{D} * \frac{v^2}{2g} \quad (10)$$

They are also used to model primary pipeline heat loss to adjust the predicted value of seawater temperature inlet and outlet (11). Heat transfers by forced convection inside, natural convection outside, and conduction through the pipeline are included (12).

$$\frac{dT}{dL} = \frac{2\pi L}{\dot{V}_{sw} c_p} U (T_{ext} - T) \quad (11)$$

$$\frac{1}{U} = \frac{1}{h_{int}} + \frac{1}{h_{ext}} + \frac{e}{\lambda} \quad (12)$$

3.2 Experimental Validation

The numerical model will be validated using the measurements of temperature, flow rate and electrical power gathered on Tetiaroa SWAC installation. The sequence of December 2021 was chosen for convenience as it is complete without data gaps. Measurement data and the simulation results are both on an hourly timestep.

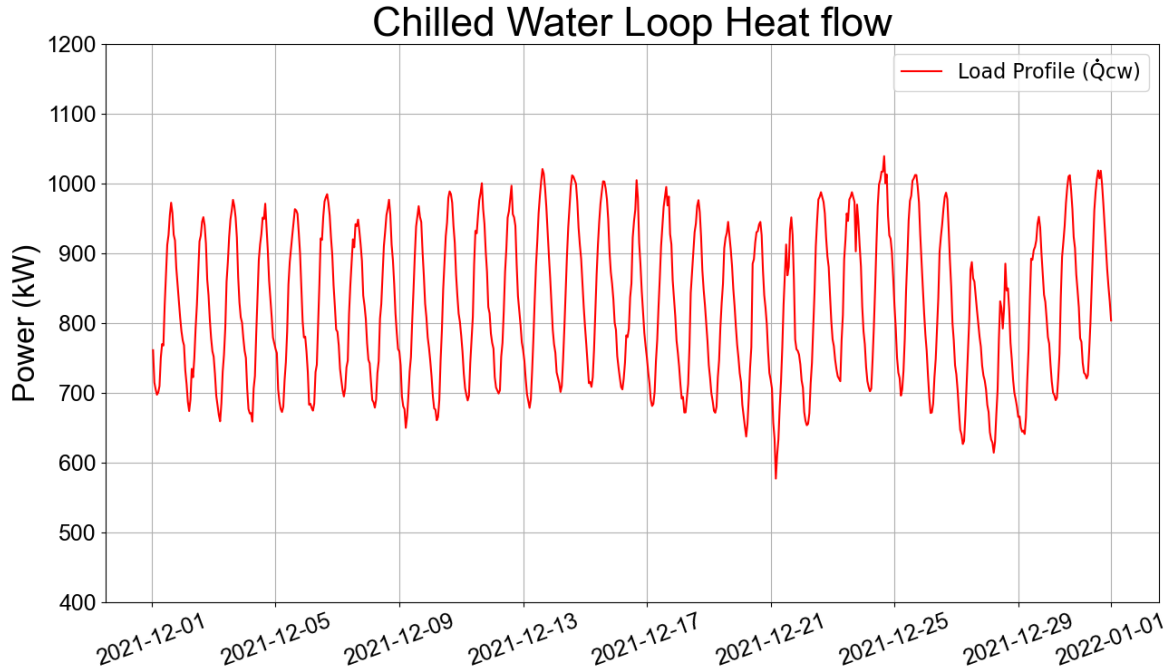


Figure 7: Validation load profile sequence

The chilled water loop heat flow measured in December will be input as a load profile in the model, replacing the building model and weather data. The cooling needs fluctuate between 600 kW and 1 MW, which is less than half of the SWAC nominal power, the installation operates with one pump instead of two. The period of measurements does not include any two-pump operation sequence thus, it is only possible to validate the single pump functioning.

$$r_i = y_i - \hat{y}_i \quad (13)$$

The numerical model results will be plotted with their residuals r_i which are the difference between the measurement y_i and its corresponding predicted value \hat{y}_i (13). The reliability of the model will be assessed by comparing the residuals to the measurement uncertainties, in order to verify that the variability of model predictions remains in an acceptable range and thus, that the model is correctly representing the system's behavior.

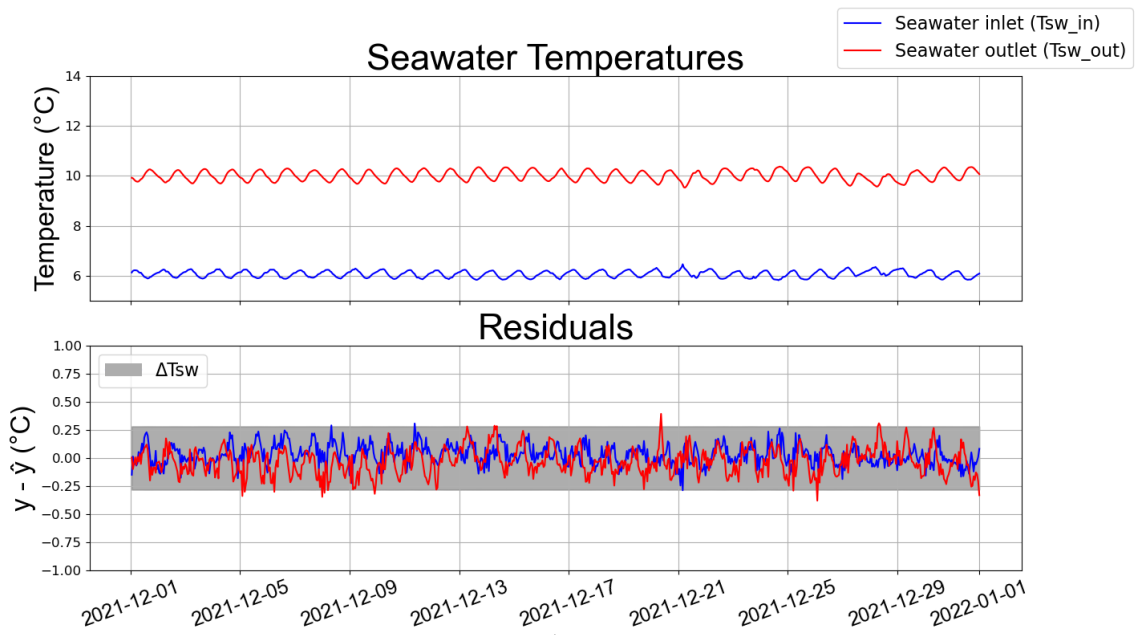


Figure 8: Modeling of seawater temperatures with residuals and measurement uncertainty

Seawater temperatures fluctuate daily around 6°C for the inlet and 10°C for the outlet. Their uncertainties are both represented by the grey band, corresponding to a relative uncertainty of +/- 0.1 % and approximately +/- 0.28°C. The two residuals remain predominantly within the range of the temperature sensor uncertainties.

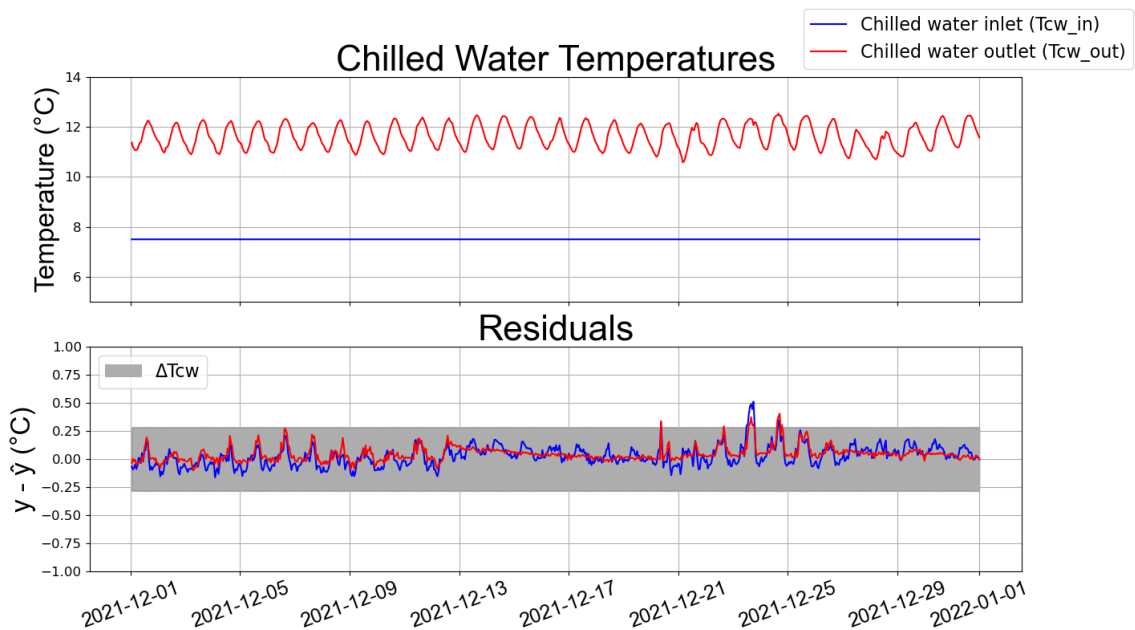


Figure 9: Modeling of chilled water temperatures with residuals and measurement uncertainty

The chilled water inlet temperature is a constant temperature setpoint adjusted to 7.5°C. The outlet temperature is oscillating daily between 11°C and 12.5°C. Residuals for the chilled water loop temperatures also stay within the uncertainty band of +/- 0.28°C, except for December 23rd. This deviation was caused by a manual intervention from the installation operator.

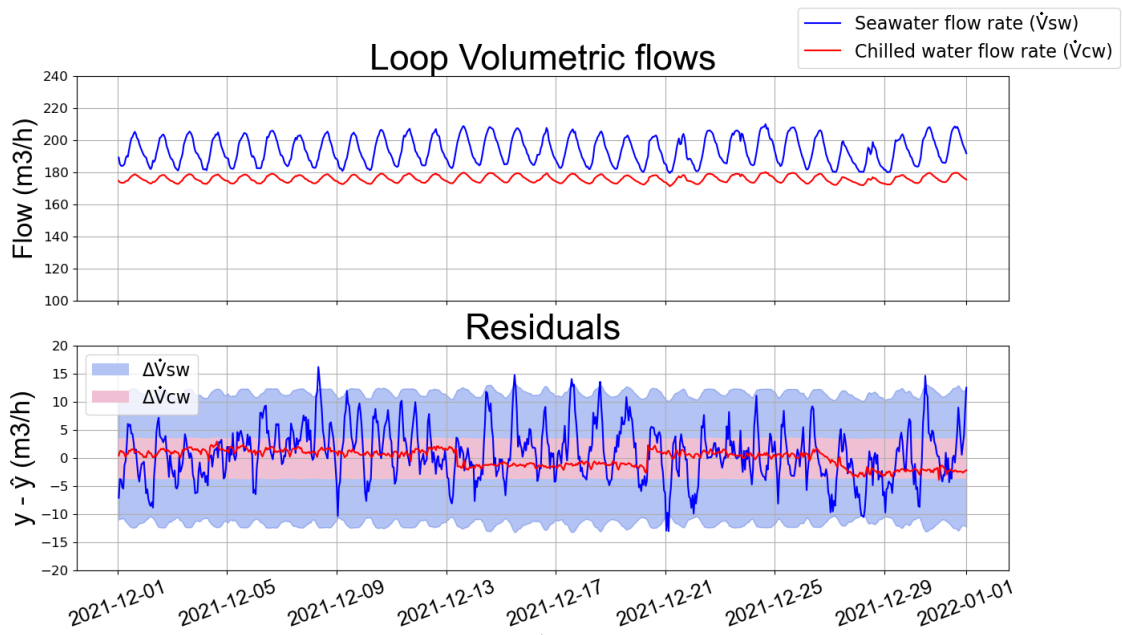


Figure 10: Modeling of loop flows with residuals and measurement uncertainty

The water flow rate of each loop represented above along with its uncertainty band, they follow the same fluctuations as the load profile with an average of 194 m³/h for the primary loop and 176 m³/h for the secondary loop. Their respective relative uncertainties are +/- 6 % (due to a suboptimal flowmeter placement) and +/- 2 %, thus approximately +/- 11.7 m³/h and +/- 3.5 m³/h.

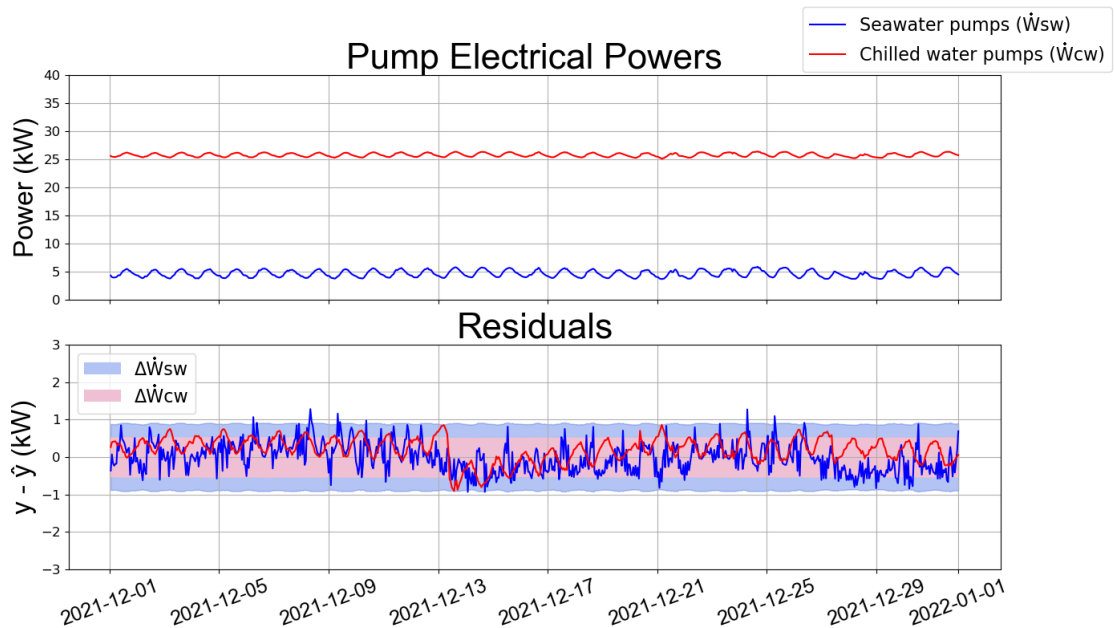


Figure 11: Modeling of pump electrical powers with residuals and measurement uncertainty

The pump electrical power consumptions have a relative uncertainty of +/- 2 %. However, the primary loop of the SWAC installation includes a vacuum pump with a nominal power of 1.6 kW. This pump operation is unknown, therefore introducing an additional random error on the primary power of +/- 0.8 kW. The uncertainty is around +/- 0.9 kW for the seawater pumps and 0.52 kW for the chilled water pumps. Small deviations can also occur because the installation includes, for each loop, 3 pumps in parallel rotating in sequence on a weekly basis, which are considered perfectly identical by the numerical model.

4 CONCLUSIONS

The SWAC provides support to a natural ventilation solution when the latter is no longer applicable or feasible due to external pollution (pollutants, noise, dust...), extreme weather conditions, or excessive internal loads. The data collected over a span of two years in The Brando hotel at the Tetiaroa site, one of the three deep Seawater Air Conditioning (SWAC) installations operating worldwide, provides us with a comprehensive understanding of the technology's performance and its seasonal variations. The primary Coefficient of Performance (COP) exhibits a range between 100 and 200, while the global COP ranges from 15 to 38. Notably, the Tetiaroa SWAC installation demonstrates an impressive Seasonal Coefficient of Performance (SCOP) of 25.44 over the two-year period, which is six times higher than the weighted average SCOP of traditional air conditioning systems, which typically ranges between 4 and 4.5 (International Energy Agency (IEA) 2018). To experimentally validate the numerical model of the SWAC system developed in EnergyPlus/Python, a data sequence of one month was used, analyzing seawater and chilled water temperatures, loop flow rates, and electrical pump consumptions predicted values. The accuracy of the model was confirmed as each residual match with its respective measurement uncertainty. In future work, this validated model, integrated with realistic cost data, will enable the exploration of design and operational variants to optimize performance and mitigate the high initial investment associated with SWAC technology. Allowing the worldwide development and adoption of SWAC in coastal areas that are traditionally deemed less favorable for such cooling systems.

5 ACKNOWLEDGEMENTS

This work was supported by the French Environment and Energy Management Agency (ADEME) and the University of French Polynesia. The authors would like to thank the Pacific Beachcomber group and especially its CEO Richard Bailey, its manager Bruno Chevallereau and Clément Capel for allowing us to exploit data from The Brando SWAC installation. Its instrumentation was funded as a part of the COPSWAC project by the ADEME and the Polynesian government which we thank as well.

6 REFERENCES

- Giraud, Melanie. s. d. « Evaluation de l'impact potentiel d'un upwelling artificiel lié au fonctionnement d'une centrale à énergie thermique des mers sur le phytoplancton ». International Energy Agency (IEA). 2018. « The Future of Cooling », 92.
- Sanjivy, Kanhan, Olivier Marc, Neil Davies, et Franck Lucas. 2023. « Energy Performance Assessment of Sea Water Air Conditioning (SWAC) as a Solution toward Net Zero Carbon Emissions: A Case Study in French Polynesia ». *Energy Reports* 9 (décembre): 437-46. <https://doi.org/10.1016/j.egyr.2022.11.201>.

Nomenclature					
cp	Heat capacity	P	Pressure	W	Electrical pump power
D	Pipeline diameter	Q	Heat flow	λ	Thermal conductivity
e	Pipeline thickness	R	Hydraulic resistance	ρ	Density
g	Gravity of Earth	T	Temperature	cw	Chilled Water
H	Hydrostatic pressure	U	Overall heat transfer coefficient	sw	Sea Water
h	Heat transfer coefficient	V	Volumetric flow rate	in/out	inlet / outlet
L	Pipeline length	v	Flow speed	int/ext	interior / exterior

The Effects of Lowering Temperature Setpoints on Perceived Thermal Comfort – An experimental study in office buildings

Beatriz Coutinho^{1,2}

*1 University of Coimbra
Paço das Escolas
Coimbra, Portugal
coutinhobeatriz20.10@gmail.com*

*2 bba Binnenmilieu B.V.
Casuariestraat 5, 2511 VB
Den Haag, The Netherlands
bc-bba@binnenmilieu.nl*

ABSTRACT

This study investigates the impact of lowering temperature setpoints on occupants' thermal comfort in office buildings, prompted by government initiatives in Europe, including the Netherlands, to reduce energy consumption. The research methodology involved a case study conducted in three office buildings in The Netherlands. Data on occupants' perception, motivation, clothing thermal insulation, activity level, discomfort, and thermal control options were collected through interviews conducted for thermal comfort surveys and building surveys. Statistical analysis revealed the importance of providing diverse control options to accommodate individual preferences, specially under temperatures outside the comfort zone. Occupants with more control options reported higher satisfaction. Variations in thermal sensation and comfort were observed among gender, age, and BMI groups, with females experiencing more discomfort and cold sensations at lower temperatures. The study emphasizes the need to consider individual differences in thermal comfort and the importance of adequate thermal control in office design and energy-saving measures. The findings contribute to the development of effective strategies for lowering temperature setpoints while maintaining occupant comfort and satisfaction.

KEYWORDS

Temperature setpoints, occupant thermal comfort, energy-saving measures, office buildings

1 INTRODUCTION

The pursuit of energy efficiency and reduction of greenhouse gas emissions has become a global priority, driven by the Russian invasion of Ukraine in 2022. Governments and building managers are exploring ways to reduce energy consumption. One widely proven approach to achieving energy savings in buildings is through human-based retrofits, specifically by adjusting HVAC temperature setpoints, which can be implemented at minimal cost (Haniff et al., 2013). Given this situation, in the beginning of April 2022, the Dutch government launched a campaign titled "Zet de knop om" ("turn the knob"), outlining plans to reduce energy consumption for room air conditioning in the short term (Rijksoverheid, 2022). The government proposed adopting a "2 degrees lower" winter setpoint of 19°C in all governmental buildings, as according to the European Commission HVAC systems in buildings account for approximately 40% of the EU's energy consumption and 36% of CO₂ emissions. However, it has also been observed that increasing the dead band results in decreased occupant thermal comfort (Jafarpur & Berardi, 2021). Neglecting comfort for energy efficiency may lead to issues like discomfort, fatigue, and reduced productivity (Ortiz et al., 2017). Humans are constantly reacting and adapting to indoor thermal surroundings. Previous studies have highlighted the role of adaptive behaviours in achieving thermal comfort and energy savings, including physiological, behavioural, and psychological responses (Sun & Hong, 2017). However, the adoption of such behaviour measures can be influenced by various factors, including occupant awareness, motivation, perceived effectiveness, convenience, and the

availability of feedback and incentives (D'Oca et al., 2017; Hu et al., 2020). Moreover, granting occupants the ability to exert control over the thermal environment has been shown to enhance their satisfaction. Leaman & Bordass (1993) found that greater occupant control access leads to higher tolerance for thermal variations in buildings. These findings highlight the complex and subjective nature of the relationship between energy-saving measures and occupants' perceived thermal comfort. Empirical studies are crucial to understanding the effects of lowering temperature setpoints on occupant comfort. This paper presents a case study in three Dutch office buildings to explore the trade-off and provide insights on lower temperature setpoints and thermal comfort. The main research question is: *"What are the effects of lowering the temperature setpoints, in Dutch office buildings, on the occupant's thermal comfort?"*. The study used thermal comfort surveys to collect data on occupant comfort levels at different temperature setpoints, focusing on behavioral responses, occupant satisfaction, and personal motivation.

2 METHODOLOGY

2.1 Design and Procedure

A thermal comfort study was conducted in three office buildings in the Netherlands to assess the impact of lowering temperature setpoints on occupant thermal comfort. The study involved conducting individual interviews, lasting around 7 minutes on average, in a dedicated room. The interviews were conducted in English and incorporated a combination of closed-ended and open-ended questions to gather extensive data. The interview process spanned approximately two days per building, resulting in a total duration of six days for the entire survey. The same questionnaire and methodology were used across all three buildings in the study.

2.2 Participants

A total of 121 participants, 65 males and 56 females, took part in the field study. Building A had 51 participants, while Buildings B and C each had 35 participants. The study focused on office workers only, excluding janitors and maintenance staff. Participants were randomly selected and provided with a brief introduction to the study and interview process. Participants who met the inclusion criteria, which included a minimum of one year of work experience in the building for winter comparisons, were invited to participate.

2.3 Buildings

The study examined three office buildings in the Netherlands: two high-rise buildings (Buildings A and C) with glass facades and air heat distribution systems, and one 3-floor office building (Building B) with air and water heat distribution systems, and a balanced window-to-wall ratio. In winter 2022-2023, all three buildings lowered their temperature setpoints, but the extent of reduction varied. Additional information on the buildings' characteristics is provided in Table 1.

Table 1: Brief description of the studied buildings

Building	Height	Location	TSet- before (°C)	TSet- after (°C)	Investigated floors	Interviews
A	149.1 m	Rotterdam	22.7	19	15	51
B	10 m	Utrecht	22	20	3	35
C	141.9 m	The Hague	21	19	10	35

3 RESULTS

The respondent group included 121 individuals, aged 18 to over 60. In Buildings A and B, the main age group was 50-59 years, while in Building C, it was 30-39 years. The majority of respondents reported being in the healthy BMI range. The following analysis combines data from all three buildings.

The analysis found that occupants adopt compensatory behaviours in response to lower indoor temperatures, such as adjusting clothing thermal insulation or using radiators. The preference for using radiators to enhance comfort raises implications for energy-saving control.

Figure 1 shows the impact of lower temperatures on thermal comfort. The analysis indicates that occupants generally experience higher comfort levels with higher temperature setpoints. A chi-square test ($\chi^2(4, N = 242) = 35.63, p < .001$) demonstrates a significant effect of lower temperature setpoints on perceived comfort. This suggests an association between indoor temperatures and thermal comfort.

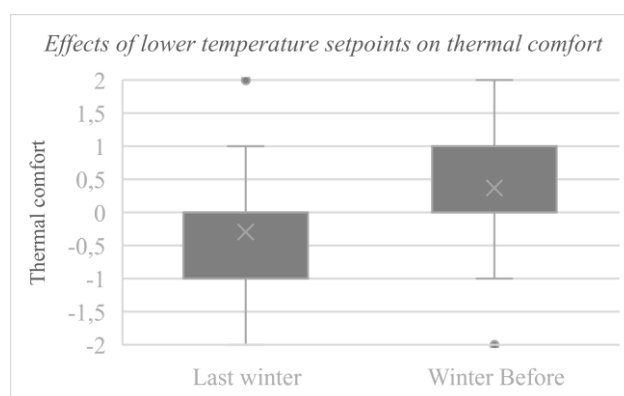


Figure 1: Box-plot illustrating the influence of lower temperature setpoints on thermal comfort. Where -2 signifies discomfortable and 2 signifies comfort. The X represents the mean.

Additionally it was found that, the majority of building occupants displayed a high motivation level (level 4) to save energy. Building B had the highest motivation (65.7%), closely followed by Building A (56.9%). Building C had a relatively lower motivation level (40%). All buildings showed an increase in motivation compared to the previous winter, with Buildings B and C having the highest percentage of occupants with changed motivation. An analysis of motivation to save energy identified sustainability as the primary driving factor across all three buildings. The second most reported motivation factor in all buildings was high energy bills.

Remarkably, the percentage of individuals motivated by the war in Ukraine was relatively low: 13.7% for Building A, 5.7% for Building B, and 9% for Building C. Despite this, when comparing the willingness to maintain low temperature setpoints across the three buildings, Building B had the highest level of willingness, with 89% of occupants committed to maintaining the setpoints even after energy prices return to regular values. Building C showed a moderate level of willingness, with 66% of occupants expressing their intention to maintain the setpoints. Building A had a lower level of willingness, with only 43.1% of occupants committed. Notably, within Building A, 31.4% of individuals explicitly stated their willingness to maintain the lower temperature setpoints only if they remained within acceptable levels of thermal comfort.

Figure 2 shows the evaluation of the "Zet de knop om" campaign in the three buildings. Building B had the most favourable evaluation, Building C had a mix of satisfied and dissatisfied occupants, and Building A had a significant percentage of occupants leaning towards being very dissatisfied, dissatisfied, or neutral in their evaluation of the campaign.

These results highlight the varying perceptions of the campaign's implementation across the buildings, with Building B displaying the highest satisfaction level.

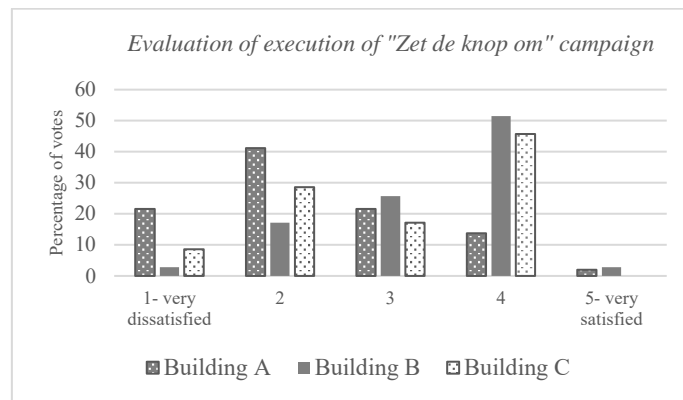


Figure 2: Evaluation of execution of "Zet de knop om" energy-saving campaign across the three buildings

A qualitative analysis identified common complaints in the three buildings: absence of feedback solicitation and perceived disregard for occupants' comfort, lack of control over the thermal environment, and unacceptable comfort levels.

Figure 3 shows the relationship between the number of control options for the thermal environment and occupant satisfaction. A chi-square test ($\chi^2(8, N = 121) = 66.65, p < .001$) revealed a significant difference in satisfaction based on the number of control options. The data suggests that occupants with more control options reported higher satisfaction levels compared to those with limited or no options.

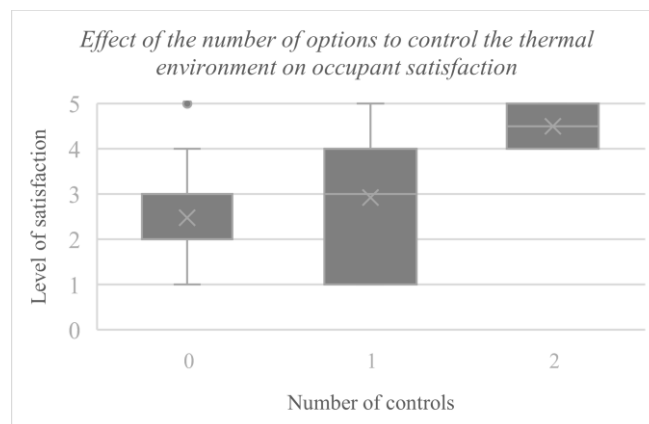


Figure 3: Box-plot depicting the effect of the number of options to control the thermal environment and occupant satisfaction. Where 0 signifies dissatisfaction and 5 signifies satisfaction. The X represents the mean.

Figure 4 illustrates the influence of gender, BMI, and age on perceived thermal comfort. A statistical analysis showed significant differences in perceived thermal comfort with lower indoor temperatures based on gender ($\chi^2(4, N = 121) = 13.67, p = 0.00843$), BMI ($\chi^2(12, N = 121) = 105.6, p < .001$), and age ($\chi^2(12, N = 121) = 57.5, p < .001$). Suggesting that females experienced more discomfort and cold sensations at lower temperatures compared to males. Moreover, no clear patterns were found for BMI and age.

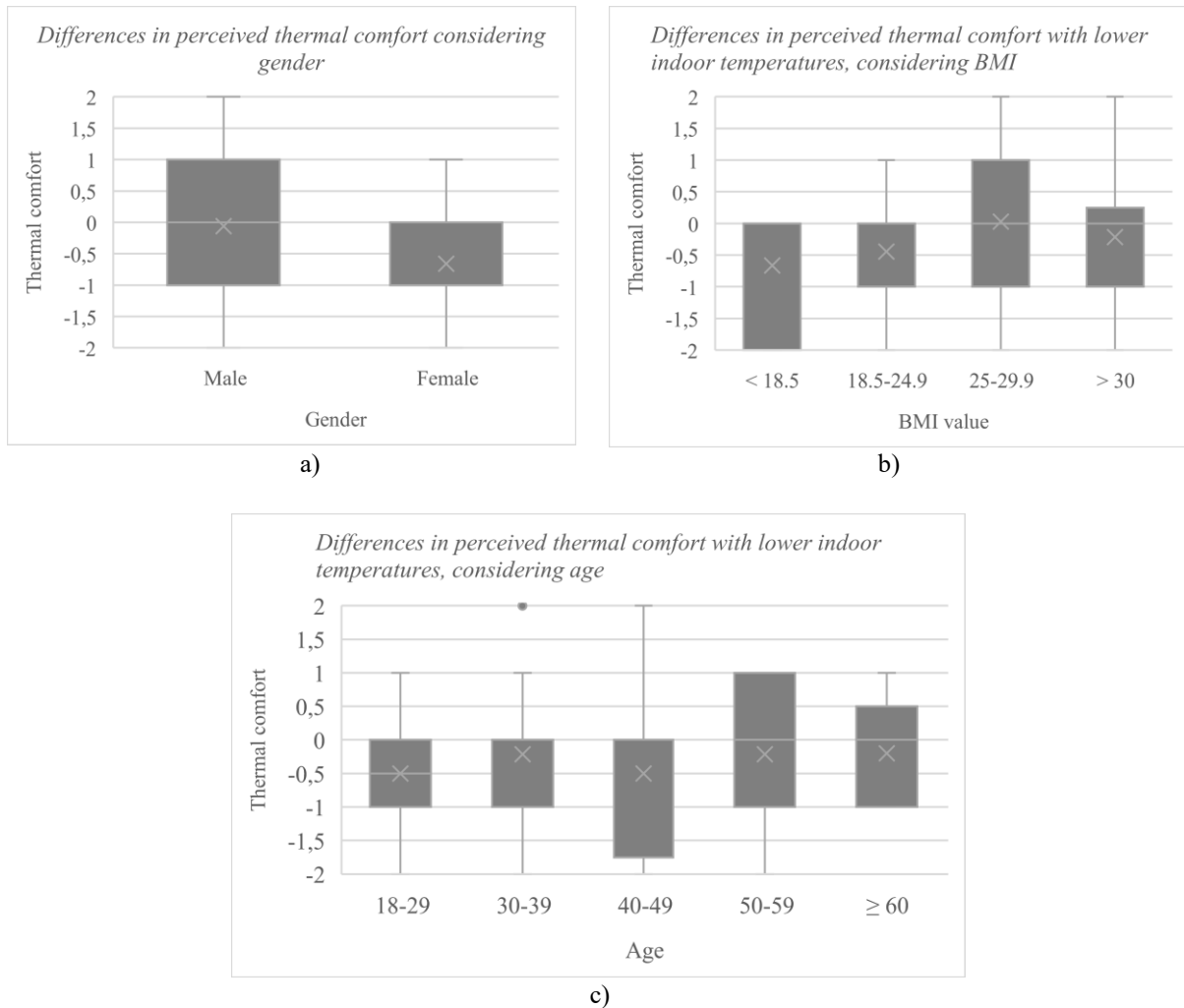


Figure 4: Box-plot illustrating the differences in perceived thermal comfort with lower indoor temperatures, considering gender (a), BMI (b) and age (c). Where -2 signifies discomfortable and 2 signifies comfort. The X represents the mean.

4 DISCUSSION

The case study yielded important findings on occupant behaviour, coping strategies, perceptions, and the impact of temperature setpoints on thermal comfort. Occupants employed compensatory behaviours like adjusting clothing thermal insulation and using radiators in response to lower temperatures, highlighting considerations for energy savings. Previous research emphasizes the role of adaptive behaviours in achieving comfort and energy savings (Butera, 1998; Sun & Hong, 2017). In line with the literature (Chun et al., 2008; Wang et al., 2018), higher temperature setpoints generally led to increased comfort, but individual experiences varied, emphasizing the importance of understanding individual preferences.

Occupants' motivation to save energy primarily stems from high energy bills rather than environmental concerns, as the majority of occupants motivation to save energy has increased since last winter, and there were variations in motivation between different settings (office vs. home), possibly due to personal responsibility for utility bills. Despite this, occupants expressed willingness to maintain lower temperature setpoints, as long as minimum comfort levels were ensured, particularly in Building A. Satisfaction with energy-saving campaigns differed across buildings, emphasizing the importance of feedback and communication. Providing diverse

control options improved satisfaction, aligning with existing literature on the positive impact of user control on comfort, satisfaction, energy savings, and productivity.

Gender, age, and BMI influenced thermal comfort, with females experiencing more discomfort in lower temperatures, consistent with previous studies by Indraganti et al., (2015) and Chaudhuri et al., (2018) highlighting women's higher dissatisfaction and sensitivity to temperature variations. Variations in comfort among different BMI and age groups call for tailored considerations. Additionally, exploring whether highly motivated individuals who actively lowered the temperature at home perceived more comfort would have been interesting. However, the data collected in this study, which consisted of participants with uniformly high levels of motivation towards energy conservation, did not allow for definitive conclusions. Without a suitable control group or participants with varying motivation levels, establishing a direct link between motivation, temperature adjustment behaviour, and perceived comfort becomes challenging. Further research with diverse participants is necessary to delve deeper into this question and obtain meaningful insights.

5 CONCLUSION

This study explored the impact of lower temperature setpoints on thermal comfort in Dutch office buildings, revealing significant effects on occupants' comfort perception. Adaptation to lower temperatures varied among individuals based on factors such as age, gender, clothing, and activity level. Control over the thermal environment and clear communication positively influenced comfort, while acceptance of lower setpoints differed across buildings. Higher comfort ratings were associated with greater acceptance, highlighting the link between comfort and energy-saving measures. The study underscores the importance of a holistic approach considering occupant preferences, energy efficiency goals, and adaptive strategies for optimal comfort. Ongoing communication and engagement are crucial for occupant satisfaction and support for sustainable, energy-efficient buildings.

6 ACKNOWLEDGEMENTS

This study was performed for my Master's thesis. I am thankful to my university and internship supervisors, Adélio Gaspar and Froukje van Dijken, as well as Atze Boerstra for this opportunity. Additionally, I am grateful for the support and resources provided by the projects: Plurianual - UIDB/50022/2020 and CLING - PTDC/EME-REN/3460/2021.

7 REFERENCES

- Afram, A., Janabi-Sharifi, F., Fung, A. S., & Raahemifar, K. (2017). Artificial neural network (ANN) based model predictive control (MPC) and optimization of HVAC systems: A state of the art review and case study of a residential HVAC system. *Energy and Buildings*, *141*, 96–113. <https://doi.org/10.1016/j.enbuild.2017.02.012>
- Butera, F. M. (1998). *Principles of thermal comfort*. *Renewable and Sustainable Energy Reviews*, *2*(1-2), 39-66.
- Chaudhuri, T., Zhai, D., Soh, Y. C., Li, H., & Xie, L. (2018). Random forest based thermal comfort prediction from gender-specific physiological parameters using wearable sensing technology. *Energy and Buildings*, *166*, 391–406. <https://doi.org/10.1016/j.enbuild.2018.02.035>
- Chun, C., Kwok, A., Mitamura, T., Miwa, N., & Tamura, A. (2008). Thermal diary: Connecting temperature history to indoor comfort. *Building and Environment*, *43*(5), 877–885. <https://doi.org/10.1016/j.buildenv.2007.01.031>
- D'Oca, S., Chen, C. F., Hong, T., & Belafi, Z. (2017). Synthesizing building physics with social psychology: An interdisciplinary framework for context and occupant behavior in office buildings. *Energy Research and Social Science*, *34*, 240–251. <https://doi.org/10.1016/j.erss.2017.08.002>

- Fadzli Haniff, M., Selamat, H., Yusof, R., Buyamin, S., & Sham Ismail, F. (2013). Review of HVAC scheduling techniques for buildings towards energy-efficient and cost-effective operations. In *Renewable and Sustainable Energy Reviews* (Vol. 27, pp. 94–103). Elsevier Ltd. <https://doi.org/10.1016/j.rser.2013.06.041>
- Hu, S., Yan, D., Azar, E., & Guo, F. (2020). A systematic review of occupant behavior in building energy policy. *Building and Environment*, 175. <https://doi.org/10.1016/j.buildenv.2020.106807>
- Indraganti, M., Ooka, R., & Rijal, H. B. (2015). Thermal comfort in offices in India: Behavioral adaptation and the effect of age and gender. *Energy and Buildings*, 103, 284–295. <https://doi.org/10.1016/j.enbuild.2015.05.042>
- Jafarpur, P., & Berardi, U. (2021). Effects of climate changes on building energy demand and thermal comfort in Canadian office buildings adopting different temperature setpoints. *Journal of Building Engineering*, 42. <https://doi.org/10.1016/j.jobe.2021.102725>
- Leaman, A., & Bordass, B. (1993). *Building design, complexity and manageability*.
- Ortiz, M. A., Kurvers, S. R., & Bluysen, P. M. (2017). A review of comfort, health, and energy use: Understanding daily energy use and wellbeing for the development of a new approach to study comfort. In *Energy and Buildings* (Vol. 152, pp. 323–335). Elsevier Ltd. <https://doi.org/10.1016/j.enbuild.2017.07.060>
- Rijksoverheid - Government of The Netherlands. (2022, April 5). *Zet okk de knop om - Bespaar nu energie*. Een Initiatief van Het Ministerie van Economische Zaken En Klimaat En Het Ministerie van Binnenlandse Zaken En Koninkrijksrelaties. <https://zetookdeknopom.nl/>
- Sun, K., & Hong, T. (2017). A simulation approach to estimate energy savings potential of occupant behavior measures. *Energy and Buildings*, 136, 43–62. <https://doi.org/10.1016/j.enbuild.2016.12.010>
- Wang, Z., de Dear, R., Luo, M., Lin, B., He, Y., Ghahramani, A., & Zhu, Y. (2018). Individual difference in thermal comfort: A literature review. In *Building and Environment* (Vol. 138, pp. 181–193). Elsevier Ltd. <https://doi.org/10.1016/j.buildenv.2018.04.040>

Long-term energy performance of dew-point indirect evaporative cooler under the climate change world scenario

María Jesús Romero-Lara*¹, Francisco Comino*², and Manuel Ruiz de Adana¹

*1 Departamento de Química-Física y Termodinámica Aplicada, Escuela Politécnica Superior de Córdoba, Universidad de Córdoba
Campus de Rabanales, Antigua Carretera Nacional IV, km 396, 14071 Córdoba, España*

*2 Departamento de Mecánica, Escuela Politécnica Superior de Córdoba, Universidad de Córdoba
Campus de Rabanales, Antigua Carretera Nacional IV, km 396, 14071 Córdoba, España*

*Corresponding author: p42rolam@uco.es
Presenting author

ABSTRACT

The progressive increase in the global average outdoor air temperature has caused an increase in the cooling demand in buildings in recent years. Given this climate change scenario, there is a need to develop efficient air-cooling systems that improve the energy efficiency of traditional direct expansion units. In this sense, ventilative cooling technologies should be tested under the climate change world scenario.

In this research study, the main objective was to evaluate the seasonal energy behaviour of a Dew-point Indirect Evaporative Cooler (DIEC) for three different climatic zones under a hostile climate change scenario. An empirical model of a DIEC system was used to obtain Seasonal Energy Efficiency Ratio (SEER) values under different climatic conditions. This DIEC model and variable air flow control of DIEC were adjusted to perform several annual energy simulations in TRNSYS17 software. Three different climatic zones according to the ASHRAE climate classification were considered in this work: 1-Very hot, 2-Hot and 3-Warm. In addition, different weather scenarios were established using a specific tool for the development of meteorological data predictions, CCWorldWeatherGen.

Based on the results, the DIEC system showed high SEER values, between 2.5 and 6.3. The lowest SEER values, between 2.5 and 5.1, were obtained for Bangkok (Thailand) – climatic zone 1 with high outdoor air temperature values and high outdoor air humidity ratio values. However, the highest SEER values, between 5.9 and 6.3, were obtained for Brasilia (Brazil) – climatic zone 2 with low outdoor air humidity ratio values and high outdoor air temperature values. These results showed that the use of a Dew-point Indirect Evaporative Cooler could be interesting under the world climate change scenario, since its SEER value improved with increasing climatic severity.

KEYWORDS

Energy simulations, evaporative cooling technology, Seasonal Energy Efficiency Ratio, world changing climate.

1 INTRODUCTION

Climate change has several implications for both human health and the energy performance of buildings (Ciancio et al., 2020; Pörtner H-O, et al., 2022). Research papers have highlighted the significant contribution of buildings to global energy consumption and carbon emissions. The heating, ventilation and air-conditioning systems (HVAC) in buildings consume approximately 36% of the global final energy and are responsible for nearly 40% of total CO₂ emissions (Allouhi et al., 2015; Xu et al., 2023). One of the main effects of climate change is the increase in the average outdoor temperature around the world. This rise in temperature has direct implications for energy demand, particularly in the areas of refrigeration and global electricity consumption (Huang and Gurney, 2016). Therefore, ensuring comfortable indoor environments with low energy consumption in buildings is a major challenge.

The development and adoption of energy-efficient cooling technologies can help reduce the reliance on fossil fuels and minimize CO₂ emissions. According to several studies, indirect evaporative cooling technology offers an interesting solution for achieving thermal comfort while simultaneously reducing energy consumption and minimizing environmental impact (Romero-Lara et al., 2021; Yang et al., 2021). Energy Efficiency Ratio (EER) is a widely used index for evaluating the energy performance of indirect evaporative coolers (IEC). EER is defined as the ratio between cooling capacity and electrical-power consumption of an IEC. In a research work, a comparative study between a traditional air-cooling system based on vapor compression and two innovative air-cooling systems was carried out (Romero-Lara et al., 2021). The main finding was that a DIEC system demonstrated three to four times lower energy consumption than the traditional air-cooling system, which translates into a higher EER value. Another work studied the correlation between the EER value of a DIEC, from 10.6 to 19.7, and different climatic conditions (Duan et al., 2017): lower EER values for high values of outdoor air humidity ratio and higher EER values for high values of outdoor air temperature.

Given the rising cooling demand in buildings, the main objective of the present work was to assess the long-term energy performance of a dew-point IEC (DIEC) considering the effects of climate change. Energy simulations were performed in the TRNSYS17 software using the DIEC experimental model. The main analysis focused on the influence of the climatic conditions of different zones on the seasonal EER (SEER) for DIEC from 1995 to 2080.

2 METHODOLOGY

2.1 Empirical model of DIEC

In this study, an experimental model of DIEC was used to obtain its long-term energy performance in terms of Seasonal Energy Efficiency Ratio (SEER). In a recent work, the authors detailed the constructive and operational characteristics of this DIEC (Romero-Lara et al., 2022). The authors also provided an explanation of the experimental setup built to examine the energy performance of the DIEC under different operational conditions. The ranges of values of outdoor air temperature (T_{OA}), outdoor air humidity ratio (ω_{OA}), and volumetric air flow (\dot{V}_{OA}) were adjusted to obtain a complete empirical model of the DIEC. High values of the determination coefficient (R^2) were shown for the empirical models of cooling capacity ($\dot{Q}_{cooling}$), electrical-power consumption (\dot{W}), and EER: 0.9991, 0.9997 and 0.9973, respectively (Romero-Lara et al., 2022). These empirical models and a variable volumetric air flow control based on outdoor temperature, see Figure 1, were used to perform several energy simulations.

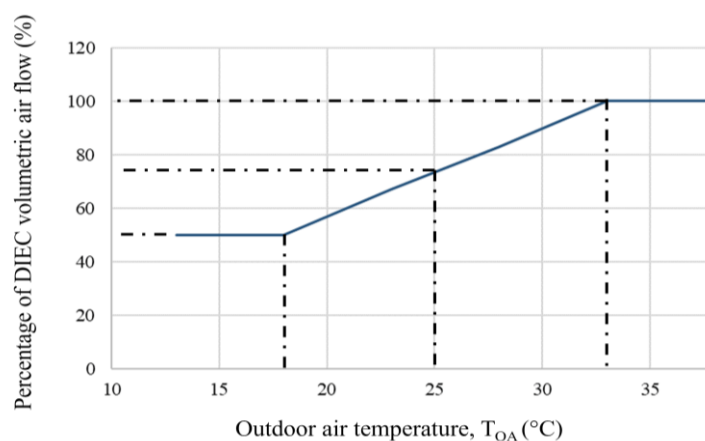


Figure 1: Variable air flow control of the studied DIEC.

2.2 Climatic zones classification

According to the ASHRAE climate classification, three different climatic zones were defined: climatic zone 1 for a very hot climate, climatic zone 2 for a hot climate, and climatic zone 3 for a warm climate (ASHRAE, 2007). This classification was made based on the thermal criteria of Cooling Degree Days (CDD), as indicated in Table 1. To ensure greater consistency in this work's analysis, two cities were selected from each climatic zone, see Table 1. In this way, a wider range of outdoor air conditions was covered.

Table 1: Classification of the climatic zones selected.

Zone number and name*	City	Country	Thermal criteria
1 – Very hot (humid)	Bangalore	India	$5000 < CDD_{10^{\circ}C}$
1 – Very hot (humid)	Bangkok	Thailand	$5000 < CDD_{10^{\circ}C}$
2 – Hot (dry)	Brasilia	Brazil	$3500 < CDD_{10^{\circ}C} \leq 5000$
2 – Hot (dry)	Brisbane	Australia	$3500 < CDD_{10^{\circ}C} \leq 5000$
3 – Warm (dry)	Valencia	Spain	$2500 < CDD_{10^{\circ}C} < 3500$
3 – Warm (dry)	Nairobi	Kenya	$2500 < CDD_{10^{\circ}C} < 3500$

*Humid = average ω_{OA} value > 11.0 g/kg. Dry = average ω_{OA} value < 11.0 g/kg. (Reference: year 1995)

Due to the selection of cities with different of T_{OA} and ω_{OA} , a more complete analysis can be performed to assess the impact of these climatic conditions on the SEER values of a DIEC.

2.3 Changing climate scenarios

Most scientific studies have used the *CCWorldWeatherGen* tool, which was developed at the University of Southampton, to generate and analyse new weather scenarios (Andrić, 2019). This tool has demonstrated to be highly valuable in simulating and modelling different climatic conditions, allowing researchers to explore and study the potential impacts of climate change on several environmental and economic factors (Ascione et al., 2022; Cruz et al., 2022; Thapa et al., 2023).

In this work, the *CCWorldWeatherGen* tool was investigated to create new weather scenarios: year 2020, year 2050, and year 2080. The reference scenario was the year 1995, since it is the year corresponding to the TRNSYS meteorological base. So, 24 cases were studied in this work, combinations of six cities in different climatic zones and four scenarios. As a summary, Table 2 provides the set of average outdoor air temperature ($T_{OA,avg}$) and average outdoor air humidity ratio ($\omega_{OA,avg}$) values for each city in each weather scenario. The cooling period considered in this study refers to the period when the T_{OA} value exceeded $18^{\circ}C$.

Table 2: Climatic conditions in changing climate scenarios of the six selected zones.

Zone number and city	1995		2020		2050		2080	
	$T_{OA,avg}$ (°C)	$\omega_{OA,avg}$ (g/kg)	$T_{OA,avg}$ (°C)	$\omega_{OA,avg}$ (g/kg)	$T_{OA,avg}$ (°C)	$\omega_{OA,avg}$ (g/kg)	$T_{OA,avg}$ (°C)	$\omega_{OA,avg}$ (g/kg)
1 – Bangalore	26.0	11.8	27.1	10.4	27.9	10.6	29.5	10.9
1 – Bangkok	26.7	13.0	28.2	11.8	29.0	11.8	30.7	12.3
2 – Brasilia	24.7	10.9	26.3	10.5	27.2	10.5	28.7	10.6
2 – Brisbane	24.2	10.8	24.2	10.5	24.5	10.5	25.1	10.6
3 – Valencia	23.6	10.9	25.1	11.0	26.1	11.1	26.8	10.7
3 – Nairobi	23.1	10.9	23.4	10.6	24.1	11.1	25.3	11.8

It can be observed a progressive increase in the $T_{OA,avg}$ values for all climatic zones, see Table 2. Climatic zone 1 shown an approximate rise of outside temperature of $2.5^{\circ}C$, while climatic

zones 2 and 3 exhibited increases of 1.8 °C and 1.7 °C, respectively, between 2020 and 2080. However, the $\omega_{OA,avg}$ values did not show any correlation. These $\omega_{OA,avg}$ values were between 10.4 and 13.0 g/kg for climatic zone 1, between 10.5 and 10.9 g/kg for climatic zone 2 and between 10.6 and 11.8 g/kg for climatic zone 3, see Table 2.

2.4 Energy performance index

In the present study, several energy simulations were performed using a DIEC empirical model and variable air flow control indicated in Figure 1. All SEER values were determined for the cooling period, using the TRNSYS17 software with a time step of 2.4 minutes for each climatic zone in each scenario (S.A. Klein, 2006).

The SEER values of DIEC were calculated according to the annual cooling energy, $Q_{cooling}$, and annual electrical energy consumption, W , of DIEC during the cooling period. For each of the 24 cases, Equations 1, 2 and 3 were used as follows.

$$\dot{Q}_{cooling} = \rho_{air} \cdot \dot{V}_{SA} \cdot (h_{OA} - h_{SA}) \quad (1)$$

$$\dot{W} = \dot{W}_{fan} + \dot{W}_{pump} \quad (2)$$

$$SEER = \frac{\sum \dot{Q}_{cooling}}{\sum \dot{W}} = \frac{Q_{cooling}}{W} \quad (3)$$

Where ρ_{air} is the density of air [kg/m³], \dot{V}_{SA} is the supply volumetric air flow [m³/s], and h_{OA} and h_{SA} are the outdoor and supply air specific enthalpy [kJ/kg], respectively. \dot{W}_{fan} and \dot{W}_{pump} are the electrical-power consumption of the fan and pump of DIEC [kW].

3 RESULTS AND ANALYSIS

The long-term energy performance of a DIEC, in terms of SEER, was performed under the climate change world scenario. Different SEER values were obtained and analysed according to the different climatic conditions across four scenarios (year 1995, year 2020, year 2050, and year 2080) for six different cities, see Table 2.

3.1 Analysis of weather scenarios

The *CCWorldWeatherGen* tool was used to develop the prediction of weather conditions in year 2020, 2050 and 2080. These scenarios and the reference scenario, year 1995, were analysed for the two cities selected in each climatic zone, during their respective cooling periods.

Figure 2 illustrates the annual variation in T_{OA} from the year 1995 to 2080 for the city of Bangalore, India, serving as a representation of climatic zone 1. It is evident that the highest T_{OA} values, ranging from 30 °C to 40 °C, occurred during the period from early April to early July, see Figure 2. For each scenario – 1995, 2020, 2050, and 2080 – the $T_{OA,avg}$ values were recorded as 26.0 °C, 27.1 °C, 27.9 °C, and 29.5 °C, respectively, see Table 2. The most significant temperature difference of 1.6 °C was observed between the years 2050 and 2080. Therefore, it should be noted both the progressive increase in outdoor air temperatures within this climatic zone 1 and the accelerated rate of increase in T_{OA} in recent years.

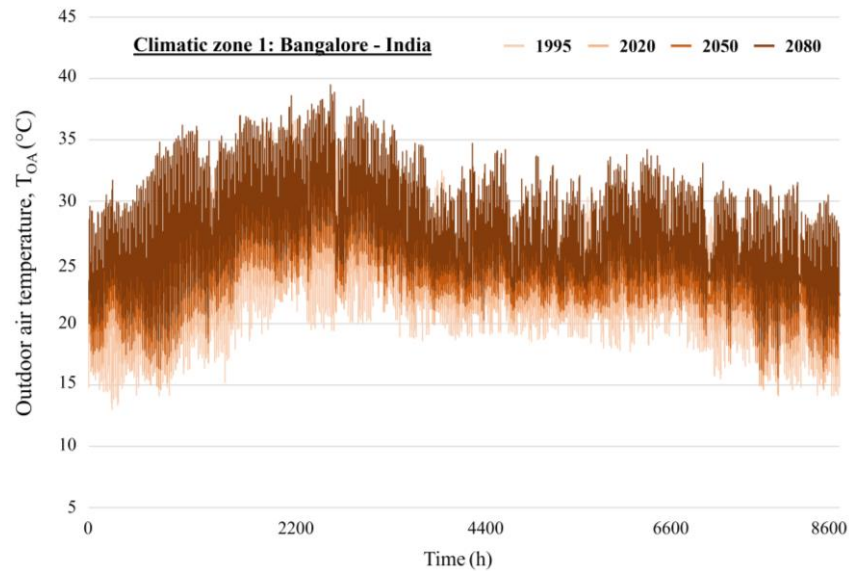


Figure 2: Hourly outdoor air temperature variation during the four weather scenarios for climatic zone 1.

According to the representation of climatic zone 2, Figure 3 displays the yearly fluctuations in outdoor air temperature for the city of Brasilia, in Brazil, from 1995 to 2080. It can be observed that high outdoor air temperature values were recorded, between 30 °C and 40 °C, throughout the year in Brasilia, see Figure 3. The $T_{OA,avg}$ values for the years 1995, 2020, 2050, and 2080 were recorded as 24.7 °C, 26.3 °C, 27.2 °C, and 28.7 °C, respectively, as shown in Table 2. The highest temperature differences were 1.6 °C between the years 1995 and 2020, and 1.5 °C between the years 2050 and 2080. This indicated that the rate of T_{OA} increase in Brasilia (climatic zone 2) was relatively more stable compared to Bangalore (climatic zone 1).

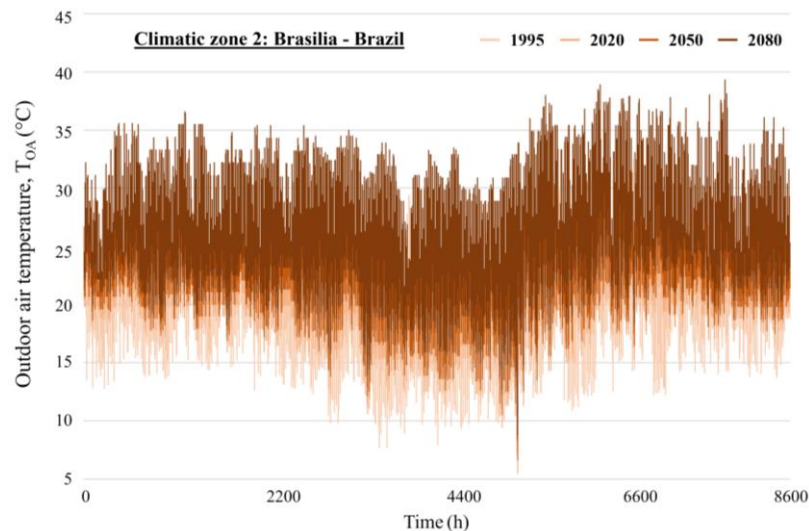


Figure 3: Hourly outdoor air temperature variation during the four weather scenarios for climatic zone 2.

Figure 4 exhibits the changes in outdoor air temperature from the year 1995 to 2080 for the city of Valencia, in Spain, serving as a representation of climatic zone 3. High T_{OA} values, ranging from 30 °C to 40 °C, were shown between the months of June (3624 hours) and October (6552 hours), see Figure 4. These months correspond to the summer season in Spain, characterized by more severe weather conditions each year. As depicted in Table 2, the average $T_{OA,avg}$ values for the years 1995, 2020, 2050, and 2080 were documented as 23.6 °C, 25.1 °C, 26.1 °C, and

26.8 °C, respectively. These findings indicate a progressive increase in outdoor temperature for climatic zone 3 as well as for climatic zones 1 and 2.

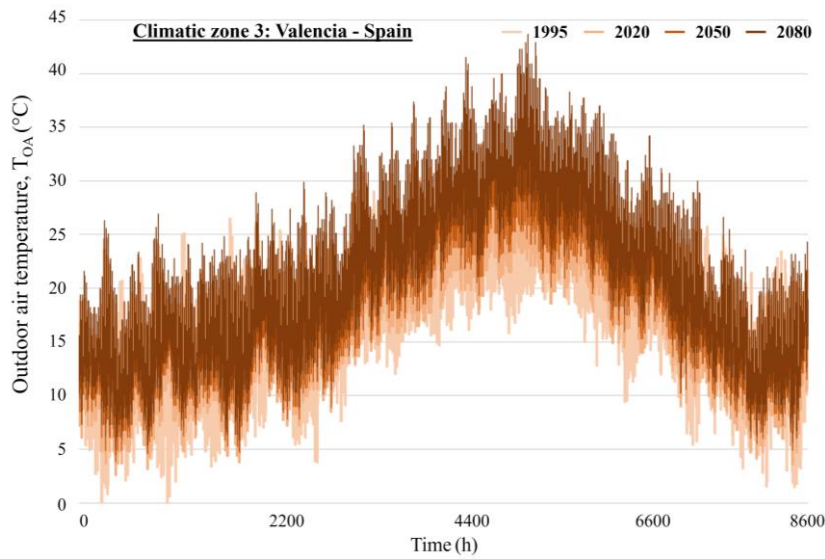


Figure 4: Hourly outdoor air temperature variation during the four weather scenarios for climatic zone 3.

3.2 Analysis of SEER for DIEC

The SEER values for the DIEC system were obtained under the changing climatic conditions of each selected city. The impact of the $T_{OA,avg}$ and $\omega_{OA,avg}$ values on SEER was grouped according to climatic zones: zone 1 in Figure 5, zone 2 in Figure 6 and zone 3 in Figure 7. Despite belonging to the same climatic zone, Figure 5 shown contrasting variations in SEER between Bangalore and Bangkok. In both cases, there was a gradual increase in $T_{OA,avg}$. However, Bangkok experienced higher levels of $\omega_{OA,avg}$ than Bangalore. For climate zone 1, the highest SEER value recorded was 6.1, under a $\omega_{OA,avg}$ value of 10.4 g/kg (Bangalore 2020). Conversely, the lowest SEER value for climatic zone 1 was 2.5, with a $\omega_{OA,avg}$ value of 13 g/kg (Bangkok 1995). Thus, it is evident that outdoor air humidity had a significant role in influencing the energy efficiency of the DIEC.

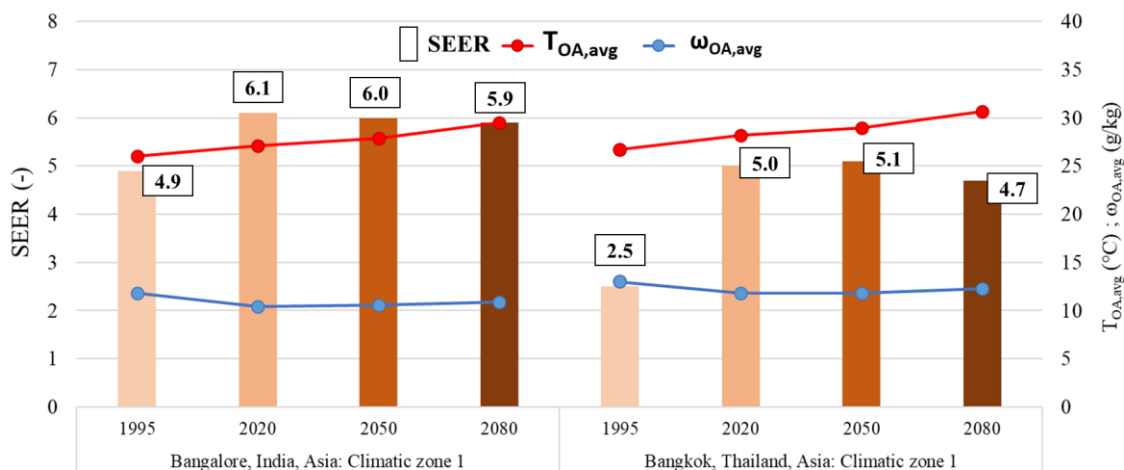


Figure 5: Impact of T_{OA} and ω_{OA} on the SEER values of DIEC for the climate change scenario in zone 1.

In the case of climatic zone 2, both the variations of $T_{OA,avg}$ and $\omega_{OA,avg}$ from 1995 to 2080 were similar for Brasilia and Brisbane, see Figure 6. The SEER variation for each city was similar in

all four scenarios, due to the stability of the $\omega_{OA,avg}$ values. Therefore, the SEER value increased with the increase in T_{OA} . The SEER values were high for all cases of the climatic zone 2, in the range of 5.5 to 6.3, see Figure 6.

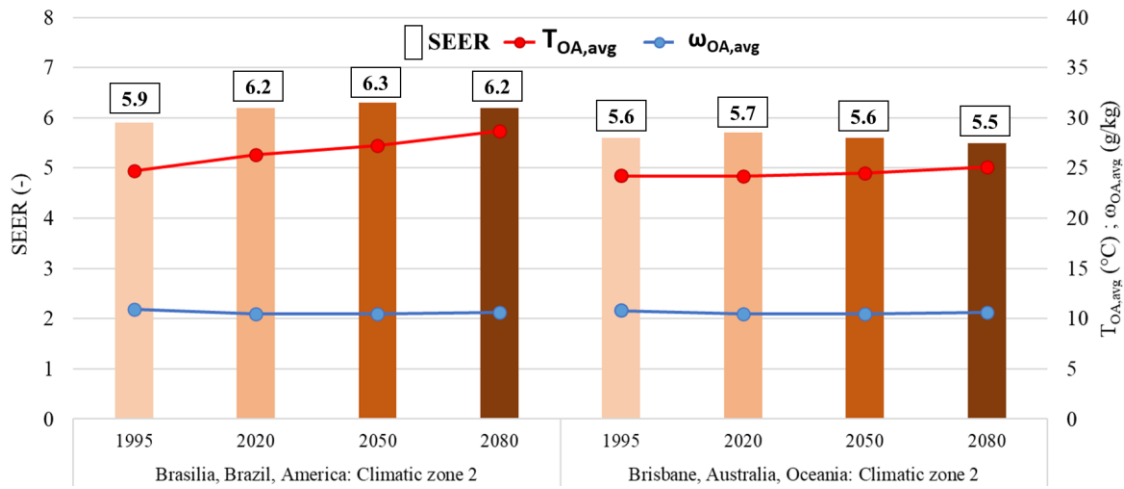


Figure 6: Impact of T_{OA} and ω_{OA} on the SEER values of DIEC for the climate change scenario in zone 2.

The SEER variation analysis carried out for climatic zone 3 confirmed the influence of T_{OA} and ω_{OA} on SEER. Research in the climate of Valencia indicated that the value of T_{OA} exhibited a progressive increase from 1995 to 2020. In contrast, the value of ω_{OA} remained constant or even decreased during that period, as shown in Figure 7. This combination of factors resulted in an overall increase in SEER of the four scenarios. However, the SEER results for Nairobi had lower SEER values in the years 2050 and 2080 due to increased outdoor humidity, see Figure 7.

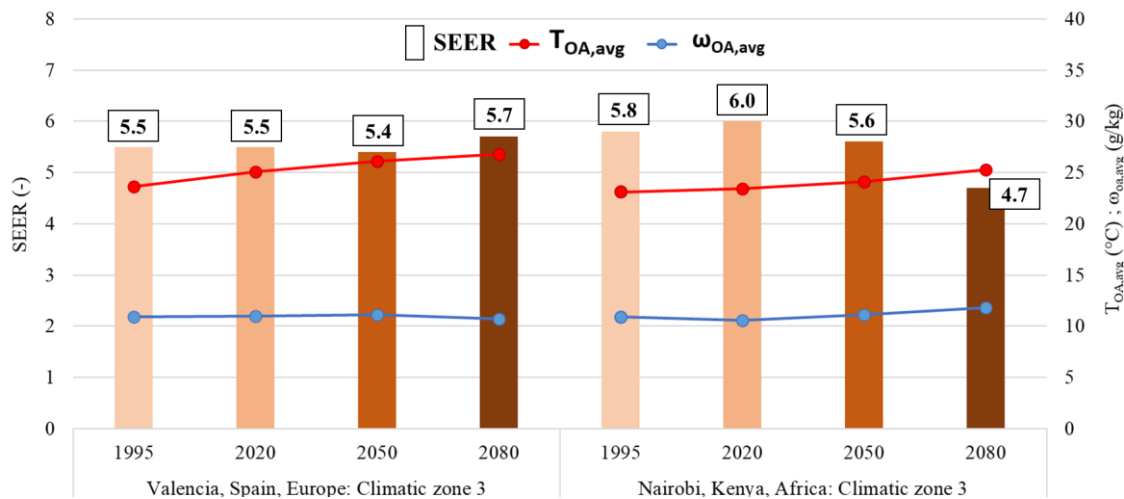


Figure 7: Impact of T_{OA} and ω_{OA} on the SEER values of DIEC for the climate change scenario in zone 3.

As a summary of the analysis carried out previously, Table 3 shows the values of $T_{OA,avg}$, $\omega_{OA,avg}$ and SEER in gradient format for the six cities and the four selected years. For the $T_{OA,avg}$ and SEER values, the green colour represented the lowest values, and the red colour represented the highest values, see Table 3. For the $\omega_{OA,avg}$ values, the white and blue colours represented the lowest and highest values, respectively. It can be observed that the lowest SEER values, between 2.5 and 5.1, were shown for Bangkok (climatic zone 1 with high $T_{OA,avg}$ values, but high $\omega_{OA,avg}$ values that penalize the SEER result of DIEC), see Table 3. However, the highest SEER values, between 5.9 and 6.3, were observed for Brasilia (climatic zone 2 with low outdoor

air humidity). Brisbane and Valencia had similar SEER values due to similar $T_{OA,avg}$ and $\omega_{OA,avg}$ values, despite being different climatic zones, see Table 3.

Table 3: $T_{OA,avg}$, $\omega_{OA,avg}$ and SEER values of DIEC for the six selected cities and for scenarios.

City	Bangalore	Bangkok	Brasilia	Brisbane	Valencia	Nairobi	$T_{OA,avg}$ and SEER Max. Min.
Climatic zone	1	1	2	2	3	3	
$T_{OA,avg}$ (°C)	1995	26.0	26.7	24.7	24.2	23.6	23.1
	2020	27.1	28.2	26.3	24.2	25.1	23.4
	2050	27.9	29.0	27.2	24.5	26.1	24.1
	2080	29.5	30.7	28.7	25.1	26.8	25.3
$\omega_{OA,avg}$ (g/kg)	1995	11.8	13.0	10.9	10.8	10.9	10.9
	2020	10.4	11.8	10.5	10.5	11.0	10.6
	2050	10.6	11.8	10.5	10.5	11.1	11.1
	2080	10.9	12.3	10.6	10.6	10.7	11.8
SEER (-)	1995	4.9	2.5	5.9	5.6	5.5	5.8
	2020	6.1	5.0	6.2	5.7	5.5	6.0
	2050	6.0	5.1	6.3	5.6	5.4	5.6
	2080	5.9	4.7	6.2	5.5	5.7	4.7

4 CONCLUSIONS

Nowadays, there is the increasing concerns about adverse weather conditions due to climate change. There is a growing need to find sustainable solutions that rely on efficient air-cooling systems. In this study, the impact of the progressive rise in outdoor air temperature and the influence of outdoor air humidity on the SEER values of a DIEC was analysed.

The main findings obtained from the energy analysis of a DIEC for three different climatic zones during the years 1995, 2020, 2050, and 2080 were as follows:

- High SEER values for DIEC were obtained for all cities studied, between 4.7 and 6.3, except Bangkok due to its $\omega_{OA,avg}$ values.
- The lowest SEER value was 2.5, obtained in Bangkok in 1995, due to the high average outdoor air humidity value that year, 13 g/kg.
- The SEER value for DIEC increased considerably in Brasilia and Valencia when the outdoor air temperature increased.

Therefore, the DIEC showed a more efficient seasonal energy behaviour for hot-dry climatic conditions. Due to the continuous increase in outdoor temperature caused by climate change scenario, this DIEC technology could be an interesting solution in terms of energy efficiency.

5 ACKNOWLEDGEMENTS

The authors acknowledge the financial support received by European Union's Horizon 2020 research and innovation programme, through the research project WEDISTRIC, reference H2020-WIDESPREAD2018-03-857801, and by the DCOOL project, reference TED2021-129648B-I00, funded by MCIN/AEI/10.13039/501100011033 and the European Union "NextGenerationEU/PRTR".

6 REFERENCES

- Allouhi, A., Y. El Fouih, T. Kousksou, A. Jamil, Y. Zeraoui, and Y. Mourad. (2015). “Energy Consumption and Efficiency in Buildings: Current Status and Future Trends.” *Journal of Cleaner Production* 109:118–30.
- Andrić, Ivan, Muammer Koc, and Sami G. Al-Ghamdi. (2019). “A Review of Climate Change Implications for Built Environment: Impacts, Mitigation Measures and Associated Challenges in Developed and Developing Countries.” *Journal of Cleaner Production* 211:83–102.
- Ascione, Fabrizio, Rosa Francesca De Masi, Antonio Gigante, and Giuseppe Peter Vanoli. (2022). “Resilience to the Climate Change of Nearly Zero Energy-Building Designed According to the EPBD Recast: Monitoring, Calibrated Energy Models and Perspective Simulations of a Mediterranean NZEB Living Lab.” *Energy and Buildings* 262:112004.
- ASHRAE. (2007). “International Climate Zone Definitions.” *ANSI/ASHRAE/IESNA Standard 90.1-2007 Normative Appendix B – Building Envelope Climate Criteria*. (cm):4.
- Ciancio, Virgilio, Ferdinando Salata, Serena Falasca, Gabriele Curci, Iacopo Golasi, and Pieter de Wilde. (2020). “Energy Demands of Buildings in the Framework of Climate Change: An Investigation across Europe.” *Sustainable Cities and Society* 60(March):102213.
- Cruz, Alexandre Santana and Eduardo Grala da Cunha. (2022). “The Impact of Climate Change on the Thermal-Energy Performance of the SCIP and ICF Wall Systems for Social Housing in Brazil.” *Indoor and Built Environment* 31(3):838–52.
- Duan, Zhiyin, Xudong Zhao, and Junming Li. (2017). “Design, Fabrication and Performance Evaluation of a Compact Regenerative Evaporative Cooler: Towards Low Energy Cooling for Buildings.” *Energy* 140:506–19.
- Huang, Jianhua and Kevin Robert Gurney. (2016). “The Variation of Climate Change Impact on Building Energy Consumption to Building Type and Spatiotemporal Scale.” *Energy* 111:137–53.
- Pörtner H-O, Roberts DC, Adams H, Adler C, Aldunce P, Ali E, et al. (2022). “Climate Change 2022: Impacts, Adaptation and Vulnerability. Intergovernmental Panel on Climate Change.” 2022.
- Romero-Lara, María Jesús, Francisco Comino, and Manuel Ruiz de Adana. (2022). “Seasonal Energy Efficiency Ratio of Regenerative Indirect Evaporative Coolers—Simplified Calculation Method.” *Applied Thermal Engineering* 220(November 2022):119710.
- Romero-Lara, María Jesús, Francisco Comino, and Manuel Ruiz de Adana. (2021). “Seasonal Analysis Comparison of Three Air-Cooling Systems in Terms of Thermal Comfort, Air Quality and Energy Consumption for School Buildings in Mediterranean Climates.” *Energies* 14(15):4436.
- S.A. Klein. (2006). “TRNSYS 17: A Transient System Simulation Program.”
- Thapa, Samar, Hom Bahadur Rijal, Wilmer Pasut, Ramkishore Singh, Madhavi Indraganti, Ajay Kumar Bansal, and Goutam Kumar Panda. (2023). “Simulation of Thermal Comfort and Energy Demand in Buildings of Sub-Himalayan Eastern India - Impact of Climate Change at Mid (2050) and Distant (2080) Future.” *Journal of Building Engineering* 68(November 2022):106068.
- Xu, Xiaoxiao, Hao Yu, Qiuwen Sun, and Vivian W. Y. Tam. (2023). “A Critical Review of Occupant Energy Consumption Behavior in Buildings: How We Got Here, Where We Are, and Where We Are Headed.” *Renewable and Sustainable Energy Reviews* 182(May):113396.
- Yang, Hongxing, Wenchao Shi, Yi Chen, and Yunran Min. (2021). “Research Development of Indirect Evaporative Cooling Technology: An Updated Review.” *Renewable and Sustainable Energy Reviews* 145(March):111082.

On the assessment of the pressure coefficient on the mixed ventilation modeling

Marcos Batistella Lopes^{*1}, Gaëlle Guyot^{2,3}, and Nathan Mendes¹

*1 Pontifical Catholic University of Paraná
R. Imaculada Conceição, 1155
80.215-901, Curitiba (Paraná), Brazil
*Corresponding author:
batistella.marcos@pucpr.br*

*2 University of Savoie Mont Blanc
Boulevard du Lac, LOCIE
73.370 Le Bourget du Lac, France*

*3 CEREMA
46 Rue Saint-Théobald
38080 L'Isle-d'Abeau,
France*

ABSTRACT

The accurate estimation of the local wind pressure coefficient is crucial in the numerical modeling of natural or mixed ventilation in buildings subjected to wind. Building ventilation modeling typically relies on average wind pressure coefficient values specific to the building façade and wind direction. While the literature provides some correlations and standards for building wall-average pressure coefficients, these values are only useful in the absence of additional information or a database, as they can vary significantly based on urban forms. Field measurements, wind tunnel tests, and numerical modeling are the available methods for estimating pressure on building facades. In the first part of this study, the wall-average pressure coefficient was validated using Computational Fluid Dynamics (CFD) for both an isolated low-rise building and a non-isolated low-rise building. Acceptable relative errors were achieved for the non-isolated building in all wind directions. However, higher relative errors were observed for the non-isolated building at surface directions of 90° and 180° for wind directions exceeding 75°. In the second part of this study, a Building Energy Simulation Test was conducted to assess the impact of the pressure coefficient on ventilation modeling, comparing five scenarios: no wind action, standard pressure coefficient, literature correlation pressure coefficient, and CFD-derived pressure coefficient for isolated and non-isolated buildings. The results indicated relative differences on the order of 7% and 6% for Air Change Rate and CO₂ average concentrations, respectively. This research contributes to the understanding of performance indicators for Indoor Air Quality (IAQ) studies, emphasizing the importance of considering both intentional and involuntary airflows in ventilation design.

KEYWORDS

Pressure coefficient. Ventilation. CFD. IAQ. Multizone model.

1 INTRODUCTION

Thermal comfort and Indoor Air Quality (IAQ) are closely tied to effective ventilation and infiltration management, which directly impact a building's energy consumption. Ventilation encompasses intentional indoor air exchange, which can occur through natural means such as opening windows and doors, or through mechanical systems involving supply and exhaust fans (ASHRAE, 2021). On the other hand, infiltration refers to the unintentional flow of outdoor air into a building through unintended openings like cracks, gaps around windows, doors, and electrical components. Conversely, when this unintentional airflow exits the indoor space, it is termed exfiltration. Both infiltration and exfiltration contribute to air leakage, representing unintentional airflows within a building.

Natural ventilation and air leakage are influenced by pressure differentials across the building envelope, which can arise from various factors such as wind, stack effect, and ventilation fans.

In the case of natural ventilation, these pressure differentials are primarily generated by external forces like wind or temperature differences. In contrast, mechanical ventilation relies on devices such as supply and exhaust fans to create pressure differences and induce airflow. In real-world scenarios, buildings experience a combination of these driving forces simultaneously, and the resulting airflow through the building envelope is a culmination of their combined effects.

To accurately comprehend the driven mechanisms of wind and stack effects, it is crucial to gain a comprehensive understanding of the airflow patterns around the building. In the case of an isolated rectangular flat-roofed building, the mean wind flow pattern reveals intricate characteristics, including the presence of horseshoe vortices, corner streams, areas of flow separation and reattachment, as well as slow rotating vortices formed behind the building due to backflow (Oke et al., 2017). The flow in the immediate wake of the building and the stagnation points upstream and downstream of the wind direction further contribute to the complexity of the airflow. Additionally, the actual airflow around buildings includes a wide range of wind speeds and directions, showcasing distinctive transient features such as the formation and dissipation of separation and recirculation bubbles, as well as periodic shedding of vortices in the wake.

The assessment and understanding of the wind load on a building can be achieved through wind tunnel tests and/or Computational Fluid Dynamics (CFD) modeling (Picozzi et al., 2022). The complex airflow surrounding buildings includes various spatial and temporal scales, and accurately representing full-scale buildings requires satisfying specific similarity criteria. These criteria include geometric, dynamic, and kinematic similarities, as outlined by Shu et al. (2020).

The complexity of CFD codes arises from their requirement to solve a set of nonlinear partial differential equations called the Navier-Stokes equations (Ferziger et al., 2020). Furthermore, the airflow around buildings typically exhibits turbulence, necessitating the modeling of turbulence closure problem (Wilcox, 2006). These turbulence models require significant computational resources and many of them are impractical for building-related problems that rely on transient boundary conditions derived from weather files.

Numerical simulations are utilized for evaluating IAQ performance indicators. Accurate modeling necessitates considering the building interior, exterior environment, and building envelope (Beausoleil-Morrison, 2021). Achieving highly accurate building modeling involves using a combination of toolboxes rather than relying on a single software, a practice known as co-simulation or coupling. In recent years, several coupling approaches have been developed, mostly aimed at assessing building energy consumption by correcting the convection heat transfer coefficient, as highlighted in Singh and Sharston (2021). However, incorporating building ventilation and infiltration into IAQ remains a challenging task, resulting in only a limited number of studies in the literature that explore IAQ and CFD coupling approaches (Kato, 2018).

Wang et al. (2010) conducted CFD simulations to predict outdoor CO concentrations in a two-story home, where the primary source was a generator located near the house. They investigated the impact of varying the distance between the source and the house. Nikolaou and Michaelides (2016) studied two indoor environments by performing CFD simulations to analyse CO transport and determine the optimal quantity and location of CO concentration sensors for occupant safety. Argyropoulos et al. (2017) employed CFD-IAQ coupling to investigate building ingress, utilizing three models to calculate pressure coefficients, and applied them to two case studies. Szczepanik-Scislo (2022) utilized the CFD-IAQ approach to study the release

of CO from an indoor gas furnace, modifying the geometry of an air terminal device to improve IAQ.

For the present study, the CFD code ‘‘CFD0 Editor’’ developed by Wang (2007) was employed. It is a plugin for Contam® (Dols and Polidoro, 2020), a software used for whole-building multizone airflow and contaminant transport analysis. Consequently, the first part of this study aims to enhance wall-averaged pressure coefficient profiles by employing CFD0-Contam indirect coupling (Wang et al., 2010). In the second part, the geometry from the Building Energy Simulation Test (BESTEST) MZ320 (Neymark and Judkoff, 2008) was selected, and boundary conditions were modified to assess the influence of wall-averaged pressure coefficients on certain IAQ indicators.

2 MODEL DESCRIPTION

2.1 Multizone model

Contam® operates on the basis of a multizone airflow network model. This model assumes well-mixed conditions within each zone, where air momentum effects, pressure, and species concentration are uniformly and homogeneously distributed. Furthermore, there is no integration with Building Energy Simulation (BES) software in this study, resulting in a constant temperature assumption. The contaminant flow balance is mathematically represented by:

$$\frac{dm_{\text{cont},i}^{\alpha}}{dt} = \sum_j \dot{m}_{\text{air},j \rightarrow i} (1 - \eta_j^{\alpha}) C_j^{\alpha} + G_i^{\alpha} + m_{\text{air},i} \sum_{\beta} K_i^{\alpha,\beta} C_i^{\beta} - \sum_j \dot{m}_{\text{air},i \rightarrow j} C_i^{\alpha} - R_i^{\alpha} C_i^{\alpha} \quad (1)$$

where $m_{\text{cont},i}^{\alpha}$ is the mass of a contaminant α in zone i , $\dot{m}_{\text{air},j \rightarrow i}$ is the rate of air mass flow from zone j to zone i , η_j^{α} is the filter efficiency of the contaminant α through the path between zones j and i , C_j^{α} is the concentration of contaminant α in the zone j , G_i^{α} is the α contaminant generation rate, $m_{\text{air},i}$ is the air mass in zone i , $K_i^{\alpha,\beta}$ is the kinetic reaction coefficient in zone i between species α and β , C_i^{β} is the concentration of the component β in zone i , $\dot{m}_{\text{air},i \rightarrow j}$ is the rate of air mass flow from the zone i to the zone j , C_i^{α} is the concentration of contaminant α in zone i , and R_i^{α} is the removal coefficient of the component α in zone i .

To discretize the mass balance equation (Equation (1)), a control volume model employing the standard implicit method is employed. The resulting set of discretized equations is solved using both an iterative biconjugate gradient (BCG) algorithm and an iterative successive over-relaxation (SOR) algorithm, as described in Dols and Polidoro (2020).

2.2 CFD model

CFD codes are capable of handling non-uniformities and heterogeneities in fluid flow, although at a significant computational cost when dealing with multizone models. The mass and momentum equations for steady-state fluid flow can be expressed in the following general form, as shown in:

$$\nabla \cdot (\rho \mathbf{u} \varphi) - \Gamma_{\varphi} \nabla \cdot (\nabla \varphi) = S_{\varphi} \quad (2)$$

where ρ is the air density, \mathbf{u} is the air velocity, φ is the transported property (mass or a velocity component), Γ_{φ} is the generalized diffusion coefficient, and S_{φ} is a source or sink term.

In certain simplified cases, such as some laminar flows, analytical solutions for the set of partial differential equations described in Equation (2) exist. However, for most flow problems, including airflow around bluff bodies, empirical and/or numerical solutions are necessary. Among the various numerical discretization methods available, the Finite Volume Method (FVM) is commonly employed. This method discretizes the domain into smaller control volumes and integrates the transport equations for each volume. To solve the convective, diffusive, and gradient terms arising from the FVM, numerical schemes are utilized. Additionally, addressing the turbulence closure problem requires numerical modeling, such as the Reynolds-Averaged Navier-Stokes (RANS) methods, which involve modeling eddies of all sizes through the Reynolds decomposition.

For dealing with incompressible airflow, the "CFD0 Editor" from Contam® comes into play. This software implements the Semi-Implicit Method for Pressure Linked Equations (SIMPLER) algorithm to determine the airflow field (Patankar, 1980). The linear eddy-viscosity model standard $k-\epsilon$ (Launder and Spalding, 1974) is employed as the High-Reynolds number turbulence model. Lastly, the convective terms are discretized using the power-law scheme.

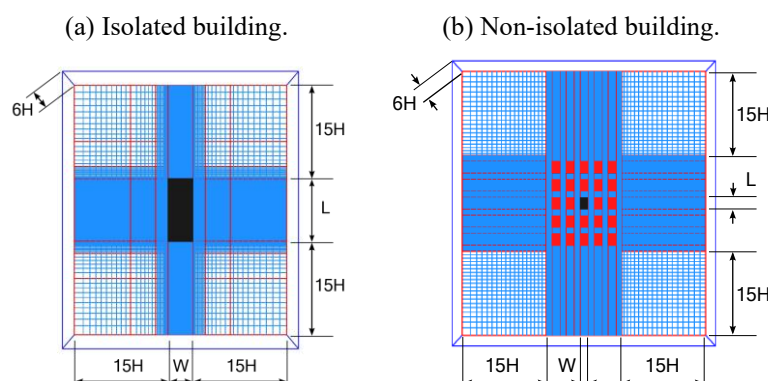
2.3 Numerical Procedure

In the first part of this study, a validation study was conducted using two low-rise building geometries from the comprehensive wind pressure database of the School of Architecture & Wind Engineering at Tokyo Polytechnic University ("TPU Aerodynamic Database", 2023). The first building, considered in isolation, has dimensions of $4\text{m} \times 16\text{m} \times 40\text{m}$, while the second building, non-isolated, has dimensions of $12\text{m} \times 16\text{m} \times 24\text{m}$, with a plan density area of 0.2 and a canyon street aspect ratio of 1.0.

Following the grid refinement factors suggested by Blocken (2015), a grid convergence study was performed with three different grid resolutions. For the isolated building, the final grid consisted of $94 \times 146 \times 46$ nodes, while the non-isolated building grid comprised $166 \times 200 \times 30$ nodes. A length scale of 1:100 was applied, and the wind velocity at the height of the building was set to 7m/s.

The CFD study incorporated specific boundary conditions. The ground boundary was modeled as no-slip, the top of the computational domain was set as a slip wall, and the sides of the domain were designed as openings with an atmospheric boundary layer profile that varied with the wind direction. Figure 1 illustrates a top view of these grids, where H represents the height, W represents the width, and L represents the length of the building.

Figure 1: Mesh



The local wind pressure coefficient is defined by:

$$C_{p,i} = \frac{P_i - P_\infty}{\frac{1}{2} \rho_\infty U_\infty^2} \quad (3)$$

where ρ_∞ is the outdoor air density, U_∞ is the approach wind speed at upwind wall height, P_∞ is the local outdoor atmospheric pressure, and P_i is the pressure in a point i for a given wall surface under wind action.

Equation (3) provides a straightforward definition, but calculating the wind pressure coefficient is a complex task due to its dependence on factors such as the building shape, wind direction, and surrounding environment. To capture an accurate representation of the wall-averaged pressure coefficient for the building facades, this study employed a wind direction increment of 15° and 22.5° .

In the second part of this study, a test was conducted using the geometry depicted in Figure 2a, featuring three distinct zones: A, B, and C. Each zone shared the same dimensions of $8.0\text{m} \times 6.0\text{m} \times 2.7\text{m}$. Zone C was equipped with an exhaust ventilation system operating at a rate of 1 Air Change per Hour (ACH), equivalent to approximately $130\text{ m}^3/\text{h}$ or 77 cubic feet per minute (cfm). Zone B had a constant emission rate of CO_2 at 18 l/h (Poirier et al., 2021) and followed a daily schedule from 5 pm to 9 am. The air leakage between zones was modeled using the power-law model based on Poirier (2023).

For the Contam® simulation (Figure 2b), the weather file for Lyon, France, was utilized, along with a constant outdoor CO_2 concentration of 400 ppm. The simulation spanned a week, starting from January 1st at 0h and concluding on January 7th at 24h, with a time step of 60 seconds.

Figure 2: Modified BESTEST MZ320

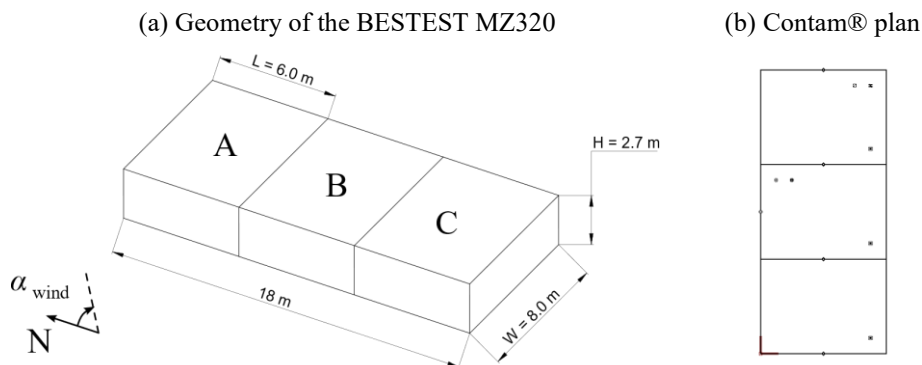


Table 1 presents the five different scenarios considered for the analysis of IAQ. The “No wind” case serves as the base case, focusing solely on mechanical ventilation, while the remaining cases involve mixed ventilation resulting from wind effects. According to the EN15242 regulation, windward facades are assigned a pressure coefficient of +0.5, while leeward facades receive a coefficient of -0.7 when no barriers are present.

Additionally, Swami and Chandra (1987) proposed a pressure coefficient correlation based on wind direction and building dimensions. Two additional pressure coefficients were obtained through CFD: one without any barriers (CFD-Isolated) and another considering a building in a

surrounding area with a plan density of 0.2 (CFD-Non-isolated). These coefficients reflect the influence of the surrounding environment on the building's airflow patterns.

Table 1: Scenarios of study

Case	Description
No wind	No wind action ($C_p = 0$)
EN15242	EN15242 pressure coefficient profile
Swami and Chandra (1987)	Literature correlation of Swami and Chandra (1987)
CFD-Isolated	CFD pressure coefficient profile for a building without any barrier surrounding
CFD-Non-isolated	CFD pressure coefficient profile for a building with a plan density area of 0.2

3 RESULTS AND DISCUSSION

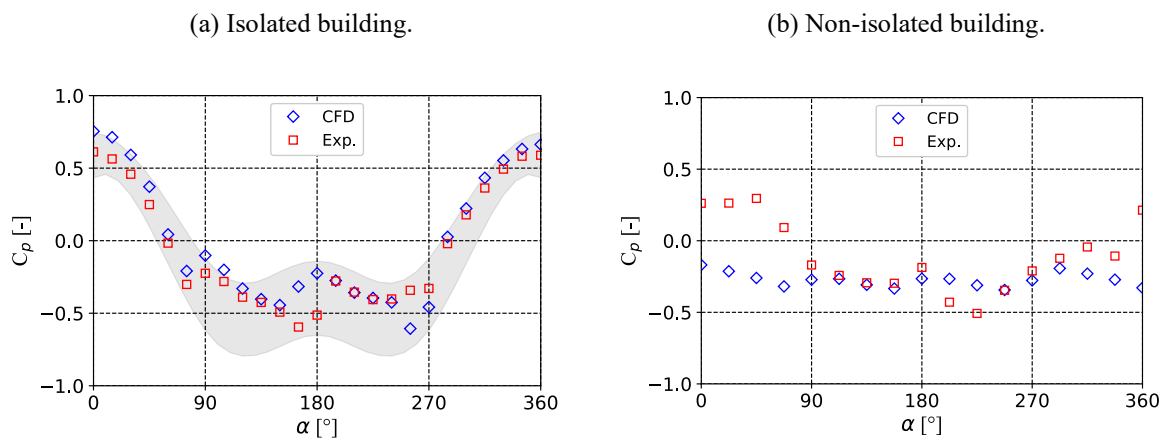
3.1 Wall-averaged wind pressure coefficient

The wall-averaged wind pressure coefficient for low-rise buildings is presented in Figure 3 in which the relative surface angle (α) is defined as:

$$\alpha = \alpha_{\text{wind}} + \alpha_{\text{surface}} \quad (4)$$

where α_{wind} is the wind direction and α_{surface} is the wall orientation.

Figure 3: Wall-averaged wind pressure coefficient



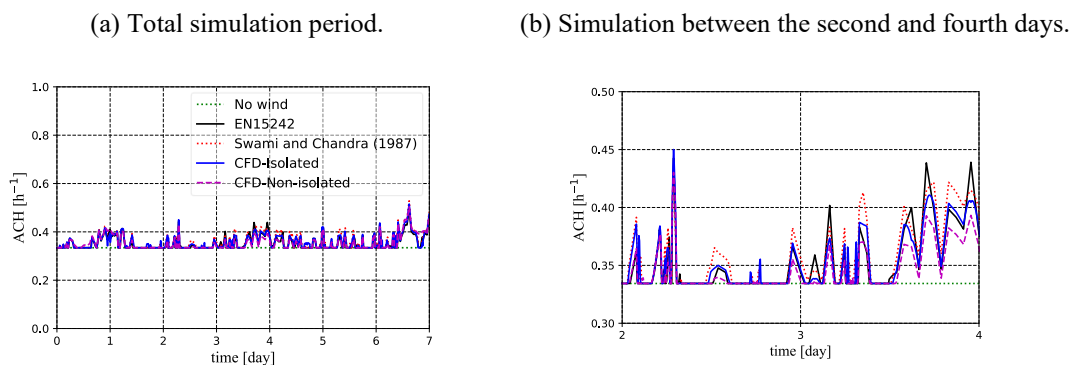
Regarding the isolated building (Figure 3a), besides the experimental data (“TPU Aerodynamic Database”, 2023) the CFD results were compared against the ASHRAE data range for low-rise buildings (ASHRAE, 2021) in which 80% of pressure coefficients are expected (the grey zone in the curve). The CFD results agreed quite well with the mean values from experimental data with higher errors in façade orientation of 90° ($90^\circ \leq \alpha \leq 180^\circ$) and 180° ($180^\circ \leq \alpha \leq 270^\circ$) with higher errors for relative surface angle near 180° and 270° (the relative error in this region is the order of 40%). These errors occurred due to the difficulty of CFD using RANS models to solve turbulence structures such as in flow separation regions and the vortices found in airflow around bluff bodies. However, almost 85% of points yielded errors as lower as 10% and the sign was the same leading to accurate pressure coefficient profiles using this CFD method for isolated low-rise buildings.

The airflow around buildings becomes even more complex when we have a neighbourhood. A building surrounded by buildings of similar height will have quite different airflow partners, i.e., different near-wall velocities and pressures. Consequently, the pressure coefficient will change and due to the large possibilities of surrounding patterns, there are fewer data found in the literature. Taking regular surroundings such as shown in Figure 1b will lead to the pressure coefficient profiles in Figure 3b. For façade orientation between 90° ($90^\circ \leq \alpha \leq 180^\circ$) and 270° ($270^\circ \leq \alpha \leq 360^\circ$), the errors were lowered, and the pressure coefficient profile was quite accurate. The CFD method of this study failed for the surface direction of 0° ($0^\circ \leq \alpha \leq 90^\circ$) mostly because for relative surface angle up to 70° the mean experiments are positive while CFD was negative. This difference in the sign is critical for natural ventilation analysis, therefore the CFD results must be improved in this façade.

3.2 IAQ in the modified BESTEST MZ320

The ACH for the whole building in Figure 2 is shown in Figure 4 in which each case was described in Table 1. When the wind action is neglected, we have $\sim 1/3$ ACH for the whole building once we have an extract ventilation of 1ACH only in Zone C. Overall, when we consider the wind action the air change rate of the whole building is around 7% higher than no wind action.

Figure 4: Air change rate (whole building)



The only contaminant in this study was the CO_2 which is associated with the air change rate and is the most common monitored building contaminant when it is important to control the building ventilation. The CO_2 concentration in Zone B is shown in Figure 5. As expected, improving the ventilation with mixed ventilation led to a reduction of the CO_2 concentration in the order of 6% for Zone B.

Figure 5: CO_2 concentration (Zone B)

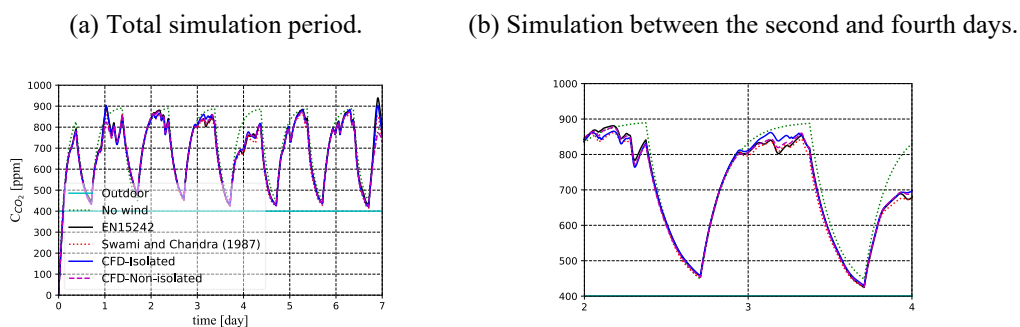


Table 2 sums up the IAQ indicators of this study in which the relative error (Er) is calculated against the case with “No wind”. The air change rate for the whole building is almost the same for the different forms to consider the pressure coefficient, therefore, for this case, there is no need to apply the CFD to obtain a pressure coefficient profile once we have almost the same outcomes regarding the straightforward correlations from the literature. Similar results were achieved for the decrease of the CO₂ concentration in Zone B and C, with lower concentrations in Zone B. In Zone A we observed a very large increase in the CO₂ due to when there is no wind, the outdoor contaminant concentration will not affect this zone. In addition, it is expected lower ventilation rates in Zone A for this building.

Table 2: Arithmetic mean of ACH (whole building) and median of CO₂ concentration

Case	ACH	Er _{ACH}	$\bar{C}_{CO_2}^{Zone A}$	Er _{$\bar{C}_{CO_2}^{Zone A}$}	$\bar{C}_{CO_2}^{Zone B}$	Er _{$\bar{C}_{CO_2}^{Zone B}$}	$\bar{C}_{CO_2}^{Zone C}$	Er _{$\bar{C}_{CO_2}^{Zone C}$}
No wind	0.334	-	59	-	754	-	497	-
EN15242	0.354	+6%	411	+599%	713	-6%	480	-3%
Swami and Chandra (1987)	0.360	+8%	409	+596%	703	-7%	476	-4%
CFD-Isolated	0.357	+7%	412	+602%	708	-6%	478	-4%
CFD-Non-isolated	0.354	+6%	411	+599%	708	-6%	482	-3%

4 CONCLUSIONS

This study performed numerical simulations employing the CFD method to obtain pressure coefficient profiles. These profiles were subsequently tested in the modified BESTEST MZ320 and compared against correlations found in the literature, as well as a case without wind effects.

To begin with, the CFD code was validated for low-rise buildings. It yielded errors as low as 10% for a building without barriers, although certain areas exhibited slightly higher errors for a building with a canyon street aspect ratio of 1.0 due to limitations in the RANS modeling technique.

Next, four pressure coefficient profiles were tested in the BESTEST MZ320 and compared with a case where no wind load was applied. This comparison focused on air change rates for the entire building and CO₂ concentrations in different zones. The results indicated an increase in the ACH of up to 8% and a decrease in CO₂ concentrations in two zones by as much as 7%.

While CFD may not be essential for this simple case, its significance is expected to be more pronounced in complex building scenarios. Therefore, future research should emphasize the importance of obtaining accurate profiles for pressure coefficients, include other IAQ indicators, explore additional scenarios such as cosimulation with BES software for non-isothermal conditions, and propose ventilation control strategies based on the most accurate boundary conditions attainable.

5 ACKNOWLEDGEMENTS

The authors would like to thank the Brazilian agency CAPES (Coordination of Superior Level Staff Improvement), of the Ministry of Education, for the financial support, the Binational Cooperation Program CAPES/COFECUB (Grant # 898/18), in collaboration with the laboratory LOCIE at the Université Savoie Mont-Blanc, France, and the Brazilian Research Council (CNPq) of the Ministry of Science, Technology and Innovation.

6 REFERENCES

- Argyropoulos, C. D., A. M. Ashraf, L. Vechot, and K. E. Kakosimos. 2017. "Coupling Multi-Zone and CFD Models for Investigating Indoor Air Quality." In *Second International Conference on Energy and Indoor Environment for Hot Climates by ASHRAE*. Doha, Qatar.
- ASHRAE. 2021. *ASHRAE HANDBOOK: Fundamentals, SI Edition*. SI ed. American Society of Heating, Refrigeration and Air-Conditioning Engineers.
- Beausoleil-Morrison, Ian. 2021. *Fundamentals of Building Performance Simulation*. Taylor & Francis.
- Blocken, Bert. 2015. "Computational Fluid Dynamics for Urban Physics: Importance, Scales, Possibilities, Limitations and Ten Tips and Tricks towards Accurate and Reliable Simulations." *Building and Environment, Fifty Year Anniversary for Building and Environment*, 91 (September): 219–245.
- Dols, W. Stuart, and Brian J. Polidoro. 2020. *CONTAM User Guide and Program Documentation Version 3.4*. NIST Technical Note 1887. NIST.
- Ferziger, Joel H., Milovan Pric, and Robert L. Street. 2020. *Computational Methods for Fluid Dynamics*. 4th ed. Springer.
- Kato, Shinsuke. 2018. "Review of Airflow and Transport Analysis in Building Using CFD and Network Model." *JAPAN ARCHITECTURAL REVIEW* 1 (3): 299–309.
- Lauder, B. E., and D. B. Spalding. 1974. "The Numerical Computation of Turbulent Flows." *Computer Methods in Applied Mechanics and Engineering* 3 (2): 269–289.
- Neymark, J., and R. Judkoff. 2008. *International Energy Agency Building Energy Simulation Test and Diagnostic Method (IEA BESTEST). Multi-Zone Non-Airflow In-Depth Diagnostic Cases: MZ320 – MZ360*. NREL/TP-550-43827.
- Nikolaou, Andreas, and Michalis P. Michaelides. 2016. "CFD Simulation of Contaminant Transportation in High-Risk Buildings Using CONTAM." In *Critical Information Infrastructures Security*, edited by Christos G. Panayiotou, Georgios Ellinas, Elias Kyriakides, and Marios M. Polycarpou, 135–146. *Lecture Notes in Computer Science*. Cham: Springer International Publishing.
- Oke, Timothy R., Gerald Mills, Andreas Christen, and James A. Voogt. 2017. *Urban Climates*. Cambridge University Press.
- Patankar, Suhas V. 1980. *Numerical Heat Transfer and Fluid Flow*. New York: McGraw-Hill Book Company.
- Picozzi, Vincenzo, Antonio Malasomma, Alberto Maria Avossa, and Francesco Ricciardelli. 2022. "The Relationship between Wind Pressure and Pressure Coefficients for the Definition of Wind Loads on Buildings." *Buildings* 12 (2). Multidisciplinary Digital Publishing Institute: 225.
- Poirier, Baptiste. 2023. "Évaluation de La Performance Globale de La Ventilation Intelligente En Logement Basse Consommation." PhD thesis. Le Bourget-du-Lac: Université Savoie Mont Blanc.
- Poirier, Baptiste, Gaëlle Guyot, Monika Woloszyn, Hugo Geoffroy, Michel Ondarts, and Evelyne Gonze. 2021. "Development of an Assessment Methodology for IAQ Ventilation Performance in Residential Buildings: An Investigation of Relevant Performance Indicators." *Journal of Building Engineering* 43: 103140.
- Shu, Chang, Liangzhu (Leon) Wang, and Mohammad Mortezaazadeh. 2020. "Dimensional Analysis of Reynolds Independence and Regional Critical Reynolds Numbers for Urban Aerodynamics." *Journal of Wind Engineering and Industrial Aerodynamics* 203: 104232.
- Singh, Manan, and Ryan Sharston. 2021. "A Literature Review of Building Energy Simulation and Computational Fluid Dynamics Co-Simulation Strategies and Its

- Implications on the Accuracy of Energy Predictions.” *Building Services Engineering Research and Technology* 43 (1). SAGE Publications Ltd STM: 113–138.
- Swami, Muthusamy V., and Subrato Chandra. 1987. *Procedures for Calculating Natural Ventilation Airflow Rates in Buildings*. FSEC-CR-163-86. Florida: Florida Solar Energy Center.
- Szczepanik-Scislo, Nina. 2022. “Improving Household Safety via a Dynamic Air Terminal Device in Order to Decrease Carbon Monoxide Migration from a Gas Furnace.” *International Journal of Environmental Research and Public Health* 19 (3): 1676.
- “TPU Aerodynamic Database.” 2023. Accessed June 27. <http://www.wind.arch.t-kougei.ac.jp/system/eng/contents/code/tpu>.
- Wang, Liangzhu. 2007. “Coupling of Multizone and CFD Programs for Building Airflow and Contaminant Transport Simulations.” West Lafayette: Purdue University.
- Wang, Liangzhu, Steven Emmerich, and Ryan Powell. 2010. *Modeling the Effects of Outdoor Gasoline Powered Generator Use on Indoor Carbon Monoxide Exposures Phase II*.
- Wang, Liangzhu, Leon, W. Stuart Dols, and Qingyan Chen. 2010. “Using CFD Capabilities of CONTAM 3.0 for Simulating Airflow and Contaminant Transport in and around Buildings.” *HVAC&R Research* 16 (6): 749–763.
- Wilcox. 2006. *Turbulence Modeling for CFD*. 3rd ed. DCW Industries.

Construction of operational control rules for an earth-to-air heat exchanger through transfer reinforcement learning

Yuki Adachi¹, Yasuyuki Shiraishi¹

*1 The University of Kitakyushu
1-1 Hibikino, Wakamatsu, Kitakyushu, Fukuoka
Japan 808-0135*

ABSTRACT

In recent years, earth-to-air heat exchanger (EAHE) systems, which is a method of pre-cooling and pre-heating outdoor air with earth-to-air heat, have been attracting attention as one of the technologies to achieve ZEB. However, at the operational phase, in order to achieve both energy saving and suppression of dew condensation control, EAHE control methods such as the timing or amount of outdoor air introduction have not been established. Recently, research on operational control by reinforcement learning (RL) has become popular and has attracted attention in the field of air conditioning control. RL is effective even in cases where future states are difficult to predict, such as EAHE. In previous studies, the unsteady CFD analysis method proposed by the authors made it possible to evaluate the annual energy savings and dew condensation in EAHE in detail. In addition, it was clarified that the RL, which uses the same CFD method as a simulator, can establish a control law that achieves both energy-saving effects and prevent indoor air pollution by suppressing dew condensation. On the other hand, RL requires a huge number of trials to construct the control law.

Therefore, the purpose of this study is to improve the learning speed and control performance. First, we adopt transfer learning (TL), which reuses a model pre-trained in RL for training in a new environment. Next, we verify the effectiveness of using this transfer reinforcement learning (TRL) as a control method for EAHE. The result showed that TRL achieved better control performance and faster learning speed than RL. In addition, it was suggested that EAHE with insufficient actual measurement data may be efficiently controlled from the first year of operation by directly using the control law established in advance. It was confirmed that RL performs well in terms of energy efficiency and air quality maintenance.

KEYWORDS

Earth-to-air heat exchanger system, CFD, Transfer Reinforced Learning, Ventilation, Outdoor air load, Condensation, Indoor air quality

1 INTRODUCTION

One of the fundamental technologies for developing zero-energy buildings is earth-to-air heat exchanger (EAHE) systems. An EAHE is a passive component of a heating, ventilation, and air conditioning (HVAC) system that utilizes the large heat capacity of the soil to pre-cool the outdoor air (OA) in the summer and pre-heat it in the winter. Further, it can reduce the heat loads of OA for air handling units or fresh air handling units (FAHU) by introducing pre-heated or pre-cooled OA through this system. The operational control of such a system is limited to control based on schedules, sequential disturbances, and internal system conditions.¹⁾ We have been using reinforcement learning (RL) to develop a control law for an EAHE system (underground pit system) to achieve energy-saving effects and prevent indoor air pollution by suppressing dew condensation.²⁾ However, RL has the problem of requiring a huge number of trials for learning convergence. For this reason, previous studies have reduced the computational load on the environment side of the RL (e.g., by reducing the number of meshes

in computational fluid dynamics [CFD] analysis), thereby enabling a large number of training cycles. Another solution to this problem that has been attracting attention in recent years is transfer learning (TL), which enables faster learning and improved learning performance by reusing previously learned models for training in a new environment.³⁾ However, few studies have applied TL to RL, and important details have yet to be clarified, such as the area (range) in which TL is effective.

The objective of this study was to construct an efficient operational control law for soil heat exchange systems using RL that utilizes TLs to speed up and improve the learning performance of RL. We do this for an EAHE, and after adapting TL to RL, we conduct a case study on the transition target to verify the effectiveness of transition reinforcement learning (TRL) as an operational control method.

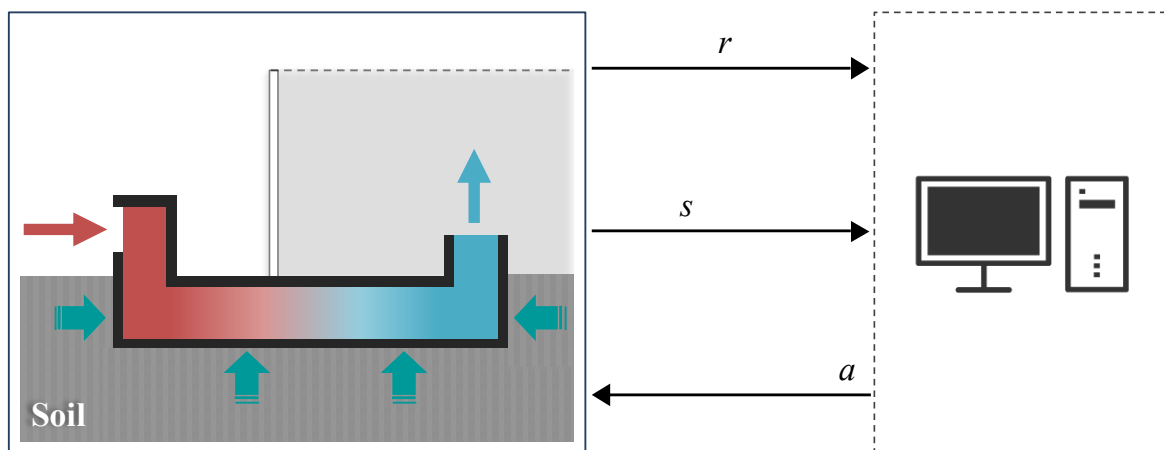


Figure 1 Diagram of RL process with EAHE as example

2 REINFORCEMENT LEARNING

2.1 Reinforcement Learning Overview

As shown in Figure 1, the RL is composed of the environment and the agents that control its operational decisions, with a reciprocal relationship between them. In RL, at a certain state s_t on the environment side, the agent manipulates the environment based on the action a_t , the output by the agent, and the next state s_{t+1} , resulting from the transition and the immediate reward r_{t+1} obtained at the transition destination (an example is an evaluation value, such as how much energy was saved), is passed from the environment to the agent. By repeating this through trial and error for the state s_t , RL learns to output an action a_t that maximizes the sum of the immediate rewards for a certain period of time.

2.2 Reinforcement Learning Problem Setup

The definitions of states s , action a , and immediate reward r are given in Table 1 as the problem set for RL. In addition to weather conditions, such as the outdoor air temperature and absolute humidity, five types of states s were used as information in the system: the condensation area ratio and surface temperatures at two representative points in the system (near the inlet and outlet ports). Action a was set to five discrete values of "MD_o / MD_e OA damper opening," that is to say the "outdoor air intake through the system," as shown in Figure 2. In the subject system, the outdoor air conditioner was assumed to have a constant air volume of 8,100 m³/h (CAV) during air intake hours. Since the control objective was to ensure energy-saving performance and to suppress condensation inside the system, the immediate reward r

was defined as two kinds of rewards: the amount of heat processed by the external controller r_1 and the condensation area ratio r_2 .

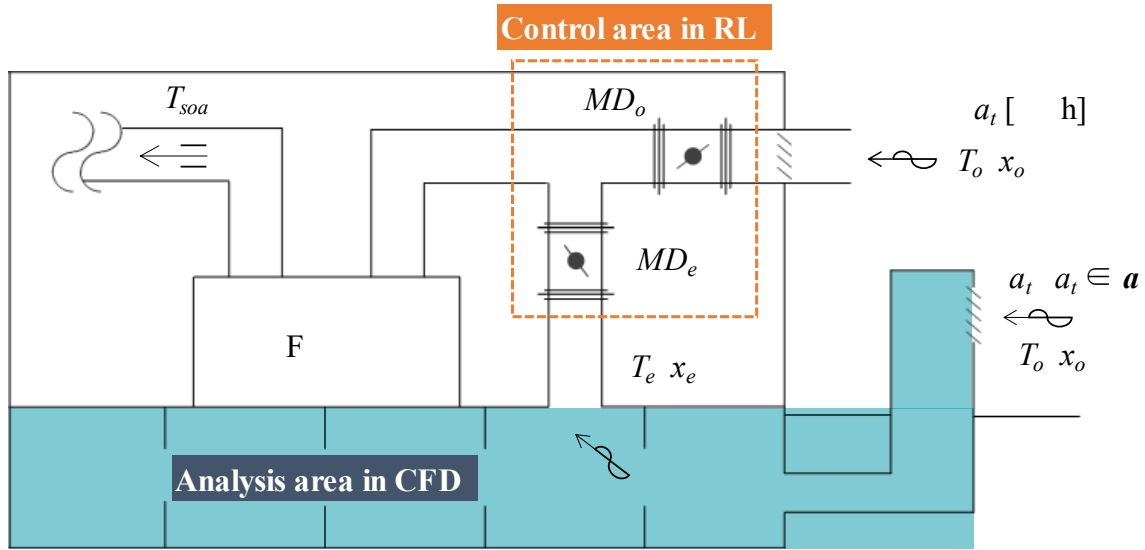


Figure 2 Diagram of EAHE

Table 1: Definition of state, action, and reward

State s	Outdoor air temperature/Outdoor air absolute humidity / Condensation area ratio / Surface temperature (2 points)
Action a	$\{0 \text{ m}^3/\text{h}, 2,025 \text{ m}^3/\text{h}, 4,050 \text{ m}^3/\text{h}, 6,075 \text{ m}^3/\text{h}, 8,100 \text{ m}^3/\text{h}\}^{\text{注1)}$
Reward r	$r = r_1 \times w_1 + r_2 \times w_2$ ($r_1 = 0.3, r_2 = 0.7$)

$$r_1 = \text{clip}\left(\frac{Q_{FAHU}}{Q_{std}}, -1.0, 0\right)$$

$$T_{OA} = \frac{T_e \cdot a + T_o(\max(a) - a)}{\max(a)}$$

$$r_1 = \Delta T = \begin{cases} T_{OA} - 22 & (\text{if winter and } T_{OA} < 22) \\ 26 - T_{OA} & (\text{if summer and } T_{OA} > 26) \\ T_{OA} - 20 & (\text{if spring / fall and } T_{OA} < 20) \\ 28 - T_{OA} & (\text{if spring / fall and } T_{OA} > 28) \\ 0 & (\text{else}) \end{cases}$$

$$Q_{FAHU} = C_p \times \rho \times \frac{\max(a)}{3,600} \times \Delta T$$

$$r_2 = \text{clip}\left(\frac{C_{area}}{C_{std}}, -1.0, 0\right)$$

$$C_{area} = \frac{S_c}{S_e} \times 100$$

Q_{std} : Standard value for r_1 [W], Q_{FAHU} : Heat load of FAHU [W], T_{OA} : h F U [°C] T_e : Outlet temp. of h [°C] T_o : Outdoor air [°C] ΔT : Difference in the blow- h F U [°C] C_p : specific heat capacity (=1.007) [kJ/(kg · K)], ρ : Air density (=1.206) [kg/m³], C_{area} : Condensation area ratio [%], S_e : Total surface area in the EAHE [m²], S_c : Condensation area in the EAHE [m²]

3. TRANSFER LEARNING

3.1 Transfer Learning Overview

TL is a framework in which the knowledge learned by the source task agent is reused by the target task agent. After incorporating TL in RL, the RL agent learns and acquires measures in the source task. Then in the target task, which is the same or a similar environment, the measures

acquired in the source task are reused, enabling faster learning and improved learning performance in the target task.

3.2 Transition Reinforcement Learning with Deep Learning

An effective method for policy reuse is the TL method using deep learning (DL). DL is a machine-learning method that uses a multi-layered neural network (NN), which is a mathematical model that mimics the network structure of neurons in the brain. NNs consist of an input layer, an intermediate layer, and an output layer, and the relationship between inputs and outputs in each layer is given by Equation (1).

$$\mathbf{y} = f(\mathbf{x}\mathbf{W} + \mathbf{b}) \quad (1)$$

Here, \mathbf{y} is the output vector, \mathbf{x} is the input vector, \mathbf{b} is the bias vector, \mathbf{W} is the weight matrix, and f is the activation function. In an NN, the output of the L-1 layer is the input of the L layer. That is, each layer computes Equation (1) independently, so the NN can extract and combine layers. In TL using DL, this feature is utilized to reuse the NN model learned in the source task for training the NN in the target task. Also, by changing the number of layers to be extracted and the positions to be combined, it is possible to respond flexibly according to the target task.

The steps involved in the TRL implemented in this paper, shown in Figure 3, are as follows. First, the optimal measures (pre-trained Q-Network) in the source model (e.g., a simple CFD model of an underground pit) are learned using Deep Q-Network (DQN). Second, all or partial layers are extracted from the pre-trained Q-Network. Next, the layers extracted from the pre-trained Q-Network are combined with newly added layers to train the target model (e.g., a CFD model of a real underground pit). Then, the weights of all or some of the layers extracted from the pre-trained Q-Network are fixed (optional). Finally, training (re-training) is performed for all the layers that were combined or only the layers that were added. Thus, by reusing the Q-Network acquired in the source model and changing the transition rate (number of layers extracted from the pre-trained Q-Network) and layers to be fixed, we expect to improve initial performance, convergence (reduction in the amount of training data), and learning performance, as shown in Figure 3.

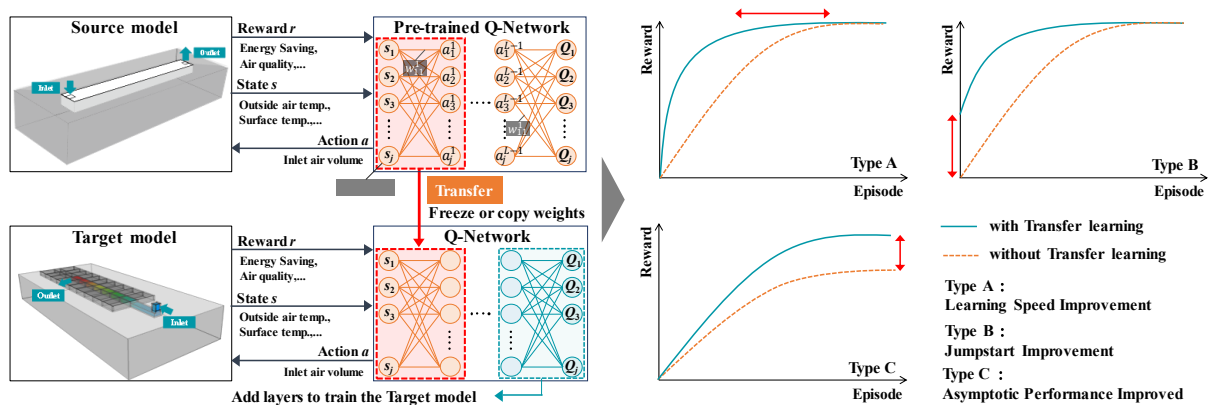


Figure 3 Diagram of Transfer Reinforcement Learning (Image of using DQN as reinforcement learning)

4. Analysis Condition

4.1 Target Building and CFD

EAHE system (underground pit system) is installed in a medium-sized office in Fukuoka Prefecture, Japan (Table 2). Outdoor air introduced into the underground pit through the inlet

protruding outdoors exchanges heat with the soil (concrete) for approximately 70 m to the outlet of the underground pit. The introduced outdoor air is pre-cooled and pre-heated and supplied to the outdoor air conditioner, contributing to energy savings in the outdoor air conditioner. Table 3 shows the CFD analysis conditions and Figures 4 and 5 show the analytical models. The outdoor air introduction period was from 9:00 to 18:00 daily. During the analysis, the amount of outdoor air introduced through the system was switched every hour according to the operational values output by reinforcement learning. CFD was employed as a simulator in the reinforcement learning environment, and the computational load reduction method of unsteady CFD, which assumes a fixed flow field, was used as the solution method.⁴⁾

Table 2: Brief Description of the Building

Location	Fukuoka
Use	Accommodations and Research Facilities
Structure	RC
Number of Stairs	1F-4F
Year Completed	July 2008
Extended Bed Area	5,498m ²
Underground Pit (W x H)	× 5 – 1.7m
Underground Pit (Length)	76.8m

Table 3: CFD conditions

Condition	Method/Parameter
Calculation period	1/1~12/31 (Approached period:1 year)
Time interval	3,600s
Domain	40.4m(X) × 13.4m(Y) × 6.9m(Z)
Mesh	Source model:6,422 (26(x) × 19 (y) × 13(z)) Target model:92,610 (70(x) × 49 (y) × 27(z))
Turbulence model, Scheme	Standard <i>k-ε</i> model, 1 st -order upwind scheme for advection term, SIMPLE algorithm
Inflow boundary	$U_{in} : a_t, T_o : \text{Outdoor air temperature}^{5)} [^{\circ}\text{C}]$ $x_o : \text{Outdoor air absolute humidity}^{5)} [\text{k} \quad \text{k}^{-1}]$ $k_{in} = 3/2(U_{in} \times 5^{-2}, \quad \varepsilon_{in} = C_{\mu}^{3/4} \cdot k_{in}^{3/2}/l_{in}$
Initial temperature	Results of the 3D pre-analysis of this system controlled by schedule
Wall boundary	Velocity and Temperature: General logarithmic function Humidity: $L \quad h \quad x = 67$
Upper side	: 22 26 °
Boundary of the pit	Heat transfer coefficient: 23.0 W/(m ² ·K)
Ground surface boundary	: [°C] Convective heat transfer coefficient: 17.9 W/m ² K

U_{in} : Inlet velocity [m/s], l_{in} : Length scale(=1.0m), k_{in} : Turbulence kinetic energy [m²/s²],
 ε_{in} : Dissipation rate of k_{in} [m²/s³], C_{μ} : Model constant (=0.09) [-]

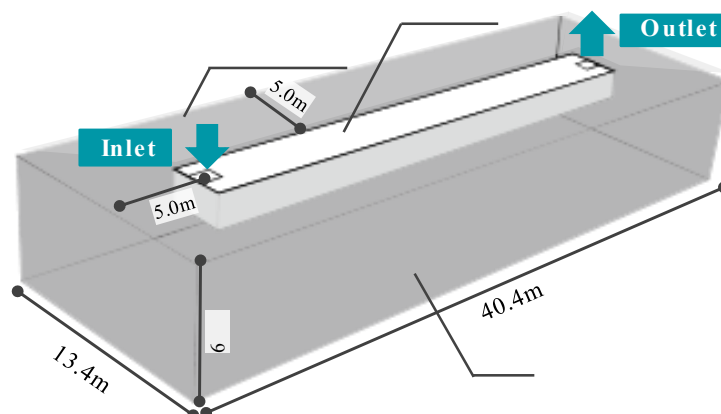


Figure 4 CFD model of EAHE system (Straight)

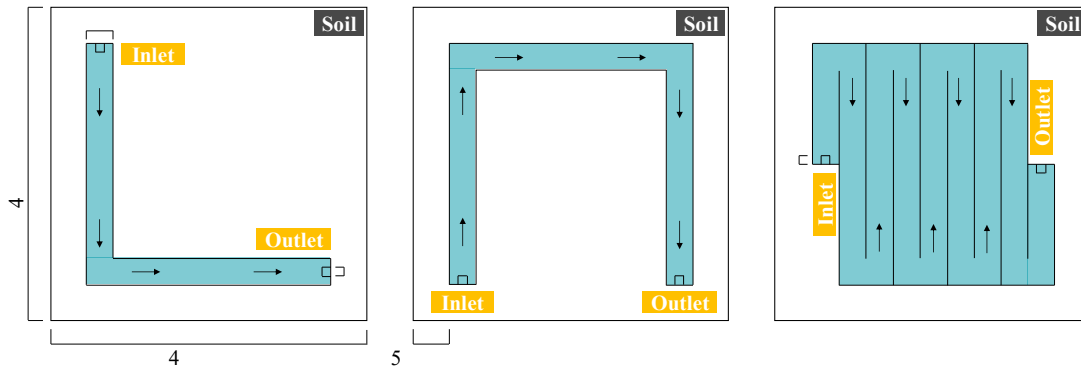


Figure 5 CFD model of EAHE system (Left: L, Mid: Corridor, Right: Meandering)

4.2 RL

The RL conditions are given in Table 4. In this study, DQN was used to implement TRL with DL. In an environment where actions are discrete, the Q function can be expressed without deepening the middle layer of the NN. Therefore, the middle layer for both the source and target

4 64×64

To speed up the learning process, the learning rate was set to 0.001 in the target model to efficiently learn the measures acquired in the source model. The ϵ -greedy method was used as the action search in the target model while using the measures acquired in the source model from the initial stage of learning.

Table 4 Conditions of reinforcement learning

Algorithm / Episode	Deep Q-Network (DQN) ⁶⁾ / 200
Discount factory	0.99
Exploration rate ϵ	ource: Linear schedule, $\epsilon_0 = 1.0$, $\epsilon_N = 0.02$ Target: Linear schedule, $\epsilon_0 = 0.5$, $\epsilon_N = 0.02$
Learning rate η	Source: 0.0005, Target: 0.001
Replay memory buffer	49,984
Q-Network / Batch size	$5 \times 64 \times 64 \times 2$ 5 2

N : Number of episode (≤ 200) [-]

4.3 TL

The similarity of the source and target is important when implementing TL. In this study, the effectiveness of TRL was verified by being conducting on various targets with measures learned with the same source model. The analysis cases are given in Table 5. The source model for each case was a straight-type CFD model. In Case 1 (transition of action), TRL from two types of airflow to five types of airflow was implemented. In the Case 2 series (shape transition), TRLs were performed from a rectilinear to an L-shape, a corridor, meandering, and for real buildings. In the Case 3 series (weather transition), TRL was conducted from Kitakyushu (warmer climate) to Fukuoka (warmer climate) and Akita (colder climate). Regarding the transition rate, the first two layers extracted from the Q-Network of the source model were combined with the new output layer because the number of nodes in the output layer was different from that in Case 1, which is a transition of action. Additionally, Cases 2 and 3 were assumed to be all layers. In all cases, the weights of the first half of the layers were fixed, and only the second half of the layers were trained. In Cases 2-4, the target model was an EAHE (straight) installed in a real building, and an analysis was conducted to directly apply the control laws constructed in the

source model to the operational control of the building to study the versatility of RL. For comparison, the analysis also included random control of RL and the outdoor air intake.

Table 5 Conditions of reinforcement learning

CASE	Source	Target	Object
1	2	5	action
2-1	Straight	L	Shape
2-2	Straight	Corridor	
2-3	Straight	Meandering	
2-4	Straight	Actual tunnel	
3-1	Kitakyushu	Fukuoka	Weather
3-2	Kitakyushu	Akita	

5. RESULTS

5.1 Progress of RL and TRL

Figure 6 shows the episode reduction rate and the number of episodes required for convergence of the RL and TRL studies for each case, and Figure 7 shows the progress of the studies from Cases 2-1 to 2-3. Figure 6 shows that Case 3-1 (Kitakyusyu to Fukuoka) resulted in the fastest learning speed and a 90-episode reduction. This is presumably because both the source and target models were straight EAHE systems, and the climates of Kitakyushu and Fukuoka are very similar, having the highest similarity between the source and target among all cases. For the Case 2 series (shape transition), more than 50 episodes were reduced in Case 2-1 (straight to L) from Figure 7. TRL also remained higher than RL with respect to total rewards. In Cases 2-2 (straight to corridor) and 2-3 (straight to meandering), the total reward remained high from the early stages of learning, which is presumably the result of efficiently utilizing the source model's measures from the early stages of learning. Cases 2-2 and 2-3 achieved an increase in learning speed of 40 episodes and 20 episodes, respectively. As in Case 2-1, TRLs showed a high sum of rewards, suggesting that they improved learning performance. This is presumably because, as in Case 3-1, the L-type had the highest similarity to the straight type. In all cases, however, TRL achieved episode reduction.

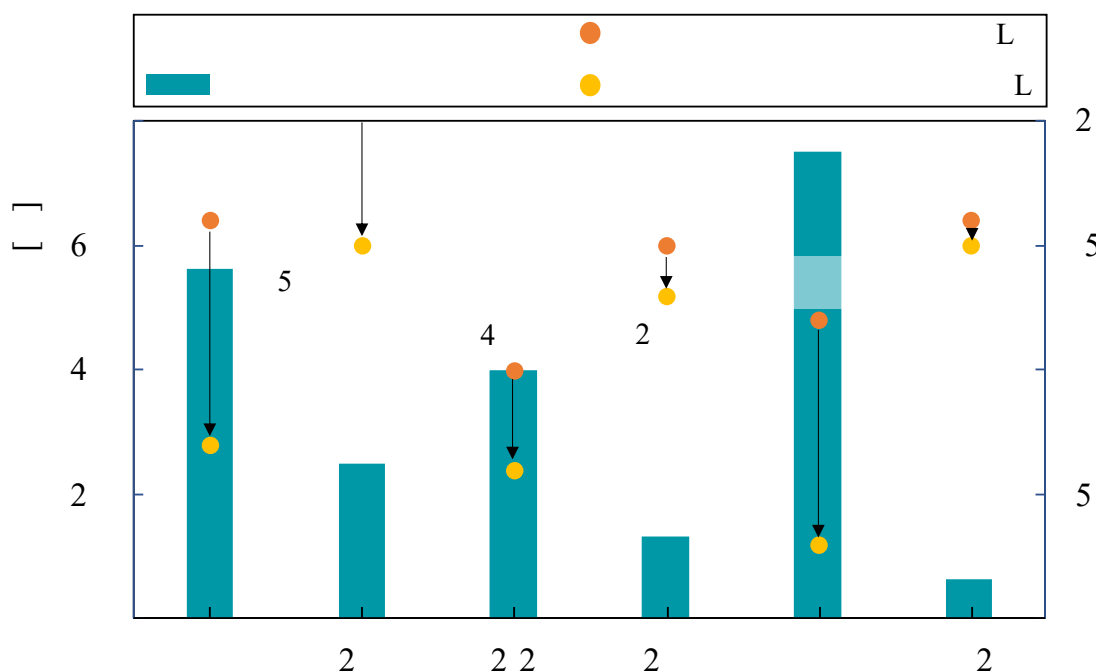
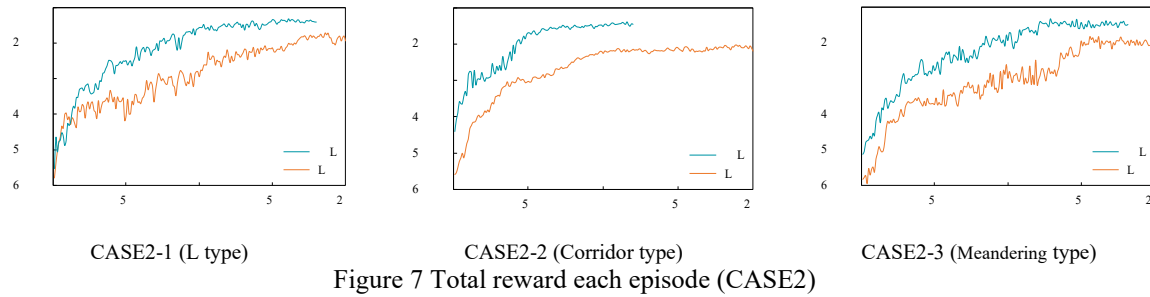
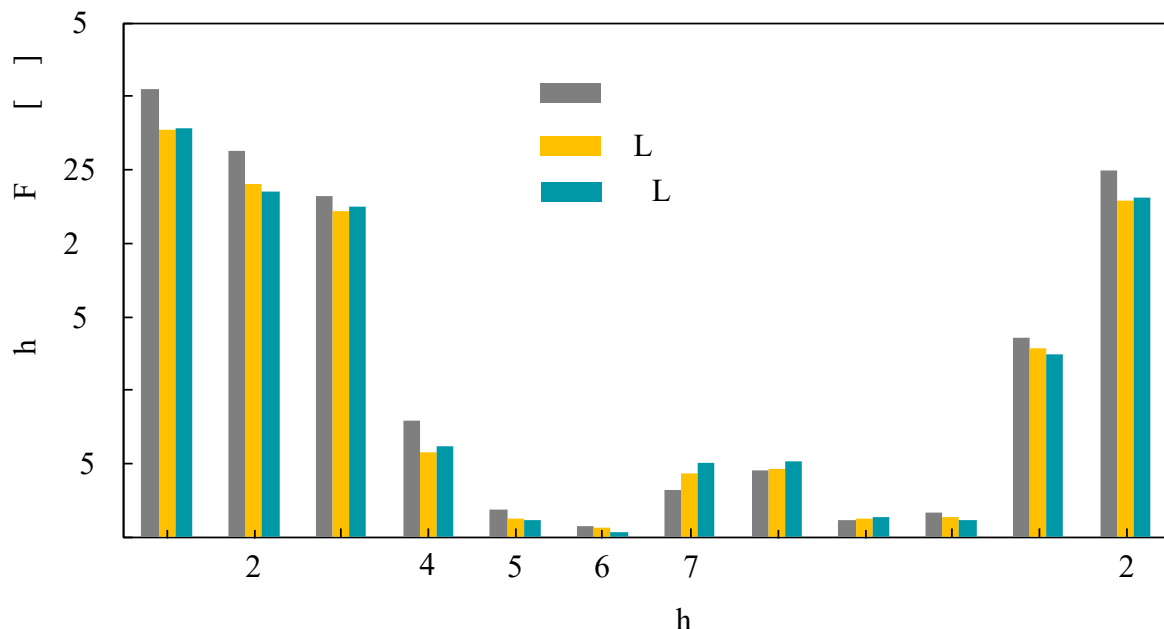


Figure 6 Episode reduction ratio / Episode of convergence



5.2 Comparison with RL and Random

Figures 8 and 9 show the heat rate and condensation area ratio of the external controller when controlled by Case 2-1, RL, and random, which are the fastest learning methods in Case 2. The condensation area percentages for Case 2-4 are also shown in Figure 10. For Case 2-1, the annual heat rates for the external air conditioner process were 128.8 GJ, 128.9 GJ, and 139.4 GJ for TRL, RL, and random, respectively, indicating that control with TRL and RL had high energy-saving performance. As for the condensation suppression effect, it was confirmed that TRL mitigated the condensation situation compared with RL and random, especially during the summer season. This confirms that TRL improved control performance. Finally, for Case 2-4, Figure 10 shows that the direct use of the source model's control law in the EAHE of a real building resulted in partial suppression of condensation compared with the random case, but the control performance was inferior to the case in which TRL was implemented. The annual heat output of the external controller was 211.9 GJ and 216.7 GJ for the random and source policies, respectively, with random being slightly higher. This may be due to the fact that the reward design prioritized the suppression of condensation. The results suggest that by reviewing the RL parameters and reward design, it is possible to obtain sufficient control performance for practical use without conducting new training.



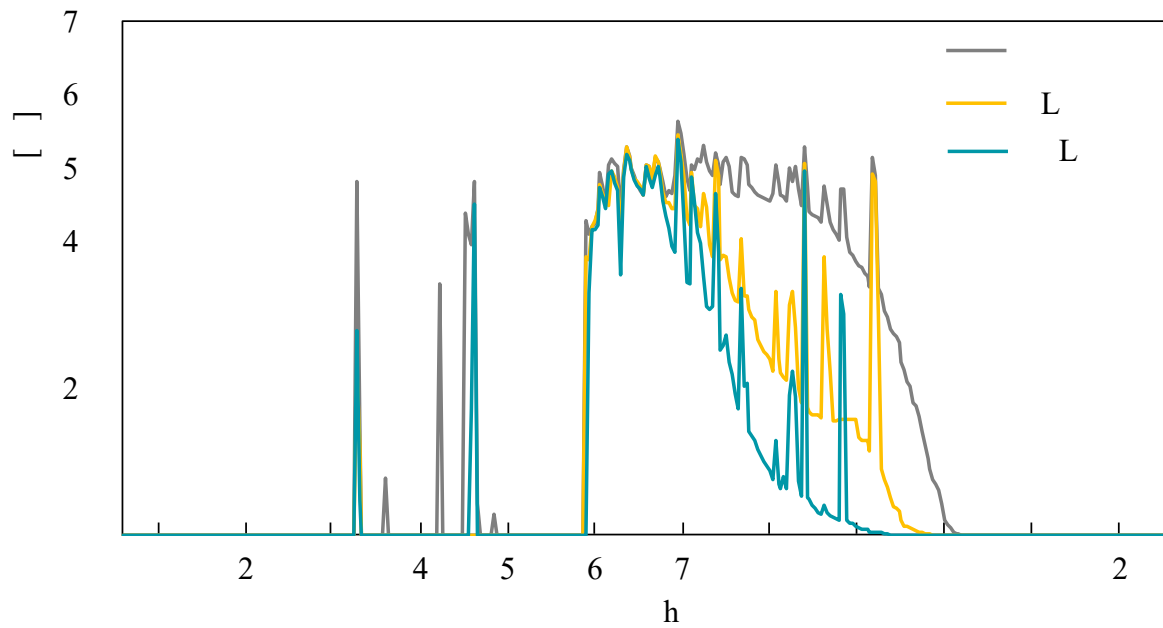


Figure 9 Condensation area ratio (CASE2-1)

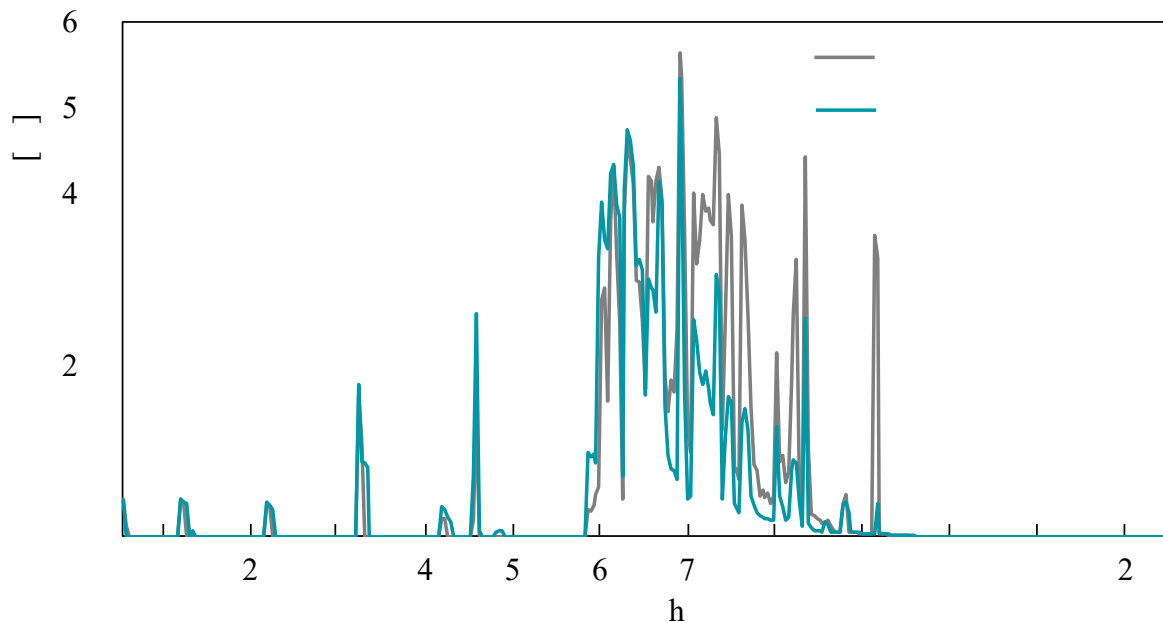


Figure 10: Condensation area ratio (CASE2-4)

6. CONCLUSIONS

By utilizing learned measures in the construction of new control laws (TRL), we were able to achieve better control performances of energy-savings and suppressing dew condensation and a faster learning speed than conventional RL. Our results also suggest that EAHEs with insufficient measured data can be efficiently controlled from the first year of operation by directly using the pre-constructed control law.

7. ACKNOWLEDGMENT

This work was supported by JSPSKAKENHI Grant Numbers 19H02301 and 20KK0102.

8. REFERENCES

- 1) Suzuki, H et al. (2021). Verification of energy and environmental performance of urban eco-campus, Part 6 Analysis of cool & heat pit energy savings in ZEB Ready buildings, Heating, Air-Conditioning and Sanitary Engineers of Japan, J-89, pp.357-360,2021.9 (in Japanese).
- 2) Motoyama, Y. (2021). Proposal for an optimal operation method for earth-to-air heat exchanger systems using reinforcement learning, Construction of control law by coupled analysis of Deep Q Network and CFD, Architectural Institute of Japan Kyusyu Chapter Architectural Research Meeting, No.60, pp.113-116, 2021.3 (in Japanese).
- 3) G Pinto et al. (2022). Transfer learning for smart buildings, A critical review of algorithms, applications and future perspectives, Advances in Applied Energy, Vol. 5, 2022.2,100084.
- 4) Tomoda, K. (2016). Annual prediction method for the thermal performance of earth-to-air heat exchanger by CFD analysis where calculation loads were reduced, Evaluation method of cooling and heating effect of an earth-to-air heat exchanger (Part 2), The Architectural Institute of Japan, 81(722), pp.393-401, 2016.4.(in Japanese).
- 5) Expanded AMeDAS Weather Data (2000). The Architectural Institute of Japan.
- 6) Mnih et al. (2015). Human-level control through deep reinforcement learning. Nature Vol.518, pp.529-533, 2015.2.

9. APPENDIX

Table 6 : List of abbreviations

RL	Reinforcement Learning
TL	Transfer Learning
TRL	Transfer Reinforcement Learning
AHU	Air Handling Units
FAHU	Fresh Air Handling Units
DL	Deep Learning
NN	Neural Network
DQN	Deep Q-Network
CFD	Computational Fluid Dynamics

Ventilation and Thermal Performance Examination of Slot Line Diffuser for Perimeter Usage by CFD Simulation

Shaoyu Sheng^{*1}, Toshio Yamanaka¹, and Tomohiro Kobayashi¹

1 Osaka University

2-1 Yamadaoka

Suita, Osaka, Japan

**Corresponding author:*

sheng_shaoyu@arch.eng.osaka-u.ac.jp

ABSTRACT

Building ventilation demand increased during the “new normal” following the Covid-19 pandemic. Rather than completely renovating existing HVAC equipment, it is more practical and cost-effective to maximize their existing ventilation performance. This study focuses on slot line diffusers, which are widely used for handling perimeter heat loads. Its long throw distance and wide coverage effectively block cold drafts and heat flow from the exterior window glass. Meanwhile, the mounting position near the glass surface and the high supply velocity can create a ventilation scenario similar to wall confluent jet ventilation (WCJV) or ceiling-supplied displacement ventilation. In order to determine the ventilation and thermal performance of the slot line diffuser, CFD simulations have been conducted using the low-Reynolds number turbulence model with fine meshes, in which a detailed velocity characteristics model derived from a full-scale experiment is used to reproduce the diffuser’s supply airflow. This study priority examined the performance under heating supply conditions. This is because buoyance reduces the throw distance of heating airflow, which obviously influences thermal and ventilation performance compared with cooling conditions. The analysis space is modelled based on a typical open space between two columns of an office building in Japan. Four human simulators are seated around a table in this space’s interior to reproduce a small-scale meeting scenario. Gas is generated by a human simulator to represent pollutants (odor or droplet nuclei) from a speaker. The diffuser’s air supply mode (full-open and half-open) and the mounting location of the exhaust are adjusted as parameters. The CFD simulation results provide a comparison of the ventilation and perimeter heating performance of this type of air terminal by listing 1: the distribution of tracer gas concentration, air temperature, and airflow distribution in the occupancy zone; 2: heating capacity, air distribution performance index (ADPI), draft rate (DR), and ventilation efficiency under different use scenarios. In conclusion, decreasing the slot line diffuser’s supply area obviously improves its heating efficiency by blocking the cold draft from the exterior window. It also enhances ventilation performance by establishing a WCJV. The vertical temperature difference and average normalized concentration in the occupied zone can be kept below 1°C and around 0.7, respectively, for office heating usage in this study.

KEYWORDS

Slot line diffuser, Perimeter thermal environment, Wall confluent ventilation, CFD simulation

1 INTRODUCTION

From the view of maximizing the ventilation and thermal performance of existing HVAC equipment, this study concentrates on the slot line diffuser, an air terminal that is widely used for perimeter heat treatment in Japan. However, studies on the slot line diffuser are mainly concentrated on its interior ventilation performance as used for stratum ventilation [1], protected zone ventilation [2], stratified air conditioning [3], etc. Regarding its perimeter usage, Lorch et al. [4] examined the perimeter air conditioning performance by mock-up tests, and Rousseau [5] tested the Air-Diffusion Performance Index (ADPI) by a full-scale experiment. Except for these two studies conducted in the early 1980s, no further studies have been found using the new measurement or simulation method in recent years, and investigation on its perimeter ventilation performance remains inadequate. Hence, our study will examine both the thermal and ventilation performance of the slot line diffuser mounted in the perimeter area with large glazing areas.

Designed with a slim geometric shape, the slot line diffuser jets air from a wide range and works as an air curtain. At the same time, a wide supply area decreases outlet velocity. This means less momentum, and buoyancy will obviously reduce the throw distance of the heating air supply, reducing heating efficiency during winter. Furthermore, this type of terminal is expected to establish wall confluent jet ventilation (WCJV) [6] or ceiling-supplied displaced ventilation to enhance ventilation efficiency. However, insufficient throw distance may have adverse effects. Therefore, in our research, two deflection panels are installed inside the diffuser's chamber to halve the diffuser's outlet area if needed. Their effect on converging airflow has been proved in our previous study [7], and their impact on the perimeter thermal environment and ventilation performance under the heating supplied condition will be examined by detailed computational fluid dynamics (CFD) simulation in this study.

In order to ensure CFD simulation accuracy, a detailed model for reproducing supply air from this type of terminal will be used. Based on the full-scale experiment in our previous study [7], this model was proposed and validated to have greater precision than the P.V. method or simple condition method. Furthermore, a linear low-Reynolds-number turbulence model [8] [9] with fine meshes will be applied. Compared with the commonly used Standard k- ϵ (SKE) turbulence model for indoor environment simulation, this turbulence model could predict the attached and separated wall shear flows and have higher accuracy in calculating the convection heat transfer. Tracer gas will be generated from a human simulator's mouth. Ventilation performance will be assessed by examining the distribution of gas concentrations in the analysis space. Furthermore, the distribution of the flow field and the age of air in this space will also be exhibited in graphs. With respect to the perimeter thermal performance, the temperature and airflow distribution in the analysis space, heat transfer rate and temperature on the glass's inner surface, heat removal rate in the perimeter zone, heat transfer/exchange rate between the perimeter and interior, and the air distribution performance index (ADPI) and draft rate (DR) index in the analysis space are enumerated. The geometry of the outlet surface in the longitudinal direction (deflection panels adjustment), and the exhaust's mounting location are adjusted as parameters. By comparing the simulation and calculation results, the thermal performance of the slot line diffuser in the glazing area during the heating period is determined. In addition, the possibility of its use as a ventilation system will be examined.

2 DETAILS OF THE CFD SIMULATION

2.1 Slot line diffuser and the detailed velocity characteristics model

The archetype of the slot line diffuser with adjustable supply area examined in this study shows in *Fig.1*. As shown in *Fig.1(a)*, closing these panels converged the airflow, thereby halving the diffuser's supply area into 550 mm longitudinal (hereinafter abbreviated as 1/2 outlet mode), as well as if the panels are opening, the supply area is 1200 mm longitudinal (hereinafter abbreviated as 1/1 outlet mode). Based on the experiment and CFD simulation in the previous study [7], under the 200m³/h, the standard supply rate of this diffuser, 1/2 outlet mode can throw the supply air into the occupied zone from the 3 meters height ceiling at a speed above 1.0 m/s. And under the same supply rate, outlet airflow of the 1/1 mode has a reversed "V" shape distribution, extending the diffusion range in the longitudinal direction, but airflow velocity in the occupied zone is less than 0.3 m/s.

Fig.2 briefly shows the airflow characteristics model and the detailed boundary division method proposed in our previous study. Each airflow boundary is defined as a "fixed velocity opening", having its unique component velocity profile in u , v , and w components calculated from the "airflow characteristics model" based on the full-scale measurement data using the X-type hotwire anemometer. Furthermore, the velocity data have also been used to calculate the turbulence kinetic k and dissipation ϵ . Mean values of k and ϵ calculated from every measurement point are used to define the turbulence statistics data under each air supply mode, respectively.

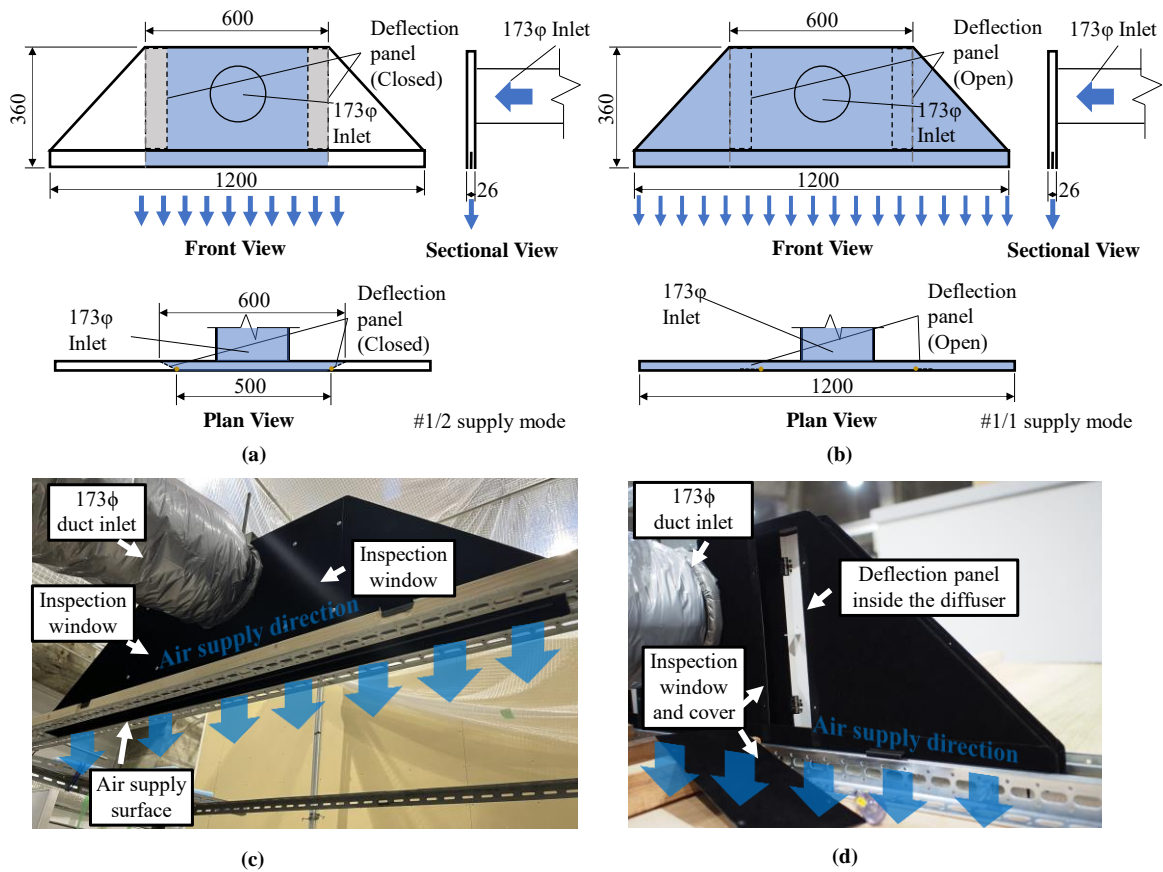


Figure 1 Slot line diffuser with deflection panel for supply area adjustment; (a) image of the 1/2 outlet mode; (b) image of the 1/1 outlet mode; (c) exterior photo of the research subject; (d) detailed view of the panel

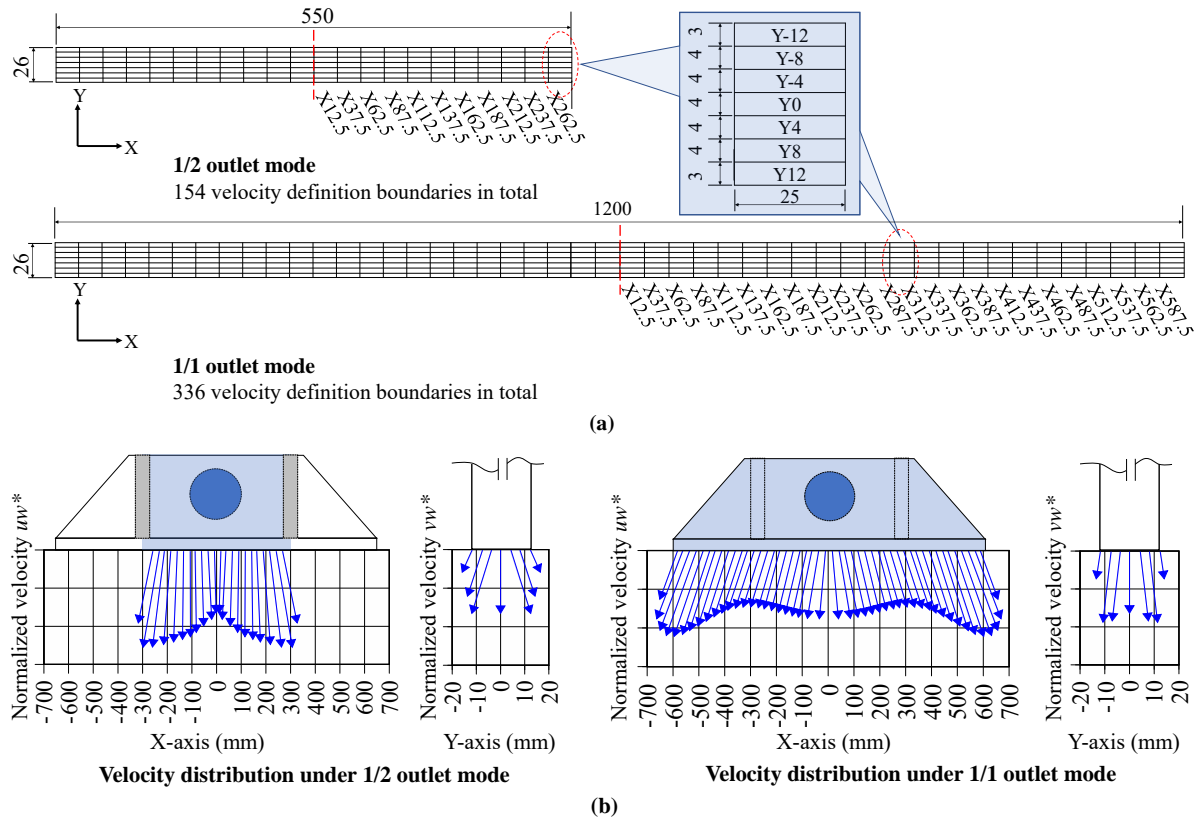


Figure 2 Airflow boundaries and the supply velocity distribution of the slot line diffuser for CFD usage; (a) layout of the velocity and turbulence specify boundaries for two supply modes; (b) normalized velocity distribution of the uw and vw component for boundaries' velocity calculation

2.2 CFD analysis space and the parameters

Fig.3 shows an overview of the analysis space in this study's CFD simulation. **Table 1** shows the CFD's parameter, and Table 1 summarizes the details of the CFD simulation. The dimension of this analysis space is modeled based on a typical open space between two columns of an office building in Japan. This space has 6 mm thick single quartz glass (thermal conductivity $K=1\text{W}\cdot\text{m}\cdot\text{K}$) on one side, considered a glass facade with poor insulation to examine the diffuser's perimeter performance. And the OA temperature is defined as 2°C , considering Japan's winter climate. The inner surface of the quartz glass is a no-slip wall and conduction heat transfer boundary due to applying the low-Renoleyd number turbulence model. Four human simulators with 75W heat generation sit in the room's interior and surround a table. Tracer gas has the same physical property as air are generate from the mouth (1.1m height from the floor) of one human simulator. Details about the heat and gas generation are shown in **Table 2**.

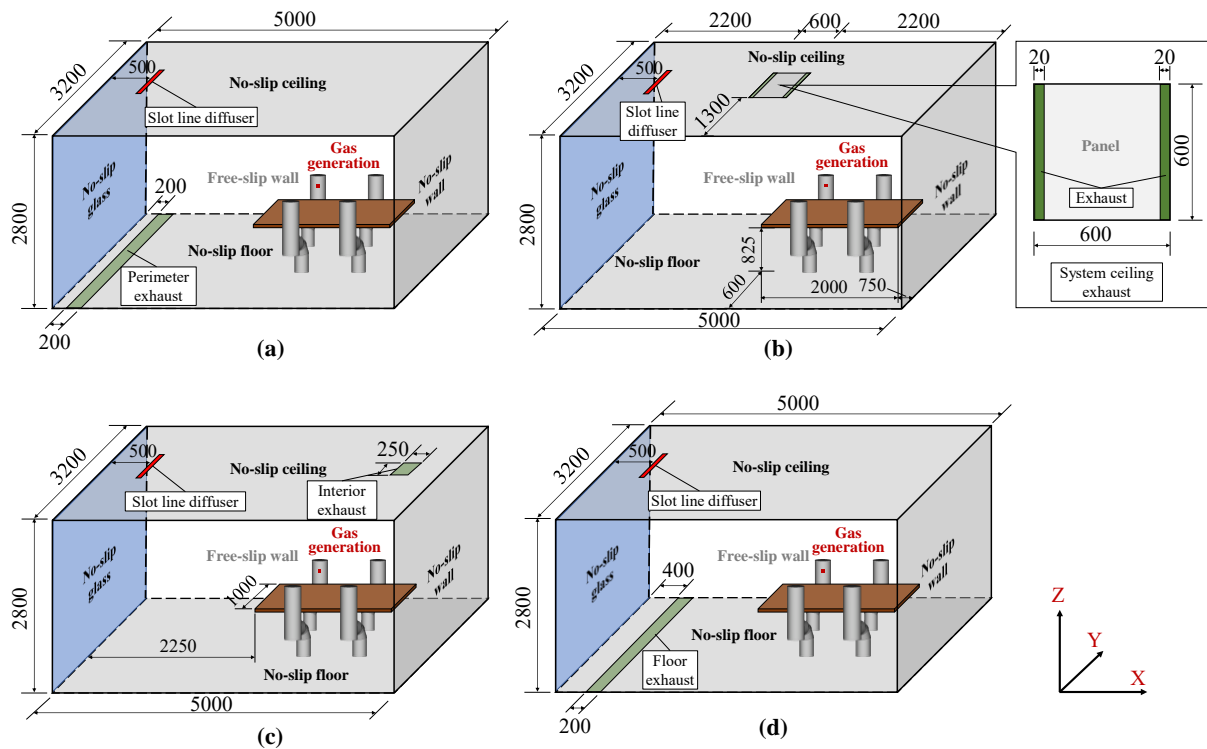


Figure 3 Image of the CFD analysis space with a slot line diffuser in perimeter glazing area; (a) perimeter floor exhaust (0.2m away from the glass); (b) system ceiling exhaust; (c) interior ceiling fan exhaust; (d) floor exhaust 0.4m away from the glass)

Table 2: Case number, abbreviation, and parameters of the CFD simulation

Cases	Parameter abbreviation	Supply mode	Supply air	Exhaust
Case1	05m (1/2) PerE_30	1/2	200m ³ /h, 30°C	Floor (0.2m from the window)
Case2	05m (1/2) CeilE_30			System ceiling (room's center)
Case3	05m (1/2) IntE_30			Ceiling fan (interior ceiling)
Case4	05m (1/2) FlrE_30			Floor (0.4m from the window)
Case5	05m (1/1) PerE_30	1/1	200m ³ /h, 30°C	Floor (0.2m from the window)
Case6	05m (1/1) CeilE_30			System ceiling (room's center)
Case7	05m (1/1) IntE_30			Ceiling fan (interior ceiling)
Case8	05m (1/1) FlrE_30			Floor (0.4m from the window)

The supply boundary of the slot line diffuser is mounted on the ceiling and 0.5m away from the glass's inner surface. In addition, four kinds of exhaust methods are used to examine their influence on perimeter environments. The first one is the 3200 mm (W) and 200 mm (L) perimeter floor exhaust, mounting on the floor 200 mm away from the window glass (**Fig. 3**

(a)). The second is the exhaust in the system ceiling generally used in Japan, and its enlarged view shows in **Fig. 3 (b)**. The third is the interior exhaust shown in **Fig. 3 (c)**, which is a 250mm square considered a ceiling exhaust fan. The last is a floor exhaust with the same scale as the perimeter floor exhaust but located 400mm from the window glass **Fig. 3 (d)**. Furthermore, all these three kinds of exhausts are defined as the natural outflow boundary.

Table 1: CFD settings and conditions used in this study

Analysis Method	CFD code		STREAM V2022
	Turbulence model		Linear low-Reynolds-number $k-\varepsilon$ model
	Algorithm		SIMPLE
	Radiation analyzed		VF method
	Discretization scheme		QUICK
	Number of calculation cycle		5,000
Meshing	Number of mesh		9,200,000
	Standard mesh size		25 mm
	Standard geometric ratio		1.1x
	First mesh from glass/wall surface	Perimeter glass	0.2 mm thickness
		Wall, ceiling, floor	0.5 mm thickness
6 mm single quartz glass		Six divisions in the thickness direction	
Glass and wall	Perimeter glass	External surface	Specifying heating transfer coefficient, $h = 23 \text{W}(\text{m}^2 \cdot \text{K})$, $\text{OA} = 2^\circ\text{C}$
		Material	6 mm single quartz glass; $K = 1 \text{W}(\text{m} \cdot \text{K})$
		Inner surface	No-slip wall boundary, Conduction, Emissivity specify = 0.9
	Ceiling, floor, and interior wall		No-slip wall boundary, Conduction, Temperature specify = 22°C , Emissivity specify = 0.9
Partition wall		Free-slip wall boundary, Temperature specify = 22°C , Emissivity specify = 0.9	
Airflow boundary	Slot line diffuser	1/1 outlet mode	550 mm (L) \times 26 mm (W), 154 inlet boundaries; Fixed velocity (around 4m/s); k and ε specify Supply air: $200 \text{m}^3/\text{h}$, 30°C
		1/2 outlet mode	1200 mm (L) \times 26 mm (W), 336 inlet boundaries; Fixed velocity (around 1.8m/s); k and ε specify Supply air: $200 \text{m}^3/\text{h}$, 30°C
	Exhaust	Perimeter exhaust	3200 mm (L) \times 200 mm (W), Natural outflow
		Interior exhaust	3200 mm (L) \times 200 mm (W), Natural outflow
		Ceiling exhaust	600 mm (L) \times 20 mm (W) \times 2 slots, Natural outflow
Furniture and occupants	Dimension	Human simulators	300 mm diameter cylinder in sitting position \times 4
		Table	2000 mm (L) \times 1000 mm (W) \times 50 mm (H)
	Heat generation	Human simulator	$75 \text{W} \times 4 = 300 \text{W}$ in total
	Tracer gas generation	Mouth size	14 mm (L) \times 13 mm (W)
Tracer gas		$9.95 \text{L}/\text{min}$; 34°C ; Physical properties same as air	

2.3 The Low-Reynolds Number $k-\varepsilon$ Model and the Meshing

The linear low-Reynolds-number model suggested by Abe., et al. [8] [9], was used in this study's turbulence calculation. The linear low-Reynolds number $k-\varepsilon$ model was confirmed to be capable of predicting the attached and separated wall shear flows in several studies and was considered suitable for this study's perimeter heat transfer calculation. A detailed mesh division is required to reproduce turbulence statistics near the wall in this model. Therefore, the mesh division of the case with 1/2 supply & interior floor exhaust is shown in **Fig. 4** for reference. All the simulation cases used the same mesh division near the glass and wall to avoid the influence of meshing dependency. The dimensionless wall distance y^+ from the glazing inner surface is ensured to be less than 0.5.

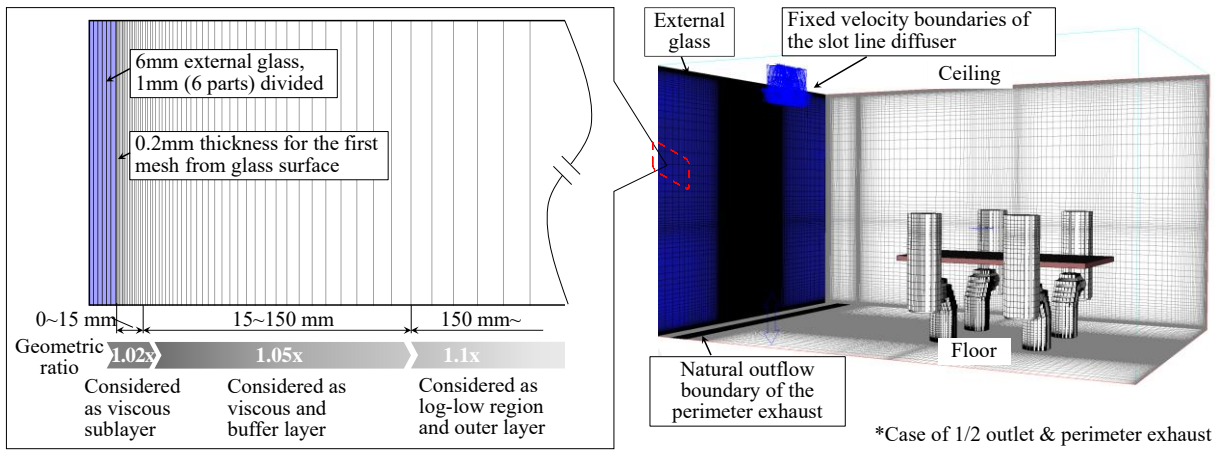


Figure 4 Image of the mesh design in the whole analysis space and the mesh division in the space near the glass surface

3 RESULTS

3.1 Thermal performance

The contour graphs of indoor air temperature and scalar velocity distribution on the vertical section of the room's longitudinal center, and the horizontal section 0.1 m above the floor are shown in **Fig.7** and **Fig.9** (diffuser's 1/1 and 1/2 supply mode, respectively). The isosurface of velocity = 0.3 m/s, the exhaust temperature, the air conditioning system's heating capacity q_{AC} , the average temperature in the occupied zone, and the glass's inner surface temperature are also summarized in these two graphs for reference.

The mean data of the air temperature, air distribution performance index (ADPI), and draft rate (DR) index shows in **Fig.5**; the vertical temperature and scalar wind speed distribution in the occupied zone shows in **Fig.6** for comparison.

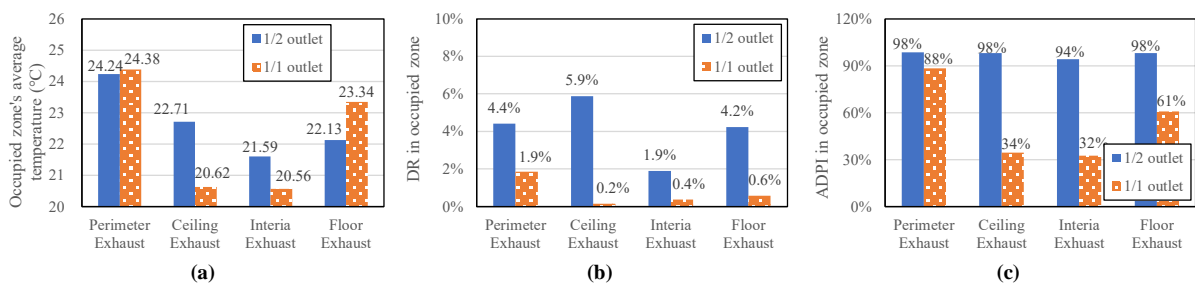


Figure 5 The ADPI, DR, and air temperature's relationship with the supply/exhaust methods (a) occupied zone's ADPI; (b) occupied zone's DR; (c) occupied zone's average temperature

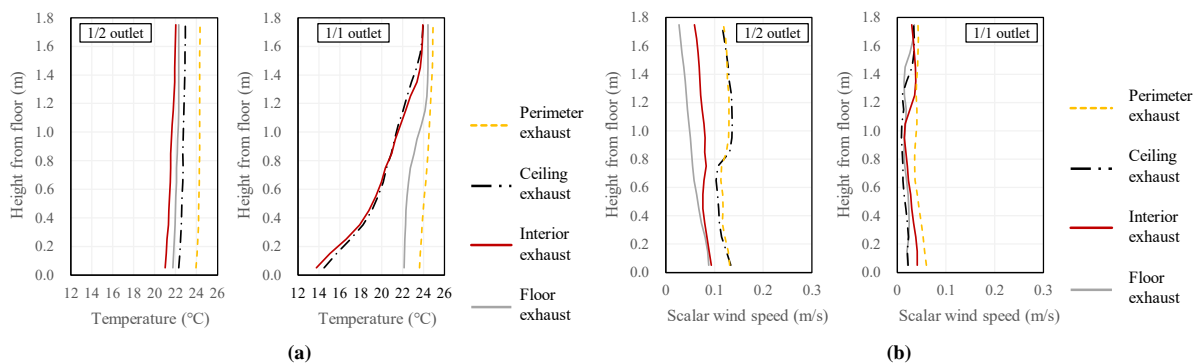


Figure 6 The air temperature and airflow vertical distribution's relationship with the supply/exhaust methods; (a) temperature's vertical distribution in the occupied zone (average of the data with the same height coordinate); (b) scalar win speed's vertical distribution in the occupied zone (average of the data with the same height coordinate)

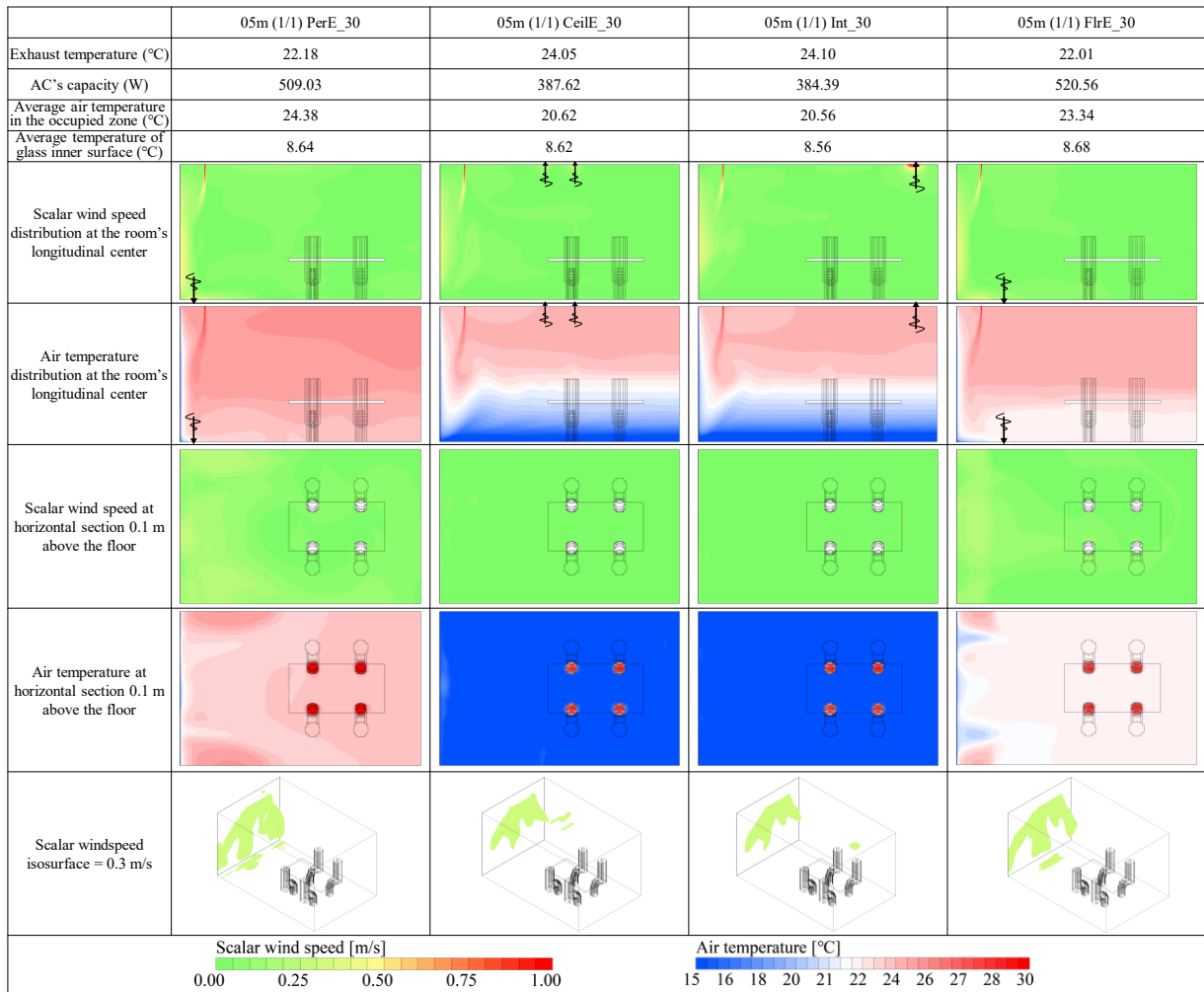


Figure 7 1/1 outlet mode of the slot line diffuser; air temperature and scalar wind speed distribution in the analysis space while using the different exhaust methods (perimeter floor, ceiling's center, interior's ceiling, and the floor exhaust)

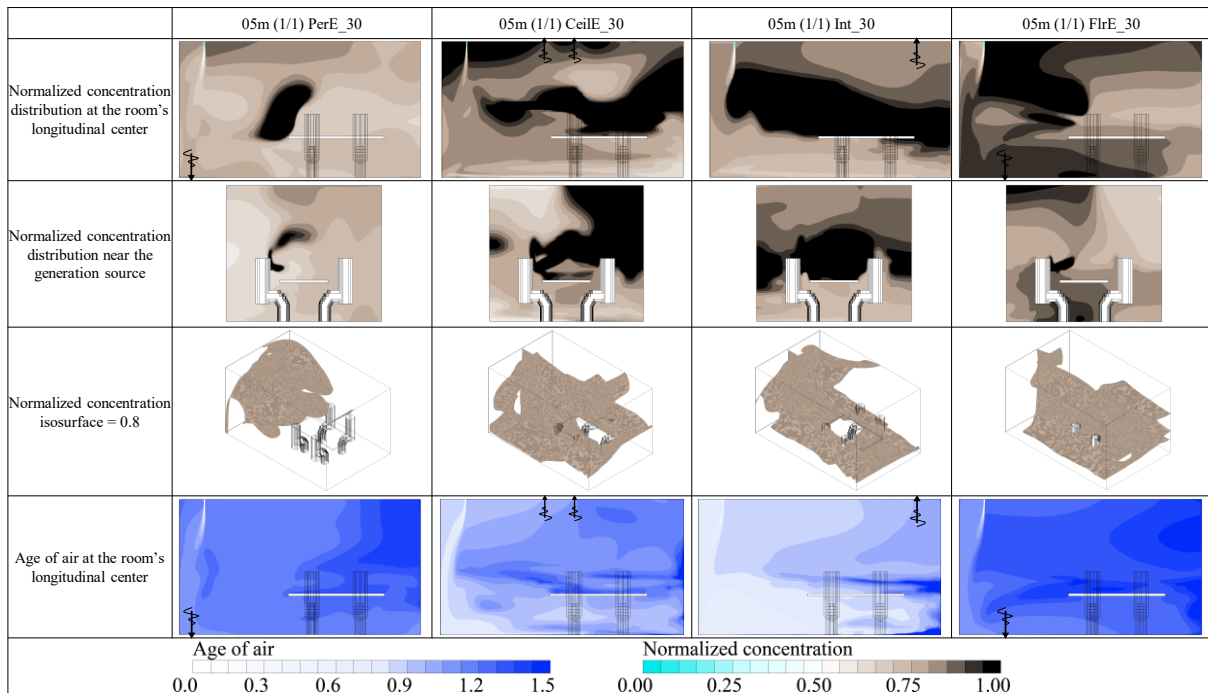


Figure 8 1/1 outlet mode of the slot line diffuser; normalized concentration and age of air's distribution in the analysis space when choosing the different exhaust methods (perimeter floor, ceiling's center, interior's ceiling, and the floor exhaust)

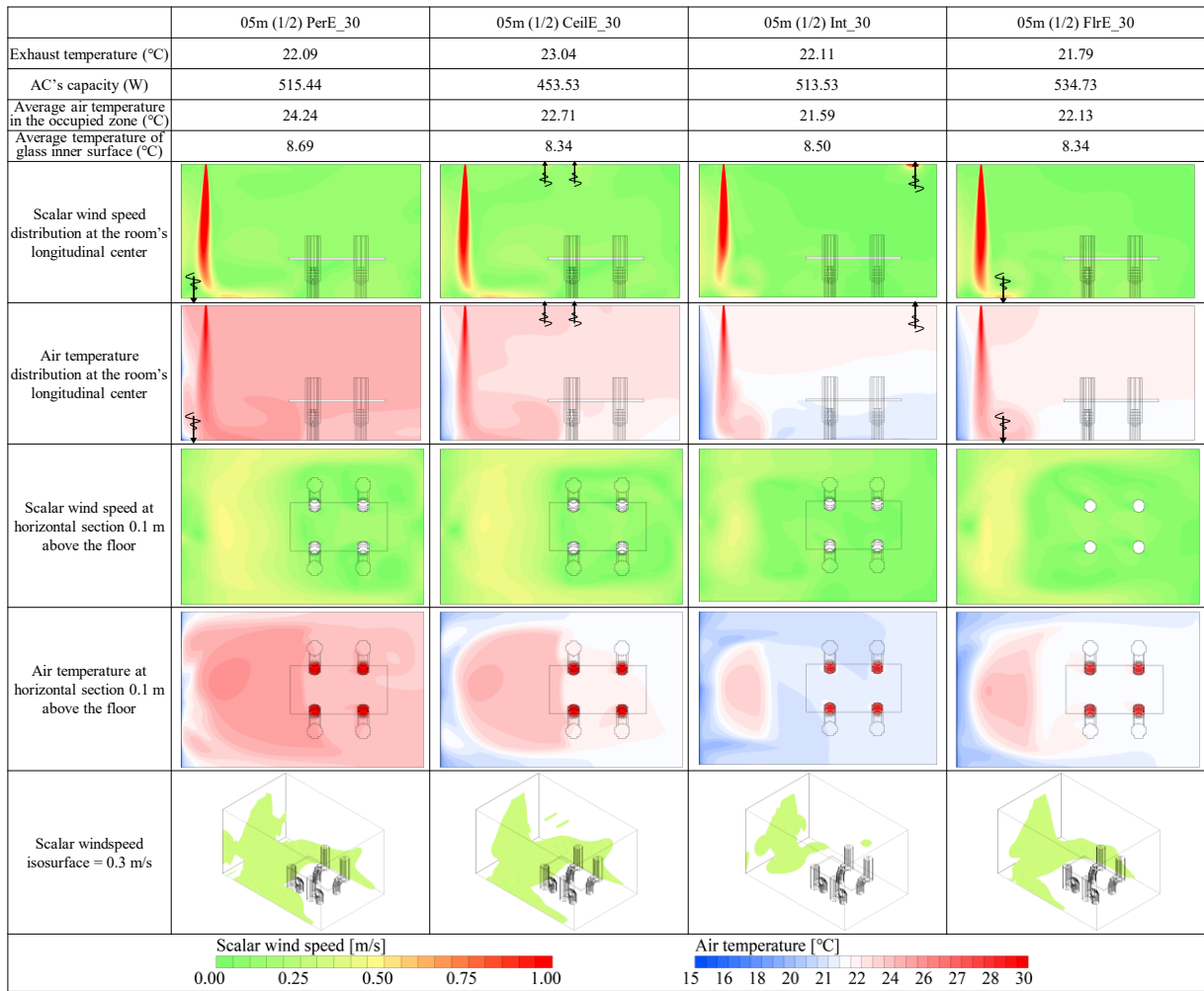


Figure 9 1/2 outlet mode of the slot line diffuser; air temperature and scalar wind speed distribution in the analysis space while using the different exhaust methods (perimeter floor, ceiling's center, interior's ceiling, and the floor exhaust)

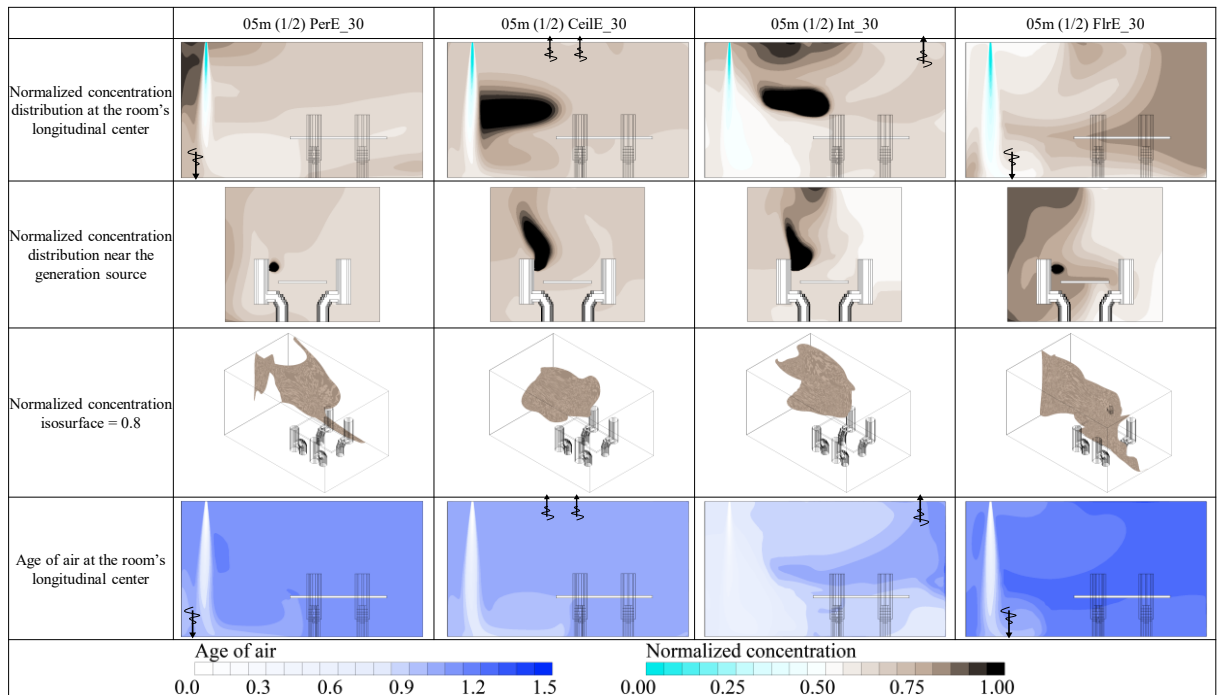


Figure 10 1/2 outlet mode of the slot line diffuser; normalized concentration and age of air's distribution in the analysis space when choosing the different exhaust methods (perimeter floor, ceiling's center, interior's ceiling, and the floor exhaust)

3.2 Ventilation performance

The normalized concentration C^* was used to represent the tracer gas concentration distribution in the analysis space. The normalized concentration C^* can be expressed by *Function (1)* below, which C_p means the concentration data of the data pickup point.

$$C^* = \frac{C_p}{C_{EA}} \quad (1)$$

Additionally, two scales for ventilation efficiency, the age of air (SVE3) and the residual lifetime of air (SVE6), are calculated and listed.

In *Fig. 8* and *Fig. 10*, the distribution of C^* is shown by contour graphs, in which the sections are located on the room's longitudinal center and vertical to the generation source (human simulator's face). The isosurface of $C^* = 0.8$ in 3D view, and the SVE3's distribution in the room's longitudinal center are also shown in these two graphs, which correspond to the diffuser's 1/2 and 1/1 supply modes, respectively. A comparison of the mean volume of C^* , SVE3, and SVE6 in the occupied zone under different supply and exhaust methods shows in *Fig. 11*.

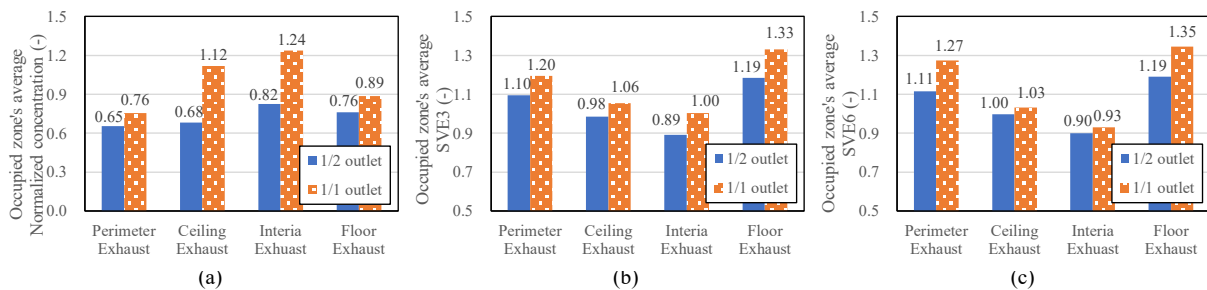


Figure 11 The normalized concentration C^* , the age of air (SVE3), and the residual lifetime of air (SVE6)'s relationship with the slot line diffuser's air supply modes and the room's exhaust methods (a) average normalized concentration in the occupied zone; (b) mean age of air (SVE3) in the occupied zone; (c) mean residual life time of air (SVE3) in the occupied zone

4 CONCLUSIONS

The heating and ventilation performance of the slot line diffuser in a typical office space with large area exterior glass is numerically investigated. Two panels are installed inside the diffuser, which is considered to improve its winter performance by converging the supply airflow. Under the diffuser's standard heating supply condition (30°C, 200m³/h, 4.5 ACPH), CFD simulations using the low Reynolds number turbulence model, the detailed air supply characteristics model, and fine meshes were conducted. The diffuser's supply mode (1/1 or 1/2 outlet) and exhaust methods are adjusted to clarify their impact. From the air temperature, airflow, and tracer gas distribution in the occupied zone and the thermal performance and ventilation efficiency index calculation, it can be concluded that:

- Converging the supply airflow by halving the slot line diffuser's supply area can obviously improve this perimeter heating and ventilation performance during the winter.
- Under the diffuser's 1/1 outlet mode, insufficient heating air flow gets into the space near the floor. It can't block cold drafts going into the room's interior without mounting a floor exhaust near the window. A vertical temperature difference of about 10°C occurred in the occupied zone when using the ceiling or interior exhaust. And it can decrease to around 2°C while using a floor exhaust.
- Under the 1/2 outlet mode of the diffuser, heated air can overcome buoyance's effect and impinge on the floor. Blocking and heating the cold draft before it enters the room's

interior. It was possible to maintain a vertical temperature difference of less than 2°C in the occupied zone when exhausting from the ceiling of the room and less than 1°C from the floor near the window.

- A flow field similar to the wall confluent jet ventilation is achieved in this office space using a slot line diffuser in 1/2 outlet mode. The mean normalized concentration in the occupied zone is less than 0.7 using the perimeter or ceiling exhaust, and less than 0.82 using other exhaust methods.
- The mean normalized concentration in the occupied zone becomes nearly equal to mixing ventilation (0.76-1.24) when the diffuser supplies the air in the 1/1 outlet mode. However, even though mixing ventilation was considered, the 1/2 outlet mode had a higher SVE performance.
- Though converging the supply air (1/2 supply mode) increased the draft rate (DR) in the interior space, it's still less than 6%, considering less impact on thermal comfort. Meanwhile, it doubled the ADPI index (94%~) compared to 1/1 supply mode, indicating better and satisfactory air distribution performance.
- Combining the ceiling exhaust mounted at the room's center with the slot line diffuser has the best ventilation performance. And mounting a floor exhaust near the exterior glass (between the glass and diffuser's direct below) has the best heating and cold draft-blocking performance.

This study validates the ventilation potential of the perimeter slot line diffuser. The best heating performance can be ensured by using a perimeter floor exhaust. And an ideal ventilation and heating performance can be achieved by combining the diffuser's 1/2 outlet with a commonly used ceiling exhaust. Future work will evaluate its ventilation performance under the cooling-supplied mode. It is intended to investigate the possibility of further improving ventilation efficiency by establishing ceiling-supplied displacement ventilation.

5 REFERENCES

- [1] Y. Cheng, Y. Cheng, Z. Lin, W. Wu and T. Yao, "Performance evaluation of stratum ventilation with slot diffuser using CFD," in *Indoor Air 2014 - 13th International Conference on Indoor Air Quality and Climate*, Hong Kong, 2014.
- [2] G. Cao, P. Nielsen, R. L. Jensen, P. Heiselberg, L. Liu and J. Heikkinen, "Protected zone ventilation and reduced personal exposure to airborne cross-infection," *Indoor Air*, vol. 25, no. 3, pp. 307-319, 2015.
- [3] B. Wei and Z. Li, "Simulation of Indoor Air Flow Fields in Buildings With Large Interior Spaces With Stratified Air Conditioning and Perforated Side Wall Diffusers," in *ASME 2010 4th International Conference on Energy Sustainability*, 2010.
- [4] F. Lorch and P. Straub, "PERFORMANCE OF OVERHEAD SLOT DIFFUSERS WITH SIMULATED HEATING AND COOLING CONDITIONS," *ASHRAE Transactions*, vol. 89, pp. 200-211, 1983.
- [5] W. Rousseau, "Perimeter Air-Diffusion Performance Index Tests for Heating with a Ceiling Slot Diffuser," *ASHRAE Transactions*, vol. 89, pp. 191-199, 1983.
- [6] S. Janbakhsh and B. Moshfegh, "Experimental investigation of a ventilation system based on wall confluent jets," *Building and Environment*, vol. 80, pp. 18-31, 2014.
- [7] S. Sheng, T. Yamanaka, T. Kobayashi, J. Yuan and M. Katoh, "Modeling of supply airflow from slot line diffuser on ceiling for CFD of thermal environment in perimeter zone," *Building and Environment*, vol. 213, no. 1, 2022.
- [8] K. Abe, T. Kondoh and Y. Nagano, "A new turbulence model for predicting fluid flow and heat transfer in separating and reattaching flows—I. Flow field calculations.," *International journal of heat and mass transfer*, vol. 37, no. 1, pp. 139-151, 1994.
- [9] K. Abe, T. Kondoh and Y. Nagano, "A new turbulence model for predicting fluid flow and heat transfer in separating and reattaching flows—II. Thermal field calculations," *International Journal of Heat and Mass Transfer*, vol. 38, no. 8, pp. 1467-1481, 1995.

Quantifying the Potential Health Impacts of Unvented Combustion in Homes – A Meta-Analysis

Jacob Bueno de Mesquita¹, Núria Casquero-Modrego^{*2}, Iain Walker²,
Brennan Less², Brett Singer¹

¹ *Indoor Environment Group, Lawrence Berkeley National Laboratory, Berkeley, CA 94720, USA*

² *Residential Building Systems Group, Lawrence Berkeley National Laboratory, Berkeley, CA 94720, USA*

**Corresponding author: NuriaCM@lbl.gov*

1. ABSTRACT

While a growing body of scientific literature describes the population health impacts of fossil fuel production and burning via climate and air pollution pathways, less is known about the health impacts of indoor combustion. This paper summarizes the results of studies from the last two decades that investigated the association between exposure to sources of unvented combustion pollutants in homes and a range of health outcomes. We found gas combustion to be associated with 6-28% (95% confidence intervals) increased odds of asthma symptoms, 4-51% increased odds of systemic symptoms, 7-81% increased odds of asthma medication use, and 3-12% increased risk of mortality. These findings can be used to improve public health, for example, by informing requirements for improved ventilation and source control, justifying switching to vented appliances, better regulation of device emissions and quantifying the benefits of electrification of end-uses. Dose-response relationships between human health, NO₂ exposure, and other by-products of combustion are not characterized with a high degree of precision. However, there is clear evidence of a wide range of health effects, even at low levels of exposure. Despite the various designs, geographic sites, length of follow-up, and study dates, we noted a level of consistency between the studies within the current meta-analysis, and with previous ones, which strengthens the level of confidence in our findings.

2. KEYWORDS

health; gas combustion; gas cooking; gas heating; meta-analysis

1 INTRODUCTION

The primary consumers of fossil fuels in homes are: heating, hot water, cooking and clothes drying. Except for cooking and unvented heaters, these end-uses are required to have a vent to outside and only contaminate indoor air if their venting system fails. While venting combustion products contributes to outside air pollution that can then enter a home, in this paper we will focus on direct indoor sources only.

It is well established that the inhalation of fossil fuel combustion products leads to a range of adverse population health effects. Cooking and unvented heating are main indoor sources of NO₂, ultrafine particles, and volatile organic compounds (VOCs) if not vented to outdoors (Lewis et al., 2023). A previous literature review (Less et al. 2022) discussing home energy performance provided a high-level summary of a few indoor air quality studies related to indoor combustion, but did not provide the in-depth health analysis that is the focus of this paper.

NO₂ is an irritant to the respiratory tract. Even short-term exposures can irritate the airways, drive inflammation, and lead to acute and chronic disease, especially among those with asthma (Barck et al., 2005; Vardoulakis et al., 2020; Lim et al., 2022). While particles are the most important contaminant of concern for health impacts, at least from Disability Adjusted Life Year (DALY) perspective (Logue et al., 2012; Morantes et al., 2022), most particle exposure is

from non-residential sources such as transport, agriculture and industry. Therefore, in this review will focus on the next important contaminant of concern, i.e., NO₂. A meta-analysis done by (Faustini et al., 2014) confirms that the effect of NO₂ was independent from PM, suggesting that NO₂ can drive health effects on its own. In addition, when the levels of NO₂ in a home are below the threshold limits, (< 15 ppb), it becomes challenging to observe any potential health effects.

Although the strong toxicological evidence for NO₂ is compelling enough to spur population health protective action, the toxicology is borne out in a number of epidemiological studies. Meta-analyses by (Khreis et al., 2017) and (Gruenewald et al., 2022) of epidemiological studies showed clear relationships with asthma development and have enabled modelling studies estimating the broader population impacts of reducing NO₂ exposures (e.g., (Knibbs et al., 2018; Achakulwisut et al., 2019; Jacobs et al., 2019; Hu et al., 2022). (Lin et al., 2013) synthesized the available literature on gas stove use and found correlations with the two health outcomes they studied, asthma development and wheeze in children. This paper provides a 10-year update to Lin et al, to build on existing dose-response findings through the inclusion of studies published through April 2023 that reported on a broader set of potential adverse health effects like hospitalization, asthma symptoms and medication use.

2 METHODOLOGY

This study reviews research since the year 2000 on the health impacts associated with exposure to combustion-related contaminants in homes. We grounded the evaluation using literature related to interventions where gas combustion appliances were replaced, or effective engineering controls were implemented, including those where measured NO₂ was taken as the main exposure variable. We grounded the review in the landmark intervention studies conducted in Australia and New Zealand (Pilotto et al., 2004; Howden-Chapman et al., 2008; Marks et al., 2010; Gillespie-Bennett et al., 2011), and a comprehensive meta-analysis focused on gas stove effects on cough and wheeze (Lin et al., 2013). We used Google Scholar to identify works citing these studies. We then applied inclusion and exclusion criteria to narrow the search to epidemiological studies that provide dose-response relationships between home combustion appliances and health outcomes.

We assessed study relevance and quality, leading to a final set of manuscripts. We included studies that used epidemiologic methods to investigate associations between health outcomes and the presence or use of unvented gas combustion appliances and/or measured NO₂ with results presented as effect estimates with confidence intervals. Studies were excluded that did not involve data collection post-2000, that did not focus on residential exposure, that had effect estimates that were already included by Lin and colleagues, and that did not include gas or oil-based cooking or heating sources. Wood burning was considered beyond the scope of this analysis, as were effect estimates of lung function. We considered meta-analyses that used pooled estimates from studies with lower risk of bias as evaluated by the WHO or other similar methodology.

In this study, the health outcomes primarily were associated with acute exposures. We categorized the health outcomes into 12 distinct categories.: 1) asthma symptoms including wheeze, cough, shortness of breath, chest tightness, respiratory symptoms, nasal symptoms, and difficulty breathing; 2) asthma symptom scores including ordinal scores 0-3 (3 as the most severe and 0 as no symptom) for wheeze, cough, overall asthma symptoms, upper respiratory, and lower respiratory symptoms; 3) systemic symptoms including poor/fair health, diarrhea, vomiting, ear infection stomach ache, eczema, sensitization, allergies, nighttime waking, and

steroid use; 4) healthcare visits that were not hospitalizations or emergency room visits or changes to asthma management; 5) hospitalization or emergency room visits, 6) medication use including asthma preventer and reliever use; 7) nonpharmaceutical interventions including limiting activity; 8) neurological disease development including schizophrenia; 9) absences from school; 10) all-cause mortality; 11) cardiovascular mortality; 12) respiratory mortality.

We converted effect estimates with continuous, independent variables to effects per 20 ppb increase in NO₂. We converted intervention studies to consider control groups as the numerator in effect estimate ratios. We used effect estimates that adjusted for confounders when available. We stratified pooled estimates by health outcome, categorical or continuous exposure, and effect estimate type (odds ratios (OR), risk ratios (RR), incident rate ratios (IRR)). We computed random effect pooled estimates where there were at least four effect estimates, accounting for variation in study populations, differences in study design, and a variety of health outcomes considered. For example, the outcome of “asthma symptoms” included effect estimates for cough, wheeze, respiratory symptoms, and others. Statistics and forest plots were generated by *R v.4.2.1* with packages *meta* and *metafor*. The data and code for reproducibility can be found at <https://gitlab.com/jacobbueno/zapdos>.

3 RESULTS

The search yielded 29 studies including 10 meta-analyses, 12 observational studies and 7 randomized controlled trials (RCTs) or quasi-experimental studies. In total, these included 184 effect estimates for a variety of health outcomes. Eleven of the studies focused exclusively on children with asthma, as part of randomized controlled trials or observational studies. An additional study included over 80% children with asthma. RCTs and observational studies often focused on unvented exposures from unvented gas heat and gas cooking. In contrast, the meta-analyses mostly focused on residential indoor NO₂ exposure from multi-year indoor air pollution monitoring. Intervention studies examined changes in exposure to combustion contaminants and associated health effects. Intervention activities included installing exhaust ventilation for combustion appliances or electric alternatives like heat pumps (Pilotto et al., 2004; Howden-Chapman et al., 2008; Free et al., 2010; Barnard et al., 2011; Gillespie-Bennett et al., 2011), a gas scrubber (Gent et al., 2022) or comparing homes with gas and appliances (Belanger et al., 2006; Willers et al., 2006; Boulic, 2012; Rice et al., 2020).

Average NO₂ level changes for unvented gas heat at home were reported in residences at 3.8 ppb (Howden-Chapman et al., 2008; Free et al., 2010), and in schools at 14.1 ppb (Marks et al., 2010), and 31.5 ppb (Pilotto et al., 2004). Belanger et al, showed an increase in average NO₂ of 17.3 ppb (Belanger et al., 2006), Comparing gas ranges with electric ranges in both multifamily and single-family homes. (Hansel et al., 2008) found that the presence of a gas stove, as well as the use of stove/oven and space heater for heat, is linked to higher indoor levels of NO₂, which suggests modifiable sources of exposure. Those with gas stoves had 15.7 ppb (95% CI 6.9-24.6) times the NO₂ concentration and those with gas heaters had 4.4 ppb (95% CI -2.8-11.6) times the NO₂ concentration. In 24 high performance California homes, (B. Less et al., 2015) measured NO₂ in kitchens that used gas and electric cooking equipment and found average 6-day integrated NO₂ concentrations of 6.6 vs. 17.9 ppb in electric and gas cooking kitchens respectively. The California Healthy Homes Indoor Air Quality Study of 2011–2013 (Mullen et al., 2016), measured combustion contaminants for 6-day periods in 352 existing California dwellings (including the homes in Less et al.). They found that kitchen NO₂ concentrations were not significantly impacted by vented combustion appliances (6.5 vs. 7.6 ppb), while unvented gas cooking with and without other vented gas appliances led to

significantly higher indoor concentrations (18 and 22 ppb, respectively). Similarly, Belanger et al 2006 found clear increases in NO₂ concentration in homes with gas versus electric cooking.

We considered NO₂ to be a main toxicant produced by indoor gas combustion (compared with electric appliances) or an indicator chemical of the combustion air pollution—including PM and VOCs—that could be related to health effects via inhalation exposure. Meta-analyses focused on indoor NO₂ concentrations found consistent relationships with all mortality with a 95% CIs of 3-12%, while a 10-year Danish birth cohort quantified risk of schizophrenia development at 2.18 (95% CI 1.69-2.85) times higher for each 20 ppb NO₂ increase (Horsdal et al., 2019). The range of health effects consistently associated with indoor, residential gas combustion over the last two decades shows that at population scale, substituting gas appliances for electric ones should reduce some adverse health effects, with associated health, economic, and social benefits. The studies highlight the elevated risk of symptoms and associated health problems for those with asthma, but also show that combustion appliance exposure could lead to asthma development and other cardiovascular, respiratory, and neurological diseases.

Samet and colleagues tracked daily symptoms in over 1,200 infants through 18 months of age and found that measured NO₂ concentrations at home, mostly below 20 ppb, were not associated with respiratory symptoms (Samet et al., 1993), suggesting there may be little risk for infants with low to modest NO₂ exposure, or among populations that are not already susceptible to respiratory health risks (e.g., those with asthma, or bronchopulmonary dysplasia). However, this study did not examine other health impacts such as respiratory infections, asthma exacerbation or initiation. Other studies included in our meta-analysis included infant populations along with older children, with mixed results (Belanger et al., 2006; Willers et al., 2006; Barnard et al., 2011; Rice et al., 2020). The 8-year prospective birth cohort by Willers et al reported a positive relationship between gas cooking and nasal symptoms, and a trend toward a positive relationship with asthma prevalence, but not eczema, wheeze, or sensitization (Willers et al., 2006). A cross-sectional study of children 12 years old or younger revealed strong, positive associations between gas stove use and wheeze, chest tightness, and shortness of breath, particularly among multi-family as opposed to single-family residences (Belanger et al., 2006). Barnard et al showed a slight risk of hospitalization associated with gas heating in a population inclusive of all ages, and Rice et al showed a nearly 600% increase in odds of hospitalization among children with bronchopulmonary dysplasia on respiratory support (Barnard et al., 2011; Rice et al., 2020). The detectable risk increases associated with indoor combustion sources appear to be modified by existing health vulnerability including asthma. The likelihood of increased risks with cumulative exposures raises concerns about health risks for communities already facing disproportionate burdens of toxic exposures, especially where there are already higher rates of asthma and other illnesses or vulnerability due to environmental exposures. Overall, the effect estimates trended toward a positive relationship between residential gas combustion, NO₂ exposure, and adverse health outcomes. There were no effect estimates with 95% CIs completely below the null, which would have been indicative of a statistically significant protective effect of the exposures on health risks.

Asthma Symptoms and Symptom Scores. The presence of gas versus electric appliances, mediated by whether the gas appliances were vented (e.g., flue for gas heater), was associated with 1.16 times the odds of reporting asthma symptoms (95% CI 1.06-1.28). There was little difference in the magnitude of effect between observational studies and RCTs, although there was greater precision among the observational studies. Table 1 summarizes odds ratios for a 20 ppb increase in average NO₂ exposure linked with combustion cooking and/or unvented heating. Each 20 ppb increase in NO₂ exposure linked with gas combustion was associated with 1.55 (95% CI 1.41-1.71) and 1.21 (95% CI 1.06-1.37) times higher odds of asthma symptoms,

for RCTs and observational studies, respectively. The pooled OR of 1.33 (95% CI 1.19-1.49) may not be reliable given the lack of overlap in confidence intervals for RCTs and observational studies, yet the confidence interval ranges demonstrate a consistent, positive association with asthma symptom risk.

Fifteen effect estimates from two RCTs (Pilotto et al., 2004; Howden-Chapman et al., 2008) showed 1.38 (95% CI 1.19-1.61) times higher risk of asthma symptoms with gas appliance exposure. A prospective cohort with six months of follow up showed that measured NO₂ at home was associated with elevated incidence rates of a range of asthma symptoms including wheeze, cough, chest tightness, limited speech, and greater correlation of these symptoms with exercise. A pooled effects model of the six effect estimates in (Hansel et al., 2008), gave an 11% (95% CI 7-15) incident rate increase per 20 ppb increase in NO₂. For each 20 ppb increase in measured indoor NO₂ level, another study reported 2.86 (95% CI 1.03-8.35) times higher odds of a unit increase in asthma symptom score (Belanger et al., 2013), and yet another (Gillespie-Bennett et al., 2011) reported 1.62 (95% CI 1.52-1.73) and 1.12 (95% CI 1.00-1.20) times higher odds of lower and upper respiratory symptoms, respectively. (Schachter et al., 2020) showed that the presence of a gas stove was associated with 2.82 (95% CI 1.10-7.24) times greater odds of an increased wintertime cough and wheeze score.

Two studies considered asthma incidence (Lin et al., 2013; Khreis et al., 2017). Pooled effect estimates and confidence intervals from Kreis and colleagues spanned above one and reached 2.08 (95% CI 1.45-2.94) for children less than 6 years of age. Lin et al., 2013 showed 32% (18-48%) and 12% (-12%-43%) increased odds of asthma incidence for presence of residential gas stove and 15 ppb NO₂ increase, respectively. Meta-analyses by Zheng and colleagues showed consistent but mild increases in emergency room visits or hospitalizations with increases in indoor NO₂ (Zheng et al., 2015, 2021). The 2015 study gave pooled risk ratios for asthma-related emergency room visits or hospitalizations of 1.07 (95% CI 1.05-1.09) for all ages. The 2021 study pooled risk ratios for the same outcome of 1.00 (95% CI 0.88-1.13) and 1.04 (95% CI 1.03-1.05) for increases in 1-hr maximum NO₂ and 24-hr average NO₂ concentrations.

It should be noted that a few studies showed no or weak associations between gas combustion or NO₂ exposure and health outcomes under study in their respective investigations. The quasi-experimental study that was included used a retrospective matched cohort for nearly 1 million New Zealanders of all ages, mostly without asthma, for 3 years of follow up and found a very slight trend toward an increase in hospitalization rate for asthma, circulatory disease, respiratory disease, or RSV among homes without a heat pump, pellet burner, or flued gas heat intervention (IRR 1.04 95% CI 1.00-1.09) (Barnard et al., 2011). The same study failed to detect an effect for hospitalization for congestive heart failure or for mortality among those hospitalized for cardiovascular or respiratory disease. A prospective cohort study with 12 weeks of follow-up in Adelaide, Australia tracked NO₂ exposure at home and in school and showed mostly weak, non-statistically significant effects (Nitschke et al., 2006). They reported some mild effects for night-time breathing difficulty and night-time asthma attacks (RR 1.06 [1.02-1.10] and 1.08 [1.00-1.14]). An intervention trial with 5 weeks of particle filtration and NO₂ scrubbing showed only marginal reductions in measured NO₂ levels and no effect between NO₂ level and asthma symptom days during the final two weeks of treatment (Gent et al., 2022).

Gas stoves and unvented gas heaters can readily produce increases in NO₂ concentration associated with adverse health effects. Relationships between gas stove use and NO₂ levels reported by Hansel et al (2008), and Belanger et al (2006), are consistent with the work of others including (Simoni et al., 2004) who examined relationships between gas stove use time and pollutant levels. We note that exhaust ventilation can reduce but not eliminate gas stove

emissions and relies upon consistent and proper operation, which is generally low (Sun & Singer, 2023). Many inner-city households are known to have gas stoves, often without exhaust ventilation (Breysse et al., 2005; Diette et al., 2007). The Baltimore home cohort conducted by Hansel et al, identified 14% of homes using gas stoves for heat, underscoring the intersection of environmental and energy injustice (Hansel et al., 2008). The higher magnitude of effects per unit increase in NO₂, reported by Belanger et al (2006), for multi-family versus single-family housing suggests that the size of the health risk may be greater at higher exposure levels associated with greater gas stove use. Field studies in homes (e.g., (Francisco et al., 2010), and IAQ analyses (Sherman et al., 2022)), have shown that NO₂ from unvented gas heaters regularly exceeds health guidelines, including spaces that meet minimum ventilation standards.

Systemic symptoms. We found evidence of a trend toward increased odds of systemic symptoms with gas combustion exposure, with a pooled OR of 1.25 (95% CI 1.04-1.51). The RCT effect estimates drove this trend in the pooled regression. Studies that reported effects as a function of continuous NO₂ exposure found similar results with OR of asthma medication use of 1.61 (95% CI 1.01-2.56) for each 20 ppb NO₂ increase.

Hospitalization, healthcare utilization and medication use. A number of other observational studies and RCTs reported on risks associated with residential gas combustion. A cross sectional study with a 2-month prospective of survey data in Maryland showed a consistent, elevated trend toward higher risk of emergency room visit or hospitalization among children with bronchopulmonary dysplasia (Rice et al., 2020). Among those with respiratory support, the odds of hospitalization were 5.95 (95% CI 1.08-32.76) times greater for homes with gas combustion. Pooled analysis of studies evaluating the use of asthma medication showed 1.39 (95% CI 1.07-1.81) times higher odds with gas combustion exposure compared with electric appliance use or the addition of exhaust ventilation.

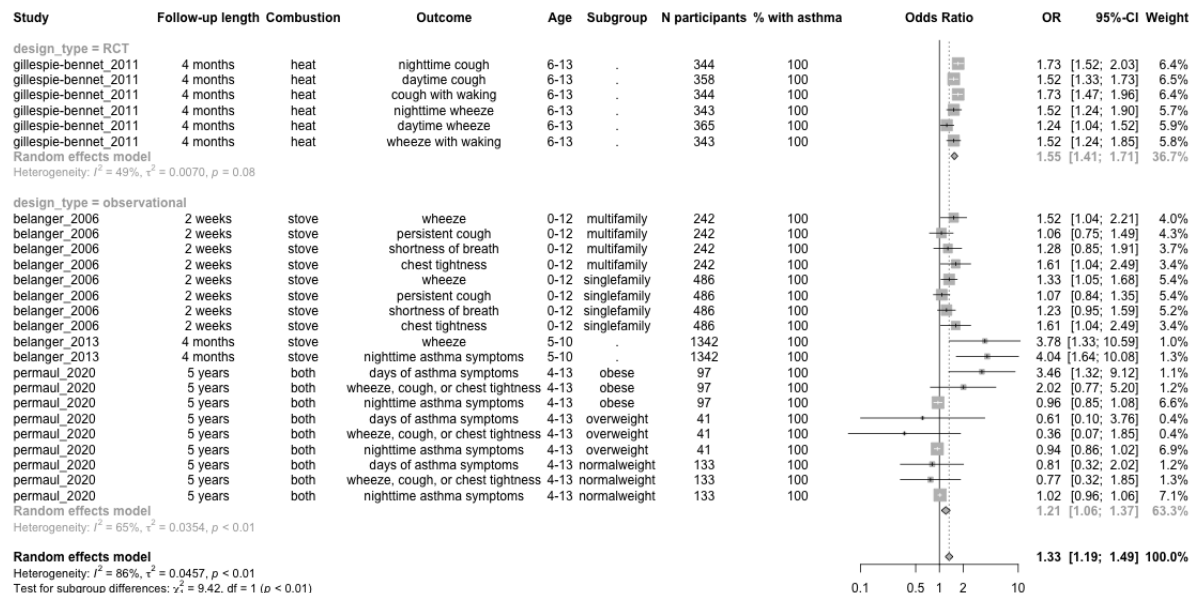


Table 1. Odds ratios for a 20 ppb increase in average NO₂ exposure linked with combustion cooking and/or heating.

A number of studies examined relationships between residential-level indoor NO₂ and population health risks. These are mostly summarized by meta-analyses, however we also included a Danish birth cohort following over 23,000 children for 10 years, which showed a 2.18 (95% CI 1.69-2.85) times higher risk for schizophrenia development for each 20 ppb increase in NO₂ (Horsdal et al., 2019). Meta-analyses mostly used a continuous NO₂ exposure variable to evaluate risk of mortality, asthma incidence, emergency room visits, and

hospitalizations. The risk of mortality was consistently elevated, with 95% CIs ranging up to 39% above the null (Table 2). The ozone-adjusted model from (Orellano et al., 2020) gave similar results to the PM-adjusted model and both were not substantially different from pooled estimates that did not adjust for co-pollutant measurements. Similarly, the effect of NO₂ was independent from PM in the meta-analysis done by (Faustini et al., 2014) according to their subset of studies that adjusted for multiple pollutants (n=7), suggesting that NO₂ can drive health effects on its own.

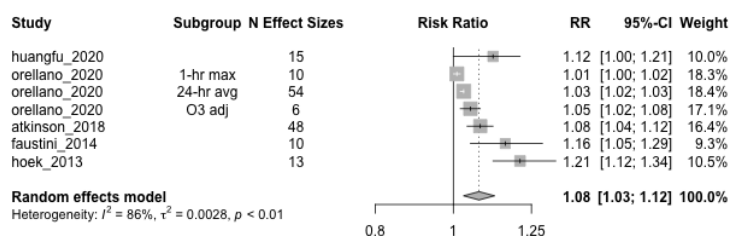


Table 2. Pooled meta-analysis all-cause mortality risk ratios for 20 ppb increases in indoor NO₂.

4 DISCUSSION

We reviewed the literature investigating associations between unvented residential gas combustion for cooking and unvented heating and potential health outcomes and found that observational studies, RCTs, and meta-analyses showed consistent increased risks for asthma symptoms, asthma development, school absence, hospitalization, and emergency room visits. Overall the health outcome with the most effect estimates for pooled analysis was the risk of asthma symptoms. The pooled estimates shows a 6-28% (95% CI) increase in risk of symptoms for unvented gas heating or presence of gas stoves compared with flued heating or electric heat or stoves. For each 20 ppb increase NO₂ concentration, the odds of asthma symptoms increased 19-49%. We observed elevated odds of asthma medication use across RCTs and observational studies with a pooled confidence interval of 7-81% higher odds with the presence of gas appliances.

Our results are consistent with a large body of scientific work in this area spanning decades. (Hasselblad et al., 1992) conducted a meta-analysis of the studies from the 1970's-1980's of indoor NO₂ exposure associated with gas stoves reported 20% increased odds of respiratory illness in children for each 16 ppb increase in NO₂ (Hasselblad et al., 1992). Lin et al considered studies through 2013 and found 6% (95% CI -1-3%) and 16% (95% CI 5-29%) increased odds of wheeze incidence with presence of residential gas stove and 15 ppb NO₂ increase, respectively. Our findings, using even more recent studies through 2023, were consistent with both of these previous meta-analyses.

Dose-response relationships between human health, NO₂ exposure, and other by-products of combustion are not well characterized. Furthermore, these relationships are mediated by numerous factors both inside and outside the built environment, including the presence and use of exhaust ventilation, the duration and types of food preparation, psychosocial stressors, and pre-existing health conditions. However, there is clear evidence of a wide range of health effects, even at low levels of exposure. A four-month prospective cohort by Belanger and colleagues showed a dose-response relationship between NO₂ exposure and wheeze, asthma symptoms, and asthma reliever medication use, with effects seen above a threshold of 6 ppb NO₂ (Belanger et al., 2013). Similarly, the year-long follow-up study by Boulic found that a 2-8 ppb increase was associated with a range of respiratory health outcomes. Perhaps it is not

surprising then, that the underpowered trial by Gent and colleagues found little relationship between health outcomes and the average 3-4 ppb NO₂ reductions, that were observed in dwellings already below health effects threshold limits.

The effect estimates, and confidence intervals presented here provide a window of reasonable risk levels for a variety of health outcomes and mortality, which can be used to extrapolate the health benefits of widespread measures to reduce the impacts of unvented combustion, including improved ventilation and source control, switching to vented appliances, better regulation of device emissions, and quantifying the benefits of electrification of end-uses. Despite the various designs, geographic sites, length of follow-up, and study dates, we noted a level of consistency between the studies within the current meta-analysis, and with previous ones, which strengthens the level of confidence in our findings. Studies were generally rigorously conducted, and variables were collected to allow for appropriate covariable adjustment. Given the small sample sizes, the pooled effect estimates are sensitive to the addition of new studies, given the small sample size. However, the reported confidence intervals are likely to be robust and provide perhaps a more helpful quantitative measure of risk given the inherent uncertainties and limitations of the epidemiologic studies required to detect population health effects in real-world conditions (Atkinson et al., 2018). New studies may be able to reduce sources of bias revealing even higher effect estimates and/or greater precision. Residential unvented combustion appliances pose a variety of serious health risks to people of all ages, but especially to children with asthma or other respiratory conditions.

5 ACKNOWLEDGEMENTS

This work was supported by the Assistant Secretary for Energy Efficiency and Renewable Energy, Building Technologies Office, of the U.S. Department of Energy under Contract No. DE-AC0205CH11231.

6 REFERENCES

- Achakulwisut, P., Brauer, M., Hystad, P., & Anenberg, S. C. (2019). Global, national, and urban burdens of paediatric asthma incidence attributable to ambient NO₂ pollution: Estimates from global datasets. *The Lancet Planetary Health*, 3(4), e166–e178. Scopus. [https://doi.org/10.1016/S2542-5196\(19\)30046-4](https://doi.org/10.1016/S2542-5196(19)30046-4)
- Atkinson, R. W., Butland, B. K., Anderson, H. R., & Maynard, R. L. (2018). Long-term Concentrations of Nitrogen Dioxide and Mortality: A Meta-analysis of Cohort Studies. *Epidemiology*, 29(4), 460. <https://doi.org/10.1097/EDE.0000000000000847>
- Barck, C., Lundahl, J., Halldén, G., & Bylin, G. (2005). Brief exposures to NO₂ augment the allergic inflammation in asthmatics. *Environmental Research*, 97(1), 58–66. <https://doi.org/10.1016/j.envres.2004.02.009>
- Barnard, L. T., Preval, N., & Howden-Chapman, P. (2011). *The impact of retrofitted insulation and new heaters on health services utilisation and costs, pharmaceutical costs and mortality.*
- Belanger, K., Gent, J. F., Triche, E. W., Bracken, M. B., & Leaderer, B. P. (2006). Association of Indoor Nitrogen Dioxide Exposure with Respiratory Symptoms in Children with Asthma. *American Journal of Respiratory and Critical Care Medicine*, 173(3), 297–303. <https://doi.org/10.1164/rccm.200408-1123OC>
- Belanger, K., Holford, T. R., Gent, J. F., Hill, M. E., Kezik, J. M., & Leaderer, B. P. (2013). Household Levels of Nitrogen Dioxide and Pediatric Asthma Severity. *Epidemiology*, 24(2), 320–330. <https://doi.org/10.1097/EDE.0b013e318280e2ac>
- Boulic, M. (2012). The association between mechanical ventilation, flue use in heaters and asthma symptoms. *Massey University*. <http://hdl.handle.net/10179/4082>
- Breyse, P. N., Buckley, T. J., Williams, D., Beck, C. M., Jo, S. J., Merriman, B., Kanchanaraksa, S., Swartz, L. J., Callahan, K. A., Butz, A. M., Rand, C. S., Diette, G. B., Krishnan, J. A., Moseley, A. M., Curtin-Brosnan, J., Durkin, N. B., & Eggleston, P. A. (2005). Indoor exposures to air pollutants and allergens in the homes of asthmatic children in inner-city Baltimore. *Environmental Research*, 98(2), Article 2. <https://doi.org/10.1016/j.envres.2004.07.018>
- Diette, G. B., Hansel, N. N., Buckley, T. J., Curtin-Brosnan, J., Eggleston, P. A., Matsui, E. C., McCormack, M. C., Williams, D. L., & Breyse, P. N. (2007). Home indoor pollutant exposures among inner-city children with and without asthma. *Environmental Health Perspectives*, 115, 1665–1669. <https://doi.org/10.1289/ehp.10088>
- Faustini, A., Rapp, R., & Forastiere, F. (2014). Nitrogen dioxide and mortality: Review and meta-analysis of long-term studies. *European Respiratory Journal*, 44(3), 744–753. <https://doi.org/10.1183/09031936.00114713>

- Francisco, P. W., Gordon, J. R., & Rose, B. (2010). Measured concentrations of combustion gases from the use of unvented gas fireplaces. *Indoor Air*, 20(5), 370–379. <https://doi.org/10.1111/j.1600-0668.2010.00659.x>
- Free, S., Howden-Chapman, P., Pierse, N., Viggers, H., & the Housing, H. and H. S. R. T. (2010). More effective home heating reduces school absences for children with asthma. *Journal of Epidemiology & Community Health*, 64(5), 379–386. <https://doi.org/10.1136/jech.2008.086520>
- Gent, J. F., Holford, T. R., Bracken, M. B., Plano, J. M., McKay, L. A., Sorrentino, K. M., Koutrakis, P., & Leaderer, B. P. (2022). Childhood asthma and household exposures to nitrogen dioxide and fine particles: A triple-crossover randomized intervention trial. *Journal of Asthma*, 0(0), 1–10. <https://doi.org/10.1080/02770903.2022.2093219>
- Gillespie-Bennett, J., Pierse, N., Wickens, K., Crane, J., Howden-Chapman, P., & Team, and the H. H. and H. S. R. (2011). The respiratory health effects of nitrogen dioxide in children with asthma. *European Respiratory Journal*, 38(2), 303–309. <https://doi.org/10.1183/09031936.00115409>
- Gruenewald, T., Seals, B. A., Knibbs, L. D., & Hosgood, H. D. (2022). Population Attributable Fraction of Gas Stoves and Childhood Asthma in the United States. *International Journal of Environmental Research and Public Health*, 20(1), 75. <https://doi.org/10.3390/ijerph20010075>
- Hansel, N. N., Breyse, P. N., McCormack, M. C., Matsui, E. C., Curtin-Brosnan, J., Williams, D. L., Moore, J. L., Cuhran, J. L., & Diette, G. B. (2008). A longitudinal study of indoor nitrogen dioxide levels and respiratory symptoms in inner-city children with asthma. *Environmental Health Perspectives*, 116(10), Article 10. <https://doi.org/10.1289/Ehp.11349>
- Hasselblad, V., Eddy, D. M., & Kotchmar, D. J. (1992). Synthesis of Environmental Evidence: Nitrogen Dioxide Epidemiology Studies. *Journal of the Air & Waste Management Association*, 42(5), 662–671. <https://doi.org/10.1080/10473289.1992.10467018>
- Horsdal, H. T., Agerbo, E., McGrath, J. J., Vilhjálmsdóttir, B. J., Antonsen, S., Cløster, A. M., Timmermann, A., Grove, J., Mok, P. L. H., Webb, R. T., Sabel, C. E., Hertel, O., Sigsgaard, T., Erikstrup, C., Hougaard, D. M., Werge, T., Nordentoft, M., Børglum, A. D., Mors, O., ... Pedersen, C. B. (2019). Association of Childhood Exposure to Nitrogen Dioxide and Polygenic Risk Score for Schizophrenia With the Risk of Developing Schizophrenia. *JAMA Network Open*, 2(11), Article 11. <https://doi.org/10.1001/jamanetworkopen.2019.14401>
- Howden-Chapman, P., Pierse, N., Nicholls, S., Gillespie-Bennett, J., Viggers, H., Cunningham, M., Phipps, R., Boulic, M., Fjällström, P., Free, S., Chapman, R., Lloyd, B., Wickens, K., Shields, D., Baker, M., Cunningham, C., Woodward, A., Bullen, C., & Crane, J. (2008). Effects of improved home heating on asthma in community dwelling children: Randomised controlled trial. *BMJ*, 337, a1411. <https://doi.org/10.1136/bmj.a1411>
- Hu, Y., Ji, J. S., & Zhao, B. (2022). Restrictions on indoor and outdoor NO₂ emissions to reduce disease burden for pediatric asthma in China: A modeling study. *The Lancet Regional Health - Western Pacific*, 24, 100463. <https://doi.org/10.1016/j.lanwpc.2022.100463>
- Jacobs, P., Borsboom, W., & Gids, W. de. (2019). *Indoor air quality in Nearly Zero Energy Buildings, reduction of exposure*. <https://www.aivc.org/resource/indoor-air-quality-nearly-zero-energy-buildings-reduction-exposure>
- Khreis, H., Kelly, C., Tate, J., Parslow, R., Lucas, K., & Nieuwenhuijsen, M. (2017). Exposure to traffic-related air pollution and risk of development of childhood asthma: A systematic review and meta-analysis. *Environment International*, 100, 1–31. <https://doi.org/10.1016/j.envint.2016.11.012>
- Knibbs, L. D., Woldeyohannes, S., Marks, G. B., & Cowie, C. T. (2018). Damp housing, gas stoves, and the burden of childhood asthma in Australia. *Medical Journal of Australia*, 208(7), 299–302. <https://doi.org/10.5694/mja17.00469>
- Less, B. D., Casquero-Modrego, N., & Walker, I. S. (2022). Home Energy Upgrades as a Pathway to Home Decarbonization in the US: A Literature Review. *Energies*, 15(15), 5590. <https://doi.org/10.3390/en15155590>
- Less, B., Mullen, N., Singer, B., & Walker, I. (2015). Indoor air quality in 24 California residences designed as high-performance homes. *Science and Technology for the Built Environment*, 21(1), 14–24. <https://doi.org/10.1080/10789669.2014.961850>
- Lewis, A. C., Jenkins, D., & Whitty, C. J. M. (2023). Indoor air pollution: Five ways to fight the hidden harms. *Nature Comment*, 614.
- Lim, Y.-H., Hersoug, L.-G., Lund, R., Bruunsgaard, H., Ketzler, M., Brandt, J., Jørgensen, J. T., Westendorp, R., Andersen, Z. J., & Loft, S. (2022). Inflammatory markers and lung function in relation to indoor and ambient air pollution. *International Journal of Hygiene and Environmental Health*, 241, 113944. <https://doi.org/10.1016/j.ijheh.2022.113944>
- Lin, W., Brunekreef, B., & Gehring, U. (2013). Meta-analysis of the effects of indoor nitrogen dioxide and gas cooking on asthma and wheeze in children. *International Journal of Epidemiology*, 42(6), 1724–1737. <https://doi.org/10.1093/ije/dyt150>
- Logue, J. M., Price, P. N., Sherman, M. H., & Singer, B. C. (2012). A Method to Estimate the Chronic Health Impact of Air Pollutants in U.S. Residences. *Environmental Health Perspectives*, 120(2), 216–222. <https://doi.org/10.1289/ehp.1104035>
- Marks, G. B., Ezz, W., Aust, N., Toelle, B. G., Xuan, W., Belousova, E., Cosgrove, C., Jalaludin, B., & Smith, W. T. (2010). Respiratory Health Effects of Exposure to Low-NO_x Unflued Gas Heaters in the Classroom: A Double-Blind, Cluster-Randomized, Crossover Study. *Environmental Health Perspectives*, 118(10), 1476–1482. <https://doi.org/10.1289/ehp.1002186>
- Morantes, G., Jones, B., Sherman, M., & Molina, C. (2022). *Health impacts of indoor air contaminants determined using the DALY metric*. 774–783.
- Mullen, N. A., Li, J., Russell, M. L., Spears, M., Less, B. D., & Singer, B. C. (2016). Results of the California Healthy Homes Indoor Air Quality Study of 2011–2013: Impact of natural gas appliances on air pollutant concentrations. *Indoor Air*, 26(2), 231–245. <https://doi.org/10.1111/ina.12190>

- Nitschke, M., Pilotto, L. S., Attewell, R. G., Smith, B. J., Pisaniello, D., Martin, J., Ruffin, R. E., & Hiller, J. E. (2006). A Cohort Study of Indoor Nitrogen Dioxide and House Dust Mite Exposure in Asthmatic Children. *Journal of Occupational and Environmental Medicine*, 48(5), 462–469.
- Orellano, P., Reynoso, J., Quaranta, N., Bardach, A., & Ciapponi, A. (2020). Short-term exposure to particulate matter (PM10 and PM2.5), nitrogen dioxide (NO2), and ozone (O3) and all-cause and cause-specific mortality: Systematic review and meta-analysis. *Environment International*, 142, 105876. <https://doi.org/10.1016/j.envint.2020.105876>
- Permaul, P., Gaffin, J. M., Petty, C. R., Baxi, S. N., Lai, P. S., Sheehan, W. J., Camargo, C. A., Gold, D. R., & Phipatanakul, W. (2020). Obesity may enhance the adverse effects of NO2 exposure in urban schools on asthma symptoms in children. *Journal of Allergy and Clinical Immunology*, 146(4), 813-820.e2. <https://doi.org/10.1016/j.jaci.2020.03.003>
- Pilotto, L. S., Nitschke, M., Smith, B. J., Pisaniello, D., Ruffin, R. E., McElroy, H. J., Martin, J., & Hiller, J. E. (2004). Randomized controlled trial of unflued gas heater replacement on respiratory health of asthmatic schoolchildren. *International Journal of Epidemiology*, 33(1), 208–214. <https://doi.org/10.1093/ije/dyh018>
- Rice, J. L., McGrath-Morrow, S. A., & Collaco, J. M. (2020). Indoor Air Pollution Sources and Respiratory Symptoms in Bronchopulmonary Dysplasia. *The Journal of Pediatrics*, 222, 85-90.e2. <https://doi.org/10.1016/j.jpeds.2020.03.010>
- Samet, J. M., Lambert, W. E., Skipper, B. J., Cushing, A. H., Hunt, W. C., Young, S. A., McLaren, L. C., Schwab, M., & Spengler, J. D. (1993). Nitrogen dioxide and respiratory illnesses in infants. *The American Review of Respiratory Disease*, 148(5), 1258–1265. <https://doi.org/10.1164/ajrccm/148.5.1258>
- Schachter, E. N., Rohr, A., Habre, R., Koutrakis, P., Moshier, E., Nath, A., Coull, B., Grunin, A., & Kattan, M. (2020). Indoor air pollution and respiratory health effects in inner city children with moderate to severe asthma. *Air Quality, Atmosphere & Health*, 13(2), 247–257. <https://doi.org/10.1007/s11869-019-00789-3>
- Sherman, M., Fahey, P., & Crawford, R. (2022). Impacts of Unvented Space Heaters. *ASHRAE Journal*, 64(5), 32-34,36,38-42,44,46-49.
- Simoni, M., Scognamiglio, A., Carrozzi, L., Baldacci, S., Angino, A., Pistelli, F., Pede, F. D., & Viegi, G. (2004). Indoor exposures and acute respiratory effects in two general population samples from a rural and an urban area in Italy. *Journal of Exposure Science & Environmental Epidemiology*, 14(1), Article 1. <https://doi.org/10.1038/sj.jea.7500368>
- Sun, L., & Singer, B. C. (2023). Cooking methods and kitchen ventilation availability, usage, perceived performance and potential in Canadian homes. *Journal of Exposure Science & Environmental Epidemiology*. <https://doi.org/10.1038/s41370-023-00543-z>
- Vardoulakis, S., Giagloglou, E., Steinle, S., Davis, A., Smeuwenhoek, A., Galea, K. S., Dixon, K., & Crawford, J. O. (2020). Indoor Exposure to Selected Air Pollutants in the Home Environment: A Systematic Review. *International Journal of Environmental Research and Public Health*, 17(23), Article 23. <https://doi.org/10.3390/ijerph17238972>
- Willers, S. M., Brunekreef, B., Oldenwening, M., Smit, H. A., Kerkhof, M., De Vries, H., Gerritsen, J., & De Jongste, J. C. (2006). Gas cooking, kitchen ventilation, and asthma, allergic symptoms and sensitization in young children – the PIAMA study. *Allergy*, 61(5), 563–568. <https://doi.org/10.1111/j.1398-9995.2006.01037.x>
- Zheng, X., Ding, H., Jiang, L., Chen, S., Zheng, J., Qiu, M., Zhou, Y., Chen, Q., & Guan, W. (2015). Association between Air Pollutants and Asthma Emergency Room Visits and Hospital Admissions in Time Series Studies: A Systematic Review and Meta-Analysis. *PLOS ONE*, 10(9), e0138146. <https://doi.org/10.1371/journal.pone.0138146>
- Zheng, X., Orellano, P., Lin, H., Jiang, M., & Guan, W. (2021). Short-term exposure to ozone, nitrogen dioxide, and sulphur dioxide and emergency department visits and hospital admissions due to asthma: A systematic review and meta-analysis. *Environment International*, 150, 106435. <https://doi.org/10.1016/j.envint.2021.106435>

How to create a performance-based regulation on ventilation – the French Experience

Valérie Leprince*¹, Baptiste Poirier², Gaëlle Guyot^{3,4}

*1 Cerema
2 rue Antoine Charial
Lyon, France*

**Corresponding author: valerie.leprince@cerema.fr*

*2 Cerema
9 rue René Viviani,
44200 - Nantes, France*

*3 Cerema
BPE Research Team, 46, Rue St Théobald, F-38080,
L'Isle d'Abeau, France*

*4 Univ. Savoie Mont Blanc,
CNRS, LOCIE,
73000 Chambéry, France*

ABSTRACT

In France, in Residential buildings, since 1982 the ventilation regulation imposes air flow rate to be continuously extracted from every room with humidity production. A boosted level of air flow rate shall be reachable in the kitchen. Since the mid-80s demand-controlled ventilation based on humidity level in each room has been allowed, provided that the system is validated by a national commission. In practice, for 40 years every new residential building has a mechanical ventilation system and 95% of them are centralised extract only systems. Since the beginning of the 2010s almost all of them have a humidity-based control. While efficient to mitigate the risk of moisture in buildings, the efficiency of those systems for other pollutants is still under investigation and the very prescriptive regulation limits the innovation possibilities to optimize the energy performance. To tackle this issue and allow the development of systems that would be more energy efficient (hybrid ventilation, low pressure systems, etc.), the French ministry for construction has set-up a working group to create a new performance-based regulation for ventilation.

This working group has defined Key Performance Indicator for ventilation systems, it evaluates the ability of a ventilation system to provide good indoor air quality through indicators on 4 criteria: humidity level, CO₂ level, fictive pollutant P1 exposure (emitted constantly) and fictive pollutant P2 exposure (emitted during cooking events). The working group has also discussed validation conditions for systems.

This new performance-based regulation gives specification for what a ventilation system shall provide. This will help to promote ventilation system in refurbishment and decrease CO₂ emissions of existing buildings which are heated through combustion appliance for more than 50% of them. It shall also foster the development of ventilation systems with less embodied energy.

KEYWORDS

Ventilation, Performance based, KPI, France

1 INTRODUCTION

The French ESSOC regulation has the objective to promote innovation in every subject including building regulation and therefore ventilation. It aims at creating performance-based regulations as an alternative to existing prescriptive regulations. Those new regulations shall allow to develop more efficient systems.

In the specific context of ventilation in residential building the French regulation is defined in the « Arrêté de 82 modified in 83 (JOFR, 1982)». This text includes requirement on the

extracted flowrate in each utility rooms (main requirements are given in annex) but does not impose anything on air inlet flowrate in each main room.

The new construction code states that “Air renewal, shall be such as, in normal condition of use, the indoor air pollution does not endanger health and security of occupants and that condensation is avoided, except temporarily”. This is respected if the system:

- Either respects Arrete de 82 requirements
- Or Fulfills Key Performance Indicators levels (named Résultats minimaux – Minimal results) as defined in a Regulatory text to be published by January 2025.

This new regulation is ambitious because defining KPI for ventilation with minimum is still a matter of research, this is worked on in IEA-EBC Annex 86.

The existing European standard EN 16798-1 “Ventilation for buildings. Indoor environmental input parameters for design and assessment of energy performance of buildings addressing indoor air quality, thermal environment, lighting and acoustics.”(CEN, 2016) describes prescriptive methods with different approaches. Nevertheless, it only deals with the definition of design flowrate. This is actually one of the objectives of the new revision to include Key Performance Indicators in the new version (the revision is in process).

When defining a regulation on ventilation and performance indicator, it is important to first define the objective of the ventilation system in the context of the regulation. Buildings need air-renewal but submarine and the international space station shows that acceptable indoor air quality can be reached without ventilation. Nevertheless, relying only on air- cleaning systems is not reasonable in buildings where pollutants emissions are not controlled.

Ventilation is air renewal by purpose-provided means which replaces the air with air coming directly from outdoors. The objective of a ventilation system can be to:

- Maintain healthy indoor air,
 - o limit indoor-produced pollutant concentration,
 - o and/or limit outdoor-produced pollutant concentration,
- Regulate humidity level to mitigate the risk of condensation and mold development (building lasting quality),
- Ensure olfactive comfort and avoid stuffiness feeling,
- Improve summer comfort,
- Etc.

Additionally, the ventilation system should not compromise acoustic comfort and significantly increase energy consumption.

Works at international level shows that views on main objectives for ventilation systems vary a lot from one country to another. In France the regulation in 1982 has been made in order to :

- First, humidity: avoid condensation,
- Second, health: limit indoor produced pollutant concentration and their transfer from utility rooms to main rooms
- Three, comfort: limit stuffiness feeling and avoid olfactive discomfort due to the transfer of odors from utility rooms (ex. Kitchen to main rooms)

Therefore, our newly defined Key Performance Indicators (KPI) and their target levels will follow this logic.

This paper presents the methodology and reasons behind choices made to create the new performance-based regulation.

2 METHODOLOGY

The current French regulation for ventilation that had little change since 1982 is based on a prescriptive approach that impose ventilation airflows to be respected. However, such prescribed ventilation airflows do not necessarily give guaranty for good IAQ. In opposition to *prescriptive approach* a performance-based approach for ventilation systems regulation could be defined based on the definition from CIB W60 commission (Gibson, 1982) frequently cited in literature in building field as :

“ The practice of thinking and working in terms of ends rather than means [...] with what a building or a building product is required to do, and not with prescribing how it is to be constructed.”

Having requirements in terms of performance rather than prescription allow the development of smart ventilation that can be defined as :

“ A process to continually adjust the ventilation system in time, and optionally by location, to provide the desired IAQ benefits while minimizing energy consumption, utility bills and other non-IAQ costs (such as thermal discomfort or noise) (Durier et al., 2018, p. 38)

The construction code states that “Air renewal, shall be such as, in normal condition of use, the indoor air pollution does not endanger health and security of occupants and that condensation is avoided, except temporarily.”. While it is a very simple statement it induces a lot of underlying questions such as:

- What is “normal condition of use”?
- What are the criteria for indoor air pollution not to endanger health and security of occupants?
- What indicator to ensure that condensation is avoided, and what “temporarily” means?

Additionally, as those performance indicators will be evaluated prior to construction, not only key performance indicators need to be detailed but also the validation protocol.

2.1 Preliminary decisions

Before starting the work on indicators, it has been decided that:

- The validation of systems shall be done building’s project by building’s project and not for a ventilation system.
 - o The agreement is valid only for a given ventilation system in a defined architecture and climate.
 - o As some parameters of local climate is difficult to anticipate (such as wind) and may change over the years, parametric study will be done on those parameters
- The ability of a system in a project to fulfill performance indicators level will be validated through preliminary simulations but not through on-site measurements.
 - o Nevertheless, the ability of indicators to be compared to on-site measurement is a criterion to define them.
- Today system that fulfill Arrêté de 82 (modified in 83) regulation shall have performance in-line with required levels for indicators but not necessarily systematically comply for all kind of dwelling/location etc.

- The performance of every existing systems will be evaluated for the 3 French climate zones and all size and configuration of dwellings to help the definition of the required level for key performance indicators
 - A performance-based regulation shall be more “safe-sided” than a prescriptive one.
- Some prescriptive requirements will be kept as a safeguard as everything cannot be planned. The following prescriptive requirements shall be kept:
 - A general and permanent minimum flowrate applying (every rooms shall be ventilated)
 - The foreseen flowrate is twice the second table of Article 4 (see annex 1)
 - A non-closable outlet in each utility rooms
 - A non-closable inlet (or outlet) in each main room
 - Existing requirements on fire-safety
 - Maintenance requirements
 - The system shall not compromise the well-functioning of combustion appliance, if any in the dwelling
 - The validation of a project will be done by an independent body with a process to be defined.

A system includes a maintenance process and the description of its inspection protocol to check and maintain its performances.

2.2 Definition of input parameters for simulations

The starting point to define input parameters for simulations was the CPT 3615 that defines simulations to be performed in the context of “Avis Techniques” (technical approbation) to be obtained for humidity-based demand control ventilation (Groupe Spécialisé n° 14.5, 2015)

In such performance-based approaches the choice for the input parameters are crucial as they directly impact the calculated performance for ventilation. Indeed, several points were questioned and defined (in Table 1) regarding:

<p>The weather and outdoor boundary conditions</p> <ul style="list-style-type: none"> - How to consider the locals weather conditions and local environment around the building? (Temperature, humidity, wind speed, solar radiation) - Which outdoor pollutants and what background level or pollution scenarios need to be considered? <p>The indoor conditions</p> <ul style="list-style-type: none"> - What are the indoor air parameters to be considered when assessing IAQ performance? - What are the activities, materials, and furniture to be considered? - And what are the associated indoor air pollutant emission scenario? 	<p>The occupancy</p> <ul style="list-style-type: none"> - How many occupants in the buildings? - What are their occupancy schedules and behaviour (windows and doors opening) for pollutant exposition calculation? - What are the bio-effluent (CO₂ and moisture) emission profiles of the occupants? <p>Building properties</p> <ul style="list-style-type: none"> - What is the level of detail needed for the envelope description (airtightness, filtration/ infiltration of pollutant from outdoor) - What is the level of detail needed for room definition (number of zones, airtightness between zone)? <p>Simulation tools</p> <ul style="list-style-type: none"> - What building simulation models is needed (aeraulic model/thermal model) ? - What are the relevant simulation period and time step?
---	--

Table 1 : Discussed inputs options and retained choice (in bold) for simulation.

Parameter	Discussed options	Complexity	Choice and reasons behind
Wheater and outdoor boundary conditions			
<i>Temperature</i>	Default temperature for a given climate zone	*	Using the standardized weather files from the RE2020; one weather file function of the climate zone ; adapted environment roughness coefficient for a given location ; elevation correction ; adapted pressure facade coefficient Cp ;
	Temperature corrected for a given location	**	
<i>Humidity</i>	Default outdoor humidity for a given climate zone	*	
	Outdoor humidity corrected for a given location	**	
<i>Wind speed</i>	Default wind speed for a given climate zone	*	
	Wind speed corrected for a given location	**	
	Wind speed corrected for a given location including buildings and vegetablizations around	***	
<i>Solar radiation</i>	Default solar radiation for a given climate zone	*	
	Solar radiation corrected for a given location	**	
<i>Number of Pollutant</i>	Solar radiation corrected for a given location with, mask and shading around the building	**	
	No outdoor pollutant interaction	-	
	Same pollutants than indoor	**	
<i>Scenario of outdoor pollutant</i>	Same pollutants than indoor with additional specific pollutants from outdoor	**	With only the CO2 as outdoor pollutant with a 400 ppm constant background level; choice limited by available data or difficulties of modelling a more dynamic pollutant level in a regulation
	Default constant background level	*	
	Dynamic pollutant level from standardized scenario or measurement	**	
	Dynamic pollutant level based on simulation	***	
Indoor conditions			
<i>Number of indoor air parameters</i>	The historical: Co2, Humidity	*	The selected KPI (described in next section) are based on CO2 and humidity; completed with two fictive pollutant P1 and P2 for background level exposure and peak emission exposure
	Historical + health risk : Formaldehyde, PM2.5, ...	***	
	Historical + specific risk : Radon...	**	
	Historical + fictive / generic pollutant	*	
<i>Activities</i>	One by pollutant	*	Moisture and CO2 emission by the occupants; additional moisture emissions from several activities breakfast, lunch, dinner, shower, laundry, laundry dry; Constant background emission for P1 pollutant; punctual emissions for P2 during cooking activities
	Pollutant with multiples activities as sources	**(*)	
<i>Scenario of pollutant emission</i>	Constant emission rate as a background average level with default values	**	
	Dynamic emission rates with default values	**	
	Dynamic with default values and interaction between pollutant	***	
<i>Materials and furniture</i>	From measurement	**	
	no interaction	*	Water vapour equivalent surface for absorption
	Hygroscopic moisture buffer effect	**	
	Furniture pollutant release / absorption	**	

...

Parameter	Discussed options	Complexity	Choice and reasons behind
Occupancy			
<i>Number of occupants</i>	Single/couple occupation: 1 occupant by room -1 if n° room >3	*	Conventional occupation hypothesis according to INSEE survey (INSEE 2006); with however an attention on the impact that could have on CO2 controlled ventilation systems
	Family occupation: 1 occupant by room and 2 in master bedroom	*	
<i>Time spends by room</i>	Standardized occupation		
	Default standardized schedules	*	Standardized occupation scenario according to GS14.5 o (Groupe Spécialisé n° 14.5, 2017); and reinforced occupation applying week-end occupation all the week
	Probabilistic models statistic behaviour	**	
<i>Doors and windows interaction</i>	No opening	*	No interaction considering the worst situation when all the windows and doors are closed, the air should be able to circulate in rooms.
	Default standardized schedules	*	
	Probabilistic models statistic behaviour	**	
<i>Occupant bio effluent profile</i>	Default standardized: same for all the occupant	*	However, an Awake and Asleep distinction is made
	Differencing function of the occupant (adult, child, morphology)	**	
Building proprieties			
<i>Room distribution</i>	Default: one zone per room	*	Regrouped zone may not be adapted for specific ventilation strategy at the room level; thus, keeping one zone per room as default.
	Regrouped: zone with room regrouped by type / space	*	
<i>Representation of airtightness (distribution)</i>	Uniform	*	Uniform distribution proportional by wall surface; using a Q4Pa permeability level of: 0.4 m3/(h.m²) in individual housing / 0.65 m3/(h.m²) for collective buildings (from median value of CEREMA data base)
	Non-uniform	**	
	From measurement	***	
<i>Air leakage between zone</i>	No air leakage	*	At this stage only the door undercutting; adapted function of the building
	Door undercutting	*	
	Uniform air leakage from the wall	**	
	Non-uniform / from measurement	***	
<i>Pollutant filtration</i>	No filtration	*	Models and knowledge on filtration through leakage still early and not ready to be implemented in regulation
	Constant filtration rate	**	
	Dynamic filtration	***	
Simulation tools			
<i>Aeraulic model</i>	Pressure code multi zone	*	
	CFD	***	
<i>Thermal model</i>	No thermal model just aeraulic	*	During the winter, the indoor temperature is constant and during the summer it is the average of the last 18 hours of the outdoor temperature.
	Coupled thermal model	**	
<i>Simulation period</i>	Default during winter heating period	*	some KPI needs the yearly calculation
	Yearly	**	
<i>Simulation time step</i>	In minutes	*	15 minutes timestep; compromising with available data and calculation time.
	Hourly	*	

2.3 Definition of Key Performance Indicators

The following questions need to be answered to define performance indicators

- On which criteria shall the system be evaluated to determine whether he fulfill the regulation
 - o Indoor air parameters – which ones?
 - o CO₂, humidity, PM_{2.5}, Radon, fictive pollutants, etc.
 - o Energy parameters
- Which indicators for each criterion?
 - o Criteria on rooms or occupant's exposition
 - o Cumulated exposure
 - o Maximum exposure
 - o A multi-criteria aggregation, in this case the impact of the weight distribution needs to be clearly explored in order to propose distribution adapted to the IAQ
 - o Else?
- Which level of requirements on indicators
 - o Absolut acceptable threshold
 - o Relative performance regarding a reference system ? (theoretical or ideal system)
 - o Else?

In the context of the French regulation on ventilation it has been decided not to evaluate performances according the energy performance as it is already included in the energy performance calculation. In France, to fulfill the objective of ventilation defined in the introduction the chosen criteria regarding indoor quality are the following :

- Humidity
- CO₂
- A fictive pollutant P1 emitted continuously in every rooms with an emission rate proportional to the area
- A fictive pollutant P2 emitted in the kitchen during cooking events at mid-day and in the evening.

Choosing fictive pollutants allows to cover multiple ones instead of picking one. Regarding humidity, the limit will be set only on high humidity level. It has been decided that it was not for ventilation to deal with low humidity level under the French climate, humidifying systems shall deal with this issue in some specific cases. It is better if for CO₂ and humidity the indicator can be measured for this regulation to be used as a reference scale.

The foreseen Key Performance Indicators are the following ones:

For CO₂:

- For each room, the CO₂ concentration (in ppm) below which it remains 67 (or 70%) of occupied time
 - o This indicator reflects the mean operating conditions
 - o An indicator in ppm is more easily readable than a cumulative exposure in ppm.h
- For each room, the CO₂ concentration (in ppm) below which it remains 95% (or 99%) of the occupied time
 - o This Indicator reflects pic conditions

For Humidity:

- For every room, a maximum percentage of time over 75% of relative humidity in the winter. The maximum value will depend on the type of room (as surface finishing standards depend on it)
- Under discussion : For every room a maximum number of hour when at least one leak is overpressures and the humidity level is above 75%

For the fictive pollutants P1 and P2:

- The mean exposure (for the most exposed person)
- The maximum exposure over one hour (moving average, for the most exposed person).
- *Under discussion:* An indicator to evaluate the transfer of pollutant P2 to the other rooms.

3 CONCLUSIONS

After 40 years, France is about to have an alternative to its prescriptive regulation on ventilation. Developing a performance-based regulation should promote smart ventilation and open the market to systems that will maintain or improve the indoor air quality, limit the energy use of building and limit their embodied energy.

In France, more than 71% of electricity is produced by nuclear plants, 21% are renewable and only 8% are from thermal plant (RTE, 2020). Therefore, the impact on CO₂ emissions of reducing electrical needs is limited. In new building heating is mostly done through electric heat pumps. Others impact of ventilation on building energy use are also mostly provided by electricity (air conditioning and fan energy). Thus, the impact of the performance-based regulation on the CO₂ emission of new building due to energy use will probably be limited.

Nevertheless, this new regulation should help decarbonize the full building stock for two reasons. First, it will at last give a framework and guidelines for refurbishment and for existing building, indeed existing regulation is not applicable most of the time in refurbishment for multiple reasons:

- Ventilation systems that respects the French prescriptive regulation usually work at high pressure (around 100 Pa), this imposes tight ductwork mostly made in galvanized steel in multi-family buildings. In refurbishment, it is usually impossible to keep existing concrete shaft and install a system consistent with the Arrete 1982.
- Installing a centralized system in refurbishment is often challenging.

Therefore, as there is no applicable legal text to refer to, ventilation is often forgotten in refurbishment projects. Having this legal framework will allow to develop ventilation systems compatible with refurbishment issues while guarantying the required indoor air quality. In 2015, gaz heats dwellings of 39% of families, fuel oil 12% and 5% for wood (INSEE, 2017). It means that for more than 50% of existing buildings optimizing the ventilation system directly decrease the impact of the building on CO₂ emissions.

Second the decarbonization of the building's sector is not only based on the reduction of the energy use but also on the reduction of buildings' materials impact. This regulation should allow the development of low-tech ventilation systems (natural, hybrid, low- pressure systems etc.). Those systems may induce as much or more energy use for the building but have less impact on embodied energy which is now considered in the French energy performance regulation RE2020.

Regarding the timeline, the objective is to define key performance indicators by the end of 2023 and to publish the regulation (including certification process) by 2025.

4 DISCLAIMER

This document gives an overview of the work performed by the French working group “ESSOC”, the information provided in this document reflects the preliminary conclusion of the group in June 2023, this conclusion may change in the coming month. Neither the ministry for construction, nor members of the GT ESSOC group can be held responsible for the content of this document.

5 ANNEX 1 : MAIN REQUIREMENTS OF ARRETE DU 24 MARS 1982

- Art. 1: The air renewal in dwelling is general and permanent at least during the heating season.
- Art2: The air renewal system shall include natural or mechanical inlet in main rooms and outlet in utility rooms. The air shall circulate between main and utility rooms
- Art 3: The ventilation system shall be able to reach, simultaneously or not the following values:

Number of main rooms in the dwelling	Extract flowrate in m ³ /h				
	Kitchen	Bathroom	Other room with water source	Toilet	
				Only one	Multiple ones
1	75	15	15	15	15
2	90	15	15	15	15
3	105	30	15	15	15
4	120	30	15	30	15
5 or more	135	30	15	30	15

- Art4: The total extract flowrate can be reduced as follow :

	Number of main rooms						
	1	2	3	4	5	6	7
Total minimal flowrate in m³/h	35	60	75	90	105	120	135
Minimal flowrate in m³/h	20	30	45	45	45	45	45

If the ventilation system automatically control flowrate to maintain an indoor air quality that is not dangerous for occupant and avoid condensation (except temporarily) the flowrate can be reduced. Provided that the system has been validated by the ministry in charge of construction

	Number of main rooms						
	1	2	3	4	5	6	7
Total minimal flowrate in m³/h	10	10	15	20	25	30	35

and health. In any case the total extracted flowrate shall at least be:

- Art.5: air inlet shall be designed to reach extracted flowrates defined at article 3. Additional requirements are set for fire safety and interaction with combustion appliance.

6 REFERENCES

CEN. (2016). EN 16798-1 *Energy performance of buildings—Part 1 : Indoor environmental input parameters for design and assessment of energy performance of buildings addressing indoor air quality, thermal environment, lighting and acoustics*

- Durier, F., Carrié, F. R., & Sherman, M. (2018, mars). *VIP 38 : What is smart ventilation? AIVC*. <http://aivc.org/sites/default/files/VIP38.pdf>
- Gibson, E. (1982). *Working with the performance approach in building (Report of Working Commission W060 CIB Publication 64)*. International Council for Research and Innovation in Building and Construction.
- Groupe Spécialisé n° 14.5. (2015). *Cahier des Prescriptions Techniques communes : Systèmes de ventilation mécanique contrôlée simple flux hygroréglable*.
- INSEE. (2017). Dossier—*La facture énergétique du logement a baissé depuis 2013 malgré la hausse de la fiscalité*.
- Arrêté du 24 mars 1982 relatif à l'aération des logements, 0073
- RTE - Direction innovation et données. (2020). *Bilan Electrique 2019. Le réseau de transport d'électricité*. https://assets.rte-france.com/prod/public/2020-06/bilan-electrique-2019_1_0.pdf

Comparative Analysis Between Indoor Temperatures of Dwellings at Urban Scale During a Typical and Extreme Summers in a Temperate Climate

Ainhoa Arriazu-Ramos^{*1}, Germán Ramos Ruiz¹, Juan José Pons Izquierdo², Ana Sánchez-Ostiz Gutiérrez¹ and Aurora Monge-Barrio¹

1 School of Architecture

Universidad de Navarra

Campus universitario s.n.

31190 Pamplona, Spain

2 Department of History, History of Art and Geography

Universidad de Navarra

Campus universitario s.n.

31190 Pamplona, Spain

**Corresponding author: aarriazu@unav.es*

ABSTRACT

This study examines the impact of heatwaves on indoor operative temperatures of dwellings in Pamplona (north of Spain) and presents a comparative analysis of a typical summer and two extreme summers with heatwaves in 2003 and 2022. The assessment was conducted in two neighbourhoods with different urban morphologies and built periods related to different energy regulations in Spain. EnergyPlus was used to simulate each residential typology for 5 months in 8 different orientations and with the constructive characteristics that correspond to its built period. The Urban Weather Generator tool was used to consider the microclimate of each neighbourhood. The results showed that dwellings in the older neighbourhood, located on top floors, with one orientation and with large windows had the highest temperatures. These results are strengthened in extreme hot summers with heatwaves compared to those derived from the typical climate series. The evaluation of indoor temperatures of dwellings in two different climatic situations highlighted the importance of assessing temperatures through summers with heatwaves to analyse dwellings' behaviour to high temperatures, even in temperate climates. The urban approach and temperature analysis in relation to building parameters allowed the identification of dwellings with higher indoor temperatures and the key building parameters (built period, floor level, orientation, window area and number of orientations) for the future objective of designing passive measures to adapt dwellings to warming conditions.

KEYWORDS

Overheating; Microclimate; Heatwaves; Building parameters; Natural cooling.

1 INTRODUCTION

The last Intergovernmental Panel on Climate Change (IPCC) report concludes that global surface temperature has reached 1.1 °C above 1850-1900 in 2011-2020 ([Intergovernmental Panel on Climate Change, 2023](#)). These increasingly higher temperatures are leading to more frequent periods of hot and warm weather, and an increase in the frequency and severity of heatwaves ([Taylor et al., 2023](#)).

Through the last 20 years, there were some events, that illustrate this phenomenon and tendency: a heatwave during August 2003 when 50,000 excess deaths were registered across Europe ([Brücker, 2005](#)); in June 2021, western North America experienced a record-breaking heatwave that caused over 1,000 deaths in Canada and around 500 deaths in the USA ([Thompson et al., 2022](#)); recently, summer 2022 was extremely warm summer characterized by a cascade of heatwaves that caused 110,000 excess deaths across Europe ([Copernicus Climate Change Service \(C3S\), 2022](#); [Vicedo-cabrera & Fischer, 2023](#)) and around 4,500 in Spain ([Tobías, Royé, & Iñiguez, 2023](#)).

The projections for southern Europe warn of more extreme warm temperatures, similar to those currently found in regions of North Africa, and suffer more tropical nights (H.-O. Pörtner, D.C. Roberts, M. Tignor, E.S. Poloczanska, K. Mintenbeck, A. Alegría, M. Craig, S. Langsdorf, S. Lössche, V. Möller, A. Okem, 2022). Besides, the probability of suffering mega-heatwaves will increase by a factor of 5-10 in the next 40 years in Europe (Barriopedro, Fischer, Luterbacher, Trigo, & García-Herrera, 2011).

The population living in urban areas accounts for 75% of the total in the European Union (Zinzi & Carnielo, 2017). In this context, it is relevant to focus on cities where Urban Heat Island (UHI) can exacerbate the effect of these extreme temperatures, heatwaves (D. Li & Bou-Zeid, 2013) and indoor thermal discomfort in summer (X. Li et al., 2019; Litardo et al., 2020; Meggers et al., 2016; Nakano, Bueno, Norford, & Reinhart, 2015; Zinzi & Carnielo, 2017).

Therefore, the interest in analysing the negative effects of high temperatures on people's health, well-being (World Health Organization, 1990, 2011) and mortality (Pathan, Mavrogianni, Summerfield, Oreszczyn, & Davies, 2017) and studying how to prevent them have increased noticeably in recent years, especially within the cities.

This paper is focused on quantifying and comparing indoor operative temperatures (IOT) of dwellings - during a typical summer (climate series 1980-2010) and two extreme ones with heatwaves (2003 and 2022) - in relation to their built period and building parameters. The assessment was conducted in two neighbourhoods of Pamplona (a city in the north Spain) considering the effect of microclimate.

Specific research aims are the following:

- To quantify the influence of microclimate on indoor operative temperatures in dwellings.
- To compare how indoor operative temperatures of dwellings are strengthened in extreme warm summers in relation to a typical climate series.
- To analyse the influence of different building parameters (built period, floor level, orientation, area of windows and number of orientations) on indoor operative temperatures.

2 METHODS

2.1 Urban context

Pamplona is a city placed in the north of Spain. It has an area of 23.55 km² with a population of 203,081 inhabitants and a population density of 8,472 inhabitants/km² (Instituto Nacional de Estadística, 2021). The city is made up of 14 neighbourhoods.

Two neighbourhoods were selected to develop the study: *Iturrama* (N1) and *Mendillorri* (N2). They are samples of different urbanism: N1 (with 9,242 dwellings and built between 1960-1980) has a high density of buildings (0.31 site coverage ratio) and they are higher (average building height: 25.45 m); in contrast, N2 (with 5,634 dwellings and built between 1990-2006) is less dense (0.17 site coverage ratio) and the buildings are lower (average building height: 10.32 m). Besides, N2 has higher percentage of green spaces (Urban ground covered in grass: 25% in N1 and 47% in N2) as it can be seen in Figure 1.

2.2 Building typologies and energy parameters definition

The building typologies classification is based on the results of the project PrestaRener (SAVIArquitectura, 2016), carried out by the research group SAVIArquitectura and previous projects analysis (Aparicio-Gonzalez, Domingo-Irigoyen, & Sánchez-Ostiz, 2020; Monge-Barrio & Sánchez-Ostiz Gutierrez, 2018). Eleven residential typologies were detected in both

neighbourhoods through a visual work using Google Earth and SITNA software (Gobierno de Navarra, n.d.-b). Figure 1 shows the residential typologies in neighbourhoods' plans: typologies 11, 12, 13, 14 and 15 refer to dwellings in multi-family buildings grouped in linear blocks; typologies 21 and 22 correspond to dwellings in multi-family buildings grouped in H-blocks; typologies 31, 32 and 34 correspond to dwellings in tower; typologies 51 are single-family dwellings.



Figure 1. Green space and residential typologies graphed in N1 (left) and N2 (right) plans.

N1 and N2 were built in different built periods related to energy requirements in Spain, so their buildings have different building characteristics as they had to comply with their energy regulation requirements for each built period:

- N1 was built before 1979 (*no energy regulation*) when there weren't any energy regulations for buildings.
- N2 was built between 1980-2006 (*CT-79 period*) with the first standard energy regulation in Spain NBE CT-79 (Ministerio de Obras Públicas y Urbanismo, 1979) which appears after the 1970s energy crisis as in other countries.

Infiltration rates were not regulated in Spain until 2019 (with the Spanish Building Code regulation) so the used values are based on previous studies (Feijó-Muñoz et al., 2019). There weren't any IAQ regulations in any of the periods and all dwellings are naturally ventilated.

Based on these envelopes' energy requirements for each built period, two types of envelopes were defined for the simulation. The parameters that defined each one are presented in Table 1.

Table 1: Used parameters and values for energy simulations

Built period / Energy regulation	Ufaçade / Uroof (W/m ² K)	Uglass / Uframe (W/m ² K)	Infiltrations (50Pa)	Solar shading system	Ventilation
N1 No energy regulation	1.39 ^a / 2.9	5.7 / 8.5	7	Blinds with low reflectivity slats ^b	Calculated natural ventilation: Windows free aperture = 15%
N2 CT-79	0.73 ^a / 0.65	3.5 / 8.5	7	Blinds with medium reflectivity slats ^b	1AM- 8AM: 4ren/h 9AM- 12PM: 0ren/h Cracks: medium

^a This value considers the influence of thermal bridges, which worsen the façade transmittance (*U*) it by 30%.

^b They are considered to be in use (completely down) when solar radiation >150 w/m²

2.3 Climate and Microclimate

Pamplona has a Cfb climate (according to Koppen-Geiger classification), temperate without dry season, "oceanic" type. Three weather files were used for energy simulations: climate series (IWEC2-based in climate series 1980-2010 of ASHRAE (ASHRAE, 2011)) and two extreme warm summers (2003 and 2022 - elaborated with available data from Government of Navarra weather stations (Gobierno de Navarra, n.d.-a)). The year 2003 registered two

heatwaves (20 days in total) the and year 2022 had three heatwaves (41 days in total) (AEMET, 2022). Figure 2 shows a summary of outdoor temperatures for the three summers.

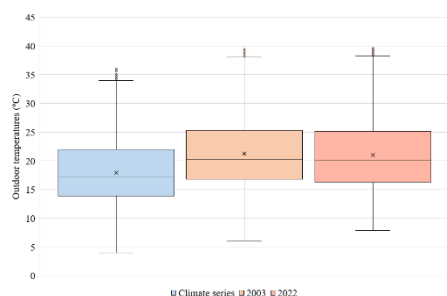


Figure 2. Box-plots showing outdoor temperatures summary for the climate series and the extreme years (2003 and 2022), during the simulation period (May to September).

As the study involves an urban scale, assessing the indoor operative temperature considering the different microclimates through each neighbourhood, was considered fundamental. For this propose, Urban Weather Generator (UWG) software was used (Bueno, Norford, Hidalgo, & Pigeon, 2013).

There are five key parameters to develop the microclimatic files through the UWG (Bueno, Norford, Pigeon, & Britter, 2011; Nakano et al., 2015):

- Urban parameters: Urban area building plan density (*site coverage ratio*); Urban area vertical to horizontal ratio (*facade to site ratio*); *Anthropogenic heat generation* (other than from buildings-traffic).
- Construction parameters: *Albedo* (roofs and soils); *Emissivity* (roofs and soils)

This research did not only consider these key parameters, but also some others more detailed ones: *average building height*, *urban ground covered in grass and trees*, and *vegetation albedo*. The parameters were calculated for the area of each neighbourhood to which a buffer of 50 m perimeter was added (to consider the affection of their surroundings).

2.4 Energy simulation and data analysis

The eleven residential typologies were modelled with their corresponding envelopes' parameters linked to their built period (Table 1). Each model was simulated for 8 different orientations. The considered simulation period was the one established by CIBSE TM-59 (CIBSE, 2013): 1 May - 30 September. The simulations were carried out for the two extreme summer climate files (2003 and 2022) and for the climate series weather file (IWEC2).

For each typology and orientation, results for two dwellings were obtained: one located on an intermediate floor (IF) and the other located on a top floor (TF) under the roof. Each dwelling was considered as a thermal zone because the scale of the research makes it unfeasible to analyse dwellings considering different thermal zones within them (Escandón, Suárez, Alonso, & Mauro, 2022) (f.e: living rooms and bedrooms). To accept this simplification, this work is based on previous studies which indicated that, when rooms do not have an active air conditioning system and the doors of all rooms are usually open (with the consequent circulation of air throughout the house) it is possible to consider the dwellings as one single thermal zone (Escandón, Suárez, & Sendra, 2019).

For each dwelling, the monthly mean operative temperatures, monthly mean maximum operative temperatures and monthly mean minimum operative temperatures were obtained for the simulation period.

Energy simulations were carried out by parameterization of building energy models developed in Design Builder and managed by a Python script (57,601 simulation combinations). Geographic Information System (GIS) was used to adjust the results to the real sample resulting

in a database of 1484 dwellings (N1 and N2) with the results of indoor operative temperature by climate weather file.

3 RESULTS

First of all, mean indoor operative temperatures (IOT) -considering or not microclimate for each neighbourhood-were compared through a TTest: differences between the three climate scenarios were found statistically significant ($p < 0.05$) in both neighbourhoods. It is important to note that the warmer the summer was, the greater this difference was (see Table 2).

Table 2. Differences between mean indoor operative temperatures (°C) considering microclimate or not considering it.

Group	Climate series	2003	2022
N1. base*	23.08 (SD. 1.61)	26.01 (SD. 2.82)	26.64 (SD. 2.00)
N1. microclimate*	23.22 (SD. 1.45)	26.95 (SD. 3.23)	27.94 (SD. 2.00)
N1. Diff.	0.13 (0.15-0.11) p<0,001	0.93 (0.97-0.89) p<0,001	1.30 (1.32-1.27) p<0,001
N2. base**	23.07 (SD. 1.59)	25.90 (SD. 2.73)	26.47 (SD. 1.96)
N2. microclimate**	23.40 (SD. 1.26)	26.96 (SD. 3.17)	27.74 (SD. 1.96)
N2. Diff.	0.32 (0.35-0.30) p<0,001	1.06 (1.11-1.01) p<0,001	1.30 (1.33-1.26) p<0,001

Based on these results, the following analyses were carried out considering the effect of microclimate in the three climate scenarios.

The mean indoor operative temperature resulted from the simulation with the climate series (1980-2010, IWEC2) and those obtained for extreme ones (2003 and 2022) showed an average difference of 4.1°C between means (1980-2010 mean: 23.6°C; 2003 mean: 27.3°C; 2022 mean: 28.1°C). This difference was even greater when only considering the three warmest months (June-August), reaching an average difference of 5.3°C between means (1980-2010 mean: 24.5°C; 2003 mean: 29.8°C; 2022 mean: 29.9°C).

If the limit of 26°C-established by the CIBSE TM-59 for bedrooms ([CIBSE TM59, 2017](#))- was considered, the n indoor operative temperature in summers with heatwaves exceeded this threshold (especially when only considering the three warmest months), while the mean indoor operative temperature derived from the simulation with the climate series was below it (see Figure 3).

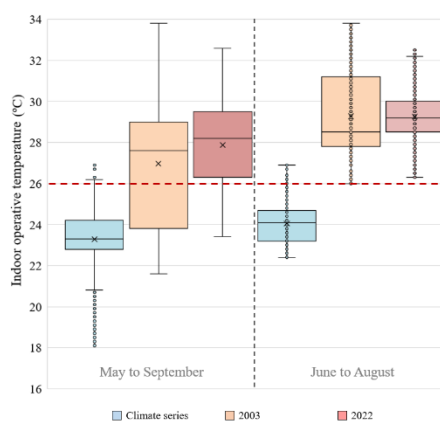


Figure 3. Box-plots showing the differences between indoor operative temperatures for the climate series and the extreme years (2003 and 2022), during all the simulation period (left) and during the warmest months (right). Monthly mean temperatures per group data.

A multilevel mixed-effects linear regression was developed to relate the dependent variable (IOT, °C) and the five independent variables analysed (built period, floor level, orientation, window area and number of orientations). This analysis was carried out for mean, maximum

and minimum temperatures. The most relevant results were found in the mean maximum temperatures (Table 3).

Table 3. Adjusted* monthly mean maximum indoor operative temperatures (°C) according to different building parameters.

Parameters**	Climate series		2003		2022		p value
	Beta Coef.	[95% Conf. Interval]	Beta Coef.	[95% Conf. Interval]	Beta Coef.	[95% Conf. Interval]	
Built period							
No regulation (N1)	0 (Ref.)		0 (Ref.)		0 (Ref.)		
CT-79 (N2)	+0.20	(+0.18 to +0.21)	-0.17	(-0.19 to -0.16)	-0.37	(-0.38 to -0.35)	<0.001
Floor level							
Top floor	0 (Ref.)		0 (Ref.)		0 (Ref.)		
Intermediate floor	+0.31	(+0.29 to +0.32)	-0.20	(-0.22 to -0.18)	-0.40	(-0.42 to -0.37)	<0.001
Orientation							
N/ NE / NW	0 (Ref.)		0 (Ref.)		0 (Ref.)		
S / SW / W	+0.20	(+0.19 to +0.21)	+0.38	(+0.37 to +0.40)	+0.44	(+0.42 to +0.46)	<0.001
E / SE	+0.13	(+0.11 to +0.14)	+0.06	(+0.05 to +0.08)	+0.03	(+0.00 to +0.05)	<0.001
Window area							
≤ 4m ²	0 (Ref.)		0 (Ref.)		0 (Ref.)		
>4m ²	+0.16	(+0.15 to +0.17)	+0.39	(+0.37 to +0.40)	+0.31	(+0.29 to +0.32)	<0.001
N° orientations							
1 orientation	0 (Ref.)						
> 1 orientation	-0.40	(-0.41 to -0.37)	-0.33	(-0.35 to -0.30)	-0.83	(-0.04 to -0.12)	<0.001

*Results are adjusted for all the variables in the table using a multilevel mixed effects linear regression.

Among the five independent variables, all of them had a statistically significant relationship with indoor operative temperature in the three climate scenarios ($p < 0.05$). The temperature differences between the reference categories and the rest of the categories of each building parameter are, in general, strengthened in warm summers compared to those derived from the climate series.

Regarding the relationship between mean maximum indoor operative temperature and the built period (according to energy standards), the dwellings built in CT-79 period (1980-2006), presented higher average maximum indoor operative temperature than those built in no energy regulation period (before 1979) for the standard climatic series. However, in extreme warm summers, this difference was reversed and the newer dwellings (no energy regulation period) had lower mean maximum temperatures (-0.37°C less in 2022).

Considering the relation between mean maximum indoor operative temperature and floor level (studying differences between apartments located in the intermediate floor and in top floor), intermediate floors presented lower indoor operative temperature than those located on top floors in warm summers with heatwaves (-0.40°C less in 2022).

Regarding the orientation of main facades, the highest mean maximum indoor operative temperature was found in dwellings facing south, west and southwest, especially in the warmest summer (+0.44°C more in 2022 than those with main orientations in north, northeast and northwest).

The size of the window area showed that the bigger it was, the higher mean maximum indoor operative temperature was found in dwellings.

Having more than one orientation in the dwelling (so there is higher potential for cross-ventilation), reduces the mean maximum indoor operative temperature by 0.83°C compared to dwellings with only one orientation in the warmer summer.

Figure 4 shows the mean maximum indoor operative temperature in the warmest month of the simulation period (August) on the plan of studied neighbourhoods. The temperature ranges have been established every 2°C with the lowest limit in 26°C (fixed limit established by CIBSE for

bedrooms (CIBSE TM59, 2017)). Temperature differences between floors and orientations are particularly noticeable in the oldest neighbourhood (N1).

CLIMATE SERIES



Figure 4. GIS plan with maximum average indoor operative temperature in August for 2022 weather files considering microclimate (left: N1; right: N2)

4 DISCUSSION

Due to the urban scale of the study - neighbourhood level- two simplifications were considered: the dwellings were considered as a single thermal zone and the temperature results were monthly.

The analyses of indoor operative temperature in relation to building parameters were aligned with previous studies. Other articles found higher overheating in dwellings located on top floors: one showed that top floors were warmer than first floors during more than 50% of summer hours (Sharifi, Saman, & Alemu, 2019); another based on CIBSE assessment demonstrated that top floor apartments failed all the criteria while those located in intermediate floors passed (Gamero-Salinas, Monge-Barrio, & Sánchez-Ostiz, 2020); and a third one which analyses mean indoor temperatures found that apartments in top floors had a mean temperature 1.2°C higher than in other floors (Vellei et al., 2017). Other studies also found that the worst orientation in relation to overheating was South and/or West: one found a statistically significant difference between indoor overheating hours (IOH) in different orientations with the highest percentage in S and W orientations (Nebia & Aoul, 2017); another found 1.5%-2% higher IOH in south-facing rooms than in north-facing rooms (Tian, Zhang, Deng, & Hrynyszyn, 2020). Regarding number of orientations (related to the potential of ventilation), other studies verified the influence of cross-ventilation in meeting CIBSE TM-59 criteria (Botti, Leach, Lawson, & Hadjidimitriou, 2022); another research, conducted in the north of Spain, concluded that the residential typology with better temperatures was the one that had double-orientation that allow crossed ventilation (on average, 1°C less than the rest of the dwellings) (Figueroa-Lopez, Arias, Oregi, & Rodríguez, 2021). Window size is also a factor that has revealed a significant relation with indoor temperatures: other studies reinforce the idea that the larger the window area is, the more it contributes to the indoor overheating problem

(Vardoulakis & Heaviside, 2012); a monitoring study in the north of Spain, concluded that dwellings with a window area larger than 4m² were almost 3 times more likely to experience IOH than those with smaller window area (Arriazu-Ramos, Bes-Rastrollo, Sanchez-Ostiz Gutierrez, & Monge-Barrio, 2022).

Future research should consider these results to propose strategies from the design (at urban and building level) to the occupants' behaviour in order to improve indoor thermal conditions throughout the summer periods.

5 CONCLUSIONS

This study presents a comparative analysis of dwellings' indoor operative temperatures (IOT) for a typical summer (climate series 1980-2010, IWEC2) and two extreme warm summers with heat waves (2003 and 2022). This research quantifies the influence of microclimate and building parameters (floor level, orientation, window area and number of orientations) on dwellings' indoor operative temperatures. The analyses are based on simulation results for dwellings in two neighbourhoods with different urban morphologies and built periods related to different energy regulations in Spain.

The difference between considering the effect of microclimate on indoor operative temperature and not considering it was statistically significant ($p < 0.05$). The indoor operative temperature was higher when microclimate was considered: this difference was greater when the summer was warmer, reaching a difference between means of 1.3°C in 2022.

The results obtained for the extreme warm summers showed higher indoor operative temperature (difference of 4.1°C on average) than those obtained for the climate series. The indoor operative temperatures in summers with heatwaves exceeded the limit of 26°C, while the temperatures derived from the simulation with the climate series were below it.

Regarding the assessment of the influence that building parameters (built period, floor level, orientation, window area and number of orientations) have on indoor operative temperature, was statistically significant ($p < 0.05$). Dwellings in the older neighbourhood (built before any energy regulation), located on top floors, with one orientation and with windows area bigger than 4m² had the highest indoor operative temperature. The most favourable orientations for summer were N-NE and NW. These results were strengthened in extreme hot summers with heatwaves compared to those derived from the typical climate series. The differences in indoor operative temperature in relation to building parameters were more pronounced in the older neighbourhood.

The indoor overheating evaluation of dwellings in different climatic situations showed that, even in temperate climates with mild summers, it is important to assess temperatures through a summer with heatwaves and considering microclimate in order to analyse dwellings' real behaviour to high temperatures. Besides, the building parameters assessment allows to identify the key building parameters for the future objective of designing passive measures to adapt dwellings to warming conditions and to help policymakers to prevent the risk of overheating within cities, especially during heatwaves.

6 ACKNOWLEDGEMENTS

This conference paper is part of the Research Project CLIMATEREADY “*Adaptation Assessment of Spanish residential buildings*” (2020-2023), funded by Convocatoria I+D+I “*Retos de Colaboración*” del Programa Estatal de Investigación, Desarrollo e Innovación Orientada a los Retos de la Sociedad. Plan Estatal de Investigación Científica y de Innovación”. Reference: PID2019-109008RB-C21. The authors would like to give special thanks to Anna Breeze, Claudia Bejerano and Carlos Jiménez, students that helped in the data collection process.

7 REFERENCES

- AEMET. (2022). *Olas de calor en España desde 1975 (actualización 2022)*.
- Aparicio-Gonzalez, E., Domingo-Irigoyen, S., & Sánchez-Ostiz, A. (2020). Rooftop extension as a solution to reach nZEB in building renovation. Application through typology classification at a neighbourhood level. *Sustainable Cities and Society*, 57(February), 102109. <https://doi.org/10.1016/j.scs.2020.102109>
- Arriazu-Ramos, A., Bes-Rastrollo, M., Sanchez-Ostiz Gutierrez, A., & Monge-Barrio, A. (2022). Building parameters that influence overheating of apartment buildings in a temperate climate in Southern Europe, 228. <https://doi.org/10.1016/j.buildenv.2022.109899>
- ASHRAE. (2011). International Weather For Energy Calculations, 2.
- Barriopedro, D., Fischer, E. M., Luterbacher, J., Trigo, R. M., & García-Herrera, R. (2011). The hot summer of 2010: Redrawing the temperature record map of Europe. *Science*, 332(6026), 220–224. <https://doi.org/10.1126/science.1201224>
- Botti, A., Leach, M., Lawson, M., & Hadjidimitriou, N. S. (2022). Developing a meta-model for early-stage overheating risk assessment for new apartments in London. *Energy and Buildings*, 254, 111586. <https://doi.org/10.1016/j.enbuild.2021.111586>
- Brücker, G. (2005, July 1). Vulnerable populations: lessons learnt from the summer 2003 heat waves in Europe. <https://doi.org/10.2807/ESM.10.07.00551-EN/CITE/PLAINTEXT>
- Bueno, B., Norford, L., Hidalgo, J., & Pigeon, G. (2013). The urban weather generator. *Journal of Building Performance Simulation*, 6(4), 269–281. <https://doi.org/10.1080/19401493.2012.718797>
- Bueno, B., Norford, L., Pigeon, G., & Britter, R. (2011). Combining a Detailed Building Energy Model with a Physically-Based Urban Canopy Model. *Boundary-Layer Meteorology*, 140(3), 471–489. <https://doi.org/10.1007/s10546-011-9620-6>
- CIBSE. (2013). The limits of thermal comfort: avoid overheating in European buildings (TM52).
- CIBSE TM59. (2017). Design methodology for the assessment of overheating risk in homes. *Technical Memoranda 59*.
- Copernicus Climate Change Service (C3S). (2022). *A wrap-up of Europe's summer 2022 heatwave*.
- Escandón, R., Suárez, R., Alonso, A., & Mauro, G. M. (2022). Is indoor overheating an upcoming risk in southern Spain social housing stocks? Predictive assessment under a climate change scenario. *Building and Environment*, 207. <https://doi.org/10.1016/j.buildenv.2021.108482>
- Escandón, R., Suárez, R., & Sendra, J. J. (2019). Field assessment of thermal comfort conditions and energy performance of social housing: The case of hot summers in the Mediterranean climate. *Energy Policy*, 128(January), 377–392. <https://doi.org/10.1016/j.enpol.2019.01.009>
- Feijó-Muñoz, J., Meiss, A., Poza-Casado, I., Padilla-Marcos, M. Á., Rabanillo-Herrero, M., Royuela-del-Val, A., ... Fernández Agüera, J. (2019). Permeabilidad al aire de los edificios residenciales en España. Estudio y caracterización de sus infiltraciones, (February).
- Figueroa-Lopez, A., Arias, A., Oregi, X., & Rodríguez, I. (2021). Evaluation of passive strategies, natural ventilation and shading systems, to reduce overheating risk in a passive house tower in the north of Spain during the warm season. *Journal of Building Engineering*, 43. <https://doi.org/10.1016/j.jobbe.2021.102607>
- Gamero-Salinas, J. C., Monge-Barrio, A., & Sánchez-Ostiz, A. (2020). Overheating risk assessment of different dwellings during the hottest season of a warm tropical climate. *Building and Environment*, 171(October 2019). <https://doi.org/10.1016/j.buildenv.2020.106664>
- Gobierno de Navarra. (n.d.-a). Meteo Navarra. Retrieved January 16, 2023, from <http://meteo.navarra.es/>
- Gobierno de Navarra. (n.d.-b). SITNA. Retrieved December 21, 2022, from https://www.google.com/search?q=sitna&rlz=1C1CHBD_esES868ES868&oq=sitna&aqs=chrome..69i57j0i13li433i512j0i512j0i10i512j0i512l6.799j0j7&sourceid=chrome&ie=UTF-8
- H.-O. Pörtner, D.C. Roberts, M. Tignor, E.S. Poloczanska, K. Mintenbeck, A. Alegría, M. Craig, S. Langsdorf, S. Löschke, V. Möller, A. Okem, B. R. (2022). *IPCC, 2022: Climate Change 2022: Impacts, Adaptation, and Vulnerability. Contribution of Working Group II to the Sixth Assessment Report of the Intergovernmental Panel on Climate Change. Climate Change 2021: The Physical Science Basis*. <https://doi.org/10.1017/9781009325844.Front>
- Instituto Nacional de Estadística. (2021). Población por capitales de provincia y sexo. Retrieved November 7, 2022, from <https://www.ine.es/jaxiT3/Datos.htm?t=2911>
- Intergovernmental Panel on Climate Change. (2023). *IPCC Sixth assessment report (AR6). European University Institute*. Retrieved from <https://eur-lex.europa.eu/legal-content/PT/TXT/PDF/?uri=CELEX:32016R0679&from=PT%0Ahttp://eur->

lex.europa.eu/LexUriServ/LexUriServ.do?uri=CELEX:52012PC0011:pt:NOT

- Li, D., & Bou-Zeid, E. (2013). Synergistic interactions between urban heat islands and heat waves: The impact in cities is larger than the sum of its parts. *Journal of Applied Meteorology and Climatology*, 52(9), 2051–2064. <https://doi.org/10.1175/JAMC-D-13-02.1>
- Li, X., Zhou, Y., Yu, S., Jia, G., Li, H., & Li, W. (2019). Urban heat island impacts on building energy consumption: A review of approaches and findings. *Energy*, 174, 407–419. <https://doi.org/10.1016/j.energy.2019.02.183>
- Litardo, J., Palme, M., Borbor-Cordova, M., Caiza, R., Macias, J., Hidalgo-Leon, R., & Soriano, G. (2020). Urban Heat Island intensity and buildings' energy needs in Duran, Ecuador: Simulation studies and proposal of mitigation strategies. *Sustainable Cities and Society*, 62(July), 102387. <https://doi.org/10.1016/j.scs.2020.102387>
- Megggers, F., Aschwanden, G., Teitelbaum, E., Guo, H., Salazar, L., & Bruelisauer, M. (2016). Urban cooling primary energy reduction potential: System losses caused by microclimates. *Sustainable Cities and Society*, 27, 315–323. <https://doi.org/10.1016/j.scs.2016.08.007>
- Ministerio de Obras Públicas y Urbanismo. (1979). Norma Básica de la Edificación: NBE-CT-79.
- Monge-Barrio, A., & Sánchez-Ostiz Gutierrez, A. (2018). *Passive Energy Strategies for Mediterranean Residential Buildings Facing the Challenges of Climate Change and Vulnerable Populations*.
- Nakano, A., Bueno, B., Norford, L., & Reinhart, C. F. (2015). Urban Weather Generator – A novel workflow for integrating urban heat island effect within urban design process. *Building Simulation Conference*, 1901–1908.
- Nebia, B., & Aoul, K. T. (2017). Overheating and daylighting; assessment tool in early design of London's high-rise residential buildings. *Sustainability (Switzerland)*, 9(9). <https://doi.org/10.3390/su9091544>
- Pathan, A., Mavrogianni, A., Summerfield, A., Oreszczyn, T., & Davies, M. (2017). Monitoring summer indoor overheating in the London housing stock. *Energy and Buildings*, 141, 361–378. <https://doi.org/10.1016/j.enbuild.2017.02.049>
- SAVIArquitectura. (2016). Proyecto PrestaRener. Pamplona, Spain.
- Sharifi, S., Saman, W., & Alemu, A. (2019). Identification of overheating in the top floors of energy-efficient multilevel dwellings. *Energy and Buildings*, 204. <https://doi.org/10.1016/j.enbuild.2019.109452>
- Taylor, J., Mcleod, R., Petrou, G., Hopfe, C., Mavrogianni, A., & Casta, R. (2023). Ten questions concerning residential overheating in Central and Northern Europe, 234(February). <https://doi.org/10.1016/j.buildenv.2023.110154>
- Thompson, V., Kennedy-Asser, A. T., Vosper, E., Eunice Lo, Y. T., Huntingford, C., Andrews, O., ... Mitchell, D. (2022). The 2021 western North America heat wave among the most extreme events ever recorded globally. *Science Advances*, 8(18). <https://doi.org/10.1126/sciadv.abm6860>
- Tian, Z., Zhang, S., Deng, J., & Hrynyszyn, B. D. (2020). Evaluation on Overheating Risk of a Typical Norwegian Residential Building under Future Extreme Weather Conditions. *Energies*, 13, 658. <https://doi.org/doi:10.3390/en13030658>
- Tobías, A., Royé, D., & Iñiguez, C. (2023). *Heat-attributable Mortality in the Summer of 2022 in Spain*. *Epidemiology* (Vol. 34). <https://doi.org/10.1097/EDE.0000000000001583>
- Vardoulakis, S., & Heaviside, C. (2012). Health Effects of Climate Change in the UK 2012: Current evidence, recommendations and research gaps. *Health Protection Agency*, 1–242.
- Vellei, M., Ramallo-González, A. P., Coley, D., Lee, J., Gabe-Thomas, E., Lovett, T., & Natarajan, S. (2017). Overheating in vulnerable and non-vulnerable households. *Building Research and Information*, 45(1–2), 102–118. <https://doi.org/10.1080/09613218.2016.1222190>
- Vicedo-cabrera, A., & Fischer, E. (2023). The footprint of human-induced climate change on heat-related deaths in the summer of 2022 in Switzerland, 1–20.
- World Health Organization. (1990). *Indoor Environment: Health Aspects of Air Quality, Thermal Environment, Light and Noise*.
- World Health Organization. (2011). *Health in the green economy: health co-benefits of climate change mitigation - housing sector*. *Medical Journal of Australia* (Vol. 195). <https://doi.org/10.5694/mja11.11023>
- Zinzi, M., & Carnielo, E. (2017). Impact of urban temperatures on energy performance and thermal comfort in residential buildings. The case of Rome, Italy. *Energy and Buildings*, 157, 20–29. <https://doi.org/10.1016/j.enbuild.2017.05.021>

Decarbonization and IAQ in Spain: a roadmap

Rafael Villar Burke¹, Marta Sorribes Gil², Daniel Jiménez González³

*1 Instituto Eduardo Torroja de ciencias de la
construcción
C/ Serrano Galvache 4
28033 Madrid
Spain
pachi@ietcc.csic.es*

*2 Instituto Eduardo Torroja de ciencias de la
construcción
C/ Serrano Galvache 4
28033 Madrid
Spain
msorribes@ietcc.csic.es*

*3 Instituto Eduardo Torroja de ciencias de la
construcción
C/ Serrano Galvache 4
28033 Madrid
Spain
danielj@ietcc.csic.es*

ABSTRACT

The presentation provides a brief overview of the current situation and a roadmap for decarbonizing the building stock under the context of EU directives. It also discusses how it could be implemented into Spanish building regulations. It examines the evolution of energy and emissions indicators and how they can help tackle the electrification of uses, generalized on-site energy generation, energy storage or building interaction with the grid. Several aspects of indoor air quality are involved in these challenges, including the increasing share of energy use due to ventilation and infiltration as well as the greater prevalence of energy recovery and free cooling capable systems. Further, additional questions arise from the differences in the scenarios used for energy efficiency and IAQ evaluation.

KEYWORDS

Decarbonization, roadmap, IAQ

1 INTRODUCTION

This article aims to provide a current overview of the decarbonisation process between now and 2050 in the European framework, and its transposition into Spanish energy policy and regulations, paying particular attention to those aspects related to building ventilation and indoor air quality.

1.1 European strategy for the decarbonisation of the building stock

The current revision of the Energy Performance of Buildings Directive 2010/31/EU [1] (EPBD) establishes a scenario for the decarbonisation of the European building stock by 2050 with the aim of mitigating climate change by reducing greenhouse gas emissions. It sets a target for all new and existing buildings to be zero-emission buildings by 2050, as well as a number of intermediate milestones, such as those committed to in the so-called European Green Pact [2], a consequence of the Paris Agreement, with a 55% reduction in net greenhouse gas emissions by 2030 compared to 1990 levels, and a further intermediate level by 2040.

The baseline scenario for the EU building stock from which to reach this target is as follows:

- 40% of the EU's final energy and 36% of its emissions are accounted for by buildings,
- 75% of the building stock is inefficient according to current building standards,
- buildings are responsible for about half of the primary fine particulate matter (PM2.5) emissions in the EU, leading to premature deaths and illness.

With this starting point, the European strategy to decarbonise the building stock is based on increasing the rate and depth of building renovations, especially of the most inefficient building stock, as well as improving information on energy efficiency and sustainability, so that this information enables end-users and technicians to make more climate-friendly decisions.

In order to achieve this global objective of climate neutrality, aspects such as the definition of a zero-emission building must be specified. According to Article 2 of the Directive itself, a zero-emission building is a building with a very high energy efficiency (determined in accordance with Annex 1, which states that it shall be expressed by an indicator of primary energy consumption per unit area per year [kWh/m²]) in which the small amount of energy that is still needed is fully covered by energy from renewable sources generated on-site, from a renewable energy community or from a district heating and cooling system in accordance with the requirements of Annex III.

Therefore the relationship between those defined so far by the EED as nearly zero-energy buildings (NZEB) and zero-emission buildings is that in the latter all the energy used must be from renewable sources, whereas previously it had to be the majority.

Other aspects of the decarbonisation strategy (as set out in the proposal to amend the Energy Efficiency Directive [3] and in Directive 2018/2001 on the promotion of the use of energy from renewable sources [4]) involve the generalisation of renewable production, taking into account the potential of buildings and on-site production, the transformation of mobility, which is also closely linked to buildings, the energy supply networks, which interact with buildings, especially the electricity grid, the potential for energy storage, etc.

1.2 Decarbonization milestones

The strategy and framework established by the directive on the energy efficiency of buildings is specified in milestones and requirements such as that new buildings must be zero-emission buildings by 2027, in the case of public buildings, and by 2030, in all other cases.

In addition, existing buildings must become zero-emission buildings by 2050, with intermediate energy efficiency targets to allow a progressive approach.

The following table shows the entry into force and expected scope of these intermediate requirements, called MEPS (Minimum Energy Performance Standards):

Table 1: Range of energy efficiency scenarios for existing buildings at the intermediate milestones (MEPS)

	Commission Approved Proposals by 15 december 2021 ⁽³⁾		European Parliament Amendments		European Council Amendments	
Public properties buildings	F in 2027	E in 2030	E in 2027	D in 2030		
Non residential private buildings	F in 2027	E in 2030	E in 2027	D in 2030		
Residential private buildings	F in 2030	E in 2034	E in 2030	D in 2033		
Residential buildings					D in 2033	B in 2040
Non Residential buildings					15% worst in 2030	25% worst in 2034

2 DECARBONISATION IN SPANISH REGULATIONS

2.1 Technical Building Code (Código Técnico de la Edificación, CTE) and Energy Certification of Buildings (Certificación energética de edificios, CEE)

Spanish regulations incorporate the latest updates of the European Directive until 2021 and are currently in the process of revision to adapt them to the latest revisions of the EPBD. It is foreseeable that an update of the affected standards may be published during 2024.

Within the state regulatory structure related to building, we have different documents and procedures that allow the total transposition of the European directive, setting the objectives established in it:

1. Within the Spanish Technical Building Code, the Basic Document on Energy Saving (DB-HE) (RD 314/2006) ⁽⁴⁾ is the one that develops and transposes a large part of the objectives of the EPBD.

It is the technical standard applicable to newly constructed buildings and existing buildings when certain interventions are carried out in them, and aims to ensure that adequate conditions of habitability and comfort of its occupants are achieved by making rational use of energy, reducing its consumption to sustainable limits and ensuring that a large part of this consumption comes from renewable sources.

The DB-HE sets, in relation to energy consumption, two global indicators, evaluated following the calculation methodology established in the UNE-EN ISO 52000-1:2019 Overall assessment of the energy performance of buildings. Part 1: general framework and procedures:

- the total primary energy consumption ($C_{ep,tot}$), which limits the total energy needs of the building, including energy from renewable sources.
- primary energy consumption from non-renewable sources ($C_{ep,nren}$), which limits the use of non-renewable resources.

The calculation of these indicators has to be done with hourly calculation procedures and so far only the consumed resources are evaluated (step A in terms of EN ISO 52000-1) and the positive impact of energy export to the grid is not taken into account (grid export factor $k_{exp}=0$).

2. On the other hand, the Energy Certification of Buildings (EEC), developed in Royal Decree 390/2021, of June 1, approving the basic procedure for the certification of the

energy efficiency of buildings [7], is established as an instrument of information to the end user, without prescriptive value. It shares calculation methodology with the DB-HE, and uses as main indicators:

- CO₂ emissions in the use phase of the building
- the consumption of primary energy from non-renewable sources ($C_{ep,nren}$), which shares with DB-HE

3. Finally, the Long-term Strategy for the Energy Rehabilitation of the Building Sector in Spain (ERESEE) [8], which was last updated in 2020, addresses the rehabilitation of the existing building stock by setting a roadmap with intervention scenarios, concrete measures and progress evaluation indicators to achieve the energy rehabilitation of the building stock and the decarbonization of the sector by 2050. It is currently being revised and transformed into a National Building Rehabilitation Plan (PNRE), the draft of which will be presented in 2025.

2.2 Evolution of technical regulations

In the roadmap towards decarbonisation, the evolution of Spanish regulations proposes to establish the following lines in line with the objectives of the EPBD:

- Progressive adjustment of the primary energy consumption limits already established in line with the zero emission buildings targets.
- Incorporation of global CO₂ emissions through LCA (Life Cycle Assessment). The current adjustment of the energy efficiency of the building in its use phase due to the development and implementation of energy saving regulations, means that it represents a smaller and smaller percentage of the total CO₂ emissions related to the building from the cradle or construction cycle (choice of materials, systems, origin of products and transport, etc.) to its demolition or demolition. Thus, the revision of Directive 2010/31/EU on the energy performance of buildings establishes the Global Warming Potential (GWP) of buildings, which must be calculated in accordance with standard EN 15978:2011. *Sustainability in construction. Assessment of the environmental performance of buildings. Calculation methods* ⁽⁹⁾, and to be incorporated in energy certificates for new buildings between 2027 and 2030.
- Electric vehicles are expected to play a crucial role in decarbonization as well as the use of soft mobility, to which building codes are already contributing and should continue to do so by:
 - the implementation in buildings of charging infrastructure in parking lots (through the obligation of pre-wiring, for example, and the minimum number of charging points in relation to the total number of parking spaces)
 - establishing requirements for a minimum number of parking spaces for bicyclesElectric vehicles are expected to play a crucial role in decarbonisation as well as the use of soft mobility, so building codes are already contributing and should continue to do so through.
- The disappearance of fossil fuel systems by 2030, prohibiting their sale and installation.
- Electrification of building uses and services (EPB uses) and decarbonisation of supply networks. The implementation in the regulations of the possibility of

exporting on-site renewable electricity production for evaluation within the energy efficiency of the building ($k_{exp}=1$), will favour and feed back into the use of electrical systems that meet the demands of the EPB uses of the building and allow the amount of energy they still need to use to be fully covered by energy from renewable sources.

Taking into consideration the export factor to the grid (k_{exp}) will imply a modification of the interaction of the building with the grid, which will affect the possibility of self-consumption of the building itself and the possibilities and facilities for thermal and electrical storage, which in the case of the electric vehicle can establish an interaction with the building as a recharge battery in one direction or the other.

3 DECARBONISATION AND ITS RELATION TO BUILDING VENTILATION

3.1 Ventilation and energy impact

3.1.1 The weight of ventilation and infiltration in energy demand

With the progressive increase in insulation levels required by regulations and the growing use of renewable inputs in services such as DHW, the exchange of air with the outside is having an increasing impact on the energy performance of the building. It is therefore important to adjust ventilation flow rates to the actual conditions of use, control air infiltration, use heat recovery and air treatment strategies or take advantage of free cooling possibilities by controlling ventilation.

The following graph shows the impact, in terms of consumption, of different ventilation flow rates and the use of heat recovery units in a residential building located in Madrid, a D3 climate with a heating degree-day (HDD18) of 2225 and a cooling degree-day (CDD25) of 175:

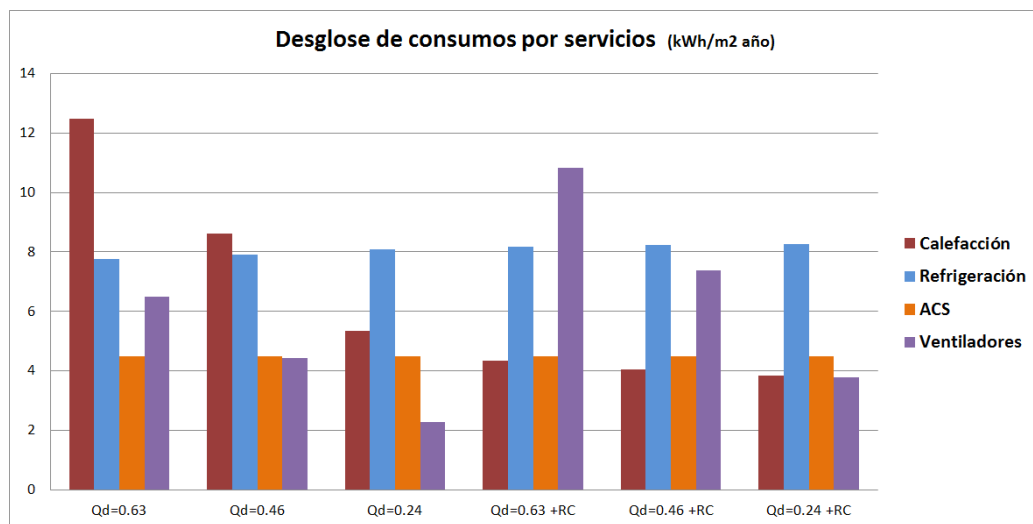


Figure 1: Graph of analysis of energy consumption broken down by services for a residential building in Madrid (D3 climate zone). Qd: Design flow rate; RC: Heat recovery unit.

3.1.2 Evolution of ventilation-related requirements

Due to the significant impact on the building's energy performance of air exchange with the outside, partly derived from ventilation requirements, it is of vital importance to adjust and control the associated consumptions.

In this line, in the evolution of the CTE DB-HE, work is being done on several fronts:

1. Adjustment of ventilation flow rates and use of demand-controlled ventilation systems;
2. Improving the airtightness treatment of the thermal envelope and the use of heat recovery systems and other ventilation techniques.
3. Ventilation systems and retrofitting

3.2 Adjustment of ventilation flow rates

3.2.1 Discrepancies in the calculation of ventilation flow rates

In the Technical Building Code [5] the energy model and the air quality model do not agree exactly in relation to the flow rates considered since:

- There are differences between the volume of the habitable premises considered for air quality purposes (CTE DB-HS / RITE) with respect to the volume of the thermal envelope of the CTE DB-HE: within the thermal envelope there may be distribution spaces, lobbies, technical rooms, etc... that are not part of the dwellings, which normally have lower ventilation needs and, although their ventilation needs should be taken into account in a differentiated manner, the reality is that they are usually assimilated to the flow rates required for the living areas, not always ensuring the same, and increasing the ventilation flow rate of the building for the purposes of the energy calculation.
- There are also differences in the use scenarios: the design flow rate for air quality control is set in relation to the maximum required flow rate and this is usually transferred mechanically as the representative average flow rate, again increasing the ventilation flow rate in the energy calculation.

As a result, unnecessarily high levels of existing ventilation flow rates are often used for energy modeling, which tend to overestimate both the energy impact of such service and the potential savings derived from its control without any benefit in terms of air quality.

It seems necessary to make progress in clarifying the calculation of ventilation flow rates to be used in the energy calculation and their relationship with those derived from air quality requirements.

3.2.2 Demand-controlled ventilation systems

Both CTE DB-HS and RITE establish their ventilation requirements to ensure the indoor air quality of buildings in performance terms, using CO₂ as the main indicator, so that a precise adjustment of ventilation needs can be reflected in better energy performance.

In recent years there has been a popularization and cheapening of ventilation equipment capable of adjusting effective ventilation levels to specific needs at any given time depending on occupancy levels or some pollutants, ensuring more reliable indoor air quality, making such a ventilation strategy feasible in more and more cases.

However, it is still relatively common that design flow rates derived from constant ventilation flow systems are still considered in the energy calculation. The use of demand-

controlled ventilation systems can be expected to play an important role in reducing energy requirements in buildings and there is a need to clarify how they should be considered for energy calculation purposes, especially in less complex buildings and with simplified assessment tools.

3.3 Improved airtightness treatment

3.3.1 Air tightness of the thermal envelope as an energy efficiency strategy

As can be seen in the table, the air tightness values of the thermal envelope currently applied to new residential buildings are not particularly demanding. However, they have served to put on the agenda of the sector's technicians the importance of this parameter in controlling energy demand and avoiding the risk of undesirable infiltration levels from the comfort point of view.

Table of air permeability requirements (n_{50}) for new residential buildings of more than 120m² of DB-HE1

Tabla 3.1.3.b-HE1 Valor límite de la relación del cambio de aire con una presión de 50 Pa,

Compacidad V/A [m ³ /m ²]	n_{50} [h ⁻¹]	
	n_{50}	
V/A ≤ 2	6	
V/A ≥ 4	3	

Los valores límite de las *compacidades* intermedias ($2 < V/A < 4$) se obtienen por interpolación.

An important issue to take into account is that, in mild climates, as is the case in much of Spain, with a reduced thermal gap between indoors and outdoors, the energy performance of more demanding levels of air tightness may be low and its interest will depend on other aspects such as the characteristics of the ventilation system, passive strategies used, etc.

While a higher level of infiltration is, in principle, favorable in terms of air quality, an excessive level is detrimental in terms of comfort and results in an unreliable supply of outside air. Moreover, in many climates, this uncontrolled air supply does not ensure minimum indoor air quality levels while maintaining a significant impact on the energy balance.

On the other hand, for the sake of energy efficiency, we must assess the potential risks associated with the lack of air permeability of buildings taking into account that, especially in residential buildings, the level of maintenance of facilities is very poor and entrusting the entire indoor air quality to increasingly complex technical systems in operation and maintenance may be questionable.

Thus, we believe that the indiscriminate tightening of the regulatory levels of airtightness of the building envelope is not advisable, having to evaluate the cases in which it is an appropriate strategy, but it seems necessary to improve the control of air permeability in some conflictive points of the envelope (passages of facilities, meeting of holes and walls, recessed boxes of facilities, etc ...) setting the obligation to adopt specific construction practices of detail in the execution of these elements, in order to minimize the problems of discomfort.

3.3.2 Use of exhaust air heat recovery systems

The reduction in regulatory levels of energy demand has made the advantages of reducing infiltration levels, to reduce the total air exchange with the outside, and the use of exhaust air heat recovery systems, to avoid energy losses due to air exchange, more interesting in

terms of economic and energy efficiency. In many climates this is already an essential strategy.

When using exhaust air heat recovery it is very important to reduce infiltration levels to guarantee the energy efficiency of the heat recovery, to ensure that there is no significant air exchange outside the recovery equipment.

Although all equipment already includes thermal bypass systems and current regulations provide for their availability, we must remember that, in many climates and for many conditions of use, this is a key aspect of the operation of a ventilation system with heat recovery, at the risk of worsening the energy performance.

It would therefore be advisable to tighten the airtightness conditions in cases where heat recovery systems are used.

3.3.3 Other ventilation-based energy efficiency strategies

The need to ensure indoor air quality requires, in almost all cases, the use of technical systems capable of ensuring such performance.

In addition to heat recovery, other ventilation techniques such as free cooling, the use of thermal bypass in the presence of recuperators, etc. also play a relevant role and, although we believe that their regulatory treatment is, in general, adequate, it is probably necessary to improve their knowledge on the part of technicians and facilitate their integration into energy calculation tools.

3.4 Ventilation and building renovation

The energy rehabilitation of residential buildings involves, in a large number of cases, the replacement of windows with higher quality carpentry and glazing, and also a lower air permeability. This often implies a reduction in the air quality of these residential spaces when it depends on infiltration, for example, in the absence of mechanical ventilation systems.

In the case of tertiary buildings, as a result of the requirements derived from the COVID-19 pandemic in relation to ventilation needs or as a result of interventions aimed at improving energy efficiency, there is often the introduction of mechanical ventilation systems, in many cases previously non-existent, including in many cases a system for heat recovery from the exhaust air.

In both cases, the need to address simultaneously and in an integrated manner the energy and indoor air quality aspects is evident, making both requirements compatible, which can serve respectively as levers to improve both performances.

Given the specific characteristics of building retrofitting, it is probably necessary to improve the knowledge of best practices and available alternatives through application guides and other tools, in order to facilitate the successful resolution of interventions and to take advantage of the opportunities they offer.

4 CONCLUSIONS

In high efficiency buildings, the consumption linked to air transport and ventilation systems is significant and comparable to that of other services, so it is essential to advance along lines of adjustment of the required flow rates, facilitate the incorporation of new technologies when appropriate, improve the efficiency of existing systems and promote best practices. Air quality and ventilation technologies are closely linked to achieving the goal of climate change mitigation and must be addressed in an integrated manner, paying special attention to building renovation.

5 REFERENCES

[1] Proposal for a Directive of the European Parliament and of the Council on the Energy Performance of Buildings (recast) (2021) (<https://eur-lex.europa.eu/legal-content/EN/TXT/?uri=CELEX%3A52021PC0802>)

[2] Communication from the Commission to the European Parliament, the European Council, the Council, the European Economic and Social Committee and the Committee of Regions. The European Green Deal (<https://eur-lex.europa.eu/legal-content/EN/TXT/?uri=COM%3A2019%3A640%3AFIN>)

[3] Proposal for a Directive of the European Parliament and of the Council on energy performance (recast) (<https://eur-lex.europa.eu/legal-content/ES/TXT/?uri=CELEX:52021PC0558>)

[4] Directive (EU) 2018/2001 of the European Parliament and of the Council of 11 December 2018 on the promotion of the use of energy from renewable sources (<https://eur-lex.europa.eu/legal-content/ES/TXT/?uri=celex%3A32018L2001>)

[5] [Royal Decree 314/2006](#), of 17 march, Spanish Technical Building Code, Basic Document on Energy Saving (DB-HE) (<https://www.boe.es/boe/dias/2006/03/28/pdfs/A11816-11831.pdf>)

[6] UNE-EN ISO 52000-1:2019 Overall assessment of the energy performance of buildings. Part 1: general framework and procedures (<https://www.une.org/encuentra-tu-norma/busca-tu-norma/norma?c=N0061777>).

[7] [Royal Decree 390/2021](#), of 1 june, approving the basic procedure for the certification of the energy performance of buildings (<https://www.boe.es/buscar/act.php?id=BOE-A-2021-9176>)

[8] 2020 Update of the Long-term Strategy for the Energy Rehabilitation of the Building Sector in Spain. (ERESEE) (https://www.mitma.gob.es/recursos_mfom/paginabasica/recursos/es_ltrs_2020.pdf)

[9] EN 15978:2011. *Sustainability in construction. Assessment of the environmental performance of buildings. Calculation methods* (<https://www.une.org/encuentra-tu-norma/busca-tu-norma/norma?c=N0049397>)

Ventilation behaviour of occupants driven by outdoor temperature: 12 case studies

Sonia Garcia-Ortega*^{1,2}, Pilar Linares-Alemparte²

*1 Universidad Politécnica de Madrid
Juan XXIII St.
Madrid, Spain*

*2 Instituto de las ciencias de la construcción Eduardo
Torroja-CSIC
4, Serrano Galvache St.
Madrid, Spain*

**Corresponding author: soniag@ietcc.csic.es*

ABSTRACT

This paper presents the results of an Indoor Environment Quality (IEQ) monitoring study (including relative humidity, temperature and IAQ in terms of indoor CO₂) in naturally ventilated dwellings (mainly based on vertical shafts and infiltrations) and the analysis of the data obtained. The aim of the study is to identify patterns that relate occupants' ventilation behaviour to outdoor temperature and to increase knowledge of occupant's perceptions of IEQ. The results could be used to improve ventilation models and building regulations.

The monitoring was conducted in 12 apartments located in Madrid, Spain, with a cold semi-arid climate, over different periods ranging from 15 to 21 days. Occupants completed surveys providing information on their habits, occupancy patterns, ventilation operations and subjective perception of IEQ.

According to the results, occupant behaviour is strongly influenced by outdoor temperature and could reverse the expected performance of the ventilation system. This influence could be significant enough to be used as a driving variable for a method of modelling human ventilation behaviour.

KEYWORDS

Natural ventilation; Occupant behaviour; Dwellings; Indoor air quality; CO₂.

1 INTRODUCTION

The traditional way of ventilating dwellings in Spain was by natural ventilation based on the operation of windows and high levels of infiltration through the building envelope, particularly through windows and window-wall joints. In the middle of the last century, the use of vertical ventilation shafts in wet rooms of dwellings became widespread and is currently the most common ventilation system in existing dwellings. This dedicated ventilation system involves the removal of stale air from wet rooms, the circulation of air from dry rooms to wet rooms and the supply of fresh outdoor air to dry rooms by infiltration. Passive stack ventilation extracts stale air from wet rooms by thermal buoyancy (temperature difference between outdoor and indoor) and Venturi effect. Since 2006, the Spanish IAQ regulation DB HS3, *Código Técnico de la Edificación* (MITMA, 2019) establishes that the reinforcement of natural ventilation with a mechanical fan is mandatory in new dwellings. However, the performance of such ventilation system can be influenced by human behaviour. It is known that occupant behaviour is one of the most important drivers of IAQ, with studies monitoring specific actions such as opening windows or room doors (Calí et al, 2016; Fan et al, 2022; Liao et al, 2022; Navas-Martín, 2023).

It would be very useful to know, on the one hand, the real IEQ of occupied dwellings where occupants modify the operation of ventilation systems. On the other hand, it would be useful to identify parameters that help predict IEQ when it is influenced by the occupants' behaviour. This paper presents the results of the monitoring and analysis of 12 dwellings that are representative of the current Spanish residential building stock. It was found that outdoor temperature is the main factor influencing the ventilation behaviour of occupants, altering the efficiency of the ventilation systems installed in dwellings.

2 METHODOLOGY

In order to focus the scope of the study on a representative sample of the current Spanish residential building stock, dwellings were selected according to the criteria of Garcia-Ortega (Garcia-Ortega, Linares-Alemparte, 2015), based on data from the National Statistics Institute (INE, 2013) on the number of occupants, living area and number of bathrooms. All of the dwellings were apartments in high-rise residential buildings, located in an integrated urban environment, in the southern plateau of the Iberian Peninsula (city of Madrid) (see Figure 1). Their ventilation systems were mainly based on natural ventilation, including occupant-driven ventilation. The façades were traditional brick masonry cavity walls with thermal insulation.



Figure 1 - Location of the monitored dwellings (black dots) and meteorological stations (red dots: belonging to the Spanish Meteorological Agency; blue dot: belonging to Madrid City Council)

A total of 42 different rooms belonging to 12 dwellings were monitored (see Table 1). Most of the rooms were monitored twice: once in summer and once in winter, with a total of 72 measurements between December 6th, 2017 and March 9th, 2020. All dwellings were occupied during the monitoring and characterisation phase.

Table 1 – Monitored dwellings

Dwelling code	Year of construction (or main retrofit)	Year/month of measurements	Vertical shafts	Permeability of envelope	Number of occupants	Occupant's behaviour patterns (general surveys)
01	1986 (2014)	17/12 18/06	Yes	low	2	Open windows 5' in the morning
02	2000	18/07	Yes	high	4	Open windows in function of outdoor temperature and thermal comfort

03	1956 (2000)	18/07	No	medium	2	Open windows 5' in the morning; all night in summer
04	1960 (2016)	18/07 19/01	Yes	low	4	Open windows for a few minutes in the morning and afternoon. Open the windows a lot in summer
05	1987	18/07 19/12	Yes	high	2	Open windows 10 - 60' in the morning; all night in summer
06	1991	18/08 18/12	Yes	high	4	No specific habits
07	1970	18/08 20/03	Yes	medium	2	Open windows in the morning. In leaving room: open window all the day except in winter (in winter only open at night)
08	1963	18/08 19/02	Yes	medium	2	No specific habits
09	1956	18/09 18/11 19/02	No	medium	1	Open the bathroom window after showering, open other windows when feel it is necessary, usually once a day
10	1982	18/09 19/01	Yes	high	2	Open windows 10' in the morning; in summer leave a small opening all day, and total open window at night
11	1960	18/09 19/03	Yes	low	4	Open windows 5-10' in the morning
12	2011	18/10	Yes	low	1	No specific habits

The Köppen or Köppen-Geiger climate classification is BSk: Dry, Semi-Arid or steppe, Cold climate. In BSk climate, winters are cold or very cold, and summers can be mild or hot. Rainfall is low. It could also be considered as a continental climate. It can be found in temperate latitudes and far from the sea, such as in inland North America or the steppes of Central Asia.

CO₂ concentration, relative humidity (%) and temperature (°C) were monitored and recorded at 5-minute intervals using Rotronic CP-011 and Wöhler CDL 210 sensors and data loggers. These monitors were placed in dry rooms, mainly bedrooms and living rooms. In some dwellings, wet rooms (kitchens and bathrooms) were also monitored. The display screens were hidden so as not to influence the occupant's behaviour.

Integrated radon measurements (Bq/m³) were also carried out in potentially problematic premises, but no significant concentrations were detected.

The correct operation of the shafts was checked using an anemometer and a capture hood model PCE-VA.

All the collected data were subjected to an analysis process to eliminate possible measurement or collection errors.

Meteorological data were obtained from stations 3195 and 3194U of the Spanish Meteorological Agency (AEMET) and from station 28079102 of the Integrated Air Quality System of Madrid City Council (Ayuntamiento de Madrid) (see locations in Figure 1):

- Air temperature: hourly and average per day (°C).
- Relative humidity: hourly and average per day (%).
- Wind speed: average per day and gust (m/s).

General surveys were conducted to identify occupant's behaviour patterns and motives that could lead occupants to deliberately alter the operation of the ventilation system. In some cases,

a short-period survey was conducted, in which recent and detailed information on ventilation operations was collected.

Parameters related to the occupants, ventilation systems, construction factors and dwellings layout were also characterised. Occupant behaviour was analysed in relation to indoor CO₂, outdoor and indoor temperatures, indoor relative humidity and average wind speed and gust. Statistical analysis was performed using R Software Version 4.2.0 (R Core Team, 2022).

3 RESULTS AND DISCUSSION

83% of the analysed dwellings have natural ventilation systems with exhaust shafts located in wet rooms in addition to infiltration through the building envelope. The rest of the dwellings have natural ventilation based just on infiltration through the building envelope.

Meteorological variables such as outdoor temperature, atmospheric pressure and wind would be expected to be the most relevant driving variables and to have the strongest influence on the efficiency of natural ventilation and consequently on the indoor CO₂ concentration.

However, this is not reflected in the monitored CO₂ results.

According to the temperatures recorded (see Figure 2), which show an important indoor/outdoor temperature gradient in winter, stack passive ventilation due to thermal buoyancy should properly perform in this season.

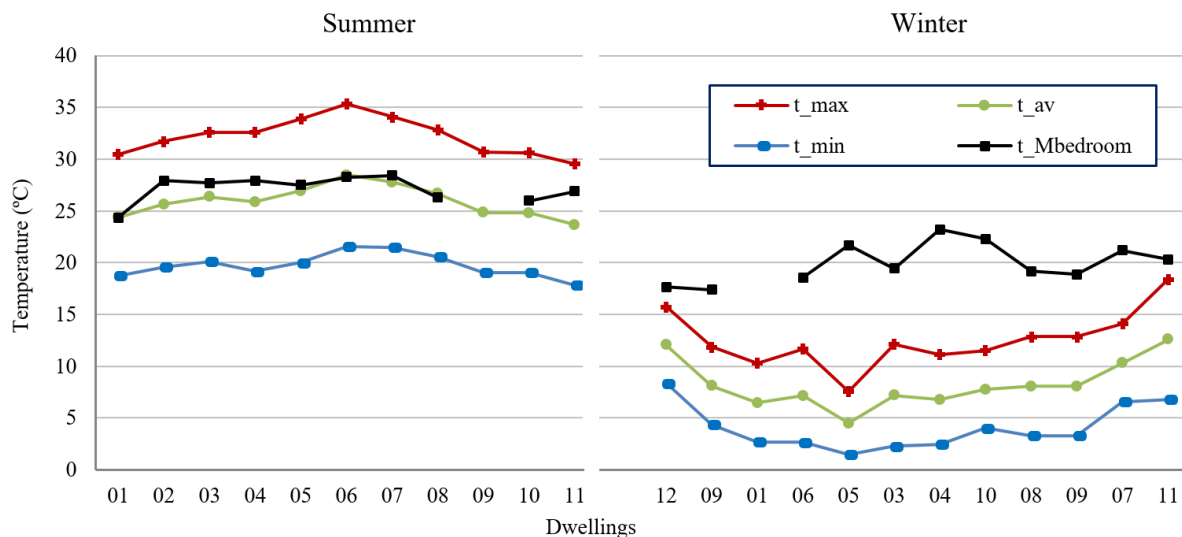


Figure 2 – Average outdoor temperatures recorded during the measurement periods for each dwelling at Station 3194U: t_{max}: of the daily maximum, t_{av}: of the daily average, t_{min}: of the daily minimum; and daily average of indoor temperature in master bedroom. Dwellings are sorted by month of measurement.

This would lead us to expect a higher ventilation rate (and lower concentration of CO₂) in winter. However, the opposite occurred: monitored data showed a significant increase in CO₂ concentration in all rooms in winter compared to the concentration in summer. Average CO₂ concentration for each room within dwellings 01 to 12 is shown in Figure 3. Basic statistics of average concentration of CO₂, number of occupants and living area per occupant are shown in Table 2.

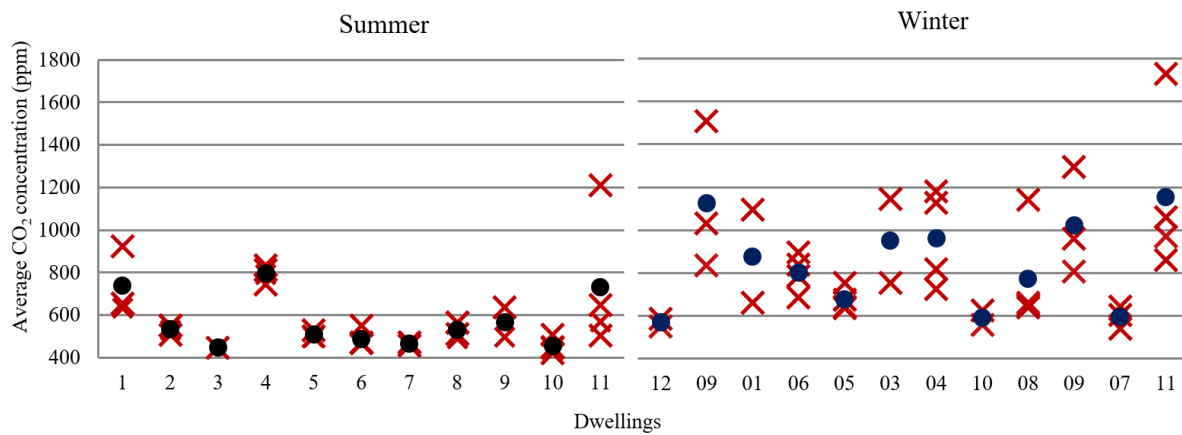


Figure 3 - Average CO₂ concentration. Red cross: for each room within dwellings 01 to 12. Black dot: per dwelling. Dwellings are displayed in the chronological ordered by month of the measurements.

Table 2 – Basis statistics of number of occupants, average concentration of CO₂ and living area per occupant.

Variable	Min.	1 st Qu.	Median	Mean	3 rd Qu.	Max.
Number of occupants per dwelling	1	2	2	2	4	4
Living area per occupant (m ² /occ) per dwelling	16.75	25.00	28.25	40.24	60.00	75.00
Average CO ₂ concentration (ppm) per room	420	508.8	639	711.4	820.8	1729

Wind and atmospheric pressure are usually recognised as other main drivers of natural ventilation. However, the analysis of the measured hourly values of wind and pressure difference between indoors and outdoors showed no correlation with concentration of CO₂ or HR. The average values of wind and atmospheric pressure over the measurement periods can be seen in Figure 4.

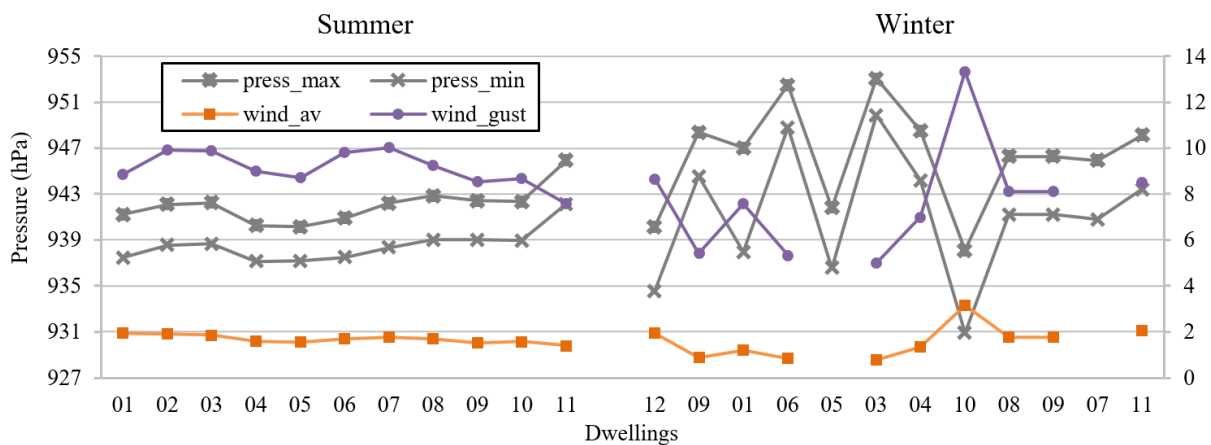


Figure 4 - Averages of the daily maximum and minimum outdoor pressure, wind and wind gust recorded during the measurement periods for each dwelling, Station 3194U. Dwellings are sorted by month of measurement.

An example of the case with the strongest wind and wind gust that occurred during the measurement of dwelling 10 can be seen in Figure 5. The highest wind speed occurred in the afternoon of January 23rd, and remained around average values during the night and the following day. However, no significant influence on the indoor CO₂ or HR concentration is observed.

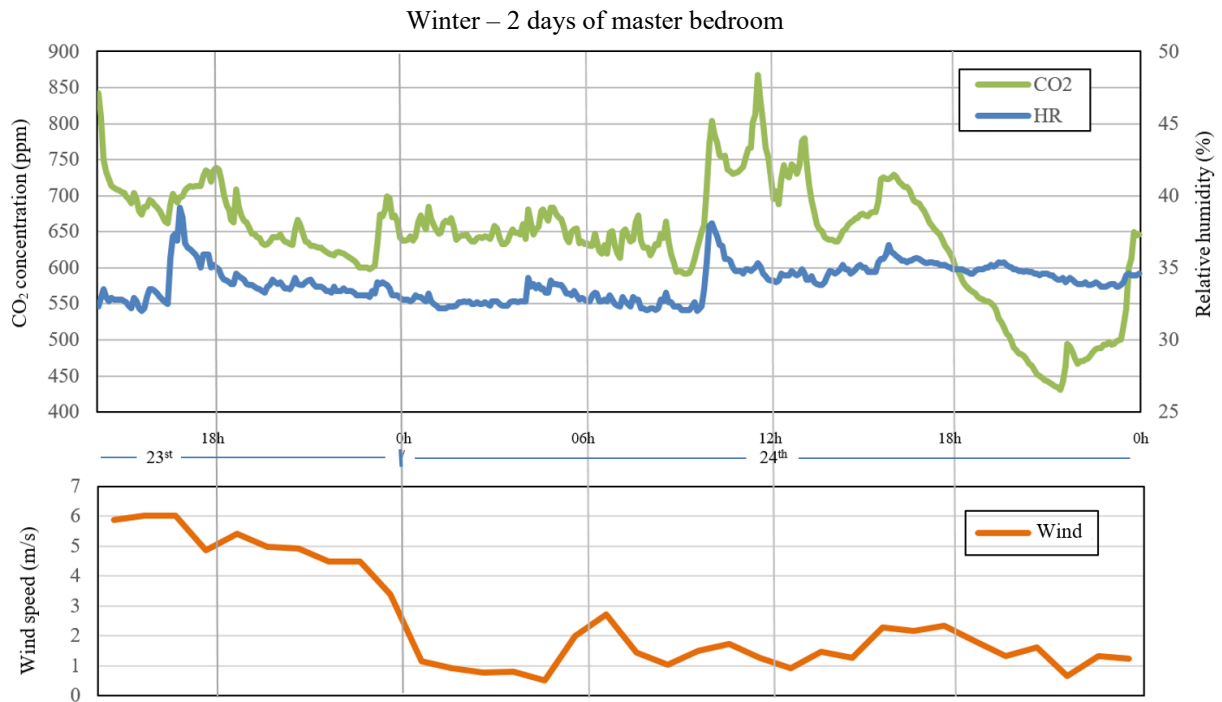


Figure 5 - CO₂ concentration and indoor temperature in the master bedroom of dwelling 10. – Data from January 23rd to 24th 2018

After this, it was assumed that other variables may have been interfering onto CO₂ concentration values, such as the behaviour of the occupants.

Some data of dwelling 01 are displayed in Figure 6 to Figure 9 and discussed below. The results are common to the rest of the case studies.

Figure 6 shows the change in occupant behaviour between June 18th and 23rd in the master bedroom with the arrival of summer and the increase in outdoor temperatures. In particular, the minimum outdoor temperatures (see Figure 7) increased by almost 7°C during this period. Due to the increase in outdoor temperatures, the indoor temperatures also increased. After reaching an indoor temperature of 27.4°C on the night of the 21st, in the short-period survey the occupants reported keeping the interior doors completely open and some windows open for long periods, including at night, thus reducing the CO₂ concentration. No clear influence of other variables such as wind was observed (see Figure 7).

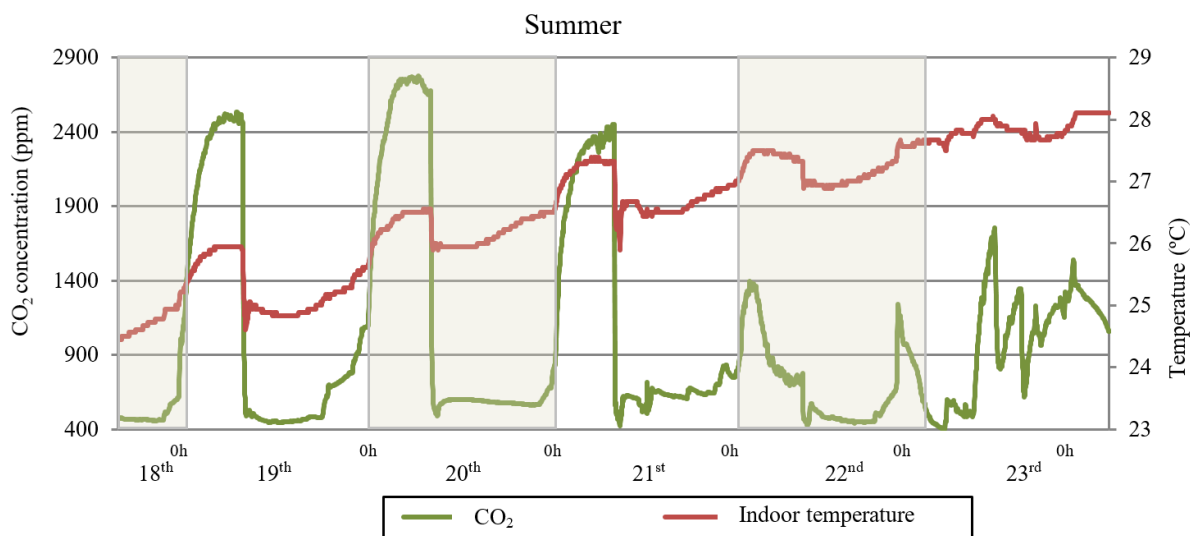


Figure 6 - CO₂ concentration and indoor temperature in the master bedroom of dwelling 01. – Data from June 18th to 23rd 2018

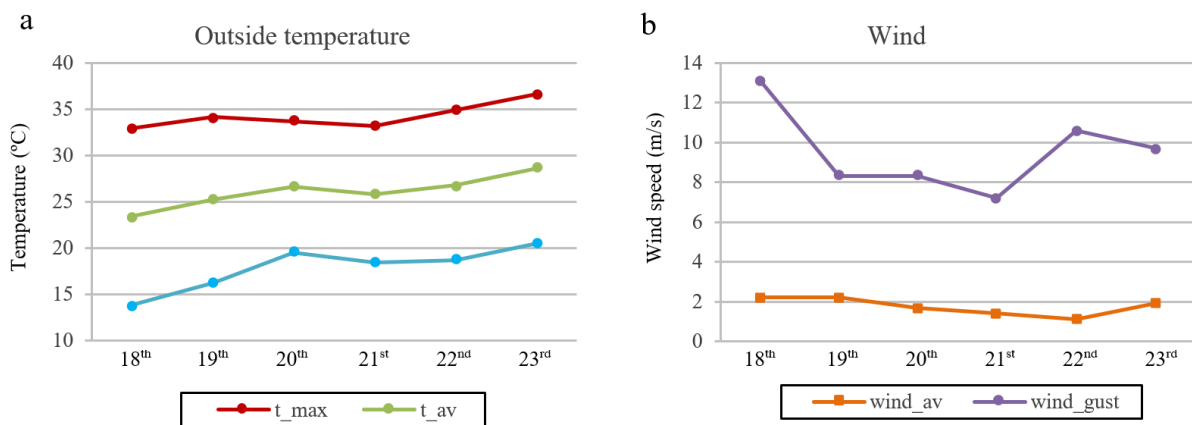


Figure 7 - a – Daily outdoor temperature: maximum, average and minimum. b – Daily wind average and wind gust. – Data from June 18th to 23rd 2018

Figure 8 shows the CO₂ concentrations measured between December 6th and 9th in the same master bedroom as in Figures 6 and 7. The occupants reported leaving the bedroom door open during the nights. However, in the short-period survey, they reported that the door was kept closed on the night from the 6th to the 7th. This resulted in a large increase in CO₂ concentration, greater than the effects derived from the other studied parameters. In addition to this, on the 7th, 8th and 9th, the occupants opened the bedroom window when they got up, which caused a rapid decrease in the concentration of CO₂ and humidity. On the 6th, however, they did not open the bedroom window in the morning, so the room was ventilated more slowly just through infiltration and stack ventilation.

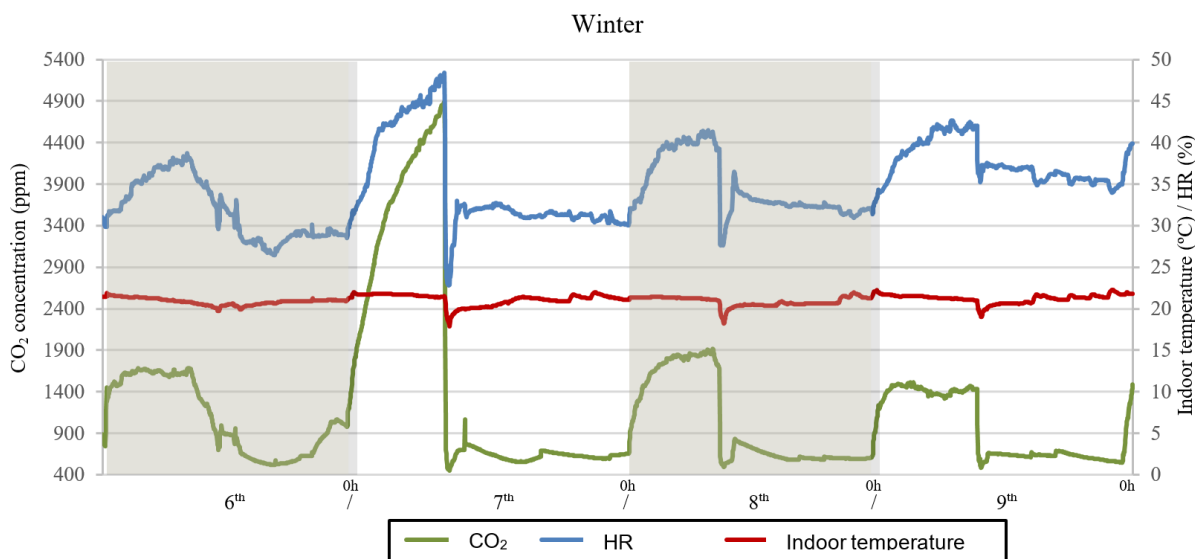


Figure 8 - CO₂ concentration, relative humidity and indoor temperature recorded in the master bedroom of dwelling 01. – Data from December 6th to 9th 2017

In Figure 9 it can be seen that on the 6th and the 7th the lowest temperatures are reached, below zero, changing the ventilation pattern of the occupants during the night of the 6th and producing the highest CO₂ concentration. The wind which occurs on the 9th (see Figure 10), does not seem to have a clear influence on the ventilation pattern neither the IAQ.

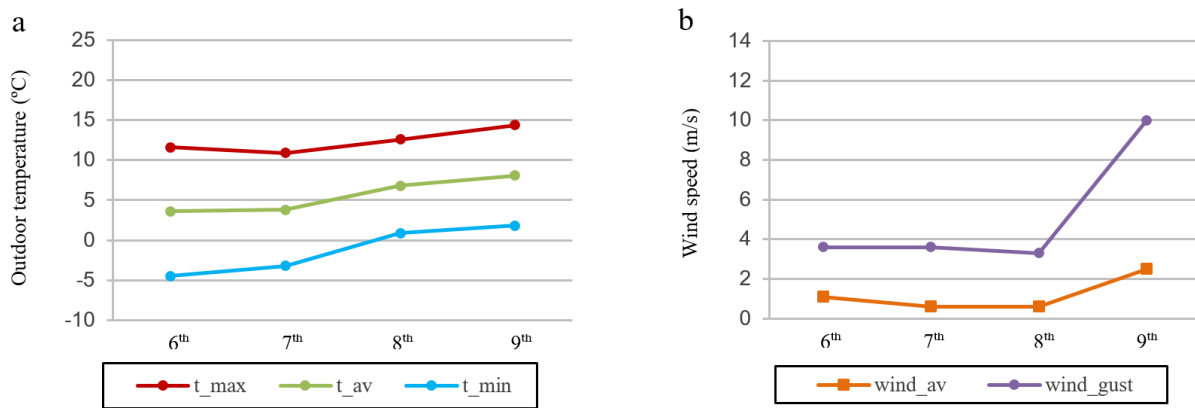


Figure 9 - a – Daily outdoor temperature: maximum, average and minimum. b – Daily wind average and wind gust. – Data from December 6th to 9th 2017

This relationship between the concentration of CO₂ and outdoor temperatures can be observed in all the monitored rooms. In view of the above analysis, it is assumed that this is due to the behaviour of the occupants.

The behaviour of the occupants in relation to the outdoor temperature seems to be behind the reversal of the expected effect of the meteorological variables on the efficiency of the ventilation systems. The occupants hinder the operation of the ventilation system in winter by closing doors, making it difficult for air to flow from the dry rooms to the wet rooms, whereas in summer they favour ventilation by opening windows and doors.

General surveys reveal a ventilation pattern based on opening the windows for 5 to 10 minutes in the morning and keeping them closed the rest of the time. Occupants tend to keep the windows open for longer periods when it is hot, not for ventilating but for providing thermal comfort.

However, when the ventilation patterns of the general surveys are contrasted against the monitored CO₂ concentration data, contradictions are found.

Only when occupants report their recent behaviour in the short-period surveys, on the same day or the day before, ventilation operations and recorded CO₂ match.

According to the surveys and monitored data, the most relevant driving variable influencing ventilation habits of the occupants is the outdoor temperature: Higher outdoor temperatures in summer cause an increase in indoor temperature, and would lead occupants to adopt behaviours such as leaving windows open for long periods, particularly at night, to cool down their homes, indirectly improving IAQ. In contrast, lower winter temperatures would lead them to keep windows and doors closed for longer periods. These results are in line with the global expectations, but they far exceed them: the influence of outdoor temperature in IEQ through occupant behaviour enhances the expected performance of the ventilation system.

In order to improve ventilation models, outdoor temperature could be used as a form of prediction of occupant behaviour.

Figure 10 shows CO₂ concentrations for different types of rooms in winter and summer.

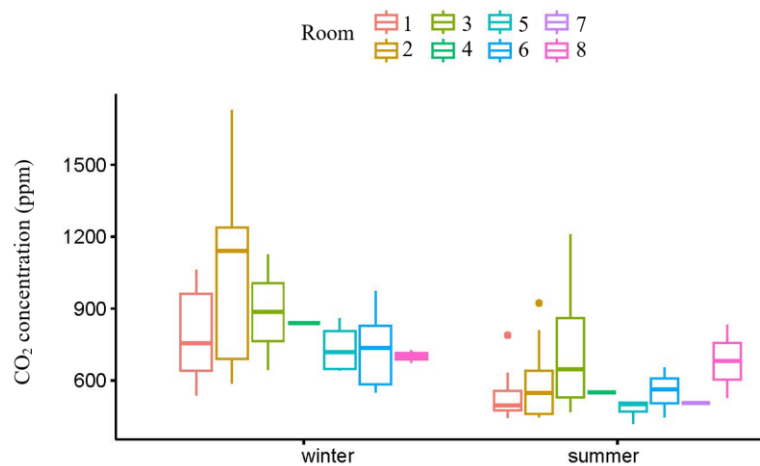


Figure 10 – Boxplot of average concentration of CO₂ per type of room in winter and in summer. Rooms: 1: Living/dining room; 2: Master bedroom, 3: 2nd Bedroom; 4: 3rd Bedroom; 6: Kitchen; 8: Bathroom; 9: 2nd bathroom; 10: Other room, e.g. a Home office or Studio

The motives of the occupants for ventilation, based on (Emmerich, 2001), are:

- IAQ control, by diluting pollutants through the introduction of fresh outdoor air;
- Cooling of overheated rooms, by introducing cooler outdoor air;
- Modifying thermal sensation, by creating a draught;
- Cooling overheated rooms at night by introducing cooler night air during hot periods.

According to the results of this study, the motivations of the occupants include thermal comfort, but not the control of IAQ reported by other authors, at least when IAQ is expressed as a function of CO₂ concentration at usual levels.

4 CONCLUSIONS

The main driver of occupant behaviour in terms of actions that can modify ventilation rates and IAQ (such as window and door operation) seems to be thermal comfort rather than IAQ control itself, at least when expressed as a function of CO₂ concentration. For practical purposes and statistical analysis, occupant behaviour in relation to IAQ could be considered as a function of average outdoor temperature.

Unfortunately, occupant behaviour is not easily captured by general surveys. This leads to doubts about the representativeness of general surveys. Only short-period surveys in which recent and detailed operation is gathered can be taken into account, deriving into further representability.

These observations may be useful to model the expected occupant ventilation behaviour in dwellings based on easily obtained variables such as outdoor temperature. This model is necessary to establish the basis and guidelines for specific retrofit policies, initiatives, regulations, etc. for naturally ventilated dwellings.

However, the results of the analysis could be extrapolated only to cases in the studied climate, with the same cultural background in relation to ventilation behaviour and with similar ventilation systems. Further research should be conducted to test the results in other climate areas and/or with other types of natural ventilation systems.

The data reported by the occupants suggest that they modify the infiltration of the dwelling during the winter in order to avoid heat losses due to the infiltration of cold air. An approach to characterisation is left for a later study.

5 ACKNOWLEDGEMENTS

We would like to thank the kind occupants and owners of dwellings who allowed us to monitor their homes in order to carry out these studies.

6 REFERENCES

AEMET. *AEMET OpenData* - Agencia Estatal de Meteorología.

Ayuntamiento de Madrid. *Conjuntos de datos - Portal de datos abiertos del Ayuntamiento de Madrid*. Sistema Integral de la Calidad del Aire del Ayuntamiento de Madrid. Portal de Datos Abiertos del Ayuntamiento de Madrid.

Cali, D.; Andersen, R. K.; Müller, D.; and Olesen, B. W. (2016). *Analysis of occupants' behavior related to the use of windows in German households*, Building and Environment, vol. 103, pp. 54–69. Doi: 10.1016/j.buildenv.2016.03.024.

Emmerich, S., Dols, W. and Axley, J. (2001). *Natural Ventilation Review and Plan for Design and Analysis Tools*. National Inst. Stand. Technol. [Online]. Available: https://www.researchgate.net/publication/239538858_Natural_Ventilation_Review_and_Plan_for_Design_and_Analysis_Tools#fullTextFileContent[accessed Mar 06 2023].

Fan, X. et al. (2022). *A field intervention study of the effects of window and door opening on bedroom IAQ, sleep quality, and next-day cognitive performance*. Building and Environment, vol. 225, p. 109630. Doi: 10.1016/j.buildenv.2022.109630.

INE (2013). *Censos de Población y Viviendas 2011*. INEbase / Demografía y población / Cifras de población y censos demográficos / Censos de Población y Viviendas 2011. Accessed: Dec. 12, 2016. [Online]. Available: http://www.ine.es/censos2011_datos/cen11_datos_inicio.htm

Liao, C. et al. (2022). *A cross-sectional field study of bedroom ventilation and sleep quality in Denmark during the heating season*. Building and Environment, vol. 224, p. 109557. Doi: 10.1016/j.buildenv.2022.109557.

MITMA - Ministerio de Transporte, Movilidad y Agenda Urbana (2019). *Documento Básico HS Salubridad. Sección HS 3: Calidad del aire interior*. Código Técnico de la Edificación, Gobierno de España. Accessed: Mar. 01, 2023. [Online]. Available: <https://www.codigotecnico.org/pdf/Documentos/HS/DBHS.pdf>

Navas-Martín, M. Á. and Cuerdo-Vilches, T. (2023). *Natural ventilation as a healthy habit during the first wave of the COVID-19 pandemic: An analysis of the frequency of window opening in Spanish homes*. Journal of Building Engineering, vol. 65, p. 105649. Doi: 10.1016/j.job.2022.105649.

R Core Team (2022). *R: A language and environment for statistical computing*. R Foundation for Statistical Computing, Vienna, Austria. [Online]. Available: <https://www.R-project.org/>

Indoor air quality in Austrian classrooms – Assessing different ventilation strategies with a citizen science approach

Simon Beck^{*1}, Gabriel Rojas¹, Elena Krois²,
Sebastian Goreth², and Christian Hechenberger²

*1 University of Innsbruck and Digital Science Center
Innrain 52
6020 Innsbruck, Austria*

*2 University College of Teacher Education Tyrol
Pastorstraße 7
6010 Innsbruck, Austria*

**Corresponding author: simon.beck@uibk.ac.at*

ABSTRACT

With many existing Austrian school buildings to be renovated in the coming years, there are debates between stakeholders, about which ventilation strategy to pursue in existing schools. Therefore, different intervention strategies such as retrofitting ventilation systems, installing CO₂-monitoring signals, or raising awareness among teachers and students should be evaluated. This paper presents the preliminary results of the project “DIGIdat” on air quality measurements in the first quarter of 2023. The “as-is” indoor air quality situation in 36 classrooms in western Austria is assessed by comparing results between different classrooms and ventilation types. To gather information on indoor air quality, data is collected using multiple low-cost air sensors per classroom that are programmed and maintained by the students under scientific supervision. The citizen science approach helps to overcome the spatial barrier between the scientists and the measurement sites, with students being “responsible” for the continuous operation of their sensor kit. Altogether 15 sensor kits, distributed over three to four classrooms, are installed in each of the ten participating schools. The sensors measure CO₂-, fine particulate matter (PM), and volatile organic compounds (VOC) concentration as well as temperature and humidity. The sensor kits were positioned and started recording after finishing programming workshops, i.e., in January and February 2023 for most schools. Statistical analysis of the measured data (with varying sample size of approx. 10 to 20 thousand five-minute averages per category) was carried out utilizing the Welch t-Test and Mann-Whitney-U-Test for differences between window airing and ventilation systems. Significantly higher CO₂ and PM_{2.5} values were found with window airing compared to ventilation systems. Somewhat less significantly, humidity was also higher in classes with natural ventilation than with mechanical ventilation. In addition to that, a correlation analysis showed a dependency between average CO₂-levels in window-ventilated classrooms and average outside temperature, whereas this was not the case with classrooms equipped with ventilation systems. The same analysis comparing inside and outside PM_{2.5} concentrations showed also the mechanically ventilated classrooms have, probably due to fine particulate filters, lower ratios of fine particulate matter between inside and outside. Boxplots and correlation regression lines confirm graphically the data analysis results and highlight the conclusions.

KEYWORDS

Indoor Air Quality, Schools, Carbon Dioxide, Ventilation, Data Analysis

1 INTRODUCTION

In densely occupied rooms ensuring adequate indoor air quality, particularly in classrooms, can prove challenging. To address this issue and quantify its effects, the project "DIGIdat" was initiated. Currently, the authors are not aware of monitoring studies that investigated long-term air quality surveys in Tyrolean (Austria) schools. Therefore, it is crucial to determine the status quo and the effects of various interventions on indoor climate and air quality, especially considering that many schools are due for renovation and adaptation to meet new legal standards. This paper presents preliminary results from the first three months of data collection in participating schools.

"DIGIdat" is a citizen science project, with different stakeholders supporting the procedures and pupils from the investigated schools participating in the data collection and maintenance of sensors. The pupils are actively taking part in the scientific process as they help work out solutions and collect data. As it is difficult to maintain good information exchange with all of the children, the discussions and project contents are carried out in two workshops per year, containing an introduction to the topic, programming the sensor-kits, exploring their school building in a rally, and analysing the measured data (see Figure 1). In between the workshops, they take ownership of the sensor kits, meaning each team is responsible for the maintenance and takes regular records of the condition and function of their sensor kit. The second pillar of the citizen science approach is discussing results and possible intervention strategies in a stakeholder workshop including building owners, architects, HVAC designers, health experts, and public authorities.

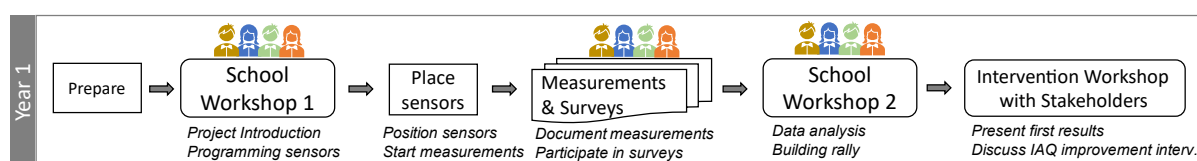


Figure 1: Citizen Science phases during the first year

The measuring instruments, supplied by "senseBox" (senseBox, 2023a), comprise a microcontroller, various air-quality sensors, and a Wi-Fi module. A total of 150 measuring devices gather air-quality data in scheduled one-minute intervals, which are then transmitted live to OpenSenseMap, a platform for publishing and visualizing open environmental sensor data (OpenSenseLab, 2023). Following the as-is situation assessment, the project aims to implement different intervention strategies such as raising awareness, providing CO₂-based warning signals, automatic window openers, and retrofitting mechanical ventilation systems. Comparisons will be drawn between air quality before and after interventions as well as across different classrooms with varying ventilation modes.

2 METHODS

2.1 Collection of data

About 137 of 150 sensor kits were programmed and positioned to measure temperature, humidity, volatile organic compounds (VOC), fine particulate matter (PM), and CO₂-levels. After sensor programming workshops with the pupils, mainly between November 2022 and February 2023, the sensor kits were positioned by the scientific project team in the different classrooms, mainly between December 2022 and March 2023. Therefore, different measurement durations (sample periods) are available for the different schools. The time intervals between measurements were set to one minute to achieve sufficient accuracy without generating unnecessarily large amounts of data. Due to data-transfer problems, the sample interval had to be increased temporarily to four minutes in several schools. With the one-minute time grid, the opening of doors or windows can be recorded well and a steep increase of e.g., the CO₂-levels, can be mapped reasonably accurately. The programming language used for the "senseBox" is a device-associated language based on "Blockly" (Wikipedia, 2019), which then is converted to "Arduino-Code" for compiling (senseBox, 2023b). As long as power supply is given, the devices save the measured data on a built-in memory card as well as load it onto the OpenSenseMap database using the matching API.

2.2 Positioning

About three to four measuring devices were placed in each of the 36 surveyed classrooms. Some schools were partially equipped with ventilation systems. In these cases, an attempt was made to select the classrooms in such a way that an equal number of classrooms with and without mechanical ventilation are represented. An outdoor measuring device was also installed in each participating school. Additional sensors were placed in other rooms, such as teacher conference rooms, computer science rooms, pupil's workshops, and also hallways which are connected to the surveyed classrooms. At least one of the devices in the classrooms and every outdoor device is equipped with a sensor for fine particulate matter.

Measurements are taken at a height of approximately 110 cm, where the main activity is seated work, and at a height of 150 cm, where the main activity is walking or standing. This also meets the recommendations of ISO16000-1 (2004), although the sensors could not be placed off the wall (as also recommended by standards) as they should not interfere with school activity and need to be securely mounted in order to be "child-proof". A highly air-permeable housing for the sensors was developed and 3D-printed as the standard mounting solution. The housings were attached to the wall with double-sided adhesive tape (see Figure 2). No effects on the VOC measurements by possibly outgassing tape glue were observed during respective tests. 110 cm for seated work was chosen to match the head height of seated students. The outdoor sensors were mounted to the exterior wall in a weatherproof place with good exposure to natural air flow while avoiding the direct vicinity of windows and doors, where indoor air could influence the measurement when opened.



Figure 2: Example of mounted measurement device (in 3D-printed housing)

Inside the classrooms, the first measurement device is usually placed on the side of the blackboard, the second on the opposite side of the blackboard, and the third on the inner wall opposite the wall with the most windows. As most of the surveyed classrooms are built in a similar way, the positioning described could be achieved in almost all classrooms. In general, measuring devices were kept as far away as possible from windows, doors, sinks, and other point sources of pollutants. The particulate matter sensor was placed inside the housing according to manufacturer specifications (Sensirion, 2019).

2.3 Sensors

In this study, a set of low-cost sensors is utilized to monitor environmental conditions. The selected sensors include the Bosch BME680, which is capable of measuring temperature, humidity, and air pressure, as well as gas resistance, which is converted into breath-VOC equivalent (b-VOC_{eq}) and a so-called Air Quality Index (not within the scope of this analysis). Additionally, the Sensirion SCD30 sensor was employed, which primarily measures CO₂-levels

but can also record temperature and humidity within the sensor. Lastly, the Sensirion SPS30 sensor was used to measure fine particulate matter in the size categories of PM_{1.0}, PM_{2.5}, and PM_{4.0}. This sensor automatically extrapolates the PM₁₀ values from the other size categories. The sensor properties for b-VOC_{eq}, CO₂, and PM_{2.5} are listed in Table 1.

Table 1: Properties of sensors for b-VOC_{eq}, CO₂, and PM

Sensor	Measurement	Method	Range	Accuracy	Source
BME680	b-VOC _{eq} *	Metal Oxide Semiconductor	0.5 – 1000 ppm**	-	(Bosch Sensortec, 2022)
SCD30	CO ₂	Nondispersive Infrared	400 – 10000 ppm	± 30 ppm	(Sensirion, 2020a)
SPS30	PM _{2.5}	Optical (light scattering)	0 – 1000 µg/m ³	± 10 %	(Sensirion, 2020b)

*calculated from correlation of typical VOCs to gas sensor resistance

**min- and max-output (tested range not available)

2.4 Underlying conditions

The microcontroller and sensors take the measurements inside a 3D-printed housing with an acrylic glass lid (see Figure 2), which both were designed in the scope of this project. Since especially the microcontroller and the Wi-Fi module emit a non-negligible amount of heat, they are placed in a separate compartment of the housing. In addition, the sensors themselves generate a small amount of heat, which offsets the BME680's temperature readings by about 0.5 - 1.5 °C above the “actual” temperature. This offset could not yet be quantified exactly, which is why the data was not adjusted in the following analysis.

The selected classrooms are all of a similar height of approximately 2.7 - 3.5 meters and provide space for 15 - 25 students. Like in most Austrian schools, the students of the participating classes spend most of the school day in “their” assigned classroom, with the exception of e.g., sports, arts, crafts, or physics lessons.

3 RESULTS AND DISCUSSION

In order to combine the multiple sensor datapoints in a classroom into a common room average, the readings are resampled into 5-minute intervals based on their time stamp. As sufficient information on classroom occupancy was not available, only the time period between 9:00 and 12:00 in the morning was analysed for the results presented herein. Within this timeframe, a full classroom occupation is very likely. In this sense, the results do not necessarily represent the average exposure concentration of the pupils.

For evaluation, measured values are then averaged within their 5-minute interval. This means that regardless of how many sensors take measurements in this 5-minute period, the mean value is always taken from the available measured values of this particular room. This makes it easy to handle rough failures and bring the data into a meaningful grid to be statistically analysed. The following data analyses and graphics were calculated and created using Python 3.0 scripts, mainly with the libraries Pandas, NumPy, and Matplotlib.

3.1 Significance

In order to analyse the existing 5-minute averages of the individual rooms, they are presented statistically in the form of a boxplot. The following boxplots show the median, the 25th

respectively 75th percentile, and the whiskers, which end at the largest and smallest measurement within 1.5 times of the interquartile range.

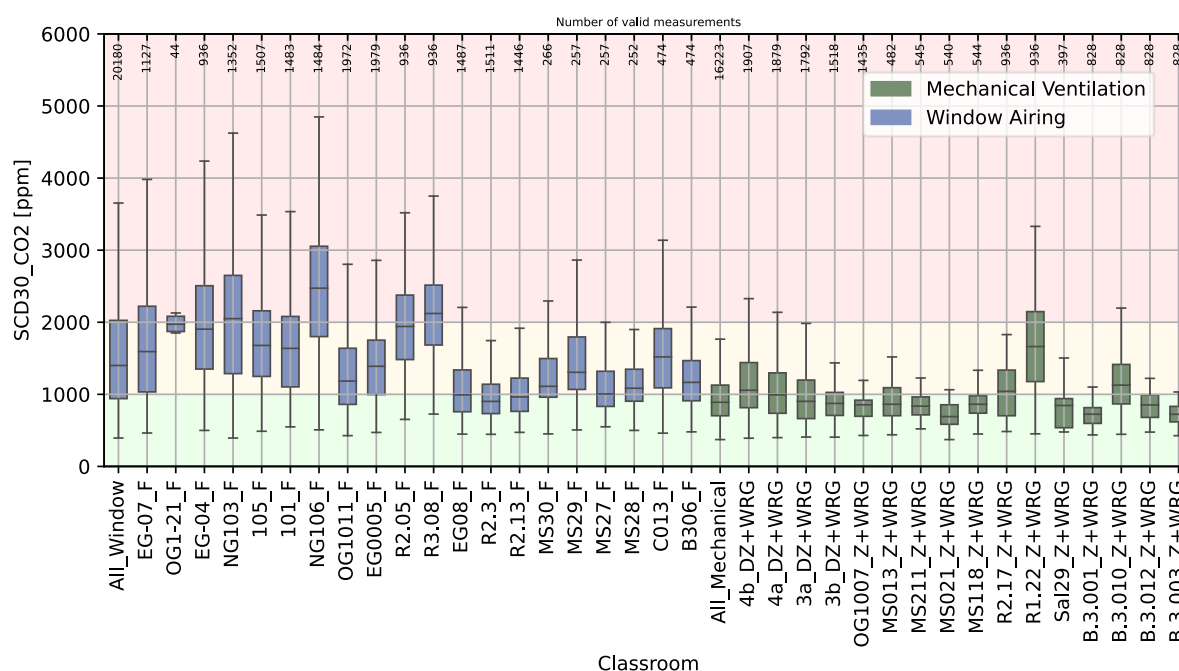


Figure 3: Boxplots of CO₂ concentration measured between 9:00 and 12:00 during schooldays

Figure 3 displays the boxplots of the CO₂ measurements for each classroom, sorted by 'mechanical ventilation' (green) and 'window airing' (blue). The first bars of the categories show the analyses of all classrooms combined for each category. It is visible that classrooms with window airing show mostly a wider range concerning the CO₂ content than those with mechanical ventilation.

The means of the underlying data are then checked for a statistically significant difference between window airing and mechanical ventilation. At first, it has to be examined, if the classroom averages are normally distributed. This is done using the Shapiro-Wilk-Test (Hedderich & Sachs, 2020). If the means are then confirmed to be normally distributed, the Welch t-Test (Hedderich & Sachs, 2020) can be a good choice for testing a significant difference, if not, the Mann-Whitney-U-Test (Spiegel & Stephens, 2018) can be more suitable. As it is not certain which is the better approach (Fay & Proschan, 2010) for the given measurement averages, the results of both tests are calculated and presented in Table 2. According to this statistical analysis, the CO₂-value is significantly higher with window airing than with mechanical ventilation (for details see Table 2). The chosen significance level for all tests is 5%.

Figure 4 displays the fine particulate matter measurements (PM_{2.5}) for each classroom. All classrooms, with one exception (see Figure 4, EG-04_F), are within an acceptable range, respectively below 10 µg/m³. The exception however consists of a classroom where only 20 five-minute interval data points could be evaluated due to data transmission problems, and should therefore be interpreted with care. With the same approach as with the CO₂-values, a statistically significant difference was tested with PM_{2.5}. Welch's t-Test and Mann-Whitney-U-Test show, PM_{2.5} levels are significantly higher in window-ventilated classrooms than in mechanically ventilated classrooms.

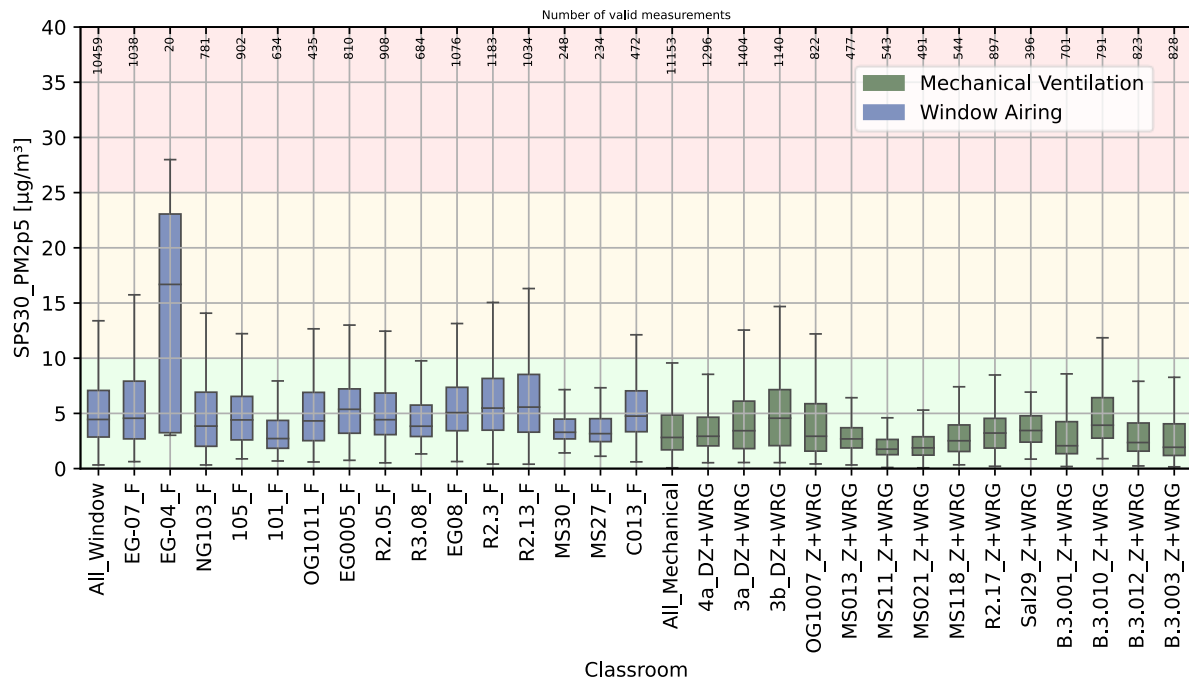


Figure 4: Boxplots of PM_{2.5} concentration measured between 9:00 and 12:00 during schooldays

In terms of relative humidity in classrooms, measurements in window-ventilated classrooms are slightly higher than in mechanically ventilated classrooms and show a slightly wider spread towards higher values (see Figure 5). The analysis of the classroom averages results that this difference is statistically significant. All classrooms examined are inside the recommended range or have at least acceptable relative humidity, with some of the lower whiskers considerably in the range of unrecommended humidity.

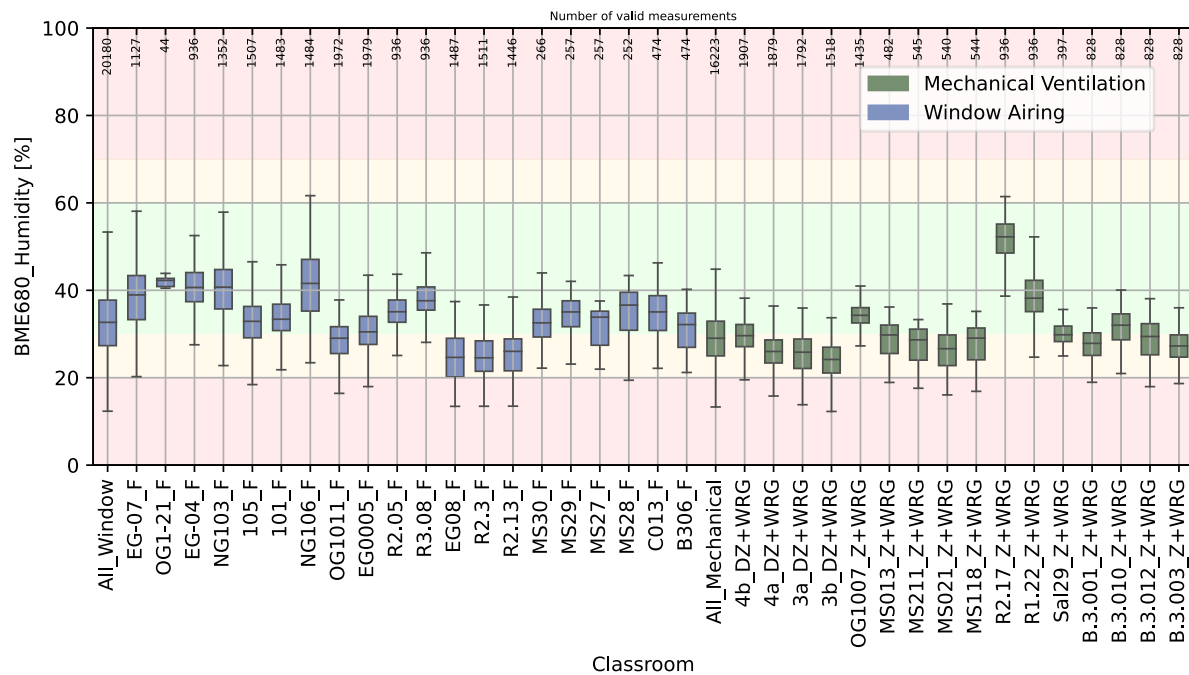


Figure 5: Boxplots of humidity levels measured between 9:00 and 12:00 during schooldays

In addition to that, also the calculated $b\text{-VOC}_{\text{eq}}$ levels were analysed and support that there is a statistically significant higher concentration of volatile organic compounds in classrooms with mechanical ventilation compared to those with window airing. This has not yet been investigated in sufficient detail, which is why the results cannot be presented or verified here. However, to complete the picture, the values are included in Table 2.

Table 2: Significance of differences: window airing vs. mechanical ventilation (significance level 5%)

Classroom Avg.	Test-Variant	p-Value Wt*	p-Value MWU**	Result
CO ₂	window airing > mechanical vent	0.0004 %	0.001 %	very significant
PM _{2.5}	window airing > mechanical vent	0.21 %	0.02 %	very significant
b-VOC _{eq}	window airing < mechanical vent	3.74 %	2.51 %	significant
Humidity	window airing > mechanical vent	4.53 %	1.14 %	significant

*Wt ... Welch's t-Test

**MWU ... Mann-Whitney-U-Test

3.2 Correlations

A further investigation concerns the correlation between indoor and outdoor measurements. For this purpose, data pairs are generated that represent the average of the measurements over the time period from 9:00 to 12:00. Figure 6 displays these data pairs for fine particulate matter (PM_{2.5}) and a regression line was created to show the trend of the highly variable data points for separate classrooms with and without mechanical ventilation. The band around the regression line represents the range within the root-mean-square deviation (short RMS, Spiegel and Stephens, 2018). This relatively small sample of data indicates a correlation between inside and outside PM_{2.5} values with a correlation coefficient for mechanical ventilation of 51.2% and for window airing of 65.3%. Both regression lines have a relatively high RMS. It can be said that this data seems to indicate the effectiveness of the particulate filters in ventilation systems.

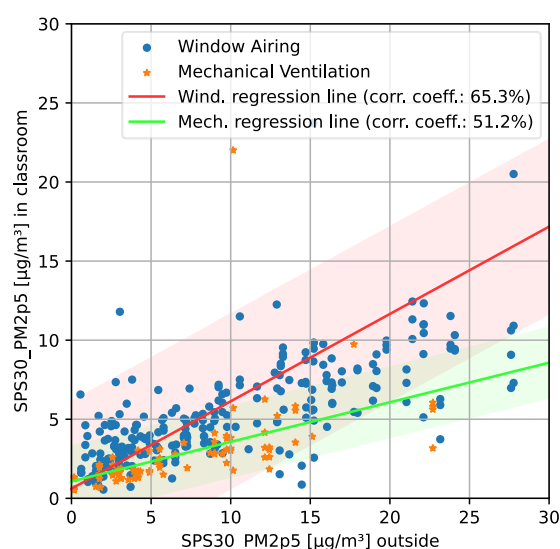


Figure 6: Correlation between avg. PM_{2.5} in classroom and avg. PM_{2.5} outside

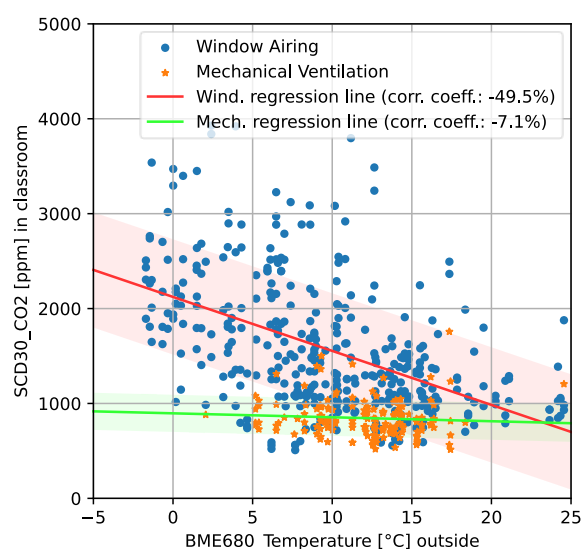


Figure 7: Correlation between avg. temperature outside and avg. CO₂-level in classroom

Figure 7 shows data pairs of the average outside temperature compared to the corresponding average CO₂-level. This correlation analysis shows a high dependency of the inside CO₂-level from the outside temperature in window-ventilated classrooms and almost no correlation in mechanically ventilated classrooms. This suggests that the colder it is outside, the less likely it is that occupants will adequately ventilate the classrooms if done by window airing. On the other hand, since most mechanical ventilation systems have heat recovery implemented the outside temperature plays a minor role given such a system. The parameters of the correlation, the regression line, and the root-mean-square deviation are listed in Table 3.

Table 3: Parameters of correlation and the regression line

Case	Ventilation	Interception*	Slope*	Correlation Coeff.	RMS
PM _{2.5} inside / PM _{2.5} outside	Window Airing	0.61 µg/m ³	0.55	65.3 %	5.57 µg/m ³
	Mechanical Ventilation	1.07 µg/m ³	0.25	51.2 %	2.28 µg/m ³
CO ₂ inside / Temperature outside	Window Airing	2123 ppm	-56.9 ppm/°C	-49.5 %	608 ppm
	Mechanical Ventilation	896 ppm	-4.2 ppm/°C	-7.1%	196 ppm

* regression line in style of $\text{value}_{\text{inside}} = \text{slope} \times \text{value}_{\text{outside}} + \text{interception}$

4 CONCLUSIONS

This work, which is based on the preliminary measurement data of the project DIGIdat, examines various air quality parameters by means of statistical data analysis. The low-cost sensor kits used have been placed in 36 classes so far and measure temperature and humidity, as well as CO₂-levels, fine particulate matter (PM), and volatile organic compounds (here as b-VOC_{eq}). Measurements were carried out at one-minute intervals, although due to problems with the database infrastructure, some classrooms had to temporarily be measured in four-minute intervals. The aim of this study was to find statistical differences between classes with and without mechanical ventilation and to investigate correlations between outdoor air and classroom air. Higher concentrations of CO₂ and PM_{2.5} were found in classes with window airing confirmed by statistical significance. There also was a statistically significant lower level of humidity in mechanically ventilated classrooms. Statistical differences were tested with the Welch t-test and Mann-Whitney-U-test at 5% significance level. The correlation for mechanically ventilated classrooms showed that fine particulate filtering is statistically visible. However, PM_{2.5} concentration is low for all classes with median values well below 10 µg/m³. For window airing, a dependence of the CO₂-levels on the outside temperature can be found. In general, the colder the outside temperature the higher the CO₂ measurements, with CO₂ concentrations above 2000 ppm in several of the window-ventilated classrooms. The preliminary analysis indicates that mechanical ventilation as installed and operated in Austrian schools reduces CO₂ concentration significantly. The goal for further analysis is to expand the data set and generate clean data for further analysis, including temperature and b-VOC_{eq}. Furthermore, the data failures are to be quantified and correlations to underlying conditions in the individual classes, such as class size, window orientation, etc., are to be established.

5 ACKNOWLEDGEMENTS

Project DIGIdat is funded by the Sparkling Science Programme of the Austrian Agency for Education and Internationalisation (OEAD) and the Federal Ministry of Education, Science and Research Austria (BMBWF). The success of the project is also due to the involvement of all the students, teachers, and helpers.

6 REFERENCES

- Bosch Sensortec. (2022). *BME680 Datasheet: Digital low power gas, pressure, temperature & humidity sensor*. <https://www.bosch-sensortec.com/media/boschsensortec/downloads/datasheets/bst-bme680-ds001.pdf>
- Fay, M. P. & Proschan, M. A. (2010). Wilcoxon-Mann-Whitney or t-test? On assumptions for hypothesis tests and multiple interpretations of decision rules. *Statistics surveys*, 4, 1–39. <https://doi.org/10.1214/09-SS051>
- Hedderich, J. & Sachs, L. (2020). *Angewandte Statistik*. Springer Berlin Heidelberg. <https://doi.org/10.1007/978-3-662-62294-0>
- OpenSenseLab. (2023). *OpenSenseMap*. <https://opensensemap.org/>
- Österreichisches Normungsinstitut (2004). *EN ISO 16000-1: Innenraumluftverunreinigungen - Teil 1: Allgemeine Aspekte der Probenahmestrategie*. Wien. Österreichisches Normungsinstitut.
- senseBox. (2023a). *Home / senseBox.de*. <https://sensebox.de/>
- senseBox. (2023b). *senseBox Blockly Editor*. <https://blockly.sensebox.de/>
- Sensirion. (2019). *Mechanical Design and Assembly Guidelines for SPS30*. https://sensirion.com/media/documents/7990F04A/616544B0/Sensirion_Part particulate_Matter_AppNotes_SPS30_Mechanical_Design_and_As.pdf
- Sensirion. (2020a). *Datasheet Sensirion SCD30 Sensor Module: CO₂, humidity, and temperature sensor*. https://sensirion.com/media/documents/4EAF6AF8/61652C3C/Sensirion_CO2_Sensors_SCD30_Datasheet.pdf
- Sensirion. (2020b). *Datasheet SPS30: Particulate Matter Sensor for Air Quality Monitoring and Control*. https://sensirion.com/media/documents/8600FF88/616542B5/Sensirion_PM_Sensors_Datasheet_SPS30.pdf
- Spiegel, M. R. & Stephens, L. J. (2018). *Schaum's outlines®: Statistics. Schaum's outline series*. McGraw-Hill Education.
- Wikipedia. (2019). *Blockly*. <https://en.wikipedia.org/wiki/Blockly>

Measurement of ventilation effectiveness and indoor air quality in toilets at mass gathering events

Ben M. Roberts*¹, Filipa Adzic², E. Abigail Hathway³, Christopher Iddon², Benjamin Jones⁴, Malcolm J. Cook¹, and Liora Malki-Epshtein²

*1 Building Energy Research Group
Loughborough University
Loughborough, UK*

*2 Department of Civil, Environmental
and Geomatic Engineering
UCL
London, UK*

*Corresponding author: b.m.roberts@lboro.ac.uk

*3 Department of Civil and Structural Engineering
University of Sheffield
Sheffield, UK*

*4 Department of Architecture and Built Environment
University of Nottingham
Nottingham, UK*

ABSTRACT

Mass gathering events were closed in 2020 to reduce the spread of SARS-CoV-2. These events included music concerts, theatre shows, and sports matches. It is known, however, that the long-range aerosol transmission of pathogens, such as SARS-CoV-2, can be reduced with sufficient ventilation indoors. This paper examines the risk of reopening these mass gathering events by measuring the CO₂ concentration, as a proxy for ventilation effectiveness, at 58 events, with a specific focus on small enclosed spaces with short occupancy. Toilets (sanitary accommodation) are spaces that are densely and continuously occupied for short durations throughout the events, such as during theatre intervals or half-time at sports events. The results showed that the average air quality in toilets was good at most events. There were, however, considerable peaks in CO₂ concentration of up to 3431 ppm in toilets at times when occupancy was presumed high, indicating that the risk of exposure to exhaled breath, which may contain virus-laden aerosols, is higher in toilets than elsewhere in the venue (although occupancy duration will be much lower). Recommendations are provided to encourage building designers and operators to be mindful of the ventilation strategies used in toilets given their occupancy and size.

KEYWORDS

Indoor air quality; ventilation effectiveness; mass gathering events; CO₂ monitoring; post-occupancy evaluation.

1 INTRODUCTION

Confined spaces with transient occupancies, such as toilets (sanitary accommodation¹), have been identified as potentially high-risk areas for the transmission of airborne pathogens (Dancer et al., 2021; Malki-Epshtein et al., 2023). At mass gathering events, these enclosed spaces can be crowded with many people mixing in proximity for brief periods, such as during half-time at sports matches or during intervals at theatres (Adzic et al., 2022). This increases the risk of both short-range and long-range airborne transmission. Person-to-person transmission of pathogens is compounded in toilets by faecal particles entering the air by flushing toilets (Best et al., 2012; Cai et al., 2022; Knowlton et al., 2018). A possible faecal-

¹ Sanitary accommodation is a space containing one or more flush toilets or urinals (HMG, 2021a) and are hereafter referred to as “toilets”.

oral SARS-CoV-2 transmission route has been identified (Guo et al., 2021) leading to toilets being considered a contact hub for community transmission of SARS-CoV-2 (Dancer et al., 2021).

Ventilation which introduces uncontaminated air into a space is an important mechanism to reduce long-range transmission of airborne pathogens, but in transiently occupied spaces the ventilation rates may not be adequate to introduce enough uncontaminated air during the brief period of dense occupancy to dilute or remove airborne pathogens (Dancer et al., 2021). In England, building regulations require sanitary accommodation to be ventilated at 6 l/s per toilet pan or urinal via extract ventilation to minimise the spread of water vapour and pollutants to other parts of the building (HMG, 2021a). The aim of the work reported in this paper was to measure the ventilation effectiveness of outdoor air in toilets at mass gathering events. The aim was achieved by measuring the carbon dioxide (CO₂) concentration in the air of 11 toilets at three venues hosting 58 mass gathering events which were run as part of the UK Government Events Research Programme in 2021 (DCMS, 2021; HMG, 2021b). CO₂ concentration is used as a proxy for exhaled breath and allows for the rapid assessment of indoor air quality (Malki-Epshtein et al., 2023).

2 METHOD

The concentration of CO₂ in the indoor air was measured in 11 toilets in three different venues at 58 live mass gathering events (Table 1). Toilets are of interest because they are usually spatially constricted areas that are densely occupied for brief periods during mass gathering events with potentially insufficient ventilation relative to the occupancy levels. The three venues (Table 1) hosted between 79 and 90,000 people at a variety of events. The snooker and football matches at the Crucible Theatre and Wembley Stadium were sporting events in which the games were played in two halves. This meant that there were three periods where toilets were densely occupied: (1) pre-event, (2) mid-event interval, and (3) post-event, although attendees were able to occupy the toilet at any time during the event. The music awards ceremony (BRIT Awards) at the O2 Arena was televised with frequent advertisement/commercial breaks of up to 15 minutes when presenters and performers would not be on stage. It was at these times that people were most likely to leave the auditorium to occupy the toilets, although they were able to visit the toilets at any time. The toilets were mechanically ventilated in all venues. This non-interventionist, observational monitoring study took place during a series of Events Research Programme pilot events which examined the risk of reopening due to long-range airborne infections after COVID-19 pandemic closures (DCMS, 2021; HMG, 2021b).

Table 1: Names and details of venues monitored.

Event	Venue	No. events	Date (DD/MM/2021)	No. toilets	No. attendees (range)	% capacity
World Snooker Championships	Crucible Theatre	46	17/04 to 03/05	6	79-862	8-88
Music awards	O2 Arena	1	11/05	3	3532	18
Football matches	Wembley Stadium	11	18/04 to 11/07	2	2700-90000	3-100

CO₂ concentration was measured at 2-minute intervals using non-dispersive infrared sensors (400-5000 ppm; ± 30 ppm) that were calibrated prior to use and routinely auto-calibrated during operation (Malki-Epshtein et al., 2023). The sensors were placed on walls at a height of 1.6 to 2.3 m above the floor, and away from vents, doors, or windows. The number of sensors installed in each space varied according to the room geometry and volume, but typically there were 1-2 sensors in each toilet.

CO₂ concentrations are of interest because elevations above typical ambient levels (420-500ppm) indicate exposure to exhaled breath, in the absence of other sources. The higher the concentration of CO₂ above typical ambient levels, the higher proportion of indoor air that has been exhaled by the occupants of the space. Ventilation is the primary removal mechanism of CO₂ in most spaces via dilution with outdoor air. Measurement of CO₂ concentration, therefore, indicates the amount of ventilation of outdoor air being received in a space relative to the occupancy levels.

Air quality classifications were used to classify each toilet by the measured mean average and maximum CO₂ concentration during each event (Table 2). Average CO₂ concentration was both the temporal and spatial average, whereas maximum CO₂ was the single point in time with the highest CO₂ concentration measured at one particular sensor location in the space. Each space was assigned a band, from Band A (high ventilation relative to the occupancy) to Band G (low ventilation relative to the occupancy). The bands were devised during the UK Government Events Research Programme to rapidly assess indoor air quality at mass gathering events (Malki-Epshtein et al., 2023). CO₂ concentration alone does not indicate a risk of transmission of airborne pathogens (Iddon et al., 2022; Jones et al., 2021) but it does allow for the rapid assessment of ventilation effectiveness relative to the occupancy levels.

Table 2: Air quality classifications and bands.

Air quality classification	Band	Range of absolute CO ₂ concentrations (ppm)
At or marginally above outdoor concentration.	A	400-600
Target for enhanced aerosol generation (e.g., singing or aerobic activity).	B	600-800
Typical air quality design standards for offices.	C	800-1000
Medium air quality.	D	1000-1200
Design standard upper limits for most schools pre-COVID-19.	E	1200-1500
Priority for improvement.	F	1500-2000
Low ventilation and/or dense occupancy. Must be prioritised for improvement.	G	>2000

3 RESULTS

3.1 Air quality classifications for all mass gathering events monitored

Analysing the spatiotemporal average CO₂ concentration showed that the majority of toilets (96%) were in air quality Band A and Band B with the remainder (4%) in Band C and Band D (Figure 1). For maximum CO₂ concentrations, however, air quality bands in toilets were in Band A and Band B for fewer events (76%) and whilst some toilets in some events were classified as Band E, Band F, and Band G, they were relatively small in number (5% of events) (Figure 1). This indicates that ventilation was generally sufficient given the occupancy levels in most toilets.

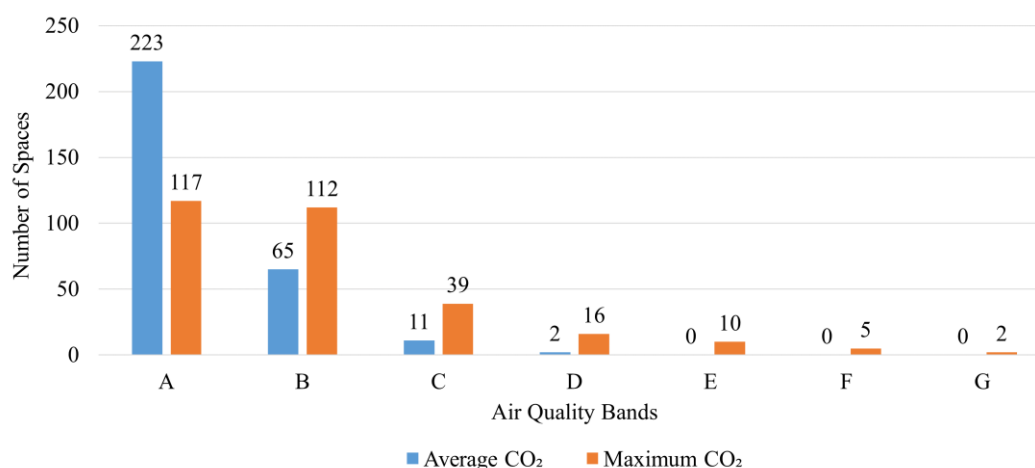


Figure 1: Air quality classification bands for toilets.

3.2 CO₂ concentration time series profiles at different events

A higher proportion of toilets are in air quality Band E, Band F, and Band G when classifying using maximum CO₂ concentration than when using average CO₂ concentration. This indicates that there are peaks in CO₂ concentration at specific times that are not sustained throughout the event. This is evidenced by investigating plots of CO₂ concentration against time (Figures 2-4).

Crucible Theatre (snooker matches)

At the Crucible Theatre, three distinct peaks in CO₂ concentration were observed which corresponded to the event starting, during the interval, and at the end of the event (Figure 2²). At other times, the CO₂ concentrations reduced to reach a quasi-steady state as most of the spectators were inside the theatre auditorium during the event.

Higher maximum and baseline CO₂ concentrations were observed in three toilets in the Crucible Theatre (unisex toilet AS7, male AS8, and unisex AS9) compared to the other toilets in the same venue (Figure 2). These three toilets were located close to the main theatre auditorium entrance, whereas the others were on floors either below or above the main entrance. Event observers confirmed that the toilets by the main entrance (AS7, AS8, and AS9) were the most visited even though event managers communicated that there were alternative toilets available on other floors. Event average CO₂ concentrations in all toilets close to the main auditorium entrance (first floor) were at least 32% higher than average CO₂ concentrations in toilets on the ground and second floor. Male toilet AS8 showed particularly high CO₂ concentrations relative to the other toilets, reaching a maximum concentration of 1600 ppm and being 400 ppm higher than the next highest concentration (Figure 2).

It was also observed that the CO₂ concentrations in toilets AS7, AS8, and AS9 did not fall below 600 ppm, even during periods assumed to be unoccupied. This is because extractor fans drew makeup air through toilet door grilles from densely occupied adjacent spaces in which maximum CO₂ concentrations of 1303 ppm were recorded.

² The example of 3 May 2021 is provided as this is the event with the highest occupancy (88% of usual capacity), but the trimodal pattern was generally observed at all events at the Crucible Theatre.

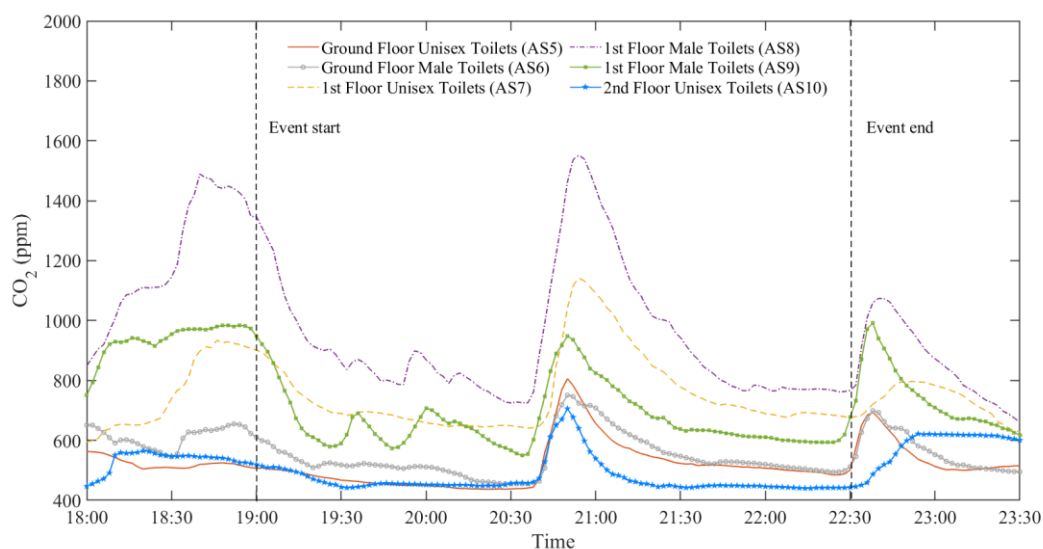


Figure 2: Measured CO₂ concentration time series profile in six toilets in the Crucible Theatre at the World Snooker Championships on 3 May 2021.

Wembley Stadium (football matches)

At Wembley, CO₂ concentration time series profiles were observed that were similar to those recorded at the Crucible Theatre with trimodal peaks before an event, at half time, and at the end of the event (Figure 3). These peaks were most pronounced at the high occupancy events but were observed even when the occupancy levels were significantly lower than usual (at 3% of usual capacity in a male toilet, Figure 3b; and 3% in a female toilet, Figure 3a). There were higher maximum CO₂ concentrations recorded during the events with higher occupancy levels. In the female toilet, the maximum CO₂ concentration was 68% higher at the 100% occupancy event compared to the 65% occupancy event (Figure 3c) and 154% higher in the male toilet comparing the 20% and 100% occupancy events (cf. Figure 3b and Figure 3d). Generally higher CO₂ concentrations were observed in the male toilet compared to the female toilet on the same floor level at the same football match due to a greater proportion of males at these events. During the 100% occupancy events, the maximum recorded CO₂ concentration was 3431 ppm in the male toilet versus 1320 ppm in the female toilet (i.e., 160% higher in the male toilet). The CO₂ concentration remained continuously elevated above 1500 ppm (classed as a priority for improvement, Table 2) for periods in male toilets at all the football matches where the occupancy was greater than 65% (Table 3).

Table 3: Comparing the occupancy to the longest continuous number of minutes where CO₂ concentration was above 1500 ppm.

Occupancy as a percentage of usual capacity (%)	Minutes CO ₂ concentration >1500 ppm				
	Before event	First half	Half-time interval	Second half	After event
65	0	0	6	2	4
72	32	0	15	6	16
100	44	0	15	4	8

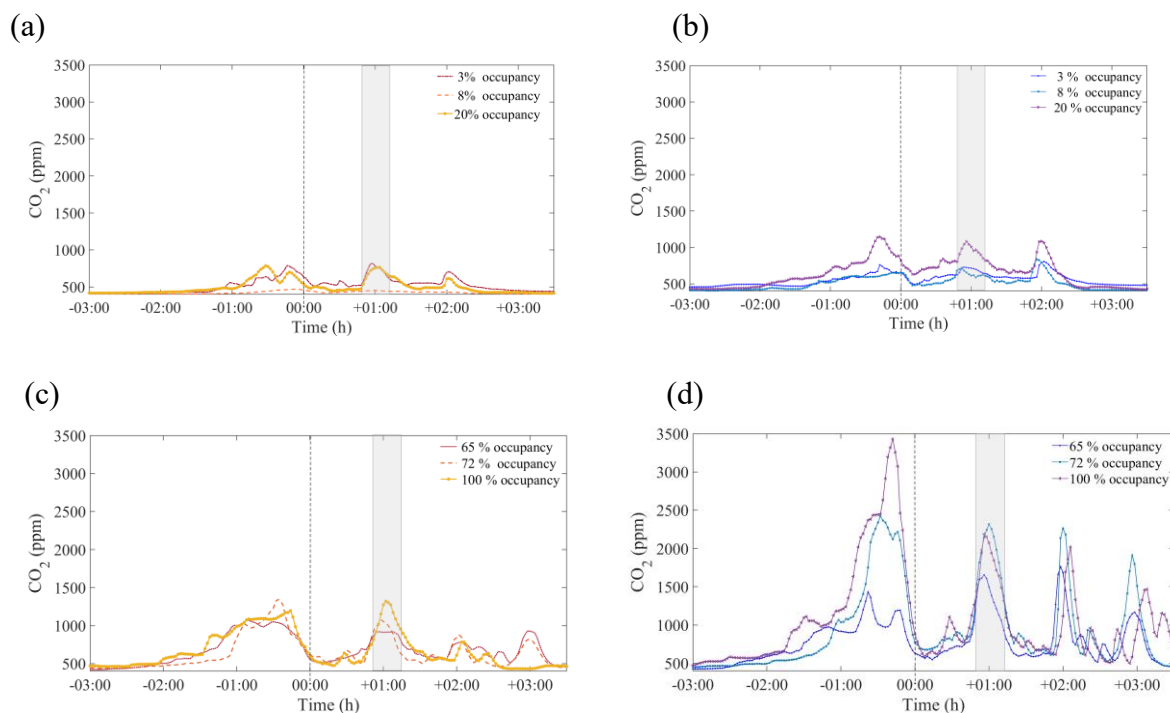


Figure 3: Measured CO₂ concentration time series profile in six toilets during football matches at Wembley Stadium with varying occupancy levels: (a) being a low occupancy event (3 to 20%) in a female toilet; (b) low occupancy event (3 to 20%) male toilet; (c) high occupancy event (65 to 100%) female toilet; (d) high occupancy event (65 to 100%) male toilet. The dashed vertical line indicates the football match kick-off time, and the shaded region is the half-time period.

O2 Arena (music awards ceremony)

Unlike the sports events held at the Crucible Theatre and Wembley Stadium, the music awards ceremony at the O2 Arena did not have a specific half-time interval, but instead a series of 15-minute advert/commercial breaks because the show was televised. Toilet visits were more evenly spaced and this is reflected in the flatter CO₂ concentration profile, which does not feature pronounced peaks during the event (Figure 4). Despite the significantly reduced occupancy (18% of usual capacity), the female toilet on Level 1 reached a maximum CO₂ concentration of 1169 ppm and was sustained above 1000 ppm for over two hours (Figure 4). The male toilets, located just next to the female toilets on Level 1, presented with a peak CO₂ concentration of 1100 ppm just prior to the event starting but then fell to an average below 750 ppm during the event. Nonetheless, the CO₂ concentrations recorded inside the toilets were considerably higher than those immediately outside the toilet (see queuing area, Figure 4).

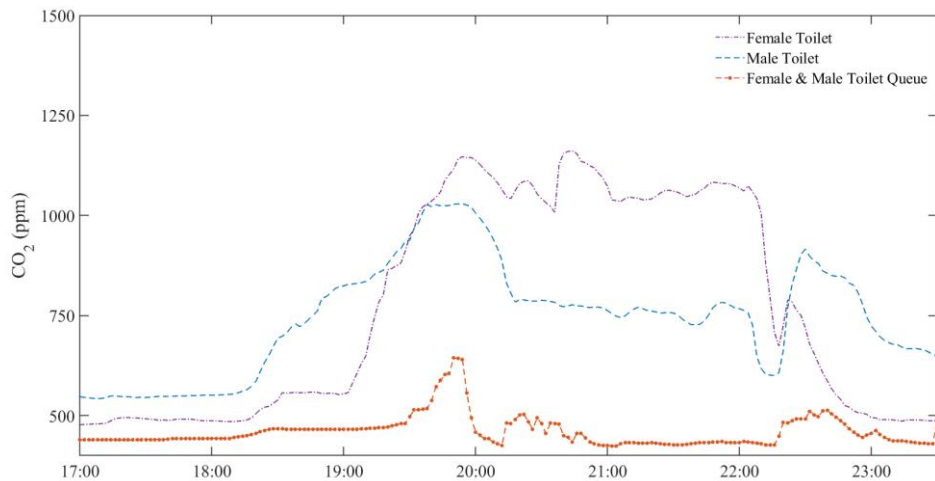


Figure 4: Measured CO₂ concentration time series on Level 1 at the O2 Arena during the music awards event at 18% of usual occupancy capacity.

3.3 Effect of occupancy levels

It has been demonstrated that higher occupancy levels drive an increase in CO₂ concentration (Figure 3 and Figure 4), as this is the only significant factor believed to change between events (the ventilation systems were otherwise operated identically). At the Crucible Theatre, where CO₂ concentration was monitored in toilets during 46 events from 8 to 88% of the venue's usual occupancy capacity, the effect of occupancy on maximum CO₂ concentration is apparent in all toilets, but especially the frequently visited toilets (those which are easily accessible due to proximity to the auditorium entrance: AS7, AS8, AS9) (Figure 5). At low occupancy events, e.g., around 10%, all maximum CO₂ concentrations were below 800 ppm, but the trend line indicates maximum CO₂ concentrations of over 2000 ppm might be expected in some toilets (AS8) at fully occupied events (Figure 5).

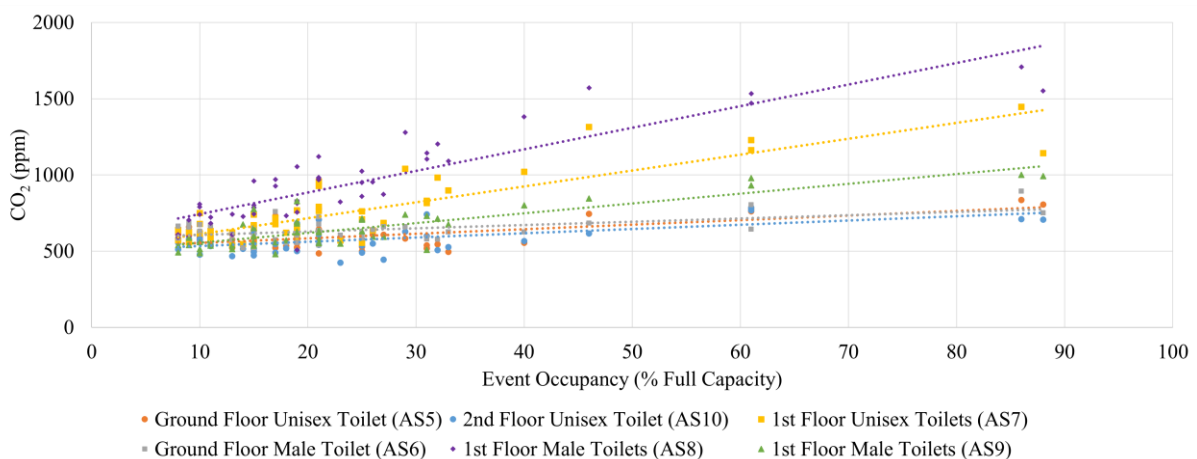


Figure 5: Event occupancy versus maximum CO₂ concentration in toilets at the Crucible Theatre.

4 DISCUSSION

The measurement of CO₂ concentration in indoor air does not indicate the risk of long-range transmission of airborne pathogens, but it is a useful way of rapidly assessing the level of ventilation relative to the occupancy of a particular space. Most of the toilets were deemed to be sufficiently ventilated, but a small number were targeted for improvement using the maximum CO₂ concentration as a performance metric. The proximity of the toilet to important areas in each venue, such as the main auditorium door in the Crucible Theatre, was also an important indicator of performance, with toilets proximate to these places more frequently occupied and so recording higher CO₂ concentrations. This perhaps suggests the ventilation systems are undersized to cope with the short periods of very high occupancy.

For structured events with a seated audience, it has previously been recommended that intervals are a useful means to reduce the CO₂ concentration in the main event space (e.g., a theatre auditorium) because it provides a period of reduced occupancy during which the space can be ventilated whilst the occupant emission rates are lower before the space becomes occupied again (Adzic et al., 2022). For toilets, however, these intervals cause brief periods of high occupancy with maximum CO₂ concentrations reaching 2250 ppm during half-time at a Wembley Stadium football match. This is compared to much lower, consistent CO₂ concentrations at the O2 Arena where toilets were visited throughout the event rather than just during the intervals. Whilst it would not be possible to introduce additional breaks in play in structured sports games, there may be other types of events where this is possible or, equally, the interval could be for a longer time to reduce the crowding that occurs in toilets with short interval durations.

Most Events Research Programme pilot events were run at reduced capacity compared to normal operations, but Wembley Stadium hosted one full-capacity event (Table 1). The measured CO₂ concentrations are influenced by both the ventilation provision and the number of occupants in the space. Reduced occupancy has a clear benefit in terms of maintaining lower CO₂ concentrations in spaces (Figure 5) but running events at such reduced capacities is not economically viable. Venue operators should instead consider ways to better disperse the event attendees around the various toilets in the venue to avoid overcrowding in any particular toilet. At the Crucible Theatre, for example, venue operators changed some toilets to unisex to reduce overcrowding in the male toilets. Alternatively, additional temporary toilets could have been installed, providing they are located close enough to the main event space to be used. Designers of new buildings to host mass gathering events could consider adding additional toilets to reduce occupant density and providing more in locations where crowds are likely to congregate, although this will result in higher construction, maintenance, and cleaning costs. Building designers should carefully consider toilet location to ensure all are used evenly or those in the densely occupied areas are larger or provided with a higher ventilation rate. Ventilation designers should also consider where makeup air is being drawn from, to avoid air being drawn from densely occupied neighbouring spaces, potentially containing virus-laden aerosols.

A limitation of this work is that not all events were run at full capacity. CO₂ concentrations are likely, therefore, to be higher when returning to full capacity than was measured in most of these examples. It did, however, provide a useful and rare opportunity to compare events with different occupancy levels in the same venue. An additional limitation is that only CO₂ concentration was considered and so the risk of long-range airborne transmission cannot be made without further analysis (Iddon et al., 2022; Jones et al., 2021). This analysis will be a

feature of future work, as will the assessment of microbiological data (air and surface samples) which were collected alongside the CO₂ measurements, but not presented here. The exposure time in toilets is likely to be low, as people do not tend to dwell there, so the risk of long-range transmission in toilets is likely to be low, irrespective of ventilation levels. However, there are other impacts of overcrowding that these data highlight, such as the scope for short-range airborne and fomite transmission in the relatively small toilet spaces. Neither of these factors were considered in this paper but will be addressed in future work. A key limitation of this work is that the exposure period of the occupants was unknown, but this has a great influence on the susceptibility of a person to infection from an airborne pathogen. Collecting data regarding this would be useful in future studies.

5 CONCLUSIONS

The mean average CO₂ concentration in 11 toilets was indicative of ventilation that was sufficient relative to the occupancy levels at 96% of the 58 events. Investigation of the maximum CO₂ concentrations, however, revealed that at some events there were intermittent periods of high CO₂, which indicated poor ventilation relative to the number of occupants. This mainly occurred during half-time intervals at the snooker and football matches, particularly during the higher occupancy events, and in toilets closest to auditorium entrances.

The key recommendations are summarised:

1. Increase the ventilation rates or the room volume in toilets which are expected to be most frequently visited (e.g., those close to auditorium entrances).
2. Increase the number of intervals, or their length in time, where possible, to spread out the occupancy of toilets over a longer period.
3. Increase the number of toilets available to reduce crowding and group them in places of high occupant density.
4. Change the admittance gender for some toilets if there is a predominantly male or female audience at a particular event.
5. Consider where supply air to toilets is being drawn from and avoid doing this from densely occupied adjacent spaces.

Future development of this work will consider translating the measured CO₂ concentration to an estimation of the risk of long-range airborne transmission of pathogens such as SARS-CoV-2 and will analyse the microbiological data measured at these events.

6 ACKNOWLEDGEMENTS

The CO₂ monitoring study was funded by the Department for Digital, Culture, Media, & Sport, who also arranged access to the venues and events; the subsequent analysis was done by the Airborne Infection Reduction through Building Operation and Design for SARS-CoV-2 (AIRBODS) consortium, funded by the Engineering and Physical Sciences Research Council (EPSRC) grant EP/W002779/1.

7 REFERENCES

- Adzic, F., Roberts, B. M., Hathway, E. A., Kaur Matharu, R., Ciric, L., Wild, O., Cook, M., & Malki-Epshtein, L. (2022). A post-occupancy study of ventilation effectiveness from high-resolution CO₂ monitoring at live theatre events to mitigate airborne transmission of SARS-CoV-2. *Building and Environment*, 223, 109392. <https://doi.org/10.1016/J.BUILDENV.2022.109392>
- Best, E. L., Sandoe, J. A. T., & Wilcox, M. H. (2012). Potential for aerosolization of *Clostridium difficile* after flushing toilets: the role of toilet lids in reducing environmental contamination risk. *Journal of Hospital Infection*, 80(1), 1–5. <https://doi.org/10.1016/J.JHIN.2011.08.010>
- Cai, C., Kim, P., Connor, T. H., Liu, Y., & Floyd, E. L. (2022). Reducing the particles generated by flushing institutional toilets. <https://doi.org/10.1080/15459624.2022.2053693>, 19(5), 318–326.
- Dancer, S. J., Li, Y., Hart, A., Tang, J. W., & Jones, D. L. (2021). What is the risk of acquiring SARS-CoV-2 from the use of public toilets? *Science of The Total Environment*, 792, 148341. <https://doi.org/10.1016/J.SCITOTENV.2021.148341>
- DCMS. (2021). *Events Research Programme: Phase I findings*. <https://www.gov.uk/government/publications/events-research-programme-phase-i-findings/events-research-programme-phase-i-findings>
- Guo, M., Tao, W., Flavell, R. A., & Zhu, S. (2021). Potential intestinal infection and faecal–oral transmission of SARS-CoV-2. *Nature Reviews Gastroenterology & Hepatology*, 18(4), 269–283. <https://doi.org/10.1038/s41575-021-00416-6>
- HMG. (2021a). *Approved Document F: Ventilation. Volume 2: Buildings other than dwellings. The Building Regulations 2010*.
- HMG. (2021b). *Science Note - Emerging findings from studies of indicators of SARS-CoV-2 transmission risk at the Events Research Programme: environment, crowd densities and attendee behaviour*.
- Iddon, C., Jones, B., Sharpe, P., Cevik, M., & Fitzgerald, S. (2022). A population framework for predicting the proportion of people infected by the far-field airborne transmission of SARS-CoV-2 indoors. *Building and Environment*, 221, 109309. <https://doi.org/10.1016/J.BUILDENV.2022.109309>
- Jones, B., Sharpe, P., Iddon, C., Hathway, E. A., Noakes, C. J., & Fitzgerald, S. (2021). Modelling uncertainty in the relative risk of exposure to the SARS-CoV-2 virus by airborne aerosol transmission in well-mixed indoor air. *Building and Environment*, 191, 107617. <https://doi.org/10.1016/J.BUILDENV.2021.107617>
- Knowlton, S. D., Boles, C. L., Perencevich, E. N., Diekema, D. J., & Nonnenmann, M. W. (2018). Bioaerosol concentrations generated from toilet flushing in a hospital-based patient care setting. *Antimicrobial Resistance and Infection Control*, 7(1), 1–8. <https://doi.org/10.1186/S13756-018-0301-9/TABLES/1>
- Malki-Epshtein, L., Adzic, F., Roberts, B. M., Abigail Hathway, E., Iddon, C., Mustafa, M., & Cook, M. (2023). Measurement and rapid assessment of indoor air quality at mass gathering events to assess ventilation performance and reduce aerosol transmission of SARS-CoV-2. *Building Services Engineering Research & Technology*, 44(2), 113–133. <https://doi.org/10.1177/01436244221137995>

Impact of the building airtightness and natural driving forces on the operation of an exhaust ventilation system in social housing in Chile.

Gilles Flamant^{*1,2}, Waldo Bustamante¹, Arnold Janssens², and Jelle Laverge²

*1 Centre for Sustainable Urban Development
(CEDEUS)*

*Pontificia Universidad Católica de Chile
El Comendador 1916*

Santiago, RM, 7520245, Chile

**Corresponding author: gilles.flamant@uc.cl*

*2 Research Group Building Physics, Ghent
University, Sint-Pietersnieuwstraat 41*

B-9000 Gent, Belgium

ABSTRACT

Chile has 1,626 social housing complexes with a total of 350,880 dwellings. Several studies have demonstrated a low thermal performance and high air permeability of the envelope of social houses throughout the country, causing surface condensation on walls, high heat losses in winter and low levels of thermal comfort for their occupants. The presence of high levels of indoor pollutants and/or indoor humidity has also been observed, causing respiratory and cardiovascular diseases in the occupants. This highlights the urgent need to renovate social housing in Chile to achieve better standards of habitability, well-being and quality of life for its inhabitants. Current retrofitting programs for social housing focus mainly on reducing heat losses and condensation problems inside the dwellings, although they also include the installation of a mechanical exhaust ventilation system with natural air inlets. However, there is currently no evaluation of the performance of such ventilation systems in the country. In fact, we do not know if the natural air inlets provide the required airflow rates to the different living areas of the dwelling and how the airflow rates are affected by the airtightness of the building envelope and the natural external driving forces (wind and thermal buoyancy).

This study has evaluated the performance of a commonly used mechanical exhaust ventilation system in a representative social house in Chile, for two sets of climatic data, using the airflow and contaminant transport calculation software CONTAM. It has highlighted the significant effect of the building airtightness and the natural driving forces, mainly the wind effect, on the performance of the ventilation system. For the house investigated in this research and considering a n_{50} -value of 10h^{-1} , the supplied airflow in one of the bedrooms is drastically reduced to almost the half of the value obtained for a perfectly airtight house when all the interior doors are open. When the doors are closed, the effect is even more pronounced. The decrease in the supplied airflows in the bedrooms leads to a significant increase in the CO_2 -exposure of the occupants. In the most unfavourable case analysed – n_{50} of 10h^{-1} with closed interior doors – the child of the family spent only 35% of his time in an indoor environment with a CO_2 concentration below 950 ppm.

These results emphasize the need to work also on improving the airtightness of social housing for a better operation of the exhaust ventilation system. They contribute to a better knowledge of the performance of the ventilation systems currently installed in the renovation of social housing in Chile, as well as to the identification of ways to improve these systems so that they can guarantee sufficient indoor air quality to the occupants.

KEYWORDS

Mechanical exhaust ventilation, indoor air quality, social housing, airtightness, wind pressure.

1 INTRODUCTION

According to the 2017 census, the total number of dwellings in Chile reaches 6.5 million. It is estimated that only 2% of the buildings meet minimum thermal performance standards (OECD, 2014) and 66% have thermal comfort problems (RedPE, 2019). Social housing is not an exception. Chile has 1,626 social housing complexes built between 1936 and 2016, with a total of 350,880 dwellings. Several studies have demonstrated a low thermal performance and high air permeability of the envelope of social housing throughout the country, causing surface condensation on walls, high heat losses in winter and low levels of thermal comfort for their occupants (de la Barrera et al., 2021). The presence of high levels of indoor pollutants and/or indoor humidity has also been observed, causing respiratory and cardiovascular diseases in the occupants. Based on a post-occupancy evaluation carried out in social housing complexes built in 2013 in the city of Concepción, Gonzalez-Caceres et al. identified 76 apartments affected by damage produced by high moisture levels out of the 400 apartments evaluated. Inadequate ventilation was identified as one of the multiple causes of this situation (Gonzalez-Caceres et al., 2019).

This highlights the enormous challenge and need to retrofit social housing in Chile to achieve better standards of habitability, well-being and quality of life for its inhabitants. Current retrofitting programs for social housing focus mainly on reducing heat losses and condensation problems inside the dwellings, although they also include the installation of a mechanical exhaust ventilation system with natural air inlets in accordance with the Chilean Ventilation Standard NCh3309 (INN, 2022). However, there is currently no evaluation of the performance of such ventilation systems in the country. In fact, we do not know if the natural air inlets provide the required airflow rates to the different living areas of the dwelling and how the airflow rates are affected by the airtightness level of the building envelope and the natural external driving forces (wind and thermal buoyancy).

This study aims to evaluate by simulation the performances of a commonly used mechanical exhaust ventilation system in a representative social housing in Chile. Specifically, the effects of the airtightness level of the building envelope and the natural driving forces on the indoor air quality are assessed using the airflow and contaminant transport calculation software CONTAM for two different outdoor climate data sets.

2 METHODS

2.1 House description

The investigated social house is a real one-story detached dwelling with a total floor area of 43m², which is typical for a Chilean social house. The house has a living-dining room with an open kitchen, two bedrooms and a bathroom, as shown in Figure 1. Bedroom 1 is assumed to face north.

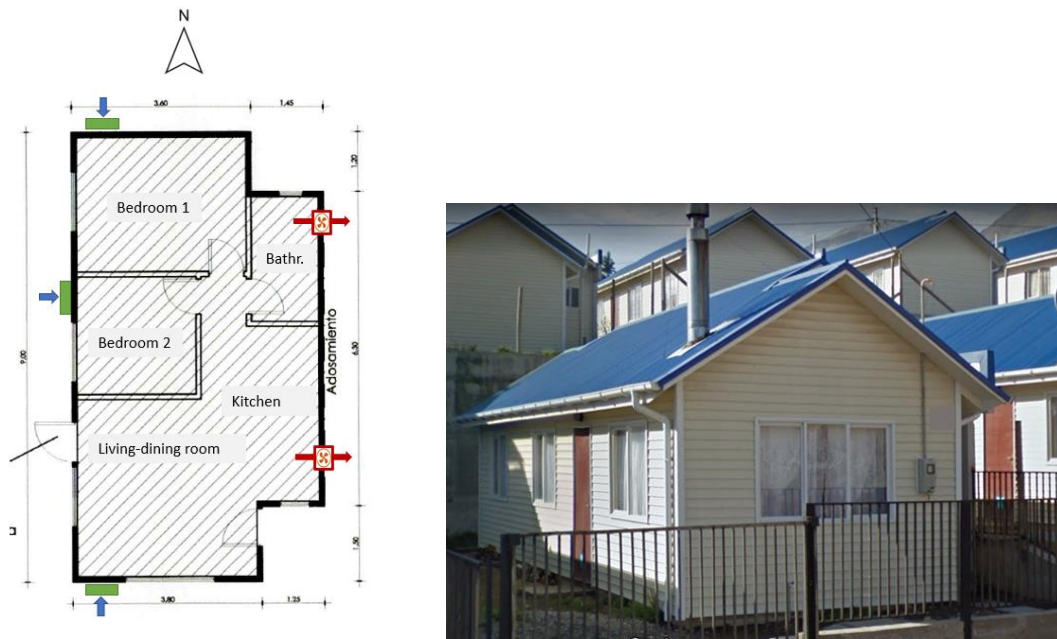


Figure 1: Plan and picture of the house investigated in this study.

2.2 Climatic data

The performance of the exhaust ventilation system was evaluated for two sets of climatic data (IWECC) corresponding to the two main cities in Chile: Santiago and Concepción. The wind speed in the IWECC data file for Santiago was modified to better match the data provided by the *General Directorate of Civil Aeronautics* for the period 2018-2022. Santiago, the capital city, is located in the central zone of Chile ($\sim 33^{\circ}\text{S}$), in the Central Valley, while Concepción is a coastal city located 500 km further south ($\sim 37^{\circ}\text{S}$). Both cities have similar average daily temperatures in winter, but different wind speeds and directions. The wind roses are shown in Figure 2 for the heating period considered in this study: from May 1 till September 30.

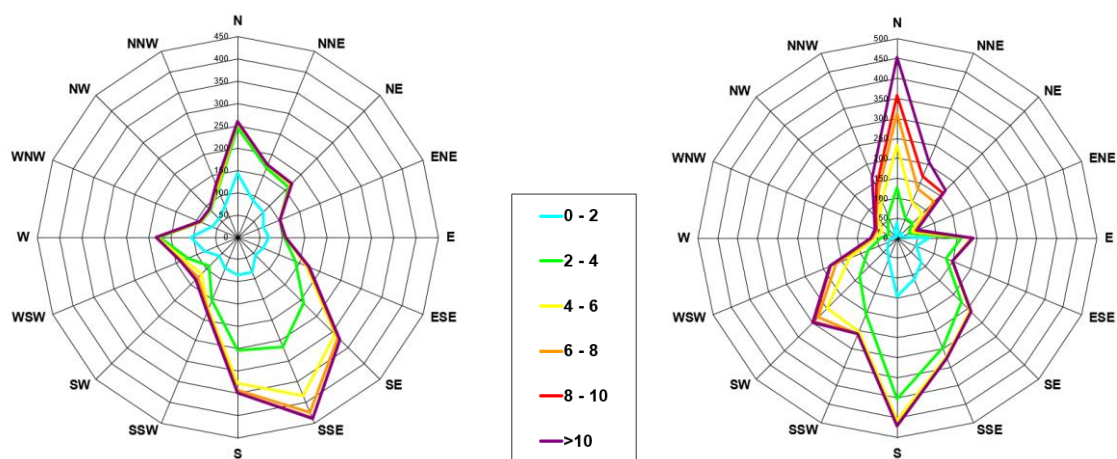


Figure 2: Wind roses for the Santiago (left) and Concepción (right) climates (wind speed in m/s).

2.3 Exhaust ventilation system

A mechanical exhaust ventilation system with constant airflow is assumed. Each bedroom and the living room are equipped with supply vents (also called ‘inlet vents’ or ‘trickle vents’) sized to provide 25 m³/h per person (category II in EN16798-1) (CEN, 2019) at 10Pa, considering two adults in the master bedroom, two children in the second bedroom and three people in the living room. The air is exhausted in the bathroom and in the kitchen with a total airflow equal to the total airflow supplied by the vents, in order to have a balanced ventilation system. As a result, the supplied airflow rates are: 50 m³/h for bedroom 1, 50 m³/h for bedroom 2, 76 m³/h for the living room; the exhaust airflow are: 50 m³/h in the bathroom and 126 m³/h in the kitchen. The location of the supply vents and exhaust fans is shown in Figure 1.

2.4 Model and assumptions

The simulations in this study used the multizone indoor air quality and ventilation analysis program CONTAM to evaluate the airflows, contaminant concentrations, and occupant exposure in the investigated building. It requires numerous input data to represent the elements of the building model, including air leakage paths (cracks, windows, doors), ventilation system elements (fans, vents), contaminant sources, etc. The main input variables are given below. A 5-minute timestep was used for the calculation and 15 minutes for the outputs.

In the absence of a detailed study of the distribution of air leakage in Chilean houses, it was assumed that air leakage is uniformly distributed over all vertical walls exposed to the ambient environment. Airflow paths were located at 3 different heights of each wall - top, middle and bottom - and modelled using the power law model with a flow exponent of 0.65. Three levels of envelope airtightness, expressed as air exchange rate at 50Pa (n_{50} -values), were considered: 10h⁻¹ corresponding to the mean value for recently built houses in Chile, 5h⁻¹, which is the current requirement applied in some cities where *Air Quality Management Plans* are in force, and 0h⁻¹ as an ideal case. Interior doors were modelled based on a two-way flow model when open, and a 1cm high air gap under the door when closed. Supply vents were modelled as a one-way flow using a powerlaw with exponent n equal to 0.5. Figure 3 illustrates the developed CONTAM model.

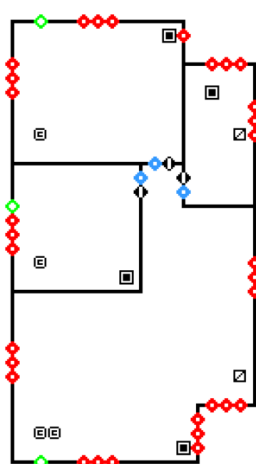


Figure 3: CONTAM model.

The wind pressure on each building surface was calculated using wind pressure coefficients from the Swami and Chandra model (Florida Solar Energy Center, 1987) and a wind speed

modifier coefficient to account for ‘suburban’ terrain. A constant indoor air temperature of 20°C was assumed.

The carbon dioxide emission rate from human respiration was calculated according to Persily (Persily & de Jonge, 2017), considering two 40-year-old adults, and 5- and 10-year-old children. The average values were: 18 L/h and 14L/h for the adults and children when they are awake, and 12 L/h and 8 L/h when they are asleep.

Due to the lack of data at the national level, a daily occupancy profile was developed, specifying the location and activity of each household member in the dwelling at each timestep, as shown in Figure 4. A permanent occupation of the dwelling by family members was assumed.

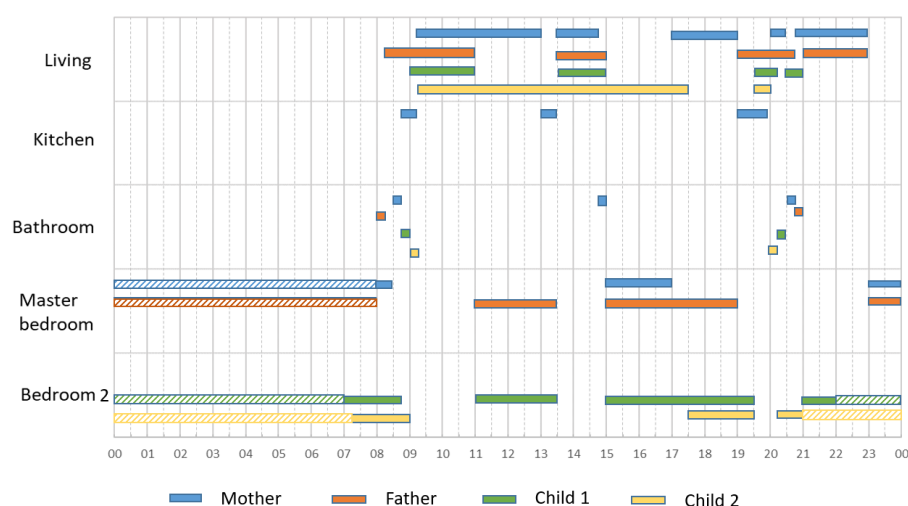


Figure 4: Occupancy profile.

2.5 Indoor Air Quality criteria

The evaluation of the performance of the ventilation system is based on the outdoor (fresh) airflow rates (AR) obtained in each room of the dwelling and the occupant’s exposure to carbon dioxide. Specifically, two CO₂-related indicators commonly used in performance-based approaches were used in this study:

- The cumulative exceeding exposure above 1000 ppm, assuming an outdoor concentration of 400 ppm
- The percentage of time spent in four CO₂ concentration classes (EN16798-1): < 950 ppm, 950-1200 ppm, 1200-1750 ppm, > 1750ppm.

Note: All average AR values mentioned in this paper are calculated per room based on all hours (occupied and unoccupied) of the heating period.

3 RESULTS AND DISCUSSION

3.1 Airflow rates

Santiago

Figure 5 illustrates the average AR over the heating period for the living room (‘Liv’), the master bedroom (‘bedr.1’) and the children’s bedroom (‘bedr.2’). When all interior doors are open, the average ARs are very close to the design values for a perfectly airtight house ($n_{50}=0$ h⁻¹): 49 m³/h for both bedrooms and 77 m³/h for the living room. The instantaneous AR (15-minute timestep) over the entire heating period fluctuates around the average values due to the effects of natural driving forces, mainly the wind forces, as shown in Figure 6. The effect of air

infiltration ($n_{50}=5$ and 10 h^{-1}) through the building envelope is different depending on the type of room. The living room is more affected by air infiltration than the bedrooms due to its higher heat losses area. In addition, the wind coming mainly from the south and southeast generates an overpressure on the facades of the living room, which explains the increase of the total fresh airflow with respect to the n_{50} for this room. On the contrary, the air infiltration for bedroom 2 represents a lower fraction of the total fresh air (infiltration + ventilation), and this room is mostly exposed to under pressure due to the wind effects. Consequently, the total outdoor air supply is drastically reduced compared to the design value: from $50 \text{ m}^3/\text{h}$ to $28 \text{ m}^3/\text{h}$ on average, when $n_{50}=10 \text{ h}^{-1}$. A higher variation of the instantaneous AR is observed for a leaky building than for an airtight one (Figure 7 versus Figure 6).

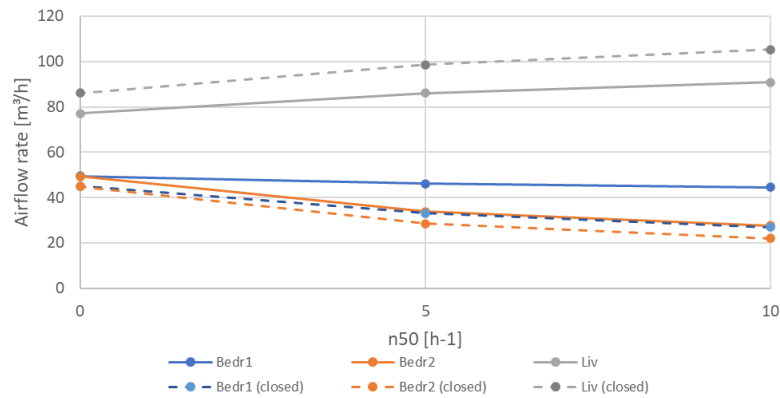


Figure 5: Average airflow rates in the living room and bedrooms over the heating period. Solid lines indicate the case with open interior doors and dotted lines the case with closed doors.

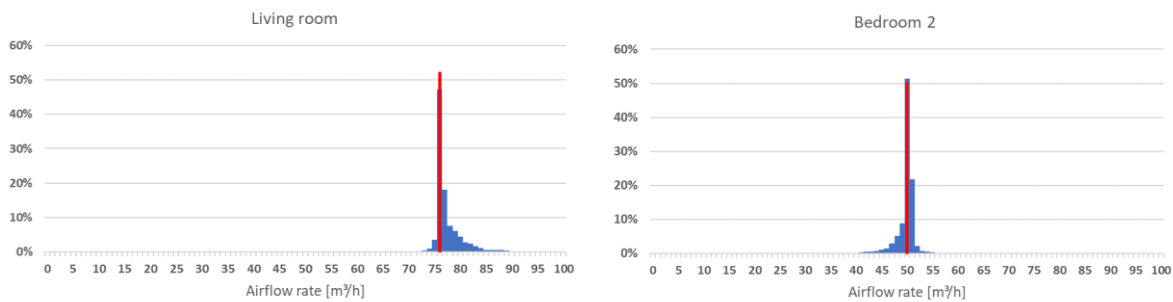


Figure 6: Frequency distribution of the outdoor airflow rates in the living room (left) and bedroom 2 (right). Perfectly airtight house, open interior doors. Vertical red line indicates the design airflow rate.

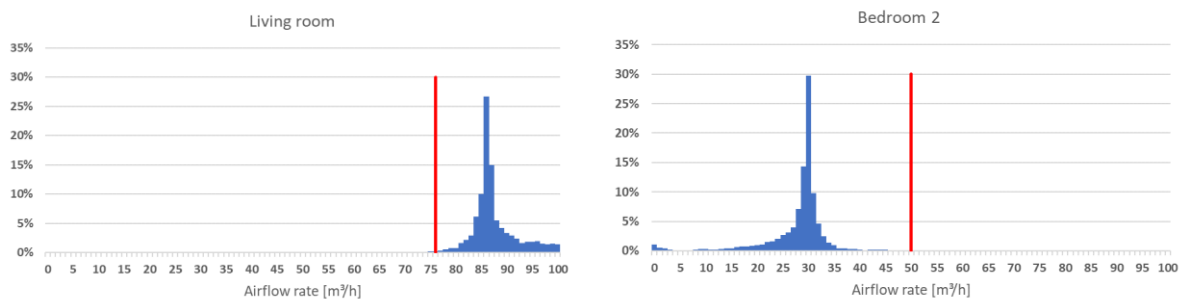


Figure 7: Frequency distribution of the outdoor airflow rates in the living room (left) and bedroom 2 (right). Leaky house ($n_{50}=10 \text{ h}^{-1}$), open interior doors. Vertical red line indicates the design airflow rate.

When all the interior doors are closed, the above effects are further accentuated. For the house under analysis, the interior doors of the two bedrooms create an additional air resistance in comparison with the living room, which facilitates the supply of air through the openings of the living room (supply vent and cracks). The average AR for bedroom 2 is only 22 m³/h at n₅₀=10 h⁻¹, less than half of the nominal airflow.

Concepción

Figure 8 shows the average AR over the heating period for the living room, master bedroom and children's bedroom. The trends observed for the living room and bedroom 2 for the climate of the city of Concepción are similar to those of the city of Santiago. However, the average ARs are higher for bedroom 1, because it is more exposed to winds – sometimes of high speed – coming from the north.

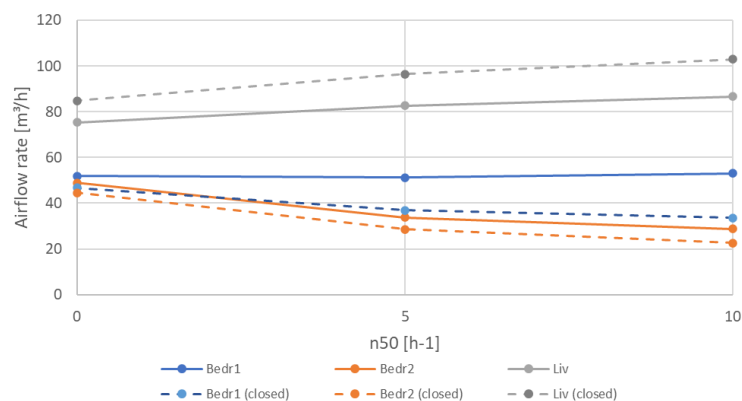


Figure 8: Average airflow rates in the living room and bedrooms over the heating period. Climatic data of Concepción. Solid lines indicate the case with open interior doors and dotted lines the case with closed doors.

In the cases simulated so far, a fixed orientation was assumed with the bedroom 1 facing north. Additional simulations were performed for other building orientations. Figure 9 illustrates the effect of the building orientation on the average AR in each room. Variations of 22%, 38%, and 7% are observed for Bedroom 1, Bedroom 2, and Living room, respectively.

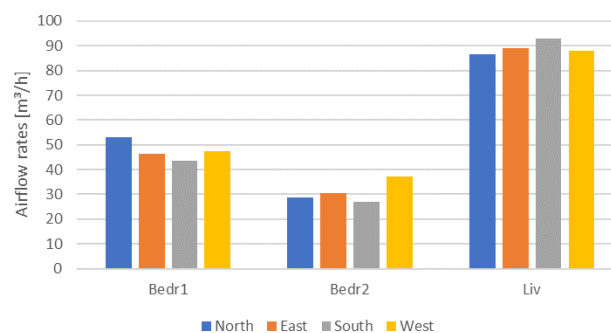


Figure 9: Effect of the building orientation on the average airflow rates. Orientation indicated in the legend of the chart refers to the bedroom 1 orientation.

3.2 CO₂-based indicators

Only the results for Santiago are presented, but the results are similar for the climate of Concepción. The cumulative exceeding exposure above 1000 ppm during the entire heating period is given in Figure 10 for the father and child₁. We also plotted the percentage of time spent in the four CO₂ concentration classes specified in EN16798-1 for the three levels of airtightness, with the interior doors open and closed (Figure 11).

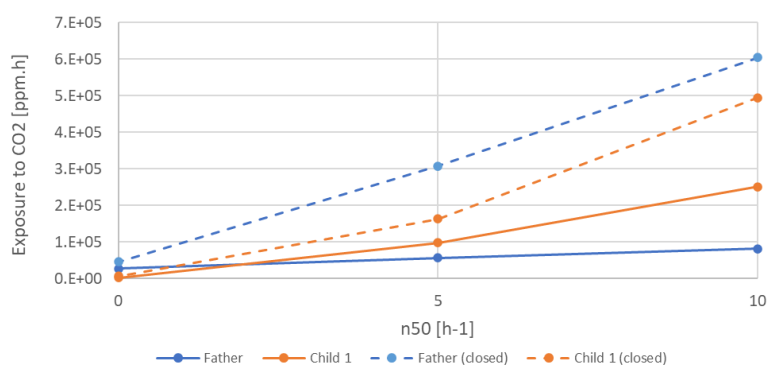


Figure 10: Cumulative exceeding exposure to CO₂ for the father and child₁.

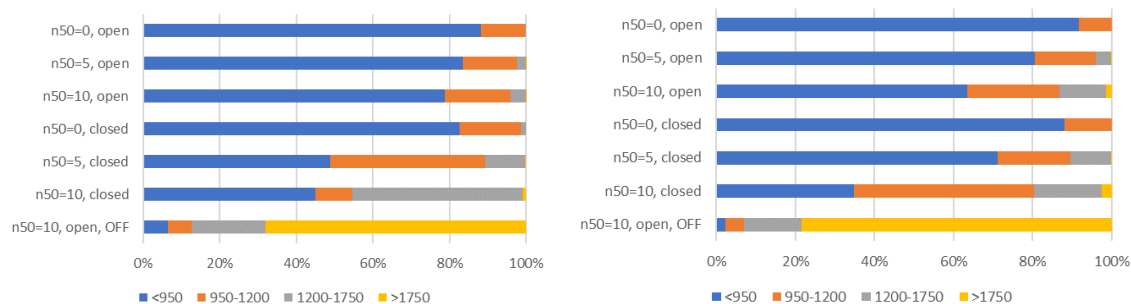


Figure 11: Percentage of time spent in four CO₂ concentration (ppm) classes for the father (left) and child₁ (right).

The decrease of the supplied airflows in both bedrooms for a leaky house leads to a significant increase of the CO₂-exposure for both father and child₁. The highest exposure values are observed for the least airtight house (n₅₀=10h⁻¹) with closed doors, which is consistent with the trends found for the airflows. In this case, the father and the child spent only 45% and 35% of their time, respectively, in an indoor space with a CO₂ concentration lower than 950 ppm, while the ventilation system was in continuous operation. On the other hand, a very good airtightness (n₅₀=0h⁻¹ in our study) makes it possible to provide the design values of the airflows most of the time and, consequently, to maintain the CO₂ concentration below 950 ppm during 92% of the time for child₁ when the doors are open and 88% when they are closed. As a basis for comparison, the case of a poorly airtight house (n₅₀=10h⁻¹) with open doors was also considered, but this time without any exhaust ventilation system (bottom bar in the figure). In this case, the indoor air quality is not guaranteed at all, as the occupant is exposed to CO₂ concentrations above 1750 ppm most of the time.

4 CONCLUSION

This study has shown the significant effect of the building airtightness and the natural driving forces, mainly the wind effect, on the performance of a mechanical exhaust ventilation system with constant airflow rate in a representative social house in Chile. For the house investigated in this research and considering a n_{50} -value of 10h^{-1} , the supplied airflow in the living room is increased by 17% on average compared to a perfectly airtight house, while in one of the bedrooms it is drastically reduced to almost the half of the value. If all the interior doors in the house are closed, the effect is even more pronounced. The decrease in the supplied airflows in the bedrooms leads to a significant increase in the CO_2 -exposure of the occupants. In the most unfavourable case analysed – n_{50} of 10h^{-1} with closed interior doors – the child of the family spent only 35% of his time in an indoor environment with a CO_2 concentration below 950 ppm. These results underline the need to work also on improving the airtightness of social houses for a better operation of the exhaust ventilation system.

5 ACKNOWLEDGEMENTS

This work was funded by the National Research and Development Agency (ANID), Chile, under research grant FONDECYT 1221666. The authors also gratefully acknowledge the research support provided by CEDEUS, ANID FONDAP 1522A0002. The paper was also developed as part of the Ph.D. program at Ghent University.

6 REFERENCES

- CEN. (2019). *EN 16798-1:2019, Energy performance of buildings - Ventilation for buildings - Part 1: Indoor environmental input parameters for design and assessment of energy performance of buildings addressing indoor air quality, thermal environment, lighting and acou.*
- de la Barrera, F., Rivera, M. I., Barraza, C., Durán, C., & Pavez, J. (2021). La Temperatura Importa: Confortabilidad De La Vivienda Social En San Pedro De La Costa 1. *Síntesis de Investigación*. <https://doi.org/10.7764/cedeus.si.13>
- Florida Solar Energy Center. (1987). *Procedure for Calculating Natural Ventilation Airflow Rates in Buildings*.
- Gonzalez-Caceres, A., Bobadilla, A., & Karlshøj, J. (2019). Implementing post-occupancy evaluation in social housing complemented with BIM: A case study in Chile. *Building and Environment*, 158(May), 260–280. <https://doi.org/10.1016/j.buildenv.2019.05.019>
- INN. (2022). *NCh3309, Ventilación - Calidad de aire interior aceptable en edificios residenciales - Requisitos*.
- OECD. (2014). *Chile's Pathway to Green Growth: Measuring progress at local level*.
- Persily, A., & de Jonge, L. (2017). Carbon dioxide generation rates for building occupants. *Indoor Air*, 27(5). <https://doi.org/10.1111/ina.12383>
- RedPE. (2019). Acceso equitativo a energía de calidad en Chile. Hacia un indicador territorializado y tridimensional de pobreza energética. In *Documento de trabajo N°5*.

Metal Oxide Semiconductor sensors (MOS) for measuring Volatile Organic Compounds (VOC) - performance evaluation in residential settings

Jakub Kolarik^{*1}

¹ *Department of Civil and Mechanical Engineering,
Technical University of Denmark
Brovej 118
2800 Kgs. Lyngby, Denmark
Corresponding author: jakol@dtu.dk

ABSTRACT

Metal Oxide Semiconductor (MOS) sensors measuring Volatile Organic Compounds (VOC) seem to be an obvious step towards broadly available Demand Controlled Ventilation (DCV). The previous research shows that MOS VOC sensors can detect high pollution events such as cleaning, painting, or high occupation density. These abilities seem to make MOS VOC sensors suitable to complement ventilation control systems, especially concerning residential ventilation. However, several questions come from the practice: “Are the MOS VOC sensors reliable and stable enough to be applied in practice?” “Are there any benefits concerning energy efficiency and indoor environmental quality?” They remain unanswered. Studies on the long-term performance of MOS VOC sensors exposed to real-life environments are lacking. Some producers test their sensors in a laboratory environment, but such data are often not publicly available. Data about the influence of ventilation control based on MOS VOC sensors on energy efficiency are also missing. The present paper reports first results from a project aiming to answer aforementioned questions having following objectives: investigate performance of MOS VOC sensors exposed to a typical residential environment. Determine sensor properties – sensitivity, linearity, hysteresis by comparing their signal with a reference measurement conducted by PID (Photo Ionization Detector). Discuss the suitability of the sensors for control of residential ventilation. We measured in a typical Danish row house occupied by a family of four. We used two sets of three commercially available sensors installed two locations-bedroom and kitchen. PID gas analyzer served as a reference measurement. The results show that all tested sensors were able to indicate the pollution events like human presence or cleaning. There was a fair agreement among the signals of the two tested sensors. These sensors produced also signals, which were in a clear relationship to the reference measurements. In the opposite, the signal from the third sensor could be clearly related neither to the reference signal nor to the other two tested sensors. This is potentially problematic for sensor’s application for ventilation control.

KEYWORDS

Residential Ventilation, Volatile Organic Compounds, Metal Oxide Semiconductor, Indoor Air Quality

1 INTRODUCTION

Today's energy efficient buildings are airtight and need therefore an efficient ventilation to maintain high quality of indoor air. Smart ventilation (Durier et al. 2018) allows for continuous adjustment of ventilation airflow in time, and optionally by location, to provide the desired indoor air quality while minimizing energy consumption. The smart ventilation is slowly but steadily finding its way into new or renovated houses across Europe, the USA and beyond. It is mostly the specific sub-type of smart ventilation, so called Demand Controlled Ventilation (DCV), which is becoming increasingly popular even in residential sector where we would not expect it to be applied some decades ago. It is mostly due to technological advances in the field building control (digital and internet enabled controllers, EC fans) as well as due to the advances Indoor Air Quality (IAQ) sensing. Sensors measuring "demand" variables like temperature, concentration of CO₂ and Volatile Organic Compounds (VOC) or relative humidity are produced cheaper and in compact dimensions. Metal Oxide Semiconductor (MOS) sensors for measuring Volatile Organic Compounds (VOC) represent such sensors (Herberger and Ulmer 2012). They offer possibility to account for air pollution related to human presence and activities as well as other pollution sources that worsen IAQ. Considering indoor air quality, it is a clear advantage. Outdoor air supply rate is increased also when pollutants originating from cleaning, cooking etc. are detected. Other advantages include low energy consumption, small dimensions and durability. Moreover, Herberger et al. (2010) developed sensor that uses data collected by Burdack-Freitag et al. (2009) correlating the measured VOC signal with human emission of CO₂. Consequently, the sensor output is converted to so-called CO₂ equivalent concentration. As "CO₂ concentration" had become known to the public as an indicator of IAQ, the intention was that the sensor signals could be more easily interpreted by building occupants. These arguments speak in favour of MOS VOC sensor technology. However, there are also, several studies, such as Won and Schleibinger (2011), which state that currently available MOS VOC sensors suffer from several drawbacks, mainly related to cross sensitivity to relative humidity, low resolution and inability to measure concentration of individual chemicals. Despite that, ventilation producers offer VOC controlled DCV also for residential applications. Studies evaluating performance of MOS VOC sensors in the field are sparse. Kolarik (2014) showed observed agreement in need for increased ventilation expressed by VOC or CO₂ sensor during 49% of occupied time. During 11% of occupied time it was only VOC sensor that indicated need for increased ventilation. Despite the fact that the study considered office spaces, it indicated that simple replacement of CO₂ sensor by VOC sensor would lead to significantly longer time with high airflows. Challenges related to direct replacement of CO₂ sensors with VOC sensors were illustrated in a field study by De Sutter et al. (2017). The results showed notable increase of ventilation rates related to the sharp peaks in the VOC signals when the same set point was used for both CO₂ and VOC based control of ventilation. The authors suggested a correction algorithm that would filter the VOC signal; however, its application was not practically demonstrated. Finally, yet importantly, besides the publication by Fahlen et al. (1992) and recent publication by Alonso et al. (2021), there are no publications dealing with evaluation of MOS VOC sensors performance characteristics both in laboratory and in the field. An objective of the present paper was to examine MOS VOC sensors during operation in realistic residential environment. Determine their properties – sensitivity, linearity, hysteresis by comparing their signal with a reference measurement conducted by PID (Photo Ionization Detector) and discuss their suitability for control of residential ventilation.

2 METHODS

2.1 Investigated sensors

Table 1 summarizes the technical parameters of tested sensors. We investigated three different sensors from established manufactures. We have chosen the sensors based on previous experiments (Kolarik et al. 2018). We purchased two specimen of each sensors and created two measuring sets. We integrated the sensors into one casing with common power supply. Arduino board with Wi-Fi module ensured wireless transfer of the measured data into a laptop equipped with the Lab View software connected to the same wireless network. The data logging interval was set to 1 minute. We used a portable photo-ionization (PID) gas detector Photo Check TIGER to conduct reference measurements of Total Volatile Organic Compounds (TVOC) concentration. We performed a custom calibration of the PID gas detector 100 ppm of isobutylene (zeroing on zero gas mixture) before the measurements. The TVOC concentrations measured by the PID device were thus representing isobutylene equivalents. Besides the MOS VOC signals, we also monitored standard indoor environmental quality (IEQ) parameters: room temperature (± 0.3 °C 5-60 °C), relative humidity (± 2 % RH 20-80 % RH) and CO₂ concentration (non-dispersive infrared, 400-2000 ppm, ± 30 ppm ± 3 % of reading). We used internet connected commercial indoor climate monitors providing measurements in 5-minute intervals. In the case of comparison between MOS VOC signals and the IEQ variables, we averaged the 1-min MOS VOC data into 5-min intervals.

Table 1: Technical parameters of investigated sensors based on manufacturer data sheets

Abbreviation	A	B	C
Output (units)	VOC index [-] ^(a)	Voltage [V]	TVOC eq. [ppb] ^(b) CO ₂ eq. [ppm]
Sensing range	0 – 500 VOC index points; 0 – 1000 ppm ethanol equivalents	0 – 3.0 V DC; 1 – 30 ppm H ₂	0 – 29206 ppb TVOC eq. 400 – 32768 ppm CO ₂ eq.
Measuring accuracy	± 15 VOC index points	NA	NA
Measurement interval/ response time	NA/ < 10 s	NA	NA
Power Supply	1.7-3.6 V DC	4.9-5.1 V DC	1.8-3.6 V DC
Communication	I ² C bus	0 – 3.0 V DC	I ² C bus
Warm up time	NA	NA	20 min
Operation temperature range	-20 – 55 °C	-10 – 50 °C	-40 – 85 °C
Operation humidity range	0 – 80 %, non-condensing	NA	10 – 95 %, non-condensing

(a) A built in proprietary algorithm processes a raw signal of the sensor, corresponding to the logarithm of the sensor resistance a “VOC index”. The index value 100 refers to the typical concentration over 24 h period.

(b) The sensor processes the raw signal into so-called TVOC and CO₂ equivalents. The algorithm is proprietary, the manufacturer states that CO₂ equivalents are determined based on the relationship between human production of VOC (bioeffluents) and CO₂.

2.2 Data processing

As each studied sensor provided different output signal, we normalized these signals to avoid the influence of the absolute value of each observation. Each observation was normalized against the difference of its maximum value and minimum value (so called min-max normalization), as shown in Equation (1):

$$y = (x - \min(x))/(\max(x) - \min(x)) \quad (1)$$

Where x is the i -th observation in the measured data and y is i -th normalized observation for the particular sensor signal. We used only the normalized data in our analyses.

According to Fahlen et al. (1992), the sensor properties can be described by so called characteristic curve. Fahlen et al. (1992) determined the curve exposing the sensor to the set of steady state concentrations of a known VOC in ascending and descending order. It is thus a linear relationship between known-reference signal and the signal from evaluated sensor. In the present paper, we established the characteristic curve by fitting the linear regression model to the data where with PID measurements as independent and respective MOS VOC data as dependent variable. Thus, the slope of the relationship represented sensor's sensitivity. The R^2 value for the linear model indicates the linearity of the sensor. To evaluate hysteresis, we selected one-day measurements from the data. We fitted linear regression model to the build-up and decay separately. Consequently, we express hysteresis as a mean distance from the two regression lines. To determine such distance, we used the obtained linear models to predict MOS VOC signal for three distinct levels of the reference signal (150 ppb, 250 ppb and 350 ppb isobutylene equivalent). The mean difference between such predictions for build-up and decay determined the hysteresis.

2.3 The test house and the measurement period

We have installed the sensor sets in a typical Danish row house occupied by a family of two adults and two children (elementary school age). We placed the sensor sets at two locations—a kitchen/dining room open to a living room and in the main bedroom (Figure 1). In the present paper we report on a part of the total measuring period. Reported measurements include September–November 2021 and February–March 2022. The whole dataset covers almost one year of measurements.

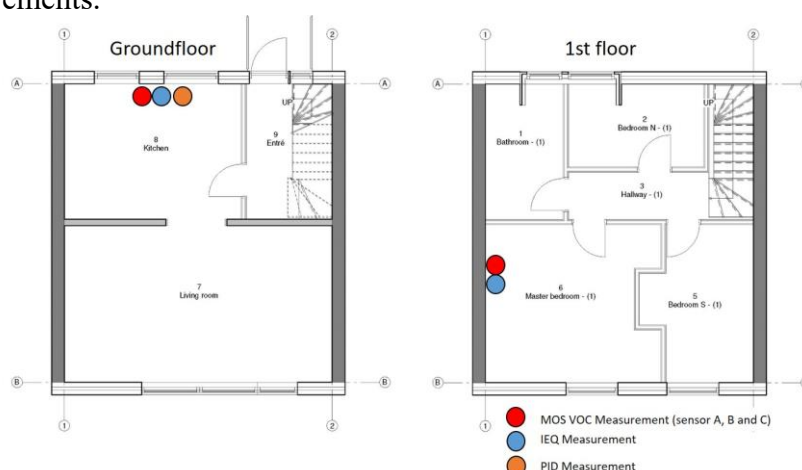


Figure 1: Placement of the sensors

3 RESULTS AND DISCUSSION

3.1 Long term data

Figure 2 gives an example of not normalized sensor signals from the kitchen. The figure illustrates a typical variability of the signal during periods when the house was empty and consequently occupied. There is a clear difference in the amplitude of the signal regardless the type of the sensor.

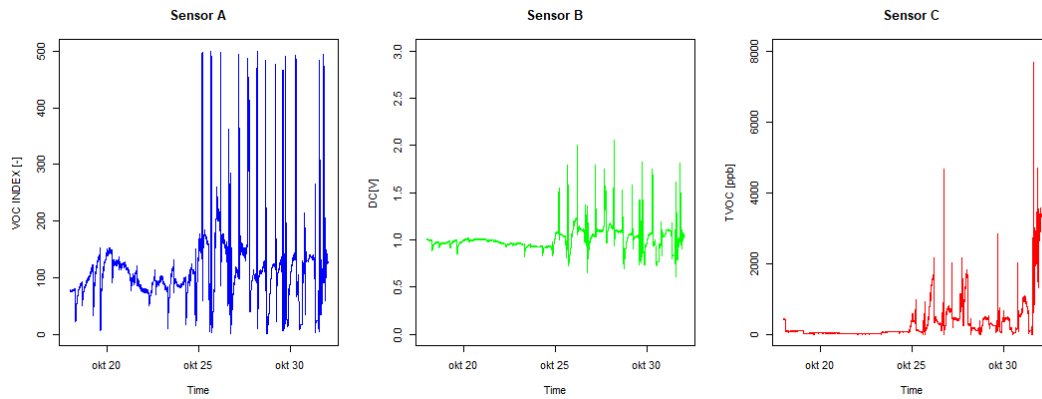


Figure 2: Absolute signal of the tested MOS VOC sensors placed in the kitchen for two weeks in October 2021 (the house was unoccupied during the first week)

Figure 3 shows the same period as Figure 2, but displaying normalized data. Using such interpretations it is possible to see that despite the fact that the trend in amplitude of the signals is the same for empty and occupied house, there is a clear difference in character of the signal. Signal from sensor C is almost zero when the house is empty, on the contrary, signals from sensors A and B still represent some development and despite the difference in amplitude of the build-ups and delays, there seems to be an agreement between these two signals. During the occupancy period, the sensor A seems to have largest fluctuations.

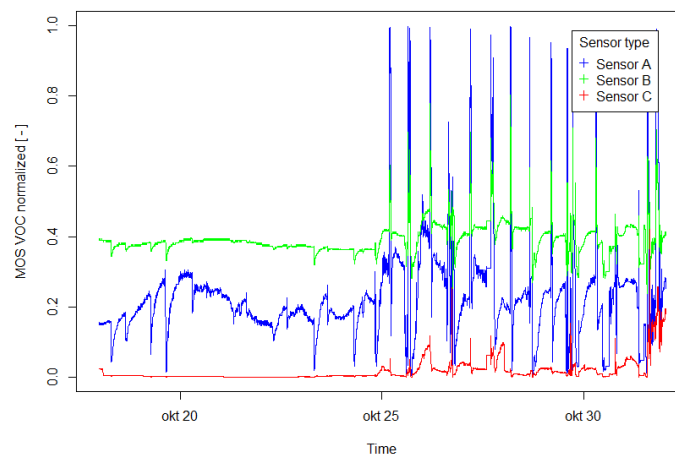


Figure 3: Normalized signals of the tested MOS VOC sensors placed in the kitchen for two weeks in October 2021 (the house was unoccupied during the first week)

Figure 4 represents a cross plot of normalized signals of the MOS VOC sensors placed in the kitchen for the same period as presented in Figures 2 and 3. It is clear from the plots, that there was a somewhat consistent relationship between responses of sensor A and B. Such relationship did not seem to exist comparing sensors A and B with sensor C. The Figure 4 shows only two weeks, but the patterns were similar through the analysed period. Analysis of the exact character of the relationship between sensor A and B is out of the scope of this paper, as it would require removal of the autocorrelation contained in the data caused by high frequency of sampling (Alonso et al. 2021).

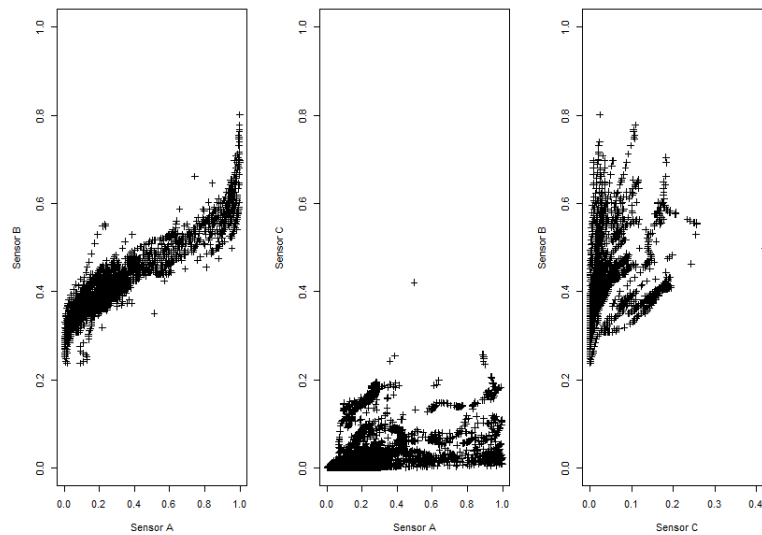


Figure 4: Cross-plot of normalized signals of the tested MOS VOC sensors placed in the kitchen for two weeks in October 2021 (the house was unoccupied during the first week)

3.2 Sensor characteristics

The Figure 5 represents characteristic curves determined using measurements from period of 7.3.2022 – 12.3.2022. The figure depicts the linear regression fit to the data in the case of sensor A (blue) and sensor B (green). In the case of sensor C, the variance explained by the linear model was too low to consider linear relationship between sensor C signal and the reference PID signal. Table 2 summarizes the sensitivity values and R^2 values of the linear regression models for particular sensors. It is clear from the table as well as from the Figure 5, that the response of the sensor C did not show any meaningful relation to the reference signal. Therefore, the sensor C seemed not to represent the indoor air quality changes in the house.

Table 2: Summary of slope and variance explained by characteristic curves

	Sensitivity (95% conf. int.)	R^2
Sensor A	2.497e-03 (2.432e-03, 2.562e-03)	0.40
Sensor B	1.383e-03 (1.350e-03, 1.416e-03)	0.44
Sensor C	7.413e-05 (2.042e-05, 12.78e-05)	0.0007

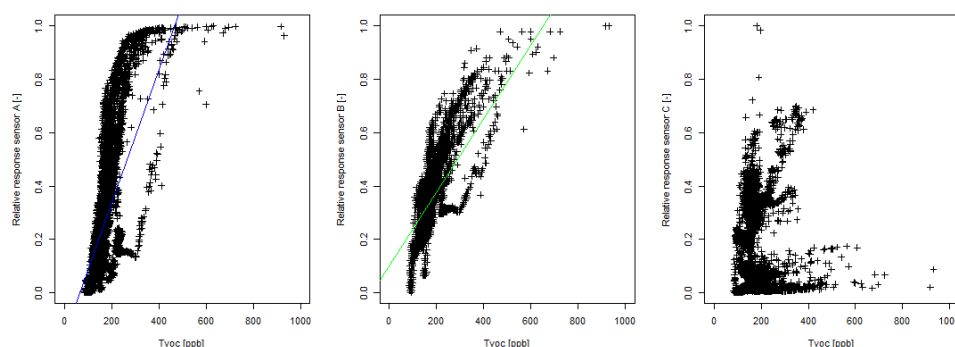


Figure 5: Characteristic curves for tested sensors determined for period of continuous parallel measurements with MOS VOC sensors and the PID monitor (7.3.2022 – 12.3.2022); regression line is not depicted for sensor C as the R^2 value does not indicate linear relationship

Analysis of the hysteresis required separation of build-up and decay periods. This is a relatively easy task in laboratory conditions, when sensors are exposed to controlled pollution events.

However, with the field data, the analysis is more demanding. For this paper, we conducted the analysis of the sensors' hysteresis on data from one particular day, Friday 11.3.2022. After 15:00 the whole family gathered at home and started weekly cleaning of the house. This initiated excitement of the sensor signals suitable for separation of decay and build-up periods. Figure 6 shows the normalized data.

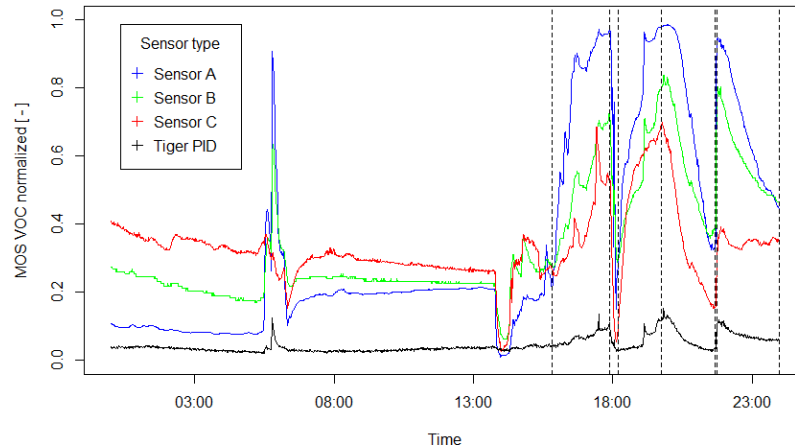


Figure 6: Data used for evaluation of hysteresis. Vertical dashed lines indicate selected build-up and decay periods during afternoon cleaning activities in the house

Figure 7 illustrates the hysteresis of the three investigated sensors for the tested period. The determined hysteresis were 0.123, 0.014 and 0.121 for sensors A, B and C respectively. The hysteresis was in general rather low, 12.3%, 1.4% and 12.1% of the measuring range, which is preferable. The sensors A and C had comparable hysteresis while sensor B showed practically no hysteresis. In the present paper, the hysteresis was evaluated only using one day measurements. In future analysis, we will analyse several days distributed through the whole dataset to determine, whether the hysteresis remained consistent. Figure 7 also shows that the relationship between the reference signal and the signal of sensor C seemed to be more consistent than when longer measurement period was considered (Figure 5).

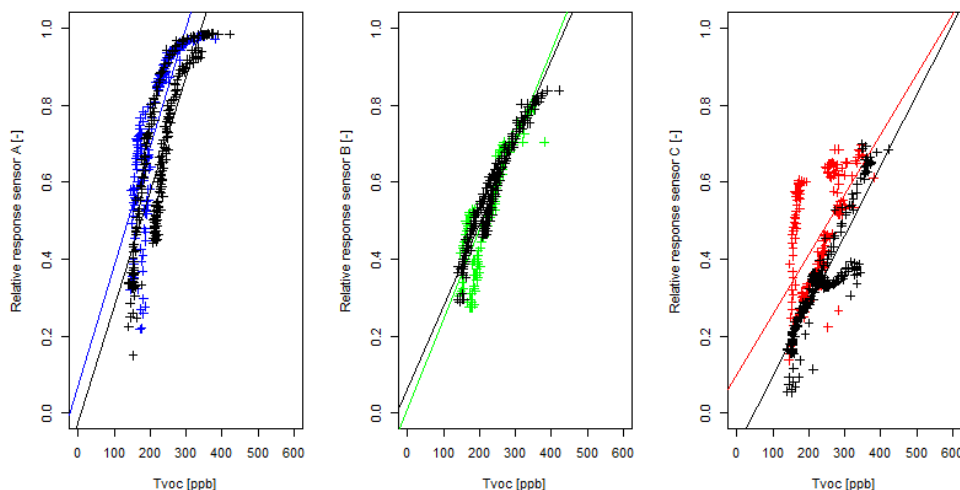


Figure 7: Separated build-up and decay periods and corresponding linear fits for the three tested sensors. Build-up is depicted in colour, decay in black

While the sensitivity determined using longer period and during one day measurements was comparable for sensors A and B, with sensor C the sensitivity differed significantly. This

indicates that the sensor C had unstable behaviour when exposed to the pollution emitted in the kitchen. The identification of reasons for this requires further analysis.

3.3 Relation between MOS VOC and CO₂ measurements, usability for control

Besides TVOC signal, offered the Sensor C also a so-called CO₂ equivalent. The Figure 8 offers a comparison between CO₂ and CO₂ equivalent signals measured in the kitchen and bedroom. It is clear, that while in the bedroom the CO₂ equivalent signal followed the pure CO₂ measurements rather closely, this was not the case in the kitchen. Human bioeffluents were the main pollution source in the bedroom, while the kitchen was the place most of the other pollutants were emitted. This was even more pronounced due to the fact that the kitchen is directly connected to the living room and represents therefore the area where the occupants of the house spent majority of time besides sleeping. It seems from the obtained data, that in the cases, where the sensor C got excited by stronger pollution event, its CO₂ equivalent signal drifted from the real CO₂ values. This would, of course represent a challenge with respect to the ventilation control. De Sutter et al. (2017) observed “overventilation” in connection with the use of CO₂ equivalent signals in their study. Further analysis of the data from the present study will focus on relationship between CO₂ and CO₂ equivalent signals for all measured data.

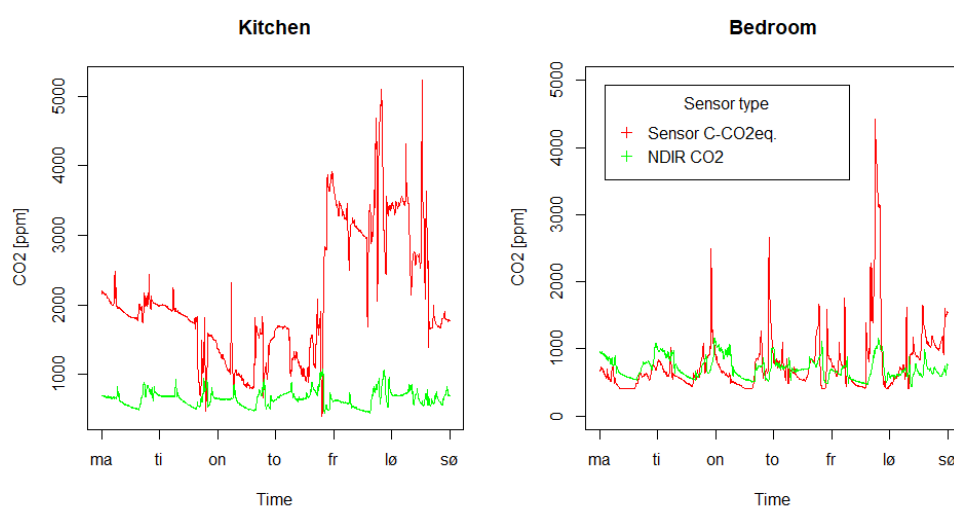


Figure 8: Comparison of CO₂ and CO₂ equivalent signal for measurements in the kitchen and bedroom

All tested sensors demonstrated ability to react on pollution events in the house. The signal from sensor C (“TVOC” signal or CO₂ equivalent) seemed to be least correlated to the reference PID measurements in the kitchen. However, in the bedroom, sensor C demonstrated rather good agreement with CO₂ measurements. As the absolute signals produced by particular sensors were different, the problem of selection of the right set point value would be apparent if they should be used in a control loop.

Utilization of PID instrument as a reference measurement in this study had its limitations. The instrument is primarily suitable for measurement of higher TVOC concentrations. As it can be seen in Figure 6, under normal pollution patterns in the house the normalized PID signal stays about 20% of the measurement range established from the whole dataset. As PID technology is also based on a relative measurement, its utilization for determination of the MOS VOC sensor characteristics has limitations. More suitable would be application of more precise analytical method like Reaction-Time of Flight-Mass Spectrometer (PTR-ToF-MS) Kolarik et al. (2018).

4 CONCLUSIONS

- All three tested sensors were able to indicate the pollution events.
- Two of the sensors had comparable behaviour in terms their sensitivity determined using reference PID measurements. There was also an obvious cross-relation between their output signals. This indicates that both sensors would behave in similar manner when used for IAQ control. There was however a difference in absolute values of the sensitivity and thus in the amplitude of their response, this needs to be taken into account in the case of their use of control.
- The third tested sensor presented somewhat unclear relationship to the reference measurements and further analysis is needed to analyse causes of such behaviour. In the analysed data, the sensor signal did not correspond to the TVOC concentrations represented in isobutyl equivalents.
- The investigated sensors had small hysteresis, which is preferable. The analysis was however conducted on relatively small sample of measurements. Analysis of broader range of build-up and decay periods is needed to confirm the results.
- The CO₂ equivalent signal corresponded to pure CO₂ measurements in the case of measurements in the bedroom. In the kitchen where the human bioeffluents were not the main pollution source, there were large discrepancies. This is not necessarily a problem for the ventilation control, but careful choice of the set point would be needed to avoid unnecessary ventilation.
- In general the results of the study indicate, that the MOS VOC sensors represent a considerable alternative to currently used sensors. This however requires that their characteristics are properly considered in control algorithms.
- Recent development in low cost sensors measuring particulate matter (PM) brings the usage of MOS VOC sensors in the new perspective. As PM is representing far the highest health risk for humans, one can expect, that low cost PM sensors will soon make their way into the residential ventilation control. However, this does not necessarily mean the disqualify VOC sensors. The future research should focus on controls that effectively combine the two types of sensors.

5 ACKNOWLEDGEMENTS

The research was supported by Bjarne Saxhofs Fond, Denmark.

6 REFERENCES

Burdack-Freitag A, Rampf R, Mayer F, Breuer K (2009) Identification of anthropogenic volatile organic compounds correlating with bad indoor air quality. *In: Proceedings of the 9th International Conference and Exhibition Healthy Buildings 2009*, Syracuse, NY

De Sutter, R., Pollet, I., Vens, A., Losfeld, F. and Laverge, J. (2017) TVOC concentrations measured in Belgium dwellings and their potential for DCV control. *In proceedings of 38th AIVC Conference*, Nottingham, UK

Durier, F., Carrié, R. Sherman, M. (2018) What is smart ventilation? *Ventilation Information Paper n 38*, INVIE EEIG, Brussels, Belgium

Fahlen P, Andersson H, Ruud S (1992) Sensor Tests, Demand Control Ventilation Systems, *SP Report ISBN 91-7848-331-331-X*, Swedish National Testing and Research Institute, Borås, Sweden

Herberger S, Herold M, Ulmer H, Burdack-Freitag A, Mayer F (2010) Detection of human effluents by a MOS gas sensor in correlation to VOC quantification by GC/MS. *Building and Environment*, 45, 2430-2439

Herberger S, Ulmer H (2012) Indoor Air Quality Monitoring Improving Air Quality Perception. *Clean-Soil Air Water*, 40 (6), 578-585

Justo Alonso, M., Wolf, S., Jørgensen, R. B., Madsen, H., & Mathisen, H. M. (2021). A methodology for the selection of pollutants for ensuring good indoor air quality using the de-trended cross-correlation function. *Building and Environment*, 209, pp. 108668

Kolarik, J. (2014) CO₂ Sensor versus Volatile Organic Compounds (VOC) sensor – analysis of field measurements and implications for Demand Controlled Ventilation. *In proceedings of Indoor Air 2014*, Hong-Kong, China

Kolarik, J., Lyng, N. L., & Laverge, J. (2018). Metal Oxide Semiconductor sensors to measure Volatile Organic Compounds for ventilation control. *Report from the AIVC Webinar: "Using Metal Oxide Semiconductor (MOS) sensors to measure Volatile Organic Compounds (VOC) for ventilation control"*. September 4, 2018

Won, D.Y., Schleibinger, H. (2011) Commercial IAQ Sensors and their Performance Requirements for Demand-Controlled Ventilation. *Report no. IRC-RR-323*, National Research Council Canada

Towards performance-based approaches for smart residential ventilation: a robust methodology for ranking the systems and decision-making

Baptiste Poirier^{*1,2,3}, Gaëlle Guyot^{2,3}, and Monika Woloszyn³

*1 Cerema Ouest
DTT Department,
F-42000 Nantes, France*

**Corresponding author: baptiste.poirier@cerema.fr*

*2 Cerema, BPE Research team,
46, rue St Théobald,
F-38080, L'Isle d'Abeau, France*

*3 LOCIE,
Univ. Savoie Mont Blanc, CNRS UMR5271, F-73376,
Chambéry, France*

ABSTRACT

Smart ventilation which provides air renewal thanks to its variable airflows adjusted on the needs can improve both indoor air quality (IAQ) and energy performance of buildings. However, such performance gains should be quantified with performance-based approaches. In this paper, we propose to extend the performance-based approach with a robust methodology to rank the ventilation systems performance. Such a methodology could be used in a decision-making tool at the design stage of buildings. Indeed, when simulations are carried out, we generally obtain a relative range of the theoretical performances, which should be achieved for each tested ventilation strategy. Nevertheless, it does not allow to rank the ventilation systems performances and to choose the most relevant one from an overall performance point-of-view. In this work the overall performance aspect was focused on IAQ and energy performance through five IAQ - and one energy - performance indicator.

We propose in this paper a simplified approach in 3 keys steps (Figure 1) adapted from existing robust assessment methods, to achieve a robust ranking of the systems based on the aggregation of performance indicators results using Simple Additive Method (SAW). In the present work, five ventilation systems have been tested with several sets of input parameters (500 simulations). In addition, three reference scenarios for input values (low, reference, high) were used for robustness assessment. We compared the ranking calculated with 500 simulations with the ranking calculated with three reference scenarios. The objective was to assess whether the three reference scenarios are sufficient to obtain a relevant ranking of ventilation systems or if more simulations are needed to achieve this goal.

Our results showed that the aggregation of the performance indicators with the SAW method is relatively accurate compared to the performance observed individually by each indicator. Then, the calculation of the design score with the minimax regret robustness method offers a clear advantage to highlight the difference between the ventilation systems, to rank them by including the uncertainty of several simulations. In addition, we show that the use of the three reference scenarios could be sufficient to obtain a relevant ranking of the ventilation systems, in comparison with 500 simulations. However, if the number of simulations is limited, we propose to perform in priority the reference scenario, for an “optimistic performance ranking”, or the reference high scenario for a “conservative performance ranking”. Nevertheless, if there are no constraint, we encourage the decision maker to simulate at least the three reference scenarios

and ideally 500 scenarios or more. The latter reinforces the validity of the calculated design score and ranking by including the uncertainty on input parameters.

KEYWORDS

Smart ventilation, residences, indoor air quality, performance, performance-based, energy

GRAPHICAL ABSTRACT

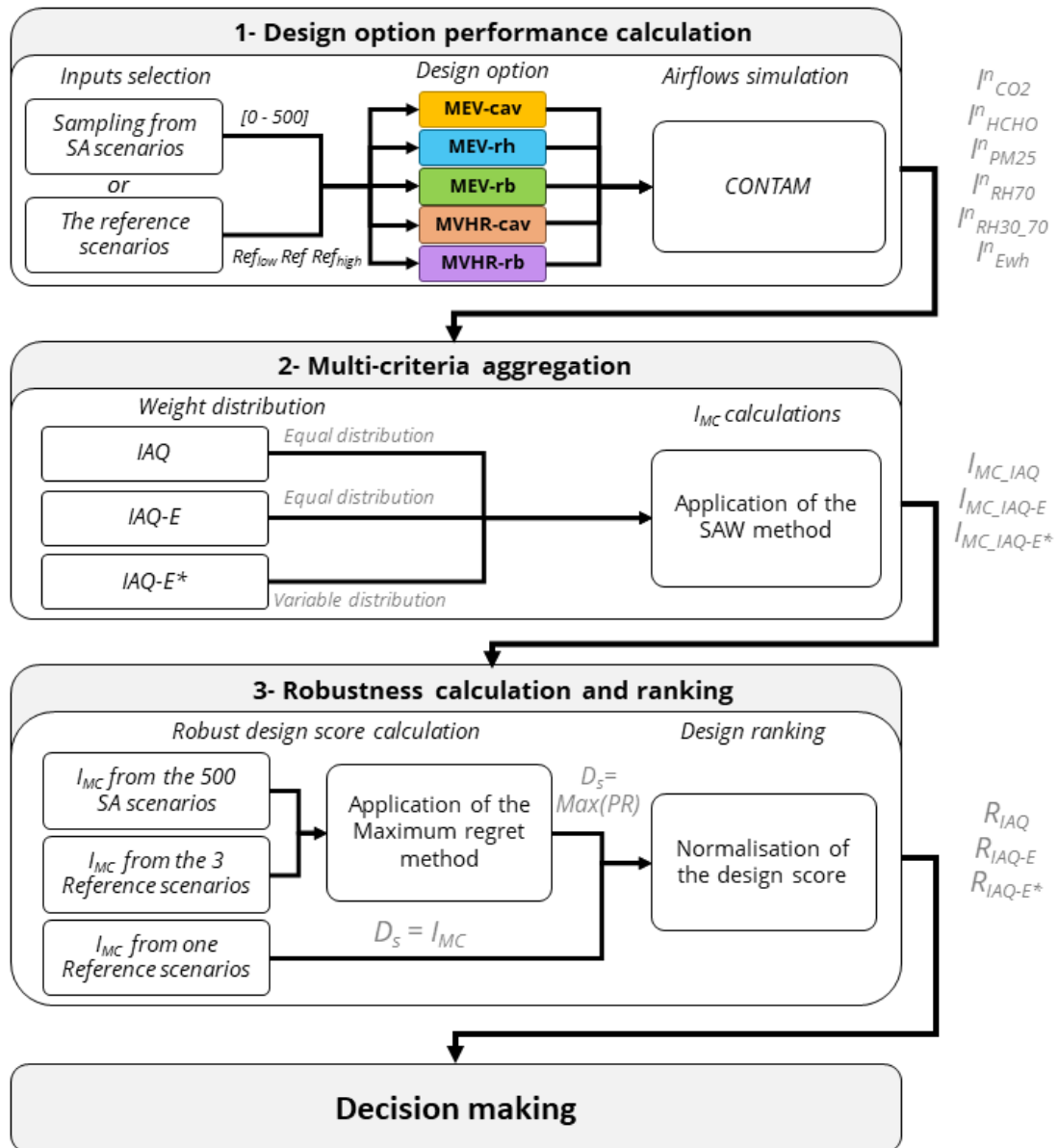


Figure 1 : Methodology for robustness calculation and ranking for decision making

1 INTRODUCTION

The assessment of ventilation performance often focuses on indoor air quality (IAQ). Nevertheless, with low energy buildings, the energy-saving potential from ventilation is becoming increasingly important. In addition, smart ventilation has been identified as a very promising way to improve both the indoor air quality and the energy performance of buildings, through the variation in time and/or place of ventilation airflows according to needs. Research efforts, such as those under in the framework of the IEA-EBC Annex 86, should make it possible to develop such smart ventilation strategies. It requires performance-based approaches in order to robustly assess the potential of gains, especially compared to more traditional constant-airflows ventilation strategies. These promising improvements need to be quantified in an overall performance way including IAQ, energy or even other relevant aspects. This paper only focusses on the IAQ and energy aspects of the overall performance of ventilation.

At the design stage, in a performance-based approach, the ventilation performance could be calculated by simulation. This assessment process consists in testing the performance of one (or several) ventilation systems according to one or (several) input scenarios; including pollutants emissions rates variations, occupant behaviours, building boundaries conditions. Due to the large possible variations in the input scenarios, we obtain a relative range of the theoretical performances. According to previous application case studies; testing IAQ or energy performance of constant and humidity controlled airflows ventilation (Poirier et al., 2022a, 2022b) ; the difference of the performances among the ventilation systems varies depending on the selected indicators. For example, differences between the ventilation systems were clearly identifiable for some indicators based on CO₂, on high relative humidity and on energy consumption. On the contrary, the performances were almost the same or very close for other indicators like the PM_{2.5} and formaldehyde exposures. Nevertheless, it does not allow to rank the ventilation systems performances and to choose the most relevant one from a global performance point-of-view.

It clearly raises the question of:

How to aggregate performance indicators and balance IAQ and energy performance assessment to provide a robust ranking of the ventilation systems?

In this paper, we propose to explore a methodology to rank the systems performance including the uncertainty from simulations; in order to complement our method for overall performance assessment (MOPA) for ventilation (Poirier et al., 2021b).

2 METHODOLOGY

As a methodology, we propose a simplified approach based on 3 keys steps to achieve a robust ranking of the systems based on performance assessment results, to help in decision making (Figure 1-Graphical abstract). These steps are based on some relevant studies on existing robust assessment methods adapted to the building sector (Kotireddy et al., 2018; Velasquez and Hester, 2013; Hoes et al., 2009; Sharma and Bhattacharya, n.d.) that seem relevant for application in the context of MOPA development.

2.1 Design option performance calculation

The first step consists in performance assessment by simulations of the different design options (D_{opt}) to be tested. In building design, several parameters could be tested, such as thermal envelope materials, compactness ratio, external shadings, building orientation, heating systems, photovoltaic panels surface, etc. (Hoes et al., 2009; Kotireddy et al., 2017; Mechri et al., 2010).

In the present work, the design options are the ventilation systems and the performance calculation were performed with multi-zone CONTAM software which have been scientifically validated (Walton and Emmerich, 1994; Emmerich, 2001). With its models, CONTAM allows to describe for example ventilation airflows with complex strategies, indoor air pollutants, occupants exposure, building airtightness and more. For this step, we based our application on the performance calculated with 2500 simulations performed in (Poirier, 2023), with a sensitivity analysis (SA) experiment using the EASI RBD-FAST method (Goffart et al., 2015; Goffart and Woloszyn, 2021). From these simulations the performance results were calculated with the following performance indicators defined in (Poirier et al., 2021b; Poirier, 2023):

I^{CO2}, Maximum cumulative CO2 exposure over 1000 ppm.

I^{HCHO}, Maximum cumulative HCHO exposure among all the occupants

I^{PM2.5}, Maximum cumulative PM2.5 exposure among all the occupants

I^{RH70}, Maximum percentage of time with RH > 70% among all the rooms

I^{RH30_70} Maximum percentage of occupant time spent with RH outside the range [30-70%]

I^{Ewh} Heat losses from total exhaust airflows calculated with equation 1

$$I_{Ewh} = H_{th} = \frac{C_{pm}}{3600} \cdot (1 - \varepsilon_{heat_{ex}}) \int q_m(t) \cdot [T_{in}(t) - T_{ex}(t)] \cdot dt \quad (1)$$

with **I_{Ewh}** the energy indicator resulting directly from H_{th} , the heat losses from exhausted air [kWh], q_m the total exhaust mass airflows in [kg.s⁻¹], C_{pm} the heat capacity of air (we used 1 kJ.kg⁻¹.°C⁻¹), $\varepsilon_{heat_{ex}}$ the heat exchanger efficiency assumed to be ideal and constant. A constant theoretical efficiency of 0.8 can, for example, be used for MVHR and 0 with no heat recovery. T_{in} is the zone temperature where the air is exhausted, and T_{ex} the external temperature [°C].

In this paper, five ventilation strategies (or referred as design option D_{opt}) were implemented in CONTAM model and implemented on French low energy house case study (Poirier et al., 2021b, 2022a) :

MEV-CAV, for mechanical exhaust-only ventilation with constant air volume

MVHR-CAV, for mechanical balanced ventilation with heat recovery and constant air volume

MEV-RH, for mechanical exhaust-only ventilation and humidity control,

MVHR-RB, for mechanical balanced ventilation with heat recovery and CO2 & humidity control at the room level

MEV-RB, for mechanical exhaust-only ventilation and CO2 & humidity control at the room as an adaption of the MVHR-rb,

For sensibility analysis, each design option 500 simulations were performed with variation on the input scenarios such occupant CO₂ and H₂O emissions, moisture emissions from activities, emissions from cooking activities, exhaust airflows and CONTAM PM_{2.5} and moisture models parameters. The sampling of the 500 input scenarios was realised with the Latin Hypercube Sampling (LHS) methods (Helton and Davis, 2003) in accordance with the EASI RBD-FAST method (Goffart et al., 2015; Goffart and Woloszyn, 2021). This sampling was carried out with a Python function implemented in the SALib library.

In addition, three reference scenarios (Ref_{low}, Ref, Ref_{high}) were also used for robustness assessment (Poirier, 2023; Poirier et al., 2021a). The objective was to compare the ranking based on the overall performance calculated with the set of 500 input scenarios and the ranking calculated with the reference and the two extreme input scenarios. This is to assess whether the three reference scenarios are sufficient to obtain a relevant ranking of ventilation systems or if more simulations are needed to achieve this goal.

2.2 Multi-criteria-aggregation

Then, we used the SAW method for the multicriteria aggregation step, that is a simple aggregation weighting method which regroups the 5 IAQ indicators and the energy indicators under one value that we named I_{MC} for “multicriteria” indicator.

The second step focuses on the method to be used to regroup the performance results from the six indicators to one aggregated value for each simulation. In the literature, the aggregation of several indicators for decision making could be found under the notion of *methods for “multi-criteria decision-making”* (MCDM)(Kotireddy et al., 2018; Namin et al., 2022; Velasquez and Hester, 2013). These methods generally propose a formulation to aggregate the multiple criteria for the tested design option under one value (here the performance indicator). We propose to name this aggregated value I_{MC} for Multi-Criteria Indicator.

According to the literature, there are numerous methods of MCDM, with for example at least 10 different methods identified in a recent review on MCDM (Namin et al., 2022). As the purpose of this work is not to test or compare all the possible methods; we decided to use the Simple Additive Weighting (SAW) method. This method is a common MCDM method widely used and seems relevant to our problem. Indeed, this method is a classical method consisting of adding up the indicators with a weighting coefficient to give more or less importance to certain indicators over others. The proposed calculation of I_{MC} with the SAW method (Equation 1) has been realised and adapted from the method described in (Podvezko, 2011).

$$I_{MC} = \sum_i \omega_i \cdot I_i \quad (2)$$

Where ω_i is the weighted normalized value ($\sum \omega_i = 1$) of the indicator I_i in [$I^{n_{CO_2}}$, $I^{n_{HCHO}}$, $I^{n_{PM_{2.5}}}$, $I^{n_{RH_{70}}}$, $I^{n_{RH_{30_70}}}$, $I^{n_{E_{wh}}}$].

The weighted values can be set in several ways depending on the priority given to the indicator by the decision maker. To show the impact of weight arrangement priority on the I_{MC} calculation we build three weight distributions to calculate an associated I_{MC} (Table 1):

I_{MC_IAQ} , corresponding to decision-making based only on the IAQ indicator, with the weight equally distributed over the five IAQ indicators ($I^{n_{CO_2}}$, $I^{n_{HCHO}}$, $I^{n_{PM_{2.5}}}$, $I^{n_{RH_{70}}}$, $I^{n_{RH_{30_70}}}$) and 0 for $I^{n_{E_{wh}}}$.

I_{MC_IAQ-E} , corresponding to decision-making for overall performance assessment based on IAQ and Energy aspects, with the weight equally distributed on the six indicators. However, this distribution gives globally an advantage to the IAQ aspect as energy aspect is represented only by one indicator against five indicators for IAQ.

$I_{MC_IAQ-E^*}$ corresponding to a decision making for overall performance assessment based on IAQ and Energy aspects, but with variable and unequally distributed weight on the six indicators in comparison with I_{MC_IAQ-E} . This distribution was built to have an equal proportion between IAQ and energy. Consequently, the weight of $I^{n_{E_{wh}}}$ is set equal to 0.5. In addition, the IAQ aspects were differentiated to give more weight to the indicators $I^{n_{PM_{2.5}}}$ and $I^{n_{HCHO}}$. Their weight is doubled in comparison to the remaining IAQ indicators. This distribution for IAQ indicator could correspond to the assumption that moisture and CO_2 have less impact on the health in comparison with $PM_{2.5}$ and formaldehyde.

Distribution For I_{MC} calculation	Weight ω_i					
	I_{CO2}^n	I_{RH70}^n	$I_{RH30_70}^n$	I_{PM25}^n	I_{HCHO}^n	I_{Ewh}^n
I_{MC_IAQ}	0.2	0.2	0.2	0.2	0.2	0
I_{MC_IAQ-E}	0.16	0.16	0.16	0.16	0.16	0.16
$I_{MC_IAQ-E^*}$	0.071	0.071	0.071	0.143	0.143	0.5

Table 1 : Weight distribution for I_{MC} calculation

2.3 Robustness calculation and ranking

Lastly, the robustness calculation step consists in integrating into one design score (D_s) all the individual performance indicators I_{MC} across the tested scenarios. Then this robust design score can be used for performance comparison of each design option (D_{opt}).

According to the comparative study for robustness method assessment of Kotireddy (Kotireddy et al., 2019); several methods exist for robustness calculations. In this study three robustness assessment methods were implemented -max–min method, best-case and worst-case method, and minimax regret method - and compared with the widely used Taguchi method.

The Max-Min method evaluates the performance spread (PS) between the maximum performance ($A_{D_{opt}}$) and the minimum performance ($B_{D_{opt}}$) of each design strategy across all the scenarios. The most robust design is the design with the smallest PS.

$$PS = A_{D_{opt}} - B_{D_{opt}} \quad (3)$$

The best-case and worst-case method evaluates the performance deviation (PD) between the maximum performance ($A_{D_{opt}}$) and the minimum performance of all design strategies (D_{min}). The most robust design is the design with the smallest PD.

$$PD = A_{D_{opt}} - D_{min} \quad (4)$$

The minimax regret method evaluates the performance regret (PR), with the difference between the performance indicators value and the minimum performance of each scenario across all designs (C_s). The performance regret is calculated for each design strategy D_{opt} across all the scenarios s . Then the MPR is the maximum performance regret of each design, and the most robust design is the design with the smallest MPR

$$PR = I_{MC,D_{opt},s} - C_s ; \text{with } C_s = \text{Min}_s(I_{MC(all_D_{opt}),s}) \quad (5)$$

$$MPR = \text{Max}_{D_{opt}}(PR) \quad (6)$$

The Taguchi method evaluates the robustness of the design strategies based on the mean and standard deviation of the performance indicators over all the scenarios. The most robust design is the design with the smallest mean and standard deviation (mean \cap std) (Hoes et al., 2009)

The max–min, best-case and worst-case, and minimax regret robustness methods for design score provide a better integration of the uncertainty across all the scenarios in comparison with the Taguchi method. That could facilitate the decision-making process by reducing the gap between simulated performance at the design stage and the real performance (Kotireddy et al., 2019).

All four methods presented above were tested for the calculation of the robust design score. Finally, we selected the minimax regret method for design score calculation and the final ranking. Indeed, the use of these three other methods had little impact on the final ranking and the minimax regret method has been identified as a less conservative approach to design decision making when risk can be accepted as a trade-off (Kotireddy et al., 2019). This is relevant for MOPA as compared to the other three methods which are more conservative.

Finally for the results analysis we calculated the design score by applying Equation 5 with the I_{MC} from the 500 SA scenarios on one hand and with the I_{MC} from the 3 Reference scenarios on the other hand. The last case is the reference scenario when the design score is directly the I_{MC} . Then this design scores were normalized In [%] by $\sum_{D_{opt}}(D_s)$ the sum of all the design scores. That facilitating the ranking and comparison between the weight distribution and the number of scenarios.

3 METHOD ANALYSIS AND RANKING RESULTS

The first step of the proposed robustness method consists in design option performance calculation and here we exploited the results from the 500 simulations per design option used for SA application case study (Poirier, 2023). The following sections next result analyses are focused on the second step (multi-criteria aggregation) and the third step (robustness design score calculation) for robust ranking.

3.1 Multi-criteria aggregation

In the Figure 2, we represent by boxplot the aggregate I_{MC} calculated with the three weight distributions (IAQ, IAQ-E, IAQ-E*) on the 500 simulated scenarios for each design option. The three reference scenarios are represented by small grey diamonds. The boxplots represent first quartile (q1) at the bottom of the box, the median in the middle and the third quartile (q3) at the top of the box; with the whiskers extend from the box by 1.5x the inter-quartile range (IQR) and the remaining outliers are represented by grey crosses.

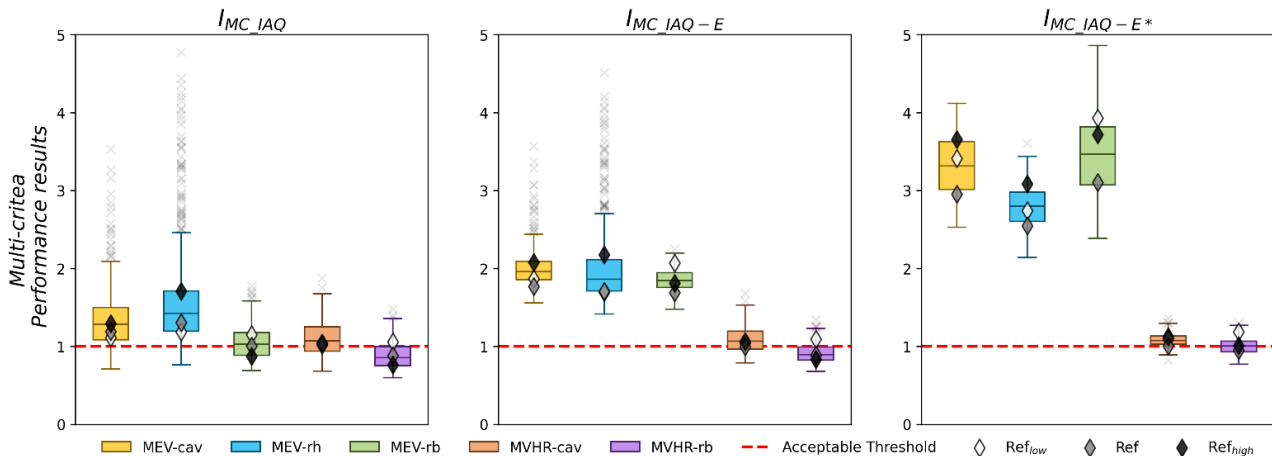


Figure 2 : Multi-criteria performance results of the five design option tested by weight distribution

This representation gives a general overview of the I_{MC} results depending on the proposed weight distribution. For the first weight distribution, including only the IAQ indicators, the aggregated performance (I_{MC_IAQ}) results in values mainly between 1 and 2 for MEV-cav and MEV-rh. For the MEV-rb and the MVHR-cav the results are centred around the acceptable threshold of 1. ; only the MVHR-rb gives the values mostly lower than 1, meaning an acceptable performance. The outliers for MEV-cav and MEV-rh illustrate that specific inputs scenarios for these systems could generate high performance assessment difference more than 4 times the

acceptable thresholds in some cases. Fortunately, the results of the reference scenarios are not outliers, which would mean that these three reference scenarios are not at all representative.

For this first case, with constant weight distribution over IAQ only, there is no clear gap between the systems in comparison with the two others weight distribution results (I_{MC_IAQ-E} , $I_{MC_IAQ-E^*}$). Such results may question the exclusive use of these IAQ indicators to rank the ventilation systems.

The introduction of the energy indicator in I_{MC_IAQ-E} underlines the difference between MEV and MVHR systems. Indeed, the values of I_{MC_IAQ-E} are distributed around the acceptable threshold of 1 for MVHR. On the opposite, the values for I_{MC_IAQ-E} are much higher than the acceptable threshold, being distributed around the value of 2 for all three MEV systems. In detail, a higher energy performance of MEV-rh (meaning lower I_{Ewh}) raised its global performance (lower I_{MC_IAQ-E} median value) in comparison with the two other systems without heat recovery (MEV). This compensates a slightly lower IAQ performance for MEV-rh. Whereas the higher I_{Ewh} of the MEV-rb increased its I_{MC_IAQ-E} value in comparison with the two other MEV. As a result, the three MEV systems have now comparable median values of I_{MC_IAQ-E} . Regarding the two MVHR systems, there is no significant change and the MVHR-rb still performs slightly better than MVHR-cav, thanks to its better IAQ performance. Thus, the distribution of IAQ-E weights highlights the energy benefit of heat recovery from MVHR systems.

In the last case IAQ-E*, with variable weight distribution, the differences between all systems are even more pronounced. Now, the MEV performance results are worse ($I_{MC_IAQ-E^*}$ range between 2.5 and 4). On the opposite, both MVHR systems exhibit performance indicator close to 1, with a narrow distribution range. In addition, the differences between the three MEV systems highlights that MEV-rh had lower energy losses than MEV-cav and MEV-rb. In this case, if energy saving is encouraged, the use of MEV-rh could be relevant in comparison with MEV-cav. In contrast if IAQ is prioritized on energy, the use of MEV-rb could be more relevant (as shows by IAQ-E distribution).

The comparison of these three weight distributions shows that the weight distribution is a clear leverage to increase the differences between systems on the final aggregated performance results. However, the uncertainty distribution from the 500 simulations performed and presented with boxplots doesn't makes systematically the ranking of the systems obvious. Moreover, in practice the use of weight distributions that voluntary increase the difference between systems to facilitate the ranking could lead to a wrong extrapolation of the simulated performance results. For example, this may question the ranking based on the IAQ-E* where the differences are mainly related to the initial pronounced differences on the I_{Ewh} .

That confirms the need of the robust design score calculation of the next step, considering uncertainty, to finalize the ranking process for decision-making.

3.2 Robust design score calculation and ranking

Figure 3 regroups, for the three tested weight distributions, the normalised design score [%] calculated with different scenarios. According to the methodology described above, the design score with 500 simulations and the three reference scenarios were calculated with the minimax regret method. The design scores for Ref_{low} , Ref , Ref_{high} , plotted in the figure, are directly the I_{MC} of each individual scenario. Then, for ranking, the best design option ($n^{\circ}1$) is the one with the lowest design score and the last ($n^{\circ}5$) is the highest design score.

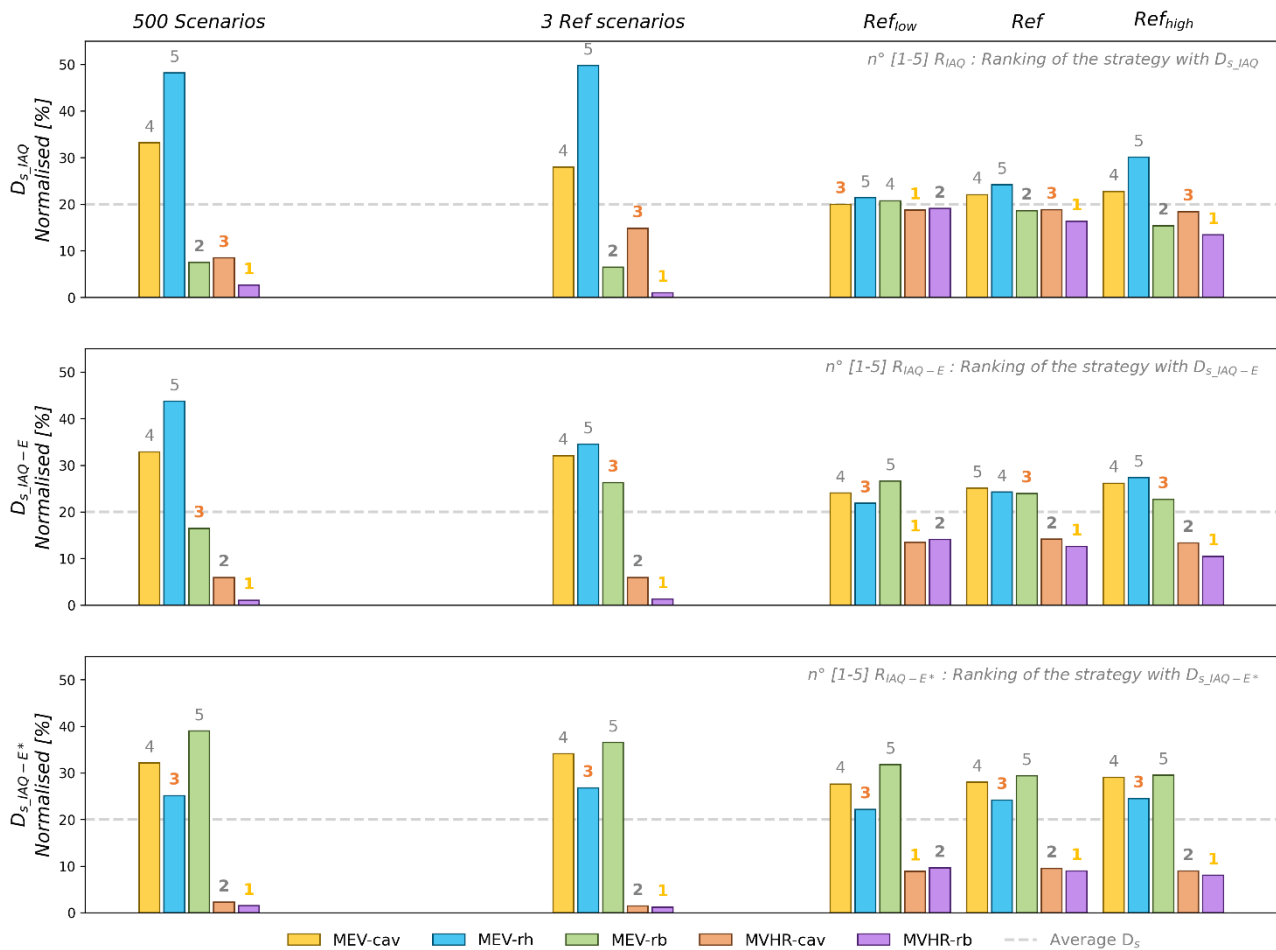


Figure 3 : Robust design score and ranking, MinMax regret method.

Different weight distributions are presented: equal IAQ (top), equal IAQ and Energy, IAQ-E (middle), and enhanced energy and health IAQ-E* (bottom).

Different scenarios are presented: 500 per system using uncertainty distribution on input parameters (left), three per system: high/ref/low (middle), and one per system, separating high/ref/low (right).

At first, the ranking order calculated from the design score is the same with 500 simulations and the 3 ref simulations. This confirms previous observations made on outliers of Figure 2 with the reference scenarios (grey diamonds) located inside the q1-q3 box. It means that the use of these 3 references scenarios for design score calculation and ranking provides the same information as the one obtained with 500 simulations design score calculation and ranking.

In detail, the ranking with design score calculated from each individual scenario (right plots), changes sometimes depending upon the weight distribution and the scenario used. For example, the ranking is inversed between MEV-cav and MEV-rh with the Ref scenario depending upon weight distribution. Another example is the Ref_{low} scenario, where ranking inversion is observed between the MVHR-cav and MVHR-rb as compared to all the other cases. In general, with Ref_{high} scenario the differences between design scores are more identifiable than for the Ref_{low} scenario.

Based on these results and the analysis made on Figure 2 we propose to :

Exclude the Ref_{low} scenarios from design scores for ranking. The risk is the loss of the uncertainty aspects, as this Ref_{low} ranking does not match with the ranking results obtained with the 500 simulations.

Keep the Ref scenario design score for an “optimistic performance ranking”, indeed the I_{MC} performance results of this reference scenario are mainly close to the q1 value and the ranking.

Keep the Ref_{high} scenario design score for a “conservative performance ranking”, indeed the I_{MC} performance results of this high reference scenario are mainly close to the q3 or the median value.

Associated together, the I_{MC} from Ref and Ref_{high} mainly cover the q1-q3 interquartile space (or at least the q1-mean). This allows to keep part of the uncertainty information and to calculate the design score with a ranking in accordance with the ranking of the 500 simulations.

Secondly, the impact of weight distribution on ranking is clearly identifiable with the design score. Indeed, the normalized design score is highly impacted for the MEV-rh from almost 50% (D_{s_IAQ}) to 25% ($D_{s_IAQ-E^*}$). An opposite evolution can be observed for the MEV-rb from almost 8% (D_{s_IAQ}) to 40% ($D_{s_IAQ-E^*}$). On the other hand, the results are only slightly impacted by the weight distribution for the MEV-cav (scores remaining around 32%), MVHR-cav (from 8% to 2%) and MVHR-rb (3% and lower). In all cases, MVHR-rb is ranked first and MEV-cav is ranked fourth, whereas MVHR-cav moves from third to second place due to the change in the ranking of MEV-rb.

This shows the importance of the weight given to the energy indicator and the priority balance between IAQ and energy. For instance, with the IAQ indicators only, the MEV-rb provides the second-best ventilation performance when it provides the worst one with the IAQ-E* distribution. Indeed, with the D_{s_IAQ-E} , the better IAQ performance of the MEV-rb is penalized because of its higher energy consumption; this explains the swapping between MEV-rb and MVHR-cav, the latter performing much better in energy consumption (thanks to heat recovery) for a slightly worse IAQ performance. On the opposite, the MEV-rh is by far the worst with IAQ performance only but it can reach a good third position with the IAQ-E* distribution. In this case, the 50% weight given for the energy indicator in the $I_{MC_IAQ-E^*}$ calculation valorizes the energy benefits of MEV-rh in comparison with the two other MEV systems which certainly provide a better IAQ.

4 CONCLUSION

To conclude, we propose a three-step method to rank different ventilation design systems and we tested it on five ventilation systems. We confirm that the performance indicators aggregation with the SAW method is relatively accurate compared to the performance observed by each indicator individually in previous study (Poirier et al., 2022a, 2022b; Poirier, 2023). Then, the calculation of the design score with the minimax regret robustness method offers a clear advantage to highlight the difference between the ventilation systems, in order to rank them by including the uncertainty of several simulations.

In addition, we show that the use of the three reference scenarios could be sufficient to obtain a relevant ranking of the ventilation systems, in comparison with the ranking obtained with 500 simulations. However, if the number of simulations is limited, we propose to perform in priority the reference scenario (Ref), if the decision making needs an “optimistic performance ranking”, or the reference scenario with the highest emission rates (Ref_{high}) for a “conservative performance ranking”. Nevertheless, if there are no constraint, we encourage the decision maker to simulate at least the three reference scenarios and ideally 500 scenarios or more. The

latter reinforces the validity of the calculated design score and ranking by including the uncertainty on input parameters.

For the MOPA, we do not retain the IAQ weight distribution as it doesn't include energy aspects for OPA. We propose to use at this stage the IAQ-E distribution in a conservative approach with balanced distribution across the six selected performance indicators. However, the IAQ-E* present a strong interest for a decision maker that would need a strictly equal proportion between IAQ and energy aspects. In future work it could be relevant to perform a more detailed sensitivity analysis on the weight distribution and then elaborate an adapted weighting selection method specifically for the six indicators (or more if added). Other MCMD could also be tested for indicators performance aggregation.

In our case, the MVHR systems presented the best overall performance with an IAQ benefit of the smart ventilation strategy (MHVR-rb). Then, depending on the decision maker priorities, the third most performant system could be the MEV-rb if IAQ is favored, or the MEV-rh or if the energy savings are more essential. In both cases the variable smart ventilation strategies present a benefit over the constant MEV-cav.

Lastly, at this stage, this ranking of the ventilation strategies shouldn't be considered as general performance ranking valid in all buildings. Indeed, the method has been applied only on one case study to demonstrate the relevance of the proposed methodology as a robust performance assessment decision-making tool for ventilation systems in buildings at the design stage.

5 REFERENCES

- Emmerich, 2001. Validation of multizone IAQ modeling of residential-scale buildings: A review/Discussion. *Ashrae Transactions* 107, 619.
- Hoes, P., Hensen, J.L.M., Loomans, M.G.L.C., de Vries, B., Bourgeois, D., 2009. User behavior in whole building simulation. *Energy and Buildings* 41, 295–302. <https://doi.org/10.1016/j.enbuild.2008.09.008>
- Kotireddy, R., Hoes, P.-J., Hensen, J.L.M., 2018. A methodology for performance robustness assessment of low-energy buildings using scenario analysis. *Applied Energy* 212, 428–442. <https://doi.org/10.1016/j.apenergy.2017.12.066>
- Kotireddy, R., Loonen, R., Hoes, P.-J., Hensen, J.L.M., 2019. Building performance robustness assessment: Comparative study and demonstration using scenario analysis. *Energy and Buildings* 202, 109362. <https://doi.org/10.1016/j.enbuild.2019.109362>
- Kotireddy, R.R., Hoes, P.-J., Hensen, J.L.M., 2017. Simulation-based comparison of robustness assessment methods to identify robust low-energy building designs. *Proceedings of 15th IBPSA conference, San Francisco, CA, USA* 892–901.
- Mechri, H.E., Capozzoli, A., Corrado, V., 2010. USE of the ANOVA approach for sensitive building energy design. *Applied Energy* 87, 3073–3083. <https://doi.org/10.1016/j.apenergy.2010.04.001>
- Namin, F.S., Ghadi, A., Saki, F., 2022. A literature review of Multi Criteria Decision-Making (MCDM) towards mining method selection (MMS). *Resources Policy* 77, 102676. <https://doi.org/10.1016/j.resourpol.2022.102676>
- Podvezko, V., 2011. The Comparative Analysis of MCDA Methods SAW and COPRAS. *Engineering Economics* 22, 134–146.
- Poirier, B., 2023. Evaluation of the overall performance of smart ventilation in low-energy housing (Génie Civil et Sciences de l'Habitat). Université Savoie Mont Blanc, Le Bourget du lac.
- Poirier, B., Guyot, G., Geoffroy, H., Woloszyn, M., Ondarts, M., Gonze, E., 2021a. Pollutants emission scenarios for residential ventilation performance assessment. A review.

- Journal of Building Engineering 42, 102488.
<https://doi.org/10.1016/j.jobe.2021.102488>
- Poirier, B., Guyot, G., Woloszyn, M., 2022a. Development of Performance-Based Assessment Methods for Conventional and Smart Ventilation in Residential Buildings, in: IAQ 2020: Indoor Environmental Quality Performance Approaches Transitioning from IAQ to IEQ. AIVC-ASHRAE, Athens, Greece.
- Poirier, B., Guyot, G., Woloszyn, M., Geoffroy, H., Ondarts, M., Gonze, E., 2021b. Development of an assessment methodology for IAQ ventilation performance in residential buildings: An investigation of relevant performance indicators. Journal of Building Engineering 43, 103140. <https://doi.org/10.1016/j.jobe.2021.103140>
- Poirier, B., Kolarik, J., Guyot, G., Woloszyn, M., 2022b. Design of residential ventilation systems using performance-based evaluation of Indoor Air Quality: application to a Danish study case. Presented at the BuildSim Nordic 2022, IBPSA Nordic, Copenhagen, Denmark, p. 8.
- Sharma, M., Bhattacharya, A., n.d. National Air quality Index. Control of Urban Series, CUPS/82/2014-2012.
- Velasquez, M., Hester, P., 2013. An analysis of multi-criteria decision making methods. International Journal of Operations Research 10, 56–66.
- Walton, G.N., Emmerich, S.J., 1994. CONTAM93: a multizone airflow and contaminant dispersal model with a graphic user interface. Air Infiltration Review 16, 6–8.

Update on Resilient cooling and indicators from the IEA EBC Annex 80

Peter Holzer¹

*1 Institute of Building Research & Innovation
Wipplingerstraße 23/3
1010 Vienna, Austria
*Corresponding author:
peter.holzer@building-research.at*

KEYWORDS

Resilient cooling, ventilative cooling, cooling strategies,

1 INTRODUCTION

The growing challenges of climate change, urbanization, and increased energy demand have underscored the critical need for sustainable and resilient cooling solutions in buildings. In response to this pressing global issue, the International Energy Agency's Energy in Buildings and Communities (IEA EBC) Annex 80 was initiated to address the multifaceted aspects of resilient cooling in the built environment. Annex 80 seeks to provide valuable insights into resilient cooling systems and their indicators, offering a pathway towards a more sustainable and adaptable future.

2 COOLING STRATEGIES

IEA EBC Annex 80 – Resilient Cooling of Buildings – has identified 16 cooling strategies that may contribute significantly to the resilience of buildings against heatwaves. Ventilative Cooling is one of them.

In the Annex deliverables these 16 strategies are described in well-structured Technology Profiles.

In the work of Annex 80, resilience has been defined as the qualities of;

- **Resistance** – The ability of a building to keep normal performance even under disruptive events.
- **Robustness** – The degree of a building's ability to keep emergency performance under disruptive events.
- **Recovery** – The character of a building in getting back to normal performance after a disruptive event.

The contribution in the Topical session will pre-present the Technological Profiles, namely the one of Ventilative Cooling, including the contributions of ventilative cooling to the resilience of a building.

3 ACKNOWLEDGEMENTS

A special thanks all the participants of the IEA-EBC Annex 80: Resilient Cooling of Buildings.

The research is supported by Det Energiteknologisk Udviklings- og Demonstrationsprogram (EUDP) under grant 64018-0578. It was also supported by the Assistant Secretary for Energy Efficiency and Renewable Energy, Building Technologies Office of the U.S. Department of Energy under Contract No. DE-AC02-05CH11231.

Ventilative Cooling Design In Practice: Where next?

Paul D O’Sullivan*, Adam O’Donovan, Maha Sohail

*Department of Process, Energy & Transport Engineering
Munster Technological University
Rossa Avenue, Bishopstown, Cork, Ireland
Corresponding author: paul.osullivan@mtu.ie

SUMMARY

Embedding robust yet accessible frameworks to evaluate ventilative cooling potential during the early/concept design stages for building practitioners can help in reducing the performance gap as well as avoiding vulnerability “lock-in” from design decisions that are based on poor or inadequate information. The challenge is to develop performance based evaluation methods that recognise the tacit approach to design in practice. Often design is iterative, non-linear and multi-agent. For this reason there is a need to harvest knowledge on design practices from industry experts as well as develop support approaches that recognise the potential lack of expert knowledge at the concept stages of design (i.e. limited ventilative cooling design expertise of planning consultants, architects and quantity surveyors). Simple and complex strategies also require different evaluation approaches as well as the need to address the wide varying performance of natural ventilation in reducing the design vs in-use performance gap.

KEYWORDS

Design, ventilative cooling, passive, practitioners, resilience.

1 CHALLENGES FOR EARLY STAGE VC DESIGN

The quality of future living circumstances for many will be contingent on how low energy indoor spaces respond to challenges from accelerated ambient warming. The most vulnerable spaces are likely to be those that adopt ventilative cooling, given the dependence on the cooling potential available in the outdoor ambient air as well as the relying on the natural driving forces present in the urban wind and indoor-outdoor buoyant exchange [Tavakoli et al, 2022]. There can be a significant design risk for building practitioners when evaluating natural/passive ventilative cooling strategies at the early and detailed design stages, particularly given the non-deterministic characteristics of the strategy. By way of example, the intermittency and short circuiting in solutions such as single sided ventilation can be problematic in guaranteeing adequate cooling supply when it is most needed.

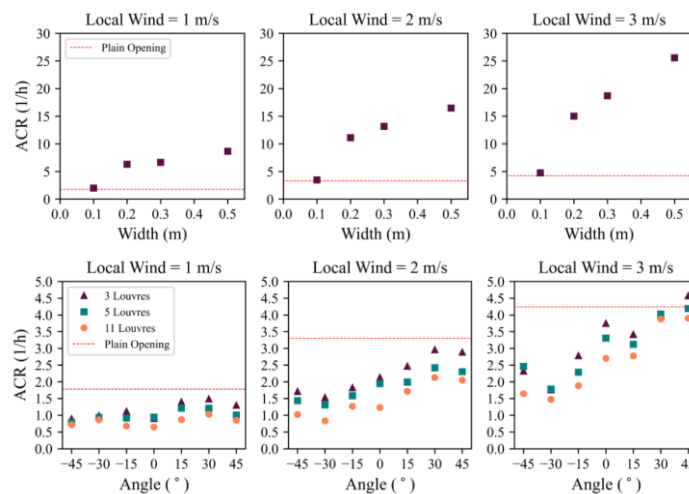


Figure 1: Wind driven SS ventilation rate performance for plain openings, louvres & guide vanes [Najafi Ziarani et al, 2023]

An example of the challenge for designers when attempting to account for VC performance at the design stages is evident from recent laboratory measurements of different window designs that highlighted a difference of over 400% [Albuquerque et al, 2021] in wind driven ventilation rates depending on window type, while a separate study reported that guide vanes were shown to outperform louvres and plain openings by a factor of over 5 [Najafi-Ziarani et al, 2023]. So there is a wide range of potential performance outcomes that design choices can influence. The issues are only examples of many that have propagating effects through design and into operation, i.e. the combined performance of thermal inertia, opening designs, hybrid and supplementary strategies, complex flows etc. Therefore, the “cooling performance gap” between design and operation is dependent on robust design approaches that better account for the cooling potential of combinations of climate-building-system as early as possible in the design process. The greater the investment in information gathering, analysis and decision making during pre-design and conceptual design phases, the fewer financial, environmental and wellbeing costs later in the project. As part of the new ventilative cooling technical specification under CEN TC156 work is progressing to define an early stage design process for practitioners that offers a performance based approach to evaluating VC potential during the concept stage. Figure 2 provides a conceptual overview of this. This will be further developed as part of the ongoing efforts of the technical specification writing group. There are many challenges around how to approach simple vs complex indoor spaces/strategies, whether a prescriptive method exists for evaluating cooling potential, how to accommodate early stage conceptual ventilation rate assessments and so forth.

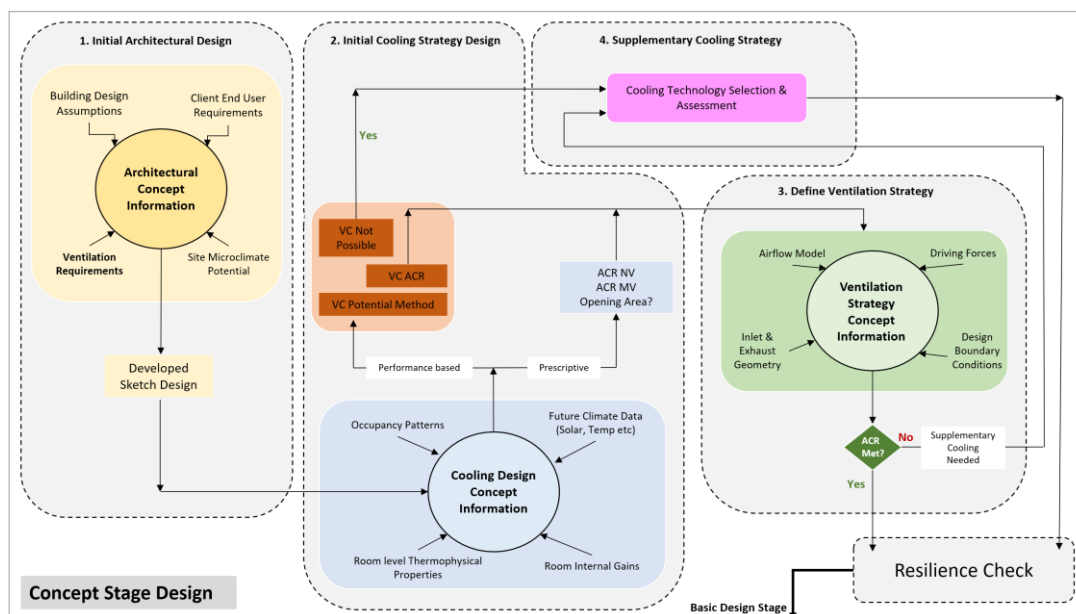


Figure 2: Evaluating Ventilative Cooling at the Concept Design Stage

2 DESIGN IN PRACTICE

Given that “design in practice” may differ from theoretical frameworks work has been completed in an attempt to map how ventilative cooling is dealt with in real design environments and whether this differs significantly from the current best practice guidance available in standards and professional body guidelines. A survey of over 30 building design practitioners has been completed which included 57 questions exploring how ventilative cooling is perceived, how the design effort is distributed throughout the design process, whether existing tools and methods are fit for purpose and what improvement are necessary to evolve VC design towards more reliable frameworks that lead to better operational outcomes for buildings [Sohail et al, 2023]. Approximately 18% of the respondents considered cooling as a design criteria but regarded it as not important. About 8% of the respondents said that it is not a design criteria in their building design practices. Around 32% of the respondents do not use any design tools to make any ventilative cooling decision and around 34% sometimes use a design tool while 34% of the respondents use the tool while making a ventilative cooling decision. It is evident that clear, reliable early stage design methods to assist designers at the concept stage to evaluate ventilative cooling potential of different strategies is important and useful to addressing the performance gap in low energy buildings. As well as the survey 10 detailed interviews with design experts have been completed and this, along with the survey work and the ongoing efforts of the writing group, should facilitate the development of a design map/ontology of how VC design is actually undertaken in practice, and how this compares to existing theoretical guidance and tools. The aim is to tailor existing frameworks and guidance to better align with the tacit knowledge of design experts and provide a

more seamless approach to evaluating ventilative cooling at the early stages through to detailed design, reducing vulnerability “lock-in” that becomes difficult to address post construction.

3 OUTLOOK

In order to reduce the performance gap for ventilative cooling it is important to first map how solutions are being selected, designed and developed in real practice based environments. Once this has been scoped and defined, it is easier to identify where there might be deficiencies in design supports, whether they be guidance documentation, evaluation tools or training and so forth. Developing support at the early stages in design, where most impact can be achieved, is key to attempting to reduce the future underperformance of ventilative cooling solutions. The new technical specification being developed under CEN TC156 aims to address this challenge by offering designers an easy to use robust, performance based approach that can evaluate VC potential early in the design to allow key decisions be made around building morphology, site microclimate exploitation, additional passive interventions, supplementary cooling requirements and so on. Good design practice will be as important as technological innovations in addressing the resilience of future indoor thermal environments.

4 ACKNOWLEDGEMENTS

This work is supported by a Science Foundation Ireland grant 18/EPSC-CDT/3586.

5 REFERENCES

Najafi Ziarani, N., Cook, M., OSullivan, P.D., *Experimental evaluation of airflow guiding components for wind driven single sided natural ventilation: a comparative study in a test chamber*. Under Review

Albuquerque, D., O'Sullivan, P.D., Carrilho Da Graca, G., (2021) *Effect of window geometry on wind driven single sided ventilation through one opening*, Energy & Buildings, Volume 245, 111060.

Tavakoli, E., O'Donovan, A., O'Sullivan, P.D., (2022) *Evaluating the indoor thermal resilience of ventilative cooling in non-residential low energy buildings: A review*, Building & Environment, Volume 222, 109376

Sohail, M., O'Donovan., Plesner, C., O'Sullivan, P.D., (2023) *A survey of building design practitioner perceptions of ventilative cooling in their building design processes to provide resilient indoor environments*, Air Infiltration and Ventilation Conference, Copenhagen, Denmark.

Life cycle assessment: A design element for ventilation system selection

Jannick K. Roth^{*1}

1 WindowMaster International A/S

Skelstedet 13

2950 Vedbæk, Denmark

**Corresponding author: jkr.dk@windowmaster.com*

ABSTRACT

A Danish office building designed with a hybrid ventilation system has been compared to a full mechanical ventilation system in the same building. The comparisons include a life cycle analysis (LCA) focussing on CO₂ equivalents (CO₂equiv.) and life cycle cost (LCC) of the two ventilation solutions. The LCA includes embodied carbon from the ventilation components and operational energy due to heating and electricity. A potential reduction of 32% in the total global warming potential (GWP) was found when using a hybrid ventilation solution instead of a mechanical ventilation solution. This includes a 46% reduction in the embodied carbon and a 26 % reduction in the operational energy. The hybrid ventilation solution was 7 % cheaper to acquire, and the life cycle cost was found to be 16 % cheaper than a mechanical ventilation solution.

KEYWORDS

Embodied carbon, operational carbon, hybrid ventilation, life cycle analysis (LCA), life cycle cost (LCC).

1 INTRODUCTION

Traditionally there has been a focus on lowering energy consumption in the building sector by reducing heat loss in the buildings through increased insulation, or development of more energy efficient ventilation systems design. These parameters are still important as this has an impact on the operational energy consumption of the building, hence the environmental impact.

Life cycle assessment (LCA) focusing on CO₂equiv.) in the design of buildings has been a well-known and used methodology for measuring adverse environmental impacts for several years. However, it is only recently that there has been a significant emphasis on the environmental impact of construction activities and its impact on our planet's climate. The focus is also led by a push from legal requirements and certification scheme tightening the requirements mainly regarding the global warming potential (GWP) using kg. of carbon dioxide equivalents (CO₂-equiv.) as an indicator.

LCA for buildings is a comprehensive approach used to evaluate the environmental impact of a building throughout its entire life cycle. This assessment considers various stages, from raw

material extraction and construction to operation, maintenance, and eventual demolition or recycling. LCA involves a systematic analysis of the building's environmental performance, considering factors such as energy consumption, resource usage, emissions, waste generation, and overall ecological footprint. The goal is to provide a holistic understanding of the building's sustainability, enabling informed decisions to minimize its environmental impact.

Only a limited number of published studies have employed LCA as a primary design consideration to determine the optimal ventilation system for a specific building.

2 METHODOLOGY

An 1230m² office building has been used as reference to compare different ventilation solutions. The office building is located in Denmark and incorporates a hybrid ventilation system which has been compared to a full mechanical ventilation system. The hybrid ventilation system consists of an automated natural ventilation solution through façade and roof windows to handle the cooling period and a downscaled mechanical ventilation system with heat recovery to fulfil the ventilation requirements during the heating period. This is compared against if the building was to be using a mechanical ventilation system, only. Both systems are sized to fulfil the same requirements regarding thermal comfort and indoor air quality.

An LCA comparison between the two systems has been establish based on embodied carbon and operational energy (heating and electricity) from the usage and products of the systems. The LCA includes eight of the total seventeen phases of the LCA. The once included in the current study are marked in blue in Figure 1.

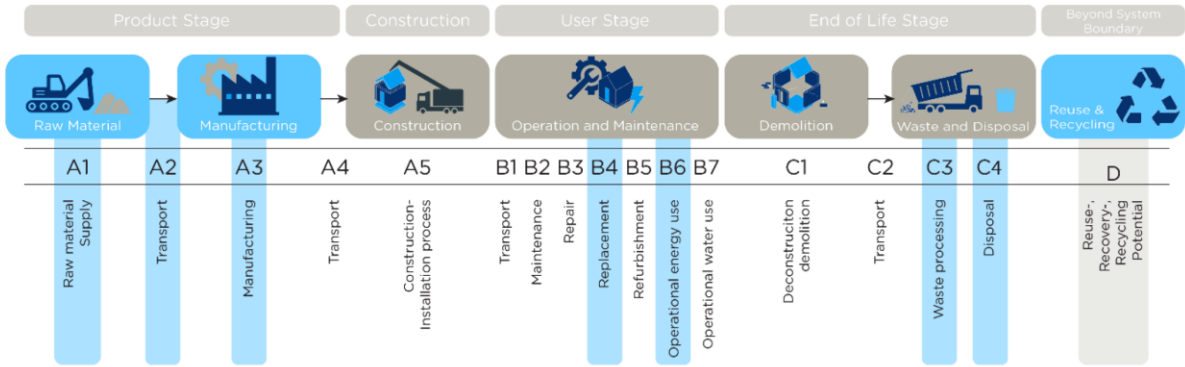


Figure 1: Included phases of the LCA.

Phase D is included in calculations, but is declared separately from the total environmental impact, as it is deemed outside the scope according to the Danish building regulation. Module D accounts potential benefits when reusing, recycling, or recovering the material after its end of life. The calculation is done in a Danish LCA tool named LCAByg using a reference period of 50 years.

The embodied environmental impact of the ventilation systems is calculated on component level for each system. The air handling units in the mechanical and hybrid ventilation systems, are simplified using generic data from the Ökobau-database that reflects the typical build-up of an air handling unit. This generic air handling unit is multiplied to the accurate weight for each scenario. The individual ventilation components used in the mechanical and hybrid ventilation systems (ducts, air handling unit, silencers, air diffusers, façade grills, air

flow dampener and regulators, end cap and control valves) are modelled into their respective raw materials. This is by using the building product declarations for the individual component build-ups. For the natural ventilation components (actuators and controllers, latter enables intelligent control of the actuators) EPD-data has been used.

A Life Cycle Cost (LCC) has been used to give an insight into the overall economic costs of the given ventilation system over its life cycle. In LCC, all costs from design, construction, maintenance, and replacements during the assessment period are included.

The ventilation systems are evaluated for the economic life cycle cost associated with design, construction, maintenance, replacements, and operational costs for electricity/heating.

2.1 Key results

Figure 2 shows the LCA results focusing on GWP with CO₂-equiv. as an indicator for the two assessed ventilation systems.

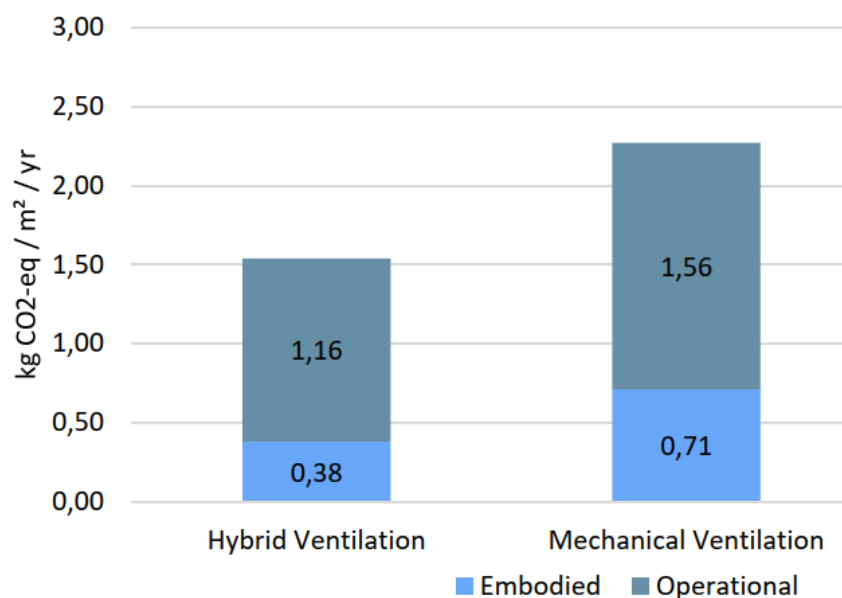


Figure 2: GWP results for the ventilation systems

Compared to the mechanical ventilation the hybrid ventilation system solution enables a:

- 46% reduction in the embodied carbon
- 26 % reduction in the operational energy
- 32% reduction in total (GWP, CO₂-equiv.)

The embodied carbon for the intelligent natural ventilation system is 0.033 kg CO₂-eq./m²/year out of the 0.38 kg CO₂-eq./m²/year in the hybrid ventilation solution.

Figure 3 shows the cumulative embodied and operation total GWP over the 50-year reference study period. The difference between hybrid ventilation and mechanical ventilation is due to the higher energy use from the mechanical system, along with a noticeably higher jump at year 2045, where most of the ventilation components are replaced.

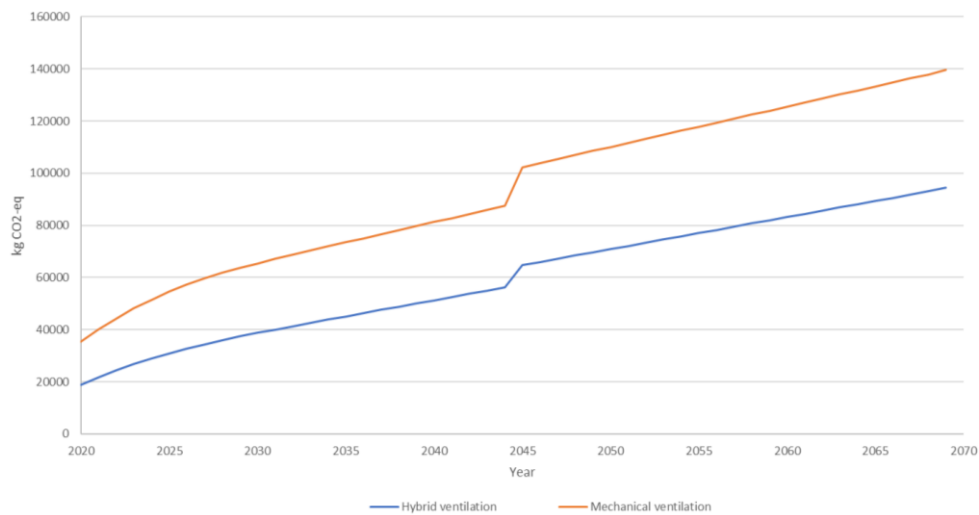


Figure 3: Total cumulative GWP, CO₂-equiv.

Figure 4 show the LCC for the hybrid and mechanical ventilation system.

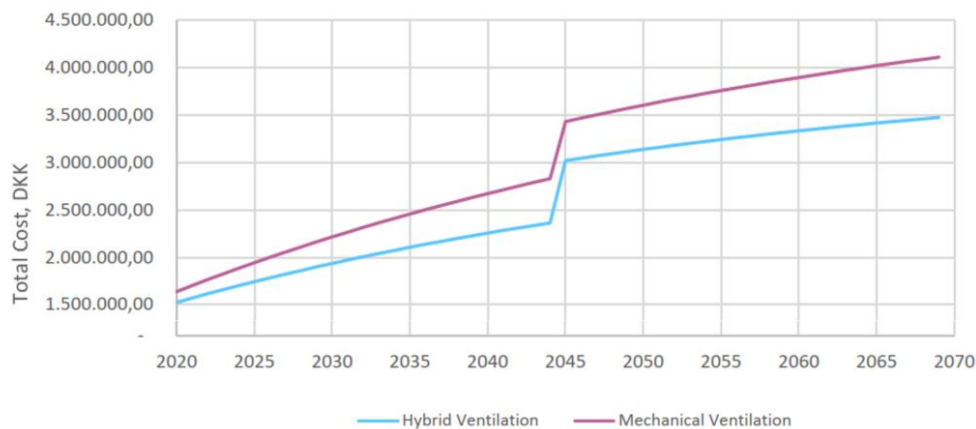


Figure 4: Cumulative cost over the 50-year assessment period, in DKK

Comparing hybrid and mechanical ventilation, hybrid ventilation is 7 % cheaper to acquire, and the overall life cycle cost is 16 % cheaper than mechanical ventilation.

3 CONCLUSION

An 1230m² office building located in Denmark has been used as reference to compare different ventilation solutions. The office building is designed with a hybrid ventilation system which has been compared to a full mechanical ventilation system. An LCA comparison between the two systems has been establish based on embodied carbon and operational energy (heating and electricity) from the usage and products of the systems focusing on CO₂-equiv.

The LCA calculations indicates that there is a significant potential for reducing the total GWP (CO₂-equiv.) by 32% choosing the hybrid ventilation system. This is due to a 46% reduction in the embodied carbon and a 26 % reduction in the operational energy.

Based on a Life Cycle Cost (LCC) including the overall economic costs of the given ventilation systems over its life cycle the hybrid ventilation was found to be 7 % cheaper to acquire, and the overall life cycle cost was 16 % cheaper than mechanical ventilation.

Lessons Learned from Irish Schools: Early-stage Insights on Overheating

Adam O’ Donovan^{1*}, Elahe Tavakoli¹, Paul D. O’Sullivan¹

*1 MeSSO Research Group, Department of Process, Energy and Transport Engineering,
Munster Technological University (Cork Campus),
Rossa Avenue, Bishopstown, Cork, Ireland
Corresponding author: adam.odonovan@mtu.ie

SUMMARY

Overheating in school buildings is likely to lead to a negative learning performance experience for occupants in these settings. In Ireland, school buildings are primarily naturally ventilated, given the relative increases in external mean temperatures that are projected to have negative effects on the potential of natural ventilative cooling going forward, it is important to assess what the current overheating status is in these buildings. Existing work has already highlighted the lack of measurement data on overheating in low energy school buildings. Additionally, the literature also supports a difference in comfort between adults and children as well differences between temperature suitable for learning performance assessments and comfort assessments in school settings. In this presentation, early-stage insights on overheating in school buildings in Ireland will be presented with a subset of data from the RESILIENCE project. A series of comfort-based and performance-based metrics will be used to contextualise this data which was gathered in 2022/2023. Additionally, lessons learned from site visits as well as inputs from a calibrated whole building simulation model will be used to determine to what extent is overheating an issue in Irish schools and are they likely to overheat in the future.

KEYWORDS

Overheating, primary and post-primary, natural ventilation, ventilative cooling, overheating

1 INTRODUCTION AND BACKGROUND

1.1 Overheating in naturally ventilated schools

Despite there being evidence in the literature to support that excess heat or overheating can have a negative effect on occupant performance in schools [1], [2], there is scarce data on the overheating performance in schools but particularly new ones [3].

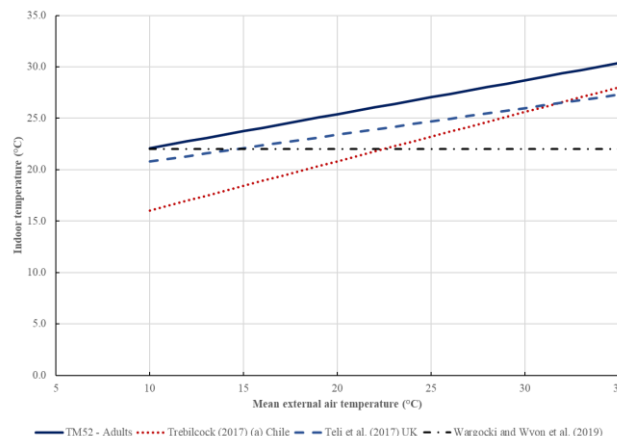


Figure 1: Comparison of adaptive thresholds for adults, children as well as thresholds reflective of relative learning performance

This mirrors the case for non-residential buildings more generally as more data is needed in this area [4]. School buildings have been examined using different metrics in the past be they for comfort [5], [6] or learning performance [2] what is evident is that adaptive standards or thresholds used for adults are not likely to be reflective of what students experience in primary schools and potentially post-primary schools also (See Figure 1). Additionally, it is also evident from the literature that passive cooling systems such as natural ventilation may not be equipped to suppress projected excesses in heat in the future [7] and this is when standardised thresholds are used. Therefore, it is important that further research be conducted in school buildings.

1.2 Project RESILIENCE and case studies

The following study is one part of project RESILIENCE, which is research project funded by the Sustainable Energy Authority of Ireland (SEAI). The focus of RESILIENCE is on overheating in naturally ventilated (NV) low energy or nZEB built environments in non-residential or commercial buildings. This research aims to:

“Systematically map and quantify how low or Nearly Zero Energy (i.e. nZEB’s) commercial building design, construction and operation in Ireland has affected or will affect indoor thermal environments in buildings that rely exclusively on passive strategies for the supply of fresh air and, more specifically, the removal of heat build-up that would otherwise lead to an unacceptable thermal experience for building occupants.”

The project has three overall building types: schools, office/educational, and healthcare. The project has targeted a total of 30 non-residential buildings (with a minimum of 2 to 3 zones per building), where data is being gathered on overheating at half-hour intervals at a minimum. The utilises data from different sources with existing BMS or Wifi-based data logging systems but in some cases standalone data loggers were used. Table 1 indicates the school buildings that were confirmed as of August of 2023. A mixture of retrofit, new built as well as extensions to existing buildings were monitored.

Table 1: List of 12 case study school buildings (as of August 2023) and monitoring systems installed

School Name	Location	Building Type	No of Zones	Monitor Type	Accuracy
PS1	South	New	5	Stand-alone	±0.3°C
PS2	South	New	5	Stand-alone	±0.5°C
PS3	South	New	>5	Wifi-based	±0.1°C
PP1	South-West	Extension	5	Wifi-based	±0.3°C
PP2	Midlands	New	>5	BMS/ Stand-alone	±0.5°C
PS4	Mid-West	Extension/Retrofit	>5	BMS	±0.5°C
PS5	South	New	5	Stand-alone	±0.5°C
PS6	South	Extension/Retrofit	5	Wifi-based	±0.3°C
PS7	North-East	Retrofit	>5	BMS	±0.5°C
PP3	South-East	Retrofit	>5	BMS	±0.5°C
PP4	South-East	Extension	5	Wifi-based	±0.3°C
PS8	West	Existing	>5	BMS	±0.5°C

As part of this presentation, data from a subset of these buildings will be presented along with some lessons learned from site visits in each building or from previous work in the simulated performance of a new NV school building in Ireland [8].

2 ACKNOWLEDGEMENTS

The research team would like to thank many stakeholders in the primary and post-primary educational sectors including, key contacts in government departments, those in regional educational and training boards as well as principals, teaching staff and caretakers for allowing access and consenting to this study. The work was approved by the MTU Research Ethics Board under approval number: MTU22032A.

3 REFERENCES

- [1] X. Li *et al.*, “Schooling of migrant children in China: Perspectives of school teachers,” *Vulnerable Child. Youth Stud.*, vol. 5, no. 1, pp. 79–87, Apr. 2010, doi: 10.1080/17450120903193931.
- [2] P. Wargocki, J. A. Porras-Salazar, and S. Contreras-Espinoza, “The relationship between classroom temperature and children’s performance in school,” *Build. Environ.*, vol. 157, no. April, pp. 197–204, 2019, doi: 10.1016/j.buildenv.2019.04.046.
- [3] S. Mohamed, L. Rodrigues, S. Omer, and J. Calautit, “Overheating and indoor air quality in primary schools in the UK,” *Energy Build.*, vol. 250, p. 111291, Nov. 2021, doi: 10.1016/j.enbuild.2021.111291.
- [4] E. Tavakoli, A. O’Donovan, M. Kolokotroni, and P. D. O’Sullivan, “Evaluating the indoor thermal resilience of ventilative cooling in non-residential low energy buildings: A review,” *Build. Environ.*, vol. 222, no. June, p. 109376, 2022, doi: 10.1016/j.buildenv.2022.109376.
- [5] D. Teli, L. Bourikas, P. A. B. James, and A. S. Bahaj, “Thermal Performance Evaluation of School Buildings using a Children-based Adaptive Comfort Model,” *Procedia Environ. Sci.*, vol. 38, pp. 844–851, 2017, doi: 10.1016/j.proenv.2017.03.170.
- [6] M. Trebilcock, J. Soto-Muñoz, M. Yañez, and R. Figueroa-San Martin, “The right to comfort: A field study on adaptive thermal comfort in free-running primary schools in Chile,” *Build. Environ.*, vol. 114, pp. 455–469, Mar. 2017, doi: 10.1016/j.buildenv.2016.12.036.
- [7] C. Heracleous, A. Michael, A. Savvides, and C. Hayles, “Climate change resilience of school premises in Cyprus: An examination of retrofit approaches and their implications on thermal and energy performance,” *J. Build. Eng.*, vol. 44, p. 103358, 2021, doi: 10.1016/j.jobee.2021.103358.
- [8] E. Tavakoli, A. O. Donovan, and P. D. O’Sullivan, “Evaluating the Resilience of VC+ Low Energy Primary Schools to Climate Change,” in *AIVC 2022*, Oct. 2022.

Resilient cooling in office buildings: case study in Belgium

Joost Declercq¹, Shiva Khosravi¹, Abantika Sengupta², Hilde Breesch²

*1 archipelago architects
Remylaan 2b, 3018 Louvain, Belgium*

*2 KU Leuven, Department of Civil Engineering,
Building Physics and Sustainable Design
Gebroeders De Smetstraat 1, 9000 Ghent, Belgium
Corresponding author: hilde.breesch@kuleuven.be

KEYWORDS

Resilient cooling, design process, building simulation, resilience assessment

1 INTRODUCTION

To achieve future-proof buildings, it is crucial to design buildings and systems that can withstand to shocks (like heat waves and power outages) and reduce the impact of shocks on thermal comfort in a building. This is known as resilience to overheating.

However, shocks are not included in daily building design practice. Practitioners still have the question: “how to design a building that is resilient to overheating?”. To answer this question, IEA EBC Annex 80: Resilient Cooling of Buildings translated its results into Resilient Cooling Guidelines (Corrado et al., 2023). The case study from these guidelines is the subject of this summary/presentation.

2 CASE STUDY DESCRIPTION

The case study is a new low-tech office building with a floor area of 1019m² on 2 floors in the city of Leuven (Belgium) designed by and for archipelago architects (see Figure 1).



Figure 1: Parkside view of the office building © archipelago architects

3 (PRE-)DESIGN PROCESS

Figure 2 presents the step-by-step design process that is applied to reach a resilient building with focus on passive design strategies and in particular the combination of solar shading, natural ventilative cooling (NVC) and exposed thermal mass. For more details about the whole design process is referred to Declercq et al. (2021).

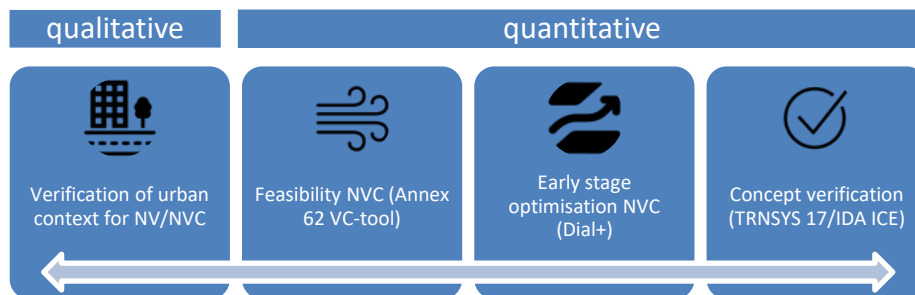


Figure 2 Step-by-step design process (including used tools) © archipelago architects

4 RESILIENCE ASSESSMENT

A building simulation model including 10 zones is built in IDA ICE v4.9.9. Thermal resilience is assessed for two open plan offices (with 32 occupants each) and one reception area by the following performance indicators: overheating escalation factor (OEF) and degree hours above a standard effective temperature (SET) of 28 and 30°C. The concerned shocks are heat waves in current and future weather conditions (mid-term and long-term projections) and a 48h power outage on the hottest day of the heat wave. Simulated scenarios include a combination of automated shading (yes/no), natural/mechanical ventilative cooling (yes/no), thermal mass (light/heavy), mechanical radiant cooling device.

5 ACKNOWLEDGEMENTS

This work has been supported by the Flanders Innovation and Entrepreneurship in the Flux50 Project “ReCOOver++: Improving resilience of buildings to overheating.”

6 REFERENCES

- Corrado, V., Psomas, T., Stern, P. (ed.), (2023) Resilient Cooling Guidelines, REHVA guidebook (to be published)
- Declercq, J., Ramon, D., Deryn, F., Allacker, K., (2021) The feasibility of natural ventilative cooling in an office building in a Flemish urban context and the impact of climate change, Proceedings of the 17th IBPSA conference, Bruges, Belgium, 1-3 sep 2021, 910-917

Design procedures for ventilative cooling integrated in new standards

Christoffer Plesner^{*1} and Jannick K. Roth²

1 VELUX A/S
Ådalsvej 99
2970 Hørsholm, Denmark

2 WindowMaster International A/S
Skelstedet 13
2950 Vedbæk, Denmark

*Corresponding author:
christoffer.plesner@velux.com

SUMMARY

Low energy buildings are highly insulated and airtight and therefore subject to overheating risks, where Ventilative Cooling (VC) could be a relevant solution in both existing and new buildings - being both a sustainable and energy efficient solution to improve indoor well-being, hereunder thermal comfort (*State-of-the-art-review*, Kolokotroni et al., 2015). VC is widely used as a key element when designing buildings to cope with overheating to assist improving thermal comfort, but can also improve the Indoor Air Quality due to higher ventilation rates in the cooling season.

VC technologies have the potential to be an effective measure to reduce the energy use in buildings, by meeting some or all of the cooling requirement of a building without the need for an active cooling system (e.g. mechanical cooling). The design of a VC system plays a significant role in the success and here fair and proper implementation of VC methods in standards, guidelines and legislation are becoming more important to enhance a proper design with a corresponding good performance.

In terms of building design, the responsiveness of a building not only includes good thermal comfort, but also resiliency and an ability to cope with the environmental impact of a certain technical solution. Amongst other things, the resilience aspect is important to include in future standards and legislation on this topic, e.g. evaluating what happens to the thermal comfort if there is a power outage.

There has generally been lacking proper ventilative cooling design integration in existing European standards and legislation and therefore New projects have started up under international standardization committees, CEN and ISO namely; CEN/TC 156 and ISO/TC 205.

KEYWORDS

Ventilative cooling, standards, legislation, compliance tools, recommendations for implementation of VC

1 EUROPEAN TECHNICAL SPECIFICATION ON VENTILATIVE COOLING IN CEN

1.1 General

There has generally been missing good ventilative cooling design integration for "system design" and "performance" aspects in existing European standards and legislation and therefore New projects have started up in New working groups under CEN/TC 156 and ISO/TC 205.

In CEN a new European Technical specification (CEN/TS) named "Ventilative cooling systems – Design" under CEN/TC 156/WG21 has started up with the goal to be the go-to European technical document for how to design ventilative cooling systems, while also ensuring a reference for ventilative cooling in the upcoming revision of EN 16798-1 named EN 16798-1-3 (for thermal comfort).

1.2 Content of CEN/TS

The purpose of the CEN/TS is to set criteria and give guidance to the design of ventilative cooling systems with main focus on thermal comfort in order to reduce cooling loads and prevent/reduce overheating in buildings. Ventilative cooling can be achieved through natural, mechanical and hybrid means.

With reference to the "VC design guide" from IEA Annex 62 inspiration has come up for input to the CEN and ISO technical documents on ventilative cooling (*Ventilative cooling design guide, IEA Annex 62, Heiselberg et al., 2018*).

In the CEN/TS, the general design procedure will consist of 3 design stages:

- Conceptual design
 - Aim: To embed VC principles and find VC potential
- Basic design
 - Aim: To determine opening areas/duct sizing and to investigate if the needed air change rate is achievable
- Detailed design
 - Aim: To investigate if the chosen ventilative cooling system actually complies with the set criteria

In the conceptual design phase will be included a method estimating the "ventilative cooling potential" early on to find when VC applications can be used throughout the year for a given climate. If VC is not sufficient, there will informatively be given information on supplementary cooling and mechanical cooling to ensure full thermal comfort in the building. The aim is to include early design evaluations with illustrated "archetypes" e.g. in terms of climate type to help the designer make valid choices early on based on simulations for VC strategies (e.g. single sided or cross ventilation).

In all design stages will be included resilience checks, ranging from simple (conceptual and basic) to possibly more detailed resilience indicators (detailed design). This resilience check will investigate if the building e.g can withstand power cuts, in order to still achieve a good thermal comfort.

2 CONCLUSION

Generally, new aspects are highlighted included in the upcoming European Technical specification on "Ventilative cooling systems - Design" in CEN/TC 156/WG21 in order for the audience to understand the need to have this information available in a new technical document and that a reference should be made to the current revision of EN 16798-1-3 (thermal comfort).

There can generally be different ways of cooling a building and here VC technologies have the potential to reduce the energy use in buildings, by meeting some or all of the cooling requirement of a building without the need for an active mechanical cooling system. The design of a VC system plays a significant role in the success of this and to this are needed fair and proper implementation of VC methods in standards, guidelines and legislation.

3 ACKNOWLEDGEMENTS

Thanks to the Venticool (International platform for resilient cooling) for their support for facilitating this workshop. (www.venticool.eu).

Some of the material presented in this topical session has been collected and developed within IEA Annex 62 on "Ventilative cooling" of the IEA Technology Collaboration Programme: Energy in Buildings and Communities and is the result of an international joint effort. All those who have contributed to the project are gratefully acknowledged. A list of participating institutes can be found in Table 1.

Table 1 - Research participants helping with input to IEA Annex 62 report

Name	Institute-Affiliation
Christoffer Plesner	VELUX A/S, Denmark
Flourentzos Flourentzou	ESTIA SA, Switzerland
Guoqiang Zhang	Centre for Sustainable Built Environment, Hunan university, China
Hilde Breesch	KU Leuven, Belgium
Per Heiselberg	Aalborg University, Denmark
Michal Pomianowski	Aalborg University, Denmark
Peter Holzer	Institute of Building Research and Innovation (TBRT), Austria
Maria Kolokotroni	Brunel University, United Kingdom
Annamaria Belleri	Eurac Research, Italy
Giacomo Chiesa	Politecnico di Torino, Italy
Guilherme Carrilho da Graca	University of Lisbon, Portugal
Hans Martin Mathisen	Norwegian University of Science and Technology (NTNU), Norway
Paul D. O' Sullivan	Munster Technological University, Ireland

4 REFERENCES

Plesner, C. (2018). *Status and recommendations for better implementation of ventilative cooling in standards, legislation and compliance tools (Background report)*. EBC Programme - Annex 62 Ventilative Cooling and Venticool platform

Kolokotroni, M., Heiselberg, P. (2015). *Ventilative Cooling - State Of The Art Review*. EBC Programme - Annex 62 Ventilative Cooling

Heiselberg, P. et al. (2018). *Ventilative Cooling Design Guide*. EBC Programme - Annex 62 Ventilative Cooling

Sensitivity Analysis of CO₂ Concentrations as Ventilation Metrics

Oluwatobi Oke*, Andrew Persily

*National Institute of Standards and Technology
100 Bureau Drive, MS8600
Gaithersburg, Maryland USA*

**Corresponding author: Oluwatobi.oke@nist.gov*

ABSTRACT

An approach has previously been developed to estimate space-specific carbon dioxide (CO₂) levels that can serve as metrics for the adequacy of outdoor ventilation rates. These metrics are based on the CO₂ concentration expected in a space given its intended or expected ventilation rate, volume, and occupant information (i.e., the number of occupants, their CO₂ generation rates, and duration of occupancy). This expected concentration can then be compared to a measured value to assess whether the actual outdoor air ventilation rate of the space is consistent with a design value, the requirement in a standard, or other recommended ventilation rate. A measured concentration higher than the expected value may indicate that the target ventilation rate is not being achieved. However, the occupant characteristics that impact the rate at which they generate CO₂ (sex, age, body mass, and level of physical activity) are difficult to know with precision, which impacts the uncertainty in the expected concentration.

This study involved a sensitivity analysis of the calculated CO₂ ventilation metric. Occupant characteristics impacting the CO₂ generation rate (body mass, ratio of male-to-female occupants, and metabolic rates) were varied by about +/- 20 % to evaluate the impact on two metric values of interest (the CO₂ concentration 1 hour after full occupancy and the steady state concentration). In addition, the space ventilation rate was varied by +/- 20 % to allow comparison to the variations associated with the other three inputs. The analysis employs the airflow and contaminant transport tool CONTAM to predict these concentrations over the range of inputs using factorial analysis. The sensitivity analysis employs a two-level full factorial design and a 10-step exploratory data approach (EDA) to identify the factors that have the most significant impacts. The result shows that outdoor ventilation rates and metabolic rates have the most significant effects on the CO₂ ventilation metric values. Varying these two parameters by +/- 20 % results in variations in the CO₂ concentrations of about 20 % to 35 %.

KEYWORDS

carbon dioxide, ventilation, metabolic rates, sensitivity analysis, CONTAM

1 INTRODUCTION

Indoor air quality (IAQ) researchers and practitioners have used indoor carbon dioxide (CO₂) concentrations to evaluate IAQ and building ventilation performance for many years (Persily, 1997), in many cases without a full understanding of the technical bases of the methods employed and the assumptions involved (ASHRAE 2022). The use of CO₂ monitoring for ventilation assessment has become more common in response to the COVID-19 pandemic given the importance of ventilation in managing the risks of infection (Persily and Oke, 2022). Many of these monitoring efforts involve the use of a single value of the CO₂ concentration for all indoor spaces, often in the range of 800 ppmv to 1000 ppmv*. However,

* In this work, CO₂ concentrations are expressed in µL/L, which is equivalent to ppmv.

using a single CO₂ concentration for all indoor spaces ignores important differences between indoor spaces, such as their size, intended use, and occupant characteristics (Persily, 2022). These differences impact the CO₂ generation rates, the timing of the concentration measurements relative to the occupancy schedule, and the outdoor air ventilation rates required by ventilation standards and building codes, which in turn influence the indoor CO₂ concentrations. An approach for analyzing space-specific ventilation rates allows users to identify CO₂ ventilation metrics based on these factors (Persily, 2022). An online tool, [QICO2](#), is available to facilitate the application of this approach (Persily and Polidoro, 2022). However, the calculation of CO₂ concentrations as ventilation metrics involves assumptions for several quantities that are inherently uncertain, such as occupant-related characteristics, and the impact of these uncertainties on the metrics is not known.

This study aims to investigate the uncertainties associated with the CO₂-based ventilation metrics proposed previously. We consider a range of values for the occupant characteristics (ratio of males to females, body mass, and level of physical activity) and outdoor ventilation rates. We use the CONTAM airflow and contaminant transport model (Dols and Polidoro, 2020) to predict CO₂ concentrations over the range of input values, with results being evaluated using factorial analysis. This analysis is intended to help practitioners understand the uncertainties associated with the indoor CO₂ concentrations used as ventilation metrics.

2 METHODS

The analysis presented in this paper involved single-zone CONTAM simulations of CO₂ concentrations in several space types. A two-level, full factorial design that was analyzed with a 10-step exploratory data (EDA) approach to identify the most important factors impacting the calculated CO₂ concentrations (NIST/SEMATECH e-Handbook of Statistical Methods). This approach allows the assessment of the impact of each input value on the calculated concentrations as well as the interactions between the input values. The analysis focused on four factors: metabolic rate, ratio of male to female occupants, body mass, and outdoor airflow rate into the space. The calculated CO₂ concentrations reveal the sensitivity to these factors after 1 hour of occupancy and at a steady state.

2.1 Single-zone simulation model

The calculation of these ventilation metrics employs a single-zone mass balance of CO₂ in each space, which is expressed in equation (1):

$$V \frac{dC}{dt} = Q [C_{out} - C(t)] + G \quad (1)$$

where V is the volume of the space being considered, C is the CO₂ concentration in the space, C_{out} is the outdoor CO₂ concentration, t is time, Q is the volumetric flow of air into the space from outdoors and from the space to the outdoors, and G is the CO₂ generation rate in the space. We ignore air density differences between the indoors and outdoors by using the same value of Q for the flow into and out of the space. In addition, the single-zone model does not account for concentration differences within and between the building zones or for CO₂ transport between zones. The solution to equation (1) is expressed in equation (2):

$$C(t) = C(0) e^{-\frac{Q}{V}t} + C_{ss} \left(1 - e^{-\frac{Q}{V}t}\right) \quad (2)$$

where $C(0)$ is the indoor concentration at $t = 0$, and C_{ss} is the steady-state indoor concentration, which is given by:

$$C_{ss} = C_{out} + \frac{G}{Q} \quad (3)$$

Note that the indoor concentration will only achieve steady state if Q and G are constant for a sufficiently long period of time, which may not occur in some spaces depending on the occupancy schedule. We used the factorial capabilities in CONTAM simulations by varying the inputs as described below to estimate the indoor CO₂ concentrations at 1-minute intervals over 24-hours.

2.2 Model Inputs

The inputs investigated in the sensitivity analysis include the following: metabolic rate of the occupants, which is a function of their level of physical activity; the ratio of male to female occupants (MF ratio); body mass of the occupants; and the outdoor airflow rate into the space. We investigated several space types from the commercial/institutional building spaces covered by ASHRAE Standard 62.1 (ASHRAE 2022). Each building space is assumed to be at an indoor temperature of 23 °C and an initial CO₂ concentration of 400 ppmv. Table 1 shows the baseline values for the occupant-related characteristics and the space ventilation rate. For the lobby, we investigated two levels of physical activity of the occupants, referred to as “active” and “mellow,” where the former is associated with a higher met rate. Also, in institutional spaces such as classrooms and lecture rooms, we examined scenarios with either a male teacher or a female teacher. The body mass values in the fourth column contain two values corresponding to the male and female occupants, respectively.

Table 1: Baseline input values for the occupant characteristics for CO₂ concentration calculations

Space type	Occupant density (#/100 m ²)	MF ratio	Body mass M/F (kg)	Metabolic rate (met)	Ventilation rate (m ³ /h)
Classroom (5 y to 8 y)	25	12 : 12 (1 adult Teacher)	Students: 26.4 / 25.8 Teacher: 93.4 / 79.6	Student: 1.5 Teacher: 2.1	185
Lecture classroom	65	32 : 32 (1 adult Lecturer)	Students: 83.6 / 73.7 Lecturer: 93.4 / 79.6	Student: 1.7 Lecturer: 2.1	277
Restaurant dining room	70	Customer: 33:33 Workers: 2 : 2	93.4 / 79.6	Customer: 1.7 Server: 2.2	356
Conference meeting room	50	25 : 25	93.4 / 79.6	1.7	155
Office space	5	2.5 : 2.5	93.4 / 79.6	1.9	42.5
Active Lobby	150	75 : 75	93.4 / 79.6	2.2	405
Mellow Lobby	150	75 : 75	93.4 / 79.6	1.9	405
Retail	15	7.5 : 7.5	93.4 / 79.6	2.1	117

To estimate the CO₂ generation from building occupants, we utilized an approach based on the basal metabolic rate (BMR) and the level of physical activity (M) (Persily and de Jonge, 2017). The BMR is influenced by sex, age, and body mass, and when multiplied by the physical activity level, provides the rate of energy expenditure. Based on that approach, the CO₂ generation, V_{CO₂}, of an individual is estimated by equation (4):

$$V_{CO_2} = BMR \cdot M \left(\frac{T}{P} \right) 0.000179 \quad (4)$$

where M is the metabolic rate, BMR is the basal metabolic rate (MJ/day), and T and P are the air temperature (K) and pressure (kPa), respectively. We estimated the volumetric flow of air into and out of the space using the Ventilation Rate Procedure in ASHRAE Standard 62.1 (ASHRAE 2022), which requires ventilation rates as the sum of a *People Outdoor Air Rate*, R_p (L/s·person) and an *Area Outdoor Air Rate*, R_a (L/s·m²) using equation (5):

$$V_{bz} = R_p \times P_z \times R_a \times A_z \quad (5)$$

where P_z is the number of people in the space, and A_z (m^2) is the net occupied floor area.

Body mass values were derived from the 2015-2018 National Health and Nutrition Examination Survey (NHANES), a comprehensive anthropometric survey representing various age groups and demographics in the United States (Fryar et al., 2021). For the adult population in all spaces, we assumed the occupants were in the range of 30 to 60 years old. The number of occupants in each space was based on the default occupant density values in ASHRAE Standard 62.1 (ASHRAE 2022) and remained constant during each simulation. Metabolic rates were calculated based on the values for activities from published literature for adults (Ainsworth et al., 2011) and youths (Butte et al., 2018).

2.3 Sensitivity Analysis

Two settings were selected for each input in the two-level design, represented as “-1” or “+1” to indicate lower and higher values, respectively. The simulations encompassed all possible combinations of high/low levels for each of the inputs. The number of simulations equals 2^k , where k is the number of factors. In this analysis, with $k = 4$, the total number of simulations was 16. The primary advantage of employing a full factorial design is that it allows for estimating both main effects and interactions among the factors. For simulation purposes, the baseline values of the studied inputs were varied by $\pm 20\%$. The 20% range is not based on specific data or analyses, but rather is intended to represent a realistic range of variation. The 10-step analysis of the results of the simulations produces graphical output that provides insights into the results. For this analysis, the steady-state CO_2 concentration and the concentration at 1 hour were selected as the outcomes or response factors.

Although the 10-step analysis generates 10 plots, we will focus on the ordered data plot and main effects plot as these are most relevant to this study (interaction effects were negligible and the plots related to fitting a model are not applicable). The ordered data plot, shown in Figure 1, shows the output values from smallest to largest for all combinations of input level for the steady-state CO_2 concentration for the classroom. This plot shows which combination of input settings yields higher or lower indoor CO_2 concentrations.

The main effects plot, shown in Figure 2, shows the mean response value for all data at a given level of a factor. For example, the “-” column for MF ratio plots the mean of all the data which have a “-” setting for MF ratio while the “+” column plots the mean of all data which have a “+” setting for MF ratio. The difference between the means for the “-” and “+” setting is the effect size for that factor (this is shown as “|Effect|” on the plot. The plot also shows the relative effect (i.e., the overall mean of the response variable divided by the effect size expressed as a percentage). The values of the effect sizes indicate the relative importance of the factors. This plot demonstrates that the outdoor ventilation rate and metabolic rate have the most significant effect, body mass has some effect (about half the size of metabolic rate and outdoor Ventilation Rate) and MF ratio has very little effect.

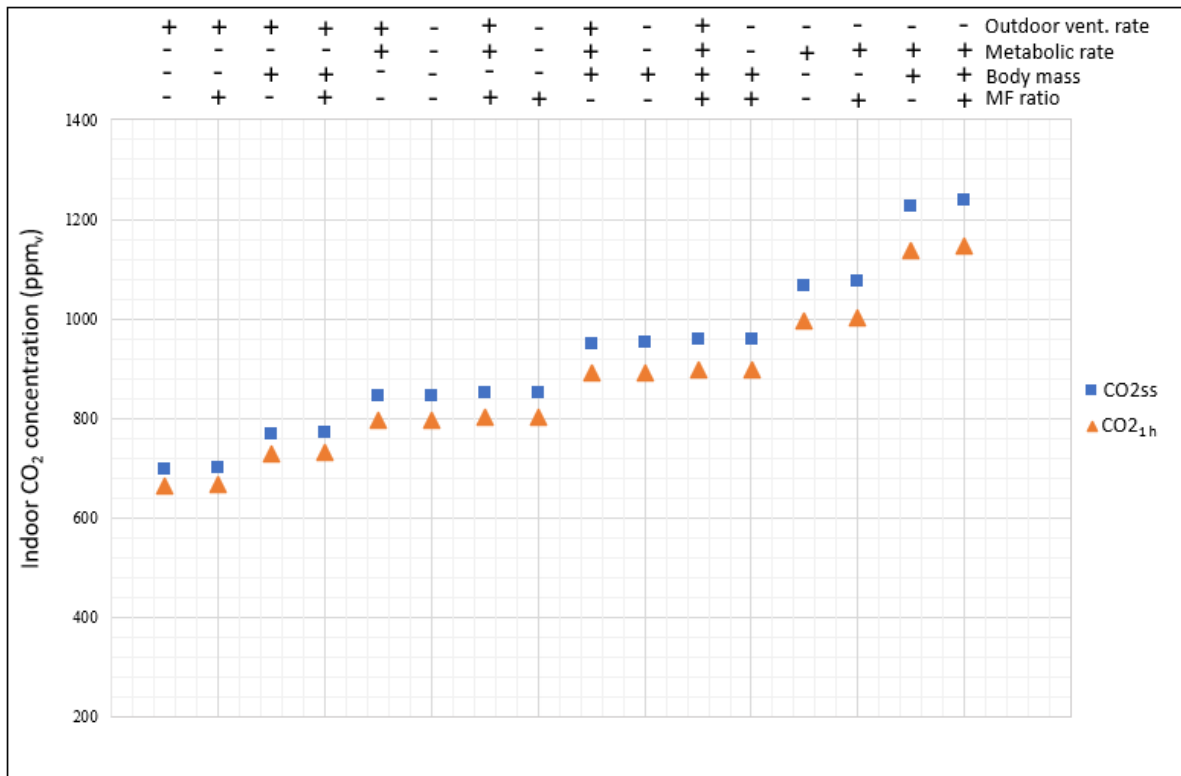


Figure 1: Ordered data plot for steady-state and 1-hr CO₂ concentration in a classroom comprising students aged 5 to 8 with an adult male teacher

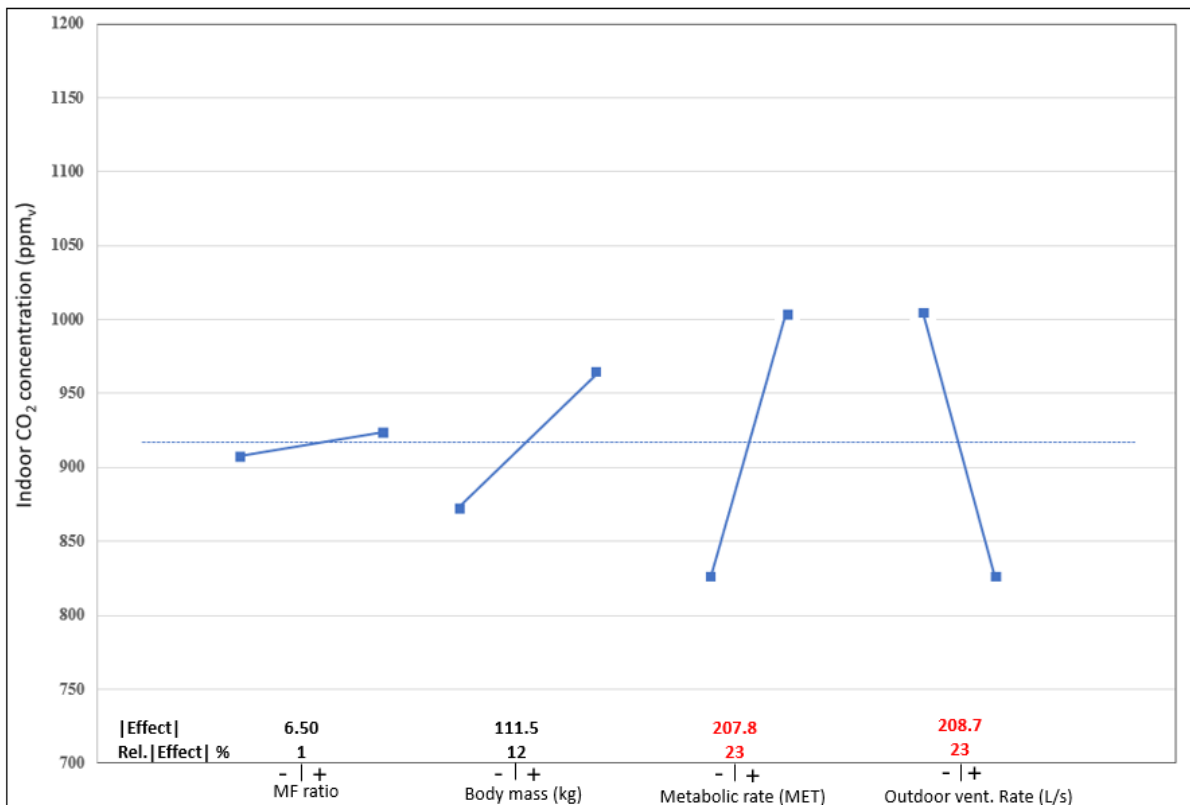


Figure 2: Main Effects plot for the steady-state CO₂ concentration in a classroom comprising students aged 5 to 8 with an adult male teacher

3 RESULTS

Table 2 displays the uncertainty analysis results for the ten spaces considered in this study for the 1-hour CO₂ concentration subject to a +/- 20% variation in each of the four input variables. Table 3 displays the results for the steady-state CO₂ concentrations. The second column of Tables 2 and 3 shows the minimum, maximum, and mean CO₂ concentrations. The remaining columns present the percent difference between the mean concentrations of the lower (-) and upper settings (+) for the four input variables.

Table 2: Percentage difference in 1h concentration for a +/- 20 % variation in the input variable

Space type	Minimum/maximum concentration (mean) ppm _v	Percent difference in 1 h concentration for +/- 20% variation in input variable			
		MF ratio	Body mass	Metabolic rate	Ventilation rate
Classroom (5 y to 8 y, male teacher)	665/1146 (865)	1	11	21	22
Classroom (5 y to 8 y, female teacher)	659/1129 (855)	1	11	21	21
Lecture classroom (male lecturer)	1175/2825 (1846)	3	21	33	31
Lecture classroom (female lecturer)	1171/2812 (1838)	3	21	33	31
Restaurant dining room	1134/2509 (1700)	3	15	31	31
Conference meeting room	1380/3312 (2170)	4	16	35	33
Office space	595/953 (742)	2	9	17	18
Active Lobby	2146/5456 (3504)	5	18	35	35
Mellow Lobby	1855/4520 (2952)	5	17	33	35
Retail	761/1546 (1074)	7	13	28	25

Table 3: Percentage difference in steady state concentration for a +/- 20 % variation in the input variable

Space type	Minimum/maximum concentration (mean) ppm _v	Percent difference in steady-state concentration for +/- 20% variation in input variable			
		MF ratio	Body mass	Metabolic rate	Ventilation rate
Classroom (5 y to 8 y with a male teacher)	697/1237 (922)	1	12	23	23
Classroom (5 y to 8 y with a female teacher)	691/1217 (910)	1	12	22	22
Lecture classroom (with a male lecturer)	1245/3043 (1976)	3	21	34	32
Lecture classroom (with a female lecturer)	1241/3030 (1968)	3	21	34	32
Restaurant dining room	11165/2598 (1755)	3	15	31	31
Conference meeting room	1561/3849 (2496)	4	17	36	34
Office space	889/1783 (1257)	4	14	26	27
Active Lobby	2246/5745 (3682)	5	18	36	36
Mellow Lobby	1938/4755 (3098)	5	17	33	35
Retail	954/2160 (1435)	8	14	32	29

These tables show that outdoor ventilation and metabolic rates impact the 1-hour and steady-state CO₂ concentrations more than body mass and MF ratio. This trend holds across all the spaces examined, although the percentage difference in CO₂ concentration varies across the different space types. For example, in the 5 y to 8 y classroom with an adult male teacher, changing the outdoor ventilation and metabolic rates by +/- 20 % leads to a 22 % and 21 %

shift in the 1-hour CO₂ concentration, respectively (Table 2). At steady state, the same adjustments result in approximately 23 % variation in the CO₂ concentrations, as shown in Table 3. For the office space, varying the outdoor ventilation and metabolic rates by +/- 20 % results in 18 % and 17 % changes in the CO₂ concentration after 1 hour of occupancy, respectively, which increases to 27 % and 26 % percent differences in the CO₂ steady-state concentration.

Body mass and MF ratio have lesser impacts on the calculated CO₂ concentration. In the 5 y to 8 y classroom with an adult male teacher, the +/- 20 % variation in body mass and MF ratio results in 11 % and 1 % shifts in the 1-hour CO₂ concentration. At steady state, the +/- 20 % percent in body mass results in a 12 % change in the CO₂ concentration, while the MF ratio yields a 1% change (Table 3). For the office space, the same variation in body mass and MF ratio resulted in 9 % and 2 % changes in the CO₂ concentration after 1 hour of occupancy and 14 % and 4 % changes in the CO₂ steady-state concentration (Table 3).

4 CONCLUSIONS

In support of the use of CO₂ concentrations as ventilation metrics, a sensitivity analysis was conducted to understand which inputs to the calculations of these metrics were most important and to estimate the impact of their variation on the calculated concentration values. This analysis involved single-zone CONTAM simulations of seven spaces using ventilation rates and default occupant density levels from ASHRAE Standard 62.1 and other parameters impacting CO₂ generation rates based on Persily (2022). The inputs of body mass, male-female ratio for some occupancies, level of physical activity or met rate, and the outdoor air ventilation rate, were all varied by +/- 20 %. The simulations employed a two-level, full factorial design that was analyzed with a 10-step EDA described above. The results showed that ventilation and met rates impact the CO₂ ventilation metric values more than the male-female ratio and body mass, with a range of 20 % to 35 % for the +/- 20 % variation in these inputs. Variations in body mass impacted the CO₂ metrics by 10 % to 20 %, and the male-female ratio variation was closer to 1 % to 8 %.

These results will help users of the CO₂ ventilation metric approach better understand the precision in the calculation of those metrics. In practice, when applying this approach, the ability to determine the required inputs will vary. In cases where one is calculating CO₂ metric values for generic space types, e.g., offices, rather than a specific office, one can only estimate the number of occupants and their characteristics that impact CO₂ generation rates. The target ventilation rate should be known with a higher degree of confidence based on the standard or guidance value one is attempting to verify, though the value may also depend on the number of occupants, as it does in ASHRAE Standard 62.1. Nevertheless, the results of this sensitivity analysis clarify the potential range in the CO₂ metric values in relation to the uncertainty in the concentration measurement. If one is evaluating a specific, existing space, they should have a better idea of the male-to-female ratio, but estimating body mass will be more difficult, requiring characterization of the occupants of the space. The met rate for the space is inherently difficult to determine as the values in the literature are based on specific activities but do not address met levels for occupied spaces, which generally are associated with a range of activities of varying durations. Therefore, the uncertainty in the CO₂ metric values associated with variations in met rates need to be explicitly acknowledged and quantitatively considered.

Additional work is planned to consider other space types, occupancy details, and other times for the CO₂ concentration calculations (as suggested in Persily 2022) to better understand the uncertainties inherent in the CO₂ ventilation metric approach. Also, developing guidance on

the use of the CO₂ ventilation metric based on this work that targets practitioners is being considered.

5 ACKNOWLEDGEMENTS

The authors would like to thank W. Stuart Dols for his assistance in the CONTAM simulations and Alan Heckert and Dennis Leber of the NIST Statistical Engineering Division for their insights on sensitivity analysis.

6 REFERENCES

- Ainsworth, B. (2011) The Compendium of Physical Activities Tracking Guide. Available from: <https://sites.google.com/site/compendiumofphysicalactivities/home?authuser=0>
- ASHRAE. (2022). ANSI/ASHRAE Standard 62.1-2022, Ventilation for Acceptable Indoor Air Quality. American Society of Heating, Refrigerating and Air-Conditioning Engineers, Inc.
- ASHRAE. (2022). ASHRAE Position Document on Indoor Carbon Dioxide. American Society of Heating, Refrigerating and Air-Conditioning Engineers, Inc.
- Butte, N. F., Watson, K. B., Ridley, K., Zakeri, I. F., McMurray, R. G., Pfeiffer, K. A., Crouter, S. E., Herrmann, S. D., Bassett, D. R., Long, A., Berhane, Z., Trost, S. G., Ainsworth, B. E., Berrigan, D., & Fulton, J. E. (2018). A Youth Compendium of Physical Activities: Activity Codes and Metabolic Intensities. *Medicine and science in sports and exercise*, 50(2), 246–256.
- Dols, W.S. and Polidoro, B.J. (2020), CONTAM User Guide and Program Documentation Version 3.4, Technical Note (NIST TN), National Institute of Standards and Technology, Gaithersburg, MD, [online], <https://doi.org/10.6028/NIST.TN.1887r1> (Accessed July 10, 2023)
- Fryar, C.D., Carroll, M.D., Gu, Q., Afful, J., and Ogden, C.L. (2021). Anthropometric reference data for children and adults: United States, 2015–2018. National Center for Health Statistics. *Vital Health Stat* 3(46). 2021.
- Lowther, S.D., (2021). Low-Level Carbon Dioxide Indoors—A Pollution Indicator or a Pollutant? A Health-Based Perspective. *Environments*. 8(11).
- NIST/SEMATECH e-Handbook of Statistical Methods, <http://www.itl.nist.gov/div898/handbook/pri/section5/pri59>, accessed June 5, 2023.
- Persily, A.K. (1997). Evaluating Building IAQ and Ventilation with Indoor Carbon Dioxide. *ASHRAE Transactions*, 103 (2), 193-204.
- Persily, A.K. and de Jonge, L. (2017) Carbon Dioxide Generation Rates of Building Occupants. *Indoor Air*. 27(5): 868-879.
- Persily, A.K. (2022). Development and Application of an Indoor Carbon Dioxide Metric. *Indoor Air*, 32(7), e13059.

Persily, A.K. and Oke, O. (2022). Application of Indoor Carbon Dioxide During the COVID-19 Pandemic. Proceedings of 42nd AIVC Conference, Ventilation challenges in a changing world: 700-709. Rotterdam, Netherlands.

Persily, A.K. and Polidoro, B.J. (2022). Indoor Carbon Dioxide Metric Analysis Tool. NIST Technical Note 2213. National Institute of Standards and Technology.

Wargocki, P. (2021) What we know and should know about ventilation. REHVA Journal. 58 (2): 5-13.

Evaluation of Uncertainties of Using CO₂ for Studying Ventilation Performance and Indoor Airborne Contaminant Transmissions

Liangzhu (Leon) Wang^{1,*}, Ibrahim Reda², Shujie Yan¹, Eslam Ali¹, Dahai Qi², Theodore Stathopoulos¹, and Andreas Athienitis¹

*1 Centre for Zero Energy Building Studies,
Concordia University, 1515 St. Catherine W., H3G
2W1, Montreal, Quebec, Canada*

*2 Department of Civil and Building Engineering,
Université de Sherbrooke, 2500 boul. de l'Université,
J1K 2R1, Sherbrooke, Québec, Canada*

*Corresponding author: leon.wang@concordia.ca

ABSTRACT

The COVID-19 pandemic has raised concerns about indoor ventilation conditions worldwide. Monitoring CO₂ concentrations in rooms has been widely used, but its relationship with outdoor air ventilation rates and ventilation performance is uncertain. Several uncertainties must be quantified, including the location and rate of CO₂ sources, sensor locations, and the dynamics of the surroundings, as well as limitations of existing simulation models, such as well-mixing assumptions. This paper presents field measurements, stochastic modeling, calibrations, and aerodynamics analysis within rooms and contaminant dispersal. Several CO₂ tracer gas tests were conducted in classrooms. Two test setups were used, one for uniformity testing and the other for evaluating ventilation performance. A proposed uniformity index (U_i) is integrated into the tracer decay method to address its limitation due to the well-mixing assumption, thereby improving the air change rate estimation by 22%. As a general rule, the outlet sampling location may represent the average of all locations in mixed-ventilated spaces. Given the small difference in peak CO₂ concentrations (2.6%) and decay periods (15%), 60% of the ventilation capacity should be used instead of the full capacity. As opposed to the instructor's location, the room midpoint yields a 7 percent higher peak CO₂ concentration, which is recommended as a dosing source to estimate air change rates using the tracer decay method. Additionally, novel simulation models have been developed for estimating ventilation air change rates in indoor environments since deterministic approaches cannot incorporate system uncertainties. It has been found that stochastic models, which combine the physical principles of a system with data collected from field measurements, are effective for resolving uncertainties, but they have not been extensively explored in terms of estimating air change rates. Therefore, we also examined the integration of stochastic differential equations (SDEs) and a Bayesian calibration model to evaluate indoor air quality and ventilation conditions in rooms.

KEYWORDS

Decay method; Tracer mixing; CO₂ monitoring; Air change rate; Bayesian calibration

1 INTRODUCTION

Poor indoor air quality (IAQ) often results from insufficient fresh air supply to building occupants. The outbreak of the COVID-19 pandemic has raised public concerns about maintaining a healthy indoor environment and limiting the spread of virus-laden respiratory aerosols. Occupied classrooms in schools, where in-person interactions are frequent, have become one of the vulnerable spaces during this pandemic. Adequate outdoor air ventilation could effectively dilute aerosol concentrations and limit the quantity of inhaled infectious

pathogens (Yan, Wang et al. 2023). Thus, ensuring proper ventilation performance in schools has become much more essential than ever before.

Over the years, improving air quality through enhanced ventilation performance has been the subject of various studies (Karava, Athienitis et al. 2012, Qi, Wang et al. 2014, Yuan, Athienitis et al. 2016, Yuan, Vallianos et al. 2018, Hou, Lin et al. 2020, Qi, Cheng et al. 2020). Characterizing ventilation rates (VR) in buildings has been an effective way for people to understand how much fresh air is delivered to the occupants. It should be noted that VR discussed in this study are in terms of the quantity of outdoor air supplied to the occupied areas, which is usually expressed as air volume per unit time (e.g., L/s) or air volume per unit time per person (e.g., L/s/person). For a lecture classroom, the ventilation design standard of the American Society of Heating, Refrigerating, and Air Conditioning Engineers (ASHRAE) recommends a VR value of not less than 4.3 L/s/person (ASHRAE 2019). Until now, few studies have paid attention to understanding the ventilation conditions of Canadian primary or secondary schools. There are several direct and indirect approaches to measuring air change rates (λ), which include airflow measurements, controlled release as well as in-situ monitoring (McNeill, Corsi et al. 2022). The direct flow measurement, which directly measures the air intake at the air-handling unit (AHU), has been widely adopted for determining the air change rate (Damiano 2010). However, this approach only works for mechanically ventilated buildings, while until recently, a large proportion of Canadian schools were naturally ventilated (Karava, Stathopoulos et al. 2006, Cheng, Qi et al. 2018).

The controlled release approach, which has been widely known as the tracer-gas technique, usually releases a designated amount of tracer gas (a single release, constant release, or controlled release) and then observes its decay with time. Due to its simplicity and less dosing volume of tracer, various studies used the concentration decay method to evaluate ventilation performance and estimate indoor air change rate. However, this method often assumes the well-mixing condition between tracer and air. In reality, the non-uniform mixing is unavoidable that caused by either short-circuiting of the inlet to the outlet or stagnant regions. Therefore, the decay method tends to underpredict λ (Van Ryswyk, Wallace et al. 2015). To fill this research gap, it is important to interpret the results of tracer gas tests in the context of a reliable mixing model.

Selecting tracer gas is important in this method e.g., CO₂ is one of the commonly used tracer gases as it appears to be safe and environmentally friendly, and its concentration could be easily measured with inexpensive sensors. In this approach, CO₂ is also an ideal choice since humans would also become the generation source, and the concentration may indicate room occupancy. In order to estimate λ using measured CO₂ concentrations in Canadian schools, traditionally, the tracer-gas mass balance equations would be used for deterministic predictions. However, during the measurement process, uncertainties would exist due to measurement noises, influence from the outdoor environments, etc., which would be ignored in the deterministic estimations. In the meanwhile, sometimes, the adoption of input parameters may be unreasonable, which would result in a large prediction bias. The stochastic grey-box model (Macarulla, Casals et al. 2018), which combines the physical principles of a system and the information generated from field measurements data, is shown to be promising in dealing with the uncertainties, whereas they have not been investigated in depth to be applied to the estimation of air change rates based on CO₂ measurements in rooms. Meanwhile, the key parameters, including room occupancy and occupant CO₂ generation rates, are often unavailable and lead to significant uncertainties, whereas these parameters may be estimated from Bayesian calibrations based on CO₂ measurements (Hou, Wang et al. 2023). These approaches help deal with uncertainties and disturbances that happen during the ventilation interpretation progress.

To address the research gaps presented above, in this study, we aim to deal with uncertainties coupled with CO₂ field measurements, mass-balance equation modeling, parameter estimations, as well as the well-mixing of tracers and airflows in reality. Although the numerical analysis was focused on single-zone cases, the extensions to multi-zone simulations were also discussed.

2 METHODOLOGIES

2.1. Field measurements in mechanically ventilated classroom

In August 2022, several CO₂ tracer tests were carried out in a classroom on the 5th floor of a 16-story institutional high-rise building (Longueuil Campus, Université de Sherbrooke, Montreal, Canada). The classroom has a volume of 266.3 m³ (8.9×8.8×3.5 m) measured using a laser meter. The entire building is served by a centralized air conditioning system controlled by a building automation system (BAS). A mixed-ventilation system is used consisting of 4 supply air ceiling diffusers (0.6×0.6 m), 6 linear slot diffusers (1.2×0.1 m), and 3 return air ceiling grilles (0.6×0.3 m). Two test setups were built. Setup (I) is designed to quantify the spatial uniformity of CO₂ concentrations by monitoring 16 locations at the breathing level (1.5 m from the floor) using the mid-point as a CO₂ source. On the other hand, setup (II) is arranged to evaluate the effect of three levels of air change rates, two source locations (mid-point and instructor desk's location), and two-door modes (opened and closed) on ventilation performance. Eight sampling locations are monitored at heights of 1.1 and 1.7 m from the floor. For both setups, the inlet (S) and the outlet (R) were also monitored.

Details regarding the tracer tests conducted using CO₂ are presented in Table 1, which is a suitable tracer as recommended by ASTM E741 (ASTM 2017). Test 01 is specified for quantifying the spatial uniformity of CO₂ concentrations, while tests 02-06 are carried out for assessing ventilation performance. Tests 02, 03, and 04 are compared to examine the effect of the air change rates. Tests 04 is compared with Tests 05 and 06 to investigate the effect of door mode and source location on ventilation performance. The BAS system was used to control the ventilation conditions, wherein the air change rate was measured (λ_{eff}) using a balometer device. Meanwhile, the CO₂ injection was controlled using a mass controller, keeping the peak concentration less than 1000 ppm.

Table 1 History of conducted CO₂ tracer tests.

Test No.	Test 01	Test 02	Test 03	Test 04	Test 05	Test 06
Test period [min]	108	70	85	75	75	75
Measured air change rate λ_{eff} [/h]	5.35 ± 0.21	8.92 ± 0.31	5.35 ± 0.21	7.25 ± 0.26	7.25 ± 0.26	7.25 ± 0.26
Source location	Mid-point	Mid-point	Mid-point	Mid-point	Mid-point	Instructor desk
Door mode	Closed	Closed	Closed	Closed	Opened	Closed
Number of sensors	18	10	10	10	10	10

2.2. Field measurements in naturally ventilated classroom

Indoor field measurements of CO₂ levels were performed in one of Montreal's primary schools from 2020 to 2021. The selected classroom has a floor area of 9.4 m × 6.6 m, which is naturally ventilated. The MX1102 (SN: 20820982) CO₂ sensor was installed at 1.7 meters height on the west internal wall right above the thermostat (1.5 m height). Table 2 illustrates the measurement information.

Table 2 Measurements information in the classroom

Location	Age (years)	Dimensions (m)	Ventilation mode	Measurement Periods	Maximum Occupancy
Montreal	5-8	9.4 × 6.6 × 3.5	Natural ventilation	2020/06/22 - 2021/06/21	16

2.3. Single-zone ventilation performance evaluation

To estimate the air change rate λ_o , the well-known decay method (Eq. 1) is commonly used. However, this method assumes a well-mixed space, which limits its accuracy. To address this research gap, a uniformity index (U_i) has been proposed (Eq. 2). By integrating U_i into the decay method, the modified decay method (Eq. 3) has been developed to improve the estimation of air change rates. This modified decay method considers the unavoidable non-uniform mixing, which might be caused by stagnant regions or short-circuiting from the inlet to the outlet. The mathematical solution of Eq. 3 was developed according to (Barber 1982, ASTM 2017).

$$\lambda_o = \frac{1}{(t-t_0)} \ln \frac{(C - C_{bg})}{(C_0 - C_{bg})} \quad (1)$$

$$U_i = \frac{C_{min}}{C_{avg}} \quad (2)$$

$$\lambda_m = \begin{cases} \frac{1}{U_i(t-t_0)} \ln \frac{(C - C_{bg})}{(C_0 - C_{bg})}, & \text{for short - circuiting when } \lambda_o < \lambda_{eff} \\ \frac{U_i}{(t-t_0)} \ln \frac{(C - C_{bg})}{(C_0 - C_{bg})}, & \text{for stagnant regions when } \lambda_o > \lambda_{eff} \end{cases} \quad (3)$$

where λ_o is estimated air change rates for uniform mixing [1/h]; t and t_0 are the final and initial elapsed time [h]; C and C_0 are the final and initial tracer concentrations [mg/m³]; C_{bg} is the background tracer concentration [mg/m³]; U_i is uniformity index; C_{min} and C_{avg} are minimum and average tracer concentrations [mg/m³]; λ_m is estimated air change rates for non-uniform mixing [1/h]; λ_{eff} is measured air change rates [1/h].

Plastic tubings (8 mm ID) were utilized to install the CO₂ injection and sampling systems. The injection flow rate was controlled with a mass controller to keep the peak CO₂ concentration under 1000 ppm. Meanwhile, an automated system monitored the CO₂ concentrations at desired locations online. A vacuum pump operating at 114 L/min continually drew fresh air samples one at a time, which were then supplied to the gas analyzer when the 18-position valve selected them for analysis. A mass spectrometer (UGA-100, Stanford Research Systems) with a quadrupole probe was used. It was also calibrated in one of Concordia's laboratories and in situ. A combination of standard gas concentrations was used for this calibration method (Blessing, Ellefson et al. 2007). According to ASTM E741, the regression curve should be within the 95% confidence level.

2.4. Single-zone air change rate predictions and calibrations

The white-box CO₂ model, which was the traditional deterministic CO₂ mass-balance model at the constant temperature, was shown as follows:

$$V \frac{dC_r}{dt} = -(C_r - C_o) \cdot Q + E \quad (4)$$

where V is the room volume [m³]; C_r is the CO₂ concentration in the room [ppm]; C_o is the CO₂ concentration of outdoor air ventilation flows [ppm]; Q is the air supply into the room [m³/h]; E is the CO₂ generation rate in the room [L/s].

The grey-box CO₂ model, which was established with the stochastic differential equation (SDE), could be expressed as follows:

$$dC_r = \frac{-(C_r - C_0) \cdot Q + E}{V} \cdot dt + \sigma \cdot dw \quad (5)$$

where σ is the incremental variance in the Wiener process; dw is a Wiener process.

In this study, the Bayesian calibration approach was adopted for the inference of air change rates in the established CO₂ white-box/grey-box model. In Bayesian calibration, the probability of the estimated parameters was inferred based on the prior distributions estimated for them. The likelihood of the estimated parameters given the measured data Y (CO₂ indoor concentration) is demonstrated as follows in Bayes's law:

$$P(Q|Y) = \frac{P(Y|Q) \cdot P(Q)}{P(Y)} \quad (6)$$

where $P(Y|Q)$ is the likelihood probability that measurement data Y (which is measured CO₂ concentration C_r in this study) occurs given the prior information of Q , $P(Q)$ is the prior joint probability of Q , and $P(Y)$ is the probability of the measurements results, which is a normalized constant. The prior distributions estimated for models were based on a previous study (Hou, Wang et al. 2023).

2.5. Multi-zone simulations and calibrations

CONTAM software (William and Brian 2015) is one of the most powerful multi-zone simulation tools for indoor air quality analysis. Thus, CONTAM is employed in this study to predict and validate CO₂ concentrations at different locations. For this purpose, the 5th floor of the Longueuil Campus (Montreal, Canada) was modeled (Figure 1). Accurate and real boundary conditions were inputted using the BAS to describe ventilation conditions in addition to considering the measured CO₂ data. Regarding the building envelope parameters, e.g., the infiltration values were obtained from the Quebec code of construction (National Research Council of and Régie du bâtiment du 2022) of 0.25 L/s/m². The model considered other different types of infiltration, such as internal wall and door infiltration. CO₂ injection was defined based on the original injection rate that was carried out during the measurements.

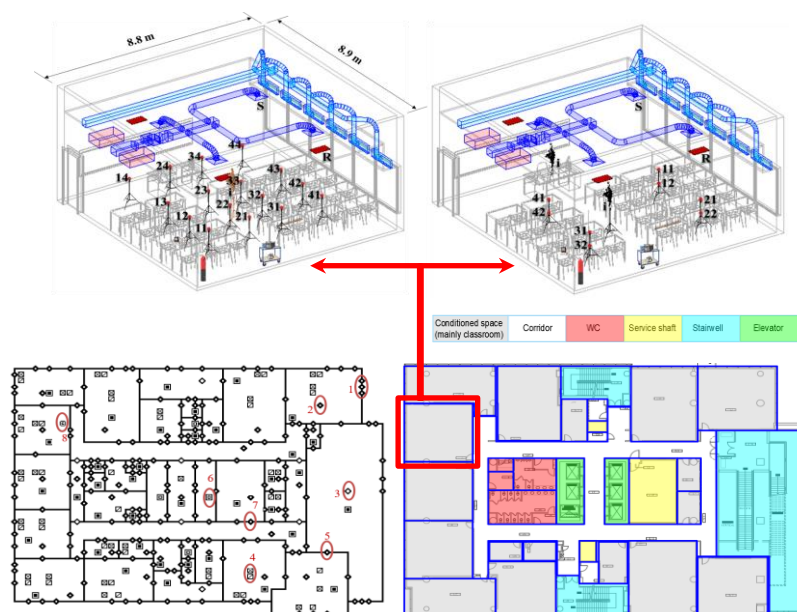


Figure 1 Architectural layout and CONTAM model of the 5th floor, Longueuil Campus, Université de Sherbrooke, Montreal, Canada (1. External wall leakage; 2. Floor leakage; 3. Stair leakage; 4. AHU supply and return; 5. Internal wall leakage; 6. Elevator shaft leakage; 7. Door leakage; 8. CO₂ injection source). Highlighted in red, are 3D views of the selected classroom showing two setups of tracer tests.

An automatic calibration method should be proposed due to the challenges involved in manually calibrating multiple parameters. To perform this, several steps should be taken. The initial step is to conduct a parametric simulation, which includes testing all possible ranges of various simulation parameters with different combinations to obtain a reasonable simulation result. To generate various combinations, a uniform distribution for all parameters was chosen using ContamFactorial 1.0, along with the necessary flagged and value files for creating different project files. A Python code was developed to execute the extracted data files and convert the simulation results into a spreadsheet format for exporting the results. Table 3 displays the parameter ranges utilized in this parametric analysis. Sampling was needed first to minimize the number of simulations. Sampling is often used to select the combinations that could be used to cover the whole range of these combinations. There are different kinds of available sampling methods. In this study, the Sobol method is used as it could be used in capturing the linear and non-linear correlations between the inputs and outputs when performing the sensitivity analysis, as discussed later. By utilizing sampling techniques, the total number of simulation cases can be reduced to 1152, which is significantly less than the millions of cases. Then, sensitivity analysis is proposed to evaluate the importance of each parameter in the results. Sobol variance-based method (Saltelli, Annoni et al. 2010) was used to evaluate the correlations between the different input parameters and output results. A sample file was first created that has all the possible combinations of the input parameters. Then, the Monte-Carlo integration was used to calculate the sensitivity index (SI) based on both the sample files and the results.

Table 3. Utilized parameter ranges for parametric analysis

Parameter	Uniform distribution range	Unit
External wall infiltration	$0.25 \pm 20\%$	L/s/m ²
Internal wall infiltration	$0.25 \pm 20\%$	L/s/m ²
Floor infiltration	$0.25 \pm 20\%$	L/s/m ²
Door infiltration	4 – 27	cm ²
Outdoor CO ₂ concentration	396 – 416	ppm
Initial indoor CO ₂ concentration	400 – 700	ppm
Indoor CO ₂ generation rate	0.002 – 0.01	L/s/ person
Occupancy	0 – 40	Number

3 RESULTS AND DISCUSSION

3.1. Single-zone measurements and simulations, calibrations

Figure 2a shows measured CO₂ concentrations at various locations with peak difference values ranging from 213 to 331 ppm. The outlet location has a peak CO₂ concentration (272 ppm) close to the average of all distributed 16 sensors at the breathing level (278 ± 33 ppm). Therefore, the outlet location is a good sampling representative of interest in this mixed-ventilated zone. Integrating the proposed uniformity index ($U_i = 0.77$) in the decay equation succeeded in decreasing the error caused by the well-mixed assumption at the outlet and the average locations from 25% to 3% (Figure 2b).

Both peak CO₂ concentration and decay period inversely correspond to increasing the air change rate (Figure 2c). When the maximum air change rate of 9 /h decreases to the minimum value of 5 /h, the peak CO₂ concentration and decay period both decrease by 39% and 63%, respectively. On the other hand, when comparing the maximum air change rate of 9 /h with the frequent operating air change rate of 7 /h, there were only minor differences observed in both the peak CO₂ concentration (2.6%) and decay period (15%). As a result, it is suggested to operate the space at 60% of its full ventilation capacity (7 /h). Opening the door reduces exposure to peak CO₂ concentration and decay period by 34% and 56%, respectively. The mid-point location is recommended as the dosing source for estimating the air change rate, rather than the instructor's desk location, as it resulted in a 7% higher peak CO₂ concentration.

Figure 3 shows (a) the measured CO₂ level in different seasons and (b) an example for evaluating the modeling approach on a selected day. During school hours (9:00 – 16:00), measurement data from 9:00 to 13:00 and 13:00 – 16:00 were used for predicting the estimated parameters and evaluating the prediction performance, respectively. The single-zone simulated CO₂ concentration with parameters estimated from the white-box and grey-box model is shown in Figure 3c. The rolling-window approach was applied for the simulation of indoor CO₂ levels (Hou, Wang et al. 2023). Results suggest that the grey-box model tends to have a better prediction performance than the white-box model. The mean average error (MAE) is 97.4 for the white-box model ppm and 48.6 ppm for the grey-box model (Table 4). This indicates that the grey-box model gives more reasonable predictions for this selected day. The results evaluated from other indices also indicate a similar trend, as shown in Table 4.

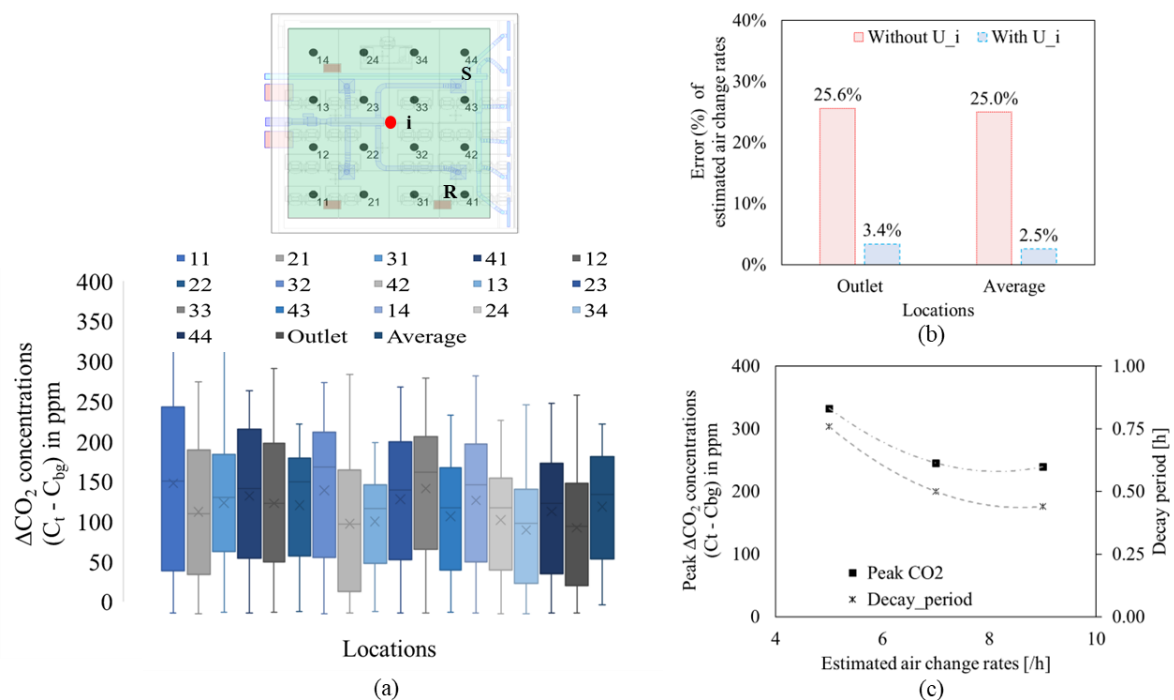


Figure 2 (a) Measured CO₂ concentrations at 16 different sampling locations in addition to the inlet and outlet. (b) Comparing the error percentage of estimated air change rates at the outlet and the average of all 16 locations at the breathing level. (c) Peak CO₂ concentrations and decay periods at various air change rates.

Table 4 Evaluations for the modeling performance

Model	MAE (ppm)	MAPE (ppm)	MSE (ppm)	RMSE (ppm)	R ²
White-Box	97.4	4.8	12791.2	113.1	0.99
Grey-Box	48.6	2.6	3361.9	58.0	0.99

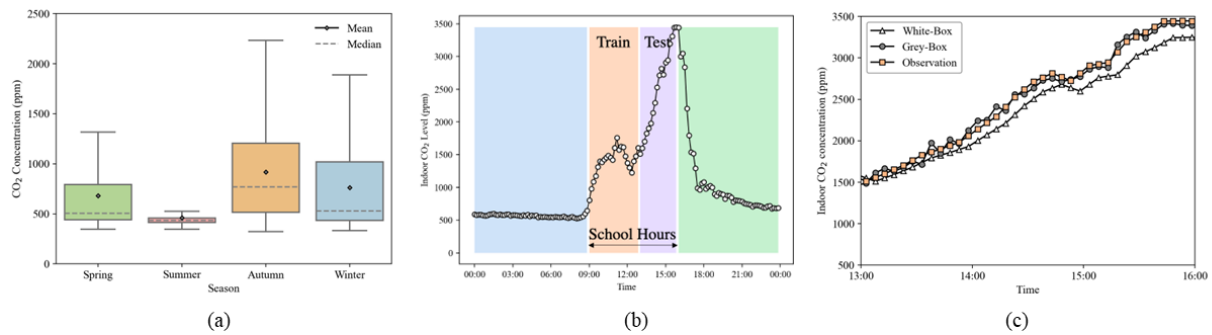


Figure 3 Measured CO₂ concentration in the classroom for different seasons (a) and for one selected day (b) Simulated CO₂ concentration with parameters estimated from the white-box/grey-box model (c).

3.2. Multi-zone simulations and calibrations

The baseline model was first validated against the measurement data. Figure 4 shows the difference in CO₂ concentration relative to the initial concentration for one sample room within the building. The results are shown for the whole measurement time, including a pre-injection period in the beginning, an injection period, and then decay. These results suggest that there has been a considerable deviation between the measurements and the simulation due to the uncertainties of the input parameters. Initially, manual calibration was explored to determine if it was feasible to adjust the input parameters based on the results. It was found that a calibration technique is necessary when dealing with such issues, particularly when there are a large number of input parameters that would make it difficult to modify each parameter individually or manually.

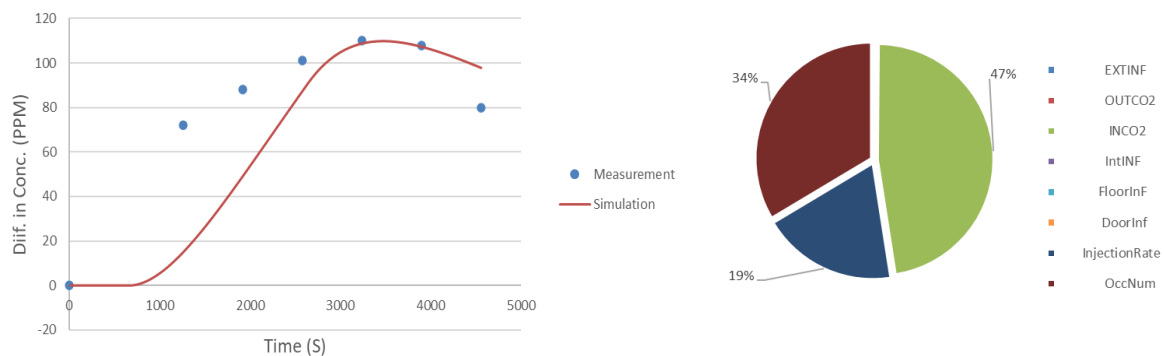


Figure 4 CO₂ concentration difference versus time (left) and sensitivity index of the input parameters (right).

After performing the parametric simulations and extracting the results, the sensitivity analysis was performed to evaluate the importance ranking of every input parameter on the output results. Figure 4 (right) shows the sensitivity Index (SI) for all the input parameters. The results suggest that the initial CO₂ concentration within the room, the occupancy, and the CO₂ generation rate are the main parameters that shall be calibrated for each zone. The other parameters will be assigned with their mean value as their influence is almost negligible. It should be noted that the proposed methodology is expected to work for the other buildings but the results may be different.

4 CONCLUSIONS

This study quantifies inevitable uncertainties coupled with monitoring and modeling CO₂ concentrations to assess ventilation performance, i.e., quantify air change rates and mitigate aerosol viral transport in buildings. A proposed uniformity index (U_i) is integrated into the decay method to reduce its limitation on uniform mixing only. Later, the effect of air change rate, source location, and door mode on ventilation performance is experimentally evaluated.

In addition, stochastic modeling and calibrations were carried out to investigate other significant factors (CO₂ injection rate and the dynamics with the surroundings). The grey-box CO₂ model was integrated with the Bayesian calibration method to support the evaluations of indoor air quality and air change rates in Canadian classrooms. By taking uncertainties from different sources into consideration, this approach would effectively estimate the air change rate from in-situ CO₂ monitoring. Additionally, this study presents a novel approach for calibrating multi-zone CO₂ simulations, which helps to identify the key parameters to be calibrated.

The following conclusions were researched through this study: The proposed uniformity index succeeded in decreasing the error caused by the well-mixed assumption from 25% to 3%. The grey-box model could give reasonable predictions for CO₂ monitoring. Three main parameters that need to be calibrated are the initial CO₂ concentration, occupancy, and CO₂ generation rate, as they have a significant impact on the accuracy of the air change rate estimation.

Future studies should be directed to developing an algorithm that can assign values to the parameters requiring calibration by utilizing measurements to minimize the error between the measurements and the simulation. Additionally, investigating the possibility of applying the same methodology to other contaminants and different ventilation systems would be beneficial.

ACKNOWLEDGMENTS

This work is supported by the Fonds Québécois de la Recherche sur la Nature et les Technologies – Team Research Project, under grant no. 2022-PR-299939 – through "*Investigation of Energy-Efficient Ventilation and Pressurization Strategies to Prevent Potential Airborne Virus Transmissions for High-rise Buildings in Québec*", and by the National Research Council Canada contract [#980615 and #999657] through "*Benchmarking test facilities for capturing aerosol movement in building spaces – an evidence-centered study (Phase I and II)*".

5 REFERENCES

- ASHRAE (2019). "Standard 62.1-2019, Ventilation for Acceptable Indoor Air Quality." American Society of Heating, Refrigerating, and Air-Conditioning Engineers: Atlanta, GA, USA.
- ASTM (2017). ASTM E741-11 (Reapproved 2017): Standard Test Method for Determining Air Change in a Single Zone by Means of a Tracer Gas Dilution, American Society for Testing Materials.
- Barber, E. (1982). "Incomplete Mixing in Ventilated Airspaces. (Part I) Theoretical Considerations." Can. J. Agric. Eng. **24**(1): 25-29.
- Blessing, J. E., R. E. Ellefson, B. A. Raby, G. A. Brucker, R. K. J. J. o. V. S. Waits, S. Technology A: Vacuum and Films (2007). "Recommended practice for process sampling for partial pressure analysis." **25**(1): 167-186.
- Cheng, J., D. Qi, A. Katal, L. L. Wang, T. J. J. o. W. E. Stathopoulos and I. Aerodynamics (2018). "Evaluating wind-driven natural ventilation potential for early building design." **182**: 160-169.
- Damiano, L. A. (2010). "Reduction of errors in ventilation rate determinations." ASHRAE Transactions **116**(2): 54-70.
- Hou, D., C.-C. Lin, A. Katal and L. Wang (2020). Dynamic forecast of cooling load and energy saving potential based on Ensemble Kalman Filter for an institutional high-rise building with hybrid ventilation. Building Simulation, Springer.

Hou, D., L. Wang, A. Katal, S. Yan, L. Zhou, V. Wang, M. Vuotari, E. Li and Z. Xie (2023). Development of a Bayesian inference model for assessing ventilation condition based on CO2 meters in primary schools. Building simulation, Springer.

Hou, D., L. Wang, A. Katal, S. Yan, L. Zhou, V. Wang, M. Vuotari, E. Li and Z. Xie (2023). "Development of a Bayesian inference model for assessing ventilation condition based on CO2 meters in primary schools." Building Simulation **16**(1): 133-149.

Karava, P., A. Athienitis, T. Stathopoulos, E. J. B. Mouriki and Environment (2012). "Experimental study of the thermal performance of a large institutional building with mixed-mode cooling and hybrid ventilation." **57**: 313-326.

Karava, P., T. Stathopoulos and A. J. I. J. o. V. Athienitis (2006). "Impact of internal pressure coefficients on wind-driven ventilation analysis." **5**(1): 53-66.

Macarulla, M., M. Casals, N. Forcada, M. Gangoellés and A. Giretti (2018). "Estimation of a room ventilation air change rate using a stochastic grey-box modelling approach." Measurement **124**: 539-548.

McNeill, V. F., R. Corsi, J. A. Huffman, C. King, R. Klein, M. Lamore, S. L. Miller, N. L. Ng, P. Olsiewski and K. J. G. Pollitt (2022). "Room-level ventilation in schools and universities." Atmospheric Environment: X **13**: 100152.

National Research Council of, C. and Q. Régie du bâtiment du (2022). Quebec Construction Code, Chapter I: Building, and National Building Code of Canada 2015 (amended), National Research Council of Canada.

Qi, D., J. Cheng, A. Katal, L. Wang, A. J. I. Athienitis and B. Environment (2020). "Multizone modelling of a hybrid ventilated high-rise building based on full-scale measurements for predictive control." **29**(4): 496-507.

Qi, D., L. L. Wang and R. Zmeureanu (2014). Verification of a multizone airflow and energy network model by analytical solutions to Stack-driven flows in buildings. eSIM Conference Proceedings (Ottawa, Canada).

Saltelli, A., P. Annoni, I. Azzini, F. Campolongo, M. Ratto and S. Tarantola (2010). "Variance based sensitivity analysis of model output. Design and estimator for the total sensitivity index." Computer Physics Communications **181**(2): 259-270.

Van Ryswyk, K., L. Wallace, D. Fugler, M. MacNeill, M. È. Héroux, M. D. Gibson, J. R. Guernsey, W. Kindzierski and A. J. Wheeler (2015). "Estimation of bias with the single-zone assumption in measurement of residential air exchange using the perfluorocarbon tracer gas method." Indoor Air **25**(6): 610-619.

William, D. and P. Brian (2015). CONTAM User Guide and Program Documentation Version 3.2, Technical Note (NIST TN), National Institute of Standards and Technology, Gaithersburg, MD.

Yan, S., L. Wang, M. J. Birnkrant, Z. Zhai and S. L. Miller (2023). "Multizone Modeling of Airborne SARS-CoV-2 Quanta Transmission and Infection Mitigation Strategies in Office, Hotel, Retail, and School Buildings." **13**(1): 102.

Yuan, S., A. Athienitis, Y. Chen and J. Rao (2016). Development of a thermal model for thermal mass coupled with hybrid ventilation in an institutional building. eSim 2016 Conference.

Yuan, S., C. Vallianos, A. Athienitis, J. J. B. Rao and Environment (2018). "A study of hybrid ventilation in an institutional building for predictive control." **128**: 1-11.

Effects of ventilation on airborne transmission: particle measurements and performance evaluation

Huijuan Chen^{*1}, Caroline Markusson¹, and Svein Ruud¹

*1 RISE Research Institutes of Sweden
Industrigatan 4
Borås, Sweden*

**Corresponding author: Huijuan.chen@ri.se*

SUMMARY

This research aims to evaluate ventilation performance on airborne transmission in buildings, by analyzing the effect of different ventilation configurations and flow rates on contaminant removal effectiveness.

KEYWORDS

Ventilation, airborne transmission, air distribution, particle measurement, ventilation effectiveness

1 INTRODUCTION AND METHOD

Airborne transmission is widely recognized as the dominant transmission route between people for many respiratory viruses. It refers to the inhalation of infectious aerosols or “droplet nuclei” (droplet that evaporate in the air). These aerosols or “droplet nuclei” are often defined to be smaller than 5 μm and can travel distances of more than 1-2 meters from the infected individual (Wang et al., 2021). Ventilation strategies, air distribution methods, and air flow rates may have significant impacts on airborne transmission (Wej et al., 2016; Qsman et al., 2022). By evaluating ventilation configurations knowledge on how to control flow path of air in buildings to provide a desired combination of occupant thermal comfort and good hygienic conditions can be obtained (Cho et al., 2019). This research aims to evaluate different ventilation configurations for control of airborne transmission in a room by laboratory measurements.

Measurements were performed at RISE Research Institutes of Sweden laboratory inside a test room with dimensions of 4.2 \times 5.0 \times 2.5 m (L \times W \times H). The test room was equipped with a ceiling swirl supply diffuser, a TV set (120 W), ceiling light (60 W) and a dummy (70 W). Different flow rates (8, 15, 30 and 40 l/s), two ventilation exhaust positions (high and low), and contaminant source location in relation to ventilation exhaust were tested; see Figure 1(a). The contaminant source was simulated by potassium chloride (KCL) aerosols generated by AGK 2000. Particle number concentrations at four positions, one close to the ventilation exhaust and three other locations (A, B and C) along the centreline of the room at the height (H) of 1.2 m, were measured by four particle counters, Optical Particle Sizer (OPS) 3330, simultaneously. All measurements were made during steady state conditions for one hour. Correlation tests were also made to assess the relative bias among the particle counters. Results were analysed by:

$$\varepsilon_p = (C_e - C_s)/(C_p - C_s) \quad (1)$$

Where ε_p is the particle removal effectiveness at point p , C_e , C_s and C_p is the particle concentration at the air exhaust, supply and a point inside the room. As the supply air was almost particle free $C_s = 0$.

2 RESULTS AND DISCUSSION

Comparisons of the particle removal effectiveness between different flow rates, for the two ventilation exhaust positions (high and low), at middle of the room (point B) with $H = 1.2$ m, is shown in Figure 1(b) and 1(c) respectively. As seen, the contaminant removal effectiveness is decreased as the flow rate is increasing from 8 to 40 l/s. With the low flow rates 8 and 15 l/s, the room air is mixed in the lower region, while in the upper region the contaminated air is accumulated, and the concentration level is high due to stratification and stagnation. A high exhaust is therefore more effective than a low exhaust to remove particles. The ventilation effectiveness is reduced from about 1.15 to 0.9 for the high exhaust (Figure 1b), while it is reduced from 1.0 to 0.8 for the low exhaust (Figure 1c). With the high flow rates 30 and 40 l/s, room air is fully mixed. The effectiveness is about 1 with 30 l/s, which is slightly reduced when increasing to 40 l/s and when moving the exhaust from a high position to a low position. This is due to short circuit which means that the jet from the supply diffuser is so strong that part of the fresh air reaches the exhaust directly without mixing with the room air. Although high flow rates result in a lower ventilation effectiveness, the absolute number of particles in the room would be less compared to low flow rates due to better dilution. This suggests that a balance between the contaminant dilution and removal should be considered when increasing flow rates to enable sufficient and effective ventilation.

As seen in Figure 1(d), moving the contaminant source close to the exhaust improves the particle removal efficiency for the high exhaust. For the low exhaust, the source location is not important as the room air is mixed in the region up to 1.2 m. Re-arranging room layout considering potential source locations could be a measure to reduce airborne transmission.

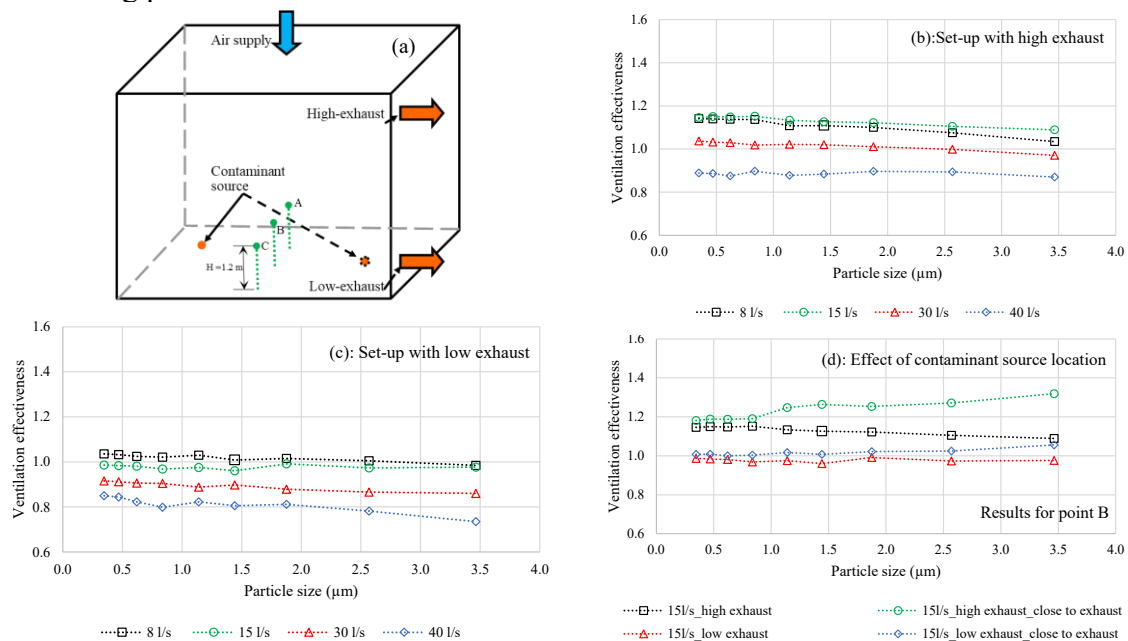


Figure 1: Measurement set-ups (a) and results (b-d)

3 REFERENCES

- Wang, C. C., Prather, K. A., Sznitman, J., Jimenez, J. L., Lakdawala, S. S., Tufekci, Z., & Marr, L. C. (2021). Airborne transmission of respiratory viruses. *Science*, 373(6558), eabd9149.
- Wei, J., & Li, Y. (2016). Airborne spread of infectious agents in the indoor environment. *American journal of infection control*, 44(9), S102-S108.
- Osman, O., Madi, M., Ntantis, E. L., & Kabalan, K. Y. (2022). Displacement ventilation to avoid COVID-19 transmission through offices. *Computational Particle Mechanics*, 1-14.
- Cho, J., Woo, K., & Kim, B. S. (2019). Removal of airborne contamination in airborne infectious isolation rooms. *ASHRAE Journal*, 61(2), 8-21.

Impact and benefits of the air cleaning measures implemented in two schools

Liang Grace Zhou^{*1}, Chang Shu¹, Justin Berquist¹, Janet Gaskin¹, and Greg Nilsson¹

¹ National Research Council Canada, Construction Research Centre
1200 Montreal Road, Building M24
Ottawa, Ontario, Canada K1A 0R6
First and Presenting author: Liang.Zhou@nrc-cnrc.gc.ca

ABSTRACT

A Canadian provincial government has initiated a collaboration with the Indoor Air Quality (IAQ) team of the National Research Council of Canada (NRC) to conduct a controlled intervention study to determine the effectiveness of portable air cleaners (PACs) in reducing indoor air contaminants in 2 schools. The study examined the presence of particulate matter of 1-, 2.5-, and 10-micron diameters (PM1, PM2.5, and PM10), carbon dioxide (CO₂), and sick days reported by staff and students under various operating conditions to determine if PACs could make a statistically significant difference in these IAQ and health indicators. This paper describes the study methods and the following key findings: 1) The indoor CO₂ concentrations were dependent on the presence of occupants and the leaks/openings through the building envelope in the space. Higher CO₂ concentrations were measured in classrooms with higher occupant densities. The CO₂ concentrations measured in both schools agreed with CO₂ concentration metrics predicted based on occupant characteristics and ASHRAE 62.1 ventilation requirements. 2) The outdoor particle sources played the most significant role in deciding the indoor particle concentrations. The presence of exterior walls and windows in a space also affected the indoor particle concentrations. 3) A particle removal efficiency index was defined and used to assess the effectiveness of filtration in removing particles. Based on the PM1 and PM2.5 removal efficiency results, the PAC units in the intervention school were able to remove some of the particles entered indoors.

KEYWORDS

Air cleaning, ventilation, occupancy, particle measurement, CO₂ concentration

1 INTRODUCTION

The NRC's IAQ team has been conducting laboratory and field studies to assess the effectiveness of air cleaning and ventilation in reducing airborne transmission of infectious aerosols and wildfire smoke exposure in buildings. Exhaled aerosols with pathogens are typically smaller than 5 µm, and a large proportion of them are smaller than 1 µm for most respiratory activities such as breathing, talking, and coughing (Fennelly, 2020; Wang et al., 2022). It is widely acknowledged that wildfires generally produce fine (<2.5 µm) and ultrafine particles (<1 µm), which pose the main health risks (Black et al., 2017; ECCC, 2023). In response to the COVID-19 pandemic, there have been many recommendations to monitor indoor CO₂ levels as an indicator of the risk of airborne transmission of pathogens and the adequacy of ventilation rates (CDC, 2021; EMG/SPI-B, 2021; REHVA, 2021).

The aim of this control-intervention study was to determine the effectiveness of deploying portable air cleaners (PACs) for improving indoor air quality and correspondingly, the health of occupants. This was primarily assessed by monitoring the concentration of particulate matter and number of reported sick days by students and staff. Additionally, the CO₂ level was also monitored to indicate whether periods of inadequate ventilation occurred in the two schools.

2 METHODOLOGY

Two schools in the same city with similar characteristics including the year built, heating, ventilation, and air conditioning (HVAC) system, number of rooms (25-30), number of teachers, and number and age of students (kindergarten to Grade 8), were selected for a field monitoring campaign. Phase 1 of the study was from March to June 2023. During this period, the control school relied solely on the existing HVAC system. Meanwhile, the intervention school relied solely on the existing HVAC system in April. After which time, one PAC was used in each classroom and the teachers lounge, and two PACs were used in the library in May and June. Air quality sensors were installed in classrooms, hallways, and other common spaces in both schools to continuously monitor the concentration of particulate matter (PM₁, PM_{2.5}, and PM₁₀), CO₂, temperature, relative humidity, and sound level in both schools. In each of the classrooms, 1 sensor was placed near the door (measurement location A), and another one was placed near an exterior wall/window (if present) or a wall on the opposite side (measurement location B). An outdoor sensor was mounted on the rooftop of each school to monitor these same parameters outdoors.

3 RESULTS AND DISCUSSION

Due to page limitations, the following sections will only display select CO₂ and particle measurements as the major indicators of IAQ.

3.1 Factors affecting indoor CO₂ concentration

Figure 1 shows the outdoor and indoor CO₂ concentrations in two classrooms in the intervention school from the last week of March to June 2023 (14 weeks). The last of week of March (week 1) was spring break. It can be observed from Figure 1 that the indoor CO₂ concentrations were primarily dependent on the presence of occupants. However, the presence of exterior walls and windows also played a role in affecting indoor CO₂ concentrations. For example, classroom INT-C-02 has exterior walls and windows, and sensor B near the windows in this room often recorded lower concentrations than sensor A near the door did. This can be seen more clearly in Figure 2. All the walls in classroom INT-C-10 were interior, and the two sensors in this room generally agreed with each other well. It is worth noting that the details about the HVAC system's operating schedule, the outdoor air intake rate, the in-duct filter efficiency, and the air infiltration through building envelopes were unknown in these classrooms. Additionally, a PAC was installed in both classrooms at the end of week 6 and has been kept on continuously after, which did not affect the CO₂ concentrations in both classrooms, as expected.

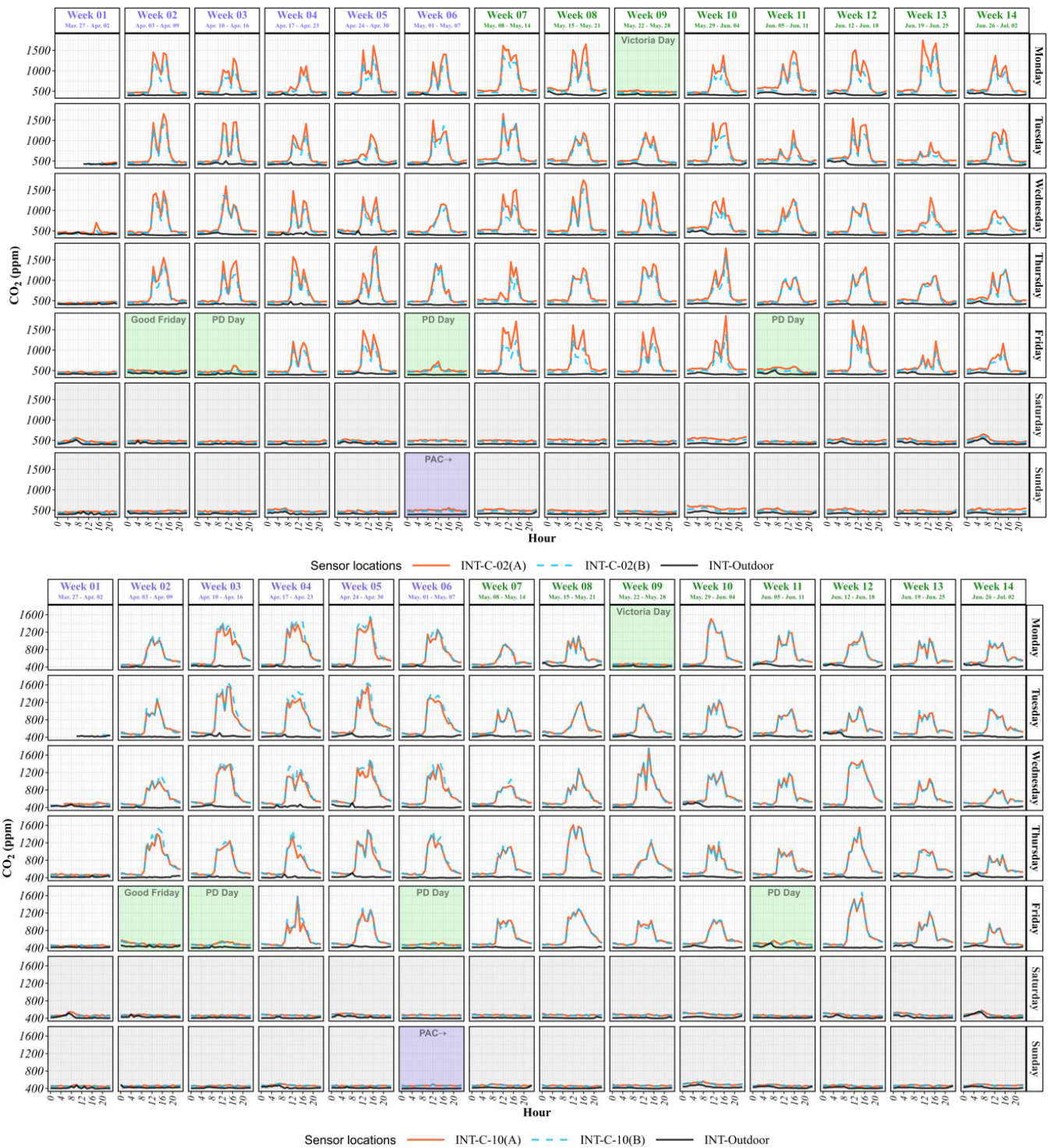


Figure 1: Outdoor and indoor CO₂ concentrations in 2 classrooms in the intervention school: with exterior windows (above) and without (below)

The CO₂ concentrations in two adjacent classrooms, INT-C-02 and INT-C-03, in the intervention school on April 11 and May 16 are plotted in Figure 2. These classrooms have similar layouts, dimensions, and HVAC system configurations. INT-C-02 had 29 students (ages 11 to 12), whereas INT-C-03 had 20 students (ages 13 to 14). The higher occupant density in INT-C-02 resulted in higher CO₂ concentrations than the levels observed in INT-C-03 between 8 AM and 4 PM when the rooms were occupied. The CO₂ concentrations measured from both schools during the occupied periods agreed with the CO₂ concentration metrics proposed by Persily (2022) for classrooms based on occupant characteristics and ASHRAE 62.1 ventilation requirements.

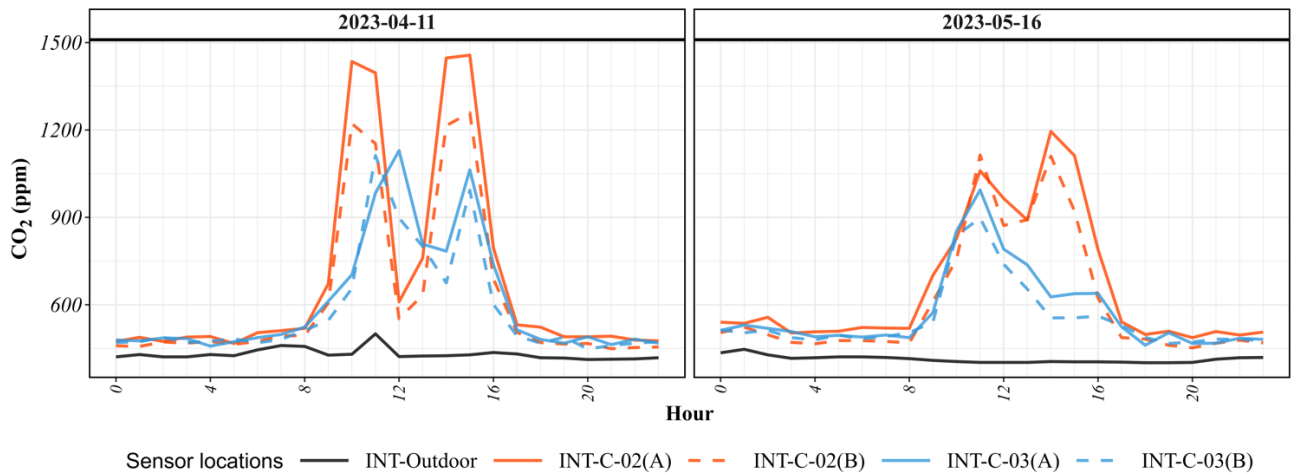


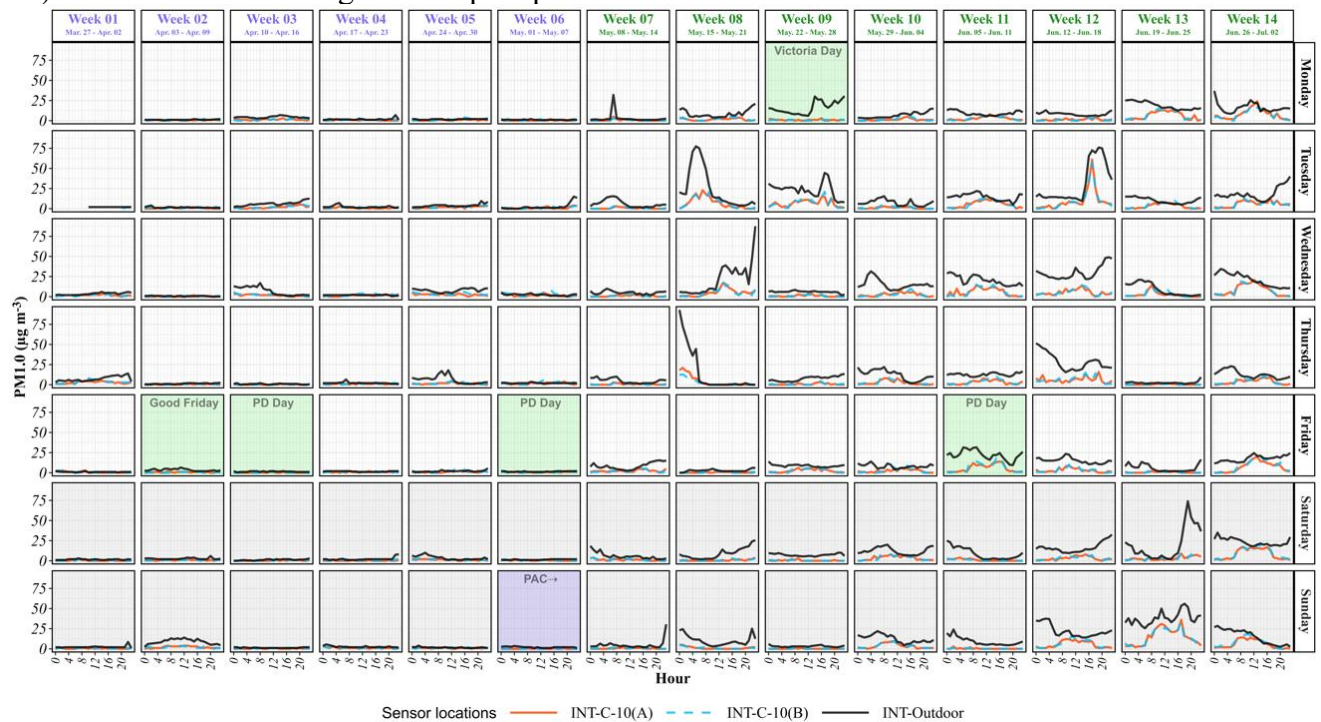
Figure 2: CO₂ concentrations in 2 classrooms in the intervention school on April 11 and May 16

The CO₂ measured on May 16 in both classrooms were lower than the readings on April 11. One possible reason for this is that outdoor air with a lower CO₂ concentration entered the space through open windows and/or the HVAC system when weather became warmer on May 16.

3.2 Factors affecting indoor PM1 and PM2.5 concentration

2.2.1 Outdoor PM1 and PM 2.5 concentration

Figure 3 and Figure 4 present the indoor and outdoor PM1 and PM2.5 concentrations measured in classrooms INT-C-10 and CTL-C-10 during the 14-week testing period from March to June. The results between weeks 7 and 12 in Figure 3 and Figure 4 demonstrate that the outdoor sources played the most significant role in deciding the indoor PM1 and PM2.5 concentrations during this period. The higher than usual outdoor particle concentrations in this period were likely correlated to the wildfire events in a neighbouring province at the same time ([2023 Alberta wildfires - Wikipedia](#)). No PAC units were used in either school between week 1 and week 6, and the concentrations of PM1 and PM2.5 in both classrooms (INT-C-10 and CTL-C-10) did not increase during the occupied period between 8 AM and 4 PM.



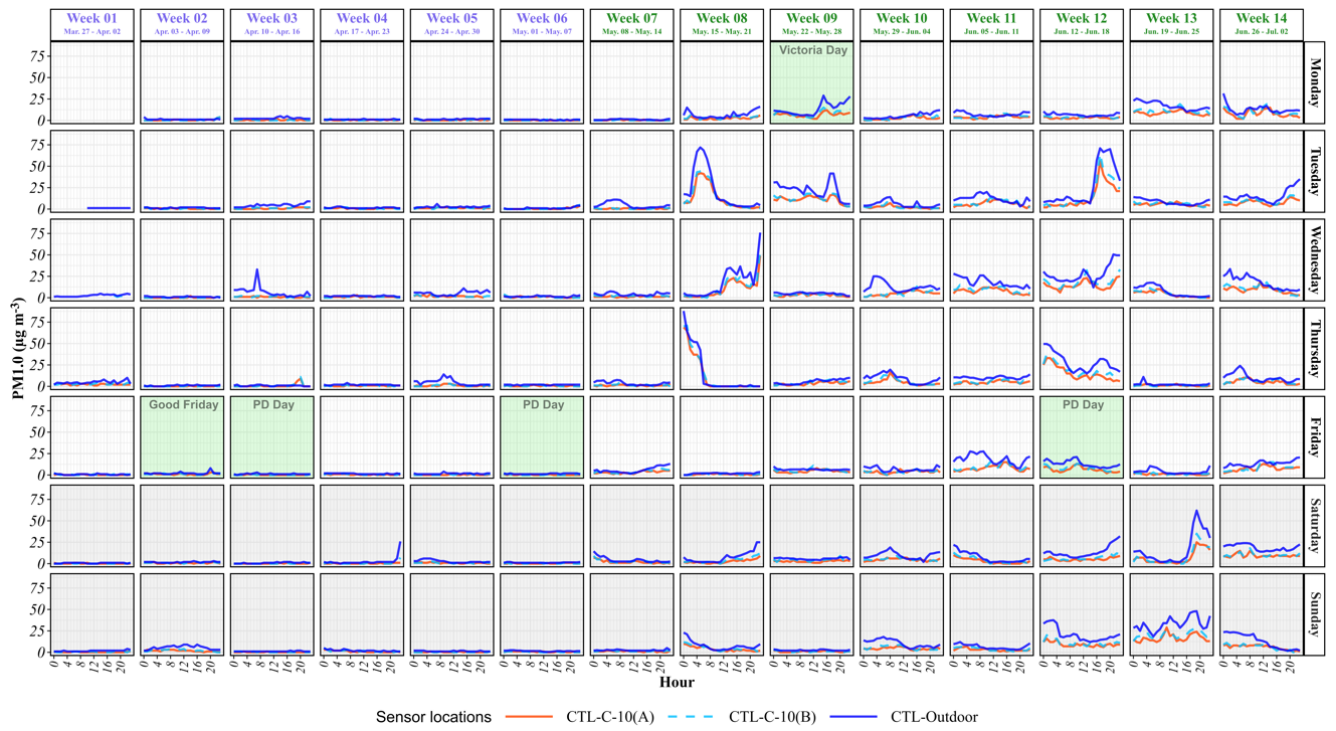
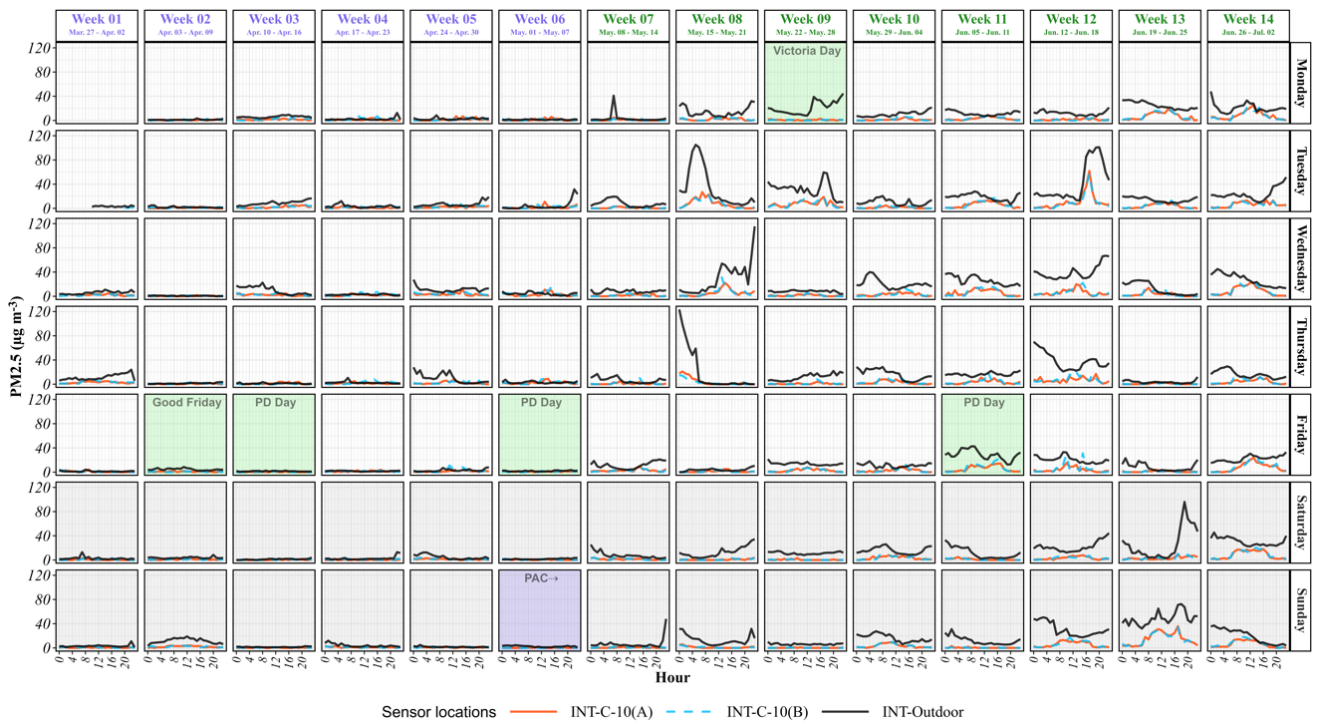


Figure 3: PM1 concentrations: a classroom in the intervention school (above) and in the control school (below)



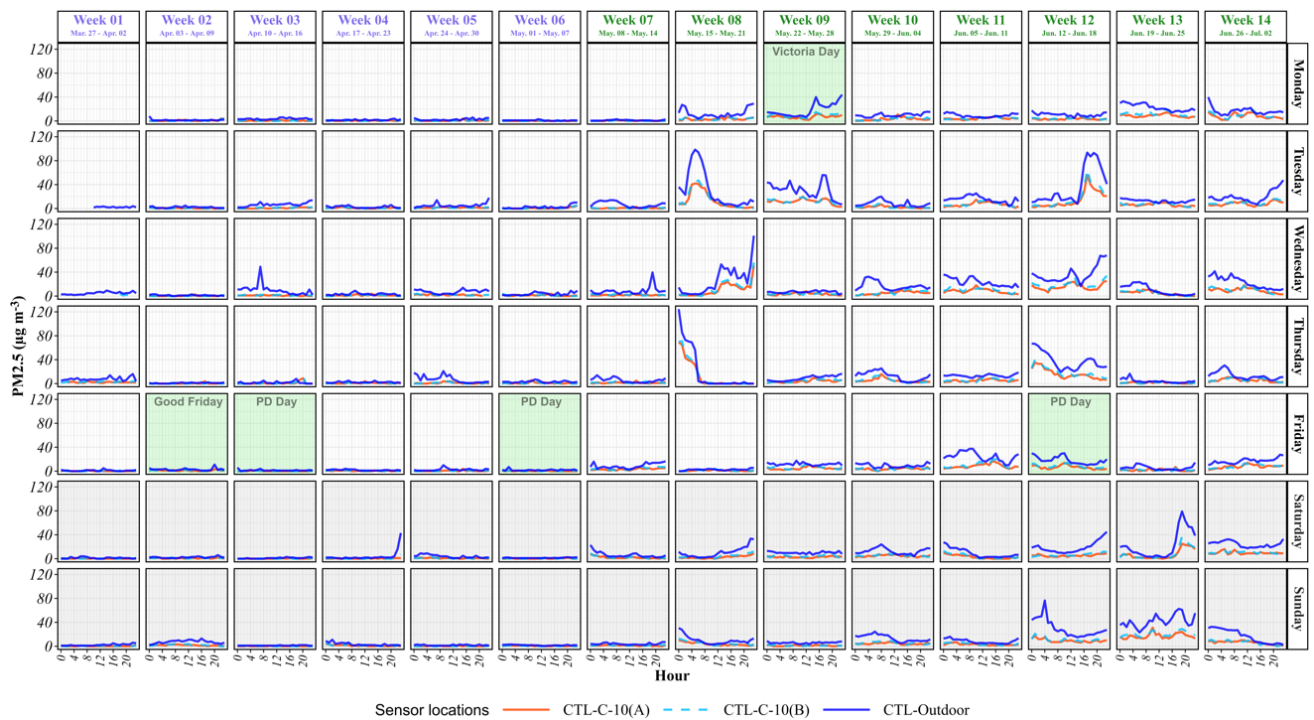


Figure 4: PM_{2.5} concentrations: a classroom in the intervention school (above) and in the control school (below)

2.2.2 Operation of PACs

The PM₁ concentrations in 2 classrooms in the intervention school on April 11 and May 16 are plotted in Figure 5. Classrooms INT-C-09 and INT-C-10 have the same layouts, dimensions, HVAC system configurations. Neither room has exterior walls or windows. The PAC in INT-C-09 was controlled by a timer to operate between 8 AM and 5 PM, whereas the PAC in INT-C-10 was operating continuously. Compared to the PM₁ results from INT-C-09, the operation of the PAC between 2 and 8 AM in INT-C-10 significantly reduced the indoor PM₁ concentration when the outdoor PM₁ levels were high during this period.

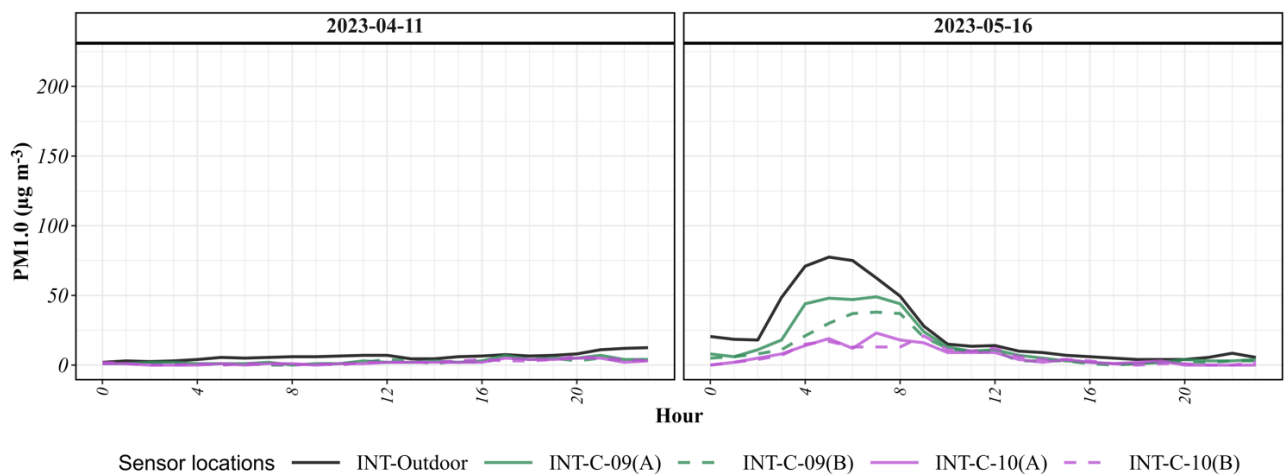


Figure 5: Effect of intermittent operation of PAC and occupancy on indoor PM₁

2.2.3 Exterior walls and windows

The PM₁ concentrations in two classrooms in the intervention school on April 11 and May 16 are plotted in Figure 6. These two rooms, INT-C-10 and INT-C-15, have the same layouts, dimensions, HVAC system configurations, and PAC operating schedules (continuous). As previously mentioned, INT-C-10 has no exterior walls, whereas INT-C-15 has. It can be seen

in Figure 6 that the concentration of PM1 in INT-C-15 was much higher than that in INT-C-10 when the outdoor PM1 concentration was high between 2 and 10 AM on May 16, indicating that PM1 particles likely infiltrated to indoors through the exterior walls and windows in INT-C-15.

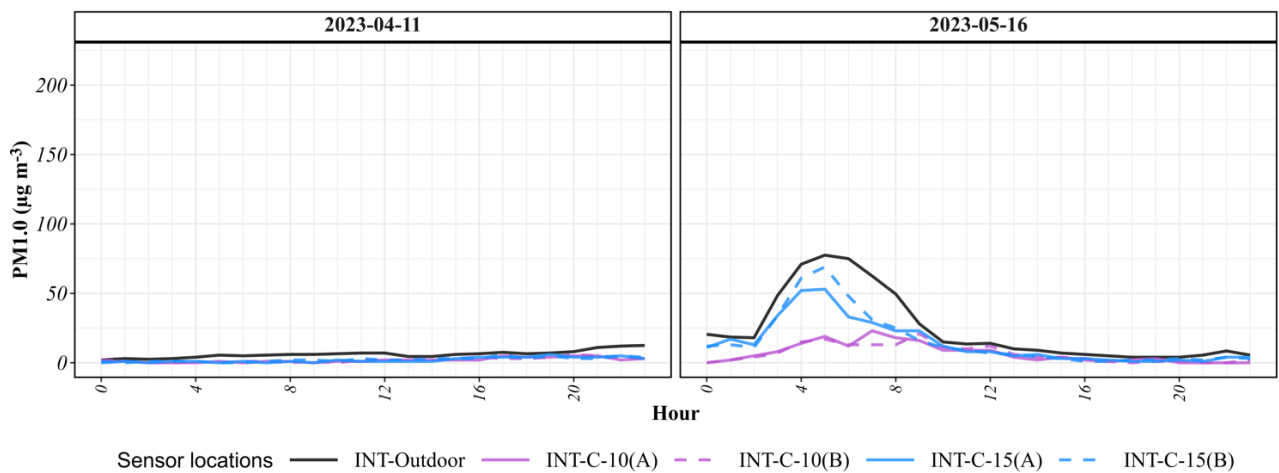


Figure 6: Effect of exterior windows/walls on indoor PM1: INT-C-10 without and INT-C-15 with

2.2.3 Operation of PAC in rooms with exterior walls and windows

The PM1 concentrations in two comparable classrooms in the intervention school on April 11 and May 16 are plotted in Figure 7. As previously mentioned, INT-C-02 and INT-C-03 share similar characteristics, and both have exterior walls and windows. The PAC in INT-C-03 was controlled by a timer to operate between 8 AM and 5 PM, whereas the PAC in INT-C-02 was operating continuously. When the outdoor PM1 concentration was high between 2 and 10 AM on May 16, the concentration of PM1 in INT-C-02 was similar to what was measured in INT-C-03, even the PAC in INT-C-02 was operating. This indicates that the capacity of the PAC unit in INT-C-02 might be insufficient to effectively remove all the PM1 particles that infiltrated through the exterior walls and windows in this room.

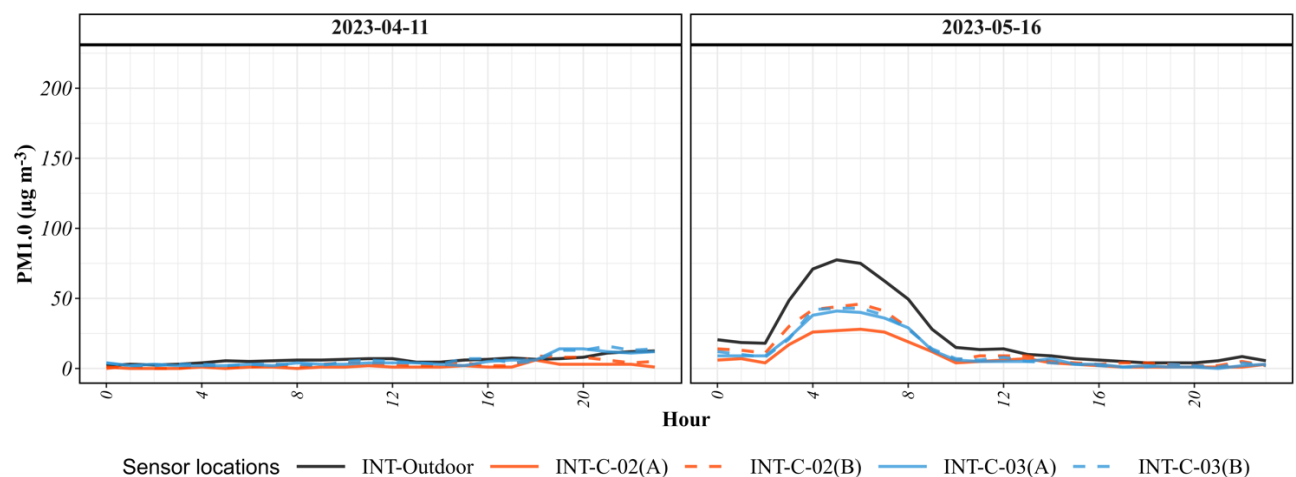


Figure 7: Operating of PAC in rooms with exterior walls and windows

3.3 PAC’s ability to reduce indoor PM1 concentration

The test results presented so far demonstrate that the outdoor sources played the most significant role in deciding the indoor PM1 and PM2.5 concentrations in both the control and the intervention schools. During the study period, the outdoor particle concentrations were

consistently higher than the indoor particle concentrations. A particle removal efficiency index can be used to assess the effectiveness of filtration in removing particles.

$$PM_{eff} = 1 - \frac{PM_{indoor}}{PM_{outdoor}}$$

In the control school, particles from outdoor sources were removed by the HVAC system in-duct filters and the building envelope. In the intervention school, particles from outdoor sources were removed by the HVAC in-duct filters, the building envelope, and the PAC units with HEPA filters after these units were deployed on May 6, 2023. Particle removal efficiencies were calculated using the time series data collected from both schools on April 11 and May 16. Table 1 presents the average PM1 and PM2.5 concentrations and removal efficiencies calculated based on the data from two classrooms (one with exterior walls/windows and one without) in each school. Wildfire events happened in a neighbouring province in May 2023, which likely contributed to the rise in the outdoor PM1 and PM2.5 concentrations. The PAC units were operating continuously in the two classrooms in the intervention school after they were deployed.

Table 1: PM1 and PM2.5 concentration and removal efficiency

School	Date	PAC (Y/N)	Outdoor PM1 conc ($\mu\text{g}/\text{m}^3$)	Indoor PM1 conc ($\mu\text{g}/\text{m}^3$)	Outdoor PM2.5 conc ($\mu\text{g}/\text{m}^3$)	Indoor PM2.5 conc ($\mu\text{g}/\text{m}^3$)	PM1 removal efficiency	PM2.5 removal efficiency
Control	April 11	N	4.53	1.54	6.70	1.70	0.66	0.74
Control	May 16	N	22.07	14.97	32.11	15.55	0.29	0.48
Intervention	April 11	N	6.22	2.16	8.81	2.31	0.65	0.74
Intervention	May 16	Y	24.65	9.26	34.07	9.69	0.61	0.70

Figure 3 and Figure 4 illustrate that the outdoor concentrations of PM1 and PM2.5 on May 16 were much higher than those on April 11. The elevated outdoor particle concentrations on May 16 resulted in much lower PM1 and PM2.5 removal efficiencies than the efficiency achieved on April 11, as seen in Table 1. On April 11, no PAC units were deployed and used in both schools. On May 16, PAC units were used only in the intervention school. Table 1 shows more pronounced decreases in particle (both PM1 and PM2.5) removal efficiencies between these two days in the control school, compared to the intervention school. Based on the considerations of all these factors, the PAC units appeared to remove some of the particles that entered indoors. To quantitatively determine the particle removal efficiency of the PAC units, comparative tests need to be carried out when outdoor particle concentration remains at a reasonably constant level.

In all scenarios, the calculated PM2.5 removal efficiencies are higher than the PM1 removal efficiencies. This is consistent with filter particle size efficiency in ASHRAE 52.2 (ASHRAE, 2017), meaning that a filter is generally more efficient in removing particles in larger size ranges. It is worth noting that the design limit of PM2.5 in ASHRAE 62.1 (ASHRAE, 2022) is $12 \mu\text{g}/\text{m}^3$, which is the annual standard for PM2.5 averaged over three years defined by the US Environmental Protection Agency.

4 CONCLUSIONS

From April to June 2023, a control intervention study was carried out in two schools with similar characteristics to determine the effect of deploying PACs with HEPA filters on IAQ and

the health of the students and staff. This paper presents the CO₂, PM₁, and PM_{2.5} measurement results under various operating conditions. The details about the HVAC system's operating schedule, the outdoor air intake rate, the in-duct filter efficiency, building envelope airtightness, and the air infiltration through building envelopes were unknown in both the control and intervention classroom. Despite these limitations, the following observations and conclusions can be made.

- The indoor CO₂ concentrations were primarily dependent on the presence of occupants. Higher CO₂ concentrations were measured in classrooms with higher occupant densities. However, the infiltration and exfiltration through building envelope can play a role in affecting indoor CO₂ concentrations and the readings recorded by the indoor CO₂ sensors, depending on where the sensors are located (i.e. the distance between the sensors and the exterior walls and/or windows). The CO₂ concentrations measured from both schools during the occupied periods agreed with the CO₂ concentration metrics proposed by Persily (2022) based on occupant characteristics and ASHRAE 62.1 ventilation requirements.
- The outdoor particle sources played the most significant role in deciding the indoor PM₁ and PM_{2.5} concentrations during the study period. The increase in outdoor particle concentrations in May and June were likely correlated to the wildfire events in a neighbouring province. The presence of exterior walls and windows in a space can also affect the indoor particle concentrations because the infiltration and exfiltration through the building envelope allow particles to enter or leave the space.
- During the study period, the outdoor particle concentrations were consistently higher than the indoor particle concentrations. A particle removal efficiency index was used to assess the effectiveness of filtration in removing particles. Based on the PM₁ and PM_{2.5} removal efficiencies calculated for both schools during the testing periods with and without the operation of PAC units in the intervention school, the PAC units in the intervention school were able to remove some of the particles that entered indoors.
- Based on the observations above, CO₂ concentration can be used to control ventilation for using outdoor air to dilute indoor air contaminants, particularly those generated by occupants, whereas outdoor and indoor particle measurements can be used to determine the needs for ventilation, filtration, and air cleaning. If CO₂ and particle readings are to be used for the control of ventilation and air cleaning, the number and the location of the sensors require careful consideration. Moreover, further research is required to better understand how particle measurements can be used to control ventilation and air cleaning systems.

In the next phase of the study, efforts will be made to examine the building envelope airtightness, HVAC system's operating schedule, ventilation rate (e.g. CO₂ decay after occupancy or other tracer gas methods), PAC airflow rates, in-duct filter efficiency, PAC filter efficiency, and sick days reported in both schools. The goal is to verify the cost and effectiveness of air cleaning and ventilation measures on IAQ and occupants' health in public spaces with shared indoor air.

5 ACKNOWLEDGMENTS

This work is supported by the federal government of Canada's Addressing Air Pollution Horizontal Initiative and the NRC International's Eureka Network under project "Reducing the risk of viral contagion from the airborne transmission of pathogens within building spaces".

6 REFERENCES

- ASHRAE. (2017) ANSI/ASHRAE Standard 52.2, Method of Testing General Ventilation Air-Cleaning Devices for Removal Efficiency by Particle Size. Peachtree Corners, GA: ASHRAE.
- ASHRAE. (2022) ANSI/ASHRAE Standard 62.1, Ventilation and Acceptable Indoor Air Quality. Peachtree Corners, GA: ASHRAE.
- Black, C., Tesfaigzi, Y., Bassein, J. A., and Miller, L. A. (2017) Wildfire Smoke Exposure and Human Health: Significant Gaps in Research for a Growing Public Health Issue. *Environ Toxicol Pharmacol.*, 55: 186–195.
- CDC. (2021). Ventilation in buildings, Centers for Disease Control and Prevention, www.cdc.gov/coronavirus/2019-ncov/community/ventilation.html.
- EMG/SPI-B. (2021). Application of CO₂ monitoring as an approach to managing ventilation to mitigate SARS-CoV-2 transmission, Environmental Modelling Group (EMG) and Scientific Pandemic Insights Group on Behaviours (SPI-B).
- ECCC. (2023). Wildfire smoke, air quality and your health. Environment and Climate Change Canada.
- Fennelly, K. (2020). Particle sizes of infectious aerosols: implications for infection control, *Lancet Respir. Med.* 8, 914–924.
- Persily, A. (2022) Development and application of an indoor carbon dioxide metric. *Indoor Air*, Volume 32, Issue 7.
- REHVA (2021). REHVA COVID-19 Guidance, version 4.1, Federation of European Heating, Ventilation and Air Conditioning Associations.
- Wang, C. C., Prather, K. A., Sznitman, J., Jimenez, J. L., Lakdawala, S. S., Tufekci, Z., and Marr, L. C. (2021). Airborne transmission of respiratory viruses. *Science*, 373(6558), abd9149.

Critical reflections on indoor-environmental quality constructs

Ardeshir Mahdavi*¹ and Christiane Berger²

*1 Institute of Building Physics, Services, and Construction, Faculty of Civil Engineering Sciences
Graz University of Technology, Graz, Austria.
a.mahdavi@tugraz.at

2 Department of Architecture, Design and Media Technology, Aalborg University, Aalborg, Denmark

ABSTRACT

The main focus of this paper can be summarized in terms of the following two presuppositions: *i*) The process through which we select and apply indoor-environmental quality (IEQ) constructs could be – perhaps should be – improved; *ii*) Such improvement would contribute to formulation of more robust IEQ standards and guidelines.

KEYWORDS

Indoor-environmental quality, measurement, constructs, proxies, scales

1 INTRODUCTION AND BACKGROUND

1.1 About IEQ constructs

A proper starting point in the indoor-environmental quality (IEQ) discourse is perhaps the generally recognized fact that a key objective of buildings is to provide comfortable conditions to the buildings' inhabitants. Indoor-environmental conditions are assumed to influence the health, comfort, wellbeing, and productivity of inhabitants. But judgements of what constitute comfortable indoor environments involve a strong subjective aspect. To make matters such as building users' comfort and satisfaction into operable criteria, that is to make them measurable, we must cast them in terms of well-defined constructs. A construct denotes here the shared understanding of how a specific aspect of IEQ is perceived and evaluated by inhabitants. In other words, a construct is a well-defined semantic place-holder for an specific aspect of IEQ. As such, for a given indoor-environmental setting, inhabitants can be asked to judge their perception of IEQ via assigning values or attributes to a suitably defined construct. For instance, perceived indoor air quality, or perceived thermal conditions can be assessed by asking inhabitants to rate the value of the corresponding constructs (e.g., thermal comfort, air freshness). Typically, various psycho-physical scales or semantic differentials are used in order to express the values of constructs in numeric terms.

1.2 About IEQ proxies and psycho-physical relationships

Professionals in the building design and operation fields cannot directly influence inhabitants' perceived IEQ and the values of the corresponding constructs. But they can influence the settings and conditions that are believed to contribute to the formation of inhabitants' perceptions and evaluations of IEQ. The operative rationale in provision of adequate IEQ is based on the assumption that certain ranges of indoor-environmental parameters are more likely to increase the probability of positive evaluation of IEQ by inhabitants. Cast in terms of relationships or comfort equations, the rationale can be formalized as follows. Salient physical features or parameters of the indoor environment act as the independent variables that can be

mapped, via psycho-physical or comfort equations, onto dependent variables, i.e., inhabitants' perception as captured via constructs and their values. The physical parameters in these equations consist of measurable variables such as air temperature, air flow velocity, water vapor and other gas concentrations, illuminance and luminance levels, and sound pressure level.

Note that, some of the mentioned measurable indoor-environmental variables (e.g., task illuminance level, CO₂ concentration) are relevant to the quality of spaces in view of IEQ requirements (e.g., visual comfort, indoor air quality), but "they do not have direct phenomenal correlates: people do not 'see' illuminance; neither do they sense CO₂ concentration. But such performance indicators may be linked to others, which do have direct perceptual corollaries" (Mahdavi 2011). However, there are also variables that are "not only relevant to human occupancy, but also correlate directly with phenomenal experience. Examples of such indicators are luminance of light sources and room surfaces, indoor air temperature, sound pressure level, and reverberation time in a room. The evaluative utility of such variables is grounded in empirically documented correspondence between the variable values and people's report on their phenomenal experience (i.e., thermal, visual, and acoustical sensations)" (Mahdavi 2011). The mapping process of the physically measurable independent variables onto the values of the construct suggests that they are viewed as physical proxies (or predictor variables) of perceived IEQ (see Table 1).

Given this background, the default engineering process of handling IEQ in buildings may be formally summarized as follows:

- Inhabitants' perception and evaluation of indoor-environmental conditions can be captured via IEQ constructs (pertaining, for example, to comfort, satisfaction, annoyance);
- Construct values are assumed to be causally related to (or at least correlated with) specific ranges of independent variables that represent physical conditions in indoor environments;
- These causal relationships (or correlations), which are sometimes expressed as comfort equations, are frequently formulated based on the results of experimental studies (typically conducted under controlled settings);
- To provide adequate IEQ and to examine if it has been delivered, specific values of specific sets of indoor-environmental variables are mandated/maintained. As such, these variables are treated as physically measurable IEQ proxies, given their assumed correlation with construct values. These correlations are typically captured via the aforementioned psycho-physical equivalence relationships and comfort equations.

Conventional thermal comfort models provide a case in point for the above process (Fanger 1972). A common construct is in this case the "thermal sensation" of inhabitants in a specific environment, as obtained via a (typically 7-point) scale that ranges from very hot to very cold. The value of this construct is assumed to be predictable via an aggregated proxy (PMV), which is a function of air temperature, radiant temperature, water vapor concentration, and air flow velocity as well as personal factors, clothing and activity. Note that the point is not the validity of this specific construct and its calculation process. Rather, the example serves to illustrate a commonly used general formalism pertaining to psycho-physical equations.

Table 1: Illustrative instances of independent variables (candidate proxies of IEQ) and constructs (variables to capture subjective evaluations) in four key IEQ domains

	Thermal	Visual	Auditory	Air Quality
Independent variables	Air temperature, radiant temperature, water vapor content, air velocity	Illuminance, luminance, contrast, colour temperature	Sound pressure level, reverberation time, frequency (spectrum)	CO ₂ and VOC concentration, Air change rate, Age of air
Constructs	Thermal sensation, thermal comfort	Visual comfort, glare rating	Loudness, annoyance	Air freshness

1.3 A note on the utility of IEQ constructs and proxies

The approach outlined in the previous sections above is operationally critical and is intended to provide accountability in designing and operating buildings with adequate IEQ. Related IEQ standards and guidelines typically entail requirements and mandates in one or both of two categories, namely prescriptive or performance-based. The former category specifies explicit mandates regarding the relevant attributes of building components and systems (e.g., the minimum window size in a room), assuming that compliance with such mandates would ensure that proxy variables of IEQ (e.g., daylight availability) can be kept in the proper ranges. The latter category spells out such ranges (e.g., the minimum illuminance level at a specific reference point in a room), leaving – to some degree – the technical details and choices to the discretion of the responsible professionals. In both cases, the assumption is that standards are firmly based on empirically established proxy-construct-correlations, and thus keeping the proxy values in the mandated ranges would ensure that a sufficiently large fraction of the population of building users would find the resultant IEQ acceptable and appropriate.

1.4 Paradigm and practice

The above remarks outline the state of the main theoretical paradigm as relevant to IEQ-related building design and operation and related standard-guided quality assurance and compliance verification procedures. However, as in many other similar areas, the state of theory and the state of actual practice are, to put it mildly, not completely aligned. This implies the need for critical reflections on the genesis and application of common IEQ constructs and the implications for IEQ standards and guidelines development processes. The next section of the paper offers a number of such reflections, addressing foundational questions regarding measurement challenges of subjective qualities, challenges in definition and operationalization of constructs, and approaches toward more transparent and evidence-based IEQ standards.

2 COMMON CHALLENGES IN IEQ DEFINITION AND ASSESSMENT

2.1 About standards

As alluded to before, the default approach toward provision of adequate IEQ in buildings involves the specification of required value ranges for selected proxy variables that are thought to be relevant to inhabitants' perception and evaluation processes. Note that a central argument in favour of this approach is the accountability exigency in the building delivery process: The stakeholders (building owners, operators, occupants) need a transparent and binding process to decide if a building's design and performance meet relevant legal and contractual obligations. Standards and guidelines are not only a primary source of related information and guidance to the practitioners, but also act as the reference documents in quality arbitration procedures. More generally, standards are often portrayed as representing the state of knowledge in the field to which they apply. In the building domain, standards may be dealing with purely technical considerations (e.g., structural resilience, construction integrity). However, IEQ-related standards go beyond purely technological issues and must consider physiological and psychological processes and phenomena involved in inhabitants' perception and evaluation of indoor environments. However, recent reviews of standards and guidelines in the IEQ domain reveal certain gaps between the explicitly stated requirements and mandates in the standards on the one side and their evidentiary basis in the scientific literature (Berger et al. 2022, 2023). These reviews suggest that standards do not routinely refer to the studies that are supposed substantiate their content, nor do they routinely disclose the procedures through which

occupant-centric constructs are selected or validated. The point of this assertion is of course not to suggest that standards should be designed in the manner of scientific dissertations or papers. But transparency regarding the lineage of the included performance indicators in general and constructs in particular would have been conducive to improving standards' credibility and their impulses toward identification of research needs.

2.2 The measurement problem

In physical sciences, the act of measurements appears to comprise a straightforward mapping of physical entities to numbers. It has been thus suggested to think of measuring length, weight, or speed of objects as representing these attributes via numbers. Hence, the relationships between physical attributes of objects can be expressed in terms of the mathematical relationships between the numbers representing those attributes. For instance, the relationship between the weights of two objects can simply be expressed by the relationship (e.g., the ratio) of the two numbers that express, in proper units, their respective weights. However, matters are arguably much more complicated when we consider concepts and entities in social sciences or psychology. A measure in economics such as GDP (Gross Domestic Product) does not represent an already existing entity in the real world, but in a sense, it constructs the very entity that it is intended to measure. This circumstance could apply, at least to some degree, to IEQ-related constructs that are meant to measure occupants' wellbeing or satisfaction. Selecting the appropriate constructs for measuring such states involves pragmatic considerations and choices, a fact, which is also reflected in the methods that are used to obtain meaningful values for the respective constructs. This is not meant to suggest that measuring IEQ-related subjective phenomena would be infeasible. Researchers in fields such as psychology have indeed developed ingenious methods to define and validate constructs pertaining to subjective feelings and sensations. However, as previously implied, the use of such methods in IEQ-related research is not always consistent and systematic. Respective studies in this field do not routinely document the provenance of the applied constructs or the reasoning for the selected methodological tools (e.g., specific scales or differentials) to obtain their values. Hence, even if different studies use the same label for the constructs they use, it is not clear if they agree on the nature of what is being measured. This can negatively impact the reliability and usability of research results. Specifically, it can impede the possibility to conduct meta-studies that would coalesce the results of multiple research efforts toward formulation of generally valid conclusions.

2.3 Construct and scales inconsistencies

As mentioned before, constructs may be interpreted as formalized containers of semantic information extracted from the results of empirical IEQ-related research involving human participants. This suggests that the practical value and usefulness of research pertaining to people's health and comfort in indoor environments depend on how rigorously constructs are defined and deployed. Specifically, obtaining and understanding occupants' evaluation of IEQ via interviews, questionnaires, and surveys needs to rely on the fidelity of constructs and the scales used to obtain them. In this context, previous findings indicate that both single-domain and multi-domain studies regarding occupants' IEQ evaluations involve a number of limitations and inconsistencies in the use of common numeric (e.g., 3-point, 5-point, and 7-point) scales to obtain the response of both participants in lab studies and occupants of actual buildings. An extensive review of multi-domain studies arrived at the conclusion that existing multi-domain studies focused mainly "on the investigation of subjective perceptual responses, most commonly through numeric scales (including 3-point, 5-point, and 7-point scales) to capture test participants' responses regarding perception, comfort, satisfaction, and preference. At

times, a different number of points and different labels were used, even though the same assessment category was involved. This, as well as the inconsistent use of dimensions in analogue scales, disables the comparison of results from different studies and poses a problem for conducting large-scale meta-analyses" (Chinazzo et al. 2022).

This suggests that, even if we assume that such scales can properly reflect occupants' perception, comfort, satisfaction, and preferences, frequent inconsistencies (e.g., scale steps, labels, dimensions) can be observed in their application in related research. However, as another recent topically similar contribution suggested, "the problem goes further, particularly if we consider the complexity of transferring research results to real-life applications: The practical fitness and interpretative potential of commonly deployed formats for eliciting and representing people's response remains a formidable challenge. We simply miss a conclusive treatment (e.g., a rigorous meta-study) of the expressive power and consistency of typical scales and formats used in IEQ research even in single-domain studies, let alone in the more challenging field of multi-domain investigations. In a nutshell, occupant-centric IEQ constructs need to be of a kind that can be obtained with low level of semantic distortion and can be applied with high level of practical usability" (Mahdavi and Berger 2023).

These reflections underline a key challenge in current studies of IEQ and its effects on building users. To achieve accumulation of knowledge in the field, it would be desirable to maintain continuity in the use of constructs, but insufficient rigor in past research's validation of constructs lessens both their reliability and the value of the findings. This problem is aggravated by the circumstance that the rigorous validation of constructs is a rather laborious endeavour.

3 SCOPE OF SOLUTIONS

3.1 General research direction and quality issues

There is perhaps no one single solution to the challenges expounded on in the previous section. However, the effectiveness of constructs is a necessary condition for the viability of research on IEQ factors and their implications for inhabitants. We discussed, in a previous paper (Mahdavi and Berger 2023), a number of measures and strategies toward enhancing IEQ-related research efforts. It would be useful to briefly revisit those as follows:

- Studies regarding the variables relevant to IEQ typically involve short-term controlled experiments. These can be very useful when queries are highly focused and narrowly defined, but their results are not directly transportable to real-life (long-term and in part chaotic) occupancy situations in buildings. To address this limitation, multiple options could be taken into consideration. One could try to render the experimental settings more realistic and the population of the test participants more representative. One could also try to conduct the experiments over longer periods of time, and under different external boundary conditions. Moreover, it would be helpful if the scope of investigation approaches is widened so as to include long-term field studies and large-scale surveys. A further option lies in the so-called living lab scenarios (Cureau et al. 2022), which can provide the opportunity to monitor inhabitants in real working environments and thus more reliably capture their views on (and intervention tendencies with regard to) indoor-environmental conditions.
- Specialized researchers in fields such as neuroscience and experimental psychology investigate response patterns of test participants to all kinds of sensory stimuli. As it has been suggested previously (Mahdavi and Berger 2023), the respective studies "are typically conducted by highly experienced researchers, who are not necessarily interested in or familiar with practical IEQ issues and associated research needs. On the other hand, experimental studies by professionals closer to building design and

operation fields display at times certain shortcomings in view of the research designs' rigor and research results' interpretation, documentation, and communication (Chinazzo et al. 2022). This implies the potential for improved research quality via collaborative efforts involving both highly qualified specialized scientists and professionals familiar with specific need and challenges in the IEQ domain."

- A further point regarding the improvement potential of IEQ-related research concerns its relevance to the practice. Viewed as a form of applied research, IEQ-related investigation should ideally focus on the kinds of constructs whose values can guide decision-making processes in building design and operation. This requirement implies "the need for the reassessment of the way constructs are defined in research designs and quantified based on research results. Ideally, the obtained values of constructs should provide useful information about how inhabitants perceive, evaluate, and react to multi-domain exposure in indoor environments and how the related processes influence their health and comfort" (Mahdavi and Berger 2023).
- A final reflection on general IEQ research quality issues pertains to the presence of underlying theoretical foundations. It is of course possible to view the relationship between the values of the indoor-environmentally relevant independent variables and the values of the constructs as mere correlational patterns and arrive at respective statistically-based comfort equations. However, grounding such regularities on explicit (e.g., causal) theories can arguably offer a deeper understanding of the underlying physiological and psychological processes. Professionals in the building design and operation domain could benefit from such deeper insights that can be obtained based on explanatory white-box models describing how indoor-environmental conditions influence inhabitants' state of mind vis-à-vis comfort and wellbeing.

3.2 Thoughts on validation of constructs

Building research in the past entails instances of explicit construct validation related to human perception. However, these efforts have not routinely followed standardized processes as recommended in psychological research. Rather, as the following two instances exemplify - they appear to have been devised in a specific – and not necessarily scalable – experimental situation:

- A study of the subjective evaluation of architectural lighting via computationally rendered images (Mahdavi and Eissa 2002) involved the use of semantic differential rating scales. The idea was to compare the test participants' subjective assessments of real spaces with those of computationally generated renderings. To this end, bi-polar pairs of terms were collected via a survey and compared with semantic differential scales developed by Flynn et al. (1973). This resulted in a set of 28 pairs of terms. In the absence of a global validation result for these bipolar scales, it was decided to test the collected set locally "using a small group of test participants who evaluated the lighting quality of a number of office spaces as projected in slides. The final metric was derived based on a statistical analysis of the results of this test. Principal component analysis (PCA) was used as a data reduction method to eliminate the redundancy among the selected scales. The resulting scales are 10 pairs of terms under seven categories", which were subsequently used to conduct the actual study (Mahdavi and Eissa 2002).
- Another study involved a construct for the judgement of the compactness of architectural objects. The traditional indicator of compactness as used in building physics is the so-called characteristic length (Mahdavi et al. 1996), which denotes the ratio of the volume of an object to its total surface area. Mahdavi and Gurtekin (2001,

2002, 2004) proposed a different indicator, namely the "Relative Compactness" (RC), which is suggested to more closely correlate with people's visual judgement of shapes' compactness. RC is derived by comparing the volume to surface area of a shape (V/A) to the volume to surface area of the most compact shape (i.e., sphere) of the same volume ($RC = 4.84 \times V^{2/3} \times A^{-1}$). Given the novelty of the RC concept and hence lack of prior validation, it was necessary to empirically explore the degree to which RC captures the subjective assessment of the compactness of building shapes. To this end, a sample of 14 representative residential building shapes were subjectively assessed by 40 participants in view of their compactness. The statistical analysis of this empirical study confirmed the viability of the proposed relative compactness construct and its perceptually relevant advantage over characteristic length indicator (Mahdavi and Gurtekin 2004).

Many such locally limited validation efforts can be cited in IEQ-related test designs, and one can understand their frequently ad hoc tendency, given the fact that external validation of constructs requires considerable time, effort, resources, and expertise. But if the state of knowledge in the IEQ field and the respective reliability of respective guidelines and standards are to be substantially improved, the underlying research efforts need to elevate the quality of research designs in general and the quality of constructs in particular. To this end, both specific – rigorously designed – case studies in experimental psychology and instructive literature on methodology (e.g., Cronbach 1990, Fowler 1993, Peterson 1999, Patten 2000, Fischer and Hüttermann 2020) can provide guidance.

4 CONCLUDING REMARK

Recent reviews of both IEQ-related standards and scientific studies regarding the effect of indoor-environmental conditions on people's health, comfort, and wellbeing point to a number of persistent limitations. The critical reflections presented in this paper point to a paucity of explicit evidence underlying the standard-based IEQ mandates, and deficiencies in the technical literature, which is expected to provide that evidence. The latter deficiencies pertain to the underlying research designs in general and the precise definition and careful validation of the deployed constructs in particular. These limitations must be addressed and mitigated if one expects major qualitative leaps in the quality of IEQ research and derivative standards. Whereas we outlined some of the necessary steps for this purpose, we have no illusions regarding the formidable nature of the task and the considerable level of required efforts. Shortcuts, piecemeal steps, and ad hoc fixes may appear as progress, but do not represent true alternatives to rigorous systematic research practices. To echo what Euclid reputedly said of geometry, there is also no *via regia* to construct validation. It requires solid knowledge of statistics, considerable experience with experimental design, as well as deep knowledge of the relevant domain (in the present context, IEQ) and its underlying theoretical foundations.

5 ACKNOWLEDGEMENTS

Ardeshir Mahdavi is supported by the FWF (Austrian Science Fund: "Der Wissenschaftsfonds") Project MuDoCo (Project I 5993). In developing the ideas underlying the present paper, the authors benefited from discussions in the framework of IEA EBC Annex 79 – Occupant-Centric Building Design and Operation.

6 REFERENCES

- Berger, C., Mahdavi, A., Ampatzi, E., Crosby, S., Hellwig, R. T., Khovalyg, D., Pisello, A. L., Roetzel, A., Rysanek, A., & Vellei, M. (2023). Thermal Conditions in Indoor Environments: Exploring the Reasoning behind Standard-Based Recommendations. *Energies*, *16*(4), 1587. <https://doi.org/10.3390/en16041587>
- Berger, C., Mahdavi, A., Azar, E., Bandurski, K., Bourikas, L., Harputlugil, T., Hellwig, R. T., Rupp, R. F., & Schweiker, M. (2022). Reflections on the Evidentiary Basis of Indoor Air Quality Standards. *Energies*, *15*(20), 7727. <https://doi.org/10.3390/en15207727>
- Chinazzo, G., Mahdavi, A., Berger, C., et al. (2022). Quality criteria for multi-domain studies in the indoor environment: Critical review towards research guidelines and recommendations. *Building and Environment*, *226*, 109719. <https://doi.org/10.1016/j.buildenv.2022.109719>
- Cronbach, L. J. (1990). *Essentials of psychological testing* (5th ed.). New York: HarperCollins.
- Cureau, R. J., Pigliautile, I., Pisello, A. L., Bavaresco, M., Berger, C., Chinazzo, G., Deme Belafi, Zs., Ghahramani, A., Heydarian, A., Kastner, D., Kong, M., Licina, D., Luna-Navarro, A., Mahdavi, A., Nocente, A., Schweiker, M., Vellei, M., & Wang, A. (2022). Bridging the gap from test rooms to field-tests for human indoor comfort studies: A critical review of the sustainability potential of living laboratories. *Energy Research & Social Science*, *92*, 102778. <https://doi.org/10.1016/j.erss.2022.102778>
- Fanger, P.O. (1972). *Thermal Comfort*. McGraw-Hill Book Company. ISBN 0-07-019915-9.
- Fischer, J.A., & Hüttermann, H. (2020). PsySafety-Check (PSC): Fragebogen zur Messung psychologischer Sicherheit in Teams. *Zusammenstellung sozialwissenschaftlicher Items und Skalen (ZIS)*. <https://doi.org/10.6102/zis279>
- Flynn, J.E., Spencer, T.J., Martyniuk, O., & Hendrick, C. (1973). Interim Study of Procedures for Investigating the Effect of Light on Impression and Behavior. *Journal of the Illuminating Engineering Society*, *3*, 87–94. <https://doi.org/10.1080/00994480.1973.10732231>
- Fowler, F. J., Jr. (1993). *Survey research methods*. Newbury Park, CA: Sage.
- Mahdavi, A. (2011). The human dimension of building performance simulation. *Proceedings of Building Simulation 2011: 12th Conference of International Building Performance Simulation Association*.
- Mahdavi, A., & Berger, C. (2023). A critical appraisal of recent research in multi-domain indoor-environmental exposure. *Proceedings of the 18th Healthy Buildings 2023 Europe Conference* (to be published)
- Mahdavi, A., & Eissa, H. (2002). Subjective Evaluation of Architectural Lighting via Computationally Rendered Images. *Journal of the Illuminating Engineering Society*, *31*(2), 11–20. <https://doi.org/10.1080/00994480.2002.10748388>

Mahdavi, A., & Gurtekin, B. (2004). Generating the design-performance space via simulation and machine learning. *Journal of Architectural and Planning Research*, 21(4) (2004) ISSN 0738-0895; 350 – 362.

Mahdavi, A., & Gurtekin, B. (2002). Shapes, Numbers, and Perception: Aspects and Dimensions of the Design Performance Space. *Proceedings of the 6th International Conference: Design and Decision Support Systems in Architecture*. Ellecom, The Netherlands. ISBN 90-6814-141-4; 291 – 300.

Mahdavi, A., & Gurtekin, B. (2001). Computational support for the generation and exploration of the design-performance space. *Proceedings of the Seventh International Building Simulation (IBPSA) Conference*. Rio de Janeiro, Brazil. Vol. I. ISBN 85 – 901939 – 2 – 6; 669 – 676.

Mahdavi, A., Brahme, R., & Mathew, P. (1996). On the Applicability of the "LEK"-Procedure for the Energy Analysis of Cooling-Dominated Commercial Buildings. *Energy and Environment*, 31(5), 409 - 415.

Patten, M.L. (2000). *Understanding research methods* (2nd ed.). Los Angeles: Pyrczak.

Peterson, R.A. (1999). *Constructing effective questionnaires*. Thousand Oaks: Sage.

Ventilation and sleep quality

Pawel Wargocki ^{*1}, Mizuho Akimoto ^{1,2}, Xiajoun Fan ¹, Shin-ichi Tanabe ²,
Chandra Sekhar ⁴, and Li Lan ³

1 Department of Environmental and Resource Engineering, Technical University of Denmark Kongens Lyngby, Denmark

3 School of Design, Shanghai Jiaotong University, Shanghai, PR China

2 Department of Architecture, Waseda University, Tokyo, Japan

4 College of Design and Engineering, National University of Singapore

**Corresponding author: pawar@dtu.dk*

ABSTRACT

We sleep more than twenty years during our lives. Sleep is essential for physical and psychological health. Yet, nearly no standards define indoor environmental quality conditions for optimal sleep. In this paper, we present a summary of studies examining the effects of bedroom ventilation on sleep quality. The results suggest that the current ventilation standards for dwellings are inadequate concerning requirements of outdoor air supply rates in bedrooms and need to be revised. They suggest that the traditionally agreed level of carbon dioxide at 1,000 ppm to achieve good air quality should be revisited, and the lower levels need to be maintained to ensure that sleep quality is not disturbed. Furthermore, the traditional recommendation of 0.5 air changes per hour also needs to be revised, as the bedroom ventilation should most likely be twice this rate. There is a need for further research and validation of these results, as well as rethinking how the ventilation air is distributed within the dwelling so that the health and sleep of building occupants are not compromised.

KEYWORDS

Dwellings, Bedrooms, Sleep quality, Carbon dioxide, Ventilation requirements.

1 INTRODUCTION

Sleep is essential for human health as it allows the body to recover and function effectively by promoting various physiological and cognitive processes. The sleep-wake cycle is generally regulated by the homeostatic physiology of circadian rhythm, which is very complex.

Sleep is traditionally monitored by measuring biological responses. For this purpose, polysomnography (PSG) is used. Although there is no accepted definition of the 'quality' of sleep, it is generally derived from the objective measurements made by PSG or subjective ratings using questionnaires. Sleep quality can be quantitatively assessed by a collection of indicators recommended by the US National Sleep Foundation.

People spend approximately one-third of their lifetime sleeping, mostly in bedrooms. Bedroom indoor air quality (IAQ) can be affected by many factors. The air pollutants present in bedrooms can have their origin outdoors or indoors.

Ventilation is commonly used to remove and dilute pollutants and is thus assumed to improve IAQ. Given the importance of ventilation in bedrooms in determining the levels of pollutants, it is surprising that only a few studies have focused on measuring ventilation rates in bedrooms. Summaries of the studies that measured bedroom ventilation rates observed that the mean air change rate (ACH) measured in bedrooms was between 0.2 to 4.9 h⁻¹, with most cases lower than 0.5 h⁻¹, traditionally considered base ventilation in dwellings.

Many standards and guidelines stipulate ventilation and IAQ requirements for buildings. However, they do not have specific ventilation requirements for bedrooms; bedroom ventilation results from the overall ventilation requirements for residential dwellings. There is no evidence of whether the prescribed ventilation requirements that are acceptable for the dwellings during the daytime are also sufficient to avoid disturbing sleep at night.

The objective of this work was to answer the following question: What is the bedroom ventilation rate to ensure undisturbed sleep?

2 METHODS

We summarized studies in which ventilation and sleep quality were measured. They included laboratory and field experiments, and cross-sectional and intervention studies. As a measure of ventilation efficiency, the measured concentration of carbon dioxide (CO₂) was used. Bedroom ventilation was obtained by a mechanical system, window, or door opening. Sleep quality was measured objectively using wrist-worn actiwatch sleep trackers and by collecting ratings of participants using the Groningen Sleep Quality Scale (GSQS). The effect on any of the objective indicators of sleep quality or an increase in GSQS score was considered an effect on the overall sleep quality. The objective measures included sleep efficiency, sleep onset latency, wake time after sleep onset, and the length and % of deep, light, and REM sleep. We did not assess the physiological consequences of the observed effects. The studies involved mainly young adults but also seniors and children.

3 RESULTS

Figure 1 shows the results of studies that measured sleep quality objectively. Figure 2 shows the results of studies that measured sleep quality using GSQS. Generally, sleep was undisturbed at the levels of CO₂ below 1,000 ppm.

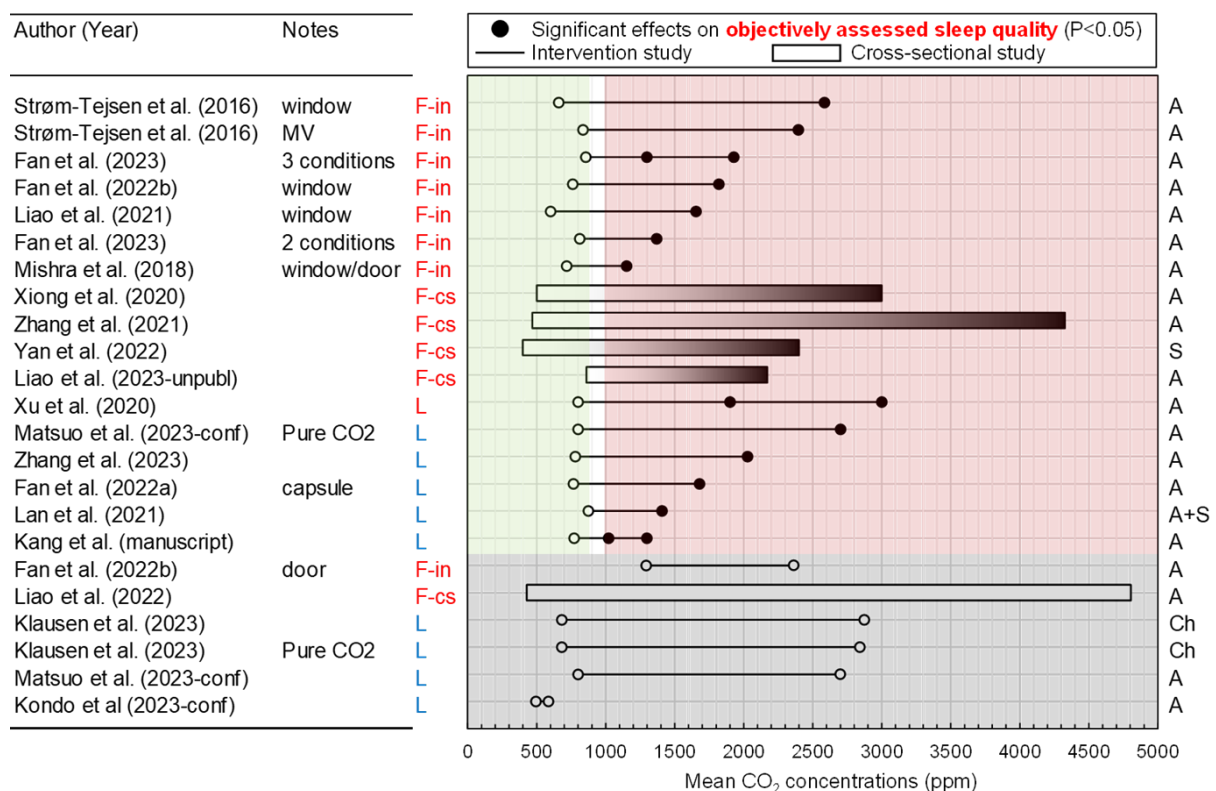


Figure 1: The relationship between sleep quality measured objectively and the concentration of CO₂, either the primary exposure or the marker of ventilation efficiency; dark dots indicate significant adverse effects, and white dots no effects.

4 CONCLUSIONS

Present results suggest that to keep undisturbed sleep quality, the ventilation rate should be above 6 L/s per person and most likely closer to 10 L/s per person (Figure 3); the latter rate is recommended for bedrooms by the standard EN16798-1 in the highest category I of indoor environmental quality. It was assumed that the emission rate of CO₂ during sleep is around 11 L/h per person, independent of age. Taking the typical size of a bedroom, this rate would

correspond to about one air change per hour, which is twice the air change rate traditionally recommended rate in dwellings. These results, however, require further validation and detailed analyses as the shape of the relationship below 1,000 ppm CO₂ is not well defined (Figure 1). Nevertheless, it is essential to note that recommendations for bedroom ventilation rates must be revisited if they exist or clearly defined if they do not exist. Additionally, advanced and novel methods securing adequate yet sustainable ventilation of bedrooms and dwellings should be developed.

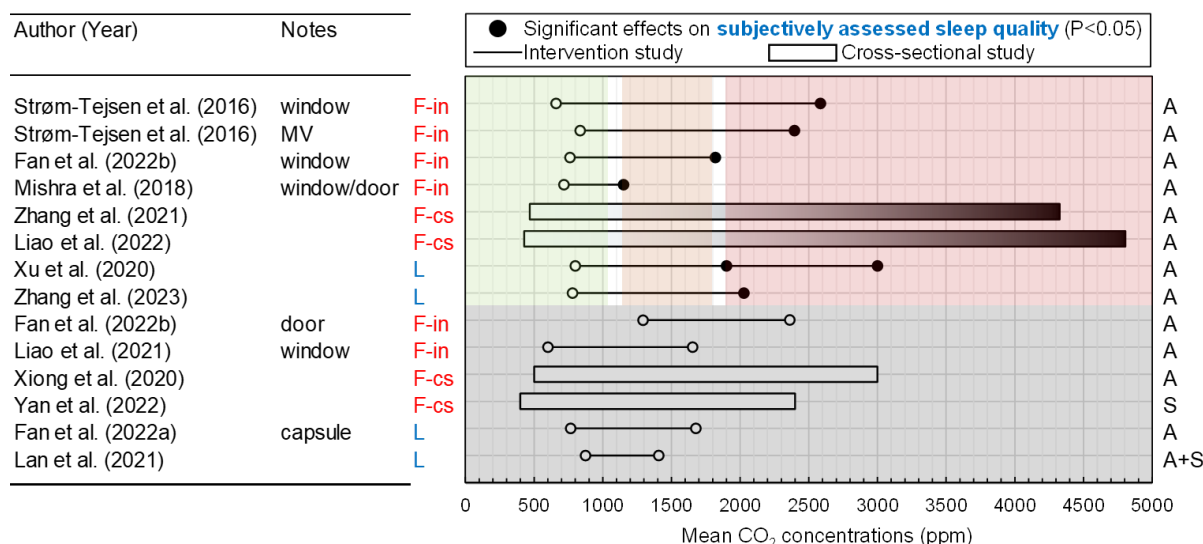


Figure 2: The relationship between sleep quality measured subjectively and the concentration of CO₂, either being the primary exposure or marker of ventilation efficiency; dark dots indicate significant adverse effects, and white dots no effects.

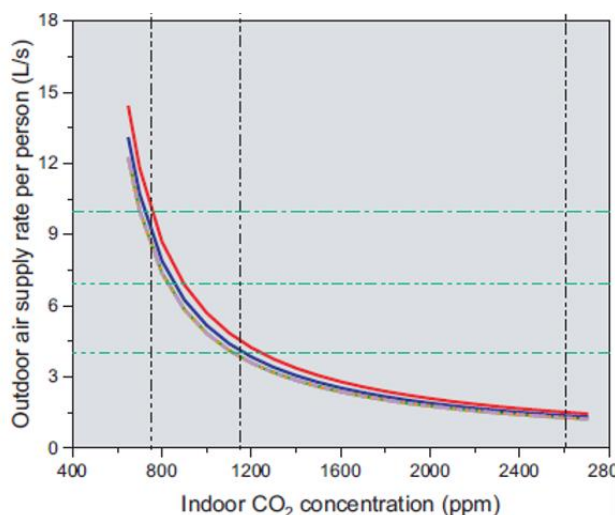


Figure 3: Estimation of ventilation rate for undisturbed sleep quality

5 ACKNOWLEDGEMENTS

Present work was partially supported by ASHRAE through project RP 1837 on "The Effects of Ventilation in Sleeping Environments" and the Danish 20th December Foundation. The Kajima Foundation is also acknowledged through the support of the "Effects of Indoor Environment on Better Sleep Quality" project and the Japan Society for the Promotion of Science (JSPS) for the Grant with the number 22KJ2956.

Applicability and sensitivity of the TAIL rating scheme using data from the French national school survey

Minh Tien Tran^{1, 2, *}, Wenjuan Wei¹, Claire Dassonville¹, Corinne Mandin¹, Mickael Derbez¹, Christophe Martinsons¹, Pascal Ducruet¹, Valérie Héquet² and Pawel Wargocki³

*1 Scientific and Technical Center for Building (CSTB), Health and Comfort Department, French Indoor Air Quality Observatory (OQAI)
77420 Champs-sur-Marne, France
Presenting author: Minh Tien Tran*

*2 IMT Atlantique, CNRS, GEPEA, UMR 6144
CEDEX 3, 44307 Nantes, France*

*3 International Centre for Indoor Environment and Energy, Department of Environmental and Resource Engineering (DTU SUSTAIN), Technical University of Denmark (DTU)
2800 Lyngby, Denmark*

ABSTRACT

The TAIL rating scheme for assessing the quality of Thermal, Acoustic, Indoor air, Luminous, and the overall environment was initially developed to assess indoor environmental quality (IEQ) in hotels and offices. To broaden the use of the TAIL rating scheme to other buildings, its applicability for schools was studied. Two additional parameters, i.e., reverberation time and nitrogen dioxide concentration, were included to account for the specificities of the building use and population. The TAIL rating scheme for schools was applied to the data collected through a national survey performed in France in 602 classrooms between 2013 and 2017 to examine the scheme's feasibility and sensitivity. The results show that using the scheme makes it possible to discriminate IEQ conditions in schools and helps identify problems that may lead to health risks or discomfort, such as insufficient ventilation or overheating during winter. It is concluded that the TAIL rating scheme adapted to schools allows tangible assessment of classroom IEQ and identification of problems requiring improvement, thus promoting a better school environment that eventually will support the proper development of children.

KEYWORDS

Thermal, ventilation, acoustic, lighting, perception

1 INTRODUCTION

Nowadays, humans stay indoors more and more. Extreme climate change can further intensify this trend. Indoor environmental quality (IEQ) is thus an important parameter. IEQ comprises the thermal environment, the acoustic environment, the indoor air quality (IAQ), and the lighting environment. A substantial number of studies have demonstrated the influence of IEQ on occupants' health, comfort, and well-being. These effects are not only limited to adults but also to children in schools. Children are more susceptible to inadequate IEQ as their bodies are still under-development. It is, therefore, essential to create a rating scheme for assessing the quality of the school environment. With this vision in mind, the TAIL-rating scheme for schools was developed. Initially, the TAIL rating scheme was developed for hotels and offices as a part

of the European ALDREN project, promoting the in-depth energy renovation of buildings [1]; the TAIL rating for schools is an adaptation of the original TAIL rating scheme with additional parameters relevant to these environments. Reverberation time for the acoustic environment and nitrogen dioxide (NO₂) concentration for indoor air quality were added; updates were made to match the new World Health Organization (WHO) air quality guidelines. A feasibility and sensitivity analysis was performed using measurement data from the French National Schools' survey (2013-2017), coordinated by the Scientific and Technical Centre for Building (CSTB).

2 RESULTS AND DISCUSSION

Table 1 presents all parameters in the TAIL rating scheme for schools, with all threshold values for each quality category. The following section presents the results of the TAIL-rating scheme, with Table 2 presenting details of the TAIL classification for each component, and parameter individually.

2.1 Thermal environment

Of the 305 schools where the thermal environment was assessed, the measurements in 237 schools were made in the heating season and 68 schools in the non-heating season. Figure 1 shows the distribution of all measurement instances for heating and non-heating seasons. While generally measured air temperatures in the non-heating season are higher than in the heating season, there were still occurrences in which recorded air temperatures from the heating season were as high as in the non-heating season. This suggests overheating in classrooms measured during the heating season. Closely examining the schools measured during the heating season, Figure 2 regroups and displays all measurement instances in the 237 schools during the heating season with colored horizontal lines corresponding to the quality level. The figure shows that a more significant variation was observed in schools having low quality according to the TAIL rating scheme. This could be due to low air temperature in the early morning and/or improper use of the heaters leading to high air temperature.

2.2 Acoustic environment

The acoustic environment was assessed using only the background noise level recorded during the school's standard period of occupation (09h00 to 17h00) but made on the weekend with no occupants. This choice is guided by the fact that the sound of the particle measurement device cannot be dissociated from the background noise level during measurements on weekdays. The results obtained show different quality levels. A Wilcoxon non-parametric test showed that compared to a school located close to medium to low traffic, schools located in high-traffic zones had a higher background noise level both on Saturdays ($p\text{-value} = 7.6 \cdot 10^{-4}$) and Sundays ($p\text{-value} = 1.27 \cdot 10^{-2}$).

2.3 Indoor air quality (IAQ)

IAQ was assessed using seven parameters: benzene, formaldehyde, visible mold RH, CO₂, NO₂, and PM_{2.5}. Figure 3 presents all CO₂ concentration measurements separated by measured season. Schools where measurements were made during the heating season, had higher CO₂ concentrations than schools measured during the non-heating season, as windows were probably less open. Figures 4 and 5 present two opposite trends in relative humidity measured during the heating and the non-heating season. From the quality category I (high) to IV (low), the measured relative humidity tended to decrease during the heating season and increase during the non-heating season. Figure 6 shows a map of all 307 schools where NO₂ concentration was

color-coded by their corresponding quality category. While most schools achieved the green-high (category I) quality level, schools located in highly populated areas achieved a lower quality level. Following the same principle, Figure 7 shows the map of the quality level of measured PM_{2.5}. Compared to the NO₂ concentration, measured PM_{2.5} quality were low but with no observed difference between urban and rural area. This resonated with previous findings, as PM_{2.5} sources are a mix of both indoor and outdoor and from its ubiquitous nature [2].

2.4 Visual environment

The visual environment assessments focused solely on measuring artificial lighting levels at students' desks and on the writing boards. The overall results for each classroom were determined on the basis of the lowest recorded measurements.

2.5 Overall IEQ

303 out of 308 schools had the lowest (category IV) red quality category, and five schools had the next to the lowest orange quality category (category III). This result will urge schools to adopt a holistic approach to assessing the current state of IEQ. They also show the advantage of considering all four components simultaneously when making decisions for IEQ improvement, which is a fundamental principle of the TAIL rating scheme, with no compromise regarding ensuring optimal IEQ in educational institutions.

Table 1: IEQ parameters included in the TAIL rating scheme for schools

Parameter	Category I	Category II	Category III	Category IV	
	Quality of the thermal environment (T)				
Air temperature	Building with mechanical cooling				
	Heating season: 22 ± 1 °C	Heating season: 22 ± 2 °C	Heating season: 22 ± 3 °C	If other quality levels cannot be achieved	
	Non- heating season: 24.5 ± 1 °C	Non- heating season: 24.5 ± 1.5 °C	Non- heating season: 24.5 ± 2.5 °C		
	Building without mechanical cooling				
	Heating season: 22 ± 1 °C	Heating season: 22 ± 2 °C	Heating season: 22 ± 3 °C	If other quality levels cannot be achieved	
	Non- heating season: Upper limit: 0.33 θ _{rm} + 18.8 + 2°C Lower limit: 0.33 θ _{rm} + 18.8 - 3°C	Non- heating season: Upper limit: 0.33 θ _{rm} + 18.8 + 3°C Lower limit: 0.33 θ _{rm} + 18.8 - 4°C	Non- heating season: Upper limit: 0.33 θ _{rm} + 18.8 + 4°C Lower limit: 0.33 θ _{rm} + 18.8 - 5°C		
	θ _{rm} : outdoor running mean temperature				
		Quality of the acoustic environment (A)			
	Background noise level	≤ 30 dB(A)	≤ 34 dB(A)	≤ 38 dB(A)	If other quality levels cannot be achieved
	Reverberation time	Classroom with volume < 250 m ³ : 0.4 - 0.6 s	Classroom with volume < 250 m ³ : 0.6 - 0.8 s	No criteria	If other quality levels cannot be achieved
Classroom with volume ≥ 250 m ³ : 0.6 - 0.8 s		Classroom with volume ≥ 250 m ³ : 0.8 - 1.2 s			

Quality of the indoor air quality (I)				
Benzene concentration	< 2 µg/m ³	≥ 2 µg/m ³	No criteria	≥ 5 µg/m ³
CO ₂ concentration	550 ppm above outdoor concentration	800 ppm above outdoor concentration	1350 ppm above outdoor concentration	If other quality levels cannot be achieved
Formaldehyde concentration	< 30 µg/m ³	≥ 30 µg/m ³	No criteria	≥ 100 µg/m ³
NO ₂ concentration	< 10 µg/m ³	< 20 µg/m ³	No criteria	≥ 20 µg/m ³
PM _{2.5} concentration	< 5 µg/m ³	≥ 5 µg/m ³	No criteria	≥ 15 µg/m ³
Radon concentration	< 100 Bq/m ³	≥ 100 Bq/m ³	No criteria	≥ 300 Bq/m ³
Relative humidity	30 – 50%	25 – 60%	20 – 70%	If other quality levels cannot be achieved
Ventilation rate	≥ (10 L/s/p + 2.0 L/s/m ² floor)	≥ 7 L/s/p + 1.4 L/s/m ² floor and < 10 L/s/p + 2.0 L/s/m ² floor	≥ 4 L/s/p + 0.8 L/s/m ² floor and < 7 L/s/p + 1.4 L/s/m ² floor	If other quality levels cannot be achieved
Visible mold inspection	No visible sign	< 400 cm ²	< 2500 cm ²	≥ 2500 cm ²
Quality of the lighting environment (L)				
Daylight factor	≥ 5.0%	≥ 3.3%	≥ 2.0%	If other quality levels cannot be achieved
Artificial illuminance (students' tables and writing board)	≥ 500 lux	≥ 300 lux	≥ 200 lux	If other quality levels cannot be achieved

Table 2: Summary of IEQ in schools using the data from the French National schools 'survey (308 schools in total)

Parameter	Category I	Category II	Category III	Category IV	Missing data
Overall classification (TAIL)	0	0	5	303	0
Thermal environment (T)	13	32	102	158	3
Air temperature	13	32	102	158	3
Acoustic environment (A)	89	99	57	49	14
Background noise level	89	99	57	49	14
Indoor air quality (I)	0	5	16	287	0
Relative humidity	44	155	87	19	3
CO ₂	3	25	67	213	0
Benzene	247	53	0	3	5
Formaldehyde	237	71	0	0	0
PM _{2.5}	1	68	0	233	6
NO ₂	200	67	0	40	1
Visible mould	290	17	0	0	1
Lighting environment (L)	1	56	97	151	3
Artificial lighting	1	56	97	151	3

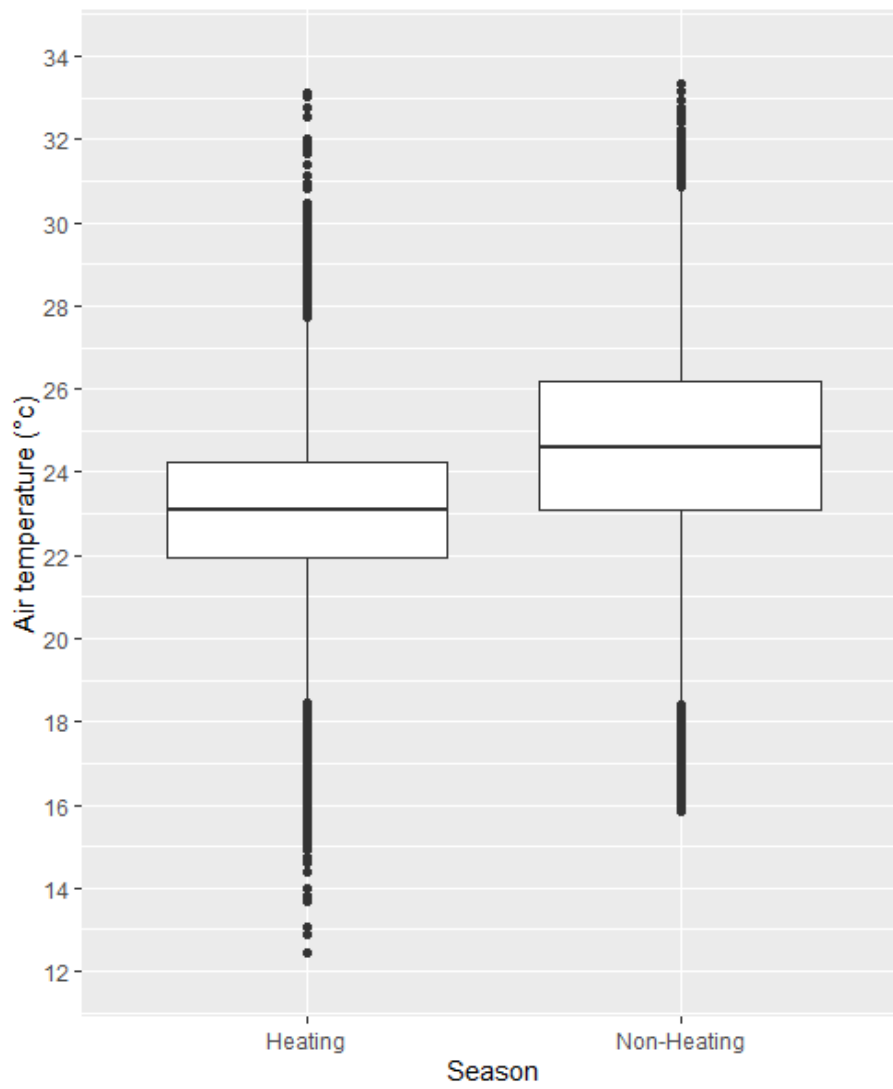


Figure 1: Distribution of the measured air temperatures in schools during the heating season (237 schools) and non-heating season (68 schools)

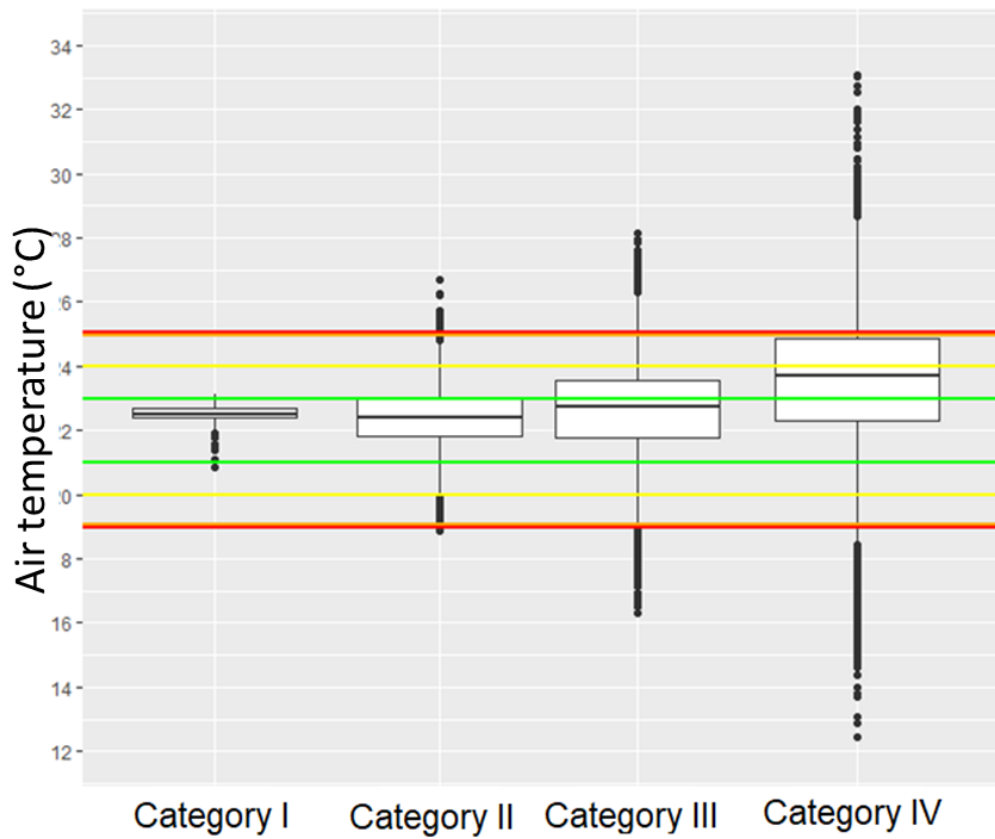


Figure 2: Distribution of measured air temperature during the heating season (237 schools) depending on the categories defined in the TAIL rating scheme

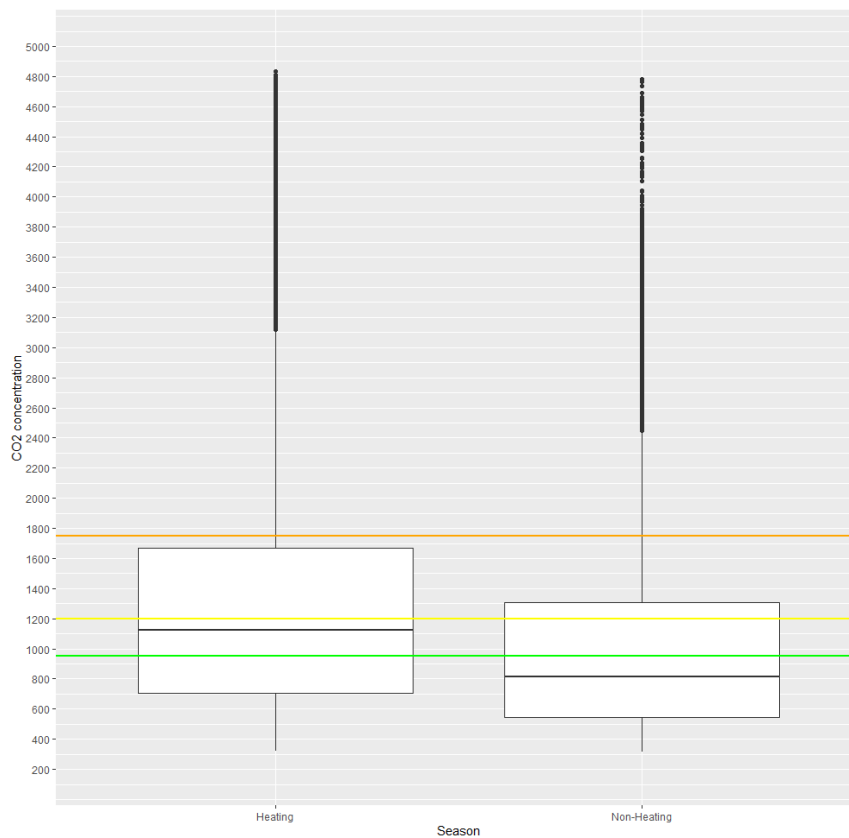


Figure 3: Distribution of measured CO₂ concentrations in schools during the heating season (238 schools) and non-heating season (70 schools)

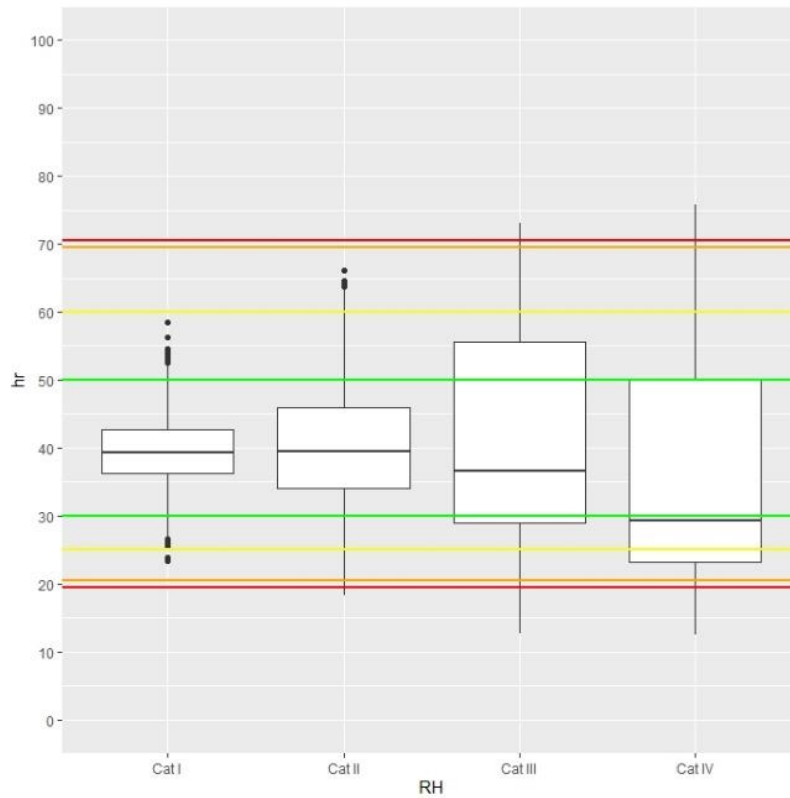


Figure 4: Distribution of measured relative humidity in schools during the heating season (237 schools) depending on the categories defined in the TAIL rating scheme

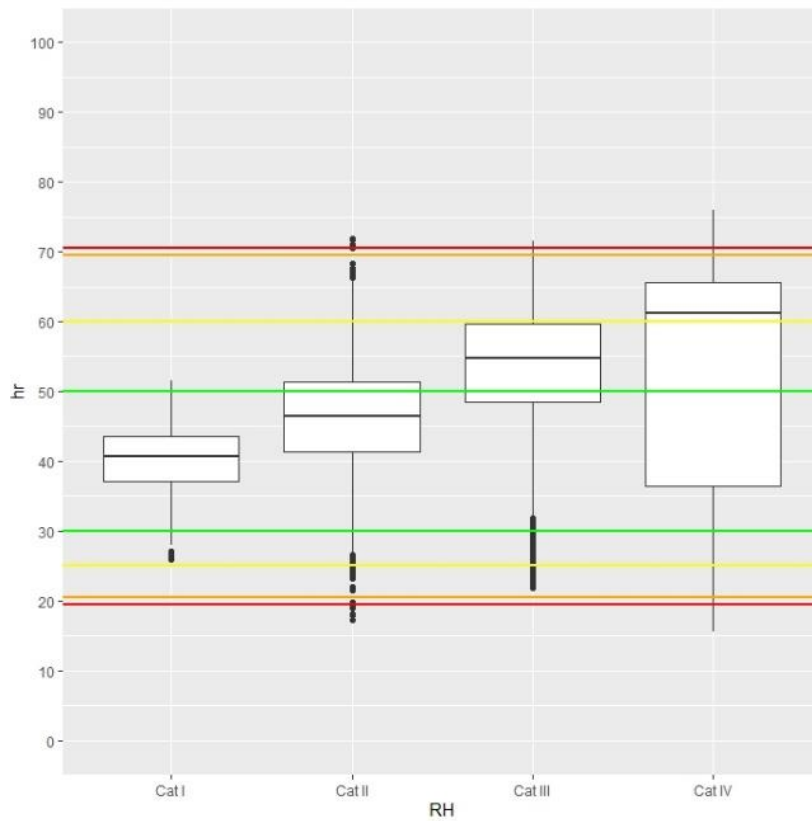


Figure 5: Distribution of the measured relative humidity in schools during the non-heating season (68 schools)

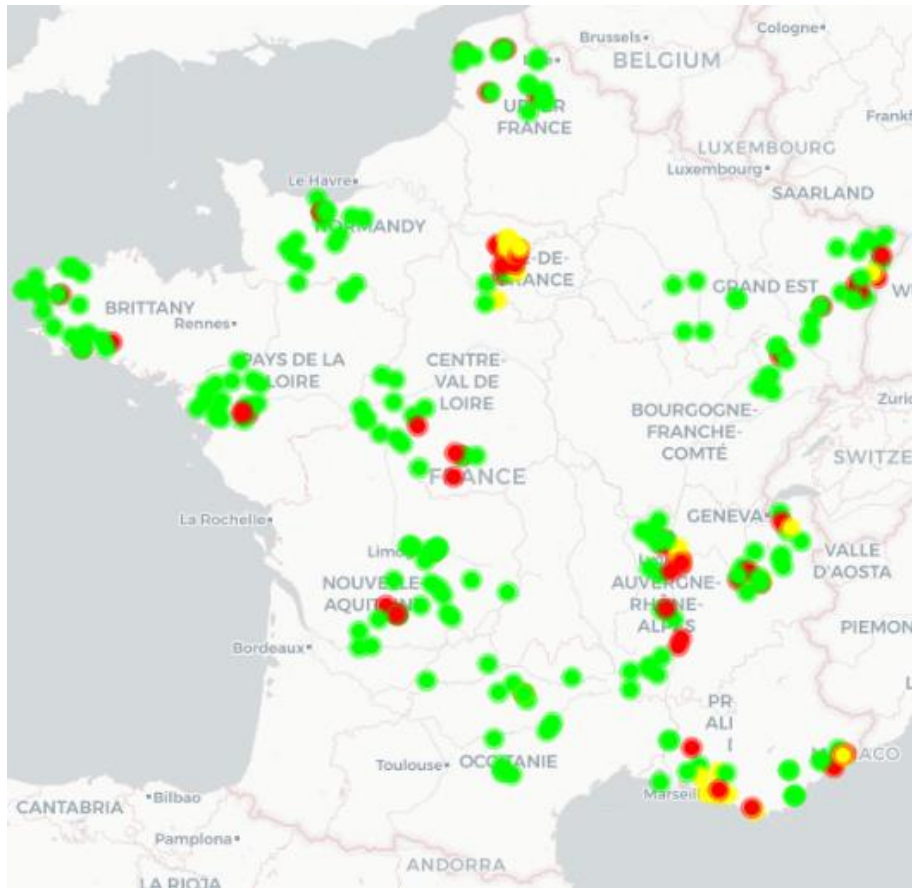


Figure 6: Schools and their corresponding color quality of the measured NO₂ concentration

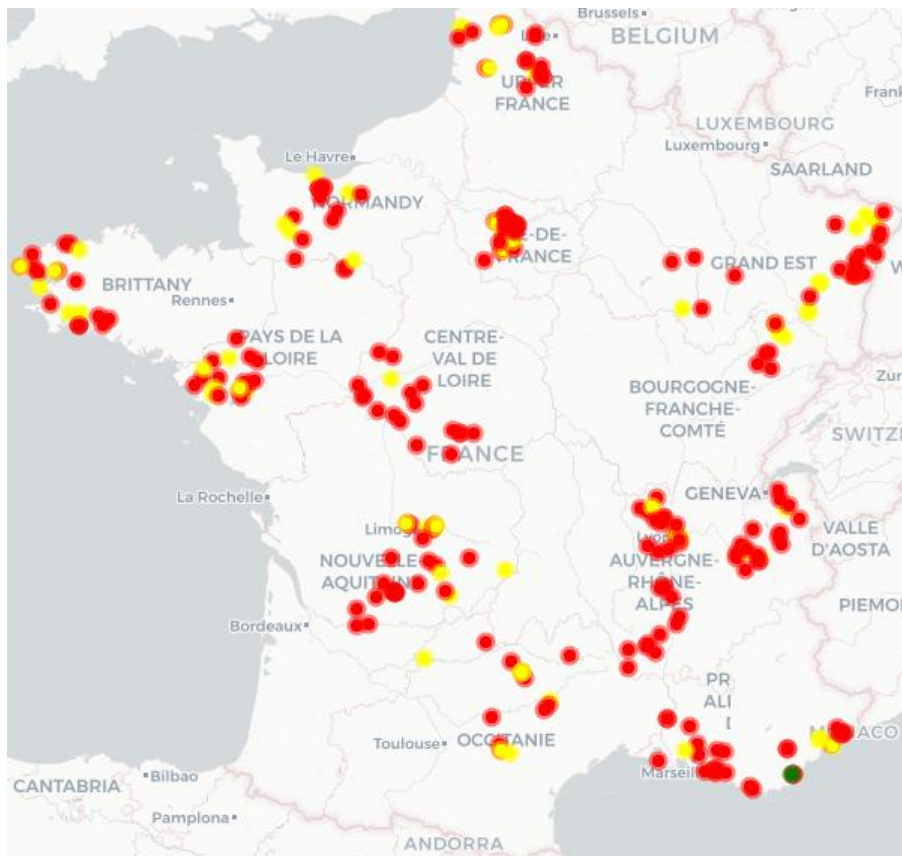


Figure 7: Schools and their corresponding colored quality of the measured PM_{2.5} concentration

3 CONCLUSIONS

The article presents the application of the TAIL rating scheme for schools using the French national survey data. From its initial development for hotels and offices, two new parameters have been added to the scheme: RT and NO₂ concentration. The reference values for different quality levels were also updated following the new AQ Guidelines by WHO. The rating scheme was shown to discriminate schools based on their overall IEQ level and specific level corresponding to the thermal, acoustic, visual environment, and indoor air quality. Analyses underlined trends, which can aid the decisions made by schools' administrations regarding IEQ improvement. There is clear evidence that the current state of IEQ is unsatisfactory. The TAIL also shows that to achieve high IEQ, no compromises should be made regarding quality levels of parameters defying IEQ. Further analyses will examine the relationship between the obtained IEQ levels defined by TAIL, building characteristics, and occupants' perceptions. A diagnostic plan can then be established, and as a result, further aiding schools in improving IEQ on their premises.

4 REFERENCES

- [1] P. Wargocki *et al.*, "TAIL, a new scheme for rating indoor environmental quality in offices and hotels undergoing deep energy renovation (EU ALDREN project)," *Energy Build.*, vol. 244, 2021, doi: 10.1016/j.enbuild.2021.111029.
- [2] F. Amato *et al.*, "Sources of indoor and outdoor PM_{2.5} concentrations in primary schools," *Sci. Total Environ.*, vol. 490, pp. 757–765, 2014, doi: 10.1016/j.scitotenv.2014.05.051.

An investigation of MVHR system performance based on health and comfort criteria in bedrooms of low-carbon social housing in Wales

Faisal Farooq^{*1}, Emmanouil Perisoglou¹, Miltiadis Ionas¹, Simon Lannon¹, Jo Patterson¹, Phil Jones¹

*1 Welsh School of Architecture, Cardiff University
Bute Building, King Edward VII Avenue,
CF10 3NB, Cardiff, UK*

ABSTRACT

Literature on the in-situ performance evaluation of Mechanical Ventilation with Heat Recovery (MVHR) in low-carbon social housing suggests that they can maintain a healthy ventilation rate in bedrooms in the UK. However, issues with noise and draught have been reported frequently. These issues may affect the sleep quality of occupants and have a detrimental effect on health and wellbeing. This research aims to present a quantification of these issues by carrying out detailed monitoring and evaluation at two case study sites in Wales, UK. The objectives are to calculate ventilation effectiveness via tracer gas experiment; predict thermal comfort using Predict Mean Vote (PMV); and predict acoustic comfort by measuring MVHR noise under different modes of operation. Results show that ventilation is effective despite the proximity of the supply vent to the door undercut; 90% of occupants are predicted to be thermally satisfied according to Fanger's thermal comfort model; and sound levels remain under the recommended value of 30dB(A) for bedrooms in all the cases. Results are followed by a discussion on experimental limitations and identification of opportunities for further investigation of the comfort indices mentioned.

KEYWORDS

MVHR, low-carbon housing, draught, noise, ventilation effectiveness.

1 INTRODUCTION

The Committee on Climate Change (2019) suggests that if UK is to meet its net zero carbon emissions target by 2050 then the housing stock needs to achieve high level of thermal efficiency which requires increased airtightness and the use of Mechanical Ventilation with Heat Recovery (MVHR) for maintaining healthy indoor air quality (pg 57). However, in-situ evaluation studies suggest that due to improper design, specification, installation, and commissioning of MVHR, a gap in performance exists. These issues have a negative impact on occupant health and comfort especially for the case of sleeping environments. This has been evidenced in the form of occupant complaints around draught and noise when trying to fall asleep (Sharpe et al., 2018, Gupta et al., 2018, Gupta and Kapsali, 2016, Gupta, 2016, ZCH, 2015), and potential short-circuiting of supply air when the vent is positioned too close to the bedroom door (Sharpe and Charles, 2015).

These studies however do not quantify the issues mentioned and were conducted at a time when MVHR was at its early stage of development, when most of the understanding on its design, installation and use was not there. This paper takes a case study approach to present the current practice of MVHR and investigates its performance in terms of occupant health

and comfort in bedroom environments. Results from tracer gas experiments, Predict Mean Vote (PMV) experiment and acoustic measurements are presented for two case study sites in Wales, followed by a discussion on how findings compare with literature, and identification of areas for further research.

2 CASE STUDY DETAILS

Two case studies sites located in Wales were chosen for this research, both of which are social housing, 2-story, 3-bedroom dwellings equipped with MVHR system (Nuair MRXBOX-ECO). Case Study A comprises of a cluster of 25 new build mid-terrace and end of terrace dwellings, whereas Case Study B is a single retrofit end of terrace dwelling. Dwellings in Case Study A have a measured air permeability of 4-5 m³/m² h @ 50 Pa, whereas Case Study B dwelling has a measured air permeability of 10.5 m³/m² h @ 50 Pa. All MVHR systems were in balance and were commissioned according to Building Regulations Part F (2021). Thermally insulated rigid ducting was used throughout except for at ends that connect the supply and extract terminal to the vents.



Figure 1: Case study sites in (a) Case Study A and (b) Case Study B.

3 METHODOLOGIES

3.1 Air Diffusion Effectiveness (ϵ_{ADE})

The relationship of supply vent/door undercut arrangement with ventilation effectiveness was evaluated using the Air Diffusion Effectiveness (ϵ_{ADE}) index developed by Fisk and Faulkner (1992). Fisk and Faulkner (1992) describe a tracer gas experimental protocol whereby a tracer gas, in this case CO₂, is filled in a room to a concentration of 2000 ppm, and is then left to decay until ambient levels are reached. The area under the curve is given by the age of air, τ , which represents the amount of time elapsed since molecules of a sample of air have entered a space, the formula is below:

$$\tau = \frac{1}{C(0)} \int_0^{t_{\text{end}}} C(t) dt \quad (1)$$

$C(0)$ is the concentration of tracer gas at initial time, t_{end} is the time at the end of the experiment, and $C(t)$ is the decay curve function. The ratio of τ at the door undercut (τ_{DU}) and breathing level (τ_{BL}) is given by the Air Diffusion Effectiveness (ϵ_{ADE}) of the ventilation strategy. If τ_{DU} is less than τ_{BL} then ϵ_{ADE} will be less than 1, and would indicate the presence of short-circuiting, a value greater than 1 would represent displacement flow pattern, whereas a value equal to 1 would indicate perfect mixing.

The experiment was run in 3 bedrooms of a single dwelling in Case Study A. Each dwelling in the cluster has the same floor plan and mechanical design. Hence results of a single dwelling would be representative of the entire cluster, as long as they are commissioned to the same ventilation rates. The experiment was set up by placing one Telaire T5100 (0-2000 ppm, ± 30 ppm) at breathing level and one at the door undercut. The breathing level in this case was chosen to be 0.6m based on the assumption that the occupant is lying in bed. Doors and windows were kept closed throughout the experiment. Figure 2 shows the experimental set-up.



Figure 2 Tracer gas set-up in rooms of different sizes and layout

3.2 Acoustic Comfort

Sound measurements were recorded with the MVHR system on and off in three bedrooms of 6 out of the 25 dwellings in Case Study A using ATP ET-965 meter (35-130 dB(A), ± 2 dB(A)). Sound and frequency measurements were recorded with the system on, off and in boost mode in three bedrooms of the single dwelling in Case Study B using Pulsar Nova 46 meter (20-140 dB(A), 31.5-16k Hz, ± 0.1 dB(A)).

Results were compared with Part F of Building Regulation's (2021) stipulated limit of 30dB(A) for bedroom environments and comments were made on whether sleep disruption is likely to be caused. Frequency measurements were recorded to analyse the change in sound quality with the system in different modes. Sound meters were placed at 0.6 m off the ground at locations where an occupant's bed is likely to be. Figure 3 shows the experimental set up for one of the bedrooms in Case Study B.



Figure 3 Experimental set-up using Pulsar Nova 46 sound level meter

3.3 Thermal Comfort

The impact of having an MVHR supply vent on thermal comfort was investigated by setting up a Predict Mean Vote (PMV) experiment based on Fanger's model given under EN ISO 7730 (2005) and ASHRAE 55 (2020) standards. The experiment was run in the Third bedroom at Case Study B for 4 nights, i.e., from 27/01/23 to 31/01/23. The timing of the experiment was chosen to be in winter because the temperature of supply air is expected to be colder. The purpose was to investigate whether the difference in room temperature and supply air temperature is likely to cause the air to sink to occupant level and lead to thermal discomfort.

The set-up included: Dantec 54R10 air velocity (0.05-5 m/s, ± 0.01 m/s) and air temperature (0 to 45°C, $\pm 0.5^\circ\text{C}$) probe and TinyTag TK-4014 radiant temperature sensor (-40 to 85°C, $\pm 0.05^\circ\text{C}$). The probe and sensor was mounted on a tripod which stood at 0.6 m off the ground. An immonit T/RH sensor (-7 to 60°C, $\pm 3\%$ of reading) was installed inside the supply vent and another one installed close to the bedroom door so that the difference in room and supply vent temperature can be recorded during the experiment. Figure 4 below shows placement of T/RH inside the supply vent (left) and mounting of the sensor and probe for the PMV experiment (right).



Figure 4 T/RH sensor in supply vent (left) and PMV experimental probe and sensor (right)

4 RESULTS & DISCUSSION

4.1 Tracer gas experiment

Decay curves are shown in Figure 5, whereas values for age of air at door undercut (τ_{DU}), breathing level (τ_{BL}) and Air Diffusion Effectiveness (ϵ_{ADE}) for the three bedrooms of a single dwelling in Case Study A are given under Table 1, respectively.

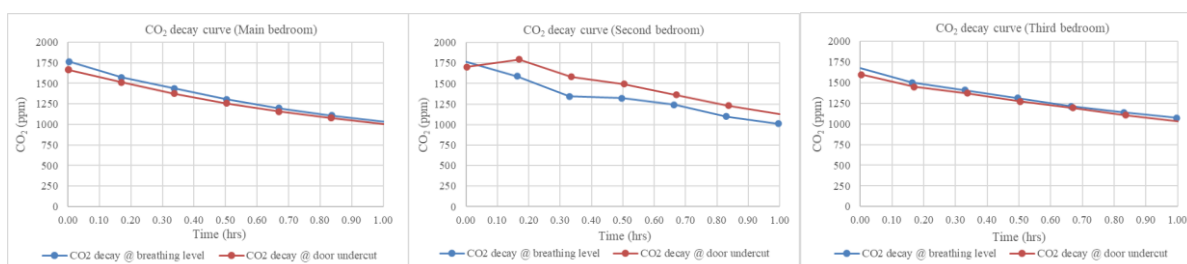


Figure 5 Tracer gas curves for the three bedrooms

Results from Table 1 show that τ_{DU} remains higher than τ_{BL} , which indicates greater air changes at breathing level than the door undercut, and hence a confirmation of ventilation effectiveness for the three bedrooms. This represents a displacement flow patterns which can be attributed to the prevalence of low air velocities in the room and to the shape of the terminal that causes the air to stick to the ceiling and walls. Computational Fluid Dynamic (CFD) modelling shall be used out to verify this further.

Table 1 Tracer gas experimental results

Main bedroom			Second bedroom			Third bedroom		
τ_{DU} (hr)	τ_{BL} (hr)	ϵ_{ADE}	τ_{DU} (hr)	τ_{BL} (hr)	ϵ_{ADE}	τ_{DU} (hr)	τ_{BL} (hr)	ϵ_{ADE}
0.78	0.76	1.02	0.84	0.81	1.04	0.81	0.79	1.02

One limitation of the experiment was the 10 min interval of recordings. Higher granularity can improve accuracy, especially for the case of bedroom 2, where unexplainable fluctuations in the curve were observed. Another limitation was that the area under the curve was calculated using trapezoid rule where curves were estimated to be straight lines.

4.2 Sound measurements

Sound level was measured with the system turned on and off in 3 bedrooms of 6 dwellings for Case Study A. No change in sound level or tonal frequency was perceived by the authors with the system on, off or in boost mode. All measurements were below 30 dB(A) as shown in Figure 6(a), which implies that sleep disruption is unlikely to be caused.

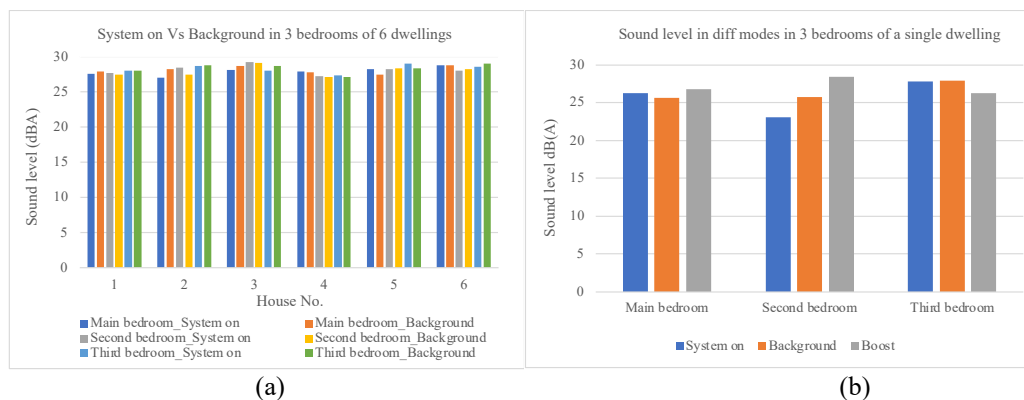


Figure 6 Sound measurements in dB(A) at (a) Case Study A and (b) Case Study B

For the case of Case Study B, sound and frequency measurements were recorded in all bedrooms with the system on, off and on boost mode. As shown in Figure 6(b), all measurements were below 30dB(A) which implies that, sleep disruption is unlikely to be caused. However, during site visits, the authors experienced a change in tonal frequency with the system on boost mode. Figure 7 shows results of the frequency distribution with the system in the three modes. Higher sound level was observed at 250 Hz for the 3 bedrooms in boost. The sound resembled that of an MVHR unit and was confirmed by the data as well as 250Hz lie within the 125-2.5kHz range which is typical of mechanical ventilation unit, according to EN BS 8233 (2014) standard.

Literature suggests that the reasons for noise and draught are due to poor levels of air tightness (Sharpe et al., 2018), overuse of flexible ducting (ZCH, 2015) and system

imbalances (Gupta and Kapsali, 2016, Gupta, 2016, Gupta et al., 2018). Although all measurements were below 30 dB(A), the change in tonal frequency observed at Case Study B could cause sleep disruption. Possible reasons for this are (a) unit located in the loft compared to being located in a dedicated utility room on the ground floor in Case Study A, and (b) air permeability being above the ideal value of 5 m³/m² h @ 50 Pa for an MVHR system to operate effectively. Greater air permeability means increased system resistance which causes the fan to run on higher than recommended speed and thus generate noise.

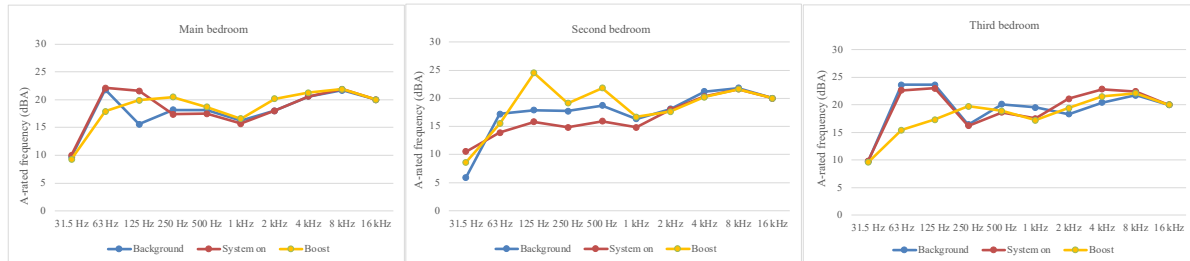


Figure 7 Frequency distribution with the system in different modes of operation at Case Study B

One limitation of the data on frequency distribution is the small sample size. Further research is required looking at a bigger sample and analysing the effect of change in tonal frequency on sleep quality. Another limitation of the work is that there are discrepancies in sound measurements for both sites. This was due to measurements being taken during morning/afternoon when background noise can be higher than night-time conditions. Another limitation was that all bedrooms were unfurnished. Furniture causes sound to dampen, which means that lower sound levels can be expected post-occupation. Future work includes carrying out an interview study with the installers, commissioners, and M&E team to verify whether a relationship between dwelling airtightness and choice of unit location exists with sound level in bedrooms.

4.3 Predict Mean Vote (PMV) experiment

PMV was calculated using Centre for Built Environment (CBE) Thermal Comfort online tool developed by Tartarini et al. (2020) based on Fanger's model. The metabolic rate chosen for the input was 0.7 and the clothing level was chosen as 3.53. A clothing level of 3.53 is representative of a typical UK bedding environment with the chest and head exposed, based on experiments conducted by Lin and Deng (2008b). Although Fanger's model given under EN ISO 7730:2005 can only be applied for a metabolic rate between 0.8-4 met and a clothing level between 0-2 clo, the online tool was used only to get an estimate for PMV.

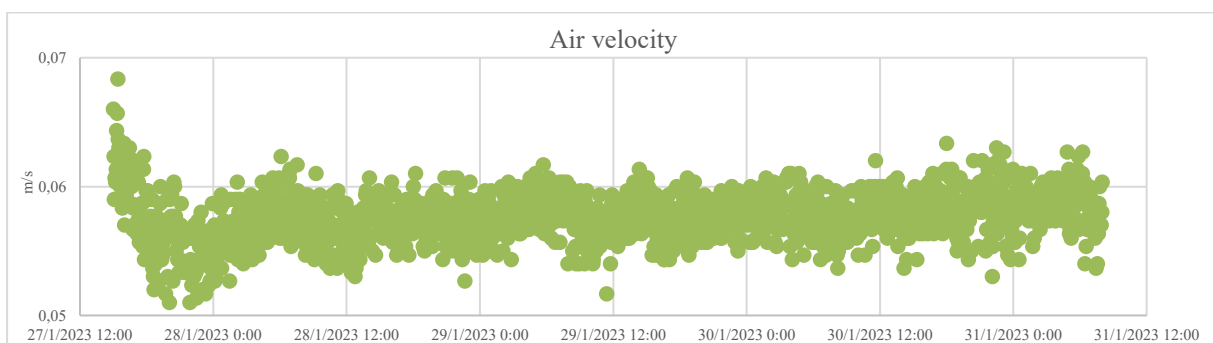


Figure 8 Results of omni-directional air velocity measurement

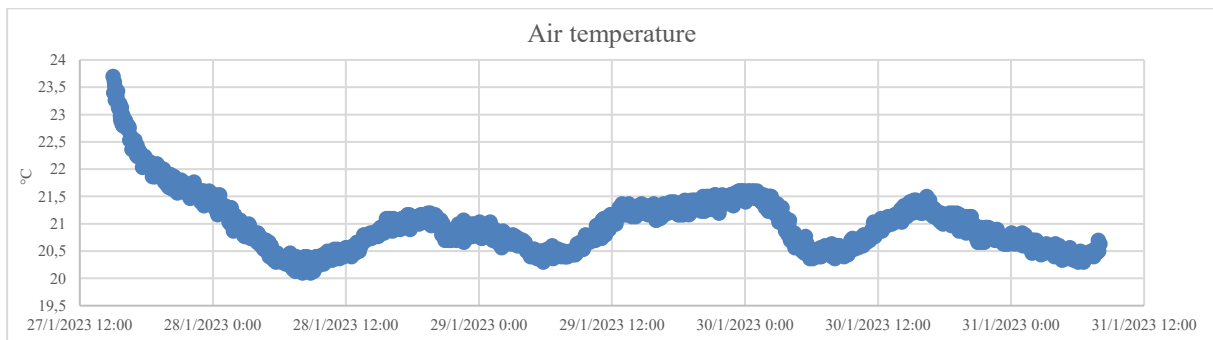


Figure 9 Results of air temperature measurement

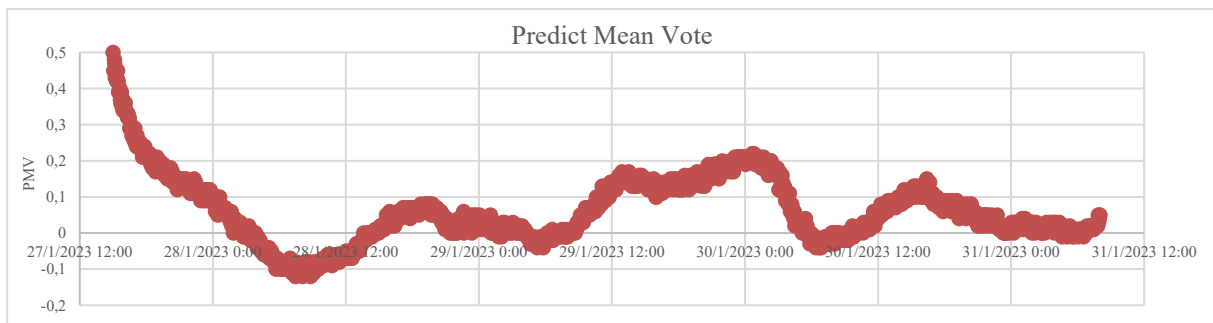


Figure 10 PMV calculated using the CBE online tool

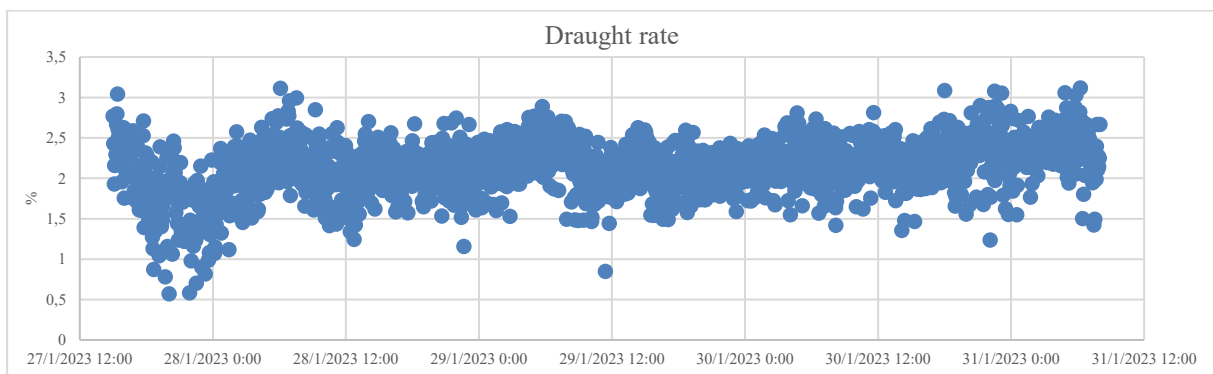


Figure 11 Draught rate calculated using EN ISO 7730 guidelines

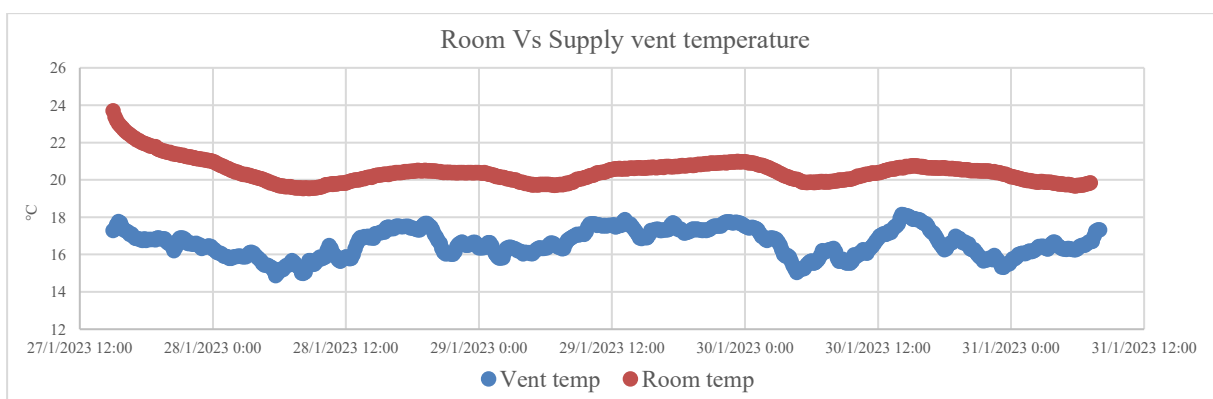


Figure 12 Comparison of room and supply vent temperature for the experiment

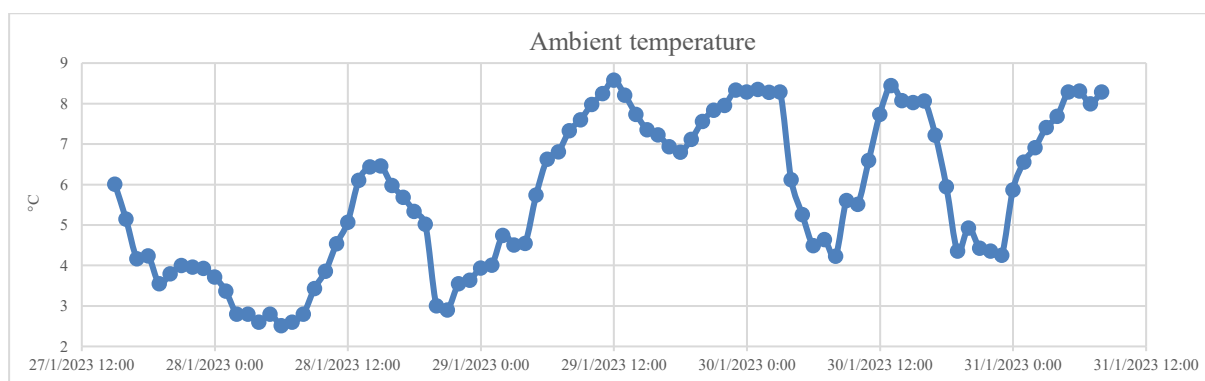


Figure 13 Ambient temperature during the experiment

At the start of the experiment, the radiator in the room was turned off so that the influence of local air currents can be avoided. This was the reason for why room temperature dropped from 24°C to approx. 21°C which was the new set point temperature for the entire dwelling, as shown in Figure 9. Results from Figure 10 show that PMV lies within ± 0.5 which means that for the set environmental conditions during the experiment, 90% of occupants are predicted to be thermally satisfied. Velocities remain under 0.07 m/s hence likelihood of draught remains low (Figure 8). This is evidenced by the draught rate results as percentage dissatisfied does not exceed 3.5% (Figure 11).

No real relationship was found between air velocity and PMV whereas a direct relationship existed between air temperature and PMV. This indicates that air from the supply vent is unlikely to drop to occupant level when there is a difference in temperature of approx. 3°C between the room and supply air (Figure 12). The system was in balance, ductwork was rigid and insulated, and unit was located in a thermally insulated loft; hence a higher factor of heat exchange efficiency was achieved, and as a result the possibility of cold air dumping remains low. Future work includes (a) applying Lin and Deng (2008a) adaptation of Fanger's model to calculate PMV for sleeping environments, (b) interviewing building professionals to further explore reasons behind draught in bedrooms, (c) carrying out CFD modelling to better understand cold air dumping by simulating air movement under different environmental conditions.

5 CONCLUSIONS & FURTHER WORK

Building performance evaluation was conducted to investigate health and comfort of having an MVHR supply vent in bedrooms of low-carbon case study dwellings for the two case studies. From a health perspective, a tracer gas experiment was carried out in bedrooms in Case Study A to investigate the relationship of supply vent/door undercut arrangement with Air Diffusion Effectiveness (ϵ_{ADE}). Results showed that ventilation was effective in all cases, despite the close proximity of the supply vent to the door undercut. This was attributed to the shape of the supply vent and to the prevalence of low velocities in the bedroom environment.

From a comfort perspective, acoustic and thermal comfort indices were considered. Results showed that sound measurements in all bedrooms on both sites were below the recommended value of 30dB(A), which means that likelihood of sleep disruption is low. However, change in tonal frequency was recorded at the Case Study B with the system on boost mode. This was attributed to (a) having the unit installed in the loft and (b) having an air permeability greater than the recommended value of 5 m³/m² h @ 50 Pa for an MVHR system to be installed.

Results from a PMV experiment conducted in one of the bedrooms to investigate the likelihood of an MVHR supply vent to cause thermal discomfort at night showed that for a difference in room temperature and supply vent temperature of approx. 3°C, more than 90% of occupants are thermally satisfied. This was attributed to the high heat exchange efficiency, which was achieved in the bedroom, mostly likely due to the system being in balance and due to the ductwork being insulated and rigid.

Further work includes recording the response of building professions who were involved at the two case study sites in MVHR design, commissioning, and installation to comment on the influence of unit location and airtightness on noise and on the impact of system imbalances and overuse of uninsulated flexible ducting on heat exchange efficiency. Lastly, CFD modelling technique will be used to investigate the difference in room temperature and supply air temperature that is likely to cause the air to sink to occupant level. The CFD model will also be used to visualise the air movement and hence aid in verifying the tracer gas experiments.

Although findings presented are of a limited sample, they provide a useful insight into the conditions that might exist in properties of similar built in Wales. Knowledge gained from this research will be useful for designers, manufacturers, installers, and commissioners on designing and specifying MVHR such that sleep disruptions can be minimised in low-carbon housing in the UK.

6 ACKNOWLEDGEMENTS

The author would like to acknowledge the Low Carbon Built Environment (LCBE) Research Team at Cardiff University for allowing access to the case study dwellings.

7 REFERENCES

- ANSI, A. & ASHRAE, A. 2020. Standard 55—Thermal Environmental Conditions for Human Occupancy. *ASHRAE, Atlanta*.
- BS 2014. British Standard BS 8233:2014 Guidance on sound insulation and noise reduction for buildings.
- CCC 2019. UK housing: Fit for the future? . UK: CCC.
- FISK, W. J. & FAULKNER, D. 1992. Air exchange effectiveness in office buildings: measurement techniques and results.
- GUPTA, R. & KAPSALI, M. 2016. Evaluating the ‘as-built’ performance of an eco-housing development in the UK. *Building Services Engineering Research and Technology*, 37, 220-242.
- GUPTA, R., KAPSALI, M. & HOWARD, A. 2018. Evaluating the influence of building fabric, services and occupant related factors on the actual performance of low energy social housing dwellings in UK. *Energy and Buildings*, 174, 548-562.
- GUPTA, R. K., M. 2016. Empirical assessment of indoor air quality and overheating in low-carbon social housing dwellings in England, UK. *Advances in Building Energy Research*, 10, 46-68.
- ISO, I. 2005. 7730: Ergonomics of the thermal environment Analytical determination and interpretation of thermal comfort using calculation of the PMV and PPD indices and local thermal comfort criteria. *Management*, 3, e615.

- LIN, Z. & DENG, S. 2008a. A study on the thermal comfort in sleeping environments in the subtropics—developing a thermal comfort model for sleeping environments. *Building and environment*, 43, 70-81.
- LIN, Z. & DENG, S. 2008b. A study on the thermal comfort in sleeping environments in the subtropics—Measuring the total insulation values for the bedding systems commonly used in the subtropics. *Building and Environment*, 43, 905-916.
- PART, F. 2021. Building Regulations. *Approved document Part F Ventilation*.
- SHARPE, T. & CHARLES, A. Ventilation provision and outcomes in mainstream contemporary new-building flats in London, UK. 1st North American Regional Conference Proceedings Healthy Buildings, 2015. 19-22.
- SHARPE, T., MCGILL, G., MENON, R. & FARREN, P. 2018. Building performance and end-user interaction in passive solar and low energy housing developments in Scotland. *Architectural Science Review*, 61, 280-291.
- TARTARINI, F., SCHIAVON, S., CHEUNG, T. & HOYT, T. 2020. CBE Thermal Comfort Tool: Online tool for thermal comfort calculations and visualizations. *SoftwareX*, 12, 100563.
- ZCH 2015. Ventilation in New Homes. London: Zero Carbon Hub.

Impact of optimized residential ventilation with energy recovery on health and well-being

Martin Kremer^{*1}, Kai Rewitz¹, and Dirk Müller¹

*1 RWTH Aachen University, E.ON Energy Research Center, Institute for Energy Efficient Buildings and Indoor Climate
Mathieustraße 10
52074 Aachen, Germany*

ABSTRACT

With rising insulation standards and air tightness in buildings, the use of mechanical ventilation becomes more relevant. In this context, energy recovery offers a significant contribution to the decarbonisation of building operations. Heat recovery systems are widely spread in residential ventilation. Moreover, enthalpy exchangers recovering sensible and latent heat have an increasing share of use in residential ventilation, especially in cold climates, as they not only reduce the energy demand but also increase the indoor air humidity in winter seasons. In moderate climates, the outdoor air provides sufficient moisture content in transitional periods. Hence, enthalpy exchangers have to be bypassed to avoid too high indoor air humidity. Since heat and moisture transfer are conjugated in membrane-based enthalpy exchangers, this leads to a decrease of recovered sensible heat as well. Consequently, the research question arises regarding how efficient moisture transfer in an enthalpy exchanger has to be in order to provide a healthy and comfortable indoor air environment with minimum energy demand. In this study, we optimize a membrane-based enthalpy exchanger regarding membrane thickness and permeability to improve the overall performance of a residential ventilation unit. Therefore, we develop a simulation setup consisting of a thermal zone model, residential ventilation unit with the enthalpy exchanger model, and the control logic for the system. This simulation setup is combined with a genetic algorithm for optimization. We define a multi-objective optimization problem in order to optimize energy demand and indoor air humidity level. The study shows that the system's energetic optimum in moderate climates (Cuxhaven) lies at a membrane thickness of 120 μm . Regarding humidity level, thin membranes with 65 μm lead to overall more comfortable humidities. In consequence, enthalpy exchanger with lower latent efficiency lead to not only better overall energetic performance in moderate climates but also more comfortable indoor air conditions. With slightly higher energy demand compared to the energetic optimum, a significant increase regarding comfortable indoor air humidities is achievable.

KEYWORDS

Enthalpy exchanger; optimization; residential ventilation; thermal comfort

1 INTRODUCTION

With rising insulation standards, buildings' air tightness is increasing. In consequence, ventilation becomes more and more relevant not only in non-residential but also in residential buildings. Typical residential ventilation systems inherit an energy recovery system as the key component. The most common form of energy recovery is sensible heat recovery. In the past decades, the usage of enthalpy recovery increased in share, especially in cold climates or warm and humid climates. Membrane-based enthalpy exchangers (MEEs) are one very common form of enthalpy recovery in residential ventilation. The membranes separate the air streams and are able to transfer heat as well as moisture. In this way, they can heat and humidify the fresh air in cold climates or cool and dehumidify the fresh air in warm and humid climates.

Many researchers have investigated membrane-based enthalpy exchangers. These studies can be divided into four different categories: investigations on the performance of MEE under different boundary conditions, investigation on different membrane materials for MEE, enhancement in flow structures of MEE, and general optimization of MEE.

Different studies address the analysis of the impact of volume flow rate, temperature and humidity boundary conditions on the effectiveness of MEE (Zhang et al., 2008; Min and Su, 2011; Nasif and Al-Waked, 2014, 2014; Al-Waked et al., 2015; Koester et al., 2017; Siegele and Ochs, 2019). They all found that sensible and latent effectiveness increase with decreasing volume flow rate. The latent effectiveness depends more on the volume flow rate than the sensible effectiveness. Moreover, the studies show that the influence of outdoor and indoor air states on the MEE's performance is dependent on the membrane material. Some membrane materials show a significant influence of the boundary conditions and others show no significant influence and perform in the same way for different boundary conditions.

This goes along with the second category of investigations regarding the influence of the membrane material. Many researchers have investigated different membrane materials in order to increase sensible and latent heat transfer in MEE (Zhang et al., 2008; Min and Su, 2010; Nasif, 2015; Koester et al., 2017; Baldinelli et al., 2019). They all show that especially the latent effectiveness is sensitive to membrane material.

Other studies address the optimization of the flow structure in MEEs in order to increase the performance of the enthalpy exchanger (Al-Waked et al., 2015; Albdoor et al., 2020a). One way to increase the performance is to increase the share of the counter-flow arrangement in the MEE. Another option is to break the boundary layer with spacers or similar geometric elements. Although these are able to increase the sensible and latent effectiveness, they also increase the pressure drop of the MEE, which leads to a higher electric energy demand for the fans.

To improve the sensible and latent effectiveness Albdoor et al. used an approach to minimize the entropy generation of MEE with a genetic algorithm (GA) (Albdoor et al., 2020b). They aim to optimize the design of an MEE. They varied mass flow rates through the MEE, length and width of the MEE, channel height, membrane thickness and thermal conductivity and the membrane material's diffusion coefficient. They could find an optimum in design that reduces the entropy generation by 20 – 30 %. Nevertheless, the optimum they found lies at very small mass flow rates. How the optimized MEE performs at nominal mass flow rates needed to ventilate the room properly is not shown in their study.

Zhang used a reliability-based approach to optimize MEE design under uncertain conditions (e.g. production tolerance) (Zhang, 2016). The aim function is the economic return of the MEE. They found that parallel-plate MEE with asymmetric polymer membranes performs best in the investigated data set. Moreover, they could show that the MEE's performance will degrade with uncertain geometric parameters compared to the exact parameters. Their study focusses on warm and humid climates. Therefore, it might not be transferable to other climatic regions.

Men et al. optimized the design of MEE with a particle swarm optimization algorithm (Men et al., 2021). Their multi-objective optimization aims to reduce entropy generation and increase economic return.

All the optimization studies have in common that they try to increase the performance of MEE. Moreover, they only consider the MEE itself for their optimization. The studies lack the investigation of the influence on the holistic system consisting of the ventilation unit and the building. Since all the studies concentrate on warm and humid or cold climates, these approaches might be sufficient. Nevertheless, in moderate climates, outdoor air humidity is sufficient for building ventilation during the spring and autumn season. During these periods, high latent effectiveness can lead to high indoor air humidities. Hence, the research question arises about how efficient the latent effectiveness of MEE has to be in order to perform best in the context of the holistic system. In this paper, we optimize the design of MEE considering the overall energy demand of the building and the indoor air comfort for different climatic regions.

2 METHODOLOGY

To optimize MEE in the context of the holistic system, we build up an optimization framework. This framework consists of a dynamic system model combined with a control algorithm. The system model is linked to a genetic optimization algorithm that varies the MEE's parameters.

2.1 Objectives and parameters used for optimization

We choose two objectives for our optimization. As first objective, we use the total use energy demand of all components. Therefore, the heating power, cooling power and electric power of the fans are integrated during the annual simulation and summed up. The GA aims to minimize the total use energy demand.

The second objective is the violation of comfortable indoor air humidity. The objective uses the two different definitions shown in Table 1. Typical international standards define a range between 30 and 65 % relative humidity for indoor air environments (Designation: Standard). (Sterling et al., 1985) investigated the impact of indoor air humidity on humans and found the range of 40 to 60 % relative humidity as a good compromise between all influences. Therefore, we choose this range as second definition (Designation: Tight). By investigating both definitions, we can analyse how the optimum design of MEE depends on the desired indoor air humidities.

Table 1 Definitions of comfortable indoor air humidity

Designation	Lower limit	Higher limit	Ref.
Standard	30 % relative humidity	65 % relative humidity	(American Society of Heating, Refrigerating and Air-Conditioning Engineers, 2020)
Tight	40 % relative humidity	60 % relative humidity	(Sterling et al., 1985)

As violations of the comfortable indoor air humidity occur dynamically during the annual operation, we define a KPI to quantify the violations. We use the *Integral Absolute Error* (IAE_{rH}) which is well known in the field of control engineering as basis for our KPI. The KPI is shown in Equation (1). Whenever the relative humidity φ in the building overshoots the higher limit φ_{\max} or undershoots the lower limit φ_{\min} , the difference will be integrated over the time the violation occurs.

$$\text{IAE}_{\text{rH}} = \int \max(\varphi(t) - \varphi_{\max}, 0) + \max(\varphi_{\min} - \varphi(t), 0) dt \quad (1)$$

To reach the optimum system performance regarding the two objectives, we choose two different design parameters – membrane thickness and membrane permeability - for the MEE as they mainly influence mass transfer only. Figure 1 shows the impact of the membrane thickness and membrane permeability on the MEE's sensible and latent effectiveness. As can be seen, the latent effectiveness is sensitive to both parameters. On the contrary, both parameters have only a small impact on sensible effectiveness. For this reason, it is possible to design the MEE's latent effectiveness without influencing the sensible effectiveness. Therefore, all results of this study can be attributed to effects caused by latent effectiveness. After a market survey on typical membrane properties, we set the range of membrane thickness to 20 - 200 μm . According to Albdoor et al., typical polymer membranes' permeability varies between 1E-13 and 1E-10 mol/(m s Pa) (Albdoor et al., 2022). Paper membranes usually have higher permeabilities. Hence, we choose a range between 1E-13 and 3E-10 mol/(m s Pa).

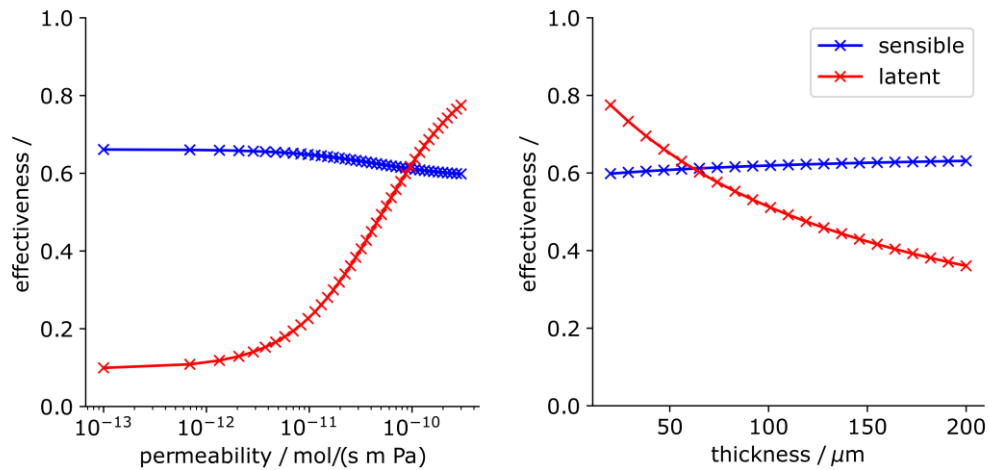


Figure 1 Influence of membrane thickness and permeability on MEE's effectiveness

2.2 Simulation model

The core of the optimization setup is a dynamic simulation model shown in Figure 2. The model consists of a thermal zone model (Lauster and Constantin, 2017) and a residential ventilation unit model. The ventilation unit model consists of a preheater model, an MEE-model and two fan models. The preheater is used to avoid frost formation in the MEE. The MEE-model (Kremer et al., 2019) consists of parallel membranes and can be varied using geometric parameters like membrane thickness, permeability of the membrane, length and width of the MEE, channel height and the number of parallel membranes.

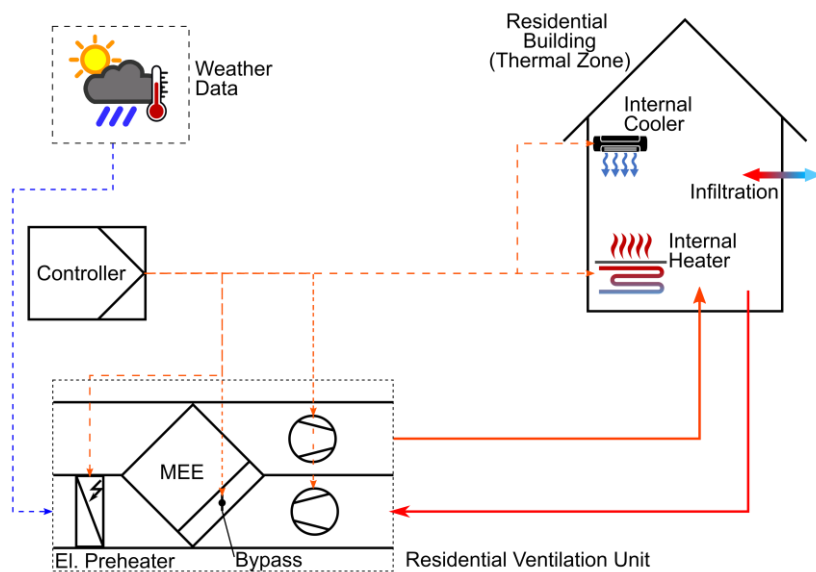


Figure 2 Structure of simulation setup used for optimization

The thermal zone model represents the building structure. The building structure is parametrized using the Tool TEASER (Remmen et al., 2018). The tool delivers typical elements according to the year of construction and translates the building structure into a thermal network (resistance-capacity-model). In this study, we choose 2015 as the year of construction.

We consider an infiltration of 0.06/h in the thermal zone model but assume no window ventilation in addition to the mechanical ventilation. The thermal zone model inherits an idealized heating and cooling model to control indoor air temperature. The ideal cooler does

not consider any condensate formation and therefore provides sensible cooling only. Internal loads such as persons, machines and light are modelled according to (Schweizer Ingenieur- und Architektenverein, 2024) considering latent heat production of persons and other sources (e.g. plants and shower).

All in all, the building energy system modelled inherits the functionality of energy recovery, heating, and cooling. No active humidification or dehumidification is applied. Therefore, indoor air temperature is fully controllable, but indoor air humidity control is limited to energy recovery. As no dehumidification is applied, the absolute indoor air humidity is always equal to or higher than the absolute outdoor air humidity due to internal gains.

2.3 System control

We develop a controller for the residential ventilation unit to control the fans and the bypass over the MEE to avoid too high indoor air temperatures and humidities. Moreover, the controller sets the cooling and heating power for the internal devices. The set point temperature for heating and cooling is derived from the German standard DIN EN 16798-1 (German Institute for Standardization, 2022). Figure 3 shows the limits for comfortable room temperature as defined by DIN EN 16798-1. We use the lower limit for a comfortable room temperature as the set point for heating and the higher limit as the set point for cooling. Since no dehumidification is considered in the simulation model, the humidity will not decrease in the building model. Hence, we use the higher limit of comfortable indoor air humidity to control the bypass over the MEE. If the indoor air humidity exceeds the limit, the bypass will open, reducing the latent and sensible heat recovered. We use two different ranges for the definition of comfortable indoor air humidity presented in Table 1.

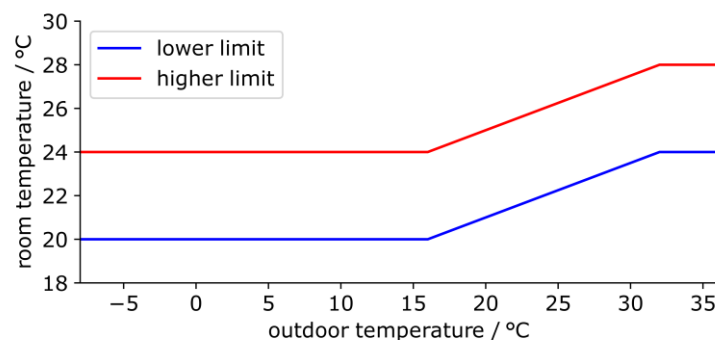


Figure 3 Limits for comfortable room temperature according to (German Institute for Standardization, 2022)

2.4 Optimization setup

Using the Dymola-API of the Python package ebcpy (Wüllhorst et al., 2022), the simulation model is linked to the optimization algorithm programmed in Python. We use a GA provided by the optimization package PyGAD (Gad, 2021) for the optimization. The parameters used for the GA are listed in Table 2. For detailed information on the parameters and their influence on the optimization, please refer to (Gad, 2021). For each parameter variation of the MEE, an annual simulation is carried out and the results are provided to the optimization algorithm. In the first step, the algorithm sets up an initial population consisting of pairs for membrane thickness and permeability values. For each pair, the simulation is carried out. The algorithm uses the results to create the next generation of parameter pairs. This process is iterated until the defined number of generations (see Table 2) is reached.

Table 2: Parameters used for the genetic algorithm

Parameter	Value
Number of generations	20
Solutions per generation	10
Number of genes	2 (membrane thickness and permeability)
Value range for genes	[20 ... 200 μm]; [1E-15 ... 3E-10 mol/(m s Pa)]
Parent selection type	steady-state-selection
Crossover type	uniform
Crossover probability	0.8
Mutation type	adaptive
Mutation probability	0.7; 0.4 (thickness; permeability)

2.5 Investigated climatic conditions

We carry out the optimization for three different locations in Europe – Sodankyla, Munich and Cuxhaven. Sodankyla, a city in Lapland (Finland), can be classified as cold and dry climate with a temperature median of 1.4 °C and a humidity median of 3.37 g/kg. The German city of Munich has a moderate continental climate (median temperature: 8.9 °C, median humidity: 5.27 g/kg). Cuxhaven on the contrary is a moderate and more humid climate (median temperature: 9.8 °C, median humidity: 6.01 g/kg) since it is a city located near the German coast. Figure 4 shows the density functions of temperature and humidity for the three locations. The x-axes show the temperature and absolute humidity respectively. The y-axes show the density of how often an interval occurs during the year. We use intervals of 1 K and 1 g/kg to calculate the densities. In Sodankyla, temperatures below 0 °C occur more often than in the German cities. Additionally, low absolute humidities occur more frequently. In Cuxhaven, temperatures between 5 and 20 °C occur more often than in Munich, whereas in Munich higher temperatures between 20 and 30 °C occur more often. Regarding humidity, both German cities have a similar density function, but absolute humidities between 5 and 10 g/kg occur more often in Cuxhaven. This interval is relevant for the operation of the MEE. Since these absolute humidities are sufficient for an indoor air environment, no humidification is needed during the times, outdoor air humidity lies in between the interval. In consequence, MEE cannot provide any benefit regarding comfort. Especially for outdoor air with absolute humidities between 8 and 10 g/kg, the risk of reaching too humid indoor air if operating an MEE is high. Therefore, the difference in optimization results between Munich and Cuxhaven will be interesting to investigate.

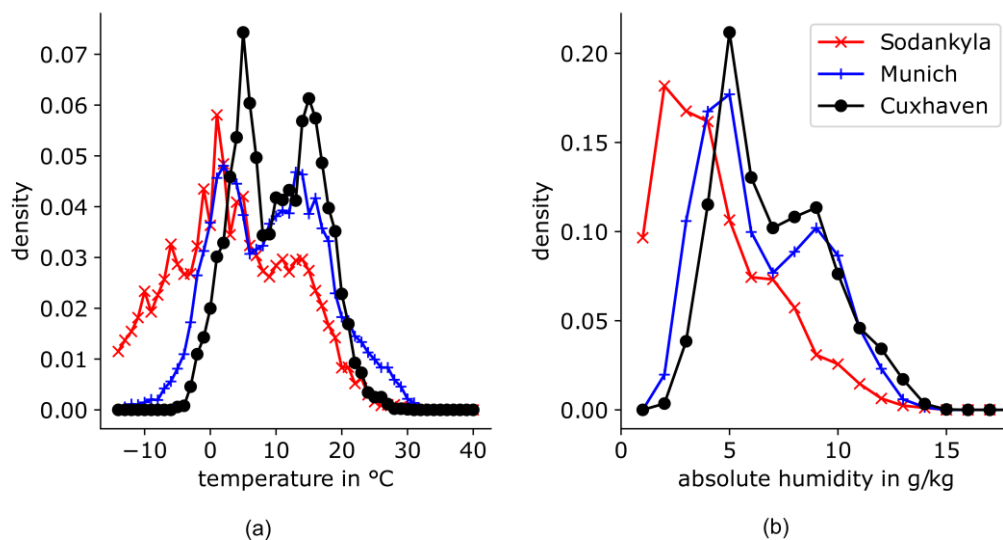


Figure 4 Density functions of temperature (a) and humidity (b) at the three investigated locations

3 OPTIMIZATION RESULTS

Figure 5 shows the results for all annual simulations carried out by the optimization for both objectives and the *Standard* comfort limits for Munich. The x-axis indicates the comfort violation as defined by Equation (1). The y-axis represents the holistic system's total use energy demand. Presented are all solutions, including the non-optimal intermediate solutions (red +). The theoretical optimum shows the best solution for the energy demand and the comfort violation, respectively. Obviously, both objectives cannot be satisfied at the same time. All solutions lying on the dotted line will be optimal design solutions depending on how both objectives are weighted. The best fit indicates the solution with the smallest distance to the theoretical optimum if both objectives are weighted equally. Since the MEE's design influences the energy demand of the residential system less than the IAE_{rH} , the best fit is found in the region with higher energy demand but a low IAE_{rH} .

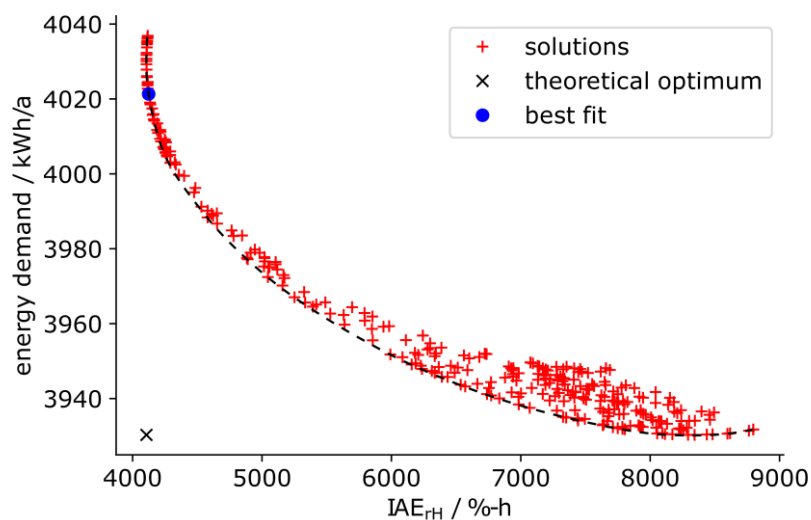


Figure 5 Pareto diagram of optimization results for Munich

Table 3 lists the found optimum design parameters for each objective and for the best fit for all investigated locations and the *Standard* comfort limits. The energy demand and the IAE_{rH} differ significantly between the three locations. While Cuxhaven (moderate climate) has the lowest energy demand and reaches the most comfortable indoor air humidities, the energy demand in Munich is slightly higher and the IAE_{rH} is higher. Moreover, the difference in IAE_{rH} between energetic optimum and comfort optimum increases. This trend is also visible for Sodankyla, the coldest and driest location in this study. Here, energy demand is more than twice as high as in Munich and Cuxhaven. The IAE_{rH} is even six to seven times higher compared to the other two locations.

The results indicate that the optimization algorithm chooses minimum membrane thickness and higher permeabilities in cold and dry climates to minimise the IAE_{rH} . This leads to an MEE with high latent effectiveness (see Figure 1). The gap between the energetic optimum and the IAE_{rH} optimum is getting higher in cold and dry climates. If the latent effectiveness is high (IAE_{rH} optimum) the risk of too humid indoor air during summer and autumn increases causing the bypass over the MEE to open. In consequence, both sensible and latent heat recovery are reduced. Especially during autumn, the outdoor air temperatures are lower. With reduced sensible heat recovery, the internal heater has to provide the energy to keep indoor air temperatures at a comfortable level. Additionally, the MEE could reduce the cooling energy demand during summer seasons when indoor air temperatures are lower than outdoor air

temperatures. Reduced energy recovery will therefore lead to higher cooling demands. In consequence, the optimization algorithm chooses thicker membranes and lower permeabilities to minimise energy demand. It has to be highlighted that the difference in energy demand for the energetic optimum and the IAE_{rH} optimum is small (0.5 – 2.5 %). For this reason, the best fit lies at a membrane thickness and permeability near the IAE_{rH} optimum. The results for a cold and dry location like Sodankyla indicate that active humidification should be considered also for residential ventilation to achieve more comfortable indoor air humidities.

Table 3 Optimal solutions for *Standard* comfort limits

Location	Optimum	Membrane thickness / μm	Permeability / $\text{mol}/(\text{m s Pa})$	Total use energy demand / kWh/a	IAE_{rH} / %-h
Munich	Energetic	155	$1,67 \cdot 10^{-10}$	3 930	8 343
	IAE_{rH}	20	$2,65 \cdot 10^{-10}$	4 030	4 107
	Best fit	20	$2,27 \cdot 10^{-10}$	4 021	4 124
Cuxhaven	Energetic	120	$1,67 \cdot 10^{-10}$	3 243	3 753
	IAE_{rH}	75	$2,09 \cdot 10^{-10}$	3 257	3 608
	Best fit	65	$1,67 \cdot 10^{-10}$	3 253	3 610
Sodankyla	Energetic	150	$1,67 \cdot 10^{-10}$	10 049	49 934
	IAE_{rH}	20	$3,00 \cdot 10^{-10}$	10 220	26 117
	Best fit	20	$3,00 \cdot 10^{-10}$	10 220	26 117

Table 4 shows the optimum design parameters for the *Tight* comfort limits for all locations. The results show that the energy demand slightly increases if the relative indoor air humidity needs to be kept between 40 and 60 %. A more frequent bypass opening over the MEE causes this. If the bypass opens more often, the internal heater has to provide the necessary heating power more often. The IAE_{rH} optimum is found for thinner and more permeable membranes compared to the *Standard* comfort limits. Especially for the location Cuxhaven, this becomes clear. In consequence, the best fit also changes to thinner and more permeable membranes. The results show a significant increase in the IAE_{rH} compared to the *Standard* limits. This is plausible and expectable as no active humidification is considered for the system.

Overall, the optimization results show that in moderate and cold climates the energetic optimum of the holistic system of a ventilated residential building is found for thicker and less permeable membranes. However, thinner and more permeable membranes need to be used for MEE to achieve more comfortable indoor air humidity. The energetic impact of MEE design is smaller than the impact on indoor air humidity. With slightly higher energy demand, significant improvement of indoor air humidity can be achieved. Especially in colder and dryer regions, MEE should be designed with thinner and more permeable membranes.

Table 4 Optimal solutions for *Tight* comfort limits

Location	Optimum	Membrane thickness / μm	Permeability / $\text{mol}/(\text{m s Pa})$	Total use energy demand / kWh/a	IAE_{rH} / %-h
Munich	Energetic	35	$3,58 \cdot 10^{-12}$	3 935	43 534
	IAE_{rH}	20	$3,00 \cdot 10^{-10}$	4 037	23 213
	Best fit	20	$2,99 \cdot 10^{-10}$	4 037	23 216
Cuxhaven	Energetic	35	$7,93 \cdot 10^{-12}$	3 277	26 311
	IAE_{rH}	20	$2,08 \cdot 10^{-10}$	3 312	18 568
	Best fit	20	$1,70 \cdot 10^{-10}$	3 307	18 580
Sodankyla	Energetic	30	$6,25 \cdot 10^{-12}$	10 058	114 344
	IAE_{rH}	20	$3,00 \cdot 10^{-10}$	10 231	70 894
	Best fit	20	$3,00 \cdot 10^{-10}$	10 231	70 894

4 CONCLUSIONS

We have presented a method to optimise the design of MEE in the context of a holistic system and applied the method to a residential building with a typical ventilation unit consisting of a pre-heater and an MEE.

The optimization results show that thicker and less permeable membranes can be used in MEE in order to reach the minimum energy demand for the holistic system. On the contrary, thinner and more permeable membranes lead to fewer violations of comfortable indoor air humidity. The influence of the MEE's design on the energy demand is not significant for the investigated use case of a residential building. With lower insulation standards or active humidification, it might increase. In consequence, the best fit to the theoretical optimum with equal weights on energy demand and comfort violation is located near the minimum comfort violation.

Further investigations could address different building types, including humidification and dehumidification and investigate locations with warm and humid climate conditions. Moreover, other geometric parameters of the MEE, like transfer area or channel height, could be investigated. Transforming the continuous variation of the permeability to discrete values of existing membrane materials is part of further work. Our KPI definition for comfortable humidity addresses only linear dependency on the humidity difference and time. For example, the risk of mould growth depends strongly on the duration of excessive humidity in the room as well as on the value of the relative humidity. Hence, the KPI definition does not provide information on the influence on human beings. This should be addressed in further studies.

5 REFERENCES

- Albdoor, A.K., Ma, Z., Al-Ghazzawi, F. and Arıcı, M. (2022). Study on recent progress and advances in air-to-air membrane enthalpy exchangers: Materials selection, performance improvement, design optimisation and effects of operating conditions. *Renewable and Sustainable Energy Reviews*, 156, 111941.
- Albdoor, A.K., Ma, Z. and Cooper, P. (2020a). Experimental investigation and performance evaluation of a mixed-flow air to air membrane enthalpy exchanger with different configurations. *Applied Thermal Engineering*, 166, 114682.
- Albdoor, A.K., Ma, Z., Cooper, P., Ren, H. and Al-Ghazzawi, F. (2020b). Thermodynamic analysis and design optimisation of a cross flow air to air membrane enthalpy exchanger. *Energy*, 202, 117691.
- Al-Waked, R., Nasif, M.S., Morrison, G. and Behnia, M. (2015). CFD simulation of air to air enthalpy heat exchanger: Variable membrane moisture resistance. *Applied Thermal Engineering*, 84, 301–309.
- American Society of Heating, Refrigerating and Air-Conditioning Engineers (2020). *2020 ASHRAE handbook: HVAC systems and equipment*. Atlanta, GA: ASHRAE.
- Baldinelli, G., Rotili, A., Narducci, R., Di Vona, M.L. and Marrocchi, A. (2019). Experimental analysis of an innovative organic membrane for air to air enthalpy exchangers. *International Communications in Heat and Mass Transfer*, 108, 104332.
- Gad, A.F. (2021). *PyGAD: An Intuitive Genetic Algorithm Python Library*.
- German Institute for Standardization (2022). Energy performance of buildings - Ventilation for buildings - Part 1.
- Koester, S., Falkenberg, M., Logemann, M. and Wessling, M. (2017). Modeling heat and mass transfer in cross-counterflow enthalpy exchangers. *Journal of Membrane Science*, (525), 68–76.
- Kremer, M., Mathis, P. and Müller, D. (2019). Moisture Recovery – A Dynamic Modelling Approach. *E3S Web of Conferences*, 111, 1099.

- Lauster, M. and Constantin, A. (2017). Verification of a Low Order Building Model for the Modelica Library AixLib using ASHRAE Standard 140, *Proceedings of Building Simulation 2017: 15th Conference of IBPSA*. IBPSA.
- Men, Y., Liang, C., Li, Z. and Tong, X. (2021). Configuration optimization of a membrane-based total heat exchanger with cross-corrugated triangular ducts considering thermal economy and entropy generation. *Case Studies in Thermal Engineering*, 28, 101446.
- Min, J. and Su, M. (2010). Performance analysis of a membrane-based enthalpy exchanger: Effects of the membrane properties on the exchanger performance. *Journal of Membrane Science*, (348), 376–382.
- Min, J. and Su, M. (2011). Performance analysis of a membrane-based energy recovery ventilator: Effects of outdoor air state. *Applied Thermal Engineering*, (31), 4036–4043.
- Nasif, M.S. (2015). Effect of utilizing different permeable material in air-to-air fixed plate energy recovery heat exchanger on energy saving. *ARP Journal of Engineering and Applied Sciences*, 10(21), 10153–10158.
- Nasif, M.S. and Al-Waked, R. (2014). Seasonal Weather Conditions Effect on Energy Consumption and CO₂ Emission for Air Conditioning Systems Coupled with Enthalpy Energy Recovery Heat Exchanger. *APCBEE Procedia*, 10, 42–48.
- Remmen, P., Lauster, M., Mans, M., Fuchs, M., Osterhage, T. and Müller, D. (2018). TEASER: an open tool for urban energy modelling of building stocks. *Journal of Building Performance Simulation*, 11(1), 84–98.
- Schweizer Ingenieur- und Architektenverein (2024). Raumnutzungsdaten für Energie- und Gebäudetechnik. Zürich.
- Siegele, D. and Ochs, F. (2019). Effectiveness of a membrane enthalpy heat exchanger. *Applied Thermal Engineering*, 160, 114005.
- Sterling, E.M., Arundel, A. and Sterling, T.D. (1985). Criteria for human exposure to humidity in occupied buildings. *ASHRAE Trans*, 91(1), 611–622.
- Wüllhorst, F., Storek, T., Mehrfeld, P. and Müller, D. (2022). AixCaliBuHA: Automated calibration of building and HVAC systems. *Journal of Open Source Software*, 7(72), 3861.
- Zhang, L.Z., Liang, C.-H. and Pei, L.-X. (2008). Heat and moisture transfer in application scale parallel-plates enthalpy exchangers with novel membrane materials. *Journal of Membrane Science*, (325), 672–682.
- Zhang, L.-Z. (2016). A reliability-based optimization of membrane-type total heat exchangers under uncertain design parameters. *Energy*, 101, 390–401.

A detailed investigation of the impact of an innovative dynamic façade system on indoor environmental quality in offices

Magdalena Hajdukiewicz^{*1,2}, Marcel G.L.C. Loomans¹

¹ *Department of the Built Environment
Eindhoven University of Technology
The Netherlands*

² *Construct Innovate
University of Galway
Ireland*

*Corresponding author: m.hajdukiewicz@tue.nl

ABSTRACT

In recent years, naturally ventilated glass façades have become a common feature in the design and retrofit of large-scale non-residential buildings, integrating architectural aesthetics and energy efficiency. These façade systems are complex and multifaceted. Thus, introducing them in buildings poses many challenges from economic, engineering, health and behavioural perspectives that can reduce optimal building performance. Building occupant behaviour and preferences are important contributors to the gap between the predicted and actual building energy performance. With people spending on average 90% of their lives indoors, the impact of indoor environmental quality (IEQ) on health, comfort, wellbeing and productivity of building occupants is vital. The use of engineering simulation, validated with data collected from operating buildings, can enable engineers, architects and facility managers to ensure optimal building design, efficient operation and improved IEQ.

This paper presents the results of a detailed investigation of the impact of an innovative adaptive façade system on IEQ in an office case study. This includes the impact of façade operation on the health, comfort and wellbeing of building occupants. The study focuses on the measurement campaign carried out in an operating office environment in the Atlas building at Eindhoven University of Technology (TU/e). This measurement campaign included physical measurements of thermal comfort and indoor air quality parameters and occupant surveys. The surveys aimed to capture the occupants' perception of the indoor environment and the effects of the dynamic façade operation on their comfort and wellbeing. The paper presents the research objectives, measurement protocol and results of the physical measurements and occupant surveys. In general, there was a good alignment between the surveyed and measured data. Furthermore, a high-resolution measurement network allowed for identification of locations where occupants' comfort may be compromised, such as beside the window where higher air temperatures occurred.

KEYWORDS

Indoor environmental quality; Thermal comfort; Air quality; Dynamic façade; Measurements; Surveys

1 INTRODUCTION

1.1 Overview

Airflow and heat transfer through naturally ventilated glass façades have a significant impact on the comfort of building occupants (La Ferla et al., 2020), which must be considered when designing and operating these systems. Optimisation and control of the façade systems is a complex problem with a multidisciplinary perspective (Bianco et al., 2018). Current approaches to designing and constructing façade systems focus on satisfying the requirements of building codes and standards in terms of structural integrity, energy efficiency and occupant-centric criteria; however, the design rarely results in optimal solutions in practice (Moghtadernejad et al., 2020). Occupant behaviour and preferences are usually not considered during the design and post-occupancy optimisation phases but are important contributors to building energy performance. It has been shown previously (Tabadkani et al., 2021) that manual controls for adaptive building systems can compromise their energy consumption, but lack of individual control could decrease the level of user satisfaction.

Adaptive building façades are façades that can interact with the environment, by reacting to its external parameters (weather and indoor environment) and building occupant behaviour, which includes ventilating for indoor air quality and comfort, insulating when required, or generating energy (Luble, 2018). As part of the previous research, Loonen et al. (2015) provided an overview of concepts and classification strategies for adaptive façades, such as dynamic exterior shading facades, glazing with phase change materials and BIPV double-skin facades. Alkhatib et al. (2021) reviewed four key aspects of current and emerging adaptive façade technologies, such as mechanisms and technologies for heat/mass transfer flows, daylight, electricity and heat generation; façade effectiveness and responsiveness; control algorithms and required sensor information. Furthermore, Attia et al. (2020) focused on future trends for adaptive façades, where occupant comfort and well-being emerged as the most important structural trend in adaptive façade technologies and solutions. This showed market demand for human-centric façade designs, which focus on healthy and comfortable working and living environments.

1.2 Research objectives

Previous research by the authors investigated the topics of indoor environmental quality (IEQ), e.g. (Boegheim et al., 2022; Zuhaib et al., 2018); the need for long-term performance monitoring, e.g. (Hajdukiewicz et al., 2015; Loomans et al., 2020); impact of IEQ on building occupants, e.g. (Brink et al., 2022); and the role of indoor climate control devices, e.g. (Boerstra, 2016). Following that expertise, this research focuses on a short-term, detailed investigation of a dynamic façade's operation and its impact on IEQ in offices and occupants' perception on the indoor environment.

The research presented here is part of the FaceINQ project (European Commission, 2023), which aims to develop new operational strategies and designs for innovative building façade systems that ensure IEQ appropriate to users, limit building related health risks and reduce energy consumption, by merging on-site measurements, qualitative user-feedback and pervasive simulation of indoor environments.

2 METHODOLOGY

2.1 Overview

The paper presents a detailed investigation of an office environment in the Atlas building at Eindhoven University of Technology (TU/e). The investigation included physical measurements of thermal comfort and indoor air quality (IAQ) parameters, and occupant surveys. The surveys aimed to capture the occupants' perception of the indoor environment and the effects of the dynamic façade operation on their comfort and wellbeing.

2.2 Atlas Living Laboratory

The research is demonstrated in the BREEAM certified (BRE, 2023) Atlas building at TU/e campus (Figure 1a). Atlas is a 'living laboratory' designed to allow new, project-specific applications to collect environmental data for academic research leading to industry innovation and reduced energy use. The 2019 retrofit of the building resulted in an 80% reduction in CO₂ emissions and transformed Atlas into the most sustainable educational building in the world (TU/e, 2019). An important aspect of the retrofit was an innovative adaptive glass façade system with parallel openable windows (Figure 1b). The façade was designed to insulate the building from excessive heat gains during the day, naturally ventilate indoor spaces at night with full horizontal opening and use natural ventilation for personal thermal or air quality purposes during daytime. However, while the building met energy efficiency targets, a further investigation of the impact of the façade operation on IEQ is needed, in order to verify and optimise future designs of novel adaptive façades (Hajdukiewicz & van Mierlo, 2023).

Thus, the objectives of the measurement campaign in the Atlas office room were to:

- Investigate IEQ parameters, including indoor thermal comfort and air quality (using CO₂ concentration as a proxy), and air temperature and velocity at window opening/ air supply in an office room throughout the day and night.
- Investigate the effect of window's operation on IEQ.
- Investigate the occupants' perception on the IEQ.
- Investigate the occupants' perception on window operation.
- Align the thermal comfort and air quality measurements with occupant surveys.

This paper focuses on the IEQ investigation in an East-facing office (plan dimensions of 5 m x 6.5 m, 2.6 m height) on the 9th floor of the building, occupied by two people between 14 – 21 April 2023. During the investigation, the occupants were asked to carry out their typical work, in this case mainly computer-based work. The office operated with a mixed mode ventilation, including a mechanical constant air volume (CAV=135 m³/h) supply and natural ventilation through a parallel openable window (1 m x 2.5 m, horizontal opening gap of 125 mm).



Figure 1: a) Atlas building at TU/e, photo by Bart van Overbeeke, (TU/e, 2019).
b) Atlas façade design with parallel openable windows (Arch Daily, 2019).

2.3 Measurement protocol

Several physical sensors measured IEQ in the office between 14 – 21 April 2023, including four thermal comfort poles, five air quality poles, and air velocity/ temperature at window and air supply. All physical measurements were synchronised in time and taken at a minimum of 1-minute time step over a full week. Figure 2a shows the measurement setup in the office.

The thermal comfort poles (Figure 3a) measured (i) dry-bulb air temperature (NTC U-type thermistor) at 0.1 m, 1.1 m and 1.7 m height, (ii) globe temperature (black sphere with NTC U) at 0.9 m height, (iii) relative humidity (RH, Serie EE08) and air temperature (NTC U) at 0.9 m height, (iv) air velocity (SensoAnemo 51XX NSF transducer) at 0.1 m and 1.1 m height. The poles were distributed in the room in the proximity of the desks (Figure 2b) to capture the conditions affecting room occupants. Pole PMV D was located beside the seat of occupant 1 and pole PMV C – beside the seat of occupant 2.

The air quality poles (Figure 3b) measured air temperature, RH and CO₂ concentration (Vaisala HMP1 and GMP252) at 1.1 m and 1.7 m height and were regularly distributed around the perimeter of the room (Figure 2b) to capture changes in the IAQ throughout the measurement period. Six NTC thermistors and six ultrasonic anemometers (Gill WindSonic) were regularly distributed around the window opening to capture parameters of the airflow through the window gap (Figure 3c). One NTC thermistor and one air velocity (SS20.250) sensor were installed at the mechanical air supply (Figure 3d). The accuracy of sensors is shown in Table 2.1. Outdoor

weather conditions, measured by the weather station located on the roof of the Atlas building, included air temperature, wind speed and direction and solar irradiance.

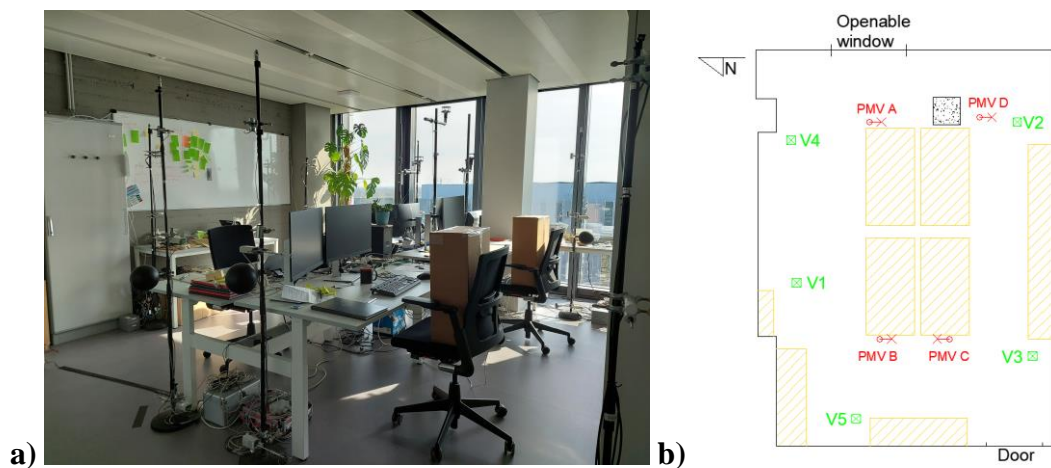


Figure 2: a) The investigated office room with the measurement equipment. b) Location of thermal comfort (PMV, red) and air quality (V, green) poles.

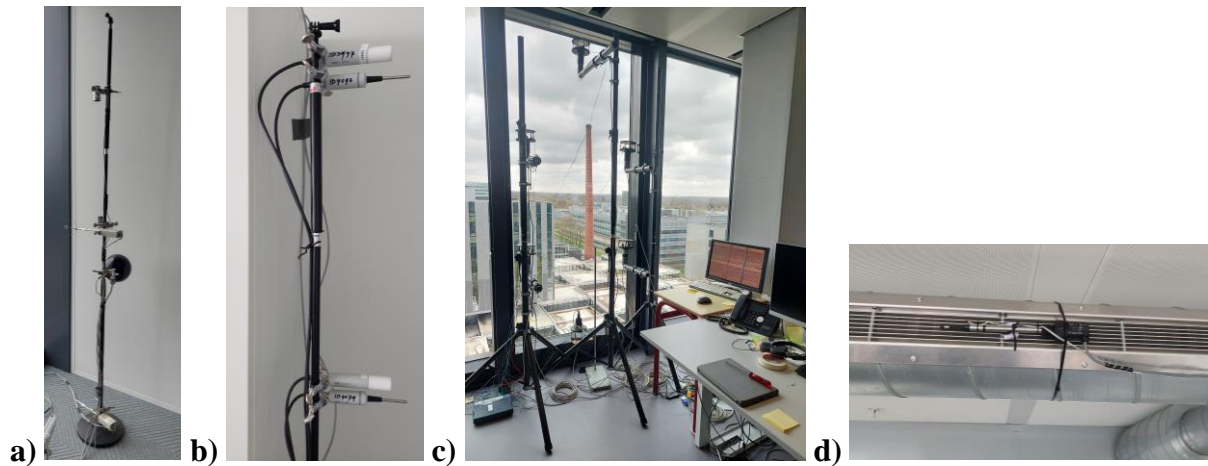


Figure 3: Measurement equipment: a) thermal comfort pole, b) air quality pole, c) window sensors and d) air supply sensors.

Table 2.1: Type and accuracy of sensors used for indoor measurements.

Sensor	Accuracy
NTC U-type thermistor	$\pm 0.05 \text{ }^\circ\text{C}$ (0-50 $^\circ\text{C}$)
Serie EE08	$\pm 2.0 \text{ \%RH}$ (0-90%, at 23 $^\circ\text{C}$)
SensoAnemo 51XX NSF transducer	$0.02 \text{ m/s} \pm 1.5\%$ of readings (in range 0.05 - 5 m/s)
Vaisala HMP1	$\pm 0.2 \text{ }^\circ\text{C}$ (at 23 $^\circ\text{C}$)
	$\pm 1.0 \text{ \%RH}$ (0-90%, at 23 $^\circ\text{C}$)
Vaisala GMP252	$\pm 40 \text{ ppmCO}_2$ (at 25 $^\circ\text{C}$ and 1013 hPa)
Gill WindSonic	$\pm 2\%$ (measured at 12 m/s, range 0-60 m/s, resolution 0.01 m/s)
SS20.250	$\pm 5\%$ of measured value + (0.4 % of final value; min. range 0.02 m/s)

2.4 Occupant surveys

The online occupant surveys were completed by two office occupants twice daily (morning at $\sim 11\text{am}$ and afternoon at $\sim 3\text{pm}$) over six days (between 14 – 21 April 2023). The surveys included questions on occupants' perceived comfort, IAQ and health symptoms. The goal was

to understand how (local) IEQ conditions are perceived when changes occur (e.g. due to window opening) and quantify those conditions through measurements.

3 RESULTS

3.1 Physical measurements

In order to analyse the indoor environmental conditions during a typical working day (occupants controlling window opening), this section presents results of the measurements taken during the working hours (9am – 6pm) of 21st April 2023. The mean outdoor air temperature during the period monitored was 13.3°C. The air supplied to the room via a mechanical system (CAV) was at a mean temperature of 21°C and velocity of 1.2 m/s (measured at the air supply grill). The building management system (BMS) setpoint for air temperature was 22°C.

Figure 4 shows the distribution of indoor air temperatures measured by the thermal comfort poles (PMV). The data clearly shows the highest variability in air temperatures measured by the pole PMV A, located closest to the window opening; followed by pole PMV D, also beside the window (Table 3.1). Those two poles indicated the highest globe temperatures in the morning, as influenced by the solar irradiance (window facing East). Air temperatures measured by the poles closer to the door (PMV B & C) showed a very similar and less variable (than PMV A & D) pattern. The maximum vertical temperature difference between head and ankles at locations of PMV B, C & D over the period monitored was 1.1°C, 0.7°C and 1.7°C, respectively; thus, less than 2°C, which was not the cause for local discomfort (ISO, 2005). At location PMV A, at 10% of the time (between 9-6pm), the vertical temperature difference between head and ankle level was between 2°C and 3.3°C. Those higher temperature differences occurred when the window was open and were caused by the cool outside air entering the warm room at the floor level. This might have caused local discomfort if an occupant was located near the open window.

According to (ISSO, 2014), the normal level of thermal comfort expectation (class B – max 10% predicted percentage of dissatisfied (PPD)) during intermediary seasons requires indoor operative temperature between 20.0°C - 24.0°C (based on calculated running mean outdoor temperature of 9.8°C, as per weather data). The operative temperature in the room during the period monitored (mean at all PMV poles locations, calculated according to (ISO, 1998)) was 23.0°C, which aligns with the thermal comfort expectation outlined in ISSO, the Dutch Building Services Research Institute (ISSO, 2014).

The mean RH measured by the thermal comfort and air quality poles was 37% and 32%, respectively. The mean CO₂ concentration measured in the room was 448 ppm.

Table 3.2 shows the mean air velocities measured at the ankle and sitting person's head level and their associated turbulence intensities ($Tu = u_n'/u_n * 100\%$) and draught rates (DR). As expected, the highest air velocities (Tu and DR) were recorded beside the open window (PMV A), where also the data had the largest spread. According to (ISO, 2005), the turbulence intensity may vary between 30 - 60 % in spaces with mixed-flow air distribution, which is seen from the periods of open window. When the window was closed, the turbulence intensities were lower, except the first period (9-10.35am) at PMV B & C, which may correspond to occupants activity in the centre of the room. At locations of PMV B, C & D, the majority of draught rates were below 10%, which is equivalent to 6% PPD. AT PMV A, the draught rates were significantly higher, particularly at the ankle level when the window was open (DR of 24% in the morning and 50% in the afternoon), which might have caused discomfort if an occupant was located there.

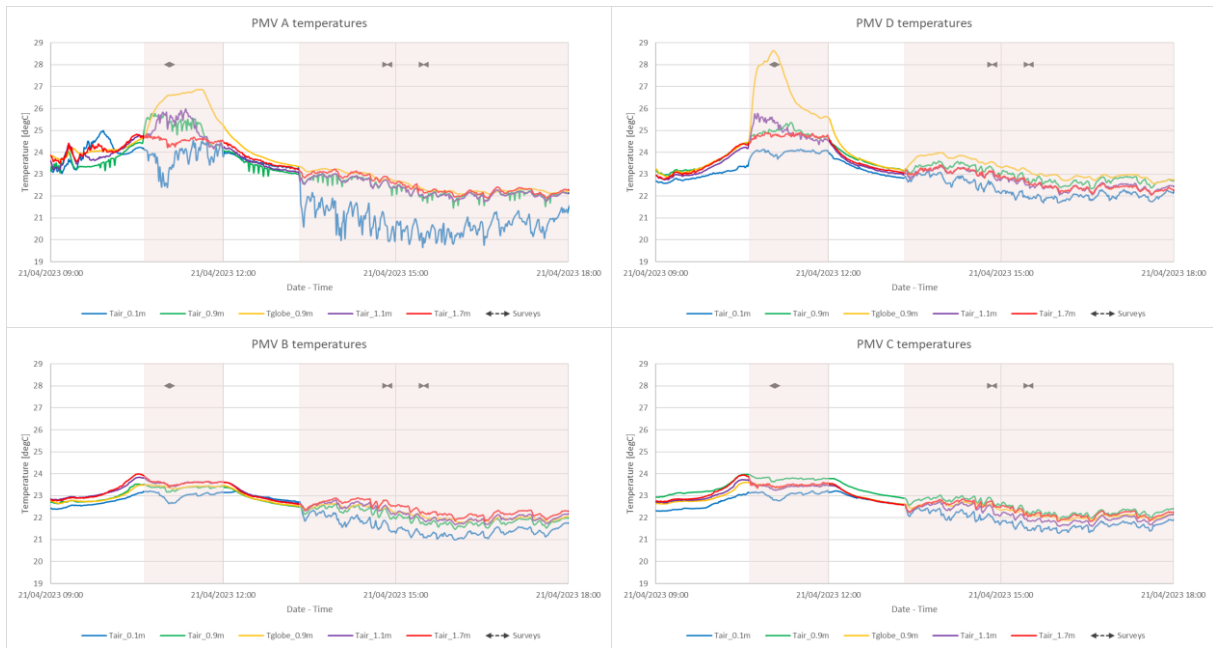


Figure 4: Indoor air temperatures measured by the thermal comfort poles (PMV); shaded orange area indicates the time of the window being open.

Table 3.1: Mean and standard deviation of indoor air temperatures (in °C) measured between 9am-6pm on 21 April 2023.

		Tair_0.1m	Tair_0.9m	Tglobe_0.9m	Tair_1.1m	Tair_1.7m
PMV A	MEAN	22.23	23.15	23.60	23.21	23.28
	ST DEV	1.59	1.09	1.38	1.11	0.92
PMV B	MEAN	22.18	22.50	22.58	22.68	22.79
	ST DEV	0.74	0.61	0.54	0.63	0.56
PMV C	MEAN	22.30	22.93	22.67	22.59	22.73
	ST DEV	0.59	0.59	0.52	0.60	0.54
PMV D	MEAN	22.79	23.44	23.89	23.25	23.26
	ST DEV	0.72	0.77	1.41	0.89	0.83

Table 3.2: Mean indoor air velocities (in m/s) measured between 9am - 6pm on 21 April 2023 and associated turbulence intensities (Tu in %) and draught rates (DR in %).

		PMV A		PMV B		PMV C		PMV D	
		V_0.1m	V_1.1m	V_0.1m	V_1.1m	V_0.1m	V_1.1m	V_0.1m	V_1.1m
Window closed (9:00-10:35)	MEAN	0.07	0.15	0.08	0.08	0.09	0.08	0.08	0.08
	Tu	16	34	56	38	60	37	28	23
	DR	3	13	6	6	8	6	5	4
Window open (10:36-12:00)	MEAN	0.17	0.16	0.09	0.09	0.08	0.08	0.11	0.10
	Tu	74	41	56	36	32	27	31	28
	DR	24	15	8	7	5	5	9	7
Window closed (12:01-1:19)	MEAN	0.10	0.10	0.06	0.09	0.08	0.07	0.10	0.08
	Tu	21	40	18	22	24	21	23	26
	DR	7	8	3	6	5	4	7	4
Window open (1:20-6:00)	MEAN	0.30	0.20	0.14	0.09	0.08	0.08	0.09	0.09
	Tu	64	34	59	29	32	43	33	28
	DR	50	19	16	6	5	6	6	6

*the measurement range was 0.05-5 m/s, thus values <0.05 m/s were assumed as =0.05 m/s

3.2 Occupant surveys

The physical measurements were broadly represented by the survey responses of two office occupants. Both surveys were taken while the window was open (Figure 4). In general, the occupants felt comfortable throughout the day and stated that they preferred the window being open. The occupants reported they did not feel any local discomfort, including thermal or draught sensation. However, as reported in the morning, the occupant 1 (located beside PMV D) felt slightly warm. This might have been due to the high air temperatures recorded at this location (mean value measured at ankle and head level of 24.6°C), including high radiant temperature (28.5°C), and relatively low air velocities of 0.1 m/s (mean at ankle and head level). In the afternoon, with decreased air temperatures (mean air temperature measured at ankle and head level of 22.2°C, and radiant temperature of 23.1°C), the occupant 1 felt neutral. Occupant 1 felt ‘neither sleepy nor alert’ in the morning and very alert in the afternoon.

Occupant 2 (located beside PMV C) also felt slightly warm in the morning (mean measured air temperature of 23.2°C and air velocity of 0.05 m/s at ankle and head level) and neutral in the afternoon (mean measured air temperature of 22.2°C and air velocity of 0.05 m/s at ankle and head level). After feeling alert in the morning, occupant 2 had some signs of sleepiness in the afternoon. Occupant 2 was satisfied with the quality of indoor air, and reported fresh air, well-ventilated room, with pleasant smell throughout the day. While occupant 1, in the morning ‘slightly agreed’ and in the afternoon ‘agreed’ that the indoor air was fresh, not stale and the room was properly ventilated.

Table 3.3 compares the surveyed and measured (and calculated based on (ISO, 2005)) predicted mean vote (PMV) values for both occupants. The authors acknowledge that the PMV is an index that predicts the mean value of the votes of a large group of persons and in such complex environments using PMV as an assessment may not be useful. However, here it is only used as an example in this specific case of an office. Table 3.3 shows a good alignment between the surveyed and measured/calculated data in the afternoon for both occupants and for occupant 1 in the morning. However, there is a small discrepancy in the data for occupant 2 in the morning, where surveyed response was ‘slightly warm’ environment and measured – rather neutral. This discrepancy might have been due to the activity of the occupant prior to taking the survey, which might have increased the occupant’s metabolic rate. Furthermore, for those investigated conditions when the window was open the measured/calculated PMV values were underestimated (on the cooler side) when compared to the surveyed values. This may result in less optimal thermal comfort conditions in reality, but still appreciated by the occupants.

The survey data for days when occupants did not have control over opening and closing the window (17 – 20 April 2023) showed that only on two occasions (2 out of 8 survey responses) the occupants felt neutral. Only half of the time the occupants felt comfortable (2 survey responses when the window was open and 2 responses when closed), with other perceptions reported as slightly uncomfortable (2 responses when the window was closed and 1 when it was open) and uncomfortable (1 response when the window was open). Further analysis is required to analyse the measured data for those dates and to understand how (local) IEQ conditions are perceived when changes occur. However, this is not the scope of this paper.

Table 3.3: Surveyed and measured PMV values.

	Occupant 1		Occupant 2	
	Survey	Measured (ISO, 2005)	Survey	Measured (ISO, 2005)
Morning survey	1	0.7	1	-0.1
Afternoon survey	0	-0.3	0	-0.4

4 CONCLUSIONS

This paper presents the research objectives, measurement protocol and the initial results of the IEQ investigation in an office room. This case study, focusing on one day results, will be replicated to analyse more extreme conditions in IEQ when the occupants are not controlling the window opening. This will allow for a point-in-time characterisation of Atlas adaptive façade operation and its impact on the occupants' perception and their comfort and wellbeing.

Furthermore, the measured parameters will provide boundary conditions and validation data to develop reliable computational fluid dynamics (CFD) models that capture the airflow and heat transfer through this novel façade system. This will be done to investigate whether the indoor environmental conditions support thermal comfort and air quality for building occupants, and to optimise future designs of novel adaptive façade systems. Previous studies utilised measurements and CFD simulations to investigate the performance of the Atlas' façade system (Hetebrij, 2021; Verbruggen, 2019). Thus, the FaceINQ project builds on those research findings.

5 ACKNOWLEDGEMENTS

The authors would like to acknowledge the financial support of the European Commission Horizon MSCA 2021 FaceINQ project (101066362). The authors would like to thank the technical staff in the Department of the Built Environment at Eindhoven University of Technology for their support in carrying out the experiments, as well as the occupants of the Atlas Living Lab for their participation in this research.

6 REFERENCES

- Alkhatib, H., Lemarchand, P., Norton, B., & O'Sullivan, D. T. J. (2021). Deployment and control of adaptive building facades for energy generation, thermal insulation, ventilation and daylighting: A review. *Applied Thermal Engineering*, 185, 116331. <https://doi.org/10.1016/j.applthermaleng.2020.116331>
- Arch Daily. (2019). *Atlas - Eindhoven University of Technology / Team V Architecture*. https://www.archdaily.com/914644/Atlas-Eindhoven-University-of-Technology-the-Netherlands-Team-v-Architecture?Ad_medium=gallery.
- Attia, S., Lioure, R., & Declaude, Q. (2020). Future trends and main concepts of adaptive facade systems. *Energy Science & Engineering*, 8(9), 3255–3272. <https://doi.org/10.1002/ese3.725>
- Bianco, L., Cascone, Y., Avesani, S., Vullo, P., Bejat, T., Koenders, S., Loonen, R. C., Goia, F., Serra, V., & Favoino, F. (2018). Towards New Metrics for the Characterisation of the Dynamic Performance of Adaptive Façade Systems. *Journal of Facade Design and Engineering*, 6(3), 175–196.
- Boegheim, B., Appel-Meulenbroek, R., Yang, D., & Loomans, M. (2022). Indoor environmental quality (IEQ) in the home workplace in relation to mental well-being. *Facilities*, 40(15/16), 125–140. <https://doi.org/10.1108/F-05-2022-0070>
- Boerstra, A. C. (2016). *Personal control over indoor climate in offices: impact on comfort, health and productivity*. [PhD]. Eindhoven University of Technology (TU/e).
- BRE. (2023). *BREEAM*. <https://www.breeam.com/> .
- Brink, H. W., Loomans, M. G. L. C., Mobach, M. P., & Kort, H. S. M. (2022). A systematic approach to quantify the influence of indoor environmental parameters on students' perceptions, responses, and short-term academic performance. *Indoor Air*, 32(10). <https://doi.org/10.1111/ina.13116>

- European Commission. (2023). *Innovative dynamic Façade systems for INdoor environmental Quality*. <https://cordis.europa.eu/Project/Id/101066362>.
- Hajdukiewicz, M., Byrne, D., Keane, M. M., & Goggins, J. (2015). Real-time monitoring framework to investigate the environmental and structural building performance. *Building and Environment*, 86, 1–16. <https://doi.org/10.1016/j.buildenv.2014.12.012>
- Hajdukiewicz, M., & van Mierlo, P. (2023). Discussion on the design of the façade system in the Atlas building. In *Private conversation*.
- Hetebrij, R. F. (2021). *CFD analysis of the night cooling capabilities of parallel openable windows including assessment of CFD modeling methodology: case study TU/e building “Atlas”* [Master]. Eindhoven University of Technology (TU/e).
- ISO. (1998). *Ergonomics of the thermal environment — Instruments for measuring physical quantities* (ISO 7726:1998).
- ISO. (2005). *Ergonomics of the thermal environment — Analytical determination and interpretation of thermal comfort using calculation of the PMV and PPD indices and local thermal comfort criteria* (ISO 7730:2005).
- ISSO. (2014). *ISSO publicatie 74. Thermische behaaglijkheid [ISSO Publication 74. Thermal Comfort]*.
- La Ferla, G., Acha Román, C. A., & Roset Calzada, J. (2020). Radiant glass façade technology: Thermal and comfort performance based on experimental monitoring of outdoor test cells. *Building and Environment*, 182, 107075. <https://doi.org/10.1016/j.buildenv.2020.107075>
- Loomans, M. G. L. C., Mishra, A. K., & Kooi, L. (2020). Long-term monitoring for indoor climate assessment – The association between objective and subjective data. *Building and Environment*, 179, 106978. <https://doi.org/10.1016/j.buildenv.2020.106978>
- Loonen, R. C. G. M., Rico-Martinez, J. M., Favoino, F., Brzezicki, M., Menezo, C., La Ferla, G., & Aelenei, L. (2015). Design for façade adaptability: Towards a unified and systematic characterization. *10th Conference on Advanced Building Skins*, 1284–1294.
- Luiblé, A. (2018). Editorial. Special Issue FAÇADE 2018 – Adaptive! *Journal of Facade Design and Engineering*, 6(3).
- Moghtadernejad, S., Chouinard, L. E., & Mirza, M. S. (2020). Design strategies using multi-criteria decision-making tools to enhance the performance of building façades. *Journal of Building Engineering*, 30, 101274. <https://doi.org/10.1016/j.jobee.2020.101274>
- Tabadkani, A., Roetzel, A., Li, H. X., & Tsangrassoulis, A. (2021). A review of occupant-centric control strategies for adaptive facades. *Automation in Construction*, 122, 103464. <https://doi.org/10.1016/j.autcon.2020.103464>
- TU/e. (2019, April 16). *BREEAM hails Atlas the world’s most sustainable education building*. <https://www.tue.nl/En/News/News-Overview/15-04-2019-Breeam-Hails-Atlas-the-Worlds-Most-Sustainable-Education-Building>.
- Verbruggen, M. (2019). *Design of a smart ventilation control strategy for Atlas* [EngD]. Eindhoven University of Technology (TU/e).
- Zuhaib, S., Manton, R., Griffin, C., Hajdukiewicz, M., Keane, M. M., & Goggins, J. (2018). An Indoor Environmental Quality (IEQ) assessment of a partially-retrofitted university building. *Building and Environment*, 139. <https://doi.org/10.1016/j.buildenv.2018.05.001>

A methodology for evaluating the ventilative cooling potential in early-stage building design

Valentina Radice Fossati*¹, Annamaria Belleri¹, Dick van Dijk²

*1 Eurac Research
Druso 1*

Bolzano, Italy

**Corresponding author:*

valentina.radicefossati@eurac.edu

2 EPB Center

Weena 505

Rotterdam, Netherlands

ABSTRACT

As a result of the new initiatives and regulations towards nearly zero energy buildings, designers are more frequently exploiting the cooling potential of the climate to reduce overheating and improve indoor well-being of people. At early stage of design, climate analysis is particularly useful for determining the most cost-effective passive cooling methods, such as ventilative cooling. However, besides the external climate conditions, building energy uses are characterized by occupancy pattern and needs, envelope characteristics and internal loads. Therefore, the climate analysis cannot be abstracted from building characteristics and use.

Within the IEA Annex 62 project, national experts worked on the development of a ventilative cooling potential tool, which aimed at assessing the potential of ventilative cooling by considering building envelope thermo-physical properties, internal gains and ventilation needs. The calculation methodology has been further developed within CEN/TC 156/WG21 TG on “Ventilative cooling systems - Design”. The main development regards the application of thermal balance calculation method from EN ISO 52016-1:2017 to calculate free-floating temperature, heating and cooling loads with and without ventilative cooling contribution, which considers also lumped thermal capacity.

The analysis is based on a single-zone thermal model applied to user-input climatic data on hourly basis. The tool predicts the percentage of hours when direct ventilation with minimum airflow rate required for indoor air quality or increased airflow rates can potentially ensure indoor thermal comfort.

Moreover, such methodology could provide building designers useful information about the level of ventilation rates needed to maintain acceptable indoor thermal comfort conditions.

The paper aims at presenting the new calculation methodology and at validating the calculation results on a reference room according to the guidelines reported in the ASHRAE Standard 140-2020.

In particular, the influence of using dynamic loads, adaptive thermal comfort model, building thermal mass and ventilation needs in the thermal balance calculation of the building are analysed. Despite the methodology is simplified, the overall goal is to provide engineers a tool for predicting in preliminary design phase and with a limited degree of uncertainty whether the building can exploit ventilative cooling to maintain indoor comfort conditions.

KEYWORDS

Ventilative cooling, early-stage design, overheating, design airflow rate, natural ventilation

1 INTRODUCTION

Climate change, economic growth, affordability of air conditioners and other increasing demographic factors (population growth, ageing and urbanization) are the main causes for the space cooling to grow faster than any other energy use in buildings (International Energy Agency, 2018). Furthermore, high energy performance standards to reduce heating demand led to high insulated and airtight buildings which can encounter overheating issues especially in heating dominated climatic regions, where there is no tradition of using external solar shadings and no cultural knowledge on how to operate them (Taylor et al., 2023). The growth of space

cooling need is not only causing an overall increase of energy demand but also of peak power, putting the electricity grid under pressure (International Energy Agency, 2018).

Ventilative cooling, meant as the use of natural or mechanical ventilation to cool indoor spaces, is considered an effective solution to reduce space cooling need in buildings and might be even a key solution to reach zero emission targets. Since it depends on the availability of suitable outdoor air conditions, climate analysis is particularly useful to support early-stage decision making on building design. However, besides the external climate conditions, space cooling uses are also characterized by solar gains control, occupancy patterns and comfort expectations, as well as by envelope characteristics and internal loads. Therefore, the climate analysis cannot be abstracted from building characteristics and use.

To this purpose, national experts worked on the development of a ventilative cooling evaluation tool within the IEA Annex 62 project (Belleri et al., 2018).

The calculation methodology has been further improved within CEN/TC 156/WG21 TG on “Ventilative cooling systems - Design”. The main improvement regards the application of thermal balance calculation method from EN ISO 52016-1:2017 to calculate free-floating temperature, heating and cooling loads with and without ventilative cooling contribution and which considers also lumped thermal capacity.

The aim of this paper is to outline the new calculation method to assess ventilative cooling potential in a preliminary design phase and its validation process.

2 METHODOLOGY FOR EVALUATING VENTILATIVE COOLING POTENTIAL (VC)

The calculation method to evaluate ventilative cooling potential is based on a single-zone thermal model applied to user-input climatic data on an hourly basis. The thermal balance calculation method from EN ISO 52016-1:2017 is applied to calculate free-floating temperature and heating and cooling loads (with and without ventilative cooling contribution) of a reference thermal zone of the building.

EN ISO 52016-1:2017 has been developed to assess the energy performance of a detailed building design or building in use. For early design phase applications, the detailed hourly thermal balance equations have been reduced to the essential (lumped) parameters, including also lumped thermal capacity. Figure 1 shows the simple 1RC model selected as the most suited model for such early design phase.

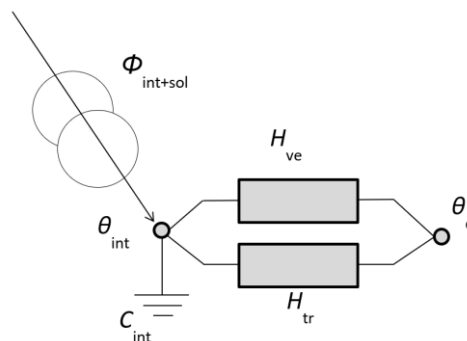


Figure 1: Simple 1RC lumped parameter model suited for the early design stage.

The previous ventilative cooling potential tool was presented by Belleri et al. (Belleri et al., 2018) and referred to the method proposed by NIST (Axley et al., 2002; Emmerich et al., 2011). Direct ventilation was considered useful to maintain indoor conditions when outdoor dry bulb temperature exceeded the heating balance point temperature. The latter parameter refers to the outdoor air temperature below which heating must be provided to maintain comfort condition within the thermal zone. However, thermal capacity of the building was not taken into account in this previous tool.

2.1 Input

The calculation requires basic information about a typical room of the building and an annual record of climatic data on hourly time resolution. The climatic data shall include outdoor dry bulb temperature, relative humidity and solar radiation.

The input data related to the building are needed to calculate the solar and internal gains, the thermal capacity of the building structure, the ventilation and transmission losses. These are calculated based on the geometry data of the reference room and window area/orientation, building use, comfort requirements and thermal properties of the envelope, as well as the presence of external shading elements.

Internal gains can be pre-calculated according to standard load profiles of occupancy, lighting and electric equipment (EN 16798-1:2019), or defined based on design needs. Furthermore, the occupant presence within the thermal zone can be indicated through the time control section.

Comfort temperatures are calculated according to the adaptive comfort model (EN 16798-1:2019). The overall heat transfer coefficient by transmission through the opaque and transparent envelope and the internal heat capacity of the zone are calculated according to EN ISO 52016-1:2017. The internal thermal capacity of the entire thermal zone corresponds to the sum of the thermal masses due to building envelope, internal partitions, air and furniture.

2.2 Thermal balance calculations

The following variables are used, with symbols and subscripts, where applicable, partially adopted from EN ISO 52016-1:2017 or specifically added to work out the methodology:

H_{tr}	= overall heat transfer coefficient by transmission (W/K);
$q_{V;t}$	= airflow rate at time interval t (m^3/s);
$\rho_a \cdot c_a$	= heat capacity of air per volume ($J/(m^3K) = 1.204 \times 1\,006$);
$H_{ve;t}$	= overall heat exchange coefficient by ventilation at time interval t (W/K);
$\theta_{int;t}$	= internal air or operative temperature at time interval t ($^{\circ}C$); NOTE: For the IRC model there is no distinction between air and operative temperature.
$\theta_{int;0;t}$	= internal air or operative temperature in free float at time interval t ($^{\circ}C$);
$\theta_{int;t-1}$	= internal air or operative temperature at previous time interval ($t-\Delta t$) ($^{\circ}C$);
$\theta_{int;set;H;t}$	= internal operative temperature setpoint for heating at time interval t ($^{\circ}C$); NOTE: Setpoint can vary in time, e.g. if the adaptive comfort model is applicable.
$\theta_{int;set;C;t}$	= internal operative temperature setpoint for cooling at time interval t ($^{\circ}C$); NOTE: Setpoint can vary in time, e.g. if the adaptive comfort model is applicable.
$\theta_{e;a;t}$	= external air temperature at time interval t ($^{\circ}C$);
$\Phi_{int;t}$	= total internal heat gain at time interval t (W);
$\Phi_{sol;t}$	= total solar heat gain at time interval t (W); NOTE: In EN ISO 52016-1:2017 the solar gains are split into direct (into the zone, through the windows) and indirect (absorbed in external constructions); for the VCP tool it is just the total. The effect of movable solar shading provisions can be taken into account on an hourly basis.
$\Phi_{HC;t}$	= heating load (if positive) or cooling load (if negative) at time interval t (W);
C_{int}	= (lumped) internal thermal capacity (J/K); NOTE: For VCP tool this is the simplified lumped capacity, covering internal capacity in the building and weighted capacity of the constructions.
Δt	= length of the time interval t (s, in casu: 3600 s);
$q_{V;min}$	= required airflow rate for hygienic ventilation (m^3/s);
$q_{m;t}$	= air mass flow rate (kg/s);

ACH_t	= volumetric air change per hour (1/h);
$q_{V;VCS;req;t}$	= required airflow rate for ventilative cooling (m ³ /s);
$\Delta\theta_{crit}$	= minimum temperature difference between indoor and outdoor temperature in order to drive natural airflow and/or to have a more than negligible cooling potential (K, i.e. 3K);
$\Phi_{HU;e;a;t}$	= relative humidity of outdoor air (%); NOTE: EN ISO 52016-1:2017 uses absolute humidity as input variable.
$\Phi_{HU;max}$	= maximum relative humidity of outdoor air for ventilative cooling (%) (e.g. 85%);
$\theta_{int;comfort;t}$	= indoor comfort temperature according to adaptive comfort model of EN 16798-1:2019 (°C).

At each timestep (*in casu* 1 hour) the heat balance of the thermal zone according to the 1RC model can be formulated as follows:

$$\left[\frac{C_{int}}{\Delta t} + H_{ve} + H_{tr} \right] \theta_{int;t} = \frac{C_{int}}{\Delta t} \cdot \theta_{int;t-1} + [H_{ve} + H_{tr}] \cdot \theta_{e;a;t} + \Phi_{int;t} + \Phi_{sol;t} + \Phi_{HC;t} \quad (1)$$

Since the unknown terms are either the node air temperature or the heating/cooling loads, the equation can be rewritten as follows, with A and B known at each time interval t .

$$A_t \theta_{int;t} = B_t + \Phi_{HC;t} \quad (2)$$

Starting from the heat balance, the potential of ventilative cooling is assessed carrying out the following steps for each time interval. The time series are first calculated in free float temperature and without the effect of ventilative cooling to have a basic case that can serve for validation purposes. The same time series are then computed considering the influence of heating and cooling needs. Ventilative cooling potential is still not evaluated. In the early design stage, the goal is just to estimate the amount of heating and cooling loads that needs to be satisfied at each hour, therefore there is no upper limit to the heating or cooling capacity. Consequently, this implies that the indoor temperature will never drop below the lower setpoint or exceed above the higher setpoint for a given interval value. In case of intermittent heating, the temperature is allowed to drop to a lower limit during intermittency. The third and last step involves the calculation of time series with heating/cooling loads and ventilative cooling potential. The goal is to reveal the ventilative cooling potential making a comparison with the second step. A one-month initialization period to avoid the influence of assumed indoor temperature at the start of the calculation has been adopted from EN ISO 52016-1:2017.

2.3 Evaluation criteria

For each hour of annual climatic record of the given location, the energy balance is calculated according to the model described previously and an algorithm splits the total number of hours when the building is occupied in the following groups:

1. **VC-mode [0]:** ventilative cooling is not required when the indoor temperature is below the lower comfort zone limit (heating is needed);

If $\theta_{int;0;t} < \theta_{int;set;H;t}$
then $q_{V;t} = q_{V;min}$ (with heat recovery)

In this mode $q_{V;t}$ is not counted as part of the ventilative cooling potential.

2. **VC-mode [1]:** direct ventilative cooling with airflow rate maintained at the minimum required for IAQ can potentially ensure comfort when the outdoor temperature is within comfort ranges;

If $\theta_{int;set;H;t} \leq \theta_{int;0;t} \leq \theta_{int;set;C;t}$
then $q_{V;t} = q_{V;min}$ (no heat recovery needed)

Unlike the previous case, $q_{V;t}$ is counted as part of the ventilative cooling potential.

3. **VC-mode [2]:** direct ventilative cooling with increased airflow rate can potentially ensure thermal comfort and indoor air quality in the air node;

If $\theta_{int;0;t} > \theta_{int;set;C;t}$, $\theta_{e;a;t} \leq (\theta_{int;set;C;t} - \Delta\theta_{crit})$ and $\Phi_{HU;e;a;t} < \Phi_{HU;max}$
then $q_{V;t} = q_{V;VCS}$

Obviously, in this case, $q_{V;t}$ is counted as part of ventilative cooling potential.

4. **VC-mode [3]:** residual discomfort hours in which ventilative cooling cannot provide benefits.

$$q_{V;t} = q_{V;min}$$

2.4 Ventilation rate assessment

The required extra ventilation rate needed to supply ventilative cooling can be assessed assuming that all cooling power is provided by extra ventilation. Then cooling loads are assumed to be null.

At each time interval, if VC mode = [2]:

$$(A_t + \Delta H_{ve;VCS;req;t})\theta_{int;t} = B_t + \Delta H_{ve;VCS;req;t} \cdot \theta_{e;a;t} \quad (3)$$

As a consequence,

$$\Delta H_{ve;VCS;req;t} = \frac{B_t - A_t \theta_{int;t}}{\theta_{int;t} - \theta_{e;a;t}} \quad (4)$$

The internal temperature $\theta_{int;t}$ of the previous equation corresponds to the cooling setpoint. Then, the required extra ventilation for ventilative cooling is equal to:

$$\Delta q_{V;VCS;req;t} = \frac{B_t - A_t \theta_{int;set;C;t}}{\rho_a c_a (\theta_{int;set;C;t} - \theta_{e;a;t})} \quad (5)$$

with $\theta_{int;t} = \theta_{int;set;C;t}$

The ventilation rate needed to provide ventilative cooling is given by the sum of the minimum required ventilation rates and the extra ventilation required.

$$q_{V;VCS;t} = q_{V;min} + \Delta q_{V;VCS;req;t} \quad (6)$$

Once the actual ventilation rate has been calculated according to VC-mode, heating or cooling loads and the internal temperature are calculated again, before moving to the next time step.

2.5 Output

The performance indicators calculated through the ventilative cooling potential methodology described in the previous sections are outlined below.

1. Percentage of time within each month when:
 - Ventilative cooling is not required (VC-mode [0]) according to the evaluation criteria described in section 2.3;
 - Direct ventilative cooling with airflow rate maintained at the minimum required (VC-mode [1]) according to the evaluation criteria described in section 2.3;
 - Direct ventilative cooling with increased airflow rate required (VC-mode [2]) according to the evaluation criteria described in section 2.3;

- Direct ventilative cooling is not useful (VC-mode [3]) according to the evaluation criteria described in section 2.3;
- 2. Required ventilation rates to cool down the building when direct ventilative cooling with increased airflow rate is required (VC mode [2]);
- 3. Monthly and annual sensible energy needs of heating and cooling with and without ventilative cooling;
- 4. Ventilative cooling capacity.

The just mentioned outputs are useful to compare the ventilative cooling potential in different climatic conditions for different building typologies and thermal masses. From design point of view, those output provide a rough estimation in early-stage design of the airflow rates needed to cool down passively the building in relation to the input provided initially, such as internal gains, comfort requirements and envelope characteristics. Statistics about extra ventilation rates needed are useful to define design ventilation rates for ventilative cooling.

3 VALIDATION

The calculation methodology has been validated according to the guidelines provided by ASHRAE Standard 140-2020 and reported in EN ISO 52016-1:2017. Two test cases (BESTEST) referring to a geometry consisting of a single thermal zone with two different types of envelopes (heavyweight and lightweight) were analyzed in the climate of Denver, USA. The test room is 8 x 6 x 2.7 m with two windows (3 x 2 m each) on South façade. All the characteristics of the reference room, such as thermophysical properties of the opaque and transparent envelope, specific heat capacity of air and furniture, boundary conditions, internal gains, ventilation and thermostat control strategies are given in detail in EN ISO 52016-1:2017. BESTEST 940 and 640 are the case identifiers present in EN ISO 52016-1:2017 to describe the heavyweight and lightweight cases respectively combined with intermittent setpoint.

All the input provided to the model are summarized in the Annex (Table 2).

The proposed methodology is validated if the calculated outputs are consistent with the BESTESTs' results reported in EN ISO 52016-1:2017. The outputs considered for validation are:

- Monthly and annual sensible energy needs for heating $\Phi_{H,nd}$ and cooling $\Phi_{C,nd}$;
- Monthly average values of the operative temperature $\theta_{op,av}$.

Regarding the BESTEST 940 and 640 reference cases, the ASHRAE Standard 140-2020 does not provide the maximum error beyond which results should not be considered reliable. On the contrary, the standard only indicates that data trends and orders of magnitude should be respected. Regardless of this, to have an accurate idea about the tool uncertainty with respect to the BESTESTs' results, taking as reference the ASHRAE Guideline 14 (ASHRAE, 2014), the Coefficient of Variation of the Root Mean Square Error (CV(RMSE)) was calculated for each output. According to ASHRAE Guideline 14, the maximum monthly acceptable calibration tolerance is equal to 15%. Generally, this error is used to calibrate and validate dynamic simulation software: since the tested methodology refers to early-stage design phase, it is plausible that the abovementioned threshold is not always respected.

3.1 Results

This section illustrates the results of the validation. The graphs in Figure 2 **Error! Reference source not found.** show the monthly sensible energy needs for heating and cooling and the monthly operative temperatures registered analysing both reference cases. The results of ISO 52016-1:2017 are directly compared with the ventilative cooling potential methodology outputs (VCT). The effect of ventilative cooling is not taken into account during the validation process. The comparison of results allows to validate the methodology output as well as to analyse the effect of thermal mass on output results. The methodology tends to overestimate the results during the winter months, in which the need of ventilative cooling potential is less crucial. On

the contrary, a good prediction of monthly cooling loads occurs during the summer period. The comparison of the results can be also seen in the Annex (Table 3 and Table 4).

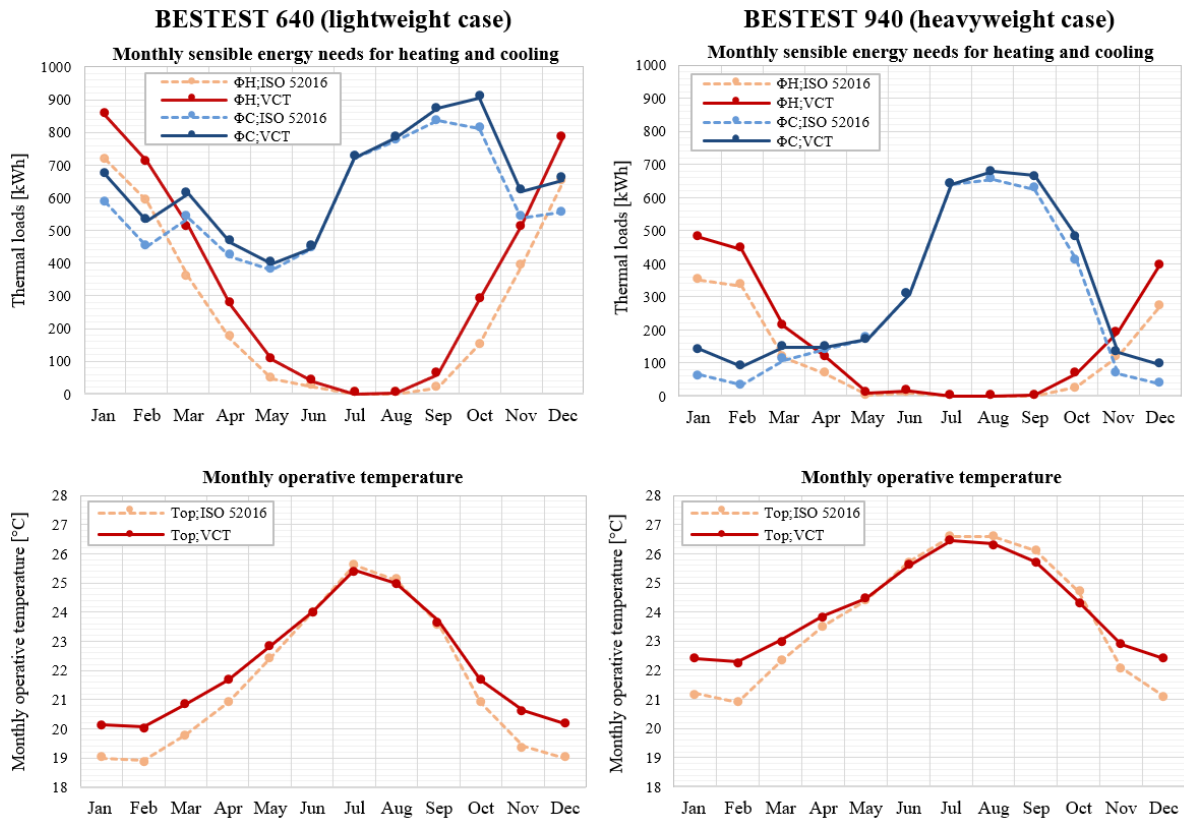


Figure 2: Validation results of BESTEST 640 and BESTEST 940. Dashed lines represent the reference results reported in EN ISO 52016-1:2017, while continuous lines represent the simple 1 RC lumped parameter model output used in the ventilative cooling potential tool (VCT).

The effect of thermal capacity is visible comparing BESTESTs monthly thermal loads. In the heavyweight reference case, characterized by a concrete-based construction system, the heating needs are lower due to the opaque envelope’s ability to store heat during the winter season so that it can be released with beneficial inward effects. On the other hand, during warm period, the high thermal capacity of envelope retards the heat flow passing through it, reducing cooling loads.

Table 1 **Error! Reference source not found.** reports the statistical error CV(RMSE) calculated and verified for all the output. According to the monthly criteria values provided by ASHRAE Guideline 14, CV(RMSE) index is respected for all the selected outputs except for the monthly sensible energy needs for heating. Overall, the errors calculated for the BESTEST 640 (lightweight case) are lower compared to the heavyweight case. The higher uncertainty in the second reference case is probably caused by the influence of higher thermal mass in the 1 RC lumped parameter model. Although the statistical error is not always respected, the methodology can still be considered validated: it is important to remember that this method is simplified compared to a building energy model (BEM) software.

Table 1: CV(RMSE) calculation and verification for all the selected output to assess model validation.

	BESTEST 640 (lightweight case)			BESTEST 940 (heavyweight case)		
Output	$\Phi_{H,vct}$	$\Phi_{C,vct}$	$\theta_{op,vct}$	$\Phi_{H,vct}$	$\Phi_{C,vct}$	$\theta_{op,vct}$
CV(RMSE)	29.71%	9.86%	3.66%	44.83%	15.03%	3.09%
	✗	✓	✓	✗	✓	✓

Charts reported in

Figure 3 show the comparison of monthly cooling needs taking into account the contribution of ventilative cooling in the two selected BESTEST cases (lightweight and heavyweight). Light blue bars represent cooling needs without the effect of ventilative cooling into the thermal zone, while blue bars represent cooling needs considering the contribution of ventilative cooling. Both graphs highlight that the implementation of ventilative cooling strategies allows to lower cooling needs consistently (reduction by 69% for lightweight case and by 60% for heavyweight case over the year), for the given climate, building and building use.

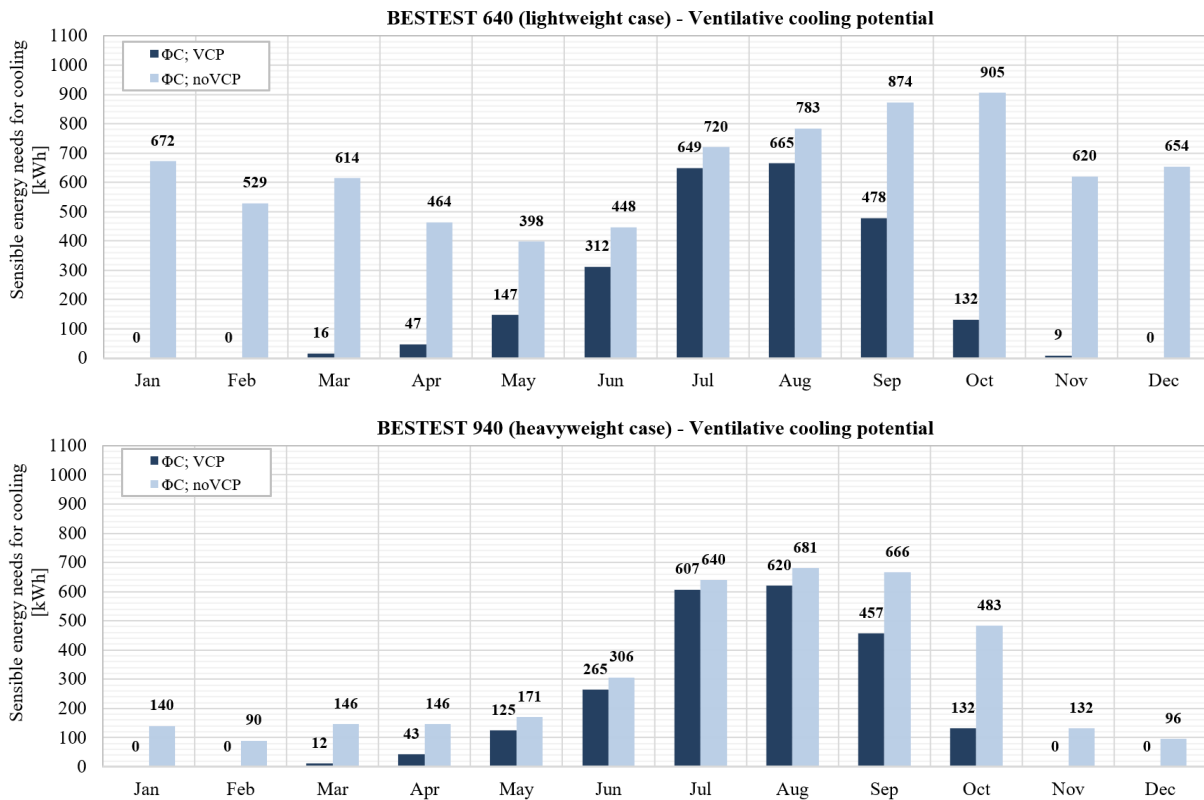


Figure 3: Comparison of sensible energy needs for cooling with and without the contribution of ventilative cooling on the heavyweight (940) and lightweight (640) reference cases.

4 DISCUSSION

A 1RC lumped parameter model was selected as the most suited model for predicting energy needs and indoor temperatures at the early design phase. The addition of more complexity to the model (as in the 3RC model outlined in EN ISO 13790:2008) may not lead to higher accuracy because most of the input data, such as details of the constructions, are unknown during early design stage. In case such input data are known, the detailed model of EN ISO 52016-1:2017 shall be applied. Although the calculation method presented and validated returns satisfactory results, some limitations are present. A limitation of the 1RC model is that indoor air temperature and indoor operative temperature are not distinguished. This limitation is acceptable in cases where air velocity is small (<0.2 m/s) or where the difference between mean radiant temperature and air temperature is small (<4 °C) (EN ISO 7730:2006). These conditions typically occur in highly insulated buildings with mechanical ventilation. Since ventilative cooling implies the use of high airflow rates to cool the environment, the assumption of air velocity smaller than 0.2 m/s might not be true. Therefore, it is important to underline

that the evaluation needs to be repeated at later design stages with more detailed calculation methods, i.e. dynamic simulations.

The analysis is carried out only on one thermal zone and assumes the air is well-mixed within the zone volume. The use of these results for the evaluation of ventilative cooling potential at building level depends on the building architecture and features and in general on how representative is the selected thermal zone for the entire building. The results obtained for the reference room can be considered valid for other building rooms with similar internal (occupancy, lighting and electric equipment density and patterns) and solar gains (same exposure, window to wall ratio and shading system). Otherwise, it is recommended to repeat the calculation for each building room.

Draft risk and localized discomfort cannot be predicted using 1RC models. In case ventilative cooling occurs to be useful during middle seasons and at low outdoor temperatures, more detailed evaluation through i.e. computational fluid dynamic models shall be carried out at later design stages.

The calculation considers only direct ventilative cooling. However, the potential of supplementary cooling solutions shall be considered within the building design to target low energy buildings. Passive night cooling, evaporative cooling, ground cooling, cooling recovery or use of smart air movement can be effective and complementary measures to ventilative cooling.

Ventilative cooling strategies shall be also future-proof and therefore it is recommended to evaluate the potential of ventilative cooling under future weather scenario to check its resiliency.

5 CONCLUSIONS

The paper presents the calculation methodology developed first within IEA Annex 62 and then within CEN/TC 156/WG21 TG on “Ventilative cooling systems - Design” to evaluate the ventilative cooling potential at early design stages. The methodology is based on a 1RC lumped parameter model that simplifies the energy balance of a reference building room. The 1 RC lumped parameter model was selected as the most suited model for predicting energy needs and indoor temperatures at the early design phase, when few information about the building features are available.

The calculation methodology has been validated according to the guidelines provided by ASHRAE Standard 140-2020 by comparing the 1RC model calculation results with the BESTEST reported in EN ISO 52016-1:2017 for two different types of envelopes (heavyweight and lightweight), in the climate of Denver, USA. The coefficient of the variation of the predicted cooling needs by the 1RC model relative to the BESTEST cooling needs reported in the EN 52016 standard is 9% in the lightweight case and 15% in the heavyweight case. The validation results are considered very promising since the level of detail of input data required for the 1RC model is very low.

Therefore, the ventilative cooling potential evaluation method is useful to compare the ventilative cooling capacity in different climates for different building typologies and thermal capacities. The outputs of the calculation can support the decision making about the application of ventilative cooling strategies and by providing an estimation of the ventilative cooling capacity and statistics about the ventilation rates needed to cool down the building in relation to internal gains, comfort requirements and envelope characteristics. The tool enables also to analyse the effect of other energy efficiency measures, like internal gains reduction, solar gains control and envelope performance, on ventilative cooling effectiveness.

6 ACKNOWLEDGEMENTS

The authors would like to thank the CEN/TC 156/WG21 TG on “Ventilative cooling systems - Design” experts for their contributions to the concept development and the interesting discussions.

7 REFERENCES

- ANSI/ASHRAE (2014). *Guideline 14-2014. Measurement of Energy and Demand Savings*.
- ANSI/ASHRAE Standard 140-2020. *Method of Test for Evaluating Building Performance Simulation Software*.
- Axley, J., & Emmerich, S. (2002). *A method to assess sustainability of a climate for natural ventilation of commercial buildings*. <https://www.researchgate.net/publication/228581659>
- Belleri, A., Avantaggiato, M., Psomas, T., & Heiselberg, P. (2018). *Evaluation tool of climate potential for ventilative cooling*. *International Journal of Ventilation*, 17(3), 196–208. <https://doi.org/10.1080/14733315.2017.1388627>
- Emmerich, S. J., Polidoro, B., & Axley, J. W. (2011). *Impact of adaptive thermal comfort on climatic suitability of natural ventilation in office buildings*. *Energy and Buildings*, 43 (9), 2101–2107. <https://doi.org/10.1016/j.enbuild.2011.04.016>
- EN 16798-1:2019. *Energy performance of buildings – Ventilation for buildings – Part 1: Indoor environmental parameters for design and assessment of energy performance of buildings addressing indoor air quality, thermal environment, lighting and acoustics*.
- EN ISO 52016-1:2017. *Energy performance of buildings – Energy needs for heating and cooling, internal temperatures and sensible and latent heat loads – Part 1: Calculation procedures*.
- EN ISO 13790:2008. *Energy performance of buildings – Calculation of energy use for space heating and cooling*.
- EN ISO 7730:2006. *Ergonomics of thermal environment – Analytical determination and interpretation of thermal comfort using calculation of the PMV and PPD indices and local thermal comfort criteria*.
- International Energy Agency. (2018). *The future of cooling: opportunities for energy-efficient air conditioners*. https://iea.blob.core.windows.net/assets/0bb45525-277f-4c9c-8d0c-9c0cb5e7d525/The_Future_of_Cooling.pdf
- Taylor, J., McLeod, R., Petrou, G., Hopfe, C., Mavrogianni, A., Castaño-Rosa, R., Pelsmakers, S., & Lomas, K. (2023). *Ten questions concerning residential overheating in Central and Northern Europe*. *Building and Environment*, 234, 110154. <https://doi.org/10.1016/j.buildenv.2023.110154>

8 ANNEX

Table 2: Model input provided for validation purpose.

Weather data	Denver, USA
Building geometry	Test room indicated in EN ISO 52016-1:2017
Thermal capacity (C)	$C_{env;940} = 15\,479\,952$ J/K $C_{env;640} = 2\,732\,538$ J/K $k_{m,int} = 10\,000$ J/m ² K (specific heat capacity of air and furniture)
Thermal transmittance (U)	$U_{o;940} = 0.3158$ W/m ² K (U-value of the opaque envelope) $U_{o;640} = 0.3167$ W/m ² K (U-value of the opaque envelope) $U_w = 2.984$ W/m ² K (U-value of the fenestration)
g-value	0.71
Shading control setpoint (Shd)	120 W/m ²
Shading factor (Y)	0
Internal gains (Φ_{int})	4.16 W/m ² (constant all year long)
Time control	From 0 to 24 (reference room is always occupied)
Intermittent setpoint	From 7 to 23 (daytime): $\theta_{int;set;H;t} = 20$ °C and $\theta_{int;set;C;t} = 27$ °C From 23 to 7 (night-time): $\theta_{int;set;H;t} = 10$ °C and $\theta_{int;set;C;t} = 27$ °C
Heating/cooling capacity	$\Phi_{H;avail} = \Phi_{C;avail} = 1000$ kW (1 000 000 W)

Table 3: Comparison of lightweight case results obtained with the methodology and ISO 52016-1:2017.

BESTEST 640						
Time	$\Phi_{H,vct}$ [kWh]	$\Phi_{H,ISO\,52016}$ [kWh]	$\Phi_{C,vct}$ [kWh]	$\Phi_{C,ISO\,52016}$ [kWh]	$\theta_{op,vct}$ [°C]	$\theta_{op,ISO\,52016}$ [°C]
Jan	853	718	672	586	20.1	19.0
Feb	711	591	529	451	20.0	18.9
Mar	513	358	614	537	20.8	19.8
Apr	273	169	464	421	21.7	20.9
May	105	47	398	380	22.8	22.4
Jun	38	22	448	446	23.9	24.0
Jul	1	0	720	720	25.4	25.6
Aug	1	0	783	775	25.0	25.1
Sep	60	19	874	835	23.7	23.6
Oct	290	151	905	812	21.6	20.0
Nov	512	389	620	538	20.6	19.4
Dec	784	646	654	557	20.1	19.0
Year	4141	3110	7680	7058	-	-

Table 4: Comparison of heavyweight case results obtained with the methodology and ISO 52016-1:2017.

BESTEST 940						
Time	$\Phi_{H,vct}$ [kWh]	$\Phi_{H,ISO\,52016}$ [kWh]	$\Phi_{C,vct}$ [kWh]	$\Phi_{C,ISO\,52016}$ [kWh]	$\theta_{op,vct}$ [°C]	$\theta_{op,ISO\,52016}$ [°C]

Jan	480	350	140	63	22.4	21.2
Feb	444	333	90	34	22.3	20.9
Mar	212	118	146	108	23.0	22.3
Apr	119	69	146	141	23.8	23.5
May	11	4	171	173	24.4	24.4
Jun	16	8	306	306	25.6	25.7
Jul	0	0	640	638	26.5	26.6
Aug	0	0	681	656	26.3	26.6
Sep	3	0	666	625	25.7	26.1
Oct	66	27	483	412	24.3	24.7
Nov	193	120	132	68	22.8	22.1
Dec	396	272	96	36	22.4	21.1
Year	1941	1301	3699	3260	-	-

Ventilation reliability: A pilot study on window opening behaviour in a primary school

Lara Tookey^{*1}, Mikael Boulic¹, Barry McDonald², Wyatt Page³,
Pawel Wargocki⁴ and Hennie van Heerden¹

¹Massey University
School of Built Environment,
Auckland, New Zealand
*l.tookey@massey.ac.nz

²Massey University
School of Mathematical and Computational Sciences,
Auckland, New Zealand

³Massey University
School of Health Sciences,
Wellington, New Zealand

⁴Technical University of Denmark
Department of Environmental and Resource
Engineering Indoor Environment,
Denmark

ABSTRACT

Most New Zealand schools are designed to be naturally ventilated, using openable windows (Ministry of Education Design Quality Standard Guidelines). Furthermore, they must meet the New Zealand Building Code Clause G4 - Ventilation. Clause G4 requires the “net openable area of windows in a classroom to be no less than 5% of the combined habitable floor area to achieve sufficient ventilation”. Although they are designed to code, there is no end-user operational or systems requirement for them to be opened. Assessing teacher behaviour in schools can improve indoor environmental quality in naturally ventilated classrooms where window operation behaviour directly impacts air exchange rates. This pilot study will use a multidisciplinary approach to monitor six naturally ventilated classrooms in one primary school in Auckland, New Zealand, during non-heating seasons. The state of the windows and external doors will be monitored using contact sensors and visual observations. Reflections on on-site management and difficulties will also be detailed. Data will be retrieved from the local meteorological station for ambient environmental data (temperature, humidity, solar radiation). The classroom environment will also be monitored (temperature, relative humidity, carbon dioxide). This data could inform on potential predictors to trigger open window/door openings. Correlational tests will be used to identify how opening of windows are affected by environmental predictors. This study will provide evidence of natural ventilation practices and their potential impact on classroom air quality.

KEYWORDS

natural ventilation; indoor air quality; indoor environmental quality; sensors; primary schools; windows; window operations

1 INTRODUCTION

Occupant behaviour plays a significant role in determining the Indoor Environmental Quality (IEQ) and energy consumption in buildings. The way, occupants interact with the building’s systems, such as heating, ventilation, and air conditioning (HVAC), can affect the overall building performance (Asadi et al., 2017).

The perceived ability or inability to adopt adaptive behaviours in a building can physiologically affect occupants and impact their overall comfort (Sundstrom & Nilsson, 2022). The psychological effect of adaptive behaviour may differ for children in classrooms compared to adults in other types of buildings. Children have different physical and

physiological needs, which can affect their perception of the indoor environment and their ability to adopt adaptive behaviours (Barrett et al., 2013). For example, children may need help understanding the control systems for heating and cooling in the classroom, which can limit their ability to adjust the indoor environment to their liking. They may also be more sensitive to noise and temperature changes than adults, impacting their comfort levels (Fanger, 1982).

Furthermore, research suggests that classroom environment factors like air quality and temperature can affect children's cognitive performance, health, and behaviour (Dadvand et al., 2015; Mendell et al., 2005; Shaughnessy et al., 2006). Therefore, it is essential to consider the psychological effects of adaptive behaviour when designing classrooms, especially for children.

To the authors' knowledge, at the time of writing this paper, there were no other studies in New Zealand (NZ) investigating the window-opening behaviours of teachers. This study aims to bridge the gap between the impact of window opening behaviour and IEQ.

This paper presents the outline of a pilot study being conducted at one Auckland primary school. By conducting this pilot study, the researcher can identify potential problems or challenges that may arise during the data collection process and make necessary adjustments before conducting the more extensive study. They can also assess the participants' acceptability of the data collection tools and test the analysis plan and determine whether modifications are necessary.

2 NEW ZEALAND CONTEXT

2.1 New Zealand climate

The New Zealand (NZ) Ministry of Education (MoE) owns more than 35,000 teaching spaces distributed over 2,100 schools (MoE, 2022). These schools are widely distributed around NZ, a long, narrow country extending 1,600 km along its north-north-east axis, with a maximum width of 400 km.

As such, there are six climatic regions, as identified in Figure 1, in which these schools operate. These climatic regions are mainly influenced by the temperate latitude, prevailing westerly winds, oceanic environment, and the Southern Alps mountains.

A series of mountain chains extending the length of NZ provides a barrier to prevailing westerly winds, dividing the country into climate regions. A summary of the mean annual values for rainfall, sunshine, temperature, frost, and wind is presented in Table 1 for consideration.

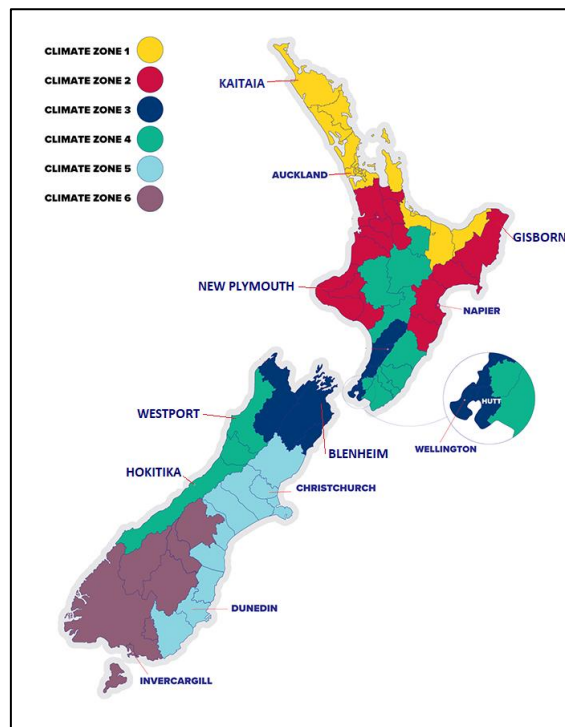


Figure 1: New Zealand climate zones (adapted from MBIE, 2023)

Table 1: Summary of Climate Information for Selected New Zealand Locations (NIWA, 2023)

Location	Rainfall	Wet-days	Sunshine	Temperature			Ground frost	Wind	Gale days
	mm	>= 1.0 mm	hours	Mean °C	Highest °C	Lowest °C	days	mean speed km/h	mean speed at least 63km/h
KAITAIA (zone 1)	1334	134	2070	15.7	30.2	0.9	1	15	2
AUCKLAND (zone 1)	1240	137	2060	15.1	30.5	-2.5	10	17	2
GISBORNE (zone 2)	1051	110	2180	14.3	38.1	-5.3	33	15	2
NEW PLYMOUTH (zone 2)	1432	138	2182	13.7	30.3	-2.4	15	20	5
NAPIER (zone 2)	803	91	2188	14.5	35.8	-3.9	29	14	3
WELLINGTON (zone 3)	1249	123	2065	12.8	31.1	-1.9	10	22	22
BLLENHEIM (zone 3)	655	76	2409	12.9	36.0	-8.8	60	13	4
WESTPORT (zone 4)	2274	169	1838	12.6	28.6	-3.5	26	11	2
HOKITIKA (zone 4)	2875	171	1860	11.7	30.0	-3.4	54	11	2
CHRISTCHURCH (zone 5)	648	85	2100	12.1	41.6	-7.1	70	15	3
DUNEDIN (zone 5)	812	124	1585	11.0	35.7	-8.0	58	15	8
INVERCARGILL (zone 6)	1112	158	1614	9.9	32.2	-9.0	94	18	18

Table 1 shows mean annual temperatures range from 9.9 °C in the south (Invercargill) to 15.7 °C in the north (Kaitiaki). Most areas experience between 648 (Christchurch) and 1249 mm (Wellington) of rainfall spread throughout the year. The wettest regions, Zone 4, received between 2274 and 2875 mm of rainfall throughout the year. The West coast of the South Island is the wettest region (Hokitika); however, just 100 km away to the east, over the mountains (Blenheim), is the driest. Wellington, and Invercargill are the windiest areas, with at least 18 days or more with a windspeed above 63 km/h.

One of the main challenges with providing ‘fit-for-purpose’ learning spaces in a geographically diverse country like New Zealand is the significant variation in climate regions. This diversity in climate can make it challenging to design and maintain learning spaces that are comfortable and conducive to learning for all students, particularly in regions

that experience extreme temperatures or high humidity levels. For example, schools in warmer regions (zone 1-2) may require cooling systems or shading to prevent overheating classrooms. Schools in colder regions (zone 3-5) may require effective insulation and heating systems to ensure that classrooms remain warm and dry. This geographic distribution of schools can present some unique challenges for the NZMoE.

When designing learning spaces in NZ, the MoE has selected passive design strategies and natural ventilation systems to provide fresh air and maintain classroom thermal comfort rather than relying on mechanical ventilation or air conditioning (MoE, 2022).

Heating systems still exist in most classrooms to ensure ‘fit-for-purpose’ learning spaces in the cooler seasons. These may include radiators or underfloor heating. It is worth noting that while air conditioning is not standard in NZ classrooms, as in some other countries, some schools have installed inverter heat pumps for cooling to help regulate temperatures during particularly hot periods (Stuff, 2020).

School window opening behaviour would vary depending on the climate in the school’s region. Generally, in warmer regions such as the north of the North Island, windows are expected to be open during the school day to allow for natural ventilation and cooling. In cooler regions, such as the south of the South Island, windows may be closed for much of the year due to colder temperatures. As such, an aspect worth noting are the reasons for the window operations. Are they in response to indoor temperature, outdoor temperature, temperature differences, humidity levels, noise or some other stimulus?

However, as mentioned previously, the MoE prefers naturally ventilated buildings. It may be likely that many schools throughout New Zealand have systems in place to encourage window-opening behaviour for natural ventilation. These systems could include window locks that allow windows to be partially opened for ventilation whilst adhering to the safety aspects (to prevent falling out of windows) or instructions to staff and students on when and how to open windows for optimal ventilation.

The COVID-19 pandemic has also brought increased attention to the importance of ventilation in indoor spaces, including schools. In response, the NZMoE has guided schools on ensuring proper classroom ventilation, which included recommendations on window-opening behaviour (MoE, 2021). One initiative introduced at this school was Aranet 4, a wireless environmental monitoring system. This system is designed to measure and monitor various environmental parameters in indoor spaces, including temperature, humidity, CO₂ levels, and atmospheric pressure. The data is collected, allowing users to monitor environmental conditions in real time. Posters were circulated to the school from the MoE, discussed at school meetings and then displayed in classrooms. Parents picking up their children after school were able to interact with these posters as well.

2.1 NZ Classroom design ventilation requirements

Most New Zealand schools are designed (following the Ministry of Education Design Quality Standard Guidelines) to be naturally ventilated, using openable windows. All classrooms must meet the ventilation rates required in the New Zealand Building Code Clause G4 Ventilation and cited standard NZS 4303:1990 (Building Performance, 2023).

The Code requires the “net openable area of windows in a classroom to be no less than 5% of the combined habitable floor area to achieve sufficient ventilation” (Building Performance, 2023). Ministry of Education’s Property Management Handbook, which guides schools on

property management, “all rooms where people are working, learning or teaching should be provided with adequate natural or mechanical ventilation, and the room should be maintained at a comfortable temperature and humidity level” (Ministry of Education, 2019, p. 22).

Although classrooms are designed to code, there is no end-user operational or systems requirement to open windows.

A survey undertaken in 40 Auckland (zone 1) primary schools in the winter of 2015 showed that only 40% of teachers open windows when they teach (Gully, 2015; Liaw, 2015). This figure dropped to 15% in a survey of 33 teachers from nine schools located in three NZ regions, namely Christchurch (N=4) (zone 5), Dunedin (N=3) (zone 5) and Hawke’s Bay (N=2) (zone 2) (Unpublished data, 2018).

Limited information is available in NZ relating to the window-opening behaviour of teachers and whether classrooms are adequately ventilated.

3 METHODOLOGY

This section of the paper outlines the methods and procedures used to conduct the pilot study. It will provide information on the research methods used, how the data was collected and how the data was analysed.

3.1 Sample selection

Convenience sampling was used. At the time of this study, there were five French-English bilingual schools in NZ. Three are in Auckland, one in Wellington and one in Christchurch. The reason for selecting French-English schools was to support the second part of the study. In the second stage of the study, the research will evaluate the impact that IEQ (carbon dioxide and thermal comfort levels) have on the cognitive abilities of primary school children. Bilingual individuals often demonstrate enhanced cognitive flexibility. Therefore, conducting research in schools that offer bilingual programmes in academic subjects in more than one language is a significant advantage. One school in Auckland opted out of the study, and the second was not a primary school. As the researcher was in Auckland, the third school was automatically selected as the pilot study. The study will be rolled out to other regions later.

3.2 School climate

The school is in a suburb in the North Shore area of Auckland. According to the Köppen-Geiger climate classification system, Birkdale has a Cfb climate (Peel et al., 2007). This means it has a warm-summer Mediterranean climate, with an average temperature above 10°C in the coldest month and no significant dry season. The average annual temperature in this suburb is around 15.6°C, with temperatures ranging from 10°C in winter to 22°C in summer. The area receives moderate rainfall throughout the year, with an average annual precipitation of approximately 1,231 mm (NIWA, 2023). The first week of observation studies were undertaken from 20th to 27th March 2023 (Autumn).

3.3 School building

The school has a roll of approximately 160 (personal communication from school administrator, 20 March 2023) students across teaching years 1 to 6. Students in these years are typically of ages 5 through 11 years old. At this school, students learn in mixed-aged classes i.e., Years 1 & 2, 3 & 4 and 5 & 6.

The school, as indicated in Figure 2, is located on an arterial road designed to handle high traffic volumes in a suburban environment. However, the main body of the school is set back from the road, and the classrooms used (identified with red X) are setback even further. Thus, the road noise is significantly diminished. To protect the privacy and anonymise data, the classrooms were named using the format “S0R1”. The first alpha number represents the school (S0), and the second the classroom number (R1). For the pilot study, this will be S0R1 – S0R7. Initially, six classrooms with identical sizes were identified for the study. After a term break, mould was discovered in one classroom (S0R3). Those students were relocated to the library (S0R7). The school building is a single-storey light timbre-framed structure which is naturally ventilated (Fig 3, Fig 4 and Fig 5).



Figure 2: Site map of school and arterial road. (Source: Google Maps, 2023)
(Red X identify the six studied classrooms)

All classrooms are on the ground floor with north-facing external doors exiting onto the playground. Cross ventilation can be achieved as there are windows on both the front (North) and back (South) walls. Table 2 details the design of the windows for the classrooms and library. The design and number of doors and windows are the same in the five classrooms, so only the details of one classroom and the library have been outlined.

Table 2: An overview of the window features of the classroom and library and their controls.

	Area (m ²)	Window Design					Window Operation
		WA ¹ (m ²)	NW ²	Window Type	MW ³	Ventilation	
Classrooms (S0R1 – S0R6)	66	3.36	1	Louvre (North)	Above head height	Double-sided at 2 levels + louvre opening	Manually with handle
		7.20	6	Side-hung outward opening (North)	0.64		Manually
		2.50	4	Top-hung outward opening (South)	1.50		Manually with handle
Library (S0R7)	175	3.36	1	Louvre (North)	Above head height	Double-sided at 2 levels + louvre opening	Manually with handle
		3.60	3	Side-hung outward opening (North)	0.64		Manually
		4.90	6	Top-hung outward opening (South)	1.00		Manually
		2.50	4	Top-hung outward opening (South)	1.50		Manually

1 = Total window area (m²) in each classroom

2 = Number of windows

3 = Minimum height of windowsill (m)



Figure 3: Design of windows in S0R2 and five other classrooms.



Figure 4: External door and windows for S0R2 (North) and Top-hung windows for S0R1 and S0R2 (South). Same design for five other classrooms.

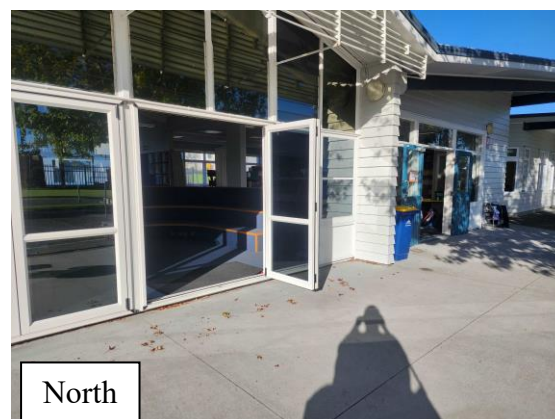


Figure 5: Louvre window and external double doors for Library/S0R7 (North)

3.4 Data acquisition

Visual observations

Three days of visual observations were conducted to ascertain the physical characteristics of the door/window open/closed status during the school day. The lead author appreciates that three days of a week is not sufficient to establish a comprehensive understanding of normal behaviour. However, due to teaching limitations throughout the semester, this was the only timeframe available. The week in March was selected as it included a day in which one class

was away on a fieldtrip. This would provide insight into how the classroom would be managed.

An observation form was developed to obtain information on the door/window open status at 20-minute intervals. By conducting these observational studies, the researcher was able to confirm the following:

- Functionality – how individuals interact with the space and whether the classrooms were in use or vacant.
- User functionality – by observing the use of space, it will be possible to identify if areas are meeting the ‘fit-for-purpose’ goal. Changes on how to improve can then be identified.
- Digital data – visual observations can provide valuable context and interpretation of the data supplied by monitoring systems, helping identify issues, validate data and improve the overall effectiveness of the monitoring system.

Visual observations were conducted to provide a general overview of the space and identify explanatory predictors influencing operations on windows and external doors. The lead author recorded the reasons for operations and the frequency through visual observations and teacher comments (Table 3).

Day: Date: Time	
S0R3	
	Back casement windows Open <input type="checkbox"/> Closed <input type="checkbox"/>
Occupancy pattern - <input type="checkbox"/> Occupied <input type="checkbox"/> Not occupied <input type="checkbox"/> On lunch/tea break <input type="checkbox"/> At the pool <input type="checkbox"/> Gone to assembly <input type="checkbox"/> Other	
Type of activity <input type="checkbox"/> Sedentary (seated) <input type="checkbox"/> Active (Running playing)	
S1R7	
Louvers	
3 Doors	
3 Front windows	
10 Back windows	
Occupancy pattern - <input type="checkbox"/> Occupied <input type="checkbox"/> Not occupied <input type="checkbox"/> On lunch/tea break <input type="checkbox"/> At the pool <input type="checkbox"/> Gone to assembly <input type="checkbox"/> Other	
Type of activity <input type="checkbox"/> Sedentary (seated) <input type="checkbox"/> Active (Running playing)	
Computer weather status and temp	

Table 3: Observation form for occupancy patterns and window opening behaviour.

To avoid disruption, the reasons for opening/closing operations were classified into general categories such as occupancy patterns, IEQ or external factors such as noise, which were obvious to observe without asking questions and intervening. In cases where the cause was unclear, the lead author would ask what the window operation was at the end of the teaching period.

Time management and weather conditions were some challenges associated with the visual observations. Due to time restrictions, the lead author could not conduct a week-long observation study; thus, the study had to be broken up over a few weeks. This was further exacerbated by a Cyclone and severe flooding, which led to school closures.

Teacher information

Before the commencement of the observational studies, the lead author was informed by two of the teachers that the students manage the opening/closing of the windows during the day based on the teacher's requests.

Window/door sensors

Window/door sensors, which incorporate Bluetooth LE5.0 technology and internal magnetic sensors, were installed on the window frame (Figure 6). Due to financial limitations, these sensors could only be installed in three classrooms. It was decided to install them in the classrooms which would form part of the second phase of the research study.

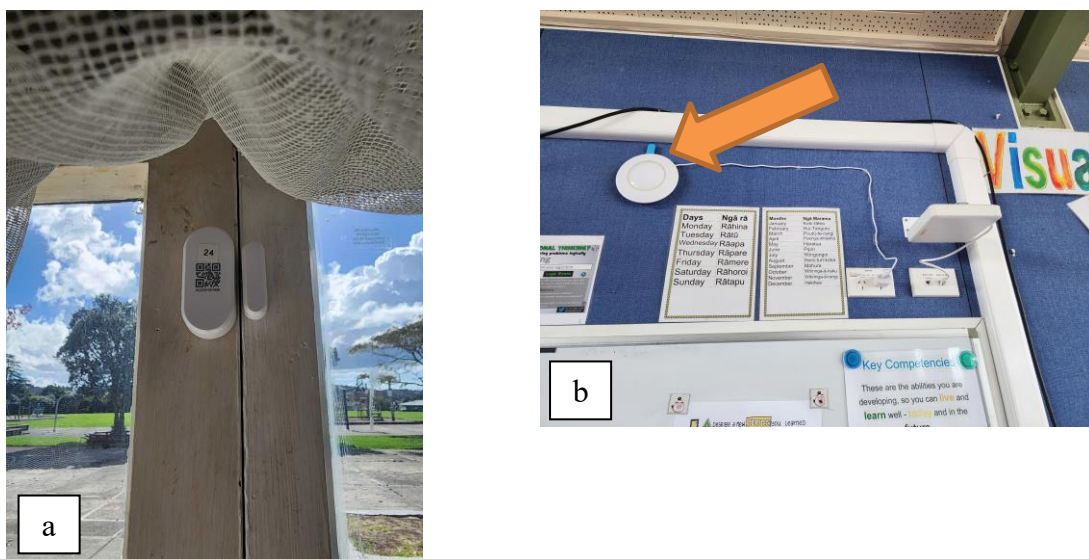


Figure 6: Placement of window sensor (a) on window frame and data logger connected to sensor through Bluetooth monitoring system (b).

These sensors assist the researcher in understanding window/door-opening behaviour by providing data on when and how often window/doors are opened and closed. The internal magnetic sensors in the sensor detect changes in the magnetic field when a window/door is opened or closed. This data is transmitted via Bluetooth LE5.0 technology to a centralised data logger (Figure 6b) as highlighted by the orange arrow.

By analysing this data, the researcher may gain insight into window/door opening behaviour, such as the frequency and duration of the window/door opening and the time of day when the window/doors are most often opened.

Some of the challenges associated with installing the sensors were related to the time management of the lead author and the logistics of working after hours at the school. The school was available for a limited time after hours because the classrooms were used for after-school workshops and community group events. Another issue was the actual construction of the window/door frame. The sensors are sensitive to rattles and frames that are not flush. Alternative fixing methods had to be developed.

Indoor Air Quality monitors

A team of researchers from Massey University, collaborating with NIWA, developed a low-cost monitoring platform, SKOMOBO (Figure 7). SKOMOBO stands for SKOol MOnitoring BOx, specifically adapted for the learning environment. Several units have been installed in the pilot study school (S0R1 – S0R3). However, as previously mentioned the students in S0R3 were moved to S0R7 due to the identification of mould. At the time of writing this paper, SKOMOBO units had not been installed in S0R7.

Figure 7a shows the pre-fieldwork co-location testing to check for data drift in the monitoring platform (SKOMOBO). The large orange arrow in Figure 7b point to a SKOMOBO monitoring platform installed in either S0R0/S0R1.

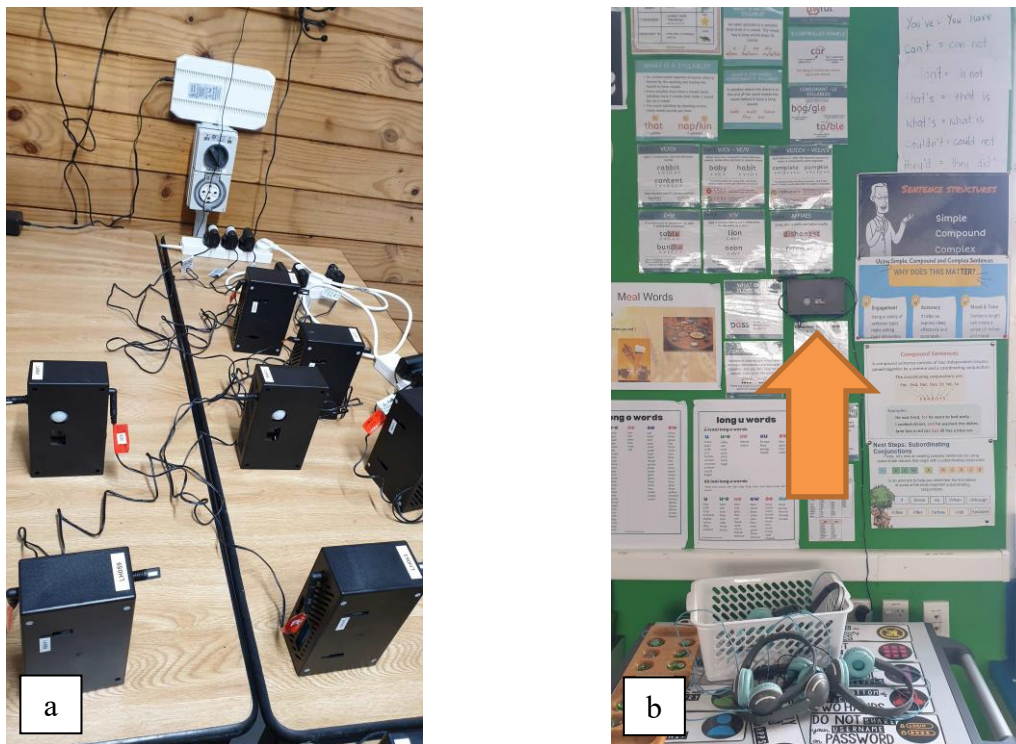


Figure 7: Pre-fieldwork co-location monitoring device at the lab (a) and Skomobo placed on the classroom wall (b)

Using a combination of the window/door sensors with the IEQ monitors it will be possible to identify periods of low ventilation, and increased carbon dioxide concentration levels, which could negatively impact on student health, learning and cognition. This data analysis forms part of the next phase of the study.

Environmental measurements

External environmental variables impacting window operations were recorded at 3-hourly intervals. This data was obtained from The National Climate Database (CLIFLO), utilising the local weather station-based in Albany North Shore (NIWA Cliflow database, 2023).

4 RESULTS

Table 4 shows the descriptive statistics of the indoor and outdoor variables over the three-day observation period. The maximum carbon dioxide (CO₂) level recorded in a classroom was 1000 ppm. The maximum indoor temperature was 26.9 °C, so this is not unexpected for an end of March (Autumn) reading. The average (across the three classrooms) CO₂ reading for the observation period was 508.6 ppm. There was a spike in the CO₂ reading for S0R2 on Day 1, the maximum (1000 ppm). The lead author assumes this is from the extra window operations made due to noise created by the swimming classes. The pool is located directed behind S0R2. This was confirmed after a conversation with the teacher (personal communication with teacher, 20th March 2023).

Table 4: Descriptive statistics of indoor and outdoor variables.

		S0R1 (SKOMOBO)			S0R2 (SKOMOBO)			Outdoor variables		
		Temp (°C)	RH (%)	CO2 (ppm)	Temp (°C)	RH (%)	CO2 (ppm)	T _{out} (°C)	Rhout (%)	Wind Speed (km/hr)
Minimum	Day 1 (9am -3pm)	19.2	54.4	410	19.5	48.1	410	14.8	58.0	1.4
	Day 2 (9am -3pm)	17.7	52.3	405	17.8	48.0	417	13.9	54.0	1.0
	Day 3 (9am -3pm)	21.1	58.6	417.0	21.7	56.9	414.0	17.9	69.0	1.1
Maximum	Day 1 (9am -3pm)	23.9	70.6	904	26.9	66.8	1000	21.8	96.0	5.0
	Day 2 (9am -3pm)	21.9	66.4	631	24.8	63.3	769	19.4	84.0	8.3
	Day 3 (9am -3pm)	24.9	75.6	701.0	25.8	72.8	718.0	21.2	94.0	6.5
Mean	Day 1 (9am -3pm)	22.2	61.3	480.5	24.2	57.2	608.5	19.1	70.7	3.7
	Day 2 (9am -3pm)	20.6	56.5	468.5	22.3	53.7	454.3	17.4	64.0	5.6
	Day 3 (9am -3pm)	23.1	68.0	525.1	23.5	65.4	515.0	20.1	79.7	3.7

Figure 8 illustrates outdoor variable conditions at 3-hourly intervals. Over the three days, no rain was recorded. On the last day there was low lying cloud, and rain was experienced in the neighbourhood, thus increasing the humidity levels at the start of Day 3. The temperatures rose steadily from day two through day three. The wind speed remained below 10km/hr.

Figure 9 details the number of window operations. Window operations are described as the number of times the windows are opened/closed during each school day (09:00 – 15:00), over the 3-day observation study. No operations occurred in S0R2 on the second day as the class was on a field trip. The windows in S0R4 and S0R5 were never opened so have not been included in Figure 9.

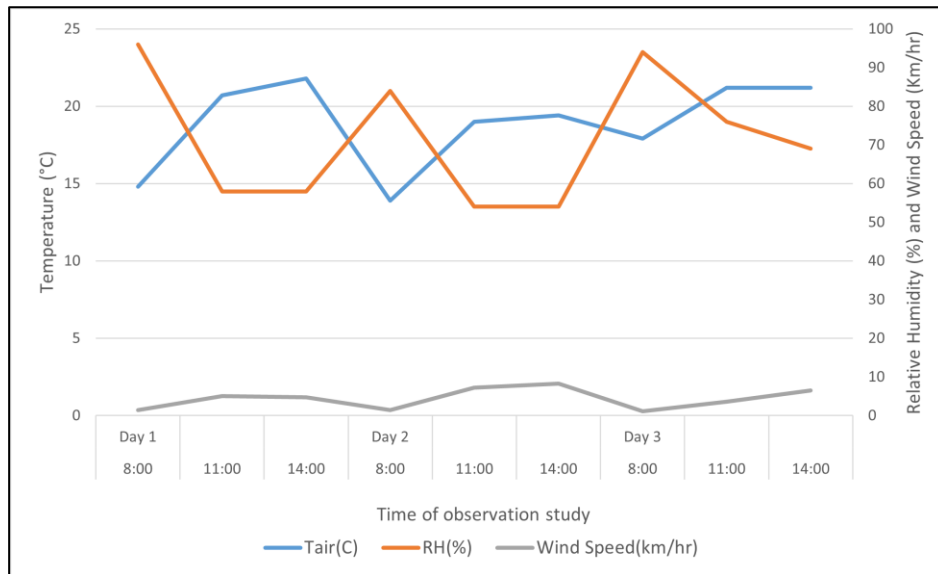


Figure 8: Three-hourly readings of outdoor environmental conditions over observation study.

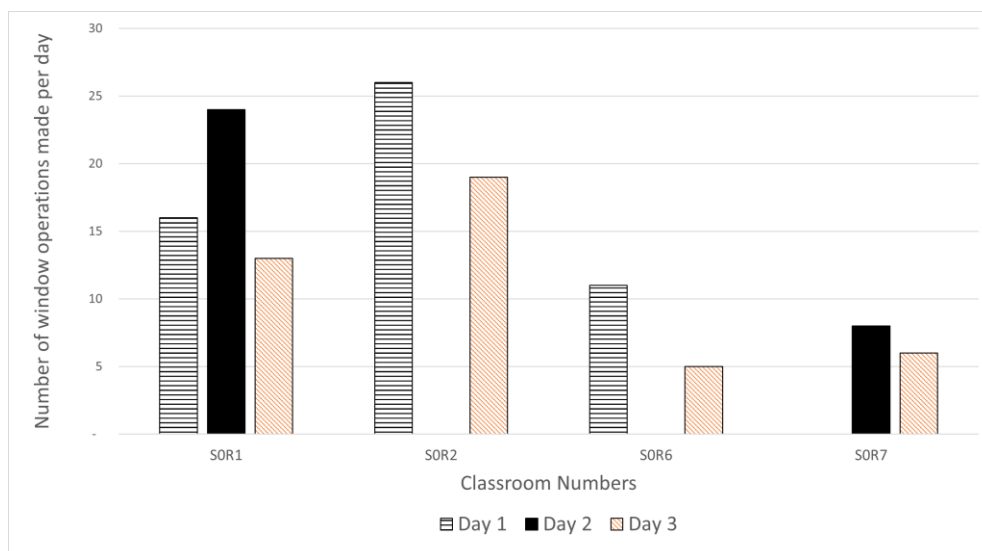


Figure 9: Number of window operations made per day over observation study.

Figure 10 shows the reasons for window operations (window opening and closing). 43% of window operations usually occurred upon teachers' arrival (usually around 8:30 am) and before students arrived in the classroom. 38% of operations occurred because of IEQ. 10% of operations (window closures) occurred due to noise. SOR2 closes the windows when the Year 1 and Year 2 students are in the pool due to increased noise.

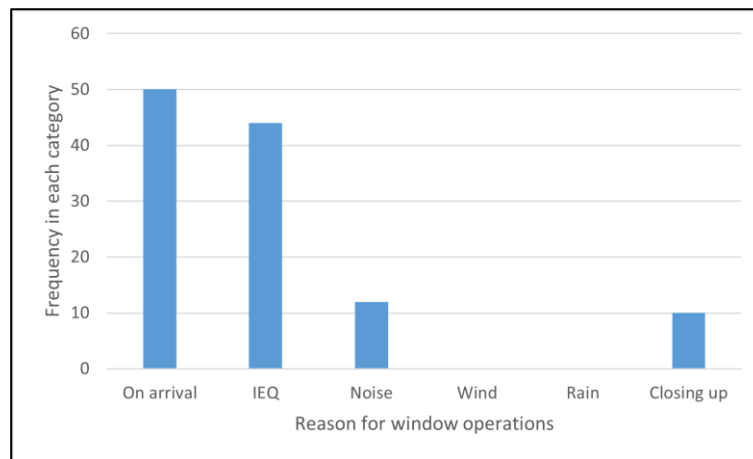


Figure 10: Reasons for window operations based on visual observations.

The caretaker opened the external doors prior to the teacher's arrival. These doors were kept open during the school's operating hours. On no occasion were windows opened by the caretaker before the teachers and students' arrival. Teachers opened their windows upon arrival. Once the windows were open, they would be kept open unless disturbing factors such as noise, rain, cold temperature or unwanted wind made them close the windows. This suggests that opening or closing windows depended on occupancy patterns (upon arrival and departure) and environmental variables. Not all window operations followed this logic; however, this closely represents the scenario in most of the classrooms in this study.

Figure 11 represents the percentage of window area that was open in each classroom for each day over the observation study period. This is based on the number of windows openable in each classroom and operations per hour.

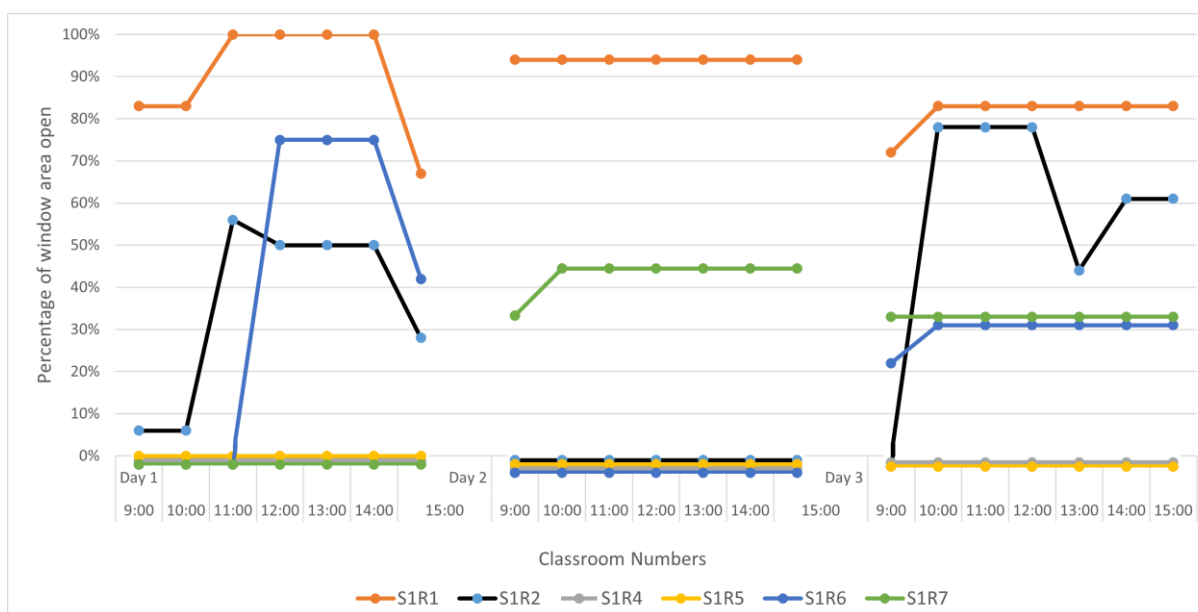


Figure 11: Percentage of window area that is open over the school day (by class) during the observation study.

The front north-facing door was open for each classroom over the three days. In classrooms S0R1 and S0R2, the teachers, consistently keep their windows open, creating well-ventilated

classrooms. The windows in S0R4 are never opened. S0R5 is combined with S0R6 (flexible teaching space with sliding partition wall). This partition wall was open throughout the observation period. Most of the teaching occurred in S0R6. The window and door usage could be more consistent in these two classrooms. This may be a result of the team teaching that occurs in this venue. This is something the lead author will investigate further.

A Spearman correlation between window open area (WOA m^2) and environmental variables was conducted to determine a more detailed analysis of window operations in response to IAQ. Visual observations showed that 38% of the windows were operated due to IAQ; therefore, environmental measured variables, including Temp, Humid (%), CO₂ (ppm), T_{out}, RH_{out} (%), and Wind Speed, were tested against WOA (m^2). The instances of operations unrelated to environmental variables from the observations (closing windows at the end of the school day) were excluded from the analysis. Table 5 shows the results of the Spearman correlation.

Table 5: Correlation and regression values between WOA (m^2) and environmental variables

Correlation/Regression of WOA with ...	Temp (°C)	Humid (%)	CO ₂ (ppm)	T _{out} (°C)	RH _{out} (%)	Wind Speed (km/hr)
R_s value	0.758	-0.341	-0.613	0.893	-0.494	0.479
P values	0.018 ^a	0.370	0.079	0.001 ^a	0.177	0.192

^a Correlation is significant (2-tailed)

Results of the Spearman correlation in Table 5 show that outdoor temperature (Spearman correlation coefficients = 0.001, $P < 0.001$) and indoor temperature (Spearman correlation coefficients = 0.018, $P < 0.001$) have the most robust relationship with WOA (m^2). Window area opening (m^2) does not correlate with outdoor windspeed. Results of the Spearman correlation in Table 5 show that WOA (m^2) negatively correlates to CO₂ and internal and external humidity levels.

5 CONCLUSIONS

The duration of time that external doors and windows are kept open will have an impact on the IEQ and ventilation in a classroom. It is interesting to note the extreme differences in practice in window opening behaviour between S0R1/S0R2 and S0R4. One would anticipate this behaviour prior to COVID-19. However, this behaviour seems unusual after the circulation of MoE guidance documents relating to window/door opening best practices.

Also, it is interesting to note the different teacher behaviour in the same school. All teachers are receiving the same information and guidance from the principal, yet their window opening behaviours are quite different.

The analysis of Spearman's correlation coefficients revealed significant relationships between the variables under investigation. A strong positive correlation was found between Variable A (window openable area) and Variable B (internal classroom temperature) ($\rho = 0.758$, $p < 0.018$), indicating a robust and consistent association between these two factors. Additionally, Variable C (Relative Humidity) exhibited a negative correlation with Variable A ($\rho = -0.341$, $p = 0.370$), suggesting an inverse relationship between these variables. Furthermore, Variable D (Carbon dioxide ppm) also exhibited a negative correlation with Variable A ($\rho = -0.613$, p

= 0.079), suggesting an inverse relationship between these variables. However, Variable E (Outdoor temperature) also exhibited strong positive correlation Variable A ($\rho = 0.893$, $p = 0.001$).

These findings demonstrate the presence of statistically significant associations between the variables A, B and E, reinforcing the hypotheses proposed in this study. The strength and direction of the correlations provide valuable insights into the relationships among the factors examined.

Overall, the observed correlations support the notion that changes in Variable A (opening of windows) are likely to impact the variations observed in Variable B (indoor temperature) and Variable D (carbon dioxide). These findings contribute to our understanding of the complex interplay between these variables and lay the foundation for further investigations in this field.

The next research phase will consider how much indoor thermal comfort (temperature and relative humidity) and indoor CO₂ levels change based on window/door opening behaviour. The third phase of the research will evaluate the impact of these changes (thermal comfort and CO₂ levels) on primary school students learning cognitive abilities.

6 REFERENCES

- Asadi, I., Mahyuddin, N. and Shafigh, P. (2017), "A review on indoor environmental quality (IEQ) and energy consumption in building based on occupant behavior", *Facilities*, Vol. 35 No. 11/12, pp. 684-695. <https://doi.org/10.1108/F-06-2016-0062>
- Barrett, P., Zhang, Y., Moffat, J., & Kobbacy, K. (2013). A holistic, multi-level analysis identifying the impact of classroom design on pupils' learning. *Building and Environment*, 59, 678-689. doi: 10.1016/j.buildenv.2012.09.016.
- Dadvand, P., Nieuwenhuijsen, M. J., Esnaola, M., Forn, J., Basagaña, X., Alvarez-Pedrerol, M., ... & Sunyer, J. (2015). Green spaces and cognitive development in primary schoolchildren. *Proceedings of the National Academy of Sciences*, 112(26), 7937-7942. doi: 10.1073/pnas.1503402112.
- Department of Building and Housing. (2011). Compliance Document for New Zealand Building Code - Clause G4 Ventilation. Wellington, NZ: Department of Building and Housing.
- Fanger, P. O. (1982). *Thermal comfort. Analysis and applications in environmental engineering*. New York: McGraw-Hill.
- Gully, F. (2015). *Windows and Doors in Schools: A study of low-decile primary schools in Auckland (Final Year Project Report)*. Auckland, NZ: Massey University.
- Liaw, F. (2015). *Doors and Windows Needs for School (Final Year Project Report)*. Auckland, NZ: Massey University.
- Mendell, M. J., Heath, G. A., & Doi, L. (2005). Indoor environmental factors associated with cognitive function in school children. *Indoor Air*, 15(Suppl. 10), 1-9. doi: 10.1111/j.1600-0668.2005.00339.x.
- Ministry of Business, Innovation and Employment. (2023). *Building Code Handbook: H1 Energy Efficiency [Brochure]*. Retrieved from <https://www.building.govt.nz/assets/Uploads/building-code-compliance/h1/h1-energy-efficiency/building-code-handbook-h1-energy-efficiency.pdf>

- Ministry of Education. (2017). Deciles. Retrieved from <https://www.education.govt.nz/school/funding-and-financials/resourcing/operational-funding/deciles/>
- Ministry of Education. (2019). Funding changes to support equity in schools. Retrieved from <https://www.education.govt.nz/news/funding-changes-to-support-equity-in-schools/>
- Ministry of Education. (2021). Ventilation and COVID-19. Retrieved from <https://www.education.govt.nz/school/property/state-schools/covid-19-property-guidance/ventilation-and-covid-19/>
- Ministry of Education. (2022). Designing Quality Learning Spaces - Indoor Air Quality and Thermal Comfort. Wellington, NZ: New Zealand Ministry of Education.
- Ministry of Education. (2023). Equity index funding summary 2023. Retrieved from https://assets.education.govt.nz/public/Documents/our-work/changes-in-education/MOE14173_Regional-Summary_Auckland_19.pdf
- National Center for Education Statistics (NCES). (2019). Condition of Education 2019. U.S. Department of Education, Washington, DC. Retrieved from https://nces.ed.gov/programs/coe/pdf/coe_toc.pdf
- National Institute of Water and Atmospheric Research. (2023). Retrieved from <https://niwa.co.nz/education-and-training/schools/resources/climate/overview>
- NIWA. (2023). Cliflo Database. Retrieved from <https://www.niwa.co.nz/climate/cliflo>
- Peel, M. C., Finlayson, B. L., & McMahon, T. A. (2007). Updated world map of the Köppen-Geiger climate classification. *Hydrology and Earth System Sciences*, 11(5), 1633-1644. <https://doi.org/10.5194/hess-11-1633-2007>
- Shaughnessy, R. J., Haverinen-Shaughnessy, U., Nevalainen, A., Moschandreas, D. J., & Sundell, J. (2006). A preliminary study on the association between ventilation rates in classrooms and student performance. *Indoor Air*, 16(6), 465-468. doi: 10.1111/j.1600-0668.2006.00450.x.
- Stuff. (2020). Retrieved from <https://www.stuff.co.nz/national/education/121817162/should-air-conditioning-be-standard-in-nz-classrooms>
- Sundstrom, E., & E. D. Nilsson. (2002). Predicting perceived control in indoor environments: The roles of environmental stimulation and attentional processes. *Journal of Environmental Psychology*, 22(3), 247-257. doi: 10.1006/jevp.2002.0243.

A survey of building design practitioner perceptions of ventilative cooling in their building design processes

Maha Sohail*^{1,2}, Adam O'Donovan^{1,2}, Christopher Plesner³ and Paul D. O'Sullivan*^{1,2}

1. *Department of Process, Energy and Transport Engineering, Munster Technological University, Cork, Ireland*
2. *MaREI SFI Centre for Marine, Climate and Energy, University College Cork, Ringaskiddy, Co. Cork, Ireland*
3. *VELUX, Ådalsvej 99 DK-2970, Hørsholm, Denmark*

*Corresponding authors: maha.sohail@mycit.ie,
paul.osullivan@mtu.ie

ABSTRACT

Buildings account for 40% of EU energy consumption and 36% of the energy related greenhouse gas emissions at present. Consequently, the net zero target set by Energy Performance of Building's Directive by 2050 for building stock is ambitious to achieve. The often default design choice to adopt mechanical cooling in non-domestic buildings highlights the lack of robust decision support tools or frameworks available to designers to properly evaluate ventilative cooling as a realistic alternative. Recent research suggests that the initial or concept design stage of a building project is a high leverage point in the design cycle to properly influence a building's design to avoid 'locking in' vulnerability at later stages due to retrospective value engineering efforts. Properly accounting for the potential of ventilative cooling solutions to mitigate risks against external disturbances to the indoor thermal environment such as heat waves as a result of climate change, as well as other performance limiting factors (i.e. air and noise pollution, power outages etc), is important to avoiding the selection of emissions intensive alternatives. A critical review of existing design processes followed by architects in practice completed as part of this study suggests that the pre-design phase and the schematic design phase of any building are the two crucial phases in any architectural design process. In these two stages, the information about a building's purpose, site, local micro-climate, client's expectations, and local legislations influences the building's overall shape, internal layout and morphology. This paper presents initial findings from a survey of industry experts about their design practices and experienced based approaches to designing ventilative cooling in low energy buildings at the concept design stages. The survey data was analysed through a mixed-methods approach (quantitative for closed-ended questions and qualitative for open-ended questions). This survey informed the ongoing development of the conceptual design framework within the Technical committee (TC) within the European Committee for Standardization (*CEN Technical Bodies - CEN/TC 156/WG 21*, n.d.; *CEN/TC 156/WG 21 - Revision of Calculation Standards EN15241, 15242 and 15243*, n.d.) scope. The framework which would be developed as an outcome of the completed study would have the potential to significantly improve the operational performance of ventilative cooling systems through early-stage interventions in building design that lead to more robust strategies that limit the need for mechanical cooling.

KEYWORDS

Design practice, design processes, ventilative cooling, design guidelines, passive cooling, building design practitioners, resilience in built environment.

1 INTRODUCTION

In the broader context of climate change and global warming, there is an increased importance of energy efficiency in buildings worldwide and a large proportion of a building's energy consumption, comes from heating, ventilation, and air conditioning (HVAC) services to make

them comfortable for human living. According to a report by the International Energy Agency (2018) focusing on The Future of Cooling (opportunities for energy-efficient air conditioning) (*The Future of Cooling – Analysis - IEA*, 2018.) carbon emissions from buildings have increased by 50% in the period between 1990 and 2019. This is partly because of urban densification and increased floor area per person caused by building more and more buildings. In addition, the global average cooling demand in commercial buildings is likely to be increased by 275% by 2050 due to rising air conditioning demands (Santamouris, 2016; *The Future of Cooling – Analysis - IEA*, 2018.) Yamina Saheb, one of the authors of the IPCC (*Summary for Policymakers of IPCC Special Report on Global Warming of 1.5°C Approved by Governments – IPCC*, n.d.) report claimed our buildings to be wrongly designed (*Our Buildings Are “Wrongly Designed,” According to IPCC Report Author*, n.d.) in the context that many of our buildings have active heating, mechanical and cooling systems that consume energy which shows a discrepancy in the way buildings are designed. There has been an increasing interest in ventilative cooling and resilient cooling concepts in recent literature and standards (Attia et al., 2021; Kolokotroni & Heiselberg, n.d.; O’ Donovan et al., 2021; Tavakoli et al., 2022) but the implementation of these concepts is still not visible in building design practices. Although, the application of ventilative cooling principles and strategies are believed to be a solution against threats of heat waves and climate change (Alonso et al., 2015; Breesch et al., 2018; Sengupta et al., 2020; Song et al., 2022). IEA EBC annex 62 State of the Art Review report (2018) recently defined VC as, ‘*The application of ventilation flow rates to reduce the cooling loads in buildings. VC utilizes the cooling and thermal perception potential of outdoor air. The air driving force can be natural, mechanical or a combination*’ (Kolokotroni & Heiselberg, n.d.).

A critical review of building design processes studied in the context of ventilation in the built environment reflects a lack of consensus among building design stakeholders in properly accounting for the cooling needs of buildings against future climate threats, such as heatwaves, at conceptual and pre-design phases, in advance of the detailed design. Participatory methods, which offer a better mode of understanding the context of how a building is designed and at what stage the decision about “cooling the building” is taken, have received less attention in this perspective. For instance, the RIBA Plan of Work (*RIBA Plan of Work 2020 Overview RIBA Plan of Work*, 2020) shows various stages of the Architectural Design Process as pre-design, schematic design to design development stages but it does not explicitly mention the considerations of indoor environmental quality at the initial stages rather sustainability checks are considered at final stages of building design such as commissioning, construction and building regulations which may include decisions of ventilation and indoor comfort. Likewise, Polat Darcin (Darcin, 2020) developed a conceptual architectural design process for ventilation in the built environment from a research perspective but did not apply it to design practice. Ahmed A.Y. Freewan (Freewan, 2019) showed an integrated design approach for passive cooling devices by a design matrix named SARS (Storing, Allowance, Removal or Slowing) but did not demonstrate its application in architectural practices. A brief review of building design and airflow modelling tools (*Best Directory | Building Energy Software Tools*, n.d.) also suggests that there is no clear design process developed that can be followed in design practices that would improve the performance (and by extension uptake) of ventilative cooling strategies from early design stages. Likewise, a brief process of design in general has been presented by CIBSE Environmental Design Guide A (CIBSE, 2015). Cevrede et al. 2020 developed a conceptual architectural design process for ventilation in built environment (Çevrede et al., 2020), a simulation based framework was developed Rahif et al. 2022 (Rahif et al., 2022) to evaluate resistivity of cooling strategies in buildings against overheating impact of climate change, yet it was not well demonstrated by multiple cooling strategies and real multi-zone reference buildings modelling. All the processes developed in these studies are not detailed and

not applied in real life scenarios to assess their application and whether they work for the industry experts.

2 METHODOLOGY

This paper presents the results from a survey targeted at Building Design Practitioners in the United Kingdom and Ireland region with the title; “Perception of Ventilative Cooling in Building Design Practices” and links it to the work done so far on ventilative cooling standards within the scope of Technical Working Group for Ventilative Cooling Standards (TC/156 WG21). The survey contains a mix of both open-ended and closed-ended questions. For this study, only the results obtained in the first three weeks of running the survey are presented, therefore, only completed responses are considered. The survey is aimed to continue for at least 3-4 months to obtain good quality data and sample size. The survey is a first step in the planned methodology of the full research study; “*Development of a building design process for improving the thermal resilience of non-domestic buildings using ventilative cooling solutions*” as is indicated in [Figure A1 \(Appendix A\)](#).

2.1 Development of the survey

The survey was developed to understand the perception of the term “ventilative cooling” in architectural and construction practices and was divided into seven parts. The overall hierarchy of the parts of the survey can be elaborated by Figure 1.

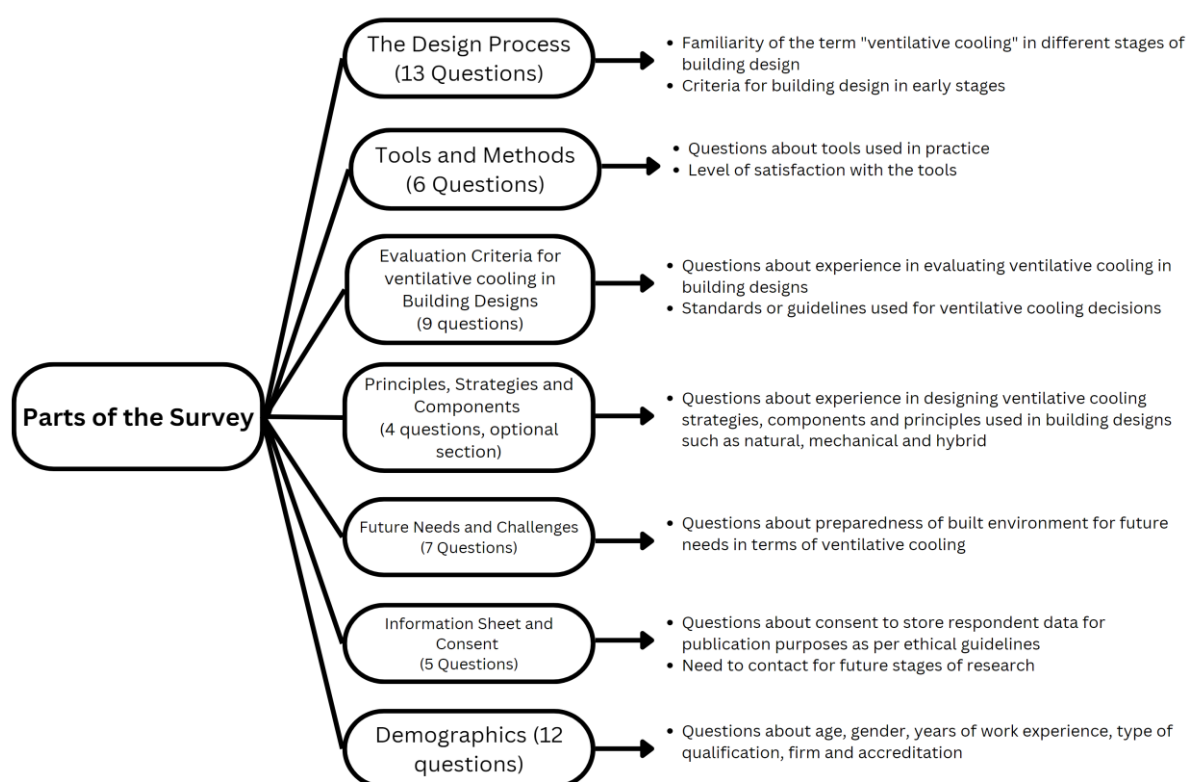


Figure 1: Summary of 57 questions used in the survey

An engineer, a researcher and a professor were identified from the network of corresponding authors of the paper to preliminary test and comment on any technical errors with the survey and to point out any issues with consistency and structure of the questionnaire. Respondents gave some suggestions about the questions which were incorporated. Overall, they were satisfied with the structure and format of the survey. Munster Technological University’s

Research Ethics Committee also approved the research in line with all ethical requirements (Approval number: MTU-HREC-MR-22-001-A).

2.2 Respondents of the survey

In this study, building design experts such as architects, building service engineers, design managers, sustainability experts in the United Kingdom and Ireland region were targeted. LinkedIn was used to identify their profiles by searching through their current job description, years of experience (more than five) and their current affiliation with an architectural design or engineering firm. Many email addresses were collected through the “contact info” section of LinkedIn profiles of respondents. In addition, many experts were identified through the professional network of the corresponding authors. Moreover, the architectural practice directory of The Royal Institute of the Architects of Ireland (<https://www.riai.ie/work-with-an-architect/find-an-architect/practice-directory/>) (*Practice Directory | RIAI.Ie (The Royal Institute of the Architects of Ireland)*, n.d.) was also used to identify architectural firms in Ireland. The response rate was consistently slow at 30% in the first two weeks, however, not all respondents answered all the questions completely. The demographics of the respondents who completed the survey is presented in Table 1. The online questionnaire was delivered through Survey Monkey link (<https://www.surveymonkey.com/r/YMNY2VT>).

Table 1: Demographics of Respondents

Demographic	Architect	Engineer	Architectural Technologist	Other	Total
Gender					
Male	7	2	1	1	11 (78%)
Female	2	0	0	0	2 (14.3%)
Prefer Not to Say	1	0	0	0	1 (7%)
Age					
35-44	2	0	0	0	2 (14%)
45-54	4	1	0	1	6 (43%)
55-64	4	1	1	0	6 (43%)
65+					
Highest Qualification					
PhD	0	0	0	1	1 (7%)
Masters or Postgraduate	7	1	0	0	8 (57%)
Bachelors	2	1	0	0	3 (21%)
Diploma	0	0	1	0	1(7%)
Other	1	0	0	0	1(7%)

3 RESULTS

The results of four sections of the survey aligning with the themes of the conference are briefly presented as follows;

3.1 The Design Process

The first question in this section was about the criteria for designing buildings and if cooling is a criterion. The results can be shown by the Table 2 where all respondents agreed that cooling is an essential criterion in their respective countries while none of them excluded it as a design criteria.

Table 2: Responses of Questions related to the term “ventilative cooling” and the “Design Process” in the Survey

Questions	Answer Option 1	Answer Option 2	Answer Option 3
Would you identify cooling of the indoor environment in buildings an important design criteria amongst your profession in your particular climate/country?	Yes, it is an important criteria(85.71%)	Yes, it is a criteria but it's not important (14.29%)	No, it's not a criteria (0%)
Are you familiar with the term “Ventilative Cooling”?	Yes (71.43%)	No (28.57%)	

The respondents were also asked whether they were familiar with the term “ventilative cooling” and it turned out a strong majority (71.43%) of the respondents were familiar with the term as shown in Table 2. Around 28.57% were not familiar. After a literature survey of the architectural design processes (*RIBA Plan of Work 2020 Overview RIBA Plan of Work, 2020; The 5 Phases Of The Architectural Design Process, Explained, n.d.; The 7 Phases of the Architectural Design Process - 2022 - MasterClass, n.d.; Saeid & Mahmoodi, 2001*); we proposed the initial question to the architects presenting a diagram in front of them where the architectural design process consists of 6 stages, i.e. pre-design phase, schematic design phase, design development phase, bidding & construction administration, commissioning and post occupancy evaluation. The initial hypothesis of this research was stated in this diagram that “*ventilative cooling decisions are not taken at the early design stages*” which we decided to test by conducting the survey. To the extent that the respondents agree or disagree with our understanding of the building design process and our hypothesis, can be seen in Figure 2, where 50% of the total respondents agreed with the process diagram presented to them, 43% disagreed (14% “strongly disagreed” and 29% “Disagreed”) and 7% had no opinion on the process and the hypothesis we stated.

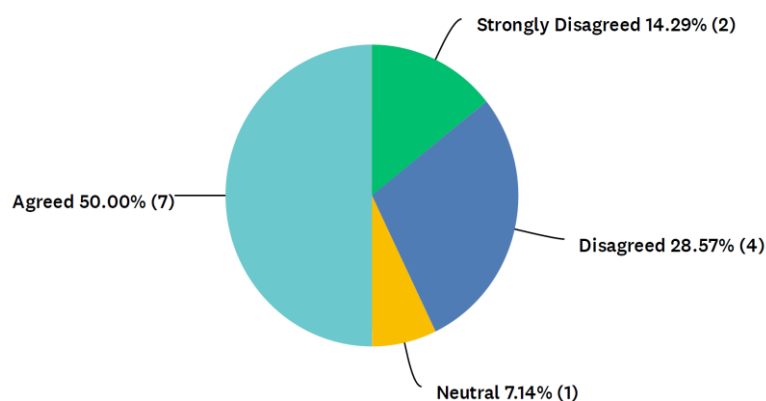


Figure 2: The extent to which respondents agreed or disagreed with the building design process diagram presented to them.

3.2 Tools and Methods

Around 21% of the respondents do not use any design tools to make any ventilative cooling decision and around 50% sometimes use a design tool while 29% of the respondents use the tool while making a ventilative cooling decision. The most popular software used by the respondents is Passive House Planning package (PHPP) with around 50% of the respondents using it, and the second most popular tool is Integrated Environmental Solutions (*Integrated Environmental Solutions / IES, n.d.*) with around 33% of the respondents using it in their design practices. The respondents who use the tools mostly use them in schematic and design

development phases. Finally, some of the respondents do not use any tools, because they do not think of themselves as experienced in using these tools and therefore, they rely on the advice of engineers on this topic

Around 54% of the respondents are not satisfied with the current tools in the market in terms of their ability to suggest ventilative cooling design options. Some of the improvements suggested by respondents to make the tools better include ability to include parametric analysis, increasing the speed and making them cost effective for use by Architects. Some Architects also believe that there is a gap between software simulations and actual performance of the building designs which needs to be reduced. Also, the ability to overestimate the mechanical cooling demand by the tools in order to follow building regulations is also a problem with the current tools highlighted by a respondent. Other than the tools, around 64% of the respondents rely on their professional experience and 28% of the respondents highlighted the importance of other means e.g. technical guidance documents, advice of engineers, cost implications and user comfort to make an efficient ventilative cooling strategy.

3.3 Evaluation Criteria for Ventilative Cooling in Building Designs

In this section the respondents were asked if they have any experience in evaluating ventilative cooling potential of their building designs and what criteria they use for the purpose. Half of the respondents were experienced and the other half were not in evaluating the ventilative cooling potential of their designs. In addition, the top two variables that the respondents consider at the early design stage for ventilative cooling systems are ventilation rate per occupant and percentage of openable area as shown in Figure 3. While evaluating comfort performance in their building designs, the majority of respondents selected “% of hours > 25°C” as the upper temperature threshold for consideration as shown in Figure 3 below.

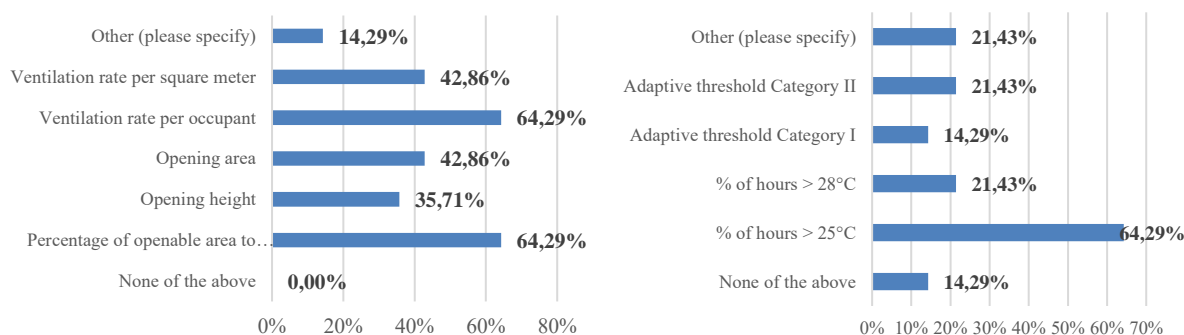


Figure 3: Results of the questions, “Which of the following metrics or variables do you consider at the early design stage for ventilative cooling systems?” and “When evaluating comfort performance in your designs, what upper temperature thresholds do you consider?” from left to right respectively.

3.4 Future Needs and Challenges

Results of some of the questions and their answers; pertaining to future needs and challenges faced by built environment professionals in improving the resilience of buildings are presented in Table 3. It can be said that the majority of respondents (93%) are familiar with the importance of ventilative cooling in delivering a carbon-neutral built environment. However, about 71% of the respondents believe that built environment design industry is not ready to design buildings for extreme climate events and the buildings of today are not ready for such events in the future.

In addition, 57% of the respondents believe that natural ventilation alone does not work satisfactorily as a cooling solution against future climate change.

Table 3: Responses of Questions related to Future Needs and Challenges of Ventilative cooling in Building Designs

Questions	Answer Option 1	Answer Option 2
Do you think that the built environment design professionals are prepared for accounting for extreme future climate events, such as heat waves, while designing buildings today that will be used many years from now?	Yes (28.57%)	No (71.43%)
In your experience does Natural Ventilation work satisfactorily as a cooling solution against future climate change?	Yes (42.86%)	No (57.14%)
Can Ventilative Cooling play a role in delivering a carbon neutral built environment?	Yes (92.86%)	No (7.14%)

An overall mind map can be generated from the overview of survey results which is represented by Figure 4. The gaps in research and future steps pertaining to easy tools or early design stages are mentioned and an interconnection between all the stages is presented by the dotted circular line. The overall result is that design is an iterative process and the core design team is always at the centre of making design decisions as the project progresses.

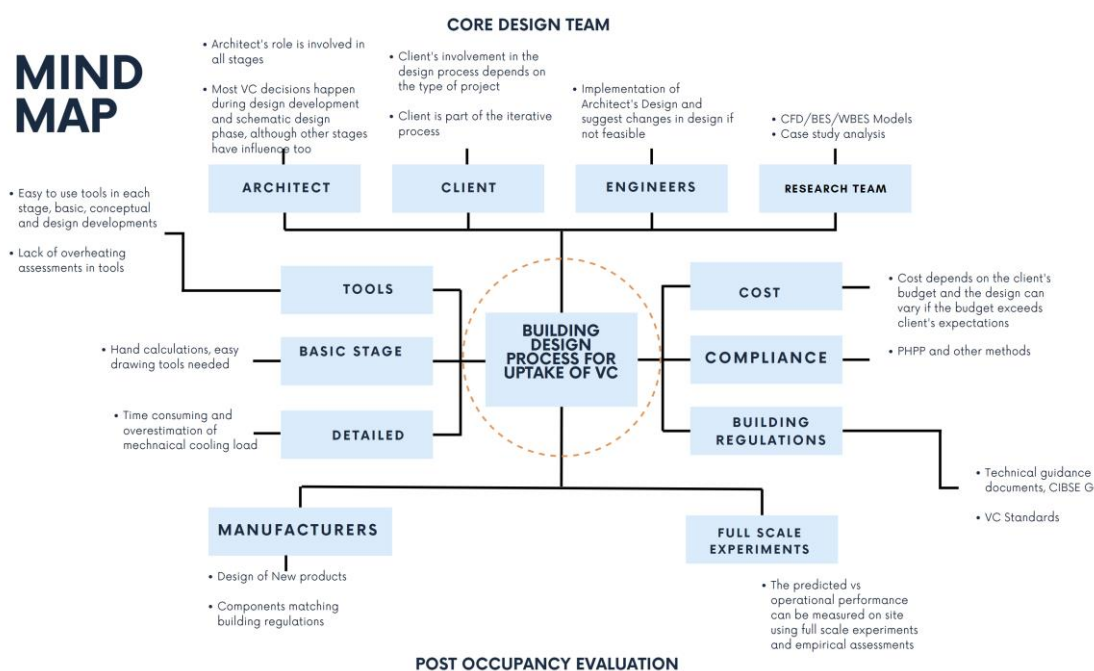


Figure 4: Visualization of the survey responses of how information flows in the design process

4 VENTILATIVE COOLING STANDARDS

Currently work is underway within TC/156 (*CEN Technical Bodies - CEN/TC 156/WG 21*, n.d.) to develop a new design guide to assist with designing ventilative cooling at building design practices. The work done by far on Ventilative Cooling standards update ([Table A1 in Appendix A](#)) was used to develop the survey questions. However, if a comparison is made between the results of the survey, the architectural design processes as covered in the section 3 and the work on standards by far, it can be inferred that Architects do not use a separate conceptual and basic design term, rather the terms used are basic as the simplest stage of design and conceptual or schematic phase is the next phase of design. In other words, the ventilative cooling standards

are more technical from the perspective of the Architects. Further stages of study would address if the Architects can find the ventilative cooling guides useful in any stage of their process and if there is a framework that can be developed further that can help in the uptake of ventilative cooling standards from the early design stages.

5 CONCLUSIONS

In this paper, only prominent results from four sections of the survey are presented to understand the perception of the term “ventilative cooling” in the overall building design process used in design practices in the UK and Ireland region. The survey results will be analysed in detail over the next few months and a statistical analyses will also be carried out on receiving a good quality data. From the results, it is evident that the building design practitioners are familiar with the term “ventilative cooling” as the name suggests but they admit the lack of decision-making frameworks and tools in promoting the uptake of VC solutions in their building designs to make buildings resilient against threats of heat waves. The results are also subject to change on receiving more responses from the industry experts in building design. This is an ongoing survey which will last for about three months providing a direction to design the next stages of the research, i.e. interviews and a possible placement at an architectural design practice to validate the design process by a case study building. This study provides an opportunity to find a case study building that has adequate ventilative cooling solutions designed and that is resistant to the effects of climate change. Identification of the design process used in such a building can help in development and verification of the design process intended in this research.

6 ACKNOWLEDGEMENTS

The research team would like to thank the survey respondents for their time and co-operation in filling out the survey. We would also like to thank many colleagues from professional network of authors of the paper who could point out the key decision makers in the United Kingdom and Ireland for this research. The writing of this paper was funded by Science Foundation of Ireland’s Centre for Doctoral Training, Energy Resilience in the Built Environment under grant number 18/EP SRC-CDT/3586.

7 REFERENCES

- Alonso, M. J., Mathisen, H. M., & Collins, R. (2015). Ventilative cooling as a solution for highly insulated buildings in cold climate. *Energy Procedia*, 78, 3013–3018.
<https://doi.org/10.1016/j.egypro.2015.11.707>
- Attia, S., Levinson, R., Ndongo, E., Holzer, P., Berk Kazanci, O., Homaei, S., Zhang, C., Olesen, B. W., Qi, D., Hamdy, M., & Heiselberg, P. (2021). Resilient cooling of buildings to protect against heat waves and power outages: Key concepts and definition. *Energy and Buildings*, 239.
<https://doi.org/10.1016/j.enbuild.2021.110869>
- Best Directory | Building Energy Software Tools*. (n.d.). Retrieved March 19, 2023, from
<https://www.buildingenergysoftwaretools.com/>

- Breesch, H., Merema, B., & Versele, A. (2018). Ventilative Cooling in a School Building: Evaluation of the Measured Performances. *Fluids*, 3(4), Article 4. <https://doi.org/10.3390/fluids3040068>
- CEN Technical Bodies—CEN/TC 156/WG 21. (n.d.). Retrieved June 21, 2023, from https://standards.cencenelec.eu/dyn/www/f?p=205:7:0:::FSP_ORG_ID:1206281&cs=156B3B1F2D53C89D0F906AC2FDA64BBEA
- CEN/TC 156/WG 21—Revision of calculation standards EN15241, 15242 and 15243. (n.d.). ITeh Standards. Retrieved June 19, 2023, from <https://standards.iteh.ai/catalog/tc/cen/4c08f95b-c2d2-432c-b38a-dfd4d16c0305/cen-tc-156-wg-21>
- Çevrede, Y., Yönelik, H., Bir, K., & Yaklaşımı, M. T. (2020). A Conceptual Architectural Design Process For Ventilation in Built Environment. *MEGARON*, 15(1), 25–42. <https://doi.org/10.14744/MEGARON.2020.84756>
- CIBSE. (2015). Environmental Design—CIBSE Guide A (8th Edition). *Environmental Design CIBSE Guide A*, 552(F-14), 1–10.
- Darçın, P. (2020). A Conceptual Architectural Design Process For Ventilation In Built Environment. *MEGARON / Yıldız Technical University, Faculty of Architecture E-Journal*. <https://doi.org/10.14744/megaron.2020.84756>
- Freewan, A. A. Y. (2019). Advances in Passive Cooling Design: An Integrated Design Approach. *Zero and Net Zero Energy*. <https://doi.org/10.5772/INTECHOPEN.87123>
- Integrated Environmental Solutions / IES*. (n.d.). Retrieved June 19, 2023, from <https://www.iesve.com/>
- Kolokotroni, M., & Heiselberg, P. (n.d.). *IEA-EBC Programme-Annex 62 Ventilative Cooling Ventilative Cooling STATE-OF-THE-ART REVIEW*.
- O’ Donovan, A., Murphy, M. D., & O’Sullivan, P. D. (2021). Passive control strategies for cooling a non-residential nearly zero energy office: Simulated comfort resilience now and in the future. *Energy and Buildings*, 231. <https://doi.org/10.1016/j.enbuild.2020.110607>
- Our buildings are “wrongly designed,” according to IPCC report author*. (n.d.). Retrieved March 19, 2023, from <https://www.fastcompany.com/90739228/ipcc-report-paints-damning-portrait-of-architecture-our-buildings-are-wrongly-designed>
- Practice Directory / RIAI.ie (The Royal Institute of the Architects of Ireland)*. (n.d.). Retrieved March 19, 2023, from <https://www.riai.ie/work-with-an-architect/find-an-architect/practice-directory/>

- Rahif, R., Hamdy, M., Homaei, S., Zhang, C., Holzer, P., & Attia, S. (2022). Simulation-based framework to evaluate resistivity of cooling strategies in buildings against overheating impact of climate change. *Building and Environment*, 208. <https://doi.org/10.1016/j.buildenv.2021.108599>
- RIBA Plan of Work 2020 Overview RIBA Plan of Work*. (2020). www.ribaplanofwork.com
- Saeid, A., & Mahmoodi, M. (2001). *THE DESIGN PROCESS IN ARCHITECTURE A PEDAGOGIC APPROACH USING INTERACTIVE THINKING*.
- Santamouris, M. (2016). Cooling the buildings – past, present and future. *Energy and Buildings*, 128, 617–638. <https://doi.org/10.1016/J.ENBUILD.2016.07.034>
- Sengupta, A., Steeman, M., & Breesch, H. (2020). Analysis of Resilience of Ventilative Cooling Technologies in a Case Study Building. *ICRBE Procedia*, 1–10. <https://doi.org/10.32438/iCRBE.202041>
- Song, G., Bivolarova, M. P., Zhang, G., & Melikov, A. K. (2022). Control of the bed thermal environment by a ventilated mattress: Human subject response. *CLIMA 2022 Conference*. <https://doi.org/10.34641/clima.2022.415>
- Summary for Policymakers of IPCC Special Report on Global Warming of 1.5°C approved by governments—IPCC*. (n.d.). Retrieved June 22, 2023, from <https://www.ipcc.ch/2018/10/08/summary-for-policymakers-of-ipcc-special-report-on-global-warming-of-1-5c-approved-by-governments/>
- Tavakoli, E., O'Donovan, A., Kolokotroni, M., & O'Sullivan, P. D. (2022). Evaluating the indoor thermal resilience of ventilative cooling in non-residential low energy buildings: A review. *Building and Environment*, 222. <https://doi.org/10.1016/J.BUILDENV.2022.109376>
- The 5 Phases Of The Architectural Design Process, Explained*. (n.d.). <https://www.casaone.com/blog/the-5-phases-of-the-architectural-design-process-explained/>
- The 7 Phases of the Architectural Design Process—2022—MasterClass*. (n.d.). <https://www.masterclass.com/articles/phases-of-the-architectural-design-process>
- The Future of Cooling – Analysis—IEA*. (n.d.). Retrieved March 19, 2023, from <https://www.iea.org/reports/the-future-of-cooling>

Can naturally ventilated office buildings cope with dusty outdoor air?

Evangelos Belias^{*1}, Flourentzos Flourentzou², Dusan Licina¹

1 Human-Oriented Built Environment Lab, School of Architecture, Civil and Environmental Engineering, École Polytechnique Fédérale de Lausanne, 1015 Lausanne, Switzerland

2 ESTIA SA, EPFL innovation Park, 1015 Lausanne, Switzerland

*Corresponding author: evangelos.belias@epfl.ch

ABSTRACT

Naturally ventilated (NV) buildings, when well designed and operated, can provide adequate indoor environmental quality (IEQ) while reducing the building energy demand. However, in dusty outdoor air, this ventilation technique may increase the penetration of outdoor particulate matter (PM) indoors, leading to adverse health effects. Given the increasing frequency of outdoor dust episodes in Mediterranean climates, an important research question is whether NV buildings can provide adequate indoor air quality (IAQ) during increased outdoor air dust episodes. We monitored indoor and outdoor concentrations of size-resolved PM for six months in an occupant-operated NV low-energy office building in Cyprus, an island with frequent episodes of airborne dust. In parallel, the building was monitored for its energy consumption, indoor air temperatures, relative humidity, and CO₂ concentrations. We also interviewed the building occupants regarding their perceived IEQ conditions. The results revealed that the NV provided adequate IAQ conditions in 4 out of 5 investigated indoor spaces for PM_{2.5} and in 2 out of 5 investigated spaces for PM₁₀. The average indoor concentrations were in the range of 4.4-5.1 µg/m³ for PM_{2.5} and 13.8-19.9 µg/m³ for PM₁₀, while the average outdoor concentrations for the same period were 7.4 µg/m³ for PM_{2.5} and 38.1 µg/m³ for PM₁₀. Additionally, unlike the outdoor air, the indoor PM concentrations respected the WHO short-term 24-hour limits, indicating that the building addressed well the dusty days. In terms of other IEQ parameters, the CO₂ levels remained below 1000 ppm for more than 90% of the time, while more than 90% of the occupants were satisfied with the thermal comfort conditions. The final actual energy consumption was ~164 kWh/m²/yr, drifting only by 7% from the predicted energy use. The results of this case study indicated that well-designed low-energy NV office buildings can provide adequate IEQ conditions, even in outdoor environments with dusty air.

KEYWORDS

passive technologies, office buildings, pollution penetration, I/O ratio, climate change

1 INTRODUCTION

Energy-efficient buildings are necessary to limit the energy demand and reduce greenhouse gas emissions globally. Natural ventilation (NV), when adequately designed and operated, can contribute to reducing the operational and grey energy demand in buildings while, in parallel, improving thermal comfort and indoor air quality (IAQ) (Flourentzou et al., 2017). Nevertheless, several studies criticize naturally ventilated buildings for not providing adequate protection to their occupants concerning outdoor air pollution, as the higher ventilation rates

and the absence of filtration increase the penetration of outdoor air pollutants indoors; hence it may lead to a deterioration of the IAQ (Stabile et al., 2017).

Among the various outdoor air pollutants, particulate matter (PM) provokes the most severe health impacts at the commonly-observed exposure concentrations (Logue et al., 2012), being listed among the top 10 risk factors for human health (Gakidou et al., 2017). Additionally, due to climate change, there is an increasing trend in airborne dust levels in the Mediterranean regions (Ganor et al., 2010). As humans spend the majority of their time indoors, they could be exposed to elevated concentrations of airborne dust if no adequate measures are taken in the design and operation of buildings.

Saraga et al. (Saraga et al., 2017) and Katra and Krasnov (Katra & Krasnov, 2020) analyzed the impact of dust episodes on the IAQ of office and residential buildings in the middle east region. Their results indicated that outdoor air is the primary source of indoor PM. However, the existing literature investigating the impact of dusty outdoor environments on IAQ is limited. Specifically, we lack knowledge regarding whether NV is appropriate in such outdoor environments to provide adequate indoor environmental quality (IEQ) conditions at a minimal energy cost.

Given that arid and semi-arid dusty environments cover ~40% of the planet's surface and are the home to ~2.1 billion people (Katra & Krasnov, 2020), this study investigated whether an energy-efficient NV building can provide adequate IAQ in an environment with elevated outdoor air dust levels.

2 METHODS

2.1 Case study building

We conducted measurements in a building located in Cyprus, an island situated in the eastern Mediterranean, which has a semi-arid Mediterranean climate with very mild winters and hot summers (classified as Csa/BSh according to Köppen (Beck et al., 2018)). During the last years and due to climate change, dust episodes coming from North African and Middle Eastern regions have increased (Achilleos et al., 2014).

The examined building (building number 3, as presented in Figure 1) is one of the four buildings of the Nicosia Town Hall complex, which is classified in energy class A according to the local energy performance certificate (EPC), and it can be characterized as low-energy, as it was designed according to the bioclimatic principles. The building hosts offices for administrative employees and is occupied from 7 am to 4 pm on weekdays. The building is not equipped with a mechanical ventilation system but relies on the manual opening of the windows by the occupants to cover its ventilation needs. For heating and cooling, the building is equipped with air conditioning (AC) units in each space that condition the air by recirculating it through the heating and cooling coils without outdoor air ventilation. Additionally, each space in the building is equipped with a ceiling fan to increase thermal comfort during summertime, and there are blinds for solar protection and daylight control. The building users have full control over these elements, being able to open/close the windows, activate/deactivate the AC and adjust its thermostat setpoints, activate/deactivate the ceiling fan, turn on/off the lights, and adjust the solar shading according to their preferences.

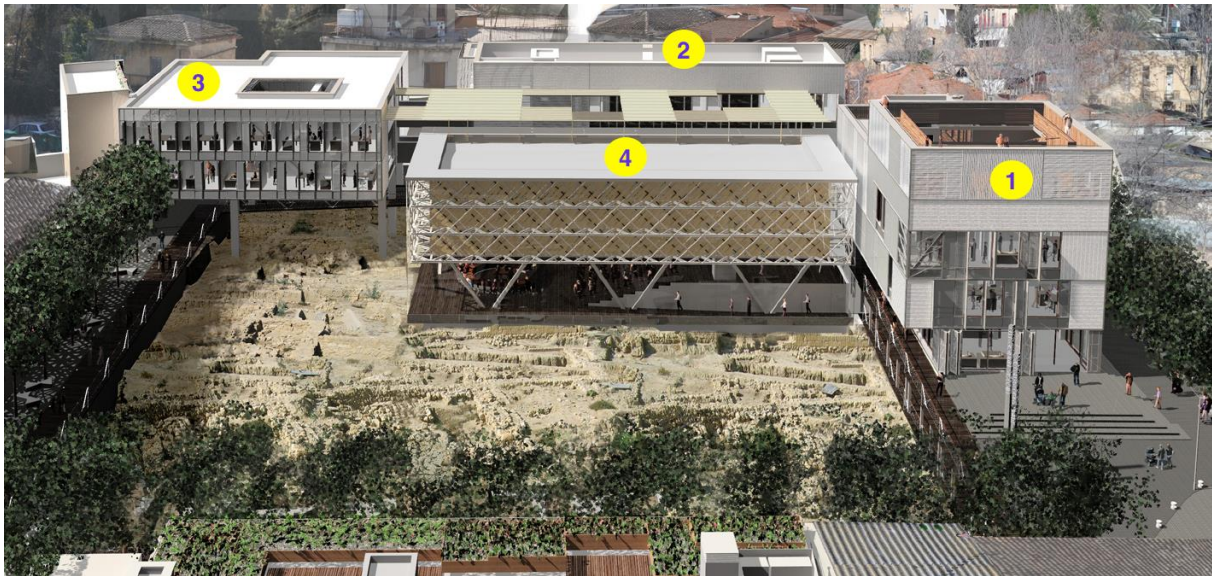


Figure 1: Nicosia Town Hall building complex. The case study building is illustrated under the number 3.

2.2 Monitoring and survey plan

Given that IEQ conditions of the passive buildings differ according to the orientation of the space, we divided the building into four different zones (North, East, South, and Center), as presented in Figure 2, where we placed the IEQ sensors. The monitored parameters were: the indoor air temperature, relative humidity (RH), CO₂, and size-resolved PM concentration. The outdoor environment of the building was also monitored for outdoor air temperatures, RH, and size-resolved PM concentrations. The positions of the sensors are equally shown in Figure 2. In parallel, the total energy consumption of the building was monitored to reveal its actual energy consumption.

The IoT-based NETATMO sensors (*Netatmo*, 2023) were utilized to measure the indoor and outdoor air temperatures and RH as well as the indoor CO₂ concentrations, as their accuracy is satisfactory compared to high-grade instruments (Demanega et al., 2021). For the PM measurements, both indoors and outdoors, it was used the Alphasense OPC-R2 sensors ("Alphasense," 2023), which were tested in a controlled environment and presented satisfactory accuracy for the PM_{2.5} and PM₁₀ concentration measurements compared to high-grade instruments.

To ensure that the sensors monitored the representative IEQ conditions of occupied zones, they were placed between 1.1-1.7 m above the floor and at least 1 m away from doors, windows, and air supply/exhaust of the recirculated air of the AC unit. A pair of indoor PM sensors was placed in the inlet and outlet of an AC unit, which was recirculating the air to condition it in order to monitor the particle arrestance efficiency of its filter. The outdoor PM sensors were placed close to the operable windows to monitor the PM concentration of the air outside the building. The outdoor T and RH sensors were placed under shade on the roof of the building and in the atrium to probe the outdoor weather conditions around the building.

The monitoring of T, RH, and CO₂ took place between April 2021 and December 2022 with a five minutes time step, while the monitoring of indoor and outdoor PM took place between July and December 2022 with a one-minute time step. This period was selected in order to capture how the building operates in the different outdoor environmental conditions of the hot, mid, and cold seasons. All data were post-processed to exclude the non-occupied hours, as our focus was on the IEQ conditions to which the occupants were exposed.

In order to collect feedback from the building users regarding their perception of the IEQ, we interviewed the users by asking them predefined questions, following the procedure described in (Flourentzou, 2022). The interviews included questions about thermal comfort satisfaction during the different seasons, air quality and ventilation satisfaction, as well as acoustic and visual comfort satisfaction to cover the whole spectrum of the IEQ and identify potential problems. Additionally, at the end of the interview, the users were asked about their global satisfaction with the building in order to record how they overall evaluate their IEQ. In total, 16 users working in 6 different spaces were interviewed and provided their feedback.

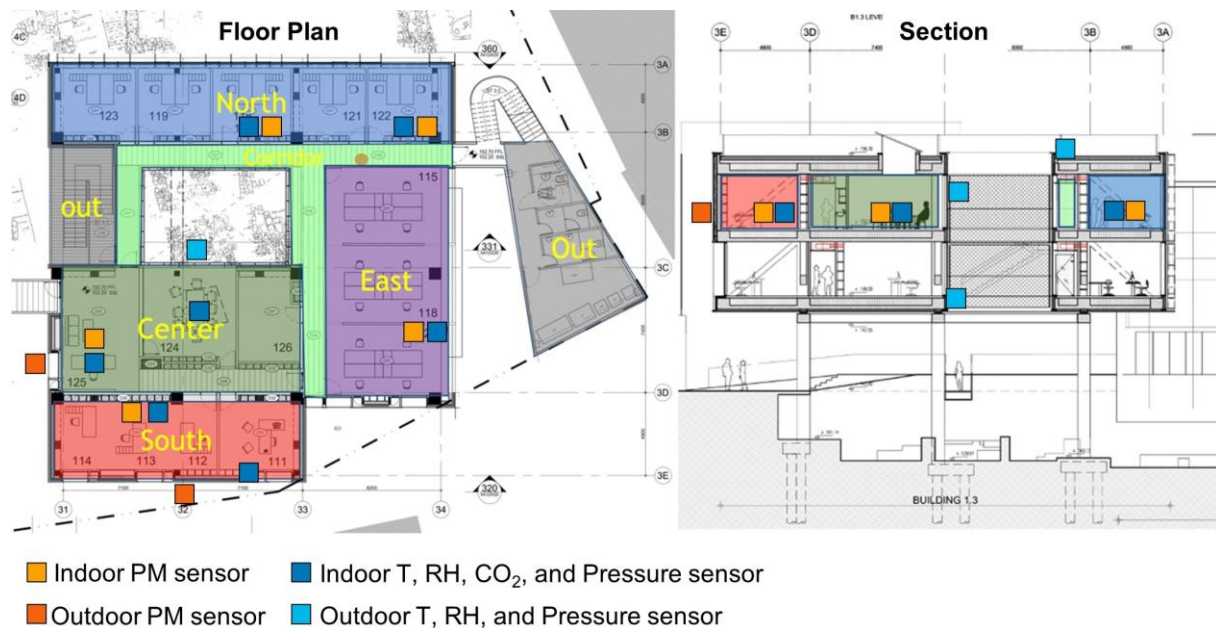


Figure 2: Sensor positions according to the buildings' zones.

3 RESULTS AND DISCUSSION

3.1 Indoor and outdoor PM levels

As presented in **Error! Reference source not found.**, the 6-month average indoor PM_{2.5} concentrations during working hours were between 4.4 and 5.1 $\mu\text{g}/\text{m}^3$ across different office spaces. PM_{2.5} concentrations were in compliance with the WHO air quality guidelines (World Health Organization, 2021) in 4 out of 5 monitored spaces. In the one space where the WHO guideline limit (5 $\mu\text{g}/\text{m}^3$) was not respected, the indoor average PM_{2.5} concentration was slightly above the threshold (5.1 $\mu\text{g}/\text{m}^3$). The average outdoor PM_{2.5} concentration was 7.4 $\mu\text{g}/\text{m}^3$.

The 6-month average indoor PM₁₀ concentrations during working hours were between 13.8 and 19.9 $\mu\text{g}/\text{m}^3$; they presented thus a significant disparity across the different spaces. The PM₁₀ levels complied with the WHO guidelines in 2 out of 5 monitored spaces, as only two spaces respected the annual average concentration limit of 15 $\mu\text{g}/\text{m}^3$. However, the average levels remained below 20 $\mu\text{g}/\text{m}^3$ in all spaces, which was the limit of the previous WHO air quality guideline, indicating generally acceptable PM₁₀ levels. The outdoor average PM₁₀ concentration for the same period was 38.1 $\mu\text{g}/\text{m}^3$.

The higher indoor PM₁₀ that did not respect the limits could be explained by the composition of the outdoor PM, which had high concentrations of coarse particles compared to the fine ones (PM_{2.5}/PM₁₀ ratio \sim 0.2). Additionally, the high indoor PM₁₀ concentrations can be explained

by the resuspension provoked by the activities of the occupants, as no other significant indoor PM source was located in the building.

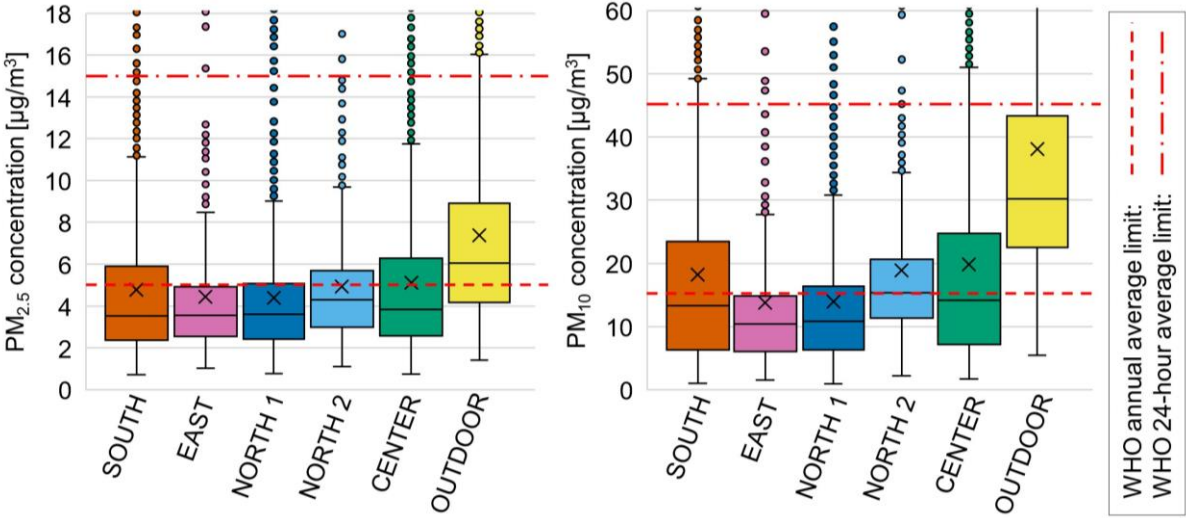


Figure 3: Indoor and outdoor PM_{2.5} and PM₁₀ concentrations during working hours. Note: Box plots indicate the minimum, 1st quartile, mean (black cross), median and 3rd quartile, maximum and outlier values.

Regarding the short-term exposure limits, as presented in Table 1, during the 183 days of monitoring, the outdoor concentrations overpassed the average daily exposure limit of PM_{2.5} (15 µg/m³) for 14 days and of PM₁₀ (45 µg/m³) for 26 days. Additionally, one severe dust episode was observed during the monitored period (daily average PM₁₀ concentration > 100 µg/m³). For the same period, the indoor daily average concentrations of PM_{2.5} overpassed the limit of 15 µg/m³ only three times, while those of PM₁₀ never overpassed the limit of 45 µg/m³. These observations indicate that the building provided satisfactory protection against short-term PM exposures for its occupants even during the days with high outdoor PM levels, as WHO air quality guidelines permit up to three exceedances of the short-term threshold limits per year (World Health Organization, 2021).

Table 1: Number of exceedance of the short-term exposure limits of the WHO guidelines during the 183 days monitoring period.

	Indoor		Outdoor	
	PM _{2.5}	PM ₁₀	PM _{2.5}	PM ₁₀
# of times exceeded the 24h limit:	3	0	14	26

The recirculation of the air through the filters of the AC units had a minor effect in reducing indoor PM, as our measurements revealed that the filters in the AC units had an arrestance efficiency of ~19% for PM₁₀, while the arrestance efficiency for PM_{2.5} was close to 0.

3.2 Hourly PM variation

As presented in Figure 4, the PM levels were not stable during the day. Regarding indoor PM_{2.5} and PM₁₀ concentrations, higher concentrations were observed during working hours (7-16h) compared to non-working hours. These higher concentrations can be explained by two mechanisms: (1) the infiltration of PM from outdoors via the NV, which was only applied during the occupied hours, and (2) the particle resuspension from the occupant activities.

The outdoor PM levels equally presented high variability through the different hours of the day. Outdoor PM_{2.5} and PM₁₀ concentrations were higher during commuting hours (7-9h and 18-21h), indicating a relationship between outdoor PM levels and traffic. The morning PM_{2.5} and

PM₁₀ concentration peaks are also visible in the indoor concentrations. These higher indoor PM concentrations can also be explained by two observations made *in situ*: (1) the occupants' habit of opening the window as soon as they arrive at the office, a time when the outdoor PM_{2.5} and PM₁₀ were high, leading to an increased outdoor PM penetration indoors and (2) the increased resuspension of particles due to occupants' movements during the first working hour. More efficient ventilation that can economize energy without deteriorating IAQ could be achieved by continuously monitoring outdoor air pollution and activating ventilation when indoor and outdoor environmental conditions are favorable (Belias & Licina, 2022, 2023).

The indoor-to-outdoor ratio (I/O) of PM_{2.5} was ~0.4 during unoccupied hours and ~0.7 during occupied hours, while the I/O of PM₁₀ was ~0.2 during unoccupied hours and ~0.5 during occupied. The low I/O ratios indicate that the primary PM source in the building was the outdoor air.

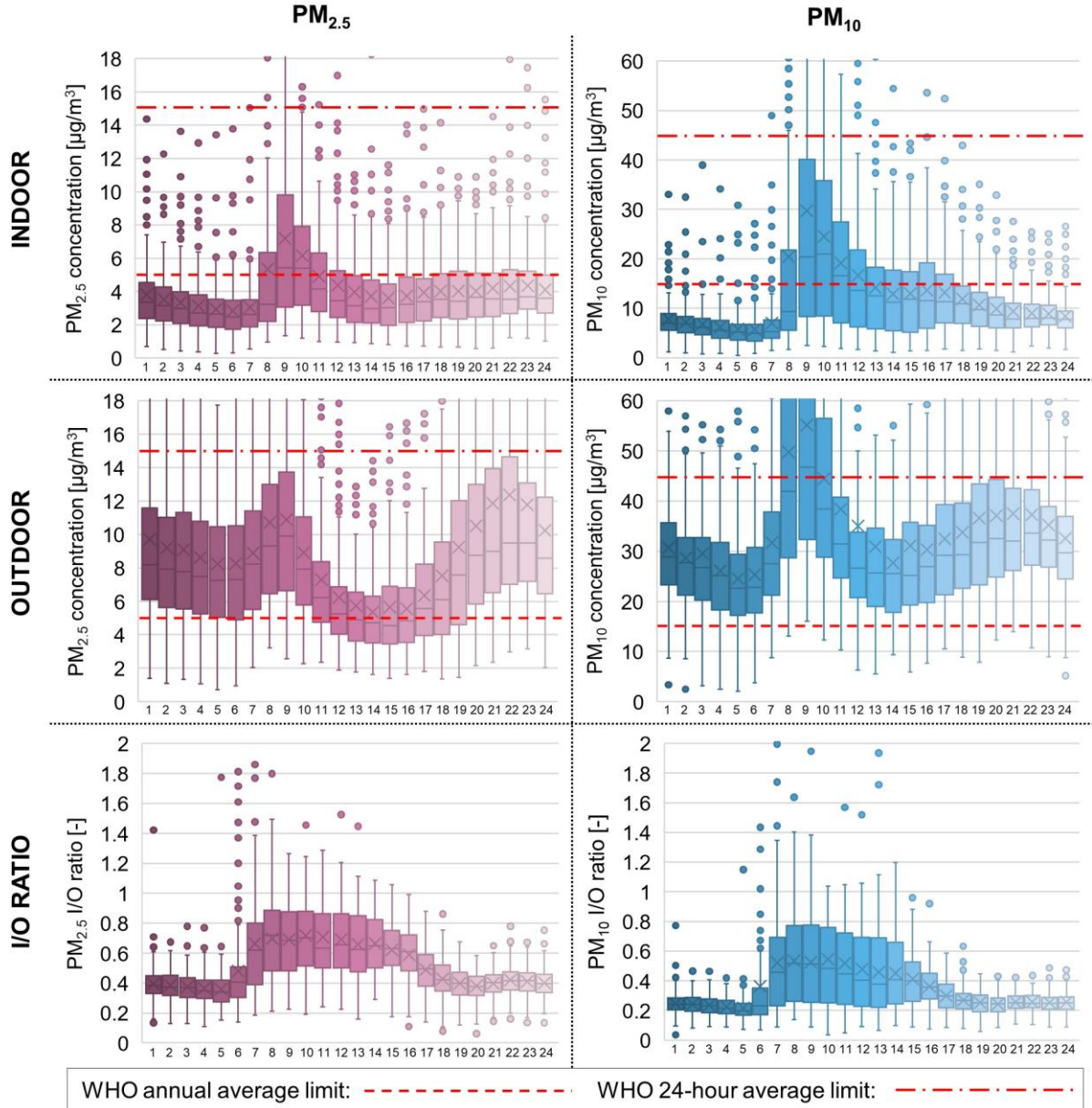


Figure 4: Hourly indoor and outdoor PM_{2.5} and PM₁₀ concentrations as well as hourly indoor to outdoor PM_{2.5} and PM₁₀ ratios.

3.3 Indoor CO₂ levels

The continuous indoor CO₂ monitoring revealed that its concentrations remained below 1000 ppm for more than 90% of the occupied time. Figure 5 presents the CO₂ levels of a typical office, where it can be observed that during the occupied hours, the CO₂ concentrations were between 450 and 1000 ppm for the majority of the time, while on some days, they overpassed the 1000 ppm, but never the 1700 ppm. When the building was unoccupied, CO₂ levels dropped below 450 ppm. These values indicate that the occupant-controlled NV performed as designed, providing sufficient ventilation for the occupants.

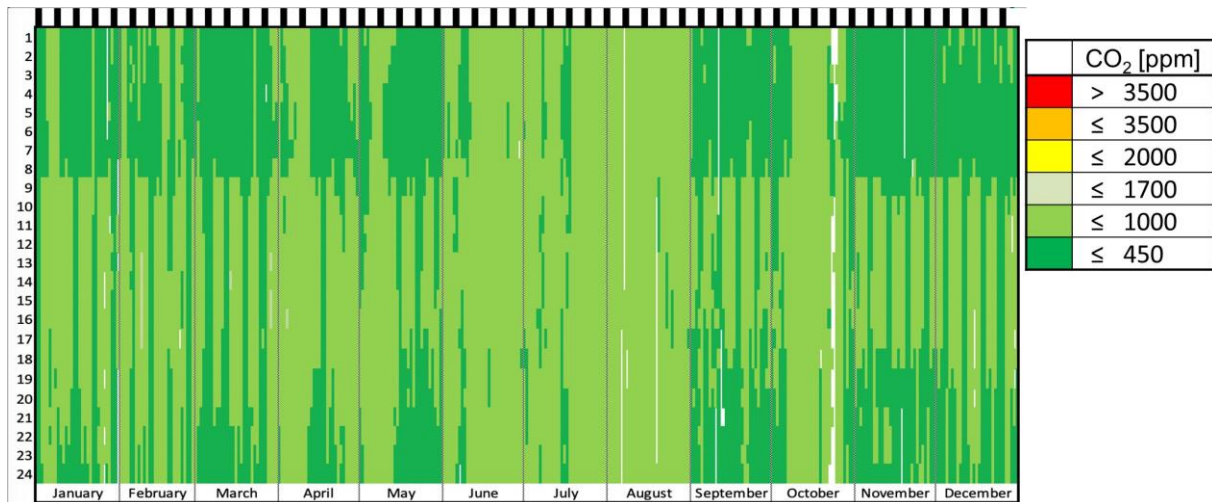


Figure 5: Indoor CO₂ levels in the south zone office. Note: weekends are represented with black on the top of the chart, hours of the day on the y-axis, and the days (grouped by months) on the x-axis.

3.4 Perceived IEQ

The feedback from the users indicated high satisfaction with the thermal environment except for one space, which was located in the northeast corner of the building, where the users reported high thermal discomfort during wintertime. This perception of thermal comfort by the users was in accordance with the measurements, as the temperatures were between the adaptive thermal comfort limits as defined by EN 16798-1 (EN 16798-1, 2019) in all the spaces except for the above-mentioned office space.

All users expressed high satisfaction regarding air quality perception, which is also in accordance with CO₂ measurements, as CO₂ concentrations remained below 1000 ppm for 90% of the occupied time. Additionally, the users reported that they found the indoor air much cleaner than the outdoor concerning the dust.

Additionally, users reported high satisfaction with the visual comfort due to the daylight from the large openings. However, the perceived acoustic quality was average, as the users reported that the sound privacy between the spaces was ineffective. Overall, more than 90% of the interviewed occupants evaluated the IEQ as exceptional and very good.

3.5 Energy consumption

Figure 6 presents the monthly expected energy consumption according to the EPC and the actual measured energy consumption for 2020-2022. The results revealed that in 2020, the building presented a significant performance gap, as it consumed more energy than predicted for several months due to the inadequate maintenance of the AC units, where the unchanged dusty filters led to malfunction and overconsumption (Siegel, 2002). Once the problem was identified and solved, the actual energy consumption was at the same levels as the predicted one, 153 kWh/m²y ±10%, indicating a class A, energy-efficient building for the Cyprus climate.

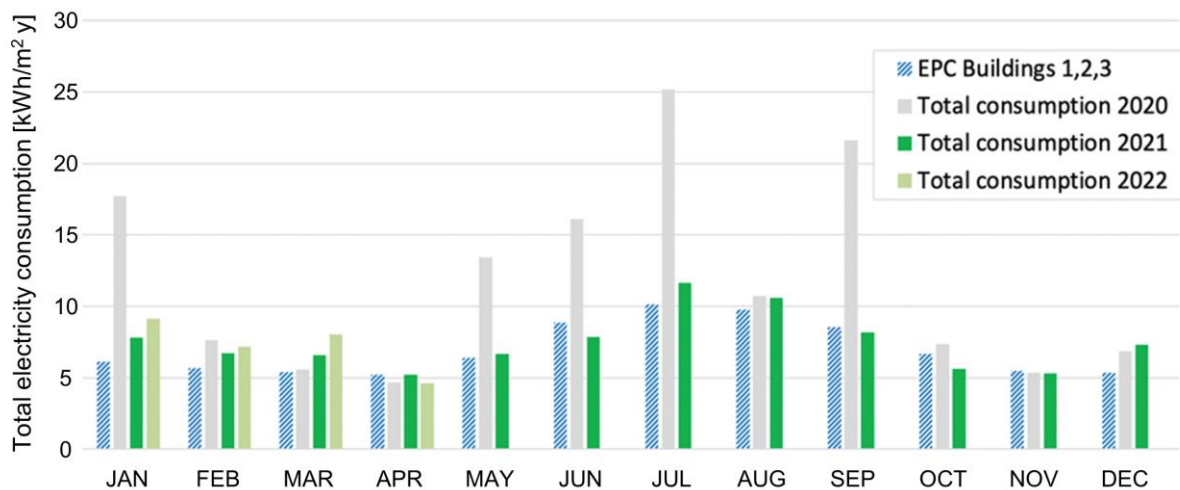


Figure 6: Monthly expected energy consumption according to the energy performance certificate (EPC) compared to the actual energy consumption during 2020-2022 years.

4 CONCLUSIONS

This study conducted measurements and occupant surveys to reveal if a low-energy, naturally ventilated (NV) office building can provide adequate indoor environmental quality (IEQ) conditions in a dusty environment characterized by a semi-arid Mediterranean climate with very mild winters and hot summers.

The results revealed average indoor concentrations during working hours in the range of 4.4-5.1 $\mu\text{g}/\text{m}^3$ for $\text{PM}_{2.5}$, while the outdoor average $\text{PM}_{2.5}$ concentration was at 7.4 $\mu\text{g}/\text{m}^3$. Indoor PM_{10} concentrations ranged from 13.8 to 19.9 $\mu\text{g}/\text{m}^3$ for an average outdoor concentration of 38.1 $\mu\text{g}/\text{m}^3$. The indoor $\text{PM}_{2.5}$ levels complied with the WHO air quality guideline in 4 out of 5 monitored spaces, while PM_{10} levels respected these limits in 2 out of 5 monitored spaces, indicating that the indoor PM levels were generally acceptable. Additionally, the indoor CO_2 concentrations remained below the 1000 ppm limit for more than 90% of the time, indicating acceptable IAQ. User-perceived IEQ was aligned with the measurements, as more than 90% of the interviewed occupants evaluated the IEQ as exceptional or very good, while the building's energy use was low, being an energy class A building. These results support that well-designed and operated energy-efficient NV buildings can provide high IEQ conditions, even in environments with dusty outdoor air.

Further studies are necessary to investigate the impact of different ventilation techniques on the IEQ and energy consumption of offices as well as other building types in environments with dusty outdoor air. These efforts will generate knowledge that will enable more sustainable building design that saves energy while providing high IEQ conditions.

5 ACKNOWLEDGEMENTS

This project has received funding from the European Union's Horizon 2020 Research and Innovation Programme under the Marie Skłodowska-Curie grant agreement number 754354, from the European Union's Horizon 2020 research and innovation programme under grant agreement No. 893945 (E-DYCE) and from EPFL.

6 REFERENCES

Achilleos, S., Evans, J. S., Yiallourous, P. K., Kleanthous, S., Schwartz, J., & Koutrakis, P. (2014). PM_{10} concentration levels at an urban and background site in Cyprus: The

- impact of urban sources and dust storms. *Journal of the Air & Waste Management Association*, 64(12), 1352–1360. <https://doi.org/10.1080/10962247.2014.923061>
- Beck, H. E., Zimmermann, N. E., McVicar, T. R., Vergopolan, N., Berg, A., & Wood, E. F. (2018). Present and future Köppen-Geiger climate classification maps at 1-km resolution. *Scientific Data*, 5(1), 180214. <https://doi.org/10.1038/sdata.2018.214>
- Belias, E., & Licina, D. (2022). Outdoor PM_{2.5} air filtration: Optimising indoor air quality and energy. *Buildings and Cities*, 3(1), Article 1. <https://doi.org/10.5334/bc.153>
- Belias, E., & Licina, D. (2023). Influence of outdoor air pollution on European residential ventilative cooling potential. *Energy and Buildings*, 113044. <https://doi.org/10.1016/j.enbuild.2023.113044>
- Demanege, I., Mujan, I., Singer, B. C., Anđelković, A. S., Babich, F., & Licina, D. (2021). Performance assessment of low-cost environmental monitors and single sensors under variable indoor air quality and thermal conditions. *Building and Environment*, 187, 107415. <https://doi.org/10.1016/j.buildenv.2020.107415>
- Flourentzou, F. (2022). *E-DYCE - D5.3: Nicosia—Cyprus case study report* (PU D5.3). https://edyce.eu/wp-content/uploads/2022/09/E-DYCE_D5.3_Nicosia_case_study-report_31.08.2022_Final.pdf
- Flourentzou, F., Pantet, S., & Ritz, K. (2017). Design and performance of controlled natural ventilation in school gymnasiums. *International Journal of Ventilation*, 16(2), 112–123. <https://doi.org/10.1080/14733315.2016.1220202>
- Gakidou, E., Afshin, A., Abajobir, A. A., Abate, K. H., ... Murray, C. J. L. (2017). Global, regional, and national comparative risk assessment of 84 behavioural, environmental and occupational, and metabolic risks or clusters of risks, 1990–2016: A systematic analysis for the Global Burden of Disease Study 2016. *The Lancet*, 390(10100), 1345–1422. [https://doi.org/10.1016/S0140-6736\(17\)32366-8](https://doi.org/10.1016/S0140-6736(17)32366-8)
- Ganor, E., Osetinsky, I., Stupp, A., & Alpert, P. (2010). Increasing trend of African dust, over 49 years, in the eastern Mediterranean. *Journal of Geophysical Research*, 115(D7), D07201. <https://doi.org/10.1029/2009JD012500>
- Katra, I., & Krasnov, H. (2020). Exposure Assessment of Indoor PM Levels During Extreme Dust Episodes. *International Journal of Environmental Research and Public Health*, 17(5), 1625. <https://doi.org/10.3390/ijerph17051625>
- Logue, J. M., Price, P. N., Sherman, M. H., & Singer, B. C. (2012). A Method to Estimate the Chronic Health Impact of Air Pollutants in U.S. Residences. *Environmental Health Perspectives*, 120(2), 216–222. <https://doi.org/10.1289/ehp.1104035>
- Netatmo. (2023). Netatmo. <https://www.netatmo.com/smart-weather-station>
- Particulate Matter Sensors | PM Sensor. (2023). *Alphasense*. <https://www.alphasense.com/products/optical-particle-counter/>
- Saraga, D., Maggos, T., Sadoun, E., Fthenou, E., Hassan, H., Tsiouri, V., Karavoltos, S., Sakellari, A., Vasilakos, C., & Kakosimos, K. (2017). Chemical Characterization of Indoor and Outdoor Particulate Matter (PM_{2.5}, PM₁₀) in Doha, Qatar. *Aerosol and Air Quality Research*, 17(5), 1156–1168. <https://doi.org/10.4209/aaqr.2016.05.0198>
- Siegel, J. (2002, August 18). Dirty Air Conditioners: Energy Implications of Coil Fouling. *Proceedings of the ACEEE Summer Study on Energy Efficiency in Buildings*.
- Stabile, L., Dell’Isola, M., Russi, A., Massimo, A., & Buonanno, G. (2017). The effect of natural ventilation strategy on indoor air quality in schools. *Science of The Total Environment*, 595, 894–902. <https://doi.org/10.1016/j.scitotenv.2017.03.048>
- World Health Organization. (2021). *WHO global air quality guidelines: Particulate matter (PM_{2.5} and PM₁₀), ozone, nitrogen dioxide, sulfur dioxide and carbon monoxide*. World Health Organization. <https://apps.who.int/iris/handle/10665/345329>

Distribution of Particulate Matter Concentration and Temperature Stratification Examined by Zonal Model and Experimental Measurements in Room with A Novel Portable Displacement Ventilation Cooling Unit

Toshio Yamanaka^{*1}, Choi Narae², Tomohiro Kobayashi³, Aya Essa³, Noriaki Kobayashi³, Miharuru Komori⁴, Nobuki Matsui⁵, Tetsuya Okamoto⁵, Takeshi Arakawa⁵, Yuki Yamoto⁵, and Shogo Otaka⁵

*1 Osaka University
2-1 Yamadaoka
Suita-shi, Osaka, Japan
yamanaka@arch.eng.osaka-u.ac.jp*

*2 Toyo University
2100 Kujirai
Kawagoe-shi, Saitama, Japan*

*3 Osaka University
2-1 Yamadaoka
Suita-shi, Osaka, Japan*

*4 Nihon Sekkei
1-23-1 Toranomon
Minato-ku, Tokyo, Japan*

*5 Daikin Industries, Ltd.
1-1 Nishihitotsuya
Settsu-shi, Osaka, Japan*

ABSTRACT

This study introduces a novel conceptual design of a mobile DV cooling unit that is aimed to support the ventilation and reinforce the thermal stratification in DV rooms. Supplying filtered chilled air from at low height, the portable DV unit (PDV unit) functions as if it is a typical DV diffuser. Moreover, the PDV unit employs heat exhausted from the heat pump to reinforce the temperature gradient by injecting the hot air flow in the upper zone of the room. Utilizing the exhaust air makes the PDV unit entirely ductless which adds to its flexibility placed in to balance the airflow. In this study, the vertical distribution of particulate matter and temperature stratification were examined by zonal model and experimental measurements in room with this novel portable displacement ventilation cooling unit. As a conclusion, from the experiment, DV capacity of PDV unit was turned out, and the effects of airflow rates of DV and PDV unit on the performance were made clear.

KEYWORDS

displacement ventilation, portable displacement ventilation cooling unit (PDV unit), zonal model, full-scale experiment, droplet nuclei

1 INTRODUCTION

Displacement Ventilation (DV) system (Nielsen, 1993) is an energy efficient ventilation system that can achieve a cleaner occupied zone compared to the regular Mixing Ventilation(MV). DV depends mainly on temperature stratification to clarify the lower occupied zone from contaminants, thus, increasing the temperature gradient results in a more efficient system. However, since DV relies on buoyancy and low velocity supply, any disturbance in the slow air flow reduces its efficiency. For example, obstacles blocking the flow can cause dead-zones of low-quality unchanged air. Another issue that can affect the

local air quality of certain zones in the room is the unbalanced heat load. These problems hinder DV system from being adopted widely despite its advantages.

In this study, the effectivity of the novel PDV unit was assessed in terms of temperature and PM distribution. Zonal model calculation and experimental measurements were carried out for this purpose. First, in the zonal model, only the thermal effect of the PDV unit was formulated. A parametric study exploring the effect of multiple variables was carried out. Secondly, field measurement was performed in which a prototype model of the PDV unit was built and operated. In the experimental measurements, the effect of various parameters was assessed by monitoring both temperature and particulate matter concentration distribution. Based on the zonal model calculations, the PDV unit's settings in the experiment were set.

2 CONCEPT OF PDV UNIT

To enhance the performance of DV system, this study addresses three points discussed by the aforementioned literature: 1- Diffusers positioning, to overcome unbalanced supply due to room shape, size or occupants seating pattern. 2- Strengthening the temperature stratification to improve the air quality and comfort of the occupied zone. 3- Integrating portable air purifiers.

To tackle the potential enhancement points, a novel air purifier unit that functions as a portable DV system is proposed. Although close ideas of merging portable air-conditioning units and air purifiers have investigated in some studies (Zhang, 2010), no similar one unit has been proposed so far, especially in DV system. The proposed machine should function as a mobile DV diffuser. It consists of a heat pump with no ducts to be connected to outdoor. Being ductless, the exhaust heat is discharged in the room to act as an additional heat source to enhance the temperature vertical stratification. Mimicking a typical DV system, supply diffuser is in the lower section of the unit while the suction port in the top section as shown in Fig. 1a. The suction port provides air for both function, cooling and exhaust heat. Moreover, to function as standalone DV system, air filters such HEPA filters function should be added to purify the return air. Placement and functioning method of the portable DV unit (PDV unit) are illustrated in Fig. 1b.

The concept of the PDV unit is examined using zonal model calculations and experimental measurements. In the following sections both methods' details and results are discussed.

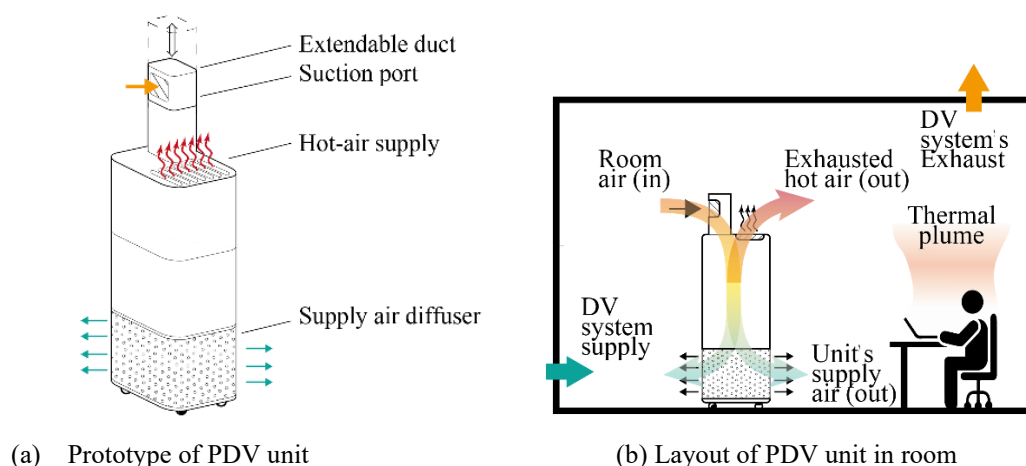


Figure 1: Outline of PDV unit

3 ZONAL MODEL

3.1 Outline of zonal model of the room with DV and PDV unit

Zonal model calculations were used in various studies to predict the thermal as well as contaminant environment in DV and other ventilation systems.

In this calculation, the basic two-layer model illustrated in Fig. 2 was adopted and the PDV unit effect was formulated in the adapted zonal model. The model assumes stratification in two layers and neglects radiation from the different surfaces as shown in Fig. 2. The thermal balance for the upper and lower zones is given by equations (1)-(2).

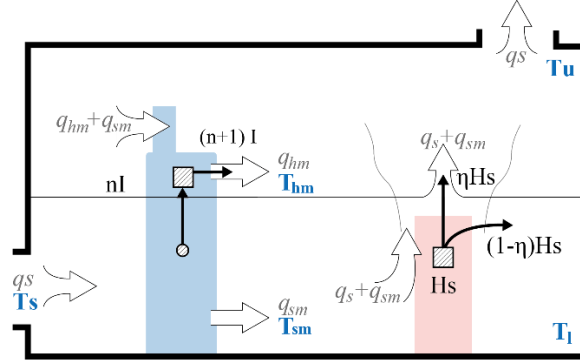


Figure 2: Zonal Model of DV room with PDV unit

For upper zone, the following balance equation of the heat can be written :

$$(n+1) I + \eta H_s + C_p \rho (q_s + q_{sm}) T_l - C_p \rho q_s T_u - C_p \rho q_{sm} T_u = 0 \quad (1)$$

For lower zone, the following equation can be written :

$$C_p \rho q_{sm} T_u - nI + (1-\eta) H_s + C_p \rho q_s T_s - C_p \rho (q_s + q_{sm}) T_l = 0 \quad (2)$$

PDV unit's cooling capacity and exhaust heat generation are shown in equations (3) and (4) respectively.

$$nI - C_p \rho q_{sm} (T_u - T_{sm}) = 0 \quad (3)$$

$$(n+1) I - C_p \rho q_{hm} (T_{hm} - T_u) = 0 \quad (4)$$

where for the DV system, q_s is the supply flowrate and T_s is the supply temperature. For the room, T_u and T_l are the air temperature of upper and lower sections respectively. C_p stands for specific heat of air (1004 J/K.kg) while ρ is the air density (1.2 kg/m³). Representing heat sources in the room, human and computer devices, H_s is the heat load generated and η is the ratio of the heat that ascends to the upper part of the room assumed to be 1. Regarding the PDV unit, n is the unit's coefficient of performance (COP), I is the input power (W), q_{sm} and q_{hm} are the machine's supply flowrate and hot air flow rate respectively. T_{sm} and T_{hm} are the supply temperature and hot-air temperature respectively.

3.2 Parametric analysis

In this single-factor analysis, some of the DV system and PDV unit specifications were changed to study the effect of each variable on the unit's performance and the room temperatures. In all cases, the assumed values are input to equations (1)-(3) to be solved simultaneously, then the resultants were used to calculate the hot air temperature using equation (4). Table 1 summarizes the set of values used in the study. The factors studied in this section are:

Cases-A: PDV unit's COP, varying from 3.0 to 4.0,

Cases-B: PDV unit supply flowrate, varying from 100 m³/h to 300 m³/h, at fixed DV flowrate,
 Cases-C: DV supply flowrate, varying from 100 m³/h to 300 m³/h, at a fixed PDV unit flowrate,
 Cases-D: PDV unit hot air flowrate, varying from 100 m³/h to 300 m³/h.

Table 1: Cases of parametric study by zonal model

		Cases-A	Cases-B	Cases-C	Cases-D
DV	q_s (m ³ /h)	200	200	300 -100	200
	T_s (°C)	20			
COP, n		3.0 – 4.0	3.5	3.5	3.5
I (W)		Dependant			
PDV unit	q_{sm} (m ³ /h)	200	100 – 300	200	200
	q_{hm} (m ³ /h)	= q_{sm}	= q_{sm}	= q_{sm}	100 – 300
	T_{sm} (°C)	20			
	T_{hm} (°C)	Dependant			

The results of the zonal model calculation of Cases A-D are plotted in this section. It should be noted that in all cases, since the idea situation of $\eta =1$ is assumed, the occupied zone temperature, T_i , is constant at 20 ° C, equal to the supply temperature.

1) PDV unit Coefficient of performance

Calculations of increasing the unit's COP from 3 to 4 at constant supply flowrate and temperature were carried out, Cases-A. From Fig. 3a, the increase in COP is seen to enhance the performance by decreasing the exhausted heat as can be. Increasing the COP from 3 to 4 reduces the required input power by a third to provide a fixed flow rate at a fixed supply temperature, as shown in Fig. 3b.

2) PDV unit supply flowrate at fixed DV flowrate

As shown in Fig. 3c and Fig. 3d, calculations with q_{sm} varying from 100 m³/h to 300 m³/h were performed, Cases-B. The 100 m³/h case requires a relatively small wattage of around 20 W. It can be observed as well that increasing the flow volume requires a steep increase in the input power of the machine. Increasing I, thus, results in exhausting air at higher temperature (T_{hm}).

3) DV flowrate at fixed PDV unit supply flowrate

Decreasing the DV supply flowrate is intended to investigate the PDV unit input power needed to compensate. As shown in Fig. 3e, the relation is exponential. At q_s 100 m³/h where the DV supply flowrate was lowest, the input power required for the PDV unit to compensate was more than 3 times that of q_s 200 m³/h. This increase in I was reflected in the hot air temperature and upper zone temperature as shown in Fig. 3f. Since T_u increased to 40 ° C making the difference between the upper and lower zone temperatures 20 ° C, this shows that the PDV unit compensation capacity is bound by the temperature difference comfort between head and feet height. However, the PDV unit location, although not represented in the zonal model, might be a major factor in this aspect.

4) PDV unit hot air exhaust flow rate

The relation between hot air flow rate and temperature is given by equation (4). For a fixed case-D, q_{hm} varying were used to calculate the hot air temperature. Fig. 3g shows that

increasing the flow rate from 100 to 300 m³/h can decrease the temperature by 10 ° C. However, the effect of this variable especially, needs to be investigated using CFD analysis or experiment measurements as the flowrate of hot air can highly affect the temperature horizontal distribution and generally the DV induced stratification.

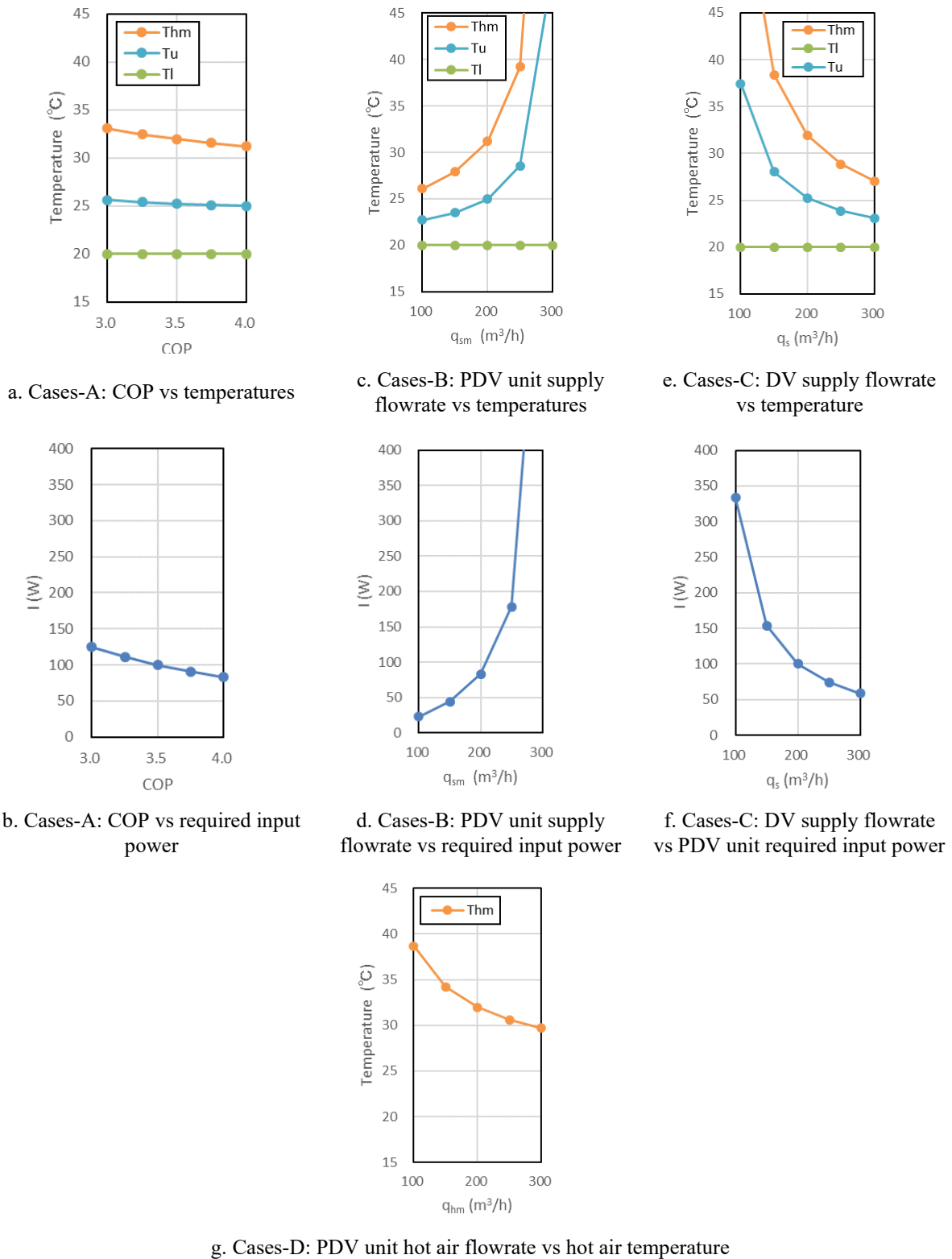


Figure 3: Relationship between PDV unit parameters (COP, PDV unit supply airflow rate, DV supply airflow rate, PDV unit hor airflow rate) and temperatures, required input power etc.

4 EXPERIMENT

4.1 Experiment room

The measurements were carried out in the period of January 26 – February 7, 2023 in a full-scaled experimental chamber made in Osaka University. This experimental room was built of insulated wooden boards. As annotated in Fig. 4, the room dimensions are 2.84 m * 2.34 m * 3.00 m, which is relatively small.

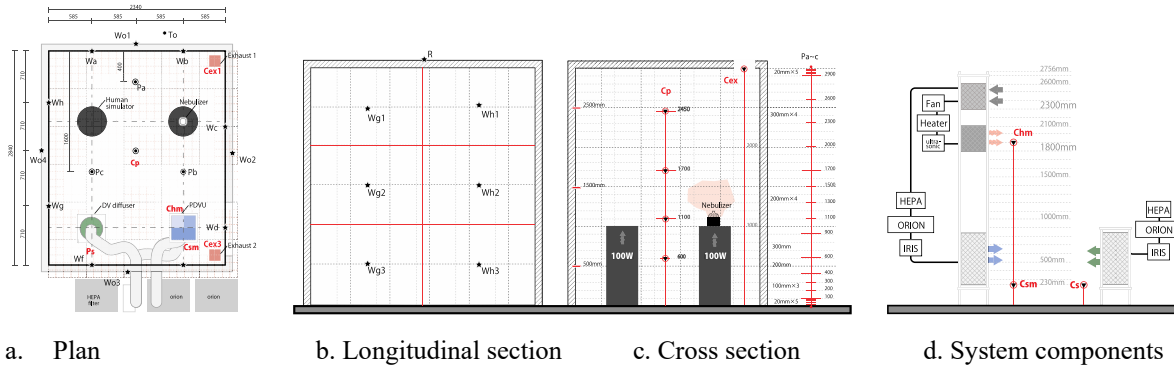


Figure 4: Experiment room and measurement points

4.2 Equipment

The PDV unit was not built as an intact one unit as designed, but broken down into its basic components with the same function as PDV unit as shown in Fig. 4d. All equipment was placed outside the room, only the diffusers, suction port, and hot-air inlet were placed inside the room.

The PDV unit components were fixed into a 2.7 m high metal frame. The suction port is 0.3 m size cube intaking air from three sides, top and bottom sides are solid while the remaining face is where the ducts were connected. The suction port is connected by 12.5 cm wide ducts to two paths; cooling and heating. The cooling and filtration function was achieved using air processor (AP-750M-C, Orion Machinery Co., Ltd.) connected to HEPA filter. Chilled and filtered air flow through the inlet duct was connected to a fabric duct to act as a circular diffuser for DV, 0.6 m high and 0.3 m in diameter. A similar arrangement was used for the room's DV system. As for the heating function, duct fan (FY-23DZ4, Panasonic) and duct heater (DM-11N, Nippon Heater Co., Ltd.) were used. The heated air flows through a 0.3 m * 0.3 m cylindrical fabric duct. The supply air flow from both DV and PDV unit are controlled by Iris dampers and monitored by low differential pressure transducer (DP-45, Validyne Engineering). The hot-air flow was monitored by ultrasonic flow meter (TRZ150D-C, Aichi Tokei Denki) connected to current data logger (RTR-505, T&D Co., Ltd.). All ducts of the system were glass fibre insulated, and the openings in the walls were tightly sealed.

Representing seated occupants as heat source, two cylindrical person simulators were operated at 100 W each, controlled by voltage regulators and monitored by watt meters. Each person simulators is 1.00 m high and of a diameter of 0.40 m. They were placed over an insulative-5 cm-foam disc in locations indicated in Fig. 4a.

Temperature was measured using T-type thermal couples connected to CADAC-3 data logger (Eto Electric Co.). The measurement points are indicated in Fig. 4a and Fig. 4b. For surface temperature, Wa1~Wh3 stand for walls inner surface points, Wo1~4 stand for the outer surface points, and R stands for the roof surface point. To measure the vertical temperature distribution in the experiment room, 22 points at each pole, Pa-c were measured. The floor and ceiling surface temperature was measured at the same poles. The surface

temperature of one heat simulator was measured as well. In addition, the air temperature of the PDV unit's supply diffuser, hot air diffuser, and suction port were measured as well as the DV supply and the exhaust temperatures. The temperature outside the experimental chamber and inside the experiment building was monitored at point To.

The contaminant simulated in this experiment was coughing droplets. Artificial saliva was prepared with 12 g salt (NaCl) and 76 g glycerine for 1 litre of distilled water. The droplets were produced by nebulizer (NE-C801, OMRON Healthcare, Inc.) and the emission rate was controlled by setting the gas flow to 2 NL/min. N₂ gas was chosen as its density is almost the same as that of air. In order to have a distributed emission, rather than a stream of droplets, the nebulizer was covered by a plastic bottle made of PET that has many holes with 0.5 mm diameter in its upper part. The bottle was heated by a bottle warmer (12.3 W) wrapped around it in order to prevent condensation and to raise the temperature of the droplet emission.

The droplets were measured using handheld particle counters (RION and Kanomax) fixed at Pd at heights 0.9 m, 1.1 m, and 1.7 m. In addition to 2.45 m which matches the suction port height. Measurements of the exhaust opening were taken as well. In addition, to confirm the supply air filters, particles count at both supply diffusers and hot-air supply were monitored.

4.3 Cases and parameters

The parameters investigated in this study were the supply flowrate of DV and PDV unit. The supply flowrate of both DV and PDV unit was tried with three variations 200 m³/h, which is 100 m³/h for one person, and one lower and one higher flowrate, 100 m³/h and 300 m³/h. The hot air flowrate was set constant to 200 m³/h regardless of the supply flowrate.

A total of 7 cases carried out are summarized in Table 2. The cases can be divided into 3 groups according to the comparative parameter. Group 1 shows the effect of changing PDV unit supply flowrate at a constant DV unit flowrate. Group 2 is a comparison between different DV supply flowrate at a constant PDV unit supply of 200 m³/h. Viewing the PDV unit as a complementary ventilation system, Group 3 compares all cases with a total supply flow rate of 200 m³/h.

As shown in Table 2, the case naming includes the system running, DV for the displacement ventilation supply, and PU is short for the PDV unit. Each system abbreviation is followed by the supply flowrate value. Here Ex1 is the name of exhaust position on the ceiling as shown in Fig.4a as Exhaust 1. (Ex2 is not listed.)

Table 2: Experiment cases

Case number	Case name*	DV supply flow rate q_s [m ³ /s]	PDV unit supply flow rate q_{sm} [m ³ /s]	DV supply flow rate q_s [m ³ /s]
1	DV200	200	0	200
2	DV200_PU100	200	100	200
3	DV200_PU200	200	200	200
4	DV200_PU300	200	300	200
5	DV100_PU200	100	200	100
6	DV100_PU100	100	100	100
7	PU200_EX1	0 (No ventilation)	200	0 (No ventilation)

*DV means Displacement Ventilation and PU means PDV unit

4.4 Measurement method

Data recordings were taken at a one-minute interval. The timeline of the measurement is illustrated in Fig. 5. The ventilation system was switched on and the temperature recordings were continued until steady state was reached, which took about 2.5 hours. Afterwards, the

nebulizer was turned on for one hour. After stopping the emission, the particles count at the exhaust was monitored until it decreased back to the background count. The emission stage was run for 2 rounds with the particle counters fixed at different heights. Finally, the ventilation system was switched off. A sample of 30 minutes in which both temperature and particles distribution were at steady state was taken for data analysis. Variation in the rounds particle count is shown in Fig.5 in the case 2 (DV200_PU200). The count variation of the exhaust air shows the unstable emission rate of nebulizer. It can be said that the absolute value of the concentration data could have deviation due to time variation of emission rate of the nebulizer.

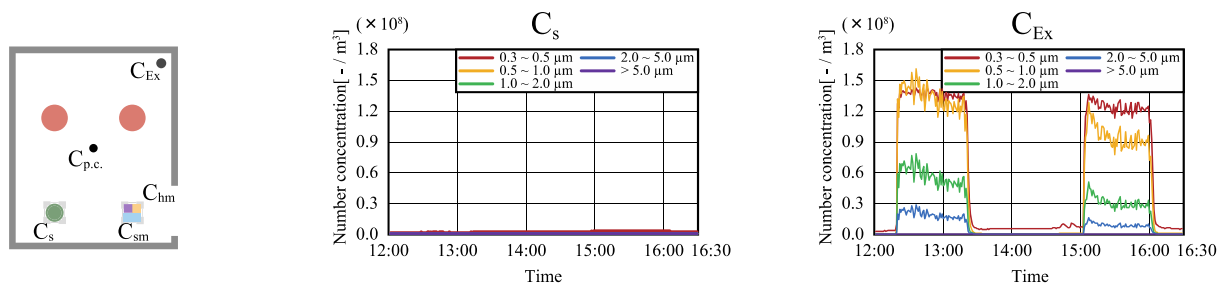


Figure 5: Variation of droplet count (Case 2 : DV200 - PU200)

5 RESULTS AND DISCUSSION

5.1 Temperature stratification

Group 1: Varying PDV unit's supply flowrate (q_{sm}) (Fig.6a)

To investigate the effect of operating the PDV unit in the room, cases of varying PDV unit supply flowrate 0 ~ 300 m³/h at constant DV flowrate are compared in Fig.6a. Comparing the cases, it can be observed that cases with PDV unit have a stronger temperature stratification. The larger PDV unit flowrate is the lower the overall temperature and especially the upper temperature peak becomes.

Group 2: Varying DV supply flow rate (q_s) (Fig.6b)

Decreasing the DV supply flowrate from 200 m³/h to 100 m³/h did not cause a major shift in the temperature curve. However, since these cases had the PDV unit in operation, it can be assumed that the PDV unit mitigated the decrease effect. Turning the DV off on the other hand, caused an increase in temperature ranging from 1 to 2°C with a stronger temperature stratification.

Group 3 Varying total flowrate ($q_s + q_{sm}$) (Fig.6c)

DV200 case displayed the lowest temperature in the upper zone. PU200 case and DV100_PU100 case showed very close results.

5.2 Particles distribution

The vertical distributions of particle concentrations in each case are shown in Fig.7. The data connected by lines are at the point of C_p in Fig.4a, and the isolated plot at the height of 1.9 m shows the concentration at the hot air supply port. This hot air is originally extracted at 2.45m+FL and heated but not filtered by HEPA. In the case of DV only (Case 1), data is not plotted, as this PDV unit is not operating.

Group 1: Varying PDV unit's supply flowrate (q_{sm}) (Fig.7a)

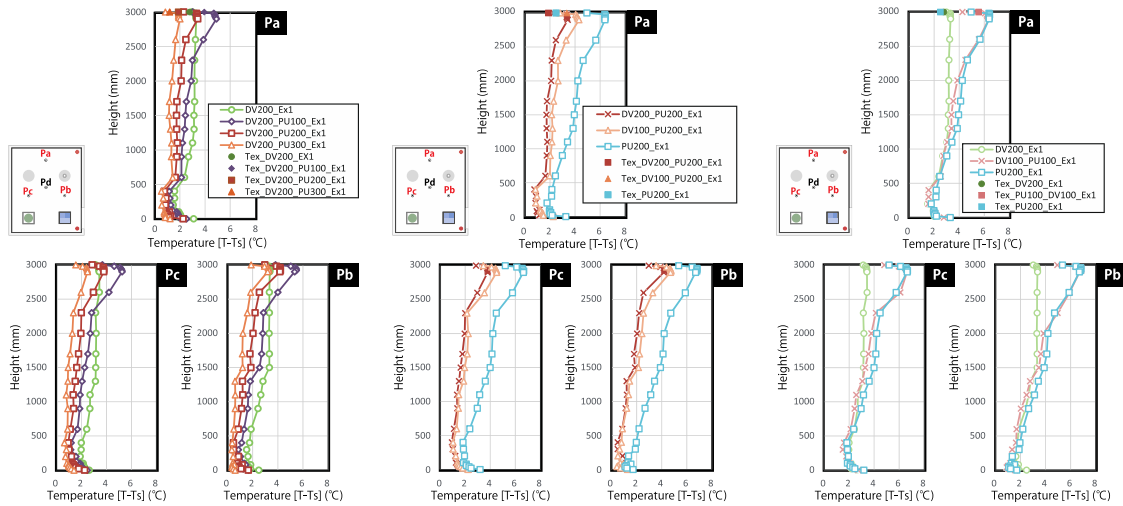
Although increasing the unit's flowrate from 100-200 m³/h caused a matching reduction of the particle count, but increasing the supply airflow rate of PUV unit has no essential effect on the particulate concentrations.

Group 2: Varying DV supply flow rate (q_s) (Fig.7b)

Decreasing the DV airflow rate had the foreseen effect of increasing the particle count and volume concentration. The increase was not confined to the higher heights and extended to the 1700 mm height. Lower heights had almost no particles even with the DV turned off, so the PDV unit has the distinct effect on the cleaning air in occupant zone and advantage of stability caused by the strong temperature stratification.

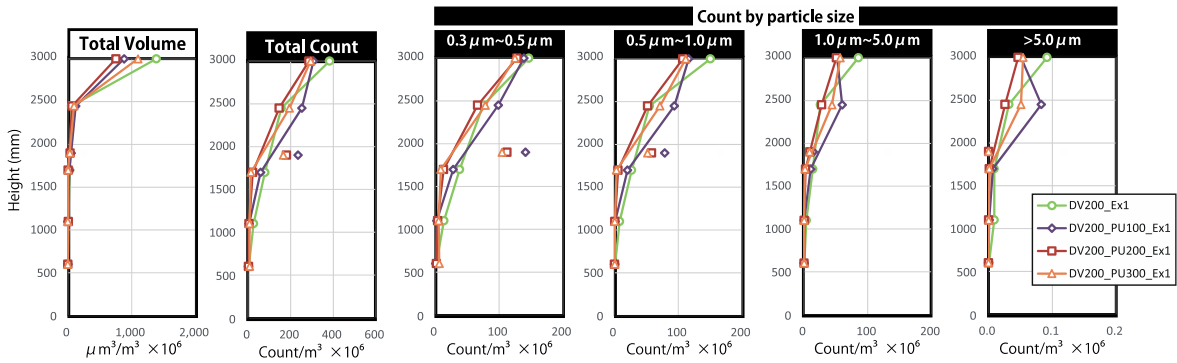
Group 3: Varying total flowrate (qs+ qsm)(Fig.7c)

Agreeing with the temperature profiles, the effect of compensating the reduction in DV airflow rate by the PDV unit airflow rate was dependent on the total airflow rate value. As shown in Fig. 7c, reducing DV airflow rate at the $q_{total}=200 \text{ m}^3/\text{h}$ causes an increase in the top zone particle count and volume. It can be said that DV is more effective than the PDV unit if the airflow rate is the same, but PDV unit has high capacity of air purification of the air in the occupancy zone.

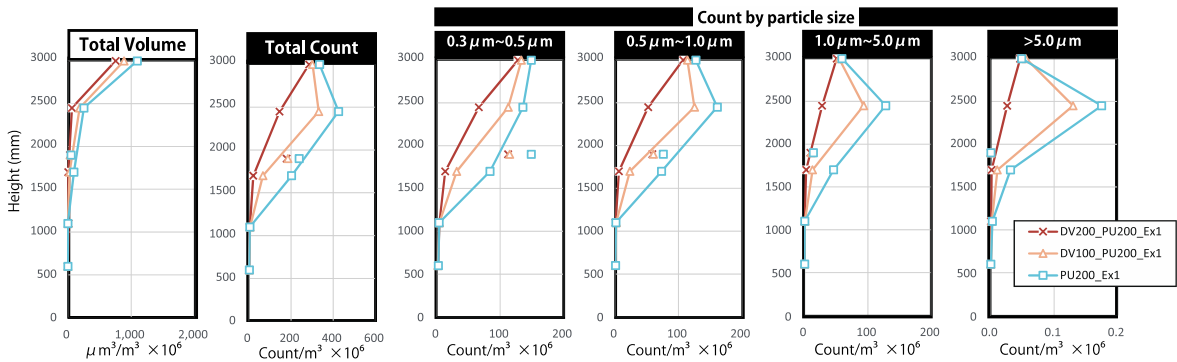


a.Group-1 (varied PDV unit supply) b.Group-2 (varied DV supply) c. Group-3 (varied supply combination)

Figure 6: Temperature Stratifications in each Group of cases



a. Group-1 (varied PDV unit supply)



b. Group-2 (varied DV supply)

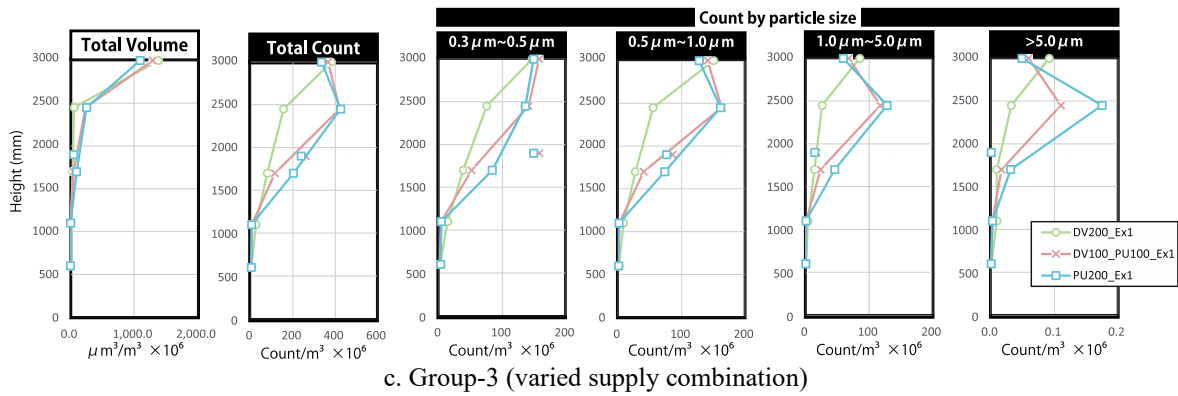


Figure 7: Vertical distributions of particle concentration (Total Volume, Total Count, Count of each particle size)

5.3 PDV unit capacity

Since the PDV unit was operated using separate systems, the heating and cooling capacities at each case were calculated using equations (3) and (4). The results are in Table 3. Q_{sm} is the cooling capacity, and Q_{hm} is the heating capacity.

The calculation shows that despite setting the heater's power Q_{hm} to 450W and monitoring it using the watt meter, the actual heat gain was not constant in all cases. Most of the cases had a lower heating capacity. Reviewing the temperature readings in Table 3, it can be noticed that the outside temperature T_o was below the supply air temperature which means that given the long ducts connections, heat seems to have been lost before arriving at the hot air supply port.

Table 3: Temperature, flowrates and PDV unit capacity by case (unit: [°C], [m³/h], [W])

Cases	T_o	T_s	T_{sm}	T_{hm}	T_u	T_{ex}	T_{Hs}	T_l	q_s	q_{sm}	q_{hm}	Q_{sm} equation (3)	Q_{hm} equation(4)
DV200_	-1.05	0	-	-	2.89	2.77	9.66	2.68	198	0	0		
DV300_	0.34	0	-	-	2.89	2.77	9.3	2.54	309	0	0		
DV200_PU100	-1.08	0	-0.21	12.19	6.03	3.94	9.37	2.13	194	104	200	217	411
DV200_PU200	-3.37	0	-0.46	10.3	5.4	1.88	8.95	1.75	193	193	201	379	329
DV200_PU300	-1.97	0	-0.54	10.07	3.9	1.18	8.35	1.31	189	288	197	428	407
DV100_PU200	-0.76	0	-0.56	11.05	4.15	3.35	9.13	2.04	119	200	196	316	454
DV100_PU100	-1.43	0	-0.35	12.83	6.62	5.54	9.38	2.73	108	98	201	228	417
PU200	2.02	-	0	13.36	7.63	-	9.86	3	0	199	201	507	385

6 CONCLUSION

From the experiment, DV capacity of PDV unit was turned out, and the effects of airflow rates of DV and PDV unit on the performance were made clear, and the zonal model is quite useful to know the mutual effect of various parameters.

7 REFERENCES

- Nielsen, P. V.(1993). *Displacement Ventilation*. Dept. of Building Technology and Structural Engineering, Indoor Environmental Engineering, No. 15
- Zhang, T. (Tim), Wang, S. , Sun, G., Xu, L., Takaoka, D. (2010). Flow impact of an air conditioner to portable air cleaning, *Building Environment*, 45, 2047–2056. doi:10.1016/j.buildenv.2009.11.006

Thermal comfort and risk of draught with natural ventilation - assessment methods, experiences and solutions

Jannick Roth^{*1}, Per Heiselberg^{*2}, Chen Zhang^{*2}

*1 WindowMaster International A/S
Skelstedet 13
2950 Vedbæk, Denmark*

*2 Aalborg University
Thomas Manns vej 23
9220 Aalborg, Denmark*

**Corresponding author: jkr.dk@windowmaster.com*

ABSTRACT

The majority of research and hence the assessment methods and tools for thermal comfort assessment of ventilation systems are not based on findings for natural ventilation solutions and do not take into account the specific characteristics of natural ventilation. This has created a lack of suitable methods for the assessment and performance evaluation of natural ventilation. This paper will focus on the evaluation of assessment methods related to estimating the risk of draught for natural ventilation systems. The key objectives and questions to be addressed are: 1) Is the current Draught Rate method suitable for the evaluation of natural ventilation and are there currently other more appropriate methods for assessing the risk of draught? 2) What are the main findings and experiences until now and to what extent can we use these? Furthermore, examples of solutions for ensuring thermal comfort in cold periods will be presented and their performance discussed based on different performance assessment methods used. This paper will conclude on the status of natural ventilation comfort performance assessment in relation to thermal comfort and the risk of draught.

KEYWORDS

Natural ventilation, air movement, draught (draft) risk, Thermal comfort, window opening.

1 INTRODUCTION

The usage of natural ventilation is now, more than ever, being pushed forward due to agendas like: reduction in CO₂ emissions including operational energy and materials as well as resiliency including focus on buildings' ability to e.g., increase the airflow rates during peak load periods and unexpected events. However, there is a risk that the current assessment methods are overestimating the risk of draught for natural ventilation systems. This is typically the case when openings directly to the outside are being used for ventilation and the temperature difference between inside and outside is more than 5K.

Draught is, in the literature and standards, defined as “the unwanted local cooling of the body caused by air movement” (Fanger 1977; ASHRAE 55; EN/TR 16798-2). Several studies have been conducted to address the main factors influencing the risk of draught like air temperature, velocity, air turbulence, exposed body parts, clothing insulation level, and overall thermal comfort (Fanger 1977; Fanger et al 1988; Houghten et al 1938; McIntyre 1979; Toftum et al 2003; Schiavon et al 2016; Liu et al 2017).

This paper evaluates the risk of draught for natural ventilation systems and compares different assessment methods used in current standards. The paper first includes a description of different draught assessment methods, then describes experiences and findings related to airflow patterns, temperatures and velocities in naturally ventilated spaces and finally

compares the estimated risk of draught by different methods and suggests technical solutions to reduce it.

2 ASSESSMENT METHODS

2.1 Overall

Most of the research conducted on thermal comfort and assessment of the draught risk of ventilation systems focuses on mechanical ventilation solutions and fails to consider the specific characteristics of natural ventilation. This has created a lack of suitable methods for assessment and evaluation of the draught risk performance of natural ventilation.

Key aspects and considerations when evaluating a natural ventilation system in terms of draught, include:

- High degree of user control: influence on the perceived indoor environmental quality.
- Visual openings/ventilation: this might lead to greater acceptance.
- Air distribution patterns: displacement or mixing depending on driving forces.
- Operation strategy: continuous or intermittent operation.

It should be noted that fulfilling the given criteria of thermal comfort and draught does not mean 100% acceptance of all occupants. Individual preferences and differences in activity and clothing levels make it difficult to satisfy everyone in space. Individual control of the thermal environment or individual adaptation (clothing, activity) increases the level of acceptance.

2.2 Risk of draught

The risk of draught is expressed in various present thermal comfort standards ISO 7730:2005, EN 16798-1:2019 and ASHRAE 55-2020. EN 16798-1 and ISO 7730 are both based on the widely used and recognised model for assessing the risk of draught developed by Fanger et al (1988). The risk of draught is evaluated by the draught rate (DR), which expresses the percentage of people dissatisfied due to draught. DR is not only determined by the local air velocity, but also influenced by air temperature and turbulence intensity, as presented in Eq. (1).

$$DR = (34 - t_{a,l})(\bar{v}_{a,l} - 0.05)^{0.62}(0.37 \cdot \bar{v}_{a,l} \cdot T_u + 3.14) \quad (1)$$

Where:

DR is the predicted percentage dissatisfied, %

t_{a,l} is the local air temperature, in degrees Celsius, 20 °C to 26 °C;

v_{a,l} is the local mean air velocity, in metres per second, < 0,5 m/s;

T_u is the local turbulence intensity, in percent, 10 % to 60 %

This model applies to people with sedentary activity and with a neutral thermal sensation for the whole body. In addition, the model is designed to predict the draught rate at the neck level, and an overestimation is expected when predicting the draught at the arm or feet level. The expected overestimation of draught at arm and feet level by Fanger et al (1988) is illustrated in Figure 1, where the dissatisfaction with draught modelled by Eq. (1) developed for neck level is compared with the measured number of dissatisfied with draught rate at feet level. There is an almost linear correlation, meaning that it is possible based on the figure and measurements to calculate both the expected draught levels at the neck, arm and feet level.

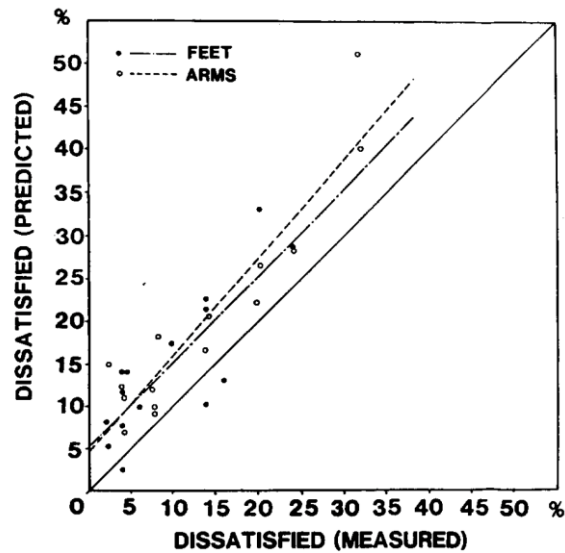


Figure 1. Comparison of predicted and measured percentages of draught risk for arms and feet (Fanger et al, 1988).

Based on a recent study from Berkeley (Schiavon et al 2016; Liu et al 2017) a new draught risk assessment method has been added in the recent ASHRAE 55-2020. The method assesses the risk of draught at the ankle region, 0.1m above floor level, valid for $clo < 0.7$ and $met < 1.3$. This method can be applied in buildings with thermally stratified systems, such as displacement ventilation and underfloor air distribution. The maximum air speed at ankle level can be derived using Eq. 2:

$$V_{\text{ankle}} < 0.35 \cdot TS + 0.39 \quad (2)$$

Where:

V_{ankle} air speed at 0.1m above floor, m/s

TS whole body thermal sensation; Equal to PMV calculated using the input air temperature and speed averaged over two heights: 0.6m and 1.1m for seated occupants and 1.1m and 1.7m for standing occupants.

Based on eq. (2) a maximum air speed of 0.39 m/s can be applied if the whole-body thermal sensation is neutral (TS=0). The online CBE Thermal Comfort Tool (Tartarini et al., 2020) can be used to assess the risk of draught at the ankle level.

3 FINDINGS AND EXPERIENCES

3.1 Assessing the airflow pattern

Openings for natural ventilation are often placed either close to the ceiling or close to the occupied zone, and the characteristics of the airflow from the openings play a crucial role in ensuring comfortable conditions. Hence, one important aspect when evaluating and improving the concept (e.g. due to draught) is to be aware of the different air distribution regimes that can occur with the chosen design. Figure 2 shows the typical air distribution conditions in a room with high positioned openings. The airflow will assume one of three primary patterns and will be dependent on the opening area as well as indoor/outdoor temperature and pressure difference.

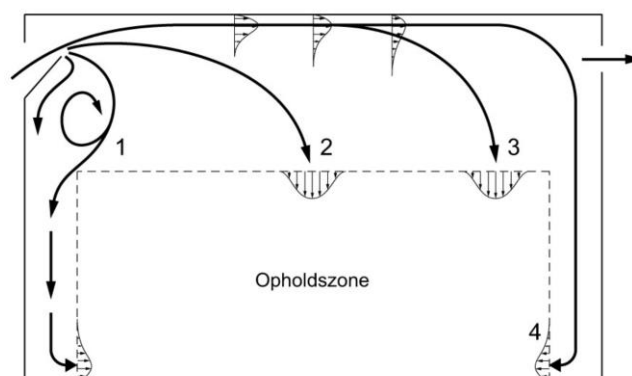


Figure 2. Typical air distribution conditions in a room with high-positioned openings (Heiselberg, 2006)

Table 1 explains when the air distribution conditions shown in Figure 2 typically occur. This explanation is found in Heiselberg (2006), which is based on several studies (Bjorn et al., 2000; Heiselberg et al., 2001 and 2002).

Table 1. Explanation of air distribution conditions in a room with high-positioned openings (Heiselberg, 2006).

Flow regime	Typically occurring	Flow pattern
1	Small driving forces (0.2 – 0.4 Pa) or low outdoor temperature supply air (high indoor/outdoor temperature difference).	Air distribution in the room will follow the displacement principle and the draught risk will be highest along the floor.
2 & 3	Driving forces ($\Delta p > 4-6$ Pa) or higher outdoor temperatures ($\Delta t < 5$ K)	Air distribution in the room will act as a thermal jet and traditional jet theory can be used to predict airflow path and draught risk will typically be highest at neck level.
4	For bottom-hung windows close to the ceiling during warmer outdoor temperatures	Air distribution in the room will act as an isothermal jet.

For low-positioned openings in the façade the aim is to distribute air to the room according to the displacement principle to achieve a high ventilation efficiency and the highest draught risk will always be close to the floor.

3.2 Risk of draught evaluation for natural ventilation

Several laboratory measurements and Computational Fluid Dynamic (CFD) simulations were carried out during the research project “Natural cooling and ventilation through diffuse ceiling supply and thermally activated building constructions” (Zhang, C. et al, 2015 and 2016). The measurement and assessment of draught risk included both a natural ventilation setup with high positioned façade openings and a setup based on diffuse ceiling supply.

Figure 3 illustrates a 2-person office room test setup and measuring positions in the room. Three bottom-hung high level inward façade openings with a dimension of 350x800mm (HxW) was located about 2.4m above floor level. The test included two heat load scenarios of around 30 W/m² and 60 W/m² with an air change rate of 2 (85,5 m³/h) and 4 (171 m³/h), respectively. Air was continuously being supplied to the room. Temperature difference (indoor/outdoor air) varied from 0-32K.

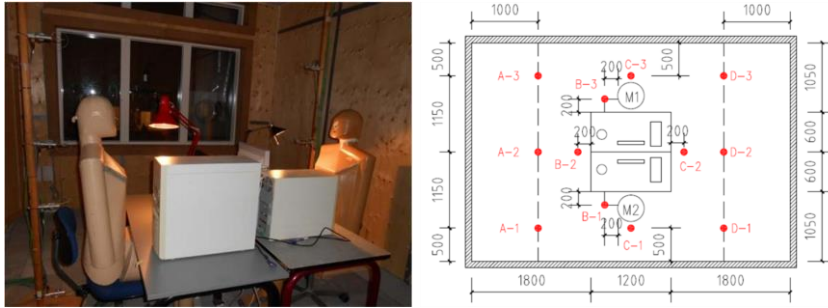


Figure 3. Test setup, measuring positions in the room and on the columns (Zhang, C. et al, 2015).

Extended results from the work are displayed in this paper, by going even further in depth with the results for the natural ventilation with high level façade openings compared to earlier shown results. It should be noted that the turbulence intensity in the study was set to 40% - for some tests some could argue to use 20% instead.

Gunnar et al (2017) conducted several experiments in a thermally insulated test room and assessed the risk of draught in a room with a high-level façade opening with a supply air flow rate of 14 and 29 l/s with an inlet temperature of around 0 °C. It should be noted that the turbulence intensity in the study was selected to be 10%, however for the current study the draught rate was re-calculated based on a turbulence intensity of 20% in order to compare results from the different studies. Figure 4 shows the test setup.

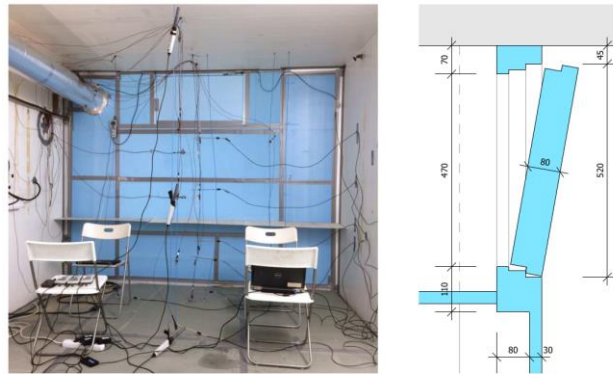


Figure 1: view inside the test room (left), section of the vent (right)

Figure 4. View inside the test room (left) and section of the opening vent (right) (Gunnar et al, 2017).

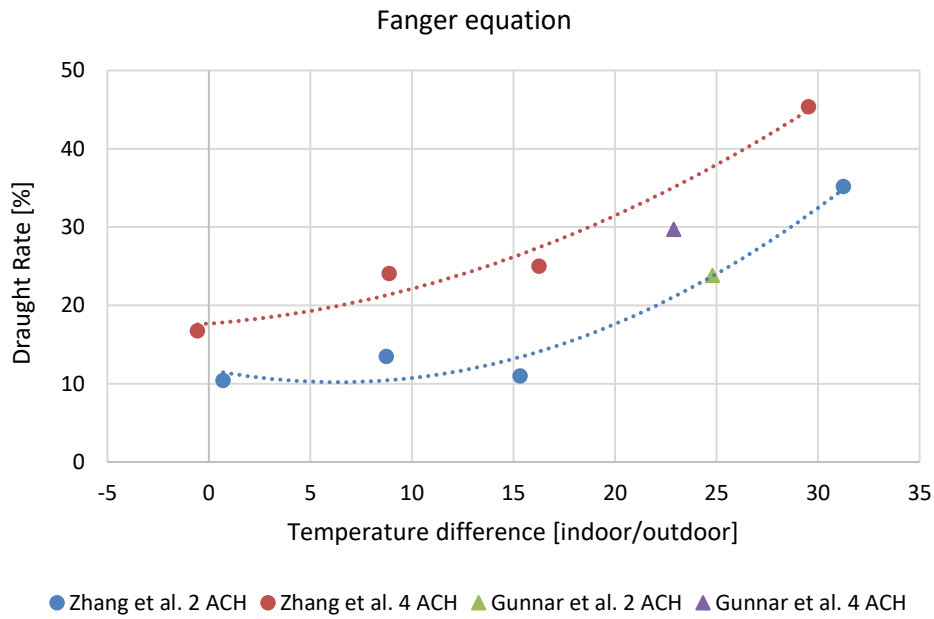


Figure 5. Calculated draught rates using Fanger's equation.

The maximum draught rates in both studies are calculated by different assessment methods as introduced in Section 2.2. Figure 5 illustrates the draught rates calculated by Fanger's equation (eq. 1). It shows, as expected, that the risk of draught increases as the temperature differences between indoor and outdoor increases. A draught rate < 20% can be achieved at a temperature difference below 6 K and 22K for 4 and 2 air changes, respectively.

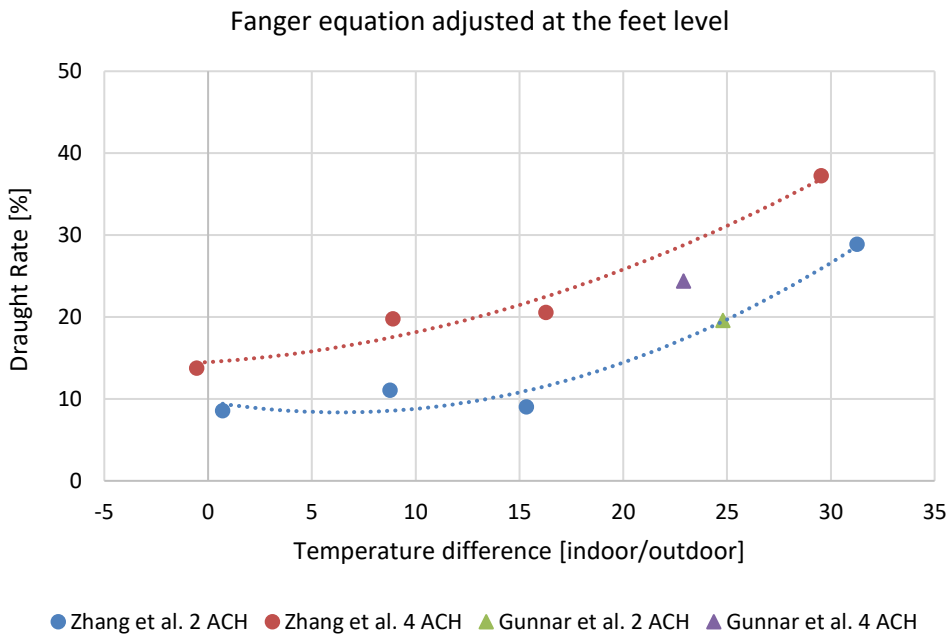


Figure 6. Calculated draught rates using adjusted Fanger's equation at the feet level.

Figure 6 shows the adjusted draught rates at the feet level based on Fanger's equation. A correlation coefficient of 0.82 is applied to the feet level, as shown in Figure 1. The reason for the lower draught rate at the feet level is that people are less draught sensitive at the feet than the head. In addition, clothing plays an important role. Normally, people have their feet and ankles covered, and the clothing layer will damp the thermal impact on the skin. The Fanger's

equation is designed to predict the draught rate at the neck level, and an overestimation is expected when predicting the draught at ankle level.

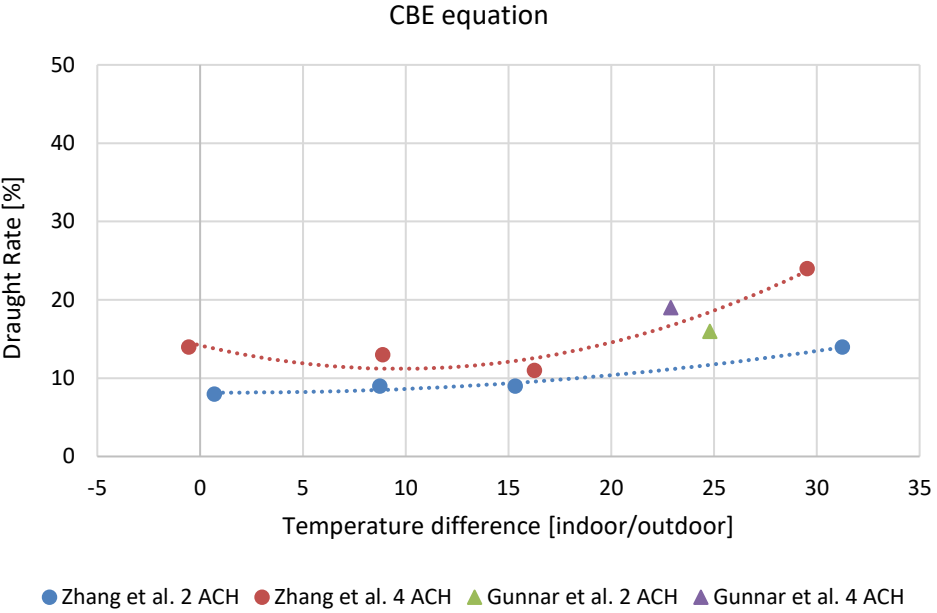


Figure 7. Calculated draught rates using CBE equation.

Figure 7 presents the draught rates calculated by the CBE equation, with an assumption of relative humidity 50%, clothing level 0.7 clo and metabolic rate 1.2 met. It could be observed that the draught rates calculated by the CBE method are much lower compared to the other two methods. The highest DR is 24% by CBE method, while the values by Fanger’s method and adjusted Fanger’s method are 45% and 37%, respectively. This is because CBE method considers both whole body thermal sensation and air speed at ankles as key parameters affecting draught, while Fanger’s method assumes people with a neutral thermal sensation and focuses on the importance of local air conditions, such as air speed, temperature, and turbulence intensity.

4 SOLUTIONS COPING WITH DRAUGHT

There are different design solutions that can be used in order to minimise the risk of draught. Table 2 gives design recommendations depending on the specific goal.

Table 2. Design options to reduce draught risk for natural ventilation.

Goal	Solution
Higher air inlet temperature	<ul style="list-style-type: none"> ▪ Double skin façade solutions
Lowered air velocities	<ul style="list-style-type: none"> ▪ Diffuse ceiling supply ▪ Obstacles e.g. a perforated plate like a window sill. ▪ Radiator below incoming air.
Higher air inlet temperature and lowered air velocities	<ul style="list-style-type: none"> ▪ Diffuse ceiling supply

Zhang et al. (2015 and 2016) developed a novel air distribution concept for air intake from the façade at the ceiling level. Outdoor air is supplied to the space between the suspended ceiling and the ceiling slab and supplied to the room through diffuse ceiling panels. Due to the large inlet opening area, the ventilated air is supplied into the room with very low velocity. The

measured results indicated that even at supply air temperatures of $-7\text{ }^{\circ}\text{C}$, the draught rate was below 10 %, as shown in Figure 8.

Gunnar et al (2017) investigated if different types of obstacles, below a high-level opening, could minimize the risk of draught. Two different windowsills were tested one was solid and the other was a perforated plate, both were located 75cm above floor level. A 30cm high vertical shelf placed on the floor approx. 30 cm from the outer wall was also tested to see if this could minimize the risk of draught. Figure 8 illustrates the flow patterns with different types of obstacles. Figure 9 shows that by introducing different obstacles below the façade openings can potentially minimise the draught rate by more than 10% points.

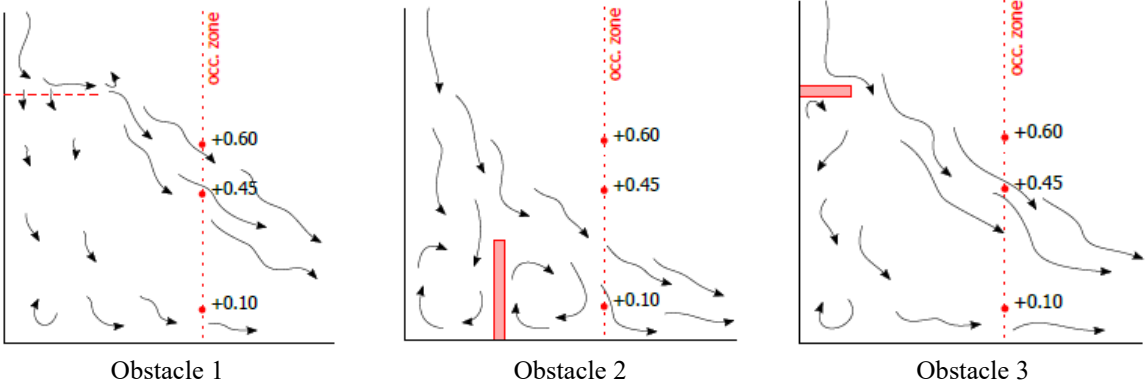


Figure 8. Qualitative visualization of the flow pattern with different types of obstacles (Gunnar et al, 2017)

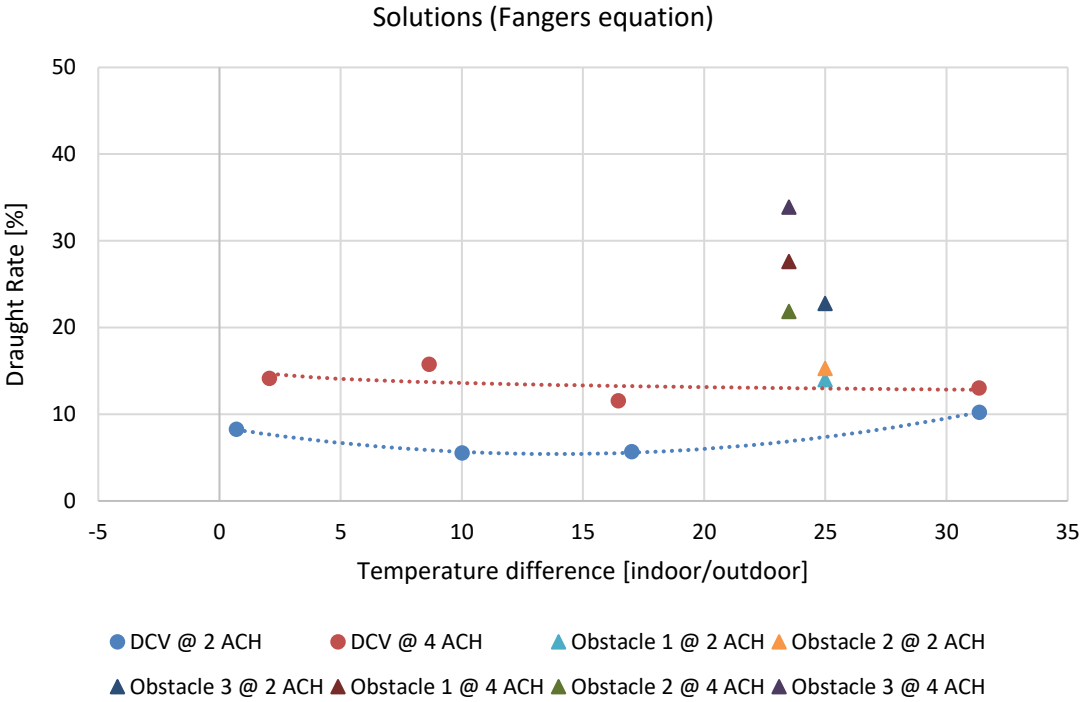


Figure 9. Risk of draught using diffuse ceiling supply (DCV) and various obstacles with Fanger's equation

5 DISSUSSION AND CONCLUSIONS

This study compared various methods proposed in current standards and literature for assessing draught rate, including Fanger's method, Fanger's method adjusted for draught risk at feet level and the CBE method. The results indicate significant deviations in predicted

draught rate when different methods are utilized. The commonly used Fanger's method tends to overestimate the draught risk associated with natural ventilation, especially in systems using displacement air distribution patterns. Further investigation is needed to identify the most suitable method for evaluating draught risk in natural ventilation systems. On the other hand, elevated air speeds do not always result in unpleasant draught. In some situations, increased air speed could enhance perceived comfort. Whether air movements lead to draught, or enhance perceived comfort depends on factors like activity level, thermal environment, overall thermal sensation, clothing, ability to personally adjust air velocities etc. Further studies are recommended to explore methods of increasing personal control on the assessment of draught risk of natural ventilation.

6 ACKNOWLEDGEMENTS

This work was supported by the project: Hybridene – Optimal hybrid ventilasjon I fremtidens bygg, financed by The Research Council of Norway (project nr. 327591).

7 REFERENCES

ISO 7730 (2005). Moderate thermal environments. Determination of the PMV and PPD indices and specification of the conditions for thermal comfort.

EN 16798-1 (2019) Energy performance of buildings - Ventilation for buildings - Part 1: Indoor environmental input parameters for design and assessment of energy performance of buildings addressing indoor air quality, thermal environment, lighting and acoustics - Module M1-6

ASHRAE Standard 55 (2020). Thermal environmental conditions for human occupancy

Fanger PO (1977) Local discomfort to the human body caused by non-uniform thermal environments. *Annals of Occupational Hygiene*, 20, 285-291.

Fanger PO, Melikov AK, Hanzawa H et al (1988) Air turbulence and sensation of draught. *Energy and Buildings*, 12, 21-39

Houghten F, Gutberlet C, Witkowski E (1938) Draft temperatures and velocities in relation to skin temperature and feeling of warmth. *ASHVE Transactions*, 44, 289-308.

Toftum J, Melikov A, Tynel A et al (2003) Human response to air movement—Evaluation of ASHRAE's draft criteria (RP-843). *HVAC&R Research*, 9, 187-202.

McIntyre, 1979. D.A. McIntyre. The effect of air movement on thermal comfort and sensation. P.O. Fanger, O. Valbjørn (Eds.), *Indoor Climate*, Danish Building Research Institute, Copenhagen, 1979, pp. 541-560.

Schiavon, Stefano, Donghyun Rim, Wilmer Pasut, and William W Nazaroff (2016). "Sensation of Draft at Uncovered Ankles for Women Exposed to Displacement Ventilation and Underfloor Air Distribution Systems." *Building and Environment* 96 (February 1, 2016): 228–36.

Liu, Shichao, Stefano Schiavon, Alan Kabanshi, and William Nazaroff (2017). "Predicted Percentage Dissatisfied with Ankle Draft." *Indoor Air*, January 2017.

Tartarini, F., Schiavon, S., Cheung, T., Hoyt, T.(2020). CBE Thermal Comfort Tool : online tool for thermal comfort calculations and visualizations. SoftwareX 12, 100563.
<https://doi.org/10.1016/j.softx.2020.100563>

Heiselberg, P. (2006). Design of Natural and Hybrid Ventilation. Department of Civil Engineering, Aalborg University. DCE Lecture notes No. 5

Heiselberg, P., Bjørn, E. (2002). Impact of Open Windows on Room Air Flow and Thermal Comfort. International Journal of Ventilation, Vol 1, No. 2, pp 91-100, October 2002.

Heiselberg, P., Svidt, K., Nielsen, P.V (2001). Characteristics of airflow from open windows. Building and Environment, 36 (2001), pp 859-869.

Bjorn, E., Jensen, J., Larsen, J., Nielsen, P.V. and Heiselberg, P. (2000). Improvement of thermal comfort in a naturally ventilated office. Proceedings of the 21st AIVC Conference, Den Haag, The Netherlands, September 22-25 (CP21). Air Infiltration and Ventilation Centre, AIVC.

Zhang, C., Heiselberg, P. K., Pomianowski, M., Yu, T., & Jensen, R. L. (2015). Experimental study of diffuse ceiling ventilation coupled with a thermally activated building construction in an office room. Energy and Buildings, 105, 60–70.
<https://doi.org/10.1016/j.enbuild.2015.07.048>

Zhang, C., Yu, T., Heiselberg, P. K., Pomianowski, M. Z., & Nielsen, P. V. (2016). Diffuse Ceiling Ventilation: design guide. Department of Civil Engineering, Aalborg University. DCE Technical Reports No. 217

Gunner, M., Justo-Alonso M., Dokka TH. (2017), Façade Improvements to Avoid Draught in Cold Climates – Laboratory Measurements. 38th AIVC Conference "Ventilating healthy low-energy buildings", Nottingham, UK, 13-14 September 2017

Evaluation of sensor-based air cleaners to remove PM_{2.5} and TVOC from indoors with pollutant sources of smoking and burning candles

Kathrine Andersen¹, Stig Koust², Freja Rydahl Rasmussen², and Li Rong^{*1}

*1 Department of Civil and Architectural Engineering
Inge Lehmanns Gade 10, 8000 Aarhus
Denmark*

*2 Danish Technological Institute
Kongsvang Alle 29, 8000 Aarhus C
Denmark*

**Corresponding author: li.rong@cae.au.dk*

ABSTRACT

Indoor air quality in residential buildings has been attracting more attention from the public. Many portable air cleaner products have been developed and are available in the market. Manufactures generally claim that those portable air cleaners can efficiently remove PM_{2.5} and/or TVOC and can also remove virus from the indoor air. However, no standards are available to have the claimed efficiency comparable and thus unclear effect in applications at homes. This study tested four air cleaners with embedded sensors by using pollutant sources of smoking and burning candles, which exist widely at homes, in a climate chamber (20 m³) without turning on the mechanical ventilation system, respectively. The concentrations of PM_{2.5} and TVOC measured by the embedded sensors were compared with the recorded data by instruments with high accuracy such as DustTrak (8533), SMPS (scanning mobility particle sizer, 3910), OPS (optical particle sizer, 3330) and Ion Science Tiger TVOC gas detector. The results showed that the embedded sensors generally underestimated the PM_{2.5} mass concentration and thus influenced the regulation of fan speeds of air cleaners. Only the embedded sensor of one air cleaner could provide comparable PM_{2.5} mass concentration with the data measured by DustTrak when the concentration was within the detected range of the embedded sensor (< 1000 µg/m³). The underestimated PM_{2.5} mass concentrations led to the air cleaners to quickly switch to the lowest fan speed although the PM_{2.5} mass concentration was still far too high. The embedded sensors cannot properly detect the mass concentrations of ultrafine particles released from burning candles. The air cleaners do not regulate its fan speeds based on TVOC concentrations measured by the embedded TVOC sensors. The obtained results highlighted the limited accuracy of the embedded low-cost sensors. It is imperative to issue standards to guide manufacturer to properly report the efficiency of their products and to clearly claim the performance of air cleaners.

KEYWORDS

Burning candles, Efficiency, PM_{2.5}, Portable sensor-based air cleaner, Smoking

1 INTRODUCTION

Nowadays people spend over 90 % of their time indoors. Ensuring indoor air quality (IAQ) is thus imperative. However, many pollutant sources exist in indoor environments, especially at home where the house owners can conduct any activities they want. Various studies have been conducted to identify the pollutant sources behind daily household activities and which ones had large impact on IAQ. One activity, which has a major influence on the emission of particles, is smoking cigarettes (Suryawanshi et al., 2016). The major pollutants from smoking are particulate matters (PM). PM_{2.5} has a harmful impact on human's health and a long-term exposure to PM_{2.5} negatively affects the lungs (Yang et al., 2021). The concentration of PM_{2.5} can be around 91 % higher in the home of smoker compared to the residence of a non-smoker (Daher et al., 2011, McCormack et al., 2008, Abdel-Salam, 2021). Smoke from tobacco have also been proven to emit VOCs, some of which have been identified to have a negative effect on people's health and can cause illnesses such as allergies

and asthma (Wang et al., 2012). Another common indoor activity is burning candles, which is the largest indoor source of ultrafine particles in Denmark (Bek. et al., 2013). Ultrafine particles have also been discovered to have a harmful impact on human's health (Schraufnagel, 2020). During the burning of candles, a large amount of ultrafine particles are emitted while $PM_{2.5}$ concentration is quite low (Hansen et al., 2018). However, when candles are lit, certain VOCs can be emitted as a by-product of the burning (Bari et al., 2015). The extinguishing of candles causes the black carbon concentration to rise, which is a by-product of soot and the largest concentration is emitted when a candle is blown out (Hegde et al., 2020).

Recently, people have become more aware of the importance of IAQ. This increased awareness has amplified the market for air-cleaning technologies. One of the popular products to improve IAQ is portable air cleaners. Besides the main filtration system, many air cleaners have additional cleaning techniques, which have been claimed to speed up the removal rate of pollutants in the air (Luengas et al., 2015). For example, it was acclaimed that virus e.g. COVID-19 and VOCs/TVOCs can also be removed from the air besides $PM_{2.5}$ (Liu et al., 2022, Chen et al., 2005). However, the removal efficiency of $PM_{2.5}$ and VOCs/TVOCs varied significantly. Besides, many test methods and standards used to quantify the portable air cleaner's efficiency are available. One study showed that the obtained efficiencies of air cleaner tested by different methods were often incomparable and could be misleading (Harriman et al., 2019). The air cleaners are also evaluated based on different performance indices, which makes it further difficult to compare results obtained from different air cleaners. Almost every test monitored different size intervals of PMs and used different pollutant sources (Afshari et al., 2022). The typical pollutant source used in those tests was cigarette smoking, road dust or pollen. The performance of the air cleaner was often evaluated based on the amount of time needed for air cleaner to clean the polluted air (Chan and Cheng, 2006). However, none of these studies have focused on pollutant sources, which could emit mostly ultrafine particles such as burning candles.

To control the portable air cleaner, embedded low-cost sensors are implemented to simplify the regulations of air cleaner by consumers (Koust and Rydahl, 2022). The most commonly used type of low-cost sensors are optical sensors, which are based on light scattering (Alfano et al., 2021), but it is not clear if the same principle has been used for those embedded sensors. The circulated ventilation rate is regulated by fan speeds based on the measured concentrations of pollutants e.g. PMs and TVOCs by embedded sensors. The accuracy of sensors and their interaction with fan auto-mode is a concern and hardly studied. The ability to measure $PM_{2.5}$ of two embedded sensors in air cleaners was investigated under two different conditions (He et al., 2020) by using a nano-sliver based surface cleaner as a pollutant source in a test chamber, and in a residential house with the pollutant source of cooking. However, the pollutant source smoking, a standardised tests of air cleaner, was not tested. The fan speed regulation under auto-mode was investigated in another study (Huang et al., 2021). The results showed that the auto-mode could be the most effective in removing particles compared to manual regulation unless a sudden high concentration arose. None of the residents in these apartments were smokers and the concentration of ultrafine particles was not monitored and analysed. The accuracy of the sensors was not investigated either.

The objectives of this study were (1) to investigate the accuracy of the embedded sensors of four selected air cleaner when pollutant sources were smoking and burning candles, respectively; (2) to study the regulation of fan speeds at auto-mode per the measured concentration of $PM_{2.5}$ and/or TVOC of the four selected air cleaner.

2 METHODOLOGY

Four air cleaner with embedded sensors to measure concentrations of PM_{2.5}/TVOC were tested with pollutant sources of smoking and burning candles in a climate chamber (20 m³) without turning mechanical ventilation system on. The surfaces of the chamber were covered by inert FEP to ensure that none of the particles could attach to the chamber wall surfaces.

The concentrations of PM_{2.5} and TVOC measured by the embedded sensors were compared with the recorded data by advanced instruments. The DustTrak (8533) measures the mass concentration of particles with size ranging between 0.1 µm to 2.5 µm, logs the data with a sampling frequency of 60 s and a time constant of 1 s. The SMPS (scanning mobility particle sizer, 3910) connected to a UCPC (Ultrafine Condensation Particle Counter, 3776) was used to measure the total number of ultrafine particles. The measured size was between 6.04 nm and up till 220.7 nm. To monitor the TVOC concentration, the Tiger (Ion Science Tiger TVOC gas detector) was employed. To ascertain similar test conditions in all measurements, the C.A 1510 was used to monitor the temperature and relative humidity in the chamber.

2.1 The selected four air cleaners

Four air cleaners were selected by using the criteria that it is possible to register the concentration of PM_{2.5} from the embedded sensors and to control the air cleaner from outside of the test chamber. Air cleaner selected in this study have been anonymised and assigned a number from 1 to 4. More information can be found in Table 1. The pre-filter is used to catch the coarse particles and activated carbon is used to remove both particles and TVOCs. The lowest level of fan speed of air cleaner 3 is only used for fan start. The sensor of air cleaner 3 can measure concentrations of PM₁ and PM₁₀ besides PM_{2.5}. Although the TVOC concentration was measured for air cleaner 4, no data could be extracted.

Table 1 Summary of four selected air cleaner

Air cleaner	1	2	3	4
Filters/cleaning technology	Pre-filter/EPA 12 combination filter/UV-C light	Pre-filter/HEPA filter/activated carbon filter	Pre-filter/EPA 12 filter/E12 filter/ionizer	Fiber mesh pre-filter/activated carbon/UV-C light
Fan speed level	4	3	5	4
TVOC sensor?	No	No	Yes	Yes*
Placement of sensors	N/A	At the back	On the top	Center of lateral side
Type of sensors	N/A	N/A	N/A	N/A

*No data can be extracted from air cleaner 4.

2.2 The experimental design

Two types of experiments were conducted and referred as type 1 and type 2, respectively. The type 1 smoking tests were conducted based on the standard ANSI/AHAM AC-1, while the type 2 smoking tests were a modified version of this standard, which was introduced later. The placement of air cleaner, pollutant source, standing fan and sampling points is shown in Figure 1. The same set-ups were followed for all measurements, namely: (1) placing the air cleaner in the centre of the test chamber, around 1.0 – 1.5 m away from the pollutant source; (2) using three identical cigarettes via smoking robots; (3) instruments such as SMPS and DustTrak were located outside the chamber, while instruments e.g. Tiger and C.A 1510 were placed on the top of the chamber, near the measuring ports; (4) before each individual measurement, the chamber were thoroughly ventilated to minimize the influence of previous measurements. This was ascertained by continuous monitoring of ultranet fine particle and PM_{2.5} concentrations until they reached the concentration of background; (5) all instruments

were zero calibrated. A mixing (standing) fan was placed next to the smoke robots in type 1 smoking tests to assist achieving a homogenized pollutant concentration in the chamber.

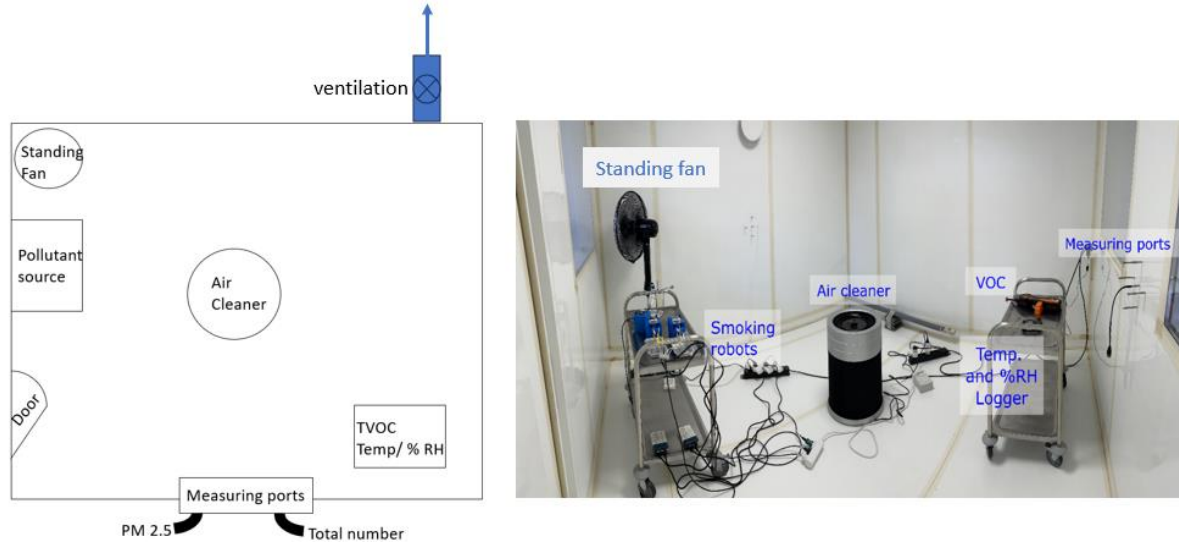


Figure 1 Sketch of placement of air cleaner, pollutant source, standing fan and sampling points in test chamber and a photo representing an example of facilities placement in a smoking test.

In smoking type 1 tests, the background concentration in the chamber was monitored for 10 minutes after the chamber was thoroughly ventilated and before the cigarettes were lit via the smoking robots which were automatically turned on from outside. When the entire cigarette was burnt out down to the white head, the smoking robots were turned off. The standing fan in the chamber was turned on for 10 minutes after no smoking was released from cigarettes. Last, the air cleaner was turned on at auto mode via APP installed in smart phone. The measured concentrations such as $PM_{2.5}$ and TOVC (if possible) by embedded sensors were recorded for minimum 30 minutes. However, there are two differences in smoking type 2 tests. The mixing fan was not used, and the air cleaner was turned on simultaneously when the cigarettes were lit. The overview of experimental cases is shown in Table 2.

Table 2 Overview of experimental cases

Air cleaner	cases	Air cleaner	cases	Air cleaner	cases	
Air cleaner 1	Smoking, type 1	Air cleaner 3	Smoking, type 1	Air cleaner 1	Candles	
	Smoking, type 1		Smoking, type 1		Air cleaner 2	Candles
	Smoking, type 2		Smoking, type 2		Air cleaner 3	Candles
Air cleaner 2	Smoking, type 1	Air cleaner 4	Smoking, type 1	Air cleaner 4	Candles	
	Smoking, type 1		Smoking, type 1			
	Smoking, type 2		Smoking, type 2			

The set-ups of candle measurements were similar with those in smoking type 1 tests. The difference was that candles were lit manually after the concentration of the chamber background was monitored for 10 minutes. The concentrations of $PM_{2.5}$ and ultrafine particles were observed to be stabilized after 40 – 45 minutes. Then the air cleaner was turned on at auto mode for 30 minutes before it was switched to highest level of fan speed manually for another 30 minutes. Afterwards, the fan speed was switched back to auto mode again and the concentration of particles was monitored for another 30 minutes. Last, the candle was extinguished via blowing and the air cleaner was still on for 30 minutes, and the data of concentrations were kept logging, which are shown in section 3.

3 RESULTS & DISCUSSION

3.1 Comparison of PM_{2.5} concentration between embedded sensors and DustTrak

Figure 2 and Figure 3 display the comparison of PM_{2.5} concentrations measured by embedded sensor of air cleaner 1 and air cleaner 3, respectively, to those by DustTrak as examples of smoking type 1 tests. The results obtained from air cleaner 2 and air cleaner 4 were not shown because they have similar trends to results achieved from air cleaner 1 and air cleaner 3, respectively. The PM_{2.5} concentrations measured by the embedded sensor were underestimated for both air cleaner 1 and air cleaner 3 compared to the values measured by DustTrak. The embedded sensor could only detect the PM_{2.5} concentration at maximum 500 $\mu\text{g m}^{-3}$ and the concentration of PM_{2.5} decayed immediately when air cleaner 1 was turned on. The embedded sensor of air cleaner 3 has detected PM_{2.5} concentration at 1000 $\mu\text{g m}^{-3}$ and PM_{2.5} concentration was maintained at 1000 $\mu\text{g m}^{-3}$ for a few minutes when it was higher than 1000 $\mu\text{g m}^{-3}$ as indicated by DustTrak, shown in Figure 3.

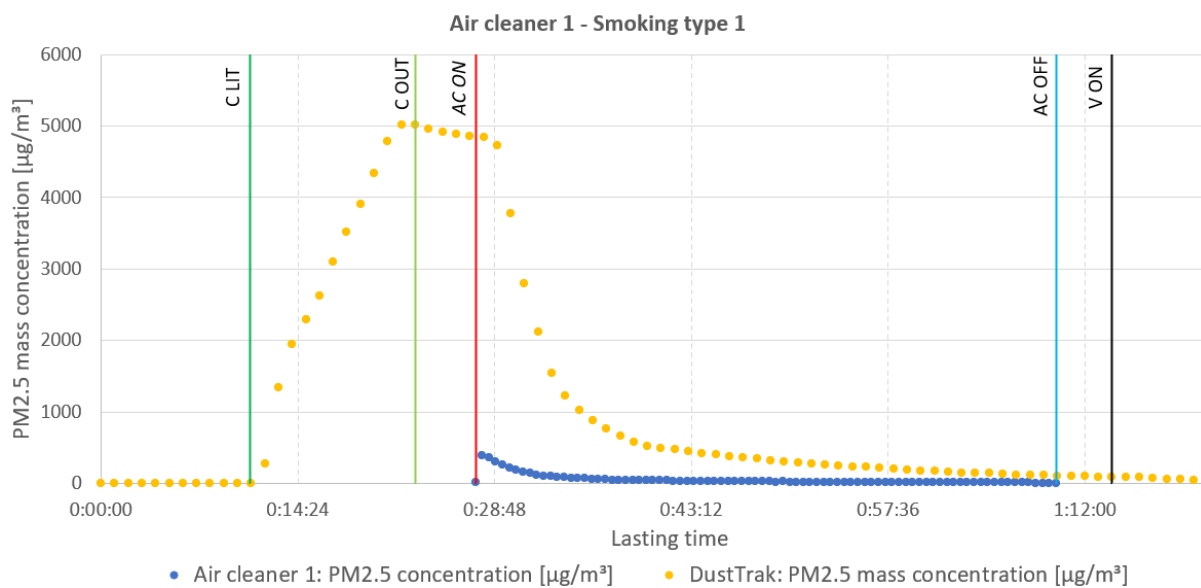


Figure 2 PM_{2.5} concentrations of smoking type 1 test conducted with air cleaner 1. The abbreviations represent the changes through the experiment. C LIT: The cigarettes were lit, C OUT: no more smoke was observed from the cigarettes, AC ON: Air cleaner turned on, AC OFF: Air cleaner was turned off, V ON: the ventilation was turned on.

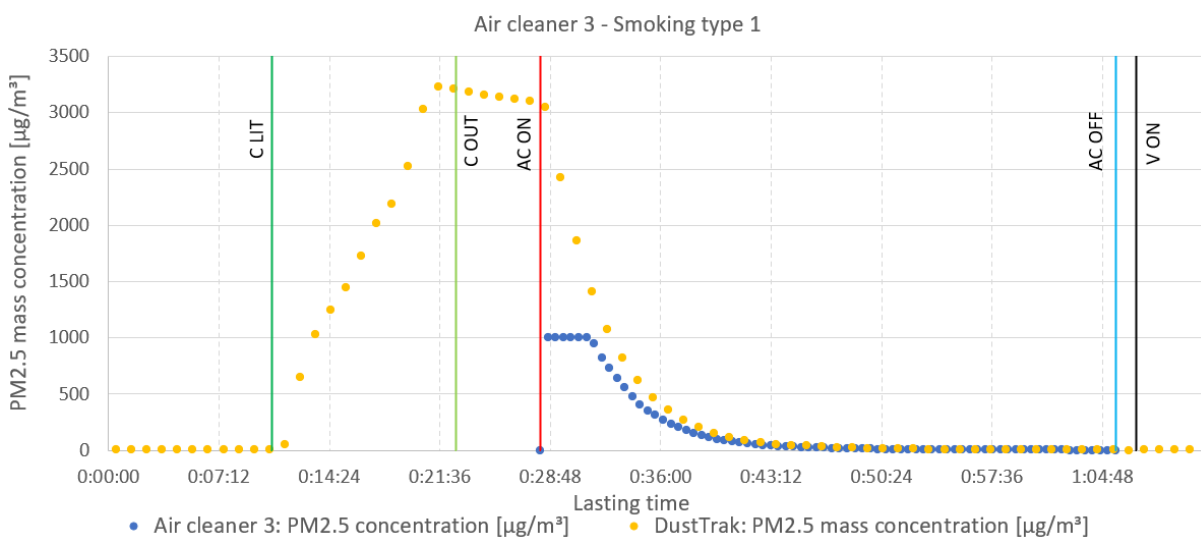


Figure 3 PM_{2.5} concentrations of smoking type 1 conducted with air cleaner 3. The abbreviations represent the changes through the experiment. C LIT: The cigarettes were lit, C OUT: no more smoke was observed from the cigarettes, AC ON: Air cleaner turned on, AC OFF: Air cleaner was turned off, V ON: the ventilation was turned on.

These results indicate that the four air cleaner were able to remove $PM_{2.5}$ after they were turned on as the $PM_{2.5}$ concentrations were decayed, and they reached to a low level after 30 min for air cleaner 1 and after 15 min for air cleaner 3.

Smoking type 1 tests for each air cleaner were repeated, shown in Figure 4 for air cleaner 2 as an example. The recorded $PM_{2.5}$ concentrations were similar in two identical repeated measurements but slightly different during the period when $PM_{2.5}$ concentration declined. The fan speed changed at almost the same timestamps for air cleaner 1, 3 and 4 in the repeated tests. However, there was a 6 min delay for air cleaner 2 and the fan speed was changed to a low level at an almost identical $PM_{2.5}$ concentration measured by the embedded sensor in the two repeated measurements. A noticeable difference of $PM_{2.5}$ concentrations measured by DustTrak was observed when the fan speed of air cleaner 2 was changed. It seems that the $PM_{2.5}$ concentration measured by the embedded sensor of air cleaner 2 was not as stable as the other three air cleaner.

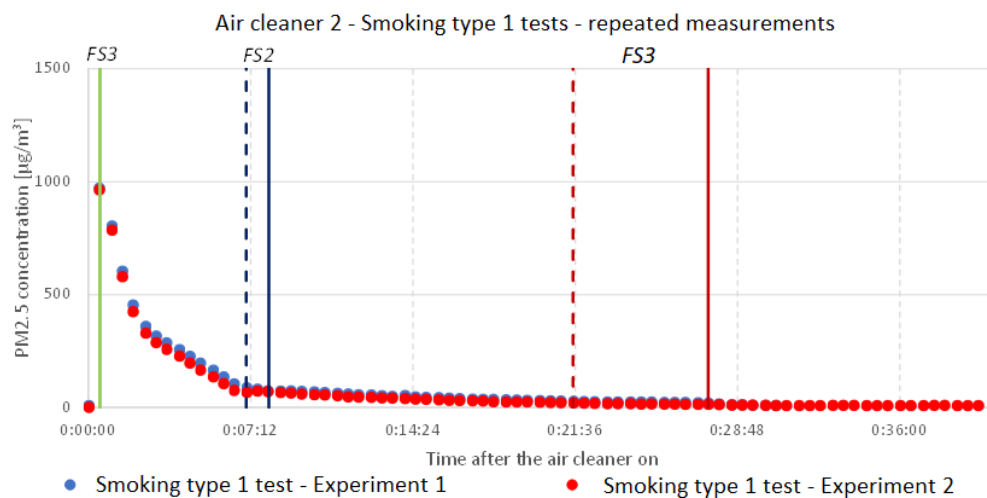


Figure 4 Comparison of $PM_{2.5}$ concentrations between two repeated measurements for air cleaner 2. The abbreviations stand for the level of fan speed (FS) that the air cleaner regulates.

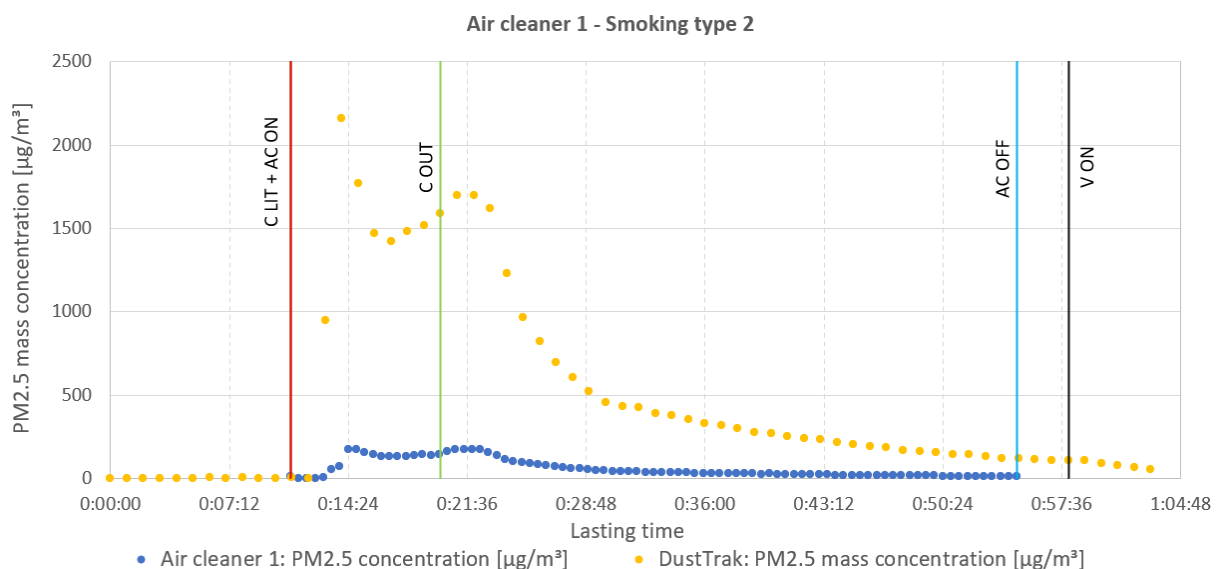


Figure 5 $PM_{2.5}$ concentrations of smoking type 2 test conducted with air cleaner 1. The abbreviations represent the changes through the experiment. C LIT: The cigarettes were lit, C OUT: no more smoke was observed from the cigarettes, AC ON: Air cleaner was turned on, AC OFF: Air cleaner was turned off, V ON: the ventilation was turned on.

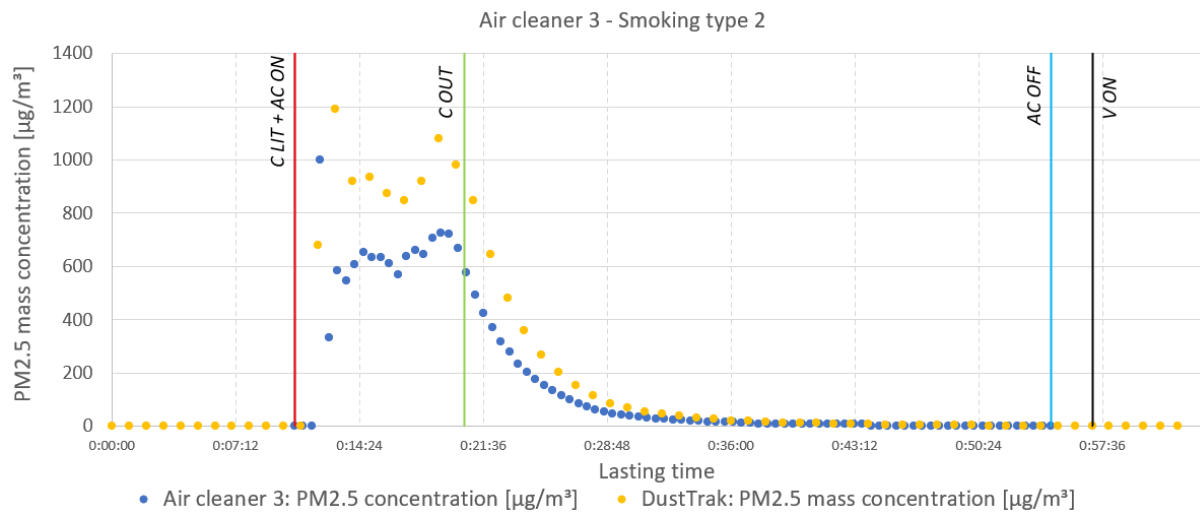


Figure 6 PM_{2.5} concentrations of smoking type 2 tests conducted with air cleaner 3. The abbreviations represent the changes through the experiment. C LIT: the cigarettes were lit, C OUT: no more smoke was observed from the cigarettes, AC ON: air cleaner was turned on, AC OFF: air cleaner was turned off, V ON: the ventilation was turned on.

Figure 5 and Figure 6 show the comparison of PM_{2.5} concentrations measured by the embedded sensors to those by DustTrak for smoking type 2 tests of air cleaner 1 and 3, respectively, when they were turned on simultaneously as the cigarettes were lit. Compared to PM_{2.5} concentrations in Figure 2 and Figure 3, they were significantly lower in smoking type 2 tests. Turning on the air cleaner during the smoking is recommended per those results. Again, the PM_{2.5} concentrations measured by embedded sensors were under-estimated for both air cleaner 1 and 3. The air cleaner 3 reduced the PM_{2.5} concentration much faster than air cleaner 1 and the embedded sensor of air cleaner 3 seems also performing better than that of air cleaner 1. This could be an advantage in terms of exposure to relatively high level of PM_{2.5} concentration in a short period.

3.2 Comparison of TVOC concentrations

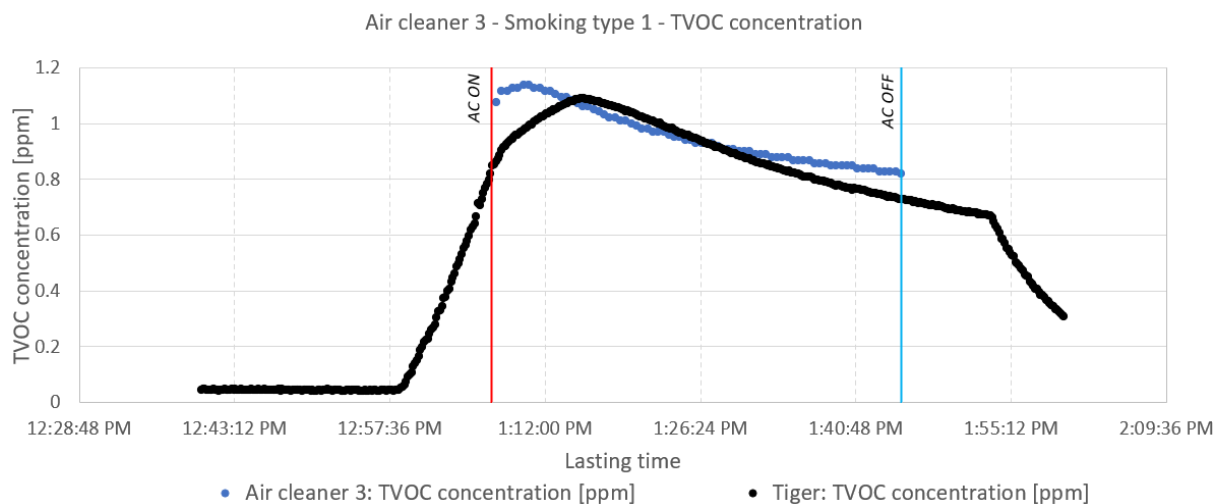


Figure 7 Variation of TVOC concentration for smoking type 1 test with air cleaner 3. The abbreviations represent the operation changes through the experiment. AC ON: air cleaner was turned on, AC OFF: air cleaner was turned off.

Figure 7 shows the variation of TVOC concentrations measured by embedded sensor and instrument Tiger in smoking type 1 tests for air cleaner 3. The measured TVOC concentrations by embedded sensor agreed well with those measured by Tiger and decayed when air cleaner 3 was turned on. The TVOC concentrations did not decay when air cleaner 1

and air cleaner 2 were turned on. But the TVOC concentrations measured by Tiger decreased as the air cleaner 3 and air cleaner 4 were turned on. Although the air cleaner 3 and air cleaner 4 did remove TVOC, the change of TVOC concentrations had little influence in regulating fan speeds.

3.3 Comparison of PM_{2.5} concentrations in tests of candle burning

Figure 8 and Figure 9 show the variation of PM_{2.5} mass concentrations and the total number concentration of ultrafine particles (total number concentration hereinafter) for air cleaner 1 and 4, respectively. The PM_{2.5} concentration was relatively low in tests of burning candle, so the air cleaner was run at a low fan speed. The total number concentration was maintained at a stable level. After the fan speed was switched to the maximum level, the total number concentration was reduced significantly. A couple of fluctuations were observed when fan was run at the maximum speed. This could be explained by the fact that the maximum fan speed disturbed the candle flames and caused unstable burning of candles. After the fan speed was switched back to the auto-mode, the fan speed was switched to the low level and the total number concentration increased again as burning candle continuously released the ultrafine particles. The changes of fan speeds hardly impacted the PM_{2.5} concentration. The extinguish of burning candle released particles with sizes larger than ultrafine particles size range so the mass concentration of PM_{2.5} significantly increased. The air cleaner 1 reduced both PM_{2.5} mass concentration and total number concentration. However, the fan speed was regulated mainly based on the PM_{2.5} mass concentration. If total number concentration of ultrafine particles was critical under certain circumstances, auto mode of fan regulation is not preferred because it does not react to high total number concentrations.

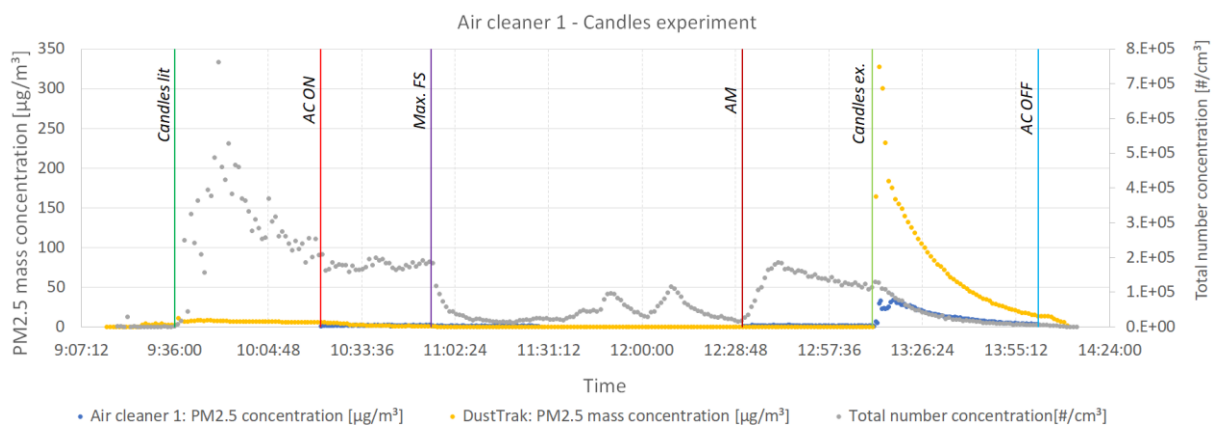


Figure 8 Total number concentration and PM_{2.5} concentration with burning candles for air cleaner 1. The abbreviations represent the changes through the experiment. Candles Lit: The candles were lit, AC ON: air cleaner was turned on, Max FS: maximum fan speed level was employed, AM: auto mode was employed, Candles ex.: candles were extinguished, AC OFF: air cleaner was turned off.

When candles were extinguished, air cleaner 1 and 2 only perceived a small change in PM_{2.5} concentration. Consequently, the fan speeds were not adjusted. Air cleaner 3 and 4 did register the change in PM_{2.5} mass concentration, as seen in Figure 9, and adjusted their fan speeds accordingly. The PM_{2.5} mass concentration and the total number concentration were reduced quickly. This resulted in the PM_{2.5} mass concentration in 10 µg m⁻³ after the candles were blown out for 15 – 20 min. For air cleaner 1 and 2, it took about 40 minutes before the PM_{2.5} mass concentration reached 10 µg m⁻³. This extended time entail that the users of air cleaner 1 and 2 can be exposed to a higher level of particles for longer time, which is a risk of their health. Another observation from burning candle tests was that none of the air cleaner turned off automatically when the embedded sensors did not register PM_{2.5} concentration. This could raise the concern to employ an air cleaner, which essentially consume electricity for no reasons.

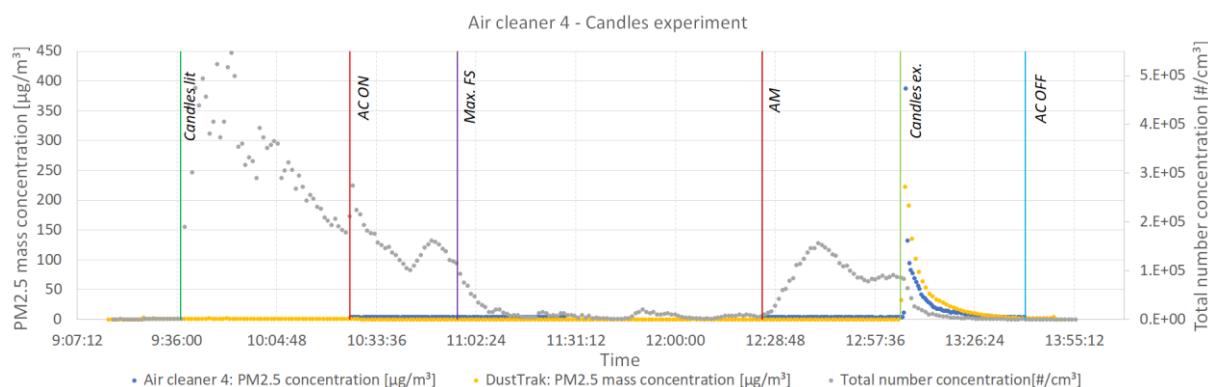


Figure 9 The result of the candles experiment conducted with air cleaner 4. The abbreviations represent the changes through the experiment. Candles Lit: The candles were lit, AC ON: Air cleaner turned on, Max FS: maximum fan speed level was employed, AM: auto mode was employed, Candles ex. Candles were extinguished, AC OFF: Air cleaner was turned off.

4 CONCLUSIONS

This study conducted experimental measurements in a climate chamber to assess the accuracy of embedded sensors of air cleaner and their influence on regulating fan speeds. Generally, the $PM_{2.5}$ concentrations were under-estimated by embedded sensors of air cleaner. The air cleaner can remove $PM_{2.5}$ when they were turned on in smoking tests and can also remove total particle concentration in burning candles tests with highest fan speed. It is recommended to turn on the air cleaner when the pollutant source of smoking is available instead of turning on the air cleaner after smoking. The customer should be reminded that the fan speed is not able to be regulated when the pollutant source is burning candles. The air cleaner being able to measure TVOC concentration cannot change its fan speed per TVOC concentration. This complete information might be suggested to be provided or the manufactory can add the feedback of TVOC concentration to fan speed regulation. It is also noticed that the embedded sensors of different air cleaner could perform diversely so standards to guide the test of air cleaner are beneficial in this industry. One of the limitations of this study is that the concentrations measured by the embedded sensors were recorded manually every 30 s. This should be improved in future studies. Little information of the embedded sensors such as the principles and types is provided, which makes more difficult to compare and discuss the results.

5 ACKNOWLEDGEMENTS

This study was part of a larger project conducted by Danish Technological Institute founded by RealDania and Grundejernes Investeringsfond, whom the authors would like to express their thanks to.

6 REFERENCES

- Abdel-Salam, M. M. M. (2021). Outdoor and indoor factors influencing particulate matter and carbon dioxide levels in naturally ventilated urban homes. *Journal of the Air & Waste Management Association*, 71, 60-69.
- Afshari, A., Mo, J., Tian, E. & Seppanen, O. (2022). Testing Portable Air Cleaning Units – Test Methods and Standards: A Critical Review. *The REHVA European HVAC Journal*, June 2022, 35-46.
- Alfano, B., Barretta, L., Del Giudice, A., et al. (2021). A Review of Low-Cost Particulate Matter Sensors from the Developers' Perspectives. *Sensors*, 21, 3060
- Bari, M. A., Kindzierski, W. B., Wheeler, A. J., Heroux, M.-È. & Wallace, L. A. (2015). Source apportionment of indoor and outdoor volatile organic compounds at homes in Edmonton, Canada. *Building and environment*, 90, 114-124.

- Bekö, G., Weschler, C. J., Wierzbicka, A., Karottki, D. G., Toftum, J., Loft, S. & Clausen, G. (2013). Ultrafine Particles: Exposure and Source Apportionment in 56 Danish Homes. *Environmental science & technology*, 47, 10240-10248.
- Chan, M.-Y. & Cheng, B. N. (2006). Performance Evaluation of Domestic Ionizer Type Air Cleaners. *Architectural science review*, 49, 357-362.
- Chen, W., Zhang, J. S. & Zhang, Z. (2005). Performance of Air Cleaners for Removing Multiple Volatile Organic Compounds in Indoor Air. *ASHRAE transactions*, 111, 1101-1114.
- Daher, N., Ruprecht, A., Invernizzi, G., et al. (2011). Chemical Characterization and Source Apportionment of Fine and Coarse Particulate Matter Inside the Refectory of Santa Maria Delle Grazie Church, Home of Leonardo Da Vinci's "Last Supper". *Environmental Science & Technology*, 45, 10344-10353.
- Hansen, J. A., Pedersen, P. B., Jensen, T. N., Poulsen, et al. (2018). Environmentally friendly candles with reduced particle emissions [Online]. *The Danish Environmental Protection Agency*. Available: <https://www2.mst.dk/Udgiv/publications/2018/11/978-87-7038-009-6.pdf>
- Harriman, L., Stephens, B. & Brennan, T. (2019). New Guidance for Residential Air Cleaners. *ASHARE Journal*.
- He, R., Han, T., Bachman, D., Carluccio, D. J., et al. (2020). Evaluation of two low-cost PM monitors under different laboratory and indoor conditions. *Aerosol science and technology*, 55, 316-331.
- Hegde, S., Min, K. T., Moore, J., et al. (2020). Indoor Household Particulate Matter Measurements Using a Network of Low-cost Sensors. *Aerosol and air quality research*, 20, 381-394.
- Huang, C.-H., Xiang, J., Austin, E., et al. (2021). Impacts of using auto-mode portable air cleaner on indoor PM_{2.5} levels: An intervention study. *Building and environment*, 188, 107444.
- Koust, S. & Rydahl, F. (2022). Mobile Air Purifiers - How good are they? [Online]. *Danish Technological Institute*. Available: <https://www.teknologisk.dk/projekter/mobile-luftrensere-hvor-godt-virker-de/44379>
- Liu, D. T., Phillips, K. M., Speth, M. M., et al. (2022). Portable HEPA Purifiers to Eliminate Airborne SARS-CoV-2: A Systematic Review. *Otolaryngology-head and neck surgery*, 166, 615-622. 88
- Luengas, A., Barona, A., Hort, C., et al. (2015). review of indoor air treatment technologies. *Reviews in environmental science and biotechnology*, 14, 499-522
- Mccormack, M. C., Breyse, P. N., Hansel, N. N., et al. (2008). Common household activities are associated with elevated particulate matter concentrations in bedrooms of inner-city Baltimore pre-school children. *Environmental Research*, 106, 148-155.
- Schraufnagel, D. E. (2020). The health effects of ultrafine particles. *Experimental & molecular medicine*, 52, 311-317.
- Suryawanshi, S., Chauhan, A. S., Verma, R. & Gupta, T. (2016). Identification and quantification of indoor air pollutant sources within a residential academic campus. *The Science of the total environment*, 569-570, 46-52.
- Wang, B., Ho, S. S. H., Ho, K. F., et al. (2012). An Environmental Chamber Study of the Characteristics of Air Pollutants Released from Environmental Tobacco Smoke. *Aerosol and Air Quality Research*, 12, 1269-1281.
- Yang, T., Chen, R., Gu, X., et al. (2021). Association of fine particulate matter air pollution and its constituents with lung function: The China Pulmonary Health study. *Environment international*, 156, 106707-106707

Developing methodology for testing of gas-phase air cleaners based on perceived air quality.

Kanta Amada ^{*1,2}, Lei Fang ¹, Bjarne W. Olesen¹, Shin ichi Tanabe ², and Pawel Wargocki ^{*1}

1 Department of Environmental and Resource Engineering, Technical University of Denmark, Lyngby, Denmark

2 Department of Architecture, School of Creative Science and Engineering, Waseda University, Tokyo, Japan

**Corresponding author: amada@fuji.waseda.jp
Presenter: pawar@dtu.dk*

ABSTRACT

The existing standards for testing gas-phase air cleaners are based on challenging them with gaseous substances. They do not describe air quality measurement using perception, and human emissions (bioeffluents) are not used as challenge pollutants. The present work examines the method that can be used as an alternative or together with other methods used for testing gas-phase air cleaners. The work is a part of the IEA's Annex 78. Three gas-phase air cleaners were tested in the Technical University of Denmark labs. Testing was conducted in rooms adapted for laboratory experiments ventilated with different outdoor air supply rates; emissions from typical building materials and people were used as challenge pollutants. The effects of using air cleaners were examined by rating the air quality's acceptability and odor intensity. For this purpose, participants (subjects) were recruited. The rating was made by entering the rooms or on the air extracted from the rooms; in both cases, the subjects were blind to exposure conditions. The air was sampled at the lowest ventilation rate for the subsequent GC/MS analysis. The results showed that air cleaners using activated carbon performed better than the ones using ion generators. The former improved perceived air quality when challenged with emissions from building materials but not when human emissions were present. The experience gained will allow for developing the standard for gas-phase air cleaners that can be compatible with the requirements for ventilation in the current standards based on sensory ratings and considering emissions from building materials and people.

KEYWORDS

Gas-phase air cleaners, Perceived air quality, Volatile organic compounds, Activated carbon, Human bio-effluents.

1 INTRODUCTION

The existing standards for testing gas-phase air cleaners use a single or mixture of selected volatile organic compounds or other pollutants to test the efficiency of air cleaners. None of them includes how air quality is tested using sensory perception. Consequently, there is an incompatibility between standards for ventilation, where requirements are mainly based on sensory perception and the performance of gas-phase air cleaners. Besides, the methods proposed in the standards do not account for the potential by-products generated in the air cleaning process that may cause air quality to be poorer than without air cleaners. This work aimed to examine the performance of various air cleaners using sensory perception of air quality and use the experience for developing the method that can be implemented in future standards for air cleaners.

2 METHODS

The experiment was conducted in March 2022 at the Technical University of Denmark. A two-stage test was carried out. In Stage 1, we examined whether the air cleaners negatively affect indoor air quality. Those who passed this stage were examined in Stage 2, comparing their performance against improved ventilation with outdoor air. We examined four portable air cleaners (PACs): PAC1a used an ion generator, PAC2p, PAC4p used activated carbon, and PAC3a used a UV/ozone reaction. They were operated at average speed (neither turbo nor

sleep). Emissions from building materials and humans (human bio-effluents) were used as a challenge pollution. We recruited eight people to source as a source of human bio-effluents. Thirty subjects were recruited during Stage 1, and thirty-one during Stage 2. They performed sensory evaluations of air quality using the scale of acceptability and odor intensity. Different experimental conditions were created in rooms adapted for experimental purposes. The volume of the experimental room was 55.7 m³: the air temperature was 23°C, and the relative humidity was 30%. The conditions were created by changing ventilation rates, setting different sources of pollution, and running or idling air cleaners. Ventilation rates (outdoor air supply rates) were set at 7.5, 12, 21 and 30 L/s. The sensory assessments were made by entering the room and on air extracted from the rooms into diffusers. The first assessment was used to rate air quality. The subjects were blind to exposure conditions. Results were analyzed using the Wilcoxon Signed Rank Test. At the lowest ventilation rates, the air was sampled on Tenax and DNPH for the subsequent chemical analyses performed by the commercial laboratory.

3 RESULTS

Figure 1 shows the selected results of the experiment from Stage 2. The sum of VOC concentrations with the PAC1a was almost the same as those without air cleaner when the pollution source was building materials or human bio-effluents. The sum of VOC concentrations with PAC2p was lower than those without air cleaners when the pollution source was building materials, human bio-effluents, and a mixture of both. Acceptability of air quality rated by the subjects with PAC1a was not significantly different when the pollution source was building materials or human bio-effluents compared with no air cleaner. It was significantly improved with PAC2p when the pollution source was building materials compared with no air cleaner; no change was seen when sources were human bio-effluents or a mixture of building materials and human bio-effluents. Similar results were seen for PAC4a. These results suggested activated carbon type air cleaners effectively reduced the VOCs regardless of pollution source and improved perceived air quality when the pollution source was building materials. However, when the pollution source included human bio-effluent, perceived air quality was not improved.

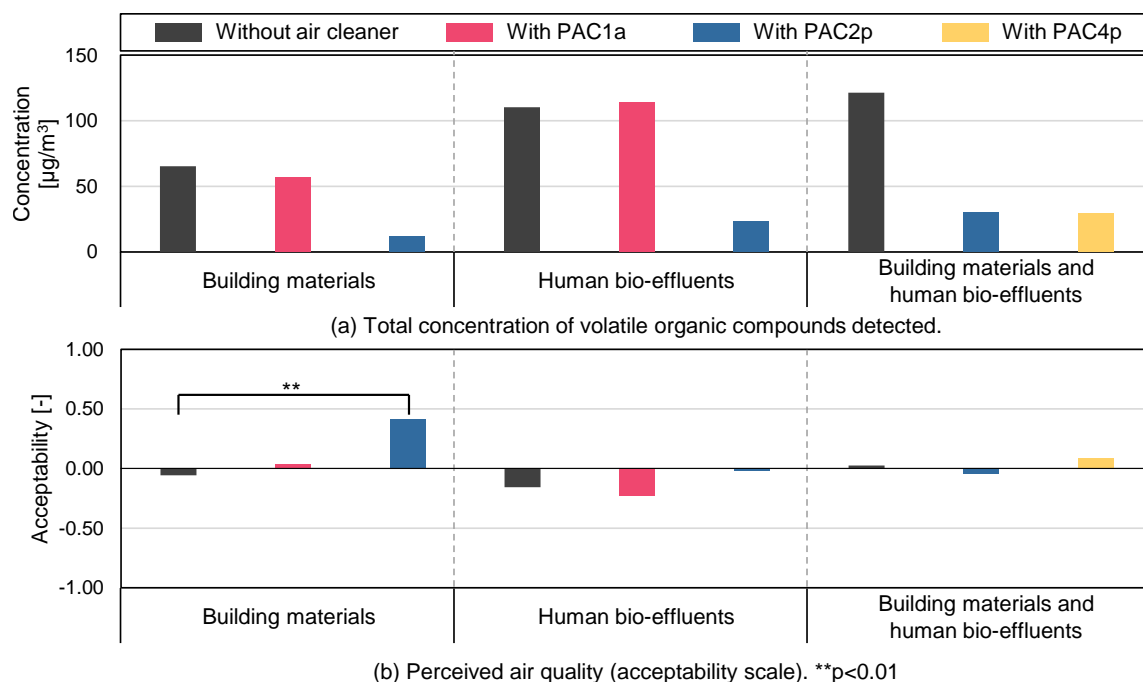


Figure 1: Results of chemical measurements (summed concentrations of VOCs) and perceived air quality (acceptability).

4 CONCLUSIONS

Present results suggest better performance of air cleaners using activated carbon but not for all pollutants. Using two two-stage assessment procedures and sensory ratings of air quality allowed for identifying air cleaners that performed poorly and even aggravated air quality. Present results require confirmation by other groups, but the experience gained can be used to develop the methodology that can be implemented in future revisions of standards that examine the performance of gas-phase air cleaners.

5 ACKNOWLEDGEMENTS

Present work was supported by the Energy Technology Development and Demonstration Programme (EUDP), providing partial support to IEA Annex 78 and Bjarne Saxhof's Foundation supporting the project on "Energy-saving potential for ventilation in buildings when using gas-phase air cleaners."

Evaluating the impact of air cleaning on bioaerosols and other IAQ indicators in Belgian daycare facilities

Sarah L. Paralovo*¹, Klaas de Jonge², Arnold Janssens², Jelle Laverge², Reinoud Cartuyvels³, Koen Van den Driessche⁴, Borislav Lazarov¹, Maarten Spruyt¹, and Marianne Stranger¹

*1 VITO
Boeretang 200
Mol, Belgium*

*2 UGent
Sint-Pietersnieuwstraat 41
Ghent, Belgium*

**Corresponding author: sarah.limaparalovo@vito.be*

*3 Jessa Hospital Clinical Lab
Stadsomvaart 11
Hasselt, Belgium*

*4 Antwerp University Hospital
Drie Eikenstraat 655
Antwerp, Belgium*

ABSTRACT

The scientific community has been aware of the importance of indoor air quality (IAQ) for many decades, but the COVID-19 pandemic has brought a significantly higher level of attention from the general public and governmental entities to this theme. However, IAQ comprises hundreds of other parameters besides infectious pathogens, many of which can equally impact the health, comfort and well-being of occupants. In this context, an intervention study was conducted in Flanders (Belgium) with the aim of investigating the potential impact of ventilation and air cleaning on the IAQ, comfort and infection risk control in Flemish public spaces. This paper describes part of this study, focusing on the IAQ assessments carried out in four daycare facilities for infants in the province of Antwerp. The two first facilities were assessed simultaneously in March 2022, while the two last ones were assessed simultaneously in September 2022. At each facility, CO₂ concentration, different size fractions of particulate matter (PM_x) concentration, temperature and relative humidity (RH) were continuously monitored in selected indoor spaces and one outdoor site for 2 consecutive weeks. Average ventilation rates were measured in each facility under different airing scenarios. Biological air samples were also collected 2 days per week, in the same spaces at each facility, for in-lab qPCR analysis of over 20 genetic markers of respiratory pathogens. Results generally highlighted the positive impact of efficient ventilation on IAQ, while the effects of air cleaning were not as prominent in each room. CO₂ concentrations up to 4200 ppm were measured in the facilities without mechanical ventilation, while they remained consistently below 800 ppm in the facility with the most effective mechanical ventilation system. SARS-CoV-2 was detected more frequently and in larger quantities in the facilities with lower ventilation rates. The variety of other pathogens was also higher in these less-ventilated facilities. The effectiveness of air cleaners in reducing airborne pathogens could not be clearly established at each location. In the sites where air cleaning clearly affected indoor PM_x, the same effect was also noticeable in the indoor pathogen levels and their variety.

KEYWORDS

Daycare facility, indoor air quality, air cleaning, ventilation, respiratory infection risk

1 INTRODUCTION

The COVID-19 pandemic has considerably increased the public attention to ventilation and CO₂ (as an indicator of ventilation) and aerosol concentrations, since it is now widely known that the SARS-CoV-2 virus spreads mainly through the air in indoor environments (Morawska and Cao, 2020; Randall et al., 2021). However, the quality of the indoor air (IAQ), and by extension of the indoor environment (IEQ), is determined by many different parameters of

varied natures (i.e. physiochemical, biological, thermal, acoustic and lighting). Similarly, the potential impact of inadequate IEQ on the health, behaviour, comfort and well-being of occupants can be very diverse. Thus, IAQ is only one of four main parameters that determine how an indoor space is experienced by its occupants. Consequently, it is perfectly possible to experience discomfort or health complaints in a room with low concentrations of typical IAQ pollutants. When evaluating strategies for improving IAQ, such as air cleaning and ventilation enhancements, it is therefore important to also consider more parameters than exclusively IAQ.

In this context, a large study was conducted in Flanders (Belgium), at the request of the Flemish Government, with the aim of investigating the potential impact of different ventilation and air cleaning strategies on the IEQ and infection risk control in Flemish public spaces, thus enabling an objective evaluation of the effectiveness and impact of such risk reduction methods. Three different types of public spaces were selected for analysis, due to their major potential for spreading infectious diseases among sizeable communities: Schools, daycare for infants and elderly care facilities. The assessments included the continuous monitoring of temperature (T), relative humidity (RH), CO₂ and particulate matter (PM_x) concentrations, the measurement of average ventilation rates (ACHs) and sound pressure levels, the application of occupant comfort surveys and the collection of bioaerosols for analysis of respiratory pathogens. The ultimate goal of this study was to substantiate selection criteria and points of attention for ventilation and air purification with objective data, and to offer actors from the respective settings a workable, low-threshold strategy to select the most suitable risk mitigation technology for a specific context. The present paper describes part of this larger Flemish study, focusing on the measurements of T, RH, ACHs and CO₂, PM_x and pathogens concentrations carried out in four daycare facilities in the province of Antwerp and the effects of air cleaning strategies over infection risk control. The assessments carried out in the other facilities, as well as the acoustic measurements and comfort surveys assessments, are to be reported elsewhere.

2 MATERIALS AND METHODS

2.1 Sampling sites

IEQ assessments were carried out during normal working-hours at four different daycare facilities in the province of Antwerp, Belgium, in a few selected locations per facility (playrooms, sleeping rooms and outdoors). The two first facilities (henceforth called C1 and C2) were assessed simultaneously during two consecutive weeks in March 2022, while the two last ones (henceforth called C3 and C4) were assessed simultaneously during two consecutive weeks in September 2022. Mobile air cleaners were placed in selected rooms. Figure 1 shows a sketch of each of the four selected facilities, with the placement of each air cleaner. Table 1 presents the main specifications of the installed air cleaners.

C1 was a naturally ventilated ground-floor space, which had formerly been a retail store, located in a residential area. A total of 13 babies and toddlers were cared for at the time of the experiment. The building featured large front windows of the unopenable shopping window type. Additionally, it had an exterior door that led to an enclosed (fenced) outdoor playground situated on the street side. Behind the indoor playroom of the toddlers (aged > 18 months), there was a kitchen with an openable window. At the back of the daycare center there was a bedroom for the children's naptime. Measurements were performed in the toddler's playroom (C1K1) and bedroom (C1K2).

C2 consisted of a terraced building located in an urban environment and had a mechanical ventilation system (based on mechanical air extraction and natural air supply). The facility provided care for 70 children in total at the time of the experiment, who were divided in groups

by age. Two rooms in the toddlers' building were selected for sampling, one on the ground floor (C2K1) and the other on the first floor (C2K2). In both rooms, there was also a duplex-style sleeping area integrated within the space (playing and sleeping areas could not be closed off from each other). Both rooms shared identical dimensions and spatial arrangements.

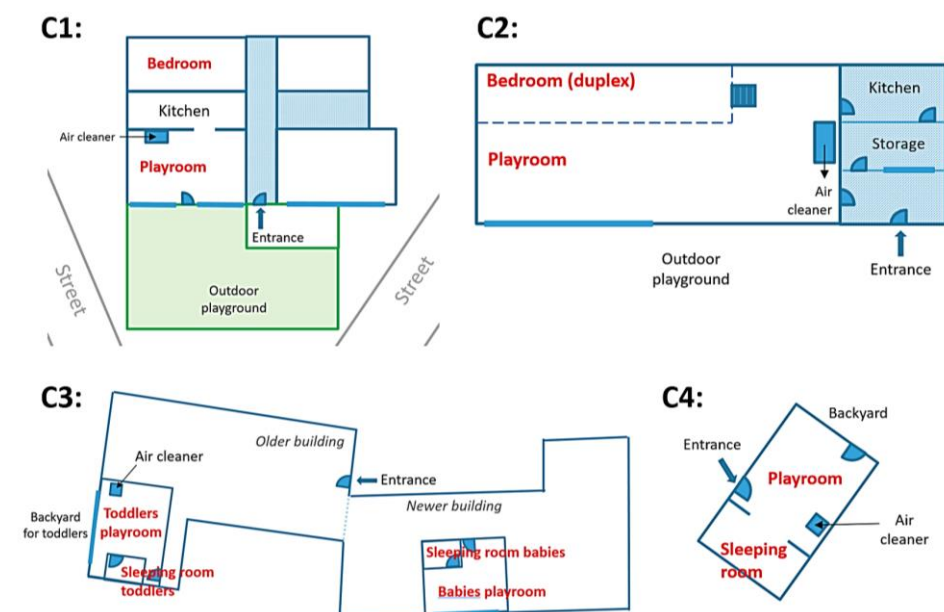


Figure 1: Sketches of each daycare facility assessed in this study (not to scale)

Table 1: Specifications of the air cleaners installed in the daycare facilities.

Facility	Basic Technology	Supplement	Airflow rate (m ³ h ⁻¹)	CADR* (m ³ h ⁻¹)	Noise level (dB)	Energy consumption (W)
C1 / C2	HEPA filter	Pre-filter and charcoal filter	736	-	28 - 58 dB	4-90 W
C3 / C4	HEPA filter	Pre-filter and charcoal filter	-	735 (pollen, smoke) >675 (dust)	27 - 55 dB	9-72 W

*CADR = Clean air delivery rate

C3 was a mechanically ventilated (with a controlled air intake and exhaust), ground-floor detached building in a residential area. A total of 101 children were cared for in the facility as a whole (considering all the available rooms), divided into 2 age groups: babies (≤ 18 months old) and toddlers (>18 months and < 3 years old). The facility consisted of a less recent building (completed in 2017, vent. sys. with heat recovery with a supply of 100% fresh air per room at design flow rate = $8.35 \text{ m}^3 \text{ h}^{-1}$ per person supply air purified with an F7 panel filter) and a more recent extension (completed in 2021, vent. sys. with heating coil, design supply air at flow rate = $30.2 \text{ m}^3 \text{ h}^{-1} \text{ person}^{-1}$ filtered with an F7 bag filter). In both older and newer constructions, every room had glass doors that can be slide opened. Two rooms were selected for air sampling in each part of the facility: Playroom for toddlers in older building (C3K1) and its adjacent sleeping room (C3K3) and playroom for babies in the newer building (C3K2) and its adjacent sleeping room (C3K4). One air cleaner was installed in C3K1.

Lastly, C4 consisted of a previously terraced house located in an urban environment and counted only on natural ventilation (door opening and infiltration). It provided care for 20 children in total (15 children > 18 months and 5 children < 18 months old), not separated by age since the facility only counts with one large playroom (C4K1) and bedroom (C4K2). Measurements were performed in both spaces, which were on ground floor and could not be

closed off from each other (the facility is one large open space, acting as a single-zone). There was a kitchen/service area in between C4K1 and C4K2, where the air cleaner was placed.

2.2 Measurement methods

In each sampling location, monitoring of T, RH, CO₂ and PM_x was carried out by stationary equipment, while the measurements of ACHs and bioaerosols were performed at specific moments according to the specific air cleaning schedules. Installations of the stationary equipment were done following the ISO 16000-1 recommendations (height of 1 to 1.5 m in the room, away from openable doors and windows or heating) as well as possible, since all areas selected for the measurements were in use and thus the devices' location should be safe for the occupants and avoid hindering daily activities. For outdoor measurements, all stationary devices were placed in a cage so that they could not be reached by the children.

The concentrations of PM₁, PM_{2.5}, PM₁₀ and TSP fractions of PM_x were measured at a 1min frequency via optical detection using GRIMM 1.108 Dust Monitors placed inside weatherproof housing. Measurements of CO₂, T and RH were performed with HUMILOG20 devices (E+E Elektronik, Austria), also at a 1min frequency, via optical detection, negative temperature coefficient and capacitive principle, respectively. Average ACHs were inferred in each assessed room via a tracer gas decay test, using CO₂ artificially injected from a pressurized cylinder as a tracer gas and several automatic CO₂ loggers scattered around the assessed room to check for air mixing (Paralovo et al., 2021). Each decay test was performed during several hours either before or after the other IEQ assessments, preferably during unoccupied hours. In each test, a few different scenarios leading from lowest to highest ventilation rates were tested (e.g. all doors and windows closed vs. all doors and windows opened), depending on the room, to provide a more comprehensive overview of the ventilation potential in each space. Air tightness of the assessed rooms was measured via standard pressurization tests (blower door test). Where available, inlet and outlet airflows from mechanical ventilation systems were measured with a FlowFinder-mk2[®] device (ACIN instruments, The Netherlands).

Bioaerosols were sampled using a Coriolis μ device (Bertin Technologies, St-Berthely, France), which collects aerosols with aerodynamic diameters between 0.5 and 20 μm via cyclonic liquid impingement (Bertin, 2012). Biological samples were collected twice per week in each daycare facility (on the same days for C1/C2 and C3/C4), aiming at collecting one sample per bedroom and two samples per playroom (one with the air cleaner active, and another with it inactive) during each sampling day (specific sampling schedules were adapted onsite depending on the facility's practicalities). Each sample was collected for 30min into 3ml of lysis buffer, at an air flow rate of 100 l min⁻¹. After sampling, the biological samples were sent to the Jessa Hospital lab (Hasselt, Belgium) for qPCR analysis. In this analysis, the following genetic markers for infectious agents were included as targets: SARS-CoV-2 RNA, Adenovirus DNA, Bocavirus DNA, Coronavirus 229E, NL63, OC43 and HKU1 RNA, Enterovirus RNA, hMPV RNA, Influenza A and B RNA, Parainfluenza 1-4 RNA, Rhinovirus RNA, RSV-A and B RNA, Herpes simplex and Varicella-zoster virus DNA, *Bordetella pertussis* DNA, *Bordetella parapertussis* DNA, *Bordetella holmesii* DNA, *Chlamydomphila pneumoniae* DNA, *Legionella pneumophila* DNA, *Mycoplasma pneumoniae* DNA and *streptococcus pneumoniae* DNA.

3 RESULTS AND DISCUSSION

3.1 Ventilation characterization

In C1 and C4, no ventilation system was present. In C2, a mechanical ventilation system was present but after assessing its vent holes, it was learnt that this system provided no measurable airflow, which was confirmed by the tracer gas decay test. C2 should thus be regarded as

without ventilation system. C3 was equipped with two separate mechanical balanced ventilation systems. All facilities enabled incrementing the ACHs by opening windows and/or doors. The average ventilation rates measured in the four daycare facilities are summarized in Table 2.

Table 2: Average ventilation rates measured in the four assessed daycare facilities under different scenarios.

C1	Air tightness	'Normal' scenario (window tilted in room next to the assessed room)			'Summer' scenario (‘Normal’ + door to outdoor playground open)				
	n50 (h^{-1} 50Pa)	ACH (h^{-1})	Vol. flow ($m^3 h^{-1}$)	ACH (h^{-1})	Vol. flow ($m^3 h^{-1}$)	ACH (h^{-1})	Vol. flow ($m^3 h^{-1}$)	ACH (h^{-1})	Vol. flow ($m^3 h^{-1}$)
K1	8.7	1.10	75.6	5.40	372				
C2	Air tightness	All doors and windows closed		'Winter' (Front door open, door to playground slightly open, storage room door closed)		'Enhanced winter' (‘Winter’ + storage room door open with window tilted)		'Summer' (Sliding windows to playground open)	
	n50 (h^{-1} 50Pa)	ACH (h^{-1})	Vol. flow ($m^3 h^{-1}$)	ACH (h^{-1})	Vol. flow ($m^3 h^{-1}$)	ACH (h^{-1})	Vol. flow ($m^3 h^{-1}$)	ACH (h^{-1})	Vol. flow ($m^3 h^{-1}$)
K1/K2	3.1	0.18	38.0	0.82	174	3.61	768	13.2	2807
C3	Air tightness	All doors and windows closed		Door to corridor open		Sliding window open (to width of mosquito screen)		Door + sliding window open (to width of mosquito screen)	
	n50 (h^{-1} 50Pa)	ACH (h^{-1})	Vol. flow ($m^3 h^{-1}$)	ACH (h^{-1})	Vol. flow ($m^3 h^{-1}$)	ACH (h^{-1})	Vol. flow ($m^3 h^{-1}$)	ACH (h^{-1})	Vol. flow ($m^3 h^{-1}$)
K1	-	0.67	167	1.20	299	2.01	501	1.80	449
K2	-	1.82	363	2.93	585	2.30	458	4.44	886
K3	-	1.23	50.0	2.57	104	-	-	-	-
K4	-	5.34	138	12.0	310	-	-	-	-
C4	Air tightness	All doors and windows closed		Door to backyard open		Window to the street side open		Door to backyard + window to street side open	
	n50 (h^{-1} 50Pa)	ACH (h^{-1})	Vol. flow ($m^3 h^{-1}$)	ACH (h^{-1})	Vol. flow ($m^3 h^{-1}$)	ACH (h^{-1})	Vol. flow ($m^3 h^{-1}$)	ACH (h^{-1})	Vol. flow ($m^3 h^{-1}$)
K1	-	<1	<140	3.33	465	1.11	155	12.0	1669

In C1, the ‘normal’ scenario led to an ACH of 1.1, which corresponds to an air supply of approx. $5 m^3 h^{-1}$ per person (average occupancy of 15 persons: children + staff). By warmer weather, the door to the playground is kept open and approx. $25 m^3 h^{-1}$ per person can be achieved. However, both scenarios are well below the guideline formulated by the Belgian Task Force Ventilation of the Corona Commissioner's Office, which recommends an air supply rate of $40 m^3 h^{-1}$ per person in any indoor environment (Flemish Government, 2022). In C2, the ‘winter’ scenario led to a ventilation rate of $8.3 m^3 h^{-1}$ per person (average occupancy of 21 persons in C2K1). In the ‘enhanced winter’ scenario, some cross-ventilation is created through the room, increasing the flow rate to $36 m^3 h^{-1}$ per person. But only in the ‘summer’ scenario the ventilation rate is above the recommended guideline (approx. $134 m^3 h^{-1}$ per person).

In C4, it was not possible to perform measurements during unoccupied hours. An exact ventilation rate for the scenario with all doors and windows closed could not be determined, but approximate values were theoretically calculated, resulting in a value of approx. $6.1 m^3 h^{-1}$ per person (average of 23 occupants: children + staff). Both scenarios with one-sided ventilation were also insufficient to achieve the recommended $40 m^3 h^{-1}$ per person. Opening windows on both sides (i.e. providing cross-ventilation) resulted in a flow rate of $72.5 m^3 h^{-1}$ per person.

In C3, a better situation was expected due to the functional mechanical ventilation system. However, the mechanical system alone was not enough to provide the minimum recommended guideline of $40 m^3 h^{-1}$ per person in neither of the playrooms (in the first scenario C3K1 reaches $8.4 m^3 h^{-1}$ per person for 20 occupants, and C3K2 reaches $30 m^3 h^{-1}$ per person for 12 occupants). In C3K2, opening the door to the corridor is sufficient to reach the recommended guideline, but

in C3K1 the guideline is not reached even with both sliding door and door to the corridor simultaneously open. Although this difference is mostly due to the lower occupancy in C3K2, there was also an imbalance in the airflows provided by the mechanical ventilation system (the newer part of the building received more airflow than the design airflow, while the older received less). This issue affected the ventilation in both bedrooms (C3K3 and K4) similarly, with the aggravation that no immediate measures can be taken to supplement the airflows (i.e. there are no windows and the doors must remain closed for the children's sleep quality).

3.2 Measurements of T and RH

According to the advice of the Flemish Indoor Environment Decree, the temperature should stay between 20-24°C during the cold season and between 22 and 26°C in the warm season. In C2, C3 and C4, the P75-values were in accordance with these recommendations, while C1 presented P-75 values < 20°C in both assessed rooms. C1 and C2 were assessed simultaneously during the cold season, but the median temperatures of both facilities differed by up to 6 degrees. C1's bedroom was significantly cooler than the playroom, while C2's bedroom was significantly warmer than the playroom. In C3 and C4, assessed during the warm season, temperatures only occasionally exceeded the maximum recommendation of 26°C.

In C3 and C4 the RH values were at least 75% of the time (i.e. P75-value) measured at acceptable levels according to the Flemish Indoor Environment Decree (40% < RH < 60% in cold season, 30% < RH < 70% in warm seasons). In C1 and C4, RH was higher in the bedrooms than in the playrooms. On the other hand, in C1's playroom the median RH was below the recommended level for the cold season (when the assessment took place). In C2 the air was remarkably dry, with RH medians < 25% in all assessed rooms, and no clear reason could be found. RH is an important comfort parameter, but more importantly a point of attention to limit the transmission of viruses indoors. Evidence shows that RH influences both evaporation kinematics and particle growth, thus in dry indoor spaces (< 40% RH) the risk of airborne transmission of SARS-CoV-2 is higher than that of humid spaces (Ahlawat et al., 2020). Recent research points to a strong negative relationship between relative humidity and the transmission of both SARS-CoV-2 and influenza (Keetels et al., 2022), partly due to the greater sensitivity of airways at lower humidity levels.

3.3 Measurements of CO₂

Figure 2 summarizes the CO₂ measurements during occupied hours at each of the assessed rooms in all 4 daycare facilities. Although C1 had the smallest group (13 children + 2 supervisors) of all facilities, the highest CO₂ concentrations were consistently measured in there, both in the playroom and bedroom, with an average peak concentration in the bedroom over the entire 2-week period of 3740 ± 360 ppm (highest peak 4250 ppm). The playroom was ventilated through a tilt window in the kitchen which remains open 90% of the day. Another possibility to boost ventilation in this room is opening the door to the playground, which is usually done for 20 minutes in the morning and in the afternoon (longer in good weather). The openable window in the bedroom is usually closed for more than half of the day. In C2, the CO₂ concentrations were generally lower than in C1, but the recommended value of 900 ppm was exceeded daily. Both C2K1 and C2K2 showed similar CO₂ profiles during the experiment. Although the ventilation characterization pointed to a non-functioning ventilation system, the concentrations also did not exceed 1500 ppm, indicating that aeration through opening windows and/or doors was reasonably effective.

C3 had generally the lowest CO₂ concentrations. However, a clear difference was noticed between the two parts of the facility. In C3K1 (18 children + 2 supervisors), the recommended value of 900 ppm CO₂ is (slightly) exceeded every day. The exceedances are more frequent and

larger in the bedroom (C3K3), where the highest measured concentration was 1150 ppm, and the ventilation rate is entirely dependent on the ventilation system. In C3K2, with 10 children + 2 supervisors and located in the newest part of the facility, with a different ventilation system, the CO₂ concentration never surpassed 800 ppm (neither in the playroom nor bedroom).

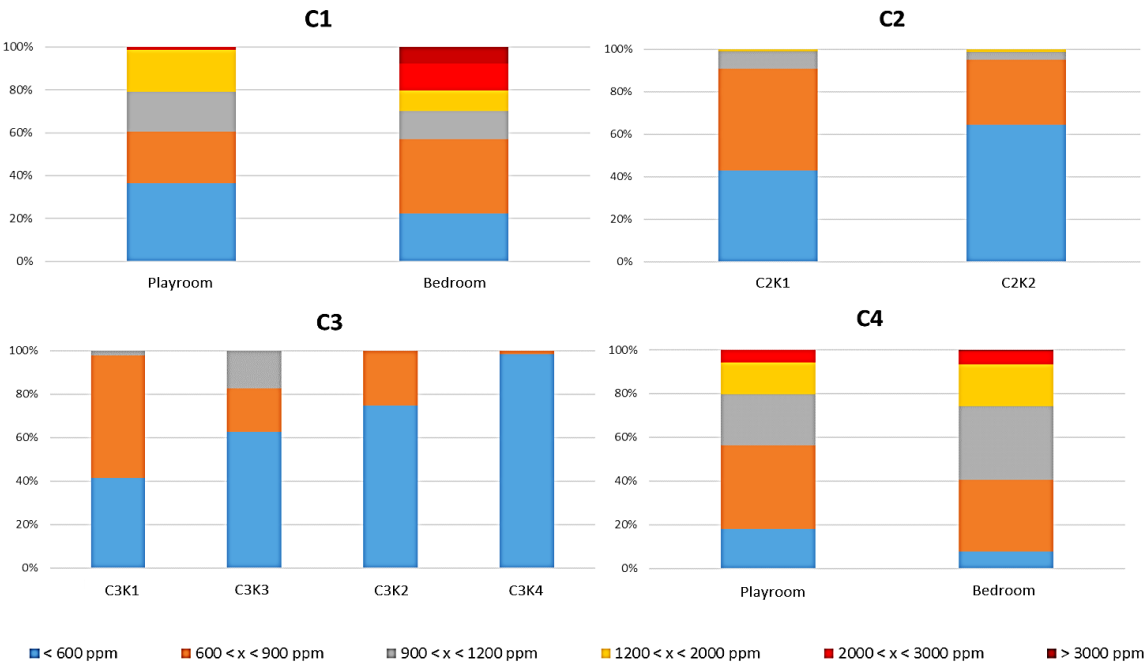


Figure 2: CO₂ measurements per concentration range during occupied hours at each assessed room.

In C4, the single-zone aspect was clearly reflected in the almost parallel CO₂ profiles in the bedroom and playroom during the measurement period (the only difference were the consistently higher peaks in the bedroom when the children were asleep). Although C1 presented the highest CO₂ peaks of all the facilities, in C4 the CO₂ concentrations were the most frequently above the 900ppm recommendation (>60% of the time in C4K2 and >45% of the time in C4K1). The 900ppm limit was exceeded daily, with greater exceedances in the second sampling week. During the first week, the good weather allowed to ventilate by opening windows and backyard door (highest concentration = 1300 ppm), but in the second week the temperature dropped, and the space was less aerated (highest concentration = 2390 ppm). On the last sampling day, the heating was switched on and all the windows/doors remained closed, and then the CO₂ concentrations rose to almost 3200 ppm. Although the construction of C4 allowed a high ACH to be achieved thanks to the possibility of cross ventilation, these measurements show that this is usually not applied in this facility.

3.4 Measurements of PM_x

The concentration of PM_x is one of the parameters by which the efficiency of air cleaning can be evaluated, since most air cleaners focus primarily on the removal of PM_x from the indoor air. In this study, the concentration of PM_x is presented in the form of indoor/outdoor ratios (I/O), which “normalize” the absolute concentrations and already account for potential outdoor environment influence indoors. I/O ratios >1 can indicate either indoor sources of PM or an accumulation of outdoor PM in the indoor environment. Table 3 summarizes the median and P-75 I/O ratios for different fractions of the PM_x calculated for each of the four facilities, considering only the rooms with air cleaners installed and only data from the days when the air cleaners were operated by the research team (i.e. intervention days, which happened 2x/week in each facility: air cleaners were switched off in the mornings and back on in the afternoons).

A consistent reduction of the different PM_x fractions due to switching on the air cleaners cannot be established in every facility. In C1, although a slightly lower I/O ratio is observed for PM₁ with the air cleaner switched on compared to the situation with air cleaner off, the I/O ratios for the larger particle fractions (TSP, PM₁₀ and PM_{2.5}) are either the same or higher with the air cleaner switched on. Similarly, in C2 the I/O ratios for all PM_x fractions in the playroom are slightly higher with the air cleaner switched on.

Table 3: Overview of the median and P-75 I/O ratios of different PM_x fractions in the four daycare facilities, with air cleaning on and off.

	C1		C2		C3		C4	
	Air cleaner status		Air cleaner status		Air cleaner status		Air cleaner status	
	OFF	ON	OFF	ON	OFF	ON	OFF	ON
	Median (P-75)							
I/O TSP	0,6 (1,2)	1,0 (2,0)	0,3 (0,6)	0,4 (1,0)	2,8 (5,5)	2,7 (5,8)	2,9 (5,1)	2,6 (4,8)
I/O PM ₁₀	0,8 (1,1)	1,2 (1,9)	0,9 (1,6)	1,3 (1,8)	1,5 (2,3)	1,4 (1,9)	1,5 (2,0)	1,1 (1,5)
I/O PM _{2.5}	0,8 (1,0)	0,9 (1,1)	0,8 (1,1)	0,9 (1,0)	0,6 (0,8)	0,6 (0,8)	1,5 (1,8)	0,9 (1,1)
I/O PM ₁	0,7 (0,9)	0,6 (0,8)	0,7 (0,8)	0,8 (0,9)	0,5 (0,6)	0,5 (0,6)	1,9 (2,4)	1,1 (1,5)

Potential reasons for this could be: inadequate configuration or location of the air cleaner in the room (in relation to PM_x sources), different activities in the facility in the morning and in the afternoon that generate different levels of particles resuspension and possibly different ventilation/airing during morning and afternoon. The latter seems to have been particularly the case for C2, which was assessed in early spring (colder mornings and warmer afternoons). Thus, the playroom door was closed in the morning with the air purifier switched on, while it was open in the afternoon with the air purifier switched off. This provided extra airing during the afternoon, possibly resulting in a reduction of the indoor PM_x concentrations unrelated to air cleaning itself.

In C3, air cleaning seems to have had virtually no effect over the I/O ratios of the measured PM_x in the playroom during the intervention days. On the other hand, in C4 a consistent decrease is observed in the I/O ratios of all PM_x fractions when the air cleaner is on, especially for PM₁₀, PM_{2.5} and PM₁. The I/O ratios of PM_{2.5} and PM₁ were reduced by 40% when air cleaning was active.

3.5 Measurements of pathogens in air

Figure 3 summarizes the results obtained after qPCR analysis of the biological air samples collected at the four daycare facilities. Cells are coloured according to the detection of SARS-CoV-2 in each sample. For the non-negative samples, the cycle threshold value (CT) is indicated. Results with a CT-value > 35.0 were considered as “limit-value”, indicating a very low viral load. For these samples, there is a higher chance of configuring a false positive result due to analytical issues or contamination during the preanalytical or analytical phase.

C1 and C2 were assessed simultaneously in March 2022, when the official daily COVID-19 incidence in Belgium was about 60/100k inhabitants, while C3 and C4 were assessed simultaneously in September 2022, when the incidence was about 15/100k inhabitants (Sciensano, 2023). Although the groups of children were different in each of the assessed rooms of each facility, it was assumed that the incidence of respiratory infections among sizeable groups of children in the same age group would be comparable in the same neighbourhood in each period, following the regional COVID-19 incidence pattern. Therefore, it was assumed that the pairs C1/C2 and C3/C4 would be comparable between themselves in terms of average emission of SARS-CoV-2, so the difference in analytical results between C1 and C2 could be attributed to the removal strategies. Moreover, it was expected that such emission would be

higher in C1/C2 than in C3/C4 due to the difference in national incidence. However, as shown in Figure 3, the facility with the most positive samples was C4, suggesting that the influence of the national incidence over the presence of pathogen (potentially infective) genetic material in the bioaerosol was smaller than initially thought.

		Week 1		Week 2		
		Day 1	Day 2	Day 3	Day 4	
C1	K1	AC ON	LV* (CT 36,6) ¹	Negative	LV* (CT 37,0)	Positive (vI* < 1000, CT 33,9) ^{1,3,4,5}
		AC OFF	-	Negative	LV* (CT 34,7)	Negative
	K2	-	Negative ^{1,2}	-	LV* (CT 35,3) ¹	-
C2	K1	AC ON	Negative	Negative	LV* (CT 36,2)	LV* (CT 39,8)
		AC OFF	-	Negative	Negative ⁵	Negative
	K2	-	Negative	Negative	Negative	LV* (CT 36,8)
		-	-	Negative	-	Negative
C3	K1	AC ON	Negative ^{6,7}	LV* (CT 39,9) ^{1,7}	Negative ¹	LV* (CT 40,9) ^{1,3}
		AC OFF	Negative	Negative ^{1,7}	LV* (CT 38,4) ¹	Negative ³
	K2	-	Negative ¹	Negative	Negative	Negative
	K3	-	Negative ⁶	-	-	Negative ^{1,3}
	K4	-	-	-	LV* (CT 37,5) ^{1,6}	-
C4	K1	AC ON	Positive (vI* < 1000, CT 30,7) ⁵	Positive (vI* < 1000, CT 32,2) ^{1,3}	Positive (vI* < 1000, CT 29,8) ^{1,3}	Positive (vI* < 1000, CT 29,6) ^{1,3,8,9}
		AC OFF	Positive (vI* > 1000, CT 27,0) ³	Positive (vI* > 1000, CT 29,0) ^{1,3,7}	Positive (vI* < 1000, CT 30,3) ^{1,3}	Positive (vI* > 1000, CT 28,1) ^{1,3,10,11}
	K2	-	Positive (vI* > 1000, CT 27,6) ^{1,3,9}	-	-	

*LV = limit value
vI = viral load

1. Streptococcus pneumoniae DNA positive	4. Enterovirus RNA at LV	7. Bordetella parapertussis DNA positive	10. Bocavirus DNA positive
2. Corona virus OC43 RNA at LV	5. Influenza A virus RNA at LV	8. Bordetella parapertussis DNA LV	11. Adenovirus DNA LV
3. Rhinovirus positive	6. Rhinovirus LV	9. Bocavirus DNA LV	

Figure 3: Results of qPCR analysis from the biological air samples collected at the four daycare facilities.

First comparing C1 and C2, in 37% of samples in C2 at least one pathogen was detected, while in C1 this rate was 67%, suggesting that the air in C2 had an overall lower infective potential than C1. While it is possible that this is due to the presence of more numerous infectious children in C1 than in C2, it is also expected to be a reflection of the better ventilation in C2 (see Table 2). Also, air cleaning did not seem to influence the presence of pathogens in the bioaerosol in either facility. In the second week, SARS-CoV-2 was detected in C1K1, C2K2 and twice in C2K1 when the air cleaner was switched on, but the subsequent samples collected in the same spaces but with the air cleaners off were negative. In all these cases, the first sample was collected earlier in the morning, when doors and windows were kept closed for thermal comfort, and the second one later in the afternoon, after the children had their outdoor playing time, during which the doors remained open, a common practice in both facilities when the weather is sunny. These results seem to suggest that a better ventilation, especially when combined with lengthier periods of airing, could be efficient in diminishing the presence of different airborne pathogens in daycare facilities, and consequently in reducing the risk of airborne pathogens transmission in these spaces.

Comparison between C3 and C4 provide a stronger indication that, in this study, a better ventilation was possibly more efficient in reducing the presence of airborne pathogens than the use of air cleaning. All samples collected at C4, arguably the less ventilated facility (according to the CO₂ measurements), were highly positive for SARS-CoV-2 (plus several other target pathogens, especially in the last week). In C3, the best ventilated of all four facilities, only 27% of the samples were non-negative for SARS-CoV-2, the lowest rate of all facilities. The presence of other targeted pathogens was also generally lower in C3 when compared to C4.

On the other hand, air cleaning did seem to have an impact, albeit less prominent, in the presence of pathogenic aerosols in the indoor air at C4. In this facility, except for day 3, the samples collected when the air cleaner was off had a higher viral load and lower CT-values than the samples collected in the same day/location when the air cleaner was on. Unlike what

happened in C1 and C2, during the C4 assessment the weather was warmer all throughout the day, and therefore there were no big changes in airing from morning to afternoon. This indicates that the different qPCR results in C4 were due to air cleaning, suggesting thus that air cleaning may be an appropriate alternative strategy when proper ventilation levels cannot be achieved. However, this alternate solution should be well-researched and adapted to the intended location, in order to provide a sufficient CADR. Moreover, attention should also be paid to the practical aspects of the installation and use of such air cleaners. Especially in C3K1, the research team had difficulties in finding an adequate location for the device, and the children interfered with it on a few occasions (i.e. shutting it on or off when not supposed to).

4 CONCLUSIONS

This paper focused on part of a larger Flemish study on IEQ in public spaces. Four daycare facilities were assessed via measurements of T, RH, ACH and CO₂ and PM_x concentrations and collection of biological air samples for in-lab qPCR analysis of over 20 respiratory pathogens. Ventilation measurements showed that most of the time the airflow rates per person were below the recommended in Belgium regarding COVID-19 spread prevention, but could generally be improved by airing. Higher CO₂ concentrations were measured in the facilities without mechanical ventilation, while they remained consistently below 800 ppm in C3, the facility with the most effective mechanical ventilation system. SARS-CoV-2 and other pathogens were detected more frequently and in larger quantities in the bioaerosol of C4, arguably the less ventilated facility (according to the CO₂ measurements). In the rooms where indoor PM_x concentrations correlated well with the air cleaning schedules, the same effect was also noticeable in the pathogen concentrations and variety. These results seem to corroborate the expected positive impact of ventilation over IAQ, while the impact of air cleaning was not as consistent in all facilities.

5 REFERENCES

- Ahlawat, A., Wiedensohler, A. and Mishra, S.K. (2020). An Overview on the Role of Relative Humidity in Airborne Transmission of SARS-CoV-2 in Indoor Environments. *Aerosol Air Qual. Res.* 20: 1856–1861. <https://doi.org/10.4209/aaqr.2020.06.0302>
- Bertin. 2012. Coriolis® µ user manual. Manual code: 05027-006-DU002-F ENG. Revised: November 2021. Bertin Technologies
- Flemish Government. 2022. *Coronavirus: verluchting, ventilatie en COVID-19*. Available at: <https://economie.fgov.be/nl/themas/ondernemingen/coronavirus/coronavirus-verluchting>
- Keetels, G. H., Godderis, L. and van de Wiel, B. J. H. (2022). Associative evidence for the potential of humidification as a non-pharmaceutical intervention for influenza and SARS-CoV-2 transmission. *Journal of Exposure Science & Environmental Epidemiology*. 32: 720 – 726. <https://doi.org/10.1038/s41370-022-00472-3>
- Morawska, L.; Cao, J. (2020). Airborne transmission of SARS-CoV-2: The world should face the reality. *Environment International*, 139: 105730. DOI: <https://doi.org/10.1016/j.envint.2020.105730>.
- Paralovo, S. L ; De Jonge, K. ; Laverge, J.; Janssens, A. (2021). Ventilation assessment in three teaching spaces at a Belgian university. *Proceedings of Healthy Buildings 2021 America*. Presented at the Healthy Buildings 2021 America, Hawaii, USA (Virtual).
- Randall, K. ; Ewing, E.T. ; Marr, L.C. ; Jimenez, J.L. ; Bourouiba, L. (2021). How did we get here: what are droplets and aerosols and how far do they go? A historical perspective on the transmission of respiratory infectious diseases. *Interface Focus*, 11: 20210049. DOI: 10.1098/rsfs.2021.0049
- Sciensano. 2023. Belgium COVID-19 Epidemiological Situation: Dashboard. Available online: < <https://lookerstudio.google.com/embed/reporting/c14a5cfc-cab7-4812-848c-0369173148ab/page/ZwmOB>> Last access: May 2023.

Removal of Odorants in Nursing Homes Using Air Cleaners

Stig Koust*, Freja Rydahl Rasmussen, Morten Stoltenberg

*Danish Technological Institute
Air and Sensor Technology
Kongsvang Alle 29
8000-Aarhus C, Denmark
Corresponding author: stko@dti.dk

ABSTRACT

This project aims to enhance the odor environment in laundry and linen rooms in nursing homes. The problem arises from the storage of soiled laundry in these rooms for several days before it is collected or washed, leading to the release of odorants. This often causes discomfort for both staff and residents, as the odors can spread to hallways and adjacent spaces. Aarhus Municipality intends to investigate whether this issue can be fully or partially resolved by installing air purifiers in the rooms.

Adsorption, specifically activated carbon, was selected as the primary technology for odor removal among the technologies utilized in air purifiers. Photocatalytic oxidation (PCO) was selected as a secondary focus area. Seven different air purifiers (6 with active carbon, 1 PCO) were selected for further testing in the laboratory. These tests were performed using acetaldehyde, as an indicator of odor, and a reduction in concentration ranging from 19% to 83% after 20 minutes was measured for the six products utilizing activated carbon. However, the product solely relying on PCO did not show a significant effect.

Degassing from the air purifiers with activated carbon filters was also examined in the laboratory and here it was found that all six products re-emitted acetaldehyde after the efficiency test. The degassing of captured acetaldehyde into the surrounding environment counteracts the intended effect and is, therefore, important to investigate. Additionally, five out of seven tested air purifiers emitted traces of other gases, characterized as byproducts, which were identified by an increase in the concentration of specific substances during testing compared to the reference experiment without an air purifier turned on. These byproducts may result from the conversion of one gas to another potentially more harmful substance. However, the concentrations of all identified byproducts were significantly lower than the instated guidelines.

Four nursing homes were chosen to have an air purifier installed in one of their linen/laundry rooms. The concentration of total volatile organic compounds (TVOC) was continuously measured throughout the project period using air quality sensors in laundry rooms at each of the four selected nursing homes. TVOCs are used here as an indicator of odor concentration.

It has been challenging to draw a conclusive statement about the effectiveness of air purifiers on odors, as numerous peaks in TVOC concentration occurred frequently, probably due to the presence of ethanol in the air, caused using hand sanitizers. This significantly influenced the sensor data, potentially overshadowing the contribution from odor compounds in the measurements that often smell even in very low concentrations.

Overall, the project has indicated that the used air purifiers can reduce the concentration of odor compounds, in the form of TVOC, at the four selected locations. The results show the most apparent effect during periods when the average TVOC concentration was highest. In these time periods, the TVOC concentration generally became lower than in the period without the air purifier. However, the average TVOC concentration is not consistently lower at the four nursing homes during the period with an air purifier installed compared to the period without.

KEYWORDS

Keywords: odor environment, air purifiers, activated carbon, VOC concentrations, indoor air pollution.

1 INTRODUCTION

Indoor air quality plays a vital role in maintaining a healthy and comfortable living environment. In recent years, there has been a growing concern regarding the adverse effects of airborne pollutants, such as odor, smoke, pollen, and infectious agents on human health. These pollutants not only cause discomfort but also pose serious health risks, ranging from respiratory diseases to the spread of pathogens. In response to this challenge, the implementation of air purifiers has emerged as a promising approach to reduce the burden of these airborne contaminants and promote a safer indoor environment^{i,ii}.

Issues related to odors have become a growing concern, particularly with respect to the working environment in eldercare. Odors and volatile organic compounds (VOCs) are closely interconnected. VOCs refer to chemical compounds that can evaporate at room temperature, thus affecting air quality. A significant portion of odors, such as those emanating from urine, are VOCs (e.g., acetone and acetaldehydeⁱⁱⁱ), while certain other odors, such as ammonia and hydrogen sulfide, cannot be classified as VOCs. The odor burden from urine and other sources of human odors consists of hundreds of different chemical compounds, making it a complex quantity to quantify.

In this project, measurements of the concentration of Total VOCs (TVOC) are used as a direct indicator of the concentration of odorous compounds. However, this approach has two main uncertainties. Firstly, as written above, not all odorants can be characterized as VOC. Secondly, the measurements will include VOCs that may not necessarily contribute to the odor issues in the specific laundry rooms under consideration. For example, ethanol from hand sanitizers is not expected to be part of the odor issues related to urine and similar sources but will show up in the measurements of TVOC. Nonetheless, both ethanol and VOCs, in general, should be minimized in terms of occupational exposure, as a wide range of VOCs can be harmful to health.

Air purifiers have gained popularity as effective devices for improving indoor air quality (IAQ) by reducing airborne pollutants. These devices utilize various technologies to capture and eliminate contaminants, providing cleaner and healthier air for occupants. However, the market for air purifiers is characterized by a significant lack of harmonized standards for testing performance. This entails that the acclaimed performance varies greatly between products, and endorsements can be misleading. This is especially the case for air purifiers utilizing filters with activated carbon^{iv}. Activated carbon is considered the main technology for eliminating gaseous contaminants such as VOCs and odorants from airstreams^v.

Low-cost sensors have gained significant attention as valuable tools for monitoring and assessing the quality of indoor air. These sensors provide real-time data on various pollutants, such as particulate matter, TVOC, CO₂, and environmental parameters that contribute to IAQ, enabling proactive measures to improve occupant health and well-being. However, like any technology, IAQ sensors possess advantages and disadvantages that need to be carefully considered for their effective implementation. IAQ sensors require regular calibration and maintenance, and failure to do so can lead to inaccurate measurements. Different sensors may vary in accuracy and have limitations in detecting certain pollutants or be sensitive to interference.

2 METHODOLOGY

2.1 Efficiency of air purifiers against odorants through laboratory test

A total of seven air purifiers were tested in the laboratory to demonstrate a documented effect on a specific VOC. The selected VOC was acetaldehyde, as it is often used as a surrogate for the carcinogenic substance formaldehyde in testing air purification solutions. Acetaldehyde can cause unpleasant odor issues at sufficiently high concentrations but can be perceived as fruity at low concentrations. It is well known that acetaldehyde is a significant component of odors emitted from urineⁱⁱⁱ. Acetaldehyde is also included in the Occupational Health and Safety Authority's threshold limit value for air pollution.

The testing of the seven air purifiers was conducted at the Danish Technological Institute in an airtight 20 m³ chamber. The test chamber is coated with Teflon to minimize the adsorption of gases and particles on the walls, making it highly suitable for testing of air purifiers. The protocol for the test was as follows:

- Prior to each test, the test chamber is thoroughly ventilated until the concentration of acetaldehyde reaches background levels.
- Acetaldehyde is dosed into the chamber until a concentration of 15-20 ppm is achieved.

- A fan in the room further mixes the air in the test chamber for an additional 5 minutes before being turned off.
- The air purifier is turned on at the highest level and runs for a period of 40 minutes, after which it is turned off.
- The test chamber is ventilated for 10-15 minutes until low VOC concentrations are reached.
- The air purifier is then turned on again, and measurements for off-gassing are taken for 15 minutes.

Throughout the entire test, the concentration of acetaldehyde is continuously measured, and air samples are collected for subsequent analysis of byproducts at the 0, 20, and 40-minute marks. Both acetaldehyde and respective byproducts are measured using a PTR-MS (Proton Transfer Reaction – Mass Spectrometry) instrument with a time resolution of 1 second.

2.2 Measurements at nursing homes

A total of 4 nursing homes at different locations were selected for this project.

Nursing home 1: The examined room is a square linen room where soiled linens (typically 3-4 carts) are stored until they are picked up for laundry. Some other items are also stored in the room. The room is enclosed with a sliding door leading to the front room where clean laundry is stored. The staff describes the room as having a foul odor, so the sliding door to the front room is usually closed. The room has no windows. **Air purifier 5** is used in this room.

Nursing home 2: The examined room is a square laundry room that contains a washing machine and a dryer. Bags and baskets with dirty laundry are stored in the room. The room has no windows, and the door is often left open as it becomes hot inside when the dryer is running. This results in the odors often spreading to the hallways. **Air purifier 3** is used in this room.

Nursing home 3: The examined room is a long, narrow laundry room that contains two washing machines and two dryers. Carts and baskets with dirty laundry are stored in the room. Additionally, clean laundry is folded and stored on table surfaces in the room. The room has the option for ventilation by opening windows. The door to the room is often closed as it is located right next to the dining area. **Air purifier 6** is used in this room.

Nursing home 4: The examined room is a square laundry room that contains a washing machine and a dryer. Carts and baskets with dirty laundry are stored in the room. The room has no windows, and the door is often closed as it is located right next to the dining area. During the project, the sensor and air purifier were moved from the originally selected room to an identical room on the floor above due to issues with the electrical network in the room. **Air purifier 7** is used in this room.

The indoor air quality was measured throughout a period of 18 weeks, which includes 7 weeks before installing air purifiers and 10 weeks with air purifiers installed. The measurements were performed with Airthings Space Pro IAQ sensors, which continuously measure the following parameters every fifth minute.

- Particulate Matter (PM1 and PM2.5) [$\mu\text{g}/\text{m}^3$]
- TVOC [ppb]
- CO₂ [ppm]
- Relative humidity [%] and temperature [°C]
- Noise [dBA] and relative light [%]

The sensors were placed at head height and with unrestricted airflow around them, as much as possible. When positioning the sensors, considerations were made for access to power and the staff's workflow. Similarly for the installation of air purifiers, considerations were made for airflow, access to power, and the staff's workflow. Additionally, the fan speed level was adjusted with respect to the noise level in the room. The noise from the air purifier was supposed to be equal to or less than other appliances inside the laundry rooms.

3 RESULTS

3.1 Efficiency in laboratory test

The efficiency of each of the seven air purifiers was examined in the laboratory. The reduction of acetaldehyde from the chamber has been calculated as the relative difference in concentration between the starting time of the test and after 20 and 40 minutes, respectively, with the air purifier running at the highest speed. The results are shown in the table below and presented in Figure 1.

Table 1: Overview of results from laboratory test of the 7 air purifiers.

Product	Technology	Reduction (20 min)	Reduction (40 min)	Degassing?
1	Active Carbon filter, EPA-filter, Ionization	32%	44%	Yes
2	Active Carbon filter, HEPA-filter, Ionization	19%	31%	Yes
3	Active Carbon filter, HEPA-filter	57%	73%	Yes
4	Photocatalytic Oxidation (PCO)	6%	8%	No
5	Active Carbon Filter, HEPA-filter	82%	86%	Yes
6	Active Carbon Filter, HEPA-filter, Ionization, PCO	83%	97%	Yes
7	Active Carbon filter and zeolite, HEPA-filter	82%	96%	Yes

Products 5, 6, and 7 have the highest reduction in acetaldehyde after 20 minutes. These three products also have the highest airflow; however, high airflow does not necessarily result in a large reduction of acetaldehyde. For example, product 5 has an airflow that is almost twice as high as product 7, but the reduction after 40 minutes for these two is 86% and 96% respectively. The reason for this is the fact that the quality and quantity of activated carbon plays a significant role in the effectiveness against acetaldehyde and other VOCs. Information about the quality and quantity of activated carbon used in air purifiers is rarely available and it has therefore not been possible to obtain for the examined air purifiers.

Furthermore, products 4, 6, and 7 also use alternative technologies (PCO and zeolite), which potentially can influence the efficiency against VOCs. Note that HEPA/EPA filters and ionization technologies are not expected to have an impact on gases, including VOCs and odors, but are very effective against particles. For products 6 and 7, it is not possible to separate and evaluate the effect of these alternative technologies since the air purifiers were tested with all technologies in place/turned on. For product 4, which exclusively uses PCO, a low reduction was measured compared to the other products that use activated carbon.

The test also shows the known fact that the effectiveness of activated carbon depends on the concentration of the gaseous pollutant. This means that the air purifiers remove acetaldehyde at a higher rate at the beginning of the experiment when the concentration is high, compared to the end of the experiment when the concentration is low. The half-life during the test thus changes continuously, which is not observed, when testing air purifiers with HEPA filters against particles. This can imply that the air purifiers can more effectively reduce peak loads (short-term high concentrations) of VOC pollution, but not to the same extent lower the background levels significantly.

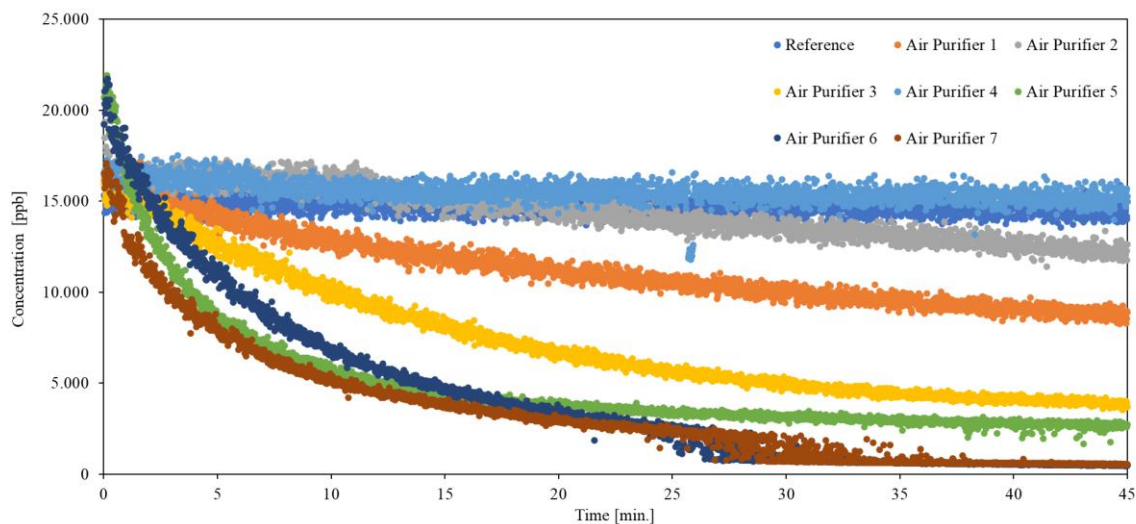


Figure 1: Concentration of acetaldehyde measured for each of the seven air purifiers and the reference in the laboratory test. The time ($t=0$) is defined as the starting time where the air purifier is turned on.

Off-gassing: Off-gassing was investigated by turning on the air purifiers in a clean test chamber shortly after completing the reduction test. If off-gassing occurs, it means that a portion of the captured acetaldehyde is released from the air purifier into the surrounding environment. The results from the test can be seen in Figure 2.

The test reveals that all products, except for product 4, release acetaldehyde after the reduction test is completed. This test is qualitative as the amount of off-gassing partially depends on the efficiency of the air purifier. For example, products 3 and 5 have captured significantly more acetaldehyde, and therefore, have the ability to release more acetaldehyde, whereas product 2 has captured less acetaldehyde, and therefore, cannot release as much. However, it can be observed that products 6 and 7, which have the highest reduction, also exhibit relatively low off-gassing. This may be due to the high quality of activated carbon used in these products.

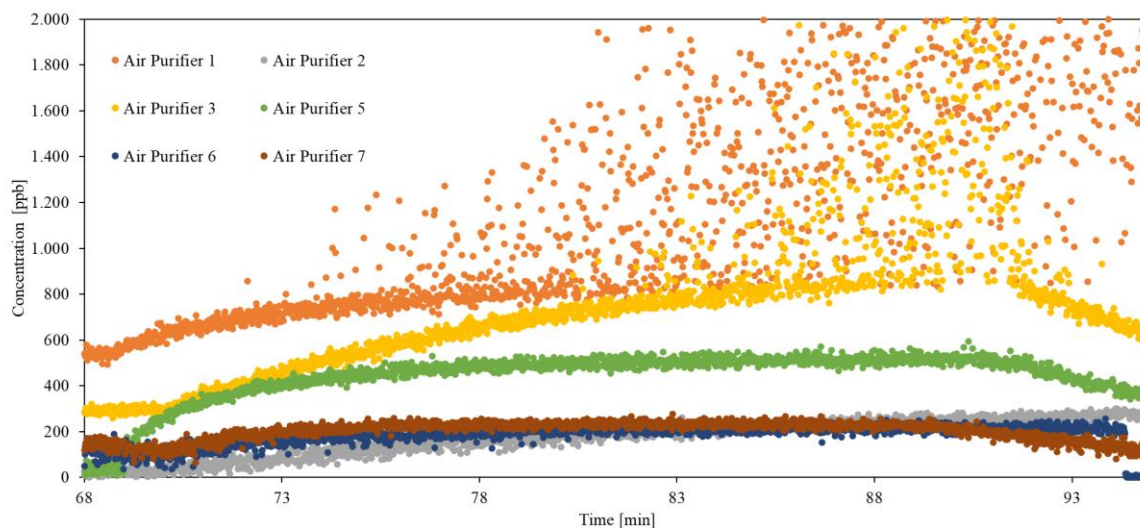


Figure 2: Concentration of acetaldehyde during off-gassing test. Reference and air purifier 4 is omitted from this graph as no adsorption occurs.

Byproducts: For products 1, 2, 3, 5, and 6, small traces of other gases, characterized as byproducts, were detected. The byproducts were identified by an increase in concentrations of specific substances in the air during the test period, which did not similarly increase during the reference test without an air purifier. Byproducts can result from the chemical transformation of gases or off-gassing from components in the air purifier (e.g., heating of plastics during operation). However, the concentrations of all identified byproducts were significantly lower than applicable guidelines (e.g., from occupational health authorities^{vi} and NIOSH^{vii}) for the respective substances. Therefore, the byproducts formed during the specific test with acetaldehyde were not considered harmful and were not a reason for the elimination of a product for further use in this project.

All air purifiers were tested for ozone emissions by measuring directly at their air outlets. None of the seven air purifiers emitted ozone.

3.2 Sensor

The total VOC concentration was measured at the 4 nursing homes with indoor air quality sensors for the entire test period and is shown in Figure 3. Data for nursing homes 1 and 2 are available for the entire period, while data for nursing homes 3 and 4 have periods excluded where the air purifier has been turned off (nursing home 4) or unexpectedly adjusted by the staff (nursing home 3). The graphs display numerous short-term high concentrations of TVOC for all nursing homes, both during periods with and without the air purifier. The exact cause of these peaks is unknown, but it is presumed that the use of hand sanitizers, which result in ethanol in the air, is a significant contributor.

For nursing homes 1, 2, and 3 there is no measured reduction in the average TVOC concentration between the periods with and without the air purifier. For nursing home 4 a reduction of 30% in average TVOC concentration was observed. However, this air purifier was only turned on for a shorter period than the other, which give rise to some uncertainty.

TVOC data for all nursing homes

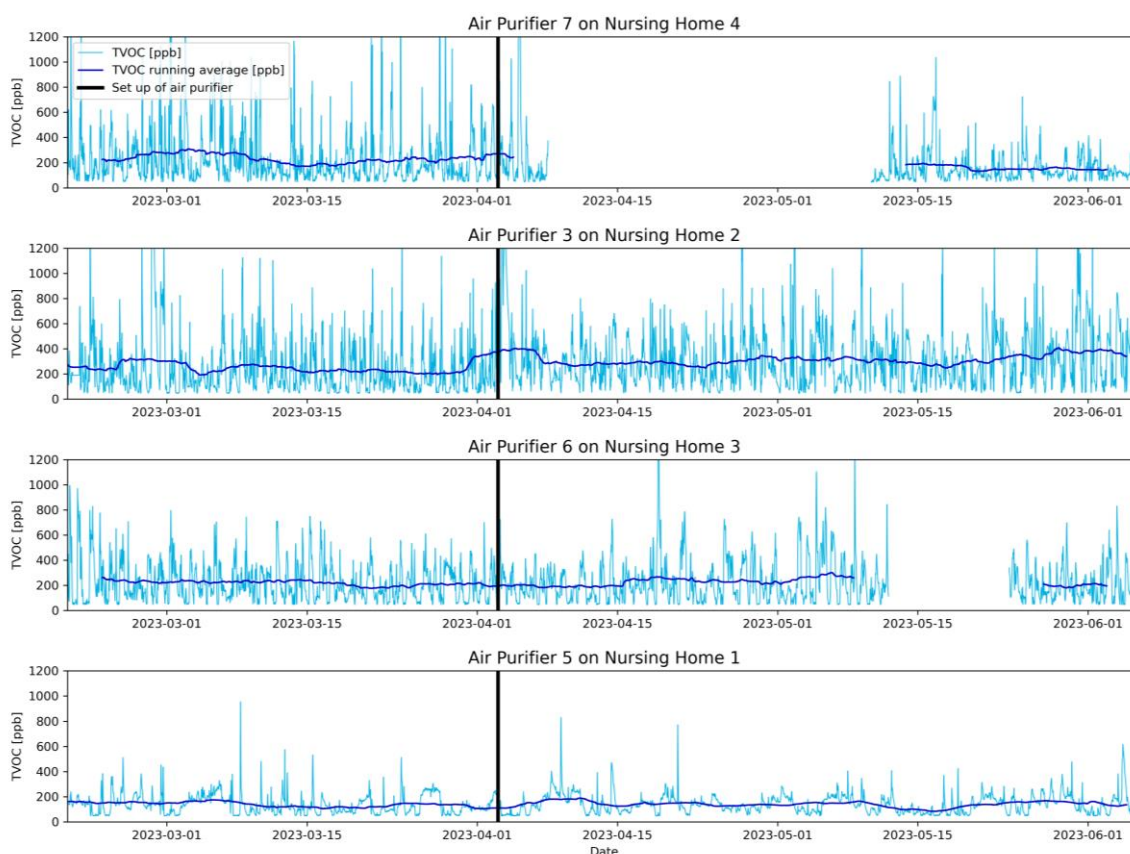


Figure 3: Measurements of TVOC concentration [ppb] for the 4 nursing homes. The vertical black line indicates the time of air purifier installation. The dark blue line running horizontally represents the rolling average. Data is available for the entire period for nursing homes 1 and 2. Data is missing for nursing homes 3 and 4 due to periods when the air purifier was set to a lower fan speed or turned off.

Table 2: Average TVOC concentration from sensor data

Average TVOC concentration	Nursing Home 1	Nursing Home 2	Nursing Home 3	Nursing Home 4
without Air Purifier	138 ppb	244 ppb	223 ppb	232 ppb
with Air Purifier	142 ppb	310 ppb	222 ppb	163 ppb

To examine any potential effect of the air purifiers, a detailed analysis of the TVOC sensor data (see Table 3) has been conducted for each of the 4 locations, which includes the following TVOC parameters for the periods with and without the air purifier:

- Maximum concentration
- Hourly average
- Number of peaks above 250 ppb^{viii} per day
- The relative amount of data points above 250 ppb

The last two parameters have been selected to investigate whether the air purifiers can limit the times when very high concentrations of TVOC are present or rapidly reduce the TVOC concentration during these periods of high air pollution.

Furthermore, the remaining measured parameters from the sensor have been qualitatively analyzed. Specifically, CO₂ and light data have been used to estimate whether the conditions regarding the use of the selected rooms were comparable in the two periods. The results show consistent CO₂ and light data for the two periods, indicating that the human activity in the rooms is comparable.

Table 3: Summary of analysis results for TVOC sensor data collected at the 4 nursing homes. Each period is indicated as a without/with air purifier turned off/on respectively and with a final difference between the two.

Parameter	Air Purifier?	Nursing Home			
		1	2	3	4
Maximum concentration [ppb]	Without	1,963	3,607	2,364	5,796
	With	946	2,515	1,866	2,667
	Difference	52%	30%	21%	54%
Number of peaks above 250 ppb per day	Without	8.1	19.8	26.4	17.6
	With	6.3	36.0	23.0	9.2
	Difference	22%	-82%	13%	48%
Relative amount of data points above 250 ppb [%]	Without	8.6	33.2	35.7	27.3
	With	6.8	52.4	32.6	13.0
	Difference	21%	-58%	9%	52%

For **nursing home 1**, all three parameters are lower during the period with the air purifier installed. The most significant difference was measured for the maximum TVOC concentration. The number of peaks and relative amount of data points above 250 ppb are similar, but still, a reduction is measured for the period with the air purifier turned on.

The hourly average of TVOC from nursing home 1 is presented in Figure 4. The average TVOC concentration is quite similar throughout all time intervals when comparing periods with and without the air purifier installed. It can be observed that there is a daily increase in TVOC concentration in the room around 08:00. This could be attributed to the staff arriving and initiating activities in the room around this time. The TVOC concentration during these hours was on average slightly higher with the air purifier installed. Only the period between 03:00 and 06:00 has a significantly lower average TVOC concentration with the air purifier turned on.

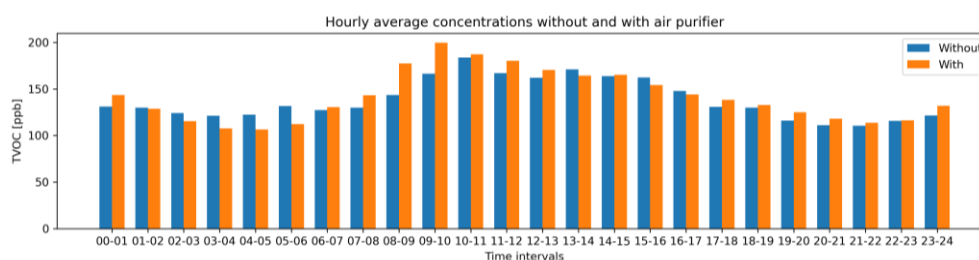


Figure 4: Hourly average of TVOC in nursing home 1.

For **nursing home 2**, higher average values for all parameters, except the maximum concentration, were measured during the period when the air purifier was turned on. Based on the available data, a clear explanation cannot be provided. Possible explanations could be the possibility of the room experiencing an increase in human activity and/or load during the period with the air purifier turned on. However, CO₂ and light data (not shown in this report) from the room suggest relatively similar activity levels in the two periods. Another explanation could be that the airflow from the air purifier results in better mixing of air in the room, leading to a higher, overall concentration observed by the sensor. Referring to the initial laboratory tests conducted on this air purifier, it is assessed that the increased concentrations are not due to the formation of byproducts from the air purifier.

The hourly average of TVOC from nursing home 2 is presented in Figure 5. It can be observed that in the period without the air purifier, the highest concentrations occur between 11:00 and 14:00. In the period with the air purifier turned on, the average TVOC concentrations measured during this period are lower. However, for most other time intervals, the TVOC concentration is higher, which may be attributed to the improved mixing of air caused by the air purifier. The air purifier is placed on a table, which could contribute to increased air mixing in the room and result in higher average concentrations measured by the sensor.

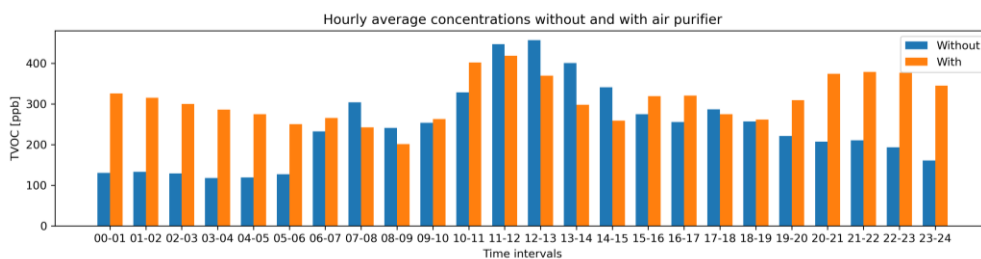


Figure 5: Hourly average of TVOC in nursing home 2.

For **nursing home 3**, the values of all three parameters during the period with the air purifier turned on were slightly lower than the period without the air purifier. This suggests a potential effect of the air purifier on reducing TVOC pollution.

The hourly average TVOC concentration for nursing home 3 is shown in Figure 6. It can be observed that there is a daily increase in TVOC concentration in the room around 06:00 lasting for approximately 3 hours. This could be attributed to the staff arriving and initiating activities in the room around this time. During the period with the air purifier turned on, the average concentrations between 06:00 and 11:00 are lower compared to the period without the air purifier. Like nursing home 2, this could indicate that the air purifier is capable of mitigating some of the peak loads during this specific period but is unable to reduce the average background level in the room.

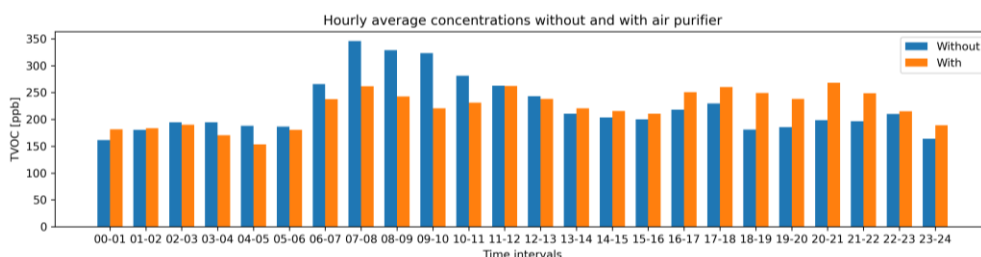


Figure 6: Hourly average of TVOC in nursing home 3.

For **nursing home 4**, it should be emphasized that the measurements during the periods with and without the air purifier were conducted in two different rooms. This introduces a significant source of error, as the human activity and load in the two rooms can be markedly different. However, considering this limitation, the average values show a significant decrease during the period with the air purifier turned on, indicating a positive effect of the air purifier.

The hourly average concentration presented in Figure 7 shows a notable decrease in TVOC concentration, particularly in the time interval from 07:00 to 11:00. This time corresponds to the period with the highest concentration during the time without the air purifier being turned on.

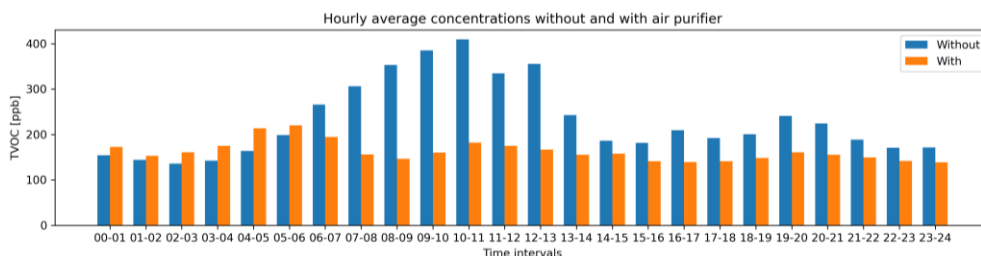


Figure 7: Hourly average of TVOC in nursing home 4.

4 CONCLUSION

Six out of the seven selected air purifiers were able to significantly reduce the concentration of acetaldehyde in the laboratory. A common feature among the six of them was the use of activated carbon filters, in addition to other air purification technologies for addressing different air pollution issues. Among these, the reduction in

acetaldehyde concentration after 20 minutes ranged from 19% to 83%. It was not possible to measure a significant effect from the product that solely utilized photocatalytic oxidation (PCO).

For all six products using activated carbon filters, the off-gassing of acetaldehyde from the product was measured. Off-gassing is defined as releasing acetaldehyde from the air purifier into the surrounding environment, thus counteracting its effect. Off-gassing should be a point of attention for future investigations into the use of air purifiers, as this was observed for all products utilizing activated carbon filters.

Additionally, for five out of the seven examined air purifiers, small traces of other gases (so-called byproducts) were detected apart from acetaldehyde. It is worth noting that byproducts are a significant point of attention for the future use of air purifiers with relevant technologies.

In this project, measurements of total volatile organic compounds (TVOCs) are performed with indoor air quality sensors at four selected nursing homes and are assumed to be a direct indicator of odor concentration. Overall, it is challenging to draw a definitive conclusion on the effectiveness of the air purifiers in mitigating odorants, as the TVOC concentration varies significantly in the sensor data analyzed during the project period. Additionally, ethanol in the air, likely from hand sanitizers, significantly affects the sensor data, which overshadows the contribution of odorants in the measurements.

For the average TVOC concentration, there is an indication of a positive effect of the air purifier in nursing home 4 (30% reduction), while nursing home 2 shows, on average, a higher TVOC concentration in the room during the period with the air purifier. For all four nursing homes, a lower maximum TVOC concentration is measured during the period with the air purifier turned on compared to the period without. Sensor data also shows that, during the period when the air purifiers were installed, there were fewer periods with a TVOC concentration above 250 ppb for nursing homes 1, 2, and 4. Particularly, a reduction in the TVOC concentration during the periods when the rooms experience a high average load is observed. The TVOC data thus suggest that air purifiers using filters with activated carbon can mitigate some of the odor peak loads during specific periods with high concentrations but is unable to reduce the average background level in the room.

5 ACKNOWLEDGEMENTS

We would like to acknowledge the collaboration with Aarhus Municipality and especially Mads Duevang Dahl and Monica Petersson Ekström.

6 REFERENCES

- ⁱ <https://www.cdc.gov/coronavirus/2019-ncov/prevent-getting-sick/improving-ventilation-in-buildings.html>
- ⁱⁱ <https://www.ashrae.org/about/news/2023/ashrae-approves-groundbreaking-standard-to-reduce-the-risk-of-disease-transmission-in-indoor-spaces>
- ⁱⁱⁱ Pandey, S. K. (2013) *Major Odorants Released as Urinary Volatiles by Urinary Incontinent Patients*, *Sensors* 2013, 13(7), 8523-8533doi:10.3390/s130708523
- ^{iv} S. Koust & F. Rydahl, (2022) Mobile Air Purifiers – How Good Are They, <https://www.teknologisk.dk/projekter/mobile-luftrensere-hvor-godt-virker-de/44379>
- ^v ASHRAE Position Document on Filtration and Air Cleaning, <https://www.ashrae.org/File%20Library/About/Position%20Documents/filtration-and-air-cleaning-pd-Feb.2.2021.pdf>
- ^{vi} Bekendtgørelse om grænseværdier for stoffer og materialer (kemiske agenser) i arbejdsmiljøet, BEK nr 1054 af 28/06/2022
- ^{vii} <https://osha.europa.eu/da/themes/dangerous-substances/practical-tools-dangerous-substances/niosh-pocket-guide-chemical-hazards>
- ^{viii} Corresponding to shift from ”good” to “medium” air quality with respect to the TVOC concentration (Umweltbundesamt - <https://link.springer.com/article/10.1007/s00103-007-0290-y>)

What can CO₂ measurements tell us about ventilation and infection risk in classrooms?

Carolanne V. M. Vouriot^{1*} and P. F. Linden¹

¹*Department of Applied Mathematics and Theoretical Physics,
University of Cambridge, Centre for Mathematical Sciences,
Wilberforce Road, Cambridge, CB3 0WA*

ABSTRACT

Indoor air quality in schools is of critical importance for the health and well-being of pupils and staff. The COVID-19 pandemic highlighted the essential role that ventilation systems play in limiting the spread of airborne diseases and consumer CO₂ monitors were deployed in UK classrooms as a cost-effective tool to help manage the ventilation supply. In such settings, which are occupied for long periods by the same group of people, CO₂ measurements have also been used to infer the risk of far-field airborne infection. Often, only a single point measurement is available and so it is crucial to understand how exposure might differ depending on the infector location and/or sensor position. This is particularly important in UK classrooms which are typically naturally ventilated, and where spatial variations in the concentration of CO₂ and infected breath can be expected.

CO₂ data gathered across 5 years prior to the pandemic from 45 classrooms in 11 different schools were first analysed and estimates of the likelihood of airborne infection were calculated. Even without accounting for the variation in disease prevalence, the data highlight significant variation in infection risk between the seasons, with January being nearly twice as risky as July. Results also show that the risk can vary widely between classrooms of the same school despite similar ventilation provisions. The second part of this work provides a detailed examination of the validity of using CO₂ as a proxy for far-field exposure. For this, a generic naturally ventilated UK classroom in wintertime was simulated using computational fluid dynamics (CFD). The ratio between actual exposure arising from a single infected individual and proxy exposure calculated from point measurements of CO₂ was also analysed. In doing so, the proxy exposure is found to be within a factor of two of the actual far-field exposure. While this factor of two might appear large, it is small relative to the typical uncertainties associated with airborne disease modelling.

KEYWORDS

CO₂ measurements; classrooms; natural ventilation; CFD;

1 INTRODUCTION

Schools are an important setting for indoor air quality. In the UK alone, 11 million pupils and staff regularly attend schools, with the majority of the time spent in classrooms. This came to the forefront of public attention during the COVID-19 pandemic. During this time, the use of carbon dioxide (CO₂) sensors became widespread in classrooms to help manage ventilation provision. In addition, CO₂ sensors have also been shown to be cheap and effective tools to assess the risk of far-field airborne infection to respiratory diseases such as COVID-19, following for instance the work of Rudnick and Milton (2003). However, in existing studies, only a limited number of measurement locations have been considered (ASHRAE, 2022) and for practical reasons often single-point measurements are available in classrooms. In naturally ventilated spaces (which includes the majority of classrooms in the UK) this can be problematic as the indoor spaces are rarely well-mixed. If CO₂ sensors are to achieve widespread success in managing indoor air quality and limiting the spread of airborne diseases, then these limitations need to be addressed.

2 METHODOLOGY

This work uses both CO₂ measurements in operational classrooms and Computational Fluid Dynamics (CFD) simulations to determine how CO₂ measurements can be used to assess the ventilation provision and airborne infection risk in UK classrooms.

2.1 CO₂ measurements in schools

A dataset of CO₂ concentration in UK schools spanning 5 years before the pandemic (2015-2020) is obtained and analysed. Measurements are made in 45 classrooms from 11 different schools across the UK in both primary and secondary schools. Following the work of Rudnick and Milton (2003), the CO₂ concentration is used to assess the rebreathed fraction and the resulting risk of airborne infection for the 32 occupants if one infector is to attend regularly the classroom for a pre- or asymptomatic period of 5 days.

2.2 CFD simulations

Simulations of a generic naturally ventilated classroom are performed using OpenFOAM. A wintertime scenario is considered where ventilation is solely buoyancy driven. The heat input (both from occupants and the heating provision) is input uniformly across the floor and drives the ventilating flow through high- and low-level vents. The presence of occupants is modelled via the addition of passive scalars at breathing height representing both the overall CO₂ output and tracers representing a potentially infected breath. This allows the comparison of both distributions to determine how exposure estimates are affected by the use of CO₂ as a proxy.

3 CONCLUSIONS

Historical measurements of CO₂ spanning 5 years in UK schools highlight the seasonal variations in ventilation provisions and resulting impact on airborne infection: notably the risk doubles in January when compared to July (the least risky month). Numerical simulations allow the measurement of the uncertainty introduced by the use of a single measurement in a naturally ventilated classroom. Although the CO₂ distribution is shown to vary spatially, point measurements are shown to be good indicators of the ventilation provision, especially when compared to other sources of uncertainties such as knowledge of the number of occupants and their activity levels. When used to assess the risk of airborne infection, using CO₂ as a proxy leads to exposure within a factor of two of exposure to infected breath. This uncertainty is lower in magnitude relative to that from other sources including estimates of the quanta generation rates which can vary by three orders of magnitude.

4 ACKNOWLEDGEMENTS

CVMV was funded via the School Air quality Monitoring for Health and Education SAMHE project (grant EP/W001411/1). Computational resources were provided by the UK Turbulence Consortium (grant EP/R029326/1). We gratefully acknowledge Fred Mendonça and his team at OpenCFD for providing support and advice on setting up the numerical simulations.

5 REFERENCES

Rudnick, S.N. and Milton, D.K., 2003. Risk of indoor airborne infection transmission estimated from carbon dioxide concentration. *Indoor air*, 13(3), pp.237-245.

ASHRAE, ASHRAE position document on indoor carbon dioxide, American Society of Heating, Refrigerating and Air-Conditioning Engineers, 2022.

Indoor air modelling and infection risk assessment in a naturally ventilated patient room

Natalia Lastovets^{*1}, Mohamed Elsayed¹, Ville Silvonen², Anni Luoto³, Piia Sormunen¹

*1 Tampere University, Faculty of Built Environment
Korkeakoulunkatu 5
33720 Tampere, Finland*

**Corresponding author: natalia.lastovets@tuni.fi*

*2 Tampere University, Faculty of Engineering and
Natural Sciences
Korkeakoulunkatu 6
33720 Tampere, Finland*

*3 Granlund Oy
Malminkaari 21
00700 Helsinki, Finland*

ABSTRACT

Sufficient ventilation in clinics is critical for diluting virus concentrations and lowering subsequent doses inhaled by the occupants. Several advanced simulation methods and tools for building physics and indoor air fluid dynamics are currently available in research and industry. However, in naturally ventilated buildings, indoor air distribution depends strongly on local and dynamically changing conditions, e.g., opening sizes and time, exhaust shaft location, and climatic and weather conditions. Therefore, considering the physical complexity of air and temperature distribution in natural ventilation rooms, new reliable and handy modelling techniques are required to predict infection risks of COVID-19 in typical naturally ventilated spaces.

This study includes field measurements and simulations of indoor air quality and building performance in a naturally ventilated hospital building. The indoor air model is built into the building energy simulation tool IDA-ICE to calculate air change rates in a naturally ventilated patient room. An initial data set was collected from the presurvey, architectural plans, and observations. The model was calibrated against indoor air measurements. Then, simulated air changes and room conditions were used for infection risk calculation. The virus-specific parameters of the infection risk model and human activity values are estimated separately using scientific literature studies.

According to measurements and simulations, natural ventilation is insufficient to dilute airborne impurities in this case study. Additionally, the infection risk analysis indicated that the infection emission rate had a significant impact on the results of different ventilation strategies. The combination of controlled ventilation and air purification reflects a comprehensive and proactive approach to managing infection risks in patient rooms and healthcare settings. The simulation tool can help engineers and designers explore different ventilation strategies and infection control measures.

KEYWORDS

Natural ventilation, infection risk assessment, patient room, COVID-19, dynamic simulation

1 INTRODUCTION

The COVID-19 pandemic has sparked extensive research on airborne transmission of diseases, virus properties, risk assessment and the role of ventilation technology and air purification in preventing airborne transmission in various indoor spaces. Hospitals and healthcare facilities, being high-risk environments, have been of particular interest in these studies. Multiple case studies have demonstrated that SARS-CoV-2 can remain viable in aerosols for several hours, further emphasising the significance of proper ventilation and air filtration in healthcare facilities (Izadyar and Miller, 2022; Zhao et al., 2022).

Ventilation systems in modern hospitals are designed to reduce airborne infection risks and prevent cross-infections. To ensure proper dilution of airborne viruses, patient rooms in hospital facilities must have 4-12 air exchanges per hour (ACH), as specified by corresponding standards and regulations (Lancet COVID-19 Commission, 2022). The COVID-19 pandemic has highlighted the limitations of natural ventilation in maintaining precise control over indoor air quality and airflow rates. In high-risk environments, mechanical ventilation with controlled airflow rates and appropriate filtration is often preferred to ensure infection control measures (WHO, 2021).

Despite the challenges brought to light during the COVID-19 pandemic, natural ventilation remains a common practice in hospitals, particularly in regions with warmer climates where it can be more easily implemented due to favourable weather conditions (Abbas and Dino, 2022; Fageha and Alaidroos, 2022). In addition, many hospitals, especially older ones, were designed with architectural features that promote natural ventilation, such as large windows, high ceilings, rooms and corridors aligned to facilitate cross-ventilation (WHO, 2009). Upgrading or retrofitting these healthcare facilities with mechanical ventilation might require significant structural modifications and compliance adjustments, which can be challenging for older facilities (Gilkeson et al., 2013). If upgrading the existing ventilation system is not immediately feasible, a combination of strategies may be needed to enhance ventilation and indoor air quality in healthcare facilities. This might involve optimising natural ventilation where feasible, implementing air purification technologies in specific areas, and considering mechanical ventilation for high-risk spaces (Fennelly et al., 2023). The design of such spaces requires careful consideration and planning to ensure that the combination of different options effectively promotes airflow and maintains a safe environment.

Virus risk assessment in naturally-ventilated indoor spaces is a complex and multifaceted problem that involves various aspects of building physics and understanding the characteristics of the specific virus in question. The transient nature of natural ventilation, combined with fluctuating outdoor and indoor conditions, makes simulation of these spaces computationally intensive and requires advanced modelling techniques. In engineering applications, it is critical to balance the level of detail in the simulation model with computational resources to meet the simulation goal. To overcome these challenges, researchers and engineers often adopt a combination of simplified modelling techniques, empirical correlations, and advanced indoor air simulation tools (Moghadam et al., 2023). When assessing virus risk in naturally ventilated settings, researchers often use a combination of building energy simulation, fluid dynamics, and contaminant transportation to determine optimal ventilation design. The design scenarios calculated by such models typically represent the effect of different building types and climate zones (Tognon et al., 2023), positions of inlet and outlet (Abbas and Dino, 2022), optimised window opening control (Grygierek et al., 2022) and occupancy scenarios (Fageha and Alaidroos, 2022) on airborne infection risk. In such design models, Wells-Riley models are commonly used to assess the impact of ventilation strategies, filtration systems, occupancy patterns, and other controls on the risk of infection transmission (Kurnitski et al., 2023).

The case studies in simulation research on virus risk with natural ventilation are usually made for educational buildings, offices, and commercial and residential buildings (Moghadam et al., 2023). However, there is a lack of evidence-based studies in hospital facilities that are strategically important and may not be closed in case of a pandemic.

This research aims to develop a straightforward engineering methodology to evaluate virus risk in naturally vented healthcare facilities. It will also provide options for possible ventilation and air purification strategies. The following sections present an infection risk assessment case study in a naturally ventilated patient room. This case study utilised measurements of indoor air parameters, dynamic simulation of natural ventilation performance and virus risk assessment. Finally, infection risk-based solutions are described using ventilation strategies and air purification combinations.

2 CASE STUDY

This case study is based on an analysis of ventilation and air purification solutions in the Matei Bals Hospital patient room in Romania, Bucharest. Background information about the case building was collected during the pre-study phase of the research (Figure 1). The hospital building has brick walls and large windows. A closed hallway separates the patient rooms on opposite sides of the building. The studied patient room is located on the second floor of a four-storey Covid Ward building. The patient room is designed for two patients. The building is ventilated only by natural ventilation, with fresh outdoor air supplied by infiltration and openings and exhaust air removed by an exhaust shaft. The patient's room is heated by a water radiator under the window connected to the district heating system.

The pre-study survey provided information about building use, approximate window opening schedules and occupancy in the patient room. In addition, information on possible diseases of patients and disinfection methods and other measures to prevent disease spread were revealed. The window opening schedule was claimed to be every two hours for fifteen minutes. A face mask is required for all hospital personnel and patients. In the infection isolation rooms, personnel wear protective suits. Hospital spaces can spread viruses due to the absence of a controlled ventilation system and air purification. Thus, further research included fresh air exchange and virus risk analysis in dynamic conditions. In addition to the survey, cloud-based indoor air quality (IAQ) monitoring was performed in the pre-study phase. Indoor air parameters fluctuated highly during the measurements. Also, measurement data quality was highly dependent on the internet connection. Therefore, further research included on-site indoor air measurements to check the quality of the data loggers.

The possible technological solutions applied in the study included the combination of portable air purifiers with existing natural ventilation. Mechanical ventilation option was also checked in the infection risk calculation.

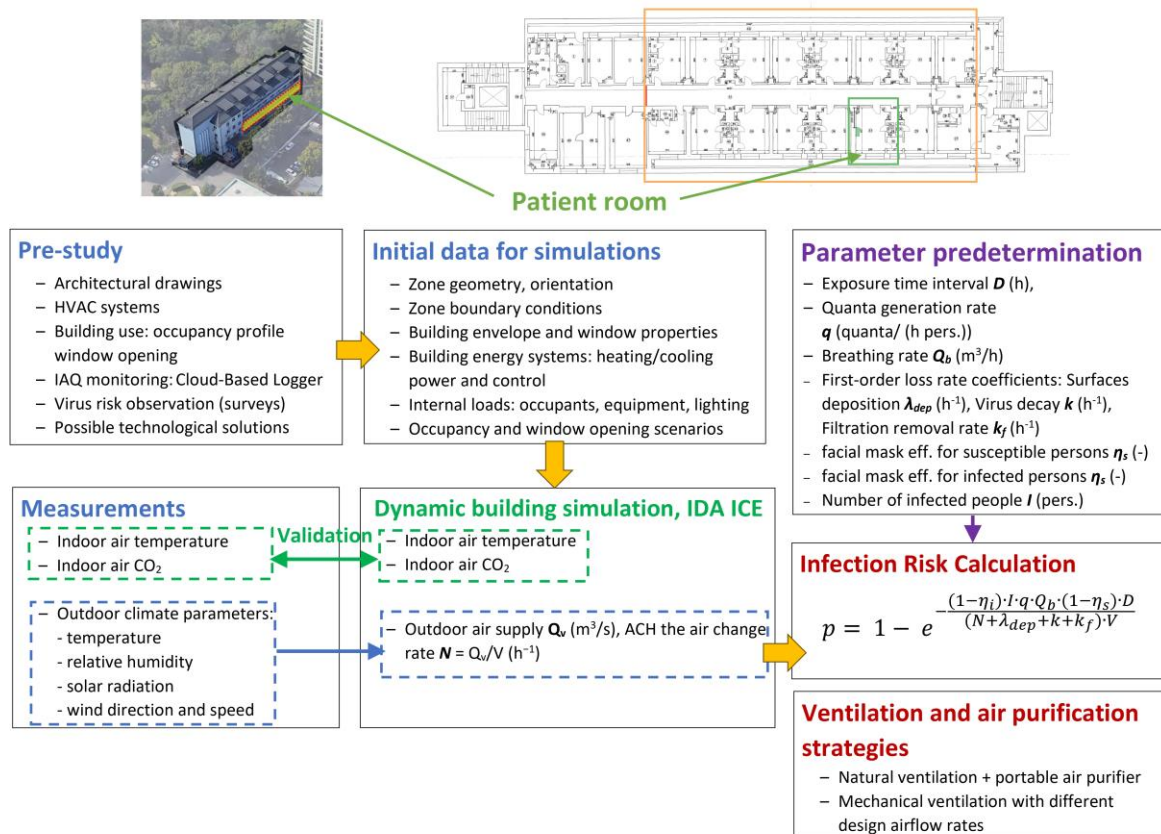


Figure 1: Case study algorithm and methods

3 METHODS

The methods applied in this section describe the research methods that followed the pre-study phase, including measurements of indoor air parameters, dynamic building simulation and infection risk calculation.

3.1 Indoor air measurements

The indoor air temperatures and CO₂ levels were measured with the cloud-based IAQ monitoring service SmartWatcher® and data loggers Onset HOBO®. The cloud-based IAQ monitoring portable device SmartWatcher® was located on the internal wall at a height of 2 meters. Three data loggers Onset HOBO® were placed on the tripod at three heights 0.5 m, 1.0 m and 1.5 m (Figure 2). In addition, during the measuring campaign the air purifier ISEC Kullas® was installed between the patient beds. The air purifier was working at 60% power, providing CADR 192 m³/h.

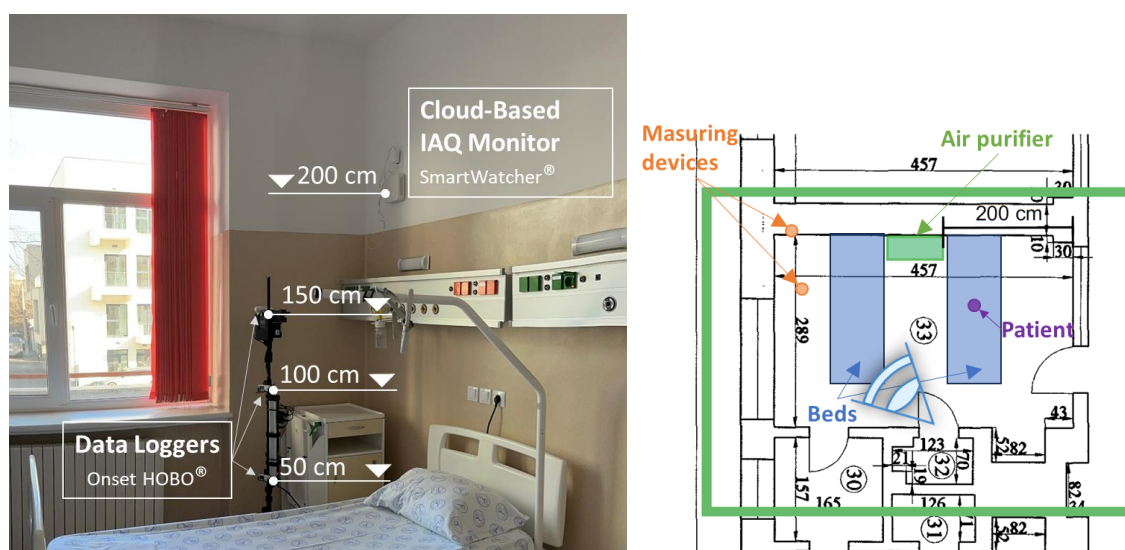


Figure 2: Patient room layout and location of the measuring devices

The SmartWatcher® IAQ Monitoring Service is a cloud-based indoor air quality monitoring service showing real-time values for the investigated parameters. The monitoring service collects data every 1 minute and stores it in the cloud every 10 minutes. The data loggers Onset HOBO® were also configured with a one-minute measurement interval. The logger's built-in memory was used to store data, which was later retrieved via USB. The outdoor air measurements were taken from the local meteorological institute, National Air Quality Monitoring Network in Bucharest. The measuring devices were validated at VTT Technical Research Centre of Finland Ltd. (<https://www.vttresearch.com/en>). Table 1 shows the technical parameters of the temperature and carbon dioxide sensors of the measuring devices.

Table 1: Measuring devices

	SmartWatcher®		Onset HOBO®	
	Air temperature °C	CO ₂ ppm	Air temperature °C	CO ₂ ppm
Range	-10 to 50 °C	0 – 10000 ppm	0 to 50 °C	0 – 5000 ppm
Accuracy	±0.1 °C	±3% of reading, ±30 ppm	±0.21 °C	±50 ppm ±5% of reading at 25 °C
Resolution	0.1 °C	1 ppm	0.024 °C at 25 °C	1 ppm

3.2 Dynamic building simulation

This section describes the initial data for dynamic simulation and the methodology for calculating the dynamic airflow rates in a naturally ventilated patient room. Figure 3 presents the initial simulation data in IDA ICE building simulation tool (Bring et al., 2000). The model utilised measured climate data to simulate the outdoor conditions. The room layout and outdoor climate parameters were measured during the measurement campaign. The parameters of the building envelope, exhaust shaft, and heat gain from lighting and equipment were estimated based on visual observation. In the building simulation, the air purifier acts as a source of recirculating air and heat gain from equipment. A zone heat balance was calculated in order to reach an average indoor air temperature of 21 °C to determine the heating power of the water radiator. Since the control and power of the heater were unknown, circuit water temperatures of 70°C at the inlet and 40°C at return were chosen based on average engineering practice. As it was not possible to observe and detect window opening times in hospital facilities, window openings were not considered in the current simulation. In addition, possible window openings didn't affect indoor air measurements, which indicates short window opening times.

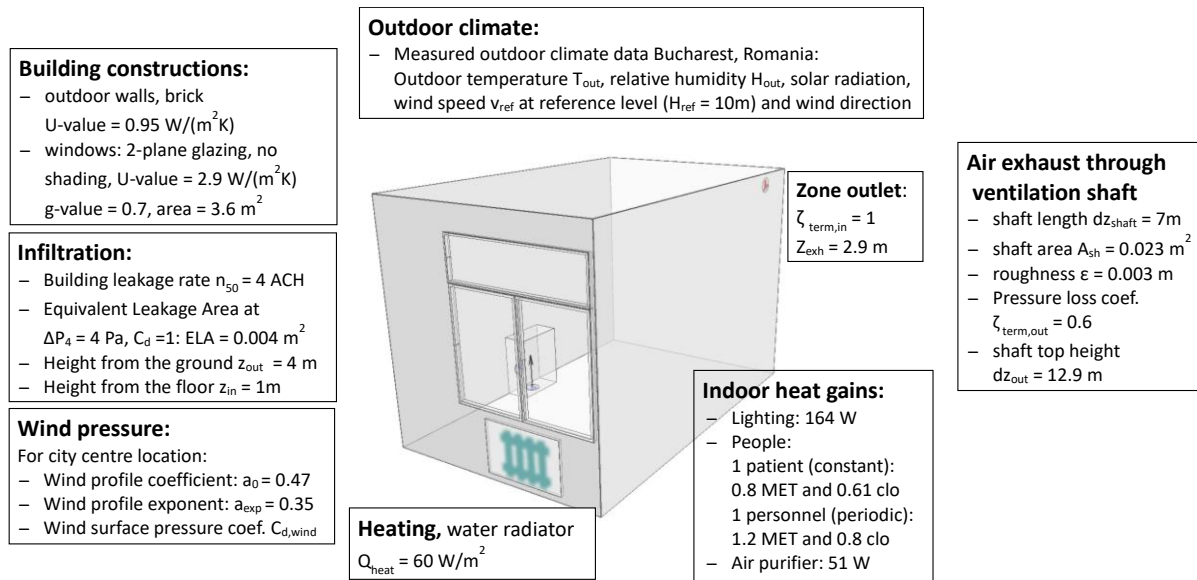


Figure 3: Initial values for dynamic simulation

Air supply was estimated through wind-driven infiltration and air leakage due to pressure differences. The infiltration rate was estimated based on measurement in a building with similar year of construction in Romania (Iordache and Catalina, 2012). In the model, the combined envelope leak area is distributed on all external walls, at z_{in} = 1 m above floor level. The wind pressure variation across the building's surfaces was estimated using wind pressure coefficients C_{d,wind}, calculated for the city centre location. The pressure difference through the leakages dp_{out-in} was defined as:

$$dp_{out-in} = (P_{in} - \rho_{in} \cdot g \cdot z_{in}) - (P_{air} + 0.5 \cdot C_{d,wind} \cdot \rho_{out} \cdot v_{wind}^2 - \rho_{out} \cdot g \cdot z_{out}) \quad (1)$$

where: P_{in} [Pa] is the static pressure of indoor, ρ_{in} [kg/m³] is indoor air density; P_{air} [Pa] is the atmospheric air pressure; ρ_{out} [kg/m³] is indoor air density.

The local wind velocity at the roof height v_{wind} was calculated with the Eq. 2. Wind profile exponents a₀ and a_{exp} are used for wind speed correction from the reference height H_{ref}.

$$V_{\text{wind}} = a_0 \cdot v_{\text{ref}} (H_{\text{build.}}/H_{\text{ref}})^{a_{\text{exp}}} \quad (1)$$

where H_{ref} [m] is height of meteorological wind measurements, $H_{\text{ref}} = 10$ m; H_{build} is the height of the building, m.

The mass flow $m_{\text{out-in}}$ [kg/s] through the infiltration was calculated with the power law equation:

$$m_{\text{out-in}} = c \cdot dp_{\text{out-in}}^n \quad (3)$$

where n [-] is the flow exponent, which is a dimensionless parameter representing the non-linearity of the airflow regime, $n = 0.6$; c [kg/(s Paⁿ)] is the power-law coefficient, which is calculated from the equivalent leakage area (ELA) as:

$$c = \text{ELA} \frac{\sqrt{2\Delta P_4 \cdot \rho_{20^\circ\text{C}}}}{\Delta P_4^{0.6}} \approx 1.35 \cdot \text{ELA} \quad (4)$$

The pressure differences from the indoor air through the exhaust shaft consist of the components related to buoyancy flows from the floor to outlet terminal $dp_{\text{in-shaft}}$, airflow inside the shaft dp_{shaft} the air outlet from the shaft towards the outdoor air $dp_{\text{shaft-out}}$ (Eq. 5-7):

$$dp_{\text{in-shaft}} = (P_{\text{in_floor}} - \rho_{\text{in}} \cdot g \cdot z_{\text{exh}}) - P_{\text{term,in}} \quad (5)$$

$$dp_{\text{shaft}} = P_{\text{shaft1}} - P_{\text{shaft2}} - dz_{\text{shaft}} \cdot g \cdot \rho_{\text{shaft}} \quad (6)$$

$$dp_{\text{shaft-out}} = P_{\text{term,out}} - (P_{\text{out,roof}} - \rho_{\text{out}} \cdot g \cdot dz_{\text{out}}) \quad (7)$$

where $P_{\text{in_floor}}$ [Pa] is the static pressure at the floor level; $P_{\text{term,in}}$ [Pa] is the static pressure at the outlet terminal in the room; P_{shaft1} and P_{shaft2} [Pa] are the static pressures on the bottom and top of the shaft respectively; $P_{\text{term,out}}$ [Pa] is the static pressure at the terminal on the top of the exhaust shaft; $P_{\text{out,roof}}$ [Pa] is the outdoor air pressure at the roof level.

The equation Eq.8 defines the mass flow $m_{\text{in-out}}$ [kg/s] through the exhaust shaft from indoor air, taking into account head pressure losses at the outlet terminal $\zeta_{\text{term,in}}$ and exhaust grill $\zeta_{\text{term,out}}$, as well as friction losses inside the shaft. Based on the flow regime depending on Reynolds number Re , surface roughness ε , and shaft dimensions A_{sh} , friction losses are presented within the combined coefficient C_{tot} (ASHRAE, 2017).

$$m_{\text{in-out}} = A_{\text{sh}} \sqrt{2 \cdot \rho_{20^\circ\text{C}}} \cdot \left(\sqrt{\frac{dp_{\text{in-outlet}}}{\zeta_{\text{term,in}}}} + \sqrt{\frac{dp_{\text{shaft-out}}}{\zeta_{\text{term,out}}}} \right) + C_{\text{tot}} \sqrt{dp_{\text{shaft}}} \quad (8)$$

$$C_{\text{tot}} = f(Re, \varepsilon, A_{\text{sh}})$$

Therefore, the ventilation rate calculation involves estimating the infiltration rate into a room due to buoyancy (stack effect) and wind-driven forces in IDA ICE building simulation software. The software uses wind profile equations and wind pressure coefficients to estimate outdoor wind speed at varying heights relevant to the building's characteristics. The stack effect takes into account differences in temperature between indoor and outdoor air, as well as pressure losses in the exhaust shaft. The calculated ventilation rates are used in the infection risk estimation described in the following Section 3.3.

3.3 Infection risk model

Infection risk calculations were conducted using the Wells-Riley model (Eq.9), which is widely used in ventilation design and indoor air quality studies to estimate infection risk, especially in

the context of infectious respiratory diseases such as influenza and COVID-19. The model parameters were chosen from the latest literature (Kurnitski et al., 2023).

$$p = 1 - e^{-\frac{(1-\eta_i)I \cdot q \cdot Q_b \cdot (1-\eta_s) \cdot D}{(N + \lambda_{dep} + k + k_f) \cdot V}} \quad (9)$$

Due to the sensitivity of the Wells-Riley model to quanta emission rates, the study examined the effects of different emission rates on the probability of infection transmission in indoor spaces in the absence of facial masks ($\eta_s = 0$ and $\eta_i = 0$) using a range of quanta emission rates from 2 to 10 quanta/hour per person (Table 2). Simulations were conducted under conditions in which one infectious ($I = 1$) and one susceptible person were constantly present.

A dynamic airflow calculation was used to simulate infection risk in natural ventilated conditions with and without the air purifier (ISEC Kullas). In addition, the mechanical ventilation cases without air purifiers were calculated with the recommended minimum (4 ACH) and maximum (12 ACH) air exchanges for patient rooms (Lancet COVID-19 Commission, 2022).

Table 2: Infection risk model parameters

Parameter	Unit	Value
Quanta generation rate per infectious person q	quanta/(h pers)	2 – 10
Breathing rate for resting people Q_b	m^3/h	0.5
Surfaces deposition loss rate λ_{dep}	1/h	0.6
Filtration removal rate from portable air purifier k_f	1/h	4.5

4 RESULTS

This section describes the results of the study. First, the measurements of indoor air temperatures and carbon dioxide were analysed and compared with the simulation results. The calculated air flow in natural ventilation was presented with the correlation to outdoor air measurements. Finally, the infection risk methodology and calculation result were shown for different parameter ranges and ventilation solutions.

4.1 Measured and simulated parameters of indoor air

The air temperatures and CO₂ levels simulated by IDA-ICE-model was compared with measurements in order to validate the building simulation model (Figure 3). The simulated air temperatures were closer to the measurement result, especially at the SmartWatcher measuring point. The temperature measured by HOBO sensors was about 1 °C higher than the simulated temperature measured by SmartWatcher (Figure 3a). This could be due to the local effect of internal heat gain sources and heating system controls that were not taken into account when calculating the heat balance. Also, the sensors' sensitive elements faced different angles toward solar radiation, heat gain sources, and airflow distribution, which resulted in different fluctuation patterns. In addition, a rapid temperature rise of 1 °C occurred due to reflected solar radiation around the same time (around 3:20 pm). Solar radiation from the eastern-facing window affected HOBO measurements in the early morning (7-8 am). Generally, the simulation model is able to capture the main patterns for indoor air temperature changes.

As the outdoor air temperature mainly determined the natural driving force for airflow, simulated air changes per hour were higher at night when the outside air was colder. Air exchanges also impacted indoor CO₂ distribution, resulting in minimal levels at night and maximum levels during the day (Figure 3b). The measured indoor CO₂ levels tended to vary throughout the day based on occupant activities, ventilation rates, and other environmental

conditions that were difficult to record and simulate. However, the model is able to present the main tendencies of dynamically changing CO₂ and calculate the mean averaged values. As a result of the validation of dynamic building simulations with measurements, it can be concluded that the simulation model is capable of predicting the thermal and mass balance with the desired level of accuracy.

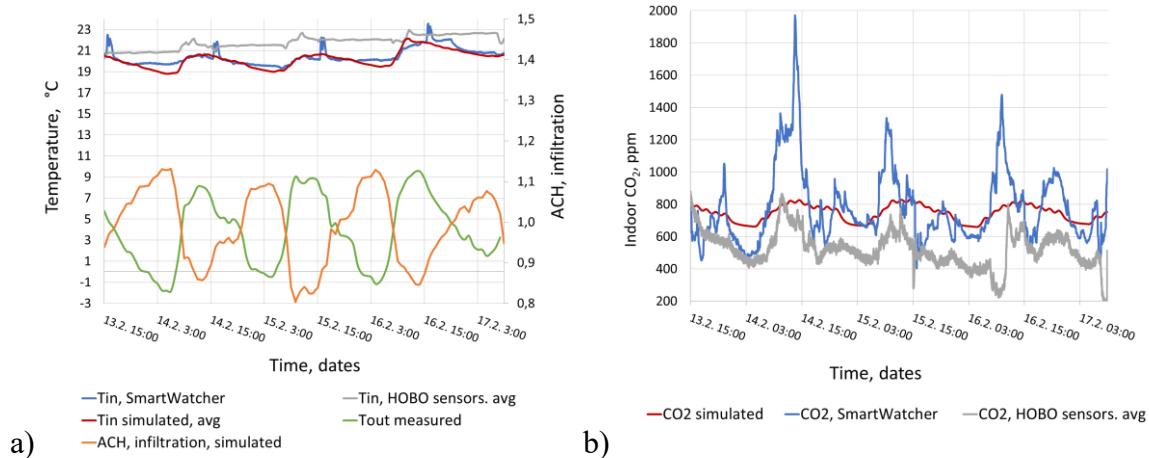


Figure 3: Measured and simulated indoor air temperatures (a) and CO₂ (b)

4.2 Infection probability calculation

Infection probabilities were calculated before and after air purifiers were installed in the patient room (Figure 4a). Infection risk results with lower quanta are more sensitive to changes in airflow rates. According to the calculations, the air purifier with 2 quanta/h pers is more effective than the one with higher quanta values. It might be because the air purifier's ability to remove infectious particles is more noticeable when emissions are lower. In cases where emission rates are higher, the air purifier might not be able to remove particles from the air as quickly as they are being emitted.

Figure 4b shows the increase in infection risk with different ventilation systems and adding the air purifier. Predictably, with natural ventilation alone the infection probability is the highest. The use of a mechanical ventilation system with a high air exchange ACH 12 demonstrates the best efficiency in reducing infection risk across different quanta emission rates. However, mechanical ventilation with lower ACH might have limitations in effectively reducing infection risk, especially in scenarios where quanta emission rates are high. In the studied case, natural ventilation combined with an air purifier can be efficient even in scenarios with high quanta emission rates.

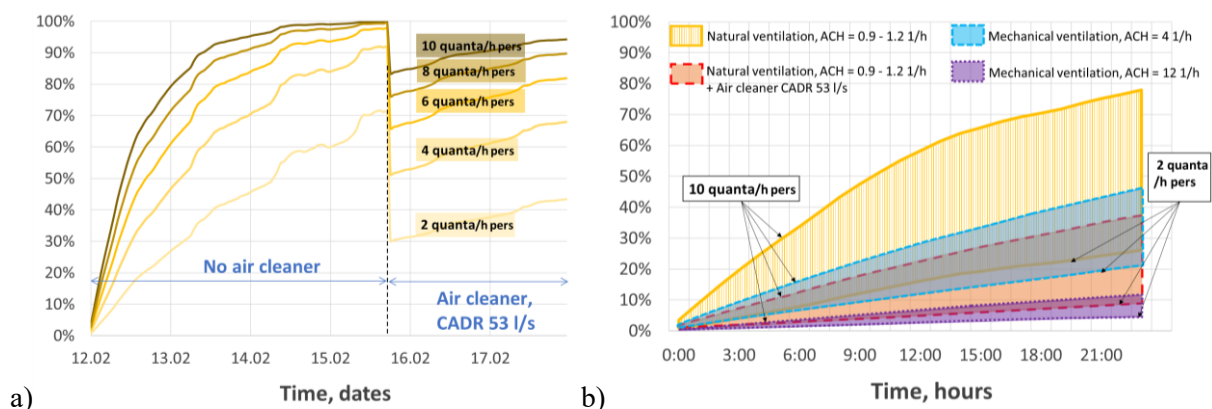


Figure 4: Infection risk probability during the measuring period (a) and with a day of exposure (b)

5 DISCUSSION

Accurate field measurements and precise simulations in real-world hospital facilities often encounter different challenges, such as limited data availability and difficulties in obtaining accurate building information. Building simulations allow you to explore various scenarios, interventions, and technologies in a controlled environment, while measurements can be used for validation and separate analysis.

Natural ventilation simulation accuracy depends on modelling assumptions. Small changes in input parameters or boundary conditions can lead to significant results differences. Validating simulation results with real-world measurements can be complex, especially for large and complex buildings with varying conditions. In this case, advanced models like CFD can be used to better understand the airflow behaviour of a building.

Within hospital settings, the Wells-Riley infection risk model has significant limitations since it does not consider disease-specific parameters, assumes a uniform distribution of infection particles, and is not suitable for dynamic scenarios. However, it is still possible to apply this model to estimate safe spaces and infection risk-based ventilation design.

While air purifiers can effectively reduce infection risks by removing airborne particles, including infectious agents, they might not inherently improve all aspects of indoor air quality (VOCs, humidity or temperature in the indoor environment). Thus, air purifiers should be used in conjunction with other measures such as ventilation, proper maintenance of the HVAC system, and other air cleaning measures.

6 CONCLUSIONS

This study investigated a naturally ventilated patient room in Bucharest, Romania. Indoor air measurements and building simulations were combined with an infection risk assessment to investigate possible ventilation and air purification technologies. A simulation model for the studied room was developed using IDA ICE software and validated with measurements. In the simulation model, dynamic airflow rates with natural ventilation were calculated and applied to infection risk estimation. These findings emphasise the significance of both emission rates and airflow rates when assessing the effectiveness of air purifiers and ventilation technologies. The results show that natural ventilation alone is not able to sufficiently dilute airborne impurities. A combined ventilation strategy and air purification are required in patient rooms to prevent infection. The simulation tool developed can be used for infection risk analysis in engineering applications to optimise hospital design and operation. The research contributes to the understanding of infection risk in indoor environments and enables finding optimised ventilation and air purification strategies to reduce the spread of airborne infectious diseases.

7 ACKNOWLEDGEMENTS

This research was supported by the Business Finland project E3 Excellence in Pandemic Response and Enterprise Solutions (www.pandemicresponse.fi) and Tampere university foundation sr.

8 REFERENCES

- Abbas, G.M., Dino, I.G. (2022) COVID-19 dispersion in naturally-ventilated classrooms: a study on inlet-outlet characteristics, *Journal of Building Performance Simulation*, 15:5, 656-677, DOI: 10.1080/19401493.2022.2063946.
- ASHRAE Standard Committee (2017). *ASHRAE Handbook: Fundamentals: SI Edition*, ASHRAE, Atlanta, USA.

- Bring, A., Sahlin, P., Vuolle, M. (2000). *Models for Building Indoor Climate and Energy Simulation: A Report of IEA SHC Task 22: Building Energy Analysis Tools; Subtask B: Model Documentation: Version 1.02*, December 1999. Kungl. Tekniska högsk.
- Fageha, M.K.; Alaidroos, A. (2022) Performance Optimization of Natural Ventilation in Classrooms to Minimize the Probability of Viral Infection and Reduce Draught Risk. *Sustainability*, 14, 14966, DOI: <https://doi.org/10.3390/su142214966>.
- Fennelly, M., Hellebust, S., Wenger, J., O'Connor, D., Griffith, G. W., Plant, B. J., Prentice, M. B. (2023). Portable HEPA filtration successfully augments natural-ventilation-mediated airborne particle clearance in a legacy design hospital ward. *Journal of Hospital Infection*, 131, 54-57. DOI: <https://doi.org/10.1016/j.jhin.2022.09.017>.
- Gilkeson, C. A., Camargo-Valero, M. A., Pickin, L. E., Noakes, C. J. (2013). Measurement of ventilation and airborne infection risk in large naturally ventilated hospital wards. *Building and environment*, 65, 35-48, DOI: <https://doi.org/10.1016/j.buildenv.2013.03.006>.
- Grygierek, K., Nateghi, S., Ferdyn-Grygierek, J., Kaczmarczyk, J. (2023). Controlling and limiting infection risk, thermal discomfort, and low indoor air quality in a classroom through natural ventilation controlled by smart windows. *Energies*, 16(2), 592, DOI: <https://doi.org/10.3390/en16020592>.
- Iordache, V., Catalina, T. (2012). Acoustic approach for building air permeability estimation. *Building and Environment*, 57, 18-27. DOI: <https://doi.org/10.1016/j.buildenv.2012.04.008>
- ISEC Kullas (webpage). Available online: <https://www.isec.fi/ilmanpuhdistimet/> (accessed on 18 May 2023).
- Izadyar, N., Miller, W. (2022). Ventilation strategies and design impacts on indoor airborne transmission: A review. *Building and Environment*, 218, 109158, DOI: 10.1016/j.buildenv.2022.109158.
- Kurnitski, J., Kiil, M., Mikola, A., Vösa, K. V., Aganovic, A., Schild, P., Seppänen, O. (2023). Post-COVID ventilation design: infection risk-based target ventilation rates and point source ventilation effectiveness. *Energy and Buildings*, 113386
- Lancet COVID-19 Commission. (2022) *Proposed Non-infectious Air Delivery Rates (NADR) for Reducing Exposure to Airborne Respiratory Infectious Diseases*. 2022. Available online: <https://covid19commission.org/safe-work-travel> (accessed on 18 May 2023).
- Moghadam, T. T., Morales, C. O., Zambrano, M. L., O'Sullivan, D. T. J. (2023). Energy efficient ventilation and indoor air quality in the context of COVID-19-A systematic review. *Renewable and Sustainable Energy Reviews*, 182, 113356, DOI: <https://doi.org/10.1016/j.rser.2023.113356>.
- Tognon, G., Marigo, M., De Carli, M., Zarrella, A. (2023). Mechanical, natural and hybrid ventilation systems in different building types: Energy and indoor air quality analysis. *Journal of Building Engineering*, 76, 107060, DOI: <https://doi.org/10.1016/j.jobe.2023.107060>.
- World Health Organization (WHO) (2009). *Natural ventilation for infection control in health care settings*. Available online: <https://apps.who.int/iris/handle/10665/44167> (accessed on 18 May 2023).
- World Health Organization (WHO). (2021). *Roadmap to improve and ensure good indoor ventilation in the context of COVID-19*. (2021). Available online: <https://www.who.int/publications/i/item/9789240021280> (accessed on 18 May 2023).
- Zhao, X., Liu, S., Yin, Y., Zhang, T., Chen, Q. (2022). Airborne transmission of COVID-19 virus in enclosed spaces: an overview of research methods. *Indoor air*, 32(6), e13056 DOI: <https://doi.org/10.1111/ina.13056>.

Performance of Local Ventilation System Combined with Underfloor Air Distribution as Preventative Measures for Infectious Diseases in Consulting Room

Jun Yoshihara¹, Toshio Yamanaka¹, Narae Choi², Tomohiro Kobayashi¹,
Noriaki Kobayashi¹, Aoi Fujiwara¹

*1 Osaka University
2-1 Yamadaoka
Suita City, Japan*

*2 Toyo University
5 Chome-28-20 Hakusan
Tokyo, Japan*

**Corresponding author:
yoshihara_jun@arch.eng.osaka-u.ac.jp*

ABSTRACT

This research introduces the local exhaust system (hood) into the consulting room to prevent airborne infection, especially for close-distance conversation. The hood's capture efficiency is mainly affected by surrounding air flow, so this research compared three various underfloor air distribution systems (UFAD); floor-supply displacements ventilation (FSDV), displacement-flow-type diffuser, and swirling flow type diffuser. FSDV is a displacement ventilation method where SA comes from the whole floor through carpets or panels, forming a tranquil up-flow. A displacement-flow-type diffuser forms thermal stratification by supplying horizontal flow along the floor. Swirling-type flow diffuser supplies up and swirling flow and mixes room air well. Droplet nuclei or microdroplets leaked from the hood should be exhausted without expanding to reduce infection risk. The lower hood capture efficiency is not directly relevant to the higher infection risk, and the route to the exhaust outlet could be significant. For this reason, FSDV is expected to reduce the infection risk for close-distance conversation compared to a swirling flow-type diffuser. Full-scale experiments were carried out in this research to reveal the relationship between the ventilation system (hood and three UFAD systems) and infection risk.

KEYWORDS

Local exhaust system, Floor-supply displacements ventilation, Wells-Riley model, Consulting room, Close-distance conversation

1 INTRODUCTION

Airborne infection caused by droplet nuclei and micro droplets moving as an aerosol is regarded as one of the possible ways to infect SARS-CoV-2 (World Health Organization, 2020). Though various measures have been taken to prevent it in many places, entire system-scale ventilation might not be enough to become the solution for preventing short-range airborne transmission (Federation of European Heating Ventilation and Air Conditioning Associations, 2020). Still, many scenarios cannot avoid close-distance conversations, for example, in a consulting (examination) room, restaurant, or crowded train. Therefore, this study proposes a novel approach combining a local exhaust ventilation system (LEV) and floor-supply displacement ventilation (FSDV)(Akimoto et al., 1997) in the consulting room. In FSDV, the conditioned air is supplied from the entire floor through many small halls or carpets, not through some diffusers. Because the capture performance of LEV is significantly affected by surrounding airflow (Komori et al., 2022), the FSDV system, which can make a calm airflow field (Akimoto et al., 1997), is expected to help LEV's performance. This report aimed to

evaluate the effectiveness of the combination of air conditioning with FSDV and a hood and its performance as an infection control measure.

2 METHOD AND MATERIALS

2.1 Measurement setting and case conditions.

A cross-sectional view of the experimental room is shown in Figure 1(a), and an isometric view is shown in Figure 1(b). The experimental room consists of $x=2,400$ $y=3,800$ $z=2,200$ mm and an under-floor chamber, where outside air cleaned by a HEPA filter is supplied under the floor and then blown into the room by a three-way floor outlet. The air supply rate is fixed at $1,000$ m^3/h (50 ACH). Exhaust air is exhausted at a total rate of 990 m^3/h through the local exhaust ventilation system (hood) shown in Figure 1(c) and general ceiling exhaust vents to balance the flow rate, and the room is designed as a clean room to maintain positive pressure. In addition, two human bodies simulating an infected person and a non-infected person (heating at 75 W/body) were placed in the room with an interval of $1,200$ mm in front of their mouths. A flanged hood is used because the flanged hood had the best capture performance under crosswind airflow in a previous study (Fig. 1(c))(Komori et al., 2022).

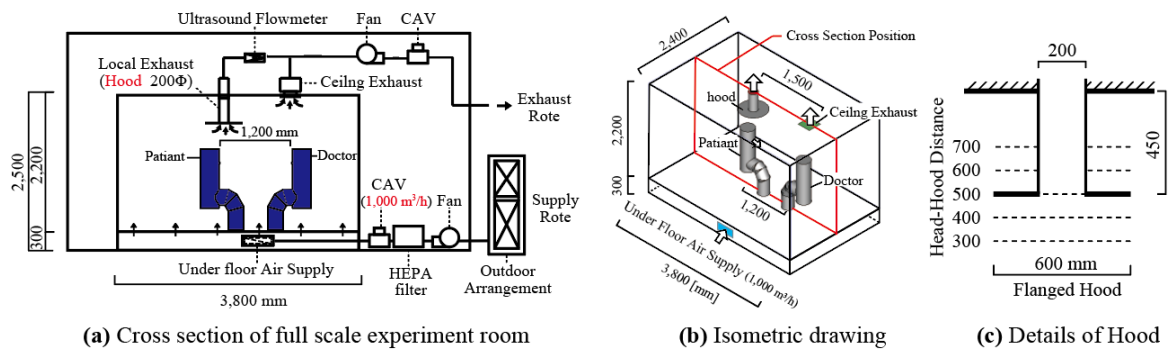


Fig.1 Full scale experiment setting

Table 1 shows the experimental conditions. The experiments were conducted assuming an examination room (Case A) and a non-examination room (Case B), and the hood exhaust volume was varied in eight ways for each of the three air supply methods. In Case A (examination room), a patient is assumed to be talking with a doctor in an infected state. In contrast, in Case B (non-examination room), since the location of the infected person cannot be specified, a hood is fixed between the human bodies, and a desk is set up as a realistic introduction position. Figure 3 shows the floor surfaces of the three air supply methods to be compared. The three air supply systems are floor-supply displacement ventilation (FSDV), swirling-flow type floor diffuser, and displacement ventilation type floor diffuser. In the FSDV system, the fresh outdoor air is supplied from the entire floor surface at a low air velocity (0.03 m/s) to form a calm airflow. In the swirling-flow type floor diffuser, the fresh outdoor air is supplied from eight swirling-flow floor diffusers with a swirl flow (air velocity: approx. $3\sim 4$ m/s) to form a well-mixed airflow. In the displacement ventilation type floor diffuser, the fresh outdoor air is supplied at an angle along the floor surface by 12 displacement ventilation type floor diffusers.

Table 1 Details of Experiment Parameter

	Air Supply Method from Under Floor Chamber	Air Flow Rate [m ³ /h] (Air Change Rate [1/h])	Hood Horizontal Position	Hood Flow Rate [m ³ /h]	Hood-Head Distance [mm]
Case A-1	Floor-supply ventilation	1,000 m ³ /h(50 /h)	above the infected person (patient)	0,50,100,150,200,300,400,500	500
Case A-2	8 Swirling flow type diffusers	1,000 m ³ /h (=125m ³ /h/diffuser×8) (50 /h)		0,50,100,150,200,300,400,500	500
Case A-3	12 Displacement flow type diffuser	1,000 m ³ /h (=83.3m ³ /h/diffuser×12) (50 /h)		0,50,100,150,200,300,400,500	500
Case B-1	Floor-supply ventilation	1,000 m ³ /h(50 /h)	middle of manikins	0,50,100,150,200,300,400,500	500
Case B-2	8 Swirling flow type diffusers	1,000 m ³ /h (=125m ³ /h/diffuser×8) (50 /h)		0,50,100,150,200,300,400,500	500
Case B-3	12 Displacement flow type diffuser	1,000 m ³ /h (=83.3m ³ /h/diffuser×12) (50 /h)		0,50,100,150,200,300,400,500	500

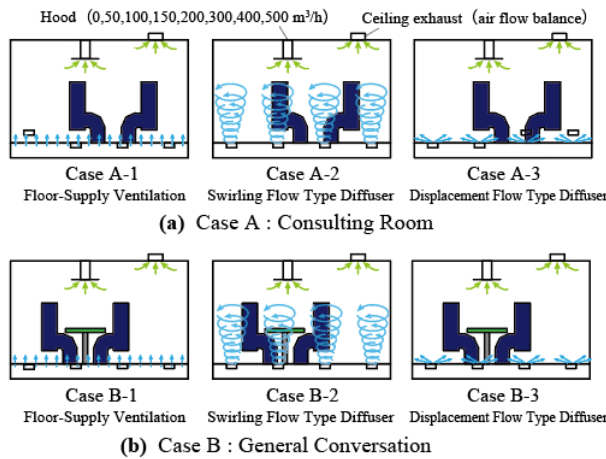


Fig.2 Concepts of Experimental Conditions

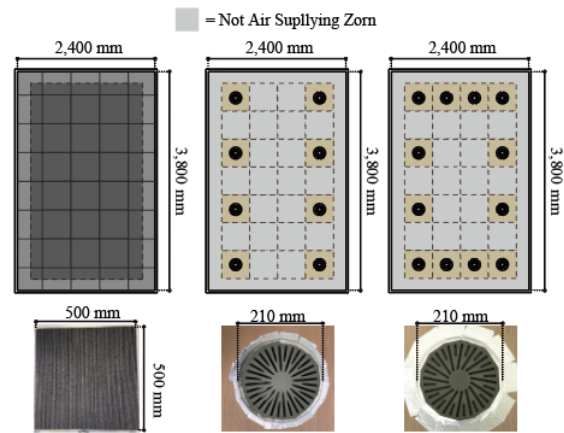


Fig.3 Floor details for each condition

2.2 Measurement point and Expiration condition

The exhaled breath of an infected person was reproduced by the simultaneous generation of CO₂ tracer gas and simulated saliva particles using a nebulizer. A conceptual diagram of exhalation generation is shown in Figure 4. CO₂ and helium were mixed at a ratio of 5:3 (CO₂: He = 3.26: 1.95 L/min) to equalize the density with that of air and generate at the height of the infected person's mouth (height: 1,100 mm) coupled with atomized simulated saliva. The expiratory volume, expiratory air velocity, and blow-off angle values during the conversation were obtained from a previous study(Zhang et al., 2022) and were set to 5.21 L/min, 0.30 m/s, and 11.9° vertical downward, respectively.

After the generation, the spatial distribution of the steady-state CO₂ concentration and the concentration in front of the mouth of non-infected subjects were measured. To account for the effects of evaporation and deposition, simulated saliva was atomized and sprayed simultaneously using a nebulizer (Figure 5). The viscosity of the simulated saliva was adjusted by adding 12 g of sodium chloride and 76 g of glycerin to 1 L of water, referring to previous research (Ogata et al., 2018). In order to reproduce the results obtained from the experiment of measuring expiratory air velocity and respiratory volume during the speech, as described in the previous report (Zhang et al., 2022), a 3D printer was used to create the air outlet (Figure 5 and Figure 7(d)).

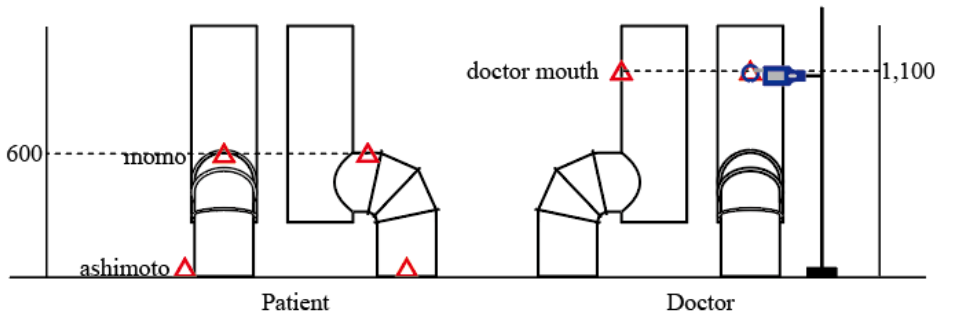
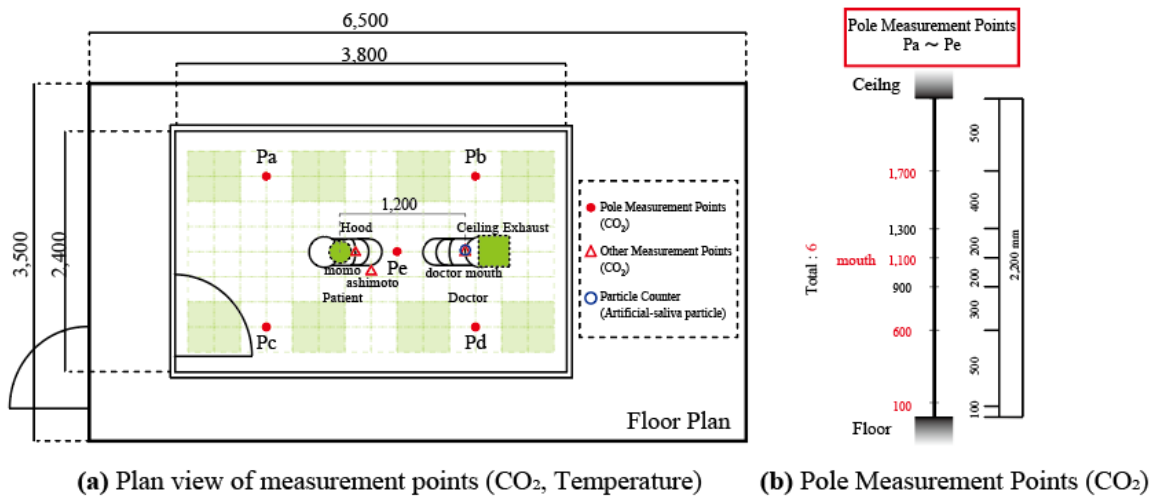
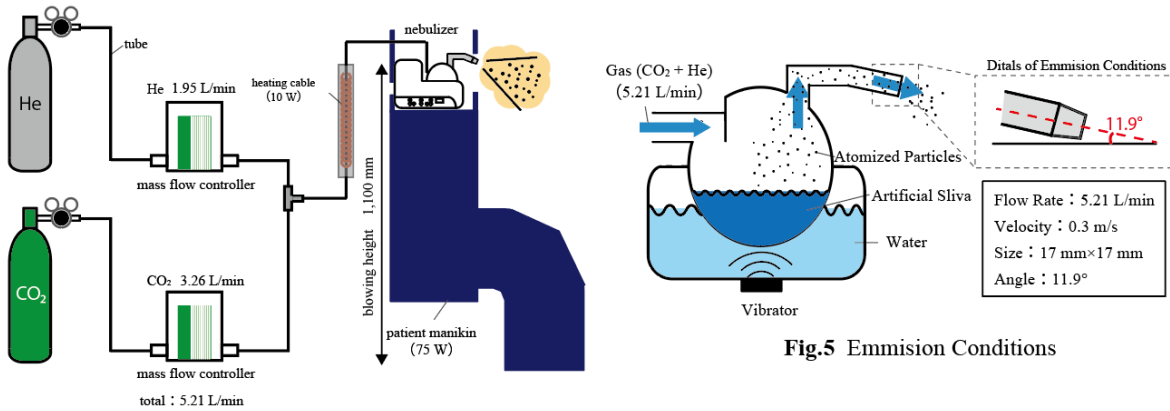


Fig.6 Measurement points (CO₂ gas concentration, Particle (> 0.3μm), Temperature)

2.3 Evaluation method

The hood capture efficiency: η , which indicates the percentage of the tracer gas generated that is collected by the hood, is calculated from Equation (1), and the effectiveness of the combination of the hood and air supply system is examined.

$$\eta = \frac{Q_h(C_h - C_{SA})}{Q_h(C_h - C_{SA}) + Q_e(C_e - C_{SA})} \quad (1)$$

where Q_h is hood flow rate [m³/h], C_h is tracer gas concentration of hood exhaust air [-], Q_e is ceiling exhaust flow rate [m³/h], C_e is tracer gas concentration of ceiling exhaust air [-], C_{SA} is tracer gas concentration of SA [-].

This study is based on the Wells&Riley model (Wells, 1955) (Riley EC et al., 1978) to evaluate infection control performance. The model defines one quanta as the unit of infectivity

that produces 63.2% of new infections in a closed space, and the basic equation is expressed in Equation (2).

$$P = 1 - e^{-n} \tag{2}$$

where P is an increased rate of the number of newly infected persons in closed space, n is the value of the quanta.

Based on the model, quanta concentration in front of the doctor's (non-infected person's) mouth; C_{qd} was calculated from equations (3). The quanta emission rate of 42 quanta/h calculated by REHVA(Federation of European Heating Ventilation and Air Conditioning Associations, 2020) was used as the quanta production rate for infected persons during the conversation.

$$C_{qd} = \frac{q}{Q} \cdot \frac{C_d}{C_{pm}} \tag{3}$$

where C_{dn} is the tracer gas concentration in front of the doctor's mouth normalized by perfect mixing concentration, C_d is the tracer gas concentration in front of the doctor's mouth, and C_{pm} is the tracer gas concentration at perfect mixing. Equation (3) can be calculated by changing C_d and C_p to CO_2 or simulated saliva particles.

Using the value of C_{qd} , the time until the infection risk of the doctor (non-infected person) reaches 5%; $t_{5\%}$ is calculated from Equation (4). Since the REHVA used the value of 5% when describing a sufficiently low risk of infection in an office. Therefore, this report uses 5% as a sufficiently low infection risk.

$$t(P\%) = -\frac{\ln(1 - P)}{n \cdot P} \tag{4}$$

2.4 Preliminary experiment on the nebulizer

To confirm the conversation reproducibility of the nebulizer, particle size and the number of particles were measured at the ceiling exhaust point (Figure 7(a)), immediately after the outbreak (Figure 7(b)), and in front of the doctor's mouth (Figure 7(c)). A hand-held particle counter (3889-01 KANOMAX) was used at the ceiling exhaust port and in front of the doctor's mouth, and a PDA (Dantec Fiber PDA) was used at the point immediately after the outbreak. D_s ; Sauter diameter was calculated using Equation (5) as representative particle size.

$$D_s = \frac{\sum n_i \cdot D_i^3}{\sum n_i \cdot D_i^2} \tag{5}$$

Where n_i is the number of pieces in each grain size category, and D_i is the representative diameter of each grain size category.

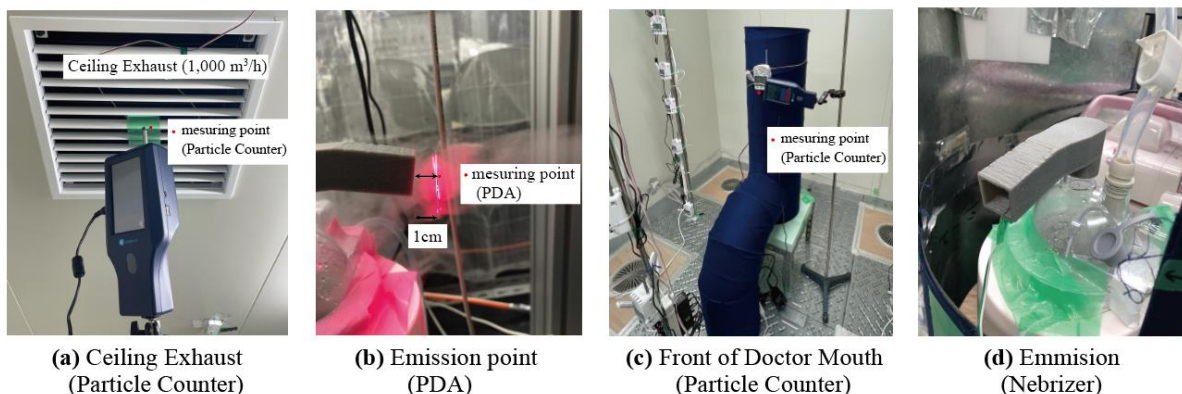


Fig.7 Picture of particle measurement

Figures 10(a), (b), and (d) show the particle size distribution and Sauter diameter calculated from the measurement results. Figure 10(c) shows the particle size distribution when counting the numbers in a previous study (Morawska et al., 2009). In the previous study, the particle size was $0.8\mu\text{m}$, while in the nebulizer used in this report, many large particles ($10\mu\text{m}$ or larger) with a strong tendency to settle out were generated. As a confirmation of steady-state conditions and a measurement of the background noise of particles, the time response variation of the number concentration measured at the exhaust point (generated over 70 minutes) is shown in Figure 8. Figure 8 shows that the background noise is low enough before and after the particle generation because air is supplied through a HEPA filter. Therefore, the particle concentration in front of the doctor's mouth was calculated, assuming the background particles were zero. In addition, even though the nominal ventilation time was only 1.2 minutes, the number concentration kept changing, suggesting that the nebulizer was not generating particles on a steady basis. After confirming that the background particle concentration was sufficiently small, the experiment was conducted with a steady-state waiting period of 5 minutes and a steady-state period of 15 minutes, as shown in Figure 9.

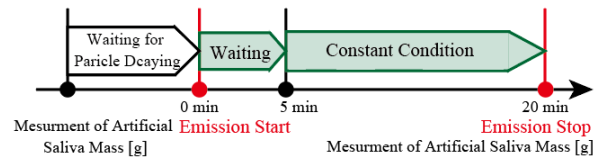
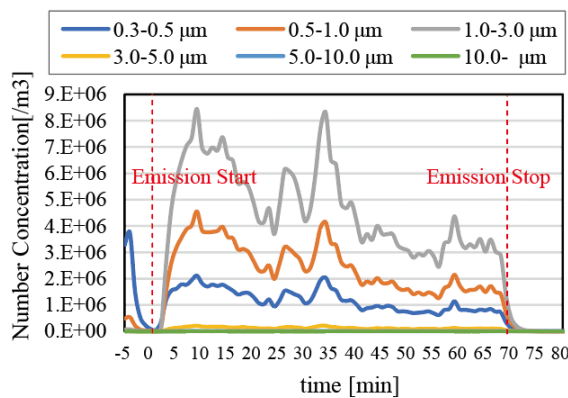


Fig.9 Experiment Time Schedule

Fig.8 Number Concentration at Ceiling Exhaust

(Hood $0\text{ m}^3/\text{h}$, Ceiling Exhaust $1,000\text{ m}^3/\text{h}$, Swirling Typr Diffuser)

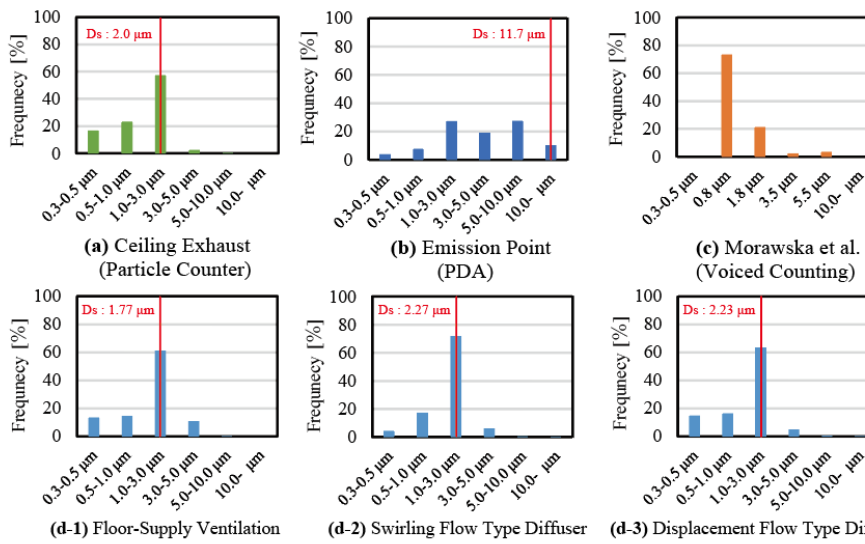


Fig.10 Frequency Distribution of Diffrent Mesurment Point (Comparson to Morawska et al.)

3 RESULTS AND DISCUSSION

3.1 The result calculated from CO₂ concentration

Figure 11 shows the spatial distribution of CO₂ tracer gas concentration normalized by the flow-

weighted concentration at the exhaust port under a hood exhaust volume of 100 m³/h (ceiling exhaust volume of 890 m³/h). In the case of FSDV, the normalized concentration is close to zero at all measurement points in both Case A (examination room) and Case B (non-examination room), indicating that exhaled air is exhausted in one direction immediately after its generation. In the displacement ventilation type floor diffuser, a concentration boundary surface was observed at some measurement points, suggesting the formation of an updraft. In the swirling-flow type floor diffuser, the existence of downward airflow is suggested near the exhalation point (Case A: Pe, Case B: Pa, Pc, Pe). At other measurement points, the normalized concentration is close to 1, and the exhaled air is mixed after descending. In the swirling flow type, the large blowing air velocity (about 3-4 m/s) is thought to cause a downward airflow due to the circulating flow between diffusers.

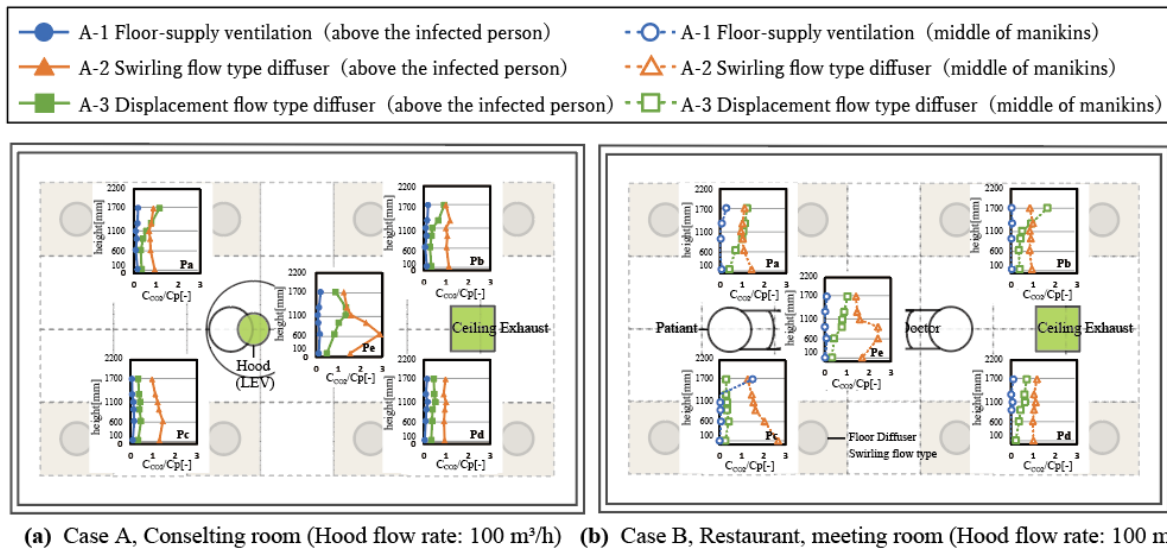


Fig.11 Normalized CO₂ concentration distribution
(C_{co2} = CO₂ concentration of each point, C_p = CO₂ concentration assuming perfect mixing)

Figure 12 shows the calculation results of hood capture efficiency and infection risk in Case A and Case B, calculated from CO₂ tracer gas using Equation (3). This indicates that the capture performance of the hood is greatly affected by the surrounding airflow. Therefore, the effectiveness of combining a hood and FSDV, which forms a quiet airflow, was confirmed. From Figure 12(c), when the infection risk is compared for each air supply method, the infection risk is lowest for the FSDV, and the value of *t*_{5%} consistently exceeds 24 hours, which is safe enough against infection. In the displacement ventilation type, when a hood is introduced (hood exhaust volume of 200 m³/h or more), the *t*_{5%} value exceeds 8 hours, assumed to be the maximum value of working hours, and can be considered relatively safe. On the other hand, for the swirling-flow type floor diffuser, the value of *t*_{5%} does not always exceed 8 hours and cannot be said to be safe.

Focusing on the results of Case B (outside the examination room) (Figure 12(a)) and comparing the results of Case A and Case B, the influence of the hood position was significant for the full-floor ventilation and displacement ventilation types, which form an upward airflow, and it is considered necessary to introduce a hood at a position where the exhaled air rises. Comparing the risk of infection for each air supply method (Figure 12(c)), the risk of infection is lowest for the FSDV, and the value of *t*_{5%} consistently exceeds 24 hours, which is safe enough against infection. In Case A, the infection risk decreases with the introduction of hoods in the FSDV and displacement ventilation type floor diffuser. In contrast, in Case B, the effect of hood introduction is negligible. Figure 13, which shows the relationship between hood collection rate and C_{qd}, also shows that in Case B, the decrease in CO₂ concentration (infection risk) with an

increase in hood collection rate is small. This indicates that even after the hood is introduced in Case B, it is not possible to collect the exhaled air of the infected person that reaches the mouth of the non-infected person. Therefore, the hoods were not effective in other areas. Therefore, careful consideration is required when installing local exhaust hoods in areas other than examination rooms.

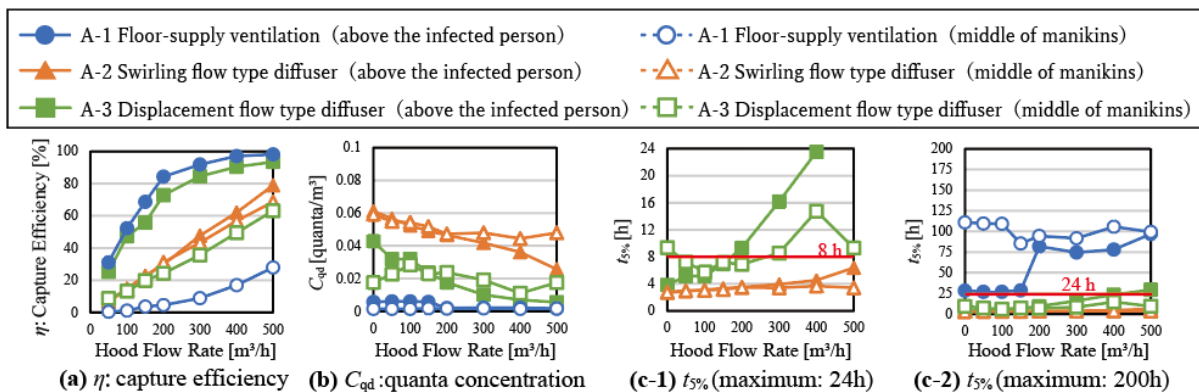


Fig.12 Calculation result of η : capture efficiency, C_{qd} : quanta concentration in front of doctor mouth, $t_{5\%}$: Time until doctor's infection probability reaches 5%, calculated by tracer gas

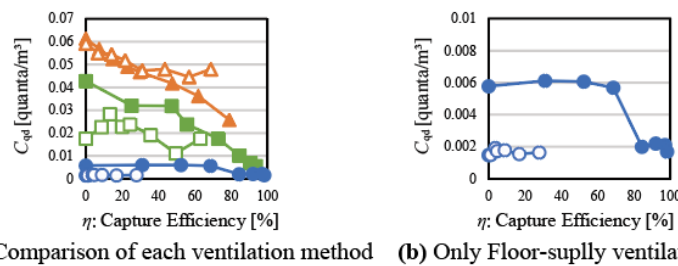


Fig.13 Relationship between η : capture efficiency and C_{qd} : quanta concentration in front of doctor mouth

3.2 The result calculated from artificial saliva

Equation (3) calculates the doctor's infection risk from the simulated saliva particles delivered to the doctor's mouth. The generated amount of simulated saliva particles is estimated by measuring the decrease in simulated saliva before and after the generation (Figure 9). When calculating the density, estimating the particle size and composition of the simulated saliva particles in a state of liquid equilibrium after water evaporation is necessary. Since previous studies (Yang & Marr, 2011) have shown that the final particle size is 0.391 to 0.502 times larger at a relative humidity of 10 to 90%, it was assumed to be 1.0, 0.40, 0.45, and 0.50 times larger. The calculations are based on the assumption that the final particle size is 1.0, 0.40, 0.45, and 0.50 times larger than the final particle size.

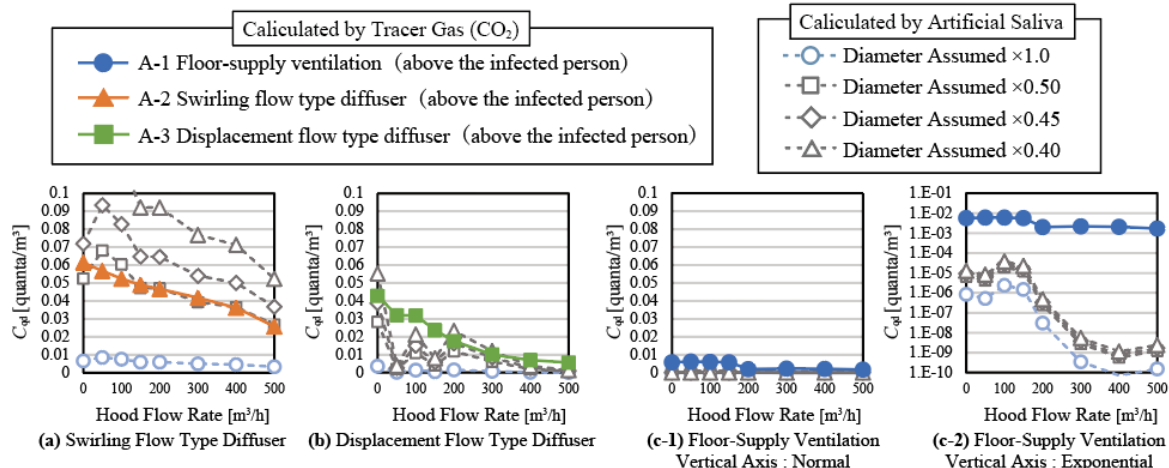


Fig.14 Comparison of C_{qd} (quanta concentration in front of doctor mouth) calculated by tracer gas or artificial saliva particle

Figure 14 shows the results of C_{qd} calculated from quanta concentration before the doctor's mouth and CO₂ when the final particle size was assumed to be 1.0, 0.40, 0.45, and 0.50 times. 0.4 times, the results obtained for the swirling flow type floor blowout (Fig. 14(a)) exceeded those calculated from CO₂. Considering the effects of deposition and adhesion, the results calculated from simulated saliva particles are expected to be smaller than those calculated from CO₂. These results may be because the amount of nebulized saliva was not stable (Figure 8) and the final particle size is not always 0.4 times larger than the final particle size of the simulated saliva particles. When 0.5 times the final particle size was used in the calculation, the C_{qd} was about the same for the swirling flow type blowout (Fig. 14(a)). Therefore, this report calculates C_{qd} and $t_{5\%}$ assuming the final particle diameter is 0.5 times larger.

C_{qd} and $t_{5\%}$ for each condition, calculated assuming that the final particle size is 0.5 times larger than the initial particle size regardless of the initial particle size, are shown in Figure 15. As in the case of the calculation based on the trend CO₂, the risk of infection is lowered in the order of " FSDV > displacement ventilation type floor diffuser > swirling-flow type floor diffuser ". This result reinforces the conclusions from the results calculated from the CO₂.

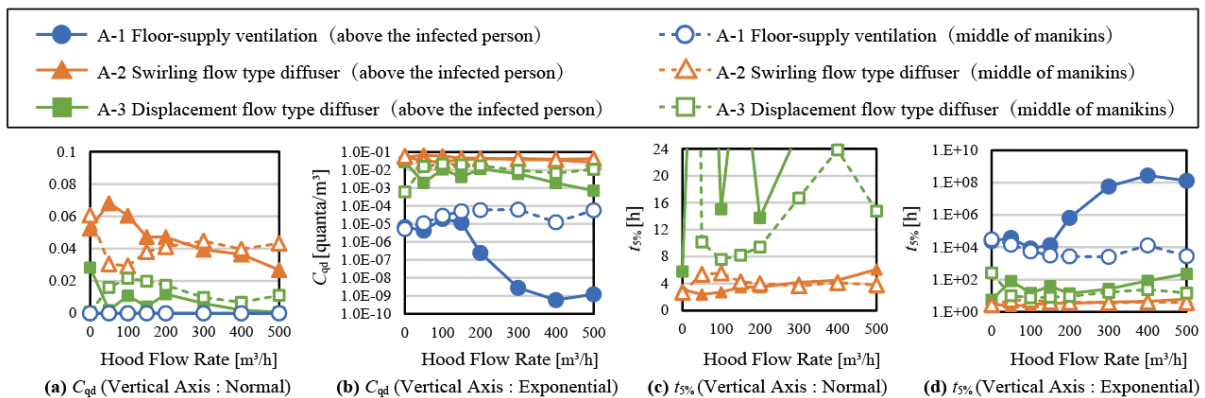


Fig.15 Calculation result of C_{qd} :quanta concentration in front of doctor mouth, $t_{5\%}$:Time until doctor's infection probability reaches 5%, calculated by artificial saliva particle (Assuming Diameter : $D \times 0.5$)

4 CONCLUSION

This study aimed to evaluate the effectiveness of the combination of air conditioning with floor-supply displacement ventilation(FSDV) and a hood and its performance as an infection control measure. The results of the doctor's infection risk calculated from CO₂ and simulated saliva droplets were also discussed. The findings of this study are summarized below.

- The effectiveness of the combination of FSDV and a local exhaust hood was confirmed in the examination rooms, and high infection control performance was confirmed in both the examination rooms and non-examination rooms.
- The high infection control performance confirmed in the non-examination rooms was strongly influenced by the large air supply volume of 1,000 m³/h for the room volume, and careful consideration is required to introduce this system in the non-examination rooms.
- These results were confirmed by both CO₂ gas and simulated saliva particles. These results were confirmed for both CO₂ gas and simulated saliva particles, and the results calculated from the simulated saliva particles were smaller than those calculated from the gas.

Future experiments should be conducted with a more stable nebulizer and closer to the particle

size distribution of the actual conversation.

5 ACKNOWLEDGEMENTS

This study was supported by Grant-in-Aid for Scientific Research (B)21H01492 and Osaka University School of Medicine Research and Development Grant for Novel Coronavirus Countermeasures in 2021.

6 REFERENCES

- Akimoto, T., Nobe, T., Tanabe, S., & Kimura, K. (1997). EXPERIMENTAL STUDY ON INDOOR THERMAL ENVIRONMENT AND VENTILATION PERFORMANCE OF FLOOR-SUPPLY DISPLACEMENT VENTILATION SYSTEM. *Journal of Architecture and Planning (Transactions of AIJ)*, 62(499), 17–25.
https://doi.org/10.3130/AIJA.62.17_3
- Federation of European Heating Ventilation and Air Conditioning Associations. (2020). *COVID-19 guidance document Version 4.0; How to operate HVAC and other building service systems to prevent the spread of the coronavirus (SARS-CoV-2) disease (COVID-19) in workplaces.*
- Komori, M., Yamanaka, T., Kobayashi, T., Choi, N., & Kobayashi, N. (2022). Development of a Design of Local Exhaust Hood with High Capture Efficiency (Part5) Prediction of Airflow under Exhaust Hood by Modeling under Passing Airflow. *Technical Papers of Annual Meeting the Society of Heating, Air-Conditioning and Sanitary Engineers of Japan*, 4, 69–72.
- Morawska, L., Johnson, G., Ristovski, Z., Hargreaves, M., Mengersen, K., Corbett, S., Chao, C., Li, Y., & Katoshevski, D. (2009). Size distribution and sites of origin of droplets expelled during expiratory activities. In *Journal of Aerosol Science* (Issue 3).
<http://eprints.qut.edu.au/>
- Ogata, M., Ichikawa, M., Tsutsumi, H., Ariga, T., Hori, S., & Tanabe, S. I. (2018). Measurement of cough droplet deposition using the cough machine. *Journal of Environmental Engineering (Japan)*, 83(743), 57–64. <https://doi.org/10.3130/aije.83.57>
- Riley EC, Murphy G, & Riley RL. (1978). Airborne spread of measles in a suburban elementary school. *American Journal of Epidemiology*, 107, 421–432.
- Wells, W. F. (1955). *Airborne Contagion and Air Hygiene: An Ecological Study of Droplet Infections - William Firth Wells -*. University of Michigan Libraries.
https://books.google.co.jp/books?hl=ja&lr=lang_ja|lang_en&id=T8nVAAAAMAAJ&oi=fnd&pg=PR7&dq=+Wells+WF.+Airborne+Contagion+and+Air+Hygiene.+Cambridge,+MA:+Harvard+University+Press,+1955&ots=dTn_tdoRGZ&sig=7xpun_61NO_NGHTJQQISJZP2fow#v=onepage&q&f=false
- World Health Organization. (2020). Transmission of SARS-CoV-2: implications for infection prevention precautions. *World Health Organization.*
- Yang, W., & Marr, L. C. (2011). Dynamics of Airborne influenza A viruses indoors and dependence on humidity. *PLoS ONE*, 6(6). <https://doi.org/10.1371/journal.pone.0021481>
- Zhang, R., Yamanaka, T., Kobayashi, T., Choi, N., Kobayashi, N., & Yoshihara, J. (2022). *Performance of Local Exhaust System as Prevention Measure of Infection in Consulting Room (Part 3) Exposure Concentration Response and Hood Capture Rate of Droplet Nuclei from Conversation and Coughing Based on Transient CFD Analysis.*

The numerical investigation of human micro-climate with different human simulators

Haruna Yamasawa^{*1}, Sung-Jun Yoo², Kazuki Kuga², and Kazuhide Ito²

*1 Osaka University
2-1, Yamadaoka
Suita, Osaka, Japan*

*2 Kyushu University
6-1, Kasuga-koen, Kasuga-city
Fukuoka, Japan*

**Corresponding and presenting author:
yamasawa@arch.eng.osaka-u.ac.jp*

ABSTRACT

The development of computational fluid dynamics (CFD) made it possible to simulate the detailed flow field and temperature field within the room. The various studies numerically investigated the flow and temperature field both inside and outside the buildings. When investigating the indoor environment, human is an important factor since it perceives the indoor environment and behaves as a source of heat and contaminant as well. Some studies investigated deeper into humans by developing detailed computer-simulated persons (CSP). However, due to the limitation of computer performance, it is still not always possible to conduct the simulation with detailed CSPs. Therefore, many studies adopted the human simulators with simplified geometry, e.g., cylinder and cuboid. However, it is necessary to understand the effect of the geometrical difference of human simulators on the simulation results. Therefore, CFD analysis with different human simulator geometry is conducted to understand the effect.

A human simulator is located in the middle of a room (3 x 3 x 3 m) with an inlet at a lower level of the room and an outlet at a higher level of the room. The air of 20 °C flows into the room via inlet boundary condition with the air velocity of 0.1 m/s. The human simulator geometry is the parameter in this study, and the studied cases are cuboid, simplified CSP, and detailed CSP. The Fanger model is applied for simulating heat generation from human skin surface; therefore, the heat generation rate differs depending on the conditions.

As a result, it was shown that the total heat generation rate and surface temperature of human simulators are almost the same, therefore, since all other walls are insulated, the exhaust air temperature also did not differ depending on the cases. However, there was some difference in the ratio between convective and radiative heat loss through the skin. In addition, although the heat generation rate is almost the same, the flow rate of thermal plume around them differed by 10% depending on the human simulator geometry.

KEYWORDS

Computer simulated person, Heat generation rate, Thermal plume, CFD analysis, Human simulator

1 INTRODUCTION

The development of computational fluid dynamics (CFD) made it possible to simulate the detailed flow field and temperature field within the room. The various studies numerically investigated the flow and temperature field both inside and outside the buildings. When investigating the indoor environment, human is an important factor since it perceives the indoor environment and behaves as a source of heat and contaminant as well. Some studies (Nielsen et al., 2003; Takada et al., 2016; Yoo & Ito, 2018, 2022) investigated deeper into humans by developing detailed computer-simulated persons (CSP). However, due to the limitation of computer performance, it is still not always possible to conduct the simulation with detailed CSPs. Therefore, many studies adopted the human simulators with simplified geometry, e.g.,

cylinder and cuboid (Lau & Chen, 2007; Yuan et al., 1999). However, it is necessary to understand the effect of the geometrical difference of human simulators on the simulation results. Therefore, to understand the effect of geometrical difference in human simulator, CFD analysis with different human simulator geometry is conducted.

2 METHODOLOGY: HUMAN SIMULATOR

The geometries of the human simulators that simulating an adult male are shown in Fig. 1, and the surface areas of the human simulators are summarised in Table 1. The studied human simulators are as follows: i) cuboid with a dimensions of 0.25 x 0.25 x 1.8 m; ii) cuboid with a dimensions of 0.15 x 0.35 x 1.8 m; iii) angular human simulator that has a head and legs; iv) detailed CSP. The model geometries were decided by fixing the human body height to be almost the same as that of *Model CSP-detailed*, i.e., 1.8 m height. The body surface area was adjusted to be around the same as that of *Model CSP-detailed* as well. The surface area of each simplified models is kept within the range of 3% from that of *Model CSP-detailed*.

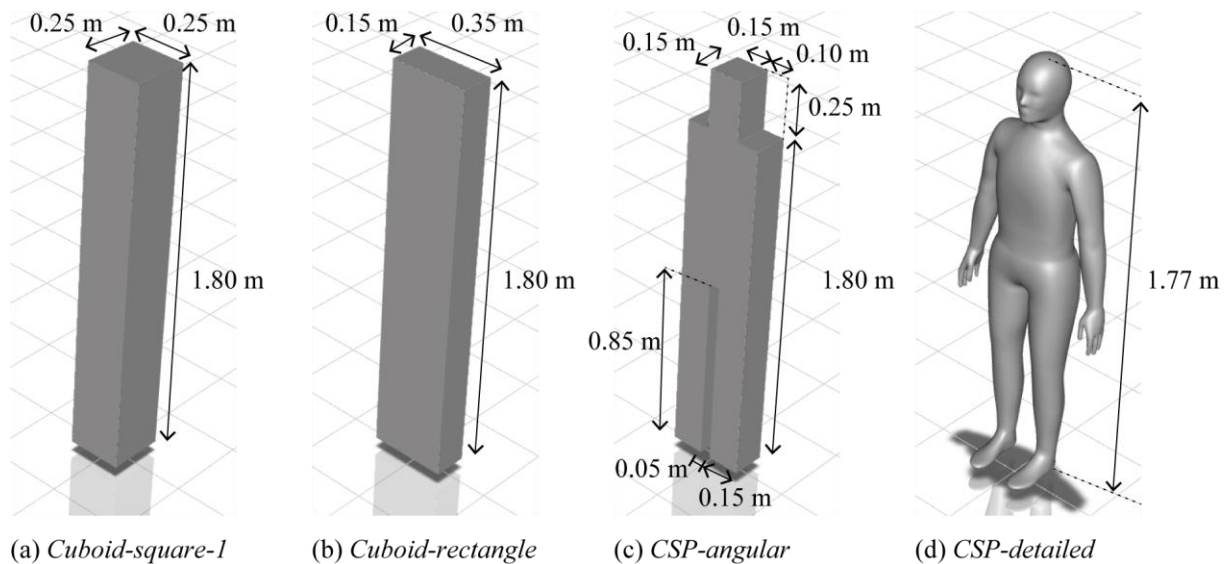


Figure 1: Geometries of the human simulators

Table 1: Geometrical information of the human simulators

Geometry	Surface area [m ²]	Height [m]	Number of cells
Cuboid-square	1.84 (-1.1%)	1.80	2,114,952
Cuboid-rectangle	1.83 (-1.6%)	1.80	2,064,930
CSP-angular	1.91 (+2.7%)	1.80	5,705,792
CSP-detailed	1.86 (Reference)	1.77	1,196,755

To investigate the difference of thermal plumes from each human simulators, skin surface temperature was controlled by adopting the Fanger's model (Fanger, 1972) to the boundary condition. The heat generation from the human simulators is expressed by the combination of core temperature and heat conductance through the core to the skin through the body. By using the simplified equations based on the Fanger's comfort equation (Fanger, 1972), the correlation between skin surface temperature T_{skin} and sensible heat generation from skin surface Q_{skin-s} can be expressed as follows:

$$Q_{skin-s} = 18.5 \times (36.4 - T_{skin}) \quad (1)$$

where, core temperature of the human body is set to be 36.4 °C and heat conductance between core of the body and the skin surface is set to be 18.5 W/m²K.

3 METHODOLOGY: ANALYTICAL METHOD

The analytical domain and the studied cases are illustrated in Figure 2. Each human simulator is located at the middle of the room with a dimensions of 3 x 3 x 3 m. The cooled air is supplied to the room through an inlet located near the floor at a wall, and is exhausted from the room through an outlet located near the ceiling at the opposite wall. Both inlet and outlet have a dimension of 0.3 x 0.3 m. Due to the detailed geometry of *Model CSP-detailed*, two cases are studied for this model: the case that (a) air inflows through the inlet at the back and outflows through the outlet at the front, and (b) air inflows through the inlet at the back and outflows through the outlet at the front.

The simulation is conducted under non-isothermal condition using commercial software, Ansys Fluent. SST $k - \omega$ model is adopted, radiative heat transfer is calculated using S2S (Surface-to-surface) model, and the second-order upwind discretization scheme is adopted.

The boundary conditions are summarized in Table 2, and the number of cells in each model are summarised in Table 1. The cells around *Model CSP-detailed* is consist of unstructured meshes, whereas the other models are consisting of structured meshes due to their simplified geometry.

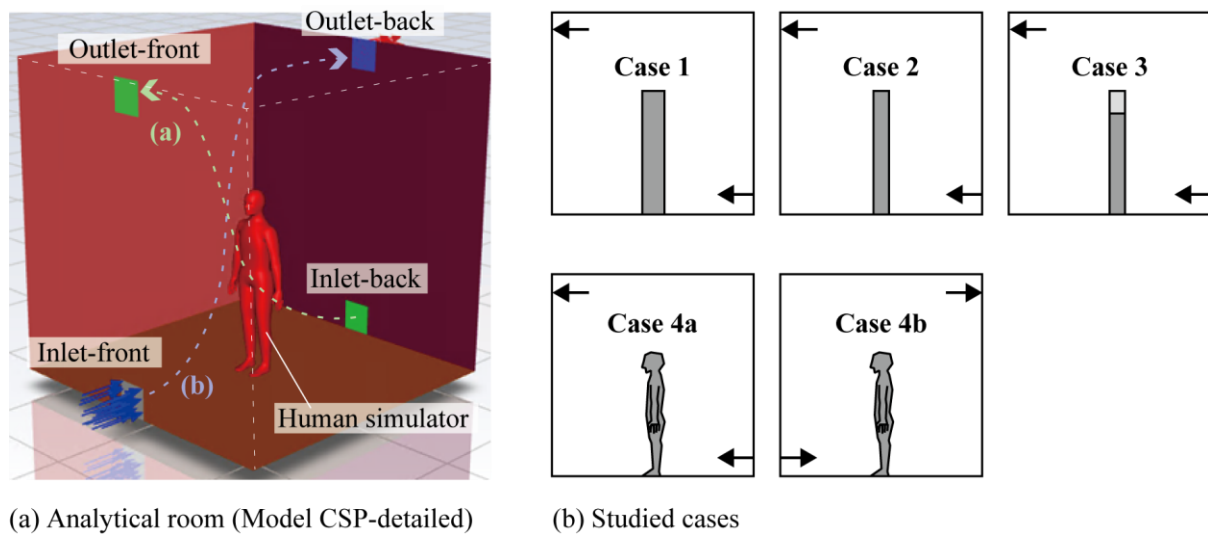


Figure 2: Geometrical configuration of studied cases

Table 2: Boundary conditions

Inlet	Velocity: 0.1 m/s, Temperature: 20.0 °C
Outlet	Gradient zero
Wall	No slip, External emissivity: 0.95, Temperature: Gradient zero
Human skin surface	No slip, External emissivity: 0.98, Temperature: Calculated by Eq. (1)

4 RESULTS AND DISCUSSIONS

The exhaust air temperature and the mean temperature of skin surface are summarized in Table 3. There is no significant difference among all the cases in terms of exhaust temperature and mean skin temperature.

Table 3: Temperature results

Case	Geometry	Exhaust temperature [°C]	Mean skin temperature [°C]	Surface area [m ²]
1	Cuboid-square	28.5	33.7	1.84
2	Cuboid-rectangle	28.5	33.6	1.83
3	CSP-angular	28.5	33.8	1.91
4a	CSP-detailed (Flow: back-to-front)	28.5	33.7	1.86
4b	CSP-detailed (Flow: front-to-back)	28.2	33.7	1.86

Figure 3 and Figure 4 illustrates the heat flux and heat generation from human simulators, respectively. The total sensible heat flux and heat are almost the same among all the cases, i.e., 49 to 51 W/m² and 92 to 94 W. However, it must be noted that the ratio between radiative and convective heat transfer from the skin was different. Figure 5 illustrates the ratio between radiative and convective heat transfer from human simulator's skin. It is shown that the heat transfer by radiation is almost double of that by convection. In addition, it is shown that the radiative component is relatively small in Case-3 and Case-4, if compared to that in Case-1 and Case-2. It is assumed to be due the reproduction of the detailed geometries; the radiative heat transfer from skin surface only goes to the surrounding cooled walls in Case-1 and Case-2, whereas the radiative heat transfer also occurs between skin surfaces in Case-3 and Case-4. Therefore, due to the simplicity of the geometry, the radiative heat transfer is assumed to be overestimated (and convective heat transfer is underestimated) in cuboid human simulators.

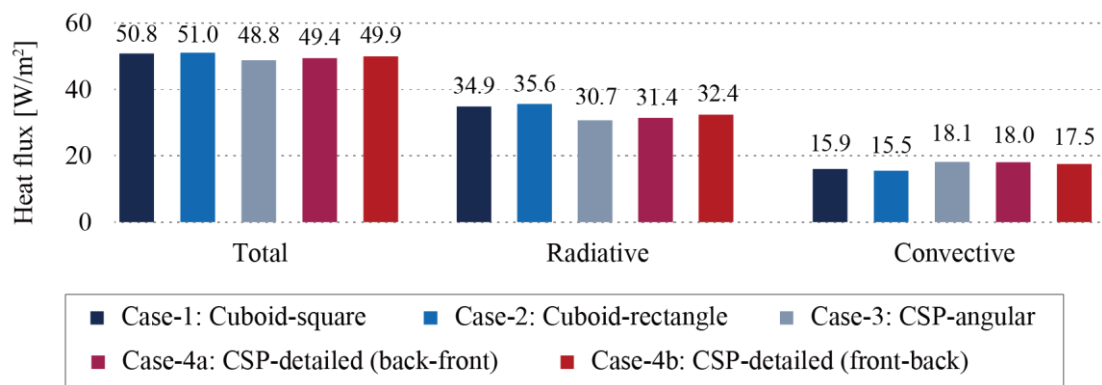


Figure 3: Heat flux from human simulators

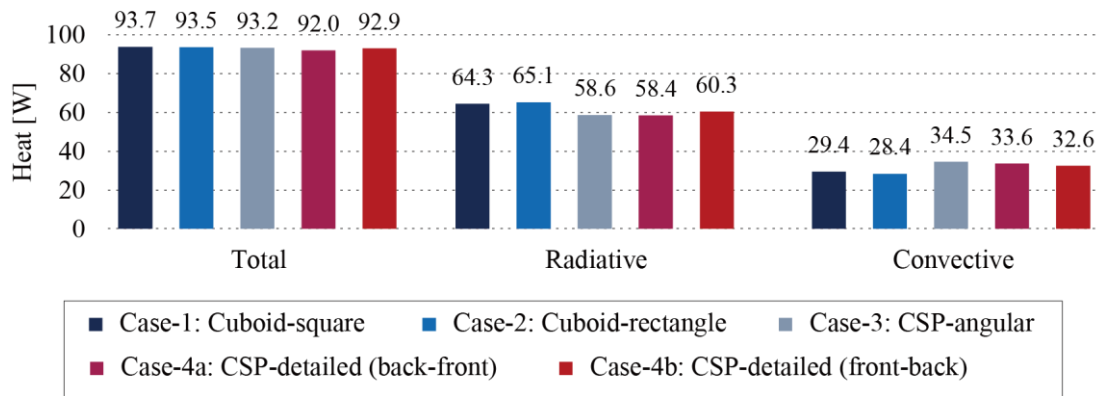


Figure 4: Heat from human simulators

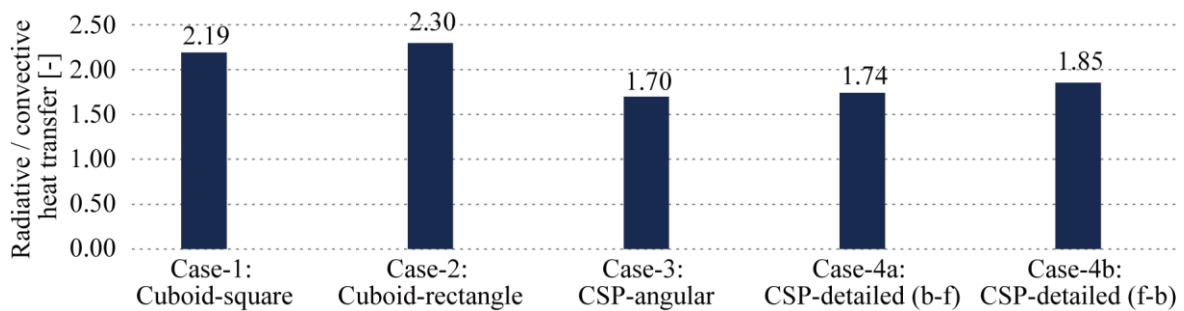


Figure 5: Ratio between radiative and convective heat transfer from human simulators

The thermal plume flow rate is shown in Figure 6. The thermal plume flow rate was calculated by conducting mass-weighted integral of upward air velocity around the human simulators. It must be noted that the velocity was integrated within the region that the upward air velocity is larger than 0.05 m/s. The plume flow rates in Case-1 and Case-2 are relatively small if compared to the other cases. It is because the convective component of heat transfer from cuboid human simulators are assumed to be underestimated as mentioned prior, which leads to the smaller drive force of the thermal plume. Moreover, it is assumed that the turbulence generated around the hip joint, also enhanced the increase of the flow rate. Additionally, the thermal plume flow rates of Case-4a and Case-4b are not identical to each other. It is suggested that more the human simulator's geometry is detailed, more the thermal plume flow rate is difficult to be simply predicted.

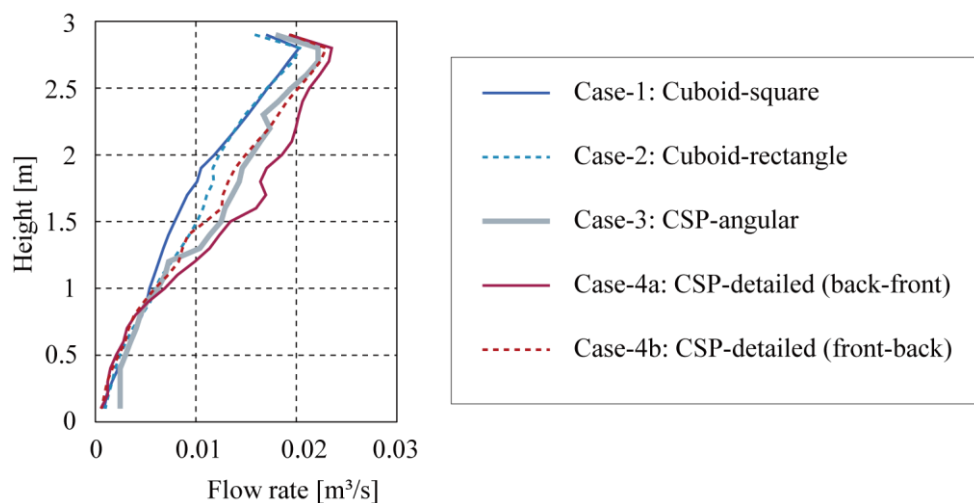


Figure 6: Plume flow rate from human simulators

5 CONCLUSIONS

To understand the effect of reproduction of the human simulators, CFD analysis was conducted with four different geometries of human simulators. The studied cases are: two kinds of cuboids, one simple CSP, and one detailed CSP. Each of the human simulators is located at the middle of the room (3 x 3 x 3 m), and the cooled air is supplied around the floor and is exhausted around the ceiling. As for the detailed CSP, two cases are conducted; (a) when air is supplied from the front, and (b) when air is supplied from the back.

It is shown that although the total sensible heat generation is almost the same among all the cases, however, the ratio between radiative and convective heat transfer differed. This also led to the difference in thermal plume flow rate.

6 ACKNOWLEDGEMENTS

This research was partially funded by the Japan Society for the Promotion of Science (JSPS) Grants-in-Aid for Scientific Research (KAKENHI) (grant numbers JP 22K18300, JP 22H00237, JP22J00743, JP22K14371, and JP 20KK0099), the Japan Science and Technology (JST), CREST Japan (grant number JP 20356547), FOREST program from JST, Japan (Grant number JPMJFR225R), and MEXT as “Program for Promoting Researches on the Supercomputer Fugaku” (JPMXP1020210316).

7 REFERENCES

- Fanger, P. O. (1972). Thermal comfort: Analysis and applications in environmental engineering. *Applied Ergonomics*, 3(3), 181. [https://doi.org/10.1016/S0003-6870\(72\)80074-7](https://doi.org/10.1016/S0003-6870(72)80074-7)
- Lau, J., & Chen, Q. (2007). Floor-supply displacement ventilation for workshops. *Building and Environment*, 42(4), 1718–1730. <https://doi.org/10.1016/j.buildenv.2006.01.016>
- Nielsen, P., Murakami, S., Kato, S., Topp, C., & Yang, J.-H. (2003). Benchmark tests for a computer simulated person. *Aalborg University, ..., October*, 1–6. http://homes.civil.aau.dk/pvn/cfd-benchmarks/csp_benchmark_test/Benchmark_Tests_071103.pdf
- Takada, S., Sasaki, A., & Kimura, R. (2016). Fundamental study of ventilation in air layer in clothing considering real shape of the human body based on CFD analysis. *Building and Environment*, 99, 210–220. <https://doi.org/10.1016/j.buildenv.2016.01.028>
- Yoo, S. J., & Ito, K. (2018). Assessment of transient inhalation exposure using in silico human model integrated with PBPK-CFD hybrid analysis. *Sustainable Cities and Society*, 40(April), 317–325. <https://doi.org/10.1016/j.scs.2018.04.023>
- Yoo, S. J., & Ito, K. (2022). Validation, verification, and quality control of computational fluid dynamics analysis for indoor environments using a computer-simulated person with respiratory tract. *Japan Architectural Review*, 5(4), 714–727. <https://doi.org/10.1002/2475-8876.12301>
- Yuan, X., Chen, Q., Glicksman, L. R., Hu, Y., & Yang, X. (1999). Measurements and computations of room airflow with displacement ventilation. *ASHRAE Transaction*, 105, 340–352.

Introduction to IEA EBC Annex 87

Bjarne W. Olesen and Ongun B. Kazanci

*Technical University of Denmark
Nils Koppels Allé, Building 402
2800 Kgs. Lyngby, Denmark
Corresponding author: bwol@dtu.dk

SUMMARY

Personalized Environmental Control Systems (PECS) have advantages of controlling the localized environment at occupants' workstation by their preference instead of conditioning an entire room. A new IEA EBC Annex (Annex 87 - Energy and Indoor Environmental Quality Performance of Personalised Environmental Control Systems) has recently started to establish design criteria and operation guidelines for PECS and to quantify their benefits. This topical session will provide an introduction to the objective/scope, activities, and intended outputs of the annex.

KEYWORDS

Personalized Environmental Control System, Indoor environmental quality, Thermal Comfort, Indoor Air Quality

1 INTRODUCTION

A new IEA EBC Annex (Annex 87 - Energy and Indoor Environmental Quality Performance of Personalised Environmental Control Systems) has recently started and has the overall objective to establish design criteria and operation guidelines for PECS and to quantify the benefits regarding health, comfort, energy, and cost performance. The scope of the annex includes all types of PECS for local heating, cooling, ventilation, air cleaning, lighting, and acoustics. Various types of PECS such as desktop systems, which are mounted on desks or integrated in a furniture, or chairs with heating/cooling and ventilation, will be covered. The annex will also include wearables, where heating, cooling, and ventilation are included in garments or devices attached to the occupants' body. This topical session will provide an overview to the activities and intended outputs planned for the annex.

2 MAIN ACTIVITIES

The annex comprises five subtasks, and their activities are described in the following sections.

2.1 Subtask A: Fundamentals

This subtask aims to define and identify requirements of PECS in terms of Indoor Environmental Quality (IEQ), i.e., thermal, air quality, lighting, and acoustics. The benefits of PECS regarding comfort, health and productivity and energy performance based on literature and new research will be shown.

2.2 Subtask B: Applications and technologies

Subtask B will summarize the working principles, capabilities and limitations of existing PECS, based on literature. Future development and improvement suggestions for PECS for optimal energy, IEQ and cost performance will be identified.

2.3 Subtask C: Control, operation and system integration

In Subtask C, existing methods for controlling PECS (including sensors used for control) will be identified and summarized. Guidelines on integrating PECS with ambient conditioning systems in buildings will be developed.

2.4 Subtask D: IEQ and Energy Performance evaluation

Existing methods of studying and testing PECS will be collected in this subtask. Generic power requirements for PECS to achieve energy savings compared to ambient conditioning systems will be identified. Universal and standardized ways of evaluating and reporting the performance of PECS will be developed.

2.5 Subtask E: Policy and advisory actions

In Subtask E, national and international building codes and standards regarding PECS will be summarized. Ways of overcoming current barriers for a wide implementation of PECS in buildings will be developed. The subtask will provide input to existing national and international standards about requirements, characteristics, and performance of PECS.

3 INTENDED OUTPUTS AND TARGET AUDIENCE

The intended outputs of the annex are as follows:

- Guidebook on requirements for PECS (Subtask A)
- State-of-the-art report on PECS (Subtask B)
- Guidebook on PECS design, operation and implementation in buildings (Subtasks C & E)
- Report on test methods for performance evaluation of PECS (Subtask D)
- Universal criteria about requirements, characteristics, and performance of PECS to be used in national and international standards (Subtask E)

The intended audience of the outputs would be consulting engineers/companies, heating, ventilation, and air-conditioning (HVAC) system and component manufacturers, researchers, building owners and tenants, and standardization bodies. Input will be given to revise relevant standards such as EN 16798 and ISO 17772 on required criteria for PECS (CEN, 2019; ISO, 2017). Development of new standards is also foreseen.

4 REFERENCES

- CEN. (2019). *EN 16798-1: Energy performance of buildings - Ventilation for buildings - Part 1: Indoor environmental input parameters for design and assessment of energy performance of buildings addressing indoor air quality, thermal environment, lighting and acoustics*. European Committee for Standardization.
- ISO. (2017). *ISO 17772-1:2017 Energy performance of buildings - Indoor environmental quality - Part 1: Indoor environmental input parameters for the design and assessment of energy performance of buildings*. International Organization For Standardization.

Indoor environmental quality (IEQ) and energy performance evaluation of PECS

Douaa Al Assaad¹, Marco Perino², Dragos-Ioan Bogatu³, Bjarne W. Olesen³

¹*KU Leuven, Department of Civil Engineering, Building Physics and Sustainable Design, 9000 Gent, Belgium*

²*Department of Energy, Politecnico di Torino, 10129 Torino, Italy*

³*International Centre for Indoor Environment and Energy – ICIEE, Department of Environmental and Resource Engineering, Technical University of Denmark, 2800, Kgs. Lyngby, Denmark*

SUMMARY

Most current environmental control systems installed in buildings aim to create a uniform IEQ, disregarding the large interpersonal and intrapersonal variability in occupants' thermal, visual, acoustics & air quality requirements. By creating occupant micro-environments that respond to individual preferences, and relaxing the surrounding space, personalized environmental control systems (PECS) can satisfy all occupants with relatively low-energy input. The performance of PECS on improving IEQ and energy use has been widely studied in different spaces using different simulation and modeling techniques, experimental methods, and field studies. Key performance indicators (KPIs) were subsequently used to quantify this performance and benchmark it with respect to conventional systems.

KEYWORDS

Personalized environmental control systems, indoor environmental quality, energy, performance evaluation methods

1 PECS PERFORMANCE

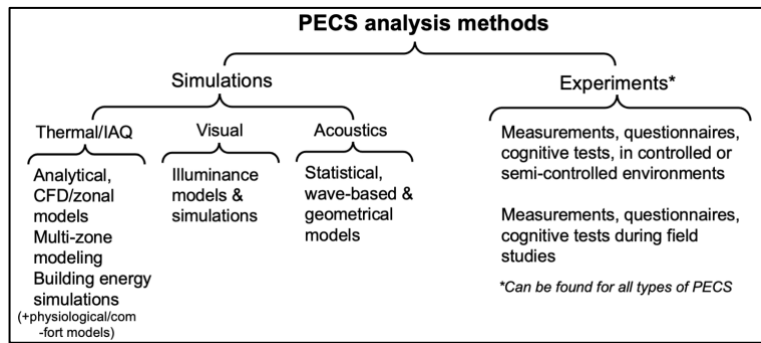
1.1 Analysis methods

Up until recent times, PECS performance evaluation methods could be classified into two major categories (Figure 1): **(i)** digital simulations that differ depending on the type of micro-environment targeted by the PECS (i.e., thermal, IAQ, acoustic, visual) or study objectives and **(ii)** experimental methods that are commonly used by all types of PECS. Combinations of simulations with select-experiments for validation of numerical prediction is also common.

Experimental techniques consist of deploying a fully functioning PECS in controlled or semi-controlled environments (e.g., climatic chamber) with either human subjects or test mannequins. Experiments also include field tests in occupied case study buildings (Kaczmarczyk, 2004; Melikov, 2007). Performance of PECS was evaluated via objective measurements of physiological (e.g., segmental skin temperature, heart rate, pupil size) and room parameters (e.g., air velocity, sound pressure) and through subjective satisfaction assessment collected from participants (e.g., questionnaires, cognitive tests, sick building syndrome, self-assessed productivity).

With every increasing hardware/software capability, computer simulation tools and modeling techniques have been widely and successfully applied to PECS research. For example, thermal/IAQ PECS (coupled to physiological comfort models) have been modeled using simplified mathematical analysis and theoretical formulations with adequate assumptions (Al Assaad 2018) or computational fluid dynamics (CFD) when more information is required about air distribution patterns as well as thermal/concentration fields in specific locations. Building energy simulation tools (e.g., EnergyPlus, IDA-ICE) are commonly used to assess the year-round energy use and potential savings for thermal/IAQ and visual PECS (Schiavon 2009). Despite the potential of digital simulation environments, they lack in their ability to simulate inter and intra individual differences between occupants and their dynamic interaction with the building.

Figure 1: Overview of PECS performance evaluation methods



1.2 Key performance indicators (KPIs)

For each PECS type (Figure 1), further subcategorization is possible. For example, thermal/IAQ PECS can be divided based on their function (heating, cooling and/or ventilation). Under this umbrella, multiple PECS exist with multiple design variations. For each type of PECS and for each evaluation method, different evaluation indices can be found. The conditions between studies were also different rendering difficult PECS comparison. Table 1 displays a summary of the main KPIs used to analyze PECS performance in simulations, experiments, or both. Common indicators found between all types of PECS include human subjective IEQ satisfaction votes often used in experimental studies

This shows the need for a universal method or standardized procedure to test and evaluate PECS performance which will be one of the main objectives of the newly formed international project “IEA EBC Annex 87 – PECS”. These procedures should include ventilation/thermal resilience performance of PECS and its environmental impact (i.e., carbon footprint).

Table 1: Summary of main KPIs used in †simulations, *experiments, °both (Shinoda 2023)

Thermal comfort ¹	Visual comfort	Acoustic comfort	Air quality	Energy
Overall/Local Thermal sensation, comfort (votes, predicted from models) [°]	Room/local visual sensation, comfort votes*	Equivalent Sound pressure levels [°]	Ventilation effectiveness [°]	Corrective energy, corrective power*
Draught index [°]	Gaze, eye movement, pupil size*	Daily noise exposure level	Personal exposure effectiveness [°]	Energy savings, energy demand [°]
Segmental/Equivalent skin temperature [°]	Luminance, luminance ratio [°]	Acceptability of system*	Intake fraction [°]	Power usage [°]
Segmental/Mean heat losses (sensible, latent) [°]	Daylight factor, daylight autonomy [°]	Speech annoyance , ability to concentrate*	Pollutant exposure reduction [°]	Heating/Cooling load [°]
Air temperature & velocity distribution [°]	Glare index [°]	Perceived privacy*	Perceived air quality*	Device-level COP*

¹Excluding heat stress related indices

2 REFERENCES

- Al Assaad et al. 2018. “Simplified Model for Thermal Comfort, IAQ and Energy Savings in Rooms Conditioned by Displacement Ventilation Aided with Transient Personalized Ventilation.” *Energy Conversion and Management* 162: 203–17.
- Shinoda et al. 2023. “Resiliency and Performance Evaluation Indicators of Personalized Environmental Control Systems (PECS).” In *18th Healthy Buildings 2023 Conference, Aachen, Germany*.
- Kaczmarczyk et al.. 2004. “Human Response to Personalized Ventilation and Mixing Ventilation.” *Indoor Air, Supplement* 14 (8): 17–29.
- Melikov et al. 2007. “Personal Ventilation: From Research to Practical Use.” In *Proceedings of Clima 2007 WellBeing Indoors*.
- Schiavon, et al. 2009. “Energy-Saving Strategies with Personalized Ventilation in Cold Climates.” *Energy and Buildings* 41 (5): 543–50.

Physiological sensing for thermal comfort assessment

Dragos-Ioan Bogatu^{*1}, Jun Shinoda¹, José Joaquín Aguilera², Bjarne W. Olesen¹,
Futa Watanabe³, Yosuke Kaneko³, and Ongun B. Kazanci¹

1 International Centre for Indoor Environment and Energy – ICIEE, Department of Environmental and Resource Engineering, Technical University of Denmark

*Nils Koppels Allé, Building 402
2800 Kgs. Lyngby, Denmark*

**Corresponding author: drabo@dtu.dk*

2 Section of Thermal Energy, Department Civil and Mechanical Engineering, Technical University of Denmark

*Nils Koppels Allé, Building 403,
2800 Kgs. Lyngby, Denmark*

*3 Mitsubishi Electric Corporation
5-1-1 Ofuna, Kamakura
Kanagawa 247-8501, Japan*

ABSTRACT

Accounting for inter- and intra-personal differences requires individual and cohort comfort models. For their development, emulators for thermal sensation of occupants are needed. Physiological signals can be acquired using both wearable and contactless devices. However, due to the widespread availability of sensing methods it is difficult to select the proper measuring method for the application. The objective of this study is to provide an overview of the capabilities of contemporary devices that measure physiological indicators used in literature and identify their capabilities and limitations. The analysis was made on a dataset of reviewed thermal comfort research studies that employed physiological sensing devices in experimental and field test campaigns. The physiological indicators investigated in literature were derived from the human thermoregulation mechanism. The physiological indicators measured were neural activity (brainwave frequency bands), heartbeat (heart rate and heart rate variability), blood flow (blood pressure, blood oxygen saturation, skin blood flow), activity (metabolic rate, activity, calorie consumption), temperature (core and skin), sweat (relative humidity, skin conductance, skin hardness, and amount of sweat). The wrist is the most investigated body part as it is a convenient area for acquiring multiple physiological indicators i.e., all physiological measurements except for ECG and EEG measurements. However, most devices are not “plug-and-play” solutions for thermal comfort assessment. As contact devices, smartbands acquire an extensive set of indicators but present 3rd party data privacy protocols which may limit their applicability. Cameras (RGB and infrared) can only be used to acquire skin temperature and heart rate but can be deployed in the space by the building owner. Further studies are required on the sensing accuracy and signal variability as a function of thermal sensation to determine the optimal measurement method.

KEYWORDS

Thermal comfort, sensing strategies, physiological indicators, wearable/contactless, sensing performance

1 INTRODUCTION

In order to deal with inter- and intra-personal differences, personal and cohort thermal comfort models were proposed (Kim, Schiavon, and Brager 2018; Quintana et al. 2022). However, these models require input from or representative of the occupant in question (Deng and Chen 2020; Laftchiev and Nikovski 2017). As thermal comfort is a function of thermoregulatory aspects, emulators such as physiological signals could be used to distinguish between thermal sensation of different people and for the same person over time (Bogatu et al. 2023; Lee and Ham 2021).

Further studies are though required on the set of indicators and their variability as a function of thermal sensation across people with different anthropometric characteristics and behaviour. With economically feasible physiological sensing methods emerging, wearable sensing devices become widespread and monitoring physiological indicators becomes simpler in both experiments and field studies. However, with a market under constant change it is difficult to select the proper measuring method for the application. The objective of this study is to provide an overview of the capabilities of current physiological indicator measuring devices used in literature and identify their benefits and limitations.

2 METHODS

The objective was to identify current physiological indicator measuring techniques in thermal comfort studies. The analysis was made on an existing dataset (Bogatu et al. 2023) where the objective was to determine relevant indicators for data driven thermal comfort prediction for HVAC control. The dataset was generated using Google Scholar, Scopus, and Web of Science, and the “reference by reference” method.

For finding relevant research studies permutations, combinations, and specific keywords such as physiological, physiology, wearable, contactless, smart control, control, smart building, thermal comfort, sensing were used. The database consisted of 94 articles that measured physiological indicators, used either physiological, environmental, behavioural, or anthropometric measurements in personal comfort model development, or integrated occupant feedback or physiological indicators in the HVAC control.

3 RESULTS

3.1 Physiological indicators

Physiological indicators used in thermal comfort studies are derived from human thermoregulation mechanism (Bogatu et al. 2023). Thermoregulation is controlled by the central nervous system, which sends nerve impulses based on signals received at skin level. The nervous system regulates blood flow through the heart and through the constriction and dilation of vessels, perspiration, and metabolic rate to regulate body temperature. Therefore, physiological indicators can be obtained from:

- Neural activity: brainwave frequency bands.
- Heartbeat: heart rate (HR) and heart rate variability (HRV).
- Blood flow: blood pressure (BP), blood oxygen saturation (SpO₂), skin blood flow (BF).
- Activity: metabolic rate (MET), activity, calorie consumption.
- Temperature: core (T_{CORE}), skin temperature (T_{SK}).
- Sweat: skin relative humidity (RH_{SK}), skin conductance (SC), skin hardness, and amount of sweat.

3.2 Physiological indicator sensing

Figure 1 shows the frequency of investigated body parts and the corresponding indicators. Most measurements were made at the wrist level, followed by the forehead, hand, upper arm, cheek, chest, forearm, thigh, ankle, neck, abdomen, waist, ankle, and calf. A collection of the sensors employed in literature and their characteristics can be found in the Appendix.

Neural activity can be recorded at the head level by an electroencephalogram (EEG) instrument consisting of electrodes which measure brain electrical activity (Pigliautile et al. 2020). Advanced instruments are available where the electrodes are attached to a headset (Kim and Hong 2020; Pigliautile et al. 2020). Although portable, these devices must be in contact with

the subject during the measurement and require dedicated software to analyse the obtained information. The analysis of the brainwaves power spectrum is made with a fast Fourier transform method to obtain the distribution of the magnitude of signals within particular frequency bands, such as Alpha, Beta, Delta, Theta, and Gamma ranges (Shan and Yang 2020). Recent devices are convenient, becoming light and easy to set up but highly intrusive if intended for long term use (Pigliautile et al. 2020; Shan and Yang 2020).

HR can be derived from HRV which can be obtained by measuring the heart's electrical activity (Chaudhuri et al. 2018; Nkurikiyeyezu, Suzuki, and Lopez 2018). **Error! Reference source not found.** The HRV is usually measured at the chest level or a combination of chest, arm, wrist, thigh, and ankle through electrodes placed on the skin (Gwak et al. 2016; Zhu et al. 2018). Since the electrodes are in contact with the skin, electrocardiogram (ECG) devices must be in occupant proximity. Although intrusive, wearable devices (medical and commodity sensors) for chest placement are available (Liu et al. 2019; Pigliautile et al. 2020). If other indicators than HR must be obtained, these devices are no longer “plug and play” and may require additional data processing.

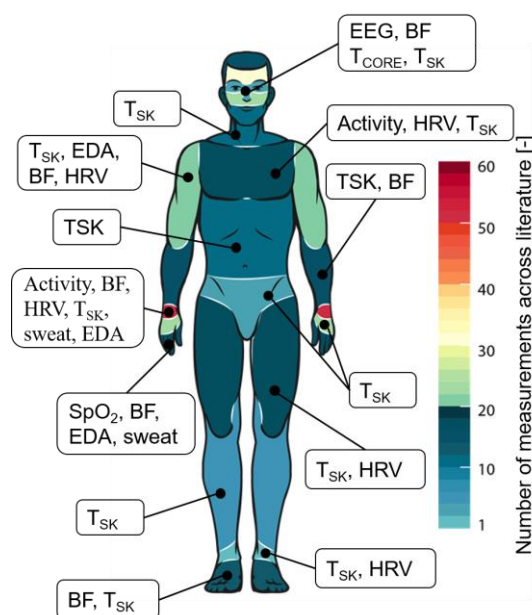


Figure 1. Frequency of physiological measurements across the human body.

Photoplethysmography (PPG) measures blood volume changes in the vessels, where light transmitted from a source onto the skin tissue is being either absorbed or reflected. The increase in blood volume is obtained based on the relative change in the light captured by the photodetector (Jung and Jazizadeh 2018b). PPG measurements can be made at the skin level, e.g., on the face where there is a high density of blood vessels (Ghahramani et al. 2016), at the wrist (Laftchiev and Nikovski 2017), or finger (Chaudhuri et al. 2020). Wrist measurements usually make use of smartbands or smartwatches equipped with a PPG sensor (Lee and Ham 2021). Blood volume changes measured at the face level are usually contactless and are obtained using Red Green Blue (RGB) cameras that track tiny colour changes in the reflected light of the region of interest (Dabiri and Jazizadeh 2014; Jung and Jazizadeh 2018a). Blood flow can be measured through laser Doppler flowmeters - similar principle to PPG using different light frequencies (Cheng, Lee, and Huang 2018). This technology was mainly used for measuring the microvascular blood flow at the finger (Cheng et al. 2018) or foot (Song et al. 2016) level. Blood pressure was measured by using a sphygmomanometer (inflatable cuff coupled to a manometer) and was rarely employed most likely due to the difficulty of obtaining a continuous measurement. SpO₂ can also be obtained through PPG at the finger level (Chaudhuri et al. 2018, 2020). An indirect measurement of blood oxygen intake, respiration,

was measured contactless using Doppler radar sensors through the motion of the chest and abdomen areas (Jung and Jazizadeh 2018a). BF, BP, and SpO₂ were investigated using medical and research grade sensors where devices were placed in contact with the skin.

The MET can be measured with a cardiopulmonary tester (Song et al. 2016). This involves a spirometry device where a mask is used to analyse the oxygen and carbon dioxide in the inhaled and exhaled air. Although portable products exist, they cannot be worn in daily life due to their intrusiveness. Activity level, representative of the MET, is usually measured instead (Lee and Ham 2021). Motion-based activity was measured using either wrist or chest connected tri-axial accelerometer devices. These sensors are relatively cheap and are usually integrated in smartwatches and smartbands (Laftchiev and Nikovski 2017). Other approaches involved the use of weight and calorie consumption estimation (Huang, Yang, and Newman 2015).

T_{CORE} is approximately measurable from the oesophagus, rectum, gastro-intestinal tract, mouth, tympanum, auditory canal regions (CEN 2021). Other options are radio-pills (Wang et al. 2007) or predicting it from heart rate measurements with high accuracy (Nazarian et al. 2021). The inner eye is also a suitable measurement point, obtainable using thermal cameras (Metzmacher et al. 2018). However, certain studies considered the eye temperature as the T_{SK} (Cosma and Simha 2019a, 2019b). A wireless non-invasive thermometer which estimates T_{CORE} based on T_{SK} and heat flux is also available, though costly (Ajčević et al. 2022).

T_{SK} can be obtained using both wearable and contactless devices (Hwang et al. 2019; Salehi, Ghanbaran, and Maerefat 2020). Except for measurements on the eye, T_{SK} represents the most investigated indicator for each human body part. The standard way of measuring T_{SK} involves the use of low-cost thermocouples (Jung and Jazizadeh 2018b; Liu et al. 2020) and resistance temperature detectors (Lopez et al. 2016) which are wired to a logging system. This method is highly intrusive and makes it difficult to perform daily activities. Wireless T_{SK} sensors are also available, consisting of button sized devices (Liu et al. 2019), which can be attached to the skin through e.g., medical tape. These devices cannot transfer data in real-time though, making them impractical for smart system integration. Smartwatches and smartbands were previously reported throughout literature as useful for measuring T_{SK} in the wrist area due to the convenient placement of the sensors (Barrios and Kleiminger 2017; Deng and Chen 2020; W. Li, Zhang, and Zhao 2019; Yoshikawa et al. 2019). Still, few newer smartwatch/smartband devices make available T_{SK} as a signal. The facial area has also drawn extensive attention due to the appearance of low-cost contactless monitoring technologies (Ranjan and Scott 2016; Warthmann et al. 2018). T_{SK} was obtained through thermal infrared cameras generally pointed at the face, a feasible non-intrusive method (Cosma and Simha 2019b; Li et al. 2020; Lu et al. 2019; Pavlin et al. 2017), or through infrared lasers which must be close to the skin level for a continuous measurement of the point of interest (Luo et al. 2018). An innovative solution was found in literature where infrared sensors were attached to a pair of glasses (Ghahramani et al. 2016). The main advantage of contactless T_{SK} measurements is that the measurement is not influenced by the sensor covering the skin area under investigation (Metzmacher et al. 2018). Skin relative humidity (RH_{SK}) was measured using button sized sensors in studies involving high physical activity (Priego-Quesada et al. 2020). Sweat rate was also directly measured with an innovative sensor (watch-type device with a capacitive humidity sensor) with low operation power and weight (Sim, Yoon, and Cho 2018). SC, or electrodermal activity (EDA), can be obtained through electrodes connected to the fingers (Pigliatile et al. 2020) or at the wrist level through smartbands (Lee and Ham 2021). Only one mention of skin hardness was found in the literature measured using a durometer (not designed for skin hardness measurements) which was placed at the skin level of the arm or wrist (Yoon et al. 2018).

3.3 Capabilities and limitations of current sensing strategies

A summary of capabilities and limitations of the physiological measurement strategies are given in Table 1. The analysis was made by comparing wearable and contactless devices. Wearable devices represent relatively cheap and mature products. They can be wired or wireless. Device examples are probes, telemetry devices, smartwatches/smartbands, and headsets. Contactless examples found in literature are RGB cameras, infrared thermal cameras, and devices employing laser Doppler velocimetry.

Table 1: Capabilities and limitations of measuring devices for physiological indicators.

Device	Capabilities	Limitations
Wearable	<ul style="list-style-type: none"> • May be integrated in a device attached to an occupant • May measure multiple parameters • Clothing does not interfere with the measurement • Mature products • May be relatively cheap • Can be placed directly on the skin • Can be placed on different and multiple body areas • Can be connected via cloud-based solutions 	<ul style="list-style-type: none"> • Measurement length dependent on the battery life and data storage capacity of the equipment • Could be intrusive and invasive (e.g., chest strap) • Accuracy issues (improper use, movement, fastening option) • Sensor accuracies may be unknown • Covers body area where measurement is made • Narrow operating ranges • Single point measurement • Influenced by physical pressure, insulation from fitting material and thermal inertia of the sensor • Inconvenient if wired
Contactless	<ul style="list-style-type: none"> • Can gather data on body areas not covered by clothing, e.g. face • Non-invasive and non-intrusive • Can capture a bigger surface area • Can detect changes from the skin naturally and directly impacted by the surrounding environment 	<ul style="list-style-type: none"> • May require a complex system consisting of multiple nodes (e.g. depth and thermal image camera) • Privacy concerns • Little flexibility regarding placement • Correction regarding clothing might be required • May not be suitable for multi-occupancy spaces due to the limited field of view • Error in detecting area of interest for measurements • Can be difficult to implement in building due to size and compatibility issues (e.g. in Building Management Systems). • Higher cost compared to wearable sensors

4 DISCUSSION

As wearables, devices designed for measuring certain physiological indicators, e.g., HRV, brainwave frequency bands, SpO₂, can be found though lacking wireless connectivity. Few commodity health monitoring telemetry devices designed to acquire multiple physiological indicators were observed (Chaudhuri et al. 2018). Smartbands/smartwatches were the most complete devices, being able to measure multiple indicators, such as T_{SK}, HR, SpO₂, and activity simultaneously. However, just as chest bands, they are commodity devices lacking standardized datasheets with information on the device's accuracy, resolution, and range. Extracting real-time data from these devices may also not be possible or would require specific knowledge. On the other hand, medical and research-grade devices are costly and usually designed for measuring specific physiological indicators, e.g., SC and brainwave sensors.

For quantifying physiological indicators in real-time, RGB and infrared thermal cameras could be feasible. RGB cameras are cheaper and usually available at the workspace. Although privacy measures such as discarding images after data collection must be taken into account when employing cameras (D. Li, Menassa, and Kamat 2019), these systems also enable pose tracking (Qian et al. 2020; Yang et al. 2019), age, and clothing estimation (Rida et al. 2023), which may complement T_{SK} and HR measurements. Infrared thermal cameras present a wider working range than contact measurements (e.g., thermocouples) but have a slightly worse correlation with the thermal sensation (Wu et al. 2019). When compared to resistance temperature sensors (usually with an accuracy of ± 0.2 °C) only a maximum of 0.5 to 0.7 K difference was observed (Metzmacher et al. 2018). Low-cost options present low image resolution, which may lead to difficulties in detecting the human profile, but information from the surrounding pixels

surrounding could reduce noise and thus improve stability. Combining RGB and infrared thermal cameras may even increase measurement accuracy as the influence of light is reduced generating clearer contours (Metzmacher et al. 2018). However, both solutions require additional data processing for obtaining the desired parameters (Dabiri and Jazizadeh 2014). From a practicality point of view, wearable devices are connected to the occupant which makes it difficult to determine ownership, operation, and maintenance responsibility. Contactless devices are deployed in the space. Although requiring the consent of the occupants, ownership, operation, and maintenance can be performed by the building owner.

5 CONCLUSIONS

Acquiring physiological indicators in real-time still represents a difficult task and thus further development of current sensing devices is required. Not all devices measuring physiological indicators present real-time data access while “plug-and-play” solutions specifically designed for thermal comfort assessment are lacking.

Contactless devices (e.g., RGB and infrared cameras) can only be used to acquire skin temperature and heart rate and require extensive data processing. Wearable devices can be used to acquire an extensive range of indicators, with the wrist area being the most versatile. Smartwatches and smartbands are mature devices used to acquire multiple physiological indicators (T_{SK} , HR, SpO_2 , and activity) simultaneously. Since they are mostly consumer products protected through 3rd party data privacy protocols, these devices cannot be deployed in buildings with ease. Measurement accuracy represents a limitation for low cost contactless solutions, which requires further investigation.

ACKNOWLEDGEMENTS

This study was financially supported by Mitsubishi Electric Corporation and by the International Centre for Indoor Environment and Energy (ICIEE), Technical University of Denmark (DTU).

REFERENCES

- Ajčević, Miloš, Alex Buoite Stella, Giovanni Furlanis, Paola Caruso, Marcello Naccarato, Agostino Accardo, and Paolo Manganotti. 2022. “A Novel Non-Invasive Thermometer for Continuous Core Body Temperature: Comparison with Tympanic Temperature in an Acute Stroke Clinical Setting.” *Sensors* 22(13):4760. doi: 10.3390/s22134760.
- Barrios, Liliana, and Wilhelm Kleiminger. 2017. “The Comfstat - Automatically Sensing Thermal Comfort for Smart Thermostats.” *2017 IEEE International Conference on Pervasive Computing and Communications, PerCom 2017* 257–66. doi: 10.1109/PERCOM.2017.7917872.
- Bogatu, Dragos-Ioan, Jun Shinoda, Bjarne W. Olesen, Futa Watanabe, Yosuke Kaneko, and Ongun B. Kazanci. 2023. “Human Physiology for Personal Thermal Comfort-Based HVAC Control – A Review.” 240(April). doi: 10.1016/j.buildenv.2023.110418.
- CEN. 2021. “EN ISO 9886 Ergonomics - Evaluation of Thermal Strain by Physiological Measurements.”
- Chaudhuri, Tanaya, Yeng Chai Soh, Hua Li, and Lihua Xie. 2020. “Machine Learning Driven Personal Comfort Prediction by Wearable Sensing of Pulse Rate and Skin Temperature.” *Building and Environment* 170(November 2019):106615. doi: 10.1016/j.buildenv.2019.106615.
- Chaudhuri, Tanaya, Deqing Zhai, Yeng Chai Soh, Hua Li, and Lihua Xie. 2018. “Random Forest Based Thermal Comfort Prediction from Gender-Specific Physiological

- Parameters Using Wearable Sensing Technology.” *Energy and Buildings* 166:391–406. doi: 10.1016/j.enbuild.2018.02.035.
- Cheng, Chin Chi, Dashang Lee, and Bi Song Huang. 2018. “Estimated Thermal Sensation Models by Physiological Parameters during Wind Chill Stimulation in the Indoor Environment.” *Energy and Buildings* 172:337–48. doi: 10.1016/j.enbuild.2018.05.005.
- Cosma, Andrei Claudiu, and Rahul Simha. 2019a. “Machine Learning Method for Real-Time Non-Invasive Prediction of Individual Thermal Preference in Transient Conditions.” *Building and Environment* 148(November 2018):372–83. doi: 10.1016/j.buildenv.2018.11.017.
- Cosma, Andrei Claudiu, and Rahul Simha. 2019b. “Using the Contrast within a Single Face Heat Map to Assess Personal Thermal Comfort.” *Building and Environment* 160(May):106163. doi: 10.1016/j.buildenv.2019.106163.
- Dabiri, Sina, and Farrokh Jazizadeh. 2014. “Exploring Video Based Thermal Perception Identification.”
- Deng, Zhipeng, and Qingyan Chen. 2020. “Development and Validation of a Smart HVAC Control System for Multi-Occupant Offices by Using Occupants’ Physiological Signals from Wristband.” *Energy and Buildings* 214:109872. doi: 10.1016/j.enbuild.2020.109872.
- Ghahramani, Ali, Guillermo Castro, Burcin Becerik-Gerber, and Xinran Yu. 2016. “Infrared Thermography of Human Face for Monitoring Thermoregulation Performance and Estimating Personal Thermal Comfort.” *Building and Environment* 109:1–11. doi: 10.1016/j.buildenv.2016.09.005.
- Gwak, Jongseong, Motoki Shino, Kazutaka Ueda, and Minoru Kamata. 2016. “Effects of Changes in the Thermal Factor on Arousal Level and Thermal Comfort.” *Proceedings - 2015 IEEE International Conference on Systems, Man, and Cybernetics, SMC 2015* 923–28. doi: 10.1109/SMC.2015.169.
- Huang, Chuan Che Jeff, Rayoung Yang, and Mark W. Newman. 2015. “The Potential and Challenges of Inferring Thermal Comfort at Home Using Commodity Sensors.” *UbiComp 2015 - Proceedings of the 2015 ACM International Joint Conference on Pervasive and Ubiquitous Computing* 1089–1100. doi: 10.1145/2750858.2805831.
- Hwang, Jongmin, Jun Kim, Kee Joon Choi, Min Soo Cho, Gi Byoung Nam, and You Ho Kim. 2019. “Assessing Accuracy of Wrist-Worn Wearable Devices in Measurement of Paroxysmal Supraventricular Tachycardia Heart Rate.” *Korean Circulation Journal* 49(5):437–45. doi: 10.4070/KCJ.2018.0323.
- Jung, Wooyoung, and Farrokh Jazizadeh. 2018a. “Towards Non-Intrusive Metabolic Rate Evaluation for HVAC Control.” *Iccbe 2018*.
- Jung, Wooyoung, and Farrokh Jazizadeh. 2018b. “Vision-Based Thermal Comfort Quantification for HVAC Control.” *Building and Environment* 142(May):513–23. doi: 10.1016/j.buildenv.2018.05.018.
- Kim, Hakpyeong, and Taehoon Hong. 2020. “Determining the Optimal Set-Point Temperature Considering Both Labor Productivity and Energy Saving in an Office Building.” *Applied Energy* 276(June):115429. doi: 10.1016/j.apenergy.2020.115429.
- Kim, Joyce, Stefano Schiavon, and Gail Brager. 2018. “Personal Comfort Models – A New Paradigm in Thermal Comfort for Occupant-Centric Environmental Control.” *Building and Environment* 132(January):114–24. doi: 10.1016/j.buildenv.2018.01.023.
- Laftchiev, Emil, and Daniel Nikovski. 2017. “An IoT System to Estimate Personal Thermal Comfort.” *2016 IEEE 3rd World Forum on Internet of Things, WF-IoT 2016* 672–77. doi: 10.1109/WF-IoT.2016.7845401.
- Lee, Jeehee, and Youngjib Ham. 2021. “Physiological Sensing-Driven Personal Thermal Comfort Modelling in Consideration of Human Activity Variations.” *Building Research and Information* 49(5):512–24. doi: 10.1080/09613218.2020.1840328.

- Li, Da, Carol C. Menassa, and Vineet R. Kamat. 2019. "Robust Non-Intrusive Interpretation of Occupant Thermal Comfort in Built Environments with Low-Cost Networked Thermal Cameras." *Applied Energy* 251(May). doi: 10.1016/j.apenergy.2019.113336.
- Li, Da, Carol C. Menassa, Vineet R. Kamat, and Eunshin Byon. 2020. "HEAT - Human Embodied Autonomous Thermostat." *Building and Environment* 178(March). doi: 10.1016/j.buildenv.2020.106879.
- Li, Wei, Jili Zhang, and Tianyi Zhao. 2019. "Indoor Thermal Environment Optimal Control for Thermal Comfort and Energy Saving Based on Online Monitoring of Thermal Sensation." *Energy and Buildings* 197:57–67. doi: 10.1016/j.enbuild.2019.05.050.
- Liu, Kuixing, Ting Nie, Wei Liu, Yiqing Liu, and Dayi Lai. 2020. "A Machine Learning Approach to Predict Outdoor Thermal Comfort Using Local Skin Temperatures." *Sustainable Cities and Society* 59(March):102216. doi: 10.1016/j.scs.2020.102216.
- Liu, Shichao, Stefano Schiavon, Hari Prasanna Das, Ming Jin, and Costas J. Spanos. 2019. "Personal Thermal Comfort Models with Wearable Sensors." *Building and Environment* 162(July):106281. doi: 10.1016/j.buildenv.2019.106281.
- Lopez, Guillaume, Takahiro Tokuda, Naoya Isoyama, Hiroshi Hosaka, and Kiyoshi Itao. 2016. "Development of a Wrist-Band Type Device for Low-Energy Consumption and Personalized Thermal Comfort." *2016 11th France-Japan and 9th Europe-Asia Congress on Mechatronics, MECATRONICS 2016 / 17th International Conference on Research and Education in Mechatronics, REM 2016* 209–12. doi: 10.1109/MECATRONICS.2016.7547143.
- Lu, Siliang, Weilong Wang, Shihan Wang, and Erica Cochran Hameen. 2019. "Thermal Comfort-Based Personalized Models with Non-Intrusive Sensing Technique in Office Buildings." *Applied Sciences (Switzerland)* 9(9). doi: 10.3390/app9091768.
- Luo, Maohui, Edward Arens, Hui Zhang, Ali Ghahramani, and Zhe Wang. 2018. "Thermal Comfort Evaluated for Combinations of Energy-Efficient Personal Heating and Cooling Devices." *Building and Environment* 143(April):206–16. doi: 10.1016/j.buildenv.2018.07.008.
- Metzmacher, Henning, Daniel Wölki, Carolin Schmidt, Jérôme Frisch, and Christoph van Treeck. 2018. "Real-Time Human Skin Temperature Analysis Using Thermal Image Recognition for Thermal Comfort Assessment." *Energy and Buildings* 158:1063–78. doi: 10.1016/j.enbuild.2017.09.032.
- Nazarian, Negin, Sijie Liu, Manon Kohler, Jason K. W. Lee, Clayton Miller, Winston T. L. Chow, Sharifah Badriyah Alhadad, Alberto Martilli, Matias Quintana, Lindsey Sunden, and Leslie K. Norford. 2021. "Project Coolbit: Can Your Watch Predict Heat Stress and Thermal Comfort Sensation?" *Environmental Research Letters* 16(3). doi: 10.1088/1748-9326/abd130.
- Nkurikiyeyezu, Kizito N., Yuta Suzuki, and Guillaume F. Lopez. 2018. "Heart Rate Variability as a Predictive Biomarker of Thermal Comfort." *Journal of Ambient Intelligence and Humanized Computing* 9(5):1465–77. doi: 10.1007/s12652-017-0567-4.
- Pavlin, Boris, Giovanni Pernigotto, Francesca Cappelletti, Paolo Bison, Renato Vidoni, and Andrea Gasparella. 2017. "Real-Time Monitoring of Occupants' Thermal Comfort through Infrared Imaging: A Preliminary Study." *Buildings* 7(1). doi: 10.3390/buildings7010010.
- Pigliautile, Ilaria, Sara Casaccia, Nicole Morresi, Marco Arnesano, Anna Laura Pisello, and Gian Marco Revel. 2020. "Assessing Occupants' Personal Attributes in Relation to Human Perception of Environmental Comfort: Measurement Procedure and Data Analysis." *Building and Environment* 177(March):106901. doi: 10.1016/j.buildenv.2020.106901.
- Priego-Quesada, Jose Ignacio, Alvaro S. Machado, Marina Gil-Calvo, Irene Jimenez-Perez, Rosa M^a Cibrian Ortiz de Anda, Rosario Salvador Palmer, and Pedro Perez-Soriano.

2020. "A Methodology to Assess the Effect of Sweat on Infrared Thermography Data after Running: Preliminary Study." *Infrared Physics and Technology* 109(April):103382. doi: 10.1016/j.infrared.2020.103382.
- Qian, Junpeng, Xiaogang Cheng, Bin Yang, Zhe Li, Junchi Ren, Thomas Olofsson, and Haibo Li. 2020. "Vision-Based Contactless Pose Estimation for Human Thermal Discomfort." *Atmosphere* 11(4). doi: 10.3390/ATMOS11040376.
- Quintana, Matias, Stefano; Schiavon, Tartarini; Federico, Kim; Joyce, and Miller Clayton. 2022. "Cohort Comfort Models - Using Occupant's Similarity to Predict Personal Thermal Preference with Less Data." *Building and Environment* 227:109685. doi: 10.1016/j.buildenv.2022.109685.
- Ranjan, Juhi, and James Scott. 2016. "ThermalSense: Determining Dynamic Thermal Comfort Preferences Using Thermographic Imaging." *UbiComp 2016 - Proceedings of the 2016 ACM International Joint Conference on Pervasive and Ubiquitous Computing* 1212–22. doi: 10.1145/2971648.2971659.
- Rida, Mohamad, Mohamed; Abdelfath, Alexandre; Alahi, and Dolaana Khovalyg. 2023. "Non-Intrusive Physiological Parameters Sensing for Personalized Human Thermal Comfort Prediction." in *Healthy Buildings Europe 2023*.
- Salehi, Behrouz, Abdul Hamid Ghanbaran, and Mehdi Maerefat. 2020. "Intelligent Models to Predict the Indoor Thermal Sensation and Thermal Demand in Steady State Based on Occupants' Skin Temperature." *Building and Environment* 169(November 2019):106579. doi: 10.1016/j.buildenv.2019.106579.
- Shan, Xin, and En Hua Yang. 2020. "Supervised Machine Learning of Thermal Comfort under Different Indoor Temperatures Using EEG Measurements." *Energy and Buildings* 225:110305. doi: 10.1016/j.enbuild.2020.110305.
- Sim, Jai Kyoung, Sunghyun Yoon, and Young Ho Cho. 2018. "Wearable Sweat Rate Sensors for Human Thermal Comfort Monitoring." *Scientific Reports* 8(1):1–11. doi: 10.1038/s41598-018-19239-8.
- Song, W. F., C. J. Zhang, D. D. Lai, F. M. Wang, and K. Kuklane. 2016. "Use of a Novel Smart Heating Sleeping Bag to Improve Wearers' Local Thermal Comfort in the Feet." *Scientific Reports* 6(January):1–10. doi: 10.1038/srep19326.
- Wang, Danni, Hui Zhang, Edward Arens, and Charlie Huizenga. 2007. "Observations of Upper-Extremity Skin Temperature and Corresponding Overall-Body Thermal Sensations and Comfort." *Building and Environment* 42(12):3933–43. doi: 10.1016/j.buildenv.2006.06.035.
- Warthmann, Alexander, Daniel Wölki, Henning Metzmacher, and Christoph van Treeck. 2018. "Personal Climatization Systems-a Review on Existing and Upcoming Concepts." *Applied Sciences (Switzerland)* 9(1). doi: 10.3390/app9010035.
- Wu, Yuxin, Hong Liu, Baizhan Li, and Risto Kosonen. 2019. "Prediction of Thermal Sensation Using Low-Cost Infrared Array Sensors Monitoring System." *IOP Conference Series: Materials Science and Engineering* 609(3). doi: 10.1088/1757-899X/609/3/032002.
- Yang, Bin, Xiaogang Cheng, Dengxin Dai, Thomas Olofsson, Haibo Li, and Alan Meier. 2019. "Real-Time and Contactless Measurements of Thermal Discomfort Based on Human Poses for Energy Efficient Control of Buildings." *Building and Environment* 162(July):106284. doi: 10.1016/j.buildenv.2019.106284.
- Yoon, Sunghyun, Jai Kyoung Sim, Noeul Park, and Young Ho Cho. 2018. "Evaluation of Skin Hardness as a Physiological Sign of Human Thermal Status." *Scientific Reports* 8(1):1–6. doi: 10.1038/s41598-018-30206-1.
- Yoshikawa, Hiroki, Akira Uchiyama, Yuki Nishikawa, and Teruo Higashino. 2019. "Combining a Thermal Camera and a Wristband Sensor for Thermal Comfort Estimation." *2019 ACM International Symposium* 238–41. doi:

10.1145/3341162.3343813.

Zhu, Hui, Hanqing Wang, Zhiqiang Liu, Duanru Li, Guangxiao Kou, and Can Li. 2018. “Experimental Study on the Human Thermal Comfort Based on the Heart Rate Variability (HRV) Analysis under Different Environments.” *Science of the Total Environment* 616–617:1124–33. doi: 10.1016/j.scitotenv.2017.10.208.

APPENDIX

Table 2. Characteristics of sensors employed in literature (T: temperature, RH: relative humidity, HR: heart rate, EDA: electrodermal activity, SC: skin conductance, ACC: accelerometer, ECG: electrocardiogram, SpO₂: blood oxygen saturation, EEG: electroencephalogram).

Type	Model	Measurable parameters	Details
Smartwatch or Smartband	Microsoft Band 2	HR, T, EDA, ACC	Smartwatch
	LG Watch R (W110)	HR	Smartwatch
	Hesvit S3 Empatica E4	HR, T (Acc. ± 0.3 °C, Res. 0.1 °C), RH _{SK} HR, T (Range -40 to +85 °C), ACC (± 2 g), EDA (Range 0.01 to 100 μ S)	Smartband Smartband
Temperature sensor or probe	Exacon D-S18JK	T (Acc. ± 0.1 °C, Range 0 to 50 °C)	Temperature probe
	TT-K-30-SLE	T (Acc. ± 1.1 °C or ± 0.4 %, Range 0-350 °C)	Thermocouple
	iButton DS1923	T (Acc. ± 0.5 °C, Res. 0.5 °C, Range -10 to 65 °C), RH (Acc. ± 5 %, Range 0 to 100%, Res. 0.6% or 0.04%)	Temperature and RH probe
	muRata NTC WZYCH4	- T (Sens. 0.1 °C)	Thermistor Temperature probe
	SBS-BTA	T (Acc. ± 0.5 °C, Res. 0.03 °C)	Thermistor
	Gigarise SG900	T (Acc. ± 0.2 °C, Range -50 to +180 °C)	-
	MLX90614 Beurer FT70	T (Acc. ± 0.5 °C, Res. 0.02 °C) T: ear (Acc. ± 0.2 °C, Range 34-43 °C), forehead (Acc. ± 0.2 °C, Range 34-43 °C), object (Acc. ± 1.5 °C, Range 0-100 °C)	Infrared sensor Medical device
CORE	T (Acc. ± 0.05 °C from 20 °C to 42 °C), T _{CORE} (± 0.28 (1 σ) ± 0.21 (MAD) – chest)	Body temperature sensor	
Heart rate sensor	Zephyr HXM-08L	HR (Acc. ± 3 %, Range 0-200 bpm)	Telemetry device
	Polar H7	ECG, HR (Acc. ± 4 %)	Chestband
	HER-BTA	HR (Freq. 5 kHz ± 10 %)	
	HRV101 BioHarness 3.0	ECG (SRate 250 Hz and 400 Hz, BW 0.05-40Hz) HR (Acc. ± 1 bpm, Range 25-240 bpm), ECG, respiration rate, body orientation, ACC	ECG Holter Physiological monitoring telemetry device
Health monitoring device	MySignals, Libelium CO.	HR (Acc. ± 5 %, Range 25 to 250 bpm), SpO ₂ (Acc. ± 2 %, Range 35 to 100%), SC (Acc. ± 5 %, Range 0-20 μ S), BP (Acc. ± 3 mmHg, Range 0 – 300 mmHg)	Pulse oximeter, Sphygmomanometer
Laser Doppler	moorVMS-LDF1	Blood flow (Acc. ± 10 %, Range: 0-1000AU)	Deeper tissue blood flow and temperature monitoring
Neural headset	EPOC+	14 ch. EEG (Res. 14 bits, DRange 8400 μ V, BW 0.2-45 Hz, BL 12 h)	14 channel EEG
	B-Alert X10, ABM	9 ch. EEG (Res. 16 bit, DRange ± 1000 μ V, BL 8+ h)	9 channel EEG
Camera	Yukai USB	Sweat area/sweat pore diameter	Digital camera with microscope
	Microsoft Kinect	RGB-DT camera (Acc. ± 4 cm at 5 m, depth range 0.8-5 m, \$48)	RGB-Depth Temperature
	FLIR A35	T _{SK} (Acc. ± 5 °C or ± 5 % of reading, Range -23 to 135 °C/-40 to 550 °C, Sens. < 0.05 °C)	Infrared
	FLIR A655sc	T _{SK} (Acc. ± 2 °C or ± 2 % of reading, \$22000)	Infrared
	FLIR T540	T _{SK} (Acc. ± 2 °C or ± 2 % of reading, Range -20 to 120 °C, Res. 464x348 px)	Infrared
	FLIR B8400 FLIR Lepton	TSK (Range -20 to 120 °C) TSK (Acc. ± 0.5 °C, Res. 0.1 °C, \$250)	Infrared Infrared

FLIR Lepton 2.5

TSK (Acc. ± 5 °C or ± 5 % of reading, Range -10 °C to 65 °C, Sens. < 50 mK, \$200)

Infrared

ASHRAE 241-2023 Control of Infectious Aerosols

Max Sherman¹, Benjamin Jones¹

¹ University of Nottingham

SUMMARY

On June 24, 2023, ASHRAE approved the publication of Standard 241-2023 *Control of Infectious Aerosols*. The purpose of Standard 241 is “to establish minimum requirements for control of infectious aerosols to reduce risk of disease transmission in the occupiable space” of buildings by defining “the amount of equivalent clean airflow necessary to substantially reduce the risk of disease transmission during infection risk management mode”. We provide a high-level overview of key aspects of the new standard as well as a discussion of its historical context and its potential impact on design and operation of buildings to achieve improved indoor air quality (IAQ).

Requirements for airborne infection risk management have been absent for a century from IAQ standards with the exception of those written for healthcare facilities and laboratories. In 1895, ASHRAE’s predecessor society, the American Society of Heating and Ventilating Engineers (ASHVE), published ventilation recommendations intended to reduce disease transmission that were incorporated in a proposed a 1914 model law and included in 22 US state codes by 1922. Since the 1930s, however, IAQ standards have focused on perceived air quality and control of chemical and particulate contaminants that have reduced minimum ventilation rates by half.

More recently, the important role that indoor environments can play in disease transmission, has been described in ASHRAE’s Position Document on *Infectious Aerosols* that was first published with the title *Airborne Infectious Diseases* in 2009. Unfortunately, this awareness did not lead to changes in standards. The great personal, societal, and economic consequences of the COVID-19 pandemic together with the evidence that poorly ventilated buildings can be high risk environments for airborne infection transmission brought the adequacy of existing IAQ standards under heavy scrutiny. Recognizing that indoor environments were not designed to mitigate risk of Covid-19 transmission, ASHRAE formed its Epidemic Task Force (ETF) early in 2020. In a matter of months, the ETF produced a large body of guidance that was well received and widely used. This guidance was not intended to set new enforceable minimum requirements but did lay the groundwork for their development, as a logical next step.

The development of Standard 241 began with the December 6, 2022 ASHRAE board motion authorizing development of a “comprehensive, consensus-based, code enforceable standard...to mitigate the risk from respiratory pathogens” on an aggressive six-month schedule requested by the US White House COVID-19 Response Team Coordinator, Dr. Ashish Jha. The committee of international experts formed to undertake this challenging task first met on February 28, 2023, delivered a public review draft on May 12 and, after evaluating over 1000 comments, recommended a final draft for publication, which was subsequently approved on June 24. This unprecedented development time of 116 days was made possible by the extraordinary commitment of the project committee and to its ability to

build on existing ASHRAE documents. Key aspects of the new standard are summarized below.

- Standard 241 applies to occupiable space in new buildings, existing buildings, and major renovations, including residential buildings and some portions of health care facilities. It sets requirements for outdoor air system and air cleaning system design, installation, commissioning, operation and maintenance.
- A prerequisite for meeting standard 241 is that minimum Indoor Air Quality be provided by complying with applicable IAQ standards such as ANSI/ASHRAE Standard 62.1, ANSI/ASHRAE Standard 62.2, or ANSI/ASHRAE/ASHE Standard 170 at the time of construction or major renovation.
- Standard 241 gives requirements that apply to *infection risk management mode* (IRMM), the operating mode when increased protection from infectious aerosol exposure is needed. Public health officials or other authorities may begin and end required use of IRMM, but it could also be used at the discretion of the building owner or occupant.
- *Equivalent clean airflow* requirements are the single most important aspect of Standard 241. The equivalent clean air flow requirement for a space is the product of space occupancy and its equivalent clean airflow rate for infection risk mitigation per person (ECA). Equivalent clean airflow is the “flow rate of pathogen-free air that, if distributed uniformly within the breathing zone would have the same effect on infectious aerosol concentration as the sum of actual outdoor airflow, filtered airflow, and inactivation of infectious aerosols”. This provides the user of the standard great flexibility to determine how requirements are met.
- The standard provides extensive requirements for mechanical filters and air cleaners. These include required testing for both performance and safety. Mechanical filters must be at least MERV-A 11 or equivalent in order to receive credit for contributing to equivalent clean airflow requirements. Prescriptive infectious aerosol removal efficiency are provided. Other air cleaners and air disinfection technologies must be tested by in-duct or chamber methods described in Normative Appendix A of Standard 241. Safety testing requires measurement of formaldehyde, ozone, and particulate matter emissions and sets target levels.
- Standard 241 includes a variety of other requirements such as air distribution, natural ventilation and for assessment, planning, commissioning, operation, and maintenance of infectious aerosol control systems, which revolves around the development of a *Building Readiness Plan* that describes the engineering and non-engineering controls used to achieve equivalent clean airflow targets for a facility. Supporting guidance and tools are provided to assist in planning and commissioning.

Standard 241 is ground-breaking in a number of respects:

- By creating a special operating mode for use when conditions warrant (IRMM), it introduces the concept of resilience into indoor air quality standards.
- Expressing control requirements in terms of a quantity, equivalent clean air, that integrates the impact of multiple controls. This is also a concept that could be adapted and applied to other indoor air quality standards.
- The requirements for filter and air cleaner testing go well beyond what is found in existing standards. They are a major step in the direction of creating uniform and effective technology-agnostic criteria for characterizing filter and air filter performance and safety that will support their effective application.

KEYWORDS

Infectious Aerosols, COVID19, Air Cleaning, IAQ

Can the Wells-Riley model universally assess airborne pathogen infection risk?

Benjamin Jones^{*1}, Christopher Iddon², and Max Sherman¹

*1 University of Nottingham
Department of Architecture and Built Environment
Nottingham, UK
*Corresponding author:
benjamin.jones@nottingham.ac.uk*

*2 University College London
Department of Civil,
Environmental and Geomatic Engineering
London, UK*

ABSTRACT

Some airborne pathogens can infect susceptible people over long distances in buildings when they are transported in small respiratory particles suspended in the air. The pathogen concentration in air can be decreased using engineering controls, such as ventilation, filtration, or inactivation. To determine their effect, it is common to use the Wells-Riley model to estimate the probability that a susceptible person is infected and is a function of the dose of infectious pathogen received and a Poisson distribution. Wells proposed a hypothetical dose unit, known as the *quantum of infection*, which is a function of the pathogen emission rate and, in turn, a function of the number of infected people and their individual pathogen emission rates. The quanta generation rate can be determined from the epidemiological data for an outbreak case of a disease in a space where the proportion of a population of people infected with a disease who were initially free of it is known. The quanta generation rate is a temporally and activity varying parameter and so this approach only represents its value at the time the infections occurred and for that space. It is also unique for every disease and disease variant, and the emission rate varies in different spaces because the probability of the presence of infected people also varies. It is unknown at the start of a pandemic, and again later when the pathogen mutation period is greater than the time taken to determine uncertainty in its value. These factors make uncertainty in its value significant and it may vary by several orders of magnitude. A Monte Carlo analysis is used to show that uncertainty in the quanta emission rate for SARS-CoV-2 varies over around 8 orders of magnitude. There is a general paucity of data of sufficient quality to reduce uncertainty in emission rates. This means that there is little confidence in the data located in the tails. The problem with this is demonstrated by applying the emission rates to the WR model to estimate that, for an 8 hour exposure in a 50 person office with an outdoor airflow rate of 10 l s^{-1} per person, the probability of infection of each occupant from long range transmission is $<1\%$ for 95% of events. It is the data in the right-tail of the emission rate distribution that leads to an appreciable probability of infection. These are just a few of several factors that make a probability of infection estimated by the Wells-Riley model unusable as a metric.

KEYWORDS

Quanta, infection risk, ventilation, far-field

1 INTRODUCTION

Some airborne pathogens can infect susceptible people over long distances in buildings when they contained in are transported in small respiratory particles with a range of sizes, some of which can remain airborne for long periods. When designing or controlling an indoor space that may contain infectious people, many of the factors of concern are fixed either by the health problem or by administrative requirements. However, the pathogens concentration in air can be decreased using various engineering controls, such as ventilation, filtration, or inactivation. To determine their effect, it is common to use the Wells-Riley (WR) model to estimate the probability that a susceptible person is infected and is a function of the dose of infectious pathogen received and a Poisson distribution. Wells proposed a hypothetical dose unit, known as the *quantum of infection*, defined as the number of infectious airborne pathogen required to infect 63% of susceptible people. Quanta comprises physical, biological, and statistical properties. It is a function of the pathogen emission rate and, in turn, a function of the number

of infected people and their individual pathogen emission rates. The quanta generation rate can be determined from the epidemiological data for an outbreak case of a disease in a space where the proportion of a population of people infected with a disease who were initially free of it is known. The quanta generation rate is a temporally and activity varying parameter and so this approach only represents its value at the time the infections occurred and for that space. It is also unique for every disease and disease variant, and the emission rate varies in different spaces because the probability of the presence of infected people also varies. It is unknown at the start of a pandemic, and again later when the pathogen mutation period is greater than the time taken to determine uncertainty in its value. These factors make uncertainty in its value significant and it may vary by several orders of magnitude. This could make a probability of infection estimated by the WR model unusable as a metric. Therefore, the aim of this paper is to quantify the uncertainty in both quanta emission rates and the probability of infection for SARS-CoV-2 to assess the ability of the WR model to universally assess airborne pathogen infection risk.

2 QUANTA DEFINED

The WR model describes the probability of becoming infected as a function of the dose of infectious agent received and a Poisson distribution (Riley 1978).

$$P(I) = 1 - e^{-n} \quad (1)$$

Here, $P(I)$ is the probability of becoming infected and n is the quanta of infectious agent the individual is exposed to. This equation is the defining relationship and can be used to make a reasonable estimate of what its value must be. The WR model assumes that quanta and the infection probability is proportional to the dose of infectious agent received. The dose of many other infectious agents is given by the amount inhaled. Then the probability of infection can be expressed as

$$n = \int QC(t) dt \quad (2)$$

where t (h) is the time variable, C (quanta per m^3) is the concentration of infectious material the individual is exposed to, Q ($m^3 h^{-1}$) is the breathing rate of an exposed person. This equation assumes that all uninfected people are equally susceptible, and they are not wearing personal protective equipment, such as a mask.

To follow an individual, the integration over time reflects what they are doing, and the quantities within it vary. To evaluate what is happening for a specific activity, Equation (2) can be simplified further by representing the quantities within the integral with their averages. Then,

$$n = \bar{Q}\bar{C}D \quad (3)$$

where D (h) is the duration of the activity and the overbars of the quantities indicate the time average over that duration.

To find the average concentration, we follow the WR model and make the assumption that the infectious material is conserved, but with a first order loss term ϕ (h^{-1}), and the only source of infectious material is infected people. In this case, the time evolution of the concentration is determined by a first order linear differential equation with the time variable assumed.

$$\frac{dC}{dt} + \phi C = \frac{1}{V} \sum_{i=1}^j q_i \quad (4)$$

Here, V (m^3) is the volume of the space, and q_i (quanta h^{-1}) is the emission rate of each of j people in the space, which is zero for those uninfected. The loss term is the sum of the outside

air change rate ψ (h^{-1}), the biological decay rate of the pathogen λ (h^{-1}), and the surface deposition rate of respiratory particles γ (h^{-1}).

$$\phi = \psi + \lambda + \gamma \quad (5)$$

The viral load of an infector evolves through the course of their infection with a particular disease; see Cevik *et al.* (2020) for SARS-CoV-2, similarly the emission rate is also seen to evolve see Zhou *et al.* (2023). It should be noted that the WR model assumes that there is an equivalent number of infected people, and that an infected person emits at a fixed rate. The emission rate term might also be reduced by any source removal mechanism, such as local capture or filtration immediately adjacent to an infected person, but it is not included here.

The average concentration can be calculated from the standard solution to a first order differential equation, but we can make the simplifying assumption that it can be treated as a steady state, when it is possible to remove the overbars so that

$$n = \frac{QD \sum_{i=1}^j q_i}{\phi V} \quad (6)$$

The quanta emission rate, q_i (quanta h^{-1}), for a single infected person can be calculated as a function of the emission rate of viable virions, G (virions h^{-1}), the fraction of virions absorbed by the respiratory tract of a susceptible person after they enter, k , and the dose constant, K , the reciprocal of the probability that a single virion initiates an infection.

$$q \equiv kG/K \quad (7)$$

If the breathing rate of a single infected person is the same as that for susceptible people, G is determined by adapting Buonanno *et al.* (2020) to be

$$G \equiv QV_{drop}^*Lv \quad (8)$$

Here, L (RNA copies m^{-3}) is the load of viral genomic material in the respiratory fluid, much of which is genomic material and not viable virus, and so v (virions per RNA copy) is the viable fraction. V_{drop}^* is the total volume (m^3) of expelled airborne respiratory particles (respiratory fluid) in 1 m^3 of exhaled air and is a function of the number of all respiratory particles per unit volume of exhaled air, C_{drop} ($\# \text{ m}^{-3}$), and the mean diameter of the exhaled respiratory particles, \bar{d} (m). An assumption is made about the hydrated volumes of the respiratory particles measured in experiments used to derive \bar{d} (see Morawska *et al.* 2009) and so an evaporation term, E , is used to account for the hydrated volume of V_{drop}^* .

$$V_{drop}^* \equiv \frac{\pi}{6} (\bar{d}E)^3 C_{drop} \quad (9)$$

3 UNCERTAINTY IN THE QUANTA EMISSION RATE

The derivation in Section 2 treats all parameters as being known precisely, although few of them are. Some, like the duration (D), can be assumed to be known because they are set as part of the design process. Others, such as the quanta emission rate (q), are known poorly. This type of parameter is best described by a distribution. Furthermore, it is preferable to predict a probability distribution for $P(I)$ rather than a simple maximum likelihood estimate. It is also the only meaningful way to understand $P(I)$ when parameter values are unknown at a moment in time, or when it is desirable to understand the uncertainty in the general risk of being in a particular space. Given that the model is the product of many assumedly uncorrelated terms, the distribution of its predictions is expected to be approximately log-normal whose variance is best described by a geometric standard deviation.

Each term in Equations 5-9 is considered separately and appropriate values and distributions are given in Table 1. The rate of aerosol emission and their origin in the respiratory tract is a function of respiratory activity, such as breathing, talking and vocalisation (singing an “*aaah*”) (Morawska *et al.* 2009). Aerosol diameters range from $<1 \mu\text{m}$ to $>100 \mu\text{m}$, and their size distribution is dependent upon the expiratory activity, usually following a log-normal distribution (Morawska *et al.* 2009). Larger respiratory particles fall ballistically under gravity in still air. Respiratory particles with an evaporated diameter of $<10 \mu\text{m}$ can remain airborne for several hours. The mean aerosol diameter (\bar{d}) is derived experimentally for people breathing for 75% of the time and talking for 25% (Morawska *et al.* 2009), and their distribution is assumed to be log-normal with a mean value of $1.84 \times 10^{-6} \text{ m}$ and an arbitrary standard deviation of 10% of the mean. Respiratory particles evaporate reducing their diameter, mass, and terminal velocity. Therefore, the diameter of the respiratory particle is likely to be greater when emitted (hydrated) than when measured and this is accounted for by the evaporation factor (E) that has limits of 2 and 5, but Nicas *et al.* (2005) advise that this is likely to be closer to 2 than 5 and so a beta distribution is used with $\alpha=2$ and $\beta=5$.

The number of all respiratory particles per unit volume of exhaled air (C_{drop}) is also given by Morawska *et al.* (2009) whose data contains concentrations of evaporated respiratory particles with a diameter of $<5 \mu\text{m}$ measured during breathing, talking and vocalisation. We assume 25% talking and 75% breathing and that C_{drop} is log-normally distributed with a mean of 9.8×10^4 respiratory particles m^{-3} and has an arbitrary standard deviation of 10% of the mean.

The viral load (L) of an infected person increases with time from the moment of infection peaking just before, or at, the onset of symptoms and decreases thereafter, normally ceasing within a week of the onset of symptoms (Cevik 2020, Cevik 2021). The magnitude of L also varies widely between people at any stage of the infection, which increases uncertainty in it (Killingley *et al.* 2022). Iddon *et al.* (2022) show the distribution of L within an infected population is unknown. Therefore, we arbitrarily use the data of Chen *et al.* (2021b) who predict that \log_{10} values of L taken from NP swabs of individuals 2 days from symptom onset are

Table 1: Uncertainty in input parameters

	Variable	Values	Source
Quanta emission rate	Breathing rate, Q ($\text{m}^3 \text{ h}^{-1}$)	LN(0.56, 0.056)	(Adams 1993)
	Respiratory activity, <i>breathing:talking</i> (%)	75:23	(Morawska <i>et al.</i> ,2009; Iddon <i>et al.</i> 2022)
	Aerosol concentration in exhaled air, C_{drop} (respiratory particles m^{-3})	LN(1.54×10^5 , 1.54×10^4)	(Morawska <i>et al.</i> ,2009; Iddon <i>et al.</i> 2022)
	Mean aerosol diameter, \bar{d} (m)	LN(1.91×10^{-6} , 1.91×10^{-7})	(Morawska <i>et al.</i> ,2009)
	Aerosol evaporation factor, E	B(2.0,5.0) [2.0,5.0]	(Nicas <i>et al.</i> 2005)
	Viral load, L (\log_{10} RNA copies ml^{-1})	N(7.0,1.4)	(Chen <i>et al.</i> 2021)
	Viable fraction, v	B(2.0,5.0) [10^{-4} , 10^{-2}]	(Killingley <i>et al.</i> 2022)
	Respiratory tract absorption fraction, k	U(0.43,0.65)	(Darquenne 2012)
	Dose constant, K	U(5,15)	(Killingley <i>et al.</i> 2022)
	Scenario	Number of infected people, j	1
Number of occupants		50	
Space volume, V (m^3)		1350	
Exposure duration, D (h)		8	
Outside airflow rate (l s^{-1} per person)		10	
Outside air change rate, ψ (h^{-1})		1.33	
Biological decay rate, λ (h^{-1})		LN(0.63,0.43)	(Van Doremalen <i>et al.</i> 2020)
Surface deposition rate, γ (h^{-1})	U(0.42,0.61)	(Thatcher <i>et al.</i> 2002)	

$N(\mu, \sigma)$, normal(mean, standard deviation); LN(μ, σ), log-normal; U(max,min), uniform; B(α, β) [min, max], beta.

Note that L needs to be converted into RNA copies per m^3 by multiplying by 10^6 .

normally distributed with a mean of 7 and a standard deviation of $1.4 \log_{10}$ RNA copies ml^{-1} . The reported values of viral load are per ml of the sample medium rather than the respiratory fluid, but it is a good surrogate for the range of viral loads.

The viable fraction (v) is not well understood, but it changes as the disease progresses, and there is heterogeneity between patients. Killingley *et al.* (2022) show that a conservative estimate of v is between $1:10^{-2}$ and $1:10^{-3}$ viable virions to RNA copies, but it could be as high as $1:10^6$. We assume that v is closer to 10^{-2} using a beta distribution with a lower limit of 10^{-4} and arbitrary values of $\alpha=2$ and $\beta=5$ to give a mean of 2.9×10^{-2} .

The respiratory tract absorption fraction (k) is a function of aerosol diameter and the breath volume. For the mean \bar{d} described earlier, Darquenne *et al.* (2012) estimates k has a range of 0.4—0.65 and, in the absence of knowledge, we assume that all values are equally probable between these limits.

There is no direct measured value of a dose constant (K) for the SARS-CoV-2 virus. A SARS-CoV-2 human challenge infected 53% of participants with a nasally applied solution of 10 TCID₅₀ (50% Tissue Culture Infectious Dose)¹ of viable SARS-CoV-2 virus (Killingley *et al.* 2022, Zhou *et al.* 2023). A crude estimate is that 1 TCID₅₀ is equivalent to 0.7 PFU indicating that the dose was 7 PFU and for the proportion infected would suggest K is approximately 9.3, for this method of application. Here, we assume that 1 PFU is equivalent to a single viable virion, although it is possible that greater than 1 viable virion is required to lead to a plaque due to probabilities of binding to the correct receptor, cell fusion and giving rise to a successful infection. Therefore, we assume K is equally probable between 5 and 15 as a reasonable assumption based on this data point.

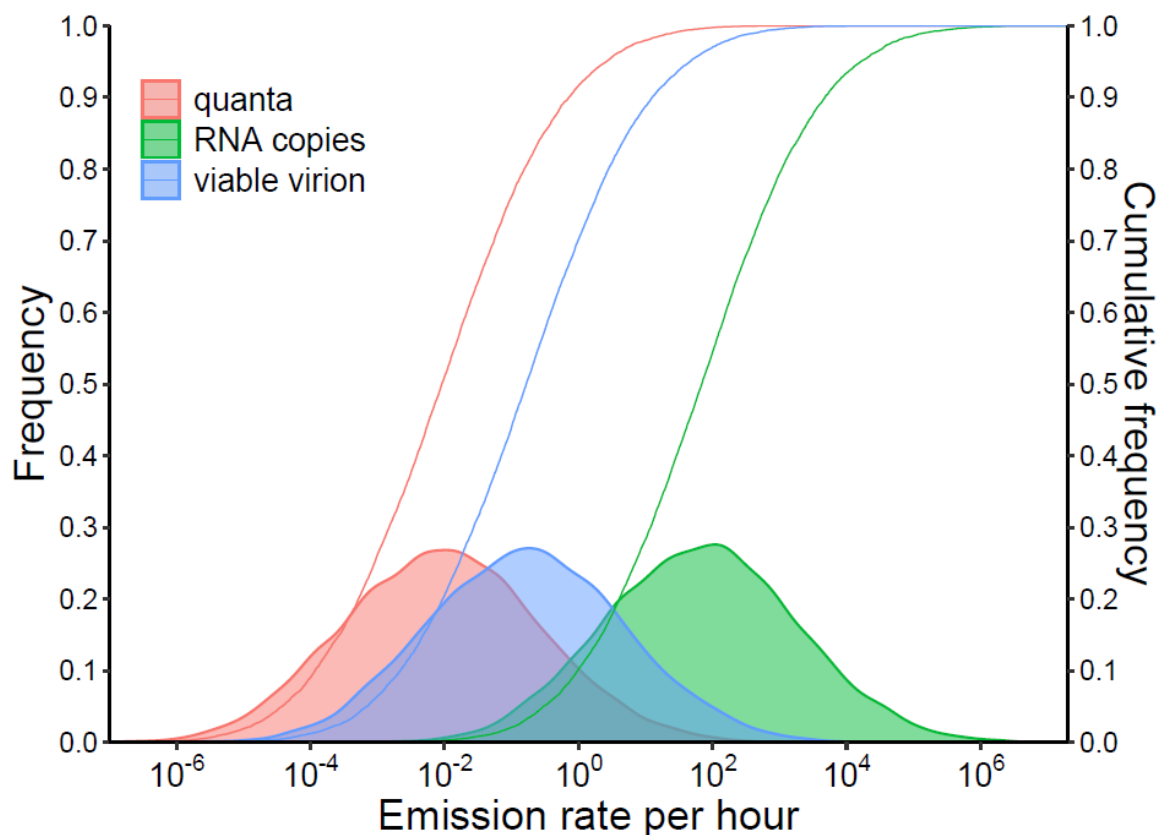


Figure 1: Emission rates of quanta, RNA copies, and viable virions (all per hour).

¹ One TCID₅₀ quantifies the amount of virus required to produce a cytopathic effect in 50% of inoculated tissue culture cells.

Table 2: Uncertainty in calculated parameters

	GM	GSD
Expelled volume ratio of respiratory particles to air, V_{drop}^*	5.9×10^{-12}	1.8
Viable virion emission rate G (virions h^{-1})	8.0×10^{-2}	28
Quanta emission rate q (quanta h^{-1})	3.5×10^{-3}	28
Removal rate, ϕ (h^{-1})	2.4	1.2
Equivalent ventilation rate (1 s^{-1} per person)	18	1.2
Probability of infection, $P(I)$	4.7×10^{-6}	29

GM: Geometric Mean; GSD: Geometric Standard Deviation

It is possible to estimate the uncertainty in the quanta emission rate (q) for a single infected person undertaking some activity that is independent of the space they occupy. Personal factors, such as L , vary relative to the population mean but average out when considered over the entire population distribution. Scenario specific factors, such as Q , C_{drop} , and \bar{d} , do not average out when considered for a population and are, therefore, unknowable. None of these parameters depend on space geometry or outside air delivery rates. Accordingly, when the quanta emission rate inputs identified in Table 1 are applied to Equations 5-9 using a Monte Carlo approach (3 consecutive sets of 10^5 samples produce identical geometric means for q and $P(I)$ when rounded to 3 significant figures), the geometric means (GM) and standard deviations (GSD) of V_{drop}^* , G , and q are calculated and given in Table 2. A probability density function (PDF) and cumulative distribution function (CDF) of q is given in Figure 1.

Figure 1 shows that q varies over around 8 orders of magnitude. The 95% confidence interval for q is between 1.4×10^{-5} and 7.0 quanta h^{-1} , which shows that the uncertainty in its value is around 5 orders of magnitude most of the time. The upper interval seems low when compared to those reported for SARS-CoV-2 superspreading events; for example, the 970 ± 390 quanta h^{-1} reported by Miller *et al.* (2020) and the 130 quanta h^{-1} (inter-quartile range of 97-155 quanta h^{-1}) reported by Vernez *et al.* (2021). Figure 1 shows that this range of values is possible for a single index case, but only for around 0.1% of the time. There is likely to be a difference in the breathing rate and the respiratory activity of the occupants reported by Miller *et al.* and Vernez *et al.* and those described here, which effect the mean aerosol diameter and the aerosol concentration in exhaled air. Future work will compare q against new empirical analyses of emission rates, such as human challenge studies.

4 UNCERTAINTY IN PROBABILITY OF INFECTION

The probability of infection, $P(I)$, in a common space type can be demonstrated using an example scenario. We consider an office space with a floor to ceiling height of 2.7m and an occupancy density of $10m^2$ per person, which contains 50 unmasked occupants who are present for 8 hours. It is mechanically ventilated with an outside delivery rate of 10 l/s per person without filtration. A single infected person is assumed present for the duration. Equation 1 is used to estimate $P(I)$. All inputs are given in Table 1 and outputs are in Table 2. The probability of infection of each occupant from a single infected person from long range transmission is $<1\%$ for 95% of the time. There are problems with this, such as the assumption of a single infected person, and in the significant uncertainty in the tails of the distribution of q , which is discussion in Section 5. It does show, however, the need to understand q better.

5 DISCUSSION

The example highlights problems with inferring quanta empirically for any airborne pathogen and applying it in the same location for the same scenario. First, it isn't always possible to know the number of infected people. The probability of any number of infected people increases with the community infection rate and the number of occupants Iddon *et al.* (2022). For low

community infection rates, the most likely number of infected people in common spaces is zero. Furthermore, the viral load varies by time and person, depending on the stage of a disease, inter-person viral dynamics and the immune response. Secondly, if the space remains unchanged but the scenario differs, then the duration and respiratory activity may vary, and consequently so do the distributions representing the breathing rate, the aerosol diameter, and the concentration of respiratory particles in exhaled air. Thirdly, for a scenario in a new space, the volume and occupancy density may change in addition to all other parameters, and consequently so does the *equivalent* ventilation rate (ϕ). Finally, by far the biggest problem that the data analysis shows, is a general paucity of data of sufficient quality to reduce uncertainty in q and $P(I)$. At the start of a pandemic the viral load, L , and hence q , are always unknown. Once a population begins to acquire immunity, the proportion of occupants susceptible to infection reduces. When infections do not confer sterilising immunity, the proportion of susceptible people is then dependent on immunity waning and the ability of a pathogen to mutate to evade immunity. The consequence of the low quality of data is that we do not know the true underlying distributions of either the inputs or the outputs and so we have little confidence in the magnitudes of the tails where there is very little supporting data. Accordingly, there is much uncertainty in the tails, and in the confidence intervals given here. They should, therefore, be considered very approximate. We report both the GM and the GSD because the distributions of the predictions are thought to be log-normal (see Section 2) and indicate where the majority of data lies and where there is more confidence in it. It is important to note that other values and distributions could be used, but these outcomes will still be true. This also applies to distributions for other pathogens, particularly those that are less well studied than SARS-CoV-2.

There are also more general and fundamental issues with inferring quanta empirically. The WR model estimates the infection risk from long range transmission, but it impossible to disaggregate it from other exposure pathways. Furthermore, quanta emission rates are derived from observational studies of high secondary attack rates of transmission resulting in the calculation of high magnitudes, which are then extrapolated to most other cases where its magnitudes are low, which introduces significant bias. Many models of infection risk use specific values of q determined from outbreaks. Figure 1 shows that q is a continuum that spans 8 orders of magnitude and so it needs to be used to estimate $P(I)$, rather than using specific values of q , if the estimate is to have any context and meaning. Even then, a distribution of $P(I)$ should only be used to show where most predictions lie.

Together, these factors make an absolute value of the personal risk of long-range airborne infection probability, $P(I)$, unusable as a metric for SARS-CoV-2 or any other airborne pathogen. It can, however, be used to give an appreciation of the magnitude of absolute risks, which we estimate to be low most of the time. When accounting for the likelihood of the presence of an infected person, the magnitude of absolute risk reduces even further; see Iddon *et al.* (2022).

6 CONCLUSIONS

The quanta emission rate of an infected person is a continuum that varies over time and between people. We find that the uncertainty in the magnitude of quanta emission rate for SARS-CoV-2 for a single infected person varies by over around 8 orders of magnitude. Unfortunately, there is a general paucity of data of sufficient quality to reduce uncertainty in emission rates. This means that there is little confidence in the data located in the tails. The problem with this is demonstrated by applying the emission rate continuum to the WR model to estimate that, for an 8 hour exposure in a 50 person office with an outdoor airflow rate of 10 l s^{-1} per person, the probability of infection of each occupant from long range transmission is $<1\%$ for 95% of events. It is the data in the right-tail of the distribution of the quanta emission rate, where there is little confidence in their magnitudes, which leads to an appreciable probability of infection.

Therefore, it is impossible to say, with any certainty, the fraction of events that will lead to some probability of infection.

These factors make an absolute value of the personal risk of long-range airborne infection probability unusable as a metric for SARS-CoV-2 or any other airborne pathogen. It can be used to give an appreciation of the magnitude of absolute risks, which we estimate to be low most of the time.

7 ACKNOWLEDGEMENTS

The authors acknowledge the Engineering and Physical Sciences Research Council (EP/W002779/1) who financially supported Jones and Iddon.

8 REFERENCES

- W. Adams, Measurement of breathing rate and volume in routinely performed daily activities, Final report, contract no. a033-205., California Air Resources Board, Sacramento (1996).
- G Buonanno, L. Stabile, L. Morawska, Estimation of airborne viral emission: Quanta emission rate of SARS-CoV-2 for infection risk assessment, *Environment International* 141 (May) (2020) 105794.
- M. Cevik, K. Kuppalli, J. Kindrachuk, M. Peiris, Virology, transmission, and pathogenesis of SARS-CoV-2, *The BMJ* 371 (2020) 1–6.
- M. Cevik, M. Tate, O. Lloyd, A. E. Maraolo, J. Schafers, A. Ho, SARS-CoV-2, SARS-CoV, and MERS-CoV viral load dynamics, duration of viral shedding, and infectiousness: a systematic review and metaanalysis, *The Lancet Microbe* 2 (1) (2021)
- P. Z. Chen, N. Bobrovitz, Z. Premji, M. Koopmans, D. N. Fisman, F. X. Gu, SARS-CoV-2 shedding dynamics across the respiratory tract, sex, and disease severity for adult and pediatric covid-19, *eLife* 10 (2021) e70458.
- C. Darquenne, Aerosol deposition in health and disease, *Journal of Aerosol Medicine and Pulmonary Drug Delivery* 25 (3) (2012) 140–147.
- C. Iddon, B. Jones, P. Sharpe, M. Cevik, S. Fitzgerald, A population framework for predicting the proportion of people infected by the far-field airborne transmission of SARS-CoV-2 indoors. *Building and Environment*. 2022;221:109309.
- B. Killingley *et al.* Safety, tolerability and viral kinetics during SARS-CoV-2 human challenge in young adults, *Nature Medicine* 28 (5) (2022) 1031–1041.
- S. L. Miller *et al.*, Transmission of SARS-CoV-2 by inhalation of respiratory aerosol in the Skaagit Valley Chorale superspreading event, *Indoor Air* 31 (2021) 314–323.
- L. Morawska, *et al.*, Size distribution and sites of origin of droplets expelled from the human respiratory tract during expiratory activities, *Journal of Aerosol Science* 40 (3) (2009) 256–269.
- M. Nicas, W. W. Nazaroff, A. Hubbard, Toward understanding the risk of secondary airborne infection: Emission of respirable pathogens, *Journal of Occupational and Environmental Hygiene* 2 (3) (2005) 143–154.
- E. C. Riley, G. Murphy, R. L. Riley, Airborne spread of measles in a suburban elementary school, *American Journal of Epidemiology* 107 (1978) 421–432.
- T. L. Thatcher, A. C. Lai, R. Moreno-Jackson, R. G. Sextro, W. W. Nazaroff, Effects of room furnishings and air speed on particle deposition rates indoors, *Atmospheric Environment* 36 (11) (2002) 1811–1819.

- N. Van Doremalen *et al.*, Aerosol and surface stability of SARS-CoV-2 as compared with SARS-CoV-1, *New England Journal of Medicine* 382 (16) (2020) 1564–1567.
- D. Vernez, S. Schwarz, J. J. Sauvain, C. Petignat, G. Suarez, Probable aerosol transmission of SARS-CoV-2 in a poorly ventilated courtroom, *Indoor Air* 31 (6) (2021) 1776–1785.
- J. Zhou *et al.*, Viral emissions into the air and environment after sars-cov-2 human challenge: a phase 1, open label, first-in-human study., *The Lancet. Microbe* 6 (2023).

Flow dynamic of human cough and measuring techniques: A review

Chen Zhang*¹, Peter V. Nielsen¹, Simon Madsen¹, Li Liu², Chunwen Xu³,
Zhengtao Ai⁴

*1 Department of the Built Environment
Aalborg University
Denmark*

*2 Department of Building Science
Tsinghua University
China*

**Corresponding author: cz@build.aau.dk*

*3 College of Pipeline and Civil Engineering
China University of Petroleum (East China)
China*

*4 Department of Building Environment and Energy
Hunan University
China*

ABSTRACT

Coughing is one of the most important respiratory activities for air transmitted pathogens. It is essential to understand the dispersion of exhaled particles when coughing to improve the prevention measure and reduce the cross-infection risk. However, cough flow structure is complex and influenced by many parameters. Simplifications are often made to the initial flow condition when simulating the transport of particles expelled during coughing in laboratory or numerical studies. This study conducts a systematic literature review on human cough, especially focusing on flow dynamic characterization. First, the measuring techniques for identifying the airflow characteristic are summarized. The boundary conditions for cough, such as flow profile, flow direction, cough duration and are compared between different studies. Finally, the vortex structure of cough and its impact on cough particle dispersion is discussed.

KEYWORDS

COVID-19, cough, respiratory infectious disease, flow dynamic, particle deposition, flow profile

1 INTRODUCTION

The COVID-19 pandemic is a respiratory infectious disease, and it has caused global health concerns. WHO has reported that the virus can spread from an infected person's mouth or nose in small particles when they cough, sneeze, speak, sing or breathe (WHO 2021). Compared with other respiratory activities like breath or speak, cough generates a higher expiratory velocity and contains a higher aerosol concentration, which leads to a potentially higher risk of cross-infection. Centers for Disease Control and Prevention (CDC 2021) has pointed out that the '2 meters (6-feet) rule' might not apply to situations involving increased exhalation, e.g. coughing. It is essential to understand the dispersion of exhaled particles when coughing to improve the prevention measure and reduce the cross-infection risk. A cough is a reflex action to clear the airways of mucus and irritants such as dust or smoke. It normally includes three phases: inspiratory, compressive, and expiratory phases. The inspiratory phase is associated with glottic opening and the inhalation of variable amounts of air. The compressive phase consists of closure of the glottis and contraction of the expiratory muscles resulting in raised intra- thoracic pressure. In the expiratory phase the glottis opens suddenly, causing an explosive release of the trapped intrathoracic air (Mahajan et al. 1994).

Cough flow structure is complex, and is influenced by many parameters such as the cougher's age, gender, and posture, which consequently affect particle dispersion indoors (Muthusamy et al. 2021). However, simplifications are often made to the initial flow condition in laboratory or numerical studies when simulating the transport of droplets expelled during coughing (Gupta, Lin, and Chen 2009a).

This study aims to conduct a systematic literature review on human cough, especially focusing on flow dynamic characterization. First, the measuring techniques for identifying the airflow characteristic of cough are summarized. The boundary conditions for cough, such as flow profile, flow direction, cough duration and are compared between different studies. Finally, the vortex structure of cough and its impact on cough particle dispersion is discussed.

2 FLOW DYNAMIC CHARACTERISTICS OF COUGH

2.1 Cough flow profile

Based on the literature (Mahajan et al. 1994)(Khan et al. 2004)(Gupta et al. 2009a)(Oh et al. 2022), the time-series cough profile can be illustrated in Figure 1. The profile indicates that the cough starts with a short inhalation, follows by a dramatic acceleration in exhalation and finally a slow decay. The inhalation volume is very small and can be neglected. The characteristic of the cough profile can be defined by the following parameters: peak flow rate (PFR) or peak velocity (PV); peak velocity time (PVT), and cough duration time (CDT) and cough expired volume (CEV) is the area under the curve. Besides the parameters mentioned above, flow direction and mouth opening are important to describe the flow characteristic of cough. Table 1 summarizes the measuring techniques and flows dynamic characteristics of cough from literature studies.

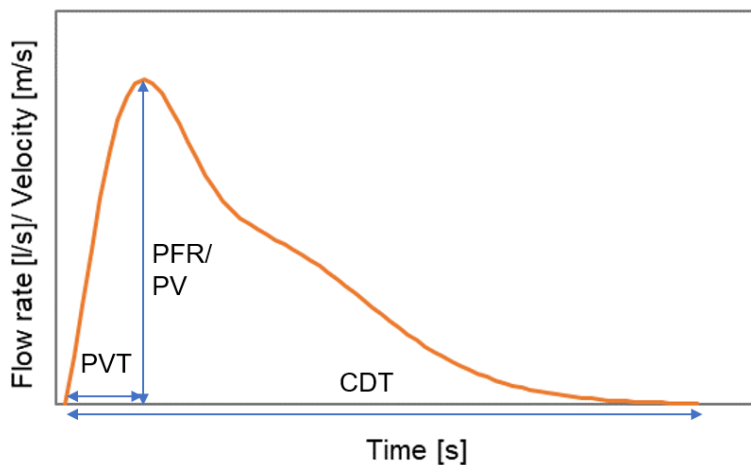


Figure 1. Cough profile as a function of time. Peak flow rate (PFR) or peak velocity (PV); peak velocity time (PVT), and cough duration time (CDT) and cough expired volume (CEV) is the area under the curve.

Depending on the measurement techniques, cough peak flow rate PFR was measured in the studies using spirometer (Lindsley et al. 2010)(Gupta, Lin, and Chen 2009b)(Mahajan et al. 1994), and peak velocity PV was measured using Schlieren imaging (Tang et al. 2012) or PIV (Han et al. 2021)(Khan et al. 2004)(Zhu, Kato, and Yang 2006)(Chao et al. 2009)(Vansciver, Miller, and Hertzberg 2011)(Kwon et al. 2012)(Wang et al. 2020). Some studies (Oh et al. 2022) attempt to convert these two parameters by considering the mouth opening area, however, assumptions have to be made by using the average mouth opening area without considering the individual difference and the mouth opening area keeps constant during the whole cough process.

Gupta et al. (2009b) measured cough flow rates from 25 subjects, and a large variation existed among the subjects, especially between males and females. For males, the PFR ranged from 3 to 8.5 l/s, while the value for females was 1.6 – 6 l/s. Lindsley et al. (2010) investigated the

influenza virus produced by coughing. The influenza-negative subjects produced slightly higher PFR than influenza-positive subjects, where the average values are 7.6 l/s and 7.1 l/s, respectively.

Table 1. Measurement techniques and flow dynamic characteristics of cough

Reference	Technique	Subjects	Cough Duration [s]	Cough peak velocity [m/s] or flow rate [l/s]	Peak velocity time [ms]	Cough Volume [l]	Flow direction	Mouth geometry
(Mahajan et al. 1994)	spirometer	10		2.8-15.8 l/s	10-50	0.5-5		
(Khan et al. 2004)	PIV	5 (4 M and 1 F)	0.9	8.1 m/s				
(Zhu 2006)	PIV	3 (3 M)	0.5	6-22 m/s Average: 11.2 m/s		0.8-2.2 Average 1.4		
(Gupta et al. 2009b)	Spirometer	25 (13 M and 12 F)	0.35-0.75	M:3-8.5 L/s F:1.6-6 L/s	M: 57-96 F: 57-110	M:0.4-1.6 F:0.25-1.25	$\theta_1=15\pm 5^\circ$; $\theta_2=40\pm 4^\circ$ (vertical spread angle 25°)	Mouth opening area: M:400 \pm 95 mm ² F:337 \pm 140 mm ²
(Chao et al. 2009)	PIV	11 (3 M and 8 F)		M:13.2 m/s F: 10.2 m/s Average 11.7 m/s				
(Lindsley et al. 2010)	Spirometer	58 (47 influenza-positive and 11 influenza-negative)	0.9	Influenza-positive 7.1 l/s Influenza-negative 7.6 l/s		Influenza-positive 2.7 Influenza-negative 3.1		
(Vansciver et al. 2011)	PIV	29 (10 M and 19 F)	0.55	1.15-28.8 m/s Average 10.2m/s				706 (D=30 mm)
(Tang et al. 2012)	schlieren imaging technique	20 (10 M and 10 F)	0.2-0.35	M:3.2–14 m/s F: 2.2–5.0 m/s;				
Kwon S. et al. (Kwon et al. 2012)	PIV	26 (17 M and 9 F)		M: 15.3 m/s F 10.6 m/s			Vertical spread angle M: 38 ° F: 32 °	
(Wang et al. 2020)	PIV	4		15 m/s				

(Han et al. 2021)	PIV	10 (5 M and 5 F)	0.52-0.56	M:6.4-18.6 m/s F: 5.0-15.7 m/s	M: 8-35 F: 8-39	Vertical spread angle M: 15.3 ° F: 15.6 ° Horizontal spread angle M: 13.3 ° F: 14.2 °	Mouth width M: 47 mm F: 39.4 mm
-------------------	-----	------------------	-----------	-----------------------------------	--------------------	--	---------------------------------------

Note: M represents male, and F represents female.

A large variation also exists in the peak velocity PV. The largest variation was observed by Vansciver et al. (2011), where the PV ranged from 1.15 m/s to 28.8 m/s from the measurement of 29 healthy subjects. The gender difference on PV was pointed out by several studies (Chao et al. 2009)(Tang et al. 2012)(Kwon et al. 2012)(Han et al. 2021). In general, PV for females was weaker than that for males. Bianchi and Baiardi (2008) further correlated PV with the subjects' gender, height, age and body mass surface through regression analysis. The differences on cough PV also exist between different measuring techniques. The PV measured by the schlieren imaging technique (3.2-14 m/s for males and 2.2-5 m/s for females) (Tang et al. 2012) was much smaller than those measured by PIV (Han et al. 2021)(Khan et al. 2004)(Zhu et al. 2006)(Chao et al. 2009)(Vansciver et al. 2011)(Kwon et al. 2012)(Wang et al. 2020). The authors claimed that subjects coughing in PIV measurement were somehow constrained and unnatural due to the measurement setup, while the cough flow was obtained more naturally in Schlieren imaging study. However, the relative temperature difference between the exhaled cough air and surrounding ambient air might influence the visualization of the cough flow, and consequently, influence the accuracy of peak velocity measurement by the Schlieren imaging technique. Therefore, the uncertainties of measuring techniques require further investigation.

The flow rate or velocity rapidly reaches a peak value early in the cough, therefore, the peak velocity time PVT is very small compared with the total cough duration time CDT. The PVT was reported by Mahajan et al. (1994), Gupta et al. (2009b) and Han et al. (2021). Large deviation exists between different studies. Gupta reported a larger PVT (57-110 ms), which is more than double the values of the other two studies. Similar to PVT, CDT also presents a large variation among different studies. The CDT value ranged from 200 ms to 900 ms, where the average value was around 500-550 m. The lowest CDT was measured by Tang et al. (2012) with the schlieren imaging technique. The authors pointed out that the limitation of such a technique is that the visibility of shadowgraphs disappeared when the exhaled and surrounding air temperatures equalized. Therefore, it is difficult to capture the entire cough process by Schlieren imaging. On the other hand, even though the peak cough flow for females was weaker than that for males, PVT or CDT didn't present clear gender difference, indicating that their cough duration times were almost the same.

2.2 Cough flow direction

Gupta et al. (2009b) measured the cough flow direction by smoke visualization. The cough flow presented as a downward jet and was defined by the angles between upper and lower boundaries to the horizontal lines, as shown in Figure 2 (a). The values of θ_1 and θ_2 were around 15 ° and 40 °, respectively. (The vertical cough spread angle θ_v was around 25 °). Different from cough flow rate, little variation in the cough spread angles were observed in this study. The jet had negligible spread in the width, where the horizontal cough spread angle was around 0 ° ($\theta=90$ °).

Velocity vectors measured by PIV was used to analyze the flow direction. Kwon et al. (2012) described the cough flow by the angles of upward vector and downward vector, as shown in Figure 2 (b). The cough flow presented as a jet almost symmetrical in the y-direction, where

the vertical cough spread angle was around 38° for males and 32° for the females. Han et al. (2021) introduced a more quantitative method to determine the cough boundaries, where the flow boundary was defined as the position where the velocity decayed to 1 % of the maximum value at the flow centerline, as shown in Figure 2 (c). The influence of the head position variations was eliminated by utilizing the fitting line method. The cough flow direction was described by vertical cough spread angles θ_V and horizontal cough spread angles θ_H . Different from Gupta's results, individual differences were significant in this study. The average vertical/horizontal cough spread angle was $15.3^\circ/13.3^\circ$ for males and $15.6^\circ/14.2^\circ$ for females. The angles were smaller than the ones measured in the other two studies.

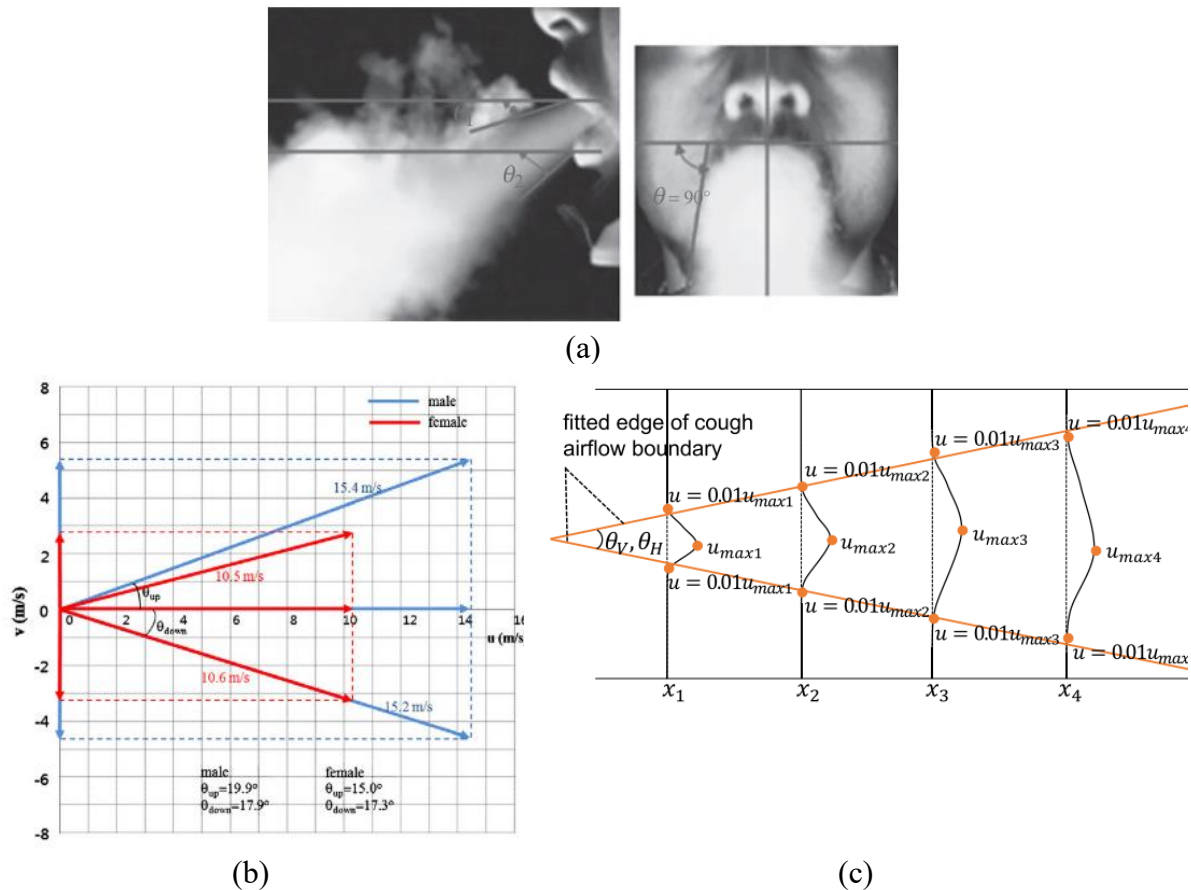


Figure 2. Schematic of determination of cough flow direction in the literature (a) Gupta et al. (2009b) (b) Kwon et al. (2012) (c) Han et al. (2021)

2.3 Mouth opening

Mouth geometry affects the cough flow dynamic, such as cross-sectional profile, hydraulic diameter, direction, and turbulence levels. Consequently, it affects aerosol distribution and penetration.

The mouth opening area during a cough is shown in Gupta et al. (2009a), as shown in

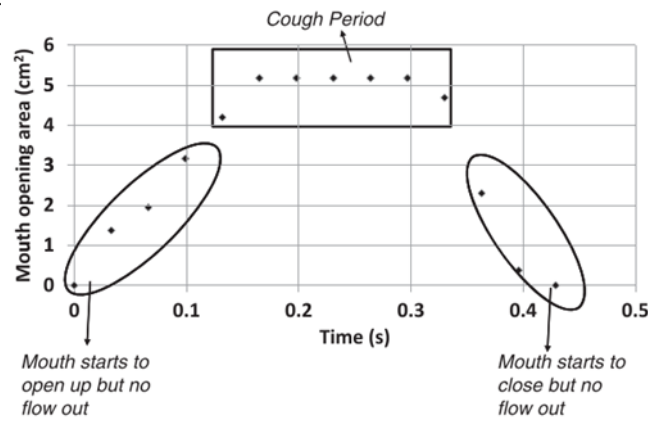


Figure 3. Even mouth opening changed during a cough, the opening area was almost constant when there was flow from the mouth. There is a variation in mouth opening area during a cough with the gender. The mean opening area for female subjects was smaller than that of male subjects, which was 3.37 cm² for females and 4 cm² for male.

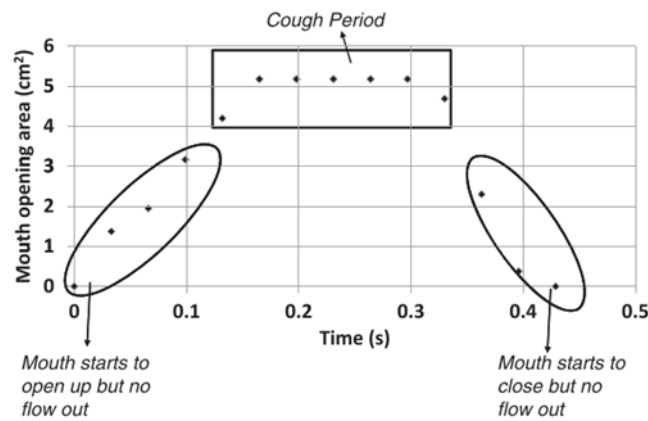


Figure 3. Month opening area during a cough (Gupta et al. 2009a)

Instead of the opening area, the mouth width was measured in Han's study (2021) and used as the boundary condition in CFD simulation. However, the measurement was done without coughing, but just as the characteristics of human subjects. In addition, the mouth width could not provide sufficient information on mouth geometry during a cough since the distance between lips also matters significantly.

It is clear to see that there are large deviations on mouth geometry between subjects and no agreement on how to report the mouth geometry during a cough. On the other hand, most studies only focus on the geometry created by lips, since it is the boundary of the mouth outlet. However, the flow travels through the trachea and oral cavity (including teeth, tongue, and lips), and the flow structure and dynamic are certainly influenced by them. Wei and Li (2017) pointed out that the difference in the spread angle of the model and human subject may be due to the missing complex oral cavity, including the effect of teeth.

2.4 Vortex structure

Several studies (Prasanna Simha and Mohan Rao 2020)(Khan et al. 2004)(Thacher and Mäkiharju 2022)(Tan et al. 2021) mentioned that the circulating motion of vortex rings produced by coughs can enhance the transport of cough droplets. Vortex rings are typically produced by injecting fluid into a quiescent medium for a short duration. The vortex rings generated by cough is due to the vibrations in the airway passage leading to periodic constrictions and relaxations, which create flow variations.

In Padmanabha's study (2020), a periodic vortex ring ejection phenomenon was observed by the schlieren imaging technique that appears as a pulsation of the cough airflow. These pulsations start several milli-seconds after the initiation of the cough. The periodic ejection and motion of vortex rings can be seen in Figure 4. The velocity of propagation of viscous vortex rings can be expressed by an analytical approach, which a function of time (t), initial radius (R), vortex ring circulation (γ), and kinematic viscosity (ν).

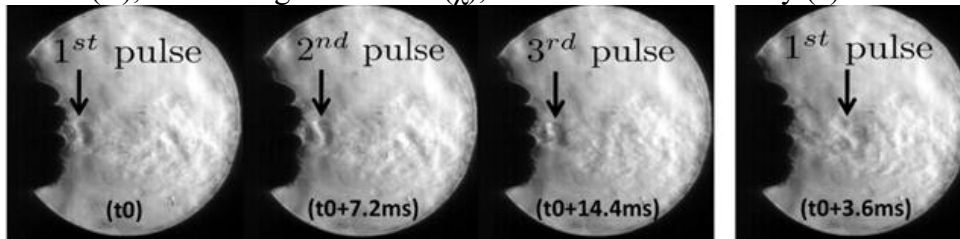


Figure 4. Periodic ejection and motion of vortex rings in coughs by Schlieren image video (Prasanna Simha and Mohan Rao 2020)

An important parameter in the dynamics of vortices is vorticity, a vector that describes the local rotary motion at a point in the fluid. The instantaneous vorticity was plotted in Figure 5 by Khan et al. (2004). It can be seen that maximum vorticity corresponds to the peak flow rate/velocity and occurs in the region of the shear layer, and the center region of cough flow is nearly void of vorticity.

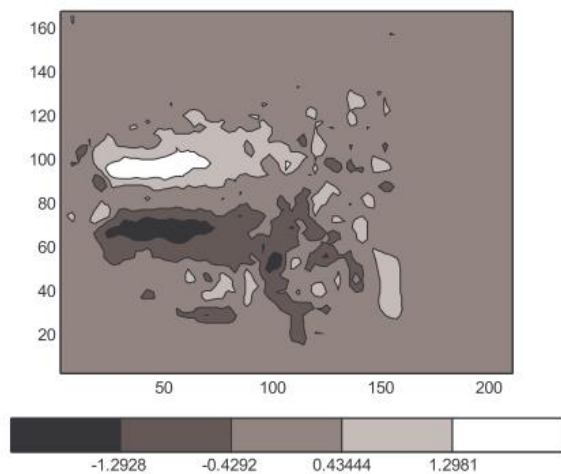


Figure 5. Vorticity contour plot displaying initial vortices (unit 1/s) (Khan et al. 2004)

Cough is often described as impulsively started jets. Tan et al. (2021) compared dispersion of aerosol particles from a loud cough with classical vortex ring formation on starting jet, as shown in Figure 6. The black particles represent virtual aerosol droplets, while the background scalar shows the out-of-plane vorticity field. From the classical vortex ring formation from impulsively started jet (Figure 6 lower), it could be seen that the flow structure depends on the stroke ratio L/D where L is the length of ejected fluid and D is the ejection diameter. When L/D is less than 4, the jet presents as a short puff and all momentum is absorbed into the vortex ring. When L/D is approximately equal to 4, the maximum amount of momentum has been absorbed and the vortex ring begins to trail a thin tail. When L/D is larger than 4, the vortex ring is unstable and sheds off smaller vortices. The L/D for a loud cough is estimated with a magnitude of 160, therefore, a loud cough contains much higher momentum than a single vortex ring could entrain.

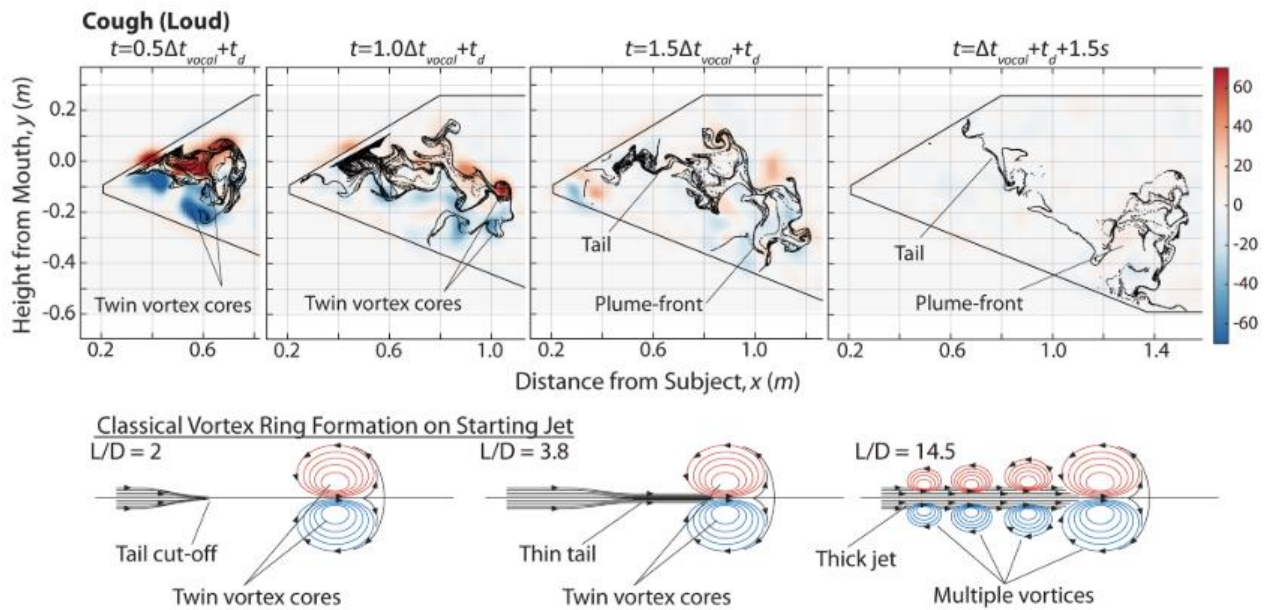


Figure 6. Dispersion dynamics of aerosol particles for a loud cough compared with classical vortex ring formation on starting jet (Δt_{vocal} is the total duration of the subject's cough, t_d is the instance that the plume enters the measurement domain, stroke ratio L/D where L is the length of ejected fluid and D is ejection diameter) (Tan et al. 2021)

Figure 6 shows, when $t=+0.5\Delta t_{\text{vocal}}$, the cough flow first presents a dominant vortex ring similar in structure to the classical impulsively start jet. The vortex ring quickly disintegrated into multiple smaller vortex cores starting at $+1.0 \Delta t_{\text{vocal}}$. At $+1.5 \Delta t_{\text{vocal}}$, the original vortex ring structure has become indistinguishable. However, the aerosol particles continued to move forward even at $+1.5s$ after cough, and the presence of a trail is an indication of high L/D impulsively started jets. Their results indicate that virus-laden aerosol ejected during coughs remain concentrated within the moving plume-front. A high exposure risk is expected with direct collision in the moving plume-front.

3 CONCLUSIONS

The literature review leads to the following conclusions:

- The airflow characteristic of human cough is normally measured by three techniques, including the Schlieren imaging technique, spirometer and PIV. Each technique has its advantages and disadvantages, and the uncertainties of measuring techniques require further investigation. On the other hand, PVT and CDT are in the order of milliseconds. In order to capture the cough characteristic, it is essential to have high-frequency measurements.
- The cough profile can be described by a gamma-probability distribution function. The characteristic of the profile can be defined by the following parameters: peak flow rate (PFR) or peak velocity (PV); peak velocity time (PVT), and cough duration time (CDT) and cough expired volume (CEV). Large deviations have been shown on PFR, PV, CEV due to subjects' gender, height, age and body mass surface, however, some deviations are due to different measuring techniques.
- Large deviations on flow direction and mouth geometry between different studies and no agreement on how to report these parameters during a cough.

- Cough creates vortex rings due to the vibrations in the airway passage leading to periodic constrictions and relaxations. The circulating motion of vortex rings can enhance the transport of cough particles in the indoor environment.

4 ACKNOWLEDGEMENTS

This research was supported by The Danish Agency for Higher Education and Science International Network Programme (Case no. 0192-00036B). It was co-supported by Martha og Paul Kernn-Jespersens Fond.

5 REFERENCES

- Bianchi, Carlo, and Paola Baiardi. 2008. "Cough Peak Flows: Standard Values for Children and Adolescents." *American Journal of Physical Medicine and Rehabilitation* 87(6):461–67. doi: 10.1097/PHM.0b013e318174e4c7.
- Centers for Disease Control and Prevention (CDC). 2021. "Scientific Brief: SARS-CoV-2 Transmission." Retrieved (https://www.cdc.gov/coronavirus/2019-ncov/science/science-briefs/sars-cov-2-transmission.html#anchor_1619805200745).
- Chao, C. Y. H., M. P. Wan, L. Morawska, G. R. Johnson, Z. D. Ristovski, M. Hargreaves, K. Mengersen, S. Corbett, Y. Li, X. Xie, and D. Katoshevski. 2009. "Characterization of Expiration Air Jets and Droplet Size Distributions Immediately at the Mouth Opening." *Journal of Aerosol Science* 40(2):122–33. doi: 10.1016/j.jaerosci.2008.10.003.
- Gupta, J. K., C. H. Lin, and Q. Chen. 2009a. "Flow Dynamics and Characterization of a Cough." *Indoor Air* 19(6):517–25. doi: 10.1111/j.1600-0668.2009.00619.x.
- Gupta, J. K., C. H. Lin, and Q. Chen. 2009b. "Flow Dynamics and Characterization of a Cough." *Indoor Air* 19(6):517–25. doi: 10.1111/j.1600-0668.2009.00619.x.
- Han, Mengtao, Ryoza Ooka, Hideki Kikumoto, Wonseok Oh, Yunchen Bu, and Shuyuan Hu. 2021. "Measurements of Exhaled Airflow Velocity through Human Coughs Using Particle Image Velocimetry." *Building and Environment* 202(May):108020. doi: 10.1016/j.buildenv.2021.108020.
- Khan, T. A., H. Higuchi, D. R. Marr, and M.N.Glauser. 2004. "Unsteady Flow Measurement of Human Micro Environment Using Time Resolved Particle Image Velocimetry." Pp. 88–100 in *Roomvent 2004*. Vol. 4.
- Kwon, Soon Bark, Jaehyung Park, Jaeyoun Jang, Youngmin Cho, Duck Shin Park, Changsoo Kim, Gwi Nam Bae, and Am Jang. 2012. "Study on the Initial Velocity Distribution of Exhaled Air from Coughing and Speaking." *Chemosphere* 87(11):1260–64. doi: 10.1016/j.chemosphere.2012.01.032.
- Lindsley, William G., Françoise M. Blachere, Robert E. Thewlis, Abhishek Vishnu, Kristina A. Davis, Gang Cao, Jan E. Palmer, Karen E. Clark, Melanie A. Fisher, Rashida Khakoo, and Donald H. Beezhold. 2010. "Measurements of Airborne Influenza Virus in Aerosol Particles from Human Coughs." *PLoS ONE* 5(11). doi: 10.1371/journal.pone.0015100.
- Mahajan, R. P., P. Singh, G. E. Murty, and A. R. Aitkenhead. 1994. "Relationship between Expired Lung Volume, Peak Flow Rate and Peak Velocity Time during a Voluntary Cough Manoeuvre." *British Journal of Anaesthesia* 72(3):298–301. doi: 10.1093/bja/72.3.298.
- Muthusamy, Jayaveera, Syed Haq, Saad Akhtar, Mahmoud A. Alzoubi, Tariq Shamim, and Jorge Alvarado. 2021. "Implication of Coughing Dynamics on Safe Social Distancing in an Indoor Environment—A Numerical Perspective." *Building and Environment* 206(April):108280. doi: 10.1016/j.buildenv.2021.108280.
- Oh, Wonseok, Ryoza Ooka, Hideki Kikumoto, and Mengtao Han. 2022. "Numerical

- Modeling of Cough Airflow: Establishment of Spatial–Temporal Experimental Dataset and CFD Simulation Method.” *Building and Environment* 207(PB):108531. doi: 10.1016/j.buildenv.2021.108531.
- Prasanna Simha, Padmanabha, and Prasanna Simha Mohan Rao. 2020. “Universal Trends in Human Cough Airflows at Large Distances.” *Physics of Fluids* 32(8). doi: 10.1063/5.0021666.
- Tan, Zu Puayen, Lokesh Silwal, Surya P. Bhatt, and Vrishank Raghav. 2021. “Experimental Characterization of Speech Aerosol Dispersion Dynamics.” *Scientific Reports* 11(1):1–12. doi: 10.1038/s41598-021-83298-7.
- Tang, Julian W., Andre Nicolle, Jovan Pantelic, Gerald C. Koh, Liang de Wang, Muhammad Amin, Christian A. Klettner, David K. W. Cheong, Chandra Sekhar, and Kwok Wai Tham. 2012. “Airflow Dynamics of Coughing in Healthy Human Volunteers by Shadowgraph Imaging: An Aid to Aerosol Infection Control.” *PLoS ONE* 7(4). doi: 10.1371/journal.pone.0034818.
- Thacher, Eric, and Simo A. Mäkiharju. 2022. “Effect of Coherent Structures on Particle Transport and Deposition from a Cough.” *Aerosol Science and Technology* 56(5):425–33. doi: 10.1080/02786826.2022.2044449.
- Vansciver, Meg, Shelly Miller, and Jean Hertzberg. 2011. “Particle Image Velocimetry of Human Cough.” *Aerosol Science and Technology* 45(3):415–22. doi: 10.1080/02786826.2010.542785.
- Wang, Hongping, Zhaobin Li, Xinlei Zhang, Lixing Zhu, Yi Liu, and Shizhao Wang. 2020. “The Motion of Respiratory Droplets Produced by Coughing.” *Physics of Fluids* 32(12). doi: 10.1063/5.0033849.
- Wei, Jianjian, and Yuguo Li. 2017. “Human Cough as a Two-Stage Jet and Its Role in Particle Transport.” *PLoS ONE* 12(1). doi: 10.1371/journal.pone.0169235.
- WHO. 2021. “Coronavirus Disease (COVID-19): How Is It Transmitted?” Retrieved November 2, 2022 (<https://www.who.int/emergencies/diseases/novel-coronavirus-2019/question-and-answers-hub/q-a-detail/coronavirus-disease-covid-19-how-is-it-transmitted>).
- Zhu, Shengwei. 2006. “Investigation into Airborne Transport Characteristics of Airflow Due to Coughing in A.” *Measurement* 112.
- Zhu, Shengwei, Shinsuke Kato, and Jeong-Hoon Yang. 2006. “Investigation into Airborne Transport Characteristics of Airflow Due to Coughing in a Stagnant Indoor Environment.” 112.

Evaluating the Impact of Air Cleaning and Ventilation of Airborne Pathogens and Human Bio-effluents at Two Primary Schools in Belgium

Klaas De Jonge¹, Marianne Stranger², Sarah L. Paralovo², Maarten Spruyt², Borislav Lazarov², Tom Geens³, Reinoud Cartuyvels⁴, Koen Van den Driessche⁵, Jelle Laverge¹ and Arnold Janssens^{1, *}

*1 Ghent University
Sint-Pietersnieuwstraat 41
Ghent, Belgium*

*2 VITO
Boeretang 200
Mol, Belgium*

**Corresponding author: Arnold.Janssens@UGent.be*

*3 Liantis
Dirk Martensstraat 26
Bruges, Belgium*

*4 Jessa Hospital Clinical Lab
Stadsomvaart 11
Hasselt, Belgium*

*5 Antwerp University Hospital
Drie Eikenstraat 655
Antwerp, Belgium*

ABSTRACT

The COVID-19 pandemic increased the awareness and importance of infectious pathogens as contaminant in the indoor air, especially for non-residential buildings with a high occupational density like schools. During the COVID-19 pandemic air cleaning is often proposed as mitigation strategy for infectious risk in these types of buildings. However, indoor air quality (IAQ) in general comprises of a large range of possible contaminants and factors that can equally impact the health, comfort and well-being of occupants. In this context, a study was conducted in Flanders (Belgium) with the aim of investigating the potential impact of ventilation and air cleaning on the IAQ and infection risk control in Flemish public spaces. This paper describes part of this larger study, focusing on the assessments carried out in two primary schools.

In the first school, which did not have a mechanical ventilation system, 4 classrooms were assessed for three weeks. In the second school, 4 classrooms connected to a centralized mechanical ventilation system were assessed in two separate measurement campaigns of 3 weeks. Between the two measurement campaigns in school 2, the defects in the mechanical ventilation system which were observed during the first campaign were corrected.

In each school, in three of the four classrooms, specific interventions were done after the first week of monitoring, among which the introduction of air cleaners. The fourth class was monitored without intervention. In each classroom, CO₂ concentrations and biological air samples were collected 2 days per week for in-lab qPCR analysis of over 20 genetic markers of respiratory pathogens. The results for SARS-CoV-2 are presented.

Unfortunately, in both schools, the effectiveness of the interventions on airborne pathogens (incl. SARS-CoV-2) could not be quantified due to the lack of infected schoolchildren and other measures like the wearing of face masks at that time resulting in mostly negative or borderline

results. In general, the results indicate the importance of proper commissioning and maintenance to mechanical ventilation systems and show an overall better expected perceived indoor air quality when the ventilation system works properly. In the school without mechanical ventilation system, manual airing through the opening of windows can achieve the same level of expected perceived indoor air quality if operated correctly.

KEYWORDS

Primary school, Indoor Air Quality, Ventilation, Airing, CO₂, COVID-19

1 INTRODUCTION

The COVID-19 pandemic increased the awareness and importance of infectious pathogens as contaminants in the indoor air in the general public and governmental agencies. In this context, the Flemish department of care (“*Departement Zorg*”) has ordered a pilot study to investigate the effectiveness of two possible IAQ management strategies namely, ventilation/airing and stand-alone air cleaning devices based on filtration. Although the main goal is to better understand the effectiveness of the two IAQ management strategies to decrease the spread of airborne pathogens, the study allowed a wider range of investigation to investigate the overall feasibility of the IAQ management strategies. A multidisciplinary consortium was assigned to investigate the IAQ (human bio-effluents(~CO₂), airborne pathogens, PM_x, RH), other parameters related to indoor health and sensation of comfort (e.g., temperature, acoustics) and record building related parameters (e.g., air change rates – ACH for different airing scenario’s)(Stranger et al. 2022).

The multidisciplinary nature of the consortium made it possible to measure and record a wide range of parameters related to the indoor air, the building and the building ventilation. The study focused on public buildings with a high occupational density and/or buildings primarily occupied by the most sensitive parts of the population (elderly and infants).

Three types of public spaces were selected: Elderly care homes, Daycares for infants and schools. This paper in particular focusses on the measurement of CO₂ and airborne pathogens carried out in two Flemish schools and their relation to the two tested IAQ management strategies. The measurements in the first school were done in February 2022, during this time the Belgian COVID-19 incidence showed a downward trend. In the second school, two measurement campaigns were done, the first one in March 2022, the second in May-June 2022. The Belgian COVID-19 incidence had an upward trend in March 2022 while it was much lower during the second round of measurements in May-June 2022 (Sciensano 2023).

The assessments carried out in the other types of buildings and other data are to be reported elsewhere (Lima Paralovo et al. 2023).

2 MATERIALS AND METHODS

2.1 Experiment design

The study was conducted in 2 primary schools, with parallel measurements in 4 classrooms of similar building typology (elementary schools, 2nd or 3rd grade):

- control class
- ventilation intervention class
- air purification intervention class

- combination ventilation and air purification intervention class.

Each measurement campaign went on for 3 weeks. On Tuesday and Thursday of each week, virus samples were taken using the Coriolis μ device (Bertin Technologies 2012). In the morning a sample was taken in each class with the intervention on. In the afternoon, in two of the classes, a second sample was taken with the intervention off. CO₂ measurements were performed with HUMLOG20-M12 devices (E+E Elektronik n.d.)

2.2 School 1

The first school is situated in a suburban, residential neighborhood close to the city of Antwerp. The 4 measured classrooms are part of the same building which was constructed around the year 2000 and is not equipped with a mechanical ventilation system. The classrooms are accessed through the gymnasium of the school and (acoustically) separated from the gymnasium by means of an intermediate space. Figure 1 shows a schematic plan of the building and the position of the different classrooms.

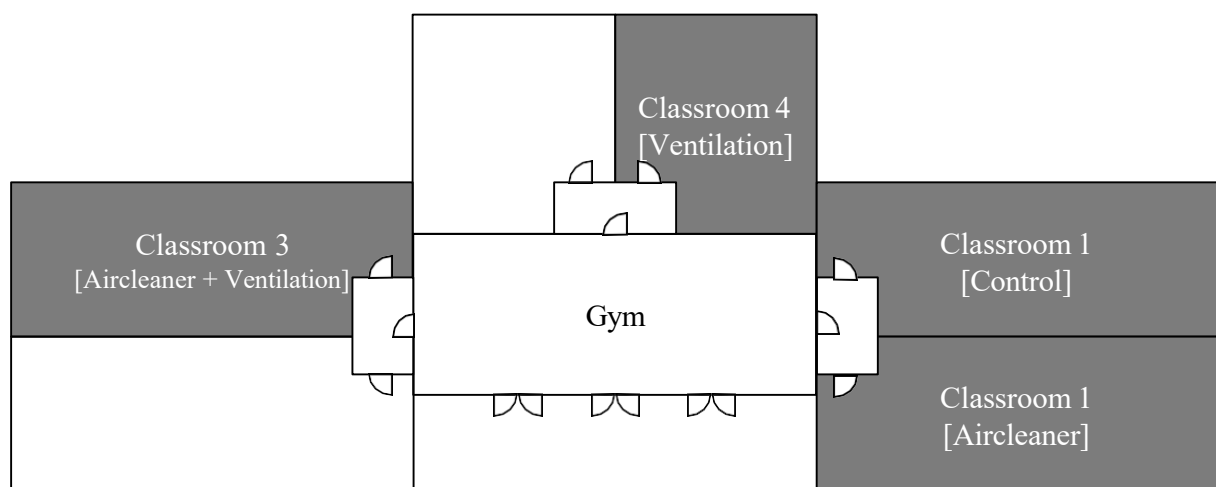


Figure 1 Plan of school 1

The 4 different classrooms are very similar in terms of occupancy density [0.31-0.41 children/m²].

The following steps were followed:

Week 0 - preparation: determination of ventilation characteristics of each classroom (ACH measured on 26/01/2022), determination of (required and effective) airflows following the guidelines published by the Belgian government (<900ppm or 40 m³/h/person) (FOD Economie 2022), selection of the desired the air cleaning systems, determination of a plausible ventilation optimization strategy to be used as 'ventilation intervention'.

Weeks 1-3: Continuous monitoring of CO₂. Collection of air samples for virus detection during 2 school days per week (to allow for (1) comparison of 4 classes within the same time span during the day and (2) evaluation of the impact of air purification intervention, ventilation intervention, and combined air purification and ventilation within the same population on the same day).

Classroom 1 served as control class and the teachers were asked to not change the window/door opening behavior during the measurements. We did not ask to ventilate less as it would be unethical to increase the risk on COVID-19 transmission intentionally.

Classroom 4, served as “ventilation-intervention” class. Because the building is not equipped with a mechanical ventilation system the intervention actually classifies better as “increased airing”. In this classroom, the windows that could not be opened anymore were fixed so the teacher had more opportunity for airing and was instructed to make use of this opportunity as much as (comfortably) possible. In this room, an additional CO₂ sensor was installed that could inform the teacher about the CO₂ levels in the room.

Classroom 2, served as “Air Cleaner intervention” class. In this classroom, a stand-alone air cleaner device with a maximum airflow rate of 800m³/h was installed. However, due to noise complaints, the air cleaner was never operated at this maximum setting.

Classroom 3 served as the room with both increased outdoor air airflow rates and air cleaning. In this room, two air cleaners with each 400m³/h maximum airflow rate were installed.

2.3 School 2

The second school is situated in a suburban, residential neighborhood close to the city of Ghent. On the campus of this school, with buildings dating mainly from the 1960-1970, one newly constructed (2018) can be found. This newer building is equipped with a balanced mechanical supply and extraction ventilation system.

Three of the measured classrooms are situated on the first level in this newer building while the control class was situated on the first level of one of the older buildings to make sure that no mechanical airflow rates were affecting the measurements in the control class. It should be noted here that the older building was less airtight than the classes in the newer building so a higher infiltration airflow rate can be expected. Figure 2 shows schematic plans of the buildings and the position of the different classrooms.

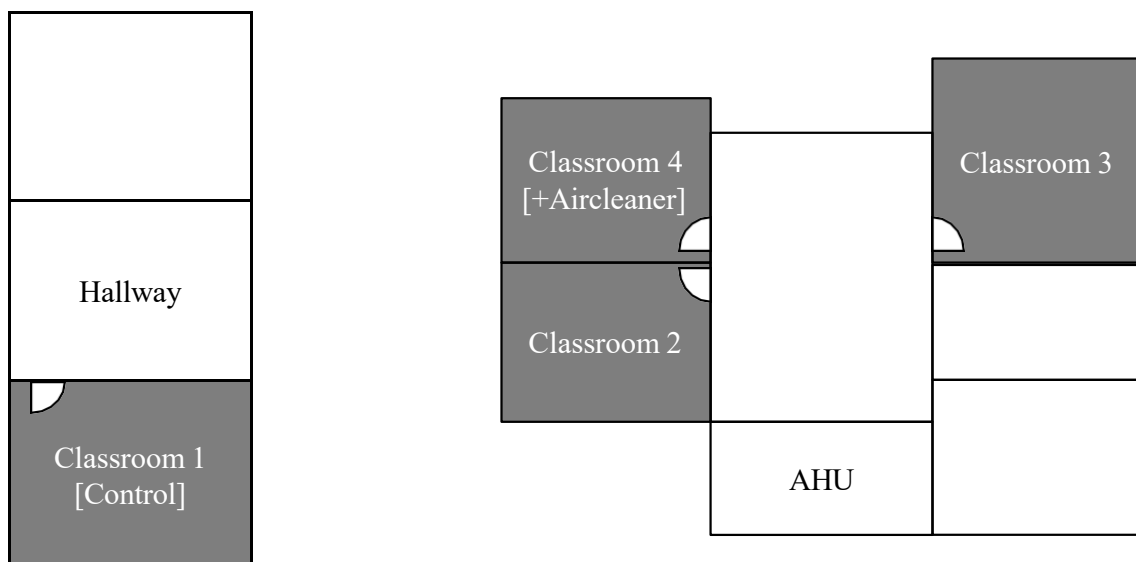


Figure 2 Plan of school 2

The 4 different classrooms are very similar in terms of occupancy density [0.33-0.36 children/m²].

In this school, 1 week of preparation (ACH measured on 1/04/2022 and 23/05/2022) was followed by 2 times, 3 weeks of measurements. In the preparation phase, technical issues were uncovered with the AHU of the building. These technical issues led to high noise complaints which made the teaching staff decide to shut off the AHU while teaching. Before the first round of measurements, some small issues were resolved. Other technical issues related to the AHU were resolved between the first 3 weeks of measurements and the second 3 weeks of measurements. This led to 3 settings in the measurements:

- No mechanical ventilation
- Better mechanical ventilation (after cleaning the filters and installing silencers)
- Optimized ventilation (after maintenance and fixes to AHU) – increased airflow rates 2-3 times.

In all cases, the teachers could also open an additional window for airing.

Classroom 1, in the older building, was selected as the control because of the absence of a mechanical ventilation system in this building. The classroom was operated using normal airing habits: windows tilted most of the time and opening the door leading to the staircase. This room is not affected by the changes to the AHU.

As classroom 2, 3 and 4 are all connected to the same AHU, the impact of the mechanical ventilation system was the same in all rooms. Therefore, the settings of the ventilation systems were varied each week:

- Week 1 No mechanical ventilation
- Week 2,3 Better ventilation
- Week 4,5,6 Optimized ventilation

In classroom 4, in addition to the variations in the ventilation, a stand-alone air cleaner was installed with a maximum airflow rate of 720 m³/h. This device was always switched on.

3 RESULTS

3.1 School 1

The continuous CO₂ measurements in all classrooms during the occupied periods are summarized as box and whiskers in Figure 3. It shows that the ventilation intervention class (classroom 4) can successfully limit the occurrence of higher CO₂ levels and that we expect the perceived air quality to be good. The box, which represents 50% of the time, is noticeably smaller for classroom 4. None of the air cleaners can have any impact on the CO₂ levels, so these measurements are a good indicator of the airing behavior in the different classes.

In all other classes, the spread in measured CO₂ concentrations is larger. Remarkably, the classrooms where an air cleaner is installed show higher levels of CO₂ than the control class indicating that the presence of the device changed the airing behavior for the worse.

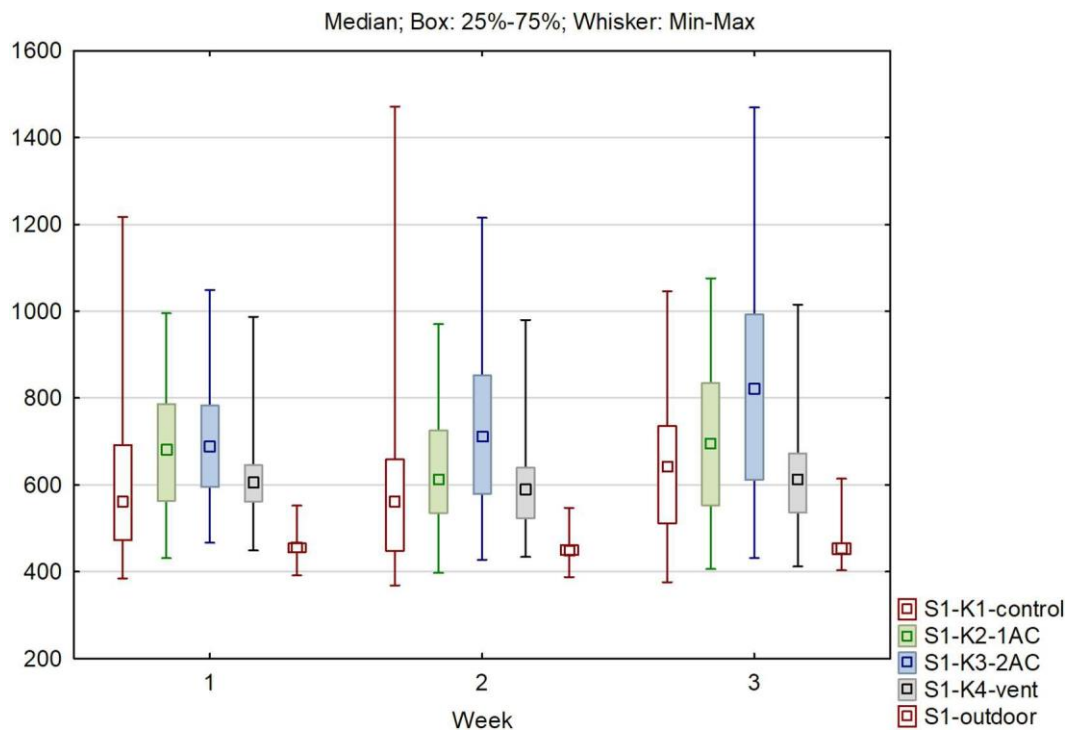


Figure 3 Box en Whiskers plot of the CO₂-concentrations [ppm] in the four classrooms and ambient air during the occupied hours from school 1

The results from the virus sampling are summarized in Table 1 showed that for most of the samples no virus was detected and for the others, virus was detected but with large uncertainties.

Although the air measurements clearly showed lower CO₂ levels in K4, the class with additional ventilation, the impact of this on virus circulation in the classroom environment cannot be determined from these measurements: no virus was detected in any sample from this class, so we assume that none of those present were infected with the virus.

With regards to air cleaning:

- During week 1 in K3, no effect of air purifier detected: both with and without air purifier, SARS-CoV-2 is detected in the air.
- During week 2 and week 3, 2 interventions found that no virus is detected with air purifier turned on, while it is detected with air purifier turned off.
- The reverse finding during week 3 (virus is detected with air purifier turned on, while it is not with air purifier turned off) may have something to do with the location of the infected person relative to the air purifier or due to a group of students that left the classroom during the second measurement of the day.

Table 1 Overview of virus sample results for school 1

SARS-CoV-2		Tuesday		Thursday	
		Intervention ON	Intervention OFF	Intervention ON	Intervention OFF
Week 1	Class. 1 - Control			Limit (ct 39.3)	
	Class 2 - Air cleaner			Neg.	Neg.
	Class 3 - Air clean + Vent.			Limit (ct 36.9)	Limit (ct 37.0)
	Class. 4 - Vent.			Neg.	
Week 2	Class. 1 - Control	Neg.		Neg.	

	Class 2 - Air cleaner	Neg.		Neg.	Neg.
	Class 3 – Air clean + Vent.	Neg.	Limit (ct 38.7)	Neg.	
	Class. 4 - Vent.	Neg.	Neg.	Neg.	
Week 3	Class. 1 - Control	Neg.		Neg.	
	Class 2 – Air cleaner	Neg.		Neg.	Neg.
	Class 3 – Air clean + Vent.	Limit (ct 39.4)	Neg.	Neg.	Limit (ct 38.3)
	Class. 4 - Vent.	Neg.	Neg.	Neg.	

3.2 School 2

All CO₂ measurements are analyzed and grouped per classroom, per setting in Figure 4. Although the control class is unaffected by the different settings, due to meteorological or behavioral differences in the measured weeks, the control can change. A first observation is that when the mechanical ventilation system is OFF (setting 1), the median CO₂ levels in the different classes are lower than the control. This is probably due to a higher sense of responsibility with regards to the IAQ when the mechanical ventilation system is OFF. Secondly, setting 2 does not seem to have a noticeable impact in comparison with no ventilation. This is due to the still relatively low airflow rates of the ventilation system in this setting. Lastly, when the full maintenance of the system was done (setting 3), the median concentration in all classrooms is 600ppm and the 75th percentile is below 1000ppm. However, higher peak concentrations up to 2500ppm did still occur.

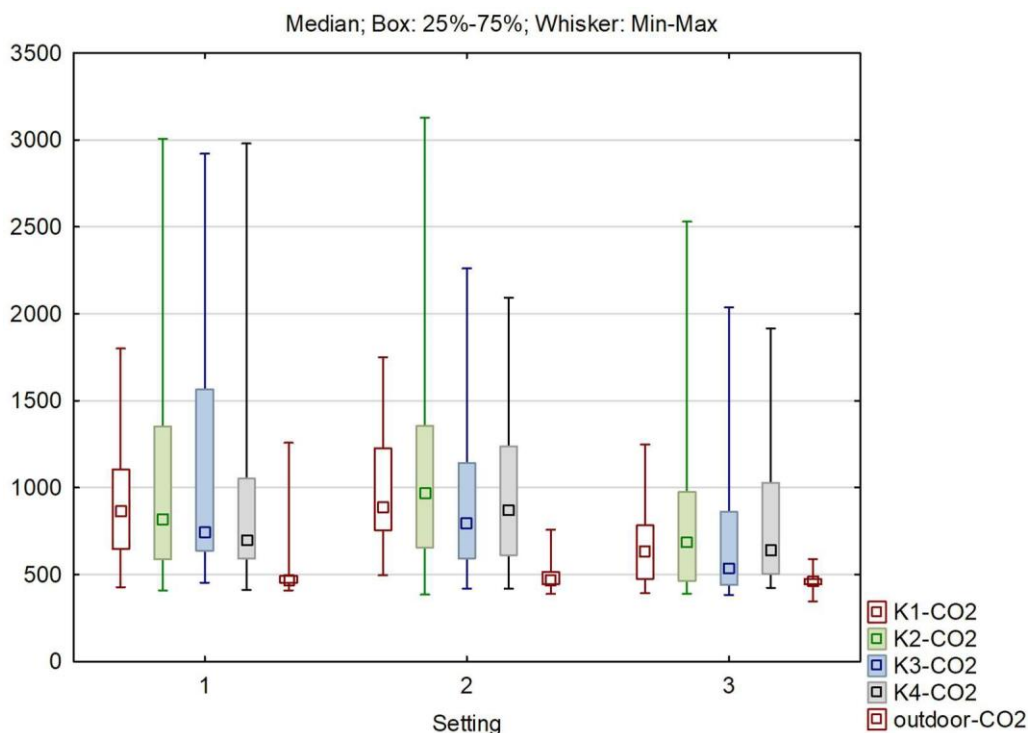


Figure 4 Box en whiskers plot of the CO₂ concentrations [ppm] recorded during the occupied hours for the 4 classrooms in school 2 for the different ventilation settings. Setting 1 = no ventilation, 2= better ventilation and 3= optimized ventilation.

Table 2 summarizes the results from the virus samples in school 2 which shows that SARS-CoV-2 was detected in most samples based on this 30-minute sampling, albeit in low concentrations. Thus, the virus circulated in classrooms mainly during the initial 3-week measurement period, reflecting the situation in Belgium at that time (Sciensano 2023).

The lower incidence in Belgium at the time of second campaign in this school can also be noticed in the lower number of samples in which SARS-CoV-2 was detected during weeks 4, 5 and 6 (although during this period the school had "optimized ventilation" which may also have contributed to a lower incidence of SARS-CoV-2 during the second measurement period).

With regards to extra ventilation as intervention, no measurable reduction of virus particles in air because of extra ventilation can be confirmed in this dataset:

- 4x no effect was detected (low viral loads detected)
- 3x there was indication of a positive effect with ventilation system turned off.
- 4x a reversed effect was observed, (higher viral load after increasing ventilation)

With regards to air cleaning, no measurable effect could be determined, and rather effect opposite to what would be expected was detected: with air purification turned on, SARS-CoV-2 was detected, while nothing was detected with air purification turned off.

Because of the low concentrations with relatively high measurement uncertainty during the second measurement period in school 2, no statement about the effect of the interventions can be formulated. Also, regarding the other pathogens measured, no effect of ventilation or air purification can be determined in school 2.

Table 2 Overview of virus sample results for school 2

SARS-CoV-2		Tuesday		Thursday	
		Intervention ON	Intervention OFF	Intervention ON	Intervention OFF
Week 1	Class. 1 - Control		Limit (ct 36.0)		Limit (ct 36.7)
	Class 2 - Mech. Vent.	Limit (ct 36.7)	Limit (ct 38.3)	Neg.	Limit (ct 38.9)
	Class 3 - Mech. Vent.		Neg.	Neg.	Limit (ct 38.5)
	Class 4 - Vent.+Air cleaner				Limit (ct 35.4)
Week 2	Class. 1 - Control	Limit (ct 38.9)		Limit (ct 39.7)	
	Class 2 - Mech. Vent.	Neg.	Limit (ct 38.7)	POS. (ct 33.0)	
	Class 3 - Mech. Vent.	Limit (ct 40.5)		Limit (ct 37.9)	Limit (ct 36.5)
	Class 4 - Vent.+Air cleaner	Limit (ct 40.7)	Neg.	Limit (ct 38.9)	Neg.
Week 3	Class. 1 - Control	Neg.		Limit (ct 40.4)	
	Class 2 - Mech. Vent.	Limit (ct 39.3)	Limit (ct 39.2)	Limit (ct 38.3)	Neg.
	Class 3 - Mech. Vent.	Limit (ct 38.5)		Limit (ct 37.4)	Limit (ct 38.2)
	Class 4 - Vent.+Air cleaner	Limit (ct 38.2)	Neg.	Limit (ct 40.0)	
Maintenance and commissioning to AHU					
Week 4	Class. 1 - Control	Limit (ct 39.1)			
	Class 2 - Mech. Vent.	Neg.		School closed	
	Class 3 - Mech. Vent.	Neg.	Neg.		
	Class 4 - Vent.+Air cleaner	Limit (ct 41.1)	Neg.		
Week 5	Class. 1 - Control	Neg.		Limit (ct 37.0)	
	Class 2 - Mech. Vent.	Neg.		Limit (ct 40.0)	
	Class 3 - Mech. Vent.	Limit (ct 38.9)	Neg.	Limit (ct 38.2)	
	Class 4 - Vent.+Air cleaner	Limit (ct 39.0)	Limit (ct 37.6)	Neg.	Neg.
Week 6	Class. 1 - Control			Limit (ct 39.5)	
	Class 2 - Mech. Vent.	Limit (ct 37.3)		Limit (ct 40.2)	Neg.
	Class 3 - Mech. Vent.	Neg.	Limit (ct 40.1)	Neg.	Limit (ct 40.0)
	Class 4 - Vent.+Air cleaner				

4 CONCLUSIONS

The virus was clearly more prevalent in the classrooms of school 2 than in school 1 at time of measurement, although according to the Sciensano SARS-CoV-2 dashboard, virus circulation in the society was similar during the measurements in school 1 and the first measurement period in school 2 (Sciensano 2023). The more effective ventilation and aeration in school 1, combined with the wearing of mouth masks in the first school, probably also contributed to the overall lower detection of SARS-CoV-2 and other viruses in the indoor air of school 1.

A relevant note to this table is that almost all the samples with detection of SARS-CoV-2 were in fact borderline, meaning that the CT values were rather high and thus the concentration in air was reasonably low (the detection limit for this qPCR analysis is CT value ≈ 40). The closer the CT value of a PCR analysis is to 39-40, the higher the measurement uncertainty of this method (e.g., CT 39.04).

For both schools, no measurable effect of increased ventilation or air cleaning on the occurrence of SARS-CoV-2 could be objectively observed for these in-situ and in-use situations. Most virus concentration in the samples were low, which can be explained by the trends in national COVID-19 disease incidence and the fact that students were wearing facemasks.

In general, the results indicate the importance of proper commissioning and maintenance to mechanical ventilation systems and show an overall better expected perceived indoor air quality when the ventilation system works properly. In the school without a mechanical ventilation system, manual airing through the opening of windows can achieve the same level of expected perceived indoor air quality if operated correctly.

5 REFERENCES

- Bertin Technologies. 2012. "Coriolis® μ User Manual. Manual Code: 05027-006-DU002-F ENG."
- E+E Electronics. n.d. "Humlog 20 Series Datasheet v2.7." Accessed July 6, 2023. https://www.epluse.com/fileadmin/data/product/humlog20/datasheet_HUMLOG20.pdf.
- FOD Economie. 2022. "Coronavirus: verluchting, ventilatie en COVID-19." FOD Economie. March 14, 2022. <https://economie.fgov.be/nl/themas/ondernemingen/coronavirus/coronavirus-verluchting>.
- Lima Paralovo, Sarah, Klaas De Jonge, Arnold Janssens, Jelle Laverge, Reinoud Cartuyvels, Koen Vandendriessche, Borislav Lazarov, Maarten Spruyt, and Marianne Stranger. 2023. "Evaluating the Impact of Air Cleaning on Bioaerosols and Other IAQ Indicators in Belgian Daycare Facilities." In . Copenhagen, Denmark.
- Sciensano. 2023. "Belgium COVID-19 Dashboard." Looker Studio. 2023. <http://lookerstudio.google.com/reporting/c14a5cfc-cab7-4812-848c-0369173148ab>.
- Stranger, Marianne, Jef Daems, Borislav Lazarov, Sarah Lima Paralovo, Maarten Spruyt, Klaas De Jonge, Janssens Arnold, et al. 2022. "Pilotprojecten ventilatie en luchtzuivering (draftversion 12/2022)." 2022/Health/R/2786. Belgium.

Review of international standards describing air cleaner test methods

Hannelore Scheipers*¹, Arnold Janssens¹, Jelle Laverge¹

*1 Building Physics Research Group, UGent
Sint Pietersnieuwstraat 41 - B4
B-9000 Ghent, Belgium*

**Corresponding author: hannelore.scheipers@ugent.be*

ABSTRACT

The offer of air cleaners has increased significantly since the SARS-CoV-2 pandemic. However, it is not clear to what extent they can contribute to indoor air quality. There are multiple standards that describe test methods for air cleaners, but no consensus can be found on how to determine the performance of the air cleaners.

This paper contains a review of test methods for several types of air cleaners, (e.g. photocatalytic devices). This allows to make a holistic analysis of the existing test methods, in order to make recommendations for legislation regarding test methods to be used on the Belgian market.

For this paper, a literature study has been conducted to investigate the similarities and differences between several standards. The investigated documents include, among others, a French standard, ISO standards, ASHRAE standards and AHAM standards.

The literature study results in a structured overview of similarities, knowledge gaps and challenges. The main differences between the standards concern the test apparatus and the pollutants used. Most of the test methods use either a test duct, which measures the single-pass efficiency, or a test chamber, where the decay of the pollutants is measured over a certain period of time. All standards define different pollutants in different concentrations that should be tested. The test pollutants consist of VOCs, aerosols, (synthetic) dust, (acid) gases and microorganisms. They also differ in the type of air cleaners being tested. Several test methods are suited for any type of air cleaner. Other methods can only be used for a specific type of air cleaner, e.g., UV-C lights. In this case the test pollutants, measurements and test apparatus are adapted to the specific kind of air cleaner.

Most standards lack a non-targeted analysis of the treated air, because this is too complicated or expensive to test. However, the by-products can be harmful and are relevant to test.

Overall, the test methods are not suitable to predict the air quality in a room where the air cleaner may be used. They provide a means to compare the performances of different air cleaners to each other, but they do not predict real life performance. Furthermore, most of the test methods do not test the long-term performance of the air cleaners. This is because the test methods are kept as short as possible to reduce the costs.

KEYWORDS

Air cleaners, test methods, literature review, indoor air quality

1 INTRODUCTION

In the context of a study commissioned by the Federal Public Service of Health in Belgium, a review has been conducted on the existing test standards for air cleaners. Since the SARS-CoV-2 pandemic the amount of air cleaners on the Belgian market has increased significantly. All the air cleaners have been tested for efficiency and safety, but many different test methods are used, and it is not known to what extent they are reliable. An extensive literature review has therefore been conducted to investigate the state of the art of the existing test standards. The review includes national and international standards that are now commonly used to test air cleaners. The technical characteristics of the test standards are compared with each other, to see to what extent they resemble or differ from each other. Therefore, this is a more technical and holistic assessment, which differs from previous research, such as the research by Afshari et al. (2022) where they focussed on test methods and standards only for portable air-cleaning units.

2 OVERVIEW OF THE INVESTIGATED STANDARDS

Table 1 gives an overview of the investigated standards, and for which type of air cleaners they are suitable.

Table 1: Overview of the test standards

Test standard	Title	Type of air cleaners
AHAM AC-1 (2020)	Method for Measuring Performance of Portable Household Electric Room Air Cleaners	Portable household electric room air cleaners
AHAM AC-4 (2022)	Method of Assessing the Reduction Rate of Chemical Gases by a Room Air Cleaner	Portable household electric room air cleaners
AHAM AC-5 (2022)	Method for Assessing the Reduction Rate of Key Bioaerosols by Portable Air Cleaners Using an Aerobiology Test Chamber	Portable household electric room air cleaners
ASHRAE 52.2 (2017)	Method of Testing General Ventilation Air-Cleaning Devices for Removal Efficiency by Particle Size	General ventilation Air-Cleaning Devices
ASHRAE 145.1 (2015)	Laboratory Test Method for Assessing the Performance of Gas-Phase Air-Cleaning Systems: Loose Granular Media	Gas-phase air-cleaning systems (tests the loose granular media)
ASHRAE 145.2 (2016)	Laboratory Test Method for assessing the Performance of Gas-Phase Air-Cleaning Systems: Air-Cleaning Devices	In-duct sorptive media gas-phase air-cleaning devices
ASHRAE 185.1 (2020)	Method of Testing UV-C Lights for Use in Air-Handling Units or Air Ducts to Inactivate Airborne Microorganisms	UV-C lights for use in air-handling units or air ducts
ASHRAE 185.2 (2020)	Method of Testing Ultraviolet Lamps for Use in HVAC&R Units or Air Ducts to Inactivate Microorganisms on Irradiated Surfaces	UV-C lights for use in air-handling units or air ducts
IEC 63086-1 (2020)	Household and similar electrical air cleaning appliances – Methods for measuring the performance Part 1: General requirements	electrically powered household and similar air cleaners
EN ISO 10121-3 (2022)	Test methods for assessing the performance of gas-phase air cleaning media and devices for general ventilation - Part 3: Classification system for GPACDs applied to treatment of outdoor air	gas-phase air cleaning devices supplying single pass outdoor air to general ventilation systems
ISO 16000-36 (2021)	Indoor air - part 36: Standard method for assessing the reduction rate of culturable airborne bacteria by air purifiers using a test chamber	Air purifiers commonly used in single room spaces
EN 16846-1 (2017)	Photocatalysis — Measurement of efficiency of photocatalytic devices used for the elimination of VOC and odour in indoor air in active mode. Part 1: Batch mode test method with a closed chamber	Photocatalytic devices or combined systems that include a photocatalytic function
NF B 44-200 (2016)	Independent air purification devices for tertiary sector and residential applications Test methods — Intrinsic performances	Any standalone air purification device

It is clear that most of the test standards only differentiate between portable air cleaners and in-duct air cleaners and not between different technologies. However, there are some exceptions to this, e.g. tests that only apply to UV-C technology. Standard ASHRAE 145.1 (2015) is also an exception, since it does not test the air cleaner itself, but the loose granular sorptive media used in the air cleaner.

3 TEST METHOD

3.1 Test apparatus

A first characteristic of the test methods is the test apparatus that is used. The two most commonly used test set-ups are the test chamber and the test duct.

The test chamber is an air-tight chamber in which the air cleaning device is placed. If the position of the air cleaner in the test standard is specified, it has to be placed in the centre of the chamber, on the floor, on a table or attached to a wall, depending on the type of air cleaner. The size of the chamber is also defined and differs among the different standards. Standard EN 16846-1 (2017) prescribes a test chamber with a minimum volume of 1 m³, where the ratio of the volume of the device to the volume of the chamber shall be less or equal to 0,10. Most other standards define larger test chambers. ISO 16000-36 (2021) states that the volume of the test chamber should reflect the later application of the air cleaner. It should be 8m³ or more and is usually between 15m³ and 30m³. AHAM AC-1 (2020), AHAM AC-4 (2022), AHAM AC-5 (2022) and IEC 63086-1 (2020) require a volume of around 30m³. NF B 44-200 (2016) is an exception to the other standards. It uses a test chamber in a test bench, which is a different way of testing than room size test chambers. It does not require a minimum volume of the test chamber, only a minimum dimension for the upstream section of the test chamber. This should at least be three times larger than the air cleaner that overruns into this upstream section.

The test duct is a duct with an air inlet and outlet in which the air cleaner is placed in a manner that the airflow has to pass through the air cleaner. The dimensions of the test duct are clearly defined in each standard. The standards ASHRAE 52.2 (2017), ASHRAE 145.2 (2016), ASHRAE 185.1 (2020), ASHRAE 185.2 (2020) and EN ISO 10121-3 (2022) (that refers to standard EN ISO 10121-2 (2013)) use a test duct for a nominal device of 610 x 610 mm, which corresponds to the dimensions of the duct. Other dimensions are also possible, if the duct is adjusted to it as described in the standards.

As mentioned earlier, standard ASHRAE 145.1 (2015) is a special case. In consequence it does not use a test chamber or test duct, but a test apparatus with a gas-phase air filtration media column, which is comparable to the test duct in terms of test set-up and test method.

3.2 Test conditions

The tests are performed under different conditions. The temperature and relative humidity of the air are prescribed and do not differ much among most of the standards. Most of the standards require a temperature from 20°C to 25°C with a deviation of 0.5 to 3°C. Two of the investigated standards are an exception to this; ASHRAE 52.2 (2017) requires a temperature between 10°C and 38°C and ASHRAE 185.2 (2020) requires to test at three different temperatures: 12.8°C, 23.9°C and 48.9°C ± 2.2°C. The required humidity of all standards is between 40% and 50% with a deviation of 1 to 10%.

For tests using test chambers, the air inside the test chamber has to meet these requirements prior to the test, but the air is not conditioned anymore once the test starts. In the case of test ducts, the supply air should be conditioned.

The tests using test chambers state that the incoming air has to be clean, which is defined as a maximum pollutant concentration that is allowed. Filters are used to clean the air that enters the test chamber. Standards using test ducts also address the background concentration of the test air. This can be done by imposing a limit for the background concentration, as e.g. standard ASHRAE 145.1 (2015) does. Here, the influent air cannot contain more than 1% of the challenge concentration of each challenge gas. Another way to handle the background concentration is filtering the influent air and measuring the background concentration, which is taken into account in the calculations of the performance. (ASHRAE 52.2 (2017))

3.3 Operational mode of the air cleaner/flow rate through the air cleaner

To test the air cleaning device in a test chamber, the air cleaner has to be turned on in a certain operational mode. Depending on this, the air cleaner has a different efficiency. Standard NF B 44-200 (2016) defines that the test sponsor shall determine the speed for the tests. The AHAM AC-1 (2020), AHAM AC-4 (2022) and AHAM AC-5 (2022) standards define that the air cleaners are tested at the highest operating mode. The last two standards also mention that it is possible to test additional modes, if this is included in the test report. IEC 63086-1 (2020) requires testing in the maximum operational mode, except if the device only has an automatic mode, then it should be tested according to the manufacturer's instructions. ISO 16000-36 (2021) requires testing for multiple operation modes. The results then have to be checked on validity (e.g. the decay rate in step one has to remain below 50%). Only valid results are taken into account. Standard EN 16846-1 (2017) does not mention an operation mode.

If a test duct is used to test the air cleaner, an airflow rate in the test duct must be specified. Standard ASHRAE 52.2 (2017) specifies that the airflow rate should be at the upper limit of the air cleaner's application range. If this has not been specified an airflow rate corresponding to 2.50 m/s is used, which is rather low for large air groups. EN ISO 10121-3 (2022) states that the rated airflow of the air cleaner should be used. If this information is not given, a face velocity of 2.54 m/s shall be used. Standard ASHRAE 185.1 (2020) and ASHRAE 185.2 (2020) prescribe a fixed air velocity of 2.54 m/s, which corresponds to an airflow rate of 3400 cmh. ASHRAE 145.1 (2015) tests at an airflow rate to achieve a residence time of 0.10 ± 0.01 s. A formula to calculate this is given in the standard.

4 DEFINITION OF PERFORMANCE

4.1 Performance when using a test chamber (CADR)

When a test chamber is used, test pollutants are usually added to the air until a certain concentration is reached. Then the supply of test pollutants stops, and the decay rate is measured. A common way of expressing the performance using this test method is the Clean Air Delivery Rate (CADR), that can be calculated by multiplying the volume (m^3) of the test chamber with the decay rate (h^{-1}) of the pollutant measured in the test chamber. As an exception, standard NF B 44-200 (2016) has a continuous supply of pollutants, since the test setup consists of a combination of a test duct and a test chamber. As a consequence, the CADR is calculated by multiplying the air flow rate of the air cleaning device with its purification efficiency.

As standard IEC 63086-1 (2020) explains, the reduction rate must be due to the operation of the air cleaner. This standard does not specify this further, but other standards do take this into account. The standards AHAM AC-1 (2020), AHAM AC-4 (2022) and AHAM AC-5 (2022) calculate the decay rate as the difference between the total decay rate with operating the air cleaner and the natural decay rate without operating the air cleaner. Standard NF B 44-200 (2016) uses a correction factor on the purification efficiency calculation to take the natural decay rate into account.

Standard ISO 16000-36 (2021) is an exception, as it uses a test chamber but only calculates the reduction rate of bacteria, without converting it into a CADR.

4.2 Performance when using a test duct

Test standards using a test duct usually have a continuous supply of pollutants for the first tests, where for e.g. the removal efficiency can be measured. Afterwards, the supply of pollutants stops, and other parameters will be measured, such as the desorption. Consequently, the performance is not expressed with a CADR. E.g. standards ASHRAE 145.1 (2015) and

ASHRAE 145.2 (2016) calculate the removal efficiency at a specific time, the penetration at a specific time and the capacity for removal for a time interval, all expressed as a percentage. From these values, other important factors can be calculated, such as the time to reach 50% breakthrough, which is the percentage of the challenge concentration that is reached at the outlet of the filter and is seen as an easy and useful indicator of air-cleaner performance (ASHRAE 145.2, 2016). Besides that, also performance curves that plot different performance parameters against the time are used. Standard EN ISO 10121-3 (2022) does not differ much from these ASHRAE standards. It calculates the (initial) removal efficiency and plots a removal efficiency versus capacity curve to define the efficiency of the air cleaner.

Standard ASHRAE 52.2 (2017) provides an extra way to express the efficiency; the Minimum Efficiency Reporting Value (MERV) for air cleaners. First the minimum particle size removal efficiency (PSE) is calculated for twelve size ranges of particles. The data points of the curves are then averaged per size range, and there are three different size ranges. The MERV value is then based on these three composite average PSE points. In this way only one value is needed to report the efficiency, instead of a curve with the removal efficiency per particle size. The MERV value should always be reported together with the test airflow rate, as it depends on it. Next to this, e.g. also the dust holding capacity of the air cleaner should be calculated. This method of expressing the efficiency is quite similar to the method used in standard EN ISO 16890-1 (2017), which is the basic standard to test in-duct filters for particulate matter. In this standard the particulate matter efficiencies (ePM) are calculated for three size ranges, based on the average fractional efficiencies and the standardized particle size distribution.

Standard ASHRAE 185.1 (2020) measures the efficiency of UV-C lights and thus has a slightly different approach. Since no filter is used, the efficiency will not differ much by time. Hence, only the single-pass bioaerosol inactivation efficiency is calculated, which is then corrected with the no-light transmission rate, where the inactivation of organisms is measured with the UV-C light turned off.

Lastly standard ASHRAE 185.2 (2020) forms an exception to the other standards. It tests UV-C lamps to inactivate microorganisms, but it has a different approach. The tests are not done with microorganisms, but the intensity of ultraviolet lamps on irradiated surfaces is measured. Hence the efficiency is expressed as the UV-C irradiance levels measured.

5 DURATION OF THE TEST

All the standards have their own practicalities, and there are also differences in measurement time. The duration of the test is often expressed in a similar way for tests using a test chamber. The following will discuss the duration from reaching and measuring the initial concentration to the end of the natural or total decay test. Some standards have a shorter measurement time, for e.g. standards AHAM AC-1 (2020), AHAM AC-4 (2022), AHAM AC-5 (2022) and ISO 16000-36 (2021) have a test time that ranges from ten minutes to an hour. The differences in measurement time are due to a faster or slower decay rate of the pollutants, characteristics of the measurement device or characteristics of the air cleaner. Standard EN 16846-1 (2017) describes a longer test duration: the test will run until 90% of the volatile organic compounds (VOCs) are removed, with a maximum test time up to 24 hours. Standard IEC 63086-1 (2020) is an exception that does not mention a test duration. This is because the standard only specifies general requirements to measure the performance, without providing a test method.

For the test methods using a test duct there is a greater difference in expressing the duration of the test. Some standards clearly specify a test duration. E.g. Standard ASHRAE 145.2 (2016) lets the standard initial performance test run for one hour, or until the penetration reaches 0.95%. The standard capacity test runs for four hours, or until a breakthrough of 95% is achieved. Then the challenge gas is removed, and desorption is monitored for 30 minutes or until the contaminant reaches 10% of the test challenge concentration.

It is also possible to test until a certain breakthrough is reached. Standard ASHRAE 145.1 (2015) runs the test until a 50% breakthrough of the initial challenge concentration is reached. There are also other ways to express a measurement time. Standard EN ISO 10121-3 (2022), that partly refers to EN ISO 10121-2 (2013), defines measurement frequencies. For the initial removal efficiency the measurement frequency is less than 2 minutes, and the test normally takes 3 hours or less. The removal efficiency versus dose test has a measurement frequency ranging from 5 min to 12 hours. The test ends when the desired end point is reached and is stable for 10 min. Lastly a retentivity determination is performed without any challenge compounds. The test runs until the downstream concentration reaches 5%, with a maximum of 6 hours. Standard ASHRAE 185.2 (2020) requires to record a one-minute average of irradiance from the sensor per grid-point location for the sensor. Standard ASHRAE 52.2 (2017) states that the number of samples and sample time are determined by a number of data quality requirements.

For standard NF B 44-200 (2016), the test time depends on the pollutant tested. For gases it has a duration of 45 minutes, for inert particulate matter, a count cycle with 15 metering steps is defined for a 30 to 60-second count-per-count window and for allergens and microorganisms no duration is defined. Standard ASHRAE 185.1 (2020) also does not specify a test duration.

6 TEST POLLUTANTS

Depending on the test, different test pollutants are used. Some standards test for a broader range of pollutants, for e.g. standard NF B 44-200 (2016) uses a test gas, microorganisms, an allergen and aerosol. Other standards have a more limited scope of test pollutants. For e.g. standard ISO 16000-36 (2021) only tests for two bacteria. An overview of the test pollutants used in the different standards can be found in Table 2.

Table 2: Test pollutants

Test standard	Pollutants	Concentration
AHAM AC-1 (2020)	Cigarette smoke with particle sizes detected from 0.10 μm to 1.0 μm diameter Commercially available test dust with particle sizes detected from 0.5 μm to 3.0 μm Paper Mulberry Pollen (non-defatted) with a particle size range of 5 μm to 11 μm , including fragments	24000 to 35000 particles/cc 200 to 400 particles/cc 4 to 9 particles/cc
AHAM AC-4 (2022)	Formaldehyde, n-Heptane, Toluene, d-Limonene, Nitrogen Dioxide, Ammonia	400 $\mu\text{g m}^{-3}$ (+20 %) 800 $\mu\text{g m}^{-3}$ (+20 %) 700 $\mu\text{g m}^{-3}$ (+20 %)
AHAM AC-5 (2022)	Bacteria: Gram-Positive (Staphylococcus epidermidis), Gram-Negative (Acinetobacter baumannii) and bacterial endospores (Geobacillus stearothermophilus) Virus: more than one bacteriophage as surrogate for human pathogenic viruses, preferred one: MS2 (with host Escherichia coli) Mold: mold spore (Aspergillus brasiliensis) Alternate microbes can also be used (should be listed in the test report): Staphylococcus aureus, Escherichia coli, Klebsiella pneumoniae, Bacillus subtilis, Phi X-174 (with host Escherichia coli), T1 (with host Escherichia coli), Phi 6 (with host Pseudomonas syringae), Penicillium citrinum, Aspergillus fumigatus, Penicillium chrysogenum, Penicillium rubens, Stachybotrys chartarum. Other microbes can also be used for specific questions.	The minimum initial concentration can vary (it depends on the microbe and the required log reduction), but will be between $5.0 \cdot 10^6$ colony forming units (CFU) and $2.1 \cdot 10^9$ CFU

ASHRAE 52.2 (2017)	Test aerosol: Polydisperse solid-phase (dry) potassium chloride (KCl) particles Synthetic loading dust: 72% ISO 12103-1, A2 Fine Test Dust, 23% powdered carbon, and 5% milled cotton linters	Is determined by initial efficiency tests, so that the total concentration level does not overload the particle counters
ASHRAE 145.1 (2015)	Challenge gases are selected from the following groups: VOC challenge gases: toluene, acetaldehyde, hexane, 2-butanone, isobutanol, dichloromethane, tetrachloroethylene Acid challenge gases: sulfur dioxide, nitrogen dioxide, nitric oxide, hydrogen sulfide, chlorine Other (common) challenge gases: formaldehyde, ozone, ammonia...	100 ± 10 parts per million by volume (ppmv) 100 ± 10 ppmv To be determined based on use application and safety considerations
ASHRAE 145.2 (2016)	A VOC: toluene , 2-butanone, acetone, benzene, cyclohexane, cyclopentane, dichloromethane, ethanol, hexane, iso-butanol, isopropanol, tetrachloroethene, m-Xylene, o-Xylene, p-Xylene An acid gas: sulfur dioxide , hydrogen chloride, hydrogen sulfide, NO ₂ ⁺ Another gas: formaldehyde, acetaldehyde, hexanal, ammonia , methylpyrrolidone, ozone , DMMP , chlorine, carbon monoxide, carbon dioxide Or another gas that is more applicable to the use of the air cleaner (Required chemicals are indicated in bold)	Low concentration: 400 parts per billion (ppb), high concentration ranging from 20 to 65 parts per million (ppm) Low concentration: ranging from 50 to 100 ppb, high concentration ranging from 5 to 35 ppm Low concentration: ranging from 75 to 100 ppb, high concentration ranging from 0.5 to 75 ppm (exception: CO ₂ : 400 ppb to 5000 ppm)
ASHRAE 185.1 (2020)	Mycobacterium parafortuitum (ATCC® 19686) Aspergillus sydowii (ATCC® 36542)	Sufficient concentration to allow measurement to show 99% inactivation
ASHRAE 185.2 (2020)	No test pollutants (only the intensity of UV-C lamps on irradiated surfaces is measured).	/
IEC 63086-1 (2020)	Only mentions that the target pollutant is a specific air pollutant with defined components, including the main categories microorganisms, gaseous pollutants and particulate matter	Not mentioned
EN ISO 10121-3 (2022)	Ozone, sulphur dioxide, nitrogen dioxide, toluene	150 ppb(v) and 3 ppm(v) 450 ppb(v) and 9 ppm(v) 900 ppb(v) and 9 ppm(v) (Values respectively for the initial efficiency determination and the efficiency vs. dose determination)
ISO 16000-36 (2021)	Bacteria: Staphylococcus aureus and Micrococcus luteus (other bacteria may be used for specific questions, but this should be listed in the test report.	Between 1.0*10 ⁴ cfu/m ³ and 3.2*10 ⁴ cfu/m ³
EN 16846-1 (2017)	VOC mixture: acetone, acetaldehyde, formaldehyde, heptane, toluene	Test is run at two concentrations: (50 ± 25%) ppbv per compound and (1000 ± 10%) ppbv per compound
NF B 44-200 (2016)	Test gas: mixture of acetone, acetaldehyde, formaldehyde, heptane, toluene A bacterium: Staphylococcus epidermidis and a fungus: Aspergillus niger	50 ppbv to 150 ppbv 10 ³ to 10 ⁴ CFU/m ³ .

Allergen: Major cat allergen Fel d 1 (<i>Felis domesticus</i> 1)	10 ng/m ³ to 150 ng/m ³
Aerosol (inert particulate matter range 0,3 - 5 µm): Particulate suspension of DEHS (DiEthylHexyl Sebacate)	Dependent on the manufacturer's requirements of the optical particle counter

The choice of the test pollutants is often based on one of the following criteria: it are commonly used test materials for air cleaners/filters, e.g. the allergen and the aerosol of standard NF B 44-200 (2016) are chosen based on this criterium, or they represent typical pollutants of indoor/outdoor air, e.g. the test gases and the microorganisms of standard NF B 44-200 (2016) are common indoor air pollutants and standard EN ISO 10121-3 (2022) uses typical outdoor air pollutants. Another possible selection criterion is mentioned in ASHRAE 185.1 (2020): the used organisms cover the range of reasonable interest for UV-C device applications.

For tests using test chambers (except for standard NF B 44-200 (2016)), the concentration given in the table above is the initial concentration before the air cleaner is turned on. The concentration is not kept constant during the test, since the decay rate is measured.

The concentration can depend on the preconditions. For e.g. standard EN 16846-1 (2017) performs a test at two different concentrations. The test with the lowest concentration searches for reaction by-products, the test with the highest concentration is to demonstrate the photocatalytic activity with monitoring of the mineralization of VOCs into CO₂. For Standard ASHRAE 52.2 (2017) and standard NF B 44-200 (2016), the concentration depends on the characteristics of the particle counters.

As mentioned before, standard IEC 63086-1 (2020) is an exception, as it only specifies the general requirements to measure the performance. As a consequence, it does not specify the test pollutants and concentration to be used. Standard ASHRAE 185.2 (2020) is also an exception, since it only measures the intensity of the UV-C lamps as performance characteristic.

7 KNOWLEDGE GAPS AND CHALLENGES

7.1 By-products

Only two of the investigated standards explicitly address the testing of by-products. Standard NF B 44-200 (2016) states that the test method can be used to measure any by-products downstream of the air cleaner. Further, the test also prescribes to measure four reaction intermediates with a corresponding limit of detection: ozone (0.5 ppbv), carbon monoxide (1 ppmv), nitrogen monoxide (0.5 ppbv) and nitrogen dioxide (0.5 ppbv). This is measured before the pollutants are added to the test air and during the test with the gas-mixture. Purpose-engineered methods should be used to measure it. Standard EN 16846-1 includes a detection procedure to measure reaction by-products and ozone. A separate test is done with a concentration of 50 ppbv per compound (aldehydes, VOC, ozone), or with a higher concentration if needed. The by-products then have to be analysed according to ISO 16000-3 and ISO 16000-6. In addition, standards AHAM AC-1 (2020), AHAM AC-4 (2022) and AHAM AC-5 (2022) refer, among others, to standard UL 867 (Standard for Electrostatic Air Cleaners), which includes a test method for ozone generation levels (AHAM AC-5, 2022).

However, as Collins (Collins, 2021) points out, air cleaners can introduce several unintended by-products in the air, such as ozone, but also other oxidants for e.g. that can be harmful to health as well. Hence, this is an important topic to address when testing air cleaners and a proper testing method for a non-targeted analysis should be set up.

7.2 Real life performance

The air cleaners are tested in a specific test chamber or test duct. The test conditions and test pollutants are pre-defined, as described in paragraph 3.2 and paragraph 6, and this does not necessarily reflect the real-life conditions in which the air cleaner will be used. As standard ASHRAE 52.2 (2017) and ASHRAE 185.1 (2020) state, the outcome of the tests should help the user to compare the performance of different devices, not predict real-life performance. The tests try to simulate the real-life operation, but field conditions are not duplicated in the test. This would also be hard since field conditions vary from location to location. As a consequence, the cleanliness of a space where the air cleaner is used, or the service life of the device cannot be predicted. Standard ASHRAE 52.2 (2017) also indicates that the synthetic dust that is used as test material is not representative for all atmospheric particulates, which may affect the test results compared to real use situations. Standard ASHRAE 145.1 (2015) further adds that performing tests at low concentrations would probably more accurately predict the performance at actual use conditions, but this would be prohibitively expensive. It is also easier to generate, analyse and control higher gas concentrations than lower concentrations.

Another characteristic of the tests that is not representative for the real use conditions, is the size of the test chamber. As declared in paragraph 3.1, the size of the test chambers typically ranges from 1m³ to 30m³, which does not necessarily represent the real use conditions. Standard ISO 16000-36 (2021) imposes that the size of the test chamber should reflect the later application of the air cleaner, but this is the only standard that does so. The manner in which the performance is measured when using a test chamber is also not very realistic, as pollutants are not continuously introduced during the test, except in standard NF B 44-200 (2016).

7.3 Long-term performance

As described before, the tests are carried out over a limited period of time. However, as standard ASHRAE 145.2 (2016) mentions, breakthrough in real life conditions may take weeks or months. Therefore, the capacity test is conducted at elevated challenge concentrations to shorten the test, hence reducing the costs. As a consequence, the performance data cannot be transferred to real use conditions directly. The results can be extrapolated, but this will not always be correct. ASHRAE 185.1 (2020) also mentions that the performance over service life cannot be predicted with the results of the test and that the equipment provider should be expected to give an estimate of the service life characteristics for the expected operating conditions.

8 CONCLUSIONS

The review points out that there are many differences between the investigated test standards. One of the main differences concerns the test method that is used. Using a test chamber or a test duct imposes a different way of testing, which also influences the test duration and the definition of effectiveness. In contrast, the test conditions and the operating mode/flow rate through the air cleaner show little difference. The test pollutants used vary widely, but this is partly a consequence of the targeted type of air cleaners to be tested. If a device using UV-C technology is tested for example, only the decay of microorganisms is relevant to test.

The test standards provide a method to compare the air cleaning devices, but they do not provide results on the real use performance or the long-term performance. A non-targeted analysis to search for potentially harmful by-products is also a knowledge gap in most of the test methods.

9 REFERENCES

Afshari, A., Mo, J., Tian, E., & Seppänen, O. (2022). Testing Portable Air Cleaning Units – Test Methods and Standards: A Critical Review. *REHVA*, 35-46.

- American Society of Heating, Refrigerating and Air-Conditioning Engineers. (2015). *Laboratory Test Method for Assessing the Performance of Gas-Phase Air-Cleaning Systems: Loose Granular Media* (ANSI/ASHRAE Standard No. 145.1-2015).
- American Society of Heating, Refrigerating and Air-Conditioning Engineers. (2016). *Laboratory Test Method for Assessing the Performance of Gas-Phase Air-Cleaning Systems: Air-Cleaning Devices* (ANSI/ASHRAE Standard No. 145.2-2016).
- American Society of Heating, Refrigerating and Air-Conditioning Engineers. (2017). *Method of Testing General Ventilation Air-Cleaning Devices for Removal Efficiency by Particle Size* (ANSI/ASHRAE Standard No. 52.2-2017).
- American Society of Heating, Refrigerating and Air-Conditioning Engineers. (2020). *Method of Testing UV-C Lights for Use in Air-Handling Units or Air Ducts to Inactivate Airborne Microorganisms* (ANSI/ASHRAE Standard No. 185.1-2020).
- American Society of Heating, Refrigerating and Air-Conditioning Engineers. (2020). *Method of Testing Ultraviolet Lamps for Use in HVAC&R Units or Air Ducts to Inactivate Microorganisms on Irradiated Surfaces* (ANSI/ASHRAE Standard No. 185.2-2020). https://ashrae.iwrapper.com/ASHRAE_PREVIEW_ONLY_STANDARDS/STD_185.2_2020
- Association Française de Normalisation. (2016). *Independent air purification devices for tertiary sector and residential applications - Test methods - Intrinsic performances* (NF B Standard No. 44-200)
- Association of Home Appliance Manufacturers. (2020). *Method for Measuring Performance of Portable Household Electric Room Air Cleaners* (ANSI/AHAM Standard No. AC-1-2020).
- Association of Home Appliance Manufacturers. (2022). *Method of Assessing the Reduction Rate of Chemical Gases by a Room Air Cleaner* (AHAM Standard No. AC-4-2022).
- Association of Home Appliance Manufacturers. (2022). *Method for Assessing the Reduction Rate of Key Bioaerosols by Portable Air Cleaners Using an Aerobiology Test Chamber* (AHAM Standard No. AC-5-2022).
- Bureau for Standardisation. (2013). *Test methods for assessing the performance of gas-phase air cleaning media and devices for general ventilation - Part 2: Gas-phase air cleaning devices (GPACD)* (EN ISO Standard No. 10121-2:2013).
- Bureau for Standardisation. (2017). *Air filters for general ventilation - Part 1: Technical specifications, requirements and classification system based upon particulate matter efficiency (ePM)* (EN ISO Standard No. 16891-1:2016).
- Bureau for Standardisation. (2017). *Photocatalysis — Measurement of efficiency of photocatalytic devices used for the elimination of VOC and odour in indoor air in active mode - Part 1: Batch mode test method with a closed chamber* (EN Standard No. 16846-1:2017).
- Bureau for Standardisation. (2021). *Indoor air - Part 36: Standard method for assessing the reduction rate of culturable airborne bacteria by air purifiers using a test chamber* (ISO Standard No. 16000-36:2018).
- Bureau for Standardisation. (2022). *Test methods for assessing the performance of gas-phase air cleaning media and devices for general ventilation - Part 3: Classification system for GPACDs applied to treatment of outdoor air* (EN ISO Standard No. 10121-3:2022).
- Collins, D. B., & Farmer, D. K. (2021). Unintended Consequences of Air Cleaning Chemistry. *Environmental Science & Technology*, 12172-12179. <https://pubs.acs.org/doi/10.1021/acs.est.1c02582>
- International Electrotechnical Commission. (2020). *Household and similar electrical air cleaning appliances – Methods for measuring the performance - Part 1: General requirements* (IEC Standard No. 63086-1).

Rethinking different ventilation strategies in a post-pandemic era: a CFD assessment

Alicia Murga^{*1}, Kazuhide Ito², and Makoto Tsubokura^{1,3}

*1 Kobe University
Nada-ku, Rokkodaicho 1-1
Kobe, Japan*

*2 Kyushu University
Kasugakoen 6-1
Kasuga, Japan*

**Corresponding author: e-mail address*

*3 Riken Center for Computational Science
Chuo-ku, Minami-machi, Minatojima 7-1-26
Kobe, Japan*

ABSTRACT

The world has experienced the devastating nature of airborne transmitted diseases through the COVID-19 pandemic. Significant actions were taken in order to reduce the number of new infections, such as quarantines, social distancing, mask wearing, frequent hand washing and surface disinfection. However, all these measures have proven insufficient to eradicate short and long-range infections, confirming the need for engineering tools to control the indoor air quality. Although the role of ventilation design in the minimization of indoor pollutants has been widely discussed, its performance has been linked to energy efficiency. General-volume ventilation strategies have been predominant. However, in a dynamic indoor environment, airflow patterns increase or decrease the risk of airborne transmission at local points, making this consideration an unsuitable option to provide clean air in the breathing zone. The present research demonstrates the purging efficiency of breathing-zone-volume ventilation against the traditional general-volume choice by comparing mixing, stratum and impinging jet ventilation. CFD has been used to predict indoor airflow, simple thermal sensation through draught discomfort and purging efficiency through age of air in a general-purpose building applying RANS modelling. Results show that breathing-zone-volume strategies significantly improve the age of air under cooling mode and sustain or slightly improve it under heating mode. However, draught sensation slightly increases in all the cases. In conclusion, a balance must be reached in this post-pandemic era to satisfy the design triad: purging efficiency, thermal comfort and energy efficiency without sacrificing one of these three elements.

KEYWORDS

Breathing-zone-volume ventilation; Age of air; Air draught; RANS; Steady-state

1 INTRODUCTION

Pandemics and epidemics have historically impacted the development of public health and the surrounding environment: the Bubonic Plague (18th century) contributed to urban planning, the Cholera epidemics (19th century) encouraged sanitary protocols, and the Spanish Flu (20th century) promoted non-pharmacological interventions as mitigation strategies for disease control (Lai et al., 2020). The recent COVID-19 pandemic (21st century) has also exposed the need for prophylactic measures and the value of non-pharmacological interventions such as social distancing, mask-wearing and the control of the built environment (Kwon et al., 2021). Furthermore, pandemics caused by airborne transmitted diseases have increased in the past decade, as evidenced by the SARS-CoV-1 outbreak in 2003 (Asia), MERS-CoV in 2012 (Middle East) and SARS-CoV-2 in 2019 (worldwide), because of technological and demographic changes (Baker et al., 2021). Following history, building design and ventilation

control are of the utmost importance to prevent and manage cross-infection and future pandemics.

Within the built environment, portable cleaners and UV light filters have been implemented, as well as an increase in minimum ventilation rates for occupied buildings. Additionally, while the role of ventilation design in the minimization of indoor pollutants – viral or otherwise – has been widely discussed, its performance has often been linked only to energy efficiency (Awbi, 2017). In this context, general-volume ventilation strategies, where the probability of infection may be assumed as independent from the location inside a room, have been predominant. However, in a dynamic indoor environment, airflow patterns increase or decrease the risk of airborne transmission at local points, making the general-volume consideration an unsuitable option to provide clean air in the breathing zone.

In contrast, breathing-zone-volume ventilation targets the circulation of fresh air in the breathing zone and can directly tackle airborne pathogens generated by human respiratory activities, minimizing cross-infection. While this type of ventilation is not new, it has often been overlooked for general-purpose building application in favour of the more conventional general-volume ventilation due to the pre-pandemic focus on energy efficiency, thermal comfort, odour control and such. In this post-pandemic era, a paradigm shift that unlocks newly purposed ventilation systems must occur (Morawska et al., 2021).

The aim of the present research is to demonstrate the application of breathing-zone-volume ventilation, specifically, stratum and impinging jet ventilation, on a general-purpose building. Performance was analysed based on purging efficiency, calculated through the Age of Air (AoA), and thermal comfort, calculated through draught sensation. A conventional general-volume, mixing ventilation strategy has also been analysed as a reference. Computational Fluid Dynamics (CFD) has been used for a RANS, steady-state analysis of the target building under heating and cooling conditions. The overarching objective of this study is to establish the basis of newly-purposed ventilation strategies that focus on infection control as well as generate discussion for future trends.

2 METHODS

The investigation utilized CFD to predict the spatial distributions of airflow and contaminant purging through AoA. The commercial software ANSYS Fluent 2021 R1 was used. Since an accurate prediction is essential to ensure reliable results, quality control and mass balance were carefully monitored while the residuals of the conserved variables were kept at 1×10^{-5} , according to the guidelines of convergence indicated in ANSYS Fluent Manual.

2.1 General-purpose building model

A simplified, empty room with dimensions of 6.0m(length)×6.0m(width) ×3.0m(height) was considered for demonstration (Figure 1). Three cases of ventilation strategies for this empty room were studied: a) mixing ventilation, as the reference general-volume ventilation; b) stratum ventilation; which supplies air to the head (breathing) level, generating a sandwiched airflow, and c) impinging jet ventilation, which delivers fresh air to a room based on a supply duct delivering air impinging onto the floor and extracts it at ceiling level, as the two types of breathing-zone-volume ventilation. Inlets and outlets dimensions, chosen according to commercially available products, are presented in Table 1 while room and mesh design are shown in Figure 1.

This room was equipped with two types of inlets/outlets: V) which refers to the ventilation system transporting outdoor air into the enclosure and subsequently discharging it directly out of the building; and, AHU) which corresponds to the recirculation system (air handling unit), assumed to have 100% filtering. Depiction of this distribution can also be seen in Figure 1.

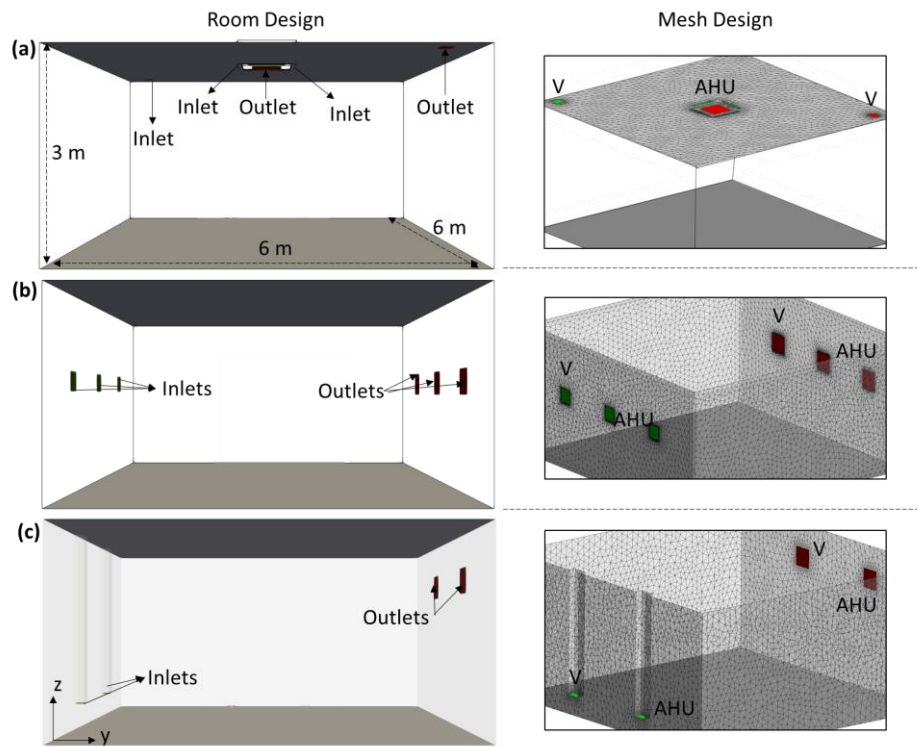


Figure 1: Room and mesh design of the general-purpose building for (a) mixing, (b) stratum and (c) impinging jet ventilation strategies

Table 1: Inlets and outlets dimensions

Cases	Inlet dimensions [m]	Number of inlets	Outlet dimensions [m]	Number of outlets
Mixing	0.2×0.2; 0.6×0.02	1; 4	0.5×0.5; 0.2×0.2	1; 1
Stratum	0.3×0.3	3	0.4×0.4	3
Impinging jet	0.3×0.15	2	0.4×0.4	2

2.2 Airflow and turbulence model

The indoor environment in this study was predicted by CFD, solving the Reynolds-averaged Navier Stokes (RANS) equations under steady state through the SIMPLE algorithm. A second order upwind scheme was chosen for the convection term and buoyancy was treated through the Boussinesq approximation. The renormalization group (RNG) $k-\varepsilon$ model was used for turbulence due to previous literature indicating its superior performance (Chen, 1995). In response to the COVID-19 pandemic, international standards have raised the minimum requirement of outdoor airflow to 10 L/s per person (European Standards, 2019). Therefore, the present study has also set this minimum requirement with an occupancy of two persons. Inlets were set as velocity inlet while outlets were considered as free-slip and the no-slip condition was assumed for all walls. Turbulent intensity was set at 10% and the length scale was defined as 1/7 of the inlet height. Adiabatic wall conditions were considered for all calculations. During summer, inlet temperature was set at 21 °C and during winter at 25 °C. As a simple thermal comfort analysis, draught sensation was calculated as:

$$D_s = \frac{v_{oc}}{v_{max}} \times 100 \quad (1)$$

Where D_s is the draught sensation, expressed as a percentage from the least (0%) to the highest discomfort (100%), v_{oc} is the velocity magnitude of air in the occupied zone (0.0 to 1.8 m) and v_{max} is the maximum velocity magnitude threshold for discomfort, set in this study at 0.2 m/s.

2.3 Age of air

The age of air is defined as the mean time taken for air molecules arriving within the indoor environment through an inlet to travel to the measurement point. In this study, the mean age of air has been calculated through a user defined function (UDF), based on the ventilation efficiency scales for spatial distribution of contaminants, proposed by Kato and Murakami (1988), where SV3 denotes the age of the supply air and is defined by the following equations:

$$SVE3 = \frac{c'_x(X)}{c_s} \quad (2)$$

$$C_s = \frac{q}{Q} \quad (3)$$

Where $SVE3(X)$ [-] is the Scale for Ventilation Efficiency 3, at position X, $C'_x(X)$ is the contaminant concentration in case of uniform contaminant generation throughout the room, q is the contaminant generation rate and Q is the airflow rate. Further details can be found in the cited literature.

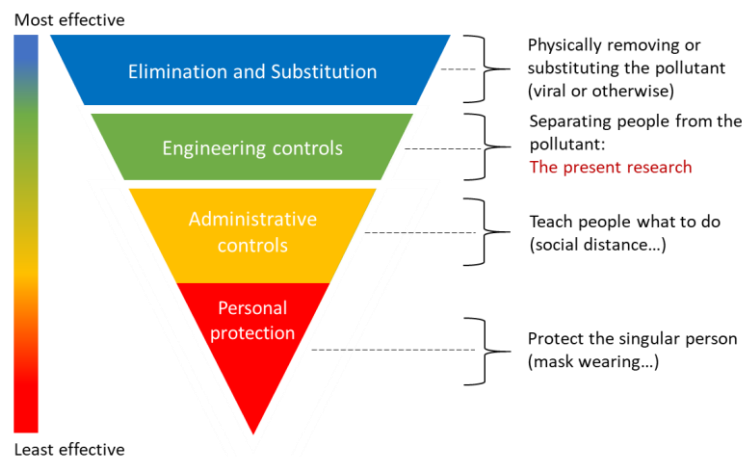


Figure 2: Infection control pyramid adapted from the CDC

3 RESULTS AND DISCUSSION

According to the US Centre for Disease Control (CDC, 2015), building ventilation is an engineering tool to reduce cross-infection and protect human life, ranking second in effectiveness, according to Figure 2. Ventilation should always consider other secondary measures like administrative controls to instruct people on what to do in case of a pandemic, and personal protection for inhabitants like masks, gloves and gowns. However, the following results only consider ventilation as an engineering control, not analysing other elements below

this level in the infection control pyramid. Furthermore, no pharmacological factors are included, such as vaccination effects.

Contours of the air velocity magnitude distribution on representative planes for different ventilation strategies under heating and cooling modes are illustrated in Figures 3 and 4, respectively. During winter, the airflow quickly tended towards the ceiling due to the higher temperature of the air supply when compared to the room air (thermal buoyancy), tending to rise above the breathing zone. The supply jet momentum was high in the direction of the inlets but rapidly lessened its impact as it distributed into the room, diminishing the probability of draught discomfort. Mixing ventilation created a more stagnant air in the occupied zoned, defined between 0.0 and 1.8 meters, while impinging jet ventilation generated more air movement. During summer, the supply jet tended towards the floor, increasing the mixed air in the mixing ventilation case as well as the penetration distance of the jet for the stratum and impinging jet ventilation cases. In all cases, a marked non-homogenous distribution of indoor air can be seen, with higher magnitudes near supply inlets and lower ones near the walls and corners of the room. The AHU of the mixing ventilation system during heating mode (Figure 3) created a Coanda effect, not allowing the filtered air of recirculation system to reach the breathing zone.

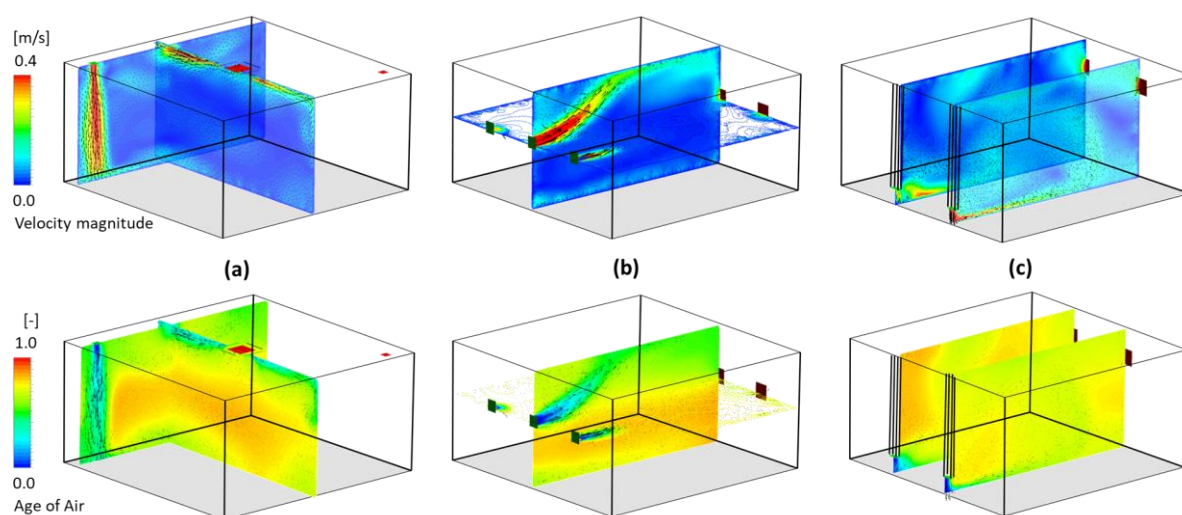


Figure 3: Velocity magnitude and normalized age of air distributions for (a) mixing, (b) stratum and (c) impinging jet ventilation strategies under heating mode

Contours of the normalized age of air also presented in Figures 3 and 4 for heating and cooling mode, respectively. In this study, “new” air was assumed to be injected from both the ventilation and the AHUs. A non-uniformity was present in both heating and cooling modes and, in the case of mixing ventilation, the age of air in the vicinity of the inlet vents was markedly lower than in the vicinity of the outlets and other parts of the room where the penetrating jet had lesser impact. For stratum and impinging jet ventilations, stratification in the age of the air was confirmed, with older air tending above the breathing zone, purging the occupied zone from older air and potential pollutants.

These results mark the relevance of local ventilation efficiency, both locally and horizontally, especially when considering airborne transmission for future ventilation design. In order to compare quantitatively the values of the age of air and draught sensation, this study has chosen as “local” environment the occupied zone (0.0 to 1.8 m) to be on the safety side.

Table 2 presents the results of the different ventilation strategies under heating and cooling mode. The table shows that in heating mode, the values of age of air were either maintained or slightly decreased when compared to the mixing ventilation strategy but the draught sensation increased when stratum and impinging jet ventilation were applied. In contrast, age of air

markedly improved when breathing-zone-volume ventilation was used under cooling mode, with a difference of more than 50% when mixing and impinging jet ventilation were compared. However, draught sensation increased for all cases when compared to the mixing ventilation one.

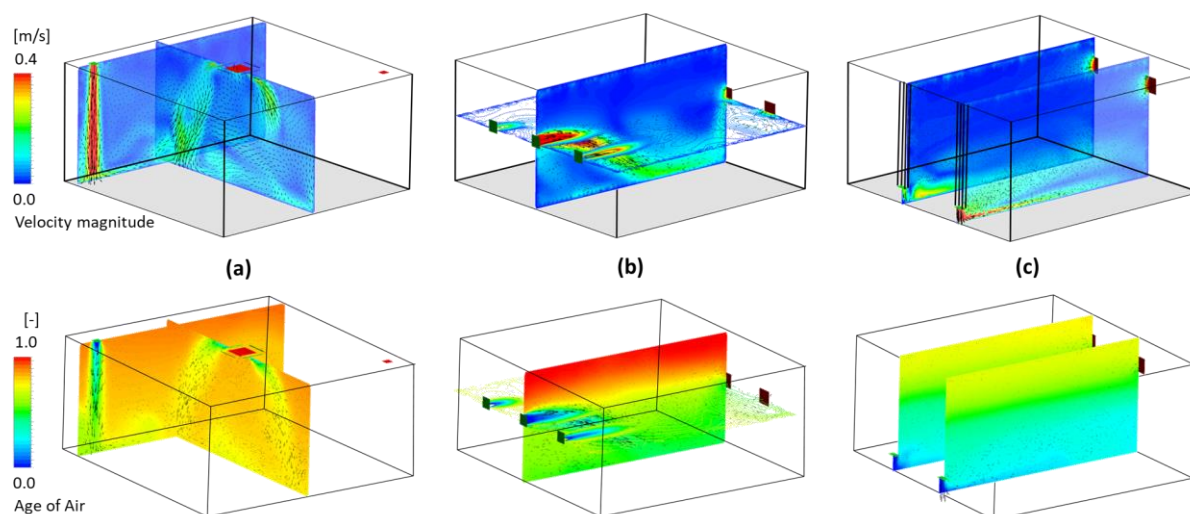


Figure 4: Velocity magnitude and normalized age of air distributions for (a) mixing, (b) stratum and (c) impinging jet ventilation strategies under cooling mode

Table 2: Volume-averaged age of air [-] and draught sensation [%] in the occupied zone

Cases	Heating		Cooling	
	Age of Air [-]	Draught sensation [%]	Age of air [-]	Draught sensation [%]
Mixing	0.68	12.88	0.74	28.93
Stratum	0.68	13.18	0.57	22.85
Impinging jet	0.63	31.28	0.33	24.11

It was confirmed that cooling mode results regarding age of air and draught sensation were generally better than heating mode results. Horizontal air strategy (stratum) and mixed air strategy in heating mode had similar results because of thermal buoyancy, allowing the warmer air to directly travel to above the breathing zone, minimizing the improvements. Furthermore, the downward flow trend of the mixing ventilation strategy in cooling did not affect the occupied zone in all cases, increasing the age of air and risk of cross-infection.

Results showed that applying breathing-zone-volume ventilation improved the age of the air circulating in the room, particularly under cooling mode; however, thermal comfort, measured through draught sensation, decreased when compared to the reference ventilation. From this point of view, a balance must be reached between thermal comfort and purging efficiency by adjusting the practical parameters of location, ventilation rate and so on.

The change of these parameters can be done by optimizing values established by the multiple guidelines, standards and regulations in the architectural field. Then, one of the coming challenges becomes the in-depth analysis of minimum ventilation requirements. Although this study has maintained the recommended 10 L/s per person in accordance with newly established regulations, is this value still adequate in a post-pandemic era or should it be increased as a prophylactic measure? The second challenge comes through the shift from general-volume to breathing-zone-volume ventilation, knowing the purging efficiency of the latter is higher, while redesigning a thermally comfortable and energy-efficient environment (a paradigm shift).

Furthermore, this study has used AoA to evaluate the indoor environment for potential contaminant behaviour, as usually done in a pre-pandemic era. However, a ventilation index that considers non-homogeneity should be considered, as proposed by Lim et al., 2013 and Ikegaya et al., 2022. Net escape velocity can reflect in detail the probability of airborne infection in a non-uniform environment and will be considered in a future stage.

Finally, while this paper presents the basis for future research, several limitations must be considered: although quality control in the simulations has been maintained, no experimental validation was carried out. Since this study is intended as an initial demonstration, no parameterisation to optimize outdoor ventilation rate, inlet/outlet location and temperature has been considered. Although a simple thermal comfort analysis has been considered through draught sensation, a more thorough approach is needed in future steps.

4 CONCLUSIONS

The current study investigated the purging effectiveness of general-volume – mixing – ventilation and breathing-zone-volume – stratum and impinging jet – ventilation under heating and cooling mode for a general-purpose building. The recently established international requirement of 10 L/s was set as outdoor airflow condition. This study showed that stratum and impinging jet ventilation greatly improved the age of air in the room under cooling mode, while sustaining – stratum – or improving – impinging jet – age of air under heating mode. Breathing-zone-volume ventilation directly provides fresh air into the breathing zone, lowering contaminants but producing a slightly stronger draught sensation which can impact thermal comfort. Although the occupied zone was able to show somewhat localized results, an exact consideration of local conditions must be used to establish a new ventilation index for non-homogeneous conditions that considers airborne transmissions.

This paper generates critical thinking in the following point: in a post-pandemic era, respiratory infection due to airborne pathogens must be recognized as a risk and consequently, ventilation design should be re-oriented to attack this issue. A balance must be sought between the existing triad in the indoor environment: purging efficiency, thermal comfort and energy efficiency.

Although valuable lessons were learned from previous pandemics, the world was still unprepared for COVID-19. Following historical trends, the next pandemic is not a remote possibility and a re-thought ventilation bedrock must be established to safeguard human health in the indoor environment while keeping a functioning everyday society.

5 ACKNOWLEDGEMENTS

Fugaku computational resources were provided by the HPCI System Research Project (ID: hp210086) as well as MEXT as “Program for Promoting Researches on the Supercomputer Fugaku” and used computational resources provided by RIKEN Center for Computational Science.

This research was partially supported by JST CREST “Creation of fundamental technologies by interdisciplinary research to coexist with infectious diseases including COVID-19” (Issue name: Development of the integrated risk assessment system for the viral droplet infection on a supercomputer and its social implementation), Grant Number JPMJCR20H7, Japan..

6 REFERENCES

Ansys Fluent. *Release 2021 R1, User Guide, Judging Convergence*, ANSYS, Inc.

Awbi, H. (2017). Ventilation for Good Indoor Air Quality and Energy Efficiency. *Energy Procedia*, 112, 277-286.

- Baker, R., Mahmud, A., Miller, I., Rajeev, M., Rasambainarivo, F., Rice, B., Takahashi, S., Tatem, A., Wagner, C., Wang, L.-F., Wesolowski, A., Metcalf, J. (2022). Infectious disease in an era of global change. *Nature Reviews Microbiology*, 20, 193-205.
- CDC. (2015). Hierarchy of Controls. Centres for Disease Control and Prevention.
- Chen, Q. (1995). Comparison of different k- ϵ models for indoor air flow computations. *Numerical Heat Transfer, Part B: Fundamentals*, 28, 353-369.
- European Standards. (2019). EN 16798-1 & 2:2019: *Energy performance of buildings – Ventilation for buildings – Part 1: Indoor environmental input parameters for design and assessment of energy performance of buildings addressing indoor air quality, thermal environment, lighting and acoustics*.
- Ikegaya, N., Sandberg, M., Ito, K. (2022). Rigorous mathematical formulation of net escape probability determining a macroscopic concentration. *Indoor Air* 32 (7) 13072.
- Kato, S., Murakami, S. (1988). New ventilation efficiency scales based on spatial distribution of contaminant concentration aided by numerical simulation. *ASHRAE transactions*, 94, 309-330.
- Kwon, S., Joshi, A., Lo, C.H., Drew, D., Nguyen, L., Guo, C.G., Ma, W., Mehta, R., Shebl, F., Warner, E., Astley, C., Merino, J., Murray, B., Wolf, J., Ourselin, S., Steves, C., Spector, T., Hart, J., Song, M., VoPham, T., Chan, A. (2021). Association of social distancing and face mask use with risk of COVID-19.. *Nature Communications*, 12, 3737.
- Lai, K. Y., Webster, C., Kumari, S., Sarkar, C. (2020). The nature of cities and the Covid-19 pandemic. *Current Opinion in Environmental Sustainability*, 46, 27-31.
- Lim, E. Y., Ito, K., Sandber, M., (2013). New Ventilation Index for evaluating imperfect mixing conditions - Analysis of Net Escalate Velocity based on RANS approach. *Building and Environment* 61, 45-56.
- Morawska, L., Allen, J., Bahnfleth, W., Bluysen, P.M., Boerstra, A., Buonanno, G., et al. (2021). A paradigm shift to combat indoor respiratory infection. *Science*, 372 (6543), 689-691.

How the COVID Pandemic and the Energy Crisis Have Influenced Indoor Environmental Conditions in non-residential Buildings

Aurora Monge-Bario¹, Ainhoa Arriazu-Ramos², María Fernández-Vigil³, Ana Sánchez-Ostiz Gutiérrez⁴

*1 School of Architecture
Universidad de Navarra
Campus Universitario 31009
Pamplona, Spain*

**Corresponding author: amongeb@unav.es*

*2 School of Architecture
Universidad de Navarra
Campus Universitario 31009
Pamplona, Spain*

*3 School of Architecture
Universidad de Navarra
Campus Universitario 31009
Pamplona, Spain*

*4 School of Architecture
Universidad de Navarra
Campus Universitario 31009
Pamplona, Spain*

ABSTRACT

Building energy behaviour and indoor environmental conditions have been changing due to different external events that have been taking place at global level from 2020, from the COVID pandemic (2020-2022) to the energy crisis (mainly from the war in Ukraine from February 2022). During these events, existing naturally ventilated (NV) buildings have had to balance minimum thermal comfort, high levels of ventilation (to reduce CO₂ concentration and risk of infection) and the lowest energy costs. Museums and schools are examples of non-residential buildings with different but high specific requirements of thermal comfort and Indoor Air Quality (IAQ). In the case of educational buildings, these requirements are demanding, since the users are children and adolescents who need to concentrate for learning and wellbeing. Schools are occupied during specific class schedules and with high levels of occupancy in the classrooms. On the other hand, demanding requirements are also characteristic of museums, which must ensure adequate indoor environmental conditions for the conservation of collections, all year during all hours of the day, but with low levels of occupancy.

This study presents three case studies, two high schools and a museum, in a location with a temperate climate in the North of Spain. They are NV buildings with low levels of energy performance, working with oil boilers without adequate control and regulation of the heating system. The analysis is based on heating energy consumption and monitoring data from 2019 (previous to the COVID pandemic), during 2020/2021 and 2021-22 (during COVID pandemic) and until 2023 (without any COVID restrictions and during an energy crisis). In addition, the study includes the analysis of questionnaires to the staff (directors and secretaries, and maintenance personnel) and managers (from the public regional administration), regarding their switch of their environmental perceptions and priorities from prior COVID to post COVID and energy crisis. In addition, some answers about their preferences in relation to the energy retrofit priorities for the buildings they have in charge were collected.

School data shows how high level of CO₂ concentration prior to the pandemic, are followed by two years of low and adequate levels for a NV buildings during COVID (mean values of 1000ppm). However, after the pandemic, CO₂ concentration levels have risen due to the new concerns for energy costs in the two case studies (to mean values of 1500ppm). In all case studies, indoor temperatures have been balanced during COVID to a minimum but with a high energy consumption (up to 30%); and finally in 2022-23, consumption has decreased a 10% since before COVID consequently worsening IAQ. The study of existing NV buildings dealing with external events, helps understanding the potential and benefits of NV. Lessons learned should be considered in the upgrade of existing buildings.

KEYWORDS

Thermal comfort, monitoring, surveys, naturally ventilated, energy consumption

1 INTRODUCTION

Existing naturally ventilated (NV) non-residential buildings have to ensure adequate Indoor Environmental Quality (IEQ) with low energy costs and without mechanical ventilation (MV). In locations with cold winters and during the external events that have affected worldwide since 2020 (COVID pandemic and energy crisis), balance thermal comfort and adequate Indoor Air Quality (IAQ) has been a challenge only possible with a high compromise of staff and/or occupants.

Monitoring systems suppose a useful tool to control the efficiency of the manual actions in these NV buildings, even low costs systems and/or covering only selected spaces of the building, to understand their global performance (Monge-Barrio et al., 2022). Schools and other public buildings opened even during pandemic in Spain (from September 2020) laying on the promotion of natural ventilation, and in some buildings supported on data of these systems registering temperatures and CO₂ concentration.

On 2022 and after the COVID pandemic, have emerged new external events as an energy crisis (affecting increasing energy prices and risk of provisions) that also affects worldwide very directly to NV buildings, that have to manage thermal comfort and IAQ with energy consumption and increasing energy costs.

This study goes throughout these four winters (from 2019-20 to 2022-23) to investigate the shift among different environmental parameters and energy performance, with three Case Studies of non-residential buildings (a museum and two high schools) through the analysis of monitoring data (temperature and CO₂ concentration), heating consumption data available of two of the buildings, and surveys to relevant staff in charge.

2 METHODS

2.1 Climate

The study analyses IEQ in three different non-residential buildings located in Pamplona, in the North of Spain, with a temperate climate without a dry season, Cfb “oceanic” according to Köppen-Geiger classification. Following data from the 1980–2010 climate series of the Spanish State Meteorological Agency, AEMET (see www.aemet.es), mean annual temperature is 12.7 °C, January being the coldest month of the year, with a monthly mean of 5.2 °C and a monthly average minimum of 1.4 °C.

2.2 Case Studies

This study is focused on two typologies of non-residential buildings with high and different requirements on indoor environmental conditions as a museum and a high school. In museums, the main objective for the collection maintenance is primarily focused on the stability of relative humidity (RH), and with some thresholds of minimum and maximum temperature and RH, always maintaining low daily swings (ASHRAE, 2011). In schools, RH swings are not relevant but maintaining adequate temperatures and IAQ within some ranges in relation to Categories of buildings. However, existing buildings naturally ventilated (without mechanical ventilation, NV, and without Air Conditioning, AC) and with heating systems, present a challenge to maintain adequate environmental conditions according to their use. While the buildings are not upgraded and during external events that have affected worldwide IEQ and consumption in

buildings, they have to balance manually thermal comfort, IAQ and energy consumption. This study analysed data and surveys of three buildings (Fig.1) that are briefly described below.

The museum of Navarra (MN) is the main public museum in the Community of Navarra, with collections from the antiquity to nowadays. The Museum of Navarre has been located in an old Hospital of sixteenth century since 1956, after two main rehabilitations in that year and later in 1990. The building has a longest wing dedicated to exhibitions, with south-west and northeast orientations without any shading, and a shortest wing with office spaces. The ground floor incorporates an old chapel (as an exhibition hall), an Auditorium, and different rooms for temporary and permanent exhibitions, and a basement under a courtyard with a large central skylight that also accommodate permanent collection.

MN building has a heating system with two diesel boilers, with manual regulation according to use and climate, and with temperature sensors per circuit, and with radiator. Only the total annual and quarterly consumption of diesel is available. The museum has portable humidifiers and dehumidifiers in some rooms to control manually RH. Only photo library in the basement, some offices in the administration area, children's workshops, and the Auditorium, have some punctual AC systems, but those rooms are not studied in this analysis (Monge-Barrio et al., 2021).

High School IES.NV (from its acronym in Spanish) was built in 1971 with a spinal typology of building, being classrooms mainly facing South-West. Only windows have been renovated during the last 10 years. The building also has an oil boiler and radiators, and the system is only regulated by on/off with a schedule per circuit (6 circuits, one per each main wing of 9 classrooms), and there are no thermostatic valves on the radiators. Heating consumption is collected manually and monthly by the staff.

High School IES.PC (from its acronym in Spanish) was built in 1944 with a squared-shaped and courtyard typology of building. Some windows are not yet upgraded, and even some of them are fixed. Unfortunately, there is not available specific heating consumption data in this school, what suppose a usual barrier to improve and optimize energy performance in existing buildings.



Figure 1: Non-residential Case Studies: Museum of Navarra, IES.NV and IES.PC High Schools

2.3 Monitoring and data consumption

In these buildings, having a monitoring system have supposed an important tool in which lean on to balance IEQ during these events. Although installed in different moments and with different parameters, all of them has *Sensonet* sensors connected via radio to a central data logger, displaying 10-min data. Summary of available monitoring data for analysis is shown in Table 1.

Table 1: Summary of available monitoring data in Case Studies

Winter	Situation	IES_NV Monitoring data	IES_PC Monitoring data	MN Monitoring data
2019-20	COVID, schools closed at March 15th 2020	3-15/03/20	NA	12/19 – 2/20
2020-21	COVID Schools opened*	12/20 – 2/21	NA	12/20 – 2/21
2021-22	COVID Schools opened*	12/21 – 2/22	12/21 – 2/22	12/21 – 2/22
2022-23	Post Covid & Energy crisis	12/22 – 2/23	12/22 – 2/23	12/22 – 2/23

Notes: *. With natural ventilation as main strategy in schools without VAC

Museo de Navarra building has a monitoring system of temperature and RH in the main rooms (and special showcases), in all floors and different orientations (accuracy $\pm 0,4$ °C in temperature and $\pm 3\%$ in RH), being available for this study data from 2019 to 2023. Heating consumption. CO₂ concentration was registered during the winter 2020-21 with mean values lower than 900ppm due to the occupancy rate, therefore this parameter is not considered in this building. A summary of available data per winter is in Table 2.

Table 2: Monitored rooms in Museum of Navarra MN and parameters

Room	Floor/ Orientation	19-20 (Dec to Feb)	20-21 (Dec to Feb)	21-22 (Dec to Feb)	22-23 (Dec to Feb)
“Prehistory and Roman”	BM / Skylight	T/HR	T/HR	T/HR	T/HR
Temporary Exhibitions	GF / -	T/HR	T/HR	T/HR	T/HR
“Middle Ages”	F1 / -	T/HR	T/HR	T/HR	T/HR
“Roman”	F1 / W	T/HR	T/HR	T/HR	T/HR
“Middle Ages, paintings 1”	F2 / W	T/HR	T/HR	T/HR	T/HR
“Middle Ages, paintings 2”	F2 / N	T/HR	T/HR	T/HR	T/HR
“Goya”	F3 / E	T/HR	T/HR	T/HR	T/HR
Room of restoration	F2 / E&S	T/HR	T/HR	T/HR	T/HR
“20 th century, paintings, 1”	F4 / W	T/HR	T/HR	T/HR	T/HR
“20 th century, paintings, 2”	F4 / W	T/HR	T/HR	T/HR	T/HR

IES.NV High School has monitored some selected classrooms till winter 2021-22 when a new system with sensors in all classrooms in the building were installed. For the purposes of this study, only the original monitored classrooms selected in different floors, were analyzed to compare (Table 3). Some classrooms on 2020-21 had PM_x measures, and some corridors in the following years, although those parameters are not studied for being installed in different spaces. During the first winter pre-COVID, data was registered with low cost mini sensors *Madge Tech* for temperature (accuracy ± 0.5 °C) and *Extech Data Loggers* for CO₂ concentration (accuracy ± 50 ppm), for not having installed the system in the building yet. Those data in March was studied, for being typical for the winter season in the location (Monge-Barrio et al., 2022).

Table 3: Monitored rooms in IES.NV High School and studied parameters

Room	Floor/ Orientation	Rate Occ. (m3/p)	19-20 (March*)	20-21 (Dec to Feb)	21-22 (Dec to Feb)	22-23 (Dec to Feb)
ESO_1C	GF / S	6,38	T/HR/CO2	T/HR/CO2	T/HR/CO2	T/HR/CO2
ESO_2B	GF / S	6,38	T/HR/CO2	T/HR/CO2	T/HR/CO2	T/HR/CO2
ESO_3A	F1 / S	6,13	T/HR/CO2	T/HR/CO2	T/HR/CO2	T/HR/CO2
ESO_3C	F1 / W	4,80	T/HR	T/HR/CO2	T/HR/CO2	T/HR/CO2
ESO_4C	F1 / S	5,80	T/HR	T/HR/CO2	T/HR/CO2	T/HR/CO2
ESO_4F	F1 / S	5,22	T/HR/CO2	T/HR/CO2	T/HR/CO2	T/HR/CO2
BACH_1D	F1 / W	7,14	T/HR/CO2	T/HR/CO2	T/HR/CO2	T/HR/CO2
BACH_2B	F2 / S	7,19	T/HR/CO2	T/HR/CO2	T/HR/CO2	T/HR/CO2
BACH_2D	F2 / S	6,56	T/HR/CO2	T/HR/CO2	T/HR/CO2	T/HR

Notes: *- March 3-13th 2020 (8 school days) before Spanish COVID lockdown, registering typical outdoor conditions for winter in the location

PC High School has a monitoring system from 2021 during the last year of pandemic and after that. Classrooms were selected in different floors and orientations, mainly facing streets with medium traffic (Table 4). Some of the classrooms have PMx measures, but was not analyzed in this study.

Table 4: Monitored rooms in IES.PC High School and parameters

Room	Floor/ Orientation	Rate Occ. (m3/p)	19-20	20-21 (Dec to Feb)	21-22 (Dec to Feb)	22-23 (Dec to Feb)
ESO_1C	GF / SW&SE	13,18	NA	NA	T/HR/CO2	T/HR/CO2
ESO_1E	GF / SW	15,00	NA	NA	T/HR/CO2	T/HR/CO2
ESO_1F	GF / SE	13,36	NA	NA	T/HR/CO2	T/HR/CO2
ESO_3F	F1 / SW	11,98	NA	NA	T/HR/CO2	T/HR/CO2
ESO_4C	F1 / SE	10,16	NA	NA	T/HR/CO2	T/HR/CO2
BACH_1B	F2 / SW&SE	8,49	NA	NA	T/HR/CO2	T/HR/CO2
BACH_1F	F2 / SW	9,67	NA	NA	T/HR/CO2	T/HR/CO2
BACH_1G	F2 / SW	12,42	NA	NA	T/HR/CO2	T/HR/CO2
BACH_2C	F2 / SE	9,33	NA	NA	T/HR/CO2	T/HR/CO2
BACH_2H	F2 / SW *	9,46	NA	NA	T/HR/CO2	T/HR/CO2

Notes: NA. Not available, because there was not any monitoring system installed; *- All classrooms face streets but BACH_2H that face a courtyard

2.4 Surveys

Some surveys to personnel in charge of the three buildings were conducted on line (through google forms) during May 2023, that is, at the end of the last winter season studied. These surveys were obtained from building staff (directors and secretaries, and maintenance staff) and managers (from the public and regional administration). The questions are related mainly to the change of their perception before COVID (2020) to post COVID and during an energy crisis (2023), on environmental conditions (indoor thermal comfort in winter and summer, relative humidity, and concentration of CO₂), satisfaction and their relevance. In addition, specific questions about natural ventilation and the relevance of heatwaves impacts in the buildings are included in the surveys.

2.5 Analysis of data

For monitoring data, mean hourly data per classroom of selected rooms in each high school, selecting only learning schedules was studied. In the museum, all data of mean hourly data of selected rooms during all days, due to the main purpose of a museum, that is the maintenance of their collections. The study is based on boxplots of mean hourly data of all spaces of each

building, comparing four winters. Also a comparison of energy consumption in the buildings with available data adjusted by HDD is done, and a summary of the responses of the surveys per kind of building.

3 RESULTS

3.1 Case Study 1. High School IES.NV

IES.NV had some monitoring data of indoor temperatures and CO₂ concentration prior to the pandemic, and all teachers and staff were very aware of the benefits of having data to improve environmental conditions and allow face to face learning of adolescents. Figure 2 shows the potential of a very conscious natural ventilation done manually in classrooms during the two years of the pandemic (mean 1.000ppm), and how it decreased from mean values higher than 2.500ppm in a pre-pandemic winter. However, and following the feedback of the teachers, CO₂ values have increased after the pandemic (1.500ppm mean values), because there is less awareness of the relevance of an adequate IAQ for the education and well-being of adolescents and adults, and due to the concern of trying to balance indoor temperatures with an exponential increase in energy costs. Temperatures are lower than adequate for educational purposes in all the studied winters, as it is established in the standards (e.g. the set point in Spain is 21°C, for new schools).

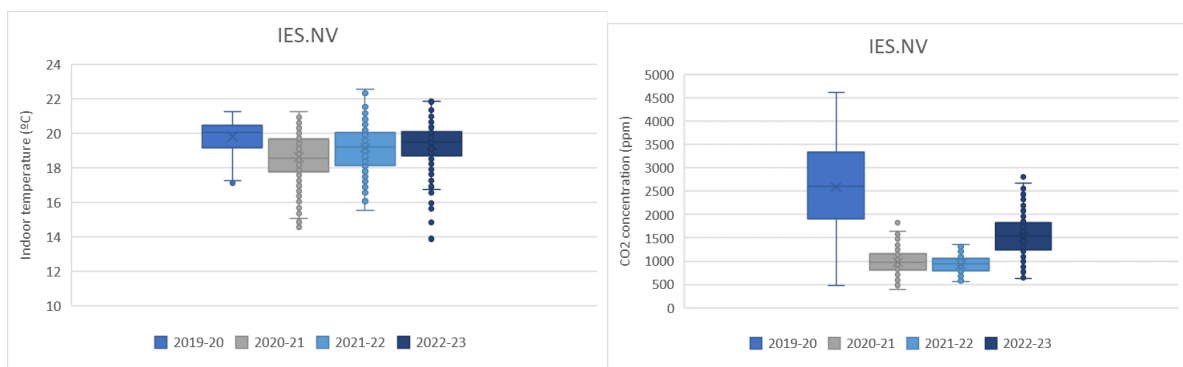


Figure 2: Monitoring data in IES.NV High School during winter months (Dec. to Feb.) of 4 years. Hourly mean values in selected classrooms of indoor temperatures (left) and CO₂ concentration (right)

3.2 Case Study 2. High School IES.PC

IES.PC had only two winter monitoring data, one during pandemic restrictions and the second one during the post pandemic situation. CO₂ concentration presents a similar situation than in IES.NV (Figure 3). During pandemic mean values of CO₂ concentration was 1.000ppm, and in the post pandemic and energy crisis situation the school has mean values near 1.500ppm. It should be noted this similarity, taking into account the differences in occupancy rates due mainly to the higher volume in IES.PC in relation to IES.NV, that should had allowed a better IAQ. Mean temperature during pandemic was lower than 19°C, and the winter post Covid has better adequate mean values for a school, higher than 21°C

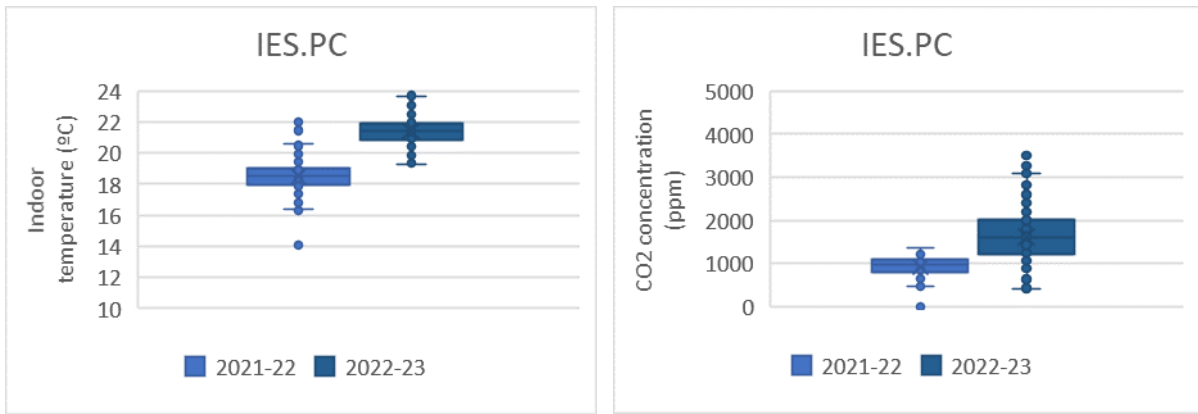


Figure 3: Monitoring data in IES.PC High School during winter months (Dec. to Feb.) of 2 years. Hourly mean values in selected classrooms of indoor temperatures (left) and CO2 concentration (right)

3.3 Case Study 3. Museum MN

MN has a monitoring system for more than 10 years mainly focused on the maintenance of their collections, therefore only with indoor temperature and relative humidity. Data of all building through mean hourly selected data during all hours of the three coldest winter months is shown in Figure 4. Temperatures are slightly higher than 19°C during the first three studied years, with a significant difference during the last year, being lower.

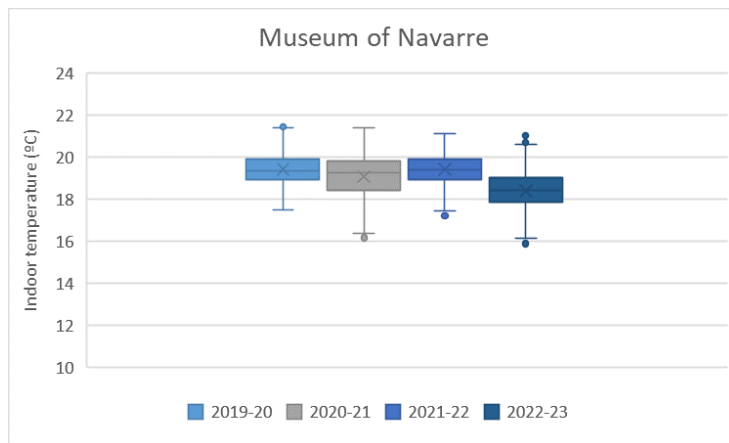


Figure 4: Monitoring data in Museum of Navarra during winter months (Dec. to Feb.) of 4 years. Hourly mean values in selected rooms of indoor temperatures

3.4 Heating energy consumption

Heating energy consumptions of the four studied winters and in two buildings (the museum and IES.NV) are analyzed in relation to the winter 2018/19 previous to the pandemic, and is summarized in Table 5.

During winter 2019/20, both buildings have 15% and 13% less, due to all buildings closed in Spain due to COVID emergency, on March 15th. During COVID, to obtain the difficult balance of minimum acceptable temperatures and the lowest CO₂ concentration to minimize illness risks, High school IES.NV has 31-27% more of normalized energy consumption. However, the museum had only a little impact on the first year, due to the use, the rates of occupancy, and the low rates of natural ventilation, due to the requirements for the conservation of collections. Finally, during Winter 2022/23, heating energy consumption has decreased in both buildings even in respect to the base year 2018/19, between 8-11%, due to the energy crisis and the final

of the COVID emergency. As natural ventilated buildings, this decrease in energy consumption resulted in the detriment of environmental conditions, and specially in relation to IAQ. It should be noted, that in this study, differences in final bills have not been studied for not having the final values.

Table 5: Summary of heating consumption in the high school IES.NV and in the museum MN

	Winter	Heating consumption kWh/m ² annual	HDD (15°C)	kWh/m ² per degree day	Normalized kWh/m ² annual	% variation in relation to winter 18/19 (pre COVID)
IES.NV	2018/19	68,4	1516	0,0451	70,74	
	2019/20	50,4	1310	0,0385	60,32	-15%
	2020/21	79,43	1488,6	0,0593	93,00	+31%
	2021/22	88,49	1548	0,0572	89,62	+27%
	2022/23	57,43	1376,8	0,0417	65,40	-8%
MN	2018/19	60,47	1516	0,0399	62,54	
	2019/20	51,21	1310	0,0391	61,29	-13%
	2020/21	73,28	1488,6	0,0492	77,18	+9%
	2021/22	67,79	1548	0,0438	68,66	-3%
	2022/23	55,06	1376,8	0,0400	62,70	-11%

3.5 Surveys to personnel in charge

Finally, 11 surveys were obtained from building staff (directors and secretaries, and maintenance staff) and managers (from the public and regional administration); 4 from the museum (including one from the collection restorer in charge), and 7 from both High Schools. A summary of them is summarized in Figure 5.

Questions related to the change in perception and summarized in Figure 5 are as follows (1-5, not important to very important):

1. Before COVID, how important was to obtain in the buildings adequate temperatures in winter? and in the actual situation?
2. Before COVID, how was your satisfaction in relation to indoor thermal conditions in winter? how is it in the actual situation?
3. Before COVID, how important was to obtain in the buildings adequate temperatures in summer? and in the actual situation?
4. Before COVID, how was your satisfaction in relation to indoor thermal conditions in summer? how is it in the actual situation?
5. Before COVID, how important was to obtain in the buildings adequate ranges of relative humidity? and in the actual situation?
6. Before COVID, how was your satisfaction in relation to relative humidity? how is it in the actual situation?
7. Before COVID, how important was to consider CO₂ concentration in your building? and in the actual situation?
8. Before COVID, how important was to naturally ventilate your building? and in the actual situation?

Questions related to the perceived importance on different measures to upgrade the buildings, that are summarized in Figure 5, are as follows (1-5, not important to very important):

- a. Substitution of oil boilers with renewable energies
- b. Renovation and improvement of the control and regulation of the heating system
- c. Installation of a new air conditioning system
- d. Installation of mechanical ventilation system
- e. Improvement or substitution of windows
- f. Improvement or substitution of shading
- g. Add insulation on opaque facades
- h. Add insulation on roofs
- i. To include more nature in the environment
- j. To reduce or eliminate traffic around the building

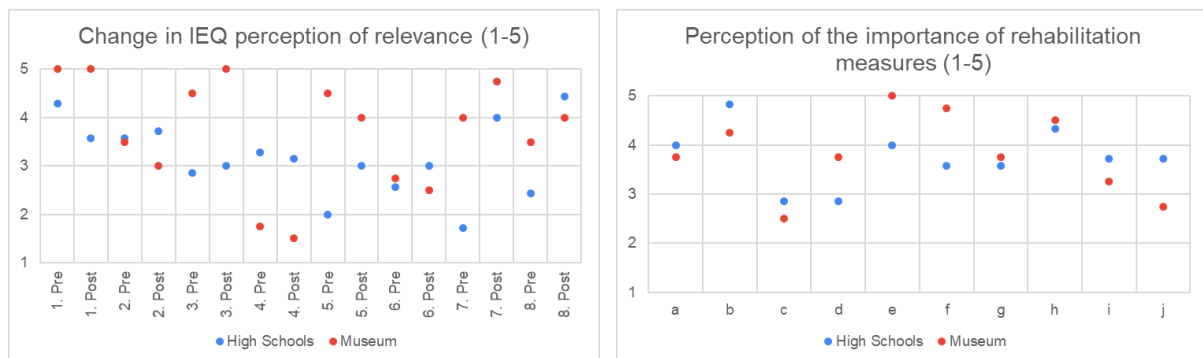


Figure 5: Graphs with summary of surveys results

From the answers of the surveys emerge mainly the change from prior COVID to post COVID and actual energy crisis, on the relevance in schools on indoor air quality (from 1,7 to 4) and natural ventilation (from to 2,4 to 4,4). However, some of them regret how fast awareness about IAQ have decay due to the urgency of maintain minimal temperatures with affordable costs, at the moment the main concern in these buildings.

Due to the specific use of each typology of buildings, there are clear differences between them, even having oil boilers and lacking mechanical ventilation and air conditioning. AC systems are not perceived as relevant in the two kinds of buildings, nor mechanical ventilation in schools. However, an improvement in the heating system, renewable energies and an improvement in the control of the system in the three case studies are the preferred upgrades. In the museum, the preferences for renovation of windows, shadings and insulation in roofs stands out regarding upgrade of thermal envelopes, while in the schools, insulation in roofs.

4 DISCUSSION

Natural ventilated existing buildings require an upgrade especially those with high demanding IEQ requirements, as schools and museums, Staff have to balance thermal comfort, IAQ and energy consumption in a different way according to the different events that have influence buildings worldwide. Upgrade of buildings with HVAC systems are needed but the potential of passive NV should be harnessed not only to rely on energy consumption. In addition, the benefits of mechanical ventilation on IEQ are not well understood as other studies found, probably due to noise, additional energy consumption and difficult of use(Monge-Barrio et al., 2022).

More studies in existing buildings are needed to allow to understand the potential and challenges of natural ventilated buildings during external events that can compromise adequate indoor environmental quality, and therefore wellbeing of occupants.

5 CONCLUSIONS

This study explores building energy behaviour and indoor environmental conditions during four years with different external events that have been taking place at global level from 2020, as the COVID pandemic (2020-2022) and the energy crisis (mainly from the war in Ukraine from February 2022). During these events, existing naturally ventilated buildings had to balance minimum thermal comfort, high levels of ventilation (to reduce CO₂ concentration and risk of infection) and low energy costs. Museum and schools are typologies of non-residential buildings highly demanding but with different requirements.

This study presents three case studies, two high schools and a museum, in a location with a temperate climate in the North of Spain. The analysis is based on heating energy consumption and monitoring data from 2019 (previous to the COVID pandemic), during 2020/2021 and 2021-22 (during COVID pandemic) and during 2022-23 (without any COVID restrictions and during an energy crisis). In addition, the study includes the analysis of questionnaires to the staff, regarding their switch of their environmental perceptions and priorities. Data shows how high level of CO₂ concentration prior to COVID pandemic, are followed by two years of low and adequate levels for a NV buildings during COVID (mean values of 1000ppm). However, after pandemic CO₂ concentration have risen due to the new concerns of the energy costs in the two case studies (to mean values of 1500ppm). Indoor temperatures have been balanced during COVID to the minimum with high energy consumption (up to 30%) even accepting low temperatures for the benefits of face to face learning. However, energy crisis has reduced energy consumption around 10% from pre-COVID consumption affecting IEQ in both kinds of buildings. The relevance of IEQ have risen through the COVID pandemic, although the perception of the upgrade of HVAC systems are mainly focused on the heating system and the renewables and not on mechanical ventilation. Much more research is needed on the performance of existing buildings specially those as schools and museums with high IEQ requirements.

6 ACKNOWLEDGEMENTS

The authors would like to give special thanks to all the directors, secretaries, managers and staff of these buildings, that have participated and supported this study throughout these four years: Museo de Navarra, IES Navarro Villoslada and IES Plaza de la Cruz.

7 REFERENCES

- ASHRAE. (2011). *Museums, libraries and archives*. In: Owen MS, editor. *ASHRAE Handbook. HVAC Appl. SI edition, Atlanta*.
- Monge-Barrio, A., Bes-Rastrollo, M., Dorregaray-Oyaregui, S., González-Martínez, P., Martín-Calvo, N., López-Hernández, D., Arriazu-Ramos, A., & Sánchez-Ostiz, A. (2022). Encouraging natural ventilation to improve indoor environmental conditions at schools. Case studies in the north of Spain before and during COVID. *Energy and Buildings*, 111567. <https://doi.org/10.1016/j.enbuild.2021.111567>
- Monge-Barrio, A., Miguel-Bellod, J. S., Arriazu-Ramos, A., González-Martínez, P., & Sánchez-Ostiz, A. (2021). Adapting Buildings to Climate Change: Case Study of a Museum in the North of Spain. In Springer Nature (Ed.), *Handbook of Climate Change Mitigation and Adaptation*. https://doi.org/10.1007/978-1-4614-6431-0_134-1

The impact of increased occupancy on particulate matter concentrations in mechanically-ventilated residential buildings in a subtropical climate.

German Hernandez^{*1,2}, Rafael Borge¹, Dan Blanchon^{2,3}, and Terri-Ann Berry²

¹ UNIVERSIDAD
POLITÉCNICA DE MADRID (UPM)
28040 Madrid, Spain

*Corresponding author: hhernandez@unitec.ac.nz

² UNITEC
139 Carrington Street,
Mount Albert, Auckland, New Zealand

³ AUCKLAND MUSEUM
The Auckland Domain, Parnell, Auckland, New
Zealand
Presenting author

ABSTRACT

Indoor air pollution can pose a serious threat to human health and can increase the risk of early mortality. Studies have shown that human exposure to indoor pollution is more common than to outdoor pollution, especially where people spend the majority of their time indoors at home. Heating, ventilating, and air conditioning (HVAC) systems are used in buildings to regulate internal climate to improve the comfort level for occupants. In addition, ventilation rates are often increased to maintain appropriate Indoor Air Quality (IAQ). Inadequate ventilation can limit the removal of substances from inside the building, leading to an accumulation of pollutants resulting from internal sources (e.g., building materials, furnishings, and personal care products). Minimum ventilation rates for buildings are prescribed in standards published by organisations such as the European Committee for Standardization and ASHRAE. However, unlike outdoor air quality, there is currently no common standard or index for IAQ.

The aim of this study is to investigate the impact of high occupancy levels, caused by stay-at-home orders under a COVID-19 lockdown, on IAQ in mechanically-ventilated residential buildings. The study focuses on particulate matter (PM_{2.5} and PM₁₀) in six residential buildings across Auckland, New Zealand's largest city, which has a subtropical climate with characteristic high humidity in the winter. Monitoring took place over a six-week period during winter: three weeks pre-COVID-19 lockdown and three weeks into the lockdown.

Indoor concentrations of PM_{2.5} and PM₁₀ were found to increase during the lockdown period in the majority of the houses (64% and 40% respectively). In contrast, outdoor PM_{2.5} and PM₁₀ concentrations decreased by 34% and 31%, suggesting internal sources were largely responsible for indoor concentrations.

KEYWORDS

Indoor Air Quality, Mechanical Ventilation, Increased Occupancy, COVID-19 lockdown, Particulate Matter

1 INTRODUCTION

Indoor air pollution can be detrimental to human health (Cohen et al., 2005; Donaldson et al., 2001) and can lead to increased mortality rates (Dockery et al., 1993; Hales et al., 2012). Numerous studies have shown that human exposure to indoor pollution is often more common than exposure to outdoor pollution (Logue et al., 2011, 2012; Weschler, 2006), especially where people spend most of their time indoors at home (Klepeis et al., 2001). A 2016 study found that New Zealanders on average spend 68.9% of their time at home indoors (Khajehzadeh & Vale, 2017). The control of indoor air quality (IAQ) inside homes is therefore an important factor for the health and wellbeing of residents.

Inadequate ventilation can prevent escape of substances from within the home and lead to an accumulation of physical pollutants arising from internal sources (e.g., building materials, furnishings, personal care products, pesticides, and household cleaners). The term “Sick Building Syndrome” describes the relationship between the IAQ and its potential effects on occupants (Bernstein et al., 2008), such as headache, respiratory infection, and cognitive function (Taptiklis et al., 2017; Tookey et al., 2019). Ventilation rates are often increased to maintain appropriate IAQ and to reduce the risk of sick building syndrome (ASHRAE, 2013; Fisk et al., 2009; Sundell et al., 2010).

Due to the growing awareness of global warming and climate change, many governments have applied pressure to reduce energy consumption and increase energy efficiency. This has motivated the building industry to innovate and improve technology, leading to more environmentally sustainable buildings. However, energy efficient buildings over the last decade have been shown to increase the concentration of some pollutants (USEPA, 2017). Similarly, despite trying to maintain or improve IAQ with ventilation, some building characteristics can negatively impact IAQ. While ventilation can help reduce concentrations of indoor pollutants, indoor concentrations of pollutants originating from outside can actually increase due to higher ventilation rates (Rackes & Waring, 2016; Weschler & Shields, 2000). A PPV (positive pressure ventilation) system uses mechanical ventilation to extract relatively dry air from the roof space, filter it and blow it into the house, creating a slight positive pressure inside. This positive pressure drives out old, stale air via gaps and cracks in the building fabric.

The Coronavirus disease (COVID-19) pandemic led to the implementation of strict lockdown policies by many countries around the world, including New Zealand, in an attempt to stem transmission of the virus. These lockdowns resulted in (with the exception of essential service workers and businesses) the general public spending the majority of their time at home. This increased occupancy has the potential to elevate concentrations of indoor air pollutants such as PM and VOCs generated by household activities such as cooking and cleaning (Cowell et al., 2023; Laltrello et al., 2022), while also increasing the likelihood of exposure to harmful pollutant levels (Adam et al., 2021; Morawska et al., 2020; Stabile et al., 2021).

New Zealand is an island country in the southwestern Pacific Ocean, divided into two main land masses (North and South Islands) with a total area of approximately 268,000 km². The population is approximately 5.2 million residents with a housing stock of approximately 2 million houses (Stats NZ, 2020a, 2023). Visible mould larger than A4 size is always present in 4.3% of New Zealand homes, while 20% of New Zealand homes suffer from damp (Stats NZ, 2019). 13% of New Zealanders suffer from asthma (Asthma Foundation NZ, 2023). Auckland is New Zealand’s largest city (by population and land mass) and one of the most remote in the world. The city is located in an isthmus in the northern part of the country and has a population

of over 1.6 million. Auckland has a humid, subtropical climate with warm, humid summers and mild winters (Hessell, 1988).

Numerous IAQ studies have investigated the effects of increased occupancy on IAQ, however these primarily focus on buildings which rely on natural ventilation. To improve understanding of the effects of occupancy on indoor pollutant concentrations, in particular where mechanical ventilation systems are installed, this study analysed IAQ parameters (PM_{2.5}, PM₁₀) in homes in Auckland, before and during a COVID-19 lockdown.

2 METHODOLOGY

2.1 Residential Data Collection, Study Location, Eligibility & Recruitment

As part of a longitudinal study, IAQ parameters were monitored for a selection of mechanically-ventilated residential homes across Auckland. The study was conducted over a three-week period prior to the COVID-19 lockdown, followed by a further three weeks during the lockdown period. Six Auckland households fitted with PPV systems were selected for this study. For standardisation, houses were selected with floor areas ranging between 120 and 273 m², comprising three to four bedrooms. Houses were selected where the number of occupants reflected the national average (three to four) (Khajehzadeh & Vale, 2017).

2.2 Air Quality Measurements

Three monitors were located indoors to measure PM_{2.5} and PM₁₀: in the master bedroom, another bedroom and the living area. Outdoor PM measurements were obtained from nearby council-owned air quality monitoring stations. Indoor monitors were positioned 1.0 m above floor level (where possible) and data was collected at five-minute intervals. Details of the monitors used are as follows:

- Type A monitors (designed and created in-house at Unitec). Type A uses a PM sensor to measure PM_{2.5} and PM₁₀ (range 0 - 1,000 µg/m³, with an accuracy of ±15%).
- Type B monitors measure PM_{2.5} and PM₁₀ (range 0 – 500 µg/m³). They were field-tested by the Air Quality Sensor Performance Evaluation Centre (AQ-SPEC) in California, and calibrated with regulatory-grade (Federal Equivalent Method) equipment.

2.3 Quality Control

The low-cost sensors used in this study were pre-calibrated against two commercial grade PM monitors (Aeroqual Dust Sentry Pro, ±5µg/m³ +15% of reading (Aeroqual, 2023)) before the monitoring period. A linear correlation assessed accuracy and provided an equation to offset the monitors, if required. Post-calibration was completed after the monitoring period, using the same monitors (Dust Sentry Pro). The equipment was isolated and co-located for one week. This data was used to run correlation tests between the low-cost sensors and the robust monitors. PM_{2.5} was well correlated with our standard monitoring equipment, yielding R² values in the 0.89 – 0.96 range.

3 RESULTS AND DISCUSSION

3.1 Household Environment, Occupancy Rates and Activity

All six houses were single-storey, open-plan timber construction, with floor and roof insulation. All windows were single-glazed. All houses had some form of heating to the main living areas (heat pumps the most common), while three houses also had heating to the bedrooms. Two households kept indoor plants (in the living and bedrooms). All households comprised at least two adults (two had three adults), while two households included two children, and two included one child. All participants reported that their homes were typically only occupied

outside of business hours (prior to lockdown) and were generally occupied full time during lockdown.

Ventilation rates, based on PPV system installed and house size, varied between 3 and 4 air exchanges per hour. Larger houses require additional fan units to guarantee this air exchange rate. The system uses a deep-pleat nano-fibre filter (F8), with filter media laminated to a nylon monofilament mesh. The filter removes all particles greater than 0.4 μm , and has been tested to meet international (Eurovent and ASHRAE) standards. The PPV system is controlled centrally using an internal algorithm that regulates fan speeds according to the temperature differential measured between rooms and the roof-space. PPV systems were set up to adjust automatically during the study period. Participants confirmed that they did not alter the controls or open windows during the study period.

Potential indoor sources of PM identified included one house with an open fire, one with a heating stove, four houses had greater than 50% floor area carpeted, and four kept dogs or cats. Two houses burned candles or similar naked flame devices indoors, while one household had smoking indoors. All occupants reported they increased the frequency of PM-inducing activities during lockdown such as cooking and vacuuming. All households had an extractor fan in the kitchen and reported using it regularly while cooking.

3.2 Indoor Particulate Matter (PM_{2.5}, PM₁₀)

The average PM concentrations (measured in the living area) across the three-week periods before and during lockdown are presented in Table 1. Three of the residential buildings (D, E and F) showed an increase in PM_{2.5} of between 25% and 62%.

Table 1 – Average indoor concentrations of PM_{2.5} and PM₁₀

Parameter	House:	A	B	C	D	E	F
PM _{2.5} ($\mu\text{g}/\text{m}^3$)	pre-lockdown	0.55	0.73	20.62	4.20	4.96	4.37
	during lockdown	0.80	1.73	21.21	5.24	8.01	5.78
PM ₁₀ ($\mu\text{g}/\text{m}^3$)	pre-lockdown	0.93	1.08	23.51	4.69	5.52	6.05
	during lockdown	0.58	0.36	21.50	6.13	9.00	7.71

This is consistent with findings by (Laltrello et al., 2022) and (Cowell et al., 2023). One house showed a substantial increase in PM_{2.5} of around 136%, while two houses showed minimal change. The change in PM_{2.5} levels for House A was close to the limit of the sensor accuracy. House C was identified as a rural/farming house, where the level of occupational activity outside the home was not affected by the lockdown. This house had the highest indoor concentration of PM_{2.5} both pre and post lockdown. In Auckland, the average household normally spends the majority of its food budget on takeaway meals (32%) (Stats NZ, 2020b). The impact of the lockdown arguably led to many more meals prepared at home than usual (due to the closure of all restaurants and takeaway food outlets), which is likely to have contributed to the observed increases in PM_{2.5}.

Indoor PM₁₀ concentrations increased following lockdown for three of the houses, between 27% and 63%, which is consistent with Laltrello et al. (2022) and Cowell et al. (2023). This may indicate the primary sources of PM₁₀ were internal for these houses. Internal PM₁₀ sources can include smoking, woodfire burning, unflued heaters and burning of candles. House F, for example, contained a fireplace. The other two houses where PM₁₀ increased were geographically sheltered from the nearest roads, so internally generated PM₁₀ is more likely to be the main component of indoor concentrations for these houses, and accordingly increase with occupancy. For the other three houses, the magnitude of change in PM₁₀ was relatively

minor ($< 1 \mu\text{g}/\text{m}^3$) for two of these, while the third house was the farmhouse mentioned previously, where day to day activities were not affected by the lockdown.

Average indoor $\text{PM}_{2.5}$ concentrations for two selected houses for the weeks immediately prior to and following COVID-19 lockdown are shown in Figure 1a and Figure 1c. These show that diurnal $\text{PM}_{2.5}$ peaks during lockdown were higher than those prior to lockdown. Figure 1b and Figure 1d show diurnal profiles for a typical day. The main diurnal peak occurred between 6 and 8pm, with a secondary peak around midday (Figure 1d). These peaks could be created during food preparation which has led to increased internal $\text{PM}_{2.5}$ levels (Laltrello et al., 2022). Background levels of $\text{PM}_{2.5}$ remained relatively low during the lockdown period as expected for people working from home, spending much of the day seated and limiting $\text{PM}_{2.5}$ emissions.

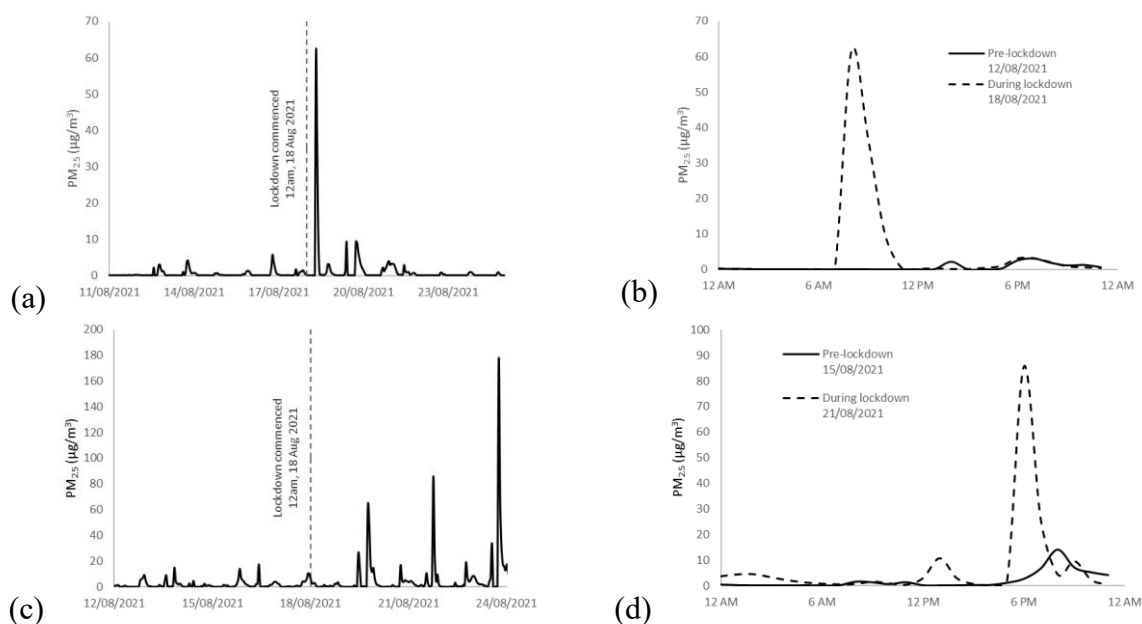


Figure 1 - Indoor $\text{PM}_{2.5}$ concentrations (a) House A, 1-week pre/post lockdown; (b) House A typical diurnal profiles; (c) House D, 1-week pre/post lockdown; (d) House D typical diurnal profiles.

Figure 2a and Figure 2c show indoor PM_{10} concentrations for two selected houses for the weeks immediately prior to and following COVID-19 lockdown. For the same two houses, Figure 2b and Figure 2d show that diurnal concentration peaks during lockdown were of similar magnitude to those prior to lockdown. In general, these occurred during mid-morning and evening time, reflecting peak traffic volumes.

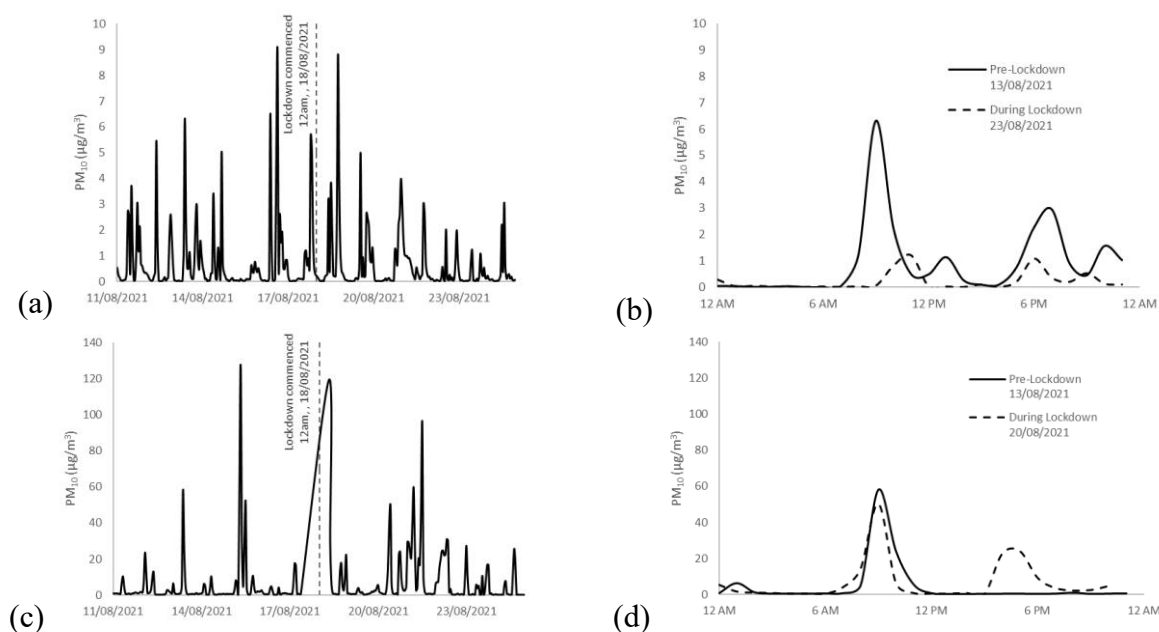


Figure 2 - Indoor PM₁₀ concentrations (a) House B, 1-week pre/post lockdown; (b) House B typical diurnal profiles; (c) House F, 1-week pre/post lockdown; (d) House F typical diurnal profiles.

Average daily PM_{2.5} and PM₁₀ concentrations for each house were compared with the corresponding WHO Air Quality Guidelines (AQG) (15 µg/m³ and 45 µg/m³ for PM_{2.5} and PM₁₀, respectively). In general, the PM_{2.5} limit was exceeded more frequently than the PM₁₀ limit. Similar studies (Algarni et al., 2021; Cowell et al., 2023) have shown that WHO limits are typically exceeded with increased occupancy, but these mostly apply to homes which only have natural ventilation. Prior to lockdown, House C exceeded the PM_{2.5} limit on 16 of the 21 days, while the only other exceedance was one day in House E. During lockdown, House C exceeded the PM_{2.5} limit 11 days out of the 3-week period, House E exceeded on two days, while Houses B and D both exceeded one day. The PM₁₀ limit was only exceeded twice, two different houses, each on a different day, both during lockdown. House C was identified as comprising residents who regularly smoked cigarettes indoors. Cigarette smoking has been shown to increase indoor concentrations of PM_{2.5} up to 28 times that for non-smoking households (Algarni et al., 2021).

The variability in indoor PM concentrations across the household was investigated by comparing PM concentrations between living areas and bedrooms. As expected, PM in bedrooms tended to be lower than in the living areas (60% lower prior to lockdown, 75% lower during lockdown), potentially due to people spending more of their time in the living areas.

3.3 Indoor Vs Outdoor PM

Outdoor PM measurements were obtained from three nearby council-owned urban air quality monitoring stations located across central Auckland. Average PM concentrations were calculated for the three-week periods immediately prior to and following COVID-19 lockdown. Average PM_{2.5} concentrations decreased by 34% (from 7.7 µg/m³ to 5.1 µg/m³), ranging between 30% and 37% for the three stations. PM₁₀ decreased by 31% (from 17.3 µg/m³ to 11.9 µg/m³), ranging between 10% and 39%. Decreases in PM₁₀ and PM_{2.5} were expected due to reduced traffic volumes and restrictions on non-essential commerce and industry during lockdown (Laltrello et al., 2022). Figure 3a and Figure 3b compare indoor and outdoor PM_{2.5} and PM₁₀ levels for a typical house and AQ monitoring station, one week prior to and one week immediately after COVID-19 lockdown. Despite a gradual decrease in outdoor PM

concentrations, indoor concentrations increased during the lockdown. Mechanical ventilation has been shown to substantially reduce indoor concentrations of outdoor-generated pollutants when compared with natural ventilation (Martins & Carrilho da Graça, 2018; Ren et al., 2017), which suggests that internally-generated pollutants are a major contributor to indoor PM concentrations.

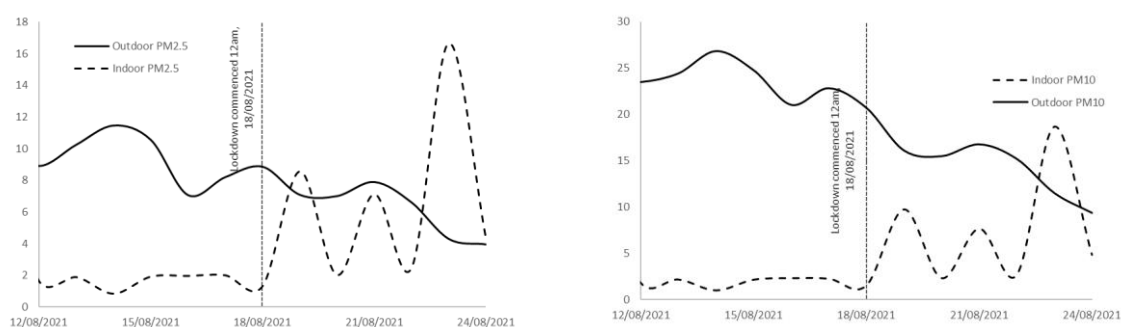


Figure 3 – Indoor vs outdoor PM concentrations, 1-week pre/post lockdown (House D) (a) PM_{2.5}; (b) PM₁₀

Average daily PM_{2.5} and PM₁₀ concentrations for each outdoor monitoring station were compared with WHO (AQG) limits, with only one site exceeding the PM₁₀ AQG for one day over the six-week study period.

PM_{2.5} indoor/outdoor ratios (I/O) were calculated, and prior to lockdown, all but one of the houses had I/O < 1. The one house with I/O > 1 was notable for having pets (two dogs and four cats) and being occupied by smokers, factors which are likely to have elevated indoor PM concentrations. During lockdown, I/O ratios increased in four houses, with three houses having I/O ratios > 1. An I/O ratio of one or less is an indicator that internal sources of PM are not likely to be significant (Lomboy et al., 2015; Yang Razali et al., 2015; Zhou et al., 2016). Where mechanical ventilation with a well-performing filter is installed, the system removes PM from the influent air to offset potential internally-generated PM (Quang et al., 2013; Wang et al., 2006). Increased I/O ratios observed during the lockdown were expected due to the increased occupancy as reported previously, consistent with previous studies (Martins & Carrilho da Graça, 2018).

4 CONCLUSIONS

This study investigates the impact of changes in occupancy rates on IAQ in homes where mechanical ventilation is installed. Outdoor concentrations of PM_{2.5} generally decreased during lockdown (34%, on average compared with pre-lockdown levels). Despite this, indoor PM_{2.5} concentrations were generally found to be between 25% and 62% higher during the lockdown period, suggesting the influence of internal sources relates to occupancy. Furthermore, mechanical ventilation has been shown to substantially limit penetration of outdoor pollutants indoors, suggesting that internal concentrations are even more likely to have originated from internal sources. Diurnal peaks were also observed to be higher during lockdown, with highest peaks typically occurring during evenings. Increased cooking activities at home may be responsible for evening PM_{2.5} spikes.

Indoor PM₁₀ concentrations generally increased during lockdown (40% average) compared with outdoor concentrations, which decreased by 31% on average. Reduced traffic emissions and industrial activity during lockdown may have been directly responsible for reduced outdoor concentrations of PM₁₀ and PM_{2.5}. Increased indoor PM₁₀ concentrations are therefore likely to be due to internal sources, mainly from combustion activities. With the exception of House C,

average daily PM concentrations rarely exceeded WHO Air Quality Guideline limits for short term exposure. Average daily PM_{2.5} concentrations inside House C exceeded the WHO limit 76% of the time prior to lockdown and 52% of the time during lockdown. Average PM concentrations in House C were five times greater than the other houses. House C was identified as a smoking household which is consistent with these results. All six of the mechanically ventilated homes were able to maintain indoor PM levels below the WHO guidelines throughout the duration of the trial, despite the increased levels of occupancy.

5 ACKNOWLEDGEMENTS

We thank HRV New Zealand, the households who participated in this study, and Joanne Low for her generous assistance with this project.

6 REFERENCES

- Adam, M. G., Tran, P. T. M., & Balasubramanian, R. (2021). Air quality changes in cities during the COVID-19 lockdown: A critical review. *Atmospheric Research*, 264, 105823. <https://doi.org/10.1016/j.atmosres.2021.105823>
- Aeroqual. (2023). *Dust Particle Counter | Measure PM10, PM2.5, PM1, AND TSP*. <https://www.aeroqual.com/products/particulate-dust-monitors/dust-sentry-pro-particle-counter>
- Algarni, S., Khan, R. A., Khan, N. A., & Mubarak, N. M. (2021). Particulate matter concentration and health risk assessment for a residential building during COVID-19 pandemic in Abha, Saudi Arabia. *Environmental Science and Pollution Research*, 28(46), 65822–65831. <https://doi.org/10.1007/s11356-021-15534-6>
- ASHRAE. (2013). *Standards 62.1 & 62.2—The Standards for Ventilation and Indoor Air Quality*. <https://www.ashrae.org/technical-resources/bookstore/standards-62-1-62-2>
- Asthma Foundation NZ. (2023). *Key statistics*. <https://www.asthmafoundation.org.nz/research/key-statistics>
- Bernstein, J. A., Alexis, N., Bacchus, H., Bernstein, I. L., Fritz, P., Horner, E., Li, N., Mason, S., Nel, A., & Oullette, J. (2008). The health effects of nonindustrial indoor air pollution. *Journal of Allergy and Clinical Immunology*, 121(3), 585–591.
- Cohen, A. J., Ross Anderson, H., Ostro, B., Pandey, K. D., Krzyzanowski, M., Künzli, N., Gutschmidt, K., Pope, A., Romieu, I., Samet, J. M., & Smith, K. (2005). The global burden of disease due to outdoor air pollution. *Journal of Toxicology and Environmental Health. Part A*, 68(13–14), 1301–1307. <https://doi.org/10.1080/15287390590936166>
- Cowell, N., Chapman, L., Bloss, W., Srivastava, D., Bartington, S., & Singh, A. (2023). Particulate matter in a lockdown home: Evaluation, calibration, results and health risk from an IoT enabled low-cost sensor network for residential air quality monitoring. *Environmental Science: Atmospheres*, 3(1), 65–84. <https://doi.org/10.1039/D2EA00124A>
- Dockery, D. W., Pope, C. A., Xu, X., Spengler, J. D., Ware, J. H., Fay, M. E., Ferris, B. G., Jr, & Speizer, F. E. (1993). An Association between Air Pollution and Mortality in Six U.S. Cities. *The New England Journal of Medicine*, 329(24), 1753–1759. SciTech Premium Collection. <https://doi.org/10.1056/NEJM199312093292401>
- Donaldson, K., Stone, V., Seaton, A., & MacNee, W. (2001). Ambient Particle Inhalation and the Cardiovascular System: Potential Mechanisms. *Environmental Health Perspectives*, 109, 5.

- Fisk, W. J., Mirer, A. G., & Mendell, M. J. (2009). *Quantification of the association of ventilation rates with sick building syndrome symptoms* (LBNL-2035E, 962711; p. LBNL-2035E, 962711). <https://doi.org/10.2172/962711>
- Hales, S., Blakely, T., & Woodward, A. (2012). Air pollution and mortality in New Zealand: Cohort study. *Journal of Epidemiology and Community Health*, *66*(5), 468–473. <https://doi.org/10.1136/jech.2010.112490>
- Hessell, J. W. D. (1988). *The climate and weather of the Auckland region*. National Institute of Water and Atmospheric Research, NIWA.
- Khajehzadeh, I., & Vale, B. (2017). How New Zealanders distribute their daily time between home indoors, home outdoors and out of home. *Kōtuitui: New Zealand Journal of Social Sciences Online*, *12*(1), 17–31.
- Klepeis, N. E., Nelson, W. C., Ott, W. R., Robinson, J. P., Tsang, A. M., Switzer, P., Behar, J. V., Hern, S. C., & Engelmann, W. H. (2001). The National Human Activity Pattern Survey (NHAPS): A resource for assessing exposure to environmental pollutants. *Journal of Exposure Science & Environmental Epidemiology*, *11*(3), 231–252. <https://doi.org/10.1038/sj.jea.7500165>
- Laltrello, S., Amiri, A., & Lee, S.-H. (2022). Indoor Particulate Matters Measured in Residential Homes in the Southeastern United States: Effects of Pandemic Lockdown and Holiday Cooking. *Aerosol and Air Quality Research*, *22*(5), 210302. <https://doi.org/10.4209/aaqr.210302>
- Logue, J. M., McKone, T. E., Sherman, M. H., & Singer, B. C. (2011). Hazard assessment of chemical air contaminants measured in residences—Logue—2011—Indoor Air—Wiley Online Library. *Indoor Air*, *21*(2), 92–109.
- Logue, J. M., Price, P. N., Sherman, M. H., & Singer, B. C. (2012). A Method to Estimate the Chronic Health Impact of Air Pollutants in U.S. Residences. *Environmental Health Perspectives*, *120*(2), 216–222. <https://doi.org/10.1289/ehp.1104035>
- Lomboy, M., Quirit, L., Molina, V., Dalmacion, G., Schwartz, J., Suh, H., & Baja, E. (2015). Characterization of particulate matter 2.5 in an urban tertiary care hospital in the Philippines. *Building and Environment*, *92*, 432–439.
- Martins, N. R., & Carrilho da Graça, G. (2018). Impact of PM2.5 in indoor urban environments: A review. *Sustainable Cities and Society*, *42*, 259–275. <https://doi.org/10.1016/j.scs.2018.07.011>
- Morawska, L., Tang, J. W., Bahnfleth, W., Bluysen, P. M., Boerstra, A., Buonanno, G., Cao, J., Dancer, S., Floto, A., Franchimon, F., Haworth, C., Hogeling, J., Isaxon, C., Jimenez, J. L., Kurnitski, J., Li, Y., Loomans, M., Marks, G., Marr, L. C., ... Yao, M. (2020). How can airborne transmission of COVID-19 indoors be minimised? *Environment International*, *142*, 105832. <https://doi.org/10.1016/j.envint.2020.105832>
- Quang, T. N., He, C., Morawska, L., & Knibbs, L. D. (2013). Influence of ventilation and filtration on indoor particle concentrations in urban office buildings. *Atmospheric Environment*, *79*, 41–52. <https://doi.org/10.1016/j.atmosenv.2013.06.009>
- Rackes, A., & Waring, M. S. (2016). Do time-averaged, whole-building, effective volatile organic compound (VOC) emissions depend on the air exchange rate? A statistical analysis of trends for 46 VOCs in U.S. offices. *Indoor Air*, *26*(4), 642–659.
- Ren, J., Liu, J., Cao, X., & Hou, Y. (2017). Influencing factors and energy-saving control strategies for indoor fine particles in commercial office buildings in six Chinese cities. *Energy and Buildings*, *149*, 171–179. <https://doi.org/10.1016/j.enbuild.2017.05.061>
- Stabile, L., De Luca, G., Pacitto, A., Morawska, L., Avino, P., & Buonanno, G. (2021). Ultrafine particle emission from floor cleaning products. *Indoor Air*, *31*(1), 63–73. <https://doi.org/10.1111/ina.12713>
- Stats NZ. (2019). *One in five homes damp*. <https://www.stats.govt.nz/news/one-in-five-homes-damp/>

- Stats NZ. (2020a). *Housing in Aotearoa: 2020*. <https://www.stats.govt.nz/reports/housing-in-aotearoa-2020>
- Stats NZ. (2020b). *Kiwis growing taste for takeaways and eating out*. <https://www.stats.govt.nz/news/kiwis-growing-taste-for-takeaways-and-eating-out>
- Stats NZ. (2023). *Population*. <https://www.stats.govt.nz/topics/population>
- Sundell, J., Nazaroff, W. W., Cain, W. S., Fisk, W. J., Grimsrud, D. T., Gyntelberg, F., Li, Y., Persily, A. K., Pickering, A. C., Samet, J. M., Spengler, J. D., Taylor, S. T., & Weschler, C. J. (2010). Ventilation rates and health: Multidisciplinary review of the scientific literature. *Indoor Air*, *21*(3), 191–204.
- Taptiklis, P., Phipps, P. R., & Plagmann, D. M. (2017). *Indoor Air Quality in New Zealand Homes and Schools—A literature review of healthy homes and schools with emphasis on the issues pertinent to New Zealand*. <https://www.aivc.org/sites/default/files/Indoor%20Air%20Quality.pdf>
- Tookey, L., Boulic, M., Phipps, R., & Wang, Y. (2019). *Air stuffiness index and cognitive performance in primary schools in New Zealand*. https://openaccess.wgtn.ac.nz/articles/conference_contribution/Air_Stuffiness_index_and_cognitive_performance_in_primary_schools_in_New_Zealand/20651283/1/files/36859050.pdf
- USEPA. (2017). *Indoor Air Quality* [Reports and Assessments]. US EPA. <https://www.epa.gov/report-environment/indoor-air-quality>
- Wang, X., Chen, D., Sheng, G., & Fu, J. (2006). Hospital indoor respirable particles and carbonaceous composition—ScienceDirect. *Building and Environment*, *41*(8), 992–1000.
- Weschler, C. J. (2006). Ozone’s Impact on Public Health: Contributions from Indoor Exposures to Ozone and Products of Ozone-Initiated Chemistry. *Environmental Health Perspectives*, *114*(10), 1489–1496. <https://doi.org/10.1289/ehp.9256>
- Weschler, C. J., & Shields, H. C. (2000). The influence of ventilation on reactions among indoor pollutants: Modeling and experimental observations. *Indoor Air*, *10*(2), 92–100.
- Yang Razali, N., Latif, M., Dominick, D., Mohamad, N., Sulaiman, F., & Srithawirat, T. (2015). Concentration of particulate matter, CO and CO₂ in selected schools in Malaysia. *Building and Environment*, *87*, 108–116.
- Zhou, Z., Liu, Y., Yuan, J., Zuo, J., Chen, G., Xu, L., & Rameezdeen, R. (2016). Indoor PM_{2.5} concentrations in residential buildings during a severely polluted winter: A case study in Tianjin, China. *Renewable and Sustainable Energy Reviews*, *64*, 372–381.

On-Site Capture Efficiency of Kitchen Range Hood Based on Particle Diameters and Exhaust Flow Rates

Shinhye Lee¹, Seongjun Park²,
Donghyun Rim², Donghwa Kang³, and MyoungSouk Yeo^{*4}

1 Department of Architecture and Architectural Engineering, College of Engineering, Seoul National University 08826 Seoul, Korea

2 Architectural Engineering Department, Pennsylvania State University, 104 Engineering Unit A, University Park, PA 1680, USA

3 School of Architecture and Architectural Engineering, University of Seoul, 02504 Seoul, Korea

*4 Department of Architecture and Architectural Engineering / Institute of Construction and Environmental Engineering, College of Engineering, Seoul National University, 08826 Seoul, Korea
Corresponding author: myseo@snu.ac.kr

ABSTRACT

Particles generated from cooking activities are the biggest contributor to the concentration of indoor particles in most homes, and they are not easily removed without natural or mechanical ventilation. As more focus is directed on human health, kitchen range hoods have drawn increasing attention and their performance in various conditions needs to be evaluated. Consequently, in this study, we performed measurements to establish the particle capture efficiency of a kitchen range hood for various particle diameters at different exhaust flow rates. The kitchen particle concentration generated by bacon-frying was measured while maintaining the differential pressure of the kitchen and adjacent zone at 0–1 Pa through the supply of outdoor air. Since the supply fan had no filter and the walls of the of the testbed were not sufficiently airtight, which is as same as typical dwellings, so an estimation of the particle concentration from the supply air or penetrated air had to be subtracted from the measured concentrations, to establish the concentration generated from bacon-frying alone. Within the particle diameter range of 0.3–10 μm , smaller particles with higher kitchen hood exhaust rate generally exhibited better capture efficiencies. Although the capture efficiencies at both exhaust rates (250 m^3/h and 350 m^3/h) were almost identical for similar particle diameters, (except for the 10 μm), the peak concentration and the time taken returning to the background concentration were reduced at an exhaust rate of 350 m^3/h .

KEYWORDS

Capture efficiency, Kitchen range hood, Particulate matter

1 INTRODUCTION

Cooking is one of the biggest contributors to indoor particle concentration, increasing it by as much as 60 times during cooking (Kwon et al., 2013). Moreover, as building envelopes have become increasingly airtight, the generated particles are not easily removed without natural or mechanical ventilation. Consequently, range hoods, which directly and effectively remove the particles generated during cooking activities, have become an essential kitchen accessory. With the wide array of range hoods available on the market, the evaluation of hood performance has become an important issue. Several studies have been conducted evaluating the performance of hoods in various conditions using gas (SF_6 , CO_2 , etc.) or particles.

Particles of diverse sizes are generated during cooking. For example, turning on a gas stove generates ultra-fine particles (UFPs), sautéing generates coarse particles, and frying generates

both (Abt et al., 2000). Different particle sizes exhibit different behavioral properties, and a hood's capture efficiency (CE) differs for fine and coarse particles. Several studies related to particle-capture efficiency have focused on UFPs (Lunden et al., 2015; Singer et al., 2012). However, the evaluation of hood performance on coarse particles is also needed, as pan frying and sautéing are common cooking methods.

The exhaust rate of kitchen range hoods is another important factor related to the reduction of particle concentration during cooking. In general, the higher the exhaust rate, the more effective the hood's air pollutant removal. However, this is only true if lower rates are inadequate: if particles can be sufficiently removed at lower exhaust rates, the use of higher exhaust rates might be unnecessary, and using lower rates can conserve energy and minimize noise. Accordingly, in this study, we analyze the CE of kitchen range hoods based on particle size and hood exhaust rate.

The goal of this study is therefore to compare the performance of kitchen range hoods by calculating the CE during performance tests using various particle diameters, ranging from 0.3–10 μm , and two different kitchen range hood exhaust rates, 250 m^3/h and 350 m^3/h .

2 MATERIAL AND METHODS

2.1 Testbed

The experiments were conducted in a testbed in Seoul over about two months in January 2020. The testbed consisted of a kitchen and two adjacent rooms, as shown in Figure 1. The dimensions of the kitchen were $3.35 \times 2.5 \times 2.4 \text{ m}^3$ (width \times length \times height), respectively, and the volume was 20.1 m^3 . A U-shaped kitchen counter, sink, chimney type range hood, and highlight cooktop, and two cabinets, were installed in the kitchen. The kitchen range hood was mounted between the two cabinets, 60 cm above the cooktop. The exhaust air flow rate of the range hood was monitored using an air flow capture hood (420, Testo). The kitchen range hood (90 cm \times 55 cm) was larger than the cooktop (60 cm \times 51 cm). The cooktop power consumption was 220 Wh/kg. It had two medium-sized burners on the front and back on the left side, and one large-sized burner in the middle on the right side. We used the front medium-sized burner for cooking in this study.

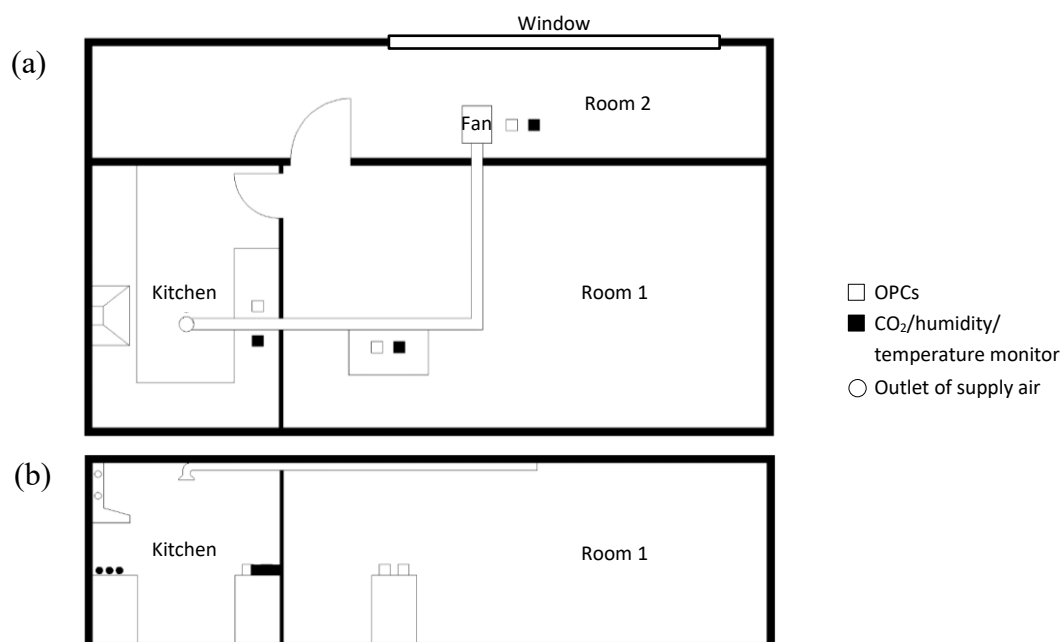


Figure 1: (a) Schematic floor plan and (b) cross-section of the testbed. Ductwork connected a fan located in room 2 with the kitchen.

Furthermore, in the testbed, there was a large window which was always kept opened, as well as a fan with no filter in room 2. Ductwork connected the fan to the kitchen to provide make-up air when operating the kitchen range hood and maintain the differential pressure between the kitchen and room 1 near zero. However, there was a construction site approximately 30 m away from the testbed, resulting in a high particle concentration in room 2. Consequently, it was expected that some of the particles from construction were delivered to the kitchen via the fan and the ductwork. Hence, the pressure of the kitchen was maintained at 0–1 Pa when the two doors (the kitchen and room) were closed during the experiments. The differential pressure of the kitchen and the room was monitored using a multifunction transmitter which had differential manometer functions (C310, Kimo).

2.2 Particulate Matter Measurement

Optical particle counters (OPCs) were placed in the kitchen and room 2, one for each zone. The OPCs used in these experiments (Aerotrak-9306, TSI Incorporated) measured particle sizes ranging from 0.3–25 μm with six channel sizes of 0.3, 0.5, 1, 3, 5, and 10 μm , respectively, at a flow rate of 2.83 L/min. The size resolution was less than 15% at 0.5 μm , and the counting efficiency was 50% at 0.3 μm . The sampling rate was set at 1 min.

2.3 Cooking Procedure

Bacon was chosen with the expectation that it would generate a similar number of particles for each cooking experiment, because of its even size, weight, and even distribution of fat. The weight of each piece of bacon was measured before every experimental case, and each piece was approximately 40 g. The bacon-frying procedure was as follows. First, the hood was turned on (or kept off, depending on the experiment). Then the pan was preheated until the surface temperature reached 210–230 $^{\circ}\text{C}$, which took about 3 minutes. Next, the bacon was cooked for 3 minutes, turned over and cooked for another 2 minutes. Lastly, the pan was covered with a lid and removed from the testbed through room 2, with the kitchen door being closed immediately. The purpose of the removal of the particle source (bacon and pan) was to prevent further particle generation. After an interval, when the particle concentration returned to the original background concentration, the testbed was ventilated and wiped with wet tissue to remove any oil and particles attached to the walls, cooktop, and kitchen range hood. All doors were closed during experiments with the hood switched on. The experiment was repeated twice for the ‘hood off’ case and three times each for the range hood exhaust rates of 250 m^3/h and 350 m^3/h . In the ‘hood on’ cases, the hood remained turned on at the same exhaust rates until the kitchen returned to the original background concentration.

2.4 Calculation of Air Change Rate

CO_2 concentration, humidity, and the temperature of the kitchen were measured using a CO_2 /humidity/temperature monitor (MCH-383SD, Lutron Electronic). The air change rate per hour (ACH) of the kitchen when the fan and the kitchen range hood was not operating was calculated by the tracer gas decay method using CO_2 . The equation for calculating the ACH is based on the mass balance equation (Cui et al., 2015):

$$ACH(t) = -\frac{1}{C_{\text{CO}_2}(t)} \frac{dC_{\text{CO}_2}(t)}{dt}, \quad (1)$$

where, $C_{\text{CO}_2}(t)$ is the CO_2 concentration of the kitchen. The calculated average ACH of the kitchen was 0.98/h, which implies low airtightness of the kitchen.

2.5 Calculation of Capture Efficiency

There is a standard test method for measuring capture efficiency of domestic range hoods, which requires tracer gas and measurement of its concentration in the exhaust air of the kitchen range hood. (ASTM E3087-18) Several studies share the equation quoted in this standard for their calculation of CE in experimental or computational fluid dynamics tests (Eom et al., 2023; Kim et al., 2018; Singer et al., 2012).

However, in some circumstances, applying this approach can be difficult since it needs the measurement of the exhaust air of the range hood. This is especially true when using particle concentration to evaluate the on-site CE, owing to the challenging nature of using OPCs to measure concentration in the supply air and the exhaust air inside the kitchen range hood. Consequently, an alternative equation was applied (Lunden et al., 2015):

$$CE = \frac{M_{captured}}{M_{emitted}}. \quad (2)$$

CE is the particulate mass (or number) exhausted through the kitchen range hood (mass captured in the hood, $M_{captured}$) divided by the mass (or number) emitted from the source ($M_{emitted}$). In this study, the number of particles were measured to obtain the CE.

To measure the mass of particles captured by the range hood, the OPC must be inserted into the exhaust duct. Furthermore, the measured particle mass by OPCs could be influenced by the large volumetric flow rate of the kitchen range hood because it does not have steady or calm airflows as the OPCs normally situates. Accordingly, the particle mass captured in the hood was calculated by subtracting the mass that was not captured in the hood but remained in the kitchen from the mass emitted by cooking:

$$M_{captured} = M_{emitted} - M_{remained}. \quad (3)$$

Where $M_{remained}$ is the mass of the pollutant in the kitchen. Substitution of Equation 3 into Equation 2 yields first-pass CE, which is used as a metric of kitchen range hood ability to pull the pollutants originated from the cooktop directly into the range hood before mixing into the indoor air, and this is the same definition and methodology that Singer et al. (2012) and Lunden et al. (2015) followed. In studies of Singer et al. (2012) and Lunden et al. (2015), they measured CO₂ concentration inside the exhaust downstream of the range hood so that they can subtract the room CO₂ concentration from it to obtain the directly captured pollutant mass and compute the first-pass CE. However, since the use of OPCs in the exhaust hood airstream is limited, the mass that did not captured and remained in the room was subtracted from the $M_{emitted}$, to compute the $M_{captured}$ indirectly.

To establish $M_{emitted}$, we measured the particle concentration in the kitchen during and after cooking with the hood and supply fan turned off. Although the kitchen was maintained at a slightly positive pressure to prevent particle penetration from the outside to the kitchen as much as possible, prior ACH measurements testify to the low airtightness of the walls between the kitchen and rooms. Hence, outside particles penetrated the room and kitchen, resulting in an increase of the kitchen particle concentration, which affected $M_{emitted}$. For $M_{remained}$, the same procedure was used, but with the hood and the supply fan turned on. As stated, the supply fan had no filter and outdoor particles were delivered to the kitchen, resulting also in an increase in $M_{remained}$.

The particle concentration of the kitchen included not only the mass generated from cooking but also the mass coming in from other zones. Moreover, as the particle concentration

of the outdoor air fluctuated, so did that of the kitchen. To account for the effects of any outdoor concentration, $M_{emitted}$ and $M_{remained}$ were converted as follows:

$$M_{emitted} = M_{hood\ off} - M_{penetrated}, \quad (4)$$

$$M_{remained} = M_{hood\ on} - M_{supplied}. \quad (5)$$

Here, $M_{hood\ off}$ and $M_{hood\ on}$ are the particle mass in ambient air of the kitchen when the hood was turned off and on, respectively; $M_{penetrated}$ is the penetrated particle mass measured in room 1; and $M_{supplied}$ is the particle mass moved from room 2 to the kitchen via the fan and ductwork.

Among the experimental studies on kitchen range hood performance regarding particulates, there is one study which was conducted in a chamber to prevent the above particulate contamination problem (Lunden et al., 2015). They equipped HEPA filters to their chamber to supply particle-free air so that they could focus only on the particles generated from cooking itself. Another laboratory study (O'Leary et al., 2019) used an HVAC unit equipped with an AFPRO F7 filter to supply air and thus evaluate the hood performance based on particle CE. Alternatively, other researchers (Rim et al., 2012) have suggested using particle reduction effectiveness, which is the ratio between the measured integrated particle concentration with the range hood on and it off, and conducted on-site experiments using this method. It is assumed that the ambient or background concentration was constant in their study. However, since, in the current study, the construction site was nearby, we considered the fluctuation of penetrated or supplied particle concentration.

Equations (2), (3), (4), and (5) can be expressed as follows, by converting mass to concentration:

$$CE = 1 - \frac{V \int_{t_0}^{tb} (C_{hood\ on} - C_{supplied}) dt}{V \int_{t_0}^{tb} (C_{hood\ off} - C_{penetrated}) dt}. \quad (6)$$

Where V is the volume of the kitchen. Since the concentrations in equation 6 indicates particle count per unit volume in the kitchen, not in the exhaust duct, so that to obtain the total particle number of the kitchen, total volume has to be multiplied and integrated with the time of measurement. The integral of concentration from the start of the experiment, t_0 , to the time taken to return to the background concentration, tb , is required because the mass in equations (1) to (4) refers to the total mass. The background concentration is the estimated concentration of the kitchen that formed due to penetrated or supplied particles ($C_{penetrated}$ and $C_{supplied}$, respectively). tb in numerator and denominator is not necessarily same value, because it should represent the mass of the captured and emitted respectively, as stated in the Equation 2, at the end.

The experimental cases and estimated parameters are shown in Table 1.

Table 1: Experimental cases and estimated parameters

Case	Supply Fan	Exhaust Flow Rates	Repeated #	Estimated Parameters	Estimated Concentration
Hood off	Not operated		2	Penetration Coefficient, Deposition Rate	$C_{penetrated}$
Hood on	Operated	250 m ³ /h 350 m ³ /h	3 3	Removal Efficiency of the Fan, Deposition rate	$C_{supplied}$

2.6 Calculation of Penetration Coefficient and Deposition Rate

To calculate the mass in the kitchen formed by factors other than emission, $M_{penetrated}$ estimation of the penetration coefficient and deposition rate is required. Penetration coefficient (P) is the rate at which the particle penetrates inside, and it can be differ by the shape or roughness of the exterior wall. Deposition rate (K) is the rate of decay due to the sink (deposition) of the particles. Both penetration coefficient and deposition rate are depend on the particle size. If the generation and resuspension of particles is ignored, the particle mass conservation equation can be expressed as follows:

$$\frac{dC_{penetrated}(t)}{dt} = aPC_{room2}(t) - (a + K)C_{penetrated}(t), \quad (7)$$

Where $C_{penetrated}$ is time-varying concentration of the kitchen depend on infiltration and deposition and does not consider the emission. a is the average ACH calculated in section 2.4 and $C_{room2}(t)$ is the time-varying particle mass concentration in room 2.

Rim et al. (2012) suggested a method for approximating $dC(t)$ in linear terms, which is permissible if the time step is relatively small (1 min for this study).

$$C_{penetrated}(t + 1) = a(t)PC_{room2}(t)\Delta t + \{1 - (a(t) + K)\Delta t\}C_{penetrated}(t) \quad (8)$$

The estimation was based on the data of two repeated experiments conducted six hours after cooking activity when the hood was off.

2.7 Calculation of Removal Efficiency of the Fan and Deposition Rate

$C_{supplied}$ can be calculated using the same method as above, this time substituting a and P for Q/V and $(1-\varepsilon)$, since any air change occurred mainly through the supply air and hood exhaust as the kitchen environment was maintained at a positive pressure.

$$C_{supplied}(t + 1) = (1 - \varepsilon)\frac{Q}{V}C_{room2}(t)\Delta t + \{1 - \left(\frac{Q}{V} + K\right)\Delta t\}C_{supplied}(t) \quad (10)$$

The estimation was based on data captured 10 minutes after cooking activity when the hood was on.

The penetration coefficient P , deposition rate K , and supply fan removal efficiency ε were approximated by the least squares method, in a way that minimizing the difference between the modeled and actual concentration using a Microsoft Excel solver. When calculating the CE, the background mass ($M_{penetrated}$ and $M_{supplied}$) was estimated and subtracted from the actual particle mass in the kitchen ($C_{hood\ on}$ and $C_{hood\ off}$).

3 RESULTS AND DISCUSSION

3.1 Removal Efficiency of the Fan and Ductwork

The particle removal efficiency of the fan and ductwork (ε) tended to increase as the particulate diameter increased, as shown in Figure 2. The larger the hood exhaust rate, the greater the supply air needed, hence the greater the required fan speed. Nonetheless, the removal efficiency was similar for both exhaust rates, 250 m³/h and 350 m³/h. In general, the removal efficiencies at 350 m³/h were slightly smaller than those at 250 m³/h for particle sizes 1–10 μm

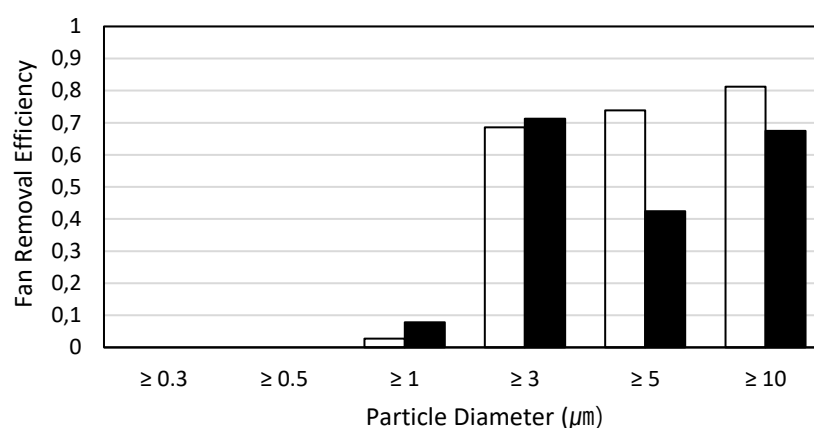


Figure 2: Particle removal efficiency of the fan and ductwork according to particle diameter and exhaust flow rate.

with some minor variations. The removal efficiency was zero for 0.3 µm and 0.5 µm at both exhaust rates.

3.2 Calculated Kitchen Concentration

Figure 3 shows the particle concentration of the kitchen calculated by subtracting the estimated background concentrations (penetrated concentration when the hood was off and supplied concentration when the hood was on) from the measured kitchen concentration to remove the effect of any outdoor concentration infiltrated from other zones (as in equations (4) and (5)). Two hood off repeated experiments display distinctive time-varying concentration patterns from each other, one of them is showing bigger peak concentration throughout the particle size bins, indicating that the emission rates might be different since the penetration coefficient and deposition rate were set to be the same. We attempted to generate same amount of particles throughout the experiments by tightly control cooking protocols, but the fat distribution of the bacon or the degree of cleanliness of the frying pan can be differ by the tests, which leads to failure of the exactly reproducible experiment. For accounting the uncertainty of the mass emitted by cooking, both hood off experiments were accounted when computing the CE.

The 0.3 µm- and 0.5 µm-diameter particles did not settle easily: the time taken for the kitchen to return to the background particle concentration was approximately 10 hours when the hood was off. When the hood was on, it took just 20 minutes for all particle sizes, except for 0.3 µm and 0.5 µm, to return to the background concentration, and this process was faster at 350 m³/h than at 250 m³/h. In particular, the particle concentration of 0.3 µm did not increase when the hood was operated at 350 m³/h. The peak concentration of all particle diameters decreased as the exhaust rate increased.

3.3 Capture Efficiency

The CEs of the range hood for various particle diameters at different exhaust flow rates were calculated for each experimental case (three cases each for the 250 m³/h and 350 m³/h flow rates and two for the ‘hood off’, for a total of eight cases), as shown in Figure 4. Note that $C_{hood\ on} - C_{supplied}$ at 350 CMH sometimes did not exceed zero concentration, (Figure 3) yielding the calculated CE over 1 (100%). This is assumed that exhaust flow rate of the range hood was adequate or higher than the kitchen needed to remove the particles. (Generated by cooking and supplied through the diffuser). One of the experiment cases with 350 CMH was

excluded in Figure 4 for this reason, to get conservative results.

CE generally improved with the range hood exhaust rate, especially for the small and large particles, owing to the CE of upward convex shape as the particle size increases at the 250 CMH, while CE decreases when the particle size increases at the 350 CMH. This implies that for both exhaust rates, larger particles are harder to remove through range hoods, but the efficiency differs by the exhaust rates for the smaller particles. In this study, it assumes that smaller particles are harder to remove with the lower exhaust rates and the efficiency improves

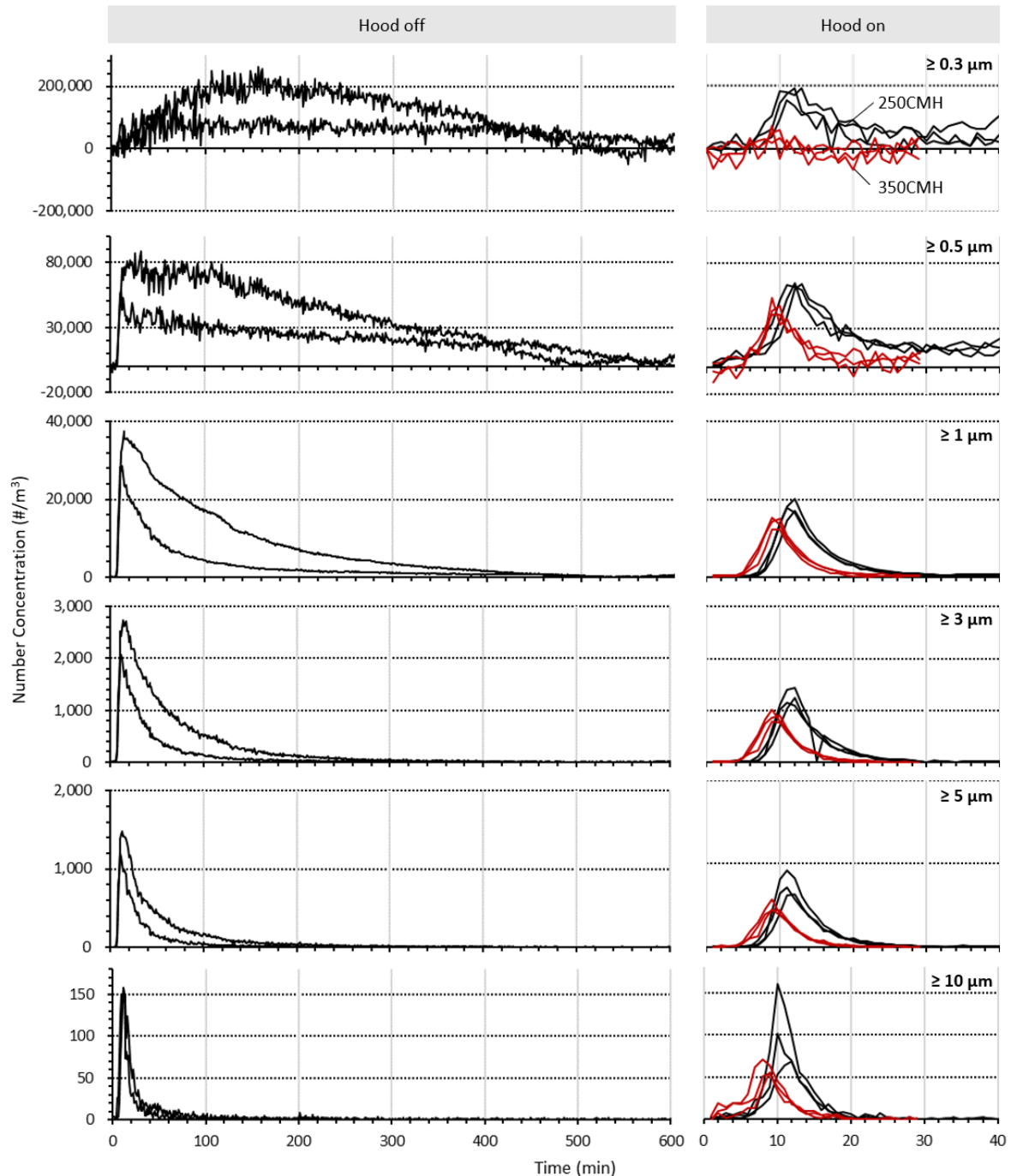


Figure 3: Measured particulate concentration of the kitchen subtracted from the estimated background concentration. Estimations were based on the approximated penetration coefficient and deposition rate for the 'hood off' case, and the removal efficiency of the supply fan and deposition for the 'hood on' case. Experiments were repeated twice for the 'hood off' case and thrice each for the 'hood on' cases at exhaust rates of 250 m³/h and 350 m³/h, respectively. All experimental cases in this study are shown in the graphs.

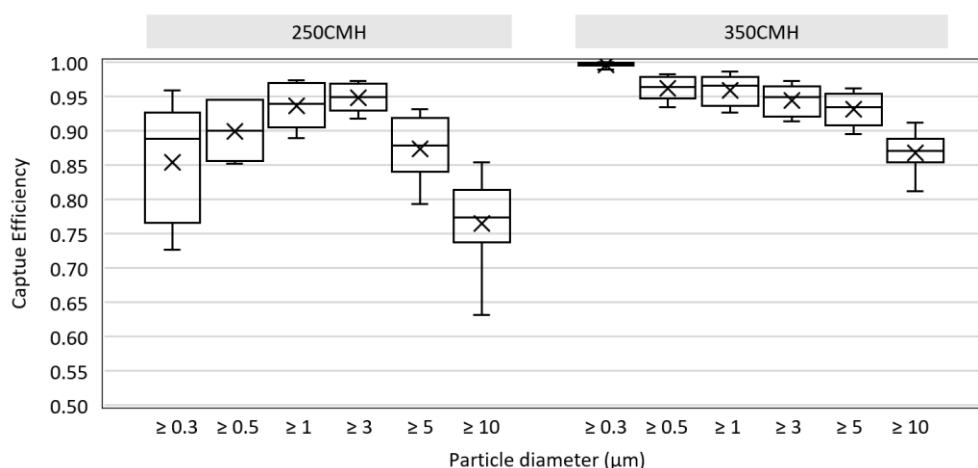


Figure 4: Capture efficiency of particles generated from bacon-cooking for the chimney type kitchen range hood at an exhaust flow rate of 250 m³/h and 350 m³/h, respectively.

sharply as the exhaust rates increases. Similar CE at the particle size between 1 µm to 5 µm was observed. (0.89 - 0.97 at 250 CMH and 0.91 – 0.99 at 350 CMH) At this particle size range, there is no substantial difference in the CE.

The positive correlation between exhaust flow rates and CEs can also be observed in other studies. Although the CE was calculated by concentration of CO₂ in the study of Singer et al. (2012), the CE also increased with increasing exhaust flow rate. Lunden et al. (2015) also found that the CE increased with exhaust flow rate for a particle size range of 6–15 µm when using the front burner (as was the case in our study) for all hood types, fan speed settings, and particle diameters. However, the CEs observed by Singer et al. were much lower than ours, being 4–39%, even though the exhaust flow rate was 51–138 l/s. (183.6–496 m³/h) This indicates that the experimental setting, location of OPCs, and calculation method can lead to different CE results.

There are some limitations in this study: (1) measurement of the ultrafine particles (UFPs) was not conducted. Cooking activity generates substantial amount of UFPs and other similar studies reported the efficiency of the range hood regarding UFPs. For example, Rim et al. (2012) showed reduction effectiveness of UFPs increased with the particle diameter up to 14 nm. (2) The complete mixing of the kitchen is not guaranteed. Some study utilized mixing fan to minimize the impact of short circuiting and to achieve generally well-mixed condition around the room. (Lunden et al., 2015) Because of the intensive generation (bacon-frying) and removal (kitchen hood exhaust) of particles in a specifically small area, a well-mixed particle concentration within the kitchen volume is difficult to achieve. Hence, the CE in equation 6 in the section 2.5 refers to the value at the measurement point, not the representative average value. However, considering the small size of the kitchen in this study, the calculated CE is expected to be similar except right below the range hood.

4 CONCLUSIONS

This study compares the coarse particle removal performance of range hoods at exhaust flow rates of 250 m³/h and 350 m³/h, respectively, based on CE. The experiments were conducted in a test testbed designed as a kitchen, but which was not completely air-tight and used an unfiltered air supply, as is common in most households. To determine the CE under these conditions, the unfiltered particle concentration was estimated and subtracted from the measured concentration to establish the contribution of cooking only to the particle concentration. The CEs of most of the evaluated particle sizes at an exhaust rate of 250 m³/h were 0.63–0.93, while those at 350 m³/h were 0.81–0.99, indicating that CEs were greater at

350 m³/h than at 250 m³/h with slight differences, except for the middle size ranged particles that showed similar CEs at both exhaust rates. The CEs of the smaller particles ($\leq 3 \mu\text{m}$) was harder to remove through the exhaust range hood when it is operating at 250 CMH, so higher exhaust rate is needed to improve the CE since most of the particles generated from the cooking activities are smaller particles.

5 ACKNOWLEDGEMENTS

This study was supported by a grant of the project for the KyungDong Navien Particulate Matter Research Task and the project for Infectious Disease Medical Safety, funded by the Ministry of Health & Welfare, Republic of Korea (grand number : HI22C1234)

6 REFERENCES

- Abt, E., Suh, H. H., Allen, G., & Koutrakis, P. (2000). Characterization of indoor particle sources: A study conducted in the metropolitan Boston area. *Environmental health perspectives*, 108(1), 35-44.
- ASTM. (2023). *ASTM E3087-18*. <https://www.astm.org/e3087-18.html>
- Cui, S., Cohen, M., Stabat, P., & Marchio, D. (2015). CO₂ tracer gas concentration decay method for measuring air change rate. *Building and environment*, 84, 162-169.
- Eom, Y. S., Kang, D. H., Rim, D., & Yeo, M. (2023). Particle dispersion and removal associated with kitchen range hood and whole house ventilation system. *Building and Environment*, 109986.
- Kim, Y.-S., Walker, I. S., & Delp, W. W. (2018). Development of a standard capture efficiency test method for residential kitchen ventilation. *Science and Technology for the Built Environment*, 24(2), 176-187.
- Kwon, M. H., Kim, S. M., Shim, I. K., Seo, S. Y., Won, S. R., Ji, H. A., & Park, J. (2013). A study on management of indoor air quality pollutants in kitchen air. *National Institute of Environmental Research*.
- Lunden, M. M., Delp, W. W., & Singer, B. C. (2015). Capture efficiency of cooking-related fine and ultrafine particles by residential exhaust hoods. *Indoor Air*, 25(1), 45-58.
- O'Leary, C., de Kluizenaar, Y., Jacobs, P., Borsboom, W., Hall, I., & Jones, B. (2019). Investigating measurements of fine particle (PM 2.5) emissions from the cooking of meals and mitigating exposure using a cooker hood. *Indoor air*, 29(3), 423-438.
- Rim, D., Wallace, L., Nabinger, S., & Persily, A. (2012). Reduction of exposure to ultrafine particles by kitchen exhaust hoods: the effects of exhaust flow rates, particle size, and burner position. *Science of the Total Environment*, 432, 350-356.
- Singer, B. C., Delp, W. W., Price, P. N., & Apte, M. G. (2012). Performance of installed cooking exhaust devices. *Indoor Air*, 22(3), 224-234.

An investigation of cooking-related pollutants in the residential sector

Daniela Mortari^{1*}, Gaëlle Guyot^{1,2}, Nathan Mendes³

¹ *University of Savoie Mont Blanc
73376 Cedex, Boulevard du Lac, 73370 Le
Bourget-du-Lac, France*

**Corresponding author: Daniela.mortari@univ-savoie.fr*

² *Cerema - Département des Transitions
Territoriales
46, rue St Théobald - CS 40128 - 38081 L'Isle
d'Abeau, France*

³ *Pontifical Catholic University of Paraná, Brazil
80215-901 Imaculada. Conceição Street, 1155
Prado Velho, Curitiba, Brazil*

ABSTRACT

In the residential sector, there are several indoor sources of pollutants related to activities such as cooking, cleaning and heating, besides those from occupants, building materials, finishing and furniture. Considering these sources, the kitchen appears as the space in the house that has the largest number of sources, with cooking being the most relevant source. In addition, meal preparation generates derivative processes related to cleaning utensils and the environment, in which detergents, air fresheners and other categories of cleaning products are used. The main goal of this study is to understand the main indoor pollutants in-kitchen, their source and transformation to further contribute to improve indoor air quality (IAQ). Therefore, an investigation focused on cooking-related pollutants is shown in the present study. The sources of pollutant related to the cooking process are separated in three main categories: the first is the type of fuel and stove, the second is related to the type of procedure used to prepare the food (frying, grilling, steaming, boiling and roasting processes) and the third is related to the type of food. The cleaning process including surface cleaners and dishwashing detergents is also discussed.

KEYWORDS

In-kitchen indoor pollutants, Cooking, Cleaning, Indoor air quality (IAQ).

1 INTRODUCTION

Until a few years ago, the biggest concern was in relation to outdoor pollution, air, water and soil. However, it has now been recognized that indoor air pollutants (IAPs) play an equally important role in human health, comfort and productivity as a result of the increasing time we spend indoors (Paleologos et al., 2021; Shayegan et al., 2022). In many situations, indoor environments can be more polluted than outdoors (Alves et al., 2021; Guyot et al., 2022; Vicente et al., 2020; Zhang et al., 2021). The concern about exposure to IAPs has worsened due to COVID-19-derived restrictions. The pandemic has changed the work dynamics, such as the increase in remote work, cleaning frequency, cooking routine, more occupation, hence, more emissions and longer occupant's exposure (Guyot et al., 2022).

In residences, there are several sources of pollution in which the kitchen appears as the space in the house that has the largest number of sources, with cooking being the most relevant (Jeong et al., 2019; Pantelic et al., 2023). Many studies in the literature have reported that heating different oils can generate a wide variety of aldehydes and ketones (Zhang et al., 2023). Depending on the procedure used, the preparation of a complete meal can generate high concentrations of PM_{2.5} (O'Leary et al., 2019), aldehydes (Alves et al., 2021) and PAHs (Saito et al., 2014). Furthermore, the type of stove/fuel also contributes to the IAPs formation (Lebel et al., 2022). Meal preparation generates derivative processes related to cleaning utensils and the environment, in which detergents and other categories of cleaning products are used.

Building materials and furniture are also important sources of VOC emissions, mainly in newly built houses (Harb et al., 2018; Poirier et al., 2021; Xu et al., 2022). The VOCs are one of the main causes of deterioration in IAQ and directly affect the health of humans harming the respiratory and nervous systems (Xu et al., 2022). Although building materials and furniture contribute significantly to the deterioration of IAQ, currently, due to the wide range of commercial products, emissions from these sources can be considered avoidable, unlike emissions from cooking processes. In this way, it is essential to develop technologies that reduce people's exposure to pollutants without changing the routine in dwellings.

This study brings an investigation of the main pollutants emitted in kitchens considering both cooking and cleaning activities. For the first one, the process involves the type of stove, the cooking procedure, and the type of food. The cleaning process considered the products related to cooking derivative activities such as cleaning utensils and the environment, hence, surface cleaners and dishwashing detergents were investigated. The information organized in this study may contribute to the development of modelling studies and implementation of policies to effectively improve indoor air quality in the residential sector.

2 POLLUTANTS RELATED TO COOKING PROCESS

In residential buildings, cooking is considered the primary source of pollutants and, in the kitchen environment, the pollutants are presented in both gas-phase and particulate-phase (Lai and Chen, 2007). The sources of pollutant related to the cooking process can be separated in three main categories: i) type of fuel and stove; ii) type of cooking procedure (frying, grilling, steaming, boiling, roasting processes, so on) and iii) type of food and its combination to compose a meal.

2.1 Type of cooking fuel

One of the first challenges is to identify the main fuels used worldwide, considering that there is a great diversity of customs within each country. Here, in this section, the most widespread ones in the literature are discussed.

Although new forms of energy have emerged to replace the use of firewood for cooking and heating, the solid fuels such as biomass and coal is still part of the energy matrix of many countries (Abdullahi et al., 2013; Gioda, 2019). According to the World Health Organization (WHO), around 3 billion people worldwide do not have access to clean cooking fuels and use open fires or simple stoves applying wood, charcoal, animal dung, crop residues, coal, and kerosene (Chomanika et al., 2022; Rupakheti et al., 2019). Kumar and collaborators (Kumar et al., 2022) performed a study in which they evaluated CO₂ exposure in kitchens of 12 major cities from 4 global regions. According to the authors, the cooking fuel type used in the homes evaluated are natural gas (NG), liquefied petroleum gas (LPG), kerosene, ethanol, electric and the different combinations of them (Kumar et al., 2022b). Likewise, in the emission inventory (EI) for the major anthropogenic sources of Indonesia performed by Permadi et al. (2017), it was shown that, in 2010, 46% of households used LPG for cooking, 39 % used fuel wood, 12% used kerosene and 3% used charcoal and coal (Permadi et al., 2017). Considering the aforementioned fuels, Table 1 presents the main emissions produced from each one.

Table 1: Main emissions related to the combustion of different fuels.

Fuel	Main emissions	Authors
Natural gas (NG)	CO ₂ , CO, steam, NO, NO ₂ , CH ₂ O, CH ₄ and PM	(Lebel et al., 2022; Singer et al., 2017; Zheng et al., 2022)
Liquefied petroleum gas (LPG)	CO ₂ , CH ₄ , CO, SO ₂ , NO, NO ₂ , PM ₁₀ , PM _{2.5} and HC	(Oke et al., 2020; Permadi et al., 2017)

Charcoal	CO ₂ , CH ₄ , N ₂ O, PM ₁₀ , PM _{2.5} , SO ₂ , CO, NO _x , black carbon (BC), organic carbon (OC), non-methane volatile organic compounds (NMVOC)	(Permadi et al., 2017)
Ethanol	CO, CO ₂ , PM _{2.5}	(Chomanika et al., 2022)
Kerosene	CO ₂ , CH ₄ , N ₂ O, PM, SO ₂ , CO, NO _x , BC, OC, NMVOC	(Permadi et al., 2017)
Coal	CO ₂ , CH ₄ , PM, SO ₂ , CO, NO _x , BC, OC, NMVOC	(Permadi et al., 2017)
Raw wood-based fuel	CO ₂ , H ₂ O, NO, NO ₂ , SO _x , CO, CH ₂ O, PM and VOCs	(Kuye and Kumar, 2023)

Many countries have implemented policies to encourage the use of cleaner fuels for cooking and heating. After a government policy for switching kerosene fuel by LPG fuel in domestic cooking, the Indonesian kerosene usage decreased by 92% in less than ten years (Thoday et al., 2018). The government of Ecuador created a campaign called National Efficient Cooking Plan (NEFC) aiming to switching 3 million of LPG based cookers to electric induction stoves (Martínez-Gómez et al., 2016). A national energy strategy has also been developing in Nigeria to replace the kerosene and biomass fuel to a cleaner fuel such as ethanol (Ozier et al., 2018). Chomanika et al. (2022) performed a study to compare the use of charcoal with ethanol briquettes by means of two different cookstoves named Chitetezo Mbaula (CM) and Kenya Ceramic Jiko (KCJ). The consumption of charcoal to prepare a complete meal in KCJ stove was high, reaching around 665 g of fuel per kg of cooked food (g/kg), while the consumption of ethanol briquettes was around 453 g/kg. The consumption of ethanol briquettes in the CM stove was 477 g/kg. The CO emissions from charcoal in the KCJ stove was 20.71 g/min while from ethanol briquettes in the KCJ and in the CM stoves the emissions rate were 0.029 g/min and 0.050 g/min, respectively. The PM_{2.5} emissions rate were 1398.03 mg/min, 0.0931 mg/min 0.1009 mg/min from charcoal in KCJ cookstove, ethanol briquettes in KCJ and ethanol briquettes in CM stove (Chomanika et al., 2022).

Zhao and Zhao (2018) compared the use of gas stove with electric stove in pollutant emission. In a commercial kitchen, the concentration of CO, CO₂, NO, NO₂, and TVOC was reduced by around 40%, 26%, 86%, 42% and 48%, respectively, by replacing the gas stove by an electric stove. The authors also stated that steaming and stir-frying may result in higher concentrations of CO, CO₂, and TVOC in domestic kitchens. In the next section of the present study, the impact of cooking procedure is discussed, but here is important to note that the emissions of CO and CO₂ were not attributed only to cooking time and methods, but also occurred as a result of burning LPG (Zhao and Zhao, 2018).

Martínez-Gómez et al. (2016) performed a study comparing LPG, electric resistance and induction cookers in terms of CO and CO₂ emissions, time spent, energy consumption and final price during the preparation of typical Ecuadorian dishes. The induction stove was more efficient in all of evaluated parameters (Martínez-Gómez et al., 2016). The discussion regarding the CO and CO₂ emissions presents high correlations with the cooking procedure and type of ingredients, which is presented in more details in Sections 2.2 and 2.3 later. However, in a general view, the CO and CO₂ emissions presented the highest concentration when LPG stove was used due to the fuel combustion. As the total emissions are also time dependent (duration of each dish cooking process), the higher calorific power used in the LPG stove during cooking, the higher the CO₂ and CO emissions (Martínez-Gómez et al., 2016). For comparative purposes, during the preparation of grilled chicken considering hood idle mode, the CO₂ emissions reached 3500 ppm to LPG stove while the concentrations to induction and electric stove were near 500 ppm. The CO concentration reached 23 ppm to LPG stove and was lower than 4 ppm to induction and electric stove (Martínez-Gómez et al., 2016). In complement, compared to induction stove, the cooking time increased between 20% and 396% (depending on the dish) to LPG stove and between 200% and 1700% to electric stove. The energy consumption increased between 44% and 170% to LPG stove and between 24% and 80% to electrical stove. Finally, the energy consumption reflects the cost for final users – compared to induction stove, the final

cost increased between 41% and 167% to LPG stove depending on the dish and, between 24% and 80% to electric resistance stove (Martínez-Gómez et al., 2016).

2.2 Type of cooking procedure

Several studies have reported that the procedure used to prepare food has a great influence on the pollutant formation. Many methods are described in the literature such as boiling, grilling, steaming, stewing, braising, stir-frying, pan-frying, deep-frying and roasting (Zhao and Zhao, 2018). According to some authors, frying and grilling produces more particulate matter than boiling and steaming food processes, especially if the food is Maillard browned or charred. Balasubramanian 2008 (apud Zhao and Zhao 2018) investigated the PM_{2.5} emissions related to different cooking methods of preparing tofu. The PM_{2.5} average mass concentrations obtained during the cooking process of 150 g of tofu were: 65,7±7.6 µg/m³, 81.4±9.3 µg/m³, 120±13 µg/m³, 130±15 µg/m³ and 190±20 µg/m³ for steaming, boiling, stir-frying, pan-frying and deep-frying processes, respectively. In some studies, the boiling process was shown to form more PM than the frying process, using the same food. However, the vapor emission can affect the performance of light scattering measurement devices. Furthermore, high relative humidity is related to hygroscopic growth of particles (aqueous aerosols), and larger particles can be more easily detected by analysers (O’Leary et al., 2019).

In addition to the preparation process itself, factors such as the type of pan also affect the indoor air pollutants. O’Leary et al. (2019) showed in their study that replacing a non-stick pan by a stainless-steel pan during meal preparation, resulted in a 940% increase in PM_{2.5} emissions. Considering that the ingredients and the method of preparation used were the same in both experiments, the justification was in relation to the thermal conductivity of the pan, its surface temperatures, and the adhesion between the food and the pan. In the stainless-steel pan, it was observed that the food stuck to the surface, being charred later. However, the PM_{2.5} formation decreased in subsequent experiments, indicating that the age of the pan may have an influence on emissions due to the changing properties of the pan's surface (O’Leary et al., 2019).

In the studies performed by Martínez-Gómez et al. (2016), it was presented that the cooking techniques, like boiling or frying, are responsible to increase the emissions of CO and CO₂. In addition, the authors showed how the frying process increased the concentrations of CO and CO₂. Although the preparation of grilled chicken was performed with the lowest final temperature, 72°C, this dish was the only one that used oil. However, the CO and CO₂ emissions resulted from this study are not only due to the cooking procedure, but also due to the LPG combustion. (Martínez-Gómez et al., 2016).

2.3 Type of food

The difficulty related to the pollutant analyses consist of all these parameters related to cooking fuel, procedure, ingredients, combination and catering types vary widely depending on the location and reflect economic and cultural factors, hence, the emission profiles cannot be generalised (Alves et al., 2021).

It is known that frying food is one of the procedures that emits the most pollutants (Liu et al., 2022). In this way, many studies have evaluated the difference among edible oils (Liu et al., 2022; Zhang et al., 2023), the effect of the addition of seasonings (Liu et al., 2017) and the combination of different ingredients to compose a complete meal (Zhang et al 2023; Alves et al., 2021; O’Leary et al., 2019). In studies carried out by Zhang et al. (2023), the formation of 13 aldehydes and ketones were identified during the use of 5 different edible oils – soybean oil, peanut oil, rapessed oil, sunflower seed oil and lard. The aldehydes and ketones identified were acetaldehyde, acrolein, propanal, methylacrolein, n-butyl aldehyde, amyl aldehyde, hexanal, acetone, methyl vinyl ketone, butanone, 2 - pentanone, 3 - pentanone and methyl isobutyl

ketone. The emission factor of aldehydes and ketones ranged from 250.87 $\mu\text{g}/(\text{goil.hr})$ to 436.12 $\mu\text{g}/(\text{goil.hr})$, being higher for rapeseed oil and lower for lard. For the 5 types of oil, the proportion of aldehydes in the total emissions varied between 61 and 78%, with acetaldehyde, acrolein and hexanal being the main compounds most formed. Liu et al. (2017) also evaluated the emissions resulting from the heating of corn oil. The main volatile organic compounds formed, dominated by aldehydes, were Ethanal, Propanal, Butanal, Methylpyrrole, Pentadienal, Toluene, 1,3-Cycloheptadiene/Phenol, Xylene/Benzaldehyde and Heptenal (Liu et al., 2017). Many authors also investigate the effect of adding seasonings on the formation of pollutants during the heating of edible oils and also during the preparation of complete meals (Liu et al., 2017; Zhang et al., 2023). The habit of stir-frying spices prior to stir-frying the food to improve the flavour of the dish is a common practice in some cultures (Liu et al., 2017). Despite the health benefits of using certain seasonings, this high-temperature stir-frying procedure can emit large concentrations of monoterpenes, which can later react with oxidants such as ozone and form a secondary organic aerosol (SOA) and thus affect health (Liu et al., 2017).

In studies carried out by Zhang et al 2023, chili powder, Chinese prickly ash and garlic slices were added to the oils. Emissions of aldehydes and ketones increased, with aldehyde being the largest proportion of total emissions, ranging between 59.3 and 71.5%. When chili powder, Chinese prickly ash and garlic slices were added to soybean oil, aldehyde emissions increased by 7.5%, 38.5% and 6.5%, respectively. When these spices were added to peanut oil, aldehyde emissions increased by 66.4%, 80.0%, and 14.9%, respectively. The authors correlated the addition of seasonings to the formation of larger molecular aldehydes; hence, their concentration was significantly greater compared to that of small molecular aldehydes (Zhang et al., 2023).

Liu et al., 2017 investigated the effects of adding garlic, ginger, myrcia and zanthoxylum piperitum (Sichuan pepper) in heated corn oil (stir-frying process). In addition to aldehydes, stir-frying spices also generated large amounts of other compounds. The stir-frying garlic process majority emitted the compounds methylpyrrole, dihydrohydroxymaltol and diallyldisulfide (DADS), the stir-frying ginger process emitted propanal, butanal, methylpyrrole, toluene, heptanal, monoterpenes and terpenoids, the stir-frying myrcia process emitted methylpyrrole, monoterpenes and terpenoids and, the stir-frying process of zanthoxylum piperitum emitted methylpyrrole, toluene, methylpyridine and monoterpenes. The addition of garlic and ginger to the heating corn oil almost had no influence on primary organic aerosol (POA) emissions. The POA concentration obtained due to the heating of pure corn oil, corn oil plus stir-frying garlic, ginger, myrcia and zanthoxylum piperitum in the reactor were approximately 42 $\mu\text{g}/\text{m}^3$, 44 $\mu\text{g}/\text{m}^3$, 46 $\mu\text{g}/\text{m}^3$, 71 $\mu\text{g}/\text{m}^3$ and 86 $\mu\text{g}/\text{m}^3$, respectively. Furthermore, garlic and ginger had no influence on SOA emissions, while large amounts of SOA were formed from the emissions of stir-frying myrcia and zanthoxylum piperitum (Liu et al., 2017).

The formation of pollutants during the preparation of complete meals is also widely studied and different emissions are reported. Zhang et al. (2023) compared the formation of aldehydes and ketones during the preparation of four different meals: Scrambled eggs with tomato and soybean oil, scrambled eggs with tomato and peanut oil, fried pork with chili and soybean oil and fried meat with chili and peanut oil. Acetone and acetaldehyde were the most abundant carbonyl compounds CCs in the kitchen. The highest acetaldehyde concentration ($12329.93 \pm 524.66 \mu\text{g}/\text{m}^3$) was obtained during the fried meat preparation while the lowest was during the scrambled eggs with tomato and soybean oil ($558.41 \pm 27.47 \mu\text{g}/\text{m}^3$). On the other hand, the last-mentioned meal presented the highest Acrolein concentration – $424.23 \pm 17.46 \mu\text{g}/\text{m}^3$ (Zhang et al 2023) being 100 times greater compared to the guidelines provided by Office of Environmental Health Hazard Assessment (OEHHA), ranging from 235.18 for scrambled eggs with peanut oil to 498.71 $\mu\text{g}/\text{m}^3$ for fried pork. O’Leary et al. (2019) compared the formation of PM_{2.5} during the cooking of (1) chicken breast fillet and pre-sliced pre-cooked potatoes fried

in olive oil and French/green beans boiled in water, (2) chicken breast fillet fried in olive oil and French/green beans and pre-sliced pre-cooked potatoes boiled in water, (3) pasta Bolognese composed of dried farfalle durum wheat pasta boiled in water, smoked lean bacon lardons, chopped onion, tomatoes and garlic fried in olive oil and minced/ground beef fried in own fat and (4) stir-fry of pre-sliced chicken breast, pre-chopped fresh vegetables, white cabbage, red pepper/capsicum leek, French/green beans, bean sprouts and straight to wok noodles all of them stir-fried in olive oil. The highest PM_{2.5} formation was obtained during the stir-fried chicken breast preparation (3.2 ± 0.24 mg/min), while the lowest concentration was obtained to meal 1 – chicken breast fillet (0.62 ± 0.041 mg/min). Saito et al. (2014) grilled different ingredients such as prawns, corn, trout, beef and pork to investigate the polycyclic aromatic hydrocarbons (PAHs) formation. The PAHs ranged from $0.0039 \mu\text{g}/\text{m}^3$ for grilled corn to $78 \mu\text{g}/\text{m}^3$ for grilled pork.

3 CLEANING PROCESS

The cleaning process involves products including floor/surface cleaners, dishwashing detergents and air fresheners (Huang et al., 2011). This study focused only on the cleaning products related to cooking process, i.e., surface cleaners and dishwashing detergents. These products are mainly sources of volatile organic compounds (VOCs), which can react with oxidants present in the environment as soon as they are emitted and generate secondary pollutants.

Huang et al. (2011) investigated the VOCs emissions from different cleaning categories including kitchen cleaners (KC) and dishwashing detergents (DD) in the household products in Hong Kong. The authors evaluated four different commercial products for each cleaning category. In addition, they evaluated the kinetic of reactions between the biogenic VOCs and the environmental oxidants hydroxyl radical ($\bullet\text{OH}$) and ozone at 298 K. The results showed that within the same category, the chemical composition and concentration of individual biogenic VOC varied widely with household products considering their different functions and scents as indicated on the labels. The identified VOCs were α -Pinene, β -Pinene, Myrcene, p-Cymene, D-Limonene, Eucalyptol, γ -Terpinene, Linalool and α -Terpineol. No association was established between the presence of fragrance in the products and the VOCs emissions (Huang et al., 2011).

Milhem et al. (2021) investigated the emissions of 6 different essential oil-based cleaning products and the correlation between their fragrance chemicals and volatile fraction. The cleaning products were classified in 5 categories: 2 kitchen degreasers, 2 general (multiuse) cleaners, 1 surface cleaner, and 1 glass cleaner. Based on information given by the manufacturer, the natural fragrance of each individual product was lemon oil, eucalyptus oil, citrus oil, lemon oil, lavender oil and eucalyptus oil for kitchen cleaner 1 (KC1), kitchen cleaner 2 (KC2), multiuse cleaner 1 (MC1), multiuse cleaner 2 (MC2), surface cleaner (SC) and glass cleaner (GC), respectively (Milhem et al., 2021). The main terpenes identified in the 6 evaluated cleaning products were α -pinene, limonene, linalool, Eucalyptol, Cymene, Bergamol, Camphor, β -pinene, γ -terpinene, α -terpineol, Menthol, and others with the mass concentration varying from 1.0 ± 0.3 to $2230.8 \pm 71.4 \mu\text{g}$ of terpene per g of product. The results showed no correlation between the total terpene mass concentrations in the liquid phase of the selected cleaning products with the total amount of terpenes transferred to the gas phase. The total gas-transferred concentrations varied from 125 ± 15 to $85225 \pm 5500 \mu\text{g}/\text{m}^3$. The multiuse cleaners (1 and 2) presented an equivalent volatile concentration in the gas phase of $27000 \mu\text{g}/\text{m}^3$ whereas their total terpene mass concentrations in the liquid phase differed by a concentration ratio of 2:1. The surface cleaner SC1 and the kitchen cleaner KC2 presented similar pattern with the gas-transferred concentrations for both products reaching approximately $80\,000 \mu\text{g}/\text{m}^3$. However, the terpene content of the surface cleaner SC1 was half of that of the kitchen cleaner

KC2 ($3200 \pm 270 \mu\text{g/g}$). In contrast, the two-household products SC1 and MC1 had equivalent terpene mass contents but gas-transferred concentrations that differed by a factor of 3 (Milhem et al., 2021).

To investigate the individual gas-transferred concentration using a microchamber experiment, the authors correlated the volatile/liquid fraction concentration ratio (V/L) with the saturation vapor pressure (VP) of the terpene pure molecules. This relationship was only met for α -pinene. For the other terpenes, the behaviour was not predictable, hence, the solvent properties showed higher influence in the transfer to the gas phase than the intrinsic properties of the pure molecule.

The experiments to evaluate the primary emissions after the application of essential oil-based product were performed under realistic application conditions, in a 1-m³ test chamber. This analysis was performed using one product from each category: SC1, MC1 and KC2. Considering the 23 TerVOCs contained in the three liquid cleaners, 19 of them were identified in the gas phase. For the three products, the results showed a fast increase after the cleaning application in which the total TerVOCs highest concentration peaks (300 ppb to SC1 and MC1 and 160 ppb to KC2) were achieved around 30 minutes. Then, a gradual decreasing was observed and, after 3.5 hours, the total TerVOCs concentration was approximately 100 ppm to SC1 and MC1 and 50 ppb to KC2. It is important to highlight that KC2 presented the highest concentration of TerVOCs ($3200 \pm 200 \mu\text{g/g}$) in the liquid phase among the three cleaners, reinforcing the lack of correlation between the total terpene mass concentrations and the total amount of terpenes transferred to the gas phase (Milhem et al., 2021).

The authors also performed a temporal evolution of the mass emission rate profiles of individual TerVOCs of the three cleaning products (SC1, KC2 and MC1) to estimate the time required to each terpene to reach the maximum emission rate, the maximum reached value and the time in which the emission source is depleted. Then, the mass emission rate profiles were evaluated considering the air exchange-corrected concentration and also air exchange plus deposition-corrected concentration. For all terpenes evaluated, the time to reach the maximum emission rate was 8 min after cleaning and the magnitude of the peak emission rate was around 710 $\mu\text{g/h}$ linalool from SC1, 1550 $\mu\text{g/h}$ eucalyptol from MC1 and 5000 $\mu\text{g/h}$ eucalyptol from KC2. Eucalyptol was the only terpene emitted from the three evaluated cleaning products, presenting a wide variation in the peak emission rate between them: $620 \pm 20 \mu\text{g/h}$ for the SC1, $4900 \pm 110 \mu\text{g/h}$ for the KC2 and $1460 \pm 30 \mu\text{g/h}$ for the MC1. Limonene was emitted from two cleaning products: $240 \pm 30 \mu\text{g/h}$ for KC2 and $1100 \pm 80 \mu\text{g/h}$ for MC1. KC2 presented the highest emission rate between the cleaning products categories and the emission of eucalyptol and menthol from KC2 was exhausted within 50 min and after 30 min for limonene. The total TerVOC emissions from SC1 and MC1 were exhausted within only 24 min (Milhem et al., 2021). The emissions of formaldehyde, acetaldehyde and acetone (the oxygenated VOCs – OVOCs) were also investigated during the experiments with SC1, KC2 and MC1. The emission values varied from one product to another presenting ranges from 6 to 18 ppb to formaldehyde, 22 to 210 ppb to acetaldehyde and 18 to 108 ppb to acetone (Milhem et al., 2021). The maximum emitted concentration of formaldehyde was observed 3.5 h after the product has been applied, indicating delayed emission kinetics that may be related not only to a primary release of the cleaning product itself but also to other factors (Milhem et al., 2021).

4 CONCLUSIONS

This manuscript provides an investigation on the main sources of pollutants in kitchens. According to the findings, the related-pollutant emissions encompass a wide range of compounds such as CO₂, CH₄, particulate matter, SO₂, CO, NO_x, volatile organic compounds (VOC), among others, varying in different concentrations depending on the type of stove, cooking fuel, cooking procedure, cooking ingredients and the cleaning products used. In many

evaluated studies, the contaminants exceeded the maximum threshold concentrations defined by the World Health Organization (WHO) based on health effects, indicating the importance of developing new strategies for reducing occupants' exposure.

5 ACKNOWLEDGEMENTS

The authors acknowledge the *Coordenação de Aperfeiçoamento de Pessoal de Nível Superior* – Brazil (CAPES – Process number: 88887.700599/2022-00) of the Ministry of Education for the financial support, the Binational Cooperation Program CAPES/COFECUB (Grant # 898/18), in collaboration with the laboratory LOCIE at the *Université Savoie Mont-Blanc*, France, and the Brazilian Research Council (CNPq) of the Ministry of Science, Technology and Innovation.

6 REFERENCES

- Abdullahi, K.L., Delgado-Saborit, J.M., Harrison, R.M., 2013. Emissions and indoor concentrations of particulate matter and its specific chemical components from cooking: A review. *Atmospheric Environment* 71, 260–294.
- Alves, C.A., Vicente, E.D., Evtyugina, M., Vicente, A.M.P., Sainnokhoi, T.-A., Kováts, N., 2021. Cooking activities in a domestic kitchen: Chemical and toxicological profiling of emissions. *Science of The Total Environment* 772, 145412.
- Angulo Milhem, S., Verrielle, M., Nicolas, M., Thevenet, F., 2021. Indoor use of essential oil-based cleaning products: Emission rate and indoor air quality impact assessment based on a realistic application methodology. *Atmospheric Environment* 246, 118060.
- Chomanika, K., Vunain, E., Mlatho, S., Minofu, M., 2022. Ethanol briquettes as clean cooking alternative in Malawi. *Energy for Sustainable Development* 68, 50–64.
- Gioda, A., 2019. Residential fuelwood consumption in Brazil: Environmental and social implications. *Biomass and Bioenergy* 120, 367–375.
- González-Martín, J., Kraakman, N.J.R., Pérez, C., Lebrero, R., Muñoz, R., 2021. A state-of-the-art review on indoor air pollution and strategies for indoor air pollution control. *Chemosphere* 262, 128376. <https://doi.org/10.1016/j.chemosphere.2020.128376>
- Guyot, G., Sayah, S., Guernouti, S., Mélois, A., 2022. Role of ventilation on the transmission of viruses in buildings, from a single zone to a multizone approach. *Indoor Air* 32, e13097.
- Guyot, G., Sherman, M.H., Walker, I.S., 2018. Smart ventilation energy and indoor air quality performance in residential buildings: A review. *Energy and Buildings* 165, 416–430.
- Harb, P., Locoge, N., Thevenet, F., 2018. Emissions and treatment of VOCs emitted from wood-based construction materials: Impact on indoor air quality. *Chemical Engineering Journal* 354, 641–652.
- Huang, Y., Ho, S.S.H., Ho, K.F., Lee, S.C., Gao, Y., Cheng, Y., Chan, C.S., 2011. Characterization of biogenic volatile organic compounds (BVOCs) in cleaning reagents and air fresheners in Hong Kong. *Atmospheric Environment* 45, 6191–6196.
- Jeong, C.-H., Salehi, S., Wu, J., North, M.L., Kim, J.S., Chow, C.-W., Evans, G.J., 2019. Indoor measurements of air pollutants in residential houses in urban and suburban areas: Indoor versus ambient concentrations. *Science of The Total Environment* 693, 133446.
- Kumar, P., Hama, S., Abbass, R.A., Nogueira, T., Brand, V.S., Wu, H.-W., Abulude, F.O., Adelodun, A.A., de Fatima Andrade, M., Asfaw, A., Aziz, K.H., Cao, S.-J., El-Gendy, A., Indu, G., Kehbila, A.G., Mustafa, F., Muula, A.S., Nahian, S., Nardocci, A.C., Nelson, W., Ngowi, A.V., Olaya, Y., Omer, K., Osano, P., Salam, A., Shiva Nagendra, S.M., 2022. CO₂ exposure, ventilation, thermal comfort and health risks in

- low-income home kitchens of twelve global cities. *Journal of Building Engineering* 61, 105254.
- Kuye, A., Kumar, P., 2023. A review of the physicochemical characteristics of ultrafine particle emissions from domestic solid fuel combustion during cooking and heating. *Science of The Total Environment* 886, 163747.
- Lai, A.C.K., Chen, F.Z., 2007. Modeling of cooking-emitted particle dispersion and deposition in a residential flat: A real room application. *Building and Environment* 42, 3253–3260.
- Lebel, E.D., Finnegan, C.J., Ouyang, Z., Jackson, R.B., 2022. Methane and NO_x Emissions from Natural Gas Stoves, Cooktops, and Ovens in Residential Homes. *Environ. Sci. Technol.* 56, 2529–2539.
- Liu, Q., Son, Y.J., Li, L., Wood, N., Senerat, A.M., Pantelic, J., 2022. Healthy home interventions: Distribution of PM_{2.5} emitted during cooking in residential settings. *Building and Environment* 207, 108448.
- Liu, T., Liu, Q., Li, Z., Huo, L., Chan, M., Li, X., Zhou, Z., Chan, C.K., 2017. Emission of volatile organic compounds and production of secondary organic aerosol from stir-frying spices. *Science of The Total Environment* 599–600, 1614–1621.
- Martínez-Gómez, J., Ibarra, D., Villacis, S., Cuji, P., Cruz, P.R., 2016. Analysis of LPG, electric and induction cookers during cooking typical Ecuadorian dishes into the national efficient cooking program. *Food Policy* 59, 88–102.
- Oke, D.O., Fakindele, B.S., Sonibare, J.A., Akeredolu, F.A., 2020. Evaluation of emission indices and air quality implications of liquefied petroleum gas burners. *Heliyon* 6, e04755.
- O’Leary, C., de Kluizenaar, Y., Jacobs, P., Borsboom, W., Hall, I., Jones, B., 2019. Investigating measurements of fine particle (PM_{2.5}) emissions from the cooking of meals and mitigating exposure using a cooker hood. *Indoor Air* 29, 423–438.
- Ozier, A., Charron, D., Chung, S., Sarma, V., Dutta, A., Jagoe, K., Obueh, J., Stokes, H., Munangagwa, C.L., Johnson, M., Olopade, C.O., 2018. Building a consumer market for ethanol-methanol cooking fuel in Lagos, Nigeria. *Energy for Sustainable Development, Scaling Up Clean Fuel Cooking Programs* 46, 65–70.
- Paleologos, K.E., Selim, M.Y.E., Mohamed, A.-M.O., 2021. Chapter 8 - Indoor air quality: pollutants, health effects, and regulations, in: Mohamed, A.-M.O., Paleologos, E.K., Howari, F.M. (Eds.), *Pollution Assessment for Sustainable Practices in Applied Sciences and Engineering*. Butterworth-Heinemann, pp. 405–489.
- Pantelic, J., Son, Y.J., Staven, B., Liu, Q., 2023. Cooking emission control with IoT sensors and connected air quality interventions for smart and healthy homes: Evaluation of effectiveness and energy consumption. *Energy and Buildings* 286, 112932.
- Permadi, D.A., Sofyan, A., Kim Oanh, N.T., 2017. Assessment of emissions of greenhouse gases and air pollutants in Indonesia and impacts of national policy for elimination of kerosene use in cooking. *Atmospheric Environment* 154, 82–94.
- Poirier, B., Guyot, G., Geoffroy, H., Woloszyn, M., Ondarts, M., Gonze, E., 2021. Pollutants emission scenarios for residential ventilation performance assessment. A review. *Journal of Building Engineering* 42, 102488.
- Rupakheti, D., Kim Oanh, N.T., Rupakheti, M., Sharma, R.K., Panday, A.K., Puppala, S.P., Lawrence, M.G., 2019. Indoor levels of black carbon and particulate matters in relation to cooking activities using different cook stove-fuels in rural Nepal. *Energy for Sustainable Development* 48, 25–33.
- Saito, E., Tanaka, N., Miyazaki, A., Tsuzaki, M., 2014. Concentration and particle size distribution of polycyclic aromatic hydrocarbons formed by thermal cooking. *Food Chemistry* 153, 285–291.

- Shayegan, Z., Bahri, M., Haghghat, F., 2022. A review on an emerging solution to improve indoor air quality: Application of passive removal materials. *Building and Environment* 219, 109228.
- Singer, B.C., Pass, R.Z., Delp, W.W., Lorenzetti, D.M., Maddalena, R.L., 2017. Pollutant concentrations and emission rates from natural gas cooking burners without and with range hood exhaust in nine California homes. *Building and Environment* 122, 215–229.
- Sun, L., Singer, B.C., 2023. Cooking methods and kitchen ventilation availability, usage, perceived performance and potential in Canadian homes. *J Expo Sci Environ Epidemiol* 33, 439–447.
- Thoday, K., Benjamin, P., Gan, M., Puzzolo, E., 2018. The Mega Conversion Program from kerosene to LPG in Indonesia: Lessons learned and recommendations for future clean cooking energy expansion. *Energy for Sustainable Development, Scaling Up Clean Fuel Cooking Programs* 46, 71–81.
- Vicente, E.D., Vicente, A.M., Evtuygina, M., Oduber, F.I., Amato, F., Querol, X., Alves, C., 2020. Impact of wood combustion on indoor air quality. *Science of The Total Environment* 705, 135769.
- Xu, L., Hu, Y., Liang, W., 2022. Composition and correlation of volatile organic compounds and odor emissions from typical indoor building materials based on headspace analysis. *Building and Environment* 221, 109321.
- Zhang, S., Ai, Z., Lin, Z., 2021. Novel demand-controlled optimization of constant-air-volume mechanical ventilation for indoor air quality, durability and energy saving. *Applied Energy* 293, 116954.
- Zhang, W., Bai, Z., Shi, L., Son, J.H., Li, L., Wang, L., Chen, J., 2023. Investigating aldehyde and ketone compounds produced from indoor cooking emissions and assessing their health risk to human beings. *Journal of Environmental Sciences* 127, 389–398.
- Zhao, H., Chan, W.R., Delp, W.W., Tang, H., Walker, I.S., Singer, B.C., 2020. Factors Impacting Range Hood Use in California Houses and Low-Income Apartments. *International Journal of Environmental Research and Public Health* 17, 8870.
- Zhao, Y., Zhao, B., 2018. Emissions of air pollutants from Chinese cooking: A literature review. *Build. Simul.* 11, 977–995.
- Zheng, Z., Zhang, H., Qian, H., Li, J., Yu, T., Liu, C., 2022. Emission characteristics of formaldehyde from natural gas combustion and effects of hood exhaust in Chinese kitchens. *Science of The Total Environment* 838, 156614.

Fine dust measurement in ducts of balanced ventilation systems

Bart Cremers^{*}, Jan de Vries

*Zehnder Group
Lingenstraat 2
8028 PM Zwolle, The Netherlands
bart.cremers@zehndergroup.com*

ABSTRACT

The measurement of particulate matter (PM) in rooms has gained interest in the last decade. However, the sensors that are currently used are intended for use in still standing air and cannot be applied to ventilation ducts with a typical velocity up to a couple of meters per second. Therefore, a prototype of a measurement module for particulate matter has been developed for use in ducts of ventilation systems. To the author's knowledge, this has not been done before.

The PM_{2.5} values as measured by the prototype in an extract duct, were compared with the values as measured in the room where the air is extracted from. The differences between the measured PM_{2.5} values were 2 to 4%, which was a sufficient accuracy for the prototype.

Three field tests were carried out in three houses with a balanced ventilation system in The Netherlands, with a distance between the houses of 50 km up to 150 km. For each field test, two PM measurement modules were installed near the balanced ventilation unit; one in the extract duct and one in the supply duct. During the measured period in the heating season, the heat recovery ensured similar temperatures in the extract and supply ducts, resulting in PM_{2.5} values that could easily be compared with each other.

The measured PM_{2.5} values in the extract ducts showed typical indoor PM sources like cooking, but also showering and steam ironing because water droplets are also measured by the sensor. In the supply air, peaks caused by incidental recirculation of chimney smoke into the fresh air intake were visible. Moreover, the effect of filter type (fine or coarse) and of filter age (old or new) within the ventilation unit could be found.

KEYWORDS

Particulate matter, air duct sensor, balanced ventilation

1 INTRODUCTION

Particulate matter in dwellings has gained a lot of interest as buildings are getting airtight and because it is harmful to a person's health. The levels of indoor particulate matter in airtight dwellings depends on indoor sources (kitchen, candles) and outdoor sources (traffic, industry, agriculture). Mechanical ventilation can reduce particulate matter levels from indoor sources and filtering of supply air reduces particulate matter levels from outdoor sources. Simulation studies have shown that penetration of PM_{2.5} outdoor pollutants can be limited by a good PM_{2.5} filter efficiency (Verheyleweghen et al., 2022). Also, in a practical study in occupied dwellings it has been shown that air supply filtration has a real impact on the levels of particles entering the dwelling (Golaz et al., 2022).

Particulate matter can be measured by low-cost sensors, but most of them are used to indicate a level in a room. Sensors for measurement of particulate matter in ducts would help to indicate the average levels of the indoor air as well as the levels of the supply air of the ventilation system.

This study aims to develop a PM sensor prototype for application in air ducts. In a test room, the PM sensor prototype in ducts is evaluated against measurement by a sensor component in a

room. After this, the PM sensor prototype is used to indicate PM levels in extract air and in supply air of a balanced ventilation system.

2 DEVELOPMENT OF A PM SENSOR FOR MEASUREMENT IN DUCTS

Commercially available low-cost PM sensor components are mostly suitable for implementation into sensors that can be placed in a room. The velocity of the air that is sampled cannot be higher than 1 m/s. This makes the components not suitable for measurement of particulate matter in ducts of ventilation systems with typical air velocity up to a couple of meters per second.

In order to measure the particulate matter in ducts, a prototype of a PM sensor for ducts has been developed. Schematically, the prototype consists of an inlet cone in which the air from the duct is drawn into the prototype in an isokinetic way (air velocity in inlet cone is equal to the air velocity in the duct). The air is directed in a direction perpendicular to the main air direction in the duct and it is slowed down to an air velocity lower than 1 m/s. This air is led over the PM sensor component after which it is directed to an outlet in the downstream direction of the air duct.

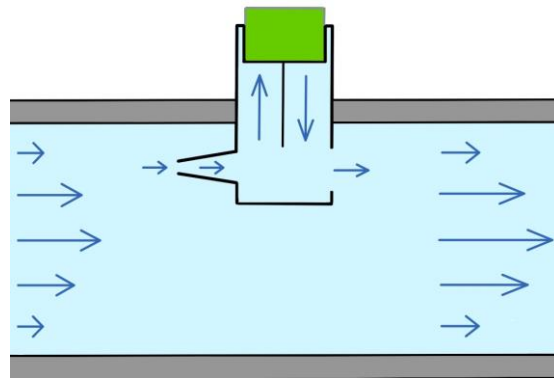


Figure 1: Schematic principle of PM measurement in a duct (blue). Blue arrows indicate air direction in the PM sensor prototype and the PM sensor component is indicated in green.

The prototype (dimensions 10 x 10 x 2 cm) was built with 3D printing. In figure 2, the prototype is shown with the inlet cone on the left. In the top, the PM sensor component (Sensirion SPS30) can be inserted into an opening in such a way that the sampled air is led via the measuring side of the sensor.

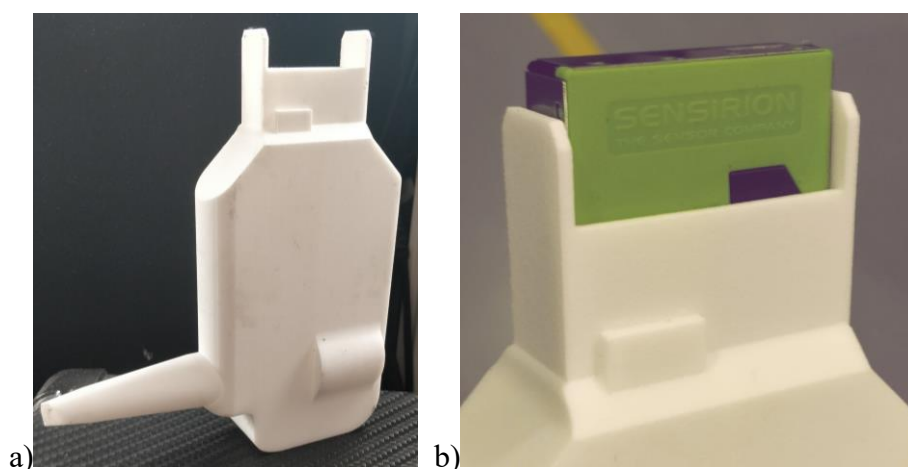


Figure 2: a) 3D printed PM sensor prototype, b) close-up of upper part of the prototype with the green PM sensor component inserted

In order to get an idea of the measured values of the prototype, an experimental set-up has been made as shown in figure 3. A test chamber (volume 19.5 m³) was provided with a PM sensor component (Sensirion SPS30). Air from the test chamber was extracted via ducts from Expanded Polypropylene (EPP) with an inner duct diameter of 160 mm. The air was extracted by a balanced ventilation unit. The supply air from the balanced ventilation unit was led back into the test chamber.

The PM sensor prototype was placed just upstream of the balanced ventilation unit, in the duct. Particulate matter was introduced in the test chamber by burning incense sticks prior to the measurement, as this is producing mainly PM_{2.5} according to literature (Goel et al., 2017).

The ventilation flow rate was varied during the 20 minute experiment. This resulted in an increasing trend of average air velocity through the duct that was 1.2 m/s (0-3 min), 2.1 m/s (3-8 min), 3.5 m/s (8-13 min) and 4.8 m/s (13-20 min).

The measured PM_{2.5} values from the sensor in the test chamber and the sensor in the PM sensor prototype were compared with each other. Figure 4 shows the decay of PM values in time. Although the experimental set-up resulted in a closed system, the PM_{2.5} values showed a decay because the test chamber was not fully airtight.

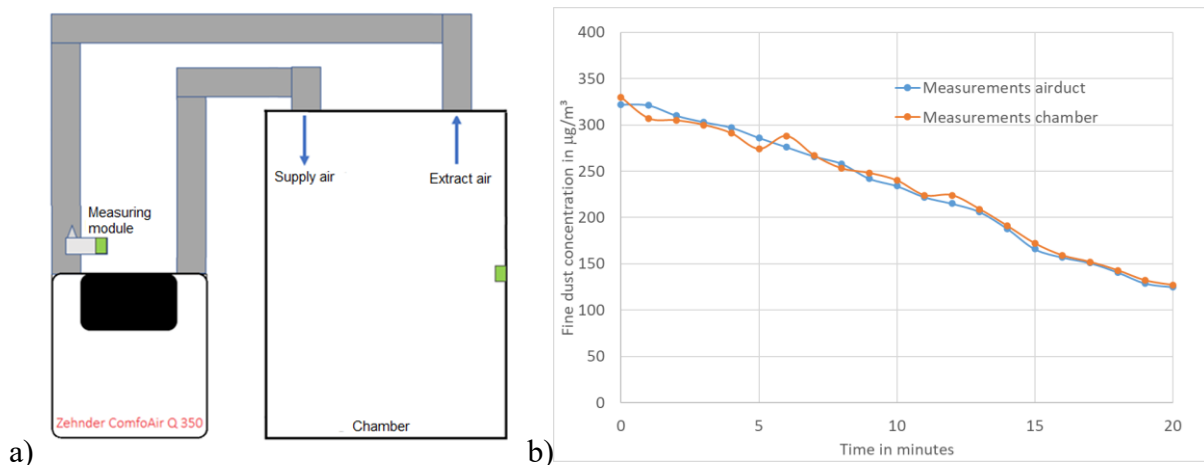


Figure 3: a) Experimental set-up of validation measurement for the PM sensor prototype and b) measured PM_{2.5} values (sensor values in test chamber in orange and PM sensor prototype values in blue)

3 DESCRIPTION OF FIELD TESTS

In order to test the PM sensor prototype in real life ventilation systems in houses, a field test was conducted. Three houses with balanced ventilation units, located in The Netherlands, were selected. They were situated in Helmond, Lettele and Zwartsluis. The distance between these houses was between 50 km and 150 km. The balanced ventilation units were provided with an EPP module and connected on top of the unit. On top of the EPP module the extract duct and the supply ducts were installed. The EPP module contained two PM sensor prototypes, one in the extract duct and one in the supply duct (see figure 4).

Placement of the PM sensor prototype in the supply duct has two advantages over placement outdoors. First, the supply duct contains air that is already filtered by the ventilation unit. This means that it is actually reflecting the PM values that are supplied to the rooms in the house. Second, measurement of particulate matter is sensitive to variations in operating temperature (Liu, 2019). Because of the heat recovery, the supply air temperature is close to the extract air temperature and therefore the PM values can better be compared with each other (as opposed to measurement in cold or warm outdoor air).

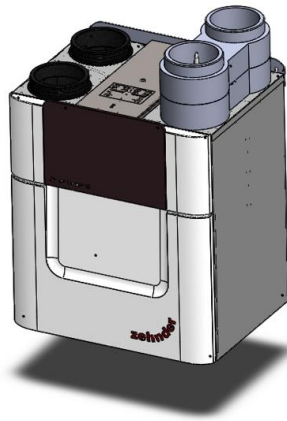


Figure 4: Schematic principle balanced ventilation system with PM measurement in extract and in supply air

4 RESULTS

4.1 Measured PM_{2.5} values in three field tests

Figure 5 shows a week of the PM_{2.5} values in the ventilation system in Helmond. The extracted air shows distinct peaks that were caused by cooking. The peak values ranged between 30 and 200 $\mu\text{g}/\text{m}^3$, depending on the prepared meal, with the exception of a peak value of 400 $\mu\text{g}/\text{m}^3$ when something had burned in the oven. There were also numerous smaller peaks that were caused by showering, and by steam-ironing.

The larger peaks of PM_{2.5} took about 3 to 4 hours before they were ventilated out of the house. The PM_{2.5} values in the supplied (filtered) air were below 12 $\mu\text{g}/\text{m}^3$ for the whole week.

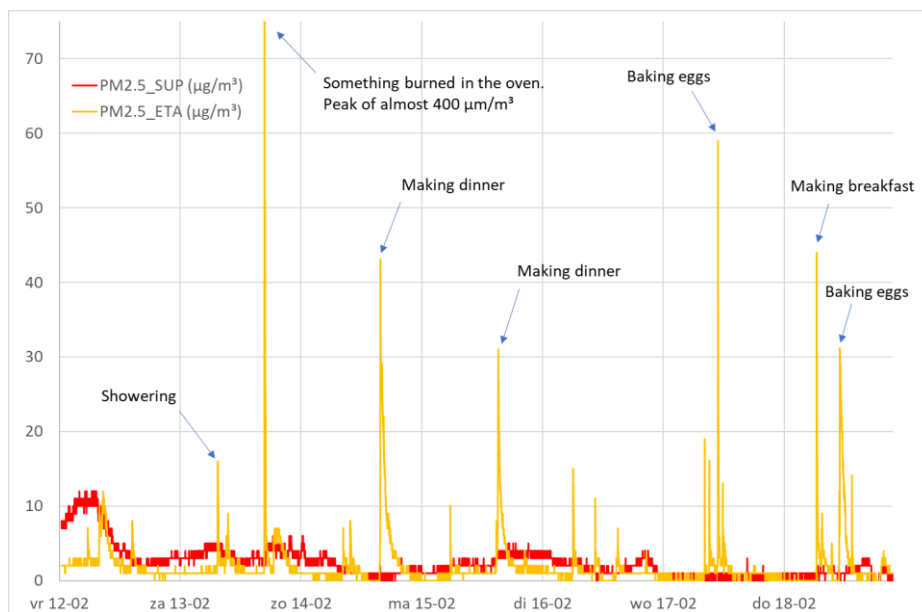


Figure 5: PM_{2.5} values in extract air (yellow) and in supply air (red) in Helmond.

Figure 6 shows a week of the PM_{2.5} values in the ventilation system in Lettele. The extracted air shows distinct peaks that were caused by cooking. The peak values ranged between 100 and 600 $\mu\text{g}/\text{m}^3$.

The larger peaks of PM_{2.5} took about 1 hour before they were ventilated from the house.

The PM_{2.5} values in the supplied (filtered) air were mostly below 30 $\mu\text{g}/\text{m}^3$ for the whole week except for a number of peaks in the supply air. The peaks in the supply air were thought to be

originating from exhaust air from a wood stove that was recirculating back into the fresh air intake on the roof.

On Feb 6th it seems that a high PM_{2.5} value in the supplied air also leads to higher values of the internal PM_{2.5} values, as reflected by the higher values in the extract.

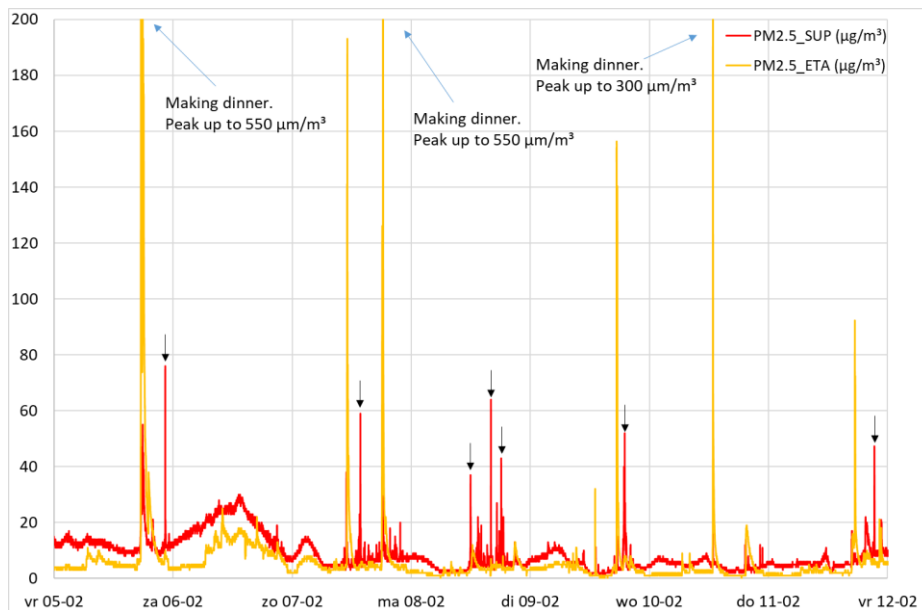


Figure 6: PM_{2.5} values in extract air (yellow) and in supply air (red) in Lettele.

Figure 7 shows a week of PM_{2.5} values in Zwartsluis. The peaks in the extract PM_{2.5} values are lower than in the other houses. This is believed to be the result of a good function cooker hood, which is working separately from the residential ventilation system. Therefore, the PM_{2.5} resulting from cooking is directly extracted by the cooker hood and brought out of the house. There is one exception with a peak value of 85 µg/m³, originating from the opening of a wood stove.

The PM_{2.5} values in the supplied air seem on average a higher value than the houses in Helmond and Lettele.

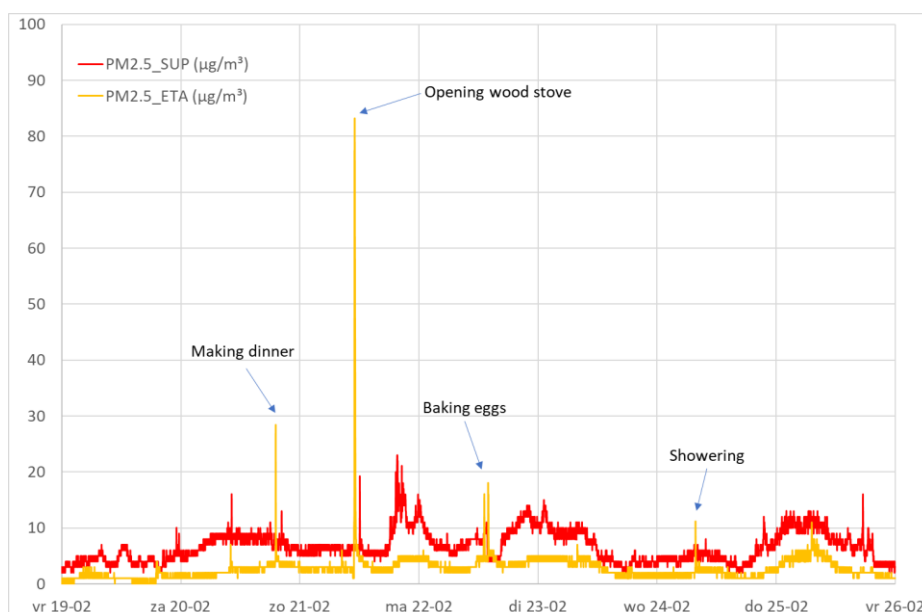


Figure 7: PM_{2.5} values in extract air (yellow) and in supply air (red) in Zwartsluis.

4.2 Comparison of PM_{2.5} values in supply air of all field tests

Interesting is the PM_{2.5} values in the supplied air during the same period in the three houses. Figure 8 shows nearly two months of PM_{2.5} values in the (filtered) supply air. It also shows the filters that are used: a new ePM1/F7 filter in Helmond and a new Coarse/G4 filter in Zwartsluis. The ventilation system in Lettele had a 3-month-old ePM1/F7 filter which was replaced by a clean ePM1/F7 filter on Feb 27th.

The results show that the trend of the PM_{2.5} values in the supply air are similar for the Coarse/G4 filter and the old ePM1/F7 filter (except for the peaks resulting from re-intake of exhaust air from a wood stove chimney). Despite the 50 km distance between the field test locations, the external PM_{2.5} values and the filter efficiency lead to a similar daily trend. Only the larger filtration efficiency of the new ePM1/F7 filter leads to low PM_{2.5} values in the supply air. After Feb 27th, when the 3 month old ePM1/F7 filter is replaced with a clean ePM1/F7 filter, the PM_{2.5} values in the supply air are suddenly getting low. After a week, the lower filtration efficiency of the Coarse/G4 filter leads to higher supply PM_{2.5} values again.

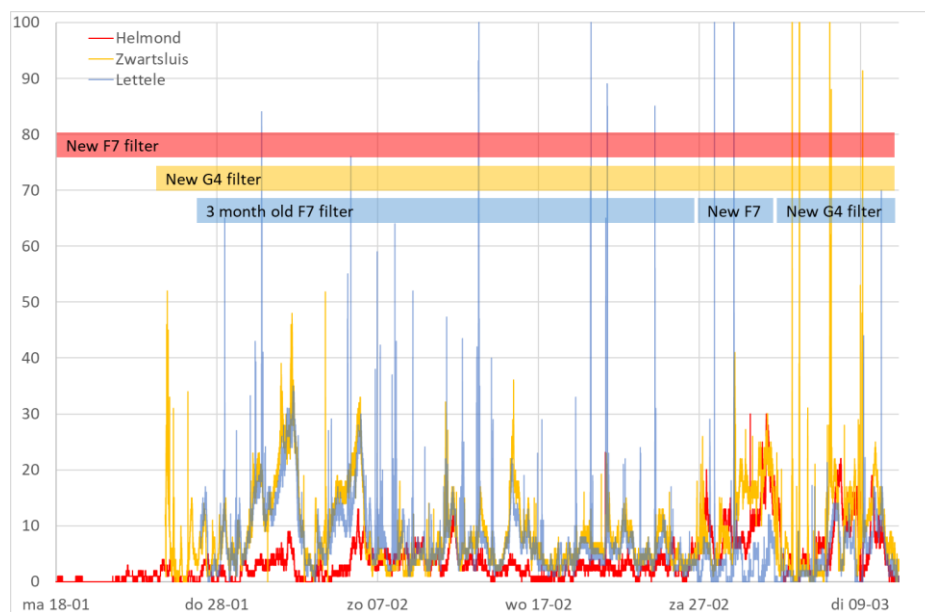


Figure 8: PM_{2.5} values in supply air in Helmond (red), in Zwartsluis (yellow) and in Lettele (blue).

5 DISCUSSION

The measurement of particulate matter in ducts proved to be a difficult task. In order to measure the right values of the PM concentration, the air has to be sampled in an isokinetic way and the air has to be slowed down before it is reaching the PM sensor component. This development has led to the application of a patent.

With the available equipment, the measurement accuracy of the PM sensor prototype could only be assessed relative to the measurement values of the PM sensor component in still standing air. The decaying PM_{2.5} signal of the PM sensor component in the room was closely followed by the PM_{2.5} signal of the PM sensor prototype. The difference between the two signals stayed within 4%. There was no clear dependency of the relative difference between the signals with the air velocity through the duct.

The measured PM_{2.5} values in balanced ventilation systems installed in three Dutch houses have been investigated.

The PM_{2.5} values in the extract air showed peaks when typical indoor sources like cooking, showering, or steam-ironing occurred. An increasing trend of the PM_{2.5} signal in the supply air (originating from increasing trend outdoors), led to an increasing trend of the PM_{2.5} signal in the extract. This indicates that the PM_{2.5} level indoors is the result of a combination of indoor sources and outdoor sources.

The PM_{2.5} values in the supply air show a trend that is largely dominated by the outdoor PM concentration. All three locations of the investigated houses, although distance between houses ranged from 50 km to 150 km, seem to be influenced by the same outdoor trend.

The exact values in the supply air are also influenced by filter efficiency. It can be seen that an ePM1/F7 filter leads to lower PM_{2.5} values in the supply air than a Coarse G4 filter. There is also the observation that the new ePM1/F7 filter leads to lower PM_{2.5} values in the supply air than a 3-month-old ePM1/F7 filter.

6 CONCLUSIONS

For measurement of particulate matter in air ducts, a PM sensor prototype has been developed. The prototype has been validated against values of a commercial sensor in still standing air and leads to good agreement.

The developed PM sensor prototype has been used to measure PM_{2.5} values in the extract air and the supply air of a balanced ventilation system. In three Dutch houses, the prototype showed values that indicate indoor sources of PM_{2.5} and outdoor sources of PM_{2.5}.

Furthermore, the measured PM_{2.5} values in the supply air seem to be dependent on the filter type and the filter age.

7 REFERENCES

- Benoit, G., Mouradian, L., Ginestet A., & Lefebvre, C. (2022). Supply air filtration and fine particle levels in indoor air of occupied dwellings. In: *Proceedings of the 42nd AIVC – 10th TightVent – 8th Venticool Conference*. Rotterdam, The Netherlands, 285-301.
- Goel, A., Wathore, R., Chakraborty, T., & Agrawal, M. (2017). Characteristics of Exposure to Particles due to Incense Burning inside Temples in Kanpur, India. *Aerosol and Air Quality Research* 17(2), 608-615. <https://doi.org/10.4209/aaqr.2016.04.0146>
- Liu, H.-Y., Schneider, P., Haugen, R., & Vogt, M. (2019). Performance Assessment of a Low-Cost PM_{2.5} Sensor for a near Four-Month Period in Oslo, Norway. *Atmosphere* 10(41). <https://doi.org/10.3390/atmos10020041>
- Verheyleweghen, S., Van Herreweghe, J., Pecceu, S., & Caillou, S. (2022). The role of ventilation in the penetration of outdoor air pollutants. In: *Proceedings of the 42nd AIVC – 10th TightVent – 8th Venticool Conference*. Rotterdam, The Netherlands, 258-267.

The Impact of Deep Energy Renovations on Indoor Air Quality and Ventilation in Irish Dwellings

Hala Hassan¹, Asit Kumar Mishra², Hilary Cowie³, Emmanuel Bourdin⁴, Brian McIntyre⁵, Marie Coggins^{*1}

*Corresponding author: marie.coggins@universityofgalway.ie

1 School of Natural Sciences & Ryan Institute, University of Galway, Galway, H91TK33, Ireland

2 School of Public Health, University College Cork, College Road, Cork, Ireland

3 Institute of Occupational Medicine (IOM), Edinburgh, EH14 4AP, UK

4 Climate Action Policy and Construction Industry Regulation Unit, Department of Housing, Local Government and Heritage, Custom House, Dublin 1, D01 W6X0, Ireland

5 Sustainable Energy Authority of Ireland, Three Park Place, Hatch Street Upper, Dublin 2, D02 FX65, Ireland

ABSTRACT

Achieving energy-efficient dwellings has become a vital part of the global climate action plan to reduce energy usage and carbon emissions. Deep energy retrofits (DER) can help reduce residential energy use significantly. However, evidence on how DER impacts on indoor air quality (IAQ), and consequently, occupant health, is scarce. More in-depth analysis of IAQ data before and after energy retrofits is essential to understand the indoor environmental challenges of adopting energy efficiency measures. DER will be required to achieve the EU target of zero emission building stock by 2050, and such studies can inform policy as retrofit strategies evolve. This study evaluates the IAQ in a sample of domestic dwellings (n=12) in Ireland before and after undergoing DER, as part of the SEAI funded research project (ARDEN). IAQ pollutants, including PM_{2.5}, carbon dioxide (CO₂), carbon monoxide (CO), formaldehyde, radon, nitrogen dioxide (NO₂), and BTEX (Benzene, toluene, ethylbenzene, and xylenes) were measured over a period of 48 hours to three months (depending on the pollutant) using continuous and passive sampling methods. This study further assesses the performance of the mechanical ventilation systems installed in the homes post DER. The results show that higher concentrations of PM_{2.5} were recorded in some homes post-retrofit compared to pre-retrofit. This was likely due to a combination of factors – increased air tightness (i.e., reduced infiltration), the new mechanical ventilation systems not achieving design flow rates, and varied occupant activities during measurement period. Overall, formaldehyde concentrations significantly increased ($p < 0.001$) post-retrofit, most likely due to the use of building materials, paints, and furnishings during retrofitting. Radon levels measured post-retrofit were below the Irish national reference level (i.e., $< 200 \text{ Bq m}^{-3}$) for most homes sampled (n=26), except for four homes which were in high radon areas. Results suggest that more emphasis is needed on improving the design, installation, commissioning and maintenance of ventilation systems, along with raising homeowner's awareness regarding IAQ, and how to operate and maintain their ventilation systems in an efficient and effective manner. This would support good IAQ in the energy efficient homes, ensuring health and wellbeing.

KEYWORDS

Indoor air quality, Deep energy retrofit, Ventilation, PM_{2.5}, Formaldehyde

1 INTRODUCTION

Ireland plans to halve its greenhouse emissions by 2030 and achieve net zero emissions by 2050. Towards this goal, the Irish programme for Government and Climate Action Plan (CAP23) have set targets to design and construct all new dwellings to Zero Energy Building (ZEB) and retrofit 500,000 existing dwellings to a building energy rating (BER) of B2 or cost-optimal equivalent by 2030. The Deep retrofit multi-annual pilot programme (DER) was introduced in 2017 and managed by the Sustainable Energy Authority of Ireland (SEAI) aiming to upgrade homes to, at least, an A3 BER by adopting a whole-house retrofit, including the requirement for a high performing fabric, reduced thermal bridging, improved air tightness ($\leq 5 \text{ m}^3 \text{ h}^{-1} \text{ m}^{-2} @ 50 \text{ Pa}$), use of renewable fuels, and installation of mechanical ventilation to support air quality.

Ventilation is a vital component of energy efficient homes, to ensure healthy indoor air quality for occupants. Increased building air tightness, post retrofit, in the absence of proper ventilation has been shown to compromise the quality of indoor air for its occupants (Wang et al., 2022). Increased concentration of pollutants, often above recommended guidelines, of particulate matter, carbon dioxide, formaldehyde, and radon have been frequently observed in homes post energy renovations (Du et al., 2019; Földvary et al., 2017). Poor indoor air quality, mainly due to inadequate ventilation, has been shown to be the most influential risk factor associated with respiratory conditions in the household (Wimalasena et al., 2021). Issues of mould growth and noise from the mechanical ventilation systems have also been reported post retrofit (Elsayed et al., 2022).

The lack of occupant knowledge on how to operate and maintain newly installed ventilation systems is another factor that will impact on indoor air quality. Coggins et al. (2022) study on indoor air quality, in deep energy retrofitted dwellings in Ireland, found that air quality was negatively impacted by improper handover and inadequate cleaning and maintenance of ventilation systems. Similarly, in the study of Pedersen et al. (2021), although tenants perceived better ventilation post renovations, many tenants were not adequately informed regarding how the ventilation systems in their homes operated.

Healthy indoor air quality in highly efficient homes can be achieved by ensuring sufficient air change rates through properly installed and maintained ventilation systems (Dovjak et al., 2022), as well as raising occupants awareness regarding IAQ and promote positive engagement with building ventilation systems.

In this study, we evaluate the IAQ in a sample of Irish dwellings (n=12), pre and post energy renovations. Furthermore, we assess the performance of the mechanical ventilation systems installed as part of the retrofit.

2 METHODOLOGY

Ethical approval for this study was obtained from the Research Ethics Committee of the University of Galway. Homes which had participated in the SEAI DER programme were recruited to participate in this study. Twelve dwellings were selected to assess the IAQ and thermal comfort pre-retrofit. The participating dwellings were located across Ireland in both urban, sub-urban and rural locations. All homes underwent a deep energy retrofit between 2019 and 2020, and were > 36-months post retrofit at the time of this study. The pre-retrofit

IAQ measurements were collected in 2019 and 2020. However, due to the COVID19 restrictions, to ensure the safety of the homeowners and the researchers, sampling was suspended during the pandemic. Post-retrofit measurements resumed in winter of 2022 and through the summer of 2023, after the pandemic restrictions had been lifted.

2.1 Indoor Air Quality Monitoring

The following IAQ parameters were measured in the bedrooms and living rooms of the recruited homes over a period of 48-72 hours: particulate matter (PM_{2.5}), total volatile organic compounds (TVOCs), carbon monoxide (CO), carbon dioxide (CO₂), temperature (T °C), and relative humidity (RH%). Concentrations were measured at 1-minute (PM_{2.5}) or 5 minute intervals (TVOCs, CO₂, CO, T, and RH). Passive samplers were used to collect formaldehyde samples (over a period of 72 hours) for the same rooms. Additionally, radon was measured for a period of 3 months in 3 homes pre-retrofit and all the 12 homes post retrofit.

Occupants were asked to complete an activity diary to trace occupant's activities during the sampling periods, and a questionnaire form to obtain feedback on the dwellings energy consumption, cleaning and cooking routines, and ventilation systems. Bedroom ventilation rates [Air Change Rates (h⁻¹) and l/s per person] were calculated using the steady-state method and night-time CO₂ concentrations, based on number of occupants and average CO₂ generation rate for sleeping occupants (Batterman, 2017; Persily & de Jonge, 2017).

3 RESULTS AND DISCUSSION

Post retrofit, all homes were upgraded to a post building energy rating (BER) of A3 or better, with post building air tightness values of between 2.7 – 5.0 m³ hr⁻¹ m⁻², as shown in Figure 1. The BER provide an indication of the energy performance of the dwelling (SEAI, 2023). Each rating corresponds to an energy use per unit floor area per year [EUI = kWh/m² year]. Eleven dwellings had oil-fired boilers and one dwelling had a gas-fired boiler as primary space heating pre retrofit. In addition, all dwellings had either an open fire or solid multi-fuel stove as secondary heating. All the retrofits involved the substitution of the previously used fossil fuel based heating systems with an air to water (A2W) heat pump.

Mechanical ventilation systems were installed in all homes. Homes either had demand control ventilation (DCV) where airflow volume was adjusted based on humidity (n = 10), or mechanical ventilation with heat recovery MVHR (n = 2). Ventilation rates, calculated using night-time CO₂ concentrations, were considerably lower in retrofitted homes (1.6 – 8.2 l/s per person; avg. = 4.0 l/s per person) compared to before the retrofit (1.4 – 32.2 l/s per person; avg. = 8.2 l/s per person). During the field surveys, many problems were observed with the newly installed ventilation systems (i.e. low pressure below design flow rates, and dust deposits on the vents).

PM_{2.5} concentrations were higher in some homes post retrofit. The 24-hr PM_{2.5} average concentration (n=24) ranged from 5.5 µg m⁻³ to 56.7 µg m⁻³ pre retrofit, and from 4.6 µg m⁻³ to 353.8 µg m⁻³ post retrofit. The maximum median concentration was recorded (3 day median = 245 µg m⁻³) in a bedroom (Home 5). This home also had the lowest measured bedroom ventilation (1.6 l/s per person) of all homes studied. Home 5 was most likely under ventilated during the sampling period. In this home, only one of the wet rooms had an extract vent (bathroom), while the extract vent in the other wet rooms (kitchen) was removed by the homeowner post retrofit due to issues related to noise and draught. Figure 2 shows a time series profile of the PM_{2.5} concentrations in the same bedroom. There were several peak

concentrations (up to $1980 \mu\text{g m}^{-3}$) during the sampling period. According to the homeowner, the bedroom door was closed during 2nd night-time, and pets were present in the room overnight.

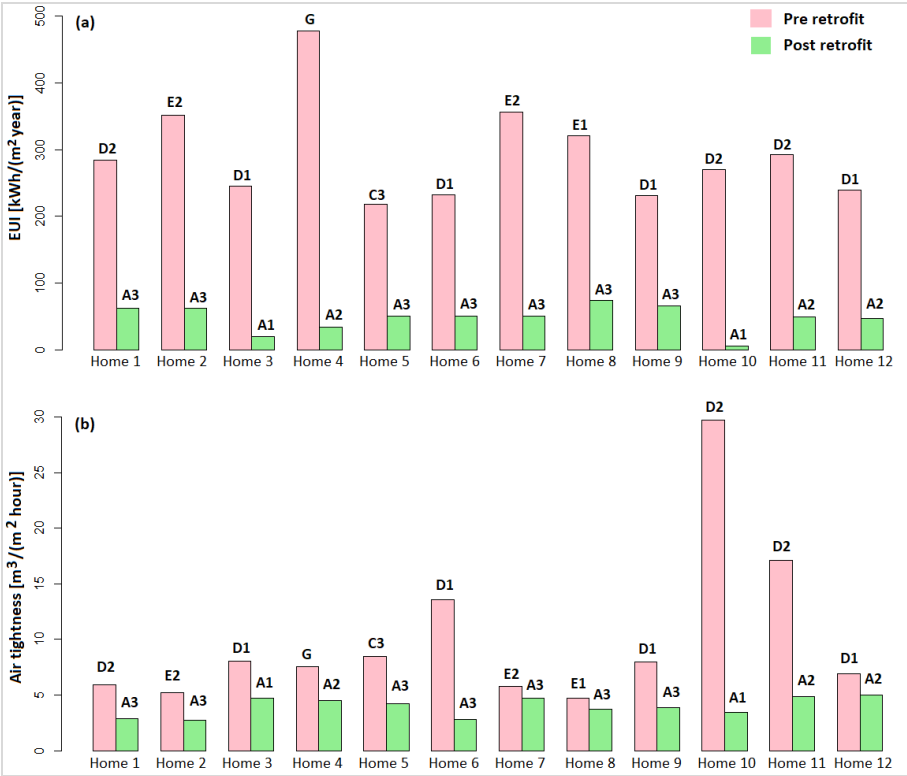


Figure 1 (a) Energy use intensity (EUI) and (b) Air tightness, pre and post retrofit for the studied homes. Each home is labelled by its BER rating for each retrofit status

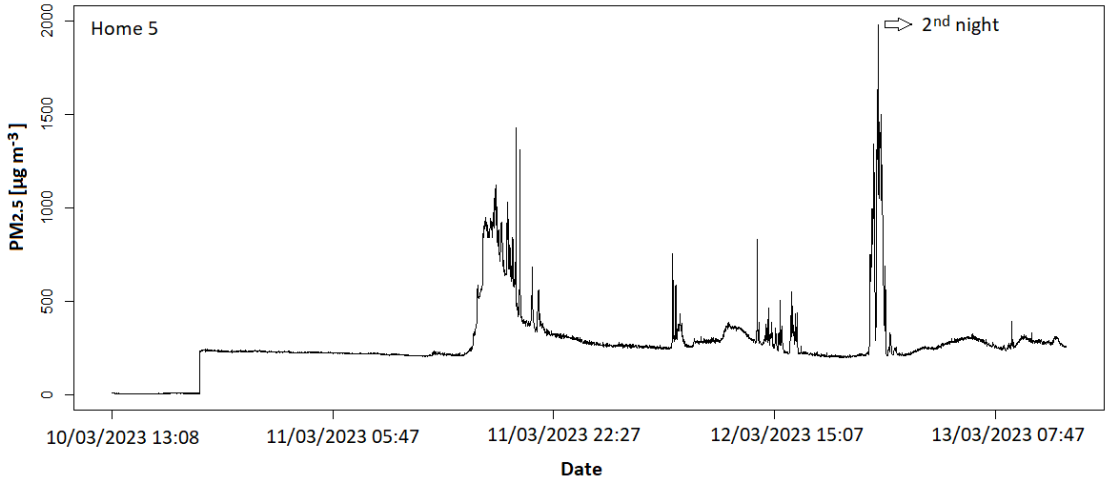


Figure 2 Time series of PM_{2.5} bedroom concentrations in Home 5 over a 3 days sampling period

Overall, there was a significant increase in Formaldehyde concentrations (72-hr average) post retrofit ($p < 0.001$) compared to pre retrofit values, with post retrofit concentrations exceeding the ATSDR annual long-term health-based guideline value of $10 \mu\text{g/m}^3$, which is also recommended by Public Health England (ATSDR, 2005; PHE, 2019). The materials used in the renovation works including furnishings, paints, and insulation materials, are major sources of formaldehyde and could be contributing to these high levels in the homes.

Radon levels were measured post-retrofit in 26 homes (14 extra homes in addition to the 12 homes in this study). Radon levels exceeding the national guideline level (i.e., 200 Bq m⁻³) were recorded in four of the homes located in high radon areas, as per EPA’s radon risk map (EPA, 2023).

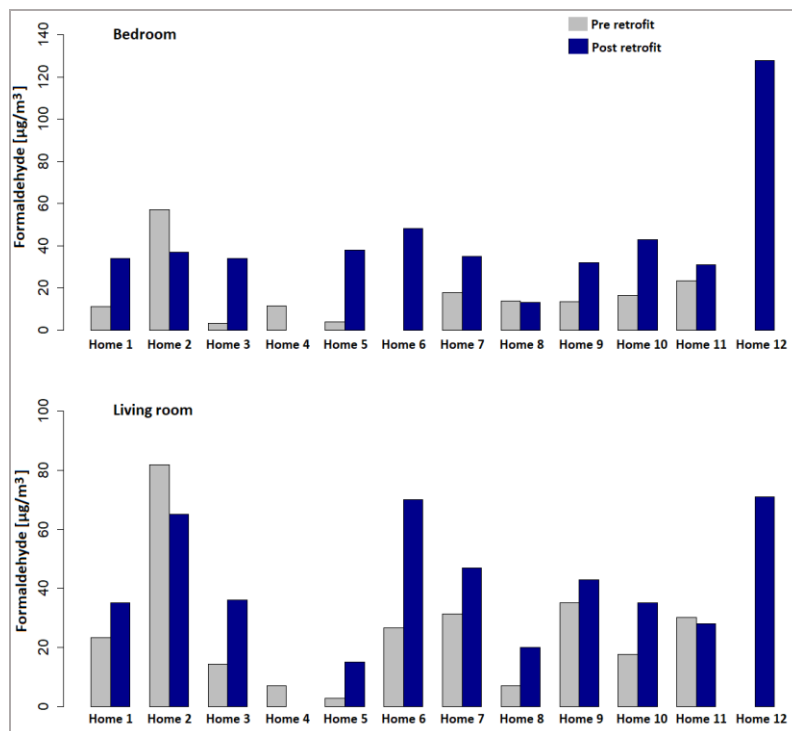


Figure 3: Formaldehyde concentrations [$\mu\text{g m}^{-3}$] in bedrooms and living areas over a 3 day period pre and post retrofit

4 CONCLUSIONS

Post deep energy retrofit assessments showed significant increases in some indoor air pollutants. Estimated ventilation rates were lower (on average) post energy renovations, which, along with occupant activity, are likely to impact on measured pollutant levels. In most of the homes, problems with ventilation systems and/or visible signs of underperformance and lack of maintenance (i.e. low pressure or dust deposits on the vents) were observed. Future work will include a statistical analysis to investigate possible associations between pollutant concentrations and factors associated with the retrofit.

5 ACKNOWLEDGEMENTS

The Government of Ireland through the Sustainable Energy Authority of Ireland’s Research, Development and Demonstration Funding Programme 2018 funds this project (RDD204).

6 REFERENCES

ATSDR. (2005). *Agency for Toxic Substances & disease Registry, USA.*
<https://www.atsdr.cdc.gov/mrls/mrllist.asp>

- Batterman, S. (2017). Review and Extension of CO₂-Based Methods to Determine Ventilation Rates with Application to School Classrooms. *Int J Environ Res Public Health*, 14(2). <https://doi.org/10.3390/ijerph14020145>
- Coggins, A. M., Wemken, N., Mishra, A. K., Sharkey, M., Horgan, L., Cowie, H., Bourdin, E., & McIntyre, B. (2022). Indoor air quality, thermal comfort and ventilation in deep energy retrofitted Irish dwellings. *Building and Environment*, 219, 109236. <https://doi.org/https://doi.org/10.1016/j.buildenv.2022.109236>
- Dovjak, M., Vene, O., & Vaupotič, J. (2022). Analysis of Ventilation Efficiency as Simultaneous Control of Radon and Carbon Dioxide Levels in Indoor Air Applying Transient Modelling. *Int J Environ Res Public Health*, 19(4). <https://doi.org/10.3390/ijerph19042125>
- Du, L., Leivo, V., Prasauskas, T., Täubel, M., Martuzevicius, D., & Haverinen-Shaughnessy, U. (2019). Effects of energy retrofits on Indoor Air Quality in multifamily buildings. *Indoor Air*, 29(4), 686-697. <https://doi.org/https://doi.org/10.1111/ina.12555>
- Elsayed, M., Romagnoni, P., Pelsmakers, S., Castaño-Rosa, R., & Klammsteiner, U. (2022). The actual performance of retrofitted residential apartments: post-occupancy evaluation study in Italy [Article]. *Building Research and Information*. <https://doi.org/10.1080/09613218.2022.2121908>
- EPA. (2023). *Radon risk map*. <https://gis.epa.ie/EPAMaps/Radon?&lid=EPA:RadonRiskMapofIreland>. [accessed July 2023]
- Földváry, V., Bekö, G., Langer, S., Arrhenius, K., & Petráš, D. (2017). Effect of energy renovation on indoor air quality in multifamily residential buildings in Slovakia. *Building and Environment*, 122, 363-372. <https://doi.org/https://doi.org/10.1016/j.buildenv.2017.06.009>
- Pedersen, E., Borell, J., Li, Y., & Stålné, K. (2021). Good indoor environmental quality (IEQ) and high energy efficiency in multifamily dwellings: How do tenants view the conditions needed to achieve both? *Building and Environment*, 191, 107581. <https://doi.org/https://doi.org/10.1016/j.buildenv.2020.107581>
- Persily, A., & de Jonge, L. (2017). Carbon dioxide generation rates for building occupants. *Indoor Air*, 27(5), 868-879. <https://doi.org/https://doi.org/10.1111/ina.12383>
- PHE. (2019). *Public Health England, Air Quality: UK guidelines for selected volatile organic compounds in the UK*. <https://www.gov.uk/government/publications/air-quality-uk-guidelines-for-volatile-organic-compounds-in-indoor-spaces>
- SEAI. (2023). *Sustainable energy authority of Ireland building energy rating certificate (BER) [Online]*. <https://ndber.seai.ie/pass/ber/search.aspx>. [accessed July 2023]
- Wang, C., Wang, J., & Norbäck, D. (2022). A Systematic Review of Associations between Energy Use, Fuel Poverty, Energy Efficiency Improvements and Health. *Int J Environ Res Public Health*, 19(12). <https://doi.org/10.3390/ijerph19127393>
- Wimalasena, N. N., Chang-Richards, A., Wang, K. I., & Dirks, K. N. (2021). Housing Risk Factors Associated with Respiratory Disease: A Systematic Review. *Int J Environ Res Public Health*, 18(6). <https://doi.org/10.3390/ijerph18062815>

Financial impact of leaky ductwork in buildings – a calculation tool to raise awareness

Nolwenn Hurel^{1*}, Valérie Leprince² and Marcus Lightfoot³

*1 PLEIAQ
2 Avenue de Mérande
73 000 Chambéry, France*

**Corresponding author: nolwenn.hurel@pleiaq.net*

*2 Cerema DTecTV/DBD
2 rue Antoine Charial
69003 Lyon, France*

*3 Ubbink Centrotherm Group
Verhuellweg 9
6984 AA Doesburg, The Netherland*

ABSTRACT

In the context of energy saving, new buildings are becoming more airtight and purpose-provided, often central mechanical ventilation is required to create and sustain a healthy indoor air quality (IAQ). This policy is summed up by the well-known energy efficiency mantra “Build tight, ventilate right”.

Central mechanical ventilation systems require ductwork systems to distribute air inside the building, but in practice, they are often not airtight. The numerous issues caused by leaky ductwork, including excessive fan energy use, acoustic discomfort and possibly even poor IAQ, if the ventilation system is not commissioned correctly, have been well outlined in literature, but there still appears to be a lack of awareness about the impact of such issues in the construction industry.

A simple tool was developed using a simplified model to estimate the financial impact of leaky ductwork in buildings over their whole life. It assumes that the design or hygienic flow rates in all habitable and wet rooms are achieved, and it is based on two previous publications from the 40th (Leprince et al., 2019) and 42nd (Hurel and Leprince, 2022a) AIVC Conferences. The purpose of this user-friendly tool is to help to raise awareness about this issue and encourage the design and installation of airtight ventilation ductwork systems, which are readily available on the market.

Case studies for 4 houses and one of the 10 AHU of a school building are presented as examples of energy and financial impact of ductwork leakage. It is found that if the fan fully compensates, a very leaky ductwork (class 3A) induces an increase of fan energy use ranging between 58% and 173% for the 4 single-family houses, and of 33% for the school AHU. The financial impact of this poor ductwork airtightness level for 80 years of operation ranges from 4.0 k€ to 33.2 k€ for the 4 single houses and reaches 74 k€ for the school AHU (out of the 10 AHU).

KEYWORDS

Ductwork leakage, calculation tool, energy savings, financial impact, case study

1 INTRODUCTION

In the context of energy saving, new buildings are becoming more airtight and purpose-provided, often central mechanical ventilation is required to create and sustain a healthy indoor air quality (IAQ). This policy is summed up by the well-known energy efficiency mantra “Build tight, ventilate right”.

Central mechanical ventilation systems require ductwork systems to distribute air inside the building, but in practice, they are often not airtight. The numerous issues caused by leaky ductwork, including excessive fan energy use, acoustic discomfort and possibly even poor IAQ, if the ventilation system is not commissioned correctly, have been well outlined in literature and summarised recently in (Leprince et al., 2020), but there still appears to be a lack of awareness about the impact of such issues in the construction industry. Measurements performed in France in the context of the Effinergie + (Moujalled et al., 2018) have shown that almost 50% of the ductwork systems in the tested houses have ductwork airtightness 2.5*class A or worse. This stresses the need to change construction habits because the ductwork in most of the tested buildings was designed to achieve at least class A (required by the Effinergie + label), but missed the target.

A simple tool was developed using a simplified model to estimate the financial impact of leaky ductwork on fan energy use in buildings over their whole life. The impact on other things, for example the heating and cooling energy losses in case the air is pre-conditioned, have not been considered. This tool assumes that the design or hygienic flow rates in all habitable and wet rooms are achieved, and it is based on two previous publications from the 40th (Leprince et al., 2019) and 42nd (Hurel and Leprince, 2022a) AIVC Conferences. It has been designed for central mechanical ventilation systems with energy recovery and central mechanical extract ventilation systems

The purpose of this user-friendly tool is to help to raise awareness about this issue and encourage the design and installation of airtight ventilation ductwork systems, which are readily available on the market.

A case study is presented using the same 4 houses as Leprince et al.(2019), as well as a school building from the PromevenTertiaire project (Hurel and Leprince, 2022b) as examples of energy and financial impacts.

2 MODEL FOR THE LEAKAGE IMPACT CALCULATION

The model used in the calculation tool is detailed below. It is based on two studies by Leprince et al. (2019) and Hurel and Leprince (2022a).

2.1 Fan energy use

The electrical AHU fan power (P_{AHU}) depends on its flowrate (Q_{AHU}) and pressure (Δp_{AHU}):

$$P_{AHU} = \frac{\Delta p_{AHU} \times Q_{AHU}}{\eta \times 3600} \quad (1)$$

P_{AHU}	W	Electrical fan power
Δp_{AHU}	Pa	Pressure induced by the fan
Q_{AHU}	m ³ /s	Flowrate delivered by the fan
η	-	Fan efficiency

The higher the pressure loss in the ductwork system, the more the fan needs to produce flowrate and pressure to compensate this resistance and meet the hygienic flowrates to ensure a good IAQ. As illustrated in Figure 1, depending on its settings and characteristics, the fan can be:

- In full compensation of leakage if the ATDs flowrates are the one expected (good IAQ but electrical overconsumption)

- In zero compensation of leakage if no additional flowrate is provided to compensate for leakage (poor IAQ but no electrical overconsumption)
- In partial compensation, with an IAQ more or less deteriorated and a more or less significant electrical overconsumption depending on the compensation rate

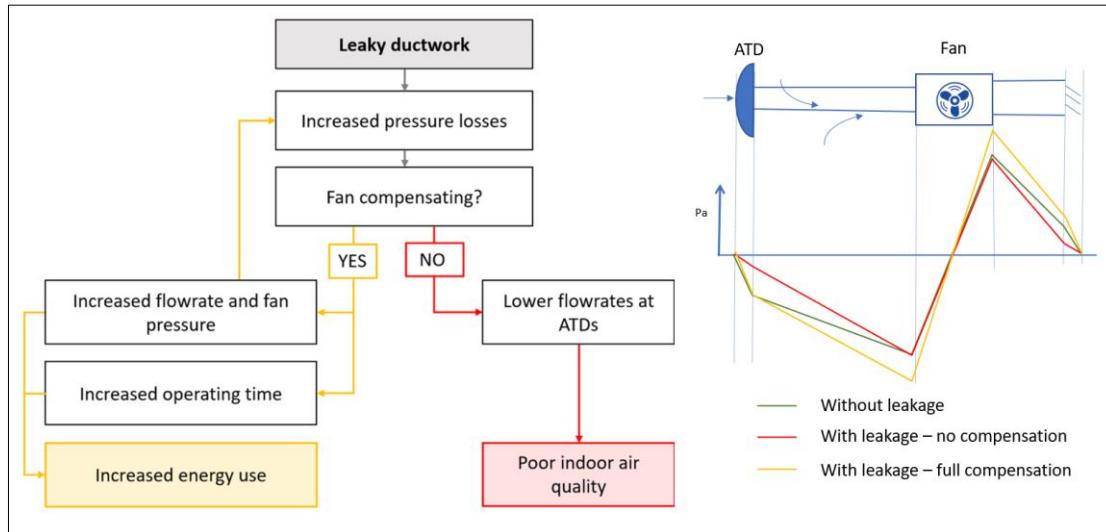


Figure 1- Impact of leaky ductwork

The fan efficiency (η) varies with its flowrate, but for simplification purposes, it is considered constant in this study whatever the airtightness level of the ductwork.

2.2 Pressure losses

Pressure drop in ductwork systems is due to the irreversible transformation of mechanical energy into heat (ASHRAE, 2013). There are two types of losses:

- friction losses (occurring along the ductwork)
- and dynamic losses (occurring at bends and junctions)

Friction losses

Friction losses occur along the entire length of duct. They are due to fluid viscosity. Friction loss can be calculated using the Darcy equation (ASHRAE, 2013):

$$\Delta p_f = \frac{1000fL}{D_h} * \frac{\rho V^2}{2} \quad (2)$$

Δp_f	Pa	Friction losses in terms of total pressure
f	-	Friction factor
L	m	Duct length
D_h	m	Hydraulic diameter
V	m/s	Velocity
ρ	kg/m ³	Air density

Friction losses are proportional to the flow velocity to the power of 2 so also to the square of the flowrate.

Dynamic losses

Dynamic losses result from flow disturbance caused by duct accessories, which change the direction of the flow (bends) and of the hydraulic diameter (adaptors) and at converging/diverging junctions.

Dynamic loss can be calculated using the following equation (ASHRAE, 2013):

$$\Delta p_t = \frac{C\rho V^2}{2} \quad (3)$$

C	-	Total loss coefficient (from all flow disturbances)
Δp_t	Pa	Total pressure loss due to dynamic losses

Total pressure loss in the ductwork

Total pressure loss in a duct section is calculated by combining friction and dynamic losses.

$$\Delta p_{loss} = \left(\frac{1000f}{D_h} + \sum C \right) \left(\frac{\rho V^2}{2} \right) \quad (4)$$

Therefore, the pressure loss in the ductwork system is proportional to the square of the flowrate and the higher the flowrate to overcome ductwork leakage, the higher resistance in the ductwork.

2.3 Electrical overconsumption calculation in full compensation conditions

The fan electrical overconsumption is estimated assuming a full compensation of ductwork leakage. The fan flowrate increases therefore with the air permeability of the ductwork:

$$Q_{AHU,real} = Q_{AHU,0} + Q_{l,real} \quad (5)$$

$Q_{AHU,real}$	m ³ /h	Fan flowrate with the real ductwork airtightness level
$Q_{AHU,0}$	m ³ /h	Fan flowrate with no ductwork leakage
$Q_{l,real}$	m ³ /h	Leakage flowrate within the ductwork

With:

$$Q_{l,real} = A_{du} \times C_l \times \Delta p_{a,du}^{0.65} \times 3600 \quad (6)$$

A_{du}	m ²	Ductwork area
C_l	m ³ /s/m ² at 1Pa	Airtightness factor of the ductwork
Δp_{du}	Pa	Average pressure difference between inside and outside the ductwork

The average pressure difference between inside and outside the ductwork is given by:

$$\Delta p_{a,du} = \frac{\Delta p_{ATD} + \Delta p_{AHU}}{2} \quad (7)$$

$\Delta p_{a,du}$	Pa	Average pressure difference between inside and outside the ductwork
Δp_{ATD}	Pa	Required pressure at air terminal devices to provide required airflow

The pressure induced by the fan Δp_{AHU} depends on the airtightness level of the ductwork as more leakage increase the total flowrate and therefore the pressure losses (see equation (4)).

To simplify the calculation and to avoid cross-reference, the ductwork leakage is calculated using equation (6) assuming a constant average pressure in the ductwork, which is the value without leakage:

$$\Delta p_{a,du} \approx \frac{\Delta p_{ATD} + \Delta p_{AHU,0}}{2} \quad (8)$$

The airtightness factor of the ductwork characterizes the level of airtightness. The limit values for each airtightness classes used in this study can be read in Table 1.

Table 1 - Classification of ductwork airtightness according to EN 16798-3 (CEN, 2017)

Airtightness classes		Air leakage limit (f _{max}) according to the test pressure (p _t) [m ³ .s ⁻¹ .m ⁻²]
Prev. name	New name	
3A	-	0,0810 x p _t ^{0,65} x 10 ⁻³
2,5A	ATC 6	0,0675 x p _t ^{0,65} x 10 ⁻³
1,5A	-	0,0405 x p _t ^{0,65} x 10 ⁻³
A	ATC 5	0,027 x p _t ^{0,65} x 10 ⁻³
B	ATC 4	0,009 x p _t ^{0,65} x 10 ⁻³
C	ATC 3	0,003 x p _t ^{0,65} x 10 ⁻³
D	ATC 2	0,001 x p _t ^{0,65} x 10 ⁻³
-	ATC 1	0,00033 x p _t ^{0,65} x 10 ⁻³

For each airtightness level, the pressure at the fan is calculated as follows:

$$\Delta p_{AHU,real} = \Delta p_{ATD} + \Delta p_{loss,real} \quad (9)$$

Yet, according to equation (4) the pressure losses inside the ductwork increase with the square of the flowrate when leakages are compensated:

$$\frac{\Delta p_{loss,real}}{\Delta p_{loss,0}} = \frac{\left(\frac{1000f}{D_h} + \sum C_t\right) \left(\frac{\rho V_{real}^2}{2}\right)}{\left(\frac{1000f}{D_h} + \sum C_t\right) \left(\frac{\rho V_0^2}{2}\right)} = \frac{V_{real}^2}{V_0^2} = \frac{Q_{AHU,real}^2}{Q_{AHU,0}^2} \quad (10)$$

Combining equations (9) and (10):

$$\Delta p_{AHU,real} = \Delta p_{ATD} + (\Delta p_{AHU,0} - \Delta p_{ATD}) \times \frac{Q_{AHU,real}^2}{Q_{AHU,0}^2} \quad (11)$$

The fan power $P_{AHU,real}$ (W) is calculated for each airtightness level using equations (1), (5) and (11):

$$P_{AHU,real} = \frac{\Delta p_{AHU,real} \times Q_{AHU,real}}{\eta \times 3600} \quad (12)$$

The power difference between the real and no leakage cases is given by:

$$\Delta P_{AHU,real} = P_{AHU,real} - P_{AHU,0} \quad (13)$$

2.4 Related extra costs calculation

The extra costs related ductwork leakage fully compensated are calculated with the fan overconsumption, the yearly operating time ($t_{AHU,y}$) and the electricity price (price_{elec}):

$$extra_cost_l = \frac{\Delta P_{AHU,real}}{1000} \times t_{AHU,y} \times price_{elec} \quad (14)$$

3 RESULTS

3.1 Calculation Tool

A calculation tool was developed using the above model. A screenshot is presented in Figure 2. The objective is to raise awareness about the negative impact of leakage and encourage the design and installation of airtight ventilation ductwork systems, which are readily available on the market. This tool is designed to be user-friendly with few simple inputs:

- **Designed fan characteristics:** flowrate, pressure and power
- **Ductwork area:** with a tool to estimate it from ductwork dimensions if the data is not available
- **Annual operating time:** with a tool to estimate it if the data is not available
- **National cost of a kWh:** to translate the energy losses into costs
- **Years of operation:** to estimate the impact through the whole ductwork lifespan, with a tool to estimate it if the data is not available according to data provided by Andersen and Negendahl (2023).

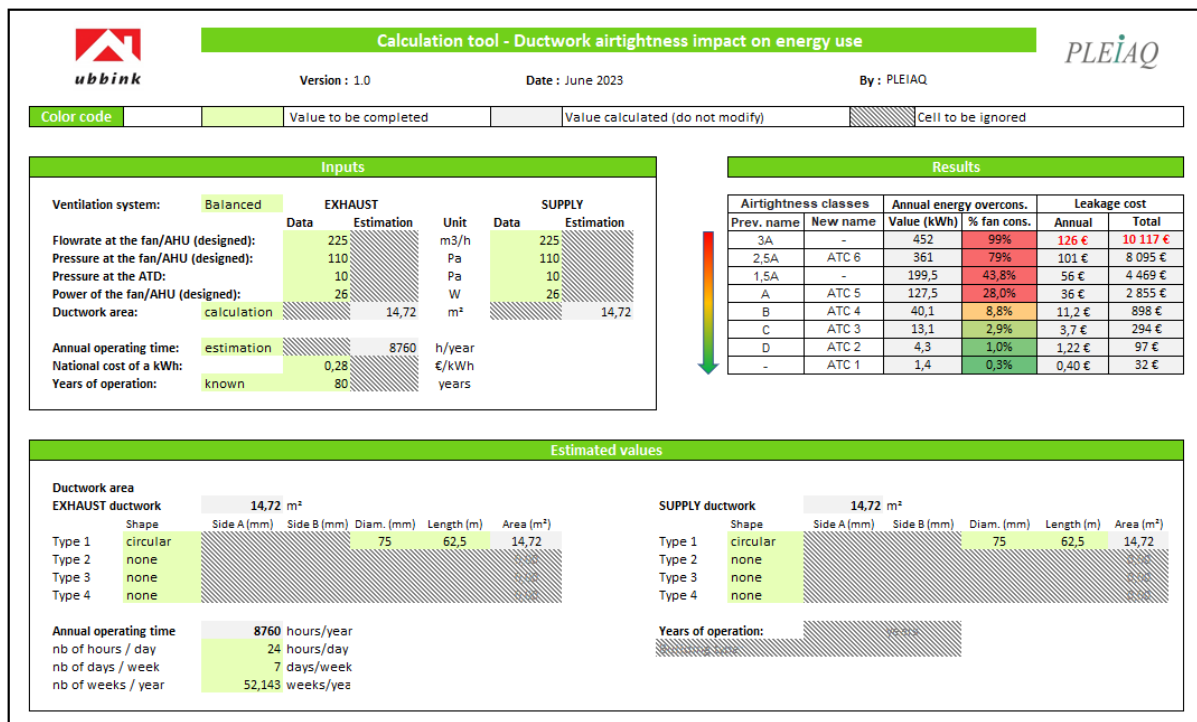


Figure 2 - Calculation tool (for the case study of house 1)

As an output, the impact of the ductwork leakage is calculated using the equations presented in section 2 for the various ductwork airtightness classes (see Table 1), with the following parameters:

- **The annual energy overconsumption** compared to a perfectly airtight ductwork given in kWh and as a percentage of the fan consumption without leakage.
- **The financial cost** of the ductwork leakage compared to a perfectly airtight ductwork, given both annually and as a total for the estimated years of operations.

3.2 Case studies

The following four scenarios have been simulated (data from (Leprince et al., 2019)):

- **House 1** is a medium-sized house with a central mechanical ventilation system with heat recovery. The ductwork system is a radial air distribution system using semi-rigid plastic ductwork. The diameter of the ductwork is 75mm and the total length is 125m. It is assumed that the ductwork is equally split between supply and extract.
- **House 2** is also a medium sized house a central mechanical ventilation system with heat recovery. The ductwork system is a trunk and branch air distribution system using metal or rigid plastic ductwork with 6m of ductwork DN160mm and 40m of ductwork DN125mm. It is assumed that the ductwork is equally split between supply and extract.
- **House 3** is a large house with a central mechanical ventilation system with heat recovery. The ductwork system is a radial air distribution system using semi-rigid plastic ductwork. The diameter of the ductwork is 75 mm and the total length is 200 m. It is assumed that the ductwork is equally split between supply and extract.
- **House 4** is a large house with a humidity-based extract only ventilation system, with self-adjusting ATD. The average flowrate is 100 m³/h. The required pressure at the ATD is 70 PA. The ductwork area is assumed to be 7.4m² (radial air distribution system).

For the houses 1 to 3, the fan power value is read from the performance curves of a ventilation unit with heat recovery with a high efficiency (provided by the manufacturer). The corresponding fan efficiency calculated according to equation (1) is 26% for houses 1 and 2, and 27% for house 3. The fan power value for the house 4 is calculated with equation (1) assuming a similar fan efficiency of 27%.

In addition, one of the 10 AHU of a 4500 m² French school building (for 500 children) has been simulated (data from the PromevenTertiaire project (Hurel and Leprince, 2022b)).

Table 2 – Parameters of the ventilation systems for the 5 case studies (for houses 1 to 3: data apply to both exhaust and supply systems)

	House 1	House 2	House 3	House 4	School (1 AHU)	
	Exh./Sup.	Exh./Sup.	Exh./Sup.	Exh.	Exh.	Sup.
Fan flowrate (m³/h)	225	225	300	100	13500	11855
Fan pressure (Pa)	110	110	160	150	130	130
Pressure ATD (Pa)	10	10	10	70	43	35
Fan power (W)	26	26	49	15.4	4701	4143
Ductwork area (m²)	14.72	9.36	23.6	7.4	317	279
Operating time (h/y)	8760				1140*	

* 2000 hours (10 h/d; 5 d/w; 40 w/y) x 57% due to CO₂ regulation (value from the Avis Technique of the ventilation system)

The annual energy overconsumption resulting from ductwork leakage is presented in Table 3 with both the value in kWh and as a percentage of the fan consumption without leakage. If the fans are able to fully compensate for leakage, the annual energy use increase for a very leaky ductwork (3A) compared to an airtight one ranges between 58% and 173% for the 4 single-family houses, and is of 33% for the school AHU.

The corresponding financial losses assuming 80 years of operation and an electricity cost of 0.28 €/kWh (EU average in the second half of 2022 according to Eurostat¹) are presented in Table 4. For very leaky ductwork (3A), they range from 50€ to 415€ per year (4.0 k€ to 33.2 k€ after 80 years) for the single-family houses, and 922€ per year (74 k€) for one of the school

¹ <https://query.no/consumer-energy-prices-in-europe/>

AHU. As there are in total 10 AHU in the school, the total financial impact would probably be in the order of magnitude of 10 k€ each year for this airtightness level.

In addition, the annual fan(s) energy uses for each building are plotted in Figure 3 according to the ductwork airtightness level. One can note that the energy use strongly decreases by improving the ductwork airtightness until ATC 4 (class B) and then tends to decrease more slowly when improving until ATC 1.

Table 3 – Annual energy overconsumption due to ductwork leakage (absolute value and percentage of fan energy use) according to the ductwork airtightness level for the 5 case studies

Airtight. classes		House 1		House 2		House 3		House 4		School (1 AHU)	
Prev.	New	kWh	%fan	kWh	%fan	kWh	%fan	kWh	%fan	kWh	%fan
3A	-	451,7	99,2%	262,6	57,6%	1482	173%	180,1	133%	3293	33%
2,5A	ATC 6	361,4	79,3%	213,0	46,8%	1164	136%	142,1	105%	2697	27%
1,5A	-	199,5	43,8%	121,1	26,6%	617,6	71,9%	76,1	56,4%	1562	15,5%
A	ATC 5	127,5	28,0%	78,6	17,2%	386,4	45,0%	47,9	35,5%	1023	10,2%
B	ATC 4	40,1	8,8%	25,2	5,5%	118,1	13,8%	14,8	10,9%	333,1	3,3%
C	ATC 3	13,1	2,9%	8,3	1,8%	38,2	4,5%	4,8	3,6%	110,2	1,1%
D	ATC 2	4,3	1,0%	2,8	0,6%	12,6	1,5%	1,6	1,2%	36,6	0,4%
-	ATC 1	1,4	0,3%	0,9	0,2%	4,2	0,5%	0,5	0,4%	12,2	0,1%

Table 4 - Annual and total (for 80 years of operation) cost of ductwork leakage according to the ductwork airtightness level for the 5 case studies

Airtight. classes		House 1		House 2		House 3		House 4		School (1 AHU)	
Prev.	New	Annual	Total	Annual	Total	Annual	Total	Annual	Total	Annual	Total
3A	-	126 €	10 117 €	73,5 €	5 881 €	415 €	33 199 €	50,4 €	4 035 €	922 €	73 772 €
2,5A	ATC 6	101 €	8 095 €	59,7 €	4 772 €	326 €	26 071 €	39,8 €	3 182 €	755 €	60 415 €
1,5A	-	55,9 €	4 469 €	33,9 €	2 713 €	173 €	13 834 €	21,3 €	1 706 €	437 €	34 999 €
A	ATC 5	35,7 €	2 855 €	22,0 €	1 760 €	108 €	8 655 €	13,4 €	1 073 €	287 €	22 924 €
B	ATC 4	11,2 €	898 €	7,1 €	565 €	33,1 €	2 645 €	4,1 €	331 €	93,3 €	7 463 €
C	ATC 3	3,7 €	294 €	2,3 €	186 €	10,7 €	856 €	1,3 €	107 €	30,8 €	2 468 €
D	ATC 2	1,22 €	97 €	0,77 €	62 €	3,53 €	282 €	0,44 €	36 €	10,26 €	820 €
-	ATC 1	0,40 €	32 €	0,26 €	21 €	1,17 €	94 €	0,15 €	12 €	3,41 €	273 €

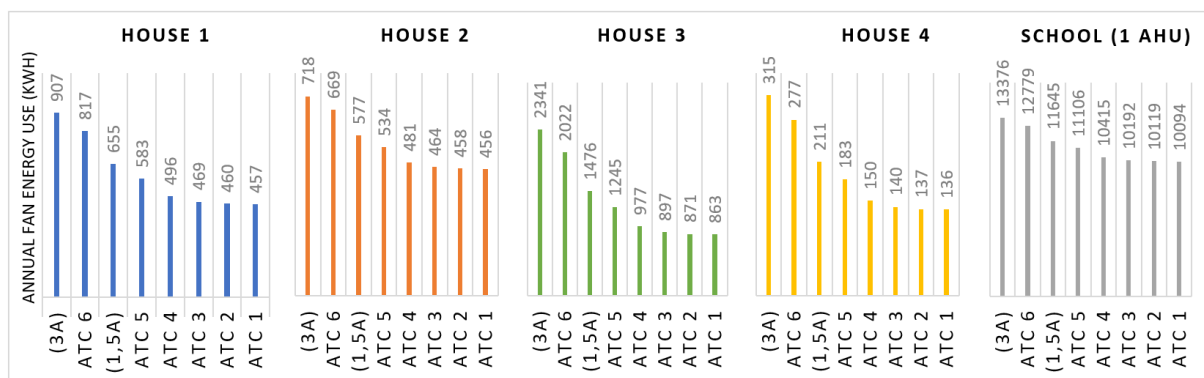


Figure 3 - Annual fan energy use for each case study according to the ductwork airtightness level

4 CONCLUSIONS

A simple tool was developed using a simplified model to estimate the financial impact of leaky ductwork in buildings over their whole life. It assumes that the design or hygienic flow rates in all habitable and wet rooms are achieved, that is to say that the fan fully compensates for ductwork leakage. The purpose of this user-friendly tool is to help to raise awareness about this issue and encourage the design and installation of airtight ventilation ductwork systems, which are readily available on the market.

It has been designed for central mechanical ventilation systems with energy recovery and central mechanical extract ventilation systems

Case studies for 4 houses and one of the 10 AHU of a school building show the significant impact of ductwork leakage on energy use and electricity bills. It is found that a very leaky ductwork (class 3A) induces:

- an increase of fan energy use ranging between 58% and 173% for the 4 single-family houses (180 to 1482 kWh) and of 33% for the school AHU (3293 kWh).
- a financial impact for 80 years of operation ranging between 4.0 k€ to 33.2 k€ for the 4 single-family houses and reaching 74 k€ for the school AHU (out of the 10 AHU).

To conclude, this tool shows the significant financial benefits of installing airtight ventilation ductwork systems in all buildings, including single-family houses with rather small ductwork areas. For larger buildings with more powerful fans and larger ductwork areas, the energy use and financial impact are vastly increased. A good level of ductwork airtightness also reduces the risks of noise and/or odour hindrance, and in case the air is preconditioned the energy and financial savings are even more substantial.

5 ACKNOWLEDGEMENTS

This work was funded by Ubbink. The views and opinions of the authors do not necessarily reflect those of Ubbink. The published material is being distributed without warranty of any kind, either expressed or implied. The responsibility for the interpretation and used of the material lies with the reader. In no event shall PLEIAQ or Ubbink be liable for damages arising from its use any responsibility arising from the use of this document lies with the user.

6 REFERENCES

- Andersen, R., Negendahl, K., 2023. Lifespan prediction of existing building typologies. *Journal of Building Engineering* 65, 105696.
<https://doi.org/10.1016/j.job.2022.105696>
- ASHRAE, 2013. *ASHRAE Handbook of Fundamentals*. Atlanta, GA.
- CEN, 2017. EN 16798-3:2017 - Energy performance of buildings - Ventilation for buildings - Part 3: For non-residential buildings - Performance requirements for ventilation and room-conditioning systems (Modules M5-1, M5-4).
- Hurel, N., Leprince, V., 2022a. Ductwork leakage: practical estimation of the impact on the energy overconsumption and IAQ. Presented at the 42nd AIVC-10th TightVent- 8th venticool conference, Rotterdam, The Netherlands.
- Hurel, N., Leprince, V., 2022b. Impact of ventilation non conformities: calculation methodology and on-site examples. Presented at the 42nd AIVC-10th TightVent- 8th venticool conference, Rotterdam, The Netherlands.

- Leprince, V., Hurel, N., Kapsalaki, M., 2020. VIP 40: Ductwork airtightness - A review. AIVC.
- Leprince, V., Lightfoot, M., Jong, J., 2019. Impact of ductwork leakage on the fan energy use and sound production of central mechanical ventilation units in houses, in: Proceedings of the 40th AIVC - 8th TightVent - 6th Venticool Conference. Presented at the From energy crisis to sustainable indoorclimate – 40 years of AIVC, Ghent, Belgium.
- Moujalled, B., Leprince, V., Melois, A., 2018. Statistical analysis of about 1,300 ductwork airtightness measurements in new French buildings: impacts of the type of ducts and ventilation systems. Presented at the 39th AIVC conference “Smart ventilation for buildings.”

Decoding 30 Years of Insights: Conclusions from ISIAQ's Landmark Webinar Series on Indoor Air Quality and Climate

Ying Xu

Department of Building Science, Tsinghua University, Beijing, China

SUMMARY

In celebration of its 30th Anniversary in 2022, the International Society of Indoor Air Quality and Climate (ISIAQ) organized a groundbreaking webinar series that spanned the entire year. This series brought together esteemed researchers who have made significant contributions to the field of indoor air sciences, as well as young and promising researchers who are shaping the future of research in this domain.

Comprising six informative webinars (<https://www.isiaq.org/webinars.php>), the series covered a wide range of crucial topics. The first webinar, titled "30+ Years of Knowledge Creation: Indoor Air 1991-2021," delved into the wealth of knowledge accumulated over three decades in the realm of indoor air quality, focusing on research published in the *Indoor Air* journal. It explored the evolution of research, advancements in technology, and the current state of understanding in the field.

The second webinar, "What We Know and What We Should Know About Indoor Environmental Quality," tackled the existing knowledge and identified areas that require further exploration and understanding in the realm of indoor environmental quality. It provided insights into the latest research findings and highlighted important knowledge gaps that need to be addressed.

Recognizing the often-overlooked exposure route, the third webinar, "Dermal - the often-overlooked exposure route," shed light on the significance of dermal exposure in indoor environments. Experts discussed the impact of various chemicals and pollutants that can affect human health through skin contact.

In light of the pressing challenges posed by energy crises, pandemics, and climate change, the fourth webinar, "Winter is coming: challenges for indoor air sciences in times of energy crisis, pandemics & climate change," explored the unique challenges faced by indoor air sciences in these complex times. It emphasized the importance of developing sustainable, resilient, and healthy indoor environments.

Shifting the focus from research to practical application, the fifth webinar, "From Research to Practice: Past Successes and Remaining Gaps," examined the successful translation of research findings into practical solutions for improving indoor air quality. It identified areas where further research and collaboration are needed to bridge remaining gaps between theory and practice.

Lastly, the series concluded with a webinar titled "The long history of airborne infection transmission: why don't we use the knowledge we have," which addressed the historical knowledge and understanding of airborne infection transmission. Experts emphasized the importance of utilizing existing knowledge and implementing appropriate measures to mitigate the spread of airborne diseases.

Overall, the ISIAQ's 30th Anniversary webinar series provided a comprehensive platform for renowned researchers and emerging talents to exchange insights, discuss pressing issues, and highlight the future directions of indoor air sciences. It celebrated the past achievements of the society while also recognizing the importance of continuous research and collaboration in ensuring healthy and sustainable indoor environments.

Calculation of the effect of ventilation measures in existing dwellings to reduce the carbon footprint

Wim Kornaat¹, Wouter Borsboom¹, Ruud van der Linden¹

*1 TNO, Molengraaffsingel 8, 2629JD Delft,
Netherlands*

ABSTRACT

To reduce the carbon footprint of the built environment, a significant overhaul of the existing housing stock is essential. This entails not only ensuring proper insulation and airtightness in residences but also optimizing their ventilation systems. To precisely gauge the impact of an advanced ventilation system, the use of a pressure node model, such as multizone ventilation models like COMIS or TNO's AirMAPs model, is indispensable. However, when dealing with existing dwellings, numerous unknown variables, including interior door usage, can introduce substantial variations in results. A simplified approach can also lead to reduced calculation times. This paper employs a simplified approach, comparing advanced ventilation solutions in a specific dwelling based on limited building and user behaviour data. We present the current progress in modelling choices, and the initial results are promising. Initial results from the first comparison between the Dutch standard ventilation method (BKN) and the single-zone model are promising. When examining manually operated mechanical exhaust and natural supply systems (C1) alongside manually operated balanced heat recovery systems (D2), the ventilation flows align well. Furthermore, the CO₂-controlled systems demonstrate a reasonable and as might be expected reduction of ventilation flows in relation to the actual CO₂-control as being used .

KEYWORDS

Simulation, ventilation system, retrofitting, energy efficiency, indoor air quality, simplified one zone, multizone models

1 INTRODUCTION

To mitigate the carbon footprint of the built environment, a substantial transformation of existing housing stock is imperative. This involves not only ensuring proper insulation and airtightness in residences but also optimizing their ventilation systems. In recent years, there has been a surge in innovative ventilation solutions in the market, enabling precise timing and location of ventilation based on occupancy patterns. This leads to a significant reduction in overall ventilation and, consequently, reduced heating requirements.

Numerous programs are available for simulating heat losses and gains and indoor environmental quality in dwellings, ranging from basic RC networks to more advanced tools such as TRNSYS or EnergyPlus. To accurately evaluate the impact of an advanced ventilation system, a pressure node multizone ventilation model such as COMIS [1] or the AirMAPs model [2] [3] developed by TNO is indispensable. However, when dealing with existing dwellings, several unknown variables, such as interior door, can introduce substantial variations in results. A simplified approach can also lead to reduced calculation times. This

paper adopts a simplified approach, comparing advanced ventilation solutions in a specific dwelling based on limited building and user behaviour data.

Moreover, there is a multitude of systems designed to recover heat or cold from exhaust air, subsequently using it to heat or cool supply air or provide hot tap water. To make informed decisions among these various ventilation system options and combinations for reducing the carbon footprint, it is crucial to understand their effects within a specific home. These effects depend on various factors, including the insulation quality of the building envelope, which influences the duration of the heating or cooling season. Additionally, factors such as infiltration and window usage play a pivotal role in determining heating and cooling demands. Furthermore, infiltration rates vary, depending on whether a balanced ventilation system or a system that creates over or under pressure is employed.

2 SIMPLIFIED MODELING APPROACH ENERGY AND IEQ

To achieve a precise evaluation of thermal comfort and energy consumption, it is imperative to employ a fine spatial resolution, involving multiple zones, in the modelling process, as opposed to using a single zone for a house. In our approach of reduced-order modelling, the primary focus is on employing a multizone RC-model (heat model). It's important to note that a multizone ventilation model demands a substantial number of input parameters and considerably extends the calculation time. Hence, we aim to integrate this multizone RC model with a one-zone ventilation model, a strategy that not only curtails the volume of required input parameters but also minimizes simulation time. The integration of models with different number of zones for the thermal and ventilation model necessitates a flexible coding framework for the comprehensive model.

2.1 Multizone RC network

In order to develop a more precise reduced RC model, we will employ a variety of standardized dwelling layouts that accurately represent the Dutch building stock. These layouts are visually depicted in figure 1 and encompass an apartment (or single-story dwelling) as well as 2-story or 3-story single-family houses. The number of thermal zones will range from 2 to 4, enhancing spatial detail. In the context of an apartment, a minimum of 2 zones is essential to replicate the influence of diverse room orientations. Typically, residents in the Netherlands tend to heat either the living room or, in some cases, both the living room and the bedroom, and occasionally even the attic. This leads to a maximum of 4 thermal zones. Each dwelling layout includes zones oriented in different directions, a crucial factor for investigating potential overheating issues.

For a specific dwelling, based on a pre-established Building Information Model (BIM), specifically gbXML in this case, an RC-model will be created [4], serving as a Building Energy Model (BEM). Given that both models function as network models, the transition from BIM to BEM is automated.

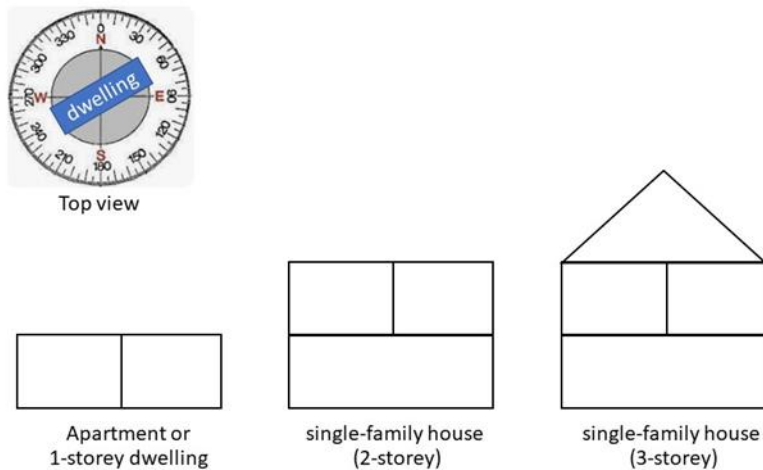


Figure 1: Reduced thermal model layouts characteristic for the Dutch building stock

2.2 Ventilation model

In order to reduce the number of input parameters of the ventilation model and reduce simulation time, we will implement a one-zone ventilation model, integrated with a multizone RC network. Within this model the ventilation features, including mechanical flows and ventilation grilles, based on the ventilation system, the envelope's leakages and the windows, will be automatically incorporated to align with the underlying multizone RC-model. This means, for instance, that the ventilation model includes envelope leakages and ventilation grilles, if present, for each zone within the thermal model. The ventilation flow in each zone is calculated by considering both the airflow through cracks, window openings, and grilles in the façade, as well as the mechanical ventilation provision within the zone. Figure 2 illustrates an example of the one-zone ventilation model for a mechanical exhaust system in a single-family house, with a 4-zone thermal RC-model delineated by a dotted line.

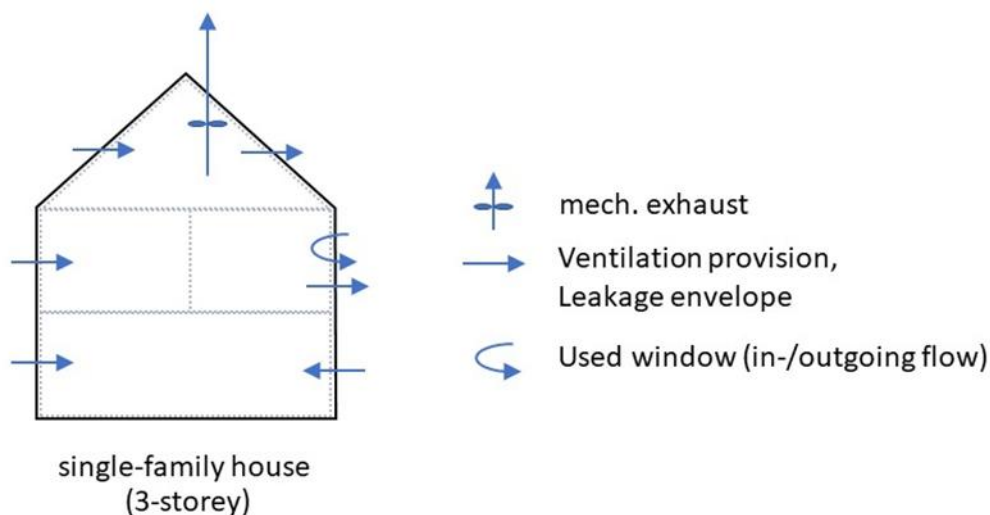


Figure 2: One zone ventilation model in combination with single-family house RC-model

2.3 Driving forces

The ventilation model will consider various driving forces, including wind pressures, thermal buoyancy and mechanical fans. To simulate wind pressures, we will create several sets of wind pressure coefficients tailored to different dwelling typologies, such as sheltered locations and non-sheltered locations. For thermal buoyancy, we will utilize the indoor temperatures calculated using the RC model and the placement of openings aligns with the BIM model.

2.4 Ventilation systems

We have integrated various types of ventilation systems and ventilation system controls into the ventilation simulation, all of which are commonly utilized in Dutch houses. Here are the details, including their respective names according to the Dutch Standard for energy performance building calculations (NTA8800):

- a) Manual control of mechanical exhaust systems with standard grilles or self-controlled grilles based on 1 Pa (Type C2 and C2a).
- b) Manual control of balanced ventilation systems (Type D2).
- c) CO₂-controlled exhaust systems (Type C4a and C4c).
- d) CO₂-controlled balanced ventilation systems (Type D3).
- e) Fans (central or decentralized) with CO₂ control on a per-room basis (Types C5b, D5a, and D5b).

These ventilation systems encompass the ones currently used in Dutch houses and those that can be implemented during renovations. They range from systems primarily operated manually to those equipped with room-level CO₂ control. For the manual control of ventilation provisions, we extract data from schedules (time series). CO₂ control is automatically simulated based upon the presence of individuals in various zones, as dictated by occupancy patterns.

2.5 Presence and occupant behaviour

The presence of individuals and their behavior regarding the manual use of ventilation systems, internal doors and windows is determined through schedules (time series). We employ hourly schedules for both weekdays and weekends. To model the utilization of ventilation systems and windows, multiple schedules are created, each assuming different usage patterns for these elements.

Regarding occupancy, it's common for people to be present for a few hours during the day or evening in the living room, and during the night in the bedroom(s). The number of bedrooms in use is determined based on the number of individuals in the household. This information is especially significant for CO₂-controlled ventilation systems, where occupancy plays a crucial role.

2.6 Indoor Air Quality

The RC-model encompasses the living and sleeping zones. By using the square meter data from the BIM file, the ventilation provisions are established in accordance with Dutch building standards for each thermal zone. This approach provides a clear understanding of the required ventilation for each zone when occupied. When combined with the concurrently simulated ventilation, it offers insights into indoor air quality throughout the simulated time period. When individuals are present in a thermal zone, we assess the Indoor Air Quality (IAQ). We calculate the IAQ by determining the ratio between the ventilation rate and the

number of individuals multiplied by the required ventilation per person, which is fixed at 25 m³/h and 70% of 25 m³/h during sleeping due to the lower metabolism.

$$\text{Formula: IAQ(zone)} = \text{ventilation} / (\text{number of persons} * 25 \text{ m}^3/\text{h}) \quad (1)$$

As KPI is considered the percentage of time with IAQ < 1 (based on the time a person is present in a zone or in the dwelling).

In cases of exfiltration, we take into account the average pollution of the rest of the dwelling and use that to determine IAQ of room.

2.7 Window modelling

We will investigate the significance of turbulent air exchange, where both ingoing and outgoing airflow occur simultaneously when windows are open (as depicted in figure 3) [5]. This turbulent air exchange is influenced by factors such as the temperature disparities between the indoor and outdoor environments, as well as the dimensions and surface area of the window [6].

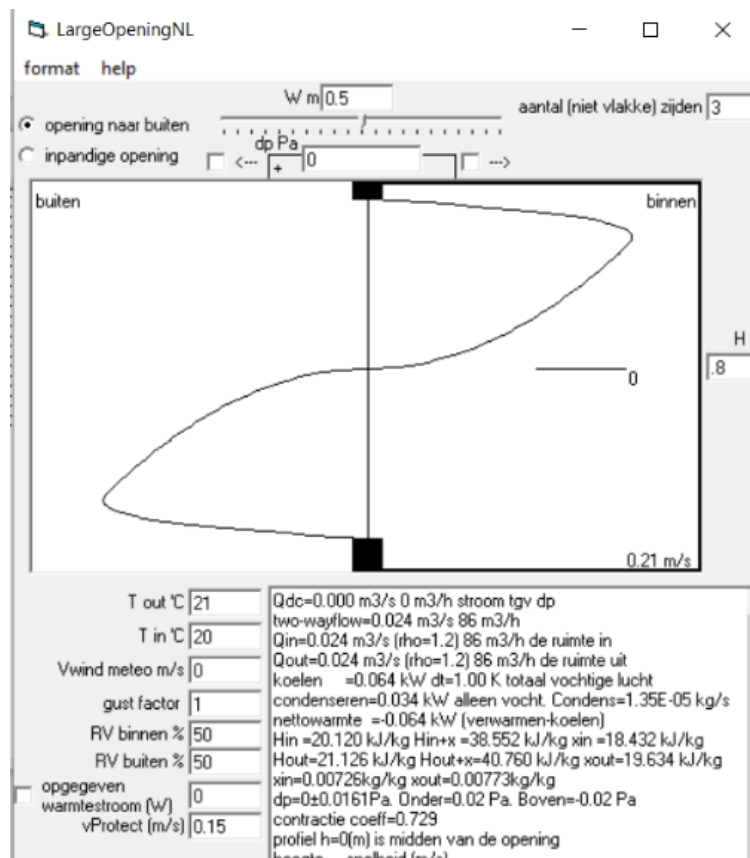


Figure 3: Turbulent air exchange open window

2.8 Internal door modelling

The state of internal doors, whether open or closed, has a substantial impact on ventilation flow, particularly when grilles or windows are open on both sides of a building. This consideration notably applies to bedroom doors. In the Netherlands, there are varying practices, with some individuals keeping them closed almost all the time while others leave them open frequently. The latter approach enhances cross-ventilation by exploiting pressure disparities created by wind affecting different building facades. We will explore scenarios with bedroom doors either consistently closed or consistently open.

In the case of closed internal doors, the ventilation model will account for additional resistance in the openings of ventilation grilles or windows. This approach addresses the typical challenges associated with ventilating bedrooms located on the leeward side of single-family houses.

2.9 Airtightness

The airtightness of a specific dwelling will be determined either through measurements, if available, or calculated in accordance with the Dutch NTA8800 standard, taking into consideration the construction year and the type/layout of the dwelling.

3 VALIDATION OF THE SIMULATION MODEL

Simulations are conducted using a ground-based row dwelling as the basis for comparison. These simulations are compared with simulations based on the multizone ventilation model COMIS, following a standardized Dutch method (BKN).

3.1 Comparison between simplified method and standardized Dutch method

A comparison is conducted using a typical row dwelling, considering both the standardized Dutch method (BKN) and the simplified method as shown in figure 4. In figure 4 the ventilation due to the ventilation system (without leakages) is given. The assessment involves scenarios for the simplified 1 zone model used by a household of 2 or 4 persons, utilizing a mechanical exhaust system with manual control and a grills in the façade (C1), as well as a manually controlled balanced ventilation system with heat recovery (D2). The ventilation flows in these scenarios align closely with each other.

Additionally, various other ventilation systems are evaluated using the simplified method, and the resulting ventilation flows appear reasonable or as might be expected. The reduction of the ventilation is in line with the reduction for the different ventilation systems according to the Dutch Standard to calculate the EPBD (NTA8800), this will be reported more extensive in future publications. Furthermore the following can be concluded:

- The flow with CO₂-controlled systems (exhaust systems C4a, C4c and C5b and balanced systems D3, D5a and D5b) are substantial reduced in relation to the manual controlled systems (respectively C1 and D2).
- Systems C4a and C4c have the same flows in case of a household with 2 persons, because these 2 persons only use the zones equipped with CO₂-control according system C4a (living room and main bedroom). So the CO₂-control in the other zones in case of system C4c (living room and all bedrooms) is not used. With 4 persons however the ventilation with system C4c increases to some extend in relation to system C4a, because of the fact that in case of 4 persons also other bedrooms (besides the main bedroom) are used. Thus the ventilation increases using system C4c, but also the IAQ improves.
- System D3 has a very low ventilation. This is due to the fact that only the living room is CO₂-controlled. When people use the bedrooms in case of system D3 the ventilation is not increased, while the system D5a and D5b have CO₂-control in all bedrooms and thus increase the ventilation in case the bedrooms are used. The system D5a and D5b thus have a higher ventilation compared to system D3, but also a better IAQ. Overall the system D5a and D5b thus are better.

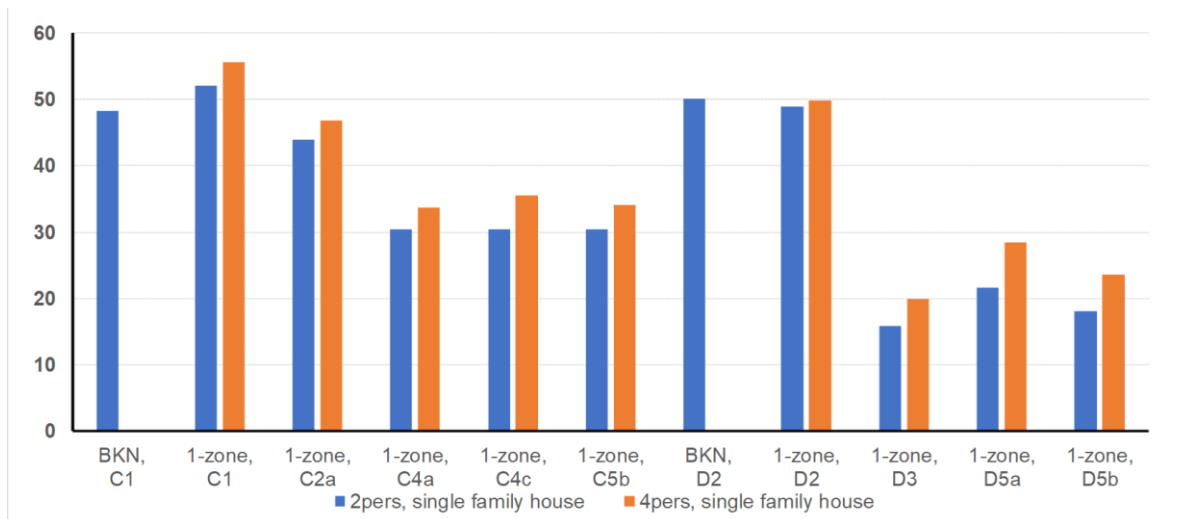


Figure 4: Average ventilation flows are compared in dm³/s between the standardized Dutch BKN method and the simplified 1 zone method for 2 persons and 4 persons household using manual controlled ventilation systems C1 and D2. Including calculations of the 2 persons and 4 persons household of the 1 zone ventilation model using different controlled ventilation systems (C2a, C4a, C4c, C5b, D3, D5a and D5b).

4 CONCLUSIONS

Initial results from the first comparison between the Dutch standard ventilation method (BKN) and the single-zone model are promising. When examining manually operated mechanical exhaust and natural supply systems (C1) alongside manually operated balanced heat recovery systems (D2), the ventilation flows align well. Furthermore, the CO₂-controlled systems demonstrate a reasonable and as might be expected reduction of ventilation flows in relation to the actual CO₂-control as being used, and these reductions are also in line with the Dutch Standard for EPBD Calculations (NTA 8800).

Additionally, more in-depth investigation is required to compare ventilation flows per zone calculated in a multi-zone model, with particular attention to the zoned ventilation system.

We will further research a one value KPI for IAQ to compare different renovation measures with end users.

5 ACKNOWLEDGEMENTS

We thank the Ministry of the Interior and Kingdom Relations (BZK) for the funding provided for the project “Renovatieverkenner”.

6 REFERENCES

In the text, references that are cited in a reference list should mention the author’s surname and the year of publication. Example:

- [1] Warren P (1996) *Multizone Air Flow Modelling (COMIS) - Technical Synthesis Report IEA ECBCS Annex 23 Energy Conservation in Buildings and Community Systems*
- [2] Borsboom W (2022), *A novel model based approach of an integrated ventilation and heating model for monitoring and control*, AIVC 2022
- [3] Kornaat W (2020) *KIP2020-Energieprestatie en binnenmilieukwaliteit, WP2: Uitbreiding digital twin met eigen ventilatiemodel (AirMAPs)*, TNO internal report

- [4] Borsboom W (2022) *Reducing peak load of renewable energy at district level with predictive twins* SBE, conference
- [5] Phaff, J.C. et al.,(1980) The ventilation of buildings. Investigation of the consequences of opening one window on the internal climate of a room. IMG-TNO, report C 448, Delft,
- [6] Gids W (1982) *Ventilation Rates and Energy Consumption due to open windows, a brief overview of research in the Netherlands*, Air Infiltration Review, vol.4, issue.1, pp.4-5
- [7] Ventilation Rates and Energy Consumption due to open windows, a brief overview of research in the Netherlands, Willem de Gids and Hans Phaff, Institute for Environmental Hygiene-TNO, Delft, Netherlands